Seismicity and large earthquake potential in southwest Bulgaria and the conterminous Balkan high hazard region

A thesis submitted for the degree of
Doctor of Philosophy

Volume 1 of 2

Thomas James Bayliss

School of Environmental Sciences,
University of East Anglia

March 2010

For my Grandfather,

There is no justice in Nature perhaps,
but the idea of justice must be sacred.

H. G. Wells (A Modern Utopia)

Abstract

A new probabilistic seismic hazard assessment is performed across southwest Bulgaria, the Balkans and selected cities. Previous analyses were limited by the age of the study, timeliness of data used, hazard maps typically stopped at political borders, they estimated hazard for a limited range of descriptors, had a different geographic coverage, or differed in the research discipline(s) they investigated. This assessment uses these limitations as drivers for the work, and aims to mitigate these shortcomings.

A new historical earthquake catalogue is developed for the region's seismicity for moment magnitude 4.0 and above. This is adopted to illustrate seismic hazard for magnitude recurrence and ground motions in the region bounded by 39°-45°N, 19°-29°E, for return periods of 50, 100 and 200 years, and these time intervals at 90% probability of non-exceedance. Peak ground acceleration and macroseismic intensity are forecast to align with EUROCODE 8. Peak ground velocity is also considered as it better represents energy flux between ground and building and a potential future EUROCODE 8 metric.

The 475-year return period hazard is estimated for each hazard descriptor, making this study compatible to EUROCODE 8 – with respect to ground acceleration hazard – and comparable with GSHAP and SESAME seismic hazard projects. Analysis is extended to consider *maximum credible magnitude* and *earthquake perceptibility* hazard. The latter combines extreme value distribution statistics with ground motion models to forecast the *most perceptible magnitude*, $M_{P(max)}$, for a range of *scenario* ground motions.

Southwest Bulgaria is dominated by the Serbomacedonian massif and Krupnik fault, with both capable of generating large-magnitude earthquakes. It is consistently estimated highest levels of magnitude and ground motion hazard. Bulgaria's capital, Sofia, is estimated a regional upper bound magnitude of 7.86 M_s (±0.75) using an extreme values statistical model, compared with a *maximum credible magnitude* of 7.76 M_s using a cumulative strain energy release model. Importantly, the former model is asymptotic, relating the upper bound magnitude to an infinite waiting time; the latter reconciles a finite time for strain energy to accumulate equivalent to the maximum magnitude. The 475-year return period PGA for Sofia (from the lead peak ground acceleration model) is 177 cm s^{-2}.

Contents

List of Figures

List of Tables

Publications and Conferences

Bayliss, T. J. and Burton, P. W., 2004. A preliminary seismic hazard analysis for Bulgaria using extreme values and cumulative strain energy release techniques. *Geophysics in Economic Activity, Environment and Cultural Heritage Investigations, Fourth National Geophysical Conference,* Bulgarian Geophysical Society, Sofia, Bulgaria, 4-5 October, p54-55.

Bayliss, T. J., 2006. Seismicity and large earthquake potential in southwest Bulgaria and the conterminous Balkan high hazard region: maximum and perceptible earthquakes. *Risk Estimation and Reduction of Natural Disasters concerning Safety of Cities in Uzbekistan (earthquakes)*, Tashkent, Uzbekistan, 19-26 February.

Bayliss, T. J. and Burton, P. W., 2006. Ground motion attenuation, extremes and perceptibility hazard of acceleration, velocity and macroseismic intensity in Bulgaria and the broad Balkan region, *Proc. First European Conference on Earthquake Engineering and Seismology*, Geneva, Switzerland, 3-8 September, p177. [Abstract and poster]

Bayliss, T. J. and Burton, P. W., 2007. A new earthquake catalogue for Bulgaria and the conterminous Balkan high hazard region. *Nat. Hazards Earth Syst. Sci.*, 7(3), 345-359.

Bayliss, T. J. and Burton, P. W., 2008. Extreme magnitude and ground motion seismic hazard in the trans-frontier political triple junction region of Bulgaria, Greece and the Former Yugoslav Republic of Macedonia, *31st General Assembly of European Seismological Commission*, Crete, Greece, p257.

Bayliss, T. J., 2009. A new historical earthquake catalogue for Bulgaria and the conterminous Balkan high hazard region. Joint meeting of the NERIES NA4 module, TASK 3.1 of the *Seismic Hazard Harmonization in Europe* (SHARE) project and the ESC Working Group "*Parametric Earthquake catalogue in Europe*": *The Making of the European-Mediterranean Earthquake Catalogue*. Thessaloniki, Greece, October 12-14.

Bayliss, T. J. and Burton, P. W., 2010. EUROCODE 8 aligned PGA, PGV and perceptibility hazard for Bulgaria and site-specific Sofia, *32nd General Assembly of European Seismological Commission*, Montpellier, France, September 6-10, 2010. [Abstract and poster]

Acknowledgements

There are many who deserve to be mentioned in relation to this work. For most the order is immaterial. But firstly, I could not have even contemplated doing this work had it not been for the belief my grandparents, Pam and Eric, had in me to help finance my MSc at Keele. I would not have been able to do this PhD without that intervention, and I will forever be indebted to them both.

I have to pay thanks for the supervisory support of Dr Paul Burton, and the continual belief he has shown in me for the last ten years or so, even when it appeared this journey may not even begin, and when I was not studying at UEA. His guidance through both bad times and good, and his ability to bring focus back to work when it appeared my mind was wandering was critical to its success. Also realising, on occasions, that sometimes I just has to do things my way and needed my 'two pence worth' of say into what this work included for it to be that bit more 'valid and justifiable' for me to do. Thanks also to Dr Yebang Xu for his supervision.

I need also to thank Qin Changyuan, Susanne Sargeant and Roger Musson of the British Geological Survey, Dr Günter Leydecker of the Federal Institute for Geosciences and Natural Resources, Germany, Rumiana Glavcheva of the Bulgarian Geophysical Society, Prof. Boyko Ranguelov of the Bulgarian Academy of Sciences, Ioannis Kalogeras of NOA, Dr Spyros Pavlides of the University of Thessaloniki and Dr Nurcan Özel of the Kandilli Observatory and Earthquake Research Center who all assisted at some point with data, advice or technical support. Also a special thanks to Jamila. Thank you.

I absolutely must thank the staff of the International Seismological Centre. I am so glad I am still in contact with them after I finished working there in 2002; I consider them all to be very close friends of mine. The advice they gave on technical issues, data issues and contacts was, as always, extremely useful. I must thank them for allowing me to use their systems on a number of occasions when I – often urgently - most needed them.

I must thank all of my colleagues and friends of ONS Geography for putting up with me boring them no end with my fascination of earthquakes and seismology, when really I should have been concentrating on issues with UK geography. Ops. I have to extend special thanks to Ali (and Anna), Alistair, Alan T, Angela, Angie, Bernie, Carolyn, Cecilia, Gary (cheers Mate ... I owe you one), Hayley, Jonathan (and Kay), Lara, Lisa, Louise, Mark, Nancy, Nathan, Nick (and Katie), Pete and Tracy for the particular and varied help they gave that got me through this, helping me through

my time at ONS. They each helped in their own particular way, too much to say here, and this would have been that so much harder without all their help.

These past six years or so, working such a distance from UEA would have been so much harder had it not been for Clare, Steve, Graeme, Khaista, Paul and Antonia. They were my '*eyes and ears'* at UEA and were always willing to go the extra distance to photocopy papers, get forms, check my post and other mundane tasks that were of no benefit to themselves at all, but all of them helped over and above the level usually expected from a student's peer group. Antonia needs a special mention for the extra assistance with GIS she gave in the final two years or so (*so, how do you digitise again?*).

I have to thank Claire, John, Kathryn, Kate, Luke, Lynette, Mark, Sarah, Vera (the '*ENV old school*'), and my family for helping me through this time. Angela C deserves a special mention also. Maybe none of them understood why I wanted or needed to do this, but they all accepted that I had to and let me get on without questioning my motives. They all put up with the unreasonably long, unfair and oft selfish silences from me, and all showed a welcomed and genuine interest in how I was doing. It was this, almost more than anything else that got me through this little adventure of mine. For this I will always be grateful to you all. Cheers guys.

Chapter 1 : Context of the thesis

1.1 Introduction

As with many other Balkan and 'Eastern Block' countries, Bulgaria has been in a state of flux in recent years attempting to become an 'Accession State' to – and member of – the European Union; this was achieved on January 1st 2007. Its location in southeast mainland Europe offers a variety of regional topographies, from mountainous areas in southwest and central Bulgaria, plains in the southeast to coastal regions on the Black Sea in the east. Such a diverse range of regions lends itself to allowing commercial and industrial sectors to prosper to the south in the border regions with Greece and the Former Yugoslav Republic of Macedonia (FYROM), sport and tourism in the mountains and Black Sea region, and expanding residential areas throughout the country.

Although Greece, Italy and Turkey are generally accepted as the more seismically active territories within Europe, Bulgaria has also contributed significantly to global and European seismic energy release. It therefore requires due consideration with respect to seismic hazard and seismic risk studies to its population and infrastructure. Bulgaria has a number of significant and populous cities in it (Table 1.1). The presence of Europe's largest magnitude shallow earthquake of the last two centuries in its borders (Kresna, 4th April, 1904, 7.1 $\rightarrow$ 7.2 M [adjusted]; Ambraseys, 2001; Pavlides and Caputo, 2004), and other significant, documented sequences provides further evidence for this need.

Mapping Bulgarian seismic hazard has been attempted periodically since 1956, when the "*Regulations for design and construction of buildings and engineering structures in the seismic regions of Bulgaria*" demanded a seismic hazard review of this region. However, this and the other early studies were limited by applying statistical methods to review only a small number of earthquake hazard descriptors; namely intensity and peak ground acceleration. Additional attempts (e.g. Bončev *et al.*, 1982; Shebalin *et al.*, 1974b; Orozova-Stanishkova and Slejko, 1994) are detailed in chapters 2 and 4, and also suffer from these and similar limitations. The Bulgarian Academy of Sciences (BAS) realised the need to update previous hazard maps to better reflect seismic source zones and support the EUROCODE 8 building code (2003), advertising this requirement in their newsletters of December 2003 (Christoskov *et al.*, 2003) and December 2005 (Nikolova *et al.*, 2005).

City	Province	Population 1991[1]	Population 2001[1]	2008 estimate	91→08 % chge	01→08 % chge
Sofia	Sofia City	1,114,925	1,196,389	1,355,366	21.6	13.3
Plovdiv	Plovdiv	341,058	340,638	379,119	11.2	11.3
Varna	Varna	308,432	314,539	352,211	14.2	12.0
Burgas	Burgas	195,686	210,316	214,193	9.5	1.8
Rousse	Rousse	170,038	162,128	174,895	2.9	7.9
Stara Zagora	Stara Zagora	150,518	143,989	162,089	7.7	12.6
Pleven	Pleven	130,812	122,149	135,440	3.5	10.9
Dobrich	Dobrich	104,494	100,379	113,894	9.0	13.5
Sliven	Sliven	106,212	100,695	111,655	5.1	10.9
Shumen	Shumen	93,390	89,054	102,473	9.7	15.1
Haskovo	Haskovo	80,700	80,870	96,180	19.2	18.9
Pernik	Pernik	90,549	86,133	90,824	0.3	5.4
Yambol	Yambol	91,497	82,924	90,782	-0.8	9.5
Pazardzhik	Pazardzhik	82,578	79,476	86,772	5.1	9.2
Blagoevgrad	Blagoevgrad	71,476	71,361	80,022	12.0	12.1
Vratsa	Vratsa	75,518	69,923	77,318	2.4	10.6
Veliko Tarnovo	Veliko Tarnovo	67,540	66,998	73,152	8.3	9.2
Gabrovo	Gabrovo	76,522	67,350	71,270	-6.9	5.8
Vidin	Vidin	62,691	57,614	66,082	5.4	14.7
Kardzhali	Kardzhali	45,793	45,729	63,079	37.7	37.9
Kazanlak	Stara Zagora	60,095	54,021	60,157	0.1	11.4
Asenovgrad	Plovdiv	52,360	52,116	60,066	14.7	15.3
Kyustendil	Kyustendil	54,431	50,243	58,658	7.8	16.7
Montana	Montana	52,476	49,368	53,725	2.4	8.8
Dimitrovgrad	Haskovo	50,977	45,918	49,992	-1.9	8.9
Lovech	Lovech	48,242	44,262	48,264	0.0	9.0
Silistra	Silistra	48,360	48,360	47,753	-1.3	-1.3
Targovishte	Targovishte	43,016	40,775	47,064	9.4	15.4
Razgrad	Razgrad	40,933	39,036	45,057	10.1	15.4
Dupnitsa	Kyustendil	41,398	38,323	42,876	3.6	11.9
Gorna Oryahovitsa	Veliko Tarnovo	38,914	35,621	38,620	-0.8	8.4
Petrich	Blagoevgrad	27,659	29,785	36,665	32.6	23.1
Smolyan	Smolyan	34,086	33,153	33,763	-0.9	1.8
Sandanski	Blagoevgrad	26,096	26,695	30,782	18.0	15.3
Samokov	Sofia	28,608	27,664	30,140	5.4	9.0
Lom	Montana	31,133	27,897	28,640	-8.0	2.7
Karlovo	Plovdiv	27,291	25,715	27,908	2.3	8.5
Nova Zagora	Sliven	26,260	25,453	27,870	6.1	9.5
Sevlievo	Gabrovo	25,494	-	27,341	7.2	-
Svishtov	Veliko Tarnovo	30,404	30,591	27,275	-10.3	-10.8
Velingrad	Pazardzhik	25,634	25,009	26,853	4.8	7.4
Troyan	Lovech	-	25,104	25,986	-	3.5
Total		4,274,296	4,263,763	4,772,271	11.7	11.9

[1] From that year's Census

Table 1.1 Cities of Bulgaria with populations estimated at greater than 25,000 in 2008

Advent of EUROCODE 8 can be interpreted as a major driver for updating Bulgaria's seismic hazard maps, as conversely, maps of seismic zoning and hazard "*are a necessary and obligatory "seismic input" for EC8 adaption* [sic.] *in Bulgaria*" (Christokov *et al.*, 2003). The initial results for Bulgaria and some of its immediate surroundings can be seen in Ardeleanu *et al.* (2005) for Romania and, more recently and relevant, Simeonova *et al.* (2006) for Bulgaria. The latter develops a probabilistic seismic hazard map for Bulgaria aimed at supporting recommendations from the EUROCODE 8 building code.

However, these authors again restrict their assessments specifically to MSK intensity hazard for a network of seismic source zones with limited geographic coverage of this region. Use of the MSK intensity scale itself limits compliance with EUROCODE 8 requirements. Cross-border compliance in methodology used for these assessments was achieved through adopting identical seismic source zone networks, earthquake data sources and common study areas (e.g. the Vrancea intermediate depth earthquake zone). This also provides retrospective consistency and comparability with Bončev *et al.* (1982). This latter work is generally accepted as a 'standard' for seismic hazard assessment for the territory of Bulgaria and it forms the basis for the new seismic source zones.

Ardeleanu *et al.* and Simeonova *et al.*'s intent to just focus upon forecasting intensity hazard can in turn be considered a strong reason for developing additional evidence of seismic hazard. Applying alternative methods to compiling new seismic hazard maps for these and other earthquake hazard descriptors will allow this. García-Mayordomo *et al.* (2004) note how many current national seismic hazard assessments are dated (some being over 20 years old), inconsistent across Europe in terms of hazard assessed and hazard descriptor used (e.g. 475-year maximum PGA, maximum MSK intensity), their method of hazard calculation or their method of estimating the maximum magnitude event. EUROCODE 8 aims to increase homogeneity between European countries by requiring each to provide estimates for one basic hazard parameter, namely the 475-year peak ground acceleration corresponding to a 50-year return period at 90% probability of non-exceedance. Any deviation from this requirement will primarily be built into ground motion models selected for each territory of Europe.

1.2 Statement of the problem

Therefore, three main ideas act as 'drivers' for this work:

- A seismic hazard assessment for Bulgaria does not currently exist that incorporates a range of suitable and complementary statistical models for earthquake recurrence, techniques to

estimate cumulative strain energy release, its associated comparable magnitude forecasts (*the maximum credible magnitude*) and earthquake perceptibility hazard.

- The conterminous political-triple junction region of Greece, the Former Yugoslav Republic of Macedonia (FYROM) and Bulgaria has not yet been subject to a full probabilistic seismic hazard assessment to date. Although a number of geologic, tectonic and seismotectonic reviews do exist for southwest Bulgaria (e.g. Bončev, 1987b; Zagorčhev, 1992a, 1992b; Burchfiel et al., 2000; Meyer et al., 2002; Georgiev et al., 2002), seismic hazard could be considered a less well-explored area of investigation. However, the need to undertake this is apparent due to its close proximity to urban centres of Sofia, Plovdiv and Blagoevgrad – and other cities in FYROM and Greece – and any potential consequences that large magnitude and damaging earthquakes may have on these locations. Although there is a second political triple junction situated north of this one (between Serbia, FYROM and Bulgaria), the former has been selected due to the inherent higher localised seismicity of north Greece and its closer proximity to the North Anatolian Fault (NAF) and Hellenic Arc and Trench system of the Aegean Sea region.

- The latest rendition to Bulgaria's accepted standard seismic hazard map presents return period seismic hazard on a different hazard metric to equivalent hazard maps for Greece and FYR of Macedonia. This will therefore result in cross-border conflict between the adopted anti-seismic building codes of the adjoining countries.

1.3 Statement of intent

Sections 1.1 and 1.2 both outline a need to develop a new and alternative probabilistic seismic hazard assessment (PSHA) of Bulgaria. Such a PSHA is developed here by applying:

1. Selected *whole* and *part process* statistical earthquake magnitude recurrence models,

2. Selected ground motion models from previous, studies that were developed specifically for the region, and,

3. Comparative seismic hazard techniques of cumulative strain energy release statistics and earthquake perceptibility.

These will contribute to previous earthquake hazard assessments of Bulgaria by concentrating upon assessing earthquake extreme hazard using a standard PSHA framework of:

- Potential earthquake magnitudes,
- Locations,
- Earthquake recurrence,
- Ground motion, and,
- Variability.

Estimates will be provided resulting from this PSHA framework for pre-selected earthquake and ground motion scenarios, with a view to providing comparable but alternative hazard forecasts for Bulgaria and specific urban centres. The broader geographic extent considered during this study is illustrated in Figure 5.1.

1.4 Structure of the thesis

This thesis is divided into seven chapters:

Chapter 2 outlines the geologic, tectonic and seismotectonic setting of Bulgaria within the context of the broader Balkan and Aegean regions. It outlines previous studies that concentrated upon these elements that are required to allow a full probabilistic seismic hazard to occur and be understood. It attempts to synthesise a range of alternative theories put forward to explain the region's geologic and tectonic evolution, and stages to reach its current geological form. Chapter 2 will continue by assessing the region's own historical seismicity, in terms of spatial and temporal distributions of the area's *parent* seismicity, and its measurement using national and international seismograph and accelerograph networks within FYROM, Bulgaria, Greece and Turkey to record seismicity levels in these countries and beyond. It continues to discuss recent regional crustal velocity models to explain active crustal deformation of the Balkan and north Aegean areas, with particular emphasis on southern Bulgaria, and suggested recent seismotectonic source models for Bulgaria and adjacent countries as mechanisms for adequately zoning the area's seismicity. Chapter 2 finishes by summarising significant large magnitude historical earthquakes.

Chapter 3 consists of two parts. The first summarises key statistical earthquake recurrence models – namely *whole process* and *part process* recurrence models – that may be used to consider seismic hazard. Particular attention is made to development and previous uses of the *whole process* cumulative frequency-magnitude distribution (Gutenberg-Richter, 1944) and the asymptotic theory of extreme values (Gumbel, 1958).

The second section summarises key historical and newer ground motion models for this region to measure ground acceleration, ground velocity and macroseismic intensity. It finishes with a brief discussion of zoned versus zone-free hazard analyses. This chapter concludes by summarising the ground motion models that will be adopted in chapters 5 and 6 to undertake a seismic hazard analysis.

Chapter 4 discusses steps to develop a new earthquake catalogue that becomes the main input to the ensuing seismic hazard assessment of Bulgaria. Details are given on previous, comparable datasets that have been developed for similar reasons, their limitations and strengths, which become governing drivers for creating this new dataset. Chapter 4 continues by outlining steps to magnitude homogenisation of all events onto the modern standard moment magnitude and surface-wave magnitude scales, and preparatory magnitude homogenization of selected key early instrumental (pre-1964) large magnitude (≥6.0 M) earthquakes. A magnitude completeness analysis is then performed on the full dataset – and subsets thereof – using standard cumulative frequency-magnitude and time-magnitude distributions. Stationarity of these data is considered for both geographic extents considered in chapters 5 and 6, as well as at a cellular level to briefly investigate magnitude stationarity at finer resolutions and its variation across the broad geographic extent.

Chapter 5 starts the probabilistic seismic hazard assessment of Bulgaria, the broader Balkan region and the political triple junction region between Bulgaria, FYROM and Greece, as well as selected key urban centres within the larger area. Chapter 5 starts with an appraisal of the earthquake catalogue developed in chapter 4 to determine *fit-for-purpose* catalogue criteria – start year, magnitude threshold and extreme interval – to adopt throughout chapters 5 and 6 to estimate realistic and stable extreme seismic hazard statistics at all geographic levels considered.

Magnitude hazard estimates are then developed using the *whole process* cumulative frequency-magnitude distribution and then compared with estimates from Gumbel's *part process* asymptotic third distribution of extreme values (after adopting specific catalogue criteria determined earlier in the chapter). Gumbel's first and third extreme values distributions are also applied to the dataset to forecast estimates for peak ground acceleration, peak ground velocity and peak macroseismic intensity at all geographic levels considered. PGA estimates are compared with GSHAP and

SESAME international seismic hazard projects. A similar sensitivity analysis will be adopted for macroseismic intensity to determine *fit-for-purpose* data constraints to forecast realistic hazard estimates. Suites of hazard maps for the Balkans and southwest Bulgaria are then created for each hazard descriptor considered.

This chapter finishes by considering these extreme hazard estimates with reference to relevant previous studies of this region, and also the 475-year return period event that is the standard adopted internationally hazard measure in EUROCODE 8.

Chapter 6 continues and finishes the seismic hazard assessment started in chapter 5 by developing estimates for the *maximum credible earthquake magnitude* and other *scenario* earthquakes using *whole process* cumulative strain energy release techniques. Magnitude hazard estimates developed will be used along with their associated waiting time statistics to determine the regions that may have experienced a complete cycle of seismicity during the time span of the developed catalogue. They will also be compared retrospectively to *whole process* and *part process* magnitude hazard estimates from chapter 5 at each geographic level considered.

Elements of magnitude extreme hazard forecasts developed in chapter 5 from Gumbel's third extreme distribution will be extracted and applied in combination with the ground motion models from chapter 3 to develop estimates for the *most perceptible earthquake magnitude*, $M_{P(max)}$ – a *design* earthquake magnitude – from investigating earthquake perceptibility and integrated perceptibility. Additional suites of hazard maps for the Balkans and southwest Bulgaria are created for these alternative hazard descriptors.

As earthquake perceptibility constitutes a form of seismic hazard disaggregation, a brief discussion of this concept is given, outlining its strengths and weaknesses and relevance to a probabilistic seismic hazard assessment such as this, and previous approaches used are adapted to consider seismic source partitioning for each urban centre considered.

Chapter 7 summarises this work and discusses key conclusions from each preceding chapter, with respect to strengths and weaknesses of the selected ground motion models (chapter 3), mechanisms to creating the input earthquake catalogue (chapter 4) and statistical recurrence and forecasting models adopted to undertake this new seismic hazard assessment of Bulgaria (chapter 5 and 6). It finishes by considering how the scope of this work may be refined and extended in the future.

Chapter 2 : Geology, seismotectonics and historical seismicity of Bulgaria

2.1 Introduction

This chapter summarises the geology, tectonic and seismotectonic regimes of southwest Bulgaria and the Balkans. Consideration will also be made to recent investigations of regional and localised crustal movements and velocity fields using Global Positioning System (GPS) data.

As in many seismic regions of the world, Bulgaria possesses a number of key industrial, commercial and residential areas. Plovdiv, Blagoevgrad, Varna as well its capital Sofia are all located in regions with varying levels of seismicity – and therefore seismic hazard and ensuing seismic risk – within Bulgaria. With increasing demands to take advantage of this country in its many forms, there is a need to better understand the natural environment that creates an earthquake hazard to them. It is through understanding geologic and [seismo]tectonic environments for sub regions in which these cities are located that it becomes possible to forecast and appreciate patterns and levels of seismic hazard to which they may be subject in the future.

Greece and Turkey to the south and southeast are generally considered more seismically active than Bulgaria. However, up until the occurrence of the 1999 Izmit earthquake (7.4 M_w, 7.5 M_s, 6.8 m_b, h = 17.0 km) Bulgaria had the dubious distinction of experiencing the strongest shallow-focus event during the 20th century (Kresna, 4th April 1904, revised surface wave estimate of 7.2 M_s and depth, h = 24.0 km; Pavlides and Caputo, 2004; van Eck and Stoyanov, 1996). This, combined with southwest Bulgaria being a sub-zone of unusually high seismicity for the country, dictates that its large earthquake potential needs to be addressed and appreciated.

Following is a brief summary of the geological and seismotectonic structures of note in this region and how their appreciation and understanding developed over time. A connection between the seismotectonic nature of the Greek and Aegean regions to the south and the southern Bulgarian seismotectonic zone will also be made.

2.2 Summary of regional geology and seismotectonics

Theories on current tectonic and geologic evolution of Bulgaria and its surrounding region were first proposed towards the end of the 19th century (Suess, 1885) and the start of the 20th century (Cvijic, 1904; Stille, 1924, 1928; Wilser, 1928; Kober, 1931). These ideas expanded views that the country and region as a whole could be sub-divided into two distinct large lithospheric crustal

plates spanning southeast Europe and Frontal Asia (Bončev, 1987b). These are the Moesian platform and Thracian Plate (Figure 2.1). Bončev *et al.* (1982) and Bončev (1987b) extend this idea by detailing fragmenting of the Thracian Plate and its development into four further geologic structural provinces. With the Moesian platform dominating much of the northern region, the geology of Bulgaria is completed by the Balkanides to the south of the Moesian platform, the Rhodopian massif extending over the southern extent of Bulgaria, the Srednogorie splitting the Balkanides and Rhodopian massif, and finally the Kraishtides to the west (Figure 2.1). These additional structures developed within what is known as the Balkanide mobile space, Balkanide conflicting (or collision) zone or Balkanide lineament bundle.

A number of theories exist, many relatively recent, that detail regional tectonics of Bulgaria and the tectonic and geologic setting of the seismic region of southwest Bulgaria (Zagorchev, 1992a, 1992b). One idea linking Bulgarian tectonics to that of the rest of the eastern Mediterranean is that the country is part of the continental margin area of Eurasia (Dabovsky, 1991). The Balkan Peninsula's Alpine region, of which Bulgaria is a part, may be a three-order collisional system consisting of a main thrust belt (the Inner Helenides), plateau (Rhodopes and Srednorgorie) and back-thrust system (the Balkanides; Orozova-Staniskova and Slejko, 1994). This is an improvement on an initial proposal in Staniskova and Slejko (1991).

The second modern idea involves Bulgaria occupying a number of units of a tectonic 'collage' along the Eurasian margin (Dabovsky, 1991). This second tectonic model again considers three first-order geologic units, but relates them to different structural zones of Bulgaria; the Moesian platform, the deformed margin of the platform (Balkanides, Srednorgorie, parts of the Kraishtides and south eastern most section of the Srednorgorie extent) and a 'collage' along the platform margin (thrust sheets in the area of Kraishtides, the Rhodopes and south eastern Srednorgorie; Figure 2.1).

Bulgarian seismicity is largely a result of the collision between the African and European plates. The resulting subduction zone is clearly defined by the Hellenic Arc-trench system, creating an Alpine mountain belt system in the south and southwest. Consequently the most seismically active region of Bulgaria, the southwest, is dominated by a fractured faulting system of Horst-Graben structures illustrated in Figure 2.2 (Georgiev *et al.*, 2002; Tzankov *et al.*, 1996) and regional extension similar in nature to that of northwest Greece (Meyer *et al.*, 2002), and encompassed by the Dinarides, Hellenides, the Rhodopes and Balkan mountain belts (Figure 2.3).

Being a predominantly extensional environment, the major Horst-Graben structures contribute significantly to the tectonic dynamics of the southwest Bulgarian region, lying as they do between

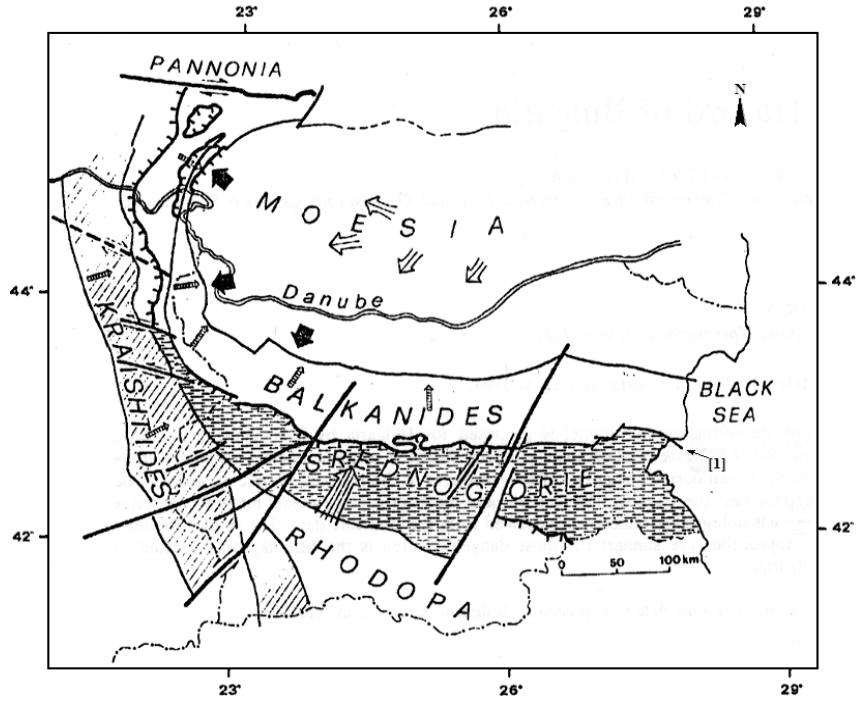

Figure 2.1 The main structural geologic zones of the Balkan Peninsula: the Moesian platform (north) and Thracian Plate (south) are divided by a line indicated at [1] (adapted from: Orozova-Staniskova and Slejko, 1994)

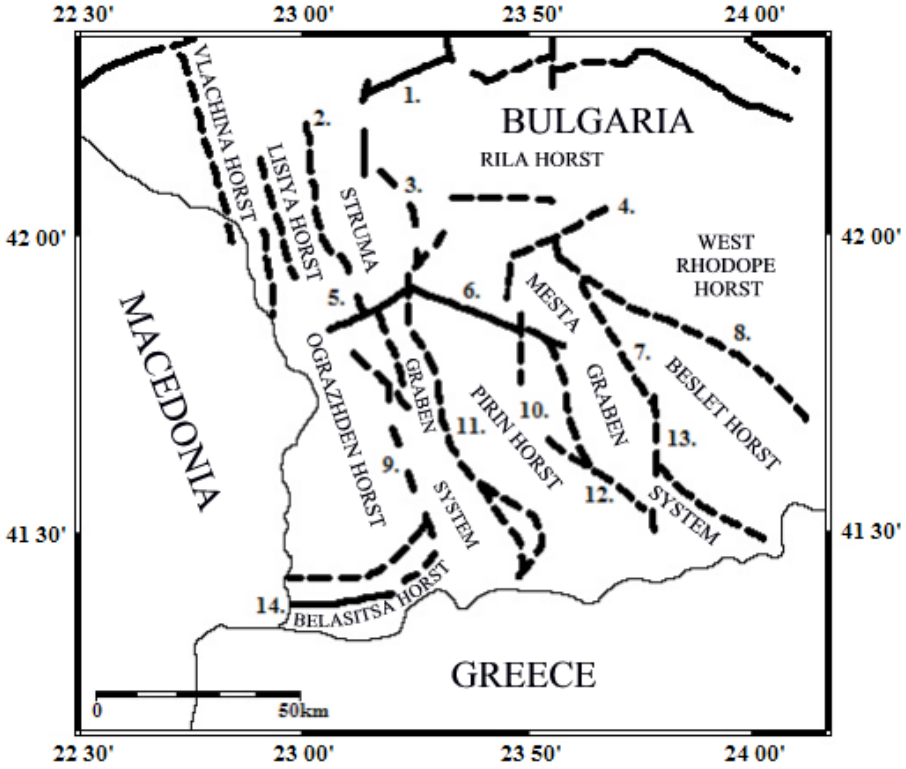

Figure 2.2 Main block and fault structures in southwest Bulgaria: 1) Klisura fault, 2) Lisiya fault zone, 3) West-Rila fault zone, 4) Semkova fault, 5) Krupnik fault, 6) Predela fault, 7) Osenovo-Ribnovo fault zone, 8) Dospat fault, 9) Ograzhden fault, 10) East-Pirin fault zone, 11) West-Pirin fault zone, 12) Gotse Delchev fault, 13) Ognyanovo-Illindentsi fault zone, 14) Petrich fault. Solid lines = recently active (present day) fault; dashed lines = neotectonic fault (adapted from: Georgiev *et al.*, 2002)

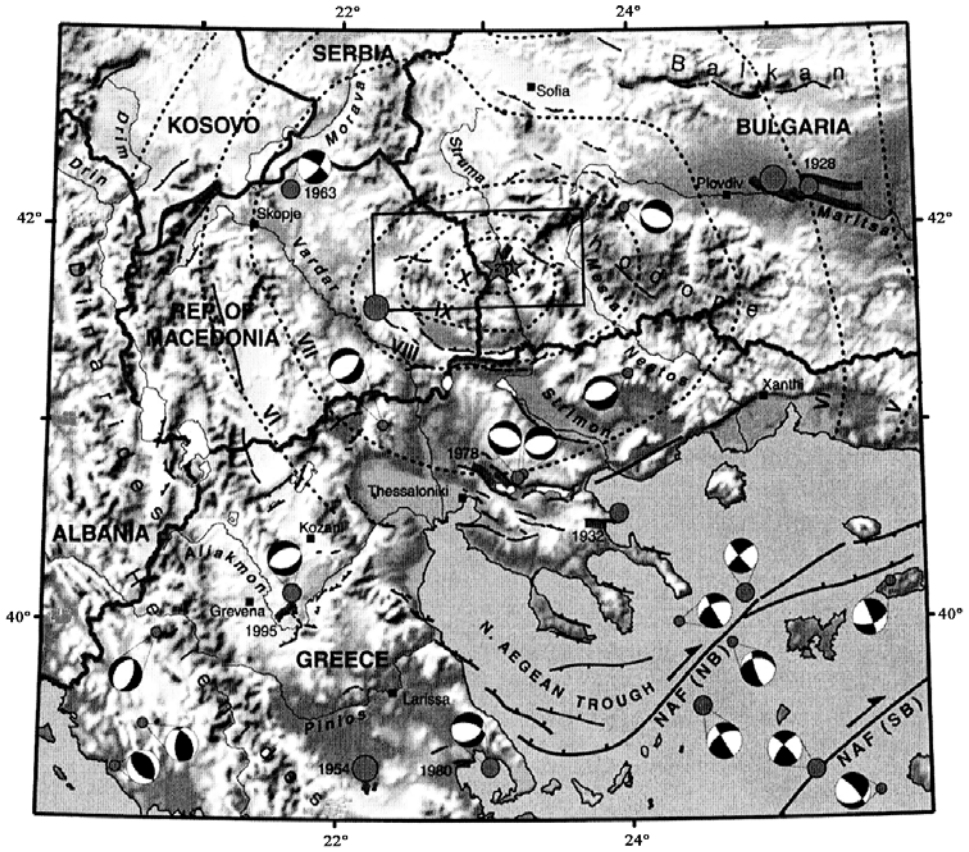

Figure 2.3 Key alpine mountain systems and seismicity of southwest Bulgaria and north Greece; NAF = North Anatolian Fault (adapted from: Meyer *et al.*, 2002)

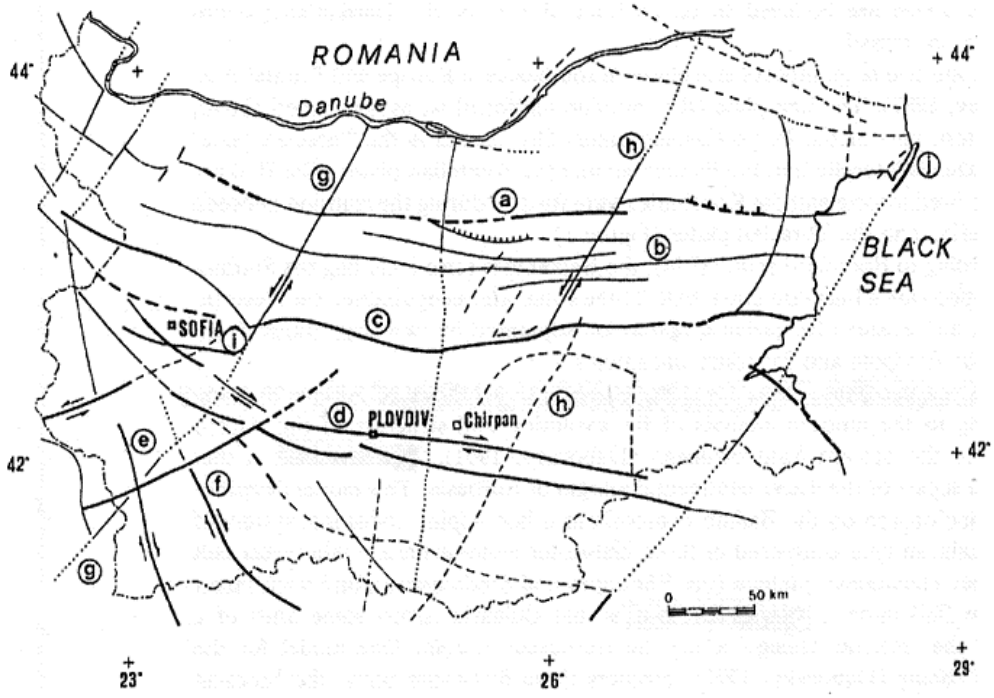

Figure 2.4 Major faults in Bulgaria; a = Fore-Balkan fault; b = Stara Planina frontal line; c = Sub-Balkan fault; d = Maritza fault; e = Struma deep fault; f = Mesta fault; g = Etropole line; h = Tvarditza line; i = Vitoshi fault; j = Black Sea cryptostructure. Heavy lines = neotectonic active faults; lines with arrows = strike-slip faults; dashed line = postulated faults; dotted lined = buried faults; lines with hatchings = normal faults or flexures (adapted from: Orozova-Staniskova and Slejko, 1994)

normal faults of the area. Normal faults will in-turn generate much of the local and regional medium and large magnitude seismicity (e.g. the 1904 Kresna earthquake). The Horst structures of the region (e.g. Osogovo, Vlahina, Kresna, Belasitsa, Rila and especially the Pirin) and the Graben structures (e.g. Blagoevgrad, Sandanski, Dupnitsa, Simitli, Razlog) characterize intensive horizontal and vertical movements, for the whole neotectonic stage, by as much as 2-3,000 metres.

A lot of the tectonic movement occurred during the Pliocene and late Miocene epochs; the west Rila fault zone experienced approximately 2,700 metres of uplift on the Rila horst relative to the Blagoevgrad Graben, while there were about 3,000 metres of uplift movement of the Pirin horst relative to the Sandanski Graben between the late Miocene and Pleistocene epochs. Further significant uplift occurred on the Osenova-Ribnova fault zone, illustrated by 1,800 metres uplift of the West Rhodope horst relative to the Mesta Graben system.

However, significant movements are not confined to these ancient periods of time. The Petrich fault – bounding the Belasitsa Horst and Strumeshnitsa Graben complex – the Predela fault that bounds the Pirin Horst and Razlog Graben and the Ognyanovo-Ilindentsi fault zone are all recently active fault zones in southwest Bulgaria.

The dominant structure in the south and southwest of the country, the Rhodope massif, can be considered either to be a stable crustal block that has been gradually broken into smaller block units over time and found between the Dinarides, Hellenides and Balkanides (Bončev, 1987a, 1987b), or as proposed more recently, a region subject to collision followed by extensional tectonics (Zagorčhev, 1992a, 1994). The former model, if correct, is the source of the suggested fracture system mentioned earlier. van Eck and Stoyanov (1996) support Jackson (1994) and Zagorčhev (1994) that southern Bulgaria appears to belong to the same seismotectonic unit as northern Greece and Aegean.

Like other tectonic environments, Bulgaria and its south and southwest regions are governed by a network of faults that create its natural seismicity and ensuing seismic hazard. The important faults in the tectonics of Bulgaria – due to their prominence, fault length and proximity to the epicentral region of the 1904 sequence – are the Fore-Balkan fault, the Stara-Planina frontal line, the Sub-Balkan Fault, the Maritza shaft and the Struma and Mesta deep faults, and the Entropole and Tzarditza lineaments (Figure 2.4). To the southwest the Kocani – crossing the border into the Former Yugoslav Republic of Macedonia – Bansko and Krupnik faults take dominance. The latter two faults are closest to the focus of the 1904 large magnitude event (Meyer *et al.*, 2002). All three are known to be normal faults of between 20 and 35 kilometres in length. No fault has been explicitly linked to generating the 1904 Kresna earthquake. However, Wells and Coppersmith

(1994) and Burton (1996) both suggest faulting of ~35 kilometres may resolve to produce an earthquake of 7.0 M. The southwest region appears to be under crustal extension (Jackson and Mckenzie, 1988; Armijo *et al.*, 1996; Burchfiel *et al.*, 2000) and is likely the northern-most section of the Aegean tectonic structure. Extensional tectonic environments initiate in northern Greece and southwest Bulgaria and then propagate into central Bulgaria on east-west striking faults.

A number of smaller faults that populate the region between Bulgaria, the FYR of Macedonia and Greece suffered surface rupturing during relatively large magnitude events in recent history. The Thessaloniki, 6.4 M_s, (1978) and Grevena, 6.6 M_s (1995) earthquakes both achieved surface rupturing of 10 kilometres or more in northern Greece. The well-documented 1928 earthquake sequence near Plovdiv in Bulgaria (6.8 M and 7.0 M respectively) broke 20 to 25 km sections of the Maritza valley faults in northeast Bulgaria (Richter, 1958). The 1978 sequence of seismicity east of Thessaloniki, northern Greece, was a result of the Serbomacedonian massif that extends north into Bulgaria (Papazachos *et al.*, 1979). This is the tectonic structure that both the 1978 Thessaloniki and 1904 Struma Valley sequences occurred on or in close proximity to in this border region. The Rhopodian geologic zone is east of the Serbomacedonian massif and the Axios-Vardar zone is to the west.

2.3 Monitoring regional seismicity

An area's seismicity is best defined as a function of the size of earthquakes (magnitude, seismic moment etc. and levels of strong ground motion, e.g. intensity, peak ground acceleration etc.) and the frequency of occurrence of these earthquakes (Papazachos, 1990). The seismicity of this study region is best considered in two distinct units, as the two main countries within it are largely governed by different tectonic regimes. That is, that covering Greece and the Aegean and generated by the Hellenic Arc to the south, its associated faulting system and the North Anatolian Fault (NAF) in the north, and that covering Bulgaria generated by the major faults detailed in Figure 2.4 and smaller fracture systems to the southwest.

Monitoring of the full region's seismicity is largely covered between the national networks of Bulgaria, the FYR of Macedonia and Greece. The National Operative Telemetric System for Seismological Information (NOTSSI; Figure 2.5) in Bulgaria consists of 14 permanent and seven local network short period seismograph stations, each also possessing single component vertical S-13 velocitygraphs (Glavcheva *et al.*, 2003). Sensitivity of installed equipment on NOTSSI allows monitoring of Bulgarian seismicity down to minimum magnitude of ≈1.0 M. The installed monitoring network within Bulgaria allows seismologists to define a "*layered*" magnitude threshold of monitoring outside the country's political boundaries, meaning the recording threshold

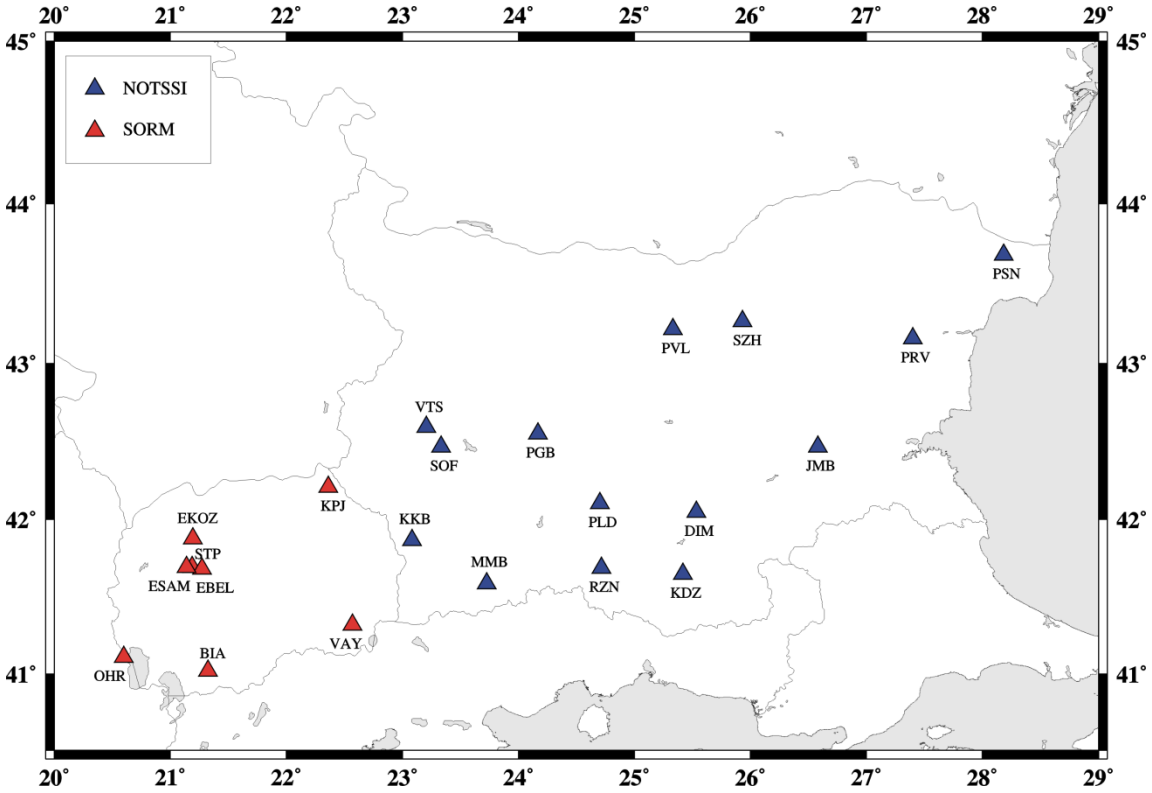

Figure 2.5 Station networks of Bulgaria (NOTSSI - National Operative Telemetric System for Seismological Information; source: after Glavcheva *et al.*, 2003) and the Seismological Observatory Republic of Macedonia (SORM)

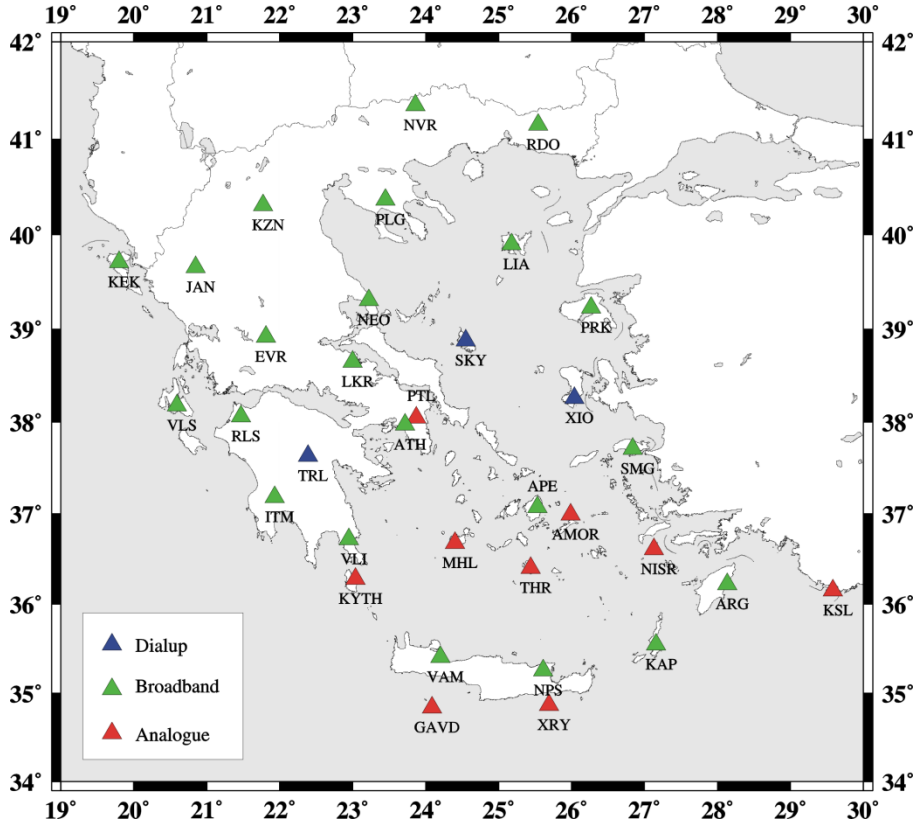

Figure 2.6 Seismological network of the Geodynamic Institute of the National Observatory of Athens (after http://www.gein.noa.gr/services/net_figure.gif)

for Bulgaria is 2.0 M, 3.0 M for the broad Balkan region, and 5.0 M for long-distance events (although this is only true for one or two of the networks stations; Ranguelov, pers. comm.).

The National Observatory of Athens (NOA) and the Geophysical Laboratory of Thessaloniki jointly run the permanent seismological network of Greece (Figure 2.6 and Figure 2.7). NOA's network consists of 22 permanent seismic stations, nine of which have digital capability. The stations at Athens and Anogeia (Crete) are both linked to international seismograph networks (WWSSN and MEDNET (MEDiterranean NETwork) respectively). An additional seven mobile radio-linked seismic stations and 10 portable seismographs compliment NOA's permanent network. The Geophysical Laboratory of Thessaloniki's seismographs network consists of 16 permanent seismograph stations; one located centrally to the network at the University of Thessaloniki, and 15 peripheral stations extending to cover the Serbomacedonian zone, north Aegean area and Ionian Islands and has been continually extended since 1981.

The FYR of Macedonia's national seismograph network contains six stations each possessing a range of seismographic recording equipment sited at Skopje, Valandovo, Ohrid, Bitola, Kriva Palanka and Stip. This network began operations on July 1st 1957.

The eastern extent of the catalogued region is predominantly covered by West Turkey (Figure 2.8; Kalafat, 2003). Turkey's countrywide seismograph network is run by the Kandilli Observatory Research Institute at the Boğaziçi (Bosphorus) University (BU-KOERI) and has been in operation since 1987 (although earthquake monitoring in Turkey began in the 1930s). At present the network consists of a total of 75 stations, consisting of 60 short period analog (1-component), 10 broadband digital (3-component) and five short period digital (3-component) stations.

Currently there is no mutual co-operation between national earthquake monitoring networks and interested institutes of Bulgaria, Greece and the FYR of Macedonia to allow transfer of earthquake information or knowledge. This excludes special cases, and organisation by individual researchers.

A number of the networks described above have realised the need to monitor micro-seismic activity in the region in addition to macroseismic events. The highly sensitive equipment used in NOTSSI (Bulgaria) – especially in southwest Bulgaria – allows regular recording of events with $M < 1.0$. Over 95% of all events recorded within the borders of Bulgaria have a magnitude $M < 3.0$, confirming this area is dominated by low and medium seismicity. Monitoring of Greek micro-seismicity is supported by mobile and portable equipment of NOA's network listed above. These are found particularly useful in monitoring aftershock activity in the region (Makris *et al.*, 2004; Karastathis *et al.*, 2005; Contadakis and Asteriadis, 2002).

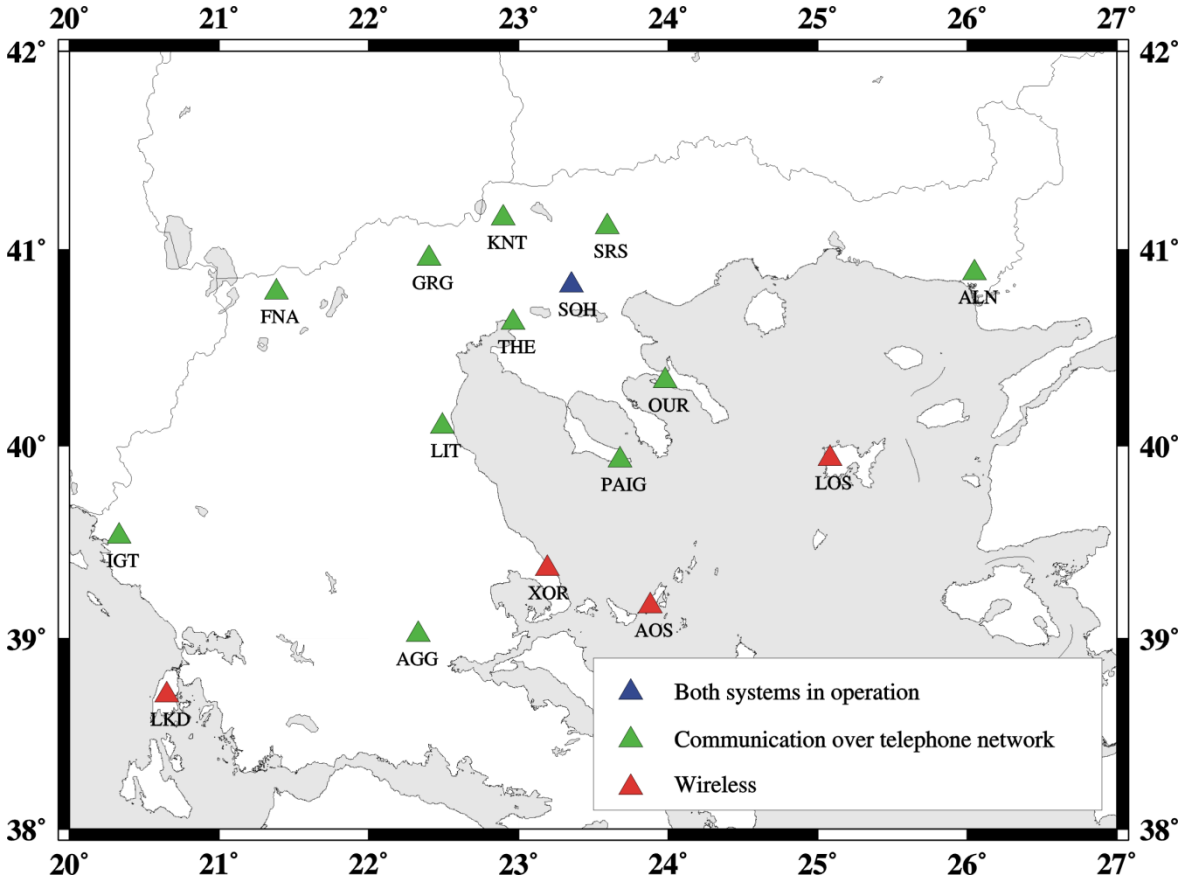

Figure 2.7 The telemetric seismological network of the Laboratory of Geophysics, Aristotle University of Thessaloniki, active since January 1st 1981 (source: after http://lemnos.geo.auth.gr/the_seisnet/en/network.htm)

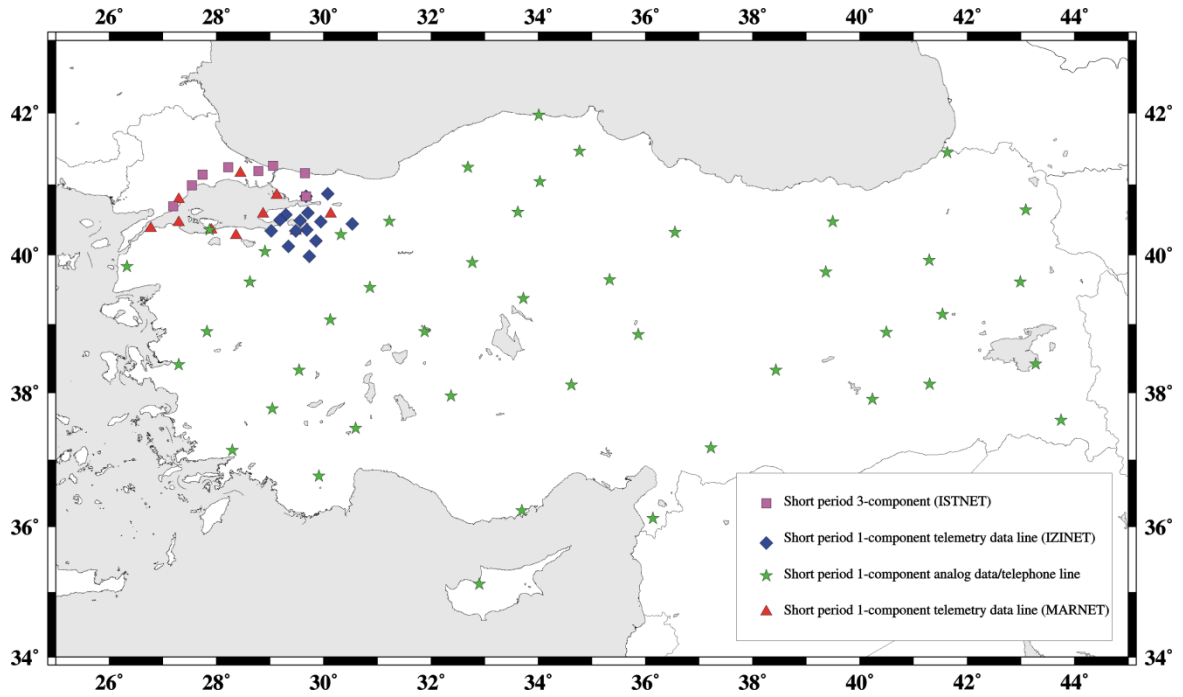

Figure 2.8 The Kandilli Observatory and Earthquake Research Institute seismic network as of April 2003

2.4 Spatial and temporal distribution of seismicity

2.4.1 Instrumental period of recording

Hypocentral distribution of Bulgaria's seismicity is shown in Figure 2.9 as represented by this catalogue. Symbol size is proportional to the homogenized surface-wave magnitude. These classes are then further divided by focal depth of $h < 10$ km, $10 \text{ km} \leq h < 30$ km and $h \geq 30$ km. It is fair to assume the event location accuracy will have improved over time with the advent of more sensitive monitoring equipment and wider coverage seismograph networks.

Approximately fifty-three percent of the seismicity in the catalogued region occurred in the southwest quarter during the time interval catalogued. Most of this is accounted for by the northern reaches of the Hellenic Arc subduction zone situated on the western coast of Albania and western and southern coastal reaches of Greece. Shallow-focus earthquakes created on low-angle thrust faults of the Hellenic Trench characterize this region's seismicity (Burton *et al.*, 2003). A second belt of high seismicity is associated with the North Anatolian Fault running across north Turkey and the Aegean Sea, to the south of the catalogued area. These belts meet at the Ionian Island network, defining a region of active shallow seismicity (Papazachos and Papazachou, 1997).

The southwest and southern regions of the country are predominantly characterized by small to moderate magnitude earthquakes (≤4.5 M), but have also experienced a small number of large magnitude events. The start of the 20th century experienced the large magnitude 1904 Kresna sequence and 1928 Plovdiv sequences. However, since these occurred, no strong events of this nature have occurred within the political borders of Bulgaria. High seismicity reduced around 1940 to 1945. This may be accounted for as a seismic gap or simple over estimation of older earthquake events, for example the 1904 Kresna event (Stanishkova and Slejko, 1991; Drakopoulos, 1976).

2.4.2 Pre-instrumental period of recording

Shebalin *et al.* (1998) and Papazachos and Papazachou (1997) are advocated here and by Burton *et al.* (2004a) as the most suitable sources of supplementary earthquake information to the Balkan and Greek catalogues respectively (Table 2.1) for the pre-instrumental (pre-1900) recording of seismicity. All events with homogenized magnitude $M_s \geq 7.0$ for instrumental and pre-instrumental periods of recording are mapped in Figure 2.10. This figure also classifies events by focal depth. Further details on earthquake parameter uncertainties for historical, early instrumental and instrumental periods of seismicity monitoring from the main data sources are given in chapter 4.

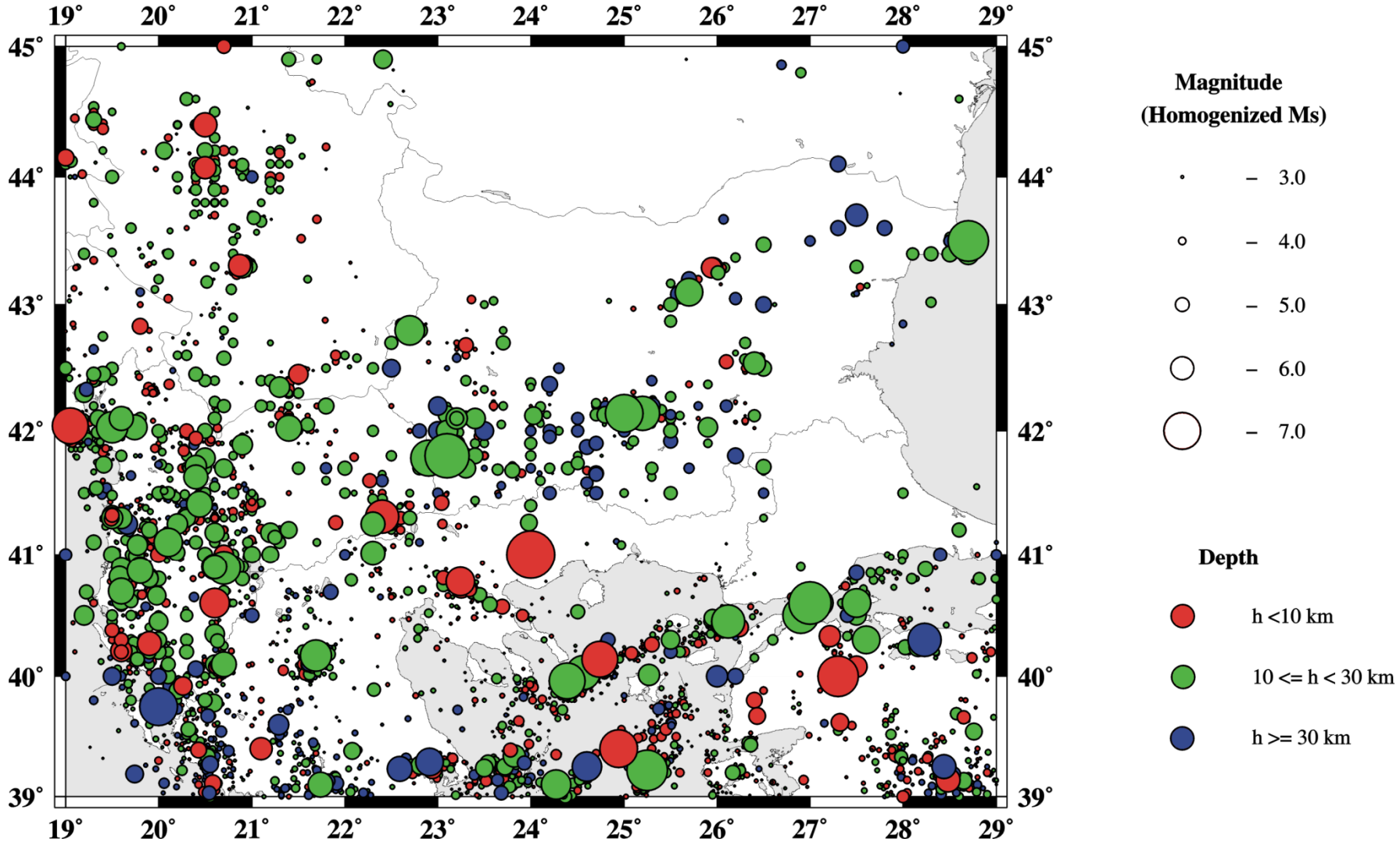

Figure 2.9 Earthquake epicentres of the Balkan region for the time interval 1900 to 2004; the early and modern instrumental periods (1900 to 2004) represent the catalogue presented in chapter 4

Criteria	Shebalin *et al.* (1998)	Papazachos and Papazachou (1997)
Full time range	342 BC to 1990	550 BC to 1995
Geographical limits	(Approx.) 38°-55°N, 10°-35°E	34.80°-42.80°N, 18.10°-31.00°E
Number of events	1,340	427
Magnitude range(s)/ magnitude thresholds	See Table 4.1	$6.0 \leq M_w \leq 8.3$
Depth range	$2.0 \leq h \leq 150.0$ km	Depth estimates are only supplied for instrumental period earthquakes. For pre-instrumental period 'n' (normal) is used for shallow earthquakes and 'i' (intermediate) is used for intermediate depth earthquakes.
Magnitude conversions to note	$M_s = 1.2m_b - 1.45$ $m_b = 0.63M_s + 2.5$	$M = M_s$ …$6.0 \leq M_s \leq 8.0$ $M = M_w$ …$5.0 \leq M_s \leq 8.0$
Main data sources	Many (50+) historical sources used including catalogues of Kárník, (1968, 1971), isoseismal atlases of Glavcheva (1993), Shebalin (1974) and Kárník and Hadzievski (1974) and others for neighbouring countries.	Macroseismic catalogues including Galanopoulos (1960, 1961); Evagelatou-Notara (1993); Guidoboni *et al.* (1994); Ambraseys and Finkel, (1995); various works of Papaioannou
Further notes	Main catalogue supplemented by additional listing of "doubtful and boundary" events (processed to same standard as main catalogue).	Sixteen events with $M \leq 6.0$ included as each has important historical relevance. Information on 18 listed events was inferred indirectly so should be used with caution. Magnitude error (events 550 BC to 1910) ± 0.3 M.

Table 2.1 Comparison of complementary pre-instrumental data sources to the presented Balkan catalogue and Greek earthquake catalogue

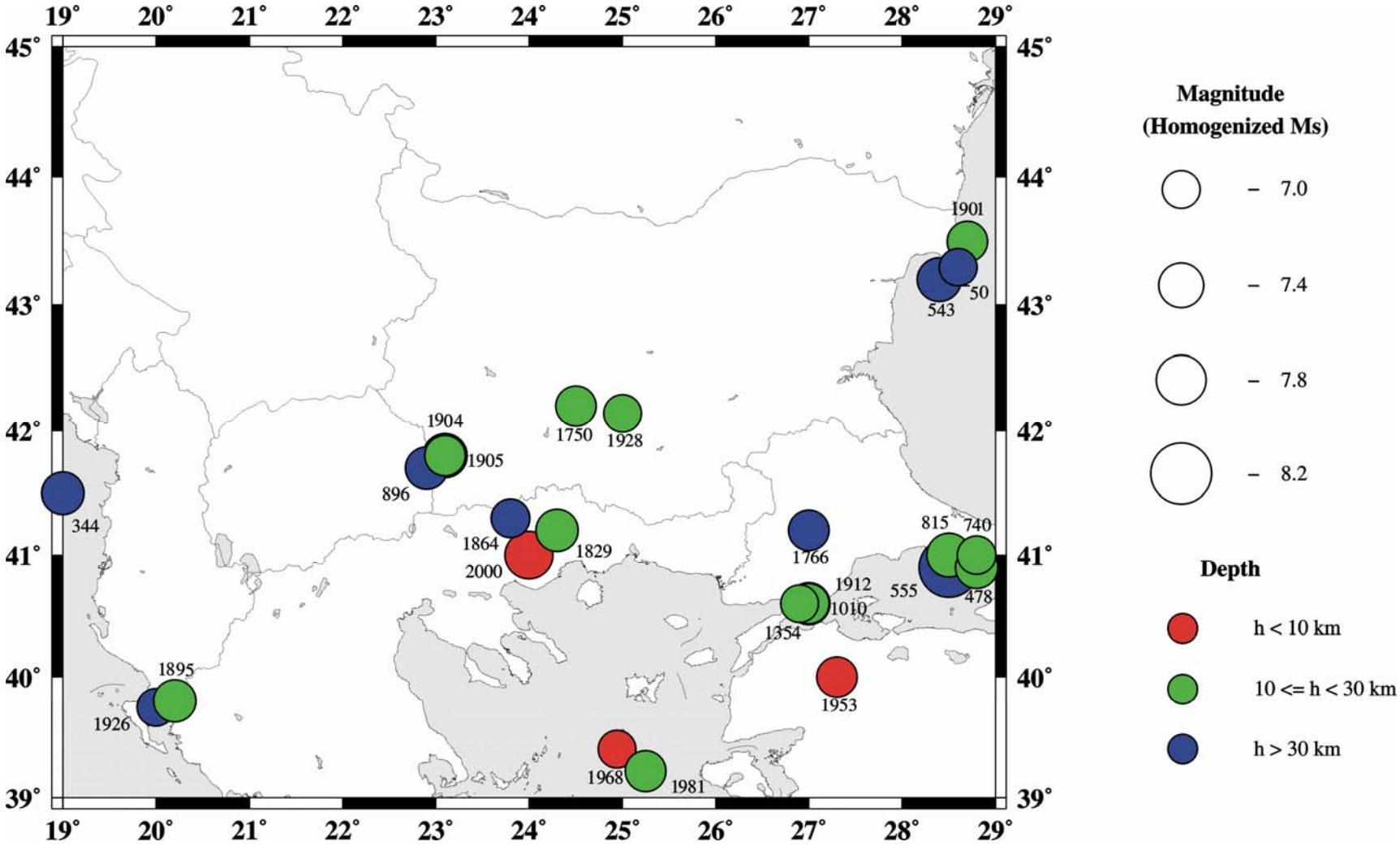

Figure 2.10 Epicentral map of seismicity that occurred in the Balkan region for the time interval 342 BC to 2004, with homogenized $M_s \geq 7.0$. Shebalin *et al*. (1998) provides the pre-instrumental period 342 BC to 1899, while the instrumental period (1900 to 2004) is represented by the catalogue of this work

The large magnitude event near Thessaloniki in 2000 can be considered anomalous in the context of all regional seismicity. This event's reported magnitude was 6.5 m_b. However, the steep gradient of the $m_b \rightarrow M_s$ magnitude conversion relation – created from the higher seismicity of Greece and the north Aegean by Burton *et al*. (2004a) and adopted in this study for the area south of the 43°N parallel common to both studies, but incorporating low-medium seismicity of southern Bulgaria – has likely generated this unusually high homogenized magnitude estimate.

Extending back into historical seismicity (Figure 2.11 illustrates back to the start of the 19th century), a number of additional large magnitude ($M_s \geq 7.0$) events are discovered, e.g.: 50 BC (7.1 M_s), 344 (7.3 M_s), 478 (7.3 M_s), 543 (7.4 M_s), 554 (8.2 M_s), 1354 (7.0 M_s), 1750 (7.0 M_s), 1766 (7.2 M_s), 1829 (7.3 M_s), 1864 (7.1 M_s), 1895 (7.3 M_s) (all years and magnitude estimates quoted here have been extracted from Shebalin *et al.* (1998) and are unhomogenized). Orozova-Staniskova and Slejko (1994) provided estimates for a small number of additional large magnitude events. These were omitted from the list above as Shebalin *et al.* (1998) revised their reported magnitude estimates to below 7.0 M. Figure 2.11 suggests the catalogue developed for this hazard assessment may have started approximately 50 years into a regional seismic cycle, as the number of events per year are broadly similar to the annual frequency in the early 20th century. This issue is considered further in chapters 5 and 6 in relation to newly formed magnitude recurrence hazard estimates.

Northwest Bulgaria is commonly agreed to be the least seismic region of Bulgaria. Loosely bounded by 42.5°-44.5°N, 22°-25°E, this region possessed only 77 earthquakes in the 105-year time interval catalogued, with none at a focal depth greater than 77 km, or magnitude greater than 6.5 M_s.

2.4.3 Mean frequency of earthquake occurrences in time

Variation in number of events per year for the full region (dark grey bars) and southwest Bulgaria (light grey bars) is illustrated in Figure 2.12. The vertical dashed line is at 1964 and is the divide between the early and modern instrumental periods of recording, while the horizontal lines indicate the mean annual number of events for the respective region. What is immediately evident from this illustration is that much of the regional seismicity is contained in the smaller southwest zone of Bulgaria. Noticeable 'spikes' are common to both plots, some of which can be tied to known, large magnitude sequences. For example, 1904 (Kresna), 1905 (north Albania and southwest Bulgaria), 1909 (Yambol/Sliven), 1921 (Skopje), 1928 (Chirpan and Plovdiv), 1963 (Skopje), 1972 (Gotse Delve, Bulgaria-Greece border), 1978 (Thessaloniki), 1983 (north Aegean Sea, west of Limnos) and 1995 (Dytiki Makedonia region, north Greece) are all visible. These sometimes close

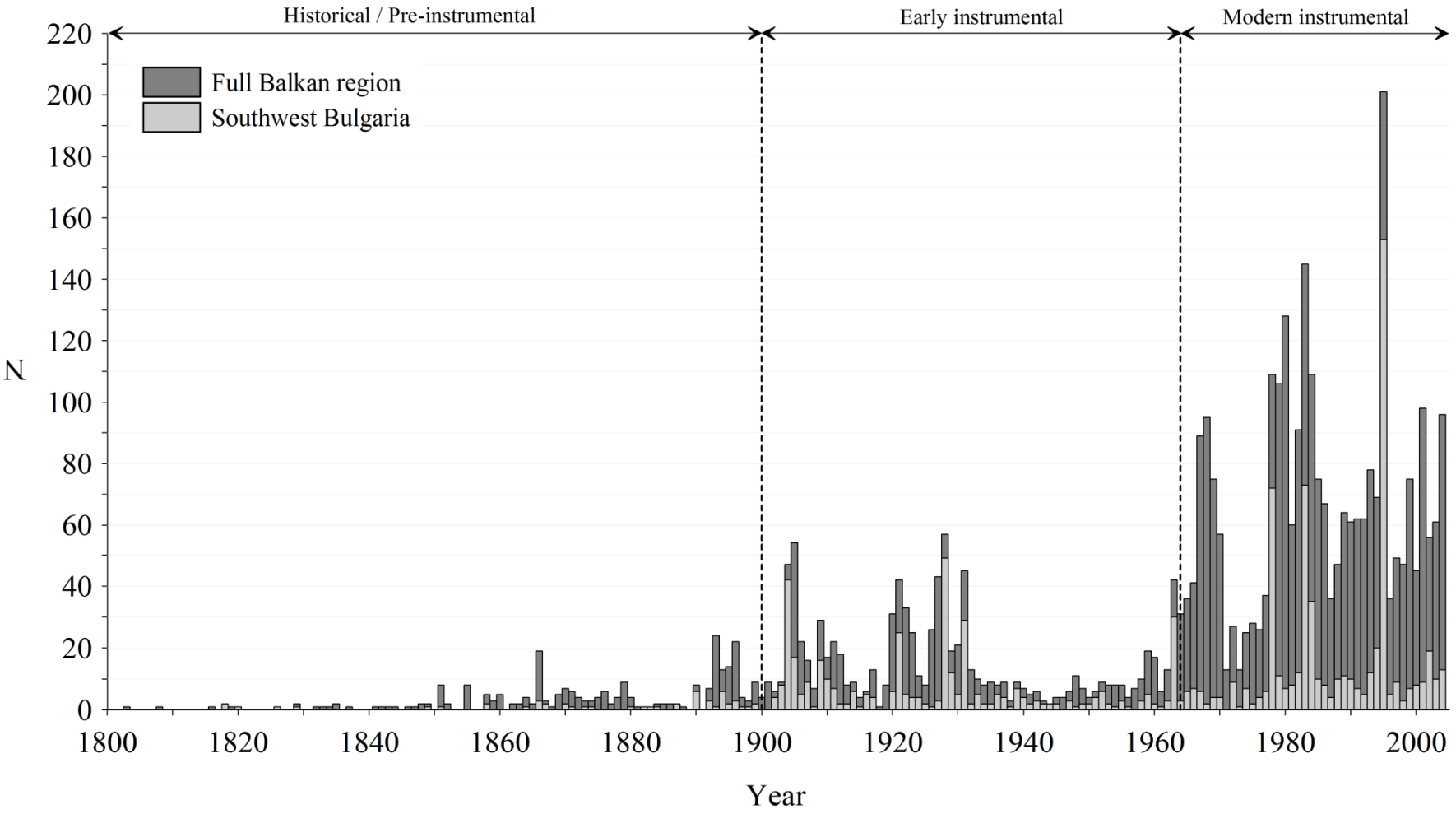

Figure 2.11 Temporal distribution of instrumental (from this work's catalogue) and pre-instrumental (from Shebalin *et al.* 1998) seismicity in the full Balkan (dark grey bars) and southwest Bulgaria (light grey bars) extents for which seismic hazard is to be considered

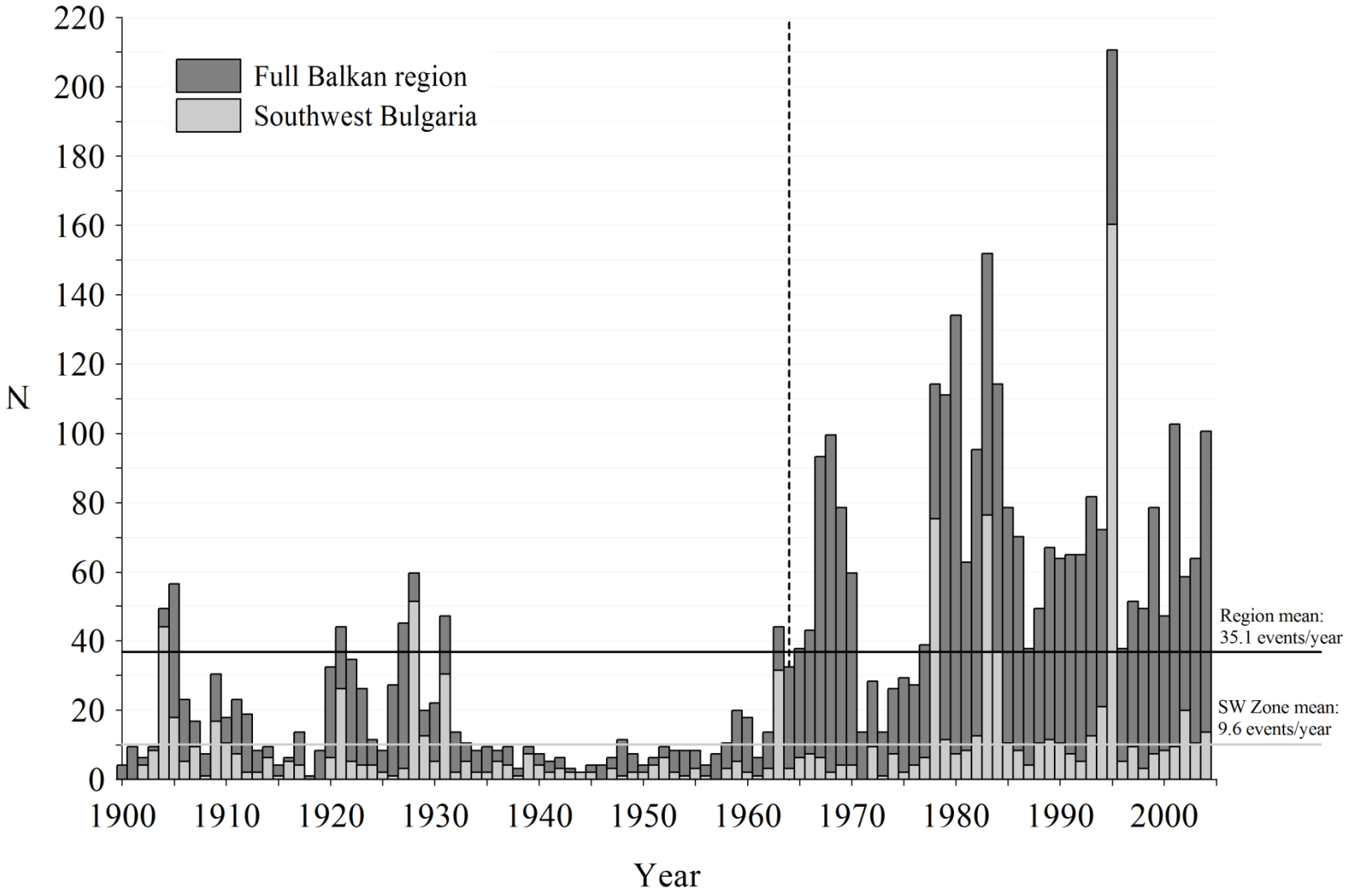

Figure 2.12 Temporal distribution of seismicity represented by the compiled catalogue. Vertical dashed line is at the separation of early instrumental and modern instrumental periods of recording

relationships indicate a large part of the broader region's past seismicity is to be found in this confined area of Bulgaria.

Frequency of regional and local seismicity is considered further in Figure 2.13, as it reports the *N*-year [rolling] mean number of earthquakes for both geographic regions (for N = 1, 2, 3, 4, 5, 6, 8 and 10-year time intervals. The *N*-year mean is reported against the ending year in each time sub interval considered; e.g. for the 5-year period 1900-1904 the *N*-year value is reported against 1904). All illustrations to Figure 2.13 highlight relative seismic quiescence during the middle of the time period considered. In the larger of the two geographic areas, no [reporting] year between 1932 and 1962 has a mean number of events great than 35.1 (the annual mean) events per N years for any value of N. In the southwest zone, no year between 1938 and 1962 has a mean number of events greater than the sub region's annual mean number of 9.6 events per year.

With respect to the southwest zone, as N increases, the number of [rolling] time intervals for which the mean number of earthquakes exceeds this smaller area's mean value are concentrated in the mid to late 1900s, late 1920s/early 1930s and the late 1970s to the end of the recording period. Each of these periods can be associated with significant historical seismic sequences; namely Kresna, Chirpan and Plovdiv and the 1978 and 2000 Thessaloniki sequences respectively.

The strong similarity between the two geographic areas extends to the mean number of events per unit area, with this being almost identical between the two geographic areas, at about 61 earthquakes per square degree. This supports further the idea that the majority of the regional catalogued seismicity is contained within the confined high-hazard southwest zone, as many of the significant seismic sequences mentioned in the previous pages occurred within its boundaries.

Figure 2.11 to Figure 2.13 all indicate a significant increase in the number of events reported after the mid-1960s. This was not due to a natural increase in seismicity in the region, but instead the introduction of the World Wide Seismological Station Network (WWSSN); this milestone allowed reporting of far more and far smaller seismic events on a global scale. Regions would be subject to minimum recording thresholds imposed by the distribution and sensitivity of the installed recording equipment. As time has progressed, these thresholds to reporting earthquakes have decreased in-line with improvements in the equipment, methods of measuring and homogenising magnitudes and expansion of seismograph station networks. A second significant increase in the number of events reported can be seen after 1980. This saw the introduction of about 12 new stations operating S13-Teledyne velocitymeters, thus increasing the accuracy and number of registered events.

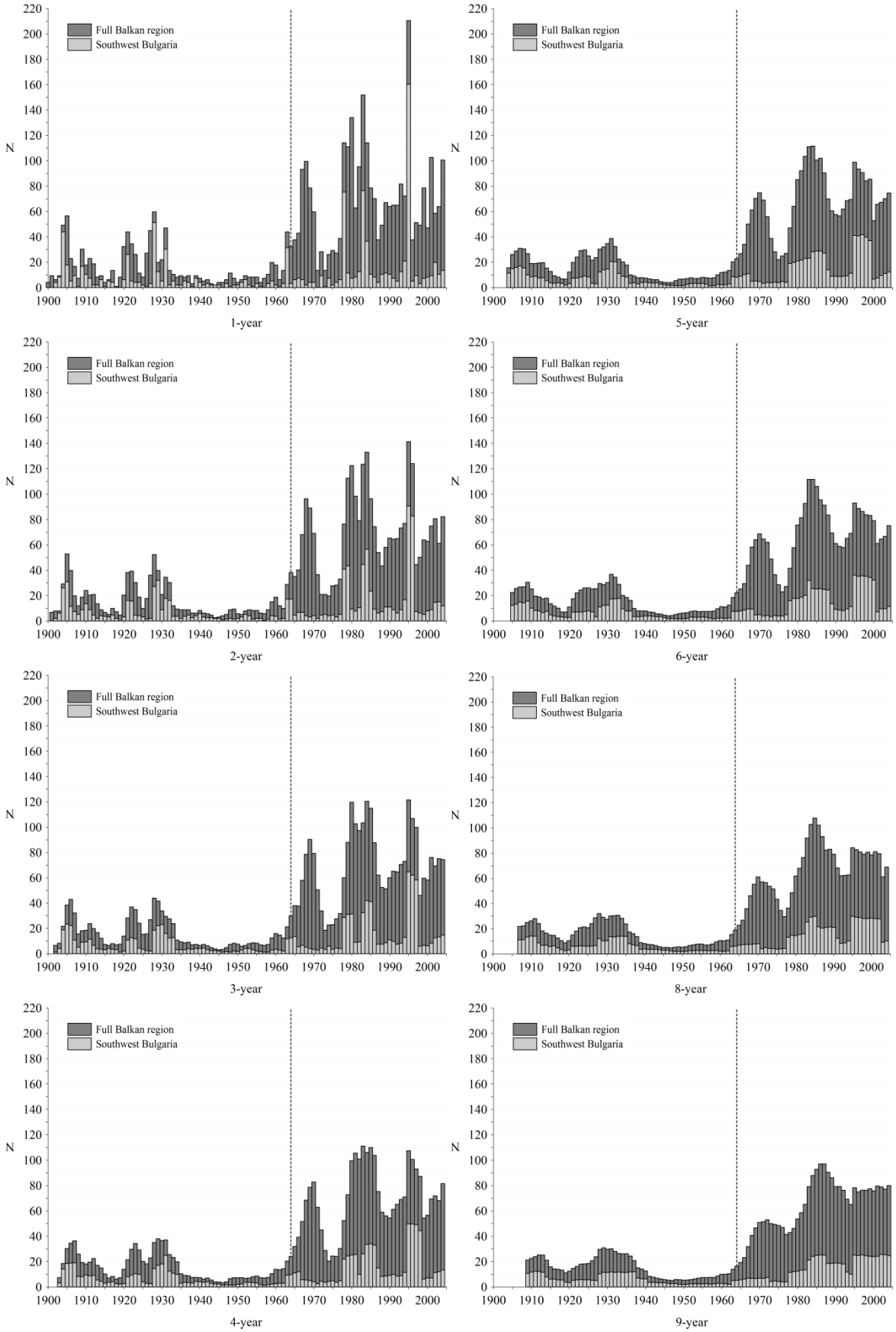

Figure 2.13 *N*-year [rolling] mean number of events for both geographic regions for which seismic hazard will be considered

The ISC contributed all data for the modern instrumental period of recording to the compiled catalogue except for the final two years. Information on network contribution to the ISC database from stations registered in Bulgaria is given in section 4.10.4.

2.5 Distribution by focal depth

The focal depth distribution of Balkan seismicity has been discussed in Bončev *et al.* (1982), Burton *et al.* (1984) and Stanishkova and Slejko (1991). Makropoulos and Burton (1984), Papazachos (1990) and Papazachos and Papazachou (1997) discuss extensively the tectonic environments of Greece and the Aegean. This region is important as the northern extent to the Hellenic Arc trench system encroaches into the southern part of the catalogued region.

Stanishkova and Slejko (1991) present data on a linear scale for depth in various forms (number of events per depth value, depth variation with magnitude), while Bončev *et al.* (1982) present magnitude versus depth plotted on a logarithmic scale. The region's seismicity is generally constrained to shallow-focus events, of which most are small to medium magnitude (≤4.5 M), with an increase in depth trending north to south (Stanishkova and Slejko, 1991). Variation in mean focal depth versus homogenized M_s magnitude is given in Figure 2.14. Mean focal depth gradually increases with magnitude up to approximately 5.5 M_s. Above this magnitude, this trend is reversed, if one excludes the anomalous entry at 7.0 M_s. The 'spike' in mean focal depth at 7.0 M_s results from a biasing effect of one small-magnitude event hypocenter located at 120 km on the subduction zone under the Albanian coast (February 21st 1968, 41.80°N, 19.10°E) combined with two shallow-focus events at this magnitude (focal depth 7 km and 14 km). The average of only these two shallow focus events is 10.5 km. In comparison, the deepest event at 401.0 km (3.3 M_s) is offset by 190 other events of equivalent size.

2.5.1 Shallow focus earthquakes (h < 30 km)

Shallow seismicity of the southern part of the region catalogued is mapped by Koravos *et al.* (2003) and Papazachos and Papazachou (1997). The latter lists macroseismic parameters for 287 shallow focus (h_{max} = 30 km) events used in a macroseismic study of the Balkan and Bulgarian regions and was extended in Papazachos and Papaioannou (1997). The northern extent of the catalogued region for the period 984 BC to 1997 (for depth h < 60 km and h > 60 km) is mapped by Oncescu *et al.* (1999). The majority of earthquakes in the catalogued region with $M_s \geq 6.5$ are within the top 30 km of the earth, and this depth interval accounts for ~87.5% of the total number of events catalogued. The surficial 10 km accounts for nearly 55% of the catalogue. The modal

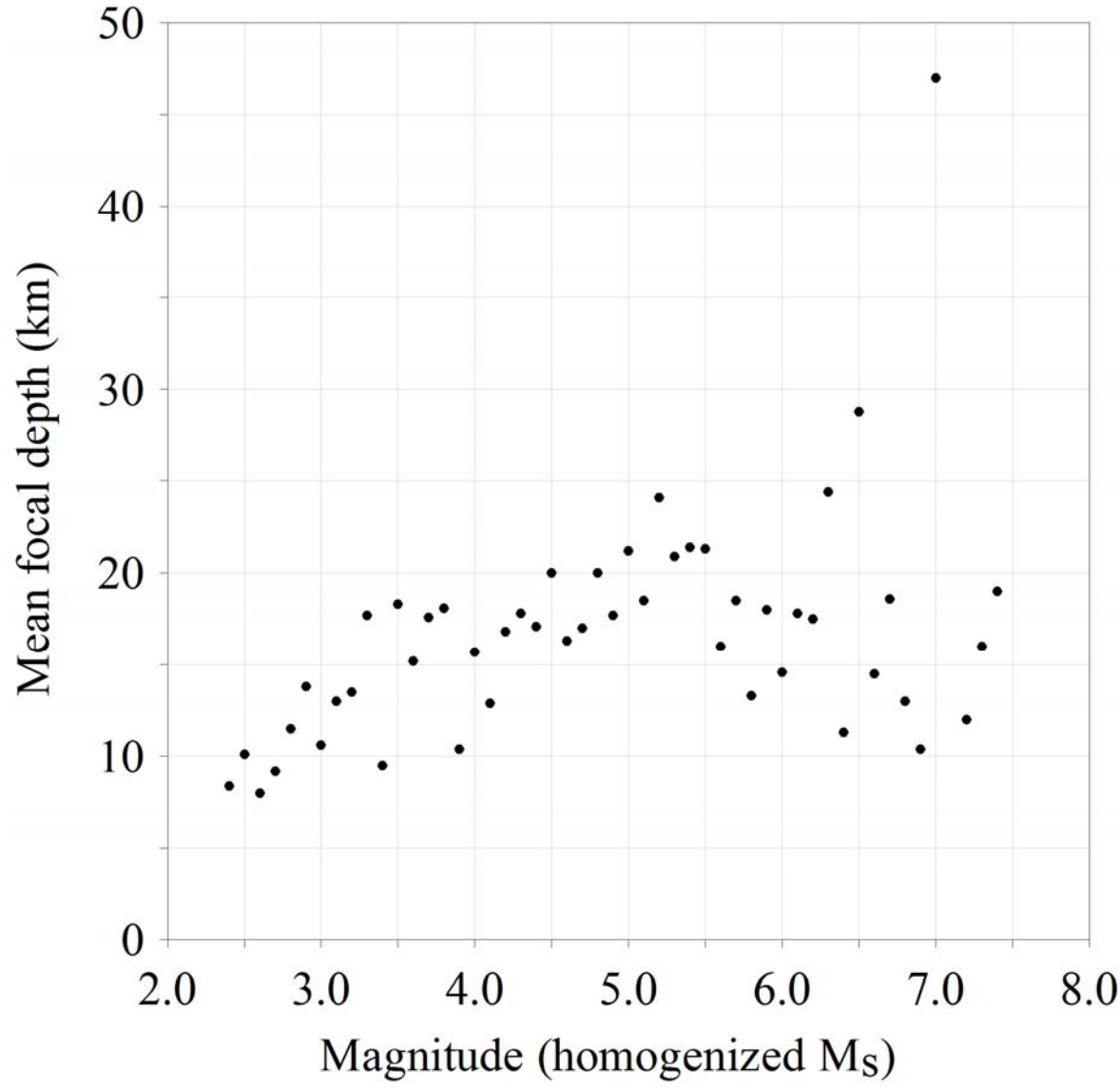

Figure 2.14 Variation in mean focal depth with magnitude of events listed in the catalogue. Note the gradual increase in mean focal depth with magnitude to 5.2 M_s before falling away. The 'spike' at magnitude 7.0 M_s is a result of biasing affect of one event at 120 km on two shallow events (average focal depth of the two shallow events alone is 10.5 km)

depth is in this depth interval at 10 km, which accounts for 617 events (16.7% of the catalogue). A significant number of events (330) have focal depth of 0.0 km, most of which are to be found in the instrumental period (i.e. the period of data provided by the ISC). The ISC will attach an arbitrary depth value of 0 km, 10 km or 30 km to an earthquake if its hypocentre cannot be constrained to a higher degree. These arbitrary depth estimates may influence further analysis of a region's seismicity and therefore seismic hazard (Stanishkova and Slejko, 1991).

2.5.2 Intermediate focus earthquakes (30 km ≤ h < 60 km)

Intermediate-focus seismicity is scarce within the borders of Bulgaria (Shebalin *et al.,* 1998). Papazachos and Papazachou (1997) catalogue and map intermediate seismicity in the southern part of this region whilst Shebalin *et al.* (1998) offers mapping of the northern section, and one of the few accounts of intermediate seismicity within Bulgaria. No events of magnitude $M_s \geq 6.7$ occurred in this depth interval between 1900 and 2004, while it accounts for 12.9% of the total catalogue.

2.5.3 Deep focus earthquakes (h ≥ 60 km)

This vertical region of seismicity has predominantly been confined to two discrete regions, i) the Vrancea region of Romania between depths of 90 to 150 km (given as the area bounded by 45°-46°N, 26°-28°E and labelled as Vrancea-Carpathian region; Purcaru, 1979), ii) the boundary between Greece and Bulgaria. There are no events in the catalogue between 90 and 150 km within Bulgarian borders.

About one percent of the catalogued events are found at focal depths of 60 km or greater. The deepest event of the catalogue is an outlier event at 401.0 km under the Adriatic Sea off the coast of Albania in 1968. The catalogue contains six additional events with focal depths of 100 km or greater (1926, 120.0 km; 1954, 100.0 km; 1961, 100.0 km; 1963, 160.0 km; 1965, 105.0 km; 1967, 124.0 km; 1968, 186.0 km; 1973, 100.0 km). All events except the 1967 earthquake are located on either the subduction zone of the Hellenic Arc or on the western reaches of the northern branch of the North Anatolian fault. Both of these zones are well outside Bulgaria's borders. The 1967 earthquake was located in northern FYR of Macedonia.

Within the borders of Bulgaria, nine events with focal depths of 60 km or greater have occurred since 1900 (Table 2.2). These are located in the southwest quadrant (six events) and northeast quadrant (three events), with none of them occurring at a depth greater than 77 km. The remainder of the catalogued region's deep-focus seismicity is predominantly restricted to the northern

Hellenic Arc region in western Greece and Albania and northwest Turkey (i.e. resulting from activity on the North Anatolian Fault).

Year	Coordinates	Location	Focal depth (km)	Magnitude (M_s[1])
1900	43.7°N, 27.5°E	Northeast Bulgaria	70.0	5.9
1909	42.0°N, 24.0°E	West of Plovdiv	62.0	4.6
1909	43.0°N, 26.5°E	Northeast Bulgaria	60.0	5.2
1909	42.0°N, 24.5°E	West of Plovdiv	60.0	4.6
1909	42.2°N, 24.8°E	Plovdiv	60.0	4.5
1913	43.2°N, 25.7°E	Northeast Bulgaria	70.0	5.1
1928	42.4°N, 25.3°E	Stara Zagora	60.0	4.5
1965	42.5°N, 23.1°E	Southwest of Sofia	77.0	3.5
1980	42.3°N, 24.2°E	West of Plovdiv	71.2	3.6

[1] Homogenized magnitude

Table 2.2 Hypocentre details for earthquakes inside Bulgaria with d ≥ 60 km

The majority of Bulgaria's seismicity is of crustal origin; generally focal depths are less than 50 km, with this being the biggest crustal thickness in the local Rhodopes areas. Therefore the deeper focal depths highlighted in Table 2.2 could be considered anomalous with respect to the parent distribution. Bulgaria's station network expanded significantly after 1980 (section 2.4.3) and it is likely that focal depths of these earlier events in Table 2.2 had high uncertainties attached to them due to poor station coverage.

Depth characteristics of the catalogued region's seismicity – in terms of distribution of events (as given by this catalogue) – are given in Figure 2.15 with respect to: 1) the number of events found at each discrete depth (km; solid line) and, 2) the cumulative increase in numbers of events with depth as a percentage of the 3,681 events listed in the catalogue (dashed line). Horizontal bars on Figure 2.15 are at 10 km and 30 km focal depth. Depth versus magnitude for all events listed in the catalogue (less the one 'outlier' event at 401 km) is in Figure 2.16, with each circle represents a single event (some discrete points will represent multiple events). Details of the deepest focus earthquakes shown on Figure 2.16 are in Table 2.3.

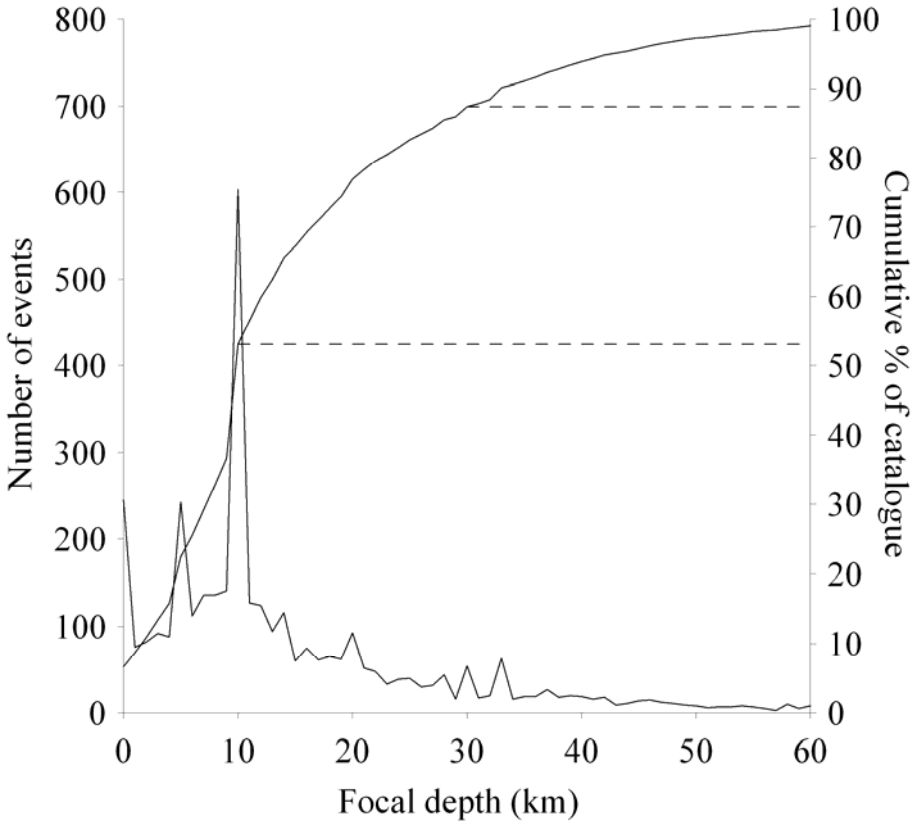

Figure 2.15 Depth distribution for Balkan seismicity (1900 to 2004): number of events versus depth (99% of catalogue)

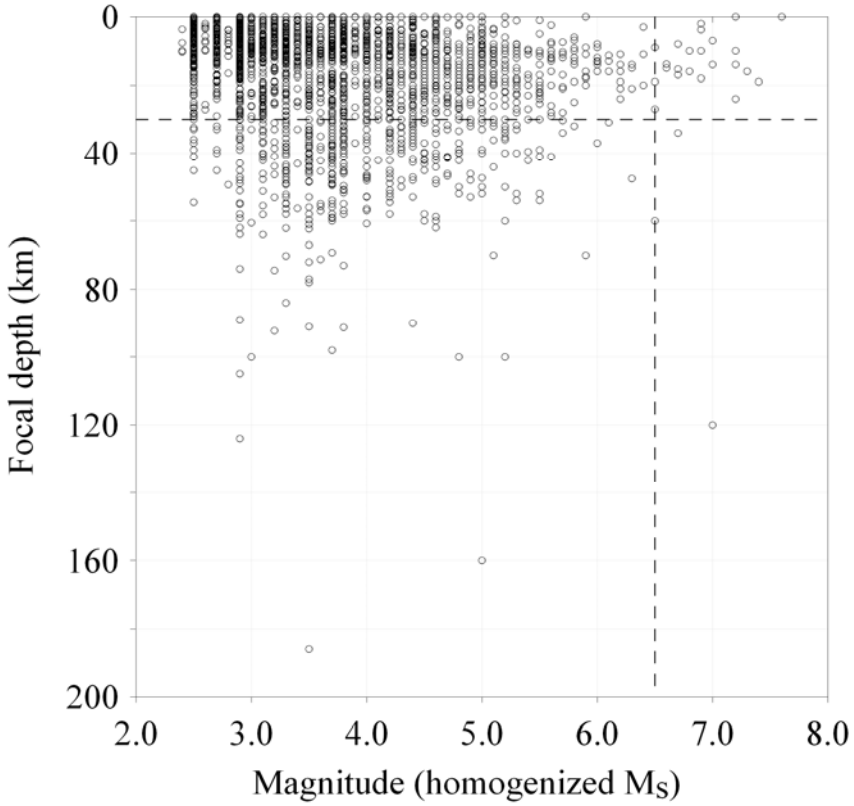

Figure 2.16 Depth distribution for Balkan seismicity (1900 to 2004): magnitude versus depth (less the 'outlier' at 401 km. horizontal dashed line is at 30 km; vertical dashed line is at 6.5 M_s)

Year	Coordinates	Location	Focal depth (km)	Magnitude (M_s[1])
1926	39.6°N, 20.0°E	Ionian Sea, Corfu	120.0	7.0
1963	40.5°N, 27.4°E	West Sea of Marmara	160.0	5.0
1965	39.6°N, 22.4°E	Larissa	105.0	2.9
1967	42.0°N, 21.7°E	North central FYROM	124.0	2.9
1968	41.8°N, 19.1°E	North Albanian coast	401.0	3.3
1968	40.0°N, 24.9°E	N. Aegean near Limnos	186.0	3.5

[1] Homogenized magnitude

Table 2.3 Hypocentre details for earthquakes within full region with focal depths >100 km

The vertical dashed line is at [homogenized] 6.5 M_s, and the horizontal dashed line is at a focal depth of 30 km. These figures both highlight that the majority of Bulgaria's seismicity is of shallow [assigned] focal depth (<30 km), probably due to the overriding presence of ISC data in the final listing. Equally, Figure 2.16 reinforces the belief that Bulgarian seismicity is small to medium magnitude in nature.

2.6 Key large magnitude historical events

Even though small and intermediate magnitude seismicity generally characterizes the catalogued region, Bulgaria has experienced some of the largest and most destructive earthquakes of the 20th century. It is useful to detail a number of these events, especially those that have occurred in south and southwest Bulgaria to better understand the geologic and seismotectonic environments here.

2.6.1 April 4th 1904 (Kresna/Krupnik, Struma Valley)

The main shock that occurred on 4th April 1904 has long been acknowledged as the largest magnitude shallow-focus event in Europe. Initially assigned a surface-wave magnitude of between 7.5 (M) (Gutenberg and Richter, 1949) and 7.8 M_s (Christoskov and Grigorova, 1968) and a body-wave estimate of 7.8 m_b (Shebalin *et al.*, 1998), this has since been re-evaluated to between 7.1 to 7.2 M_s by Pavlides and Caputo (2004) and 7.2 M_s by Ambraseys (2001). Its main foreshock had been assigned magnitude estimates of 7.1 m_b and 7.3 M_s by different authors, but later re-evaluated to between 6.8 and 6.9 M_s by Pavlides and Caputo (2004). This event is important not only for its magnitude, but also its proximity to the political triple junction between Bulgaria, the FYR of Macedonia and Greece.

The region affected by this event straddles the FYROM-Bulgaria-Greece borders. The intensity VI contour extends east-west from southern Italy to Istanbul, Turkey, and north-south from southern Romania to Volos, Greece (Papazachos *et al.*, 1997a). Maximum intensities estimated were X.

This region is interspersed with faults of varying size. The three most important to the 1904 Kresna sequence are the Kocani fault of eastern FYROM, Krupnik and Bansko faults – east of Krupnik fault – in southwest Bulgaria. All three extend for 20 km or more, with estimates obtained from both satellite imagery and field observations (Meyer *et al.*, 2002, 2007). The Kocani fault strikes approximately EW in two sections for 25 km, Krupnik fault (suggested to be the most probable location of the main shock) striking NE-SW for 20 km and Bansko fault strikes NW-SE for 30 km. Until the studies of Ambraseys (2001) and Meyer *et al.* (2002), neither the surface breaks nor these three source faults had been pinpointed.

Meyer *et al.* determined an epicentral intensity (on the MSK scale), I_0, of X that is well constrained by a large number of observations, as are contours at I = VII and below. The contour at I = VII is the first (extending down the intensity scale) to extend significantly into both the FYR of Macedonia and north Greece showing the extensive regional effect of this event.

However, even though this single event has been reviewed many times, there is still much uncertainty on this event's magnitude; different methods derive distinctly different estimates. For example, Ranguelov *et al.* (2000b) re-evaluated this event using 12 alternative methods (e.g. macroseismic data, length of aftershock sequence, old instrumental data and geodetic data). Each returned estimates in the range of 6.4 M (extreme values method) to 7.9 M (macroseismic data). The mean estimate – from both averaging the maximum and minimum estimates and averaging all estimates together – is approximately 7.2 M, further supporting the decision to adopt 7.2 $M_{(s)}$ as the event's revised magnitude estimate in chapter 4.

2.6.2 June 14th 1913 (Gorna Orjahovitza)

The first ever seismic moment estimates for the June 14th 1913 event located near Gorna Orjahovitza were estimated by Dineva *et al.* (2002). They used original seismograph records and bulletin data from a range of global seismological stations to re-compute origin time, location, seismic moment, surface and moment magnitudes for this and three other noteworthy large earthquakes of the early instrumental period of recording (including the 1904 Kresna earthquake). All revised estimates were systematically lower than any original estimates, e.g. those of Gutenberg and Richter and Kárník. These estimates were also supported by work of Abe and Noguchi (1983a, 1983b) and Pacheco and Sykes (1992). Dineva and colleagues re-computed this event's magnitude

to 6.30 M_s (± 0.25) – after using methodology of Abe (1988) – and 6.38 M_w (± 0.13) – after using methodology of Hanks and Kanamori (1979) – down from between 6.75 and 7.1 M by Kárník (1968), Gutenberg and Richter (1949) and Christoskov and Grigorova (1968). They also attached a mean estimate for M_0 of 4.61 ± 2.04 x 10^{18} Nm.

2.6.3 April 14th and 18th 1928 (Chirpan and Plovdiv)

The 1928 earthquake sequence near Chirpan and Plovdiv is another example of large destructive seismicity in the catalogued region. Being more recent that he 1904 Kresna earthquake, it was recorded more accurately and has consequently better studied. This sequence consisted of two shocks, both generally considered to be main shocks (and not a foreshock – main shock sequence) with magnitudes of 6.8 M and 7.0 M assigned by Kárník (1968), and located in close proximity to the cities of Chirpan, and Plovdiv and Duvanja respectively in the Maritza Valley. Both events had shallow focal depths of approximately 10 km and 15 km respectively.

The cumulative effect of these two main shocks and their aftershocks was felt over about 3000 km^2, affecting five major towns and 240 villages. The first shock occurred on a south-dipping fault with constant slip of 0.7 m (Dimitrov *et al.*, 2004), whilst the second larger event produced maximum slip of 2.6 m on a north-dipping fault. The larger 7.0 M shock also accounted for approximately 75% of the sequence's seismic moment. An epicentral intensity of I_0 = X (MSK) was experienced. Paleoseismologic investigations specifically of this foreshock have also been undertaken (Vanneste *et al.*, 2006).

Fault activation during this seismic sequence was somewhat unusual. Neither event managed to rupture the area's main fault (Asenovgrad fault), and only managed to reactivate more minor localised faulting. However, fault breaks of up to 105 km were reported. The April 14th event is thought to have initiated two rupture zones. This consisted of a continuous 38 km surface rupture striking N95° and dipping south between Trakia and Orizovo. The distributed destruction pattern of towns in the region is clearly indicative of the 38 km of rupturing being associated with fault activation by this first event (Dimitrov *et al.,* 2004). The second rupture zone associated to the first event has been linked to a 62 km long discontinuous sequence of faulting a few kilometres south of initial rupturing and following the Maritxa River from Nadeja and Belozem.

Along with a failure of the region's main Asenovgrad fault to rupture, new surface ruptures appeared after the April 18th event, extending for 53 km on what has come to be called the Popovitza fault. Starting south west of Parvomai, it ran in an approximate N118° direction before altering to N144° near the Striama River. This stretch of surface faulting experienced vertical uplift

of between 1.5 m and 3.5 m along its length. A number of focal mechanism solutions have been proposed for this event (e.g. Glavcheva, 1984; Dimitrov and Ruegg, 1994; van Eck and Stoyanov, 1996; Dimitrov *et al.,* 2004). The last of these offer a fault mechanism of strike = 300°, dip = 67°, and rake = -124°, suggesting the north dipping plane corresponds well to direction of main surface rupture.

This two-event main sequence on 14th and 18th April 1928 was further characterized by a main aftershock of 5.7 M on April 25th, and an additional 15 aftershocks greater than 5.0 M for one month.

2.7 Seismotectonic and seismogenic source zone solutions for the Balkans

Developing a new seismotectonic framework against which to assess seismic hazard is outside the scope of this study, and it is perhaps a moot point as it will in practice adopt zone-free techniques to forecasting hazard (section 3.9). Seismotectonic (seismogenic) source zones (SSZ) are more appropriate to practicing hazard analysis in relation to specific known tectonic structures.

However, it is useful to highlight four recent attempts to group the region's historical seismicity, and view how they relate to the new earthquake catalogue discussed in chapter 4. Most recently Simeonova *et al.* (2006; Figure 2.17(a)) updated the SSZ models of Bonchev *et al.* (1982), Sokerova *et al.* (1992) and Dachev *et al.* (1995), and encompass seismicity within an approximate 200 km radius of Bulgaria, to also include Romania, Greece and [former] Yugoslavia. This was in response to EUROCODE 8 recommendations. The seismic sources of the NAF, Serbomacedonian massif, southwest Bulgaria, Vrancea and Adriatic/Ionian Sea coasts are all incorporated. Hypocentre distribution of all 30 zones is governed by crustal seismicity ($h < 60$ km) with a maximum depth in southwest Bulgaria of 50 km. Figure 2.17(b) shows a generalisation of a tectonic source zone model developed by Holt *et al.* (2000) to study velocity fields in the Aegean.

Holt *et al.* concentrated explicitly on velocity fields of this region, whereas a more comprehensive review of active fault systems in Greece is found in Goldsworthy *et al.* (2002). These zones were used by Koravos *et al.* (2003) to assess perceptibility hazard in terms of acceleration, velocity and intensity. Since SSZ zone 14 in Koravos *et al.* (2003) approximates to the southwest sub-region considered in chapter 6, and this reference text adopts the same ground motion descriptors and ground velocity and acceleration models as this study, the SSZ model of Holt *et al*. (2000) will be taken forward to allow comparison between Koravos et al. (2003) and this PSHA.

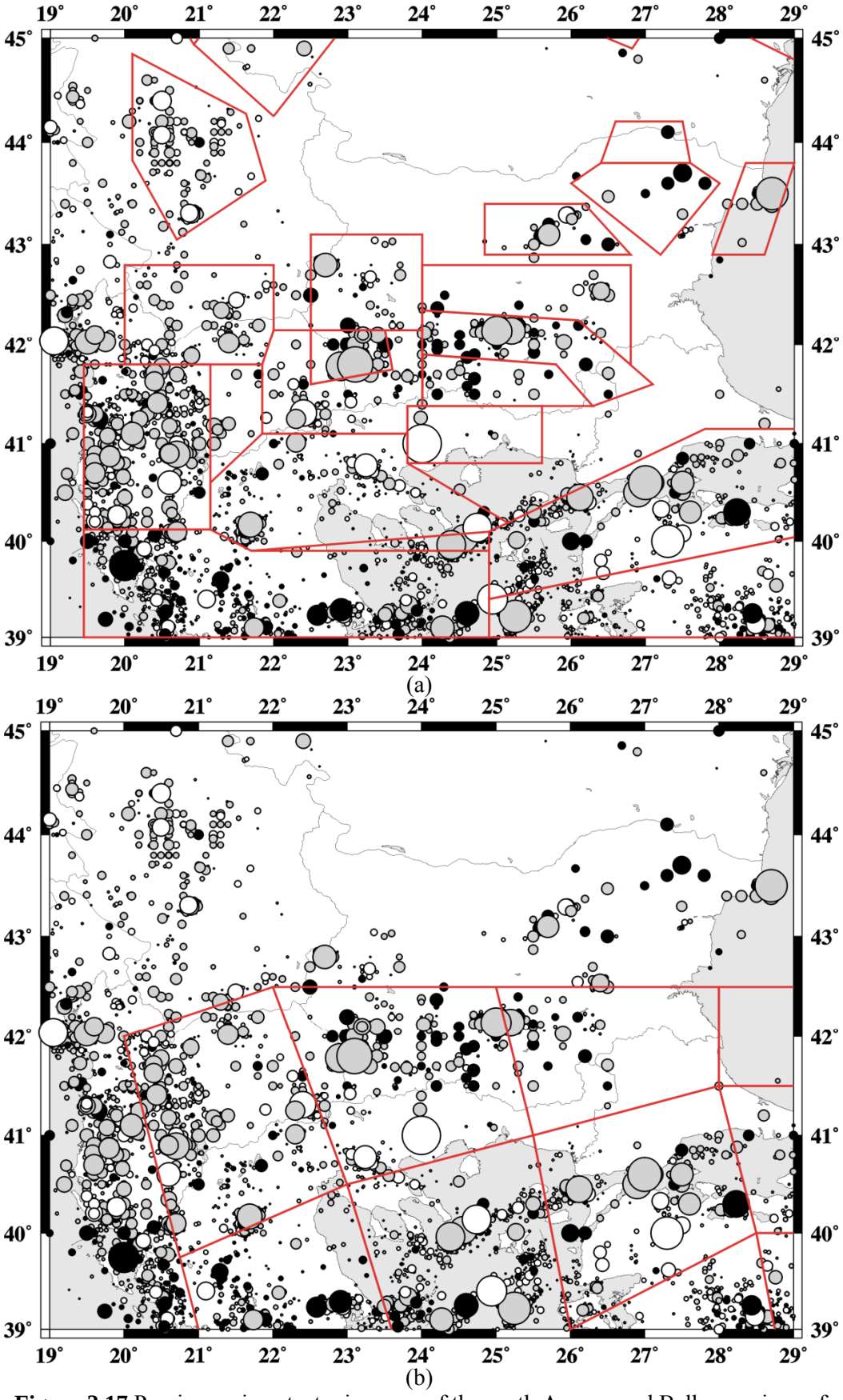

Figure 2.17 Previous seismotectonic zones of the north Aegean and Balkan regions of continental Europe: (a) Simeonova *et al*. (2006) and (b) Holt *et al*. (2000)

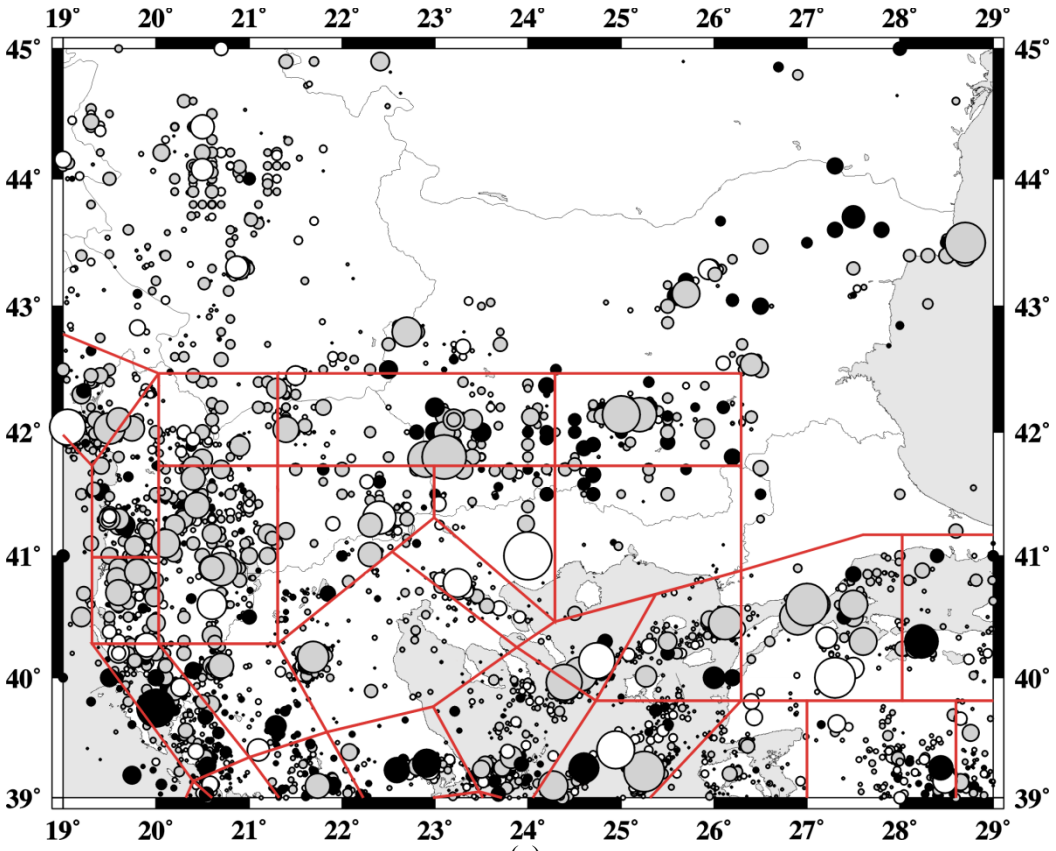

(c)

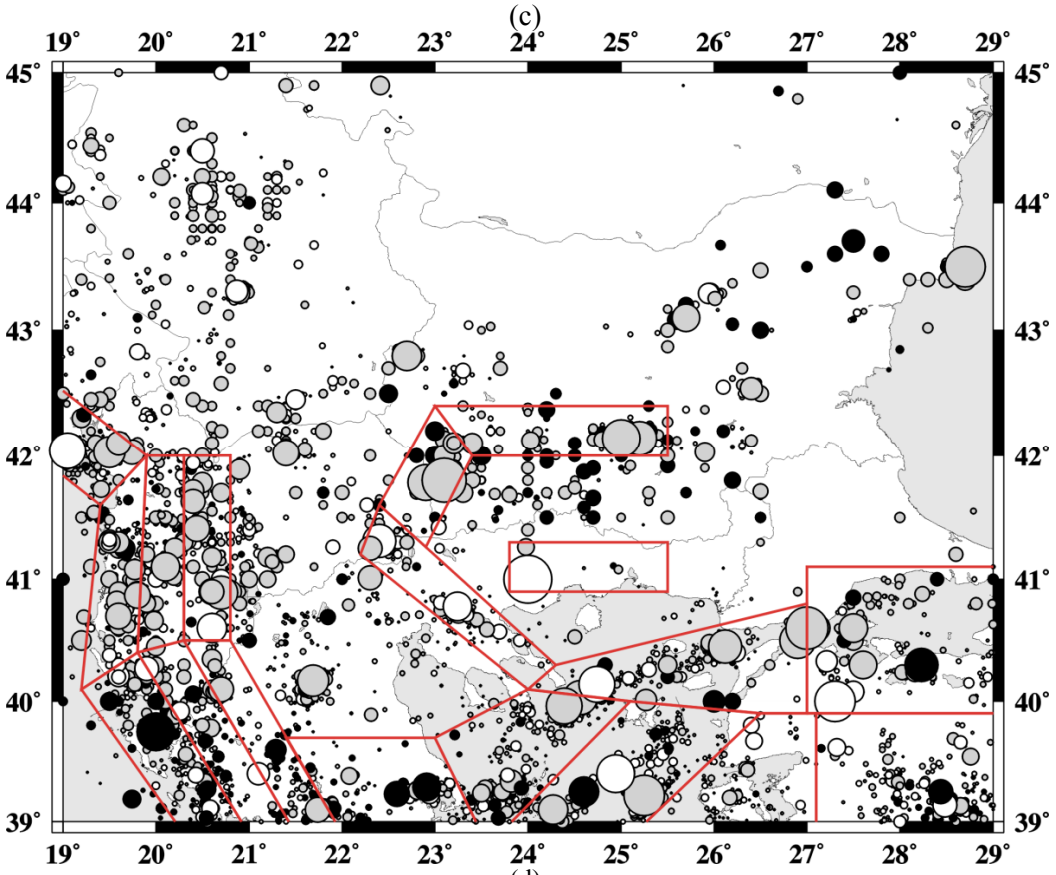

(d)

Figure 2.17 (contd) Previous seismotectonic zones of the north Aegean and Balkan regions of continental Europe: (c) Papazachos and Papazachou (1997) and (d) Papazachos (1990)

Sources zones used by Papazachos and Papaioannou (1997) and Papazachos (1990) for the Aegean and south Balkan regions are illustrated in Figure 2.17(c) and (d). Burton *et al.* (2004b) apply source zones of Figure 2.17(c) to assess regional extreme magnitude and perceptibility seismic hazard. The models in Figure 2.17(a)-(d) all extend beyond the geographic scope of the considered region, and hardly incorporate seismicity north of central Bulgaria (≈43°N).

2.8 Previous seismic hazard analyses

Four previous papers assessing seismic hazard of Bulgaria need highlighting (Bončev *et al.*, 1982; Stanishkova and Slejko, 1991; Orozova-Stanishkova and Slejko, 1994; van Eck and Stoyanov, 1996).

A new method for compiling prognostic maps that integrates geologic, geophysical, geodetic and seismological data with space image information is developed by Bončev *et al.* (1982). Over the area bounded by 40°N-46°N, 21°E-30°E (for they reason that a large considered region was necessary for a better understanding and estimation of all seismoactive zones within and around Bulgaria) they created a suite of hazard maps that mapped seismotectonic potential, major fault lineaments, activity, relative seismic danger, seismic source zones (according to geologic and seismological data) and observed earthquake sources of the region. These led to forming 1,000 and 10,000-year intensity shakability maps for the region (and also selected sub-regions). For a long time this single work formed the basis of seismic hazard knowledge to Bulgaria and became the benchmark study.

Stanishkova and Slejko (1991) present a seismotectonic review for Bulgaria. Although no contoured hazard maps are presented, a number of epicentre and sub-surface geology maps are provided. These continue the pattern of only presenting information within the country's border limits.

Six hazard maps reviewing seismic hazard of Bulgaria are developed in Orozova-Stanishkova and Slejko (1994). All maps relate to the 100-year return period event, with 37% probability of non-exceedance (Figure 2.18 and Figure 2.19). Contour maps are presented for: 1) maximum observed intensity since 1800, 2) maximum intensity with 37% probability of non-exceedance in 100 years using Gumbel's first distribution, 3) maximum intensity with 37% probability of non-exceedance in 100 years using Gumbel's third distribution, 4) maximum PGA with 37% probability of non-exceedance in 100 years using Cornell's approach, 5) maximum PGA with 37% probability of non-exceedance in 100 years using fault rupture model, and 6) maximum intensity with 37% pnbe in 100 years by taking envelope of isointensity lines from items (2) to (5).

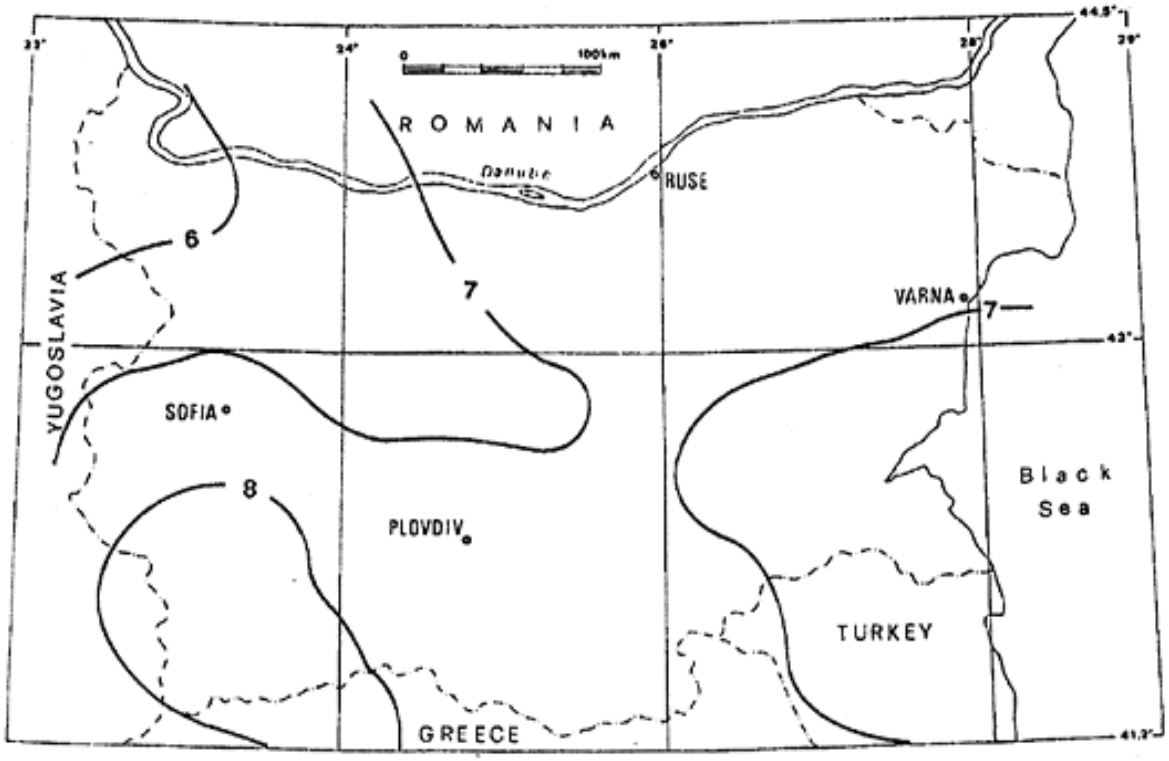

Figure 2.18 Previous attempts at mapping Bulgarian and Balkan seismic hazard: maximum intensity with 37% probability of non-exceedance in 100 years using Gumbel's first extreme distribution

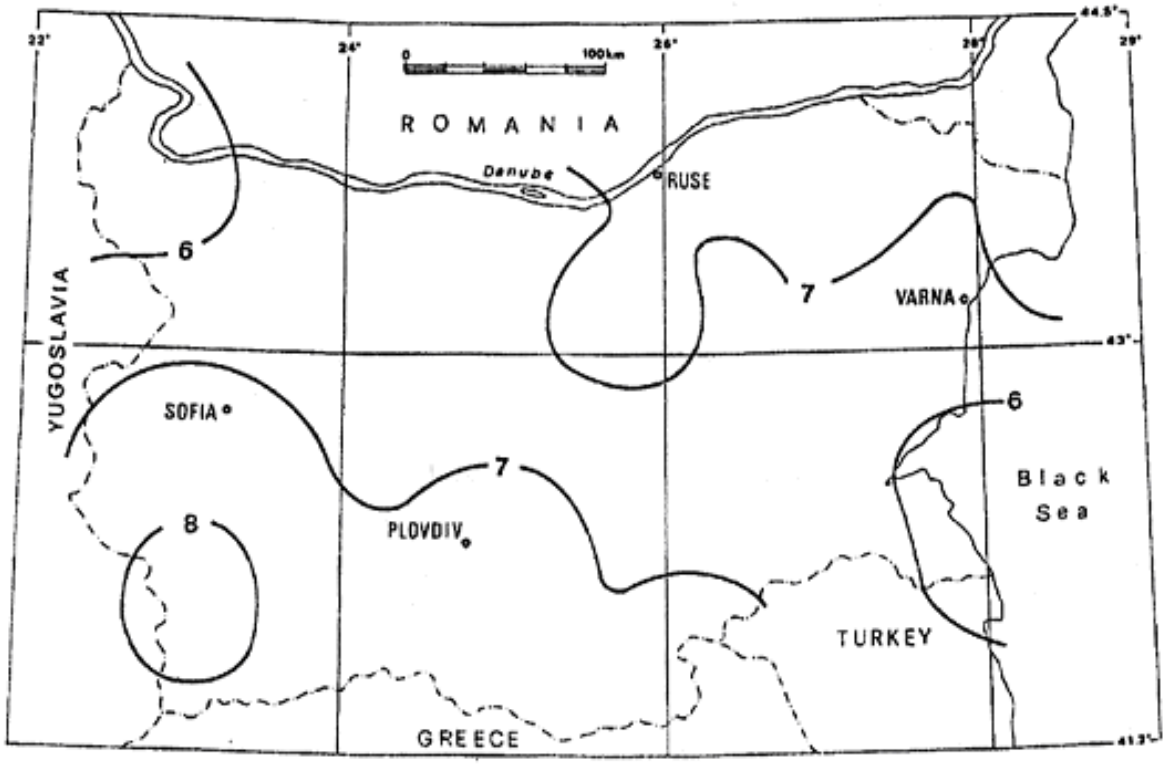

Figure 2.19 Previous attempts at mapping Bulgarian and Balkan seismic hazard: maximum intensity with 37% probability of non-exceedance in 100 years using Gumbel's third extreme distribution (source: Orozova-Stanishkova and Slejko, 1994)

Lastly, van Eck and Stoyanov (1996) approach Bulgaria's seismic hazard by applying their own earthquake catalogue, and is discussed briefly again in chapter 4. A primary output of their work is a contoured map forecasting horizontal PGA in Bulgaria with an annual exceedance probability of 0.01 (that is, 99% probability of not being exceeded). This they felt provided a direct comparison to Bončev *et al.* (1982).

Mapping of seismicity for Greece and the Aegean region is done by Makropoulos and Burton (1985a, 1985b) and contours magnitude recurrence and peak ground acceleration (PGA) respectively. Magnitude recurrence was in terms of the 80-year most probable event and the event with 70% probability of not being exceeded in 100 years; PGA was contoured for 100 and 200-year forecasts at 70% probability of non-exceedance. Burton *et al.* (2003, 2004b) continues to contour hazard for Greece for PGA and extreme and perceptible magnitudes respectively.

These seismic hazard assessments are noteworthy as they are specific to Bulgaria or sub regions of this country. Two larger scale studies – the "*Global Seismic Hazard Assessment Program*" (GSHAP; Giardini and Basham, 1993; Giardini, 1999), and "*Seismotectonics and Seismic Hazard Assessment of the Mediterranean Basin*" (SESAME; Jiménez *et al.*, 2001) – are important as they not only cover Bulgaria and the Balkan extent, but they adopt strongly similar ground motion models as this studies hopes to use, while adopting distinctly different seismic zonation models and assumptions. These studies are discussed in detail in section 5.5.4 with respect to this PSHA.

2.9 Active crustal deformation of southern Bulgaria

Developments in Global Positioning System (GPS) networks on a national and continental scale provide seismologists with a wealth of information to understand present day kinematics within and around Bulgaria. These networks allow researchers to link ideas on regional and localised tectonic and geologic behaviour to earthquake patterns, focal mechanism solutions and onto crustal movements, strain accumulation and velocity fields. This section summarises recent and current investigations into crustal motion and strain accumulation of Bulgarian tectonic regimes using such GPS network data.

Much recent work exists detailing this region's crustal motion and strain accumulations (e.g. Georgiev *et al.,* 2002; Nocquet and Calais, 2003; Shanov, 2005; Burchfiel *et al.,* 2006; Kotzev *et al.*, 2001, 2006; Caporali *et al.*, 2008). Importantly, most of these provide solutions beyond the boundaries of this explicit study area and the political borders of Bulgaria, and acknowledge the broad effect of multiple geologic and tectonic regimes on each other and allow them to be tied to the seismicity listed in the developed catalogue.

A number of international and regional GPS station networks are developing to allow monitoring of crustal motions and velocities. The International GPS Service (IGS), the Central European GPS Reference Network (CERGN) the EUREF Permanent GPS Network (EPN), the *Réseau GPS Permanent* (RGP) and REGAL networks all currently contribute to defining the International Terrestrial Reference Frame (ITRF; its latest incarnation being ITRF2000) across mainland Europe. However, results from the majority of these are adopted to review crustal motion in west Europe.

In a similar vein to needing new homogenous earthquake catalogues to comprehensively assess modern day seismicity for the Balkans, additional local and regional GPS networks have been constructed to allow crustal movements to be measured in this broader region (Kotzev *et al.* 2001; Georgiev *et al.*, 2002; Burchfiel *et al.*, 2006).

Crustal velocities generally increase as one moves east and south from the FYR of Macedonia. Burchfiel *et al.* (2006; Figure 2.20) recognize a near uniform 3-4 mm/year southward velocity for the FYR of Macedonia relative to Europe, with the FYR of Macedonia moving as a single crustal block. These result from 0-2 mm/year slip rates on strike-slip faults of the country. Velocities in southwest and south Bulgaria remain approximately constant at between 1 to 2 mm/year in a south to south-southeast motion with respect to the more stable north and east regions of Bulgaria and southern Romania (Kotzev *et al.*, 2006; Figure 2.21). However, it is important to note that faulting is significantly more fractured in southwest Bulgaria than the FYR of Macedonia, with the latter appearing to be more of a single block movement.

Velocities increase further in central, south, south central and Bulgaria, to 3-5 mm/year (in the Sub-Balkan Graben region and Thracian basin into the Stara Planina mountains), 3-4 mm/year (S) and 3mm/year (ESE) respectively. This marks a transition from the Southern Balkan Extensional Regime (SBER) to the Aegean extension region to the south of the study area (Kotzev *et al.*, 2001; Figure 2.22). Velocities increase dramatically in northern Greece, moving towards the North Anatolian Fault, with this movement estimated at 25 mm/year (S) (Burchfiel *et al.*, 2006). More recent results from GPS analysis (Caporali *et al.*, 2008) covering the full study area are shown in Figure 2.23. These results suggest that, specifically in relation to stations in Bulgaria and Romania, velocities of 2-4 mm/year in a south to southeast orientation are similar to those of other work detailed here for this region. The increased velocities exhibited in the Sub-Balkan Graben system is indicative of how stress and strain maybe transferred between neighbouring regions by faults and fault segments (Papadimitriou *et al*., 2007) and thus across political borders.

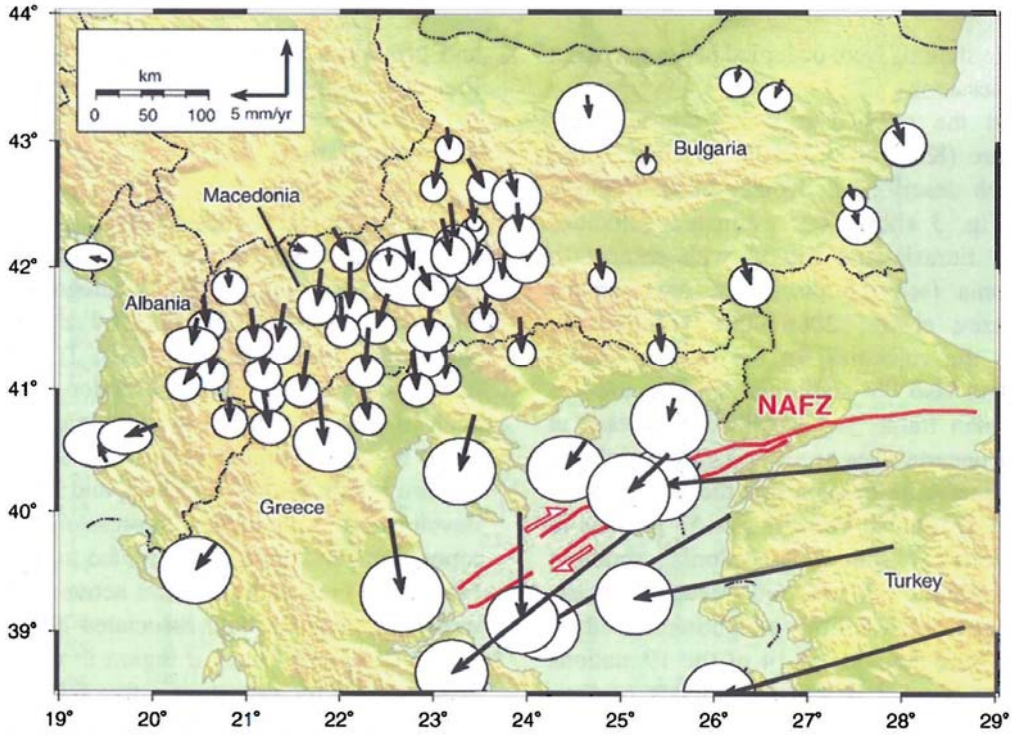

Figure 2.20 GPS velocities in southeast Europe with respect to a Eurasian reference frame (source: Burchfiel *et al.*, 2006)

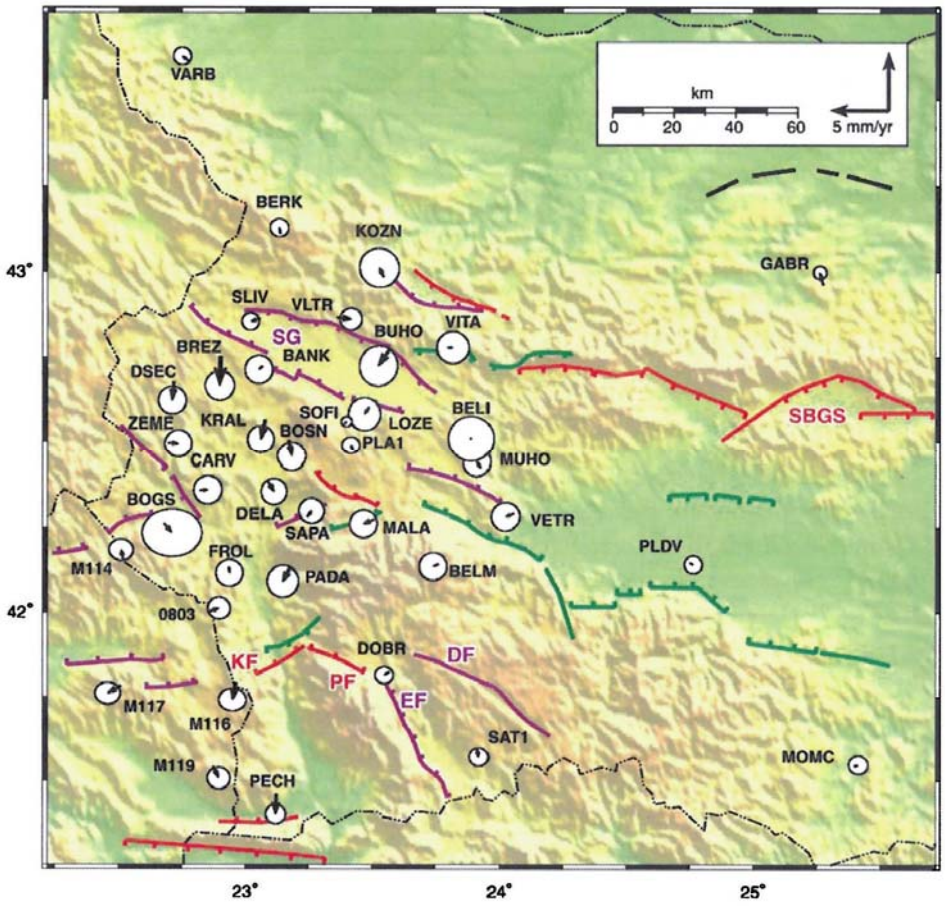

Figure 2.21 GPS velocities in southeast Europe with respect to a West Bulgaria reference frame (source: Kotzev *et al.*, 2006)

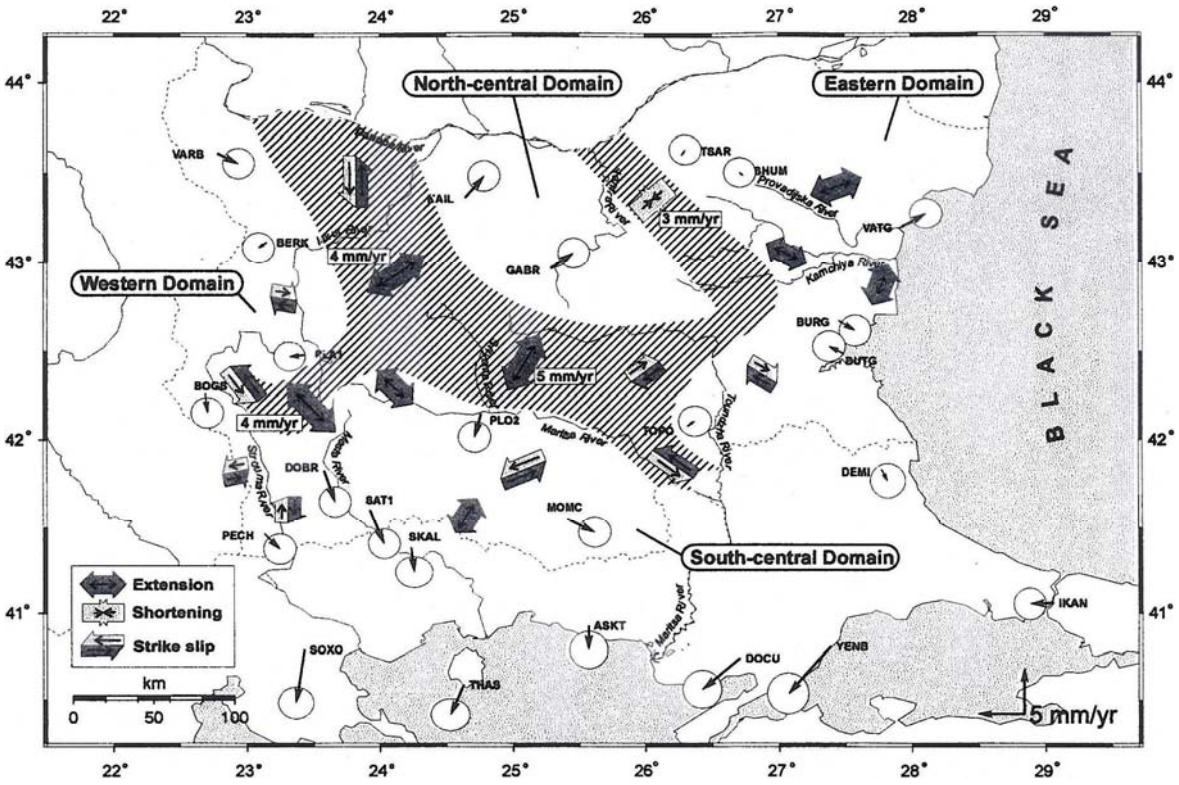

Figure 2.22 GPS velocities with respect to a Eurasian reference frame (source: Kotzev *et al.*, 2001)

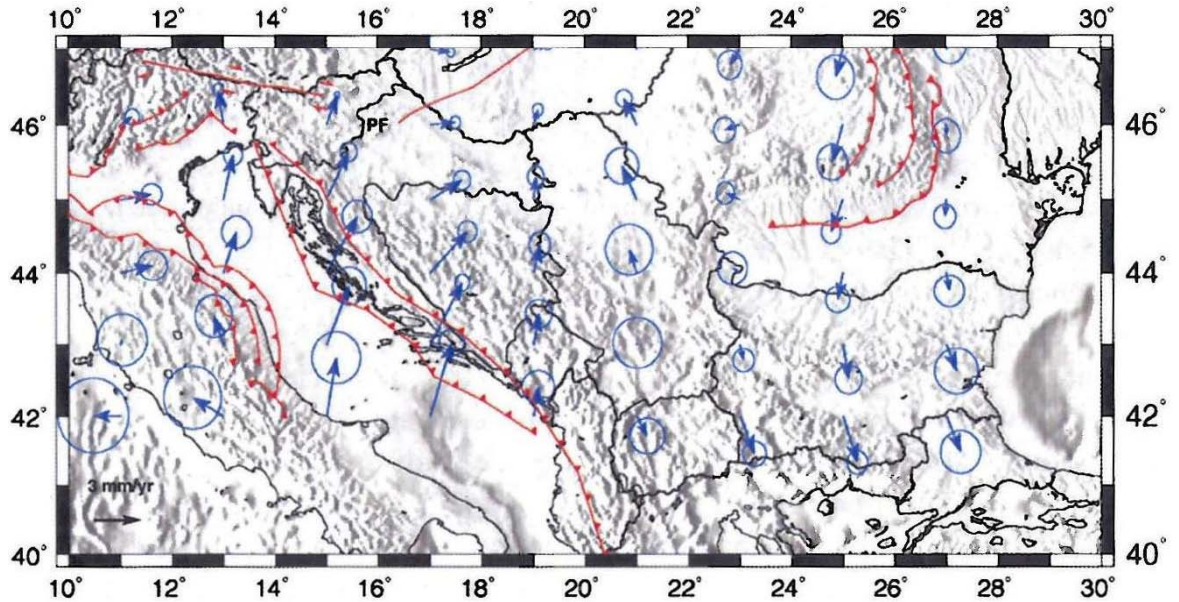

Figure 2.23 Interpolated GPS [horizontal] velocities in southern Europe (adapted from: Caporali *et al.*, 2008)

2.10 Summary

The new catalogue described in chapter 4 provides an opportunity to view regional seismicity in Bulgaria and its surrounding region. It has confirmed that the region is dominated by shallow focal depth ($h < 30$ km) and small to moderate magnitude ($M \leq 4.5$) seismicity created by the tectonic environment characterized by Horst-Graben structures and short (a few tens of km), segmented faults.

It is not until considering this region's seismicity extends east and south (into the FYR of Macedonia and Greece) that deeper-focus events are found on the Hellenic Arc system. The seismotectonic setting within Bulgaria and the surrounding Balkan area is illustrated in Figure 2.24 using the catalogue listing developed in chapter 4 and shows known major normal, strike-slip, thrust and undefined faults.

A limitation common between many previous hazard mapping outputs for this region is their inability to adequately bridge the political borders between the FYR of Macedonia, Bulgaria and Greece. This region of southern Europe is known to be one of medium to high seismicity generated by the NAF and Hellenic Arc system, although Bulgaria itself is predominantly small to medium-level seismicity. However, previous maps often fail to represent the full and simultaneous contribution of seismicity from these three bordering countries. This high seismicity straddles their political borders, with the 1904 Kresna sequence being just one example of this. Additional maps highlighting this limitation in mapped forecasted seismic hazard are given in Figure 2.25 and Figure 2.26.

Chapter 3 outlines a range of key statistical models that have been adopted in previous seismic hazard assessments for this and other regions. Selected models are applied in chapters 5 and 6 to review seismic hazard in southwest Bulgaria and the surrounding Balkan. The hazard assessment will be supplemented with a review at key selected urban centres including the capital Sofia.

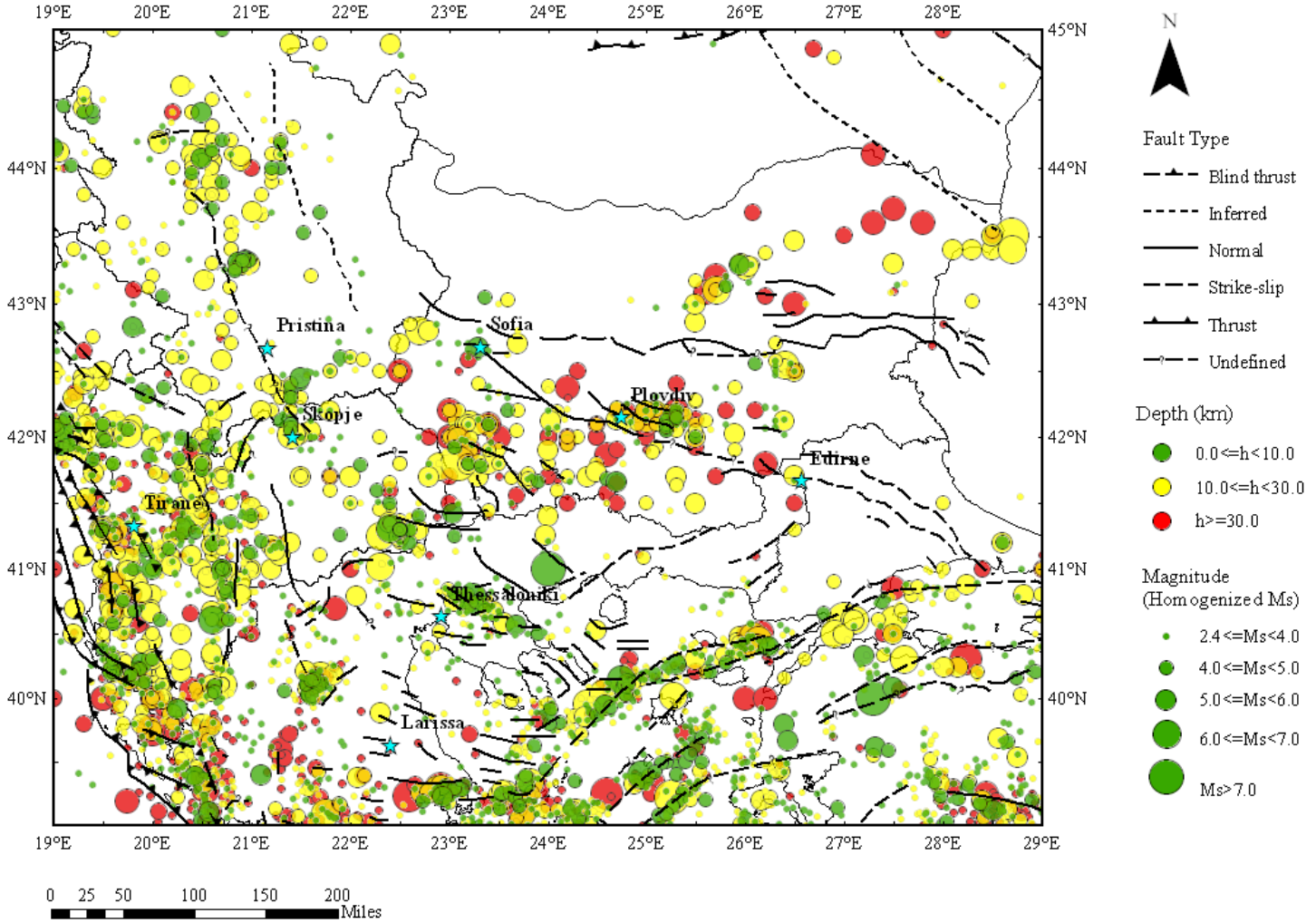

Figure 2.24 Seismotectonic environment of Bulgaria and the surrounding Balkan region. Major strike-slip, normal, thrust and undefined geological faults are shown along with catalogued seismicity discussed in chapter 4 (after: Geodynamic map of the Mediterranean, Commission for the Geological Map of the World; CGMW)

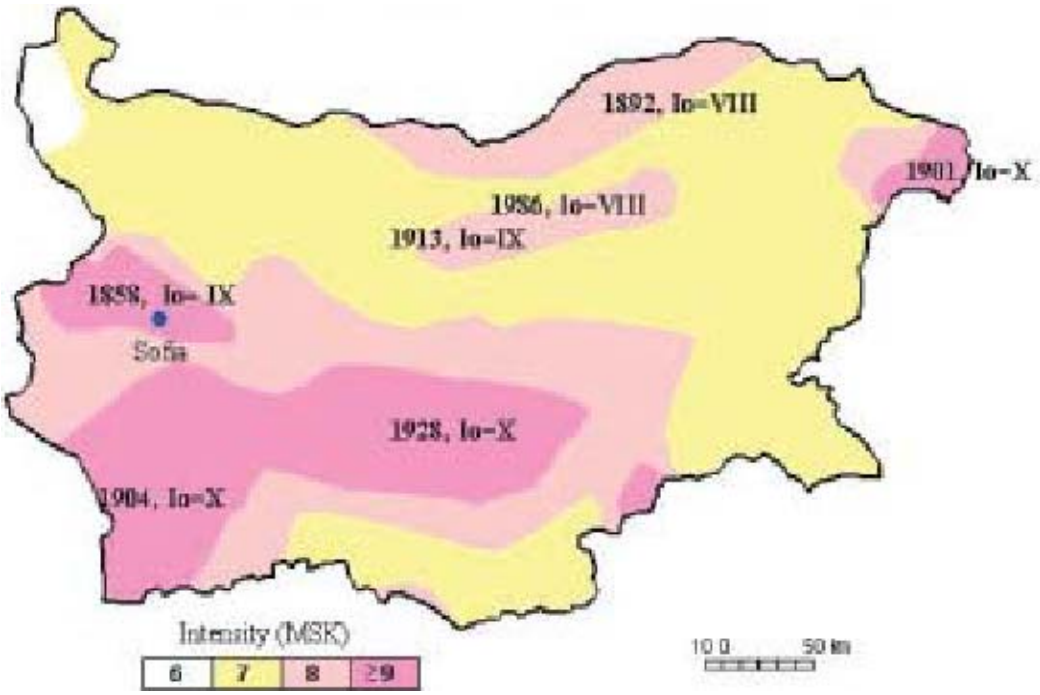

Figure 2.25 1,000 year intensity shakability map for Bulgaria and the nation's strongest events (source: Glavcheva *et al*., 2003)

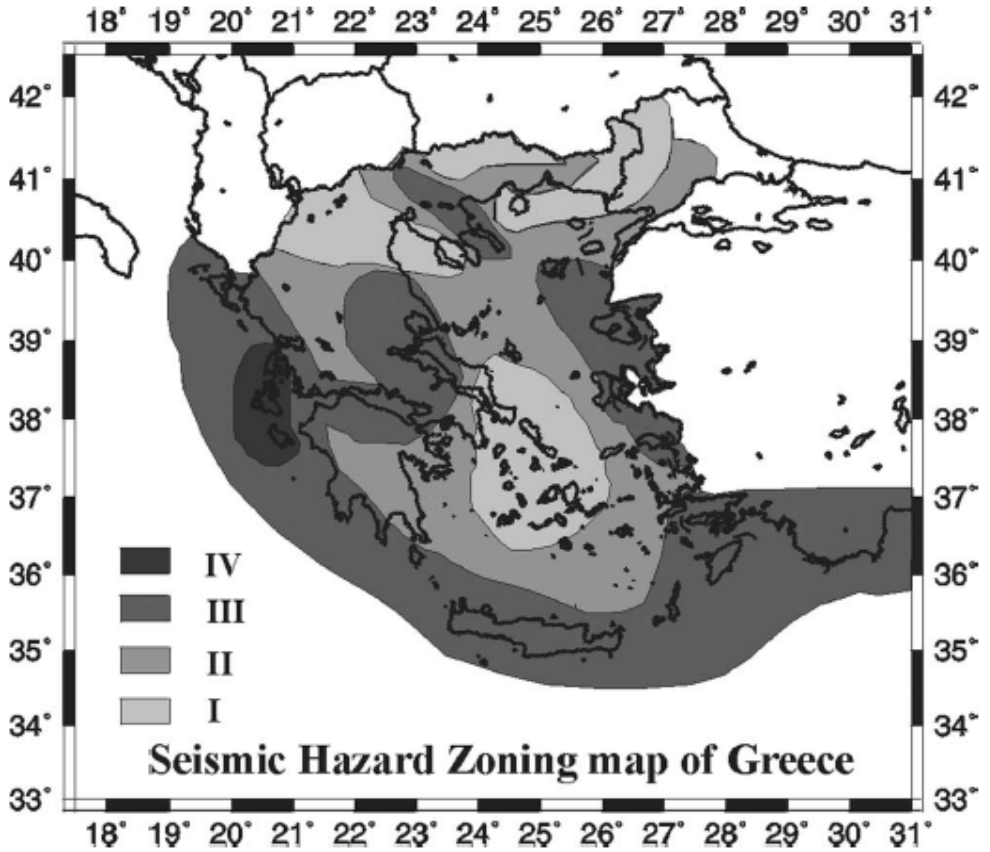

Figure 2.26 Seismic hazard zoning map for Greece derived New Greek Seismic Code (NEAK). Contours relate to zones associated to forecasted average horizontal peak ground accelerations of 12%g, 16%g, 24%g and 36%g (zones I to IV respectively) for the 475-year return period event (adapted by: Burton *et al.*, 2003)

Chapter 3 : Seismicity, statistical hazard and regional ground motion models

3.1 Introduction

Seismic hazard assessments across broad regions like the Balkans often require a number of statistical approaches to be applied to fully and successfully model its seismicity and estimate resultant hazard. Statistical recurrence models make use of one or more characteristic defined by Lomnitz (1974) for earthquake state space, and as such a region's seismicity: size (in terms of earthquake magnitude, energy release or other quantifiable statistic), latitude, longitude, depth (combined to provide knowledge of spatial distribution in three dimensions), the number of earthquakes and time (the temporal distribution).

This chapter is divided into two sections; it starts by discussing a number of familiar and widely adopted statistical approaches that are to be used in this hazard assessment. In doing so, it acknowledges a need to tailor a seismic hazard assessment to suit its specific needs from a selection of available – but often limited – tools and methods. Discussing each statistical model involves key steps in their historical development, past applications to seismic hazard, their limitations and benefits, understanding of uncertainties involved when reviewing results and, where possible, the current situation regarding its development and application. Special attention is given to reviewing the first and third asymptotic distributions of the theory of extreme values (Gumbel, 1958) and cumulative strain energy techniques then and how they can be used to develop methods to forecasting a region's seismic hazard in terms of expected extreme earthquakes.

The second section focuses upon reviewing important steps in the development of models to assess peak ground motion. In this instance it was decided to focus upon macroseismic intensity, ground acceleration and ground velocity to review Bulgarian seismic hazard. Following is a review of previous work on ground motion models relevant to these ground motion hazard descriptors.

Appendix 1 contains a full listing of hazard nomenclature used in chapters 4 to 7 of this thesis.

3.2 Seismicity models and statistical methods

Applying statistical models to a particular *scenario* can either be in isolation or as a suite of techniques to assess seismicity and seismic hazard. The latter option – to consolidate techniques together in a single study – should be preferred as it will invariably be the most beneficial, through making more effective use of information gathered for a particular region (Burton, 1990).

A broad review for a range of probabilistic statistical models currently available to seismic hazard researchers is discussed in Burton (1990). In applying the umbrella term 'pathways' to this range of statistical models, he discusses the cumulative frequency-magnitude distribution, Gumbel's first and third asymptotic extreme values distributions and cumulative strain energy release techniques.

These are used – by demonstration – to develop ideas for peak ground motion and earthquake perceptibility as measures of seismic hazard in both high and low seismicity regions. Geographic examples are made of other previous work covering Turkey (Burton *et al.*, 1984), Greece (Makropoulos and Burton, 1985a, b) and the North Sea area (Burton *et al.*, 1983), demonstrating the broad geographic and seismic applicability of these methods. These earthquake characteristics are selected as they were considered of most benefit to earthquake engineers in these situations. It is shown how from a single input earthquake catalogue one could achieve rigorous and compatible estimates for earthquake statistics pertinent to engineering needs. In summary, "*The corollary of this* [that is, the discussion put forward in the publication's text] *is that different pathways to assessing seismic hazard should be encouraged and exploited rather than assuming that one pathway provides ideal results*".

Additionally, Makropoulos (1978) outlines a need to check the validity of statistical models with a region's past seismicity record. As all models used here apply – to some degree – a new historical earthquake catalogue to estimating seismic hazard, this will be possible later on in this work. Development of some statistical methods beyond their original intended use has seen further benefits provided to assessing seismic hazard. For example, inspecting the stability of parameters of Gumbel's third extreme distribution to assess catalogue completeness and constraints on data usage (Burton, 1981) is one extra dimension that may be considered. This aspect will also be included in this chapter's discussion, and adopted in chapter 5.

3.3 Magnitude modelling of earthquake seismicity

The most commonly used *whole process* model is the Gutenberg-Richter cumulative frequency-magnitude distribution (Gutenberg and Richter, 1936, 1942, 1944, 1949; Richter, 1935, 1958), defined by Eq. (3-1):

$$\log N(m) = a - b(m) \qquad (3\text{-}1)$$

Where N(m) is the number of events per unit time with magnitude greater than or equal to m, and a and b are zone dependent constants; a is dependent upon the time span of a catalogue and on a

region's level of seismicity, and will be in a wide value range whilst b is typically between 0 and 1. Due to the importance of the b-value in describing a region's seismicity, section 3.5.1 is devoted exclusively to its discussion. A good summary of the cumulative frequency distribution and its characteristics is given by Makropoulos (1978) and Makropoulos and Burton (1983). Readers should refer to that text and references therein, for a fuller understanding of this magnitude recurrence model.

What is important here is concern surrounding inclusion or exclusion of earthquake foreshock and aftershock sequences; that is, non-independent seismic events. The main caveat to a cumulative frequency-magnitude distribution is that it should only consider independent, naturally occurring seismic events. Those events known to be non-independent and not of a natural origin (for example quarry blasts or nuclear explosions) within a given seismic sequence should be removed by applying a proven statistical filtering method.

A number of previous studies have applied cumulative frequency distributions to regions globally. For example, Miyamura (1962) discusses its relation to geotectonics, and Lazarov and Christoskov (1981) assesses the time-space independence of seismicity within Bulgaria and the central Balkans using revised earthquake catalogue that is Poissonian. By applying procedures outlined in Knopoff (1971) and Gardner and Knopoff (1974; and much of Gardner and Knopoff's other related work) to remove earthquake aftershocks and swarms – in principle the smaller magnitude events of a region's seismicity – they attempt to improve completeness of their earthquake catalogue. Spatial and temporal windows specified in kilometres and days respectively were applied, along with a decay parameter to enforce a cut-off to event aftershocks to their catalogue. This high and low truncation was suggested for events of $M < 6.0$ and $M \geq 6.0$. A certain number of events are then systematically "*restored*" to prevent a loss of effect of the region's natural background seismicity. Their work highlights that restoration of a catalogue's level of completeness is more important for higher activity zones as it has a more significant effect. For their catalogue, only a small number of events were "*restored*", thus not affecting the Gutenberg-Richter parameters 'a' and 'b' significantly.

Data typically shows the linear nature of Eq. (3-1) does not hold for high and low magnitudes (Makropoulos, 1978). Cumulative frequency distributions tend to 'tail-off' at these magnitude extremes. This is a result of small magnitude events generally being poorly recorded and reported, and an infrequency of large magnitude events making real-time observed seismicity not hold to this linear ideal. Consequently, Eq. (3-1) is not valid at every magnitude, and is restricted to the range $m_{min} \leq m \leq m_{max}$ (Yilmaztürk *et al.*, 1998; Bender, 1983).

Equally, a cumulative frequency-magnitude distribution may not be Poissonian in nature, as, if it accounts for all recorded events, it loses the assumption of independence between events. A better fit of the plotted curve to individual data points will also be obtained if only independent events are considered after foreshocks and aftershocks are removed.

3.3.1 The b-value

b-values have been important in seismology and seismic hazard assessment for a long time. b-values are important measures of a regions seismicity, as it is the ratio of large to small magnitude events. A higher b-value indicates smaller magnitude earthquakes rather than large ones are more likely to occur (Yilmaztürk and Burton, 1999) and vice versa. Put differently, a higher b-value indicates a smaller fraction of the total earthquakes occurring at higher magnitudes. Estimates for b-values will vary from region to region. As an earthquake catalogue is a direct representation of a region's seismicity, and therefore a source of estimating its b-value, this estimate is a direct result of manipulation of one or more of the following factors:

- Minimum and maximum magnitude thresholds imposed on catalogue;
- Size of earthquake population considered in time and space;
- Magnitude interval considered;
- 'Fitting' method applied to data (e.g. least-squares, maximum likelihood);
- Handling of anomalous data entries in a dataset, e.g. 'zero' observations in a magnitude interval used, or entries known to be suspicious or have low confidence levels.

Due to its importance in seismic hazard analysis, methods for quantifying b-values have been discussed extensively. Aki (1965) and Utsu (1966, 1971) suggest alternative methods for finding b-values for a region. b-value estimates may be dependent upon the interval, ΔM (Utsu, 1971). When ΔM is large, b is systematically small using maximum likelihood estimation.

Although general agreement has been reached on the basic meaning of a b-value in the context of a region's seismicity, a number of authors have suggested alternative or more appropriate interpretations and uses for it. b-values may relate to deformation energy density and rates of acceleration respectively (Neunhofer and Gueth, 1989; Bender, 1983). The latter compares two

maximum likelihood formulas, two least-squares formula and an X^2 formula as different methods for deriving estimates for b, noting that different fitting methods are better for handling 'grouped' or 'continuous' earthquake data.

3.4 Part process statistics (fitting of extreme values)

Whole process models such as the Gutenberg-Richter distribution suffer from the need to be aware of the full earthquake population down to a known magnitude threshold. This is often not practical due to a lack of accuracy, homogeneity and incompleteness (Makropoulos, 1978). A need is therefore apparent for models that represent spatial and temporal distributions of only extreme events in a region's seismicity, as these are the events typically of most interest in seismic hazard analyses. Gumbel's theory of extreme values is sufficient to meet the needs for a model of largest events within a temporal and spatial dataset, thus countering limitations outlined in section 3.3.

'Extreme' distributions developed by Gumbel benefit over the *whole process* Gutenberg-Richter model by not requiring full knowledge of the earthquake history (the process); hence their moniker as *part process* models. As hazard analyses tend to be interested in extreme events in a given distribution, only knowledge of these extreme occurrences should really be required. These are often more accurately reported and homogenous than smaller related events of the parent distribution (Lomnitz, 1974; Makropoulos, 1978; Burton, 1979, 1990). Additionally, this typically has the added effect of automatically removing the foreshock and aftershock distributions, making these maxima independent of the parent distribution and each other, thus making the retained listing nearer to being Poissonian in nature. As well as these benefits over *whole process* models, extreme values theory is governed by three key assumptions (Gumbel, 1935; further developed in 1945a, 1945b, 1958):

1. That the conditions prevailing in the past must also be valid in the future;

2. That the observed largest events in a given interval are independent;

3. That behaviour of the largest earthquakes in a given interval in the future will be similar to that in the past.

It is useful to outline briefly development of Gumbel's theory of extreme values. An extended review of theory is given in Appendix 2, although the salient points are retained below.

Gumbel's theory of extreme values is described by three equations, termed $G^{(I)}$, $G^{(II)}$ and $G^{(III)}$. The first asymptotic distribution, used extensively in Makropoulos and Burton (1985b) and Burton *et al.* (2003) takes the form of Eq. (3-2):

$$G^{(I)}(x) = \exp[- \exp(-\alpha(x - \mu))] \qquad \alpha > 0 \qquad (3\text{-}2)$$

where x is the earthquake variate (e.g. peak ground acceleration or peak ground velocity) under consideration, α is the extremal intensity function, μ is the characteristic largest value such that:

$$\phi^{(I)}(\mu) = 1/e$$

and also being the mode of the largest values.

Gumbel's second asymptotic distribution concerns the use of a lower bound asymptote. As earthquake hazard statistics are generally interested in largest events, Gumbel's second distribution is of no relevance here and will not be considered further. Gumbel's third asymptotic distribution is given by Eq. (3-3):

$$G^{(III)}(x) = \exp\left[-\left(\frac{\omega - x}{\omega - \mu}\right)^{k}\right] \qquad k > 1,\ x \le \omega,\ \mu < \omega \qquad (3\text{-}3)$$

where $G^{(III)}(x)$ is the cumulative probability of the variate less than or equal to x; x takes on the same meaning as before, by representing the variate considered (in the instance of a $G^{(III)}(x)$ distribution though, x is typically magnitude, or another bounded earthquake descriptor such as intensity, thus $G^{(III)}(x)$ becomes $G^{(III)}(m)$). k is again a function of the curvature parameter λ (with $k = 1/\lambda$), μ is the characteristic largest value, and ω is the limiting upper bound value with Eq. (3-4),

$$\phi^{(III)}(\omega) = 1 \qquad (3\text{-}4)$$

When m tends to its upper limit ω, the function $G^{(III)}(m) \rightarrow 1$, whereas when m decreases, $G^{(III)}(m) \rightarrow 0$; μ is the characteristic largest value (but not the modal value in this distribution) such that,

$$\phi^{(III)}(\mu) = \frac{1}{e} \qquad (3\text{-}5)$$

The variate described by Gumbel's first distribution is not limited by an upper or lower bound (Figure 3.1). It is therefore of theoretically infinite range, making it relatable to the inferred linear regression nature of the Gutenberg-Richter distribution and 'extreme' ground motions.

Gumbel's first extreme distribution favours modelling of ground motion hazard such as peak ground acceleration, peak ground velocity or displacement, whose variate is not bounded by upper or lower limits. Gumbel's third distribution is limited by an upper bound, ω, to the variate considered, making it compatible with the acknowledged behaviour of world seismicity (Esteva, 1976). This distribution can typically be safely applied to intensity and magnitude as each is represented by a range using clearly defined limits.

3.4.1 Plotting point probability rules

Gumbel's extreme distributions select annual [or other *N*-year interval] extreme values, m_i, from an earthquake catalogue of *N*-years in length. These are then ranked in ascending order such that $m_1 \leq m_2 \leq \ldots \leq m_n$ where m_n is the largest extreme value selected. Gumbel (1958) and Gringorten (1963) offer solutions to successfully plotting these discrete points by assigning probabilities to each instance, e.g., Gumbel (1958) – Eq. (3-6) and Eq. (3-7) – found,

$$P(m_i) = (i - 1/2)/N \qquad \text{for i} = 1\ldots N \qquad (3\text{-}6)$$

$$P(m_i) = i/(N + 1) \qquad \text{for i} = 1\ldots N \qquad (3\text{-}7)$$

while Gringorten (1963) offers Eq. (3-8),

$$P(m_i) = (i - 0.44)/(N + 0.12) \qquad \text{for i} = 1\ldots N \qquad (3\text{-}8)$$

which is considered suitable when $N \geq 20$. This last option is the most commonly used in modern extreme values distribution analyses. Developing a new plotting point rule is considered outside the scope of this work, so Eq. (3-8) will be taken as the plotting point rule used here.

Regardless of the plotting point rule invoked, there may be *j* years for which no value for m_i is available, therefore the distribution is calculated over $i = j + 1, \ldots n$. From Eq. (3-8) the plotting point probability for the lowest extracted extreme value becomes,

$$P(m_i) = (j + i - 0.44)/(N + 0.12)$$

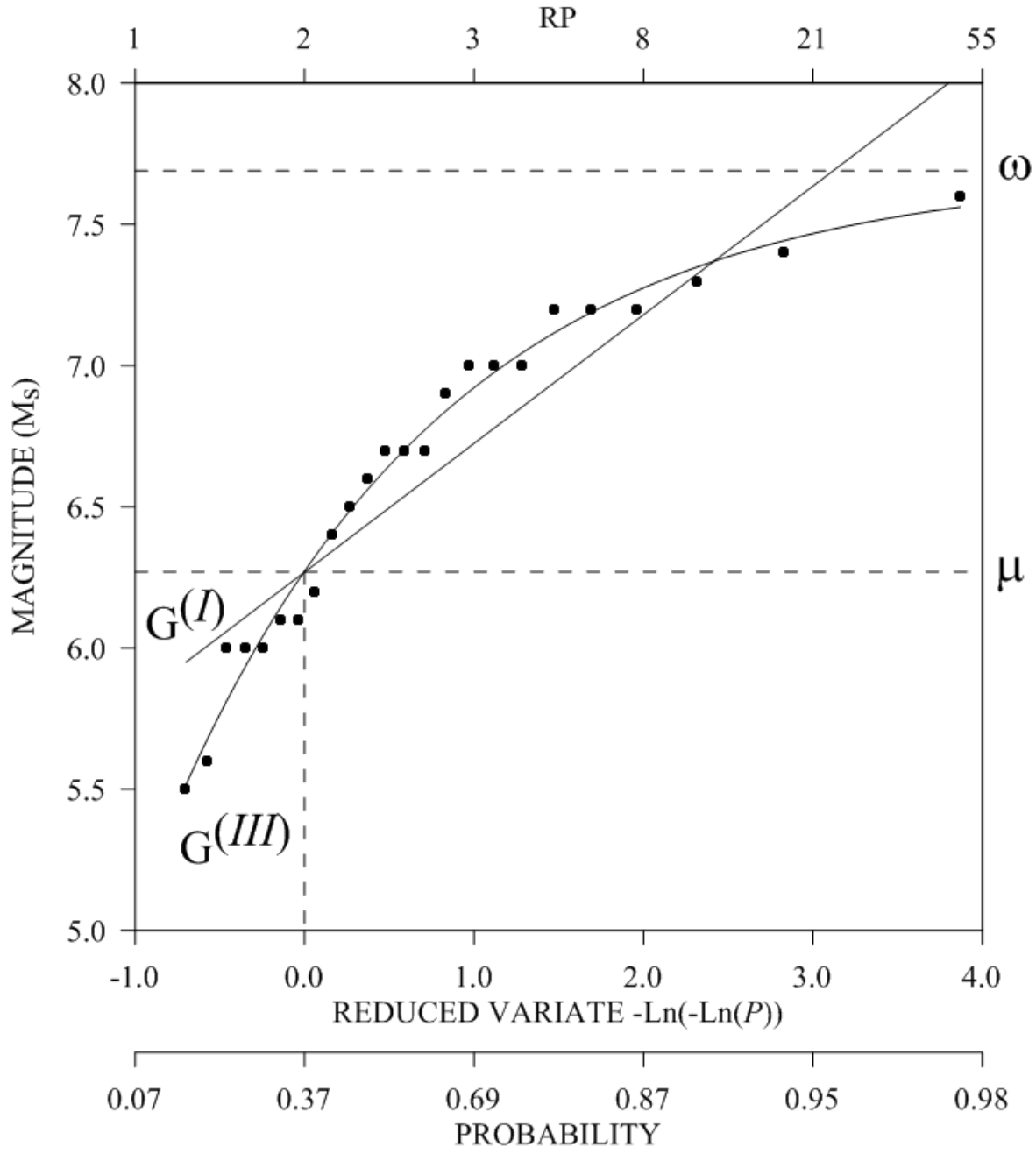

Figure 3.1 Graphical relation between Gumbel's first and third asymptotic extreme values distributions using an arbitrary set of extreme values

This rule is often accepted suffice sufficient extreme data is available from the considered catalogue. This is typically such that $j \leq N/L$, with L equal to 3 or 4 usually being accepted, and is generally achievable if extreme intervals longer than 1 year are considered.

In chapters 5 and 6 j will be referred to as 'LIMIT' to denote the minimum proportion of years acceptable for which no extreme value is available in an adopted earthquake catalogue.

3.4.2 Previous applications of Gumbel's 1st distribution to earthquake hazard

Earthquake ground motion descriptors that Gumbel's first extreme distribution is most suitable for modelling are given in section 3.4. Epstein and Lomnitz (1966) was one of the first to apply a first-type distribution to earthquake data. Although Nordquist (1945) was the first to apply Gumbel's extreme values theory to earthquake data, his text does not explicitly state a preference between first and third-type distributions. After fitting available data for California between 1932 and 1962, Epstein and Lomnitz show their data had good agreement with both this statistical model and data analysed by Gutenberg and Richter (1949).

Gumbel's first [and third-type] extreme distribution was critically assessed by Dessokey (1985) against the triple exponential and Johnston distributions on Turkey, China and New Zealand. Return periods for a number of magnitude values are returned and compared between the different models. High values of M are found for the first-type distribution and so this is rejected for magnitude extreme estimation. Uncertainty is however noted over the ideal model between Gumbel's third-type distribution, triple exponential and the Johnston distribution. All three statistical models gave good fits to observations in New Zealand. Similarly, all models gave poorer fits to Turkish data, suggesting data more than the statistical model selected governs results of seismic hazard analysis. Burton (1978a) applies the Institute of Geological Sciences (IGS; now the British Geological Survey database) to study ground motion. Selected formulae were chosen to assess peak ground acceleration, peak ground velocity, epicentral intensity and ground displacement. Gumbel's distributions were directly compared using this data to determine the appropriateness of each for forecasting magnitude recurrence, in terms of return periods, for a selection of magnitude values. The linear form of Gumbel's distribution offers more conservative estimates of risk than the third distribution at higher magnitudes, due to best-fit plots of $G^{(I)}$ to data approaching the upper bound estimate, ω, to $G^{(III)}$ at lower values for the reduced variate, $-\ln(-\ln P)$.

3.4.3 Previous applications of Gumbel's 3rd distribution to earthquake hazard

Many texts endeavour to apply Gumbel's third extreme distribution to earthquake data, and to attempt to model regional extreme seismicity and have been given already in section 3.4. The main aims of a number of these are elaborated on here.

Direct comparisons between Gumbel's first and third asymptotic extreme distribution are attempted by Dick (1964), Epstein and Lomnitz (1966), Yegulalp and Kuo (1966) and Yegulalp and Kuo (1974) to determine their suitability to forecasting a region's magnitude hazard. Applying the third distribution in isolation to data for the Aleutian Islands and West Alaska is discussed by Yegulalp (1974), and suggests a *scenario* magnitude for buildings constructed at that time. Applications for Gumbel's third distribution to seismic risk across high seismic regions of Europe (Greece, Turkey and Aegean regions) and Asia are trialled by Makropoulos (1978), Burton (1979), Burton *et al.* (1984), Makropoulos and Burton (1985a), Yilmaztürk and Burton (1999), and Burton *et al.* (2004b). All show the third-type distribution is consistently a better model for magnitude recurrence seismic hazard over the first-type distribution. Similar work – but on a global scale – is outlined by Tsapanos and Burton (1991) to estimate maximum magnitude events with a 85-year return period for fifty geographic cells of seismicity located around the world, using data specific for the study and the third distribution.

Burton *et al.* (2004b) extends Makropoulos and Burton (1985a) by assessing specific catalogue parameters (i.e. extreme interval, minimum magnitude threshold and time span) used for the work. This method of refining final hazard results by altering selection criteria of earthquake data used is also discussed by Burton (1981) and Yilmaztürk (1993), and will be used in this study to produce more realistic statistical forecasts for seismic hazard in the region than was previously achieved.

Past applications of Gumbel's third type distribution to central Europe and the Balkans cannot be dismissed. Kárník has undertaken a significant amount of research into earthquake hazard on the European mainland. His seminal earthquake catalogue is discussed in chapter 4, and comparable seismic hazard assessments for central Europe are detailed in Kárník and Hubnerová (1968), Kárník and Schenková (1977) and Schenková and Kárník (1978). Return periods were determined by Kárník and Hubnerová (1968) for maximum earthquakes for 15 of the 39 seismic zones defined using shallow-focus events of magnitudes >4.5 M. In doing so they suggest the largest [probable] event had already occurred in most regions. The latter two texts highlighted curvature of the third-type distribution results in longer return periods than an equivalent application of a first-type distribution to the same data, and advocated the third distribution for assessing magnitude recurrence hazard.

Estimates for maximum earthquakes and 75-year return period magnitudes in addition to their uncertainties are developed by Burton (1977) using the third distribution. This is performed for the region bounded by 32°-48°N, 4°-36°E. Using a cellular '*moving cell*' approach, estimates are found for all cells with sufficient data. Covariance matrices highlight many data cells that exhibited little curvature of fit (small λ) to follow the $G^{(III)}$ distribution, resulting in estimates of ω with large uncertainties. This was attributed to using data with an insufficient time span not being able to establish curvature a $G^{(III)}$ distribution should exhibit, reinforcing results of Dick (1964).

3.5 Inspection of parameters from Gumbel's 3rd extreme distribution

Gumbel's third distribution of extreme values is suitable for highlighting annual [or other time interval] magnitude extremes in an earthquake population at an acceptable cost of excluding the smaller magnitude events of the parent population. This is typically the desired situation as the larger magnitudes of a region generally produce peak earthquake characteristics of most interest to earthquake engineers, e.g. peak ground accelerations, velocities and intensities.

Authors usually chose annual extremes. However, this assumes data is of good enough quality and to a suitable degree of completeness – even after lower magnitude events of the parent distribution are removed – for annual extremes to provide reliable forecasts. Use of annual or other relatively short extreme intervals may not mitigate the effect of years with no data – a problem more apparent in early instrumental and historical periods of earthquake monitoring – or the inclusion of '*dummy*' observations, or introduction of non-dependent events (Burton *et al.*, 2004b). Using overly long extreme intervals to select extremes may not only disregard 'true' earthquakes that should more appropriately be included, rather than excluded, in the final extreme sample, but may also reduce an extreme distribution's fit to data, thus increasing statistical error; i.e. decreasing the efficiency of the system. Longer intervals decrease the number of extreme intervals with '*null*' entries (sometimes called '*dummy*' observations) that must be discarded from an extreme subset due to not having an associated extreme value. These intervals are not devoid of earthquakes, but have extreme events falling below the cut-off magnitude imposed, M_{CUT}, on the catalogue but are above the magnitude of completeness for the data set, so no extreme can be attributed to that interval.

There needs to be some means to assess data and the effects of restricting its application to a Gumbel distribution. This analysis can then be invoked as a preparatory step on an earthquake catalogue before its application to an extreme values distribution analysis. This would be with the aim of obtaining reliable forecasts for earthquake extremes. The next section outlines such a method for discriminating suitable data restrictions to apply.

3.6 Stability of $G^{(III)}$ distribution parameters

Burton (1981) investigates the effect on dependence of the three parameters (ω, μ, λ) of a $G^{(III)}$ distribution and their first-order uncertainties on variations in a) extreme interval used, b) cut-off magnitude M_{CUT}, and c) start year used. Data used were primarily from the Institute of Geological Sciences and LOWNET seismograms (Burton and Neilson, 1978, 1980). The intentions of this method are therefore three-fold:

- To ensure variations in ω, μ and λ are as a result of the natural extreme distribution tested, and not from incorrectly applied restrictions imposed upon earthquake data, nor inclusion of '*dummy observations'* of extremes in the statistical distribution model applied.

- To obtain reliable and robust values for the extreme interval (NPER), cut-off magnitude (M_{CUT}) and start year of data.

- To obtain realistic estimates for ω, μ and λ (and their associated uncertainties) of Gumbel's third asymptotic extreme distribution.

This methodology is adopted in Burton *et al.* (2004b) in an updated analysis of extreme earthquake and perceptibility hazard for Greece and the Aegean. In doing so, they highlight its relevance for applying to areas of lower seismicity, by suggesting longer extreme intervals (large sample interval) are required to remove the effects of '*null*' years (years without earthquakes above the imposed magnitude threshold) and smaller magnitudes inherent to a region's background seismicity, so improving the model fitting to the third distribution. An extreme interval of never less than six years was finally selected for this region to ensure stability. Six-year intervals were also applied in Burton (1981). Due to an obvious difference in levels of natural seismicity in these regions, it is possible to suggest incomplete data or a significantly shorter time span to covering British seismicity may result in these identical extreme intervals of sampling.

Selecting catalogue criteria is done as follows: a suitable set of extreme interval, cut-off magnitude and start year for data is chosen based upon instances in plots of variation of (ω, μ and λ) against the variate where each parameter is realistic in terms of catalogued seismicity and uncertainties attached are small or within accepted limits. When the variate is the extreme interval, μ should show curvature, as it represents the *characteristic* magnitude over the *N*-year interval (Figure 3.2). For all variates, estimates of (ω, μ and λ) should have reached a stable 'plateau' of forecasts.

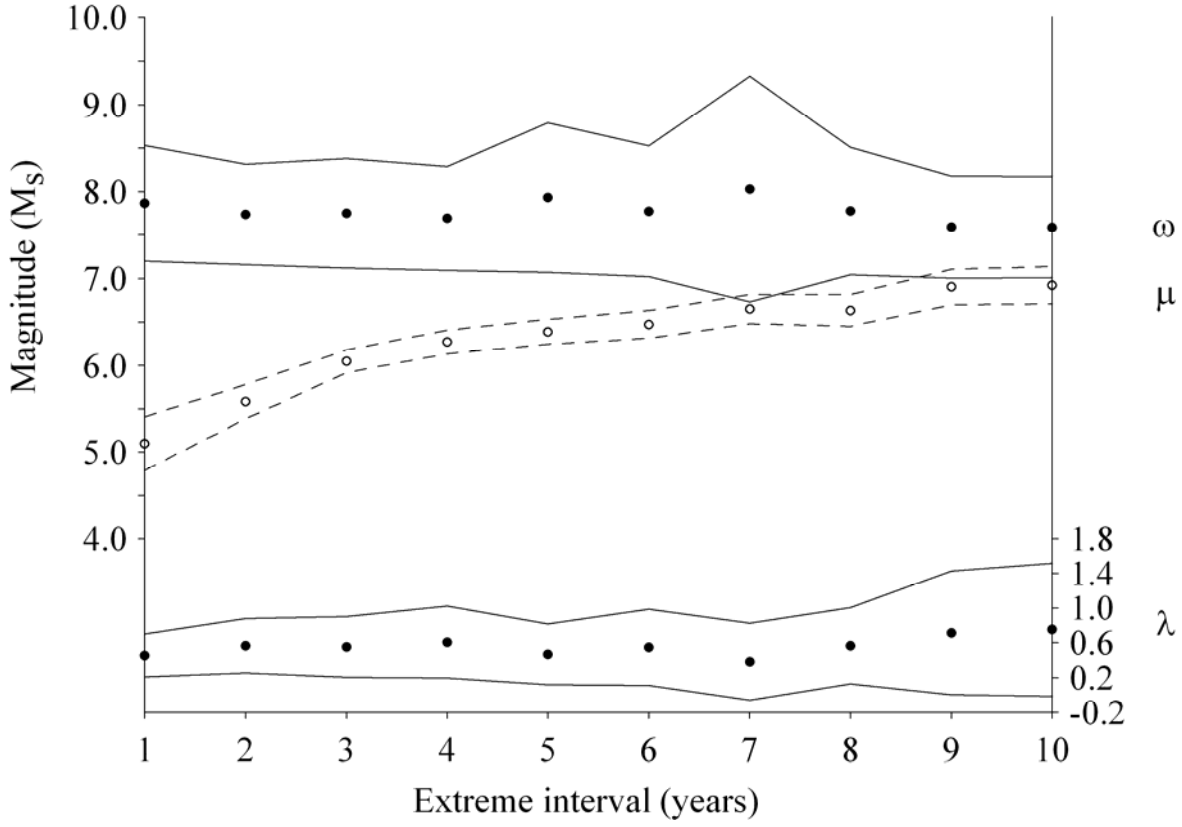

Figure 3.2 Stability of (ω, μ and λ) and their first order standard deviations of Gumbel's third asymptotic extreme values distribution (after Burton, 1981). In this instance, variation in seen with change in the extreme interval applied is shown, although the x-axis may alternatively refer to start year or lower magnitude threshold imposed

Methodology outlined in Burton (1981) for critically assessing catalogue characteristics to use in an extreme values hazard assessment therefore ideally lends itself to application to these areas. Consequently, it will be applied to earthquake data in chapter 5 to allow development of a seismic hazard assessment for southwest Bulgaria and the broader Balkan region.

3.7 Cumulative strain energy release techniques

3.7.1 Theory and methodology

Early attempts to relate seismic energy release to the *whole process* cumulative frequency-magnitude law of Gutenberg and Richter (1944), Eq. (3-1), and the event's magnitude focus upon their magnitude-energy law, Eq. (3-9):

$$\text{Log } E = A + Bm \tag{3-9}$$

Where E is energy release in ergs, m is the earthquake magnitude and A and B are zone-dependent constants. Gutenberg and Richter (1956) derived the early standard and accepted equation form of log E = 11.8 + 1.5M from which most early estimates for energy release in ergs of individual earthquakes were obtained.

Benioff (1951a, b), Benioff (1955) and Båth and Benioff (1958) use examples of the White Wolf fault, Kern County, United States and the 1952, 8.5 M Kamchatka earthquakes to develop relations between the cumulative frequency-magnitude distribution and seismic wave energy to investigate using strain release curves for predicting future event magnitudes. By extrapolating creep strain release curves for the Kern County earthquake of July 21st, 1952, this work was able to predict a) the magnitude of expected shock, and b) the waiting time for the next event of equal magnitude. Equation (3-10) represents strain energy release from a seismic sequence over a time interval, t, as being proportional to the square root of the energy, J:

$$\Sigma J^{1/2} = A + B \log t \tag{3-10}$$

where J is energy release in ergs, A and B are constants and t is time since main earthquake. The authors introduced the power to ½ to simulate time variations of the relationship between M and J. $\Sigma J^{1/2}$ represents the sum of the strain release increments, instead of a summation of the absolute energy releases from each earthquake, which is now accepted to be a more appropriate model to adopt.

The aftershock sequence to the Kamchatka earthquake could be represented by three distinct traces, shown by Figure 3.3(a) and (b). Each trace represented different rates of energy release and time intervals, with each trace holding to Eq. (3-10). Data were filtered of magnitudes $M < 6.0$ as it was considered omission of these lower magnitudes would not adversely alter strain characteristics plotted.

Galanopoulos (1972) and Båth (1973) both return to the issue of energy release from individual earthquakes; the latter adopted Eq. (3-11) to represent energy release, E, in terms of magnitude, M:

$$\text{Log } E = 12.24 + 1.44M \tag{3-11}$$

Inconsistencies between three standard magnitude scales (local, body-wave and surface-wave) were realised by Gutenberg and Richter (1956), Kanamori (1977) and Hanks and Kanamori (1979), and a need to define new scales to solve this problem. The latter two sought to resolve this by developing a new magnitude scale (moment magnitude, M_w) that eradicated problems of saturation on standard magnitude scales at large magnitudes (large events defined as possessing fault ruptures greater than 100 km). Noting that seismic moment, M_0, of an earthquake is one of the most accurately determined values – long period body-waves make this possible – the energy-magnitude relation of Gutenberg and Richter (1956) was adopted with a term for strain energy drop of an earthquake, W_0, Eq. (3-12) to derive this new moment magnitude scale, Eq. (3-13):

$$W_0 \sim M_0 / (2\text{x}10^4) \tag{3-12}$$

$$M_W = 2/3 \log M_0 - 10.7 \tag{3-13}$$

This magnitude scale is important to modern seismic hazard analyses due to its ability not to saturate at any magnitude, providing a consistent term that can relate the size of one earthquake directly to another. The correctness of Eq. (3-13) to estimate an event's moment magnitude is supported by Thatcher and Hanks (1973) and Purcaru and Berckhemer (1978) when they obtained similar M_o/M_s relations.

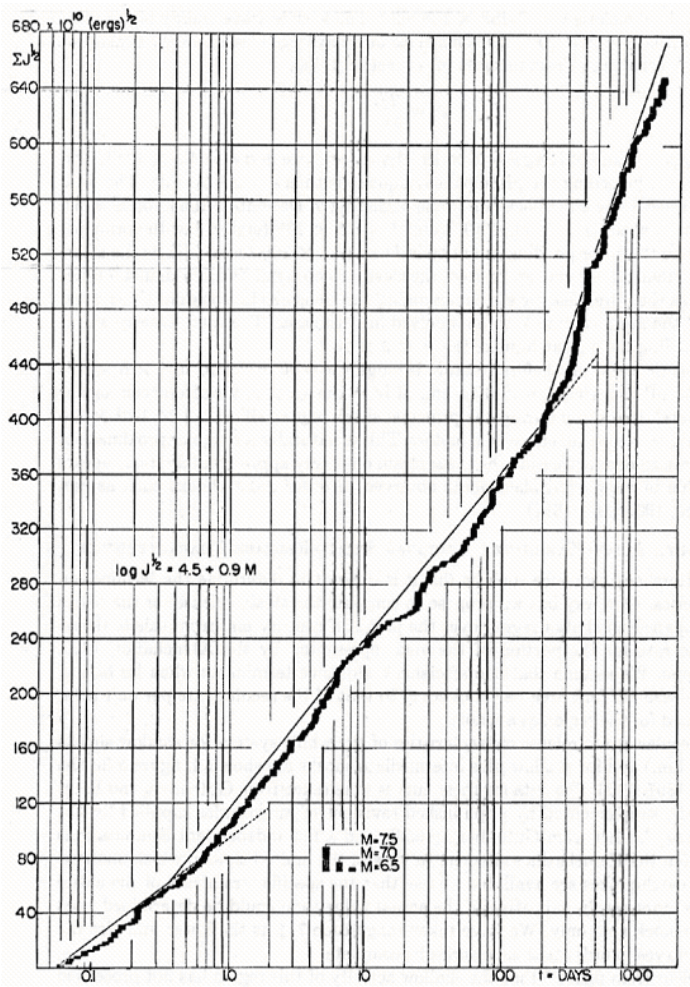

(a)

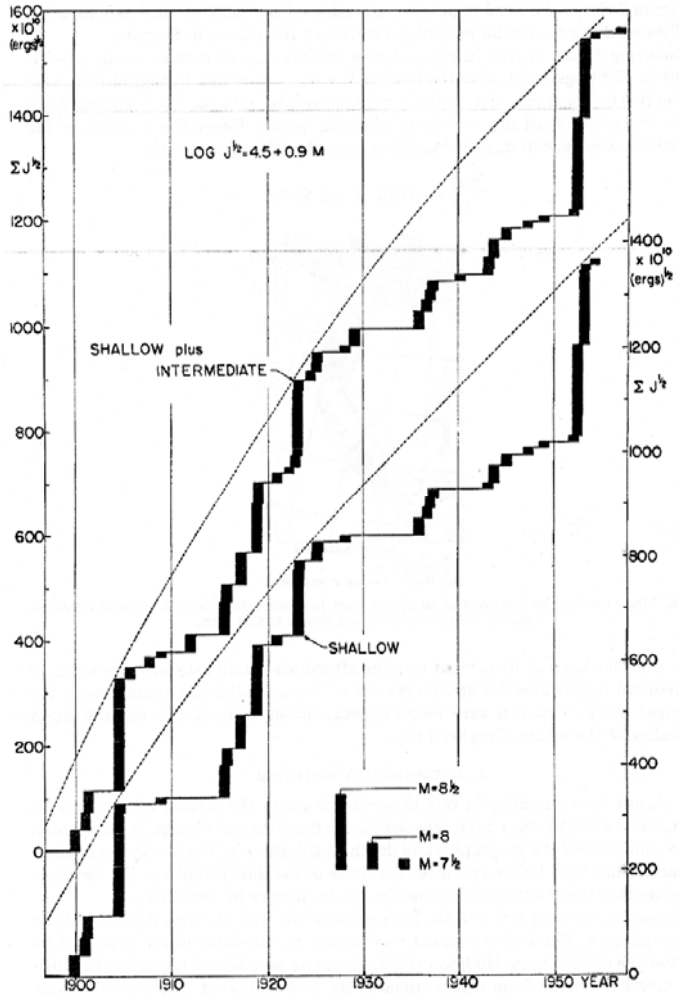

(b)

Figure 3.3(a) Strain-release characteristics for the aftershock sequence to the 1952 Kamchatka earthquake, outlining application of Eq. (3.18); (b) regional strain accumulation for the Kamchatka-Kurile Islands region for shocks M ≥ 7 ¼ (source: Båth and Benioff, 1958)

Modern expressions for cumulative strain energy release statistics for assessing *maximum credible magnitude* hazard have their genesis in work of in Makropoulos (1978) and Makropoulos and Burton (1983). This work was first to propose analytical methods for linking expected maximum magnitudes (and other magnitude statistics) to energy release statistics. Three values were proposed – M_1, M_2 and M_3 – that state specific earthquake magnitudes in terms of regional energy releases from an earthquake sequence. These three values are defined as:

- M_1 – the most probable annual maximum magnitude (mode), which from Eq. (3-1) equals a/b;
- M_2 – the magnitude that corresponds to the mean annual rate of energy release;
- M_3 – the analytical upper bound for the earthquake magnitude for the region.

Energy release from an earthquake sequence can be described easily in a graphical sense, with elements of a cumulative strain energy release plot representing M_2, M_3, the energy equivalent to M_3 (that is, all energy released in a single instance), and a waiting time, T_w, for this energy to accumulate.

Makropoulos and Burton (1985a) use their 1981 Greek catalogue to establish relationships between cumulative strain energy release and a $G^{(III)}$ distribution for Greece. Close agreements found led them to indicate a close relation between $G^{(III)}$ and cumulative strain energy release statistics provided at least one clearly defined cycle of seismic periodicity is present in data used. Contouring results enables confirmation of the effect of λ (the curvature parameter), and how it varies between locations, implying each area possesses its own magnitude distribution to reach its forecasted upper bound. In addition to contouring regional magnitude extremes, third asymptote distributions were directly compared alongside cumulative strain energy release techniques for six urban centres of Greece (Athens, Thessaloniki, Patras, Rodhos, Heraklion and Corinth) for cells of differing radii. These are converted into estimates relating to waiting times (return periods) for magnitude extreme estimates, and incremental magnitude intervals.

Considered graphically, Figure 3.4 illustrates M_1, M_2 and M_3 as energy release for a sequence of individual earthquakes in a given region for time interval, T (Burton, 1990).

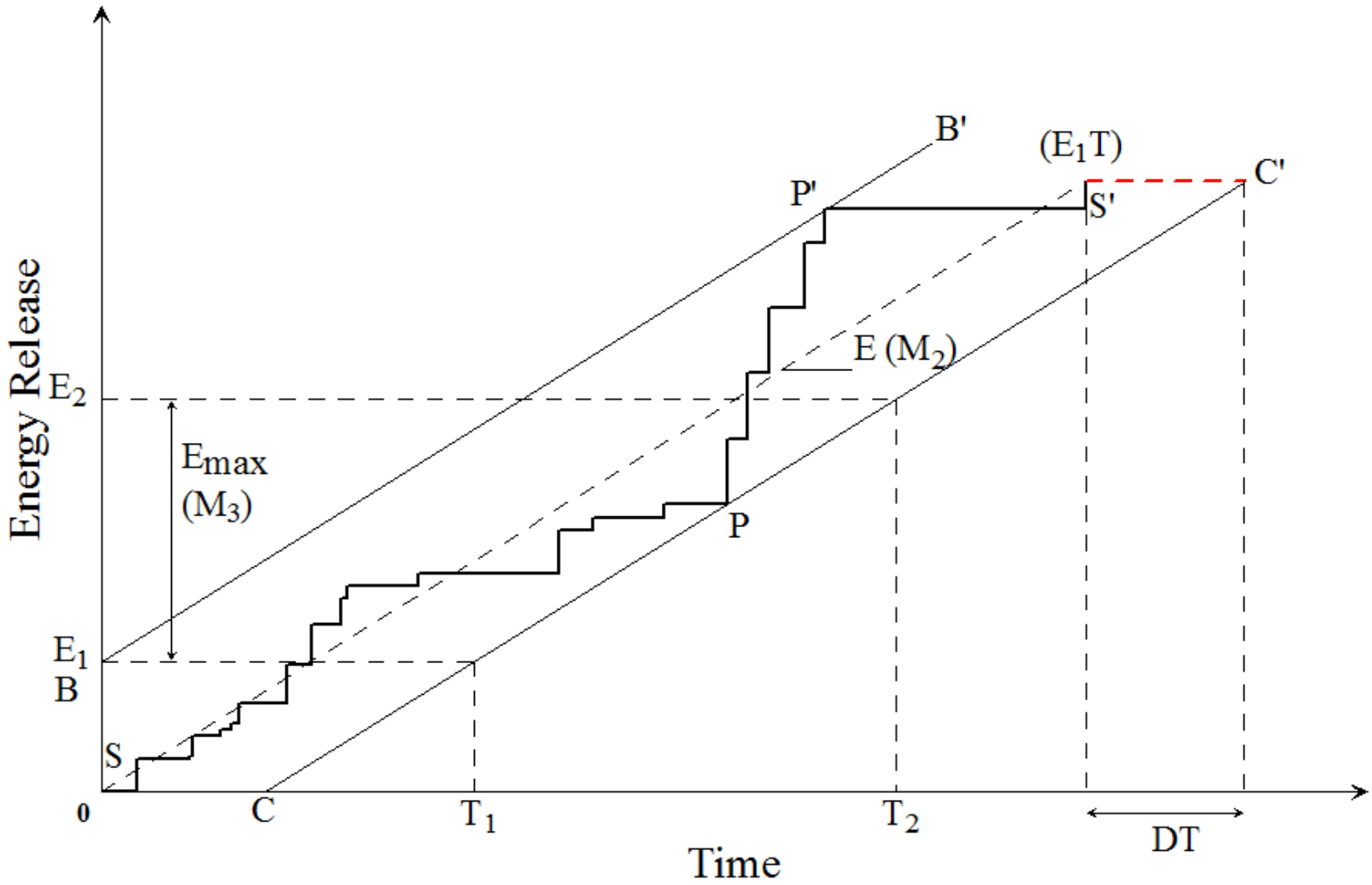

Figure 3.4 Graphical illustration of a region's cumulative strain energy release, and statistics available (adapted from Makropoulos and Burton, 1983) and incorporating the concept of waiting time (DT; Tsapanos, 1998)

- Slope $\Delta E/\Delta T$ represents the annual rate of energy released in a region per unit time, (M_2).

- The vertical line E_1E_2 represents the upper limit E_{max} for the energy release of a region if it were released as a singular event. This corresponds to M_3;

- Waiting time, T_w, for all energy to accumulate (assuming no earthquake events in the mean time), and equivalent to M_3, is defined by horizontal distance, T_1T_2 between parallel enveloping lines BB' and CC'.

The ensuing seismic hazard assessment in chapters 5 and 6 will determine robust, realistic and comparable estimates for magnitude hazard using the *part process* third extreme values distribution of Gumbel and the cumulative strain energy release techniques outlined in this chapter. Whilst doing so, it is important to understand a fundamental difference between these two techniques.

Burton and Makropoulos (1985) state "*it is clear that ω is notionally equivalent to M_3…, no matter whether M_3 is determined analytically…. or graphically from the cumulative strain energy release diagrams…*". Further, ω and M_3 differ fundamentally in that ω represents a maximum magnitude from an infinitely long waiting time, as $G^{(III)}$ is asymptotic; M_3, corresponds to a finite waiting time, i.e. the time which it takes for all strain to accumulate in the region. Thus, it is fair to assume M_3 is approximate to, but less than ω of $G^{(III)}$, such that:

$$\omega - M_3 \geq 0 \qquad (3\text{-}14)$$

3.7.2 Previous applications of cumulative strain energy release techniques

Relatively new expressions for cumulative strain energy release for seismic hazard practices were discussed in section 3.7.1. Consequently, a number of authors have sought to take advantage of them. Aside from work already outlined earlier, certain others are useful to mention. Burton *et al.* (1984) use this method to assess M_3 against ω for Turkey, the Aegean and east Mediterranean for a 75-year return period using data of the Kandilli Observatory and ISC up to 1978. Using limitations of ω outlined in section 3.7.1 as reason for using strain energy release techniques, they compare directly results for these two models. Strain energy release techniques reveal waiting times of 15- to 70-years to enable all energies to accumulate. Regional cellular estimates for M_3 (the magnitude equivalent to total release of all accumulated strain) are mapped to provide graphical comparison to M_{75} (i.e. largest magnitude event expected in a 75-year time interval) and each cells *most perceptible magnitude*; the idea that M_3 is consistently less than ω is confirmed by the data used.

Tsapanos (1998) restricts his study of seismic hazard to seven seismic regions, ranging from regions of the Eurasian belt to Japan and California and "*can be considered as a follow up to Makropoulos and Burton (1983) work*". He validates the idea of M_2 and M_3 representative magnitudes for aspects of cumulative strain energy release. Tsapanos introduces a new term for an alternative waiting time, DT, defining the time (in years) between the upper bound line (of energy-time diagrams) and the time since the end of the last seismic activity. Graphically this will be obtained by extending the lower envelope line (line CC' of Figure 3.4), and the strain energy release line of the plot until they intersect one another, and is often referred to as the 'residual time'. This estimate of waiting time now equates to the next time sub-interval within which the event with magnitude less than or equal to M_3 will occur. Results of Tsapanos reinforce Makropoulos and Burton (1983) in stating M_2 and M_3 have a difference of approximately one magnitude unit.

3.8 Regional ground motion modelling

Earthquakes are usually assumed to be point source processes in time and space, although other models can be adopted. However, radiating energy allows an earthquake to have significant impact at great distances from its hypocentre. Damaging effects experienced from energy released is most pronounced within the first 100 to 200 km as it radiates from the earthquake's focus. Once this seismic energy reaches the Earth's surface, it manifests itself in any of the following forms: a) felt and observed macroseismic intensity, b) ground acceleration, c) ground velocity and d) ground displacement.

Determining the size of any ground motion characteristic at a distance from an earthquake requires derivation of appropriate ground motion laws. These will typically be in terms of earthquake magnitude, or epicentral intensity, I_0, and some distance element (e.g. focal or hypocentral distance is most often used, although Douglas (2003) state a further eight options) as a minimum requirement; other variables may also be included at the user's discretion and *scenario* in question. Magnitude is typically quoted using the surface-wave magnitude scale, although more recently favour has swung towards using the moment magnitude scale, due to reasons outlined earlier. This is particularly useful as smaller-magnitude events may have comparable effects, in terms of ground motion, at the Earth's surface if they have shallow focal depths, as larger magnitude earthquakes do at deeper focal depths.

Four key urban centres within the southwest zone of interest considered are situated in what could be considered to be close proximity to sites of previous large magnitude (i.e. ≥6.0 M) earthquakes that occurred during the catalogued time interval of 1900 to 2004. Sofia, Thessaloniki, Blagoevgrad and Plovdiv have all experienced significant damaging earthquakes within 100 km of them. In reviewing Bulgarian seismic hazard this assessment will focus upon macroseismic intensity, ground acceleration and ground velocity. Following is a review of previous work on attenuation of these ground motion characteristics.

3.8.1 Attenuation of macroseismic intensity

3.8.1.1 Determining epicentral intensity

There are generally two acknowledged means for estimating intensity attenuation. Kövesligethy (1906, 1907) develops a method to estimate differences in intensities between source and site (i.e. epicentral intensity, I_0, and site intensity at distance r, I_i, respectively in Eq. (3-15)), with assistance from others (e.g. Jánosi, 1907; Blake, 1941) when trying to develop a relation between macroseismic intensity and focal depth of an earthquake:

$$I_0 - I_i = 3 \log (r/h) + 3\alpha M(r-h) \quad (3\text{-}15)$$

where r is the radius of an isoseismal of intensity, I_i, and M is log e. Refer to Musson (2002) for a brief summary of how Eq. (3-15) evolved amongst contributors. This method has been adopted in the past by Burton *et al.* (1985) and Papazachos (1992).

A more common means to estimate site intensity is to describe it as a function of earthquake magnitude and epicentral (or hypocentral) distance. Crudely, these equations will take the form of I = f (M, R), with a more descriptive general form in Eq. (3-16):

$$I = a M + b \log R + c R + d \quad (3\text{-}16)$$

where R is hypocentral distance, and a, b, c and d are constants (alternatively given as SI = C1 + C2M – C3f (logR) – C4f (R) in Papaioannou (1986) where SI is a general term, "Seismic Intensities", created by the author and C4 is an anelastic co-efficient). This approach has been adopted by a number of authors, and is generally favoured for developing intensity ground motion equations. Previous works using this approach include Papaioannou (1984), Papazachos and Papazachou (1997), Papazachos and Papaioannou (1997) and Shebalin *et al.* (1998).

Fundamental to a lot of intensity ground motion models is knowledge of the epicentral intensity, I_0, of an earthquake of a known or estimated magnitude (and, optionally, at a known focal depth). Intensity estimates are rarely obtained at the exact earthquake epicentre, no matter how desirable knowledge of this value is. Consequently, epicentral intensity needs to be determined by other means. For example, this may be via extrapolation of data from nearest points with measurements, or, estimation of a fractional intensity estimate from equations such as Eq. (3-15).

This study focuses upon three neighbouring countries – Bulgaria, Greece and the Former Yugoslav Republic of Macedonia – and as such, previous work detailing estimation of epicentral intensities for all should be considered where available. These can then be applied in combination with any of the intensity ground motion laws discussed later.

Glavcheva (1997) proposes Eq. (3-17) for epicentral intensity in Bulgaria:

$$I_o = 1.37M_L - 1.97\log h + 2.00 \quad (3\text{-}17)$$

where M_L is the local magnitude of an earthquake. Equation (3-18) estimates epicentral intensity in a suite of intensity equations adopted by Shebalin *et al.* (1998) while developing their historical catalogue of Bulgaria:

$$I_0 = bM_s - \upsilon \log h + c \quad (3\text{-}18)$$

where b, c and υ are numeric parameters, with their region-dependent values are in Table 3.1.

	B	υ	c
φ ≤ 47°N	1.5	4.0	3.8
φ > 47°N	1.5	3.5	3.6

Table 3.1 Numeric values for parameters of intensity relations from Shebalin *et al*. (1998)

Ground motion models for the FYR of Macedonia cannot be ignored. Even as the most aseismic and smallest country of the three considered, it has still experienced large magnitude events in history (518 AD, May 13th 1995, 6.5 M_s; Ambraseys and Jackson, 1998). Being part of the political triple junction of interest and contributing to its regional tectonics and seismicity, dictates that past modelling of its intensity ground motion also demand attention. Hadzievski (1975) suggests Eq. (3-19) for this country:

$$I_{max} = 1.8M - 4.2 \log h + 3.3 \quad (3\text{-}19)$$

where I_{max} is upper intensity threshold (not epicentral intensity), M_L in Eq. (3-17), M_s in Eq. (3-18) and M in Eq. (3-19) are earthquake magnitudes and h is focal depth of the earthquake in Eq. (3-17) to Eq. (3-19) above.

Equation (3-20), also of Papazachos and Papaioannou (1997), is a linear relation between I_0 and M and resolves situations where focal depth is not known:

$$I_0 = b\,M + a \quad (3\text{-}20)$$

a and b are variables that need determining and are specific to a region, and M is an earthquake's moment magnitude. Equations for Greece, Albania, Yugoslavia, Bulgaria and Turkey are provided. Those of interest here, for Greece and Bulgaria, are Eq. (3-21) and Eq. (3-22) respectively:

$I_0 = 1.43M - 0.93$ Greece (3-21)

$I_0 = 1.43M - 0.15$ Bulgaria (3-22)

These assume geometric spreading and anelastic attenuation from the earthquake focus, and anisotropic radiation at the source.

3.8.1.2 Previous macroseismic intensity seismic hazard studies

A large suite of isoseismal maps for the Balkans and western Turkey for pre-1800 to 1970 is presented in Shebalin *et al.* (1974a), in addition to his record of magnitude seismicity for mainland Europe, with $I_0 > VI$ for 1901 to 1970, $I_0 > VII$ for 1801 to 1900 and $I_0 > VIII$ for before 1800. These isoseismal maps has long been regarded a main source of information for many subsequent studies of Balkan seismic hazard.

Drakopoulos (1976) highlights a need for more knowledge of temporal and spatial distributions of moderate and more frequent earthquakes of Greece and the whole Balkan region, and assesses these characteristics using the maximum intensity-frequency relation for this combined region. Stepp's model of completeness was found to hold for intensity estimates, suggesting a minimum time interval was also required to reach a mean recurrence rate that increased with intensity class. The maximum intensity-frequency and cumulative frequency-magnitude distributions show strong similarity to each other; each possesses area-dependent constants such that $b_M \equiv b_{I_0}$ (the b-value for magnitude and b-value for epicentral intensity respectively), and each can be illustrated by plotting distribution curves of a similar form.

Magnitude data is sparse for all but the most recent 20 to 30 years, and this is given as reason enough not to test for magnitude recurrence rates. Drakopoulos attempts to use maximum intensities to replace magnitude as the earthquake descriptor. Consequently, he finds b_{I_0} to be systematically lower than the equivalent b_M due to the different geologic conditions each are related to. Magnitude [and b_M] relates to physical properties of fracture process within the earth. Intensity is directly related to surface conditions and its response to ground motion. Maximum intensity-frequency distributions of all shocks for both areas of interest do not adhere to the law when $I_0 >$ IX, and so describe similar characteristics as magnitude in the cumulative frequency-magnitude law, by 'tailing-off' at high values.

Many previous authors have had difficulty in finding robust relations between scales of observed intensity and [peak] ground acceleration in the past, due to the former being a descriptive measurement of earthquake severity, and by its nature subjective, whilst ground motion is a recorded value. This problem was first attempted to be resolved by Cancani (1904). Trifunac and Brady (1975) found that peak accelerations and intensity estimates did not correlate well, and exhibited large scatter in the data; a view that is supported by Grünthal (1998). Glavcheva (1990) attempts to find an optimised correlation between these two earthquake characteristics. Seismograph records – specifically maximum amplitude, a_{max}, visible period, T, and duration of the 'intensive' phase τ - were compared against macroseismic intensity estimates for 11 large magnitude events for the time interval 1986 to 1987. Glavcheva found best correlations between macroseismic intensity and peak amplitudes, a_{max}, and good correlations also with vertical and horizontal components of a_{max}.

Papoulia and Stavrakakis (1990) undertake a seismic hazard assessment specifically for the city of Patras using a modified version of the approach of Cornell based on applying a number of intensity ground motion models for this area. Cornell considers seismic sources as either point, linear or areal sources, and seismicity of each source is considered homogenous. Using multiple regression techniques on macroseismic data for three linear and three areal seismic sources, intensity attenuation relations are obtained, given in terms of magnitude and hypocentral distance. Comparison of each to an 'averaged' law derived from them, Papoulia and Stavrakakis conclude that the 'averaged' law returns unrealistic estimates compared with each individual relation, due to a higher degree of uncertainty being introduced, suggesting use of individual local attenuation laws over 'averaged' relations due to increases in uncertainty with the latter forms. This is however contrary to Makropoulos and Burton (1985b), while considering peak ground acceleration instead.

Papazachos (1992) tries to model anisotropic radiation patterns of macroseismic intensities for Greece to enable estimating an 'averaged' attenuation structure for the seismic and predominantly shallow extent of the upper crust of Greece. This modelling relied on observed macroseismic intensities that are reliant upon earthquake source properties such as radiation pattern, size and focal depth, geometrical spreading and anelastic attenuation characteristics. Data from Shebalin *et al.* (1974b), isoseismal maps of the University of Thessaloniki for 1902 to 1981 and reports from the Bulletin of the Seismological Institute of the National Observatory of Athens (BSINOA) are used. Macroseismic intensity conversion equations to convert original estimates provided on other scales (e.g. MSK and MCS (Mercalli-Cancani-Sieberg)) onto the Modified Mercalli (MM) scale are adopted. They found that in general determinations of intensity attenuation co-efficients from an anisotropic spreading model were more reliable than those obtained from an isotropic model.

More objective methods to evaluating isoseismal radii and for developing parameters for an attenuation relation by estimating equivalent radii, D_i, from point intensity data are outlined by Cella *et al.* (1996). Data from 55 earthquakes were classified based on similar attenuation characteristics before an intensity ground motion model of Grandori *et al.* (1987, 1991) was applied to define all parameters for each earthquake. Three key reasons are given for undertaking this work. First, it constituted a contribution to the Italian Macroseismic working Group of the National Project for Seismic Prevention (GNDT). Second, and arguably a debatable point, the authors believe intensity decay to be the most important aspect to seismic hazard assessment, and finally; realisation that the majority of isoseismal maps for any given earthquake are often different due their subjective nature of creation by different workers, providing a range of estimates for the radii of each isoseismal.

Papazachos *et al.* (1997a) reviewed many previous works (for example, Seiberg 1932a, 1932b; Galanopoulos, 1941, 1949, 1950; Papazachos *et al.*, 1982) in addition to isoseismal maps produced by NOA and the Geophysical Laboratory of the University of Thessaloniki. This exercise recognised the necessity to draw up revised synthetic isoseismal maps for 176 historical ($M \geq 5.5$ and $h < 60$ km) events in Greece and its surrounding region, extending north to approximately 46°N. Again, macroseismic scale conversions offered by Shebalin *et al.* (1974b) and methods proposed by Papazachos (1992) to draw synthetic isoseismals are used in compiling their maps.

Finally, Ardeleanu *et al.* (2005) take the catalogue of Shebalin *et al.* (1998) to develop probabilistic seismic hazard maps for Romania based on probability of exceedance of 10% in 50 years (the 475-year return period event) and 10% in 10-years (a 95-year recurrence period event). By applying the ground motion model of Kövesligethy (1907), with a new factor Ω included to account for anomalous deep focus events such as the Vrancea sequence their work attempted to account for effects of crustal zones of seismicity as well as those anomalous sequences at greater depth.

3.8.1.3 Regional intensity ground motion models

Intensity ground motion models attempt to relate physical and observed effects of earthquakes, and are borne out of consolidating initial reporting and observation work ‘in the field’ in the immediate aftermath of an earthquake with post-event mapping activities of an earthquake isoseismals. Models aim to provide links between regional geology and near-surface strata to key earthquake parameters such as magnitude, distance from the earthquake focus (i.e. either epicentral distance or hypocentral distance) and focal depth, if hypocentral distance is to be used, and sometimes inclusion of some function relating to epicentral intensity.

There have been many such studies for this broad region in addition to those discussed earlier that also offer useful intensity-attenuation relations; some are discussed below. A broader selection of those considered most relevant to this work is given in Table 3.2, with a refined selection illustrated in Figure 3.5.

The ground motion model of Papazachos and Papaioannou (1997) will be applied, in conjunction with their epicentral intensity relation for Bulgaria (Eq. 3-22) to assess macroseismic intensity hazard to the region (chapter 5) and earthquake intensity perceptibility hazard (chapter 6). Reasons for selecting the relation of Papazachos and Papaioannou (1997) are two-fold:

- Its use will allow direct comparison to work of Burton *et al.* (2004b) for the high-hazard region of Greece adjacent and to the south of this study area;

- The relation omits any reference to earthquake focal depth; with the catalogue that will be used for the hazard assessment containing a large amount of data from the ISC, who are known to assign approximate depth estimates to events for which focal depth cannot be determined to a high degree of accuracy, it was felt using a relation that did not reference a depth parameter would improve resultant hazard forecasts.

Therefore:

$$I - I_0 = -3.59\log(\Delta + 6) + 3.19 \qquad (3\text{-}23a)$$

becomes,

$$I = 1.43M - 3.59\log(\Delta + 6) + 3.04 \qquad (3\text{-}23b)$$

Ground motion model	Comment	Reference
$I = 1.063 + 1.5222M_s - 1.1021 \text{ Ln } (\Delta^2+h^2)^{1/2} - 0.0043 (\Delta^2+h^2)^{1/2}$	Developed from relation of Musson (2000) and specific to region of the Aegean region south of 43°N. Used to developed perceptibility curves for 14 separate tectonic zones recognised in Holt *et al.* (2000)	Koravos *et al.* (2003)
$I = 1.063 + 1.5222M_s - 1.1021 \text{ Ln } R - 0.0043R$	Developed using database of seismicity for Turkey, but applicable to the broad Aegean region. I = site intensity (Medvedev-Sponheuer-Kárník (MSK) or EMS-98 scale); R = hypocentral distance; M_s = magnitude	Musson (2000)
$I = 1.87 + 1.69M - 3.94\log (D+30)$	Specific to intermediate depth earthquakes in southern Aegean.	Papazachos and Papazachou (1997)
$I = 6.59 + 1.18M_s - 4.50 \log (\Delta+17)$	An 'average' relation developed whilst assessing intensity attenuation characteristics for 19 seismic zones for shallow earthquakes of the southern Balkan region.	
$I_i = 2.42 + 1.69M_s - 4.31 \log (\Delta+30)$ $I_i = 0.78 + 1.69M_s - 3.37 \log (\Delta+30)$ $I_i = -0.09 + 1.69M_s - 2.85 \log (\Delta+30)$	Based upon macroseismic intensity work of Tassos (1984). Relations are specific to the concave, Hellenic Arc and convex directions of the Hellenic Arc (top to bottom)	Papaioannou (1984)
$dI_i = -0.22 + 2.40\text{x}10^{-3}(R_i-h) + 2.85\log(R_i-h)$ $dI_i = 0.27 + 3.6\text{x}10^{-3}(D_i) + 2.43\log(D_i) - 2.64\log(h)$	dI_i = variation in intensity between site in question and epicentral intensity, I_0; D_i = epicentral distance; h = focal depth. Borne out of need for simpler relation of the form $dI = (I_0 - I_i) = b \text{ Log } [(R_i/h)^n \exp(a(R_i-h))]$ (h = focal depth; R_i = focal distance).	Ambraseys (1985)
$I - I_o = -3.227\log\sqrt{1+\frac{\Delta^2}{h^2}} - 0.0033\left(\sqrt{\Delta^2+h^2} - h\right)$ $I - I_0 = -3.59 \text{ Log } (\Delta + 6) + 3.19$	Δ = Epicentral distance (in km), h = Focal depth. (Top) Applicable to a broader Balkan area (Greece, Albania, Yugoslavia, Bulgaria and western Turkey); (Bottom) Relation is specific to the Balkan region	Papazachos and Papaioannou (1997)

Table 3.2 Selected macroseismic intensity ground motion models relevant to the Balkan and Aegean regions; relations given in the table below are illustrated in Figure 3.5

Ground motion model	Comment	Reference
$I_i = bM_s - \upsilon Log\ r_i + c$ $I_0 - I_i = \upsilon - Log\ (r_i/h)$	General equations developed by authors. Values for parameters b, υ and c are determined for regions north and south of 47°N.	Shebalin *et al.* (1998)
$I_{max} - I_i = 4.2\ log\ (R_i/h)$	I_{max} = epicentral intensity, I_0; R_i = radius of isoseismal, i, (in km); h is focal depth, (in km).	Hadzvieski and Pekevski (1975)

Table 3.2 (continued)

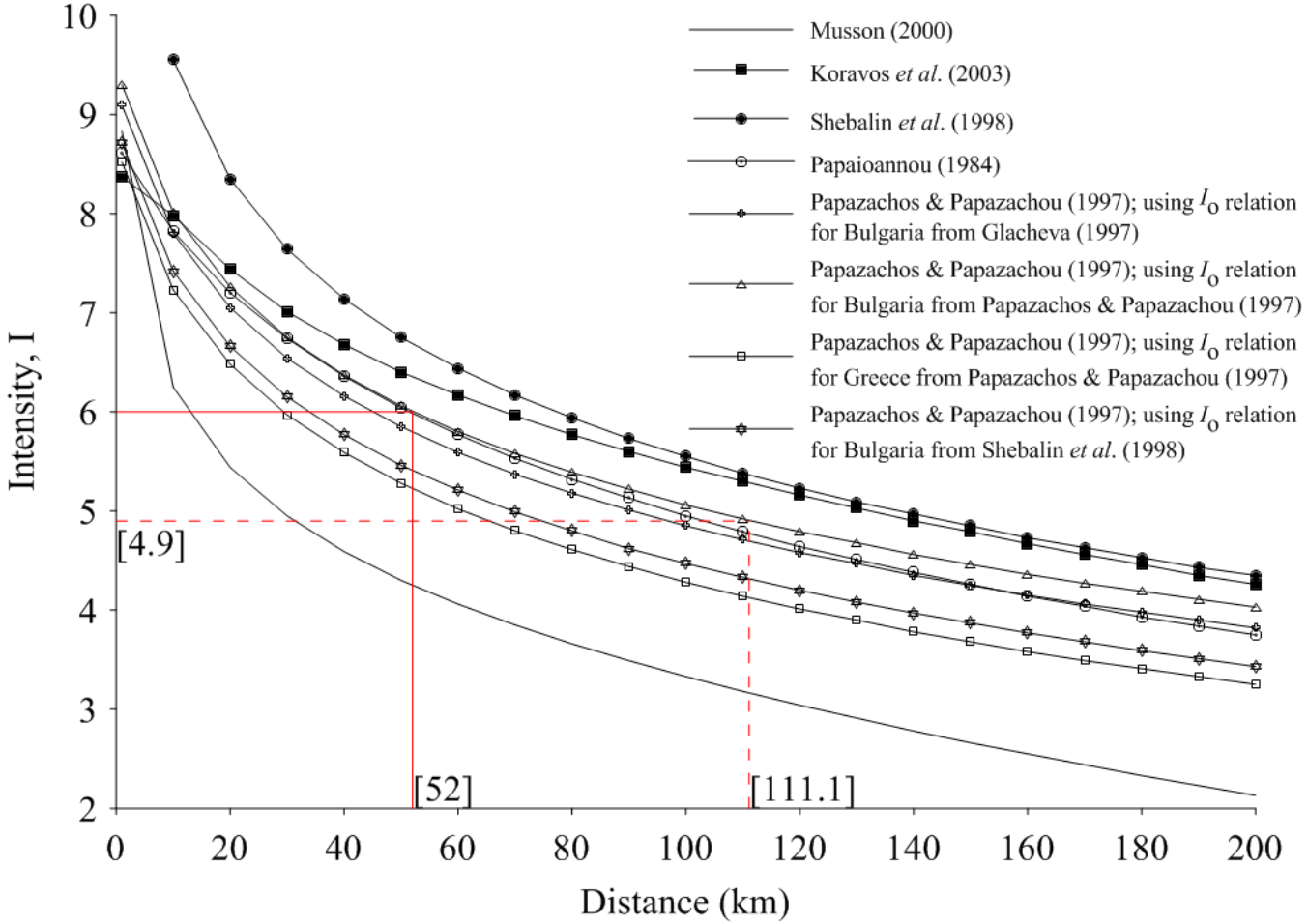

Figure 3.5 Selected macroseismic intensity attenuation curves for the region of interest. All macroseismic intensity models are plotted for a nominal earthquake of magnitude 6.5 M and focal depth h = 10 km; solid red lines illustrate epicentral distance at which intensity VI will be felt, while dashed red lines highlight the intensity felt at 111.1 km (≅ 1° of latitude)

3.8.2 Attenuation of ground acceleration

3.8.2.1 Ground acceleration models – general forms

Understanding a region's peak ground acceleration would ideally be developed from a suitably complete collection of strong motion records, such as the European strong-motion database (http://www.isesd.cv.ic.ac.uk/ESD/frameset.htm). This however is rarely possible due to lack of sufficient quality data for most regions of the world. Relations must be described between known earthquake parameters, such as magnitude, and a description of distance and often an additional element describing the effects of site geology.

A generalised relation, Eq. (3-24), is proposed by Esteva and Rosenblueth (1964) between magnitude, m, and peak ground acceleration, a:

$$a = b_1 e^{b_2 m} e^{-b_3} \tag{3-24}$$

Much of the work that followed this simply presented modifications of this general form of attenuation relation, rather than suggest distinct alternatives. However, Orphal and Lahoud (1974) took an alternative approach to propose the general form to a ground acceleration model, Eq. (3-25):

$$A = \lambda\, 10^{\alpha M} R^{\beta} \tag{3-25}$$

λ, α and β are constants to be determined. This develops from work of Murphy and Lahoud (1969) on peak ground motion derived from nuclear explosions, by consolidating a relation for ground motion with explosion yield, W, and focal distance, R ($A = K\, W^n\, R^m$) with one for relating explosion yield to local magnitude ($M = a + b.\log W$). The functional form of Eq. (3-25) is discussed in Table 3.3.

Joyner and Boore (1981) propose another alternative general solution, Eq. (3-26), to predicting peak ground accelerations, which has been used extensively for reviewing peak acceleration in Europe (for example, in much work of Ambraseys and colleagues). Utilizing a reference to site geology in it, their equation in a general form is:

$$\log(a) = \alpha + \beta M - \log(r) + br + \sigma P \tag{3-26}$$

Ground motion model	Comment	Reference
$a = 6.6x10^{-2}\ 10^{0.40M}\ R^{-1.39}$	R = focal distance; M = local magnitude; a = PGA in g; $\sigma = 1.99$. From a statistical analysis of peak horizontal accelerations from 1971 San Fernando event using data of Hudson (1971)	Orphal and Lahoud (1974)
$a = 2164e^{0.70m}(r+20)^{-1.80}$	a = PGA in cm s^{-2}; m = magnitude; r = hypocentral distance Derived by averaging selected attenuation equations (Donovan, 1973; Orphal and Lahoud, 1974; Esteva, 1974; and Båth, 1975) due to limited number of strong motion records for study region.	Makropoulos (1978), Makropoulos & Burton (1985b)
$Log\ A = 3.78 + 0.39M_s - 2.37log\ (\Delta+30)$	Obtained from 14 [corrected] accelerograms. Extended further in Papaioannou (1986) to incorporate the southern Balkan region	Papaioannou (1984)
(a) $Log\ (a_h) = -1.09 + 0.238M_s - log(r) - 0.00050r + 0.28P$ (b) $Log\ (a_v) = -1.34 + 0.230M_s - log(r) - 0.27P$ (c) $Log\ (a_h) = -0.87 + 0.217M_s - log(r) - 0.00117r + 0.26P$ (d) $Log\ (a_v) = -1.10 + 0.200M_s - log(r) - 0.00015r + 0.26P$	For vertical and horizontal ground accelerations (in g) in Europe. Were generated from a refined subset of 529 triaxial strong motion records obtained for 219 European shallow earthquakes from European Earthquake Strong Motion Database; (a) and (b) do not account for focal depth; (c) and (d) do account for focal depth.	Ambraseys and Bommer (1991)
$log\ \gamma_m = 1.77 + 0.49M - 1.65log\ (\Delta+15)$	γ_m = PGA (cm s^{-2})	Theodulidis (1991)
$ln\ a_g = 3.88 + 1.12M_s - 1.65\ ln(R + 15) + 0.41S + 0.71P$	a_g = PGA (cm s^{-2}); R = epicentral distance (km), S = site effect, (0 at 'alluvium' sites; 1 at 'rock' sites); P is equal to 0 for 50-percentile values, and 1 for 84-percentile values. Obtained using 105 horizontal components of data for 36 events in Greece with magnitude $4.5 \le M \le 7.0$, and 16 horizontal components from four shallow subduction earthquakes with magnitude $7.2 \le M \le 7.5$ in Alaska and Japan.	Theodulidis & Papazachos (1992)
$a = exp\ (1.163M_s + 2.222)\ R^{-1.43}$	R = average hypocentral distance; $\sigma = 46.2$; obtained by converting intensity values of the Kövesligethy relation for selected historical events into PGA estimates, using isoseismal maps of Shebalin *et al.* (1974) and intensity-acceleration relations for events of Voutkov *et al.* (1986). Is an isotropic attenuation relation since no acceleration data for that region was available	Orozova-Staniskova and Slejko (1994)

Table 3.3 Selected ground acceleration models relevant to the Balkan and Aegean regions; relations given in the table below are illustrated Figure 3.6

Ground motion model	Comment	Reference
$a = \exp(1.163M_s + 2.222)\, R^{-1.43}$	R = average hypocentral distance; $\sigma = 46.2$; obtained by converting intensity values of the Kövesligethy for selected historical events into PGA estimates, making use of isoseismal maps of Shebalin *et al.* (1974a) and intensity-acceleration relations for worldwide earthquakes of Voutkov *et al.* (1986). Is an isotropic relation since no acceleration data for the region could be obtained	Orozova-Staniskova and Slejko (1994)
$\text{Log}(a_h) = -1.429 + 0.245M_s - 0.00103r - 0.786\log(r) + 0.241P$	$4.0 \le M_s \le 7.3$, without depth control; $r^2 = d^2 + h_0^2$, $h_0 = 2.66$	Ambraseys (1995)
$\text{Log}(a_h) = -1.242 + 0.238M_s - 0.00005r - 0.907\log(r) + 0.240P$	$5.0 \le M_s \le 7.3$, without depth control; $r^2 = d^2 + h_0^2$, $h_0 = 4.04$	
$\text{Log}(a_h) = -1.060 + 0.245M_s - 0.00045r - 1.016\log(r) + 0.254P$	$4.0 \le M_s \le 7.3$, with depth control; $r^2 = d^2 + h^2$ (r = slant distance)	Ambraseys (1995)
$\text{Log}(a_h) = -0.895 + 0.215M_s - 0.00011r - 1.070\log(r) + 0.247P$	$5.0 \le M_s \le 7.3$, with depth control; $r^2 = d^2 + h^2$ (r = slant distance)	
$\log(a_h) = -1.05 + 0.245M_s - 0.001r - 0.786\log(r) + E\log(V_s30) + 0.23P$	a_h = peak acceleration in g; P = 0 at 50-percentiles, P = 1 at 84-percentiles; r = hypocentral distance (in km). Covers region from Italy to Greece. Component E $\log(V_s30)$ defines a site-dependent magnification co-efficient dependent upon shear-wave velocities experienced within the top 30 metres of surface strata. Used only 14 (of 268) strong motion records with source distances > 40 km.	Ambraseys (1997)
$\text{Ln } A = 5.571 + 0.937M_s - 1.256\ln R - 0.0069h$	R = hypocentral distance (in km); A= PGA (in cm s^{-2}). Derived from three earthquakes of the Vrancea region (southern Romania).	Lungu *et al.* (1997)
$\text{Ln } A = 6.470 + 0.923M_s - 1.403\ln R - 0.0007h$		
$\text{Ln } A = 8.136 + 0.876M_s - 1.657\ln R - 0.0076h$		
$\text{Ln } A = 4.150 + 0.913M_s - 0.962\ln R - 0.006h$		
(a) $\text{Ln } A = -1.15 + 0.923M_s - 1.403\ln R - 0.0004R$	A =PGA (in g); R = anelastic attenuation parameter. Specific to north Balkan region. Relate to directional affects of attenuation from (a) Bucharest, (b) Cernavoda and (c) Moldova.	Musson (1999)

Table 3.3 (continued)

Ground motion model	Comment	Reference
(b) Ln A = 0.33 + 0.876M_s – 1.657ln R – 0.0004R	A =PGA (in g); R = anelastic attenuation parameter. These models are specific to the [considered] anomalous Vrancea intermediate-depth seismic sequence, whose earthquakes of 1977 were significantly deeper (80-90 km) than the rest of the immediate surrounding region. Relate to directional affects of attenuation from (a) Bucharest, (b) Cernavoda and (c) Moldova.	
(c) Ln A = -3.1 + 0.913M_s – 0.962ln R	The relatively high forecast PGAs at greater distances from the source compared with other models results from; i) lack of large magnitude earthquakes to model from; ii) large variation in rates of attenuation in some azimuths; iii) inability to include terms for anelastic attenuation in these models. Equations are considered incompatible at short distances as each were regressed individually.	Musson (1999) (continued)
ln a_g = 4.37 + 1.02M_s – 1.65ln(Δ + 15) + 0.31S + 0.66P*	Δ = epicentral distance (in km), S = site affect (taking 0 for 'alluvium' sites, and 1 at 'rock' sites); P* accounts for scatter of data about its best fit line (P* = 0 for 50-percentile values and P* = 1 for 84-percentile values). Derived from shallow earthquakes in and the broad Aegean region	Koravos *et al.* (2003)
ln (a_h) = 4.09 + 1.12M_s – 1.65 ln(R+15)	a_h = PGA (in cm s^{-2}); R = epicentral distance; M_s = earthquake magnitude. Developed from work of Ambraseys (1995, 1997) after advice from Theodulidis, by taking S = 0.5 and P = 0 (i.e. a stiff soil, average attenuation relation) to better simulate near-surface geology of the Aegean region	Burton *et al.* (2003)

Table 3.3 (continued)

a is peak ground acceleration in g, M is magnitude and $r = (d^2 + h_0^2)^{1/2}$, where d is the shortest distance from station to the surface projection of the fault rupture (km) and h_0 is a constant to be determined from α, β and σ. σ is the standard deviation of log(a) and P is a constant that alters depending on whether 50-percentiles or 84-percentiles are required. Equation (3-26) has been developed further by Ambraseys and Bommer (1991) in their work on Europe-wide ground accelerations (Table 3.3).

3.8.2.2 Regional PGA ground motion models

An extensive review of strong ground motion relations and past studies on a global level is given in Douglas (2003), citing that little agreement has been reached concerning 'best practice' procedures in this particular area of research, due to scarcity and variability of ground motion data on a regional level. Douglas makes effort to review criteria employed to establish and refine ground acceleration laws. For example, such criteria as a) source to site distance, b) minimum magnitude, c) estimated intensity experienced at recording site, d) minimum peak ground acceleration (PGA), e) time-history quality, f) distribution of acceleration records used, g) event depth and, h) site conditions have been employed by past workers in isolation or in unison to achieve estimates of regional PGA estimates. Key relations are listed below, while Table 3.3 briefly discusses a wider selection of additional ground motion models relevant to this region, while a number of historical ground acceleration models considered are also illustrated in Figure 3.6. Relations described herein all refer to horizontal ground acceleration, although a few may also be applied to the vertical component of ground acceleration.

Orphal and Lahoud (1974) undertake a statistical analysis of peak horizontal accelerations from the 1971 San Fernando earthquake, and a number of other events of the region. Using a good set of data from Hudson (1971) and assuming that peak accelerations observed here were regionally typical, Eq. (3-27) was derived:

$$a = 6.6\text{x}10^{-2}\, 10^{0.40M}\, R^{-1.39} \qquad \sigma = 1.99 \qquad (3\text{-}27)$$

where R is the focal distance, M is local magnitude and a is peak ground acceleration in g's.

Makropoulos (1978) and Makropoulos and Burton (1985b) took a rarely adopted approach to develop a peak ground acceleration model by averaging a number of past equations (e.g. Donovan, 1973; Orphal and Lahoud, 1974; Esteva, 1974; Båth, 1975) to arrive at Eq. (3-28):

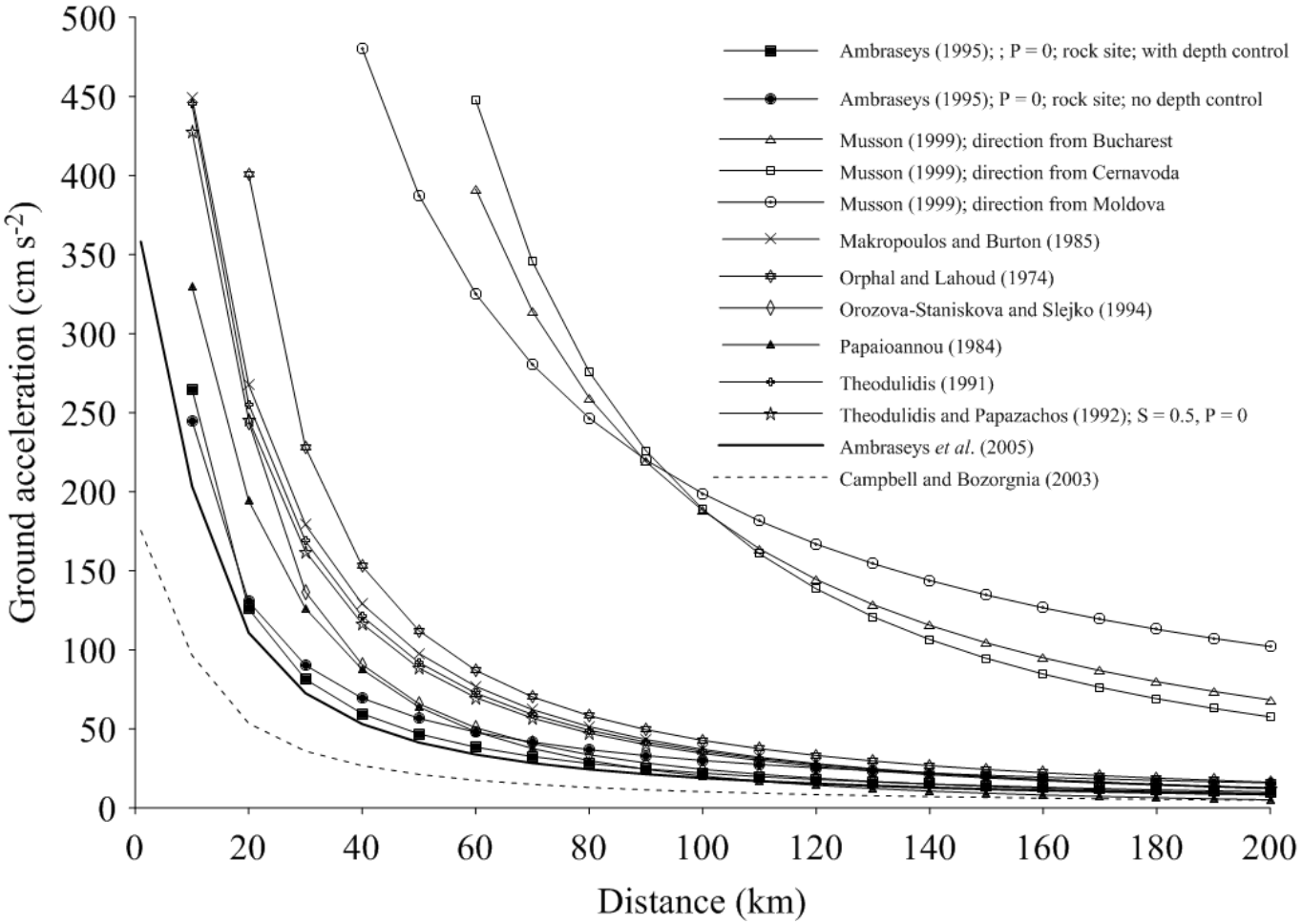

Figure 3.6 Selected ground acceleration curves for the region of interest. All ground acceleration models are plotted for a nominal earthquake of magnitude 6.5 M and focal depth h = 10 km, with accelerations in cm s^{-2}. High PGAs for models of Musson (1999) result from; i) lack of large magnitude earthquakes to model from; ii) large variation in rates of attenuation in some azimuths; iii) inability to include terms for anelastic attenuation in these models. Equations are considered incompatible at short distances as each were regressed individually

$$a = 2164.e^{0.70m}(r + 20)^{-1.80} \quad (3\text{-}28)$$

a is peak ground acceleration in cm s^{-2}, m is earthquake magnitude, and r is hypocentral distance. The method of 'averaging' a number of regional ground motion models for ground acceleration was preferred due to a limited number of strong motion records for this region at the time. An issue that is still a problem for many regions of the world today. The resultant equation was consistent with the existing observations of ground acceleration in Greece.

To provide direct comparability and geographic extension to work of Burton *et al.* (2003, 2004a and 2004b) the following horizontal ground acceleration ground motion models are selected to apply in the ensuing seismic hazard study. For the magnitude interval $5.0 \leq M_s \leq 7.3$, with depth control (Ambraseys, 1995),

$$\log (a_h) = -0.895 + 0.215M_s - 0.00011r - 1.070 \log(r) + 0.247P \quad (3\text{-}29)$$

and also (Theodulidis and Papazachos, 1992),

$$\ln (a_h) = 4.09 + 1.12 M_s - 1.65 \ln(R + 15) \quad \text{with } P = 0, S = 0.5 \quad (3\text{-}30)$$

Although some consider Bulgaria and the immediate surrounding region to be a region of moderate seismicity, the following facts suggest use of relations describing earthquake data with higher magnitudes as a suitable solution for the purpose of this new hazard assessment:

1. Large and damaging earthquakes (≥7.0 M) have occurred in recent history;

2. For the time interval of the catalogue (1900 to 2004), 82 of the 105 (~78%) annual extremes exceed (homogenized) 5.0 M_s suggests use of relations relevant to a higher magnitude range over alternative models representing lower magnitude ranges, and;

3. The new analysis will make use of extreme values statistics to assess the region's seismic hazard.

3.8.2.3 More recent peak ground acceleration models

Although peak acceleration ground motion models selected in section 3.8.2.2 provide compatibility with previous and recent seismic hazard assessments for neighbouring and overlapping regions, they are noticeably old and have since been superseded by more recent ground motion models that have been proposed. Many of these are borne out of modern strong [ground] motion and associated earthquake, station and waveform-parameters databases that are developed to better represent a given area's seismic history. These allow ever more uniform ground motion models to be developed, incorporating specific criteria to refine them with respect to source-to-site distances (e.g. hypocentral, epicentral, shortest distance to rupture plain), soil type conditions or faulting mechanisms (e.g. rock, stiff soil, soil, alluvium) or magnitude scale adopted.

Two newer ground acceleration models exist that are currently very relevant to Bulgaria and the Balkans (Schmitt; pers. comm.). These are given below, with their defining characteristics in Table 3.4. Popular in current Balkans research is Ambraseys *et al*. (2005), whose functional form is:

$$\text{Log } y = a_1 + s_2 M_w + (a_3 + a_4 M_w) \log (d^2 + a_5^2)^{1/2} + a_6 S_S + a_7 S_A + a_8 F_N + a_9 F_T + A_{10} F_O,$$

a_1 to a_{10} are constants dependent upon whether PGA or spectral acceleration is considered. M_w is moment magnitude, S_S and S_A are soil type variables and F_N, F_T and F_O are fault mechanism variables.

This ground motion model is extremely flexible. It allows the user to consider causative faulting mechanism, soil type and source-to-site distance, allowing an alternative source-to-site option if the ideal solution (Joyner-Boore distance) is not possible. It is also designed for seismicity with magnitudes ≥5.0 M_s originating at shallow crustal focal depth and was developed from the European Strong Motion Database, of which sixty-two per cent of its strong-motion records were recorded in Europe (Italy, Turkey, Greece and Iceland), although none were in Bulgaria. A nominal number of strong-motion records were also recorded in other European countries.

The second model is Campbell and Bozorgnia (2003). This more complex ground motion model accommodates more and different soil types and faulting mechanisms and is most relevant to shallow crustal earthquakes – of most interest to this work. It is more limited than Ambraseys *et al*. (2005) in that it is holds over shorter source-to-site distances (<60 km). It is also developed from fewer recorded ground motions that are more geographically disparate (i.e. predominantly the continental United States) compared with the European ones adopted for Ambraseys *et al*. (2005), and the dominant faulting mechanisms for earthquakes in the dataset are thrust and strike-slip.

Ground motion model	Underlying database	Magnitude	Source-to-site distance type	source-to-site distance of... (km)	Soil type factor	Faulting mechanism factor
Ambraseys *et al*. (2005)	Europe and Middle East (ESM Database)	≥ 5.0 M_w	Joyner-Boore[1]	<100	soft soil; stiff soil	normal; odd; thrust
Campbell and Bozorgnia (2003)	Worldwide (mainly California)	$4.7 \leq M_w \leq 7.7$	Shortest distance to rupture/seismogenic source	<60	firm soil; very firm soil; soft rock; firm rock; generic soil; generic rock	strike-slip/normal; reverse; thrust; reverse or thrust

[1] Refer Joyner and Boore (1981); where the location of the fault is unknown, it is acceptable to adopt the epicentral distance instead

Table 3.4 Alternative new peak acceleration ground motion models for Bulgaria and the Balkans

Campbell and Bozorgnia's model is generalised as:

$$\ln Y = c_1 + f_1(M_w) + c_4 \ln [f_2(M_w, r_{seis}, S)]^{1/2} + f_2(F) + f_4(S) + f_5(HW, F, M_w, r_{seis}) + \varepsilon,$$

Details of the component parameters are fully explained in the associated text. Both Ambraseys *et al*. (2005) and Campbell and Bozorgnia (2003) are also illustrated in Figure 3.6 alongside the older ground acceleration models.

Due to the flexible nature of both Ambraseys *et al*. (2005) and Campbell and Bozorgnia (2003), quite strong generalisations are required to accommodate them in this work. Ambraseys *et al*. (2005) is refined in Figure 3.6 to consider stiff soil site conditions and earthquakes from normal faulting mechanisms (causative fault information is not available in the adopted catalogue; chapter 4). These changes align soil conditions with Theodulidis and Papazachos (1992) and also reflect the Commission for the Geological Map of the World (CGMW) that the majority of faulting in the Balkan and Aegean areas around southwest Bulgaria is predominantly normal faulting in character (also see Dimitrov and Ruegg, 1994; Tzankov *et al.*, 1996; Van Eck and Stoyanov, 1996; Kotzev *et al.*, 2001, 2006; Goldsworthy *et al.*, 2002; Vanneste *et al.*, 2006; Papadimitriou *et al.*, 2007 as well as a number of historical studies relating to specific historical events or seismic sequences).

Further, Ambraseys and colleagues selected a range of data representing faulting mechanisms to derive their ground motion model. Thirty two per cent of their subset (191 of 595 earthquakes) occurred on normal faults, and was the largest proportion for an individual faulting mechanism. Forty per cent of the selected data represents stiff soil local site conditions; again, the largest proportion for a single site condition (also considered are very soft soil; soft soil; rock). Accepting these generalisations sets Ambraseys *et al.*'s relation to:

$$\log(y) = 2.522 - 0.142M_w + (-3.184 + 0.314M_w) \log(d^2+7.6^2)^{1/2} + 0.134$$

Campbell and Bozorgnia's model can be simplified to the following, if one generalises it for firm soil (note: the author's do not acknowledge 'stiff soil' as a possible soil type, as do the models of Theodulidis and Papazachos and Ambraseys. Instead they opt for firm or very firm soil, soft or firm rock as available options), and normal faulting mechanisms, and using epicentral distance as the source-to-site distance (r_{seis}).

$$\ln Y = -4.033 + 0.812M_w + 0.036(8.5 - M_w)^2 - 1.061 \times \ln[r_{seis}^2+0.041^2 \times \exp([0.766M_w + 0.034(8.5-M_w)^2])^2]^{0.5}) + \varepsilon,$$

The model of Ambraseys *et al*. (2005) is currently favoured for estimating Bulgarian peak ground accelerations over Campbell and Bozorgnia (2003) since the latter requires knowledge of complex faulting characteristics such as hanging wall effects. Knowledge of this characteristic is difficult to ascertain for faults in the southeast European region (Schmitt; pers. comm.). Ambraseys *et al*. (2005) will therefore also be taken forward to consider with respect to peak ground acceleration hazard against the older models selected in section 3.8.2.2.

What is immediately apparent from Figure 3.6 is that both newer ground motion models undercut all other historical models. This may simply be due to the over-zealous simplification of these models to accommodate them in this work, the underlying ground motion datasets used to initially develop them or adopting a single nominal magnitude for illustration purposes.

3.8.2.4 Comparison of peak ground acceleration models

All models use the surface-wave magnitude except for Ambraseys *et al.* (2005) which adopts the moment magnitude. However, the agreement between the M_w and M_s magnitude scales is generally very close, and a number of previous studies suggest the one-to-one relation of $M_s = M_w$ holds for some areas of the Balkans. For example, Grünthal and Wahlström (2003) and Bungum *et al.* (2003) find the equality $M_w = M_s$ to hold for central and northern Europe. Oncescu *et al.* (1999) also adopt this equality. Kanamori (1977, 1983) and Wells and Coppersmith (1994) note these magnitude scales to be approximately equivalent between $5.0 \rightarrow 7.5$ and $5.7 \rightarrow 8.0$ respectively. These magnitude ranges are relevant to an extreme values analysis that: 1) spans a high hazard region subject to large earthquakes of comparable magnitudes; 2) adopts cut-off magnitude thresholds above 5.0 M_s for both regions considered; 3) uses the newer model of Ambraseys *et al.* (2005) due to its applicability for magnitudes $M_w \geq 5.0$.

Variability in peak ground accelerations forecast for specimen magnitudes of 5.0 M, 6.0 M and 7.0 M is illustrated in Figure 3.7 for the three models of Theodulidis and Papazachos (1992), Ambraseys (1995) and Ambraseys *et al*. (2005), and their underlying characteristics are outlined in Table 3.5. What is most apparent from Figure 3.7 is the acceleration model predicting the highest or lowest ground motions is dependent upon magnitude and source-to-site distance. Although Ambraseys *et al*. (2005) under-cuts the other laws for a 6.5 M earthquake (Figure 3.6), and indeed a 6.0 M event (Figure 3.7(b)), lower magnitudes estimate this newer law to produce higher ground motions than Theodulidis and Papazachos (1992; Figure 3.7(a)).

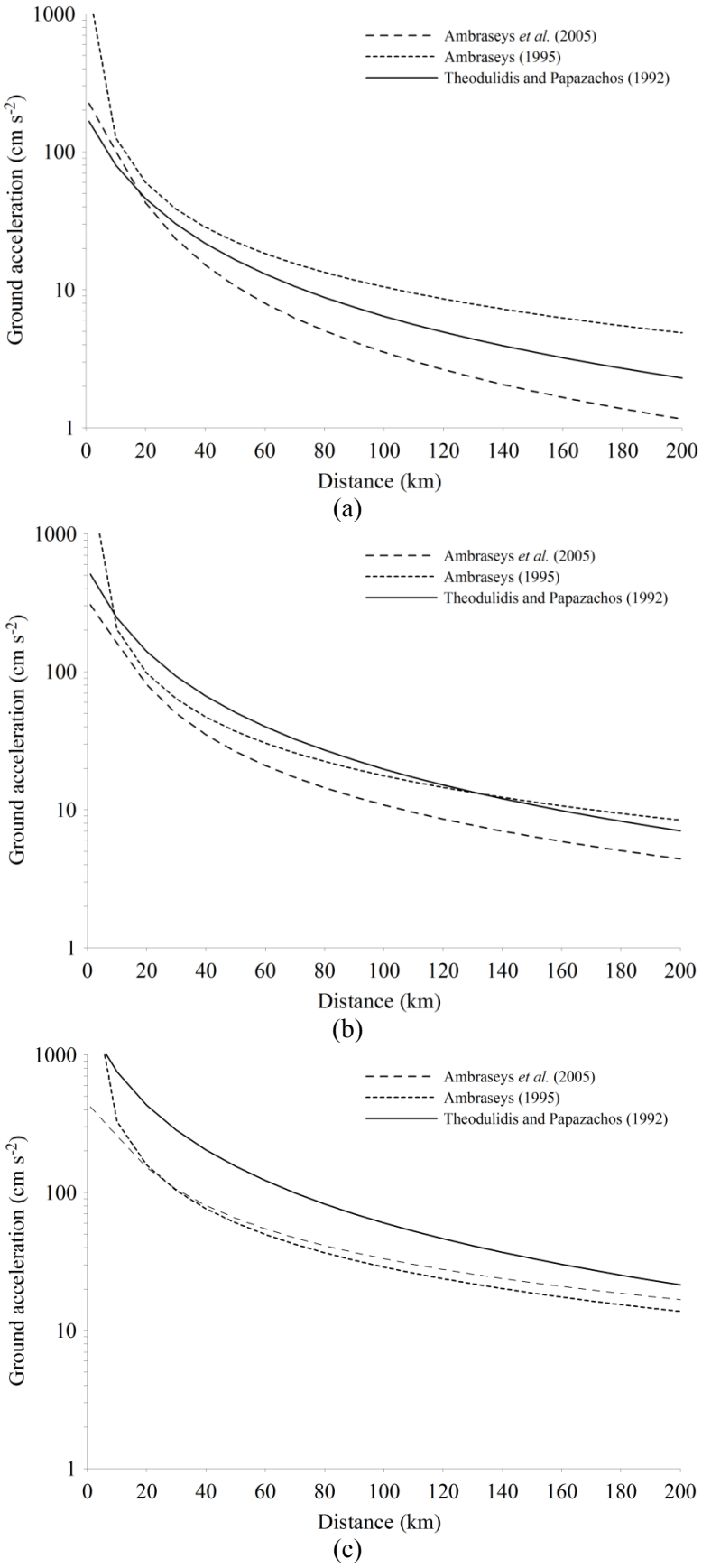

Figure 3.7 Variability in peak ground accelerations for *scenario* earthquakes of magnitude (a) 5.0 M, (b) 6.0 M and (c) 7.0 M for a nominal focal depth of 10 km

Source	Site conditions	Depth control	Depth function	Distance function	Magnitude scale	Magnitude range	Percentile	Faulting mechanism modelled for
Theodulidis and Papazachos (1992)	Stiff soil	No	No	Epicentral	Surface-wave	Unspecified[1]	50th	n/a
Ambraseys (1995)	No	Yes	Focal	Hypocentral	Surface-wave	$5.0 \leq M_s \leq 7.3$	50th	n/a
Ambraseys *et al.* (2005)	Stiff soil	No	Focal	Epicentral[2]	Moment-wave	Unspecified[3]	n/a	Normal[4]

[1] Model was developed from data of $4.5 \leq M_s \leq 7.0$; [2] Simplification made to relation as causative fault information not available in adopted earthquake database; [3] Model was were developed from data of $M_w \geq 5.0$; [4] Model is aimed to be flexible with respect to faulting mechanism of each individual earthquake in the adopted catalogue. However, as this information is not known, it was simplified to reflect seismicity deriving from Normal faults

Table 3.5 Summary of adopted peak acceleration ground motion models

Ground motion model	Comment	Reference
$\ln v_g = -0.18 + 1.29M_s - 1.62\ln(\Delta + 10) + 0.22S + 0.73P^*$	a_v = PGV; Δ = epicentral distance (in km), S = site affect (taking 0 for 'alluvium' sites, 0.5 for 'stiff soil' sites 1 at 'rock' sites); P* accounts for scatter of data about its best fit line (P* = 0 for 50-percentile values and P* = 1 for 84-percentile values).	Koravos *et al.* (2003)
$v = 7.26 * 10^{-1}\ 10^{0.52M}\ R^{-1.34}$	R = focal distance; M = local magnitude; v = PGV (in cm s^{-1}); σ = 1.89. Used insufficient data being available to scale relations. Made assumption that assumption: that peak velocities [and for that matter displacements] attenuate over distance in an identical fashion to those seen for nuclear explosions (Wiggins, 1964; Murphy and Lahoud, 1969).	Orphal and Lahoud (1974)
$\log \upsilon_m = -0.39 + 0.61M - 1.62\log(\Delta+10)$	υ_m = PGV; Δ = epicentral distance; M = magnitude. Derived for Greece	Theodulidis (1991)
$\ln v_g = -0.79 + 1.41M_s - 1.62\ln(R + 10) - 0.22S + 0.80P$		Theodulidis and Papazachos (1992)
$\ln v_g = -3.02 + 0.79I_{MM} + 0.04S + 0.70P$		

Table 3.6 Selected ground velocity models relevant to the Balkan and Aegean regions; relations given in the table below are illustrated in Figure 3.8

These models swap forecasting lowest ground motions at approximately 20 km source-to-site distance for a 5.0 M event. Also noticeable is that for the three magnitudes considered in these illustrations, Ambraseys *et al*. (2005) and Theodulidis and Papazachos (1992) largely decay at similar rates, and exhibit the largest variability in predicted ground acceleration with increasing magnitude. Ambraseys (1995) exhibits far greater decay in the very near-field (≤20 km) and also the smallest change in estimated PGA with increasing magnitude.

In the near-field, Ambraseys (1995) estimates far higher hazard than the other two models for moderate earthquakes. The two models that predict for stiff soil conditions are nearly identical, and both approximately a factor of five less than Ambraseys (1995). This pattern is very similar in the far-field. Ambraseys (1995) continues to give most importance to of the three models considered at a magnitude of 5.0 M, and still approximately five times that of Ambraseys *et al.* (2005).

Conversely, Ambraseys (1995) gives least importance to large magnitude (7.0 M) earthquakes in the far field, although the difference from the other models is far less than for smaller magnitude earthquakes. Ambraseys *et al.* (2005) forecasts significantly lower hazard of the three models in the near-field (<20 km), but models a rate of ground motion decay comparable to that predicted by Theodulidis and Papazachos (1992).

These observations suggest that in sub regions dominated by larger magnitude earthquakes, such as southwest Bulgaria, the north Aegean, northern Greece and eastern Turkey they will be forecast significantly lower estimates for ground acceleration using Ambraseys *et al*. (2005) than the earlier variant from Ambraseys and Theodulidis and Papazachos.

The strong similarity between Theodulidis and Papazachos (1992) and Ambraseys *et al*. (2005) in terms of both ground motion decay rates and estimated ground motions in the near-field and far-field is likely due to both being simplified to model stiff soil site conditions, and the underlying strong motion data being relatively similar (Theodulidis and Papazachos use 105 horizontal components from 36 shallow Greek earthquakes between $4.5 \leq M_s \leq 7.0$, while Ambraseys *et al*. use 595 European strong motion records).

3.8.3 Attenuation of ground velocity

3.8.3.1 Regional PGV ground motion models

Attenuation of peak ground velocity (PGV) is perhaps the least explored aspect of the three ground motion characteristics of earthquake hazard in the Balkan region. This is reflected in the limited number of ground velocity models listed in Table 3.6 and illustrated in Figure 3.8.

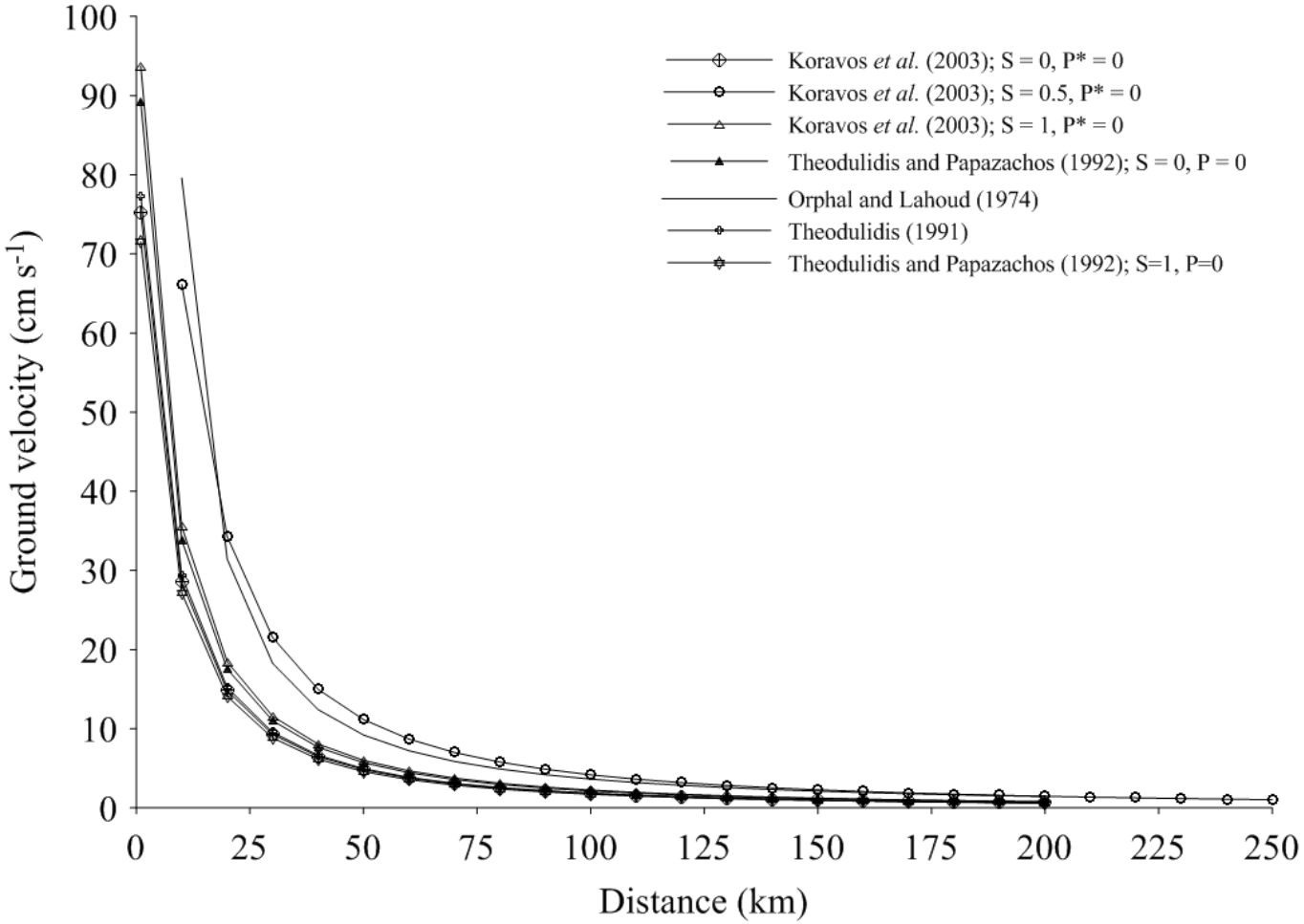

Figure 3.8 Selected ground velocity curves for the region of interest. All ground velocity models are plotted for a nominal earthquake of magnitude 6.5 M and focal depth h = 10 km, with velocities in cm s^{-1}

The model of Theodulidis and Papazachos (1992), Eq. (3-31) is selected to assess ground velocity hazard. As no velocity ground motion exists specifically for Bulgaria or the immediate surrounding region, it is entirely appropriate to apply one for the neighbouring region of Greece.

$$\ln v_g = -0.79 + 1.41M_s - 1.62\ln(R + 10) - 0.22S + 0.80P \quad (3\text{-}31)$$

3.9 Techniques to seismic hazard analysis

Typically, a seismic hazard analysis can be described as either probabilistic or deterministic in nature, although a combination of the two may be applied where deemed necessary or beneficial. Many of the individual hazard analyses described in this chapter are probabilistic in nature, and in being so have made choices to apply methods described by Cornell (1968).

Cornell's approach is a much-advocated method to review a location's seismic hazard that was developed after realising there is a need to determine and account for a range of additional factors that can be incorporated into assessing earthquake hazard. For example, Cornell realises a need to allow for source and site geology, historical data and the geographic relation between earthquake source and the particular site in question, and not just account for the frequency and occurrence of the earthquake. Solutions were determined for scenarios involving hypothetical point, line and areal seismic sources and the site under review. The main focus of this work was to develop relations between a specified ground motion variate, such as intensity, peak ground velocity, peak ground acceleration and average return periods at a site.

Cornell's method can be considered a zoned hazard analysis technique. That is, earthquake epicentres [hypocentres] are grouped together and constrained based on geographic and geologic beliefs and spatial patterns. It can also be adapted and altered as new information on a *scenario* is obtained, or to incorporate alternative assumptions (e.g. changes in activity rates, variation in attenuation characteristics of a region, magnitude distribution in terms of time or size etc.).

The alternative solution to zoned hazard analyses is a zone-free analysis; this will be the technique applied in this study. Zone-free hazard analyses rely on grouping earthquakes based on proximity to a point of interest and filtering by any number of earthquake descriptors (e.g. depth, magnitude, event time). Typically epicentres [hypocentres] are grouped into circular or rectangular cells of a known dimension. Cell size considered will likely vary depending upon the earthquake descriptor being considered. Magnitude recurrence hazard is specific to a point, whereas ground motions can have influence at several hundred kilometre's distance from a site.

The difference between a zoned and zone-free hazard analysis is illustrated in Figure 3.9(a) and (b). A zone-free hazard analysis has advantage over a zoned version as it does not require any source characterisation (e.g. determining fault or seismic source dimensions) prior to its application, so may be more appropriate when information on seismicity is limited.

3.10 Summary

This chapter reviews previous seismic hazard assessments that concentrate upon macroseismic intensity, ground acceleration and ground velocity for the broad region of the Balkans and the Aegean. From these studies, it has been possible to extend discussion onto specific ground motion models for these three earthquake descriptors. It has then been possible to select suitable ground motion models based upon past uses, limitations and the geographic region to which they are most relevant, to take forward into an updated assessment of seismic hazard for Bulgaria. The selected ground motion models are outlined below. These will be used to revise seismic hazard by Gumbel's extreme values theory in chapter 5.

The single ground acceleration model of Theodulidis and Papazachos (1992; Eq. (3-30); $TP92_A$) is taken forward as the primary model for reviewing peak ground acceleration (PGA) seismic hazard. However, the two alternative models of Ambraseys (1995; Eq. (3-29); AM95_WDC) with depth control and Ambraseys *et al*. (2005; AM05) will also be adopted in a more limited nature to consider ground acceleration hazard at site-specific levels only.

Concerns have been documented (e.g. Burton *et al.*, 2003) that ground accelerations estimated using the model of Theodulidis and Papazachos (1992) set up for a 'rock' soil type may be biased resulting from an initial wrong characterization of the prevailing soil type of the region. This could result in over-estimation of peak ground accelerations in the near-field (Figure 3.6). This led Burton *et al.* (2003) to adopt a 'stiff soil' set-up to counter this affect (such that $S = 0.5$). Throughout this work, a conscious effort will be made to provide as much compatibility with Burton *et al.* (2003, 2004b) in terms of developing the earthquake catalogue, ground motion models adopted and geographic extent considered. Consequently, even though using Theodulidis and Papazachos (1992) has caused concern in previous works, it was felt achieving strong compatibility between these seismic hazard assessments and the ensuing benefits gained outweighed any potential advantages gained and inconsistencies introduced from using an alternative and newer ground acceleration relation.

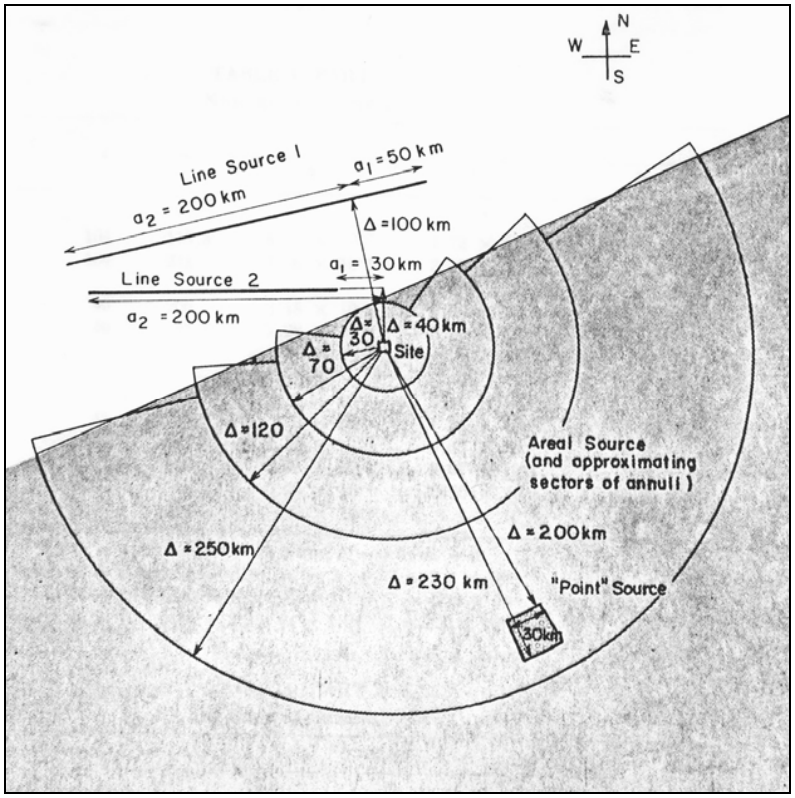

(a)

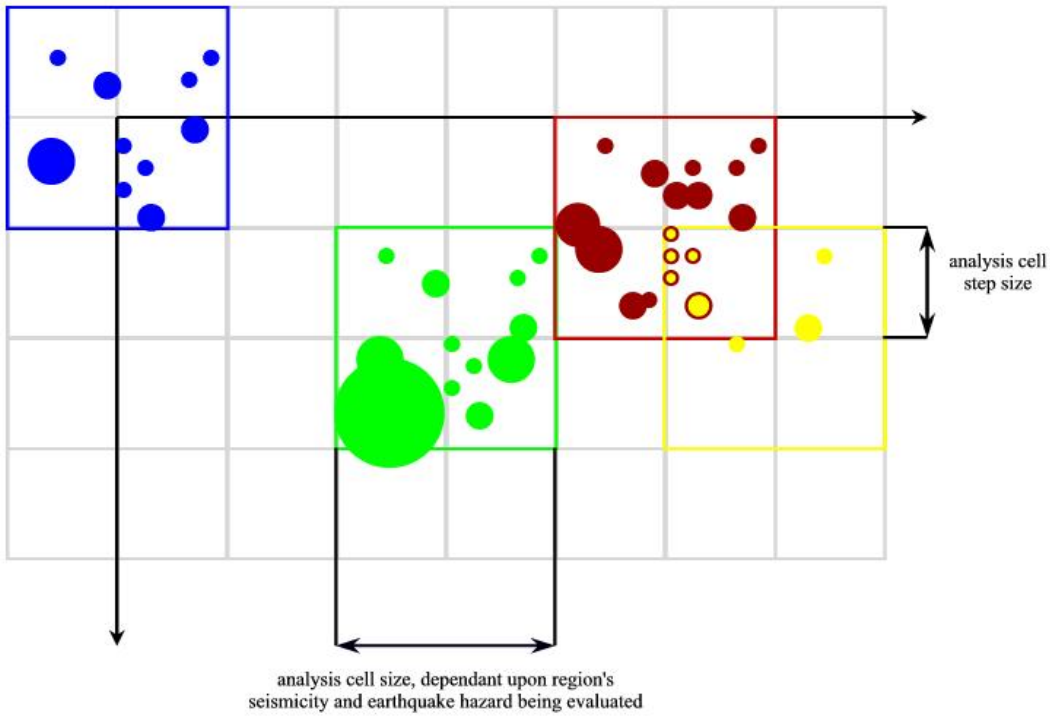

(b)

Figure 3.9 Techniques of (a) a zoned seismic hazard analysis (after Cornell, 1968), and (b) a zone-free seismic hazard analysis

Due to the age of the two lead peak ground acceleration models mentioned above, the newer model of Ambraseys *et al*. (2005) will also be considered at points alongside to allow comparability between ground motion models of different times and with different means to their development.

Equation (3-31) of Theodulidis and Papazachos (1992) will be taken forward for assessing peak ground velocity seismic hazard in terms of estimates of peak ground velocities (PGV).

Equation (3-23b), an aggregation of epicentral intensity and intensity relations from Papazachos and Papaioannou (1997), will be taken forward to assess intensity-based seismic hazard in chapter 5. It has been selected to provide direct comparison with work of Burton *et al.* (2004b), differing only in the epicentral intensity relation used with it. Intensity, PGA and PGV hazard will be forecast at a regional, localised (southwest) and point (city) level.

Chapter 6 will continue the assessment of seismic hazard by applying principles of earthquake perceptibility and integrated perceptibility for acceleration and velocity ground motion, in addition to macroseismic intensity as described above. Each will be assessed for a) the catalogued region and, b) the southwest border region respectively, with results for both areas contoured to produce hazard maps suitable for ascertaining the seismic hazard to these areas. These will then be supplemented with a similar analysis for selected urban centres selected in the full-catalogued region, with each representing different levels of seismicity across the full region of interest. Output for point locations will be in the form of peak perceptibility and integrated perceptibility curves for each ground motion model adopted for intensity, ground acceleration and ground velocity, which will then provide estimates for the most perceptible earthquakes at selected levels of ground motions, and their associated probabilities.

Chapter 6 will develop the hazard assessment further by applying cumulative strain energy techniques to obtain extreme magnitude estimates consistent with finite waiting times, and are directly comparable to theoretically infinite return periods of Gumbel's third asymptotic extreme values distribution.

Chapter 4 : An earthquake catalogue for Bulgaria and the broader Balkan extent

4.1 Introduction

Shebalin *et al*. (1998) mention that the "*…territory of Europe as a whole is not covered by a system of homogenous earthquake catalogues*". This is also supported by Musson (1999; "*…the absence of a reliable, homogenised catalogue for the whole [North Balkan] region...*"). Interest is often biased towards more seismically active provinces. This is reflected in Bulgarian seismicity not having the same luxury as more seismically active, and consequently more familiar, neighbours in the region – e.g. Italy, Greece and Turkey – with regards to the extent to which it has been catalogued in the past. It is often only partially covered or excluded entirely from catalogued areas, and as such, seismic hazard assessments and risk mitigation will both suffer for this. During the second half of the twentieth century, a number of authors have taken steps to rectify this shortfall, notably by Drakopoulos (1976), Shebalin *et al*. (1998), Grünthal and Wahlström (2003) and Burton *et al*. (2004a).

Earthquake catalogues need to represent an area's seismicity as accurately and as completely as possible. This demand generally restricts the time interval of analysis to the instrumental period, i.e. from the start of the 20th century. Extending further back in time requires access to extensive macroseismic and seismotectonic data, early historical records, public reports, and palaeo-seismicity records. An improvement in quality and distribution of seismograph stations through time has enabled a consistent improvement in earthquake data recording. A sharp increase in the numbers of events reported was seen during the 1960s when the World Wide Seismological Station Network (WWSSN) was introduced. This provided for the first time a reliable global source of recorded earthquake data for researchers to access and use for many disciplines including creating earthquake catalogues. Selected key earthquake catalogues from recent times that cover mainland Europe are shown in Figure 4.1(a) and (b). Such catalogues need to be created for a seismic hazard assessment of a region to occur. This problem is approached here through development of a new earthquake catalogue that is considered homogenous within itself and also to other recent catalogued data for a specific adjacent seismic region.

The need to create this earthquake catalogue and its structure is governed by seven criteria considered key in *developing a robust and suitable tool for seismic hazard assessment*. These are born out of limitations that are considered present in previous attempts at cataloguing Bulgarian and Balkan seismicity, 'best practice' principles of earthquake cataloguing and the intended end use of this catalogue. These reasons and criteria are:

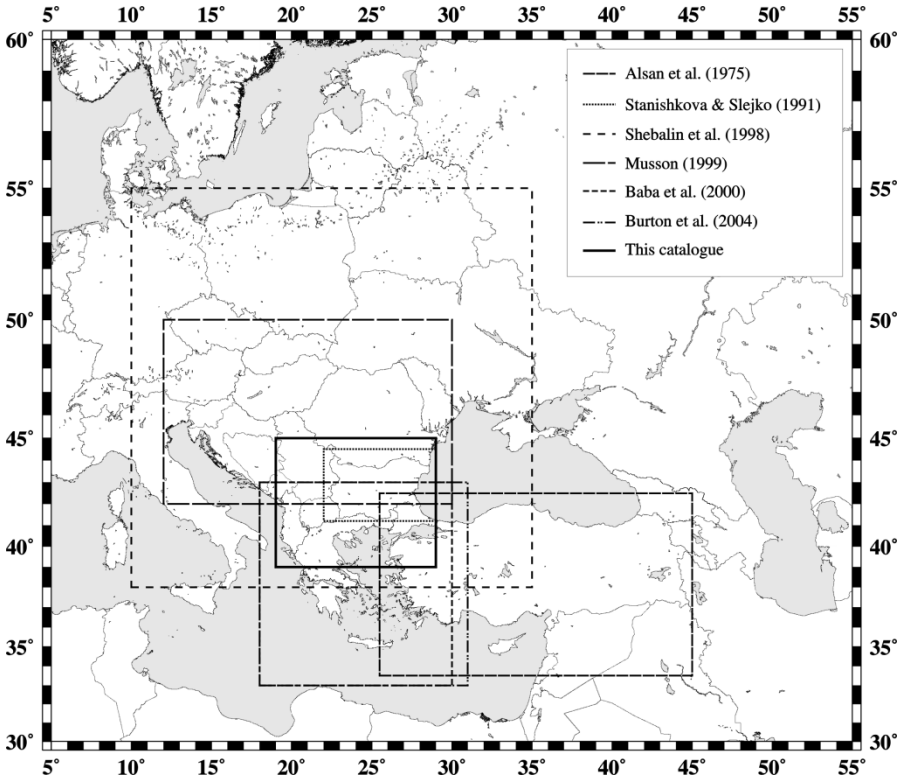

(a)

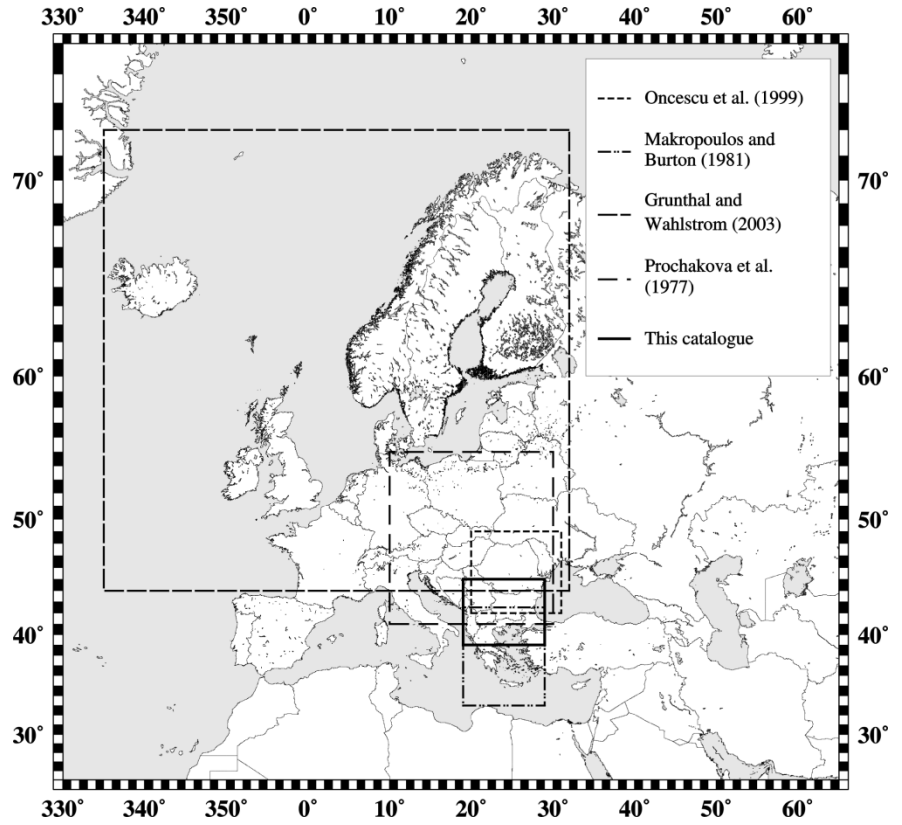

(b)

Figure 4.1(a) Selected catalogued areas of the north-west European, Balkan and Aegean regions. In each figure, the presented catalogue is outlined by the solid black rectangle. The geographic extent represented by Figure 4.1(b) is equivalent to that of Kárník (1968, 1971)

1. Currently there exists no catalogue using the best available data that covers the selected study area;

2. A need to span political boundaries since earthquake sequences do not adhere to them (Alsan *et al.*, 1975; Giardini, 1999; Baba *et al.*, 2000);

3. Catalogues that do cover portions of this study region are often created by merging many data sources together, many of which themselves would have been derived in this manner. Creation of a historical earthquake catalogue requires use of several other resources to form a resource that is consistent, complete and adheres to specific criteria. However, overzealous use of an excessive number of secondary resources may introduce new and unnecessary problems such as event duplication and inclusion of fake entries (Musson, 1999). The aim here has been to use resources economically and effectively to avoid these issues, especially with few resorting to secondary resources;

4. Ultimately it is intended for this catalogue to be used in a seismic hazard assessment over a specific larger area, in unison with a second catalogue. Its physical format is therefore strictly governed by that defined in Burton *et al.* (2004a) to enable tasks outlined in point 7;

5. Catalogues that are currently best representations of this region's seismicity (e.g. Kárník 1968, 1971; Shebalin *et al.* 1974b, 1998; the British Geological Survey's hypocentre database) are known to possess fake and duplicate entries, have missed events, poorly assigned magnitudes, or suffer from the other issues specified above (Sargeant, Musson; pers. comm.; Shebalin *et al.*, 1998);

6. A desire to make a magnitude homogenous catalogue for the area of study using carefully selected magnitude conversion equations depending upon the time and area in question;

7. To create a catalogue that is homogenous and compatible with the Greek catalogue of Burton *et al.* (2004a) covering the adjacent Greek and Aegean region, thus providing an extension to Burton *et al.*'s catalogue. This will enable seismic hazard assessments over a wider area of interest, for a longer time interval than is currently possible with any single earthquake catalogue currently available or either catalogue used in isolation, through consolidation of these catalogues.

Therefore this chapter describes in detail the creation of a new historical earthquake catalogue for the Balkan region. Limitations with previously developed catalogues for this region and those adjacent to it are discussed and related to this work. A description of magnitude conversion equations used, with particular emphasis on conversion from $m_b \rightarrow M_s$ magnitude scales, is provided along with magnitude conversion hierarchies. A comprehensive assessment of catalogue completeness is also provided. This catalogue forms the main data source for the forthcoming probabilistic seismic hazard assessment (PSHA) and is considered homogenous with the catalogue of Burton *et al.* (2004a).

4.2 Previous cataloguing of Balkan seismicity

Cataloguing Bulgarian and Balkan seismicity has been approached on a number of occasions in the past. Each is characterised by their content, its intended use and the form in which it is presented. Key data sources relevant to this study are outlined here. Kárník (1968) presents a catalogue for Europe and the Mediterranean region for the time interval 1901 to 1955 consisting of events with macroseismic intensities $I_0 \geq$ VI or magnitudes $\geq$ 4.5 M as part of the European Seismological Commission's Project of the Seismicity of Europe. It seeks to achieve uniform magnitude determinations for the European area (defined approximately as 25°-75°N, 30°W-65°E) by applying calibration curves with station and depth corrections, and aims to provide data homogeneity in terms of space, time and seismic energy source. This work is limited by the fact that it was a compilation of a large number of other works detailing regional seismicity. For each of the countries covered, epicentral accuracy is provided, where possible, in full or part degrees, minutes etc. These were given to a resolution of 1′ for macroseismic epicentres in Bulgaria, representing the centre of the meizoseismal area or the location of I_{max}. Romanian events are given to an accuracy of 0.1°; Turkish events to 0.1° and 1°; Greek events to 1°, ½°, 1/4° and 0.1°. The sub-project that provided data for the region of interest, i.e. seismicity of the "Baltic Shield", presented a seismotectonic map for Europe and a study of the seismicity of the Carpathian and Balkan region.

Kárník followed up this work in 1971, focusing on events with macroseismic intensities $I_0 \geq$ VII for the time interval 1801 to 1900. Again, this catalogue was a result of merging a number of regional and national catalogues together. Due to the period in question, this work differs fundamentally by being purely orientated to providing macroseismic data for each event. Absence of seismological stations in the 19th century prevents statistical homogeneity with respect to time, space and intensity being achieved, and events of specific types (e.g. oceanic events) may be missed or misrepresented. Additional work of Kárník applied Gumbel's theory of extreme values to forecast

estimates of maximum and minimum earthquakes in specific regions. Using one-year intervals, and data of only shallow earthquakes, return periods were forecast for a range of magnitude values.

The UNDP/UNESCO Survey of the Seismicity of the Balkan Region produced the long respected Shebalin *et al.* (1974b) catalogue. This presents a collection of the main earthquake parameters for Balkan events in the time interval 1901 to 1970, with $M \geq 4.0$ or $I_0 \geq VI$. The main sources used to derive its content were listings of Galanopoulos (1960, 1961, 1963), Kárník (1968, 1971) and Papazachos and Comninakis (1971).

Western Turkey is also of interest to this work. The first computerized earthquake catalogue for Turkey was provided by Alsan *et al.* (1975), covering the region 35.5°-42.5°N, 25.5°-45°E for the period 1913 to 1970. This pursued the highest possible magnitude homogeneity and completeness through application of P-wave readings from the British Association for the Advancement of Science, Bureau Central International de Sèismologie (BCIS), the International Seismological Summary (ISS) and, after 1963, the International Seismological Centre (ISC). Earthquake epicentres were reliant on the Herrin earth model and magnitudes were obtained on a homogenized M_s magnitude scale.

The rectangular region loosely bounded by 41°-55°N, 10°-30°E is covered by Prochazkova *et al.* (1977), although the southwest extent of this region was disregarded (the area covering the former Yugoslavia, Northern Italy, Austria and Albania). Its content was derived from Kárník (1968, 1971), International Seismological Centre (ISC) Bulletins for the period 1970 to 1972 and an unpublished event list of Kárník, to cover the time interval 1800 to 1972. This published catalogue was accompanied by an Atlas of Isoseismals. Intensities were mapped on the MSK-64 intensity scale.

Makropoulos (1978) develops a catalogue of Greek earthquakes for the time interval 1901 to 1978, for the region 33°-42.5°N, 19°-29°E. Work relocated 605 events for the period 1917 to 1963 using master events and phase arrival data from the ISS. Phase arrival data was sought from the bulletins of the British Association for the Advancement of Science, and ISS and ISC records to re-determination hypocentres throughout the entire catalogue. Makropoulos found it possible only to relocate hypocentres for the period 1917 to 1963 due to poor station coverage in the preceding period. Test relocations of ISC data showed a mean general improvement of <10 km in 95% confidence limits. Hypocentre re-determinations were achieved using single event ('Geiger' method) and Joint Epicentre Determination (JED; Douglas, 1967) programs. More data were extracted from bulletins of the Seismological Institute at Uppsala (SIU) for stations at KIR and UPP, the National Earthquake Information Service (NEIS), Shebalin *et al.* (1974b) and ISC

database to homogenize data onto the M_s magnitude scale. These data can be considered complete down to 5.5 M_s for 60 years, and 4.7 M_s for 17 years. This work is further detailed in Makropoulos and Burton (1981) and added to in Makropoulos *et al.* (1989).

A catalogue for the region 41.2°-44.5°N, 22°-29°E is compiled by Stanishkova and Slejko (1991), containing 2,541 events for the time interval 340 to 1989 using data from the National Oceanographic and Atmospheric Administration (NOAA), ISC and data of the important Strazhitza seismic sequences of 1986. ISC data was preferred to NOAA data when both sources provided information on the same event.

Shebalin *et al.* (1998) supersedes Shebalin *et al.* (1974b). This earthquake Catalogue for Central and Southeast Europe (CSEE) was compiled within the framework of the Russian-German project '*Reevaluation of the earthquake data for the areas between the EU countries and the territory of the FUSSR (former USSR)*'. This comprehensive earthquake catalogue covers the time interval 342 BC to 1990, and 38°-55°N, 10°-35°E for the countries: Poland, Czech Republic, Slovakia, Hungary, Slovenia, Croatia, Bosnia and Herzegovina, Serbia, Montenegro, FYR of Macedonia, Albania, Romania and Bulgaria in their entirety as well as western Turkey. Over 50 articles and publications were consulted to allow reporting of 3,949 earthquake magnitudes in one of four formats: M_s derived from macroseismic and mixed determinations (including rough estimation from observed maximum intensity, I_{max}, and depth); M_s derived from direct measurements; M_s converted from SP, LP etc. phases; and m_b derived from direct measurements. Each earthquake is assigned one magnitude estimate, and one epicentral intensity estimate (based on the MSK-64 – Medvedev-Sponheuer-Kárník – scale), with each having an inferred uncertainty attached. Intensity and magnitude thresholds applied are given in Table 4.1.

	Intensity	Magnitude
Earthquakes with sources in the lithosphere, h < 75km	$I_0 \geq 5.0$	any
	$I_0 < 5.0$	$M_s \geq 5.0$, $m_b \geq 4.5$
Earthquakes with sources in the mantle, h ≥ 75km	any I_0	$M_s \geq 5.0$, $m_b \geq 4.5$
	$I_0 \geq 5.0$	Any

Table 4.1 Lower thresholds applied to intensity and magnitude to create the CSEE catalogue

Southern Romania constitutes much of the northern region of this study region that is not common with Burton *et al.* (2004a). Thus, cataloguing its seismicity is of interest here. Many studies have proceeded to form catalogues of this region (Purcaru, 1979; Radu, 1979, 1991; Constantinescu and Marza, 1980; Trifu and Radulian, 1991; Oncescu *et al.*, 1999). Being the most recent work, Oncescu *et al.* (1999) is the most noteworthy. This work covered the time interval 984 BC to 1979,

using data from Constantinescu and Marza (1980), and loosely covers 42°-49°N, 20°-31°E. Historical events were not re-interpreted, and instrumental events between 1980 and 1997 were relocated using digital data picks (predominantly surface-wave). Magnitudes are presented on the moment magnitude scale, M_w, (Kanamori, 1977; Hanks and Kanamori, 1979) and recalculated in line with a conversion hierarchy scheme. The authors hoped to achieve magnitude homogeneity between all large and small crustal and intermediate depth earthquakes.

The region bounded by 33°-43°N, 18°-30°E (termed "southern Balkan area") is detailed by Baba *et al.* (2000), for the time interval 1964 to 1995, and reports 60,473 shallow-focus events with surface-wave and body-wave magnitude estimates drawn from the ISC and National Earthquake Information Center (NEIC). Additionally, local magnitudes reported by the Geodynamic Institute of the National Observatory of Athens (NOA), the Geophysics Laboratory of Thessaloniki University (GLAUTH) and the seismological stations of Kandili, Istanbul (ISK), Tirana (TIR), Titograd (TTG) and Skopje (SKO) are cited and used to develop relations between local magnitudes obtained from each station. Scaling relations between reported M_L estimates of local networks and the corresponding seismic moment magnitudes were also used to reach magnitude homogeneity in terms of M_w.

Fifty-five individual studies and catalogues are merged by Grünthal and Wahlström (2003) to create an M_w-based composite earthquake catalogue for the region bounded by 44°-72°N, 25°W-32°E (approximately equivalent to GSHAP (Global Seismic Hazard Assessment Program) Region 3; Giardini and Basham, 1993) and time interval 1300 to 1993. Data for approximately 5,000 events are provided and calibrated onto a homogenized M_w magnitude scale by applying a hierarchical conversion system. Values for epicentral intensity, I_0, are also provided. This catalogue is truncated at a lower magnitude threshold of 3.5 M_w, though this should not be considered the data's magnitude completeness threshold.

Burton *et al.* (2004a) extend Makropoulos and Burton's (1981) catalogue through an additional 18 years data from ISC, NEIC, Institute of Geodynamics National Observatory of Athens (NOA) and Harvard-Centroid Moment Tensor (HRVD-CMT) databases. A number of magnitude conversion equations from m_b, M_s, M_w and M_L magnitude scales onto homogenized M_w and M_s scales are tested to ensure magnitude homogeneity and provide 5,198 events during 1900 to 1999 on homogenized M_s and M_w scales, along with originally reported m_b, M_s, M_w and M_L. No attempt is made to relocate the additional data due to evidence already described above from Makropoulos and Burton (1981). This gave credence to using unaltered ISC earthquake hypocentre estimates. This revised catalogue facilitated the SHIELDS earthquake early warning project being developed around Athens and to provide a foundation for revised seismic hazard analysis in Greece.

4.3 Data sources

Data sources selected to create this catalogue depend upon the time interval and geographic region in question. Those used can be further classified into early instrumental and modern instrumental data sources. Data from each source were handled according to criteria outlined in Burton *et al.* (2004a).

4.3.1 Instrumental period (1964 to present day)

The International Seismological Centre's (ISC) hypocentre database is generally accepted to be the definitive source of earthquake location and magnitude data for the modern instrumental period of earthquake recording. Revised event locations and magnitudes are published 15 to 18 months behind real time to allow the greatest number of phase readings possible to be collected before analysis. Typically earthquakes are reported on the body-wave magnitude scale, m_b. In addition, surface-wave magnitudes, M_s, are often reported, occasionally moment magnitudes, M_w, are reported, and rarely local magnitude, M_L, and duration magnitude, MD, estimates are also reported.

Data were collected from the ISC hypocentre database for the time interval 1964 to 2002. Primary hypocentres were selected for those earthquakes located in the region of interest regardless of the agency that computed them. After removing events with no reported magnitudes, filtering to the study region, and adopting a homogenized magnitude threshold of 4.0 M_w, ISC data accounted for 2,569 events. Reported magnitudes provided in the catalogue were extracted from the ISC bulletin on a hierarchical basis:

1. If the ISC had computed an estimate (for any magnitude type used) that was selected;

2. If no ISC estimate was available, an estimate from the NEIC was sought;

3. If no NEIC estimate was available, magnitudes computed by the University of Athens (ATH) were sought.

4. If none of the above were available, a magnitude calculated by any other reporting station was accepted.

All events are within a magnitude range $4.0 \leq M_w \leq 7.2$ between 1964 and 2002 and a focal depth range 0.0 to 401.0 km for the region bounded by 39°-45°N, 19°-29°E.

The ISC's processing time-lag prevented adopting their data to the end of the desired final year of 2004. To allow the required time interval to be represented by this catalogue, data for 2003 was required from the National Earthquake Information Center (NEIC). NEIC report earthquake locations and magnitudes in near real time, and are assigned one of either M_L, m_b, M_s, MD or M_w magnitude estimates (reported by any one of a number of reporting stations or agencies; e.g. ISK, ATH, IST, BRK, ATU, SKO, TRI, TIR, RMP, GRF). NEIC data provided an additional 61 events in the moment magnitude range $4.0 \leq M_w \leq 5.5$ and focal depth range 0.0 to 72.0 km.

The final year of the catalogue, 2004, is represented by data contributed by Institute of Geodynamics, National Observatory of Athens (NOA). NOA cites earthquakes on the local magnitude scale (M_L). NOA provides a further 96 events in the moment magnitude range $4.0 \leq M_w \leq 5.8$ and focal depth range 2.0 to 98.0 km.

Data has not been filtered to remove quarry blasts within the catalogued region. Necessary inclusion of these event types, due to uncertainty in event type assigned by analysis (e.g. by the ISC during their evaluation) will likely influence hazard forecasts estimated in the ensuing analysis chapters. However, a brief review of source ISC data extracted for the period 1964 to 2002 shows there were no known and accepted quarry blasts in the considered region during this time, although there was a small number of other known human-induced events (i.e. known chemical or experimental explosions; Harris, pers. comm.).

4.3.2 Early instrumental period (1900 to 1963)

Further data sources were needed that represented the early instrumental period of recording and considered reliable to maintain magnitude homogeneity with the remainder of the instrumental period of seismology. Many sources were considered, including (with reasons for their rejection):

- The catalogue of Shebalin *et al.* (1974b; superseded by Shebalin *et al.* (1998) and known to possess missed events, fakes and duplicates);
- The catalogues of Kárník (1968, 1971; superseded by Shebalin *et al.*, 1974b, 1998);
- The hypocentre database of the BGS (known to contain duplicate and fake events).

Much emphasis is finally placed upon the recent catalogue of Shebalin *et al.* (1998). This catalogue becomes the sole source of earthquake data for the early instrumental recorded period of recording from 1900 to 1963. After filtering the events to regional boundaries and to a minimum moment

magnitude threshold of 4.0 M_w, Shebalin *et al.* (1998) provides an additional 955 events in the homogenized magnitude range $4.0 \leq M_w \leq 7.2$ and focal depth range from 0.0 km to 160.0 km.

4.3.3 Historical period (pre-1900)

To provide additional data describing the region's historical seismicity, pre-instrumental data from Shebalin *et al.* (1998) has been homogenized to allow it to be appended to the main catalogue of seismicity for the instrumental period. Data available spans the time interval 342 BC to 1899 and provided 411 additional events. All reported earthquakes in this time interval were reported with surface wave magnitude estimates, making rendering onto homogenized moment and surface-wave magnitude scales easy using identical methods to those used for early instrumental and instrumental periods. Inclusion of a period of pre-instrumental data enables the time window of analysis to be lengthened, and in doing so, will decrease uncertainties in earthquake extremes forecasted (Musson, *http://www.quakes.bgs.ac.uk/hazard/hazguide.htm*, 2002).

4.4 Geographical coverage

This catalogue loosely corresponds to the Flinn-Engdahl (seismic regionalization) regions 30 and 31 (Flinn and Engdahl, 1965; Flinn *et al.*, 1974); "Middle East-Crimea-E. Balkans" and "Western Mediterranean Area" respectively, and is located at the boundary of GSHAP seismic regions 3 and 4. A conscious effort was made to exclude the seismic regions of the [southern] Hellenic Trench and the Vrancea-Carpathian region of Romania (Radulian *et al.*, 2002; Purcaru, 1979). This was to exclude two anomalous regions of high seismicity that may bias correlation between magnitude scales and hence future earthquake extreme forecasting practices in the principle study area. However, the catalogued region was extended far enough beyond the political borders of Bulgaria to limit "edge" effects within the territorial boundaries of the country in any ensuing seismic hazard assessment.

4.5 Adjusting reported magnitudes of significant historical events

Re-evaluating magnitude estimates originally reported by seismological agencies is commonplace with the advent of more data and time. This is particularly true of larger magnitude, destructive events – those events of importance in this study – as they will tend to be those annual or other *N*-year extreme events that are used in the final analysis. Similarly, it will often be older events of the early instrumental and historical periods that are re-evaluated due to an initial lack of a comprehensive review of macroseismic or instrumental data.

One event for which the magnitude has long been a source of contention, and is of importance here, is the April 4th 1904 Kresna [Krupnik fault] event. This event was reported with a body-wave magnitude estimate of 7.8 m_b (±0.2 m_b) by Shebalin *et al.* (1998), making it the strongest shallow focus earthquake in Europe of the last two centuries (Sledzinski, 2000; Ranguelov *et al.*, 2000b). Much work has focused upon re-evaluating this earthquake's magnitude. For example, Grigorova and Grigorov (1964), Christoskov and Grigorova (1968), Ranguelov *et al.* (2000a, 2000b; 2001), Rizhikova *et al.* (2000), Toteva *et al.* (2000), and Meyer *et al.* (2007) and references therein all report revised magnitude estimates for this event, the seismic sequence in which it occurred and the seismic potential of the localised Kresna-Krupnik seismic zone. Ranguelov *et al.* (2000b) especially makes effort to highlight how a number of previous studies apply alternative methods to appraise this earthquake's magnitude, producing estimates in the range 6.4 M to 7.9 M using neotectonic movements and observed macroseismic intensity estimates respectively.

S. Pavlides has re-evaluated this magnitude to 7.1 to 7.2 M_s (pers. comm.; Pavlides and Caputo, 2004) using historical and fault rupture measurements, and following the revision of Ambraseys (2001), Meyer *et al.* (2002), and Papazachos (1990) and application of empirical formulae from Ambraseys and Jackson (1998) and Wells and Coppersmith (1994). Dineva *et al.* (2002) estimates this event's surface-wave magnitude as 7.2 M_s, in agreement with Abe and Noguchi (1983b; after revision from 7.3 M_s; Abe and Noguchi, 1983a) and Pacheco and Sykes (1992). Consequently, this new estimate of 7.2 M_s is attached to the 1904 Kresna event, in addition to the original body-wave magnitude estimate of Shebalin *et al.* (1998; Event No. 40, p414). These studies intended adjustment of the magnitude of this event (along with other large magnitude early instrumental events that are detailed later) to counter the effect of using undamped narrow-band seismometers (Koravos *et al.*, 2003).

To maintain consistency across large magnitude events in this catalogue, additional earthquakes of note were reviewed to determine if their magnitudes had been re-evaluated by past authors. Attention was paid specifically to the early instrumental period, 1900 to 1963, and events with a reported magnitude of M ≥ 6.0 (where M is a generic reported magnitude scale representing m_b, M_s, ML, and M_w). The modern instrumental period (1964 to present) was not reviewed further as this period is covered largely by data from the International Seismological Centre (ISC). Invoking their processing time lag implies these estimates may be considered definitive for this time period. A number of studies have re-evaluated ISC data, notably Makropoulos and Burton (1981), Engdahl *et al.* (1998) and Pérez (1999) to relate hypocentre locations and teleseismic reporting, completeness and magnitude homogeneity determination. This particular task is considered outside the scope of this study. Engdahl *et al.* (1998) achieved similar results to Makropoulos and Burton

(1981) for their re-determined hypocentres. ISC hypocentres were deemed acceptable to adopt without further analysis.

The events in this catalogue to have their magnitude estimate(s) re-evaluated are:

- **1904 April 4th (Kresna) 6.9 M_s/6.8 M_w:** Pavlides and Caputo (2004) re-evaluate the main foreshock to the 1904 event. This was re-assigned with a surface-wave magnitude estimate of 6.8 to 6.9 M_s (Shebalin *et al.* (1998) report this event with a magnitude of 7.1 m_b ±0.3, estimated from direct measurements; Event No. 32, p415). Consequently this study's catalogue reports the M_s magnitude for this event as 6.9 M_s, in addition to the original estimate by Shebalin *et al.* (1998) of 7.1 m_b. A second magnitude estimate for this event of 6.8 M_w (Dineva *et al.*, 2002) was also attached to this event's listing in this catalogue.

- **1913 June 14th (Gorna Orjahovitza) 6.3 M_s**; Event No. 262, p418**:** The 14th June 1913 Gorna Orjahovitza event is also discussed by Dineva *et al.* (2002). They suggest 6.3 M_s as an alternative to the 7.0 M_s estimate by Shebalin *et al.* (1998). Additionally, Bungum *et al.* (2003) suggests 6.8 M_s using Pasadena seismological observatory data. The revised estimate of 6.3 M_s by Dineva *et al.* (2002) was adopted for this study's catalogue, as source parameters have been used to derive the estimate, instead of analog and digital records by Bungum *et al.* (2003).

- **1928 April 14th and 18th (Plovdiv) 6.8 M_s and 7.0 M_s**; Event Nos. 531 and 538, p421**:** Dimitrov *et al.* (2004) re-evaluated the Chirpan and Plovdiv events of 14th and 18th April 1928. These were initially assigned surface-wave estimates of 6.8 M_s and 7.0 M_s respectively by Shebalin *et al.* (1998). Dimitrov *et al.* obtain moment magnitude estimates of 6.7 M_w and 7.0 M_w respectively for these events. These re-evaluations are included in the catalogue, in addition to retaining the magnitude estimates of Shebalin *et al.* (1998). Also noteworthy is Karakostas *et al.*'s (2006) attempt to determine slip distribution and fault geometry using surface faulting and deformation. This enables them to derive alternative and comparable moment magnitude estimates – not attached to this catalogue – of 6.5 M_w and 6.9 M_w for the Chirpan and Plovdiv events respectively.

In addition to the re-evaluated events discussed above, Bungum *et al.* (2003) assess a number of events by looking at long-period ground motions for large magnitude European earthquakes of the 20th century. The following events are of note in their work:

- **1905 January 6th (42.0°N, 19.5°E) 6.6 M_s:** assigned 6.6 M_s by Shebalin *et al.* (1998), Kárník (1971) and Bungum *et al.* (2003). The magnitude estimate of Shebalin *et al.* (1998) and others is adopted;

- **1906 March 1st (41.1°N, 20.1°E) 6.4 M_s:** assigned 6.4 M_s by Shebalin *et al.* (1998), and 6.5 M_s by Kárník (1971) and Bungum *et al.* (2003). Magnitude estimate of Shebalin *et al.* (1998) was retained;

- **1953 March 18th (40.0°N, 27.3°E) 7.2 M_s and 7.2 M_w**: not reported by Shebalin *et al.* (1998) and assigned 7.2 M_s and 7.2 M_w by Pacheco and Sykes (1992). Full event details from Pacheco and Sykes (1992) were adopted;

- **1960 May 26th (40.5°N, 20.6°E) 6.5 M_s**: assigned 6.2 M_s by Shebalin *et al.* (1998) and 6.5 M_s by Pasadena Seismological Observatory and Bungum *et al.* (2003). The magnitude estimate of Pasadena Seismological Observatory and Bungum *et al.* (2003) was retained.

Revised magnitude estimates for the events discussed above are summarised in Table 4.2, in relation to the original magnitude estimates provided by Shebalin *et al.* (1998) and the resulting homogenized magnitude estimates on moment and surface-wave scales.

4.6 $m_b \rightarrow M_s$ magnitude conversion

The International Seismological Centre's (ISC) database provides a rich source of data from which to derive magnitude regression equations, with the magnitude scales the ISC report on for any given earthquake – and thus users can access – outlined earlier. Consequently, provided a study region is significantly large enough to contain a reasonable number of such events, there is opportunity to develop regression equations between these two magnitude scales. This method has been approached a number of times in the past using ISC data (and data derived from original ISC data).

Alsan *et al.* (1975) use 110 events with ISC m_b and M_s magnitude estimates to give Eq. (4-1):

$$M_s = 1.55m_b - 2.49 \quad (4\text{-}1)$$

Makropoulos and Burton (1981) uses ISC data for 126 earthquakes for the time interval 1964 to 1975 to obtain Eq. (4-2) (with a standard deviation of 0.41):

									Reported magnitudes[1]		Additional estimates		Homogenized magnitudes[2]	
Year	Month	Date	Hour	Minute	Second	Latitude	Longitude	Depth	m_b	M_s	M_s	M_w	M_w	M_s
1904	04	04	10	02	34.00	41.78	22.90	18.0	7.1[3]		6.8 - **6.9**[4]	**6.8**[5]	6.8	6.9
1904	04	04	10	25	55.00	41.80	23.10	24.0	7.8[6]		7.1 - **7.2**[7]		7.1	7.2
1905	06	01	04	42	15.00	42.03	19.50	15.0		6.6	**6.6**[8]		6.6	6.6
1906	03	01	17	45	00.00	41.10	20.10	20.0		**6.4**	6.5[9]		6.4	6.4
1913	06	14	09	33	00.00	43.10	25.70	14.0		7.0	**6.3**[10]		6.3	6.3
1928	04	14	08	59	57.00	42.14	25.20	16.0		**6.8**		**6.7**[11]	6.7	6.8
1928	04	18	19	23	47.00	42.14	25.00	14.0		**7.0**		**7.0**[12]	7.0	7.0
1953[13]	**03**	**18**	**19**	**06**	**13.00**	**40.00**	**27.30**	**0.0**			**7.2**	**7.2**	7.2	7.2
1960	05	26	05	10	11.00	40.60	20.60	9.0		6.2	**6.5**[14]		6.5	6.5

[1] Original magnitude estimates from Shebalin *et al.* (1998); [2] Estimates derived from adopted magnitude estimates and magnitude conversion equations (section 4.7) and hierarchies (Section 4.9); [3] Original magnitude estimate from Shebalin *et al.* (1998) of 7.8 m_b (±0.3); [4] Alternative estimate from Pavlides & Caputo (2004) and adopted in this catalogue; [5]Alternative estimate from Dineva *et al.* (2002); [6] Original magnitude estimate from Shebalin et al. (1998) of 7.1 m_b (±0.3); [7] Alternative estimate from Pavlides and Caputo (2004); Magnitude of 7.2 M_s agreed by Dineva *et al.*, (2002) and adopted in this catalogue; Meyer *et al.* (2006) offer "M_s *~7.1*"; [8] Original estimate agreed by Kárník (1971) and used in this catalogue; [9] Alternative estimate from Kárník (1971); [10] Alternative estimate from Dineva *et al.* (2002); [11] Alternative estimate from Dineva *et al.* (2002); [12] Alternative estimate from Dimitrov *et al.* (2004); [13] Full event not reported in Shebalin *et al.* (1998). Event details obtained from Pacheco and Sykes (1992) and added to the catalogue; [14] Alternative estimate from Bungum *et al.* (2003).

Table 4.2 Summary of magnitude estimates reported by previous authors for selected large magnitude historical events. Event details used in final analysis are highlighted in bold

$$M_s = 1.31m_b - 1.41 \quad (4\text{-}2)$$

Rezapour and Pearce (1998) use data for 13,903 earthquakes with ISC data to derive Eq. (4-3):

$$M_s = (1.8782 \pm 0.0222)m_b - (4.6046 \pm 0.1102) \quad (4\text{-}3)$$

Shebalin *et al.* (1998) is of interest to this study on many levels. Not only is it the most recent and currently the most comprehensive historical earthquake catalogue for this region, they adopt a similar method for deriving $m_b \rightarrow M_s$ conversion equations for ISC data also. Here they use ISC data to obtain Eq. (4-4):

$$M_s = 1.2m_b - 1.45 \quad (4\text{-}4)$$

Burton *et al.* (2004a) derive Eq. (4-5) and Eq. (4-6) from 591 events with both ISC m_b and M_s estimates using single-error and York (1969) double-error regression respectively;

$$M_s = 1.306\ (\pm 0.070)m_b - 2.037\ (\pm 0.32) \quad (4\text{-}5)$$

$$M_s = 3.05\ (\pm 0.10)m_b - 10.22\ (\pm 0.47) \quad (4\text{-}6)$$

Additionally, Gutenberg and Richter (1956) derive Eq. (4-7):

$$M_s = 1.59m_b - 3.97 \quad (4\text{-}7)$$

To obtain uniform estimates for magnitudes of European earthquakes Ambraseys (1990) re-evaluates events with $3.0 \leq M \leq 8.0$ to derive orthogonal regression relationships between m_b, M_L and M_s (also see Bormann *et al.*, 2002). The relation for m_b to M_s – with m_b being determined according to the ISC procedure from short-period P-wave recordings – is given by Eq. (4-8):

$$0.86\ m_b - 0.49\ M_s = 1.94 \quad (4\text{-}8)$$

The compiled catalogue here contains 638 events with both M_s and m_b ISC magnitude estimates. Regressing M_s values on m_b for these earthquakes, results in Eq. (4-9) and Eq. (4-10), again, derived from single and York double-error techniques respectively:

$$M_s = 1.4311\ (\pm 0.040) m_b - 2.4394\ (\pm 0.178) \quad (4\text{-}9)$$

$$M_s = 1.9418\ (\pm 0.0443) m_b - 4.7256\ (\pm 0.2002) \quad (4\text{-}10)$$

Single error regression assumes uncertainty only in data of the y-axis variable. York (1969) presents reasoning for the least squares quadratic to be used in generalised forms when it is found that errors in the y-coordinate of a given point is correlated to errors in the x-coordinate through the data range. He applies this principle to isochron fitting for meteorite age determination.

The 638 events contained in this study's catalogue with both m_b and M_s magnitude estimates by the ISC are plotted in Figure 4.2 along with a selection of $m_b \rightarrow M_s$ conversion equations outlined already in this section, Eq. (4-9) and Eq. (4-10) that are specific to this new dataset.

However, with modern analysis techniques favouring applying M_w estimates to conceive robust seismic hazard forecasts, it is also useful to consider relationships between reported and homogenized M_s and M_w magnitude scales. Figure 4.3(a) and (b) plot reported and homogenized M_s and M_w magnitudes of the catalogue respectively. Few earthquakes were present within the catalogue region that possessed M_w estimates; consequently only 79 events are plotted in Figure 4.3(a) and support principles of using alternative methods to homogenizing earthquakes on the M_w scale. Kanamori (1983) and Wells and Coppersmith (1994) note these magnitude scales to be approximately equivalent in the range $5.0 \rightarrow 7.5$ and $5.7 \rightarrow 8.0$ respectively. Unfortunately, with a lack of events reporting M_w magnitudes in the range $5.7 \rightarrow 6.4$ and M_s magnitudes in the range $5.6 \rightarrow 6.4$ it is not possible to suggest such a range of equality. Figure 4.3(b), that plots all 3,681 events of this catalogue, indicates a range of equality between approximately $5.6 \rightarrow 7.0$ M_s.

This small magnitude range in which no earthquake is reported on both M_w and M_S estimates is noteworthy. The 79 earthquakes present in this data extract occurred predominantly in the late modern instrumental period recorded solely by the ISC; 73 occurred after 1990 with a further three between 1981 and 1983. The remaining three events are from the large magnitude seismic sequence of Kresna and Plovdiv in 1904 and 1928 respectively, and only have estimates reported on both magnitude scales due to their homogenisation in section 4.5. These final three may be excluded from consideration because of this reason. The presence of these three anomalous events in the early 1980s could be explained by either the ISC experimenting with reporting magnitudes on the M_w scale – these events were significantly larger magnitude than those after 1990, or the decision by the ISC to habitually only consider estimating M_w for small-moderate magnitudes.

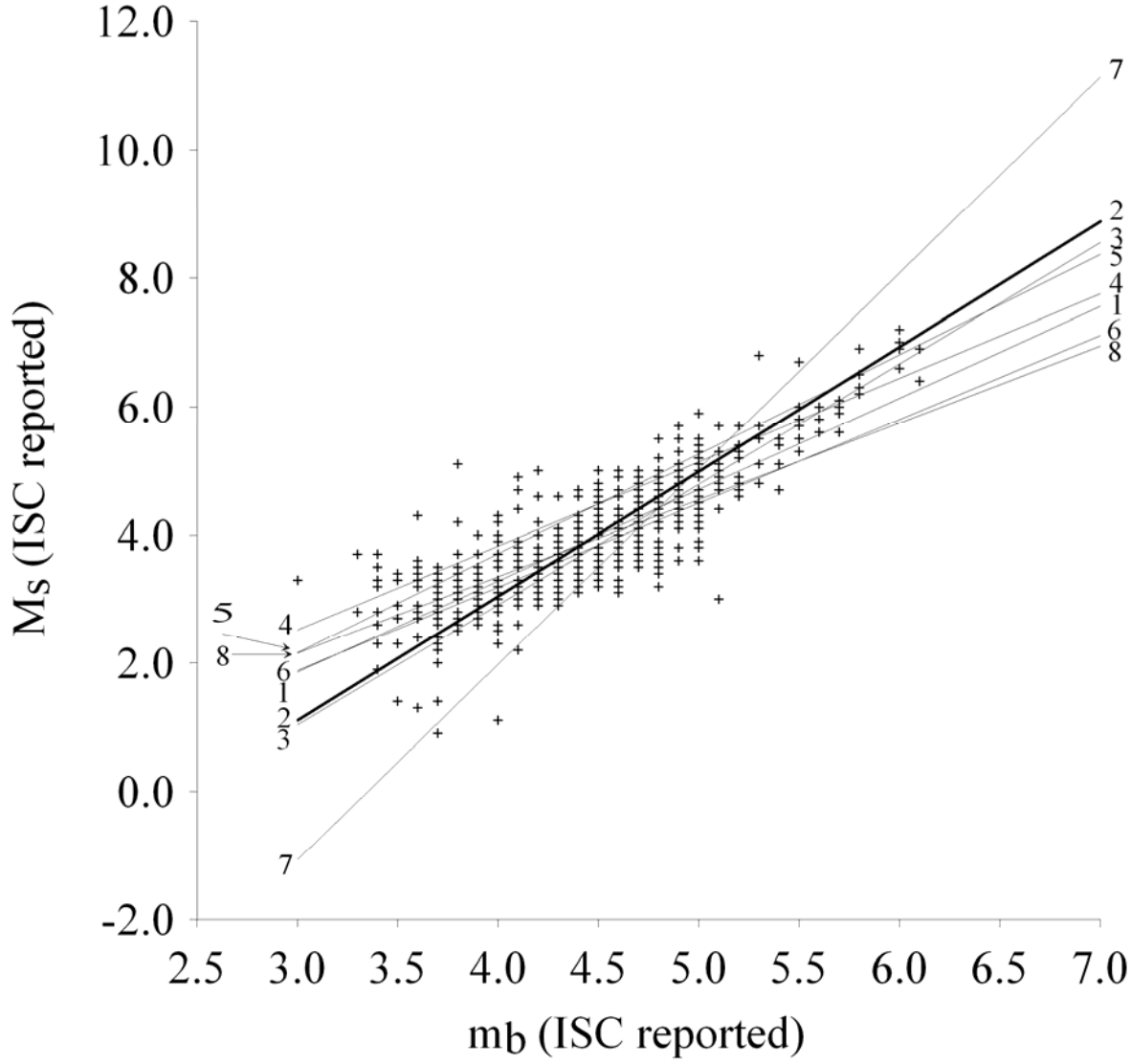

Figure 4.2 Selected $m_b \rightarrow M_s$ magnitude conversion equations for the region of study. Individual points are 638 ISC prime events with reported estimates for both m_b and M_s scales. Line 1 - This catalogue (single error; Eq. (4-9)); Line 2 - This catalogue (double error; Eq. (4-10)); Line 3 - Rezapour and Pearce (1998); Line 4 - Makropoulos and Burton (1981); Line 5 - Alsan *et al.* (1975); Line 6 - Burton *et al.* (single error; 2004a); Line 7 - Burton *et al.* (double error, 2004a); Line 8 - Shebalin *et al.* (1998)

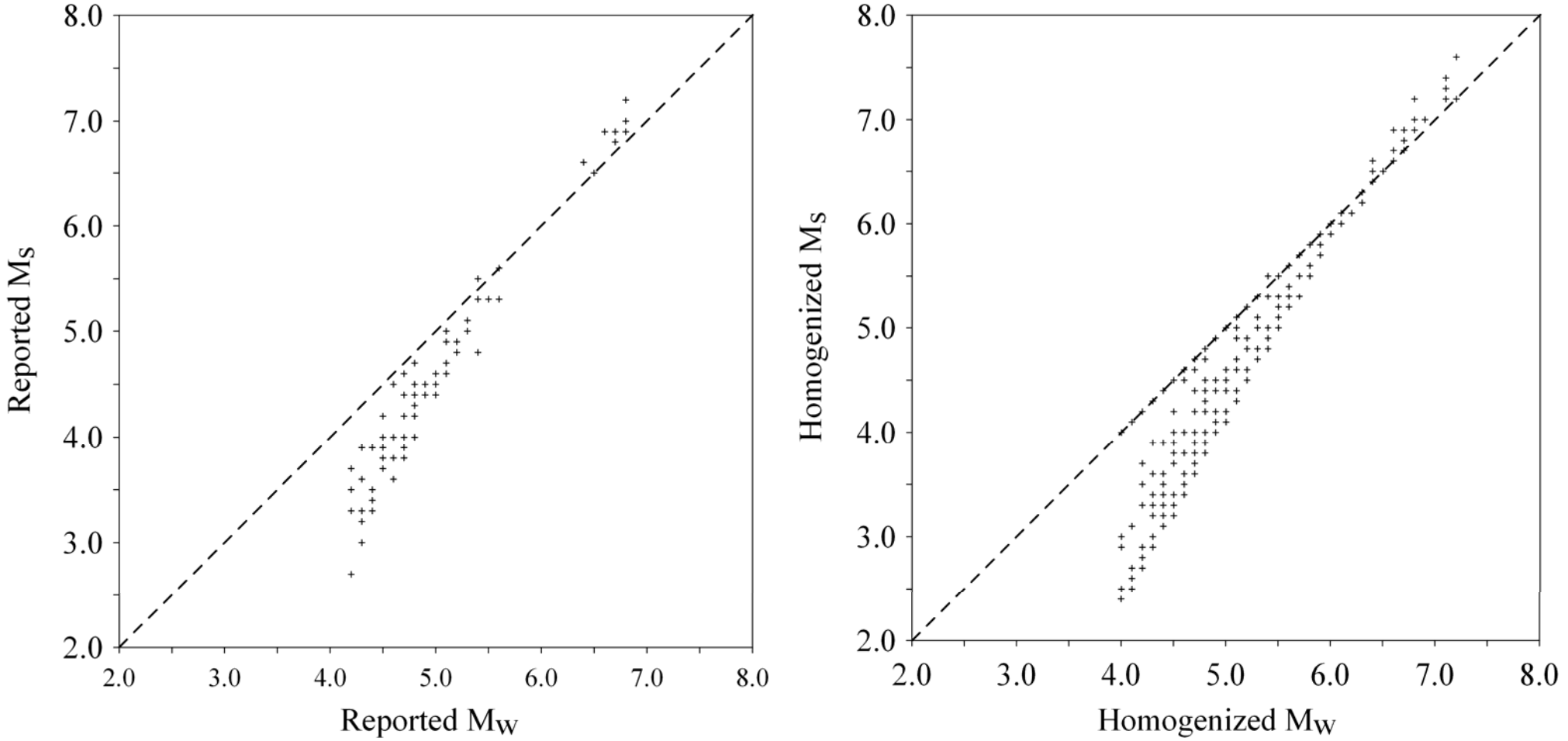

Figure 4.3 Surface-wave magnitude (M_s) versus moment magnitude (M_w): (a) the 79 events from the newly developed earthquake catalogue that possess reported estimates for both M_s and M_w magnitude types by the reporting agency or literature source; (b) all 3,681 events of the catalogue plotted using homogenized M_s and M_w magnitude estimates. In each plot, the dashed line indicates magnitude equality (i.e. a 1 to 1 slope)

Figure 4.3(b) plots homogenized M_s versus M_w magnitudes for all 3,681 events of this catalogue, and indicates a range of equality between approximately 5.6 $\rightarrow$ 7.0 M_s. This highlights a systematic underestimating of M_w at low M_s, changing to a systematic over-estimation at higher surface-wave magnitudes. Larger magnitude events are symptomatic of larger-scale fault movements and energy release; therefore recalibration of an earthquake M_s magnitude to the moment magnitude scale will invariably increase its original estimate due the strong relationship between fault rupture dynamics and energy release.

4.7 Magnitude determination

Clearly, many alternative magnitude scale conversions for the region have been proposed and this is inevitably an on-going situation as more, and better data accumulates. Although the $M_s \leftrightarrow m_b$ pairing is vital, other scale conversions are required to finish this catalogue. Conversion equations to be used here are governed by five key points:

1. The existence of a 'common' area 39°-43°N, 19°-29°E overlapping with the catalogued region of Burton *et al.* (2004a), and their equivalent conversion equations;

2. Whether the sub-region in question is north or south of 43°N (the boundary between the area common with Burton *et al.* (2004a) and that which is not);

3. The magnitude type;

4. The magnitude scale conversion required;

5. Conversion equations used in past studies.

Equations used to render each earthquake in this catalogue onto the required magnitude scales for the region south of 43°N are set as those used in Burton *et al.* (2004a). Using these aims to maintain magnitude homogeneity between this catalogue, the Greek catalogue of Burton *et al*. and the M_s re-evaluation performed for the Makropoulos and Burton (1981) catalogue. To convert onto the moment magnitude scale, M_w, from M_s use (Papazachos and Papazachou, 1997):

$$M_w = 0.56M_s + 2.66 \qquad 4.2 \leq M_s \leq 6.0, \qquad (4\text{-}11)$$

When $M_s \geq 5.3$ (Burton *et al.*, 2004a):

$$M_w = 0.804M_s + 1.28 \qquad 5.3 \leq M_s \leq 7.2, \qquad (4\text{-}12)$$

From M_L use (Baba *et al.*, 2000; Margaris and Papazachos, 1999):

$$M_w = M_L + 0.43 \qquad (4\text{-}13)$$

From m_b use (Papazachos and Papazachou, 1997; Papazachos *et al.*, 1997b):

$$M_w = 1.28m_b - 1.12 \qquad (4\text{-}14)$$

To enable conversion onto the surface-wave magnitude scale, M_s, from M_w use Eq. (4-11) and Eq. (4-12); from m_b, use Eq. (4-3) (Rezapour and Pearce, 1998), and from M_L use (Burton *et al.*, 1991):

$$M_s = 1.70\ (\pm\ 0.05)M_L(\mathrm{ATH}) - 3.59\ (\pm\ 0.22) \qquad (4\text{-}15)$$

where M_L(ATH) is the local magnitude scale as recorded at the Athens Observatory (NOA).

The region north of 43°N requires detailed homogenizing for this study. This region is dominated geographically not only by Bulgaria, but also by southern Romania and Serbia, and as such, conversion equations derived in previous studies of seismicity for these territories are of interest here, as are regressions that can now be determined from data within this catalogue itself. Grünthal and Wahlström (2003) and Bungum *et al.* (2003) find the equality $M_w = M_s$ to hold for central and northern Europe. Oncescu *et al.* (1999) also adopt this equality. If m_b is reported by the data source, use Eq. (4-14). If M_L is reported use (Baba *et al.*, 2000):

$$M_w = M_L + 0.43 \qquad (4\text{-}16)$$

To convert onto the M_s scale from M_w use Eq. (4-11) and Eq. (4-12) as appropriate. If M_L is reported, use Eq. (4-14). If m_b is provided, use (from this work) Eq. (4-10).

4.8 Uncertainty in earthquake parameter estimation of sources

The majority of this new catalogue is accounted for by two main data sources: the catalogue of Shebalin *et al.* (1998) and the hypocentre database of the ISC. Together these account for nearly 96% of the total number of earthquakes reported for the period 1900 to 2004. These two data

sources account for two distinctly different periods of seismicity monitoring, and as such, it is important to understand how earthquake parameter estimation and their uncertainties has been calculated and changed over time and the reason behind these variations.

4.8.1 Uncertainties in parameter estimation during early instrumental period

Data from Shebalin *et al.* (1998) accounts for the full period of early instrumental (pre-1964) earthquake recording. As this catalogue is made from many component parts (i.e. other studies, catalogues, macroseismic and historical data) the authors realise a need to fully account for and justify development of their work in the context of earthquake parameters and their uncertainties ("*6.4. All main parameters of an earthquake should be accompanied by their error limits*"; Shebalin *et al.*, 1998). Although extensive in nature, it is useful to extract and repeat a number of keys points from the text. Following on from Point 6.4 above, Point 6.5 states "*To estimate the source parameters we should use all available data. The discrepancies among them are much more informative than the coincidences…. These discrepancies help to estimate to possible parameter errors*".

Section 7 of Shebalin *et al*. continues to outline development of source parameter estimations and uncertainties, but only ever making discrimination between historical and instrumental period events, not historical, early instrumental and instrumental periods of recording, as is necessary here. As this data source was only used to form the time interval 1900 to 1963 of this catalogue, we need only to discuss further parameter estimation of "instrumental data", and in that, only time of occurrence, epicentral location, magnitude and depth.

Estimation of occurrence time was undertaken in the following manner; "*All time taken from various initial data sources are converted into the new calendar and are given in GMT [Greenwich Mean Time]. We considered the dependence of the old to the new date correction in the century when the country changed its calendar. Possible time errors depend upon the accuracy in time determination and discrepancy in various references*".

As with many data sources a hierarchy of preference was imposed to estimate each earthquake's characteristics as accurately as possible. This can be summarised as follows:

- If macroseismic data were unavailable, time and position of an epicentre are determined by averaging as many data source estimates as are available. Errors are duly estimated from the associated discrepancies amongst them;

- If macroseismic data were available, special allowance was made for discrepancies in the estimation of an epicentre's location. Here Shebalin *et al.* (1998) suggest a macroseismic epicentre that corresponds to the position of the source epicentroid (the point over a source centroid) describes more accurately an event's true location than an equivalent instrumental epicentre (the latter only being a point on the surface over the rupture start point). Consequently, they take the epicentre to be the centre of the first isoseismal where the error is equal to the distance between macroseismic and instrumental estimates;

- To constrain magnitudes, an event's surface-wave magnitude was preferred. Where this was not possible a body-wave magnitude was derived from Eq. (4-18) using ISC data in a similar fashion to that used earlier, or its own estimate was retained for some smaller events:

$$m_b = 0.83\ M_s + 1.2 \qquad (4\text{-}18)$$

- Uncertainty in the magnitude estimate was derived from the number of reporting stations used in its determination. If there were discrepancies between data sources, the magnitude was averaged and included an assigned weighting factor of their creation;

- Instrumental depths were only used since 1965 in this catalogue. To derive depth estimates for 1900 to 1963 one of two methods was adopted: either using I_o and I_i in a macroseismic equation, Eq. (4-19), but restricted themselves to attaching focal depth estimates of 5, 10, 20, 30 or 50 km to each earthquake, to avoid inferring undue accuracy on estimates:

$$I_o - I_i = v - \log (r_i/h) \qquad (4\text{-}19)$$

- where I_o and I_i are epicentral intensity and intensity at distance r_i respectively, h is focal depth and v is a numerical parameter (taken as 4.0 here), or using M_s and I_o in Eq. (4-20):

$$I_o = b - Ms - v - \log h + c \qquad (4\text{-}20)$$

- Where b and c are additional numerical parameters taking values of 1.5 and 3.8 respectively. Discrepancy between the two methods formed the estimated error, as a ratio of results from Eq. (4-19) and Eq. (4-20).

4.8.2 Uncertainties in parameter estimation during instrumental period

After 1963 the International Seismological Centre (ISC) comes into its own with regards to earthquake data processing. It is this data source that contributed most to the instrumental period of monitoring in this catalogue. Over time the ISC has been at the forefront of promoting best use of traveltime models, opting for a least-square derivative of the radially stratified Jefferys-Bullen (JB; Jefferys and Bullen, 1988) tables in calculating earthquake hypocentre locations based primarily upon P-wave arrivals. JB tables have been used throughout the existence of the ISC (and its previous incarnation, the International Seismological Summary, ISS). Due to this limitation in using only teleseismic (non-upgoing ray paths) P-waves to estimate hypocentre location, focal depths could never be well constrained, thus limiting their application in areas of research where knowledge of focal depths is vital.

At the start of the 21st century attempts were made to update these traveltime models by integrating a 3-D earth model into standard calculations. It has been realised by many recent authors that knowledge of precise locations of key events is needed to allow calibration and comparison between different earth models and travel-time tables. Such events generally constitute man-made events such as explosions (particularly nuclear events) where exact locations are already known and can be well constrained. Engdahl *et al.* (1998) reassessed ISC data (including 1,166 nuclear explosions and 83 earthquakes) with later phase arrivals, a modernized earth model - ak135 – that accounted for the heterogeneous nature and discontinuities of the upper mantle, and station specific traveltime corrections. They estimated an average mislocation vector of 9.4 ± 5.7 km.

The ISC developed a ‘control’ set of 157 well known events from IASPEI’s (International Association of Seismology and Physics of the Earth’s Interior) collection of Ground-Truth (GT) events. Ground-Truth is nomenclature introduced by Bondár *et al.* (2001; discussed further in Bondár *et al.*, 2004) where GTX (e.g. GT0, GT5, GT10 etc.) describes the believed accuracy of a given event within ‘X’ kilometres of the estimated epicentre. It is against these “Ground-Truth” events that the ISC’s new traveltime earth models are compared.

Hypocentre uncertainties are further constrained based upon distribution of station traveltime residuals (Storchak, pers. comm.), but are limited by being considered only as mathematical uncertainties. Bondár *et al.* (2004) assesses location accuracy for local, near regional, regional and teleseismic networks. The latter two scenario’s difference in accuracy between natural events and explosions is between 5 and 10 km. They also assess depth and origin time, finding that testing synthetic arrivals of a simplified velocity model creates hypocentre mislocations of only 0.5 km, but with uncertainties of nearly 5 km in focal depth and 0.6 seconds in origin time when using only

P-wave arrivals. Including S-wave arrivals reduces depth and origin time errors at a cost to epicentre location.

Limitations in focal depth estimations originally achieved by the ISC have already been briefly discussed. However, it is useful to know that the organisation now assigns focal depths of 0, 10, 33 and 100 km or at 50 km increments thereafter. These are now assigned either based upon ISC primary data sources, or on up-going depth phases. The latter will be well constrained if stations are located within 30 to 50 km of the event. P and S waves are used to assist in these estimations.

4.9 Magnitude conversion hierarchies

The importance of using a magnitude conversion hierarchy to develop earthquake catalogues cannot be overstated. Strategies to form homogenous magnitude scales have been adopted by Alsan *et al.* (1975), Oncescu *et al.* (1999), Grünthal and Wahlström (2003) and Burton *et al.* (2004a). A magnitude conversion hierarchy was also considered necessary in the GSHAP Project (Basham and Giardini, 1993; Johnston and Halchuk, 1993). The hierarchy employed by GSHAP is in Table 4.3.

No.	Method
1	M derived directly from M_0
2	M estimated from standard teleseismic magnitudes
3	M estimated from measured isoseismal areas
4	M estimated from regional or non-standard instrumental magnitudes
5	M estimated from quoted intensity areas, radii or magnitudes
6	M estimated from number of recording stations
7	M estimated from epicentral intensity, I_0
8	M assigned by judgement

Table 4.3 Magnitude conversion hierarchy in GSHAP (Basham and Giardini, 1993; Johnston and Halchuk, 1993)

These texts continue to discuss detailed methods for employing conversion hierarchies, with each step taking precedence over steps directly below it. Magnitude conversion hierarchies are important as they homogenize a catalogue onto specific magnitude scales and counteract inhomogeneity resulting from merging multiple catalogues that may represent two different political, geographical or seismotectonic regions. This thereby effectively removes existence and impact of any divide that is present.

Hierarchies used in this catalogue are largely restricted since a significant percentage of the area covered by it is common with that the catalogue of Burton *et al*. (2004a), and are loosely described in Table 4.4. Strategies for converting to homogenized moment and surface-wave magnitude scales are in Table 4.5 and Table 4.6 for south of 43°N and Table 4.7 and Table 4.8 for north of 43°N.

No.	Method
1	Accept source's magnitude estimate if magnitude type required is given;
2	Used relevant equation from section 4.7 to determine M_w from M_s or M_s from M_w
3	Accept m_b, use relevant equation from section 4.7 to determine M_w or M_s as appropriate
4	Accept M_L, use relevant equation from section 4.7 to determine M_w or M_s as appropriate

Table 4.4 Generalised magnitude conversion hierarchy for the creation of this catalogue

4.10 Catalogue completeness

A key requirement of any historical earthquake catalogue is to be complete and homogenous with respect to magnitude, intensity or another accepted earthquake parameter as far as possible down to a known threshold for a known time span. A number of standard methods exist that may be employed to obtain estimates for catalogue completeness. Data completeness and homogeneity is largely dependent upon availability (Makropoulos, 1978) and as such is governed by such factors as the time interval in question, geographical region, and recording instrumentation used. It is fair to assume that with time, data availability will improve in most geographical regions with implementation of more and superior monitoring methods. This will result in a gradual move away from an initial bias towards reporting only larger magnitude events. Consequently, a move away from selecting only the very extreme magnitude events being reported will allow inclusion of lower value extremes into the compiled earthquake history, thus making an '*extreme values*' analysis more representative of the regions seismicity. To incorporate as many small magnitude events as possible for the region and to provide the truest representation of its seismicity, this catalogue was truncated at a moment magnitude of 4.0 M_w (as 4.0 $M_w \cong$ 2.4 M_s whereas 4.0 $M_s \cong$ 4.9 M_w; truncating at 4.0 M_s would remove a significant number of small magnitude but well determined events; Burton *et al.*, 2004a).

The threshold to catalogue completeness is the magnitude, notionally termed after here as M_c (i.e. completeness magnitude) above which it is considered fully reported. The traditional method for estimating completeness of a catalogue uses the cumulative frequency-magnitude distribution of Gutenberg and Richter (1944; Richter, 1958). This method will be discussed and applied below as well as a standard time-magnitude distribution.

From	Comments	Conversion equation	Source
M_w		M_w	
M_w	If $M_s < 5.3$ If $M_s \geq 5.3$	$M_w = 0.56M_s + 2.66$ $M_w = 0.804M_s + 1.28$	Papazachos and Papazachou (1997) Burton *et al.* (2004a)
m_b		$M_w = 1.28M_s - 1.12$	Papazachos and Papazachou (1997) Papazachos *et al.* (1997b)
M_L		$M_w = M_L + 0.43$	Baba *et al.* (2000)

Table 4.5 Strategy for converting onto the moment magnitude scale south of 43°N

From	Comments	Conversion equation	Source
M_s		M_s	M_s
M_w	If $M_s < 5.3$ If $M_s \geq 5.3$	$M_w = 0.56M_s + 2.66$ $M_w = 0.804M_s + 1.28$	Papazachos and Papazachou (1997) Burton *et al.* (2004a)
m_b		$M_s = (1.8782 \pm 0.0222)m_b - (4.6046 \pm 0.1102)$	Rezapour and Pearce (1998)
M_L	M_L(ATH) is the local magnitude scale as recorded at the NOA.	$M_s = 1.70\ (\pm 0.05)M_{L(ATH)} - 3.59(\pm 0.22)$	Burton *et al.* (1991)

Table 4.6 Strategy for converting onto the surface-wave magnitude scale south of 43°N

From	Comments	Conversion equation	Source
M_w		M_w	
M_s		$M_w = M_s$	Oncescu *et al.* (1999), Grünthal and Wahlström (2003)
m_b		$M_w = 1.28m_b - 1.12$	Papazachos and Papazachou (1997) Papazachos *et al.* (1997b)
M_L		$M_w = M_L + 0.43$	Baba *et al.* (2000)

Table 4.7 Strategy for converting onto the moment magnitude scale north of 43°N

From	Comments	Conversion equation	Source
M_s		M_s	
M_w	If $M_s < 5.3$ If $M_s \geq 5.3$	$M_w = 0.56M_s + 2.66$ $M_w = 0.804M_s + 1.28$	Papazachos and Papazachou (1997) Burton *et al.* (2004a)
m_b		$M_s = 1.9418\ (\pm 0.0443)m_b - 4.7256\ (\pm 0.2002)$	This work
M_L	M_L(ATH) is the local magnitude scale as recorded at the NOA.	$M_s = 1.70\ (\pm 0.05)M_L(ATH) - 3.59(\pm 0.22)$	Burton *et al.* (1991)

Table 4.8 Strategy for converting onto the surface-wave magnitude scale north of 43°N

4.10.1 Cumulative frequency-magnitude modelling (Balkan extent)

Investigating an earthquake catalogue's level of completeness is critical, and concerns many areas of seismological study. The commonest method for assessing magnitude distribution and completeness of an earthquake catalogue is the Gutenberg-Richter cumulative frequency-magnitude law (i.e. $\log N_c(m) = a\text{-}bm$, where $N_c(m)$ counts the number of earthquakes with magnitude greater than M and a and b are zone-dependent constants related to seismicity of the zone). This distribution is illustrated in Figure 4.4(a)-(d) for the full catalogue (3,681 events) at cut-off magnitudes, M_C, of 4.6 M_s, 5.0 M_s, 5.4 M_s and 5.8 M_s respectively, with data presented for all magnitudes in the catalogue. Three time intervals are considered: the full catalogue (1900 to 2004), early instrumental (1900 to 1963) and modern instrumental (1964 to 2004).

Figure 4.4(a) suggests the lowest magnitude this catalogue could be considered complete in is 4.6 M_s [homogenized]. Below this value the distribution curve [for the full catalogue] starts to deviate from linearity, indicating a likely under-reporting of smaller magnitude events. This is a common characteristic of many earthquake catalogues. Viewing this catalogue in this manner suggests a lower threshold to its magnitude completeness of at best ≈4.6 M_s.

Additional lines on Figure 4.4(a) to (d) denote the b-value for each time interval considered. b-values for each section of the catalogue are an important measure of regional activity that is often used in seismic hazard studies to characterise earthquake populations (Utsu, 1971; Vere-Jones, 1970). Data representing the full time interval, and with magnitudes ≥4.6 M_s, has an a-value of 4.62 (±0.18) and b-value of 0.822 (±0.03; by least squares). Lower b-values may correspond to time intervals or geographic regions relatively dominated by larger earthquakes (Yilmaztürk *et al.*, 1998; Yilmaztürk and Burton, 1999). It is interesting to note therefore the b-value for the early instrumental period is 0.759 (±0.02), and this is the period of the large magnitude 1904 Kresna-Kroupnik, 1928 Plovdiv, and 1913 Gorna Orjahovitza earthquakes; however, a similar b-value of 0.792 (±0.02) is returned for the modern instrumental period. Although the difference between modern instrumental and early instrumental b-values is small, they can still be considered to adhere statistically to suggestions of Yilmaztürk *et al.* (1998) and Yilmaztürk and Burton (1999). b-value estimates of the frequency-magnitude distribution for similar regions from previous studies are listed in Table 4.9, allowing direct comparison with estimates obtained for the full catalogue for data above 4.6 M_s.

This catalogue however has not been filtered of its foreshock and aftershock activity (i.e. those events that are causally connected to a larger, parent earthquake) to make it Poissonian in nature. This was a conscious decision to maintain its flexibility and applicability to other areas of

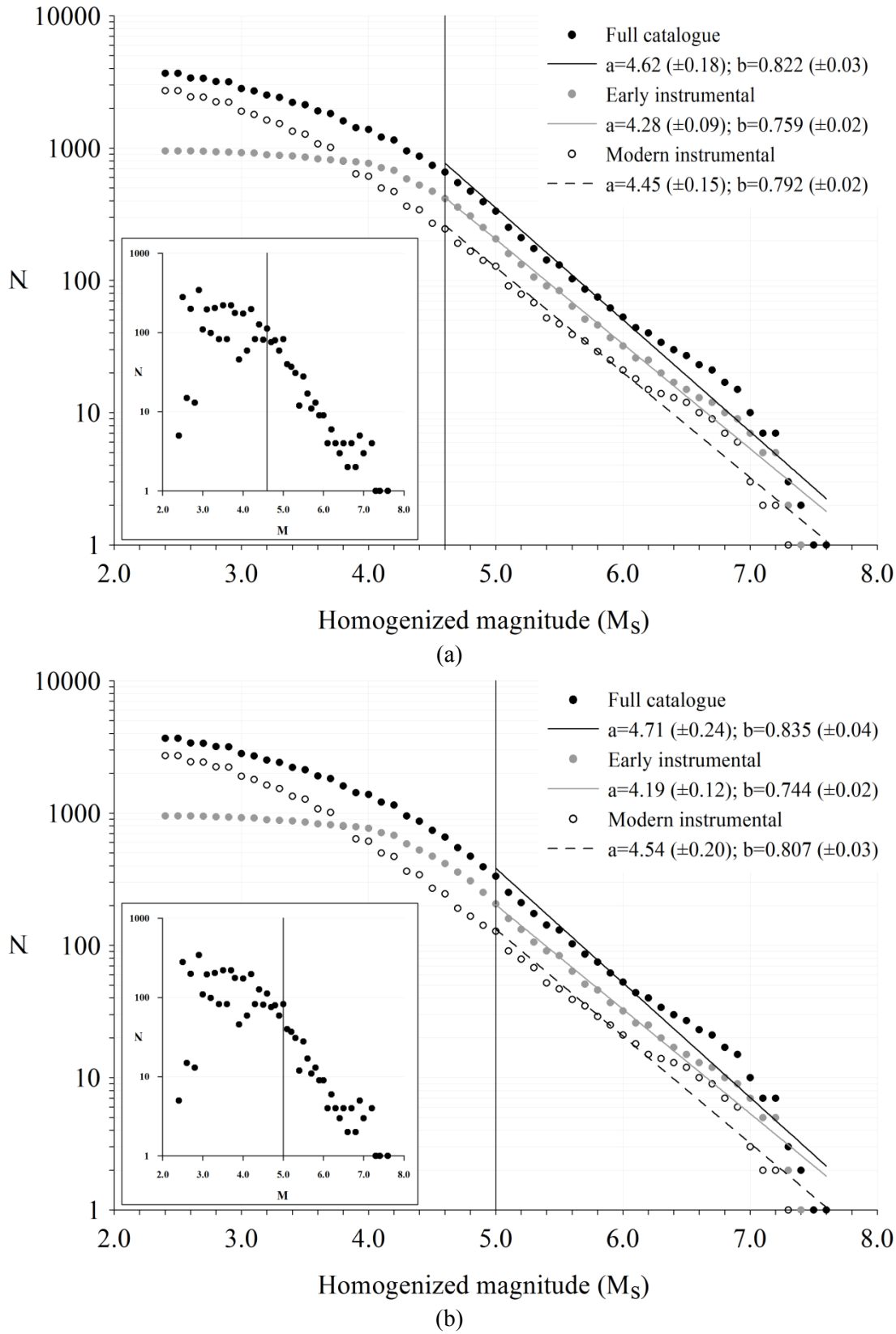

Figure 4.4 Frequency-magnitude distributions for the full Balkan catalogue: statistics given using M_C of (a) 4.6 M_s and (b) 5.0 M_s. Solid circles represent the full catalogue (1900 to 2004), grey circles the early instrumental period of recording (1900 to 1963) and hollow circles the instrumental period of recording (1964 to 2004). Data are shown for all homogenized magnitudes. Insets show magnitude-density distributions for all data with vertical lines at M_C

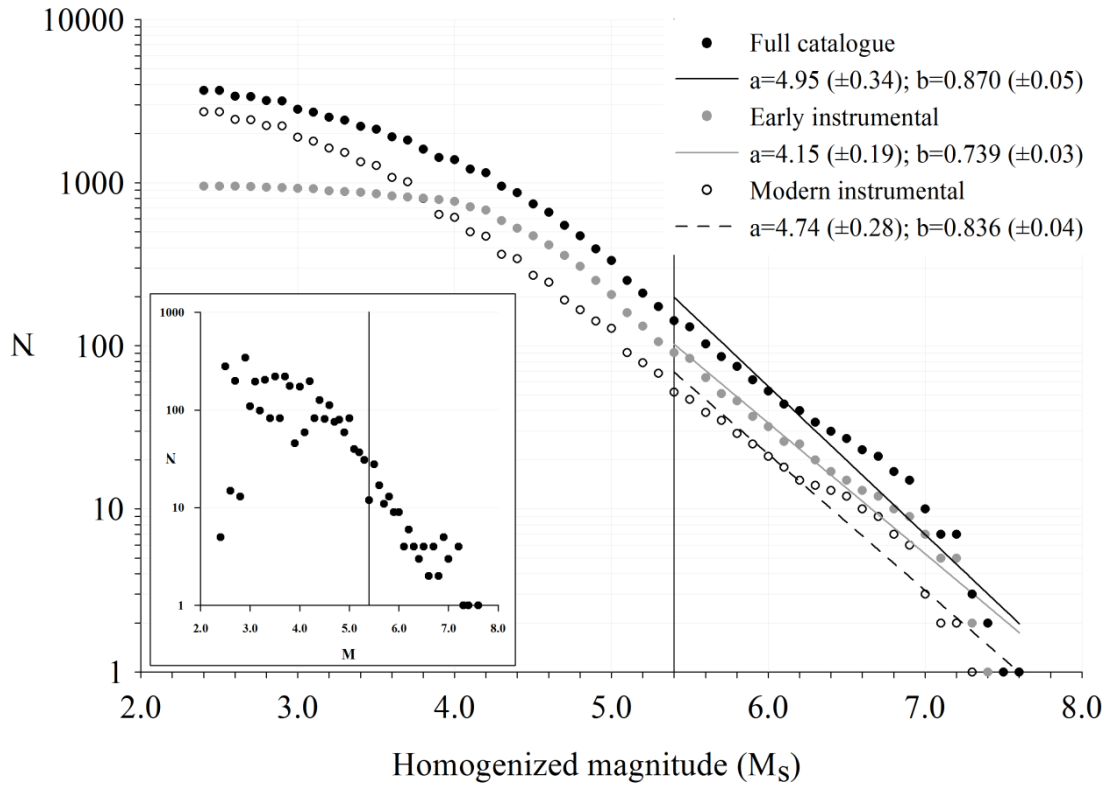

(c)

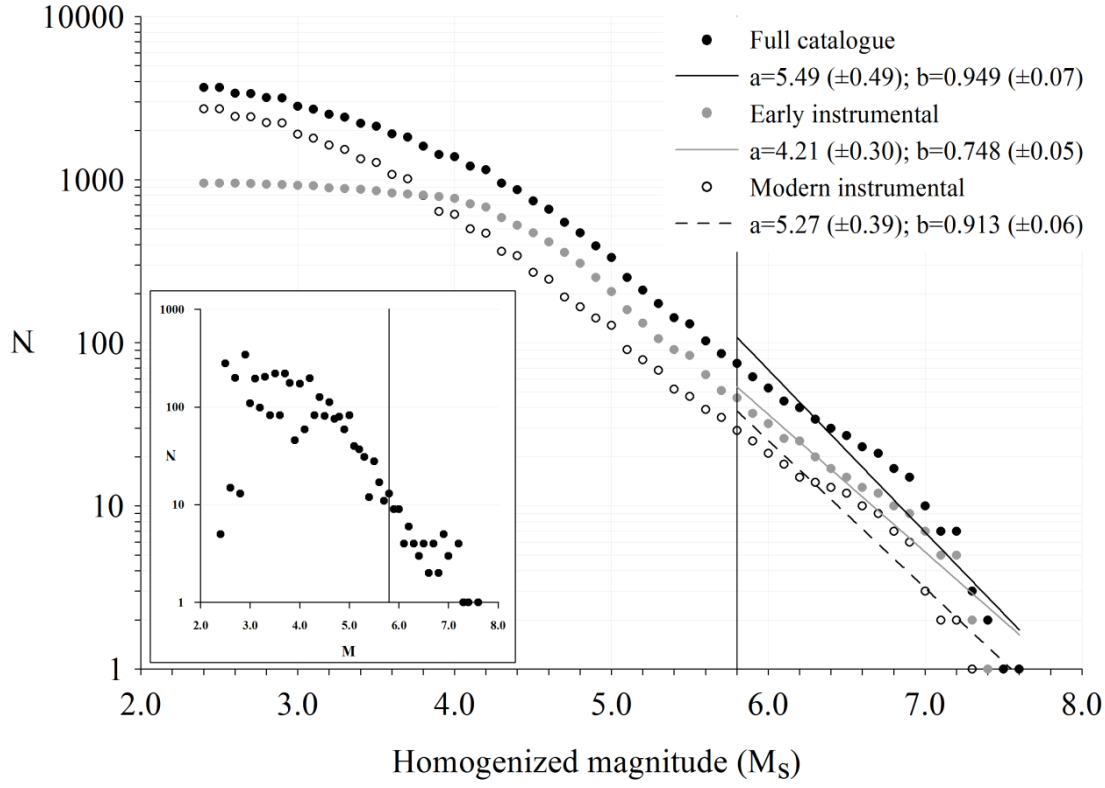

(d)

Figure 4.4 (continued) Frequency-magnitude distribution plots for the full Balkan catalogue: statistics given using an M_C of (c) 5.4 M_s and (d) 5.8 M_s, otherwise illustrations are as in (a) and (b)

Source	Geographic region	b-value	Comments
Presented catalogue	Bulgaria, the Balkans	0.822 (±0.03)	Full catalogue (1900 to 2004); using lowest realistic value for M_C of 4.6 M_s [homogenized]
Presented catalogue	Bulgaria, the Balkans	0.759 (±0.02)	Early instrumental period (1900 to 1963); using lowest realistic value for M_C of 4.6 M_s [homogenized]
Presented catalogue	Bulgaria, the Balkans	0.792 (±0.02)	Modern instrumental period (1964 to 2004); using lowest realistic value for M_C of 4.6 M_s [homogenized]
Alsan *et al.* (1975)	Turkey	0.68 (±0.01), 0.78 (±0.02)	Early instrumental and instrumental; obtained graphically
Christoskov (1982)	Bulgaria	0.83	
Papazachos (1990)	Struma and Maritsa zones	0.60	
Sokerova *et al.* (1992)	Maritsa zone	0.90 (±0.04)	
Orozova-Staniskova and Slejko (1994)	Bulgaria	0.34 (±0.03), 0.44 (±0.01), 0.39 (±0.01), 0.60 (±0.01)	Varna, Sofia, Struma, Vrancea
van Eck and Stoyanov (1996)	South Bulgaria	0.77 (±0.04) / 0.66 (±0.05)	Maximum likelihood used including/excluding aftershocks
Baba *et al.* (2000)	South Balkans, Greece and Aegean	1.17 (±0.01)	Different magnitude scale used, most similar; region to this work.
Musson (1999)	North Balkans	0.550 to 1.155	50 seismic source zones in study region (mean = 0.794).

Table 4.9 Gutenberg-Richter b-value estimates for Bulgaria and surrounding region from the presented catalogue and previous work of note derived from Figure 4.4

seismological research. Suggesting a completeness threshold, M_c, of 4.6 M_s might therefore seem ambitious. Filtering earthquake catalogues of foreshock and aftershock activity is likely to improve distribution statistics. Consequently, distribution statistics for higher magnitude thresholds are now considered. These are offered in Figure 4.4(b) to (d) for thresholds of 5.0 M_s, 5.4 M_s and 5.8 M_s respectively. It is evident from these that, for the time intervals 1900 to 2004 and 1964 to 2004, the data's b-value gradually increases systematically, while b-values for the time interval 1900 to 1963 are seen to fluctuate slightly at higher M_C after starting at a high of 0.759 at 4.6 M_s. These decreasing b-values for increasing M_C during the early instrumental period of reporting is further indication that this time interval is dominated, to some degree, by higher magnitude events, if Yilmaztürk *et al.* (1998) and Yilmaztürk and Burton (1999) ideas are accepted.

Statistics for the full time interval begin to approach values offered by Christoskov (1982), Sokerova *et al.* (1992) and Musson (1999) at and above 5.0 M_s. The most recent of these studies, Musson (1999), made his catalogue Poissonian by applying a 'space-time' window to flag potential fore and aftershock activity. Had this work's catalogue been made Poissonian its b-value would be higher so it is reasonable to suggest that its M_c is greater than 5.0 M_s, highlighting good agreement between this catalogue and other related work. Poissonian declustering of this catalogue, on both the M_s and M_w magnitude scales, to remove '*accessory*' shocks (Musson, 1999) is considered further in section 4.10.2 using recognised filtering procedures.

A magnitude-density distribution provides an alternative means by which to estimate an earthquake catalogue's lower threshold of completeness. This method was adopted by van Eck and Stoyanov (1996) on their homogenized catalogue for southern Bulgaria, and Willemann (1999) compares completeness of International Seismological Centre Bulletin data for 1994 and 1995 for a number of global seismic regions. Here Willemann (1999) suggests that where several hundred magnitude estimates are available an objective estimate for the lower bound to data completeness is indicated by the maximum of the density distribution. Insets to Figure 4.4 give such a density distribution for all data of this catalogue (with the vertical lines placed at the respective magnitude threshold).

Using the assumption outlined by Willemann (above), and noting that the distribution curve's general pattern also holds for the cumulative frequency distribution (Main, 1995) a completeness threshold of 2.9 M_s might be suggested. However, this is too low to suggest with any real confidence. This severe deviation from the Gutenberg-Richter relation therefore suggests:

- An alternative estimate for the completeness threshold of this catalogue can be suggested from this illustration. The inset to Figure 4.4(a) becomes approximately linear above 4.6 M_s, loosely following a frequency-magnitude distribution at this same magnitude. Below this

magnitude, data are widely scattered, suggesting a number of discrete magnitudes are not fully reported. However, this estimate may be biased through using the $m_b \rightarrow M_s$ conversion equation, Eq. (4-10) on approximately one third of the catalogue, and its steep gradient (Figure 4.2).

- Alternative methods for estimating catalogue completeness are required.

4.10.2 Poissonian declustering and earthquake stationarity

4.10.2.1 Bulgaria and the Balkans

The previous section assessed this catalogue's cumulative magnitude distribution in its raw form, such that any '*accessory*' shocks reported in its original data sources would have migrated over into the final formed catalogue if they met all other earthquake selection criteria invoked when compiling it. This, together with the broader catalogued region combining input from a number of neighbouring earthquake populations (e.g. Adriatic subduction zone, the North Anatolian Fault, Gulf of Corinth and Aegean area), clearly makes the data collected non-Poissonian (Gardner and Knopoff, 1974). Data collected may be non-Poissonian from one area, but Poissonian in others due to either: different – or difficult – data collection strategies; uncertainty or disagreement on the completeness magnitude for a specific sub region; having recorded an incomplete cycle of seismicity for a particular area, or; incorrect or different declustering algorithms adopted for different areas.

A catalogue unclustered of 'accessory' shocks is heterogeneous in the seismicity it captures with respect to time (Corral, 2006). The number of events retained after declustering will depend upon the number of events considered as 'main' shocks. As the emphasis of this study is to undertake a new seismic hazard assessment for the selected region using extreme value statistics, developing a new declustering algorithm to remove dependent seismic events is beyond the scope of this work. Also, declustering an earthquake catalogue before using any extreme values statistics methodology as the recurrence model, such that only *N*-year extreme magnitudes are considered, could be considered a moot issue and an inappropriate allocation of effort.

Regardless of the statistical recurrence model(s) adopted, a PSHA should assume a Poissonian distribution of the parent seismicity considered as input to the assessment. That is, each event retained in the final dataset should satisfy the fundamental need to be an independent main shock, free of all its fore- and after-shocks. PSHAs are underpinned by the general assumption they have been created from a Poissonian declustered listing of independent events. Thus the hazard itself can

be assumed to represent hazard that would emanate from independent earthquakes. Consequently, Poissonian declustering is often considered a vital preliminary step to performing a PSHA.

Three historical but still actively applied declustering algorithms that each apply different selection logic to data will therefore be adopted here to investigate the effect of removing (purging) 'accessory' shocks has on this catalogue's distribution statistics if applied to both homogenized M_s and homogenized M_w scales. These methods are summarised in Table 4.10.

Revised frequency-magnitude distributions for data filtered using the algorithms listed in Table 4.10 on (a) M_s and (b) M_w homogenized magnitude scales are shown in Figure 4.5, with indicative distribution statistics given for cut-off magnitudes of 5.0 M_s and 5.0 M_w respectively. Figure 4.5(a) is comparable to Figure 4.4(b) for unclustered data. Reporting a- and b-values at this M_C is considered acceptable as (a) the complete catalogue is considered complete at some magnitude ≥5.0 M_s and (b) previous authors (e.g. Oncescu *et al.*, 1999; Grünthal and Wahlström, 2003) note that it is acceptable to use the equality $M_s = M_w$ to convert between these scales in the region considered.

Two points are important to note from Figure 4.5. Firstly, a- and b-values are notably higher after applying each declustering algorithm on the moment magnitude scale than those for the unfiltered data (Figure 4.5(b)), thus making each slope shallower in nature (Musson, 1999), but not so on the surface-wave scale (Figure 4.5(a)). Higher b-values also indicate a higher ratio of larger magnitude events (Yilmaztürk *et al.*, 1998; Yilmaztürk and Burton, 1999), which seems logical due to exclusion of many smaller swarm events. Secondly, the downturn in all three curves at 4.0 M_w (Figure 4.5(b)) is simply a function of this catalogue's data being truncated at this lower threshold value when compiling it. Further, insets of the magnitude density plot to Figure 4.5 give good indication that the magnitude threshold to completeness is ≥5.0 M.

b-value estimates at 0.2 M_s increments between $4.6 \leq M_s \leq 5.8$ are given in Table 4.11 for the full data compared against filtered versions using methods outlined in Table 4.10. The most important pattern to appreciate on Table 4.11 is that b-values for each cut-off magnitude applied to full unclustered data are always higher than the equivalent b-values from all declustered options.

Having removed '*accessory*' shocks, data adheres closer to the ideal Poissonian distribution, such that events can now be assumed independent of each other in space due to declustering. However, for the catalogue to be truly Poissonian, event independence is required in both the space and time domain. To be independent with regards to time implies earthquake stationarity and is often a difficult requirement to achieve (Powell and Duda, 1975). Stationarity of the Poissonian process,

Source	Criteria for 'Accessory shocks'	Purging on M_w	Purging on M_s
Gardner and Knopoff (1974)	- Only removes after shocks - Sizes of distance and time windows dependent upon size of main shock, such that: M Km Days 2.5 19.5 6 3.0 22.5 11.5 3.5 26 22 4.0 30 42 4.5 35 83 5.0 40 155 5.5 47 290 6.0 54 510 6.5 61 790 7.0 70 915 7.5 81 960 8.0 94 985	- 1,854 events removed	- 1,738 events removed
Reasenberg (1985)	- Removes foreshocks and aftershocks - First event in sequence is main shock - Subsequent larger magnitude is 'larger main shock' - Fixed time window applied regardless of main shock's magnitude (320 days)	- 705 events removed	- 567 events removed
Musson (1999)	- Removes foreshocks and aftershocks - Largest magnitude in sequence is main shock - First event of two equal, largest magnitudes is taken as main shock - Fixed time window (100 days) applied regardless of main shock's magnitude	- 1,972 events removed	- 1,765 events removed

Table 4.10 Summary of selected declustering algorithms

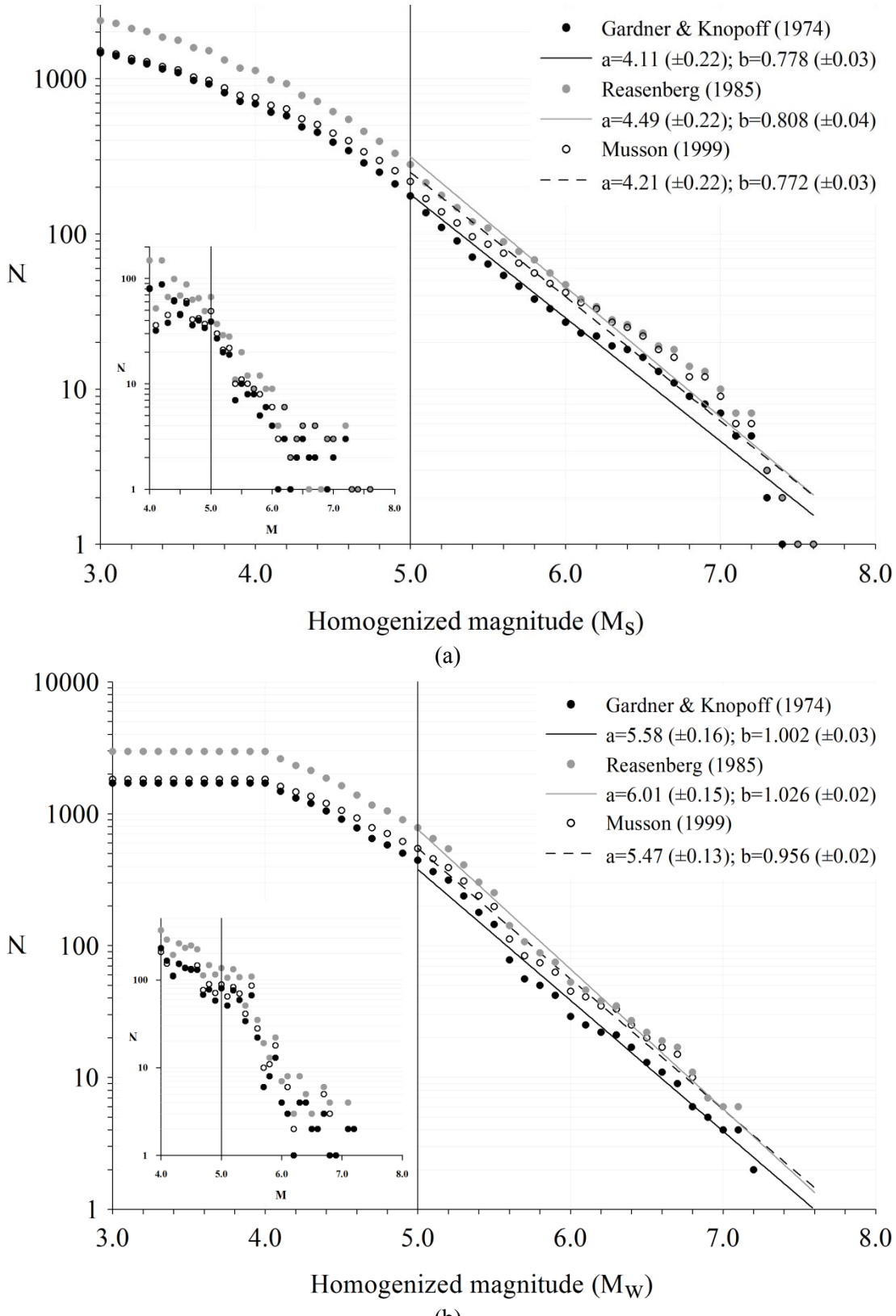

Figure 4.5 Cumulative frequency-magnitude distributions for versions of this regional catalogue Poissonian declustered using methods of Gardner and Knopoff (1974), Reasenberg (1985) and Musson (1999) on the (a) M_s and (b) M_w magnitude scales, for a cut-off magnitude, M_C, of 5.0 M_s or 5.0 M_w (depending on the declustering model adopted). The inset shows a magnitude density distribution for each solution to declustering these data

Catalogue time interval	Declustered?	# of events considered	Cut-off magnitude threshold (M_C; homogenized M_s)						
			4.6	4.8	5.0	5.2	5.4	5.6	5.8
Full catalogue (1900-2004 inc.)	No; All data	3,681	0.822 (±0.03)	0.829 (±0.03)	0.835 (±0.04)	0.847 (±0.04)	0.870 (±0.05)	0.901 (±0.06)	0.949 (±0.07)
Early instrumental (1900-1963 inc.)		955	0.759 (±0.02)	0.754 (±0.02)	0.744 (±0.02)	0.737 (±0.02)	0.739 (±0.03)	0.736 (±0.04)	0.748 (±0.05)
Modern instrumental (1964-2004 inc.)		2,726	0.792 (±0.02)	0.799 (±0.02)	0.807 (±0.03)	0.817 (±0.04)	0.836 (±0.04)	0.870 (±0.05)	0.913 (±0.06)
Full catalogue (1900-2004 inc.)	Gardner and Knopoff (1974)	1,943	0.776 (±0.03)	0.778 (±0.03)	0.778 (±0.03)	0.780 (±0.04)	0.793 (±0.05)	0.821 (±0.06)	0.857 (±0.07)
Early instrumental (1900-1963 inc.)		488	0.715 (±0.01)	0.705 (±0.01)	0.687 (±0.01)	0.672 (±0.01)	0.674 (±0.01)	0.688 (±0.01)	0.702 (±0.02)
Modern instrumental (1964-2004 inc.)		1,455	0.705 (±0.02)	0.698 (±0.02)	0.689 (±0.03)	0.672 (±0.03)	0.656 (±0.03)	0.645 (±0.04)	0.638 (±0.05)
Full catalogue (1900-2004 inc.)	Reasenberg (1985)	3,114	0.798 (±0.03)	0.803 (±0.03)	0808 (±0.04)	0818 (±0.04)	0838 (±0.05)	0867 (±0.06)	0908 (±0.07)
Early instrumental (1900-1963 inc.)		787	0.725 (±0.01)	0.719 (±0.02)	0.708 (±0.02)	0.701 (±0.02)	0.707 (±0.03)	0.715 (±0.03)	0.730 (±0.04)
Modern instrumental (1964-2004 inc.)		2,327	0.783 (±0.02)	0.788 (±0.02)	0.793 (±0.02)	0.796 (±0.03)	0.803 (±0.03)	0.821 (±0.04)	0.841 (±0.04)
Full catalogue (1900-2004 inc.)	Musson (1999)	1,916	0.757 (±0.03)	0.765 (±0.03)	0.772 (±0.03)	0.783 (±0.04)	0.807 (±0.05)	0.845 (±0.05)	0.891 (±0.06)
Early instrumental (1900-1963 inc.)		529	0.678 (±0.02)	0.670 (±0.02)	0.656 (±0.02)	0.645 (±0.02)	0.650 (±0.03)	0.662 (±0.03)	0.672 (±0.04)
Modern instrumental (1964-2004 inc.)		1,387	0.771 (±0.02)	0.785 (±0.03)	0.802 (±0.04)	0.818 (±0.04)	0.840 (±0.05)	0.877 (±0.06)	0.923 (±0.07)

Table 4.11 b-value estimates at selected cut-off magnitudes [homogenized M_s] for presented catalogue for the full Balkan extent obtained from least squares method of Aki, and declustering algorithms from Table 4.10

$$\Pr[N = x] = \frac{\lambda^x}{x!} e^{-\lambda}, \qquad x = 0, 1, \ldots$$

$$\Pr\left[T < x \leq T + \Delta T\right] = \lambda e^{-\lambda x} \Delta T$$

is such that the rate of process, λ, is not a function of time (Lomnitz, 1966) but only the total number of events in time, *t*, resulting in the physical dependence between large events is likely to be weak; an assumption that itself advocates use of extreme values theory (Lomnitz, 1994).

Plotting the accumulated number of events with respect to time is a quick and simple method to estimate and suggest periods of stationarity. Linear behaviour of this plot indicates stationarity, with the curve's slope a measure of the rate of seismicity. This particular distribution is shown in Figure 4.6(a) for all unclustered data and the three declustered versions considered in Table 4.10 and Table 4.11, and above specific cut-off magnitudes in Figure 4.6(b) (for all data only).

The full catalogue clearly has non-stationary behaviour over its entire length. This is a characteristic often seen with 'hybrid' catalogue compilations and also likely to be a result of this geographically large catalogue spanning many different zones of seismicity. However, it approaches stationary behaviour for distinct shorter time intervals; regardless of whether data is raw or declustered (Figure 4.6(a)).

However, care needs to be taken when suggesting stationary periods of seismicity, since as the time interval shortens the catalogue will start to show sub periods of 'pseudo clustering' of earthquakes, indicated by the more common shorter inter-event times, compared with rarer, longer intervals between events. Both of which an earthquake sequence must have to be a truly random process. If one considered only data above specific magnitudes, Figure 4.6(b), data appears to approaches stationary behaviour over increasingly longer time intervals as M_C increases. For example, lower M_C exhibit more distinct, smaller time intervals of possible stationarity than higher M_C. Lines plotted in Figure 4.6 start to approach linearity over the longer time intervals necessary to confidently suggest magnitude stationarity for $M_s \geq 5.0$ and $M_s \geq 5.5$. The slight increase seen at 1928 for $M_s \geq 5.0$ in Figure 4.6(b) is less apparent for $M_s \geq 5.5$, suggesting this increase in M_C results in removal of a number of larger magnitude accessory shocks relating to the 1928 Plovdiv sequence.

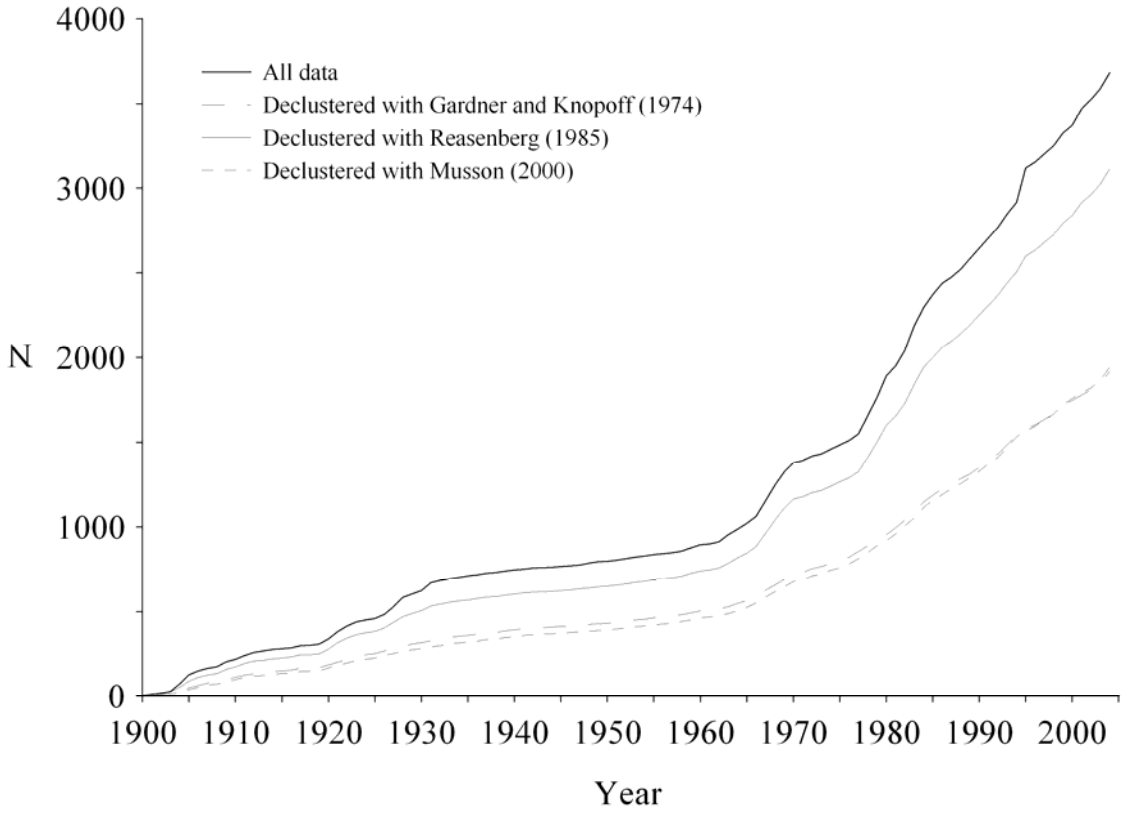

(a)

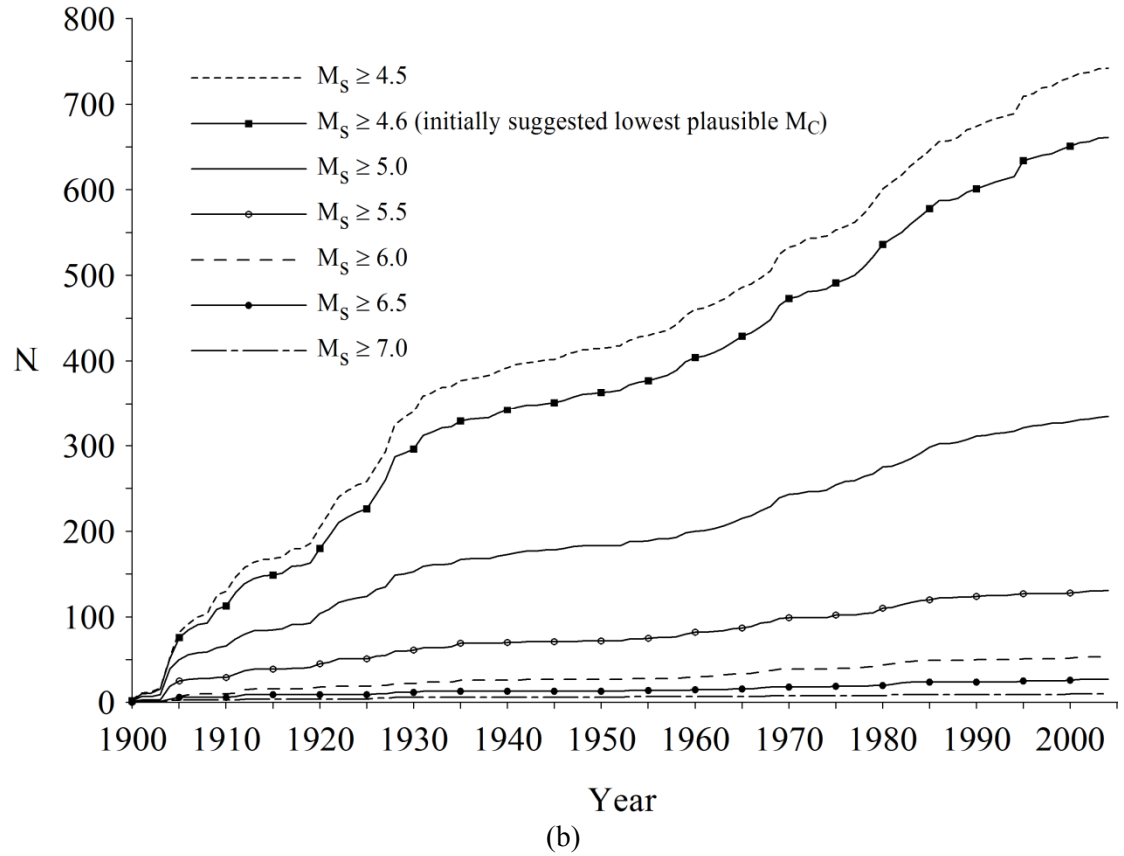

(b)

Figure 4.6 Cumulative number of earthquakes with respect to time for (a) all magnitudes and (b) all magnitudes above selected cut-off magnitudes (on the homogenized M_s magnitude scale) for the full catalogue

Seismicity rates for data truncated at a lower threshold, M_C (e.g. ≤5.0 M_s), are characterised by periods of high activity in the first 30 years of the catalogue, some of which can be related to well-known seismic sequences (e.g. 1904 Kresna and 1928 Plovdiv sequence). Plots using a cut-off of ≤5.5 M_s are clearly affected by the 1904 sequence, while the 1928 sequence is evident on plots for $M_C \leq 5.0$ M_s. As M_C increases beyond 5.0 M_s, each plot of the cumulative number of events tends to 'smooth out' to better reflect stationary earthquake behaviour.

It is important to acknowledge however, different data sources provide coverage for earlier and later portions of the full catalogue. ISC data is used in isolation for the period 1964 to 2002, and during this time interval, the magnitude threshold invoked by the ISC to review events decreased. This may account for – in part at least – the distinct changes to seismicity rates seen under lower cut-off magnitudes later in the catalogue time span. Use of ISC data for this latter period of recording could therefore be considered to '*mask*' true seismicity rates, and variation of these seismicity rates, during the modern instrumental period of recording. As the cut-off magnitude considered increases, the period of apparent stationarity extends back from 2004 to increasingly earlier time prior to 1964, so seeming to remove the effect of using different data sources for the early and modern instrumental periods of recording.

Further, if stationarity is present within the catalogue, frequency-magnitude statistics should remain constant as the time interval, seismicity or geographic area considered changes if one is considering a sufficiently long time interval to avoid issues of pseudo-clustering. Viewing distribution statistics of Figure 4.4(a) to (d)shows that as the magnitude cut-off imposed increases from 4.6 M_s to 5.0 M_s, a- and b-values of all three time intervals considered remain approximately constant (to within 0.10 M_s and 0.01 M_s respectively). Increasing the magnitude cut-off from 5.0 M_s to 5.4 M_s sees the early instrumental period retains this stable statistical behaviour, while the full catalogue and modern instrumental period of recording are forecast larger differences between a- and b-values. This continues to be true for the magnitude interval $5.4 \leq M_s \leq 5.8$.

Section 4.10.2.2 considers similar characteristics for southwest Bulgaria, while section 4.10.3 considers the effect of varying the geographic area considered upon stationarity of this catalogue.

4.10.2.2 Southwest Bulgaria

Figure 4.7(a)-(h) and Table 4.12 reproduce frequency-magnitude distributions and statistics for southwest Bulgaria bounded by 40°-43°N, 21.0°-25.5°E. This sub-catalogue contains 1,008 discrete events, the first of which occurred on January 29th 1902.

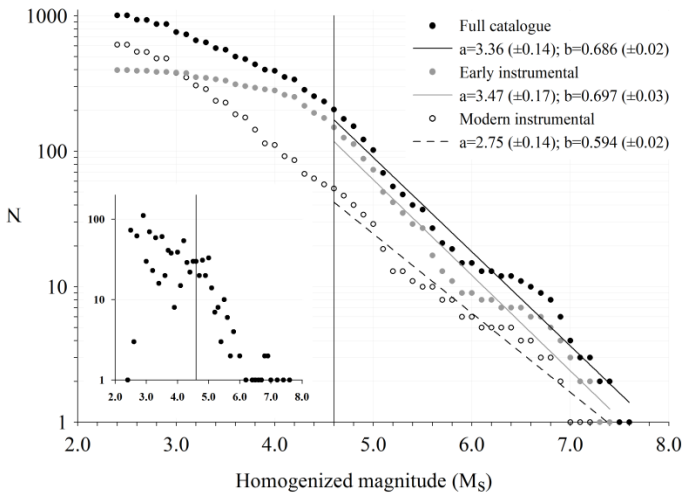

(a)

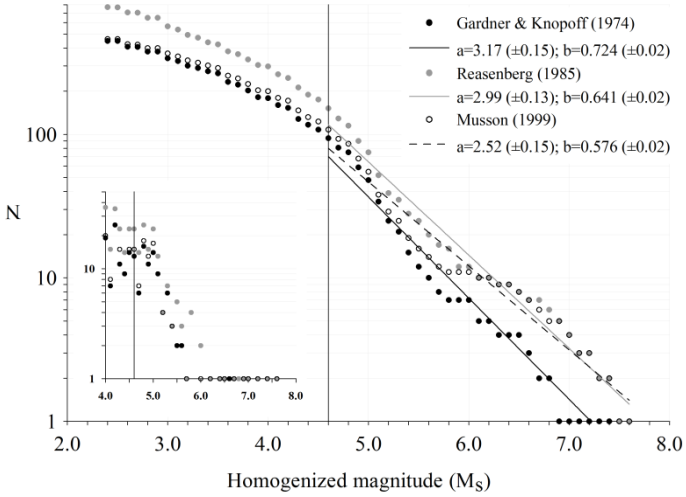

(b)

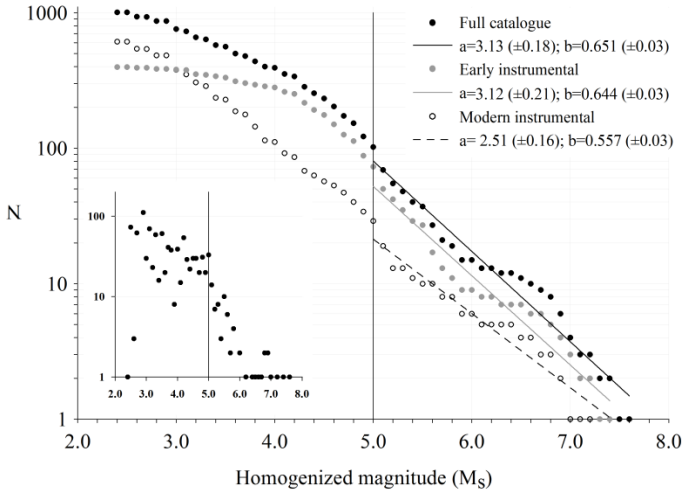

(c)

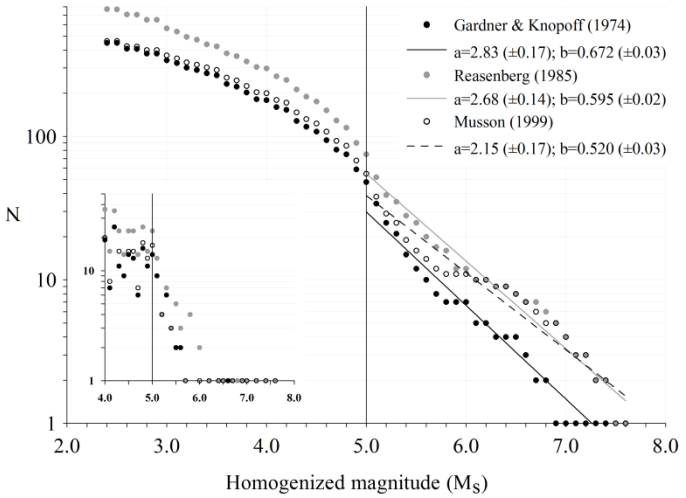

(d)

Figure 4.7 Selected frequency-magnitude distribution plots for southwest Bulgaria: statistics for cut-off magnitudes of (a)-(b) 4.6 M_s and (c)-(d) 5.0 M_s, otherwise illustrations are as in Figure 4.4. Distributions using full data are on the left; those using declustered data for 1900 to 2004 only are on the right (all use the M_s scale)

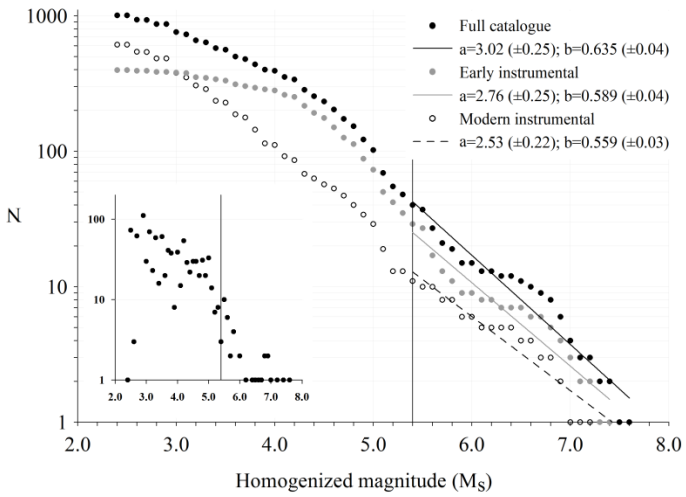

(e)

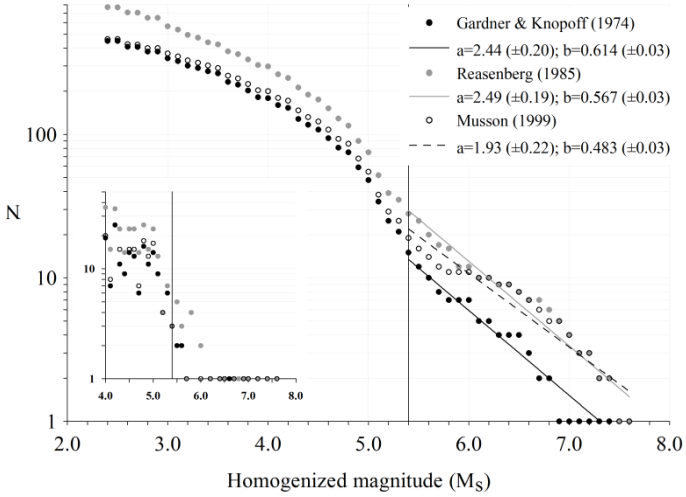

(f)

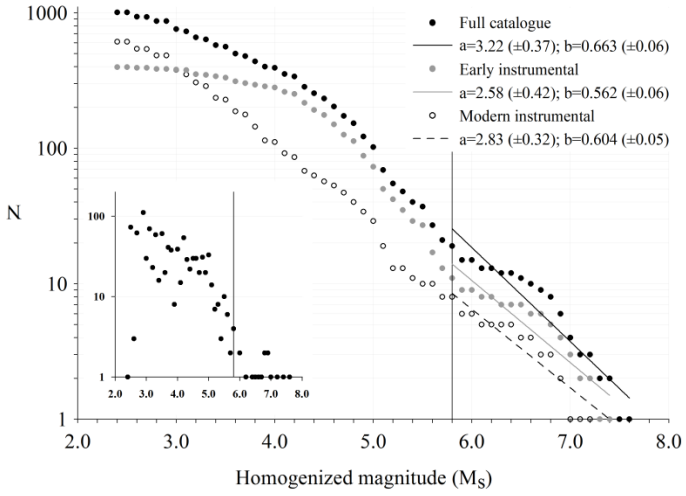

(g)

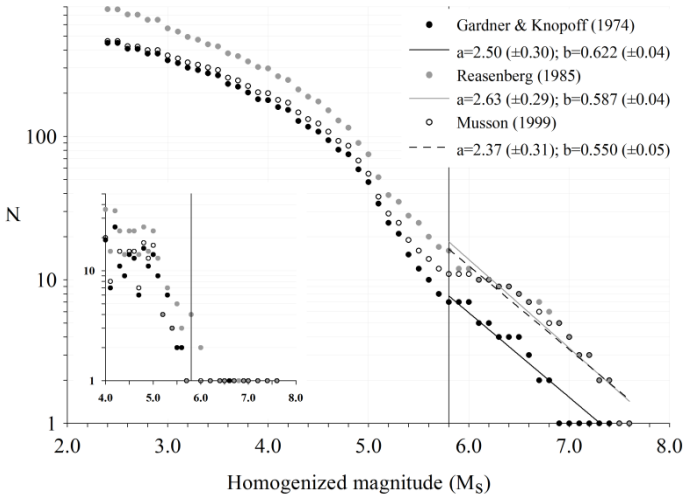

(h)

Figure 4-7 (continued) Selected frequency-magnitude distributions for southwest Bulgaria: statistics for cut-off magnitudes of (e)-(f) 5.4 M_s and (g)-(h) 5.8 M_s. otherwise illustrations are as in (a) to (d). Distributions using full data are on the left; those using declustered data for 1900 to 2004 only are on the right (all use the M_s scale)

Catalogue time interval	Declustered?	# of events considered	Cut-off magnitude threshold (M_C; homogenized M_s) 4.6	4.8	5.0	5.2	5.4	5.6	5.8
Full catalogue (1900-2004 inc.)	No; All data	1,008	0.686 (±0.02)	0.672 (±0.03)	0.651 (±0.03)	0.636 (±0.03)	0.635 (±0.04)	0.633 (±0.05)	0.663 (±0.06)
Early instrumental (1900-1963 inc.)		396	0.697 (±0.03)	0.676 (±0.03)	0.644 (±0.03)	0.615 (±0.04)	0.589 (±0.04)	0.551 (±0.05)	0.562 (±0.06)
Modern instrumental (1964-2004 inc.)		612	0.594 (±0.02)	0.578 (±0.02)	0.557 (±0.03)	0.542 (±0.03)	0.559 (±0.03)	0.582 (±0.04)	0.604 (±0.05)
Full catalogue (1900-2004 inc.)	Gardner and Knopoff (1974)	448	0.724 (±0.02)	0.705 (±0.03)	0.672 (±0.03)	0.638 (±0.03)	0.614 (±0.03)	0.609 (±0.04)	0.622 (±0.04)
Early instrumental (1900-1963 inc.)		190	0.869 (±0.03)	0.844 (±0.04)	0.786 (±0.04)	0.725 (±0.04)	0.664 (±0.05)	0.647 (±0.04)	0.718 (±0.08)
Modern instrumental (1964-2004 inc.)		258	0.524 (±0.03)	0.505 (±0.03)	0.468 (±0.03)	0.417 (±0.03)	0.384 (±0.03)	0.355 (±0.03)	Insufficient data
Full catalogue (1900-2004 inc.)	Reasenberg (1985)	769	0.644 (±0.03)	0.622 (±0.02)	0.595 (±0.02)	0.572 (±0.02)	0.567 (±0.03)	0.567 (±0.03)	0.587 (±0.04)
Early instrumental (1900-1963 inc.)		315	0.641 (±0.02)	0.614 (±0.03)	0.576 (±0.03)	0.545 (±0.03)	0.526 (±0.03)	0.513 (±0.04)	0.537 (±0.05)
Modern instrumental (1964-2004 inc.)		454	0.574 (±0.02)	0.559 (±0.02)	0.531 (±0.02)	0.498 (±0.02)	0.488 (±0.02)	0.477 (±0.03)	0.453 (±0.03)
Full catalogue (1900-2004 inc.)	Musson (1999)	461	0.576 (±0.02)	0.553 (±0.03)	0.520 (±0.03)	0.494 (±0.03)	0.487 (±0.03)	0.505 (±0.04)	0.550 (±0.05)
Early instrumental (1900-1963 inc.)		211	0.579 (±0.03)	0.537 (±0.04)	0.478 (±0.03)	0.427 (±0.03)	0.393 (±0.03)	0.392 (±0.04)	0.433 (±0.05)
Modern instrumental (1964-2004 inc.)		250	0.507 (±0.02)	0.504 (±0.02)	0.490 (±0.02)	0.474 (±0.02)	0.476 (±0.03)	0.490 (±0.03)	0.515 (±0.04)

Table 4.12 b-value estimates at selected cut-off magnitudes [homogenized M_s] for presented catalogue for southwest Bulgaria obtained from least squares method of Aki, and declustering algorithms from Figure 4.10

These estimated b-values are considerably lower for this area than the broader extent considered in earlier. Each reporting period considered exhibits reduced b-values with increasing M_C until a particular magnitude point, after which they begin to increase again. For both full and early instrumental reporting periods, this switch occurs at about 5.6 M_s, while the modern instrumental period exhibits this trend at about 5.2 M_s.

This sub-catalogue's magnitude plotting points approach linearity for data during the full time span at approximately 5.0 M_s (Figure 4.7(c) and (d)). It would appear that magnitudes greater than 6.0 M_s may be overestimated due to the homogenization process as points plotted deviate from linearity between approximately $6.2 \leq M_s \leq 7.0$. As for the full geographical extent considered, Table 4.12 provides b-value estimates for finer increments of $4.6 \leq M_s \leq 5.8$ for this sub-catalogue, compared against filtered versions using the same methods. Figure 4.8(a) and (b) plot accumulated number of events over time, in a similar fashion to the full-catalogued region in the previous section. Again, adopting lower M_C prevents periods of stationarity to be confidently suggested due to issues of pseudo-clustering of earthquakes in shorter time intervals, and predominance of shorter inter-event gaps. Stationary periods can only reasonably be suggested for higher values of M_C, which for southwest zone of interest appears to be $\geq$6.0 M_s.

4.10.3 Distribution statistics and stationarity for example analysis cells

Chapters 5 and 6 will develop a seismic hazard assessment by applying a zone-free cell analysis (Figure 3.9) to the two geographic areas. This technique applies a '*moving cell*' approach across an area using cells of a known and constant size with constant cell separation. Generally these individual cells are of 2° half-width or radius to reflect the agreed nature of general ground motion attenuating mostly within this distance.

However different cells sizes may accommodate other specific geographic or seismotectonic knowledge or a specific end aim (e.g. site specific hazard analysis; Makropoulos and Burton (1985a) and Burton (1977) respectively).

Assessing completeness over such a broad geographic area as considered here will not highlight subtle variation in sub-catalogue completeness, as it incorporates the full area seismicity within a single cell. Applying analysis cells of different sizes at a localised level has four benefits:

1. To indicate the impact of applying this earthquake catalogue on magnitude completeness at a finer resolution than before across the region considered;

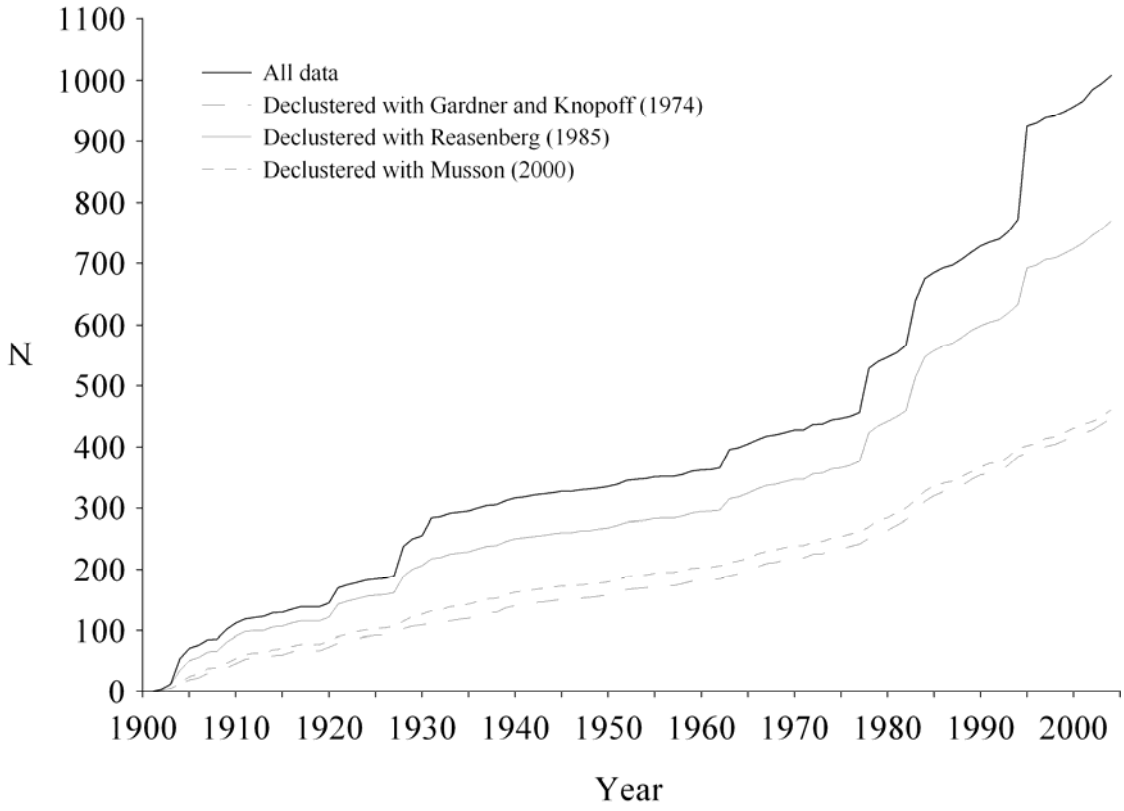

(a)

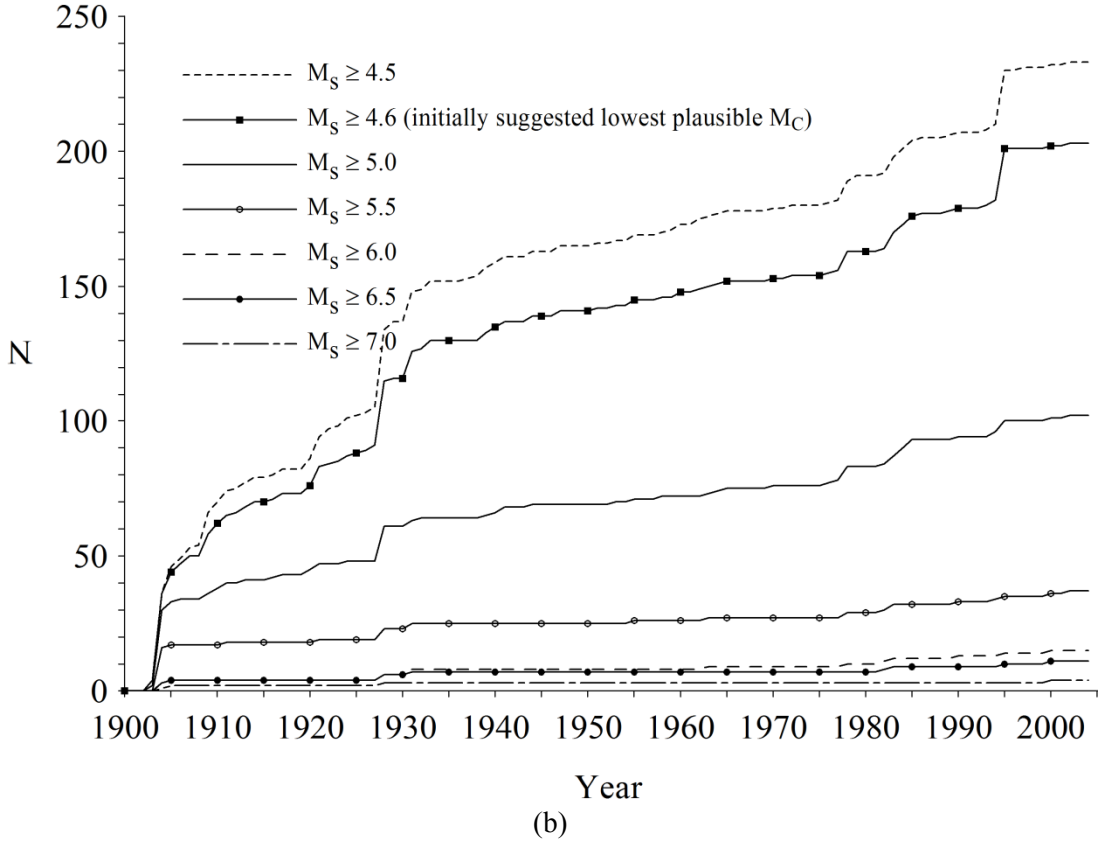

(b)

Figure 4.8 Cumulative number of earthquakes with respect to time (a) all magnitudes and (b) all magnitudes above selected cut-off magnitudes (on the homogenized M_s magnitude scale) for southwest Bulgaria

2. To help understand the low- and high-magnitude content of the region's [catalogued] seismicity in specific areas and impacts on distribution statistics at a cellular level;

3. To help define the presence, or lack thereof, of stationarity for the most important, larger magnitude events of the catalogue;

4. To help form an understanding of the ideal analysis cell size to adopt in chapter 5 and 6 (this item will be considered in greater detail in chapter 5).

For the purposes for this exercise, three points are selected in a pseudo-random nature within which the immediate area's seismicity is considered different (Figure 4.9). These are labelled '*low*' (43°N, 26°E), '*moderate*' (42°N, 23°E) and '*high*' seismicity (41°N, 21°E), and loosely reflect the number of earthquakes found within them. Seismicity present within 1° and 2° half-width cells is then assessed using frequency-magnitude distributions with a nominal M_c of 4.6 M_s (Figure 4.10(a)-(f), Figure 4.11(a)-(f) and Figure 4.12(a)-(f) respectively). In each case, distributions for all data (full, early instrumental and modern instrumental time intervals) and declustered data (full time intervals only) are presented, with declustering on the homogenized M_s scale, along with cumulative event counts using identical magnitude thresholds as in previous sections.

A nominal cut-off magnitude of 4.6 M_s to analysis was adopted in this section for two reasons; firstly, Figure 4.4 and Figure 4.6 indicate that this magnitude is the lowest that magnitude completeness could realistically be suggested for the full catalogue, and secondly, as the catalogue covers a number of different seismogenic regimes, the level of magnitude completeness is likely to vary geographically. Setting M_C to 4.6 M_s here will ensure all regions are fully considered.

This section investigates specifically the affect of varying the geographic area, and so the seismicity content within. The following discussion focuses upon images (a) and (d) of Figure 4.10 to Figure 4.12, as these represent the full catalogue; (b), (c), (e) and (f) are purely for illustrative purposes and allow comparison against the declustered versions mentioned earlier. For (c) and (f) the same logic used in sections 4.10.1 and 4.10.2 can be applied here concerning time intervals of stationary behaviour.

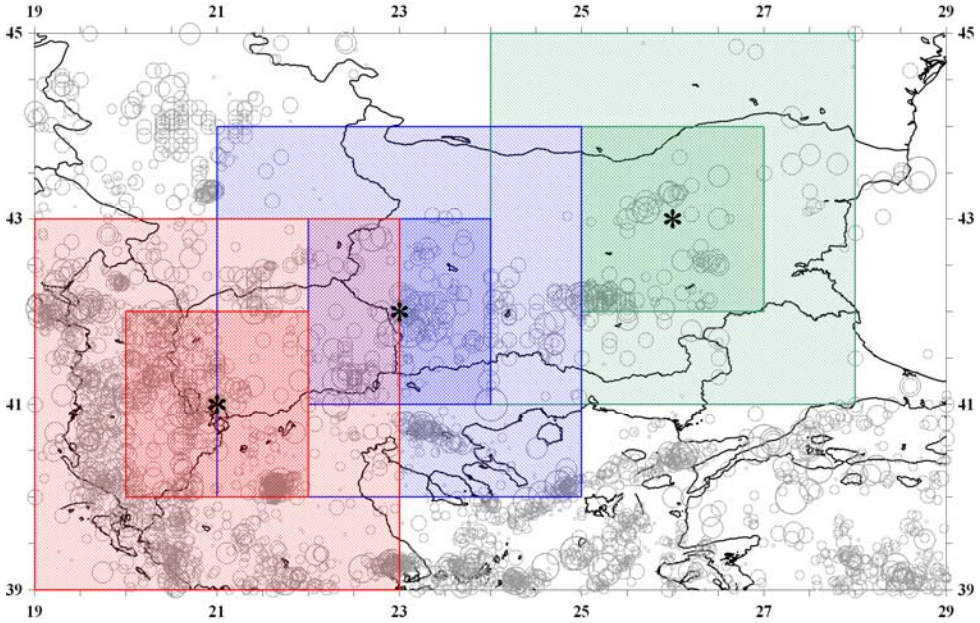

Figure 4.9 Pseudo-randomly selected points for different seismicity levels around which 1° and 2° half-width analysis cells are placed to consider magnitude completeness at a cellular level; Green frames are 'low' seismicity cells, blue are 'moderate' seismicity, red are '*high*' seismicity

The main point to note from Figure 4.10 ('*low*' seismicity) are the relatively low a- and b-values for both 1° and 2° half-width cells ((a) and (b)) when compared with Figure 4.11 and Figure 4.12. This is indicative of a bias towards both lower magnitudes and frequency levels of seismicity, with the majority contained during the early instrumental period (shown by grey circles shadowing black circles closely in both Figure 4.10(a) and (b)). It would be reasonable to expect some analysis cells not to contain enough seismicity to allow forecasting of extreme hazard, creating blank areas of '*null*' forecasts. If this were the case, one might expect the northern and eastern edges of the broad region (Figure 4.9) to be lacking any hazard forecasts.

Curves of the cumulative number of events above specific cut-off magnitudes for each cell size considered, (c) and (f) in Figure 4.10 to Figure 4.12, offer interesting insight into stationarity across the region. For '*low*' seismicity cells (Figure 4.10), the full catalogue (heavy black line) approximates to the same distribution for both 1° and 2° half-width cells. After the early period up to 1928, seismicity rates for both cell sizes approximate to a lower, more constant rate of seismicity, with the only noticeable rate change punctuating this during 1986, due to seven individual events of that year.

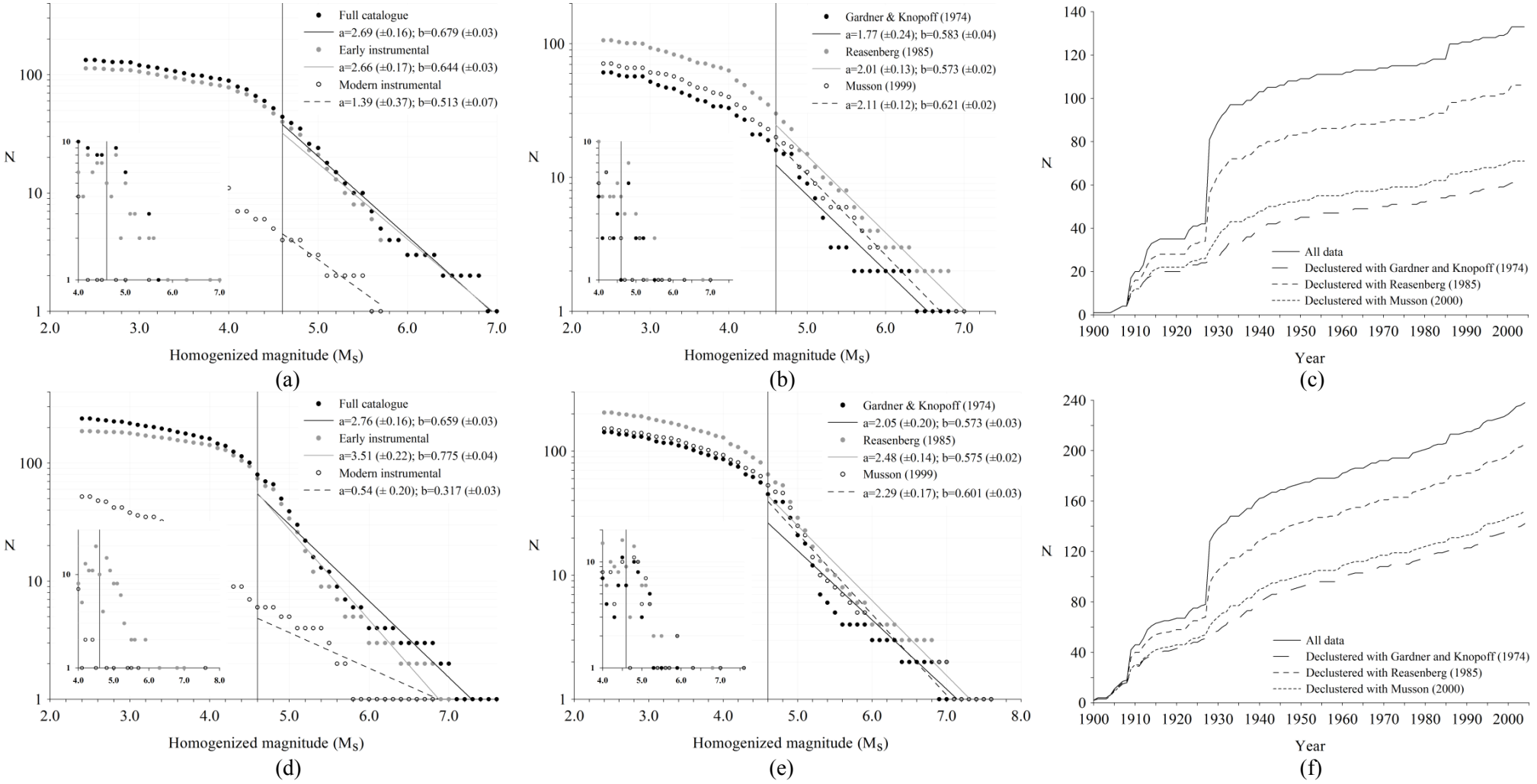

Figure 4.10 Frequency-magnitude distributions for hazard cells centred on 42°N, 23°E with (a)/(b) 1° half-width and (d)/(e) 2° half-width, for a cell of 'low' seismicity within the full area. Distributions for full data with statistics using cut-off magnitude of 4.6 M_s are on the left; those for declustered data (1900 to 2004 only) are in the centre. The cumulative number of events with respect to time are shown in (c) and (f)

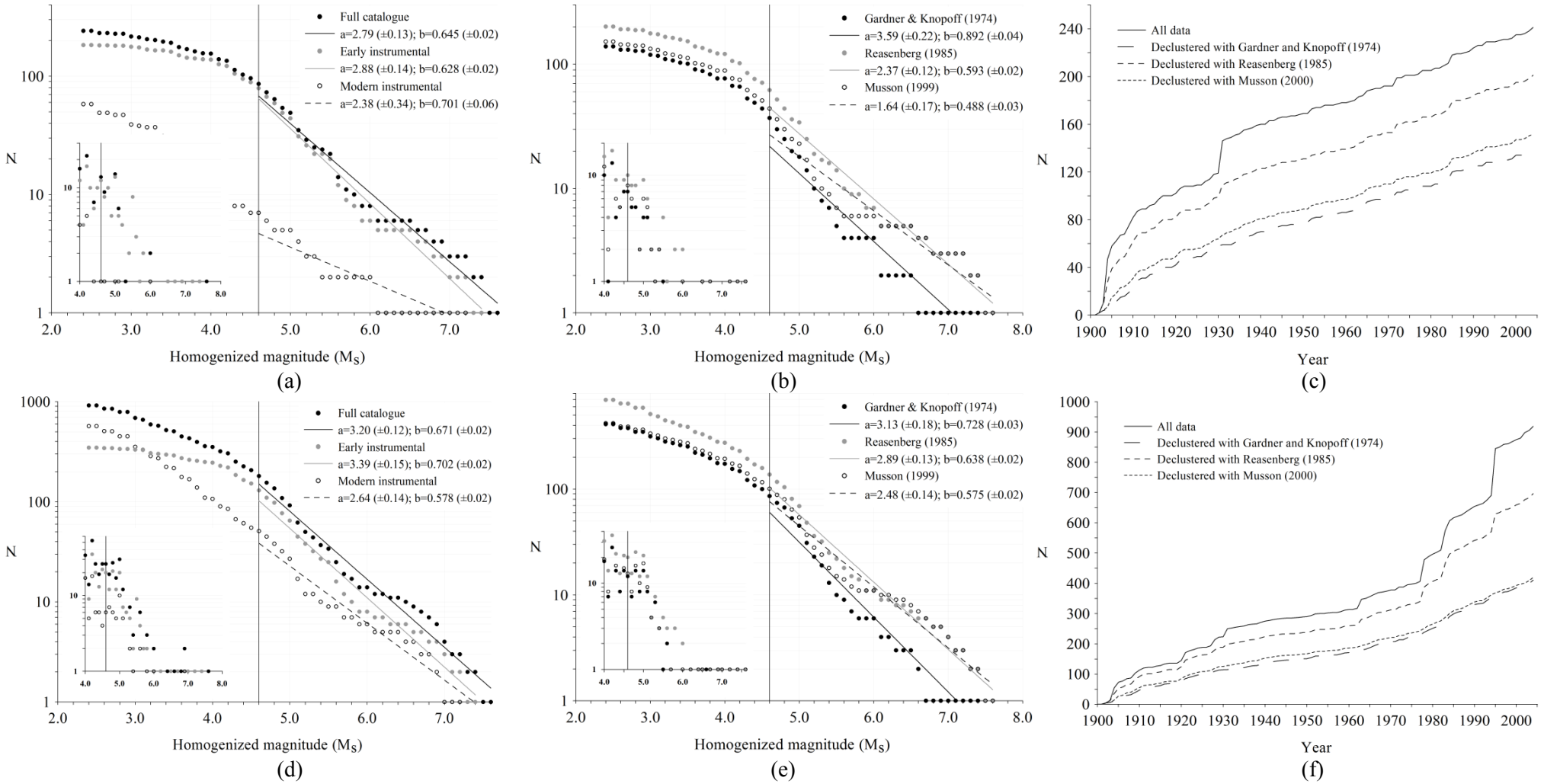

Figure 4.11 Frequency-magnitude distributions for hazard cells centred on 42°N, 23°E with (a)/(b) 1° half-width and (d)/(e) 2° half-width, for a sub-region of 'moderate' seismic activity within the full area. Distributions for full data with statistics using cut-off magnitude of 4.6 M_s are on the left; those for declustered data (1900 to 2004 only) are in the centre. (c) and (f) are as in Figure 4.10

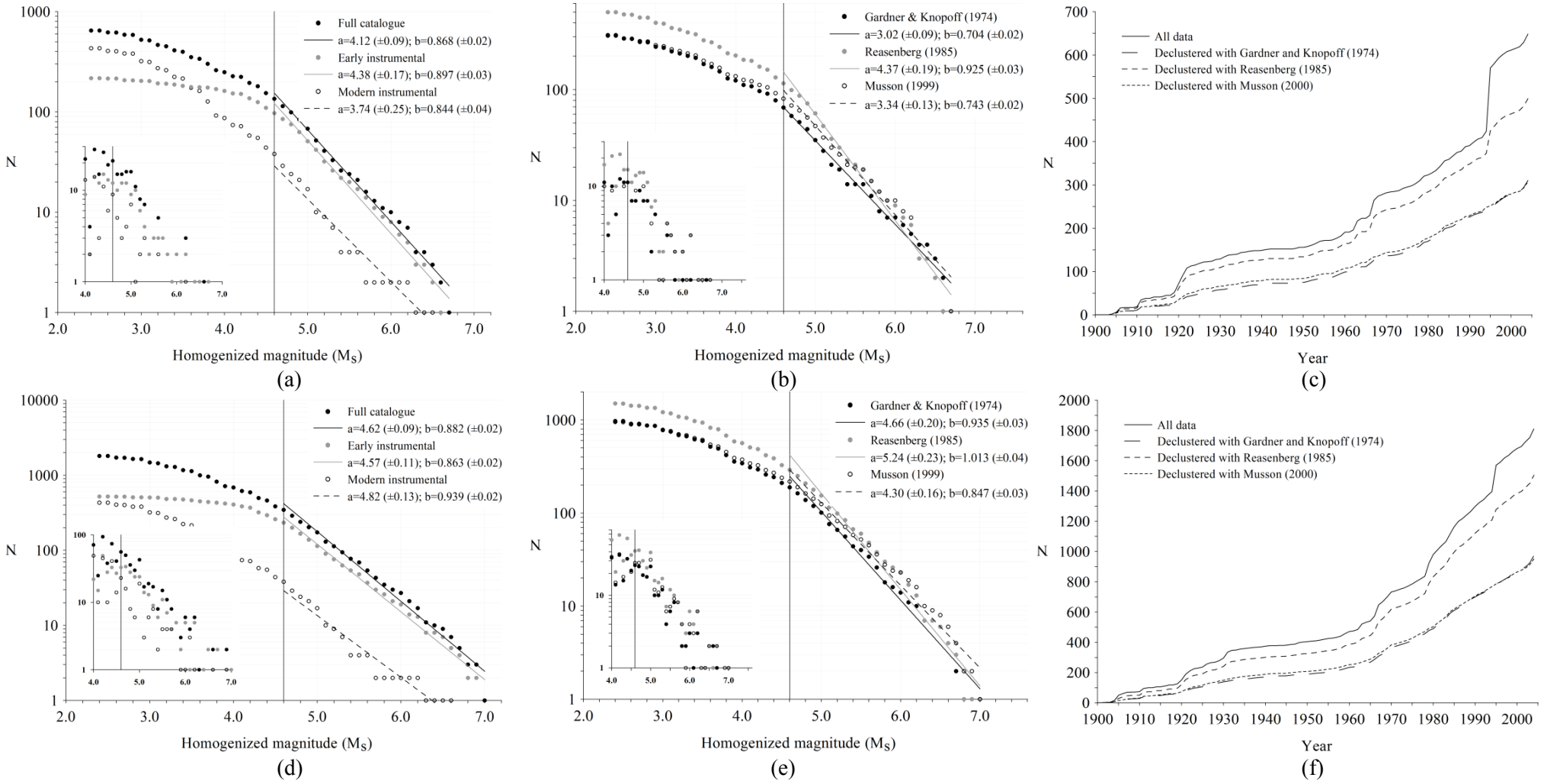

Figure 4.12 Frequency-magnitude distributions for hazard cells centred on 41°N, 21°E with (a)/(b) 1° half-width and (d)/(e) 2° half-width, for a sub-region of 'high' seismic activity within the full area. Distributions for full data with statistics using cut-off magnitude of 4.6 M_s are on the left; those for declustered data (1900 to 2004 only) are in the centre. (c) and (f) are as in Figure 4.10

'*High*' seismicity cells (Figure 4.12) also appear to follow similar patterns of seismicity rate change for both cell sizes. Again, the most noticeable rate changes are seen at the same points, with a general trend of seismicity rates increasing with time. In both (c) and (f), a pronounced increase in seismicity rates is seen during the 1960s and 1970s. These changes may relate to the introduction of the WWSSN and improvements by the ISC in collecting and reviewing earthquake phase data. If this were the case however, one might expect to observe similar marked increases in seismicity rates during this time interval in (c) and (f) of all three figures, but this is not so. It is unlikely that the WWSSN would have such a localised effect as to monitor seismicity in one sub-region of a country, but not in another at only [approximately] 600 km in the same country.

'*Moderate*' seismicity cells exhibit notably different patterns of seismicity rates between 1° and 2° half-width cells, with the 1° cell approximating to the distribution of '*low*' seismicity cells, and the 2° cell approximating to the distribution of '*high*' seismicity cells. This apparent divide would suggest cells of approximately 2° half-width may be most suited for considering this region's seismicity, if one expects some sub-regions may not provide suitable forecasts to contour if smaller cells are used.

Poissonian stationarity of this catalogue over its full time span appears to reduce as the analysis cell size increases. Considering only the full time interval (black) in each case, a- and b-values of both analysis cell sizes differ by only 0.1 M_s and 0.02 for the '*lowest*' seismicity case. These increase to 0.4 M_s and 0.03 for '*moderate*' seismicity, while the '*high*' seismicity case only sees an increase in difference between the a-values of 0.5 M_s. The difference between b-values in this last instance is only ~0.01, suggesting stationarity may be being approached in this situation.

Finally, it is interesting to briefly discuss images (b) and (e) of Figure 4.10 to Figure 4.12, for declustered data. In each, declustering has the noticeable effect of bringing plotted lines for each considered time interval nearer each other. Earlier discussion suggested most of the unfiltered catalogue's content was to be found in the early instrumental period, 1900 to 1963. By declustering data, the distribution curves moved closer to each other, indicating the early period of recording – obtained solely from Shebalin *et al.* (1998) – was dominated by a significant amount of clustering that were not systematically removed by magnitude thresholds (Table 4.1) imposed during compilation of their original data (notably data cut on unhomogenized – m_b and M_s – magnitude scales as opposed to homogenized – M_w and M_s – scales).

It is important to remember that the preceding discussion only considers six analysis cells, selected randomly across the region of interest, and only incorporates two different cell sizes. Suggestions outlined above are therefore only indicative of the full region's seismicity.

4.10.4 Time-magnitude distribution

Time-magnitude distributions have been used before to assess catalogue completeness. Makropoulos and Burton (1981) and Stepp (1973) both use this method on homogenized Greek magnitude estimates, and epicentral intensities for the Puget Sound region of Canada respectively; a similar method is used here. The numbers of earthquakes reported in this catalogue per decade are shown (except for the final time sub-interval, which covers 5 years) for specific magnitude intervals, in Figure 4.13. The values used to create the time-magnitude distribution plot and provide a synopsis of catalogue content are given in Table 4.13.

Events are classified into seven magnitude intervals: $M_s \leq 4.0$, $4.0 \leq M_s < 4.5$, $4.5 \leq M_s < 5.0$, $5.0 \leq M_s < 5.5$, $5.5 \leq M_s < 6.0$, $M_s \geq 6.0$ and *all* magnitudes. Figure 4.13 suggests that all events in magnitude interval $4.5 \leq M_s < 5.0$ are reported back to the decade 1930 to 1939, and events in magnitude interval $5.0 \leq M_s < 5.5$ are fully reported throughout the catalogue time span. A gradual fluctuation in the numbers reported at this magnitude interval (i.e. $5.0 \leq M_s < 5.5$) suggests time-varying seismicity might be occurring during the period of the catalogue. Two distinct peaks are seen at 1920 to 1929 and 1970 to 1979/1980 to 1989, suggesting a shorter periodicity for events in this magnitude interval. The magnitude interval $4.5 \leq M_s < 5.0$ exhibits similar fluctuations across the full time interval suggesting a shorter time interval for a complete seismic cycle for events in this magnitude to that suggested for the interval above; one should expect short term fluctuations in seismicity if a random process is assumed. A gradual decrease in the number of events reported for magnitudes of $M \geq 5.5$ over the full time interval suggests this may be only part of a longer period of time-varying seismicity for this magnitude interval, i.e. longer than the length of the catalogue.

Had the data only shown a gradual increase in numbers reported for a particular magnitude interval over time, it might be plausible to suggest this was resulting from an increasing sampling time interval. However, with Figure 4.13 showing gentle fluctuations in two different magnitude intervals ($4.5 \leq M_s < 5.0$ and $5.0 \leq M_s < 5.5$), it is more likely to be a result of a statistical fluctuation in activity.

Significant increases in the total number of reported events in the decade 1960 to 1969 and thereafter simply reflects the introduction of the WWSSN in this decade, and the proliferation of globally seismological data. Since then, the number of smaller magnitude earthquakes with magnitudes ≤ 4.0 M_s reported has increased significantly as a result of a continual increase in sensitivity of recording stations, number of recording stations accessible and geographical coverage of seismological stations improving.

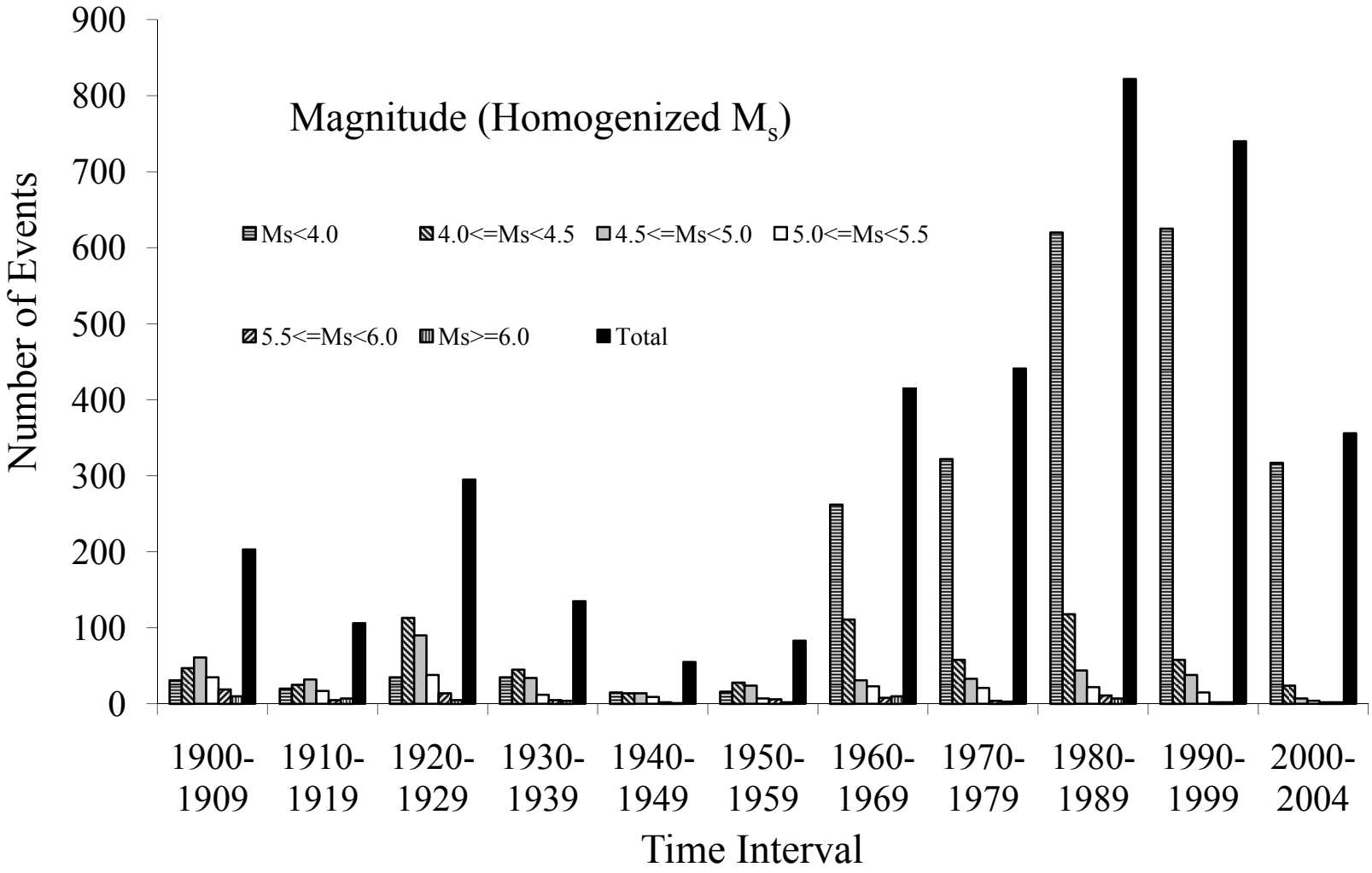

Figure 4.13 Catalogue completeness; this catalogue presented in discrete magnitude and time intervals. All data are represented (i.e. 1900 to 2004, homogenized $M_s \geq 2.4$)

Period	$M_s \leq 4.0$	$4.0 \leq M_s < 4.5$	$4.5 \leq M_s < 5.0$	$5.0 \leq M_s < 5.5$	$5.5 \leq M_s < 6.0$	$M_s \geq 6.0$	Total
1900-1909	31	47	61	35	19	10	203
1910-1919	20	25	32	17	5	7	106
1920-1929	35	113	90	38	14	5	295
1930-1939	35	45	34	12	5	4	135
1940-1949	15	14	14	9	2	1	55
1950-1959	16	28	24	7	6	2	83
1960-1969	262	111	31	23	8	10	445
1970-1979	322	58	33	21	4	3	441
1980-1989	620	118	44	22	11	7	822
1990-1999	625	58	38	15	2	2	740
2000-2004	317	24	7	4	2	2	356
Total	2,298	641	408	203	78	53	3,681

Table 4.13 Time-magnitude distribution statistics for the presented catalogue: the number of events is given in discrete magnitude intervals of 0.5 M_s, and for time-intervals of 10 years (except for the final time interval which is five years)

A progressive expansion of the Bulgarian seismograph monitoring network was seen through the 1960s, 1970s and 1980s. This is reflected in the increased numbers of magnitude $4.0 \leq M_s < 4.5$ events being reported to between 55 and 112 for a decade. The 1960s and 1970s saw Bulgaria's network expand using 3-component seismometers to encompass more of the seismogenic zones (Glavcheva *et al.*, 2003). A further expansion of the network was seen in mid-1980 after the 1977 Vrancea earthquake sequence. This significant increase in numbers of events reported with magnitude <4.5 M_s after 1960 suggests that reporting of these events is severely incomplete before this time. The use of the expanded network of seismometers within Bulgaria obviously has an effect on the threshold of magnitude completeness able to be reported. Finally, it is worth noting the ISC started receiving data from Sofia, Bulgaria in December 1952. However, data provision was very infrequent (amounting to a few deliveries in 1952 and 1964) until continuous supply commenced in January 1991 until the present day. To compensate for this, estimates of earthquake hypocentres were derived from other agencies contributing phase data at the time.

4.11 Catalogue format

The format of this catalogue follows that outlined in Burton *et al*. (2004a). Strictly adhering to these criteria should allow consistent and easy joining of these two catalogues to enable probabilistic seismic hazard studies of a region of greater extent than is possible through using any one of these catalogues in isolation. It is useful at this point to briefly clarify the order and formatting of this and the Greek catalogue's fields:

YEAR (F4.0), MONTH (F3.0), DATE (F3.0), HOUR (F4.0), MINUTE (F3.0), SECOND (F7.2), LATITUDE (F8.2), LONGITUDE (F8.2), DEPTH (F7.1), HOMOGENIZED_MW (F8.1), HOMOGENIZED_MS (F8.1), MB_REPORTED (F8.1), MS_REPORTED (F8.1), MW_REPORTED (F8.1), ML_REPORTED (F8.1)

HOMOGENIZED_MW and HOMOGENIZED_MS are moment and surface-wave magnitude calculated from the reported m_b, M_s, M_w and M_L magnitude estimates, and using the magnitude conversion equations and magnitude conversion hierarchies outlined earlier. The above format is consistent with Burton *et al.*'s (2004a) catalogue.

Homogenized magnitude estimates on both moment and surface-wave scales are provided for two reasons. First, a need for consistency between the Greek catalogue and this is required (as detailed above); second, to enable consistent hazard calculations with past studies in the magnitude scale(s) used.

However, this second point, i.e. which magnitude scale(s) are best to use for calculations, is still a contentious issue as even now authors are in two minds regarding this. Grünthal and Wahlström (2003) state "*Seismic hazard calculations are currently based mostly on M_w magnitudes, which, unlike other magnitude concepts, do not saturate for strong events. Most strong motion relations refer to M_w*". Their work was strongly based around the Global Seismic Hazard Assessment Program (GSHAP) which itself was based heavily on use of the seismic moment, M_0. This measurement can be closely tied to the moment magnitude scale M_w. Burton *et al.* (2004a), in agreement with Grünthal and Wahlström (2003) points out that preparation of an earthquake catalogue should logically be on the moment magnitude scale, M_w, to enable consistent description of an earthquake size. However, they then provide pragmatic reasoning behind supplementing each event with a homogenized surface-wave scale as "*...seismic hazard attenuation laws are still more often expressed in terms of M_s than M_w*".

Consequently, this catalogue reports all earthquakes on both homogenized M_w and M_s magnitude scales, and results in chapters 5 and 6 are – unless otherwise stated – reported using M_s.

4.12 Summary

A new earthquake catalogue for the instrumental period of seismological recording has been created for the central European and Balkan region bounded by 39°-45°N, 19°-29°E. Given limitations with previous catalogues in terms of time intervals covered, magnitude inhomogeneity and completeness, geographical extent and data content, the task was set to derive a new data source that met explicit requirements for this seismic province and defined as complete as possible the seismicity of the region for the time interval 1900 to 2004.

Data sources used have been restricted to those considered as accurate and complete as possible for the time sub-interval and geographical region considered. Only one data source was used to represent any given time interval (i.e. no two sources were merged) down to individual years. These data sources in the catalogue presented here are:

- 1900 to 1963: 39°-45°N, 19°-29°E – historical catalogue of Shebalin *et al.* (1998);
- 1964 to 2002: 39°-45°N, 19°-29°E – hypocentre database of the International Seismological Centre;
- 2003: 39°-45°N, 19°-29°E – hypocentre database of the National Earthquake Information Center, USGS;

- 2004: 39°-45°N, 19°-29°E – hypocentre database of the Institute of Geodynamics, National Observatory of Athens (NOA).

Reported magnitudes for all 3,681 events have been converted onto homogenized moment magnitude and surface-wave magnitude scales using a selection of carefully chosen magnitude conversion equations, and magnitude conversion hierarchies have been developed to enable consistent conversion from reported m_b, M_s, M_w and M_L magnitude estimates onto these homogenized moment and surface-wave scales. All these steps enable magnitude homogeneity to be retained across the data throughout the geographical region.

International Seismological Centre data has often been used to derive $m_b \rightarrow M_s$ magnitude regression equations for regions of the world. New region-specific regression equations have been developed from relevant ISC data to enable conversion from the m_b magnitude scale onto the M_s magnitude scale. These have then been compared to previously created equations derived for similar regions of study and data sets.

Catalogue completeness is a major issue of concern for seismologists using earthquake catalogues as a tool to develop seismic hazard analyses. Completeness is strongly governed by data availability, which in turn is linked to the geographical region in question and time interval considered. A number of standard methods have been adopted here to suggest possible limits on completeness in the catalogue presented. Each differ from the others, depending upon whether they suggest a magnitude completeness threshold for the full catalogue, or a sub-interval of time and magnitude within it. An approximate agreement for the lowest possible completeness magnitude, M_c, of approximately 4.6 M_s – at best – is suggested by a cumulative frequency-magnitude distribution and the time-magnitude distribution histogram for this catalogue. However, extreme caution must be taken with this estimate due to the conscious decision not to filter this database of fore and aftershock sequences prior to completeness analysis.

It is therefore more reasonable to expect M_c to be $\geq$5.0 M_s for both geographic regions considered in this chapter. This is supported by additional analysis shown in Figure 4.4, Figure 4.6, Figure 4.7 and Figure 4.8. Knowledge relating to the catalogue's likely threshold to magnitude completeness, M_c, may be taken forward into chapter 5 to further refine its estimate and continue to determine a precise value for the cut-off magnitude, M_{CUT}, at which catalogue data should be truncated to perform an extreme values-orientated seismic hazard analysis. M_c and M_{CUT} may not necessarily be identical due to the effects of *whole* and *part process* magnitude models.

Section 4.10.2 covers the vital issue of declustering an input data catalogue of fore- and aftershocks to define a parent distribution of independent main events, and continues to perform some exploratory analysis on the affects of three current declustering algorithms, and the affect of analysis cell size and contributing levels of seismicity. Although declustering earthquake catalogues is an agreed vital step to performing a PSHA, adopting an extreme values approach to hazard analysis is considered to mitigate the need to actively clean the data in this instance. Therefore, the full data catalogue will be used in the final analysis (chapters 5 and 6), after determining fit-for-purpose catalogue filtering criteria (section 5.3).

The final content of this catalogue in terms of epicentral location and event magnitude is plotted in Figure 4.14(a). It is this catalogue that will be used to develop a full probabilistic seismic hazard assessment of Bulgaria and its surrounding region, before focusing upon the southwest region of the country using extreme values, cumulative strain energy release techniques and perceptibility. Figure 4.14(b) plots the earthquakes found in the southwest Bulgarian “triple junction” region. Appendix 3 summarises the dimensions of this new catalogue and provides its full listing.

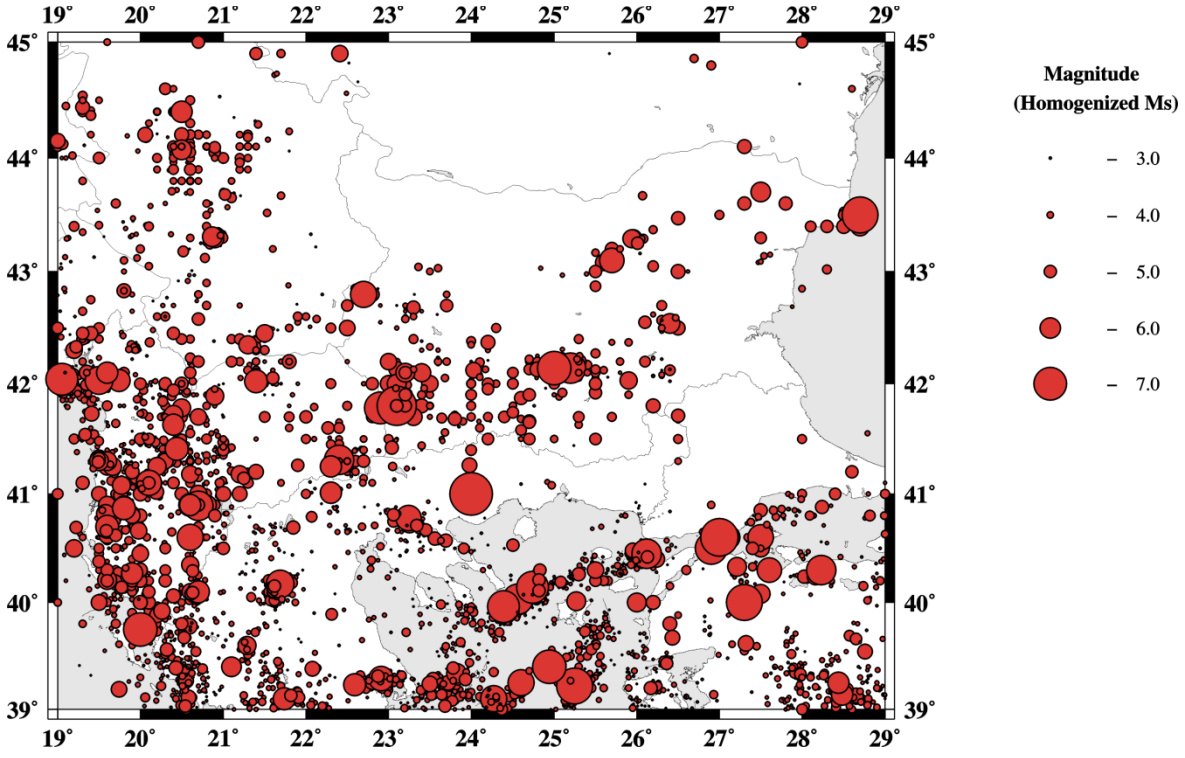

(a)

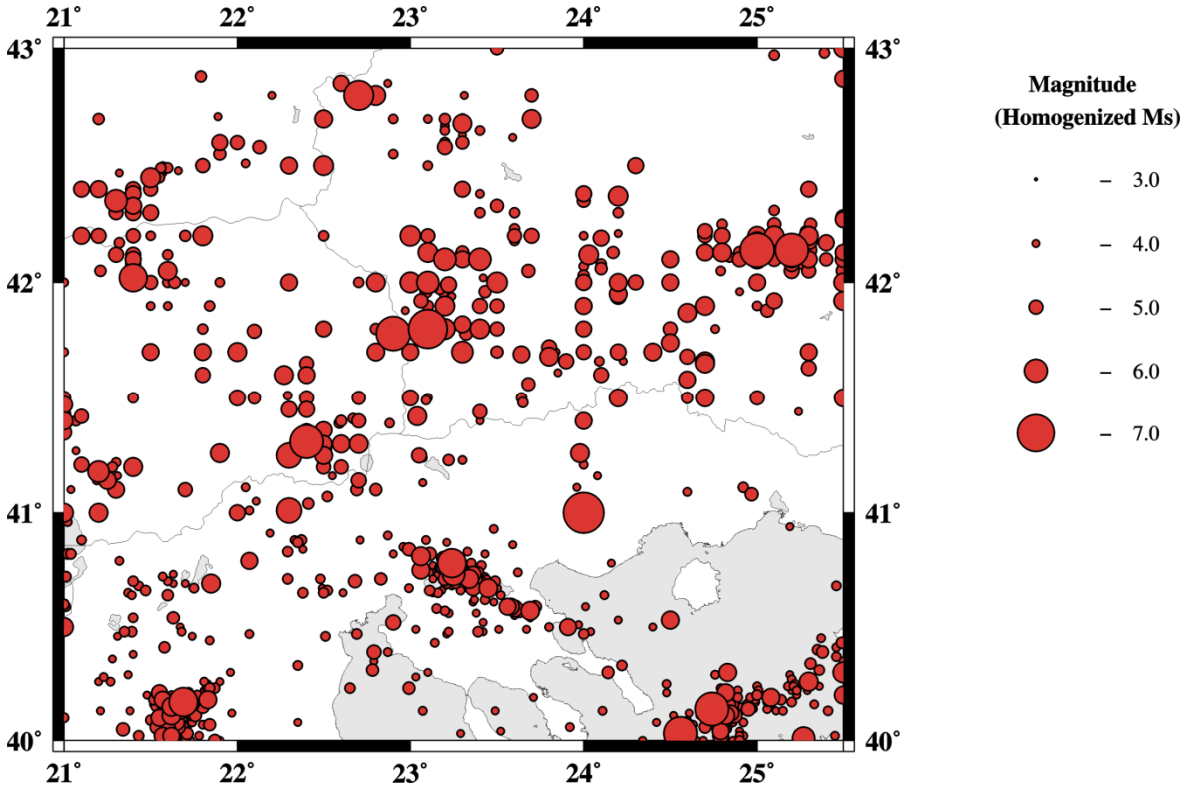

(b)

Figure 4.14 Earthquake epicentres for all events in the developed catalogue in (a) the Balkan and southeast European region and (b) southwest Bulgaria

Chapter 5 : Earthquake extreme magnitude and ground motion hazard

5.1 Introduction

Seismic hazard to Bulgaria and the surrounding Balkan region has been a major concern for many years. Hazard is predominantly generated by the collision environment between the Eurasian and African tectonic plates, and the resulting Alpine mountain orogeny extending through Greece, the FYR of Macedonia and Bulgaria. The Hellenic Arc Trench system to the south also has a dominating affect on the area. Of particular interest here though are the central area of the study region containing the convergence of the political borders between the FYR of Macedonia, Greece and Bulgaria.

Limitations in the geographical coverage of previous *state-of-the-art* hazard analyses by Bončev *et al.* (1982), Stanishkova and Slejko (1991), Orozova-Stanishkova and Slejko (1994) and van Eck and Stoyanov (1996) have already been discussed in chapter 2. These limitations may be considered a direct concern for seismic hazard studies across this region, earthquake engineering practice and retro-fitting of critical structures alike. They are relatively modern – having all been developed within the past 25 years – and they are of limited geographic extent, or are constrained in geographic coverage by political borders. Justification for this work is therefore borne out by using these limitations in historical work as the drivers for this alternative and contemporary probabilistic seismic hazard assessment.

The new earthquake catalogue described in the previous chapter will be used to estimate seismic hazard for southwest Bulgaria and the broader Balkan area. A preliminary analysis of key catalogue characteristics (magnitude threshold, extreme interval and start year) will be undertaken to determine an optimum configuration of data to use for forecasting earthquake extremes, and to develop realistic forecasts of hazard. This will allow the ensuing hazard analysis to consider suitable extreme events without including an excessive number of '*dummy*' observations (extreme intervals with '*null*' entries or unrepresentative low-magnitude extreme values), background seismicity or over-zealous removal of genuine extreme events. This procedure uses Gumbel's third asymptotic extreme values distribution and is described in detail in sections 3.5 and 5.3.

This chapter contributes to a new study of Bulgaria by focusing upon earthquake extreme hazard using a standard probabilistic seismic hazard assessment (PSHA) framework of: 1) potential earthquake magnitudes, 2) locations, 3) earthquake recurrence, 4) ground motion and 5) variability. Hazard forecasts are provided as suites of contoured hazard maps for the region bounded by 39.0°-

45.0°N, 19.0°-29.0°E, and for the southwest region between 40.0°-43.0°N, 21.0°-25.5°E. Hazard forecasts are presented for; 1) magnitude recurrence, 2) peak ground acceleration (PGA), 3) peak ground velocity (PGV) and 4) macroseismic intensity with respect to:

1. The maximum modal event expected in 50, 100 and 200 years (i.e. M_{50}, M_{100}, M_{200}).

2. The maximum modal event with 90% probability of not being exceeded (pnbe) in 50, 100 and 200 years (i.e. M_{P50}, M_{P100}, M_{P200}).

50-, 100- and 200-year return periods are selected as these are standard measures adopted when considering seismic hazard affecting non-critical urban structures. These have been used many times in the past, e.g. Makropoulos and Burton (1985a, b) and Burton *et al*. (2003, 2004a) and so allow easy direct comparison between studies. The 50-year return period at 90% pnbe (the '*475-year return period event'*) also allows the specific EUROCODE 8 hazard metric to be considered.

Peak ground accelerations will primarily be calculated using Theodulidis and Papazachos (1992; $TP92_A$) for stiff soil conditions (S = 0.5) at the 50th percentile (P = 0). Occasionally the models of Ambraseys (1995; AM95_WDC) for rock sites with depth control at the 50th percentile (P = 0) and Ambraseys *et al*. (2005; AM05) constrained to represent seismicity developed from normal faulting regimes (F_N = 1) and stiff soil conditions (S_A = 1) will also be considered for comparison.

Peak ground velocities will be calculated using Theodulidis and Papazachos (1992; $TP92_V$) for stiff soil conditions (S = 0.5) at the 50th percentile (P = 0).

Macroseismic intensities will be calculated using the aggregated form of intensity attenuation and epicentral intensity relations of Papazachos and Papaioannou (1997; PP97).

Reasons for selecting these ground motion models have already been given in section 3.10.

Urban areas are becoming increasingly complex through expansion of commercial, industrial and residential areas and their infrastructures that characterise them. Consequently seismic hazard assessments are an increasingly integral part to developing and designing anti-seismic structures in many parts of the world; this is certainly true of Bulgaria. Each section that follows considers a particular measure of seismic hazard and will also incorporate equivalent estimates for hazard at eight key urban centres (Figure 5.1; Table 5.1) within the study region. Where necessary, hazard maps will be supplemented by site-specific estimates for the large earthquake potential at a site.

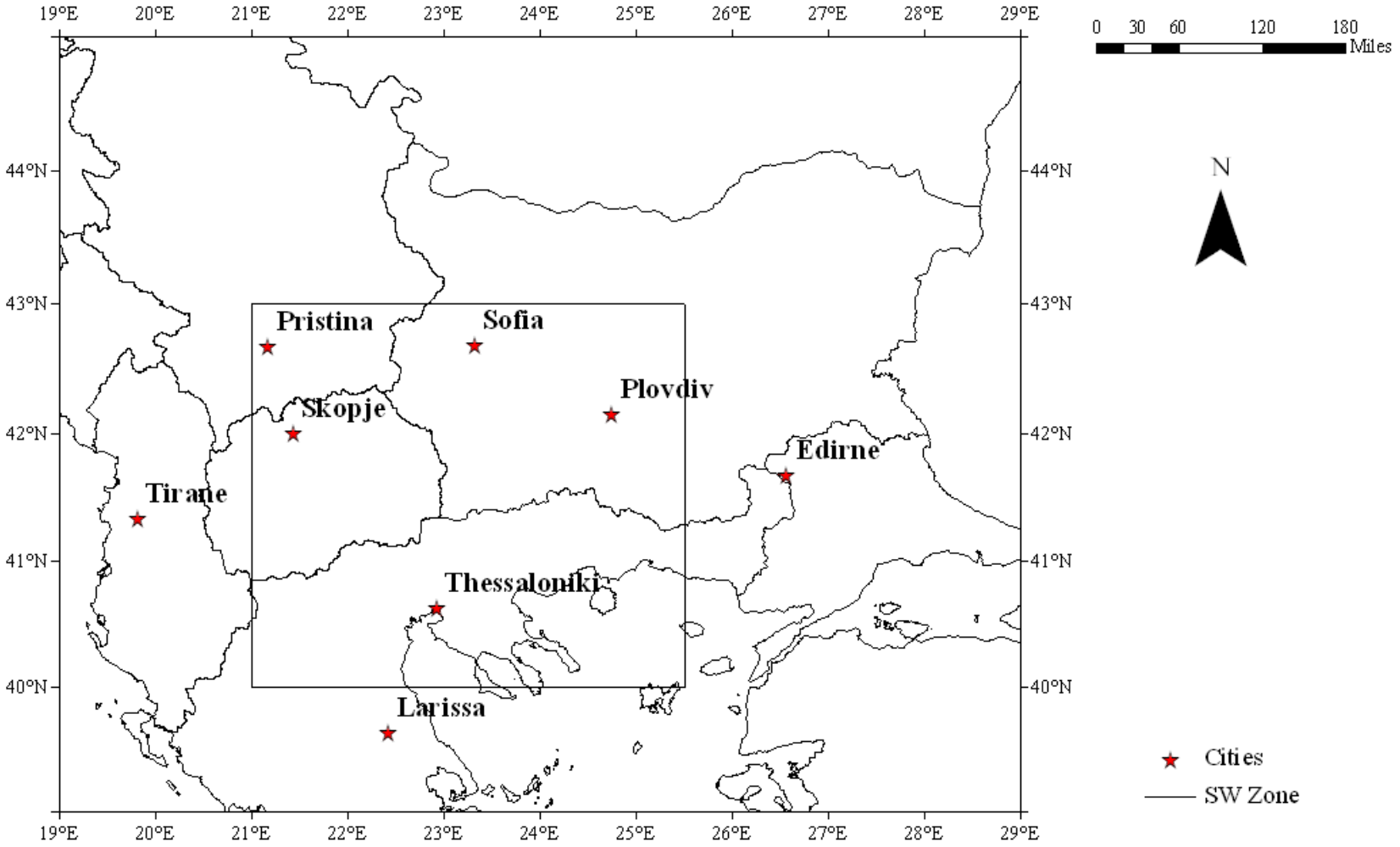

Figure 5.1 The eight urban centres for which seismic hazard will be estimated. The internal rectangle outlines the sub region to be considered as southwest Bulgaria

City	Geographical co-ordinates	Elevation (m)	Estimated population[1]
Edirne	41.67°N, 26.57°E	48	139,919
Larissa	39.63°N, 22.42°E	67	132,924
Plovdiv	42.15°N, 24.75°E	164	379,119
Pristina	42.67°N, 21.17°E	652	206,686
Skopje	42.00°N, 21.43°E	240	478,725
Sofia	42.68°N, 23.32°E	550	1,355,366
Thessaloniki	40.63°N, 22.93°E	20	351,367
Tirane	41.33°N, 19.82°E	90	399,999

[1] 2008 estimate

Table 5.1 Urban centres selected to consider seismic hazard in the Balkan region (Figure 5.1)

Seismicity present within a 2° half-width cell centred on the city in question will be considered for magnitude, peak ground acceleration, peak ground velocity hazard and intensity.

5.2 Contouring hazard

Hazard maps will be developed using a zone-free analysis method, by applying a '*moving cell*' approach similar to that used in Burton *et al.* (2003, 2004b) and Makropoulos and Burton (1985a, b). Two-degree half-width (i.e. rectangular) cells will be placed at 0.5° intervals of latitude and longitude to fully cover the region, ensuring full overlap between analysis cells. Cells of 2° half-width will be used as attenuation of seismic energy from earthquakes will have decayed significantly over an epicentral distance of ~222 km. One degree of latitude is approximately 111 km.

Earthquakes occurring within each analysis cell will be extracted from the new catalogue. *N*-year extremes will then be considered from this subset to estimate hazard forecasts for magnitude, ground acceleration and velocity and macroseismic intensity. The *N*-year extreme interval to be used for both geographic regions considered, and each city, will be selected in this chapter along with the start year and magnitude threshold, M_{CUT}, (or intensity threshold, I_{CUT}, if intensity hazard is considered) of the catalogued data.

Hazard estimates will be calculated using Gumbel's third asymptotic extreme distribution appropriate for bounded hazard scales (magnitude and intensity). Gumbel's first asymptotic extreme distribution will be used for the unbounded hazard scales of ground acceleration and velocity. Distribution parameters and their associated uncertainties will also be obtained.

Forecasts for extreme PGA and PGV hazard will be calculated using Eq. (A2-8) to estimate the *T*-year ground motion maximum. Equation (A2-9) will be used to calculate peak ground motions with probability *P* of not being exceeded in *T*-years.

For magnitude recurrence hazard, Eq. (A2-14) will be used to estimate the annual modal maximum event, Eq. (A2-15) will be applied to forecast the *T*-year modal maximum earthquake magnitude, m(*T*). Equation (A2-16) will be used to obtain estimates of the magnitude with probability *P* of being a maximum, not being exceeded in the next *T* years. Where relevant, $P = 0.9$ for 90% pnbe, and $T = 50$, 100 or 200 years as required. $T = 25$ years will also be used when forecasting hazard at the eight urban centres.

5.3 Sensitivity analysis for extreme distribution parameterisation

For such an important final product as a seismic hazard assessment, users will need to consider justify base parameters on which it has been founded. Procedures previously developed by Burton (1981) for reviewing the stability of (ω, μ, λ) from Gumbel's third extreme values distribution with respect to: 1) cut-off magnitude (M_{CUT}), 2) extreme interval (NPER), and 3) start year of catalogue data used are discussed in section 3.5. Further, Figure 5.2 attempts to define the conditional ordering and relationships between these statistical components and the numerous statistical and seismotectonic factors relevant to governing the final selection of these, and extends to recommend a hierarchical order against which to evaluate them.

Discussion of the final selection for: 1) cut-off magnitude (M_{CUT}), 2) starting values of (ω, μ, λ), 3) extreme interval (NPER), and 4) analysis cell size is given in sections 5.3.2 to 5.3.5 to allow a seismic hazard assessment based on extreme values statistics using the earthquake catalogue data. Before this, section 5.3.1 briefly discusses how parameter stability curves are developed in terms of the geographic and seismic context. Sections 5.3 and 5.5.3 consider magnitude recurrence hazard specifically. A similar process is considered specifically for intensity recurrence hazard in section 5.5.6.

5.3.1 Choice of earthquake data

All earthquakes within the boundaries of each region for which seismic hazard will be considered in chapter 5 and 6 will be included in this analysis; for the full region this totals 3,681 events, and for southwest Bulgaria this is 1,008 events. For urban centres this will constitute the specific subset of events within the analysis cell described in section 5.1.

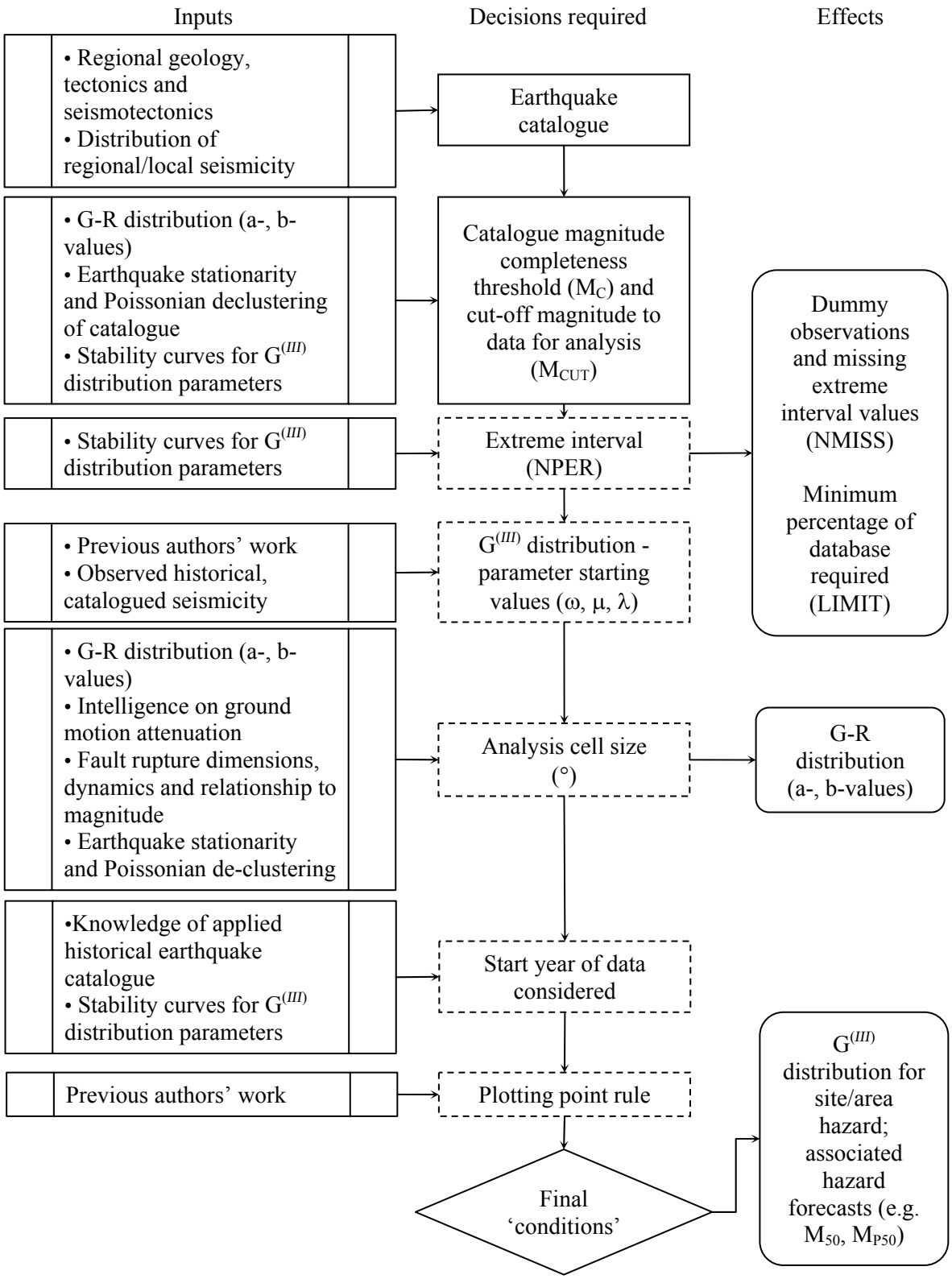

Figure 5.2 Conditional ordering of decisions required to rationalize '*fit-for-purpose*' conditions to developing a zone-free statistical seismic hazard analysis using a historical earthquake catalogue in tandem with Gumbel's distributions of extreme values. Solid rectangles denote decisions that are characteristic of the catalogue used; dashed rectangles denote decisions that can be defined by the 'user'. Curved rectangles denote factors affected by earlier decisions made

A single rectangular analysis cell will be located at the centre of each geographic extent to capture all seismicity within its boundary (42.0°N, 24.0°E for the full area, and 41.5°N, 23.25°E for southwest Bulgaria). Each cell used is large enough to incorporate each area's entire seismicity. These data will be used to develop estimates for (ω, μ, λ) and the associated statistics using procedures outlined in the following sections.

5.3.2 Choice of M_{CUT}

Magnitude completeness, M_C, is an inherent characteristic of any earthquake catalogue, regardless of whether it is the full data or has been declustered of fore and aftershocks prior to use. Typically this is the lower magnitude threshold at which earthquake data should be truncated in pre-analysis prior to a full seismic hazard assessment taken place, and will assume data has been Poissonian declustered of fore- and aftershock sequences beforehand. However, occasionally the cut-off magnitude, M_{CUT}, that is most suitable to actually adopt and invoke on data may differ slightly from this completeness magnitude due to the magnitude resolution of analysis adopted to determine M_C, and known [or unknown] uncertainties in the magnitudes listed in the constructed dataset. Further, M_C may differ from M_{CUT} depending on whether a *whole process* or *part process* magnitude model is adopted. Here M_C will be used in relation to *whole process* statistical distribution – that is, the parent distribution – while M_{CUT} relates to *part process* statistical analysis.

Here we are interested in determining the cut-off magnitude, M_{CUT}, for data catalogued in chapter 4. Possible statistical tools for determining M_C are discussed in chapters 3 and 4, with those adopted in chapter 4 each offering different estimates for this critical value. However, final selection of M_c, and therefore M_{CUT}, from any of these statistical analytical approaches will still always be somewhat dependent upon judgement 'by-eye'.

Determining M_C using frequency-magnitude distributions, in both its raw and declustered forms is given in section 4.10 and subsections therein, and suggests this value to certainly be above 4.6 M_s, and more likely in the magnitude interval $5.0 \leq M_s \leq 6.0$. M_c is likely to increase after removing dependent *accessory* sequences due to removal of these smaller magnitude events. a- and b-values will increase (Table 4.11 and Table 4.12), so resulting in a higher ratio of larger magnitude events. Filtering earthquake data of dependent events prior to an extreme value statistical analysis is a somewhat moot issue as applying an extreme values analysis is typically expected to have similar effects on M_{CUT}; this issue is investigated further here.

Knowing the likely magnitude interval M_{CUT} will appear in allows the magnitude range to be refined in which to consider stability of (ω, μ, λ) and their first order standard deviations for suites

of specific extreme intervals (NPER) and magnitude thresholds (M_{CUT}) using Gumbel's third extreme distribution to perform a *sensitivity analysis*.

NPER was tested for 1-year (annual) to 6-year extremes, at thresholds in the magnitude interval $4.5 \leq M_s \leq 6.0$. This interval for NPER was chosen in response to Burton *et al.* (2004b) selecting never less than 6-year extreme intervals to assess magnitude hazard and perceptibility for Greece and the Aegean extent. Appreciating the Balkan region to the north has a generally lower level of seismicity, it is likely a shorter extreme interval will be best suited and help model extreme magnitudes of the earthquake dataset in a better fashion. The test interval for M_{CUT} was selected to encompass the high and low extremes for the likely value of M_{CUT}.

Parameter stability curves are illustrated in Figure 5.3 for what are considered to be the most suitable ideal set of M_{CUT} and NPER values; (a) illustrates stability in (ω, μ, λ) with respect to M_{CUT}, for 4-year extreme intervals of data for the full Balkan extent; statistics which construct Figure 5.3 are tabulated below the illustration and are consistent with a 50-year return period event.

Values for the number of missing years of data considered (NMISS), the percentage factor dependence of extreme data required to allow the selected plotting point procedure to be achieved (LIMIT), and the 50-year return period (RP) magnitude forecast (M_{50}) and its uncertainty (σ_M) are also presented. Similarly, Figure 5.4 illustrates 50-year return period statistics for southwest Bulgaria, with respect to M_{CUT}, for 5-year extreme intervals (with statistics given below).

Evidence for the most suitable values for M_{CUT} for (a) the broad Balkan extent and (b) southwest Bulgaria are provided in Figure 5.3 and Figure 5.4, with mutually supporting evidence from *whole process* statistics of chapter 4. Vertical red lines in each figure highlight these values, and have been selected as they provide the most stable (ω, μ, λ). Although some consideration for suitability of NPER needs to be included here, choice of final NPER for both areas will be considered further in section 5.3.9.

5.3.3 Choice of NPER

This section investigates the effect of varying the extreme interval (NPER) on (ω, μ, λ) and their uncertainties. M_{CUT} should be set at 5.5 M_s for the Balkans and 5.3 M_s for southwest Bulgaria (section 5.3.2). Having plotted parameter stability with respect to M_{CUT} specifically for 4-year and 5-year extreme intervals respectively, a logical progression for this pre-analysis is to plot stability with respect to NPER. This will help confirm whether these particular extreme intervals at which parameter stability were plotted earlier are viable selections, or recommend suitable alternatives.

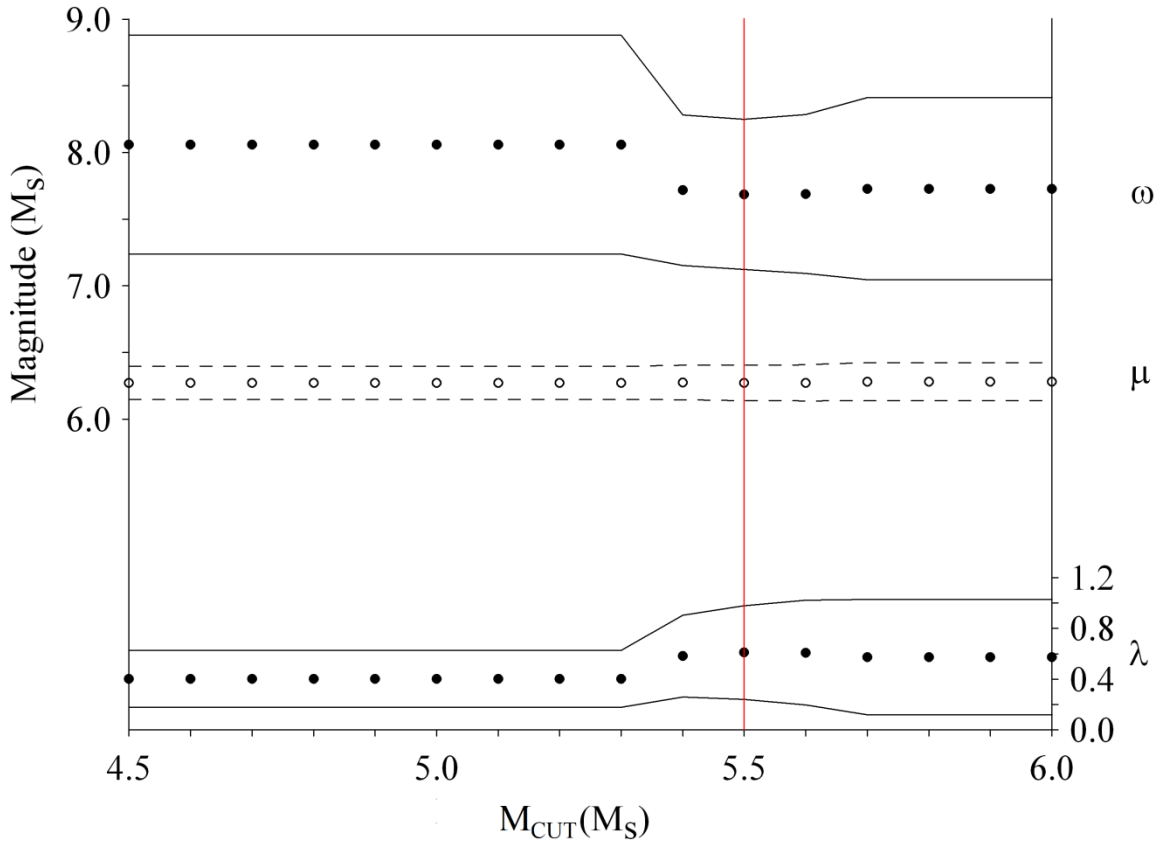

NPER	START	M_{CUT}	ω	σ_ω	μ	σ_μ	λ	σ_λ	M_{50}	σ_M	X^2	NMISS	LIMIT
4	1900	4.5	8.059	0.821	6.273	0.123	0.403	0.223	7.759	0.615	0.060	0	1/2
4	1900	4.6	8.059	0.821	6.273	0.123	0.403	0.223	7.759	0.615	0.060	0	1/2
4	1900	4.7	8.059	0.821	6.273	0.123	0.403	0.223	7.759	0.615	0.060	0	1/2
4	1900	4.8	8.059	0.821	6.273	0.123	0.403	0.223	7.759	0.615	0.060	0	1/2
4	1900	4.9	8.059	0.821	6.273	0.123	0.403	0.223	7.759	0.615	0.060	0	1/2
4	1900	5.0	8.059	0.821	6.273	0.123	0.403	0.223	7.759	0.615	0.060	0	1/2
4	1900	5.1	8.059	0.821	6.273	0.123	0.403	0.223	7.759	0.615	0.060	0	1/2
4	1900	5.2	8.059	0.821	6.273	0.123	0.403	0.223	7.759	0.615	0.060	0	1/2
4	1900	5.3	8.059	0.821	6.273	0.123	0.403	0.223	7.759	0.615	0.060	0	1/2
4	1900	5.4	7.718	0.565	6.275	0.130	0.583	0.322	7.630	0.467	0.029	2	1/2
4	**1900**	**5.5**	**7.686**	**0.562**	**6.272**	**0.132**	**0.611**	**0.368**	**7.613**	**0.478**	**0.033**	**3**	**1/2**
4	1900	5.6	7.689	0.597	6.273	0.135	0.608	0.412	7.615	0.523	0.034	4	1/2
4	1900	5.7	7.729	0.683	6.282	0.144	0.573	0.454	7.635	0.616	0.030	5	1/2
4	1900	5.8	7.729	0.683	6.282	0.144	0.573	0.454	7.635	0.616	0.030	5	1/2
4	1900	5.9	7.729	0.683	6.282	0.144	0.573	0.454	7.635	0.616	0.030	5	1/2
4	1900	6.0	7.729	0.683	6.282	0.144	0.573	0.454	7.635	0.616	0.030	5	1/2
4	1900	6.1	7.593	0.548	6.218	0.225	0.752	0.652	7.567	0.587	0.016	8	1/2
4	1900	6.2	7.606	0.633	6.235	0.357	0.725	0.812	7.575	0.763	0.016	10	1/2
4	1900	6.3	7.670	0.831	6.303	0.431	0.620	0.883	7.604	0.993	0.012	11	1/2
4	1900	6.4	7.670	0.831	6.303	0.431	0.620	0.883	7.604	0.993	0.012	11	1/2
4	1900	6.5	7.698	0.968	6.332	0.530	0.581	0.976	7.613	1.176	0.013	12	1/2

Figure 5.3 Stability in (ω, μ, λ) with respect to M_{CUT} for 4-year extreme intervals of data for the full Balkan extent

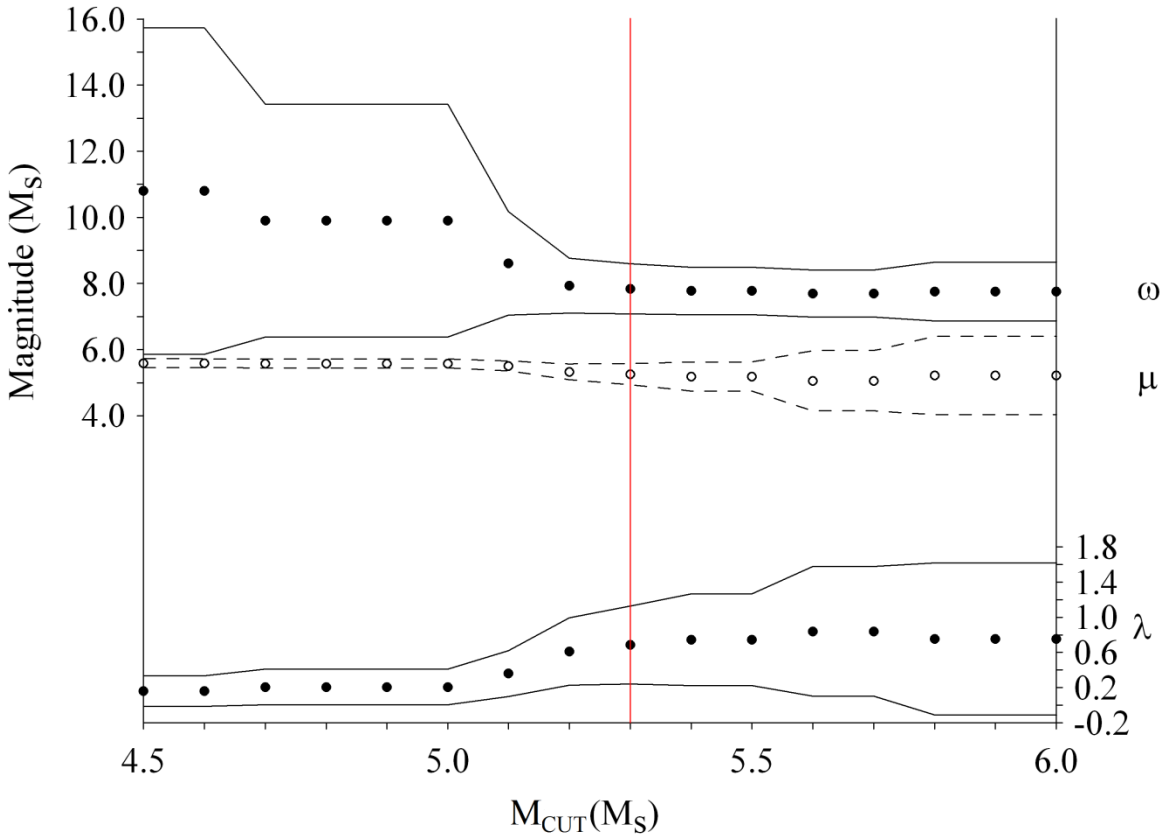

NPER	START	M_{CUT}	ω	σ_ω	μ	σ_μ	λ	σ_λ	M_{50}	σ_M	X^2	NMISS	LIMIT
5	1900	4.5	10.79	4.937	5.593	0.131	0.162	0.174	8.113	2.123	0.183	0	1/2
5	1900	4.6	10.79	4.937	5.593	0.131	0.162	0.174	8.113	2.123	0.183	0	1/2
5	1900	4.7	9.903	3.520	5.579	0.134	0.208	0.204	8.078	1.850	0.175	1	1/2
5	1900	4.8	9.903	3.520	5.579	0.134	0.208	0.204	8.078	1.850	0.175	1	1/2
5	1900	4.9	9.903	3.520	5.579	0.134	0.208	0.204	8.078	1.850	0.175	1	1/2
5	1900	5.0	9.903	3.520	5.579	0.134	0.208	0.204	8.078	1.850	0.175	1	1/2
5	1900	5.1	8.608	1.566	5.507	0.149	0.360	0.259	7.964	1.187	0.106	3	1/2
5	1900	5.2	7.933	0.830	5.329	0.240	0.613	0.383	7.801	0.842	0.030	6	1/2
5	**1900**	**5.3**	**7.840**	**0.759**	**5.259**	**0.318**	**0.684**	**0.444**	**7.759**	**0.846**	**0.021**	**7**	**1/2**
5	1900	5.4	7.777	0.722	5.188	0.441	0.745	0.519	7.726	0.896	0.018	8	1/2
5	1900	5.5	7.777	0.722	5.188	0.441	0.745	0.519	7.726	0.896	0.018	8	1/2
5	1900	5.6	7.699	0.708	5.060	0.912	0.840	0.736	7.678	1.138	0.008	10	1/2
5	1900	5.7	7.699	0.708	5.060	0.912	0.840	0.736	7.678	1.138	0.008	10	1/2
5	1900	5.8	7.759	0.893	5.219	1.186	0.752	0.864	7.712	1.481	0.004	11	1/3
5	1900	5.9	7.759	0.893	5.219	1.186	0.752	0.864	7.712	1.481	0.004	11	1/3
5	1900	6.0	7.759	0.893	5.219	1.186	0.752	0.864	7.712	1.481	0.004	11	1/3
5	1900	6.1	7.789	1.063	5.298	1.594	0.711	1.034	7.725	1.865	0.004	12	1/3
5	1900	6.2	7.789	1.063	5.298	1.594	0.711	1.034	7.725	1.865	0.004	12	1/3
5	1900	6.3	7.831	1.345	5.417	2.108	0.655	1.257	7.739	2.418	0.003	13	1/3
5	1900	6.4	7.831	1.345	5.417	2.108	0.655	1.257	7.739	2.418	0.003	13	1/3
5	1900	6.5	7.867	1.717	5.514	2.863	0.612	1.569	7.747	3.173	0.003	14	1/4

Figure 5.4 Stability in (ω, μ, λ) with respect to M_{CUT} for 5-year extreme intervals of data for southwest Bulgaria

Stability of (ω, μ, λ) for the full Balkan extent with respect to NPER at M_{CUT} of 5.5 M_s is shown in Figure 5.5, while Figure 5.6 gives the same for southwest Bulgaria at M_{CUT} of 5.3 M_s. Statistics used to construct both illustrations are also given.

Extreme intervals from 1 (annual) to 10 years are applied to data for a time interval of 1900 to 2004. Data are assessed at $4.6 \leq M_{CUT}$ (M_s) ≤ 6.0 M_s at intervals of 0.1 M_s, noting some higher values for M_{CUT} may not be represented by the full time interval of data available due to an inadequate number of data extremes. The lowest value for M_{CUT} is set at 4.6 M_s due to the majority of annual extremes in the catalogue being >4.5 M_s (104 are >4.5 M_s and 82 of 105 annual extremes are >5.0 M_s).

Changing NPER has a systematically identical effect through $4.6 \leq M_{CUT} \leq 6.0$. ω gradually decreases with increasing NPER and M_{CUT}. Typically ω decreases by between $0.5 \rightarrow 1.0$ M_s when M_{CUT} increases by one magnitude unit from 4.6 to 5.6 M_s for any given NPER. For higher M_{CUT}, realistic estimates for ω based on observed seismicity of the region are approached using moderate extreme intervals of 3-, 4- and 5-year for the full-catalogued region (Figure 5.5).

For southwest Bulgaria, only an NPER of 5 years provides realistic estimates for ω when compared against regional historical seismicity. Interestingly, longer extreme intervals of 8, 9 and 10 years produce similar ω in both areas, but these are associated with a larger uncertainty attached to λ. Due to this, these longer extreme intervals can be safely excluded from further consideration.

Both figures show μ gently increasing through the range of extreme intervals for all M_{CUT}, with its curve becoming less pronounced at longer NPER and lower M_{CUT}. This represents its function as the characteristic magnitude over an *N*-year time interval, with probability of $P_N(\mu) = 1/e$ of being the extreme event. Generally σ_μ decreases slightly through the same range. Both μ and σ_μ are seen to begin to noticeably plateau to stable and realistic values for the Balkan and southwest Bulgaria extents at NPER of 4-year and 5-year respectively.

Two other points are worth noting concerning variation in and selection of NPER for the areas:

1. In both Figure 5.5 and Figure 5.6, higher NPER are associated with wildly inflated estimates of σ_λ, with this being most noticeable for data of the full Balkan extent.

2. Viewing the statistics below each illustration shows LIMIT, the minimum percentage of extreme data required for forecasting purposes needs to be reduced to provide forecasts at shorter NPER for southwest Bulgaria, at an M_{CUT} of 5.3 M_s.

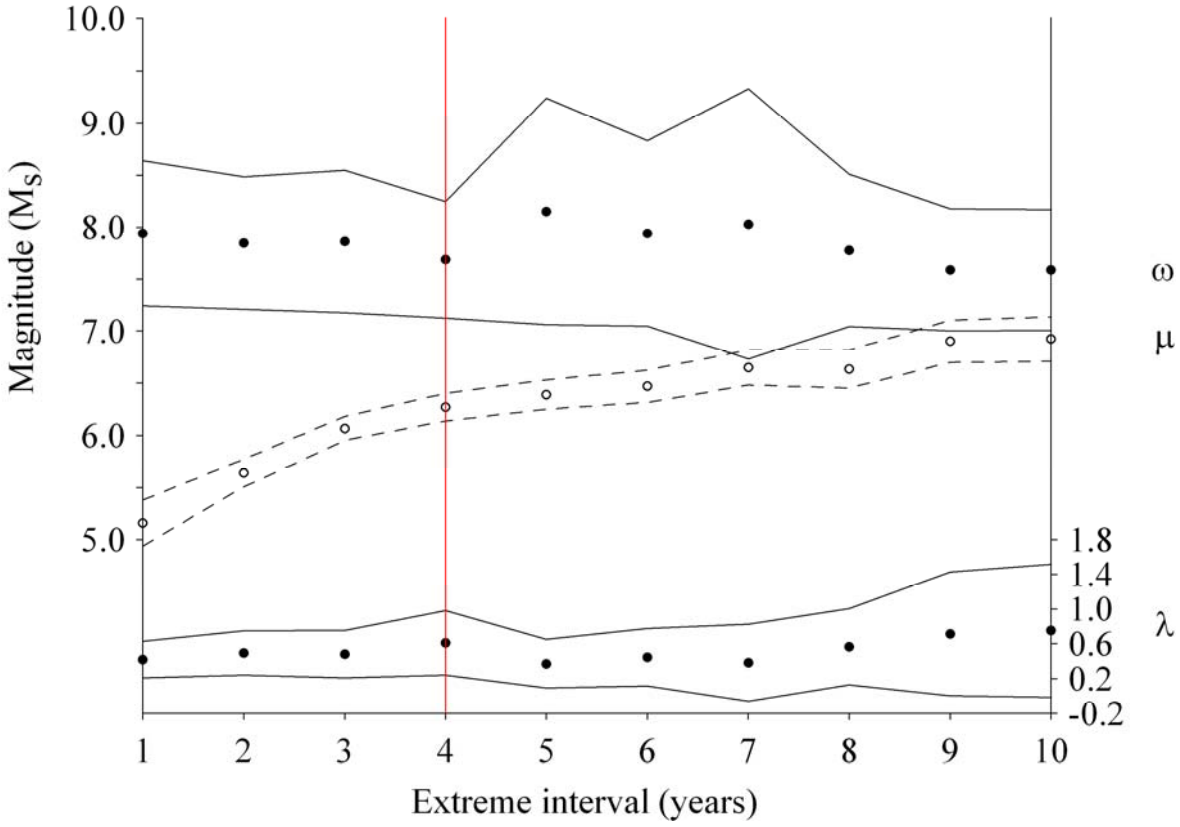

NPER	START	M_{CUT}	ω	σ_ω	μ	σ_μ	λ	σ_λ	M_{50}	σ_M	X^2	NMISS	LIMIT
1	1900	5.5	7.940	0.698	5.160	0.221	0.419	0.209	7.511	0.684	0.012	46	1/2
2	1900	5.5	7.847	0.638	5.643	0.135	0.495	0.255	7.620	0.593	0.019	14	1/2
3	1900	5.5	7.861	0.685	6.070	0.113	0.482	0.272	7.663	0.568	0.025	4	1/2
4	**1900**	**5.5**	**7.686**	**0.562**	**6.272**	**0.132**	**0.611**	**0.368**	**7.613**	**0.478**	**0.033**	**3**	**1/2**
5	1900	5.5	8.150	1.089	6.392	0.139	0.373	0.279	7.807	0.796	0.062	0	1/2
6	1900	5.5	7.938	0.893	6.471	0.154	0.448	0.330	7.743	0.691	0.044	0	1/2
7	1900	5.5	8.029	1.297	6.649	0.167	0.384	0.438	7.774	0.960	0.042	0	1/2
8	1900	5.5	7.777	0.733	6.634	0.181	0.567	0.437	7.700	0.585	0.026	0	1/2
9	1900	5.5	7.589	0.587	6.902	0.203	0.715	0.711	7.572	0.465	0.026	0	1/2
10	1900	5.5	7.587	0.582	6.923	0.214	0.752	0.763	7.575	0.458	0.025	0	1/2

Figure 5.5 Stability in (ω, μ, λ) with respect to NPER for M_{CUT} of 5.5 M_s for the Balkan extent

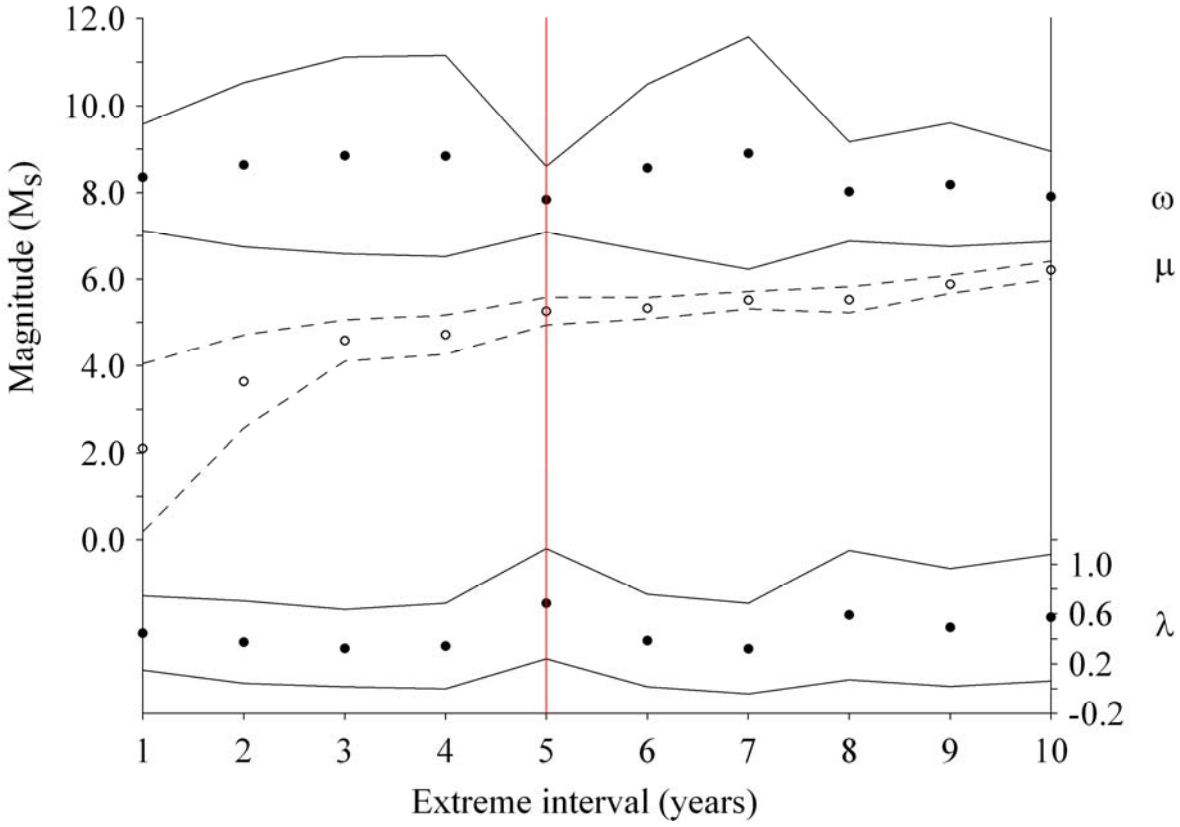

NPER	START	M_{CUT}	ω	σ_ω	μ	σ_μ	λ	σ_λ	M_{50}	σ_M	X^2	NMISS	LIMIT
1	1900	5.3	8.348	1.231	2.114	1.932	0.447	0.296	7.517	2.042	0.099	82	1/5
2	1900	5.3	8.639	1.893	3.643	1.068	0.375	0.330	7.671	2.085	0.072	35	1/3
3	1900	5.3	8.851	2.266	4.583	0.477	0.326	0.310	7.803	1.886	0.082	17	1/2
4	1900	5.3	8.836	2.319	4.713	0.453	0.343	0.342	7.905	1.961	0.083	12	1/2
5	**1900**	**5.3**	**7.840**	**0.759**	**5.259**	**0.318**	**0.684**	**0.444**	**7.759**	**0.846**	**0.021**	**7**	**1/2**
6	1900	5.3	8.567	1.923	5.328	0.248	0.386	0.370	7.975	1.602	0.140	5	1/2
7	1900	5.3	8.905	2.676	5.511	0.202	0.322	0.363	8.056	1.945	0.112	3	1/2
8	1900	5.3	8.025	1.144	5.524	0.297	0.593	0.520	7.880	1.152	0.059	4	1/2
9	1900	5.3	8.181	1.428	5.878	0.208	0.491	0.474	7.939	1.233	0.069	2	1/2
10	1900	5.3	7.906	1.043	6.205	0.207	0.572	0.508	7.794	0.876	0.085	1	1/2

Figure 5.6 Stability in (ω, μ, λ) with respect to NPER for M_{CUT} of 5.3 M_s for SW Bulgaria

> Conventionally, previous work has shown a LIMIT of 1/3 or ¼ to be sufficient, such that a minimum of one third or one quarter of possible extremes observations is required to forecast distribution parameters.

A lower LIMIT is characteristic of extracting annual extreme intervals for southwest Bulgaria data, such that the number of missing years of annual extreme magnitudes, NMISS, in the data considered is unsuitably high (i.e. 82 years) to warrant such a decrease in LIMIT. For NPER = 2 years LIMIT increases to 1/3, with only 35 missing years (section 3.5) of *N*-year extreme data apparent from the data. It would not have been possible to plot shorter extreme intervals had LIMIT been set at 1/3.

A 4-year extreme interval should be used for the larger geographic area as it provides: 1) a realistic estimate for ω with smallest σ_ω, 2) μ starting to plateau at realistic values (with small σ_μ) and 3) a high curvature parameter λ (Figure 5.5).

A 5-year extreme interval should be used for southwest Bulgaria as it provides: 1) the lowest value for ω (and realistic in terms of observed historical seismicity) with smallest σ_ω and 2) a high curvature parameter λ (Figure 5.6).

The relationship between NPER and NMISS and to a lesser extent LIMIT and M_{CUT} will be explored in more detail in section 5.3.9.

5.3.4 Choice of starting values for (ω, μ, λ) [magnitude recurrence hazard]

ω's starting value is set at 7.7 M_s in response to two key events in the catalogue: the homogenized 7.2 M_s Kresna earthquake of 1904 (41.8°N, 23.1°E) and the homogenized 7.6 M_s Thessaloniki earthquake of 2000 (41.0°N, 24.0°E). Earlier chapters outline how the Kresna earthquake has for a long time been considered the largest shallow-focus earthquake of mainland Europe during the 20th century. Shebalin *et al.* (1998) report this at 7.8 m_b (with an uncertainty of ±0.2 m_b), and is the reported body-wave magnitude estimate adopted by this work for this event. This estimate has often been questioned by others, who suggest it to have been over-estimated; after homogenisation using more recent evaluations this reduced to 7.2 M_s. The Thessaloniki earthquake was only reported on the body-wave scale (6.5 m_b), but resulted in an homogenized surface-wave of 7.6 M_s. Gumbel's third extreme distribution dictates ω cannot be less than or equal to the largest data value considered.

Consequently 7.7 M_s was selected as a compromise between both historically reported and homogenized magnitudes for these extreme earthquake events, and to accommodate requirements of the statistical distribution model to be used.

The choice of a suitable starting value for μ is less clear-cut. The characteristic largest magnitude μ is not strictly known until some form of statistical analysis has been done. Few previous works offer suggestions for this parameter for this geographic region. Burton (1977) provides estimates for a number of 4° analysis cells across mainland Europe to which such a statistical distribution is applied. For those three cells possessing any common area with this broader study area, estimates of μ range from 3.92 M (±0.15) to 5.59 M (±0.10) from applying annual or 2-year extreme intervals.

The parameter μ is a function of many geographic, seismotectonic and statistical factors. In a zone-free extreme hazard study like this, the important determinates are cell size – and so the levels of seismicity contained in these – and the extreme interval adopted. Chapter 4 applied a preliminary analysis of seismicity statistics with respect to M_c and analysis cell size, using a random sample set of cells across the considered region. While section 5.3.5 considers cell size in fuller detail, it is expected this study will use smaller half-width cells than Burton (1977) for reasons relating to ground attenuation (chapter 3). It therefore seems practical to reduce the value of μ to 4.5 M_s from a mean value of 4.92 M in Burton (1977) to account for this change in cell size.

The curvature parameter λ may take any value less than 1 (as, from Eq. (3-3), $k = 1/\lambda$ and $k > 1$) and is a measure of the distribution's curvature indicating how quickly the curve approaches ω. As $\lambda \to 0$, $k \to \infty$. A typical value for λ is 0.3. When $\lambda = 0.3068$ the modal and median values of Gumbel's third distribution are equal (Burton, 1977). Generally, when $\lambda > 0.31$ the mode is lower than the median and when $\lambda < 0.31$ the mode will follow the median value. After testing potential values for λ, a value of 0.5 was found to allow the distribution to better fit extreme data considered. Consequently $\lambda = 0.5$ will be used for λ; final choices for each parameter are given in Table 5.2.

$G^{(III)}$ parameter	Starting value
ω	7.7
μ	4.5
λ	0.5

Table 5.2 Starting values for (ω, μ, λ) of a $G^{(III)}$ distribution to assess Balkan magnitude hazard

5.3.5 Analysis cell size and cell migration

The analysis cell size selected to use in the following zone-free hazard analysis is governed by:

1. Respecting ground motion decay patterns as a function of distance;

2. Surface and subsurface fault rupturing;

3. Stationarity as a function of cell size and M_{CUT} applied.

Ground motion decay (point 1 above) is generally most prevalent over the initial 200 km (approximately 2° of latitude) from an earthquake source, so it is convenient to simplify cell size selection to either 200 km or 2°. However, a number of modern ground motion models predict rapid decay over a much shorter distance, e.g. Musson (2000) for intensity ground motion, Theodulidis and Papazachos (1992) and Orphal and Lahoud (1974) for acceleration ground motion or any of the ground velocity models illustrated in Figure 3.8. Some previous works have found smaller analysis cells more suitable for including localised seismicity (e.g. Makropoulos and Burton (1985a) use 100 and 150 km radius cells for magnitude recurrence hazard while Makropoulos and Burton (1985b) applies cells of the same size for ground acceleration hazard), while others (Burton, 1977; Burton, 1979; Burton *et al.*, 1984) apply larger cells of 4° radius (or half-width).

Some previous studies have tried to relate event magnitude to resulting surface and sub-surface fault rupture lengths (point 2). This is also a useful tool to confirm the correct cell size to apply during a zone-free seismic hazard assessment. Wells and Coppersmith (1994) explore relations between moment magnitude and surface rupture length (in km). Their Figure 9 illustrates regression of surface rupture length on M_w for their worldwide database of source parameters for 421 historical earthquakes. Correlating a magnitude 7.2 M_w event – the largest homogenized moment magnitude in this work's catalogue – on this graph approximates to a surface rupture of 80 km. Indeed, their database shows that historical events of a similar magnitude never ruptured more than 80 km at the surface (although the 7.23 M_w Dasht-e-Bayaz earthquake on 31/08/1968 did created a 110 km *subsurface* rupture).

Burton (1996) models hypothetical subsurface ruptures resulting from surface-wave magnitudes to answer claims of the 'VAN' group to predict earthquakes during the early 1980s. Figure 3 of that work predicts rupture lengths for $5.0 \leq M_s \leq 8.0$ at half-magnitude intervals taking regression relations from the Wells and Coppersmith text mentioned earlier. Rupture lengths are estimated at 74 km for a 7.5 M_s event and only ~7 km for a 5.5 M_s event.

Historically, a general preference has been seen for cell shape to move from circular to rectangular cells. Circular cells have a distinct limitation in that they need to be large enough so as to avoid gaps falling between them where hazard may not have been forecast. Evidently, spacing between analysis points strongly dictates this minimum cell size. A typical procedure for zone-free analysis will see cells migrate across a region at 0.5° steps. Incorporating this approach with rectangular 2° half-width cells will see cells overlap neighbouring cells by approximately 7/8 to achieve a contour '*smoothing*' effect. Contouring will become coarser the wider analysis points are spaced.

Point 2 in the shortlist above is also considered to a limited degree in section 4.10.4, looking at *whole process* frequency-magnitude and earthquake stationarity statistics of full and declustered magnitude data, with respect to 1° and 2° half-width cells. Illustrations and previous work indicate 2° half-width rectangular analysis cells are most appropriate to resolving realistic estimates for the a- and b-values. 2° half-width rectangular cells will be used throughout this hazard analysis against which seismic hazard will be assessed. Point 3 has already been considered in section 4.10.3.

5.3.6 Choice of start year

(ω, μ, λ) stability curves for the Balkan extent using NPER of 4 years and M_{CUT} of 5.5 M_s (Figure 5.7) show consistent estimates for ω (~7.5 M $\rightarrow$ ~8.0 M) when the start year is set early in the catalogue's time span. These estimates for ω are realistic, considering observed seismicity, especially during the first half of the 20th century. Parameters ω and σ_ω generally increase as the time interval shortens and these also begin to vary wildly.

The start year could be between 1915 and 1925, as Figure 5.7 indicates ω and σ_ω both achieve realistic estimates during this time interval. However, starting the time interval at 1905 or after removes the large magnitude 1904 Kresna event (homogenized 7.2 M_s) from analysis; this main 1904 event would be an annual extreme. A number of earthquakes of similar magnitudes have occurred in the catalogued region since the 1904 event, so it would be misguided to consider this a '*rogue*' event or sequence of seismicity as, for example, the Vrancea seismic sequences of 1940 and 1977 are considered to be (Radulian *et al.*, 2002).

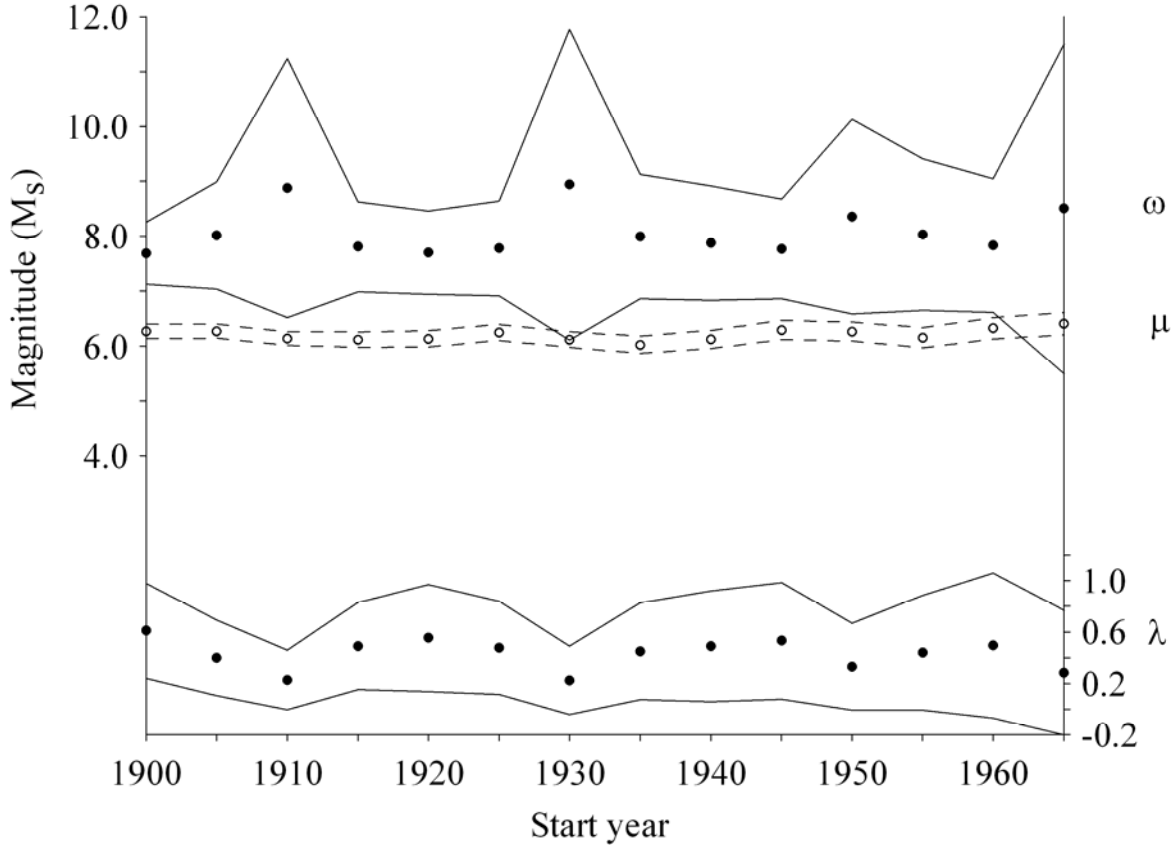

NPER	START	M_{CUT}	ω	σ_ω	μ	σ_μ	λ	σ_λ	M_{50}	σ_M	X^2	NMISS	LIMIT
4	**1900**	**5.5**	**7.686**	**0.562**	**6.272**	**0.132**	**0.611**	**0.368**	**7.613**	**0.478**	**0.033**	**3**	**1/2**
4	1905	5.5	8.014	0.975	6.274	0.128	0.400	0.292	7.717	0.742	0.022	1	1/2
4	1910	5.5	8.880	2.360	6.140	0.124	0.229	0.231	7.824	1.320	0.081	0	1/2
4	1915	5.5	7.803	0.817	6.122	0.138	0.490	0.338	7.625	0.670	0.053	2	1/2
4	1920	5.5	7.696	0.754	6.136	0.147	0.555	0.416	7.583	0.651	0.032	3	1/2
4	1925	5.5	7.778	0.862	6.253	0.147	0.478	0.362	7.606	0.690	0.044	1	1/2
4	1930	5.5	8.939	2.832	6.120	0.141	0.226	0.265	7.840	1.572	0.108	0	1/2
4	1935	5.5	7.990	1.131	6.029	0.157	0.451	0.375	7.734	0.922	0.067	2	1/2
4	1940	5.5	7.871	1.040	6.126	0.164	0.490	0.431	7.686	0.869	0.027	2	1/2
4	1945	5.5	7.767	0.906	6.297	0.174	0.532	0.454	7.644	0.744	0.041	1	1/2
4	1950	5.5	8.354	1.771	6.267	0.171	0.330	0.338	7.852	1.232	0.119	0	1/2
4	1955	5.5	8.029	1.379	6.156	0.183	0.440	0.445	7.769	1.100	0.123	1	1/2
4	1960	5.5	7.829	1.212	6.327	0.194	0.496	0.563	7.676	0.997	0.044	1	1/2
4	1965	5.5	8.503	3.002	6.408	0.203	0.285	0.486	7.880	1.939	0.041	0	1/2

Figure 5.7 Stability in (ω, μ, λ) with respect to start year for M_{CUT} of 5.5 M_s for the Balkans

As advancing the start year by 5 years removes this key extreme event from consideration, it is justifiable to retain 1900 as the start year, equivalent to the start of the early instrumental period of recorded seismicity. This proposal is reinforced by the gradients of ω and σ_ω steepening sharply from an acceptable and realistic value of 7.69 M_s (±0.56) to 8.01 M_s (±0.98) between 1900 and 1905, and on to 8.88 M_s (±2.36) in the following 5-year interval to 1910, as the 1904 and then the large magnitude extreme event of 1905 are excluded from consideration.

Equivalent stability curves for data of southwest Bulgaria are given in Figure 5.8 using NPER of 5 years and M_{CUT} of 5.3 M_s. ω is estimated at <8.0 M_s when the start year is between 1900 and 1910. However, σ_ω increases markedly after 1925, while the modal magnitude μ rises gradually as expected as the time interval shortens. Selecting a suitable start year for considering data in the southwest zone suffers from the same concerns as the broader extent. Moving the start year forward for considering the extremes from the catalogue removes some [annual] year's largest magnitude events – notably the 1904 and 1905 earthquakes in southwest Bulgaria – that ordinarily would be considered extreme magnitudes of the catalogue. Consequently, the start year selected for this smaller region of analysis will also be set to 1900.

5.3.7 Stability of forecasted distribution statistics – validating parameterisation

Estimates for (ω, μ, λ), their uncertainties, chi-square (X^2) and the off-diagonal elements $\sigma^2_{\omega\mu}$, $\sigma^2_{\omega\lambda}$, $\sigma^2_{\lambda\mu}$ of Gumbel's third extreme distribution's covariance error matrix, ε, for the broader Balkan extent are given in Table 5.3. Statistics are given for NPER of 4-, 5- and 6-year extreme intervals, for $4.6 \leq M_{CUT} \leq 6.0$ at 0.1 M_s intervals. Equivalent data for southwest Bulgaria over the same intervals of NPER and M_{CUT} are given. In each table, an individual row represents a single application of Gumbel's third distribution against extracted extreme observations that result from the listed NPER and M_{CUT} imposed on all data captured for the geographic area considered.

Each NPER set is characterised by a distinct value for M_{CUT} at which notable downturns in ω and σ_ω are seen. Each M_{CUT} is emphasised by large values of ω before this magnitude, which can be considered unrealistic based upon observed seismicity. After these magnitudes ω begins to approach the regional observed maximum magnitude. As NPER increases, these critical magnitudes that exhibit distinct improvements to the forecast distribution statistics also increase. For example, when considering the full Balkan data (Table 5.3), for a 4-year NPER this change is at 5.4 M_s, while for a 5- and 6-year NPER it is at 5.6 M_s. ω is estimated at between 7.69 and 8.15 M_s, with σ_ω ranging between 0.56 and 1.09, across all distributions considered.

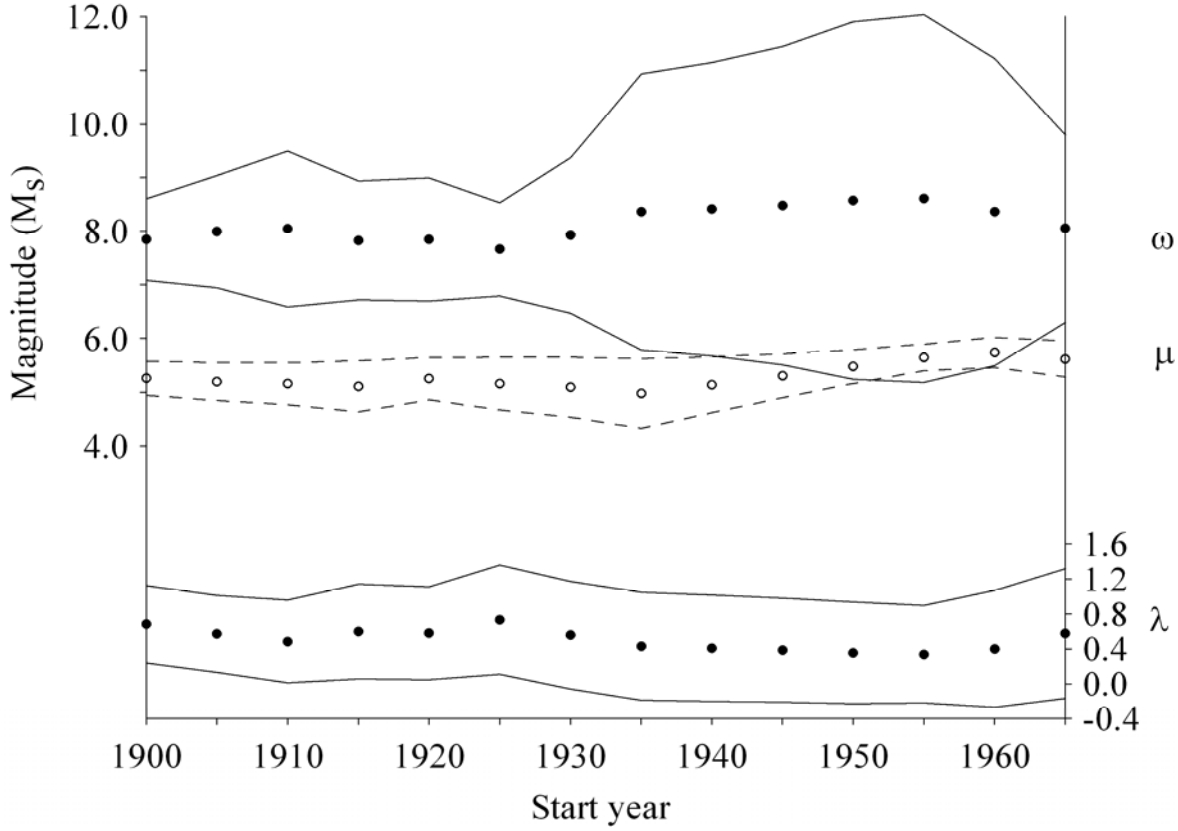

NPER	YEAR	M_{CUT}	ω	σ_ω	μ	σ_μ	λ	σ_λ	M_{50}	σ_M	X^2	NMISS	LIMIT
5	**1900**	**5.3**	**7.840**	**0.759**	**5.259**	**0.318**	**0.684**	**0.444**	**7.759**	**0.846**	**0.021**	**7**	**1/2**
5	1905	5.3	7.988	1.045	5.197	0.352	0.572	0.442	7.804	1.117	0.029	7	1/2
5	1910	5.3	8.039	1.454	5.159	0.391	0.485	0.474	7.725	1.461	0.038	7	1/2
5	1915	5.3	7.822	1.109	5.108	0.477	0.600	0.544	7.672	1.271	0.040	7	1/2
5	1920	5.3	7.845	1.149	5.253	0.392	0.579	0.534	7.682	1.240	0.038	6	1/2
5	1925	5.3	7.661	0.869	5.160	0.491	0.734	0.623	7.607	1.064	0.068	6	1/2
5	1930	5.3	7.922	1.452	5.094	0.558	0.558	0.615	7.719	1.625	0.088	6	1/2
5	1935	5.3	8.361	2.575	4.976	0.648	0.428	0.619	7.862	2.512	0.058	6	1/2
5	1940	5.3	8.408	2.735	5.140	0.521	0.409	0.609	7.874	2.504	0.057	5	1/2
5	1945	5.3	8.473	2.968	5.306	0.408	0.384	0.596	7.889	2.533	0.056	4	1/2
5	1950	5.3	8.571	3.334	5.476	0.314	0.353	0.581	7.904	2.626	0.054	3	1/2
5	1955	5.3	8.608	3.425	5.648	0.249	0.338	0.559	7.921	2.559	0.053	2	1/2
5	1960	5.3	8.358	2.862	5.739	0.283	0.401	0.668	7.914	2.362	0.116	2	1/2
5	1965	5.3	8.049	1.753	5.619	0.336	0.578	0.744	7.895	1.693	0.110	2	1/2

Figure 5.8 Stability in (ω, μ, λ) with respect to start year for M_{CUT} of 5.3 M_s for southwest Bulgaria

NPER	M_{CUT}	ω	σ_ω	μ	σ_μ	λ	σ_λ	$\sigma^2_{\omega\mu}$	$\sigma^2_{\omega\lambda}$	$\sigma^2_{\mu\lambda}$	X^2	NMISS	LIMIT
4	5.0	8.06	0.82	6.27	0.12	0.40	0.22	-0.053	-0.175	0.016	0.06	0	1/2
4	5.1	8.06	0.82	6.27	0.12	0.40	0.22	-0.053	-0.175	0.016	0.06	0	1/2
4	5.2	8.06	0.82	6.27	0.12	0.40	0.22	-0.053	-0.175	0.016	0.06	0	1/2
4	5.3	8.06	0.82	6.27	0.12	0.40	0.22	-0.053	-0.175	0.016	0.06	0	1/2
4	5.4	7.72	0.57	6.28	0.13	0.58	0.32	-0.035	-0.168	0.022	0.03	2	1/2
4	**5.5**	**7.69**	**0.56**	**6.27**	**0.13**	**0.61**	**0.37**	**-0.031**	**-0.191**	**0.020**	**0.03**	**3**	**1/2**
4	5.6	7.69	0.60	6.27	0.14	0.61	0.41	-0.025	-0.227	0.015	0.03	4	1/2
4	5.7	7.73	0.68	6.28	0.14	0.57	0.45	-0.015	-0.289	0.003	0.03	5	1/2
4	5.8	7.73	0.68	6.28	0.14	0.57	0.45	-0.015	-0.289	0.003	0.03	5	1/2
4	5.9	7.73	0.68	6.28	0.14	0.57	0.45	-0.015	-0.289	0.003	0.03	5	1/2
4	6.0	7.73	0.68	6.28	0.14	0.57	0.45	-0.015	-0.289	0.003	0.03	5	1/2
5	5.0	8.15	1.09	6.39	0.14	0.37	0.28	-0.081	-0.292	0.022	0.06	0	1/2
5	5.1	8.15	1.09	6.39	0.14	0.37	0.28	-0.081	-0.292	0.022	0.06	0	1/2
5	5.2	8.15	1.09	6.39	0.14	0.37	0.28	-0.081	-0.292	0.022	0.06	0	1/2
5	5.3	8.15	1.09	6.39	0.14	0.37	0.28	-0.081	-0.292	0.022	0.06	0	1/2
5	5.4	8.15	1.09	6.39	0.14	0.37	0.28	-0.081	-0.292	0.022	0.06	0	1/2
5	5.5	8.15	1.09	6.39	0.14	0.37	0.28	-0.081	-0.292	0.022	0.06	0	1/2
5	5.6	7.93	0.86	6.39	0.14	0.47	0.35	-0.061	-0.284	0.026	0.05	1	1/2
5	5.7	7.93	0.86	6.39	0.14	0.47	0.35	-0.061	-0.284	0.026	0.054	1	1/2
5	5.8	7.74	0.70	6.38	0.15	0.60	0.49	-0.035	-0.315	0.021	0.047	3	1/2
5	5.9	7.74	0.70	6.38	0.15	0.60	0.49	-0.035	-0.315	0.021	0.047	3	1/2
5	6.0	7.74	0.70	6.38	0.15	0.60	0.49	-0.035	-0.315	0.021	0.047	3	1/2
6	5.0	7.94	0.89	6.47	0.15	0.45	0.33	-0.074	-0.280	0.031	0.044	0	1/2
6	5.1	7.94	0.89	6.47	0.15	0.45	0.33	-0.074	-0.280	0.031	0.044	0	1/2
6	5.2	7.94	0.89	6.47	0.15	0.45	0.33	-0.074	-0.280	0.031	0.044	0	1/2
6	5.3	7.94	0.89	6.47	0.15	0.45	0.33	-0.074	-0.280	0.031	0.044	0	1/2
6	5.4	7.94	0.89	6.47	0.15	0.45	0.33	-0.074	-0.280	0.031	0.044	0	1/2
6	5.5	7.94	0.89	6.47	0.15	0.45	0.33	-0.074	-0.280	0.031	0.044	0	1/2
6	5.6	7.77	0.75	6.47	0.16	0.55	0.43	-0.060	-0.306	0.038	0.040	1	1/2
6	5.7	7.82	0.92	6.48	0.16	0.51	0.52	-0.056	-0.452	0.029	0.040	2	1/2
6	5.8	7.82	0.92	6.48	0.16	0.51	0.52	-0.056	-0.452	0.029	0.040	2	1/2
6	5.9	7.82	0.92	6.48	0.16	0.51	0.52	-0.056	-0.452	0.029	0.040	2	1/2
6	6.0	7.82	0.92	6.48	0.16	0.51	0.52	-0.056	-0.452	0.029	0.040	2	1/2

Table 5.3 Parameter stability for selected distribution statistics for the full Balkan extent

Similarly, λ is in the range 0.37 to 0.61, with σ_λ between 0.22 and 0.52. Lower values for M_{CUT}, in the range 4.6 $M_s \rightarrow$ 5.5 M_s, generally return higher estimates for ω, σ_ω, while λ is markedly lower.

Parameters ω and λ only reduce at higher M_{CUT} for shorter extreme intervals. M_{CUT} of 5.4 M_s (specifically for an extreme interval of 4-years) may be considered such a critical magnitude, after which ω generally decreases in-line with shorter extreme intervals. It is likely that at this M_{CUT}, missing years held in the data start to be excluded by the statistical model, resulting in more realistic hazard estimates. The effect of missing years and their relationships with NPER and M_{CUT} is considered in section 5.3.9. Increasing M_{CUT} by 0.1 to 5.5 M_s for a 4-year NPER reduces ω from 7.72 M_s to 7.69 M_s with no noticeable change to σ_ω (0.57 to 0.56) while λ increases from 0.58 to 0.61 with σ_λ changing from 0.32 to 0.37.

Noteworthy improvements to ω and λ using 5- and 6-year extreme intervals are only introduced at M_{CUT} of 5.6 M_s for both extreme intervals. However, estimates of ω and λ for both of these condition suites (M_{CUT} = 5.6 M_s with 5-year extremes and M_{CUT} = 5.6 M_s with 6-year extremes) suggest that the distribution provides a poorer fit to data extremes, with higher ω, σ_ω, σ_λ and lower λ compared with the conditions of M_{CUT} = 5.5 M_s with 4-year extremes.

If one considers the region's seismicity and the dominant seismicity here, conditions of M_{CUT} = 5.5 M_s with 4-year extreme intervals may be realistic due to the region's lower seismicity levels compared with Greece, west Turkey and the Aegean to the south and east. For example, Burton *et al.* (2004b) adopted never less than 6-yearly extremes at M_{CUT} of 5.5 M_s for their hazard analysis of this area, so a lower extreme interval may seem reasonable here (Burton *et al.*, 2004b).

Data for the area bounded by 21°-25.5°E, 40°-43°N are considered in Table 5.4. Lower NPER (4 and 5 years) and an M_{CUT} of <5.0 M_s produce wildly inflated, physically unrealisable estimates for ω in excess of 9.0 M_s, and occasionally in excess of 10.0 M_s. Without further investigation these would suggest Gumbel's first distribution might be better suited to modelling magnitude recurrence hazard of this sub region. This particular *scenario* is considered in more detail in section 5.3.11. The upper bound ω begins to stabilise and approach realistic values with respect to observed seismicity for M_{CUT} > 5.0 M_s and NPER of 4, 5, and 6 years. Again, a distinct critical magnitude can be seen at a specific M_{CUT} for each NPER considered, and for southwest Bulgaria this occurs at 5.1 M_s for NPER of 4 and 5 years and 5.2 M_s for an NPER of 6 years. For an NPER of 4 years, there are generally insufficient extreme data to establish Gumbel's third distribution for an M_{CUT} greater than 5.6 M_s without decreasing the minimum percentage of extreme values necessary (LIMIT; section 3.4.1).

NPER	M_{CUT}	ω	σ_ω	μ	σ_μ	λ	σ_λ	$\sigma^2_{\omega\mu}$	$\sigma^2_{\omega\lambda}$	$\sigma^2_{\mu\lambda}$	X^2	NMISS	LIMIT
4	5.0	9.99	4.52	5.15	0.13	0.18	0.21	0.013	-0.955	-0.002	0.196	4	1/2
4	5.1	8.81	2.26	4.95	0.22	0.30	0.27	0.207	-0.597	-0.031	0.142	8	1/2
4	5.2	8.84	2.32	4.71	0.45	0.34	0.34	0.726	-0.776	-0.123	0.083	12	1/2
4	5.3	8.84	2.32	4.71	0.45	0.34	0.34	0.726	-0.776	-0.123	0.083	12	1/2
4	5.4	8.11	1.22	4.15	1.05	0.57	0.48	0.960	-0.554	-0.452	0.037	15	1/3
4	5.5	7.97	1.06	3.86	1.48	0.65	0.55	1.190	-0.548	-0.755	0.031	16	1/3
4	5.6	7.84	0.99	3.41	2.98	0.77	0.78	2.317	-0.715	-2.223	0.013	18	1/4
4	5.7	7.84	0.99	3.41	2.98	0.77	0.78	2.317	-0.715	-2.223	0.013	18	1/4
4	5.8	7.89	1.25	3.75	3.68	0.70	0.95	3.797	-1.124	-3.361	0.019	19	1/4
4	5.9	7.89	1.25	3.75	3.68	0.70	0.95	3.797	-1.124	-3.361	0.019	19	1/4
4	6.0	7.89	1.25	3.75	3.68	0.70	0.95	3.797	-1.124	-3.361	0.019	19	1/4
5	5.0	9.90	3.52	5.58	0.13	0.21	0.20	-0.169	-0.710	0.009	0.175	1	1/2
5	5.1	8.61	1.57	5.51	0.15	0.36	0.26	-0.039	-0.394	0.004	0.106	3	1/2
5	5.2	7.93	0.83	5.33	0.24	0.61	0.38	0.051	-0.296	-0.040	0.030	6	1/2
5	**5.3**	**7.84**	**0.76**	**5.26**	**0.32**	**0.68**	**0.44**	**0.094**	**-0.310**	**-0.084**	**0.021**	**7**	**1/2**
5	5.4	7.78	0.72	5.19	0.44	0.75	0.52	0.158	-0.342	-0.165	0.018	8	1/2
5	5.5	7.78	0.72	5.19	0.44	0.75	0.52	0.158	-0.342	-0.165	0.018	8	1/2
5	5.6	7.70	0.71	5.06	0.91	0.84	0.74	0.407	-0.469	-0.578	0.008	10	1/2
5	5.7	7.70	0.71	5.06	0.91	0.84	0.74	0.407	-0.469	-0.578	0.008	10	1/2
5	5.8	7.76	0.89	5.22	1.19	0.75	0.86	0.740	-0.711	-0.915	0.004	11	1/3
5	5.9	7.76	0.89	5.22	1.19	0.75	0.86	0.740	-0.711	-0.915	0.004	11	1/3
5	6.0	7.76	0.89	5.22	1.19	0.75	0.86	0.740	-0.711	-0.915	0.004	11	1/3
6	5.0	15.70	27.37	5.57	0.14	0.07	0.21	-1.464	-5.616	0.011	0.247	0	1/2
6	5.1	12.06	10.72	5.53	0.14	0.12	0.23	-0.409	-2.470	0.008	0.209	1	1/2
6	5.2	8.92	2.55	5.40	0.20	0.31	0.33	0.094	-0.819	-0.018	0.155	4	1/2
6	5.3	8.57	1.92	5.33	0.25	0.39	0.37	0.163	-0.692	-0.043	0.140	5	1/2
6	5.4	8.28	1.46	5.23	0.33	0.48	0.42	0.227	-0.596	-0.087	0.126	6	1/2
6	5.5	8.03	1.10	5.06	0.48	0.60	0.50	0.293	-0.516	-0.175	0.112	7	1/2
6	5.6[1]	7.69	0.69	4.41	1.31	0.96	0.77	0.583	-0.470	-0.899	0.058	9	1/3
6	5.8	7.85	1.35	5.10	2.33	0.70	1.23	2.496	-1.572	-2.690	0.035	11	1/3
6	5.9	7.85	1.35	5.10	2.33	0.70	1.23	2.496	-1.572	-2.690	0.035	11	1/3
6	6.0	7.85	1.35	5.10	2.33	0.70	1.23	2.496	-1.572	-2.690	0.035	11	1/3

[1] A $G^{(III)}$ distribution failed to fit when NPER = 6 years and M_{CUT} = 5.7 M_s

Table 5.4 Parameter stability for selected distribution statistics for southwest Bulgaria

Of these combined sets of M_{CUT} and NPER considered, an M_{CUT} of 5.3 M_s and NPER of 5 years seems the most suitable for application as they return the most realistic estimates of ω and higher μ with smaller σ_μ and σ_λ. Although marginally higher values for M_{CUT} return reduced estimates for ω, σ_ω and σ_μ, σ_λ is higher, so casting some doubt over the rigorousness of ω.

Distribution curves for both geographic areas considered that result from NPER and M_{CUT} criteria discussed and selected in this and previous sections are given in Figure 5.9 with a fuller discussion given in section 5.3.8 with respect to the choice of distribution plotting point rule.

5.3.8 Choice of extreme probability plotting point rule

A number of historical probability distribution plotting point rules are available to use with extreme observations extracted from a parent distribution and are in outlined section 3.4.1. Having selected suitable values for M_{CUT}, NPER and start year of data to consider, along with starting values for Gumbel's third distribution parameter set (ω, μ, λ), the next step is to plot all extreme values that will be extracted under these conditions to illustrate how these plotting point rules differ. Variations for the Balkan extent and southwest Bulgaria are shown in Figure 5.9(a) and (b) respectively.

In both instances Gumbel's plotting point rule given by Eq. (3-6; dashed line and crosses), has the lowest curvature to these data, resulting in the highest ω forecast. Gumbel's alternative solution given by Eq. (3-7; grey line and open circles) and Gringorten's alternative recommendation for when $N \geq 20$ (Eq. (3-8); solid line and solid circles) are identical to each other, to within 0.1 M, and show the strongest distribution curvature. For these reasons, and as it is the most commonly used distribution plot point rule at the current time and also holds for when sample sizes are less than 20, Gringorten's solution will be used to provide estimates for the distribution's reduced variate, $-\ln(-\ln(P))$, average return periods of extreme events and the probability, P, of these extremes occurring.

Unsuitable suites of M_{CUT} and NPER would not only manifest themselves with inaccurate estimates for (ω, μ, λ) but also visually with lower magnitude extreme observations deviating from the distribution's 'best-fit' curve, and weaker distribution curvature.

5.3.9 NPER and NMISS

Choice of NPER used against any given magnitude data will have a strong bearing on the number of extreme observations that are extracted and used from a parent distribution. Selecting a longer extreme interval will exclude a higher proportion of extreme observations from consideration.

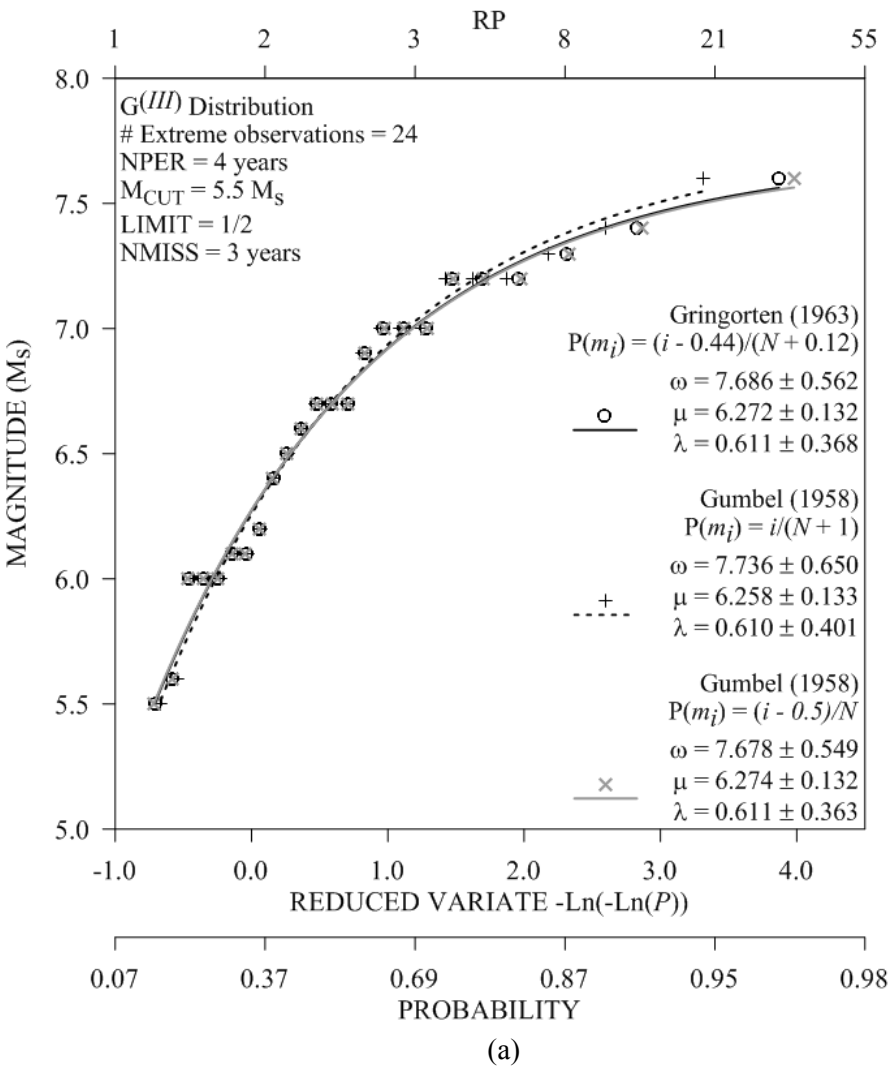

(a)

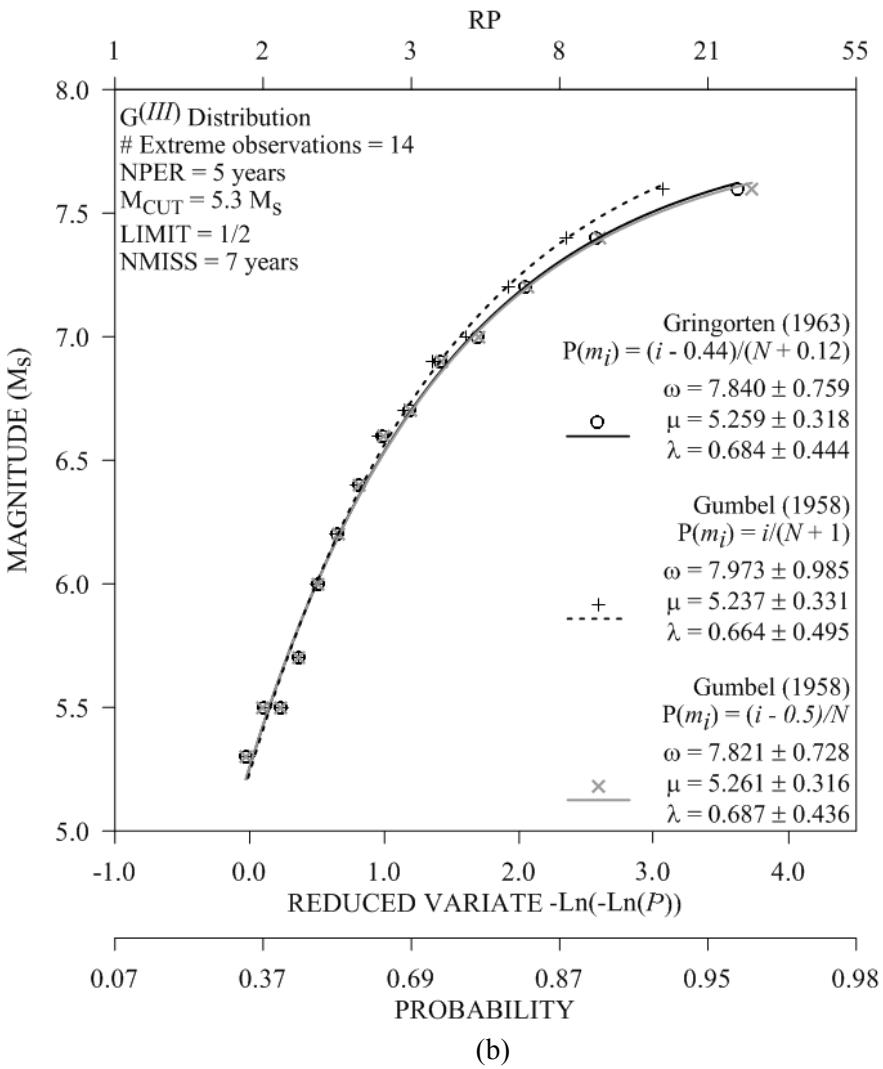

(b)

Figure 5.9 Comparison of selected extreme probability plotting point rules using the finalised parameterisation and catalogue data choices for (a) the full Balkan extent and (b) southwest Bulgaria; starting values for each distribution parameter are as in Table 5.2

This should be done intentionally to remove missing years from the ensuing analysis; i.e. those years with largest magnitude events still considered annual extremes – that are above the threshold of magnitude completeness, M_c (a characteristic property of a catalogue), but below the imposed cut-off magnitude, M_{CUT} – but are excluded as these are located in, for example, periods of quiescence.

A potentially adverse effect of setting NPER is to set it too high so as to exclude several true extreme observations that warrant consideration. Selection of a correct NPER will improve the efficiency of the statistical system (Burton *et al.*, 2004b). Extending NPER decreases the number of extreme intervals necessary to cover a particular time interval. This will typically decrease the number of intervals for which no extreme can be found ('*null*' entries or '*dummy*' observations), thus increasing the efficiency of the system. The number of intervals considered that are not assigned an *N*-year extreme interval equals NMISS. It should be the worker's intention to determine NPER such that only '*dummy*' extreme observations or artificially low, misleading annual extreme observations are excluded from statistical consideration.

However, it is not only NPER that directly affects NMISS and the stability of forecasted (ω, μ, λ). Raising M_{CUT} will also progressively exclude more extreme observations. This is illustrated in Figure 5.10 for the broader Balkan extent and southwest Bulgaria. These illustrate:

1. All observed annual extreme magnitudes (grey line) for the area concerned, disregarding any M_{CUT} or NPER. The lowest extreme observations are 4.5 M_s (1943 and 1987) and 3.1 M_s (1934 and 1942) for each geographic region respectively;

2. Extreme observations retained after applying only NPER selected in section 5.3.3 (blue line);

3. Extreme observations retained after applying both NPER (as in point 2) and the cut-off magnitude, M_{CUT}, selected in section 5.3.2 (red line).

Of importance to note in both figures are those extreme observations that are considered by point 2 above, but excluded by point 3. Considering Figure 5.10(a) as an example, one would expect 105 [years of data]/4[-year NPER] = 27 [26.25] extreme observations to be considered. Imposing M_{CUT} of 5.5 M_s excludes the three lowest extreme observations (1939, 1946 and 1997). These therefore are the three NMISS years of this particular suite of conditions. Similarly, the seven NMISS values (1917, 1939, 1941, 1947, 1953, 1965 and 1970) associated to the final selected conditions of southwest Bulgaria are highlighted (blue line) in Figure 5.10(b).

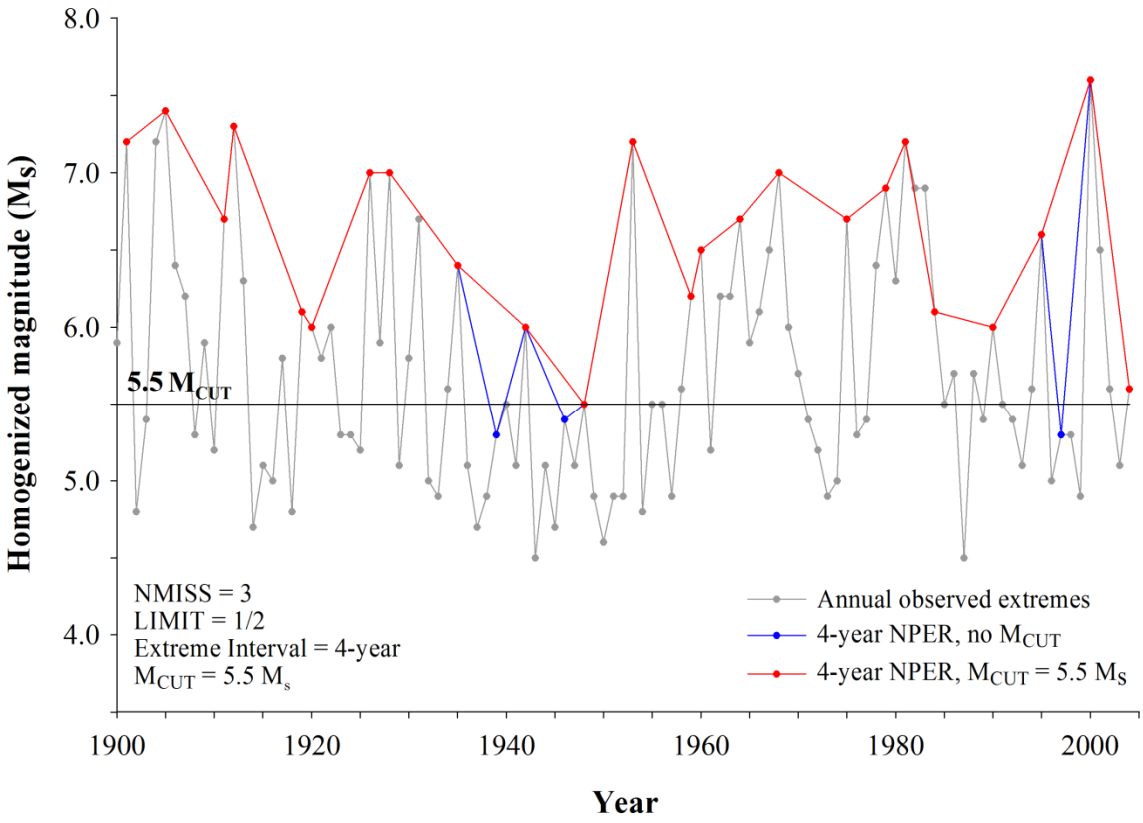

(a)

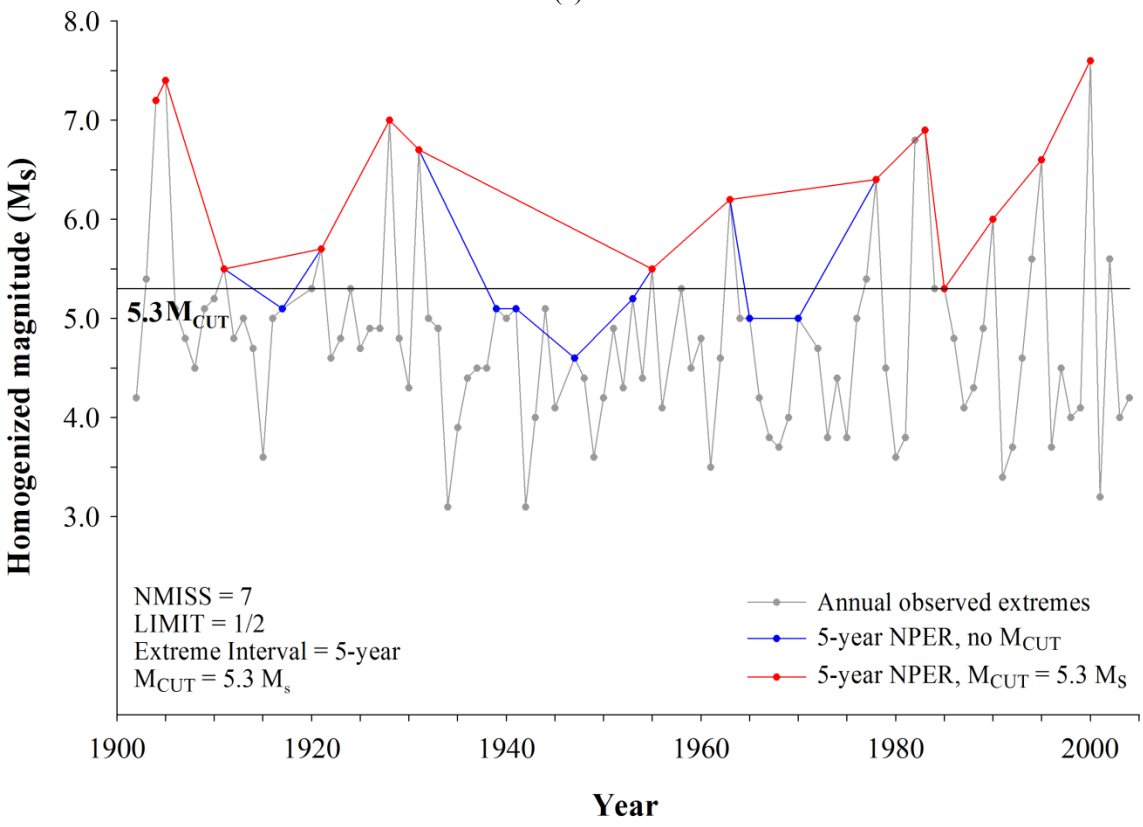

(b)

Figure 5.10 Extreme magnitudes considered (red line) and excluded (blue line) from analysis with respect to annual extreme values [grey line; when M_{CUT} set at lowest homogenized M_s of catalogue in its raw state] and M_{CUT} applied, for (a) full Balkan extent and (b) southwest Bulgaria

As the number of excluded extreme observations increases due to altering NPER and M_{CUT}, the proportion of total available observed extreme values statistically considered will reduce. In this situation, there comes a point when the extreme values set considered become insufficient to forecast extreme values statistics. To counter this, one may reduce the minimum proportion (LIMIT) of extreme data accepted from the initial parent distribution. Such a practice may prove acceptable and beneficial in forecasting (ω, μ, λ) and associated uncertainties, but at a cost of unrealistically large X^2 and off-diagonal elements of the error matrix, ε (Table 5.3). Therefore, only analysis cells that with LIMIT ≥ 1/3 will be accepted and taken forward to contour all forms of seismic hazard considered in chapter 5 and 6.

5.3.10 Rationalizing Gumbel's third distribution to cells when λ ≥ 1

Certain suites of higher M_{CUT} and NPER values fail to resolve to Gumbel's third distribution due to λ being forecast ≥ 1 for a small selection of analysis cells (e.g. 5.7 M_{CUT} with NPER = 6 years for data of southwest Bulgaria). This is mathematically unacceptable (Gumbel, 1958) and is not compatible with his third distribution of extreme values. Equation (3-3) states Gumbel's third distribution and the acceptable values for its three parameters (ω, μ, λ). As k (i.e. 1/λ) must be greater than 1 (so $0 < \lambda < 1$), cells that are forecast λ ≥ 1 need an alternative treatment to ensure this is achieved. The case k [λ] = 1 is the exponential function. Setting k [λ] = 1 reduces Eq. (3-3) to Eq. (5-1), with λ = 1;

$$G^{(III)}(m) = \exp\left[-\left(\frac{\omega - m}{\omega - \mu}\right)\right],$$

$$G^{(III)}(m) \equiv \exp[1/\lambda + am], \qquad \text{where } 1/\lambda \text{ (constant)} = -a\omega, \text{ with } a = 1/(\omega - \mu) \qquad (5\text{-}1)$$

As $\lambda \rightarrow 1$, the $G^{(III)}$ curve approximates to the two-parameter (α, μ) first-type distribution. Resolving earthquake extreme data to Gumbel's first distribution will be considered in section 5.3.11. Such occurrences of λ forecast ≥1 provide opportunity to investigate effects of remedying analysis cells for which λ was estimated ≥1. This situation is likely to arise when Gumbel's third distribution cannot be fitted to extreme data, due to insufficient numbers of extremes in the sample, resulting from long extreme intervals, and a high cut-off magnitude. Although the increase above 1.0 for λ is typically minor, the fact it occurs compromises use of the third distribution as a possible statistical magnitude recurrence model.

Two solutions are investigated to resolve analysis cells that are forecast $\lambda \geq 1$; 1) setting $\lambda = 1$, and, 2) setting λ to the last estimate of $\lambda < 1$ from the applied distribution algorithm. Both solutions are applied here to the specific condition set of 5.7 M_{CUT} with NPER = 6 years for data of southwest Bulgaria. Estimates for (ω, μ, λ) and X^2 for both solutions to $\lambda \geq 1$ are given in Figure 5.11.

Immediately it is important to recognise that setting $\lambda = 1$ (solid line) is limited as a suitable option due to all return period magnitudes being forecast the same value (in this instance 7.64 M_s). That aside, these possible solutions to instances of $\lambda \geq 1$ appear remarkably similar. ω is identical, with σ_ω varying by <0.01 M_s, while μ and σ_μ differ by <0.01 M_s and 0.01 M_s respectively. Similarly, forecast maximum and pnbe return period magnitudes differ by < 0.001 M_s.

As there is little discernable difference between estimates of (ω, μ, λ) and their uncertainties, one has to base a recommendation for the solution when $\lambda \geq 1$ on the effect that setting $\lambda = 1$ has on maximum return period forecasts by setting them to identical values. Consequently if a correction to λ is required to contour magnitude hazard, in a particular analysis cell, λ will be set to the last estimate of $\lambda < 1$. Fitting Gumbel's first extreme distribution is considered in section 5.3.11.

5.3.11 Rationalizing Gumbel's first distribution to earthquake data when $\lambda \geq 1$

The *whole process* cumulative frequency-magnitude distribution (Eq. (3-1); Gutenberg and Richter, 1944, 1949; Richter, 1958) provides the conventional approach to assessing magnitude seismic hazard. This method notionally suggests a linear distribution to magnitude recurrence throughout the observed magnitude range. However, experimental data show a cumulative frequency-magnitude distribution does not hold at high magnitudes due to the infrequency of large magnitude events. It is also difficult to fit the distribution at low magnitudes due to incomplete event recording. Consequently data will typically *tail off* from the linear ideal for this distribution at high and low magnitudes.

Due to its unbounded nature, Gumbel's first extreme values distribution can be linked to the full process cumulative frequency-magnitude distribution, but holds for initial distributions unlimited in both directions. The cumulative frequency-magnitude distribution holds best if assumed it is Poissonian in nature for the number of earthquakes with m > 0, and m is a random variable distributed with a cumulative distribution function,

$$F(m) = 1\text{-}e^{-\beta m} \qquad m \geq 0 \qquad (5\text{-}2)$$

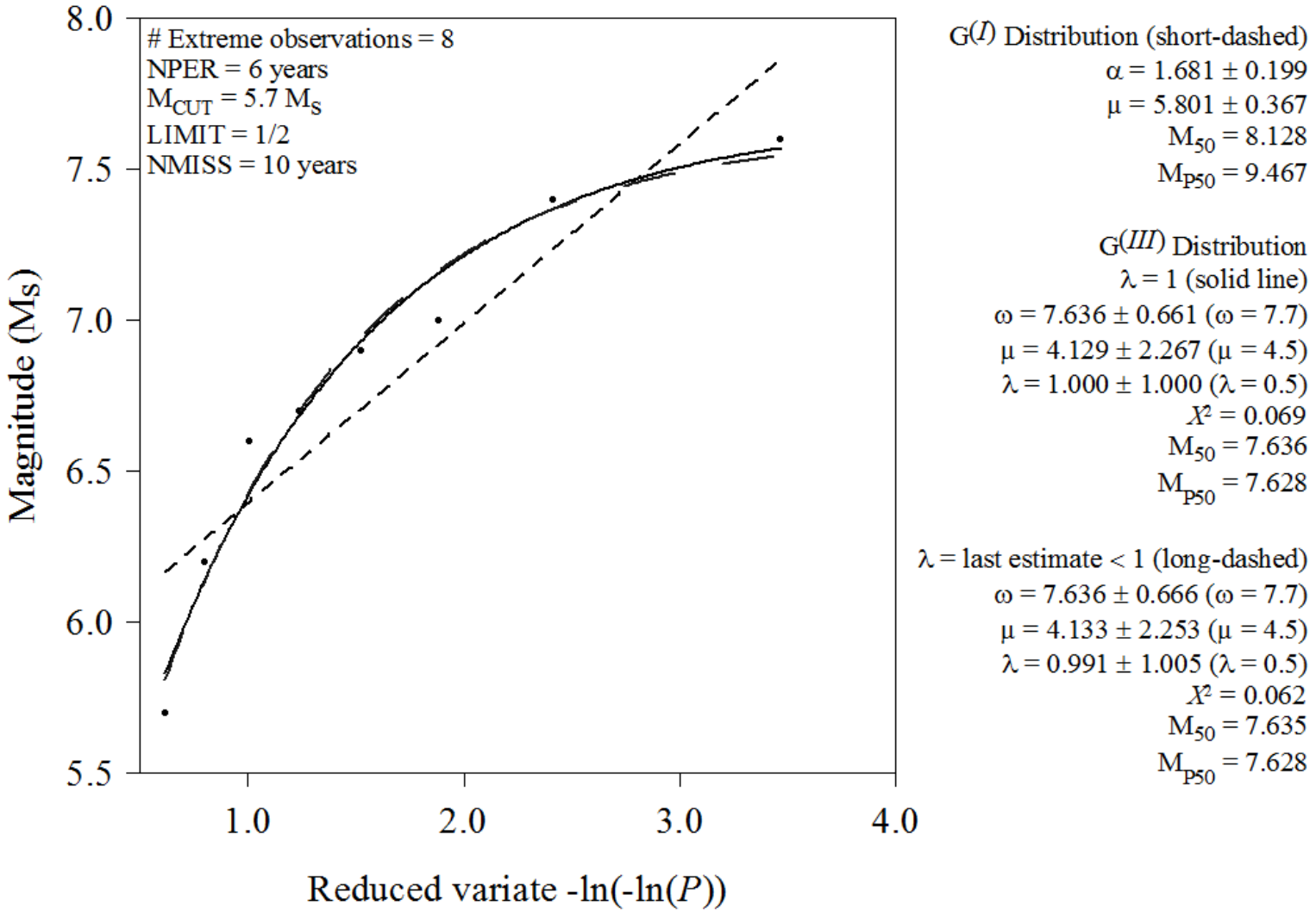

Figure 5.11 Fitting Gumbel's first and third extreme values distributions with two solutions considered for when $\lambda \geq 1$ for the third distribution

From this, the largest annual magnitude will be distributed with a cumulative distribution function,

$$G(m) = \exp[-a \exp(-\beta m)] \qquad m \geq 0 \qquad (5\text{-}3)$$

and corresponds to Eq. (3-2) giving Gumbel's first distribution of extreme values. The existence of an upper bound magnitude needs to be recognised mathematically in any statistical distribution applied to earthquake data (Esteva, 1976). Doing so will counter a major limitation of the *whole process* cumulative frequency-magnitude distribution which is in theory unbounded by a limiting upper magnitude.

Gumbel's first distribution is applied to the example set of M_{CUT} and NPER values for which the third distribution failed in Table 5.4. Observations in section 5.3.7 of unrealistically large estimates for ω suggest this may be an acceptable alternative approach to use. A specimen illustration of a $G^{(I)}$ 'curve' (short dashed line) superimposed on equivalent $G^{(III)}$ curves for the same extreme observations for the set of M_{CUT} and MPER considered, along with estimates for (α, μ), their uncertainties and maximum and 90% pnbe return period extreme magnitude forecasts is in Figure 5.11.

Calculating M_{50} and M_{P50} provides direct comparison between these two distributions for identical data. Estimates for both M_{50} and M_{P50} from a $G^{(I)}$ distribution are both larger than those derived from the $G^{(III)}$ distribution. All are outside the range of observed seismicity, with M_{P50} outside the acknowledged limit on the surface-wave magnitude scale for global seismicity. Due to this and observations in preceding sections, a $G^{(III)}$ distribution should be used for magnitude hazard.

5.3.12 Stability in *T*-year modal maximum earthquake forecasts

Stability in 50-year modal maximum magnitudes from conditions selected in the previous sections is shown in Figure 5.12 for the Balkans with (a) M_{CUT} of 5.5 M_s and start year of 1900, (b) 4-year NPER and start year of 1900, (c) M_{CUT} of 5.5 M_s and 4-year NPER, and for southwest Bulgaria for data of (d) M_{CUT} of 5.3 M_s and start year of 1900, (e) 5-year NPER and start year of 1900, (f) M_{CUT} of 5.3 M_s and 5-year NPER. These illustrations support decisions made earlier and summarised in section 5.3.13 relating to NPER and M_{CUT} to apply to data for both geographic regions considered.

5.3.13 Solution to parameterisation for Balkan earthquake extreme data

Conditions that have been selected to use during the ensuing seismic hazard assessment for (a) the Balkans, and (b) southwest Bulgaria, based on the preceding discussion are listed in Table 5.5.

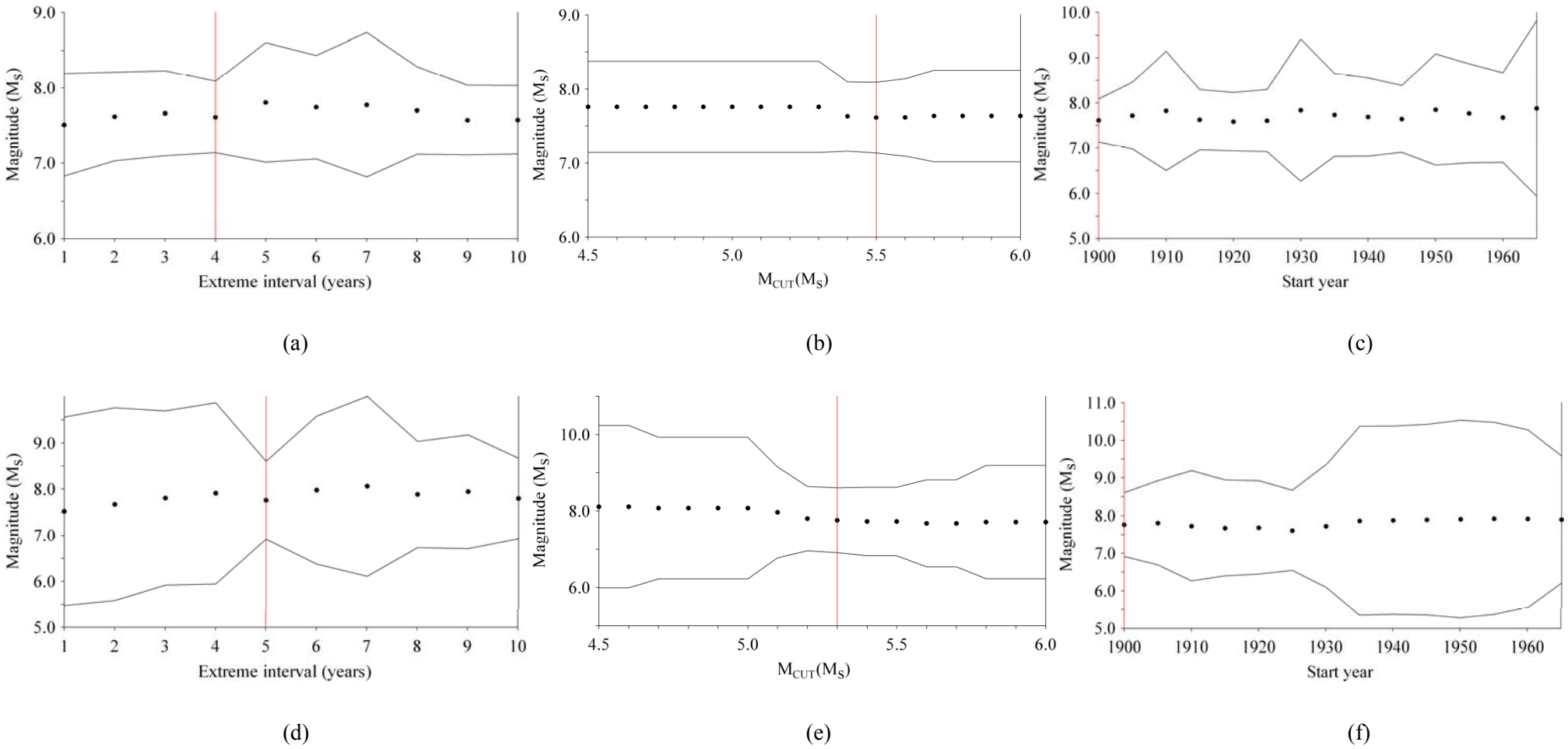

Figure 5.12 Variation in forecasted 50-year modal maximum magnitude M_{50}, for the selected data conditions (Table 5.5) considering data for the broad Balkan region with (a) M_{CUT} of 5.5 M_s and start year of 1900, (b) 4-year extreme interval and start year of 1900, (c) M_{CUT} of 5.5 M_s and 4-year extreme interval, and for southwest Bulgaria with (d) M_{CUT} of 5.3 M_s and start year of 1900, (e) 5-year extreme interval and start year of 1900, (f) M_{CUT} of 5.3 M_s and 5-year extreme interval. Vertical red lines indicate the final conditions selected

	The Balkans	Southwest Bulgaria
Statistical distribution	$G^{(III)}$	$G^{(III)}$
Solution to $\lambda \geq 1$	Last estimate of iteration < 1	Last estimate of iteration < 1
Analysis cell size (°)	2	2
M_{CUT} (M_s)	5.5	5.3
NPER (years)	4	5
Start year	1900	1900
ω_{START}	7.7	7.7
μ_{START}	4.5	4.5
λ_{START}	0.5	0.5

Table 5.5 Rationalized statistical conditions for considering Balkan extreme seismic hazard

The earthquakes in the catalogue that are retained in each area from adopting these criteria are given in Figure 5.13 and Figure 5.14 respectively and help estimate (a) *whole* and (b) *part process* hazard estimates (green spheres $\Rightarrow$ focal depth h <10 km; yellow spheres $\Rightarrow$ focal depth 10 km $\leq h \leq$ 20 km; yellow spheres $\Rightarrow$ focal depth 10 km $\leq h \leq$ 20 km; grey spheres $\Rightarrow$ focal depth $h \geq$ 30 km).

The most significant focal depth range to appreciate in Figure 5.13 and Figure 5.14 is that representing seismicity in the focal depth range of 10 km $\leq h \leq$ 20 km (yellow spheres). This encompasses seismicity considered to contribute the majority of the extreme seismic hazard (Figure 2.14). Consequently, these are the maximum and minimum *scenario* focal depths to be considered in all earthquake perceptibility and integrated perceptibility plots in chapter 6 and Appendices 18 to 29 (inc). The other focal depth ranges highlighted are standard divisions adopted between shallow and intermediate depth seismicity and these dominate regional Balkan seismicity (section 2.5).

5.4 Site-specific extreme distribution magnitude parameterisation

Cities in Figure 5.1 need to be considered using the sensitivity analysis adopted in section 5.3. This will ensure site-specific hazard estimates result from statistical extreme distributions that are well-constrained to the extreme sample for each city considered, and are realistic with respect to seismogenic sources relevant to the city in question. Site-specific parameterisation to be adopted for each city is summarised in Table 5.6. Starting values for (ω, μ, λ) are as given in Table 5.5.

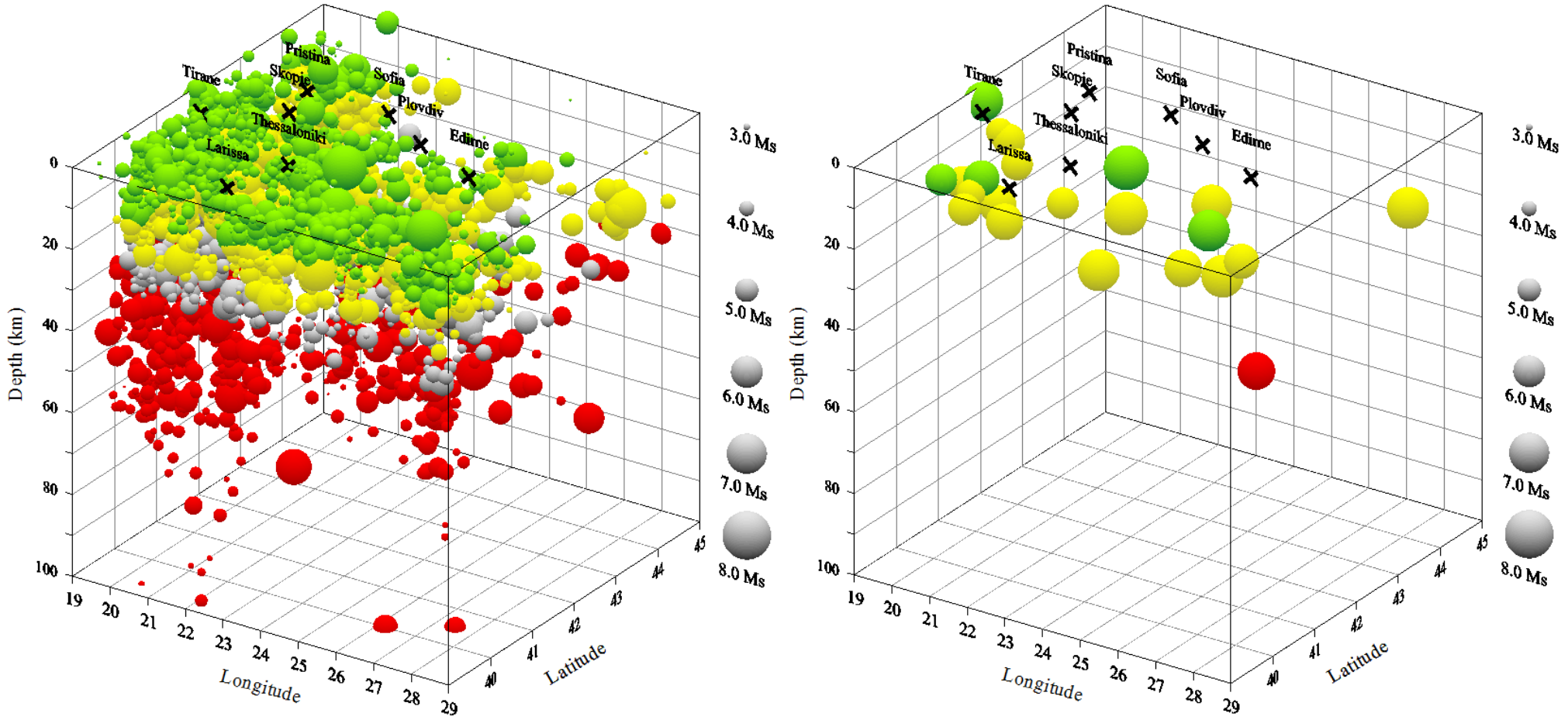

(a) (b)

Figure 5.13 Earthquake hypocentres for the broader Balkan extent that will be considered for (a) *whole process* and (b) *part process* hazard statistics from the composed catalogue retained after adopting filtering criteria outlined in Table 5.5 (green spheres $\Rightarrow h$ <10 km; yellow spheres $\Rightarrow$ 10 km $\leq h \leq$ 20 km; grey spheres $\Rightarrow$ 20 km < h < 30 km; red spheres $\Rightarrow h \geq$ 30 km)

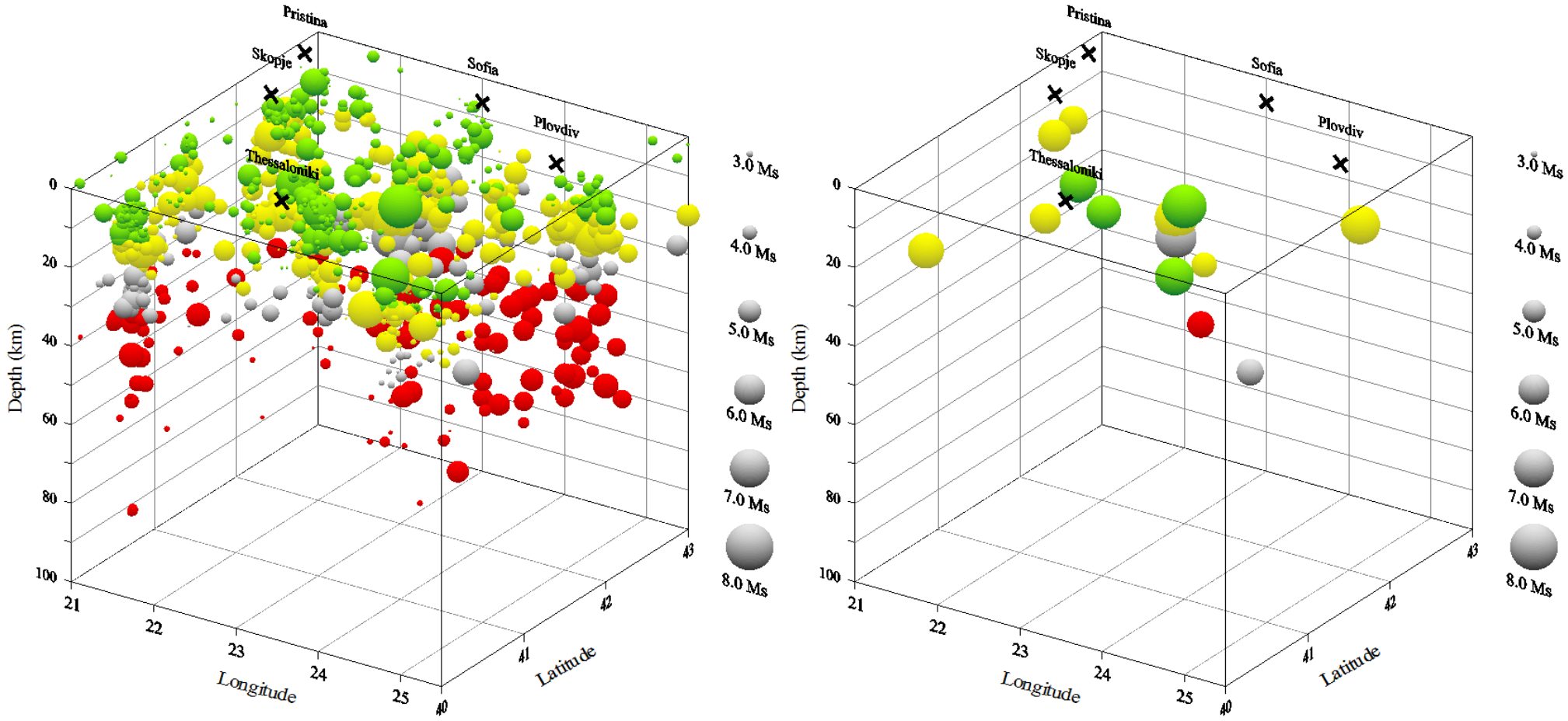

(a) (b)

Figure 5.14 Earthquake hypocentres for the southwest Bulgaria that will be considered for (a) *whole process* and (b) *part process* hazard statistics from the composed catalogue retained after adopting filtering criteria outlined in Table 5.5 (green spheres $\Rightarrow h$ <10 km; yellow spheres $\Rightarrow$ 10 km $\leq h \leq$ 20 km; grey spheres $\Rightarrow$ 20 km $< h <$ 30 km; red spheres $\Rightarrow h \geq$ 30 km)

City	NPER (years)	Start year	M_{CUT} (M_s)
Edirne	6	1900	5.2
Larissa	5	1900	5.0
Plovdiv	6	1900	5.6
Pristina	2	1900	4.9
Skopje	2	1900	5.0
Sofia	5	1900	5.3
Thessaloniki	5	1900	5.4
Tirane	6	1900	5.6

Table 5.6 Site-specific $G^{(III)}$ distribution parameterisation for urban centres for which magnitude, PGA and PGV seismic hazard will be considered

Sofia will be used as a site-specific example throughout chapters 5 and 6 for each hazard descriptor considered. This is an important city in the context of this region due to its central location in the southwest region of interest, its proximity to the borders of Bulgaria, FYR of Macedonia and Greece and large magnitude historical earthquakes, and has national importance as the capital of Bulgaria. Site-specific extreme distribution curves are presented in the main text for this city, while equivalent illustrations for the other cities are given in related appendices. Site-specific hypocentral distributions extracted to estimate hazard around each city are in Appendix 4 (Sofia's *whole* and *part* hypocentral distributions are illustrated in Figure 5.15).

5.5 Extreme earthquake hazard

Three geographical aspects of interest run through this seismic hazard assessment of the full broader Balkan extent regardless of the measure for seismic hazard considered. These are: 1) the region north of 43°N; 2) the region south of 43°N offering direct comparison to work of Burton *et al.* (2003, 2004b) for ground acceleration and magnitude and perceptibility hazard respectively; and 3) the sub region containing the political triple junction between Bulgaria, Greece and the FYR of Macedonia. These will each be considered throughout the following chapters.

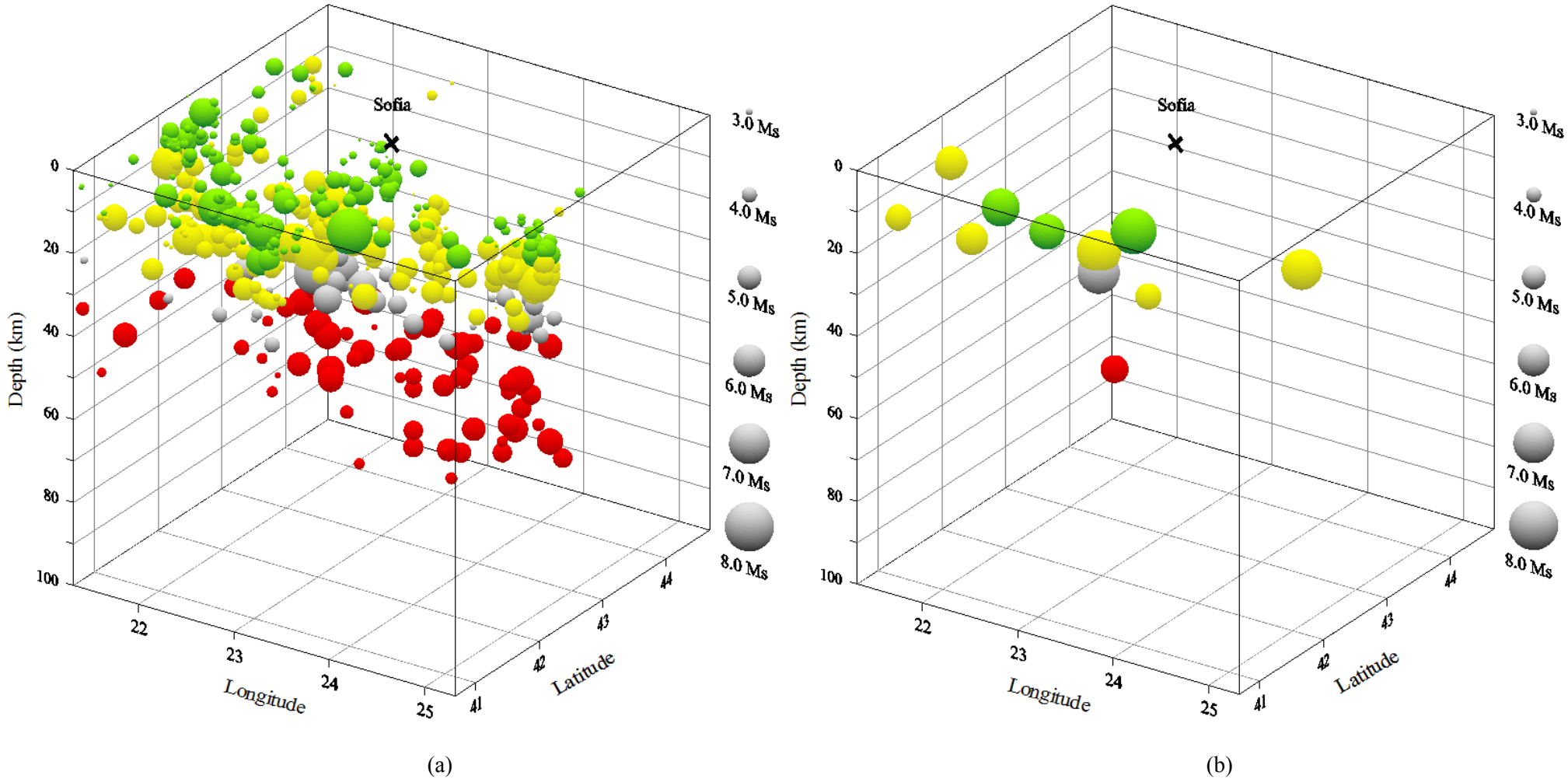

Figure 5.15 Site-specific hypocentral distributions contributing to (a) *whole process* and (b) *part process* seismic hazard statistics for Sofia (green spheres ⇒ h <10 km; yellow spheres ⇒ 10 km ≤ h ≤ 20 km; grey spheres ⇒ 20 km < h < 30 km; red spheres ⇒ h ≥ 30 km)

5.5.1 'Edge' effects

Cell size selected by the user to contour hazard are largely governed by the 'need' of the seismic hazard analysis, e.g. is magnitude recurrence or ground motion hazard to be investigated? In-depth knowledge of an area's seismicity will also impact upon cell size selected. A larger cell may be desirable to incorporate more seismicity in a low-seismicity environment. Smaller cells may be adopted to accommodate an area's ground motion characteristics, or to capture ground motions that have most effect on an area's characteristic building type (Makropoulos and Burton, 1985a).

The larger the cell size is, the higher the likelihood significant portions of it will occur outside the study area's border, and therefore the reach of the adopted earthquake catalogue, as one is usually synonymous with the other. This relationship will increase the proportion of analysis cell for which no recorded seismicity exists, in the context of the adopted catalogue.

A 'worst-case' *scenario* exists where insufficient extreme data are extracted against which either extreme distribution may be fitted. This will result in hazard forecasts being unobtainable, and areas of '*null*' forecast areas being present on the final hazard maps. These areas of '*null*' forecasts are the results of methodological limitations, although this does not mean these sub areas are devoid of hazard.

Therefore, the inner dashed rectangle to each hazard map that covers the broader area in chapters 5 and 6 represents the area within which all analysis cells are fully contained by the study area. The impact of 'edge' effects can be excluded from consideration when investigating these analysis cells. The effects on an extreme value analysis of increasing the proportion of an analysis cell lying outside a study area (notionally termed the cell's '*null area'*) is summarised in Figure 5.16.

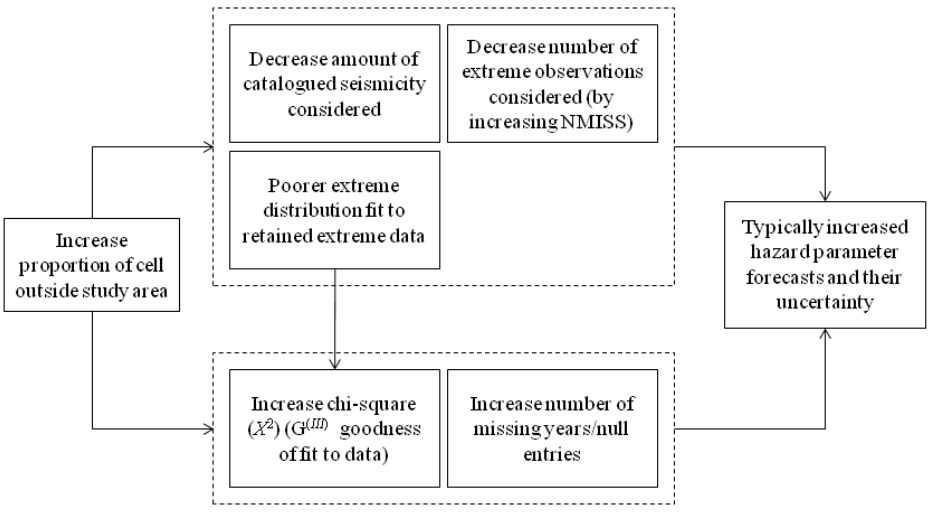

Figure 5.16 Impact of increasing a cell's '*null area*' outside a catalogued area

5.5.2 Nomenclature of hazard forecasts

Chapters 5 and 6 will adopt specific notation to discriminate between:

- Extreme forecasts for specific time intervals (M_{50}, M_{100}, M_{200});
- Extreme forecasts for specific time intervals at particular confidence levels (M_{P50}, M_{P100}, M_{P200});
- Adopted ground motion models (e.g. $TP92_A$, AM95_WDC, AM05, $TP92_V$, PP97), and,
- Earthquake perceptibility magnitude and probability forecasts (e.g. $M_{PI(VII)} = 6.6$, $P_{PI(VII)} \approx 2.1E{+}10^{-4}$; $M_{PA(150)} = 6.6$, $P_{PA(150)} \approx 1.1E{+}10^{-3}$; $M_{PV(5)} = 6.8$, $P_{PV(5)} \approx 1.1E{+}10^{-3}$).

A full nomenclature of hazard forecasts is provided in Appendix 1.

5.5.3 Magnitude (M_s) recurrence

Magnitude recurrence hazard is contoured in Figure 5.17 in terms of the modal maximum earthquake magnitude expected in (a) 50, (b) 100 and (c) 200 years using contour intervals of 0.25 M_s. Magnitude hazard equivalent to the earthquake with 90% probability of not being exceeded (pnbe) is contoured in Figure 5.18. The underlying statistics that create Figure 5.17 and Figure 5.18 are listed in Appendix 5, and this lists parameters (ω, μ, λ) and their uncertainties of Gumbel's third extreme distribution, and the maximum magnitudes for the time intervals stated above for the 156 computation nodes at which hazard could be established. The estimates for magnitudes at 90% pnbe for these same time intervals are also listed. Finally, estimates for the annual modal maximum earthquake, m(1), the maximum observed event contained in the analysis cell from the catalogue, M_M, values for the off-diagonal elements $\sigma^2_{\omega\mu}$, $\sigma^2_{\omega\lambda}$ and $\sigma^2_{\mu\lambda}$ of the extreme distribution's covariance error matrix, ε, and chi-square (X^2) are also provided. X^2 is a measure of the goodness-of-fit of the observed data extremes with Gumbel's third distribution to which they are fitted. Appendix 6 provides full covariance matrices for each computation node used to contour magnitude hazard across the regional extent using the zone-free approach described in section 3.9.

It is perhaps most useful to start discussing magnitude hazard by reviewing 100-year return period hazard (M_{100}; Figure 5.17(b)). As the final catalogue covers the region's seismicity for 105 years, this map is closest to the time span of observed seismicity represented by the adopted catalogue.

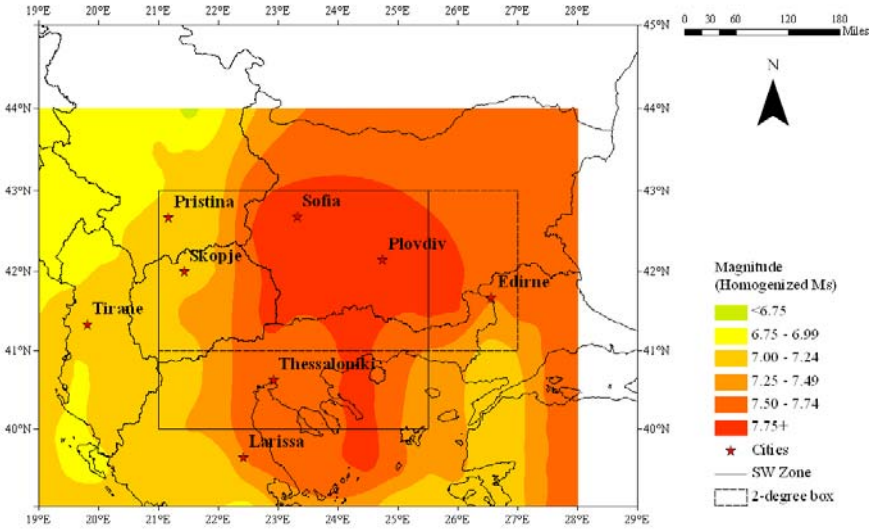

(a)

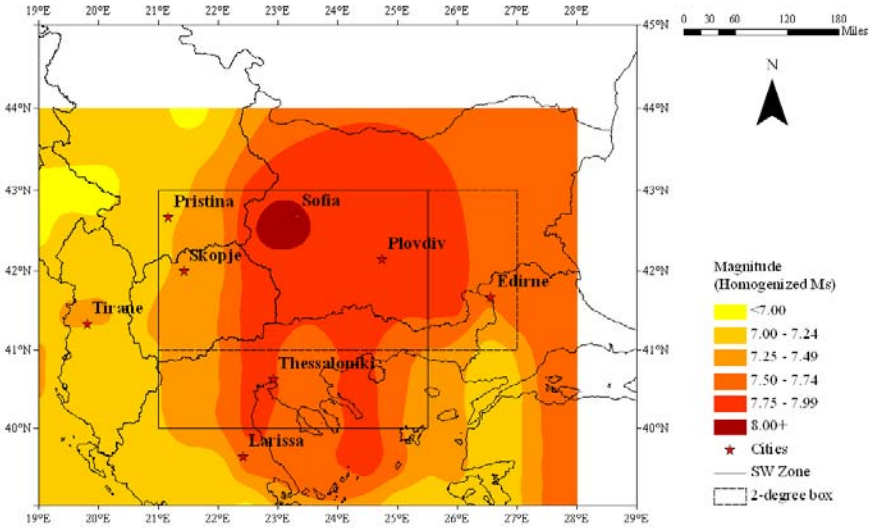

(b)

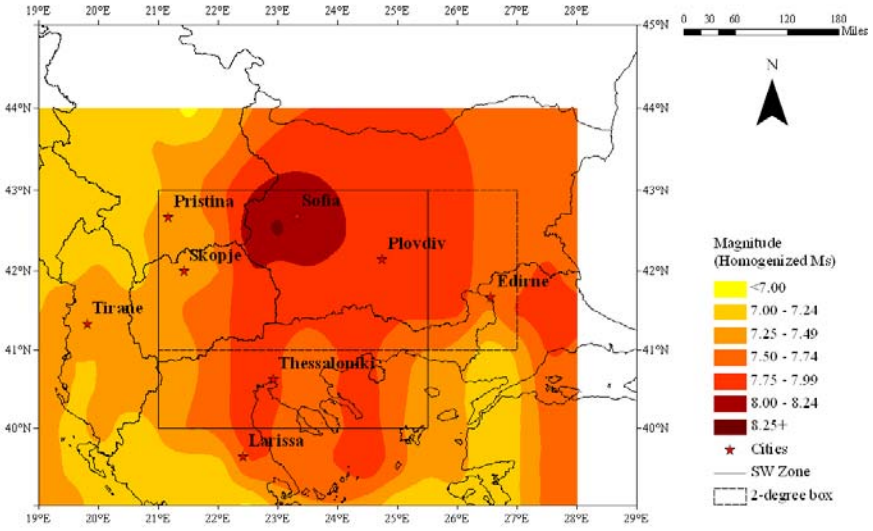

(c)

Figure 5.17 The modal maximum earthquake magnitude within (a) 50, (b) 100 and (c) 200 years. Contours are at intervals of 0.25 M_s

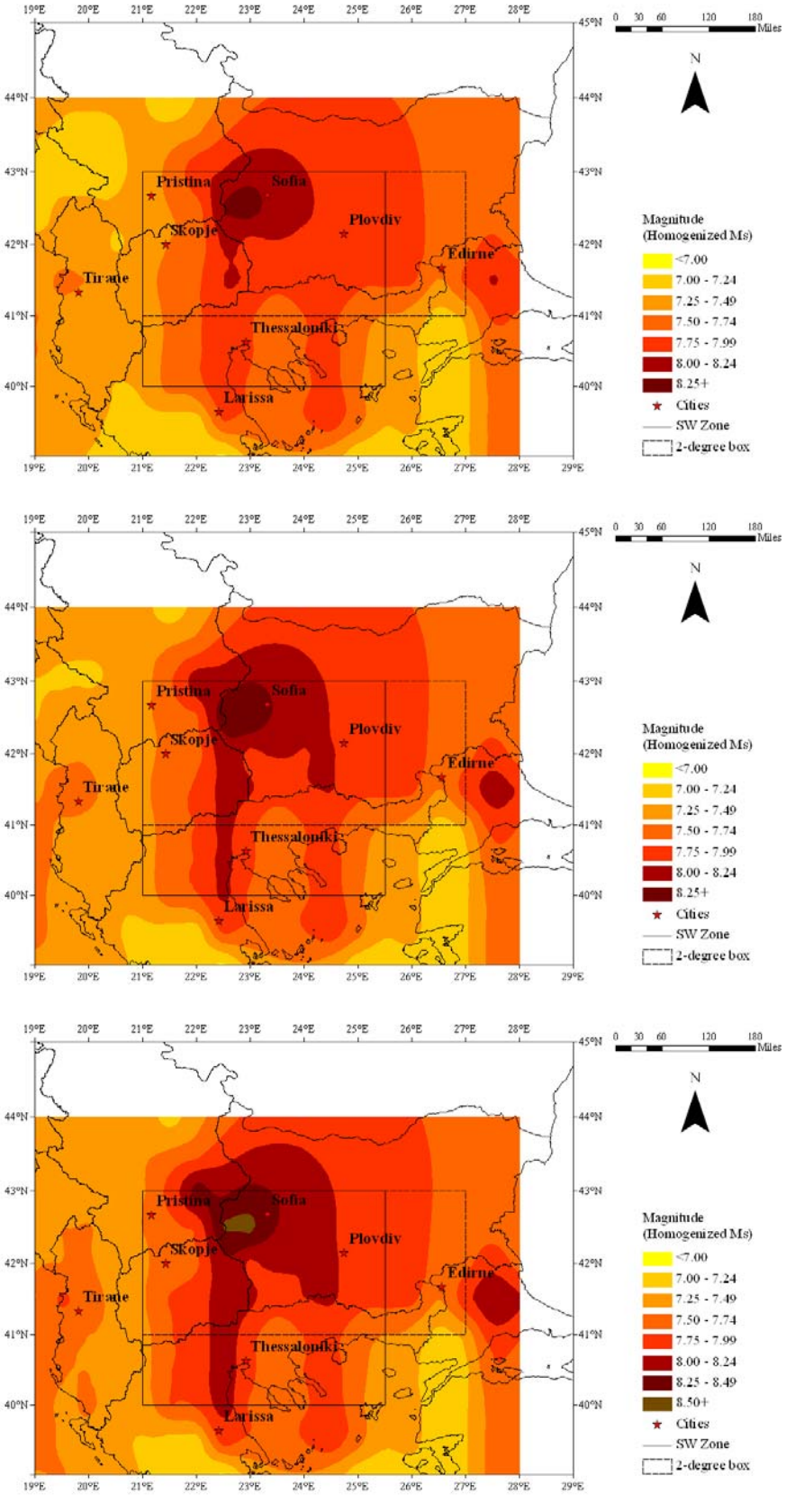

Figure 5.18 Magnitudes expected within (a) 50, (b) 100 and (c) 200 years, with 90% probability of being a maximum or not being exceeded. Contours are at intervals of 0.25 M_s

Hazard cannot be contoured for the entire region. It is evident from Figure 4.14 that there is clearly not enough catalogued seismicity in the northern and eastern-most 1° of the territory to support fitting an extreme distribution to cellular data after it has been refined using criteria outlined in Table 5.5 to return hazard estimates.

The first confined zone of highest extreme hazard is a localised area exceeding 8.00 M_s situated immediately over Sofia, northeast of the political triple junction (Figure 5.17(b)). This is encompassed by the 7.75 M_s contour that covers most of west and central Bulgaria and extends south into north Greece over Thessaloniki and the northern Aegean Sea. This larger area of high hazard also extends north to the Bulgaria-Romania border. No part of Bulgaria, except for the extreme northwest of the country is forecast magnitude hazard of less than 7.50 M_s in 100 years.

The majority of the area for which magnitude hazard can be forecast is estimated to be subject to extreme magnitudes of 7.00 M_s or greater. Only a very confined area in the extreme northwest over Serbia is forecast $M_{100} < 7.00$ M_s. A second zone of lower magnitude hazard ($M_{100} \approx 7.00$-7.50 M_s) is seen extending north-south over west Turkey.

The confined zone of highest hazard located northeast of the triple junction area increases to $M_{P100} \geq 8.25$ M_s when considering magnitude hazard at 90% pnbe (Figure 5.18). The 8.00 M_s contour has enlarged to encompass much of eastern FYR of Macedonia and western Bulgaria, as far east as Plovdiv. A thin zone of 8.00 M_s hazard also extends south into Greece as far as Larissa. Two further zones of high hazard also start to appear at the extreme west (7.00 $M_s \leq M_{P100} \leq 7.50$ M_s) and east (8.00 $M_s \leq M_{P100} \leq 8.25$ M_s) of the study region. The former is centred over Tirane and loosely follows the subduction zone of the Adriatic Sea.

The northeast corner of Bulgaria containing Varna, Shumen, Burgas and Ruse is forecast highs of 7.50-7.75 M_s in 100 years, rising to 7.75-8.00+ M_s at 90% pnbe in small pockets of high hazard. This is realistic with respect to the seismicity in the adopted catalogue. Central Bulgaria increases to 7.75-8.00 M_s (>8.0 M at 90% pnbe). Regions with lowest forecasted magnitude hazard are in the extreme northwest, local to north Serbia at <7.00 M_s (7.00-7.50 M_s).

The peaks of magnitude hazard have a strong similarity to the observed epicentral distribution of the region. As with ground acceleration hazard (section 5.5.4), zones of increased magnitude hazard are found at locations of high-magnitude and frequently occurring seismicity, e.g. southwest Bulgaria, along the coast of the Adriatic and Ionian Seas to the west of the region, and marking the North Anatolian Fault (NAF) across the Aegean Sea into Turkey.

Unlike a $G^{(I)}$ distribution, which has a linear characteristic associated with it between ground motion modelled and the logarithm of time, a $G^{(III)}$ distribution exhibits curvature to the extreme data, resulting in an asymptotic value for the upper bound magnitude ω. This characteristic varies significantly from location to location. ω for each analysis cell possesses a strong covariance with the curvature parameter, λ (as k = 1/λ in Gumbel's third distribution; that is, they are the inverse of each other). For individual computation nodes, values of λ are found to be in the range from 0.08 to 0.99. Evidently a number of analysis cells required λ to be reassessed in accordance with section 5.3.13. Co-varying values of ω also show significant differences. ω is in the range from 6.94 M_s (±0.64) to 12.46 M_s (±45.29). Similarly, values for σ_ω vary between 0.42 to 45.29 while σ_λ varies by 0.38 to 1.14. This fact is highlighted when viewing the sequence of contour maps of Figure 5.17. As the curvature of Gumbel's third distribution is not linear, variation in contoured patterns become negligible for smaller differences between return periods due to each analysis cell approaching its own value for ω at different rates. However, significant difference is seen between hazard contour patterns associated to longer time intervals (e.g. comparing Figure 5.17(b) to Figure 5.17(c) for 100 and 200 years respectively).

The covariance error matrix, ε, associated to extreme distribution parameters estimated from fitting Gumbel's third distribution to earthquake extreme data can yield stronger evidence of the quality of hazard forecasts obtained. General rules apply to elements of ε (Burton, 1979) and how they relate to each other. σ_ω^2 is usually the largest diagonal element to ε as ω is usually difficult to determine, especially with insufficient catalogue data, and is also associated to a physically unrealisable magnitude. σ_λ^2 is usually small and comparable to λ. σ_μ^2 is unique to the distribution in that it is the only one of the three distribution parameters that is physically realisable, leading σ_μ^2 to be typically small in value. It also has small dependence upon the other two parameters of Gumbel's distribution. μ should be well constrained and realistic in terms of observed seismicity, more so with a greater number of extreme intervals considered in the catalogue.

Further correlated relationships can be given between the three distribution parameters (Yegulalp and Kuo, 1974), by the off-diagonal elements to ε. Typically $\sigma_{\omega\lambda}^2$ is large and negative, $\sigma_{\omega\mu}^2$ is small and negative (such that $|\sigma_{\mu\lambda}^2| < |\sigma_{\omega\mu}^2|$) while $\sigma_{\mu\lambda}^2$ is small and positive. The error matrix, ε, for the broad region is given below (akin to a single analysis cell encompassing all regional seismicity):

$$\varepsilon = \begin{bmatrix} 0.316 & -0.131 & -0.191 \\ -0.131 & 0.017 & 0.020 \\ -0.191 & 0.020 & 0.135 \end{bmatrix}$$

σ_{ω}^{2} (upper left element of ε; Appendix 2) is relatively small in this instance to develop the single value for ω of 7.69 M_s (±0.56). This is possible due to the curvature parameter λ being high (0.61 ± 0.37) with relatively low σ_{λ}, suggesting the distribution is well-defined and achieves a good fit to extracted extreme data (Figure 5.19(a)). It is also a result governed by the number of missing years, NMISS (3), being relatively small (approximately 11%) compared with the number of extremes expected (27) for the data conditions adopted (NPER = 4; M_{CUT} = 5.5; start year = 1900).

All analysis cells used to contour magnitude hazard exhibit the generally large and negative values expected for $\sigma_{\omega\lambda}^{2}$. These range from -25.05 for cell 43.0°E, 22.0°N (located in a relatively aseismic area of south eastern Serbia near Nis) to -0.27 for cell 40.5°E, 25°N (in the northern Aegean in Thrakiko Pelagos, southeast of Thasos). These are associated to ω of 12.46 M_s ± 45.29 (with λ = 0.08 ± 0.55) and 7.60 ± 0.52 (with λ = 0.81 ± 0.60) respectively, supporting the inverse relationship between ω and λ.

$\sigma_{\omega\mu}^{2}$ generally adheres to the pattern it is believed to follow. For all cells except the low seismicity cell at 43.0°E, 22.0°N which has high ω, σ_{ω} and low λ (whose $\sigma_{\omega\mu}^{2}$ is 16.36), values are between -0.003 and 7.4. Eighty nine (58%) of the 156 computation nodes used to contour hazard have $\sigma_{\omega\mu}^{2}$ less than 1.00 and 119 (76%) are less than 2.00. $\sigma_{\omega\lambda}^{2}$ is contoured in Figure 5.20(a) while variation in ω contoured in Figure 5.20(b). The anomalous extreme high in Figure 5.20(b) is at 43.0°E, 22.0°N. Upper bound statistics are considered further in chapter 6 in relation to the modal magnitude M_1 and the *maximum credible magnitude* M_3.

Extreme magnitude hazard for southwest Bulgaria in 50-, 100- and 200-year time intervals (M_{50}, M_{100}, M_{200}) is contoured in Figure 5.21(a)-(c) with Figure 5.21(d)-(f) repeating these time intervals for magnitude hazard at 90% pnbe (M_{P50}, M_{P100}, M_{P200}). All hazard maps are contoured using seismicity present within 2° half-width cells located at 0.5° intervals of latitude and longitude (with cell-specific hazard statistics given in Appendix 7). Unlike the broader study area, all analysis cells will be subject to edge effects, due to the relatively large size of analysis cells with respect to the study area size.

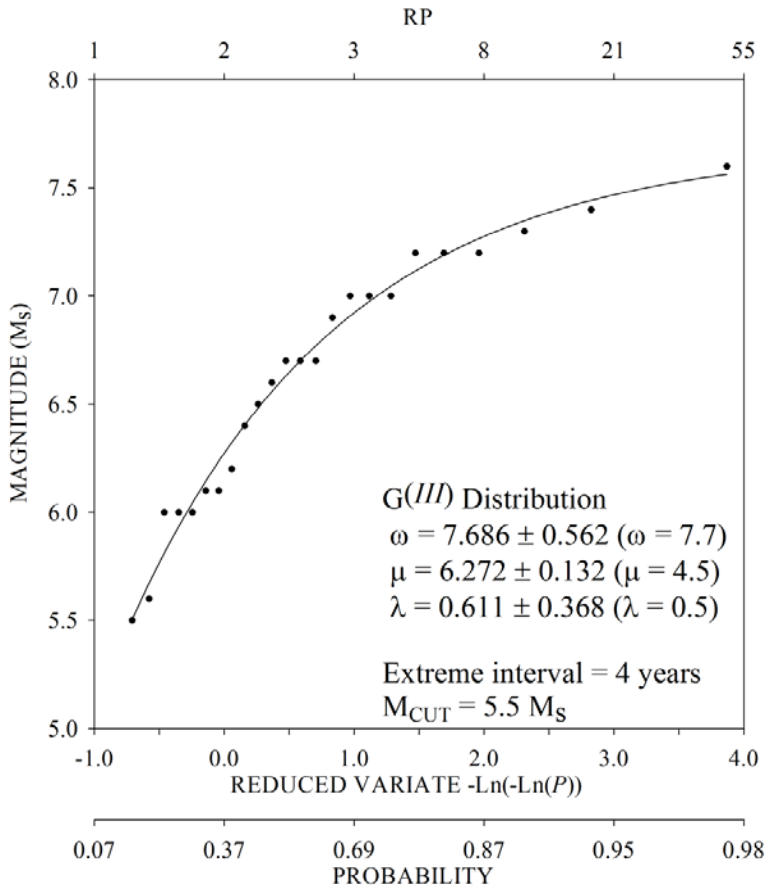

$$\varepsilon = \begin{bmatrix} 0.316 & -0.031 & -0.191 \\ -0.031 & 0.017 & 0.020 \\ -0.191 & 0.020 & 0.135 \end{bmatrix}$$

(a)

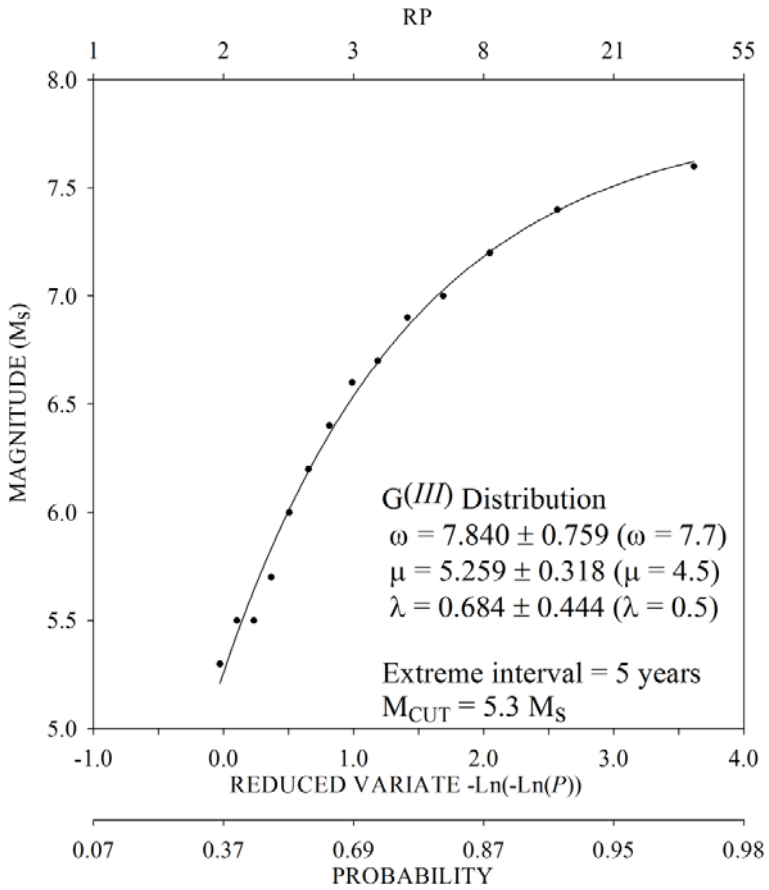

$$\varepsilon = \begin{bmatrix} 0.657 & 0.449 & -0.300 \\ 0.449 & 0.734 & -0.296 \\ -0.300 & -0.296 & 0.163 \end{bmatrix}$$

(b)

Figure 5.19 Gumbel's third extreme distribution fitted to final extreme magnitude data and covariance error matrix, ε, for (a) the Balkans and (b) southwest Bulgaria

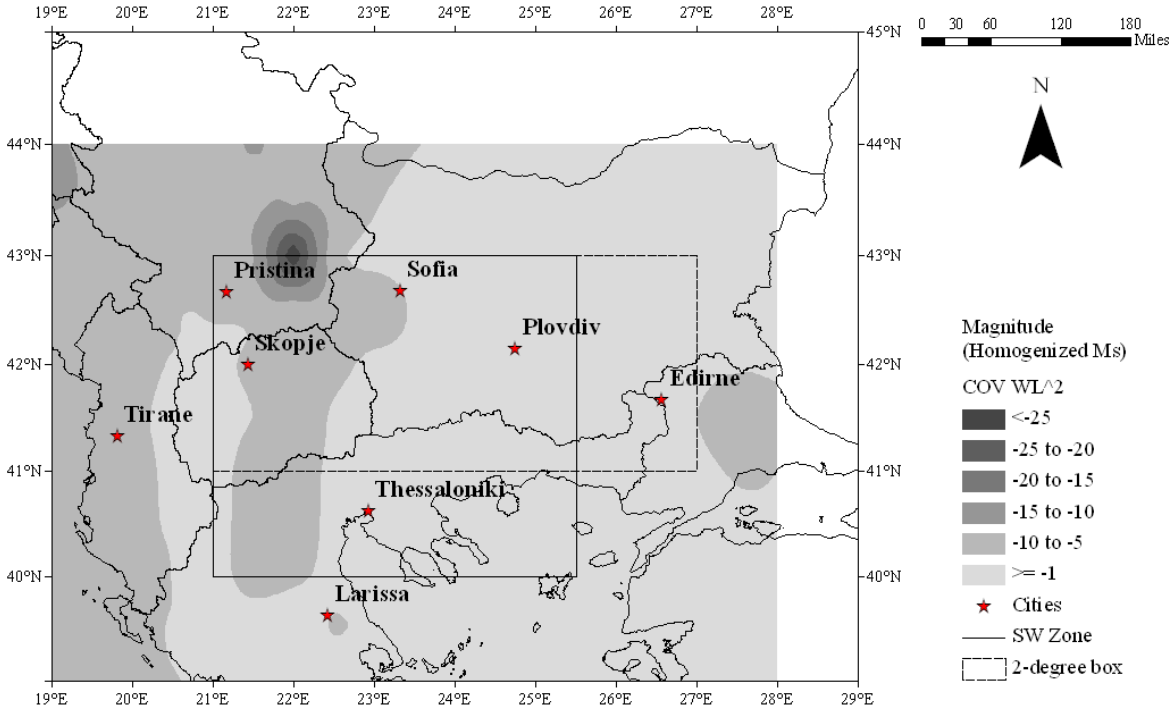

(a)

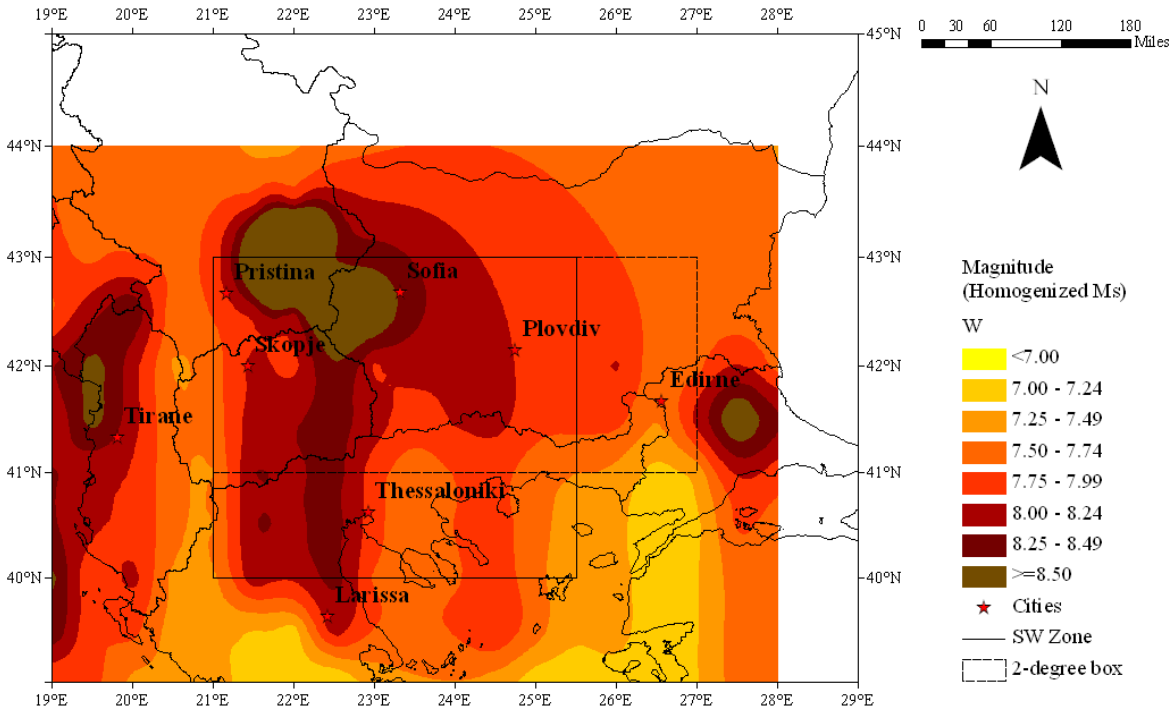

(b)

Figure 5.20(a) covariance between ω and λ ($\sigma^2_{\omega\lambda}$) from error matrix, ε, of Gumbel's third distribution (all contours to Figure 5.20(a) are at intervals of 5 units except for -1); (b) upper-bound magnitude, ω, of Gumbel's third extreme distribution for the broad Balkan region

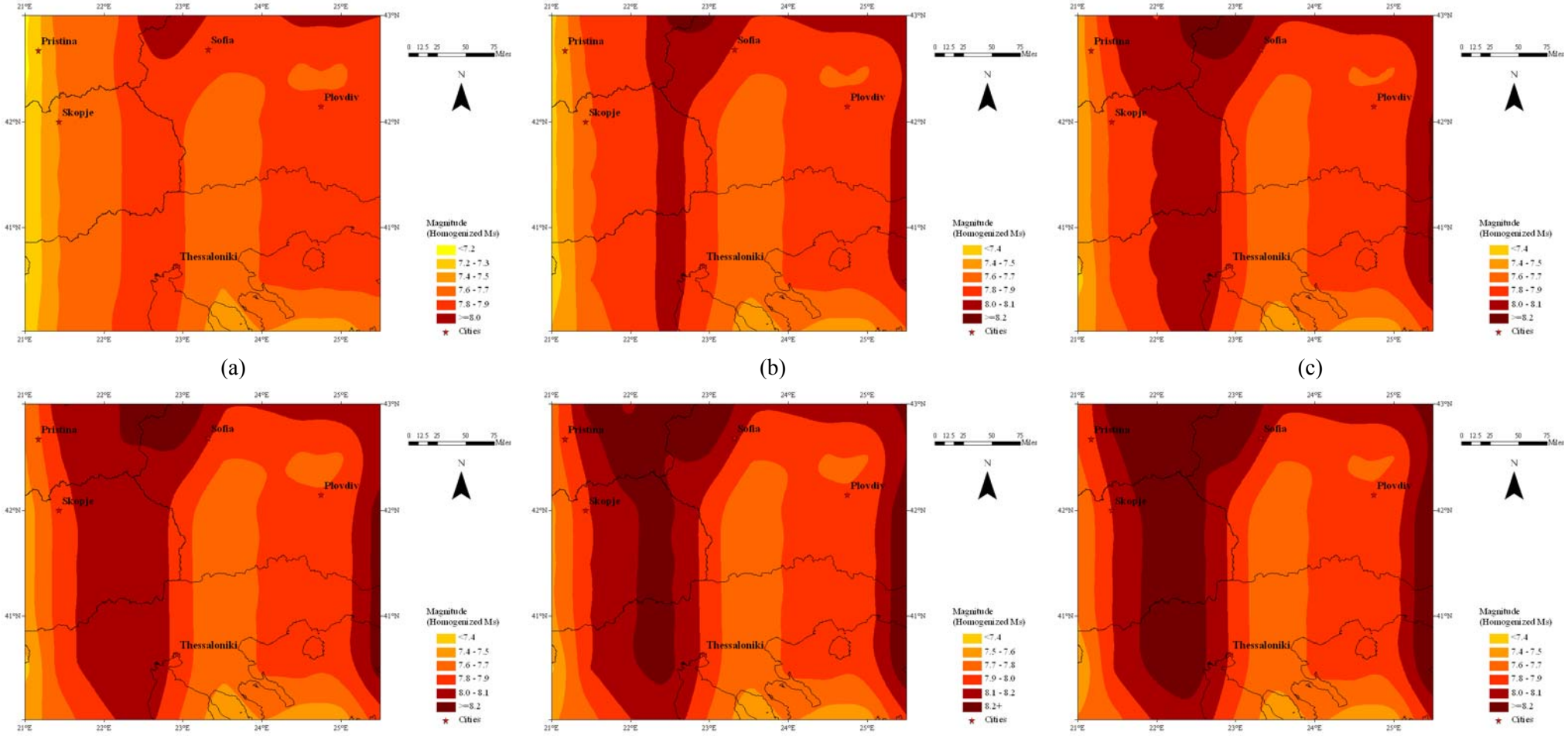

Figure 5.21 Magnitude hazard in the southwest zone; the modal maximum earthquake magnitude within (a) 50, (b) 100 and (c) 200 years, and magnitudes expected within (d) 50, (e) 100 and (f) 200 years, with 90% probability of not being exceeded (a 1 in 10 chance of being exceeded; contours are at intervals of 0.2 M_s)

These maps will not simply be a larger scale replication and enlargement of hazard forecast for the broader Balkans since different earthquake distributions from different input catalogues have been used to derive estimates. The larger area requires the full earthquake catalogue (3,681 events) while magnitude hazard for southwest Bulgaria considers only the 1,008 events located within the borders of this sub region itself, since magnitude is a point process not a field process. Consequently, catalogue parameters used for extreme interval, magnitude threshold and start year are different (section 5.3.13).

There is a tendency for magnitude hazard to increase west to east. For the 50-year return period hazard (M_{50}), the area is dominated by the 7.9 M_s contour, with a maximum of 8.2+ M_s forecast close to the central north boundary to the area considered. The confined zone of peak magnitude remains at 8.2+ M_s in 50 years at 90% pnbe (M_{P50}), but it has expanded in size. All elements to Figure 5.21 also exhibit a high magnitude zone of hazard running north-south through the FYR of Macedonia in between Skopje and Blagoevgrad.

This confined zone of magnitude hazard appears to loosely follow the direction of the Serbomacedonian massif, although the strict north-south direction of the contouring is more likely a legacy of analysis cell spacing and controlled by the cell distribution and size used to derive hazard estimates and contour them. Four particular distributions, or instances, of historical seismicity may have had enough influence on the distribution of localised seismicity to produce this trend; 1) the earthquake of 21st March 2000 with a magnitude of homogenized 7.6 M_s (the largest homogenized magnitude in the catalogue); 2) the seismicity distribution east of Thessaloniki running along the arcuate zone of the Serbomacedonian massif; 3) the dense distribution of seismicity around Plovdiv (bounded approximately by 42.0°-42.3°N, 24.5°-25.0°E), and, 4) the dense distribution of seismicity around the island of Limnos in the northern Aegean.

Covariance error matrices of Gumbel's third distribution for each 2° half-width cell used to determined magnitude hazard for southwest Bulgaria are provided in Figure 5.22 with the associated values of $\sigma^2_{\omega\lambda}$ contoured across southwest Bulgaria in Figure 5.23(a), and ω contoured in Figure 5.23(b). The single $G^{(III)}$ distribution curve that considers all seismicity within the southwest zone is given in Figure 5.19(b) from data with an M_{CUT} of 5.3 M_s and 5-year extreme interval. The curve is again well defined. Like Figure 5.19(a) μ is well constrained with a small standard deviation σ_μ (5.26 M_s ± 0.32) and ω (7.84 M_s ± 0.76) is compatible with the homogenized magnitude of the 2000 Thessaloniki event (7.6 M_s).

21.0°E	21.5°E	22.0°E	22.5°E	23.0°E
$\begin{bmatrix} 9.931 & 2.048 & -1.598 \\ 2.048 & 0.679 & -0.379 \\ -1.598 & -0.379 & 0.266 \end{bmatrix}$	$\begin{bmatrix} 24.387 & 4.270 & -3.479 \\ 4.270 & 1.062 & -0.661 \\ -3.479 & -0.661 & 0.507 \end{bmatrix}$	$\begin{bmatrix} 10.507 & 2.966 & -1.771 \\ 2.966 & 1.234 & -0.559 \\ -1.771 & -0.559 & 0.309 \end{bmatrix}$	$\begin{bmatrix} 5.023 & 1.067 & -0.896 \\ 1.067 & 0.426 & -0.225 \\ -0.896 & -0.225 & 0.168 \end{bmatrix}$	$\begin{bmatrix} 5.023 & 1.067 & -0.896 \\ 1.067 & 0.426 & -0.225 \\ -0.896 & -0.225 & 0.168 \end{bmatrix}$
$\begin{bmatrix} 10.681 & 1.511 & -1.505 \\ 1.511 & 0.381 & -0.242 \\ -1.505 & -0.242 & 0.219 \end{bmatrix}$	$\begin{bmatrix} 24.387 & 4.270 & -3.479 \\ 4.270 & 1.062 & -0.661 \\ -3.479 & -0.661 & 0.507 \end{bmatrix}$	$\begin{bmatrix} 5.944 & 1.635 & -1.283 \\ 1.635 & 0.747 & -0.408 \\ -1.283 & -0.408 & 0.291 \end{bmatrix}$	$\begin{bmatrix} 1.966 & 0.702 & -0.604 \\ 0.702 & 0.516 & -0.273 \\ -0.604 & -0.273 & 0.203 \end{bmatrix}$	$\begin{bmatrix} 1.966 & 0.702 & -0.604 \\ 0.702 & 0.516 & -0.273 \\ -0.604 & -0.273 & 0.203 \end{bmatrix}$
$\begin{bmatrix} 7.996 & 0.650 & -1.153 \\ 0.650 & 0.138 & -0.111 \\ -1.153 & -0.111 & 0.172 \end{bmatrix}$	$\begin{bmatrix} 6.413 & 1.193 & -1.457 \\ 1.193 & 0.410 & -3.15 \\ -1.457 & -0.315 & 0.346 \end{bmatrix}$	$\begin{bmatrix} 3.882 & 0.659 & -0.887 \\ 0.659 & 0.252 & -0.183 \\ -0.887 & -0.183 & 0.214 \end{bmatrix}$	$\begin{bmatrix} 2.416 & 0.351 & -0.578 \\ 0.650 & 0.154 & -0.108 \\ -0.578 & -0.108 & 0.148 \end{bmatrix}$	$\begin{bmatrix} 0.792 & 0.196 & -0.366 \\ 0.196 & 0.179 & -0.134 \\ -0.366 & -0.134 & 0.194 \end{bmatrix}$
$\begin{bmatrix} 7.996 & 0.650 & -1.153 \\ 0.650 & 0.138 & -0.111 \\ -1.153 & -0.111 & 0.172 \end{bmatrix}$	$\begin{bmatrix} 6.413 & 1.193 & -1.457 \\ 1.193 & 0.410 & -3.15 \\ -1.457 & -0.315 & 0.346 \end{bmatrix}$	$\begin{bmatrix} 3.882 & 0.659 & -0.887 \\ 0.659 & 0.252 & -0.183 \\ -0.887 & -0.183 & 0.214 \end{bmatrix}$	$\begin{bmatrix} 2.416 & 0.351 & -0.578 \\ 0.650 & 0.154 & -0.108 \\ -0.578 & -0.108 & 0.148 \end{bmatrix}$	$\begin{bmatrix} 0.792 & 0.196 & -0.366 \\ 0.196 & 0.179 & -0.134 \\ -0.366 & -0.134 & 0.194 \end{bmatrix}$
$\begin{bmatrix} 7.996 & 0.650 & -1.153 \\ 0.650 & 0.138 & -0.111 \\ -1.153 & -0.111 & 0.172 \end{bmatrix}$	$\begin{bmatrix} 6.413 & 1.193 & -1.457 \\ 1.193 & 0.410 & -3.15 \\ -1.457 & -0.315 & 0.346 \end{bmatrix}$	$\begin{bmatrix} 3.882 & 0.659 & -0.887 \\ 0.659 & 0.252 & -0.183 \\ -0.887 & -0.183 & 0.214 \end{bmatrix}$	$\begin{bmatrix} 2.416 & 0.351 & -0.578 \\ 0.650 & 0.154 & -0.108 \\ -0.578 & -0.108 & 0.148 \end{bmatrix}$	$\begin{bmatrix} 0.792 & 0.196 & -0.366 \\ 0.196 & 0.179 & -0.134 \\ -0.366 & -0.134 & 0.194 \end{bmatrix}$
$\begin{bmatrix} 7.996 & 0.650 & -1.153 \\ 0.650 & 0.138 & -.1113 \\ -1.153 & -0.111 & 0.172 \end{bmatrix}$	$\begin{bmatrix} 2.536 & 1.142 & -1.018 \\ 1.142 & 0.915 & -0.561 \\ -1.018 & -0.561 & 0.915 \end{bmatrix}$	$\begin{bmatrix} 3.882 & 0.659 & -0.887 \\ 0.659 & 0.252 & -0.183 \\ -0.887 & -0.183 & 0.214 \end{bmatrix}$	$\begin{bmatrix} 2.416 & 0.351 & -0.578 \\ 0.351 & 0.154 & -0.108 \\ -0.578 & -0.108 & 0.148 \end{bmatrix}$	$\begin{bmatrix} 0.792 & 0.196 & -0.366 \\ 0.196 & 0.179 & -0.134 \\ -0.366 & -0.134 & 0.194 \end{bmatrix}$
$\begin{bmatrix} 2.420 & 1.120 & -0.752 \\ 1.120 & 0.927 & -0.428 \\ -0.752 & -0.428 & 0.253 \end{bmatrix}$	$\begin{bmatrix} 5.228 & 3.257 & -1.604 \\ 3.257 & 2.919 & -1.147 \\ -1.604 & -1.147 & 0.521 \end{bmatrix}$	$\begin{bmatrix} 1.037 & 1.235 & -0.571 \\ 1.235 & 2.655 & -0.904 \\ -0.571 & -0.904 & 0.364 \end{bmatrix}$	$\begin{bmatrix} 1.354 & 0.599 & -0.484 \\ 0.599 & 0.599 & -0.281 \\ -0.484 & -0.281 & 0.194 \end{bmatrix}$	$\begin{bmatrix} 0.430 & 0.387 & -0.313 \\ 0.387 & 0.900 & -0.439 \\ -0.313 & -0.439 & 0.287 \end{bmatrix}$

23.5°E	24.0°E	24.5°E	25.0°E	25.5°E
$\begin{bmatrix} 0.907 & 0.773 & -0.429 \\ 0.773 & 1.323 & -0.498 \\ -0.429 & -0.498 & 0.236 \end{bmatrix}$	$\begin{bmatrix} 0.907 & 0.773 & -0.429 \\ 0.773 & 1.323 & -0.498 \\ -0.429 & -0.498 & 0.236 \end{bmatrix}$	$\begin{bmatrix} 1.179 & 2.000 & -0.555 \\ 2.000 & 5.628 & -1.225 \\ -0.555 & -1.225 & 0.302 \end{bmatrix}$	$\begin{bmatrix} 1.179 & 2.000 & -0.555 \\ 2.000 & 5.628 & -1.225 \\ -0.555 & -1.225 & 0.302 \end{bmatrix}$	---
$\begin{bmatrix} 0.469 & 0.633 & -0.343 \\ 0.633 & 1.916 & -0.701 \\ -0.343 & -0.701 & 0.315 \end{bmatrix}$	$\begin{bmatrix} 0.469 & 0.633 & -0.343 \\ 0.633 & 1.916 & -0.701 \\ -0.343 & -0.701 & 0.315 \end{bmatrix}$	$\begin{bmatrix} 0.455 & 1.706 & -0.388 \\ 1.706 & 12.410 & -2.209 \\ -0.388 & -2.209 & 0.435 \end{bmatrix}$	$\begin{bmatrix} 0.455 & 1.706 & -0.388 \\ 1.706 & 12.410 & -2.209 \\ -0.388 & -2.209 & 0.435 \end{bmatrix}$	---
$\begin{bmatrix} 0.283 & 0.204 & -0.262 \\ 0.204 & 0.506 & -0.330 \\ -0.262 & -0.330 & 0.323 \end{bmatrix}$	$\begin{bmatrix} 0.511 & 0.257 & -0.307 \\ 0.257 & 0.393 & -0.239 \\ -0.307 & -0.239 & 0.224 \end{bmatrix}$	$\begin{bmatrix} 0.530 & 0.654 & -0.348 \\ 0.654 & 1.767 & -0.635 \\ -0.348 & -0.635 & 0.282 \end{bmatrix}$	$\begin{bmatrix} 0.530 & 0.654 & -0.348 \\ 0.654 & 1.767 & -0.635 \\ -0.348 & -0.635 & 0.282 \end{bmatrix}$	$\begin{bmatrix} 9.343 & 4.077 & -1.630 \\ 4.077 & 2.472 & -0.794 \\ -1.630 & -0.794 & 0.294 \end{bmatrix}$
$\begin{bmatrix} 0.283 & 0.204 & -0.262 \\ 0.204 & 0.506 & -0.330 \\ -0.262 & -0.330 & 0.323 \end{bmatrix}$	$\begin{bmatrix} 0.511 & 0.257 & -0.307 \\ 0.257 & 0.393 & -0.239 \\ -0.307 & -0.239 & 0.224 \end{bmatrix}$	$\begin{bmatrix} 0.530 & 0.654 & -0.348 \\ 0.654 & 1.767 & -0.635 \\ -0.348 & -0.635 & 0.282 \end{bmatrix}$	$\begin{bmatrix} 0.530 & 0.654 & -0.348 \\ 0.654 & 1.767 & -0.635 \\ -0.348 & -0.635 & 0.282 \end{bmatrix}$	$\begin{bmatrix} 9.343 & 4.077 & -1.630 \\ 4.077 & 2.472 & -0.794 \\ -1.630 & -0.794 & 0.294 \end{bmatrix}$
$\begin{bmatrix} 0.283 & 0.204 & -0.262 \\ 0.204 & 0.506 & -0.330 \\ -0.262 & -0.330 & 0.323 \end{bmatrix}$	$\begin{bmatrix} 0.511 & 0.257 & -0.307 \\ 0.257 & 0.393 & -0.239 \\ -0.307 & -0.239 & 0.224 \end{bmatrix}$	$\begin{bmatrix} 0.530 & 0.654 & -0.348 \\ 0.654 & 1.767 & -0.635 \\ -0.348 & -0.635 & 0.282 \end{bmatrix}$	$\begin{bmatrix} 0.530 & 0.654 & -0.348 \\ 0.654 & 1.767 & -0.635 \\ -0.348 & -0.635 & 0.282 \end{bmatrix}$	$\begin{bmatrix} 9.343 & 4.077 & -1.630 \\ 4.077 & 2.472 & -0.794 \\ -1.630 & -0.794 & 0.294 \end{bmatrix}$
$\begin{bmatrix} 0.283 & 0.204 & -0.262 \\ 0.204 & 0.179 & -0.330 \\ -0.262 & -0.330 & 0.323 \end{bmatrix}$	$\begin{bmatrix} 0.511 & 0.257 & -0.307 \\ 0.257 & 0.393 & -0.239 \\ -0.307 & -0.239 & 0.224 \end{bmatrix}$	$\begin{bmatrix} 0.530 & 0.654 & -0.348 \\ 0.654 & 1.767 & -0.635 \\ -0.348 & -0.635 & 0.282 \end{bmatrix}$	$\begin{bmatrix} 0.530 & 0.654 & -0.348 \\ 0.654 & 1.767 & -0.635 \\ -0.348 & -0.635 & 0.282 \end{bmatrix}$	$\begin{bmatrix} 9.343 & 4.077 & -1.630 \\ 4.077 & 2.472 & -0.794 \\ -1.630 & -0.794 & 0.296 \end{bmatrix}$
$\begin{bmatrix} 0.304 & 0.986 & -0.411 \\ 0.986 & 7.160 & -2.206 \\ -0.411 & -2.206 & 0.772 \end{bmatrix}$	$\begin{bmatrix} 0.344 & 0.988 & -0.364 \\ 0.988 & 6.205 & -1.684 \\ -0.364 & -1.684 & 0.522 \end{bmatrix}$	$\begin{bmatrix} 0.329 & 3.261 & -0.409 \\ 3.261 & 64.494 & -6.675 \\ -0.409 & -6.675 & 0.734 \end{bmatrix}$	$\begin{bmatrix} 0.329 & 3.261 & -0.409 \\ 3.261 & 64.494 & -6.675 \\ -0.409 & -6.675 & 0.734 \end{bmatrix}$	---

Figure 5.22 Magnitude covariance error matrices, ε, for southwest Bulgaria. For presentation purposes, the geographic area represented has been split into two halves between the 23.0°E and 23.5°E meridians. The rows of each table represent – from bottom to top – parallels 40.0°N to 43.0°N at 0.5° steps. Cells with '*null*' forecasts are also given. Matrix elements of ε are:

$$\varepsilon = \begin{bmatrix} \sigma_{\omega}^{2} & \sigma_{\omega\mu}^{2} & \sigma_{\lambda\omega}^{2} \\ \sigma_{\omega\mu}^{2} & \sigma_{\mu}^{2} & \sigma_{\lambda\mu}^{2} \\ \sigma_{\omega\lambda}^{2} & \sigma_{\mu\lambda}^{2} & \sigma_{\lambda}^{2} \end{bmatrix}$$

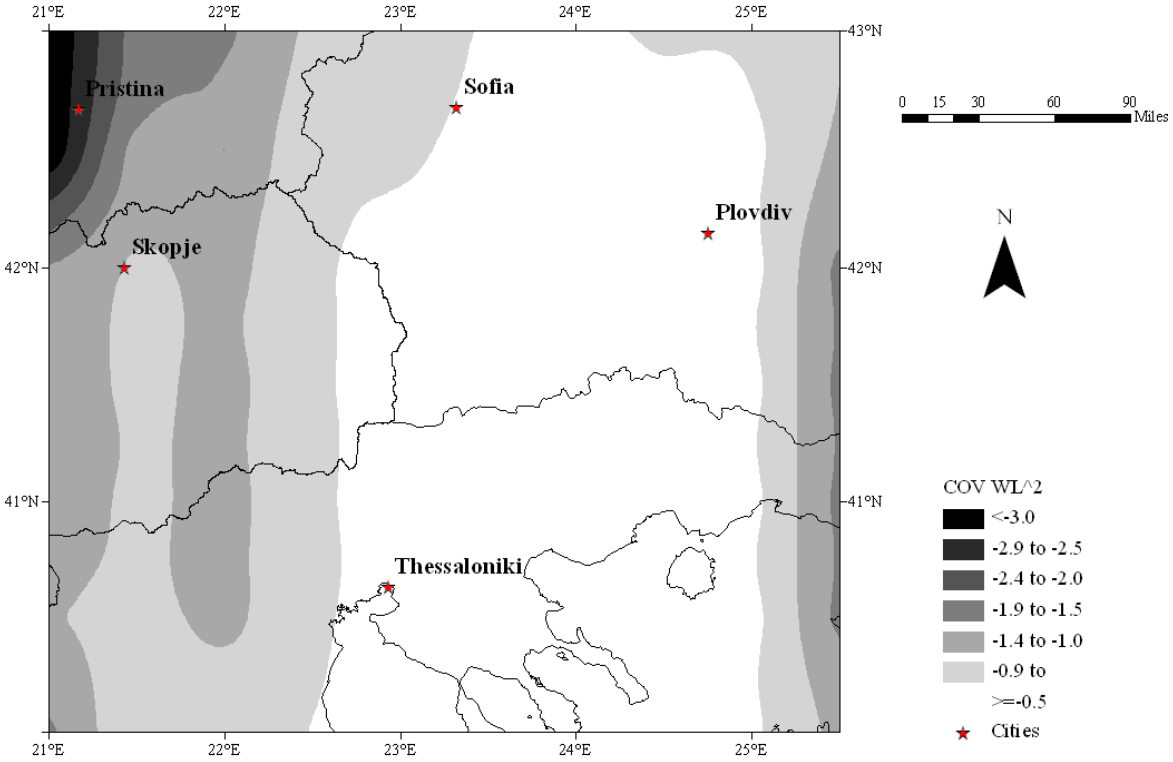

(a)

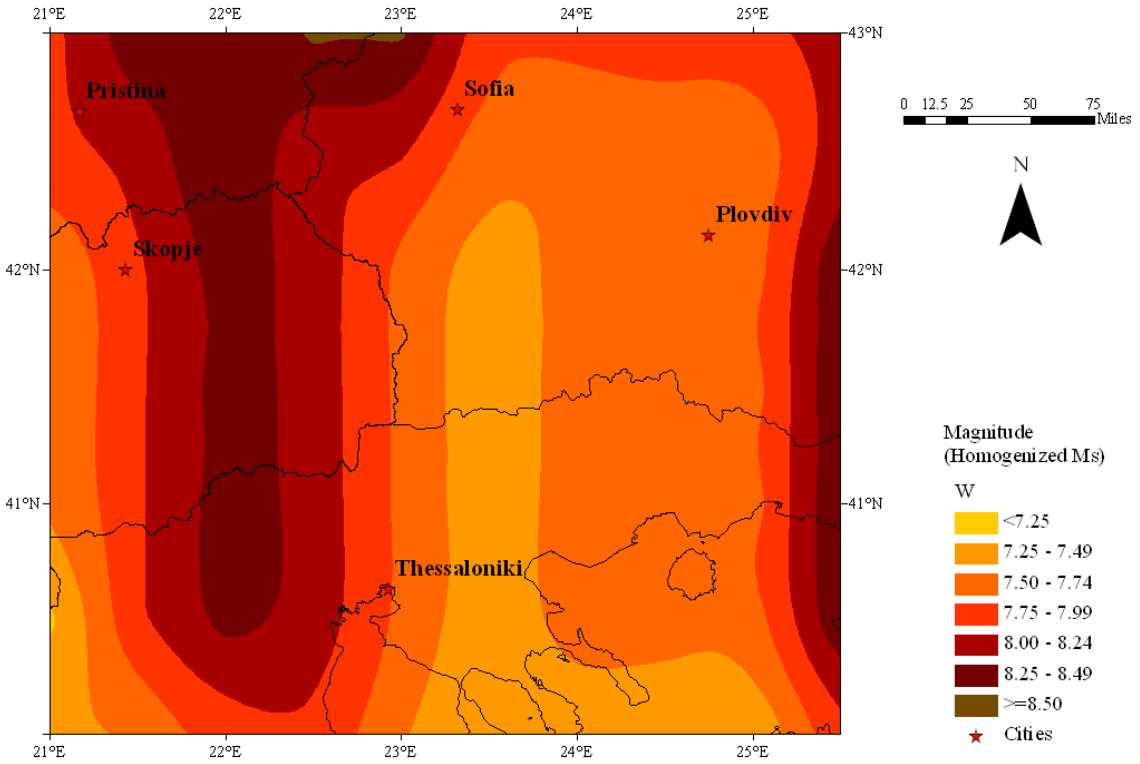

(b)

Figure 5.23(a) Covariance between ω and λ ($\sigma^2_{\omega\lambda}$) from error matrix ε of Gumbel's third distribution (all contours are at intervals of 0.5 units); (b) upper-bound magnitude, ω, of Gumbel's third extreme distribution for southwest Bulgaria (all contours are at intervals of 0.20 M_s)

Extreme magnitude hazard forecasts for the eight urban centres considered for time intervals of 25, 50, 100 and 200 years as well as these return periods at 90% pnbe are in Table 5.7, and allow the quality of hazard forecasts to be considered at a lower geographic level and in conjunction with magnitude hazard maps of southwest Bulgaria. Average return periods for specific magnitudes, and the number of exceedances expected in 50 and 100 years of each magnitude level as well as the maximum observed magnitude, M_M, from the catalogue and the modal magnitude, M_1, from cumulative strain energy release statistics (equivalent to a/b from the Gutenberg-Richter relation) are given in Table 5.8. It is evident that Sofia and Thessaloniki are located in the most seismically active area of this border region (Figure 5.21).

Sofia is subject to seismicity of the Struma Valley (notably the strong earthquake sequences of 1904 to 1906). Thessaloniki is prone to seismicity generated by the highly active Serbomacedonian geologic massif east of the city. This is the same massif that generated the 1904 Kresna sequence further north in Bulgaria. This seismic zone was particularly active during the 1970s, especially May-June 1978, and has been reviewed by a number of previous authors (Papazachos *et al.*, 1979; Tranos *et al.*, 2003).

The 2° half-width cell considered surrounding Sofia may possibly expect an earthquake of 5.0 M_s to occur about every 2 years, and a magnitude 7.0 M_s event every 7 years (Table 5.8). This suggests an earthquake the size of the 1904 Kresna main shock (homogenized 7.2 M_s) will require approximately 9 years to occur. If the larger historical magnitude estimate of 7.8 m_b (Shebalin *et al.*, 1998) had been selected to represent this event the time interval would increase to 169 years. These estimates for waiting time compare to equivalent estimates for the waiting time T_w from cumulative strain energy release of 74 years (section 6.2).

Four earthquakes of homogenized magnitude ≥7.0 M_s occurred in the southwest zone of Bulgaria considered here (1904, 7.2 M_s; 1905, 7.4 M_s; 1928, 7.0 M_s; and 2000, 7.6 M_s) suggesting that the homogenized magnitude estimate for the 1904 Kresna earthquake is compatible with the observed seismicity, although the waiting time developed from strain energy release techniques is more realistic than return periods from extreme values theory. Also, the two 7.0+ M_s earthquakes in the first 30 years of the 20th century may represent a period of pseudo clustering of seismicity, before a long period of quiescence for the area's largest magnitude earthquakes leading up to the earthquake of 2000. This is likely due to the former being akin to a finite waiting time maximum magnitude while the latter relates to an infinite return period. The statistically short return time from the distribution for a Kresna-sized event may be due to reasonably high uncertainties on ω and λ.

City	NPER	M_{CUT}	ω	σ_ω	μ	σ_μ	λ	σ_λ	$\sigma^2_{\omega\mu}$	$\sigma^2_{\omega\lambda}$	$\sigma^2_{\mu\lambda}$	X^2	NMISS	M_M
Full region	4	5.5	7.69	0.56	6.27	0.13	0.61	0.37	-0.03	-0.19	0.02	0.03	3	7.6
SW Bulgaria	5	5.3	7.84	0.76	5.23	0.32	0.68	0.44	0.09	-0.31	-0.08	0.02	7	7.6
Edirne	6	5.2	7.57	0.71	5.31	0.25	0.73	0.47	0.03	-0.31	-0.04	0.07	5	7.3
Larissa	5	5.0	7.89	1.26	5.51	0.17	0.43	0.35	-0.01	-0.43	-0.01	0.06	4	7.6
Plovdiv	6	5.6	7.96	1.21	4.47	1.54	0.69	0.76	1.40	-0.87	-1.07	0.03	10	7.6
Pristina	2	4.9	7.68	1.46	5.08	0.13	0.29	0.24	0.05	-0.34	-0.01	0.04	13	7.4
Skopje	2	5.0	7.89	1.70	5.25	0.10	0.26	0.22	0.02	-0.37	-0.01	0.03	10	7.4
Sofia	5	5.3	7.86	0.75	4.18	0.89	0.81	0.52	0.42	-0.35	-0.39	0.05	10	7.6
Thessaloniki	5	5.4	7.90	0.94	5.26	0.42	0.62	0.50	0.21	-0.44	-0.15	0.03	8	7.6
Tirane	6	5.6	7.35	1.29	5.91	0.17	0.44	0.60	-0.03	-0.74	0.01	0.03	3	7.0

City	NPER	M_{CUT}	m(1)	M_{25}	M_{50}	M_{100}	M_{200}	σ_M	M_{P25}	M_{P50}	M_{P100}	M_{P200}	σ_{MP}	M_M
Full region	4	5.5	6.89	7.57	7.61	7.64	7.65	0.48	7.10	8.20	7.66	7.67	0.58	7.6
SW Bulgaria	5	5.3	6.67	7.71	7.77	7.79	7.81	0.85	7.70	7.75	7.79	7.81	0.74	7.6
Edirne	6	5.2	6.70	7.49	7.52	7.54	7.55	0.73	7.53	7.55	7.56	7.56	0.70	7.3
Larissa	5	5.0	6.01	7.42	7.54	7.63	7.70	1.06	7.66	7.72	7.77	7.80	1.18	7.6
Plovdiv	6	5.6	6.40	7.79	7.86	7.90	7.92	2.00	7.88	7.91	7.93	7.94	1.21	7.6
Pristina	2	4.9	5.33	6.76	6.93	7.07	7.18	1.01	7.15	7.25	7.33	7.39	1.23	7.4
Skopje	2	5.0	5.44	6.81	6.99	7.13	7.26	1.06	7.24	7.34	7.43	7.51	1.35	7.4
Sofia	5	5.3	6.88	7.79	7.82	7.84	7.85	1.17	7.81	7.83	7.84	7.85	0.75	7.6
Thessaloniki	5	5.4	6.44	7.70	7.77	7.81	7.84	1.08	7.81	7.84	7.86	7.87	0.93	7.6
Tirane	6	5.6	6.23	7.08	7.15	7.20	7.24	1.07	7.22	7.25	7.28	7.30	1.20	7.0

Table 5.7 (ω, μ, λ) and uncertainties for a $G^{(III)}$ distribution for selected cities. M_M is maximum observed magnitude; m(1) is annual modal magnitude; M_{25}, M_{50}, M_{100} and M_{200} are modal maximums in 25, 50, 100 and 200 years. M_{P25}, M_{P50}, M_{P100} and M_{P200} are these at 90% probability of non-exceedance (σ_M and σ_{MP} are their uncertainties). $\sigma^2_{\omega\mu}$, $\sigma^2_{\omega\lambda}$ and $\sigma^2_{\mu\lambda}$ are off-diagonal elements of the covariance error matrix, ε. NMISS is number of extreme intervals of missing extreme data; X^2 is goodness of fit measure

Location	M_{CUT}	Return Period (years)						ω	m(1)	All data[1]			$M \geq M_{CUT}$[2]			M_3[3]	M_M
		5.0	5.5	6.0	6.5	7.0	7.5			a	b	M_1	a	b	M_1		
Full region	5.5	1.1	1.1	1.4	1.9	3.8	28.2	7.69	6.89	3.504	0.640	5.48	5.061	0.887	5.70	7.815	7.6
SW zone	5.3	1.5	1.7	2.2	3.1	5.7	19.9	7.84	6.67	2.714	0.580	4.67	3.024	0.636	4.75	7.755	7.6
Edirne	5.2	1.4	1.7	2.2	3.3	7.0	114.8	7.57	6.70	2.293	0.522	4.39	2.709	0.596	4.55	7.401	7.3
Larissa	5.0	1.3	1.6	2.3	4.0	10.5	68.6	7.89	6.01	3.104	0.674	4.61	4.068	0.830	4.90	7.600	7.6
Plovdiv	5.6	1.8	2.2	2.8	4.1	7.0	19.3	7.96	6.40	2.527	0.563	4.49	2.292	0.539	4.25	7.754	7.6
Pristina	4.9	1.5	2.4	5.0	15.6	100.1	9204.9	7.68	5.33	3.036	0.634	4.79	4.534	0.882	5.14	7.589	7.4
Skopje	5.0	1.3	2.0	4.2	12.9	71.5	1785.0	7.89	5.44	3.199	0.650	4.92	4.949	0.938	5.30	7.589	7.4
Sofia	5.3	1.9	2.3	2.9	4.0	6.6	18.5	7.86	6.88	2.408	0.543	4.43	2.627	0.587	4.48	7.759	7.6
Thessaloniki	5.4	1.5	1.7	2.3	3.3	6.2	21.9	7.90	6.44	2.951	0.615	4.80	3.448	0.698	4.94	7.756	7.6
Tirane	5.6	1.1	1.2	1.7	3.9	25.7	-	7.35	6.23	3.139	0.646	4.86	5.686	1.075	5.29	7.112	7.0

Location	M_{CUT}	Number of exceedances expected in 50-years						Number of exceedances expected in 100-years					
		5.0	5.5	6.0	6.5	7.0	7.5	5.0	5.5	6.0	6.5	7.0	7.5
Full region	5.5	45-46	45-46	35-36	26-27	13-14	1-2	90-91	90-91	71-72	52-53	26-27	3-4
SW zone	5.3	33-34	29-30	22-23	16-17	8-9	2-3	66-67	58-59	45-46	32-33	17-18	5-6
Edirne	5.2	34-35	29-30	22-23	15-16	7-8	-	69-70	58-59	45-46	30-31	14-15	-
Larissa	5.0	39-40	31-32	22-23	12-13	4-5	0-1	79-80	63-64	44-45	24-25	9-10	1-2
Plovdiv	5.6	27-28	22-23	17-18	12-13	7-8	2-3	54-55	45-46	35-36	24-25	14-15	5-6
Pristina	4.9	33-34	20-21	9-10	3-4	0-1	0-1	66-67	41-42	19-20	6-7	0-1	0-1
Skopje	5.0	37-38	24-25	11-12	3-4	0-1	0-1	75-76	49-50	23-24	7-8	1-2	0-1
Sofia	5.3	25-26	21-22	17-18	12-13	7-8	2-3	51-52	43-44	34-35	25-26	15-16	5-6
Thessaloniki	5.4	34-35	28-29	22-23	15-16	8-9	2-3	68-69	57-58	44-45	30-31	16-17	4-5
Tirane	5.6	47-48	41-42	28-29	12-13	1-2	-	95-96	82-83	57-58	25-26	3-4	-

[1] Uses least squares on all unclustered catalogue data; [2] Uses least squares on unclustered catalogue data of $M \geq M_{CUT}$ for time span 1900-2004; [3] see chapter 6

Table 5.8 Average return periods (years) for selected magnitudes for 2° half-width cell centred on each urban centre. Also given are number of exceedances expected in 50- and 100-year time intervals; ω is the upper bound to Gumbel's third distribution; m(1) is the annual modal [or most probable] maximum magnitude estimated using Gumbel's third distribution; M_1 is the most probable annual maximum magnitude (modal) magnitude estimated from a and b of cumulative frequency-magnitude distribution; M_3 is the analytical upper bound magnitude from strain energy release statistics; M_M has same meaning as in Table 5.7

The number of exceedances expected around Sofia with respect to equivalent estimates for the Balkan region and southwest Bulgaria are in Table 5.9. The long return period estimated from extreme values of 169 years (for the unhomogenized estimate of 7.8 m_b) is nearly two-thirds longer than the catalogue, again suggesting this it does not represent a full cycle of seismicity in the region considered. Using the homogenized magnitude estimate of 7.2 M_s suggests there will be five or six such magnitude events in the 105-year time interval of the catalogue, which is within one (7 observed) of the number of events with $M \geq 7.2$ M_s (homogenized) in the applied catalogue.

Mean return periods, T_{AVE}, for earthquakes at 90% pnbe in the time interval specified, calculated using Eq. (A2-18), are in Table 5.10, and provide means to interpret estimates in Table 5.8 and Table 5.9.

	The Balkans			Southwest Bulgaria			Sofia		
M	50-yr	100-yr	Observed	50-yr	100-yr	Observed	50-yr	100-yr	Observed
5.0	45-46	90-91	334	33-34	66-67	102	25-26	51-52	78
5.5	45-46	90-91	131	29-30	58-59	37	21-22	43-44	30
6.0	35-36	71-72	53	22-23	45-46	15	17-18	34-35	12
6.5	26-27	52-53	27	16-17	32-33	11	12-13	25-26	8
7.0	13-14	26-27	10	8-9	17-18	4	7-8	15-16	4
7.5	1-2	3-4	1	2-3	5-6	1	2-3	5-6	1

Table 5.9 The number of exceedances expected at selected magnitudes for the broad Balkan region, southwest Bulgaria and Sofia. 'Observed' implies considering all events in the adopted catalogue's 105-year time span

pnbe \ T_{AVE}	25	50	100	200
0.90	238	475	950	1899

Table 5.10 Average return period, T_{AVE}, corresponding to T-year events with 90% probability of not being exceeded (pnbe)

The $G^{(III)}$ distribution curve for data from 5-year extreme intervals and magnitude threshold of 5.3 M_s (unsurprisingly identical to the configuration adopted for the southwest Bulgaria zone considered earlier) for the area immediately surrounding Sofia from seismicity present within a 2° half-width cell is in Figure 5.24 (with distribution curves for the other cities given in Appendix 8). Figure 5.24 shows a good third type asymptotic behaviour to extreme data and this is reflected in a small X^2 of 0.05, is in the mid-range of value for X^2 for the eight considered cities (Table 5.7) and is a legacy of a well-defined distribution curve to the extreme data.

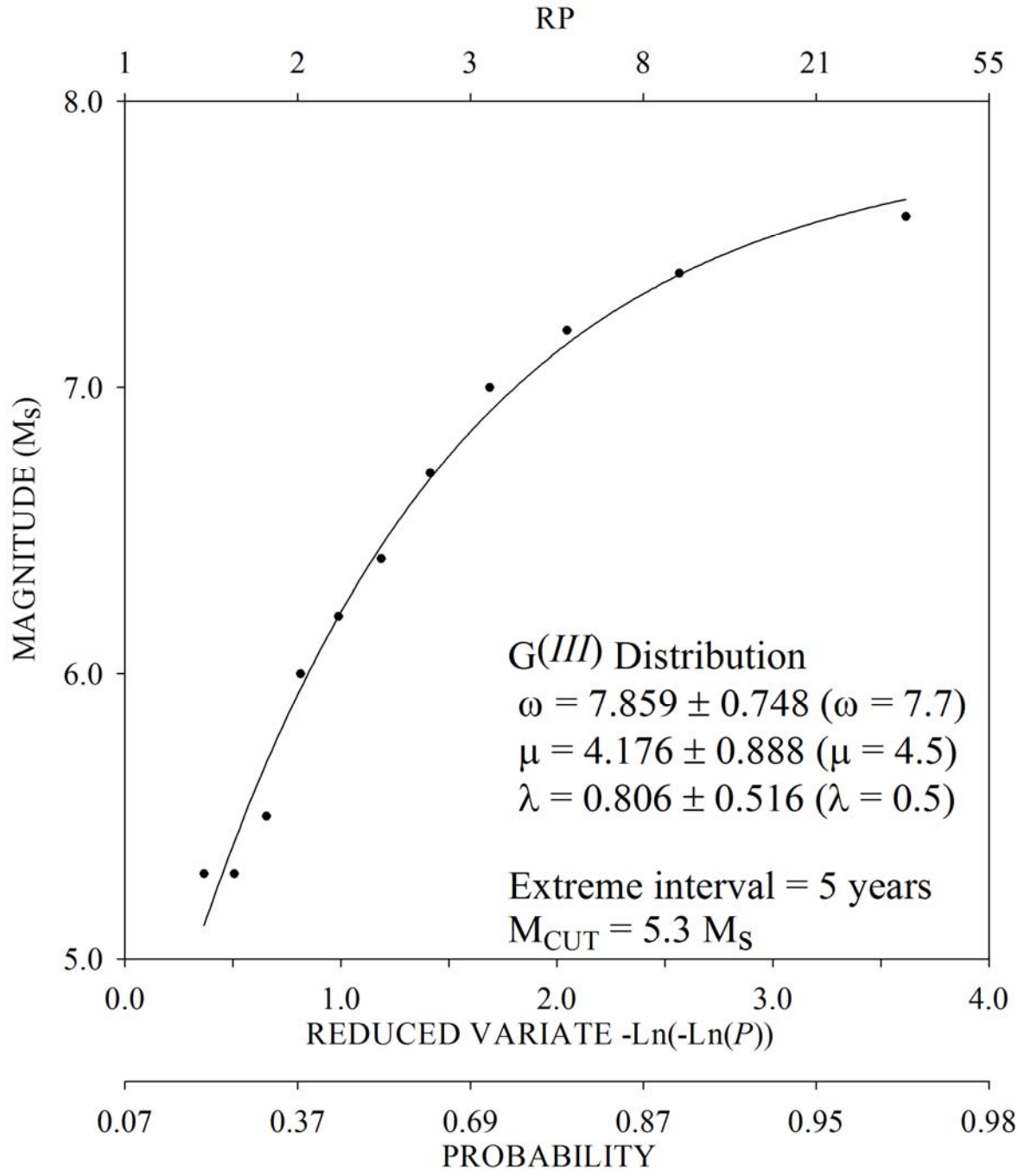

$$\varepsilon = \begin{bmatrix} 0.560 & 0.423 & -0.351 \\ 0.423 & 0.788 & -0.394 \\ -0.351 & -0.394 & 0.267 \end{bmatrix}$$

Figure 5.24 $G^{(III)}$ distribution curve of extreme value data and associated covariance error matrix, ε, for the area of 2° half width box cell centred on Sofia

Sofia is forecast a realistic value for ω with a small uncertainty (7.86 M_s ± 0.75), in the context of the large magnitude reported events in the catalogue and previous work of other authors. Thessaloniki (7.90 M_s ± 0.94) and Edirne (7.57 M_s ± 0.71) are also estimated realistic upper bound magnitudes producing good asymptotic distribution behaviour. As these cities are in areas of very high seismicity, it is likely these well-defined estimates are a result of this high seismicity helping constrain estimates.

Statistically, the areas immediately around Plovdiv, Pristina, Tirane, Larissa and Skopje exhibit the poorest distribution fit to data, with relatively high uncertainties on the distribution's upper bound that are greater than 1 (ranging from 1.21 for Plovdiv to 1.70 for Tirane). No great significance can be attributed to individual values of ω compared between the cities as they are individually constrained by the high-magnitude earthquakes in that city's subset of extreme values extracted from the catalogue. For example, ω for Tirane is 7.35 M_s, but this acknowledges the maximum observed event in the 2° analysis cell is only 7.0 M_s. Conversely, Thessaloniki is attached with ω of 7.90 M_s but experienced the largest magnitude event in the 105-year time span of the catalogue (7.6 M_s). The upper bound, ω, is between 0.3 and 0.5 M_s greater than M_M for all cites considered.

As low standard deviations on ω may be attributed to the ability for a localised area's high seismicity to constrain these values, so may high standard deviations be attributed to cities being located in regions of lower seismicity. Although Plovdiv did experience the destructive sequence of 1928, it has not been subject to any other large magnitude seismicity in the immediate vicinity during the catalogued time span. The Struma Valley is at the extreme of the 2° analysis cell from which its site-specific hazard forecasts are developed. Seismicity within its immediate area is typically ≤5.0 M_s (Figure 4.14).

This lower general seismicity, together with very few large magnitude historical events and a starting value for ω of 7.7 M_s may have produced its relative high uncertainty on ω. Plovdiv also exhibits larger uncertainty on μ (1.54 M_s) than any other city. All other cities are below 1.0, supporting these selected catalogue criteria (NPER, starting year and M_{CUT}) and parameter estimates, as μ is the only physically realisable parameter to Gumbel's third distribution.

The five cities exhibiting higher standard deviations on ω are also attached with either lower estimates for the distribution's curvature parameter, λ, (e.g. Skopje, $\lambda = 0.26$; Pristina, $\lambda = 0.29$) or acceptable values for λ but which are attached with equivalent or higher values for its standard deviation (e.g. Tirane with $\lambda = 0.44 \pm 0.60$; Plovdiv with $\lambda = 0.69 \pm 0.76$); both situations that help provide higher uncertainties on ω and poorer distribution fit to extreme data.

Regional faulting systems that cross large territories permit individual earthquake populations to more readily affect neighbouring geographic areas. Thus, one region may be affected by multiple earthquake populations superimposed on each other, leading to heightened perhaps misleading hazard levels. Makropoulos and Burton (1985a) consider a chi-square for Thessaloniki of 0.159 (for a 150 km radius centred cell) to be high, consistent with a poorly fitted distribution curve and attribute this to superposition of two earthquake populations, namely those of north and south Greece. Here an improved chi-square of 0.03 is achieved (for a 2° half-width analysis cell, the nearest equivalent between studies) leading to a lower ω of 7.90 M_s (Makropoulos and Burton forecast 8.57 M_s). Although part of this difference may be attributed to difference in cell size and shape, it is more likely due to the effect of adopting different extreme data filtering criteria on the raw earthquake catalogue to exclude '*null*' entries and artificially low, unrepresentative annual extremes from consideration. Makropoulos and Burton do not apply any conscious filtering to their catalogue, instead relying on cell size to reflect their desire to capture ground motion hazard most applicable to the building types that characterise Greece. Therefore three points can be suggested:

1. The poorer asymptotic behaviour of Larissa, Tirane, Pristina and Skopje may be attributable to superposition of two or more earthquake populations due to their relative close proximity to one another and the seismogenic sources of north Greece, south Bulgaria and potentially that of Albania and the nearby Adriatic coast.

2. Although Sofia is close to cities listed in (1), it is subject less to superposition of two earthquake populations as it is surrounded by very localised, very high seismicity produced by the tectonics of the Struma Valley and southwest Bulgaria. This may have suppressed the effects of seismicity from further afield on statistical hazard forecasting. For example, with respect to a *whole process* distribution, its surrounding locality would bias the cumulative frequency-magnitude distribution to the higher end of the magnitude range, or have similar effects on a *part process* model by introducing higher magnitudes to the extreme sample not necessarily present in more distant earthquake population.

3. Adopting data constraints in section 5.3.13 has excluded enough background seismicity and unrepresentative annual extremes from statistical consideration that Edirne and Sofia are deemed not to be affected by superposition of two earthquake populations (e.g. that of north Greece and southwest Bulgaria, or north Greece and Turkey) leading to well-constrained distribution curves to its extreme data.

The region contains a number of trans-border, even trans-continental faulting systems. Turkey, Greece and the north Aegean are dominated by the North and South Branch of the North Anatolian Fault (NAF; Figure 2.3). Southwest Bulgaria contains the Krupnik fault extending westwards into the FYR of Macedonia (Figure 2.2). South central and southwest Bulgaria is cut by many faults capable of producing moderate to large magnitude earthquakes (e.g. the Mesta fault and Etropole line running north-south from Bulgaria to Greece; Figure 2.4). Thessaloniki is to the western end of the NAF (Meyer *et al.*, 2002) and also the closer Serbomacedonian massif (Papazachos *et al.*, 1979) that runs north into Bulgaria. Thessaloniki therefore appears subject to two or three different faulting systems.

5.5.4 Peak Ground Acceleration (PGA)

Section 3.8.2.2 considers previously adopted peak ground acceleration models for Bulgaria and the Balkans, with Figure 3.6 plotting a selection of these over a distance of 200 km for a nominal earthquake of 6.5 M at 10 km focal depth. The classical model of Theodulidis and Papazachos (1992; $TP92_A$) for stiff soil conditions (site effect variable S = 0.5) at the 50th percentile (P = 0) will be adopted to aid comparison between this work and hazard analyses of Makropoulos and Burton (1985b) and Burton *et al.* (2003). Ambraseys *et al*. (2005; AM05) for earthquakes derived in normal faulting mechanisms (F_N = 1) for stiff soil conditions (site effect variable S_A = 1) will also be considered to update this hazard analysis alongside Ambraseys (1995; AM95_WDC) for rock sites with depth control at the 50th percentile (P = 0). Illustrations and tables are however largely only presented for the lead ground acceleration model of Theodulidis and Papazachos (1992).

As PGA hazard is modelled using Gumbel's linear first extreme values distribution, ensuing hazard forecasts will also follow a linear trend. Variability between related contoured hazard maps using different ground motion models will be seen in absolute values for estimated PGA – a result of important changes in soil type adopted by the different models – but geographic coverage of the hazard distribution will be largely similar between each. Consequently, hazard maps are generally only presented here for the lead ground acceleration model of Theodulidis and Papazachos (1992).

PGA hazard (in cm s^{-2}) estimated using Theodulidis and Papazachos (1992) is contoured across the broader region in Figure 5.25 for the same return periods against which magnitude hazard was forecast in section 5.5.3. Figure 5.26 repeats this at 90% probability of non-exceedance with cell-specific statistics for parameters α, μ and uncertainties and the forecast maximum accelerations in *T* years, and *T* years at 90% pnbe given in, with cellular estimates that create these maps given in Appendix 9.

Small increases in PGA estimates using Ambraseys (1995) suggest conservative estimates for PGA. Absolute values forecast for PGA, as well as their change with increased return period, could be considered lower than might be expected for this area, considering its highly active tectonics. This concern is highlighted in Burton *et al.* (2003); therefore, the Theodulidis and Papazachos '*stiff soil*' model is applied to extreme data as the lead ground motion model to critically assess.

An often-used benchmark for reporting ground acceleration seismic hazard is the 475-year return period event, and is promoted in EUROCODE 8 (2003) as the standard measure to adopt across Europe. This is equivalent to the maximum event forecast in a 50-year time interval at 90% probability of non-exceedance (A_{P50}). 475-year forecasts are shown to be systematically higher using Theodulidis and Papazachos than Ambraseys (Figure 5.26(a)).

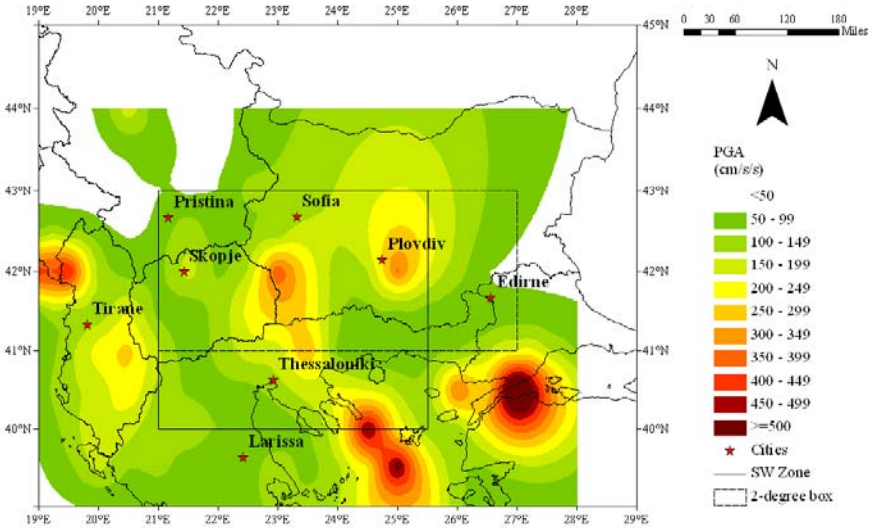

(a)

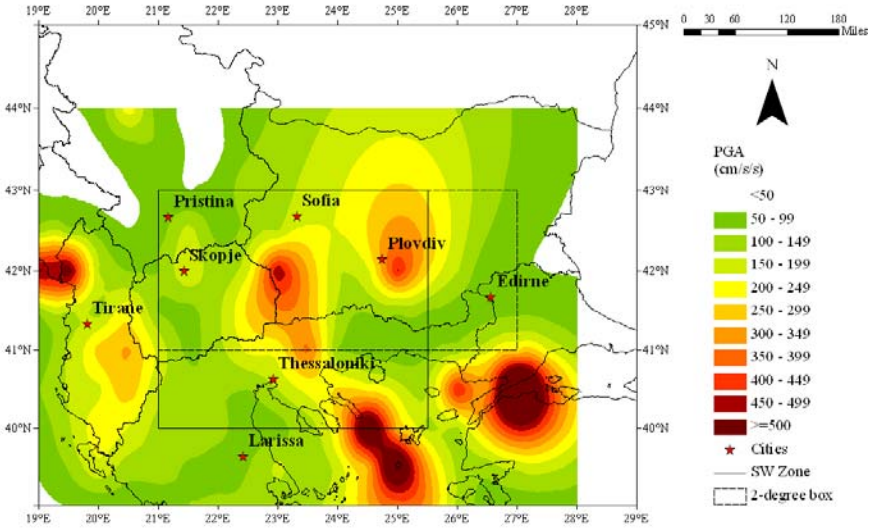

(b)

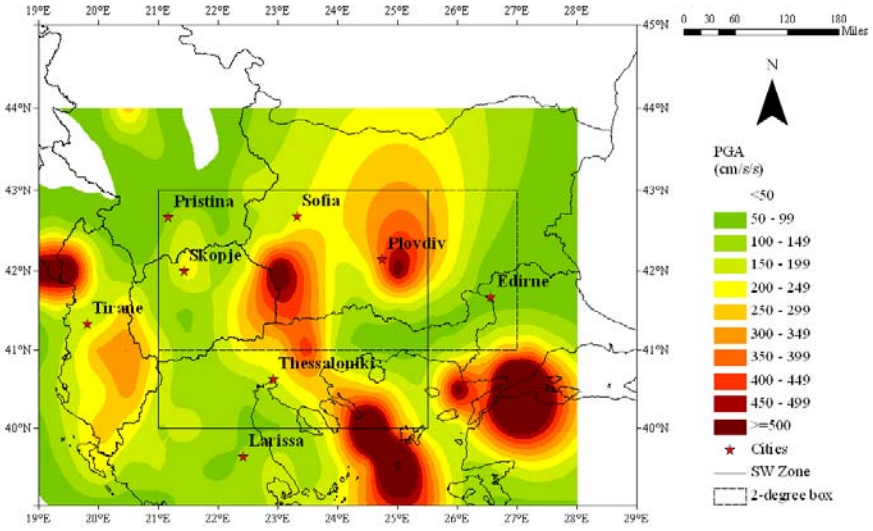

(c)

Figure 5.25 PGAs in (a) 50, (b) 100 and (c) 200 years using Theodulidis and Papazachos (1992) for stiff soil conditions (S = 0.5) at the 50th percentile (P = 0). Contours at intervals of 50 cm s^{-2}

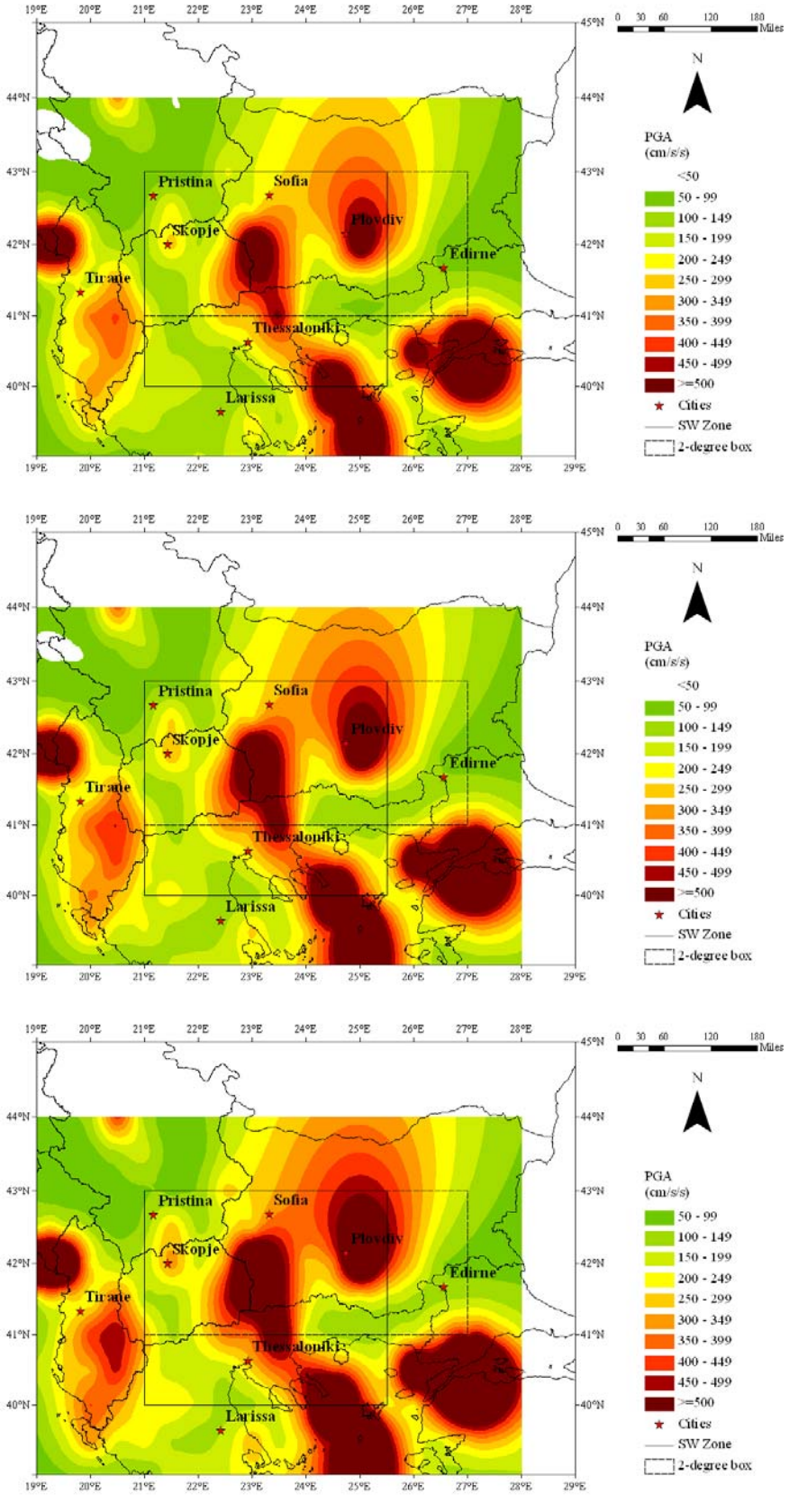

Figure 5.26 PGAs in (a) 50, (b) 100, (c) 200 years at 90% pnbe from Theodulidis and Papazachos (1992), stiff soil conditions (S = 0.5), 50th percentile (P = 0). Contours at 50 cm s^{-2} intervals

Typically, accelerations increase by between 50 and 100 cm s^{-2} at the northeast Bulgaria-Romania border and central Serbia, 100 to 200 cm s^{-2} at the Albania-Serbia border and as much as 350 cm s^{-2} in west Turkey. The highs of southwest Bulgaria and Plovdiv increase by approximately 100 cm s^{-2} and 125 cm s^{-2} respectively.

Maximum accelerations using Theodulidis and Papazachos (Figure 5.25) show the areas of high forecasts highlighted earlier are still present; however forecasts are typically lower than the equivalent 90% pnbe forecasts by approximately 100 to 300 cm s^{-2} using Theodulidis and Papazachos. It is also interesting to relate equivalent PGA and magnitude hazard maps by locations of high and low forecast hazard. For example, the region immediately west of Sofia possesses the highest magnitude recurrence hazard for a 50-year return period at 90% pnbe ($M_{P50} > 8.25$ M_s; Figure 5.18(a)). The area immediately south of Sofia is forecast systematically lower magnitude hazard. However, west of Sofia is forecast significantly lower ground acceleration hazard than the more southerly area. South of Sofia is dominated by higher accelerations, that extend uninterrupted southeast to Thessaloniki (Figure 5.26(a)) and is likely due to the seismicity resulting from Serbomacedonian massif. This may also be due to variation in focal depths between these two selected areas. Underlying seismicity considered after filtering earthquake data for the area immediately south of Sofia and around Thessaloniki is also considerably higher in terms of absolute number and magnitude than that west of Sofia.

One governing reason for undertaking this study is that many previous studies failed to extend observations and hazard forecasts across the political borders between these countries. Due to this, full seismotectonic regimes may not have been fully considered in these seismic hazard analyses, as earthquake populations are not constrained by country. Contour maps often stop at borders and may not fully reflect a region's seismicity. The NEAK map (Figure 2.26) is a good example of this. As its geographical extent was tightly restricted a full and direct comparison between it and this work cannot be made. Peak ground accelerations of Figure 5.26(a) that are common with NEAK are those in the vicinity of Limnos and Turkey's west coast, and over Corfu and west coast of mainland Greece. Here NEAK forecasts PGAs of 24%g (~235 cm s^{-2}), for both sub regions. Ambraseys forecasts significantly lower maximums here of 50-100 cm s^{-2}, whilst Theodulidis and Papazachos estimates are less than NEAK at 50-100 cm s^{-2}.

Although comparing with NEAK has its limitations, it is possible to compare forecasts obtained here to those from two other studies; 1) the "*Global Seismic Hazard Assessment Program*" (GSHAP; Giardini and Basham, 1993; Giardini, 1999), and; 2) "*Seismotectonics and Seismic Hazard Assessment of the Mediterranean Basin*" (SESAME; Jiménez *et al.*, 2001). Both these projects were designed to span political boundaries, assessing seismic hazard on an international

scale; GSHAP is on a global scale, while SESAME is limited to the Mediterranean area. These projects differ in that GSHAP aimed to develop hazard maps independently for each country through combining multiple previous, independent country-specific seismic hazard assessments. These were then consolidated into one final PGA hazard map that became the project's main product. SESAME aimed to aggregate neighbouring seismic populations and seismotectonic and seismogenic source models together to create new cross-border seismic sources, with the hope they would be more representative of the region's true seismicity. Each project developed maps forecasting acceleration hazard akin to the 475-year return period event, making both equivalent to Figure 5.26(a) of this study.

GSHAP (Figure 5.27(a)) assessed Balkan seismic hazard in their combined Europe-Africa-Middle East seismic hazard map. Although maps of the GSHAP project were always going to be relatively low resolution due to the large geographic coverage they provided, it is still possible to crudely make out similar patterns of high and low peak ground accelerations. The high of ~2.0-3.0 m/s located on the Albanian coast is present and similar in value (>200 cm s^{-2}) with Theodulidis and Papazachos while peak accelerations in southwest Bulgaria are also comparable in size, coverage patterns and also tracing the Serbomacedonian massif. West Turkey is forecast peak accelerations in excess of 4.0 m/s along the southern edge of the Marmara Sea.

SESAME forecast the 475-year return period PGA (Figure 5.27(b)) and spectral acceleration for the full Mediterranean region using the stiff soil relation of Ambraseys *et al.* (1996). This brings even closer compatibility between these study and SESAME as both using the Ambraseys model used herein and by Burton *et al.*. Although SESAME's map for 475-year return period peak ground accelerations (A_{P50}) also illustrate peak accelerations on the Albanian coast and west Turkey similar to estimates derived here, by Burton *et al.* and the GSHAP study, southwest Bulgaria is forecast estimates by SESAME significantly higher than this and the other studies quoted, although one must acknowledge the inherent difficulty of interpolating accurate hazard estimates from a smoothed colour ramp such as that used in SESAME. Peak accelerations estimated by Theodulidis and Papazachos are broadly comparable to SESAME across the region.

These differences may be explained by either: the conscious decision for SESAME not to harmonize the adopted individual seismogenic models; a single uniform seismic behaviour being determined for each seismogenic zone; the incomplete coverage provided by the Bulgaria-specific seismogenic zones of van Eck and Stoyanov (1996); adoption of a more seismogenic-orientated probabilistic methodology (e.g. McGuire, 1993; Muir-Wood, 1993); or adopting different input earthquake data.

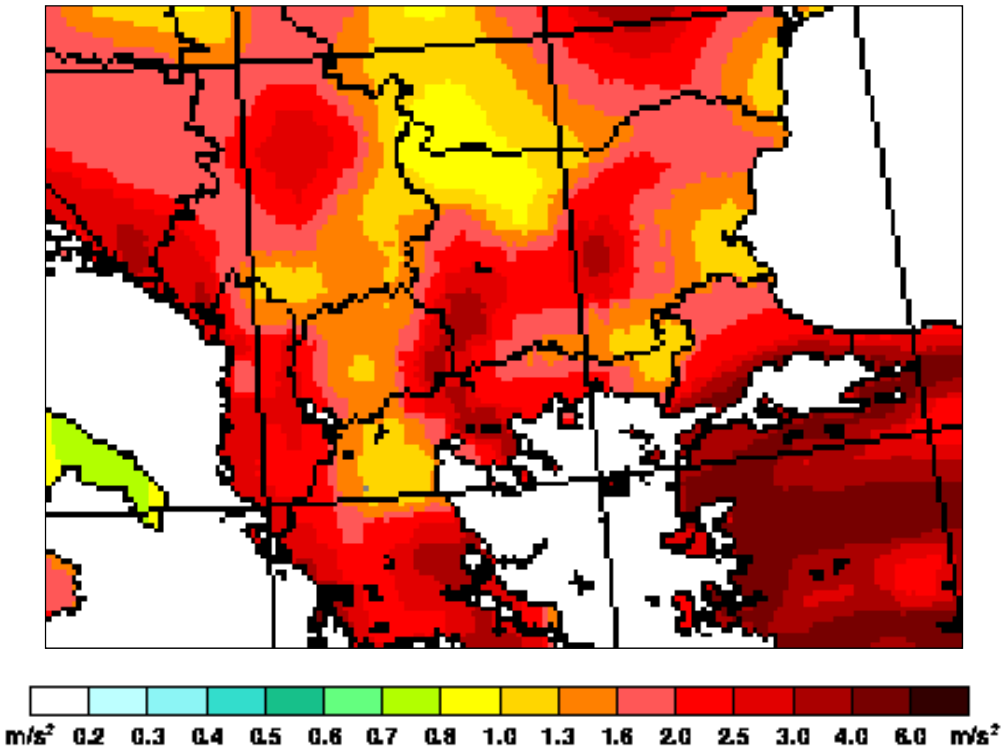

(a)

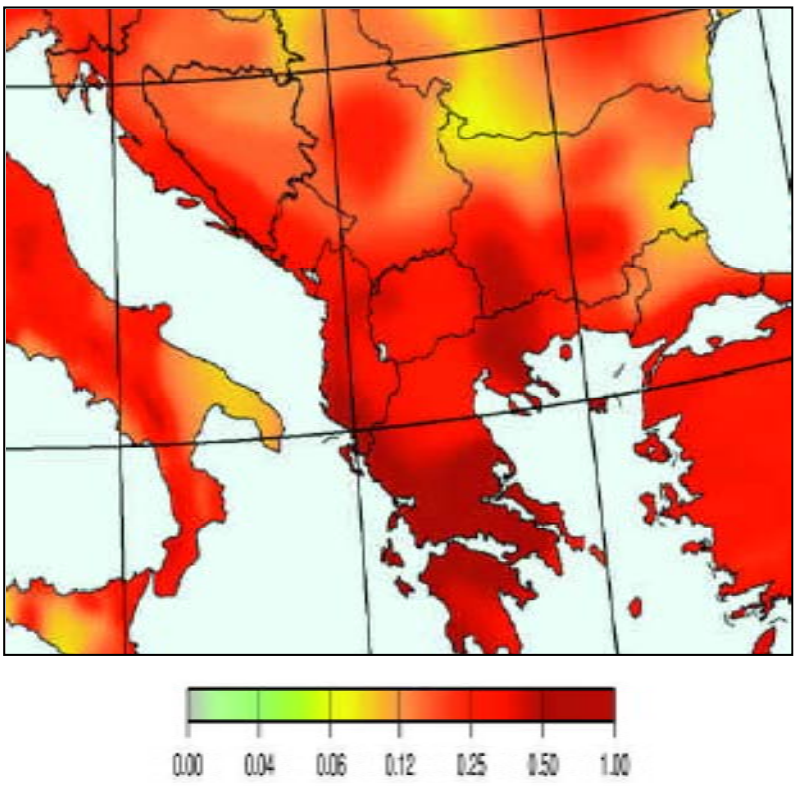

(b)

Figure 5.27 Extracts from (a) GSHAP and (b) SESAME international seismic hazard projects. Both projects presented maps for the 475-year return period peak ground acceleration (i.e. 90% probability of non-exceedance in 50 years)

Longer return period accelerations for Theodulidis and Papazachos are provided by Figure 5.25(b)-(c) and Figure 5.26(b)-(c). These continue the near linear nature of acceleration extremes using Gumbel's first extreme values distribution, reflected in similar isoline patterns created (Makropoulos and Burton, 1985b). Horizontal accelerations increase across this broader region by up to 200 cm s^{-2} from Theodulidis and Papazachos at the Serbia-Albania border, 100 cm s^{-2} in the Struma Valley of southwest Bulgaria near the political triple junction and 100 cm s^{-2} in the Aegean Sea and western Turkey areas respectively at 90% confidence levels. The epicentral distribution of the adopted catalogue (Figure 2.10 and Figure 4.14) shows that patterns of peak ground accelerations follow the population distribution of significantly larger earthquakes in this region. Namely the east coast of the Adriatic Sea, the FYR of Macedonia-Bulgaria-Greece border region in the centre and the demarcation of the NAF by earthquake epicentres located across the north Aegean Sea into west Turkey are all highlighted. Peak accelerations in Figure 5.26 are produced by populations dominate in moderate to large magnitude ($\geq$5.0 M_S; Figure 4.14) and shallow-focus ($h \leq 30$ km) earthquakes (Figure 2.14 to Figure 2.16).

Uncertainties on ground acceleration return period hazard forecasts at each cell grid point used to contour hazard vary markedly across this broader mapped region. These range from 0.22 to 0.61 regardless of the attenuation law adopted. σ_α, the standard deviation on the logarithm of α, varies from 0.148 to 0.40 while σ_μ varies between 0.10 and 0.19.

Peak ground acceleration hazard in southwest Bulgaria is given on a larger scale in Figure 5.28 for time intervals of (a) 50 (b) 100 and (c) 200 years, and at 90% pnbe for the same time intervals ((d)-(f)) after adopting the model of Theodulidis and Papazachos (Appendix 10 lists cell-specific estimates for this ground motion model). These figures highlight clearly how this particular region is dominated by its historical high seismicity and how ground acceleration estimates are governed by key seismic sequences, notably the 1904 Kresna sequence to the centre of the region, the 1928 Plovdiv sequence on the area's eastern fringe, and the western end of the North Branch of the NAF in the Aegean.

Plovdiv (42.15°N, 24.75°E) and Sofia (42.68°N, 23.32°E) are prone to the highest ground accelerations of the five urban centres considered in this smaller area of the Balkans. Both locations are forecast to experience accelerations in excess of 100 cm s^{-2} for Theodulidis and Papazachos in a 50-year time interval. This rises to a minimum of 450 cm s^{-2} at 90% pnbe around Plovdiv and 250 cm s^{-2} around Sofia. Neither city sits exactly on a grid point used to contour PGA hazard for this smaller region, therefore these estimates are only interpolated from the hazard contours and should be used with caution.

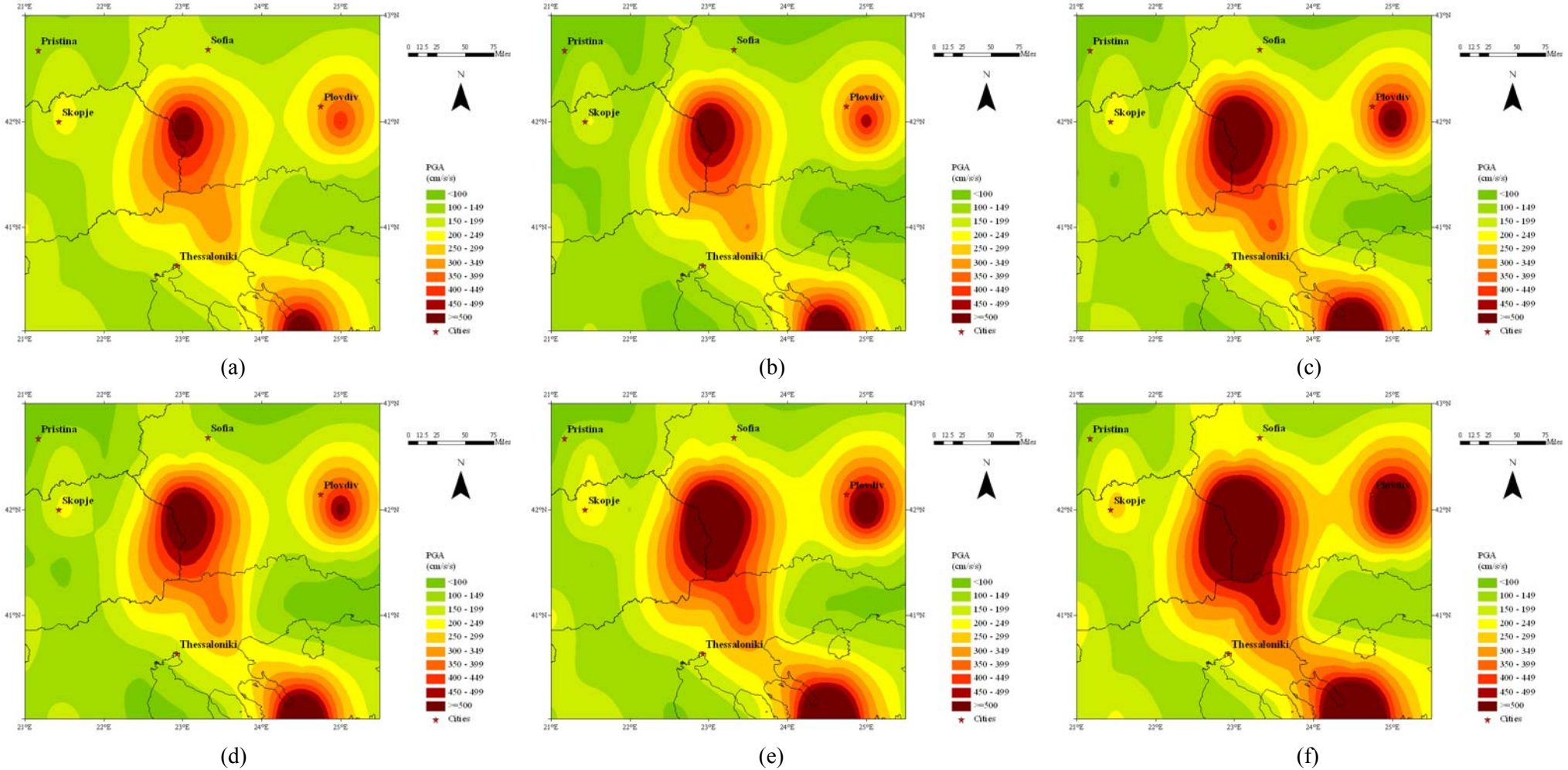

Figure 5.28 Peak ground accelerations in the southwest zone for time periods of (a) 50, (b) 100 and (c) 200 years and (d) 50, (e) 100 and (f) 200 years with 90% probability of not being exceeded (that is, a 1 in 10 chance of being exceeded). Forecasts are obtained using Theodulidis and Papazachos (1992), for stiff soil conditions (S = 0.5) at the 50th percentile (P = 0). All contours are at intervals of 50 cm s^{-2}

Site-specific PGA estimates from Theodulidis and Papazachos at Plovdiv of approximately 370 cm s^{-2} are ~120 cm s^{-2} more than the interpolated equivalent estimates (at 250 cm s^{-2}) for 50-year maximum accelerations. This gap increases to nearly 300 cm s^{-2} at 90% pnbe, but with the interpolated estimate now lower than the site-specific estimate (with a site-specific estimate of 750 cm s^{-2} and interpolated estimate of ~450 cm s^{-2}). Estimates from Theodulidis and Papazachos at Sofia differ to a lesser degree, with 50-year maximums varying by approximately 40 cm s^{-2} (site-specific of 108 cm s^{-2}; interpolated of 150 cm s^{-2}) and 50-year 90% pnbe estimates different by ~75 cm s^{-2} (site-specific of 177 cm s^{-2}; interpolated of ~250 cm s^{-2}).

PGA results for Thessaloniki from Burton *et al.* (2003) and this work are compared in Table 5.11, while Table 5.12 and Table 5.13 provide PGA estimates for same-size analysis cells positioned precisely here and at the other urban centres, so providing *site-specific* estimates for these cities. Site-specific estimates at Thessaloniki are systematically higher in this study than Burton *et al.* (2003) by almost identical ratios, regardless of the return period considered. Forecasts using Ambraseys are typically ~76-78% those of this study using the same ground motion model, while Theodulidis and Papazachos are nearer 68-71% of this study's estimates. This is a function of the linear nature of Gumbel's first asymptotic distribution used to model PGA hazard.

	T	A_{25}	A_{50}	A_{100}	A_{200}	Comment
Thessaloniki 40.63°N, 22.93°E	Absolute PGA	109.76	122.57	135.37	148.18	AM05
		72.99	83.14	93.29	103.44	AM2_2[1]
		149.38	171.82	194.25	216.69	NTP_2[1]
		96.10	108.20	120.30	132.39	AM95_WDC
		219.22	248.15	277.08	306.01	$TP92_A$
	Percentage difference[2]	76.0	76.8	77.5	78.1	AM95_WDC
		68.1	69.2	70.1	70.8	$TP92_A$

[1] Specific notation used by Burton *et al.* (2003) denoting data of $M_s \geq 5.5$ and 1900-1999 used; [2] Percentage estimates AM2_2 or NTP_2 are of AM95_WDC and $TP92_A$ respectively

Table 5.11 PGA estimates at 90% probability of non-exceedance in *T* years, for Thessaloniki based on AM95_WDC, $TP92_A$ and AM05 models from this work and the equivalent models from Burton *et al.* (2003; except for AM05) applying data within a 2° half-width cell. Each estimate in the lower pair of attenuation laws is directly comparable to the equivalent set from the upper pair of laws (e.g. AM95_WDC of this work compares to AM2_2 of Burton *et al*.; 2003)

City	α	σ_α	μ	σ_μ	A_{25}	A_{50}	A_{100}	A_{200}	A_{P25}	A_{P50}	σ_{PA}	A_{P100}	A_{P200}
Edirne	7.49	0.20	0.16	0.14	28.26	32.73	37.20	41.67	42.78	47.25	0.35	51.72	56.19
Larissa	7.44	0.16	0.12	0.11	33.45	39.05	44.65	50.25	51.63	57.23	0.29	62.83	68.43
Plovdiv	-30.74	0.37	0.03	0.20	87.82	113.35	138.88	164.41	170.70	196.24	0.56	221.77	247.30
Pristina	4.33	0.11	0.13	0.07	28.67	33.91	39.15	44.39	45.69	50.93	0.18	56.17	61.41
Skopje	0.05	0.10	0.05	0.07	60.85	73.95	87.04	100.13	103.36	116.45	0.15	129.55	142.64
Sofia	2.27	0.28	0.10	0.16	35.51	42.67	49.83	56.99	58.76	65.91	0.45	73.07	80.23
Thessaloniki	0.66	0.22	0.06	0.14	56.83	68.93	81.03	93.12	96.10	108.20	0.38	120.30	132.39
Tirane	22.92	0.17	0.06	0.12	75.04	86.26	97.49	108.71	111.48	122.70	0.30	133.93	145.15

Table 5.12 Parameters (α, μ) and their uncertainties of a $G^{(I)}$ distribution for eight urban centres considered in the catalogued region. A_{25}, A_{50}, A_{100} and A_{200} are the maximum accelerations expected in 25-, 50-, 100- and 200-year time intervals respectively. A_{P25}, A_{P50}, A_{P100} and A_{P200} are ground accelerations at 90% probability of non-exceedance in the time interval specified (a 1 in 10 chance of exceedance) from Ambraseys (1995) for rock sites with depth control at the 50th percentile (P = 0). σ_{PA} is uncertainty on A_{P50} only. Accelerations are given in cm s^{-2}. Estimates derived from the distribution of seismicity present within a 2° half-width cell of the city are given

City	α	σ_α	μ	σ_μ	A_{25}	A_{50}	A_{100}	A_{200}	A_{P25}	A_{P50}	σ_{PA}	A_{P100}	A_{P200}
Edirne	4.79	0.20	0.06	0.14	54.53	65.25	75.96	86.67	89.31	100.02	0.35	110.74	121.45
Larissa	5.39	0.16	0.06	0.11	55.85	66.72	77.59	88.46	91.14	102.01	0.29	112.87	123.74
Plovdiv	-132.26	0.37	0.01	0.20	281.40	370.48	459.56	548.64	570.60	659.68	0.56	748.76	837.84
Pristina	0.92	0.11	0.09	0.07	35.08	42.43	49.78	57.14	58.95	66.31	0.18	73.66	81.02
Skopje	-15.03	0.10	0.02	0.07	126.34	156.79	187.23	217.67	225.18	255.62	0.14	286.06	316.51
Sofia	-14.00	0.28	0.03	0.16	85.98	107.51	129.04	150.57	155.88	177.41	0.45	198.94	220.47
Thessaloniki	-9.05	0.22	0.02	0.14	125.29	154.22	183.15	212.08	219.22	248.15	0.38	277.08	306.01
Tirane	30.89	0.17	0.03	0.12	139.27	162.61	185.95	209.29	215.04	238.38	0.30	261.72	285.06

Table 5.13 Site-specific peak ground acceleration estimates the eight cities considered. Fields provided are as in Table 5.12. Estimated derive from ground motion model of Theodulidis and Papazachos (1992), for stiff soil conditions (S = 0.5) at the 50th percentile (P = 0). Forecasted accelerations are given in cm s^{-2}

As ratios are nearly identical regardless of the *T*-year return period considered and as the ground motion models used are identical this constant pattern has to be attributed to variability imposed by the respective input catalogues to each study, and their different coverage of the seismotectonic regimes and related seismicity. Using identical cut-off magnitudes of 5.5 M_s helps align these PGA estimates still further.

Site-specific peak ground accelerations in terms of the 475-year return period hazard (A_{P50}) are further explored in Table 5.14 – and in Figure 5.29 for both geographic areas – after adopting the newer model of Ambraseys *et al*. (2005). Regardless of the geographic resolution considered, Ambraseys (1995) systematically estimates significantly lower PGA than Ambraseys *et al*. (2005). PGA estimated by the newer model is approximately 50-150 cm s^{-2} higher in southwest Bulgaria, while at a site-specific level PGA estimates for areas around Skopje, Plovdiv and Edirne have increased the most.

Hazard maps for southwest Bulgaria show clearly the dominance of the same three high seismicity zones highlighted in the regional hazard maps (Figure 5.25 to Figure 5.26). Those of the Struma Valley in the extreme southwest of Bulgaria, the Rila and Rhopodi mountain complexes in central south Bulgaria and Chalkidiki Peninsula southeast of Thessaloniki. These are in close enough proximity to each other, and the seismicity distributions are of shallow enough focal depth, that accelerations resulting from each earthquake population ensure a major proportion of the region is forecast at least 100 cm s^{-2} ground motion in 50 years. Contours obtained here support findings of Burton *et al.* (2003) using their Greek catalogue for mutually covered geographies.

Unusually, more variability is seen comparing Ambraseys *et al.* (2005) with Theodulidis and Papazachos (1992). Only Edirne, Pristina and Skopje are estimated lower PGA by the latter model. Interestingly, those cites that are forecast higher PGA by Theodulidis and Papazachos are those in close proximity to large magnitude historical earthquakes or sequences (e.g. Sofia to the 1904 Kresna sequence; Plovdiv to the 1928 sequence; Thessaloniki to the 2000 [largest catalogued] earthquake), thus highlighting this model's propensity for perhaps over-estimating near-field ground acceleration in response to large magnitude catalogued historical earthquakes.

City	α	σ_α	μ	σ_μ	A_{25}	A_{50}	A_{100}	A_{200}	A_{P25}	A_{P50}	σ_{PA}	A_{P100}	A_{P200}
Edirne	0.50	0.15	0.03	0.11	102.45	124.41	146.36	168.32	173.73	195.69	0.26	217.64	239.60
Larissa	8.87	0.15	0.09	0.11	44.00	51.56	59.13	66.69	68.56	76.12	0.28	83.69	91.25
Plovdiv	13.05	0.13	0.02	0.10	164.94	197.64	230.35	263.06	271.12	303.83	0.23	336.53	369.24
Pristina	11.50	0.13	0.11	0.10	41.83	48.37	54.90	61.43	63.04	69.57	0.24	76.10	82.64
Skopje	11.19	0.13	0.02	0.10	184.89	222.29	259.70	297.10	306.32	343.73	0.21	381.13	418.53
Sofia	7.58	0.14	0.09	0.11	43.96	51.79	59.63	67.46	69.39	77.23	0.26	85.06	92.89
Thessaloniki	8.72	0.13	0.06	0.10	66.23	78.62	91.00	103.39	106.44	118.83	0.23	131.21	143.60
Tirane	33.85	0.13	0.04	0.10	116.48	134.28	152.07	169.87	174.26	192.05	0.24	209.85	227.64

Table 5.14 Site-specific peak ground acceleration estimates the eight cities considered. Fields provided are as in Table 5.12. Estimated derive from ground motion model of Ambraseys *et al*. (2005), for stiff soil conditions (S_A = 1) and earthquakes of normal faulting mechanisms (F_N = 1). Forecasted accelerations are given in cm s^{-2}

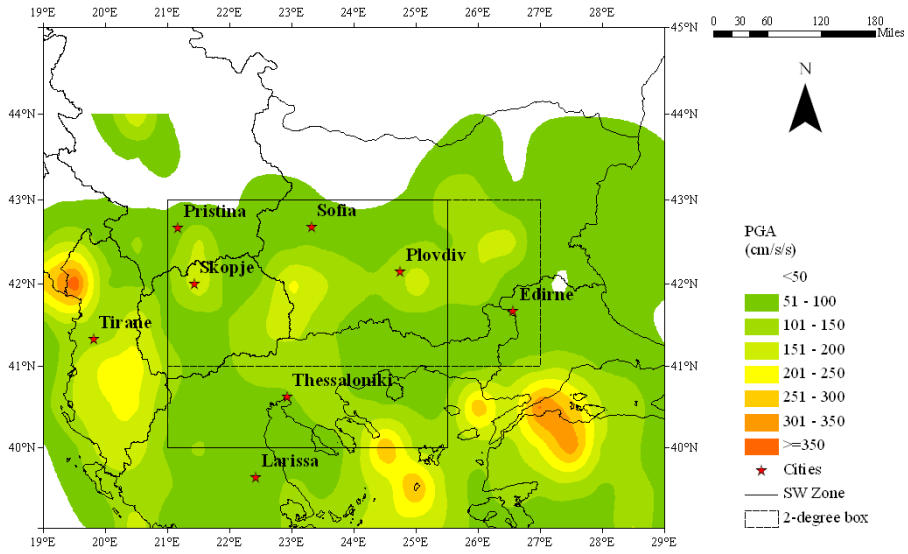

(a)

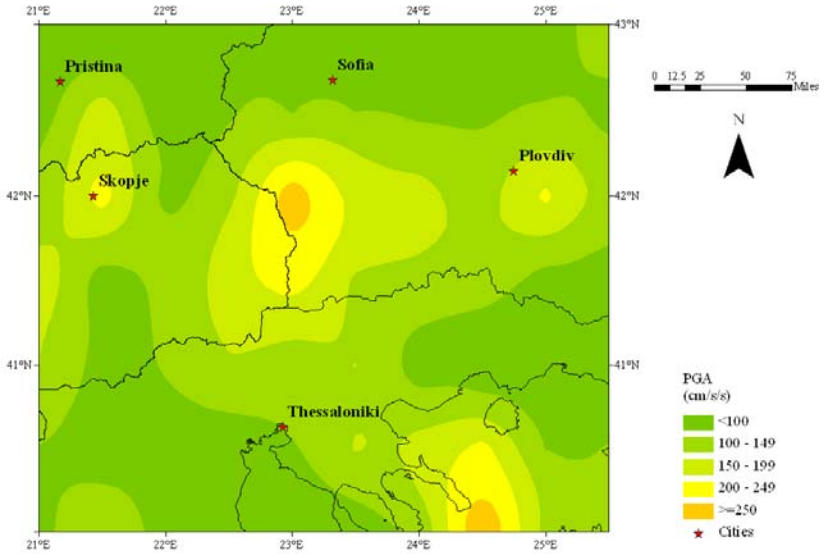

(b)

Figure 5.29 Peak ground acceleration estimates using Ambraseys *et al.* (2005) for (a) the Balkans and (b) southwest Bulgaria. Estimates are the 475-year return period peak ground accelerations (A_{P50}). Contours are at intervals of 50 cm s^{-2}

5.5.5 Peak Ground Velocity (PGV)

The horizontal velocity ground motion model of Theodulidis Papazachos (1992; $TP92_V$) for stiff soil conditions (S = 0.5) at the 50^{th} percentile (P = 0), will be applied to estimate horizontal ground velocity hazard. The site effect variable, S, was set to 0.5 for two reasons:

1. Koravos *et al.* (2003) used the same value in their assessment of perceptible earthquakes in the Aegean region, and,

2. Burton *et al.* (2003) took advice from Theodulidis that S = 0.5 better represents site geology of the Greek and Aegean regions. However they used it in modelling peak ground acceleration modelling using the equivalent PGA model from Theodulidis and Papazachos (1992).

Maximum ground velocities (in cm s^{-1}) are shown in Figure 5.30 for 50-, 100- and 200-year return periods (V_{50}, V_{100}, V_{200}), while these time intervals at 90% pnbe hazard are shown Figure 5.31 (V_{P50}, V_{P100}, V_{P200}). Appendix 11 tabulates the parameters α and μ and their uncertainties of a $G^{(I)}$ distribution along with the forecasted maximum velocities in *T* years, and *T* years with 90% pnbe for each analysis cell. It is these estimates that produce Figure 5.30 and Figure 5.31. As with magnitude recurrence and PGA hazard presented earlier, Balkan ground velocity hazard is dominated by peak forecasts in southwest Bulgaria, Plovdiv and the northern reaches of the Aegean Sea, the Serbia-Albania border region and western Turkey. These zones of high ground velocities are all in excess of 10 cm s^{-1} for a 50-year time interval. The peak ground velocities estimated in these latter three regions exceed 20 cm s^{-1} in confined pockets.

Extending to 475-year return period velocities, PGV contours increase by 10 cm s^{-1} to produce near identical hazard contour patterns, again reflecting the linear nature of Gumbel's first distribution used to fit against extracted extreme data. Much of southwest Bulgaria around the Struma Valley region is now dominated by the 20 cm s^{-1} contour that extends into east Macedonia. Peak velocities covering the north Aegean Sea and western Turkey increase to 40 cm s^{-1}, with confined pockets at 50 cm s^{-1}.

Lengthening the return period from 50 to 200 years shows peak velocities rising by 5 cm s^{-1} to achieve maximum PGV of 20 cm s^{-1}at 90% pnbe. Zones of high hazard covering the Struma Valley and Plovdiv in southern Bulgaria are now linked together by the 10 cm s^{-1} contour, with a new 10 cm s^{-1} high starting to appear in the Lovech Province, north central Bulgaria. The highest forecasts are in north Aegean and west Turkey at ~50 cm s^{-1}.

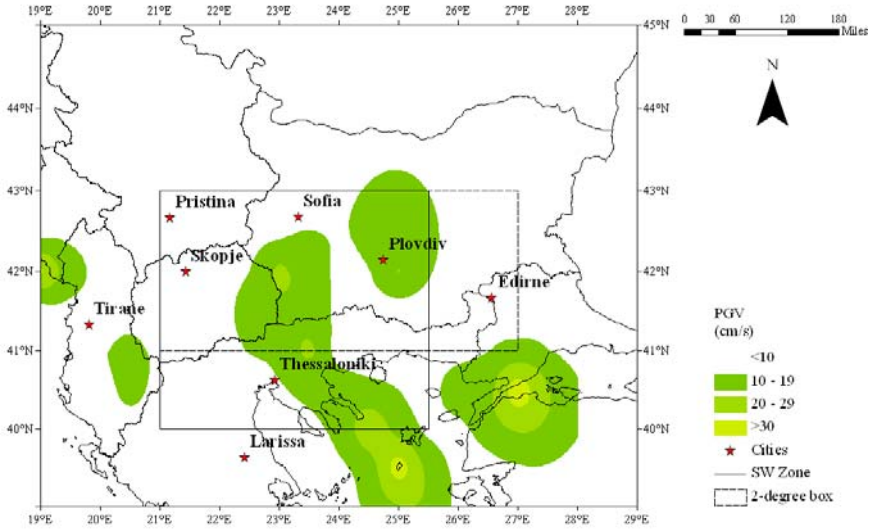

(a)

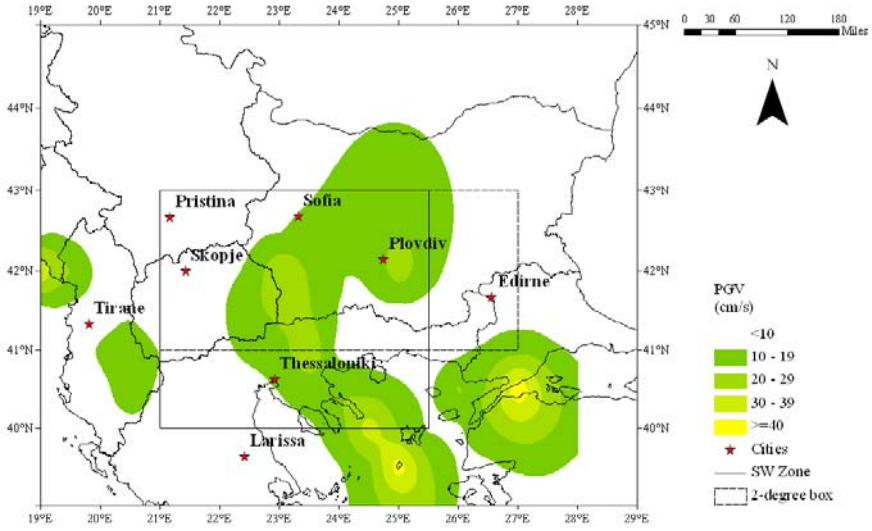

(b)

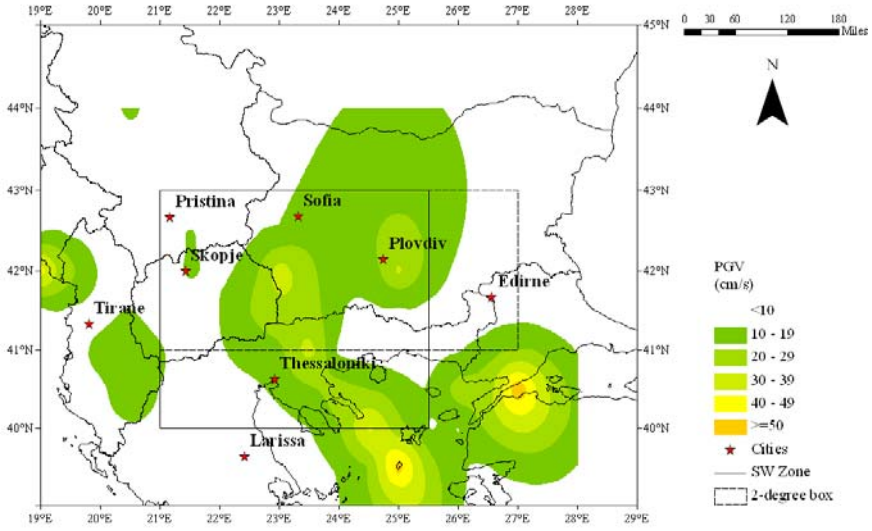

(c)

Figure 5.30 PGVs in (a) 50, (b) 100 and (c) 200 years using Theodulidis and Papazachos (1992), stiff soil conditions (S = 0.5) at the 50th percentile (P = 0). Contours at 10 cm s^{-1} intervals

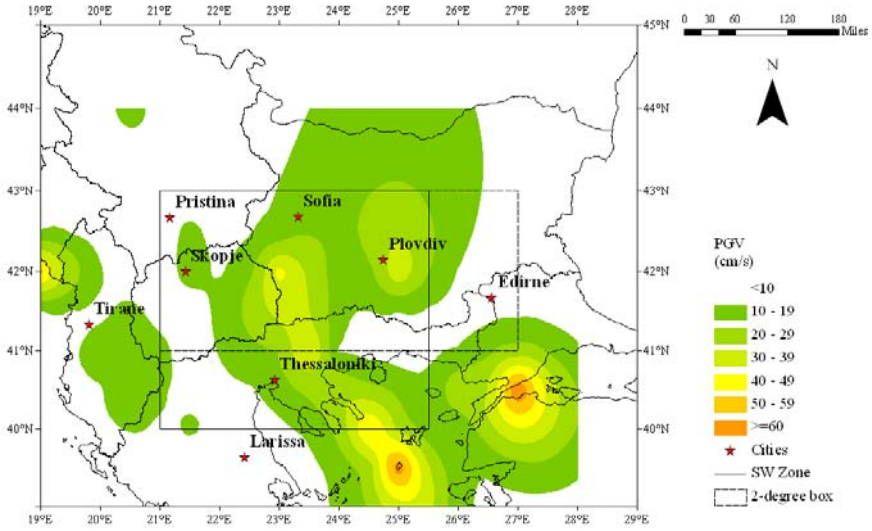

(a)

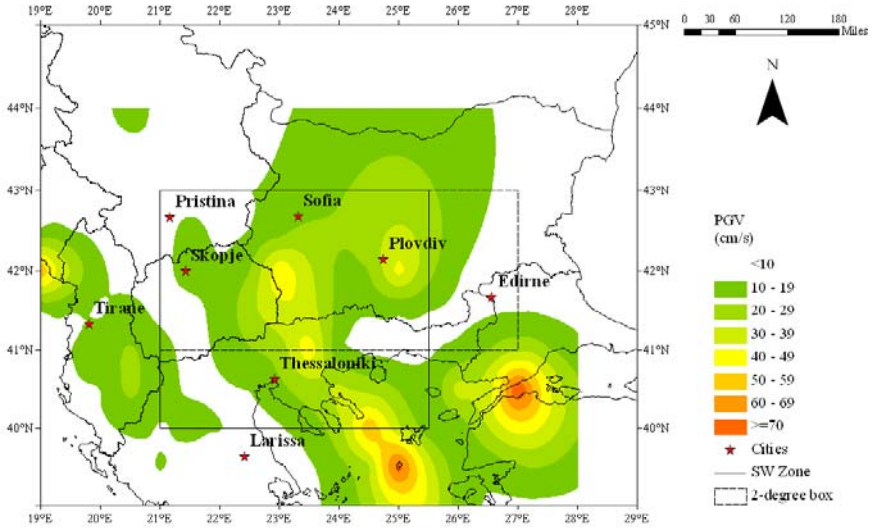

(b)

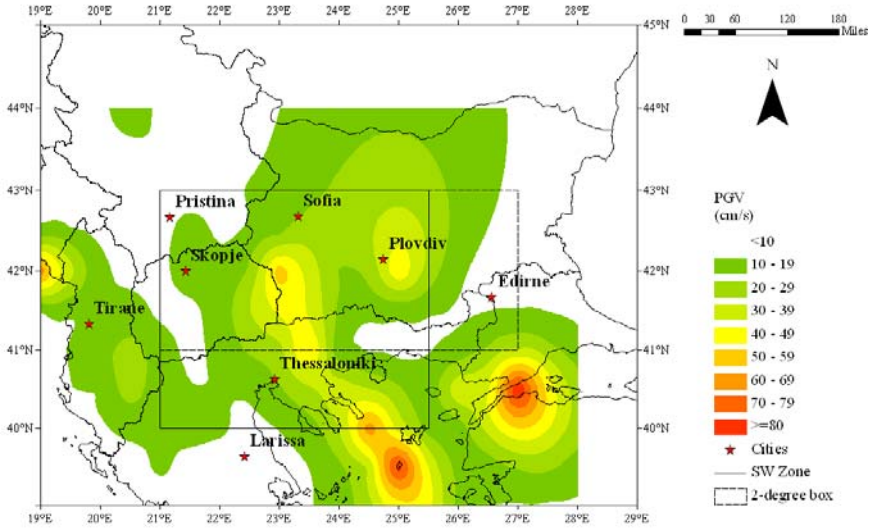

(c)

Figure 5.31 PGVs in (a) 50, (b) 100, (c) 200 years, at 90% pnbe from Theodulidis and Papazachos (1992), stiff soil conditions (S = 0.5) at 50th percentile (P = 0). Contours at 10 cm s^{-1} intervals

Ground velocity hazard specific to southwest Bulgaria for time intervals of 50, 100 and 200 years is contoured in Figure 5.32(a)-(c) respectively using the model of Theodulidis and Papazachos; (d) to (f) contour velocity hazard for the same time intervals at 90% probability of non-exceedance. Unlike magnitude recurrence hazard (section 5.5.3), patterns of ground motion hazard for this confined zone will be closer to that of the broader Balkan area due to the full catalogue of 3,681 events being applied. The same distribution of seismicity has been applied to both areas to counter 'edge' effects as ground motion hazard is a field effect, not point process. However, different values for extreme interval, magnitude threshold are used due to the different geographic extent considered (section 5.3.13).

General hazard patterns created are consistent with that of ground acceleration hazard. The most significant regions of extreme ground motion are seen in: 1) the centre at the border of Bulgaria and Macedonia (approx. 23°E, 42°N); 2) centred on Plovdiv in the east, and; 3) west of Limnos. Lengthening the time interval areas of hazard bound by the same level contour (e.g. 20 cm s^{-1}) gradually enlarge, merge and connect together such that Figure 5.32(c) and (f) (200-year return period (V_{50}) and 200 years at 90% pnbe (V_{P50})) are dominated by the 10 cm s^{-1} contour and – to a lesser degree – the 20 cm s^{-2} contour. The peak velocity forecast in 50 years is 20 cm s^{-1}, rising to 40 cm s^{-1} in 200 years. At 90% probability of non-exceedance, this rises to 60 cm s^{-1} in 200 years. Statistics that underpin hazard maps for southwest Bulgaria are given in Appendix 12.

Table 5.15 provides extreme velocity estimates for the standard eight urban centres of the region. As expected, the four localities within the high seismicity region of southwest Bulgaria are forecast the highest ground velocities, with Plovdiv expecting the highest velocities at ~89 cm s^{-1} for the 475-year mean return period event (V_{P50}). Sofia, being located in a band of marginally lower hazard is forecast 27 cm s^{-1} for this hazard measure.

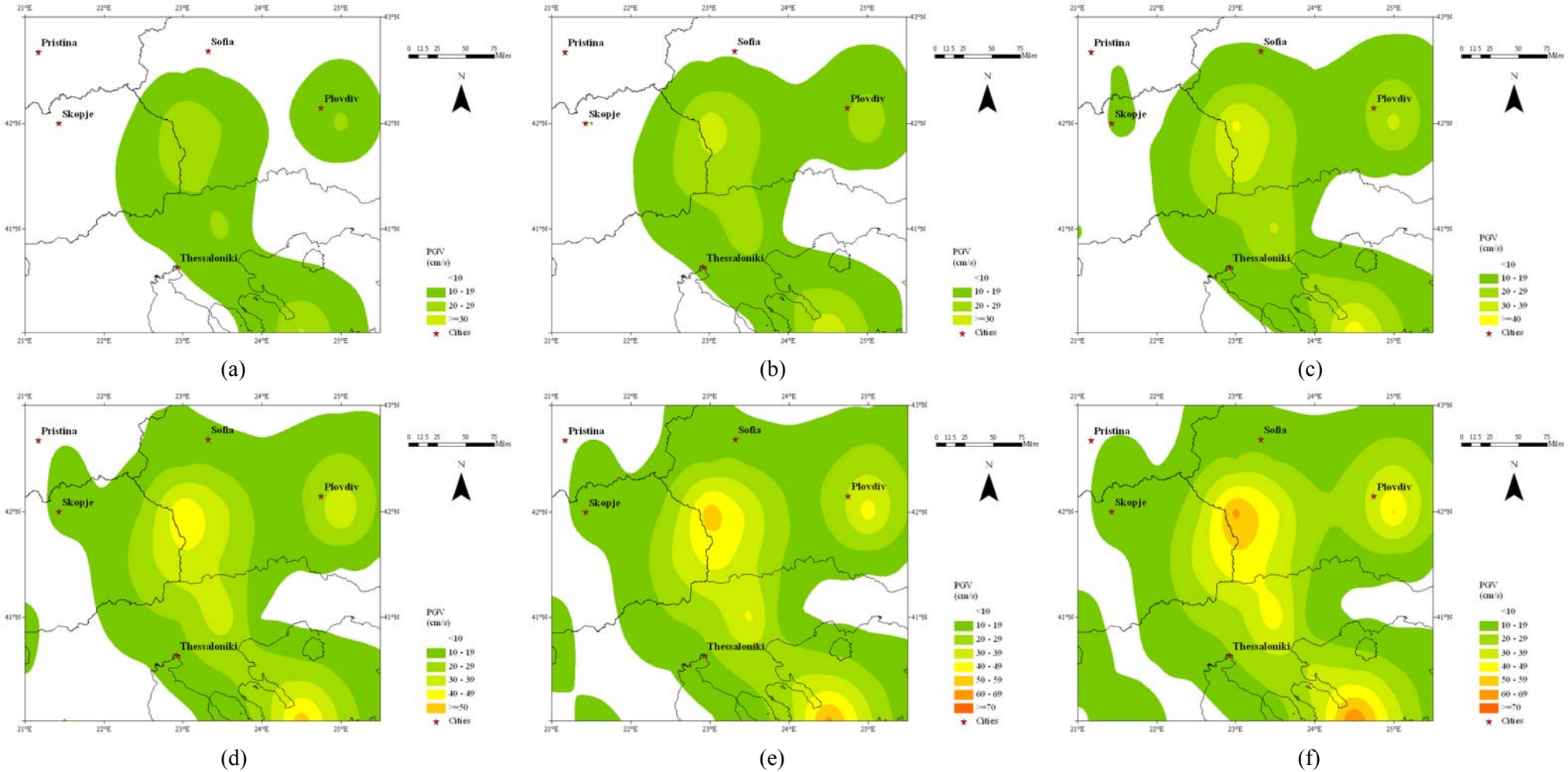

Figure 5.32 Peak ground velocities in the southwest zone for time periods of (a) 50, (b) 100 and (c) years and (d) 50, (e) 100 and (f) 200 years with 90% probability of not being exceeded (a 1 in 10 chance of being exceeded). Forecasts are obtained using Theodulidis and Papazachos (1992) for stiff soil conditions (S = 0.5) at the 50th percentile (P = 0). Contours are at intervals of 10 cm s^{-1}

City	α	σ_α	μ	σ_μ	V_{25}	V_{50}	V_{100}	V_{200}	V_{P25}	V_{P50}	σ_{PV}	V_{P100}	V_{P200}
Edirne	-0.69	0.25	0.39	0.15	7.47	9.22	10.98	12.73	13.17	14.92	0.41	16.68	18.43
Larissa	0.29	0.20	0.51	0.13	6.60	7.95	9.31	10.67	11.01	12.36	0.35	13.72	15.08
Plovdiv	-20.90	0.40	0.06	0.20	36.34	48.67	60.99	73.32	76.36	88.69	0.60	101.01	113.34
Pristina	-0.02	0.11	0.81	0.07	3.94	4.80	5.65	6.51	6.72	7.57	0.18	8.43	9.28
Skopje	-1.13	0.10	0.27	0.07	10.98	13.59	16.19	18.80	19.45	22.05	0.15	24.66	27.27
Sofia	-2.83	0.28	0.21	0.16	12.82	16.19	19.56	22.94	23.77	27.14	0.45	30.51	33.88
Thessaloniki	-1.88	0.22	0.16	0.14	18.54	22.94	27.33	31.73	32.81	37.21	0.38	41.61	46.00
Tirane	3.14	0.17	0.34	0.12	12.55	14.58	16.60	18.63	19.13	21.16	0.30	23.18	25.21

Table 5.15 Parameters (α, μ) and their uncertainties of a $G^{(I)}$ distribution for eight urban centres in the catalogued region. $V_{25,}$ $V_{50,}$ V_{100} and V_{200} are the maximum velocities expected in 25-, 50-, 100- and 200-year time intervals respectively. V_{P25}, V_{P50}, V_{P100} and V_{P200} are forecasts for ground velocities at 90% probability of non-exceedance in the time interval specified (a 1 in 10 chance of exceedance). Estimates are obtained using relation of using Theodulidis and Papazachos (1992) for stiff soil conditions (S = 0.5) at the 50^{th} percentile (P = 0). σ_{PA} is uncertainty on V_{P50} only. Velocities are given in cm s^{-1}. Estimates derived from the distribution of seismicity present within a 2° half-width cell of the city are given

5.5.6 Macroseismic intensity

An earthquake's epicentral intensity, $I_{0,}$ is akin to its magnitude as an alternative pseudo source parameter estimate. However, unlike magnitude, it can be applied to a known area to relate ground motions to observed physical and emotional effects of earthquakes. Many intensity ground motion models already discussed in section 3.8.1.3 take advantage of knowing I_0 to estimate macroseismic intensity at a known distance from the earthquake. This section assesses macroseismic intensity hazard of the Balkans through selected intensity laws and the third extreme distribution of Gumbel.

5.5.6.1 Evaluation of extreme distribution parameters

Being an alternative pseudo source parameter of earthquakes, epicentral intensities for each earthquake allows investigation using the approach described in section 5.3. Surface-wave magnitude estimates for each earthquake will be converted to I_0 estimates using Eq. (3-22). A very small number of previous studies (e.g. Orozova-Stanishkova and Slejko, 1994) have examined intensity hazard modelled with a $G^{(I)}$ distribution. Some seismic regions are better suited to this model due to the nature of their parent seismic distributions. Figure 5.33 illustrates $G^{(I)}$ and $G^{(III)}$ distributions applied to converted I_0 estimates for the catalogue, using a range of data scenarios (refer to figure caption for details). Each plot is also accompanied by estimates for the parameters and their uncertainties from the two statistical distributions used.

Macroseismic intensity is an integer scale. However intensity values may be interpolated notionally between points of known intensity and given decimal fractions if using ground motion models of the form of either Kövesligethy (1906) or Blake (1941). For this preparatory analysis, the resulting intensity estimates from the source surface-wave magnitude values will be stored both to one decimal place and rounded down to the next whole integer intensity value and investigated to see whether Gumbel's first or third distribution is better suited to model these data.

In response to Figure 5.33 (with particular emphasis on (d)), I_0 estimates rounded down to the next integer value will be retained and modelled using a $G^{(III)}$ distribution to determine fit-for-purpose values for extreme interval, epicentral intensity threshold (I_{CUT}) and catalogue start year to return stable estimates for ω, μ and λ. Figure 5.33(d) illustrates this configuration returns realistic ω – with respect to catalogue content – and smallest standard deviation on ω, with realistic μ and λ.

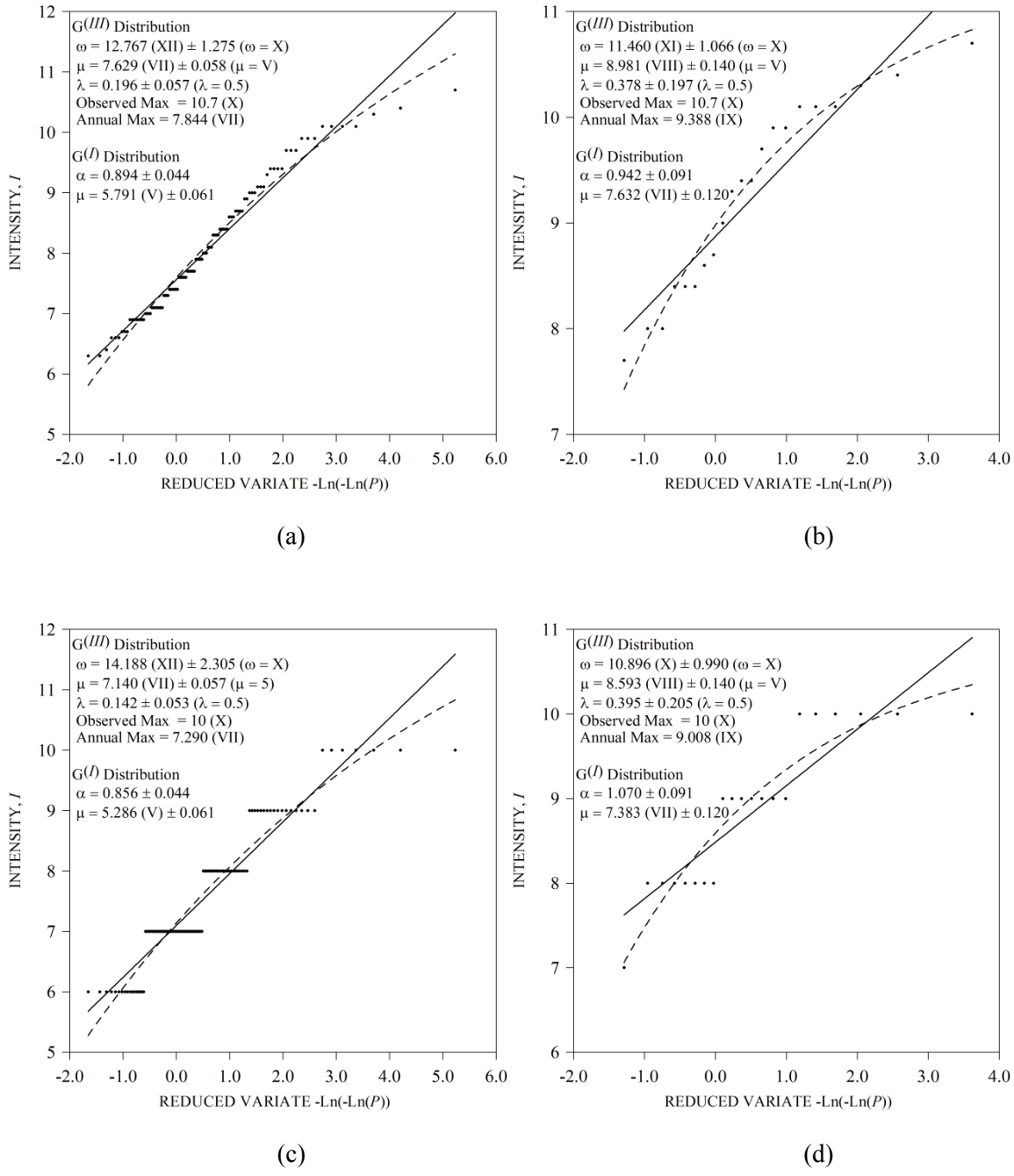

Figure 5.33 $G^{(I)}$ and $G^{(III)}$ distributions (solid and dashed lines respectively on each plot) for the full Balkan area using epicentral intensity estimates given to one decimal place and (a) 1-year extreme intervals, and (b) 5-year extreme intervals; using epicentral intensity estimates rounded down to the next integer value and (c) extreme intervals of and (c) 1-year extreme intervals, and (d) 5-year extreme intervals

5.5.6.2 Cumulative frequency-*intensity* modelling (Balkan extent)

Having determined the functional form of the epicentral intensity estimates to adopt for earthquakes in this catalogue, an indicative estimate for the catalogue's likely intensity threshold of completeness can be given in a similar fashion as used for magnitude completeness in section 4.10.1 by using a cumulative frequency-*intensity* distribution curve. These are shown in Figure 5.34 for the Balkan and southwest Bulgaria (cumulative frequency-*intensity* statistics for different values of I_{CUT} are given in Table 5.16). Both curves indicate data completeness tails off at intensities less than VI.

5.5.6.3 Variation in $G^{(III)}$ distribution parameters

The next stage to determining suitable intensity characteristics is defining the intensity threshold (using knowledge from section 5.5.6.2), extreme interval and start year of catalogue data. Figure 5.35 illustrates variability in $G^{(III)}$ distribution parameters while changing the same variables used on earthquake magnitude in section 5.3 for the full Balkan region. Where applicable the intensity threshold, $I_{CUT,}$ was set to IV, the minimum [computed] epicentral intensity of the catalogue.

- (a) shows change with variation in extreme interval applied for $I_{CUT} \geq$ VI

- (b) shows change with variation in I_{CUT} for 4-year extreme interval data

No plots of (ω, μ, λ) against start year have been given since a conscious decision was made to retain 1900 as the start year to ensure the 1904 and 1905 extreme events were incorporated into the analysis if the adopted extreme interval and intensity threshold permitted. ω begins to plateau using data of 4-yearly extreme intervals when I_{CUT} = VI (10.9 ± 0.8). By this cut-off intensity μ has stabilised to increase at a steady rate with constant σ_μ (8.3 ± 0.1) and λ, and acceptable σ_λ (0.41 ± 0.15). These patterns are also identical for I_{CUT} = VI (Figure 5.35(a)), and little change is seen after extreme intervals of 4 years when I_{CUT} = VII.

Figure 5.35(b) indicate realistic estimates for (ω, μ, λ) and uncertainties will be returned when I_{CUT} = VI, reinforcing evidence from Figure 5.34 that intensity completeness is around VI. Although a more realistic upper bound intensity is seen when I_{CUT} = VIII, uncertainty on the curvature parameter is more than double equivalent uncertainties at I_{CUT} = VI and VII. Increasing I_{CUT} to intensity VIII also reduces the number of earthquakes considered (from the full data set) by approximately 90%.

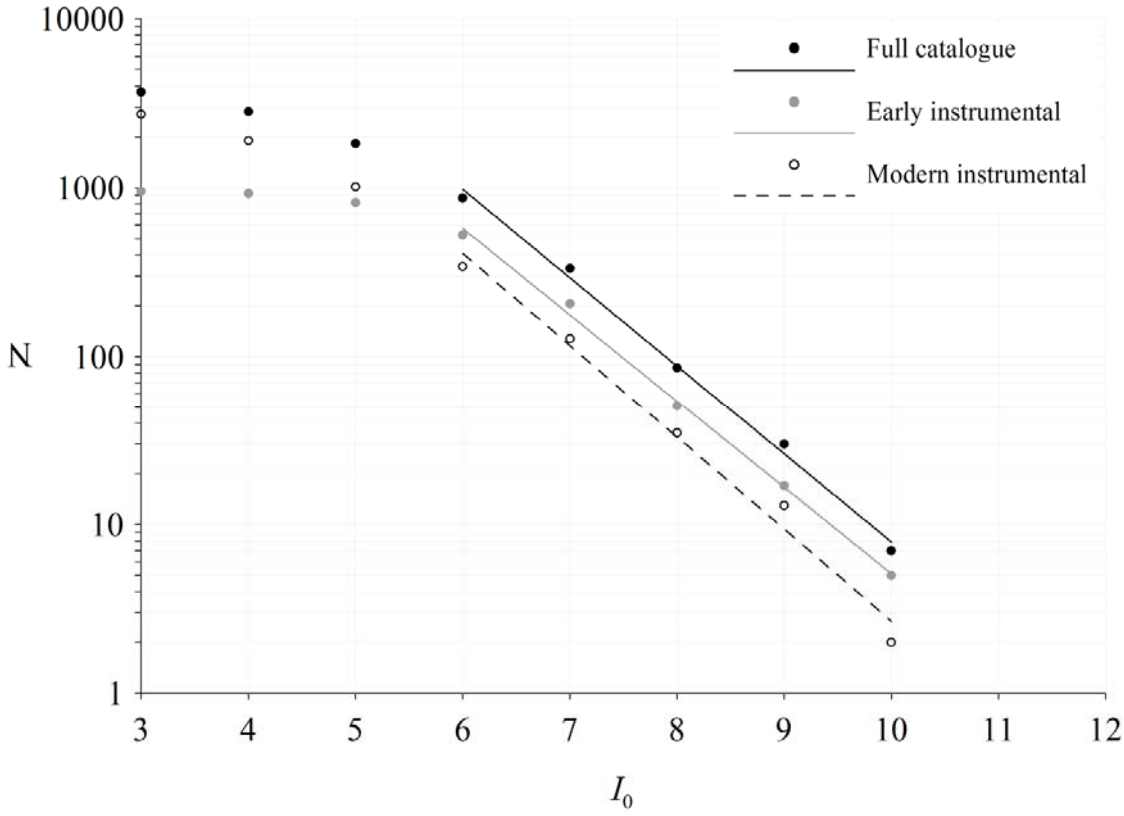

(a)

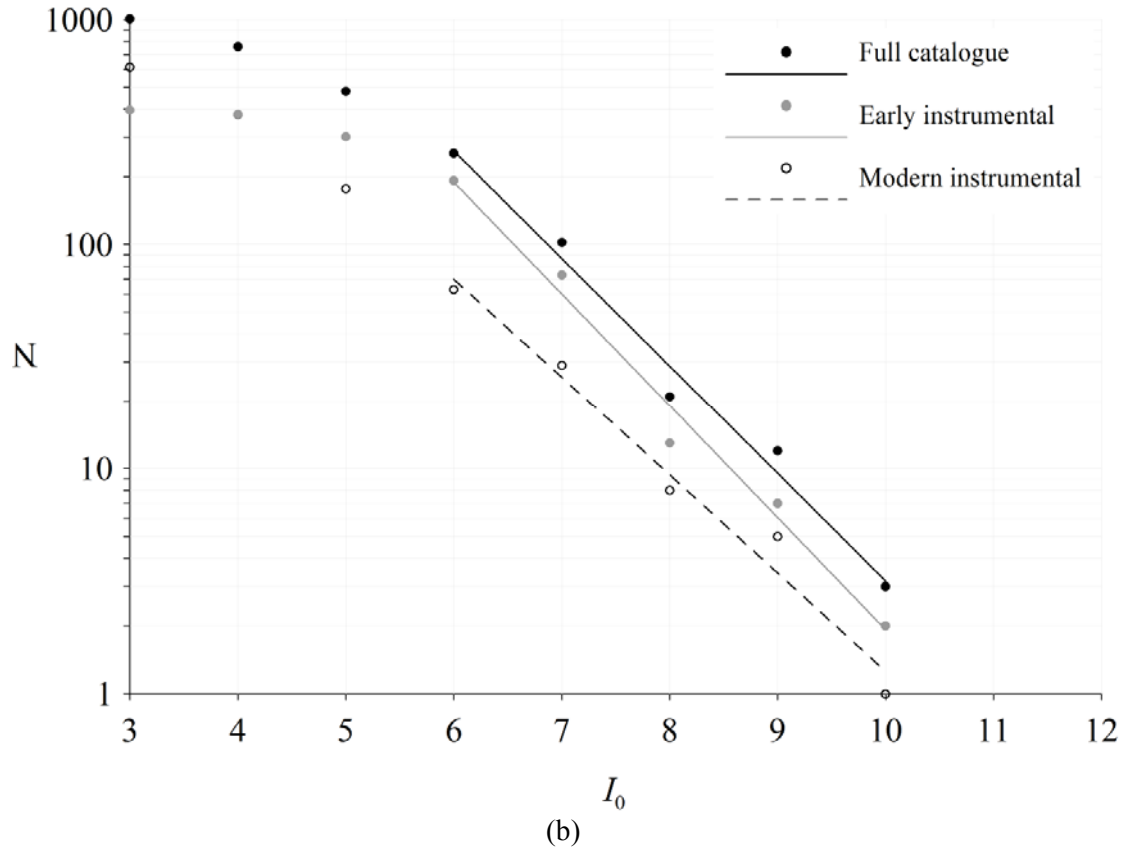

(b)

Figure 5.34 Cumulative frequency-intensity distribution curves for (a) the Balkans and (b) southwest Bulgaria. Lines of best fit are illustrated from the inferred lower limit of intensity completeness to the data maximum

Intensity threshold (I_{CUT})	a-value	b-value	Modal intensity	Comments
IV	III (3.5 ± 0.1)	0.473 (±0.01)	VII (7.3 ± 0.4)	Full unfiltered catalogue (3,681 events)
V	III (3.7 ± 0.1)	0.507 (±0.02)	VII (7.4 ± 0.5)	Full unfiltered catalogue (3,681 events)
VI	III (3.9 ± 0.1)	0.528 (±0.02)	VII (7.4 ± 0.9)	Full unfiltered catalogue (3,681 events)
VII	III (3.8 ± 0.3)	0.516 (±0.02)	VII (7.4 ± 0.9)	Full unfiltered catalogue (3,681 events)
VIII	-	-	-	Insufficient data
IX	-	-	-	Insufficient data
X	-	-	-	Insufficient data

Intensity threshold (I_{CUT})	a-value	b-value	Modal intensity	Comments
IV	II (2.7 ± 0.1)	0.436 (±0.01)	VI (6.2 ± 0.1)	Southwest Bulgaria unfiltered sub-catalogue (1,008 events)
V	II (2.9 ± 0.1)	0.465 (±0.02)	VI (6.3 ± 0.1)	Southwest Bulgaria unfiltered sub-catalogue (1,008 events)
VI	II (2.9 ± 0.2)	0.469 (±0.02)	VI (6.3 ± 0.1)	Southwest Bulgaria unfiltered sub-catalogue (1,008 events)
VII	II (2.5 ± 0.3)	0.410 (±0.04)	VI (6.0 ± 0.4)	Southwest Bulgaria unfiltered sub-catalogue (1,008 events)
VIII	-	-	-	Insufficient data
IX	-	-	-	Insufficient data
X	-	-	-	Insufficient data

Table 5.16 Cumulative frequency-intensity distribution statistics for integer intensity values derived from applying Eq. (3-22) to surface-wave magnitude estimates of each earthquake. Statistics are developed using least squares method of fitting for (a) the full Balkan extent and (b) southwest Bulgaria (a-values are given to one decimal place)

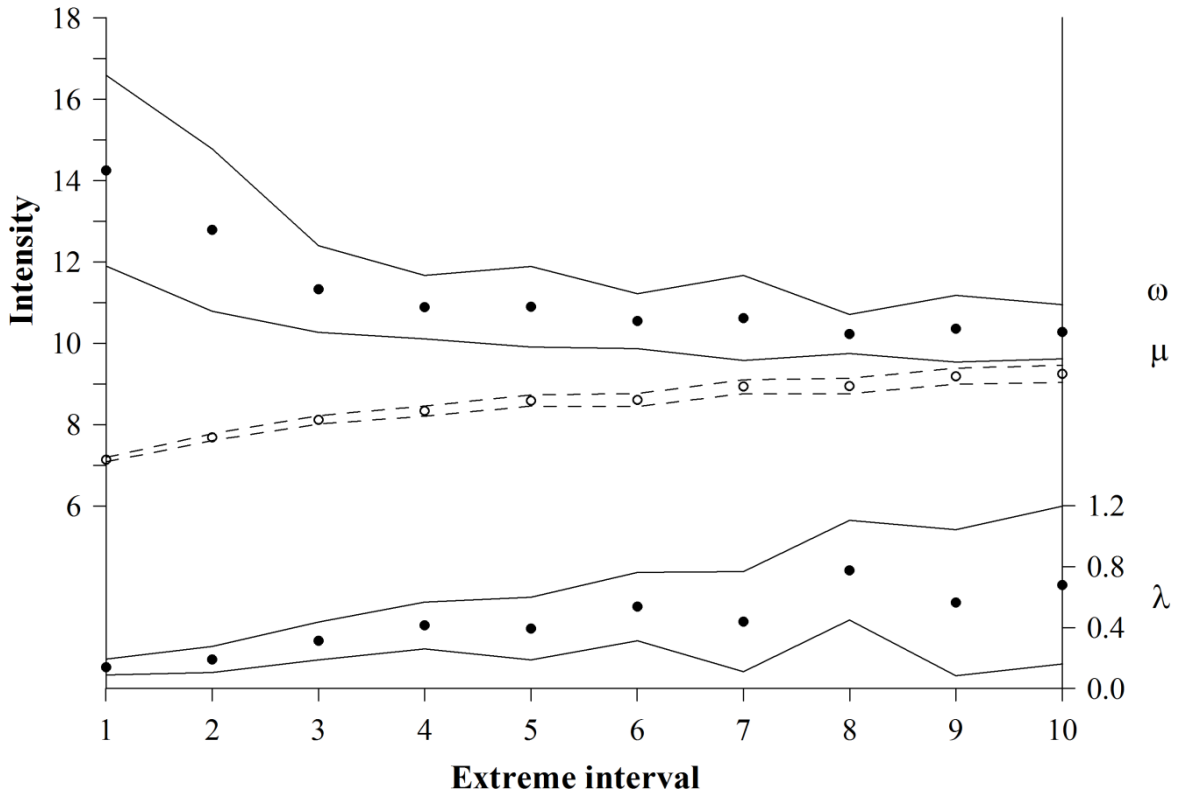

(a)

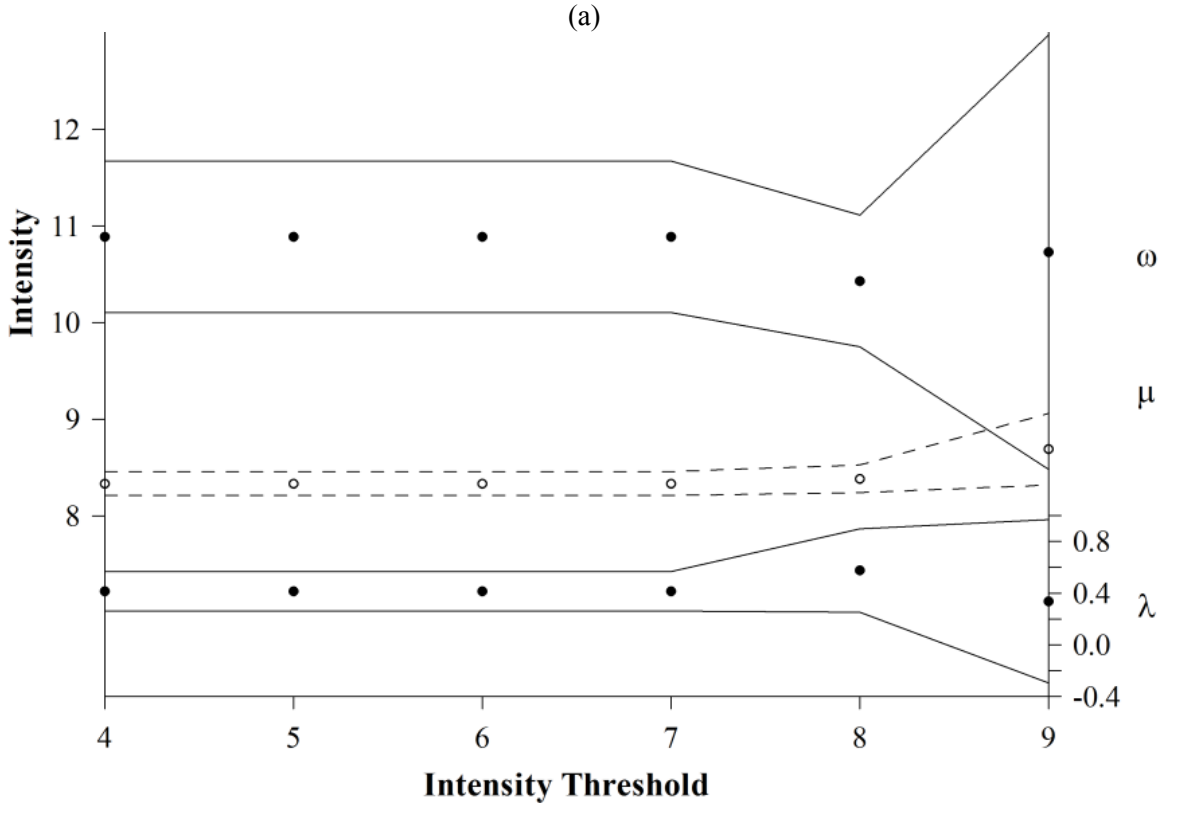

(b)

Figure 5.35 Variation in parameters of a $G^{(III)}$ distribution for the Balkans with variation in (a) interval using data with $I_{CUT} \geq$ VI, (b) epicentral intensity threshold using data of 4-year extreme interval

Southwest Bulgaria statistics are in Figure 5.36. Extreme interval, I_{CUT}, and start year of data and parameter starting values for Gumbel's third distribution for both areas are in Table 5.17.

	The Balkans	Southwest Bulgaria
Statistical distribution	$G^{(III)}$	$G^{(III)}$
Analysis cell half-width (°)	2	2
I_{CUT} (I)	VI	VIII
NPER (years)	4	5
Start year	1900	1900
ω_{START}	XI	XI
μ_{START}	V	V
λ_{START}	0.5	0.5

Table 5.17 Final catalogue parameters for $G^{(III)}$ distribution starting values for intensity hazard

5.5.6.4 Selecting the starting value for ω

As intensity in an accepted integer scale, it is fair to assume ω's starting value will also take this form. As the maximum [converted and homogenized] epicentral intensity in the adopted catalogue is X, ω_{START} could also realistically be set at XI. However, due to the iterative nature of the hazard forecasting programs used, it is possible to set ω_{START} to 10.1. Both scenarios were tested to determine the correct value for ω_{START} (integer or decimal) to adopt for analytical purposes, along with the integer-based catalogue selected in section 5.5.6.1. Selected responses (e.g. 50-year modal (I_{50}) and 50-year modal at 90% pnbe (I_{P50})) to this specific variation in ω_{START} are in Table 5.18.

	ω_{START} = XI					ω_{START} = 10.1				
City	ω	σ_ω	I_{50}	I_{P50}	X^2	ω	σ_ω	I_{50}	I_{P50}	X^2
Edirne	10.1	0.6	10.1	10.1	0.6	11.0	1.3	11.0	11.0	1.3
Larissa	10.0	0.9	9.9	10.0	0.5	11.0	1.0	10.8	10.9	1.0
Plovdiv	10.4	1.1	10.3	10.3	0.4	11.4	0.9	11.4	11.4	0.9
Pristina	10.5	0.9	9.4	9.8	0.4	11.6	0.8	10.0	10.7	0.8
Skopje	11.0	1.2	9.4	10.0	0.4	15.5	0.7	10.2	11.7	0.7
Sofia	11.2	1.2	10.6	10.9	1.1	12.7	2.3	11.7	12.2	2.3
Thessaloniki	10.4	0.7	10.3	10.4	0.7	11.5	1.3	11.3	11.4	1.3
Tirane	9.4	0.4	9.0	9.2	0.4	10.0	0.8	9.4	9.7	0.8

Table 5.18 Responses to different values for ω_{START} when forecasting intensity recurrence hazard

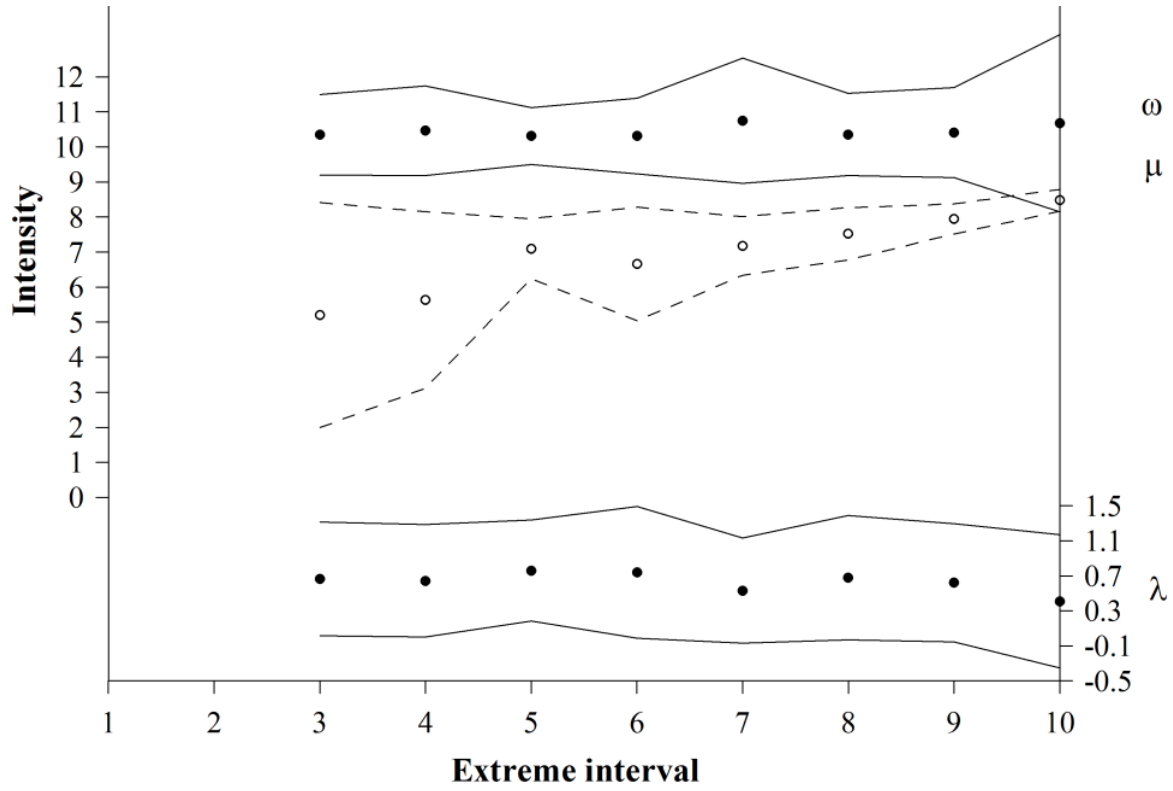

(a)

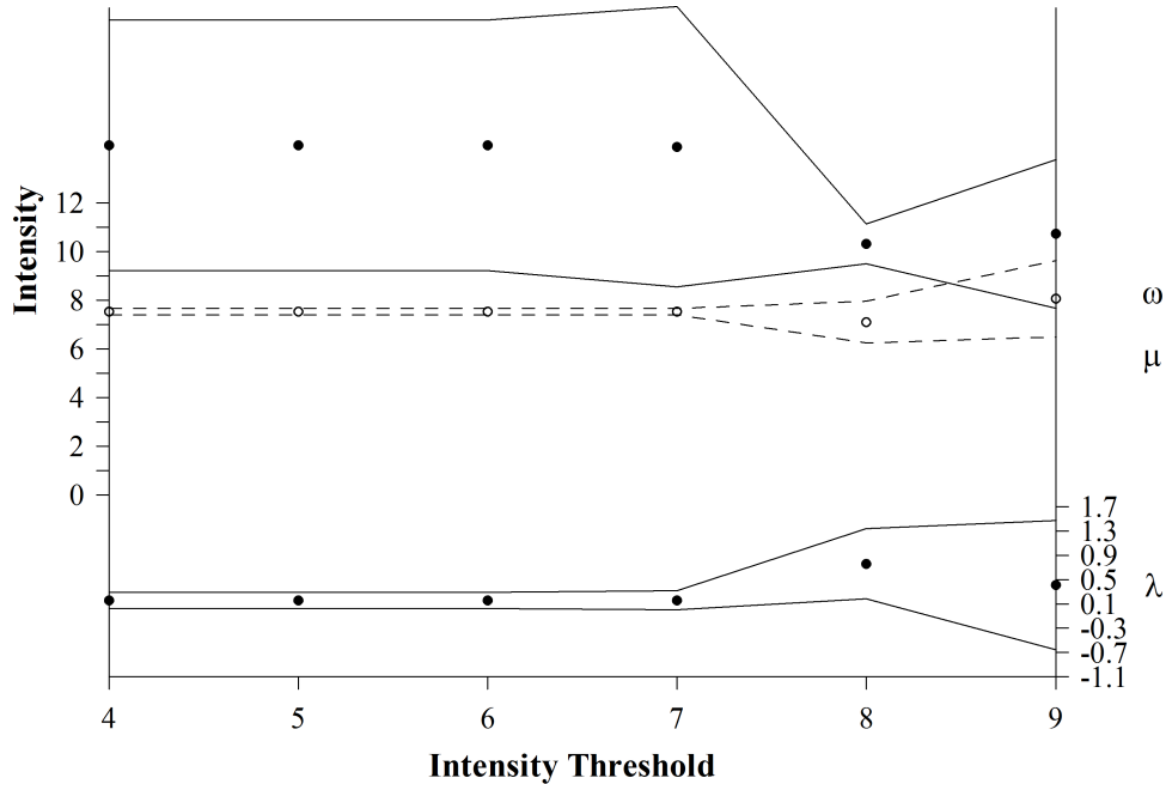

(b)

Figure 5.36 Variation in parameters of a $G^{(III)}$ distribution for southwest Bulgaria with variation in (a) extreme interval using data with $I_{CUT} \geq$ VIII, (b) intensity threshold using data with 5-year extreme interval

It is immediately evident from Table 5.18 that adopting ω_{START} = 10.1 returns more unrealistic estimates than when ω_{START} = XI. All return period forecasts for the urban centres are higher using ω_{START} = 10.1 than ω_{START} = XI. In absolute terms this equates to increases of between 0.4 and 2.1 intensity points, equating to as much as a 21% increase. Plovdiv, Skopje and Sofia habitually return the highest differences in hazard estimates between the two conditions, with estimates for the latter two cities exceeding the intensity range. Similarly, ω is higher by 0.6 to 4.5 intensity points (7 to 41%) – as is X^2 – for all cities considered.

Interestingly however, hazard and distribution parameter estimates for both geographic regions considered are quite similar. Little significant change is seen in the distribution parameters when changing ω_{START} from XI (11) to 10.1 for either considered geographic extent, and consequently, little significant change to the individual elements to each covariance matrix, ε (below).

$$\varepsilon = \begin{bmatrix} 0.462 & -0.015 & -0.142 \\ -0.015 & 0.021 & 0.002 \\ -0.142 & 0.002 & 0.050 \end{bmatrix} \qquad \varepsilon = \begin{bmatrix} 0.657 & 0.448 & -0.300 \\ 0.448 & 0.734 & -0.296 \\ -0.300 & -0.296 & 0.163 \end{bmatrix}$$

Full Balkan extent **Southwest Bulgaria**

Further, little variation is observed in the 50-year modal (I_{50}) and 50-year modal at 90% pnbe (I_{P50}) extreme intensity hazard, with only marginally lower hazard in isolated areas (decreasing from I = XI to I = X) over the north Aegean.

These significant and adverse changes (e.g. exceeding the intensity scale's acknowledged upper limits) in estimates for the distribution's upper bound magnitude, ω, for all cities cannot support changing approach to adopting ω_{START} = 10.1.

Similarly, changes for all annual modal and return period modal values, and increases for X^2 for all cities when ω_{START} = 10.1, go further to support the recommendation not to alter ω_{START} from XI (11).

Lower values for $\sigma^2_{\omega\lambda}$ across the north Adriatic Sea and Albanian coast are not on their own enough to justify adopting ω_{START} = 10.1 for forecasting extreme intensity hazard. This area is a great distance from the main areas of interest (Bulgaria and the southwest political triple junction).

5.5.6.5 Site-specific extreme distribution intensity parameterisation

The site-specific sensitivity analysis for the third distribution's parameters was repeated on computed estimates for epicentral intensity. Values for the extreme interval, NPER, and the threshold to epicentral intensity, I_{CUT}, adopted for each city considered are given in Table 5.19.

City	NPER (years)	Start year	I_{CUT}
Edirne	10	1900	VII
Larissa	9	1900	IV
Plovdiv	7	1900	VIII
Pristina	2	1900	V
Skopje	1	1900	VI
Sofia	8	1900	IV
Thessaloniki	8	1900	IV
Tirane	1	1900	IV

Table 5.19 Site-specific $G^{(III)}$ distribution parameterisation for urban centres for which intensity seismic hazard will be considered

5.5.6.6 Macroseismic intensity hazard

The $G^{(III)}$ distribution along with estimates for (ω, μ, λ) and associated uncertainties resulting from catalogued intensity extremes extracted after adopting criteria from Table 5.17 with integer intensity values for the Balkan extent is shown in Figure 5.37(a).

Macroseismic intensity hazard for the broad Balkan region is contoured in Figure 5.38 and Figure 5.39 (at 90% pnbe), applying the same '*moving cell*' approach adopted for magnitude recurrence, PGA and PGV hazard earlier in this chapter. Underlying statistics to these are given in Appendix 13. Immediately it is apparent that sufficient extreme intensity values exist above the adopted threshold of VI (with 4-yearly extreme intervals) to forecast hazard levels across the entire region.

Areas of peak intensity hazard loosely follow those of magnitude hazard, with lower peak intensities forecast to the west of the region, where generally $I <$ XI for the 50-year modal intensity (I_{50}), than the centre and eastern extent ($I >$ XI). The northern reaches are also forecast lower intensity hazard for this time interval. For 50-year return periods (I_{50}; Figure 5.38(a)) Bulgaria is dominated by intensity X. As the return period lengthens to 200 years (I_{200}; Figure 5.38(c)), intensity contours migrate westwards, creating an intensity '*high*' of $I >$ XII over the south central and south east part of the region, covering the southern half of Bulgaria, eastern Greece and western Turkey.

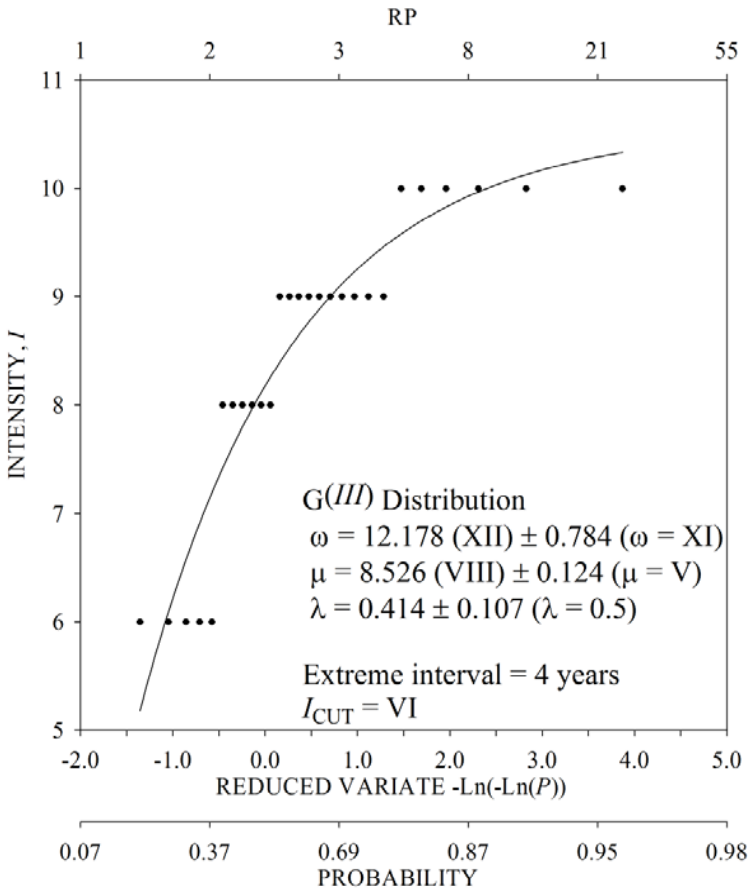

$$\varepsilon = \begin{bmatrix} 0.614 & -0.051 & -0.080 \\ -0.051 & 0.015 & 0.008 \\ -0.080 & 0.008 & 0.012 \end{bmatrix}$$

(a)

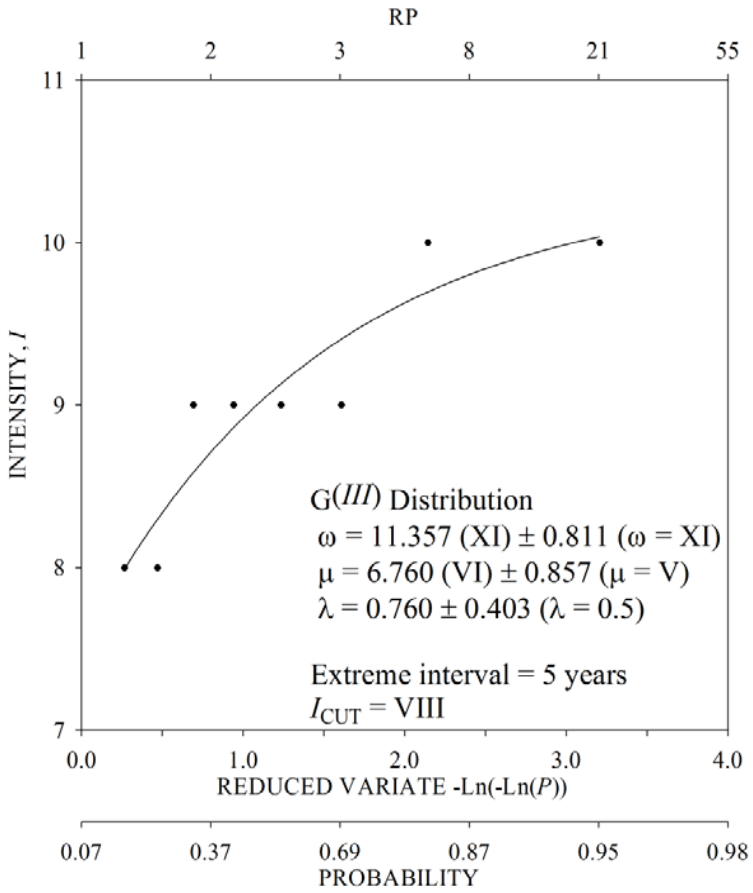

$$\varepsilon = \begin{bmatrix} 0.576 & 0.094 & -0.310 \\ 0.094 & 0.101 & -0.084 \\ -0.310 & -0.084 & 0.197 \end{bmatrix}$$

(b)

Figure 5.37 Gumbel's third extreme distribution fitted to final extreme intensity data and covariance error matrix, ε, for (a) the Balkans and (b) southwest Bulgaria

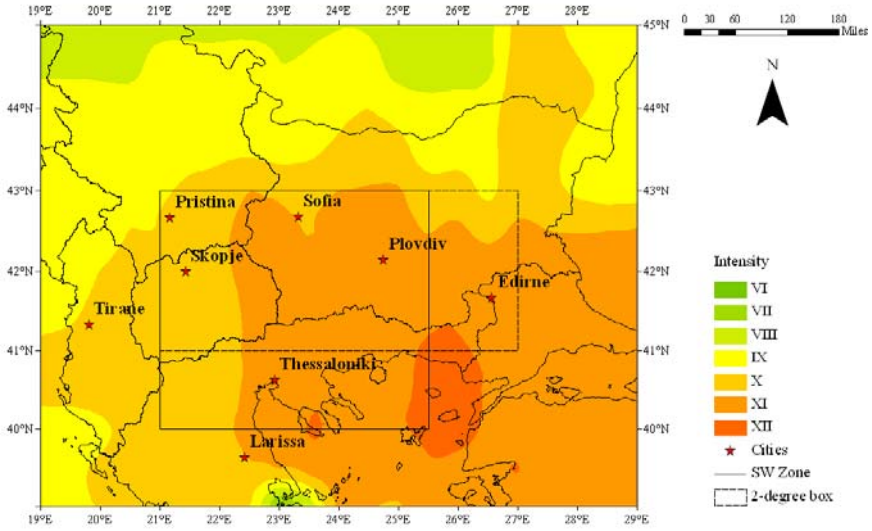

(a)

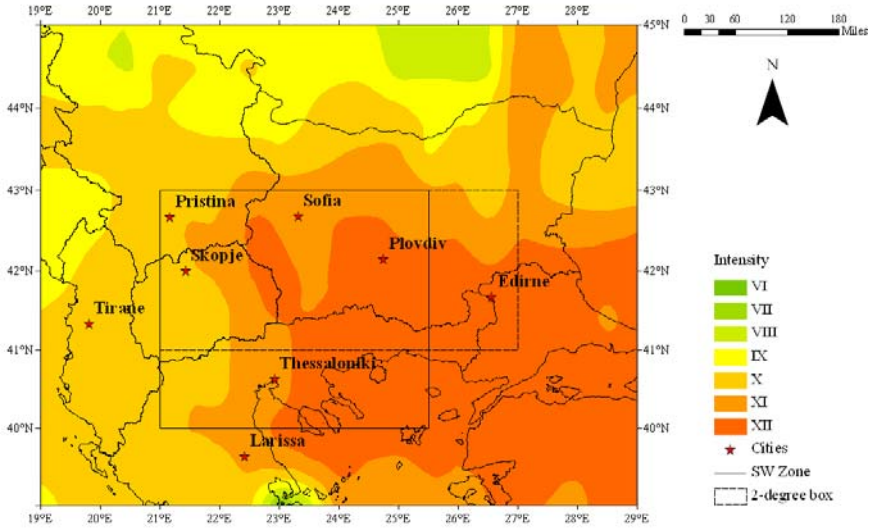

(b)

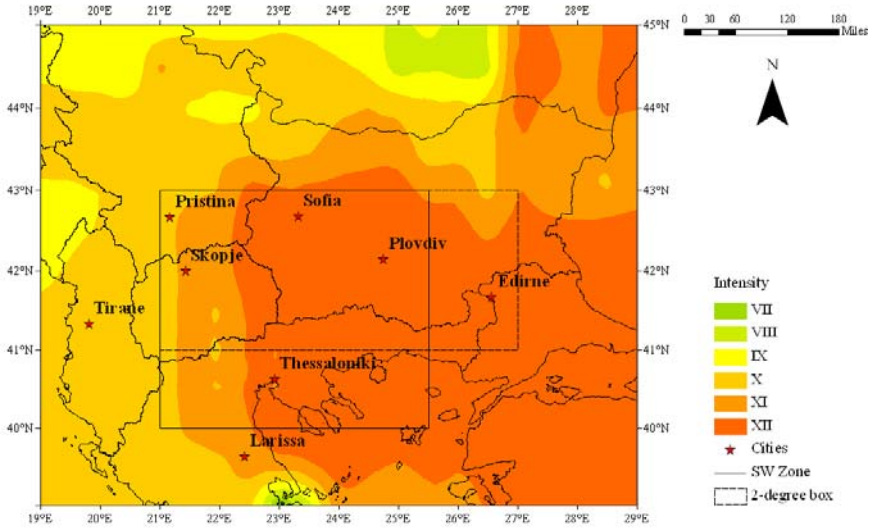

(c)

Figure 5.38 The highest intensities expected in (a) 50, (b) 100 and (c) 200 years using Papazachos and Papaioannou (1997). Contours are at single intensity intervals

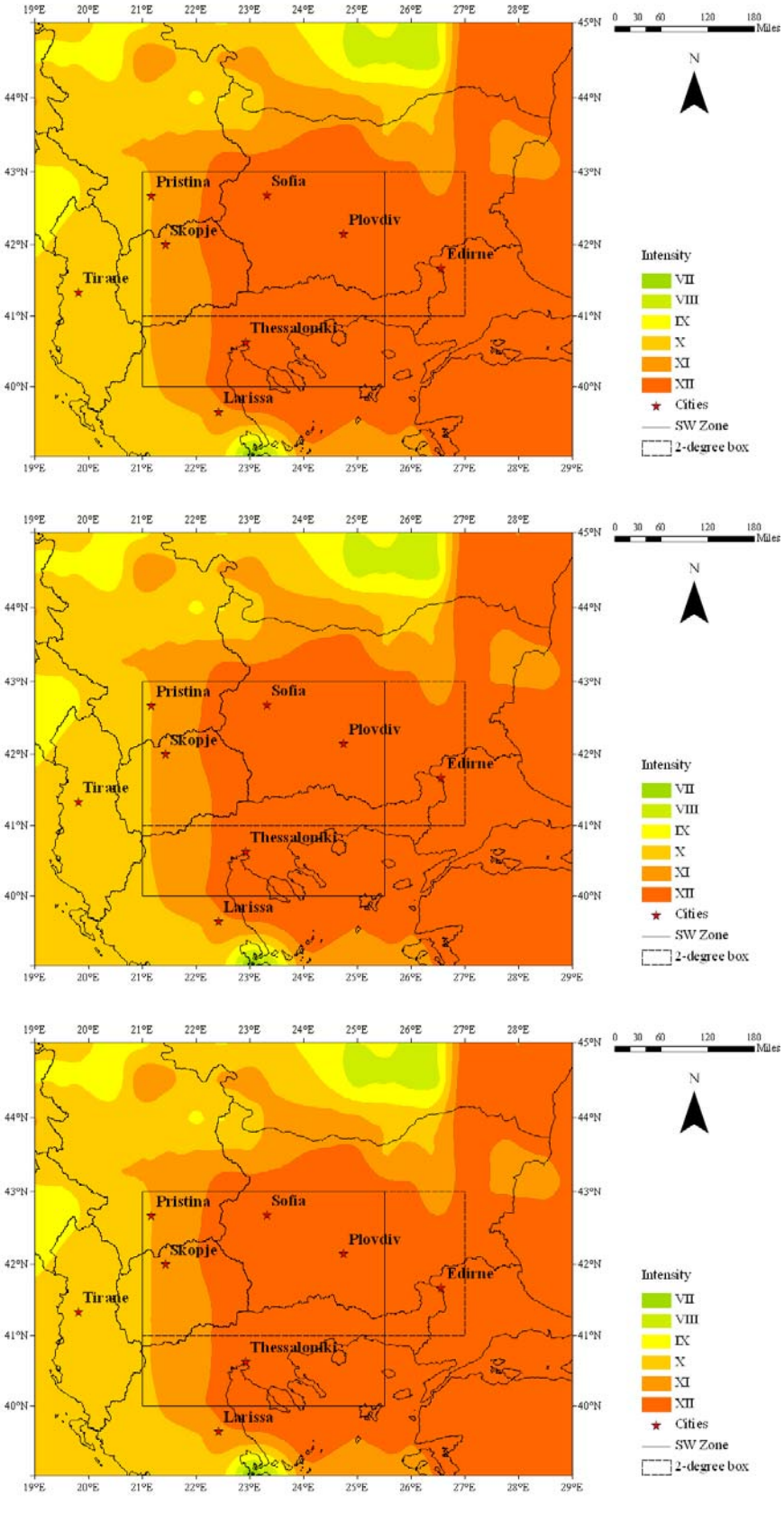

Figure 5.39 Intensities expected in (a) 50, (b) 100 and (c) 200 years with 90% pnbe (a 1 in 10 chance of being exceeded) by Papazachos and Papaioannou (1997). Contours at single intensity intervals

A lot of this zone of high intensity hazard is found outside the central zone where an entire analysis cell's extent is contained within the study region considered. Thus, this peak intensity of XII may in part be due to '*edge*' effects experienced and the inflated values σ_ω and $\sigma^2_{\omega\lambda}$ this may bring. For a 200-year return period (I_{200}), the majority of this region is forecast peak intensities of X or more. The far eastern edge of this intensity X contour is noticeably aseismic along the coast of the Black Sea (Figure 4.14), and suggests analysis cells in this region will be forecast unrepresentative peak intensities with large uncertainties, as their forecasts will not be constrained by as many observed historical extreme intensities as cells nearer the centre of the region. This appears to be the case, with $13.4 \leq \omega \leq 26.1$ and $1.6 \leq \sigma_\omega \leq 51.2$ for analysis cells in the area 41°N-43°N, 27°E-29°E.

The southwest Bulgarian sub region is dominated by peak intensities of XI for all return periods and probabilities of exceedance considered. Hazard contour patterns vary little through return periods considered; suggesting intensity hazard has a degree of 'stationarity' in this area. Further, no hazard map is forecast intensity hazard of <IX, which is likely a result of the high intensity threshold, I_{CUT}, adopted to epicentral intensity data in the first instance (Table 5.17). Hazard forecasts are also restricted to the area bounded by the meridians at 21.5°E and 24.0°E. Again this is most likely due to I_{CUT} being set at VIII.

The 475-year return period measurement for intensity (Figure 5.39(a)) peaks at I > XII covering the majority between 22.0°E-29.0°E, 39.0°N-43.5°N (i.e. the majority of Bulgaria) and slightly enlarged on that of the 200-year maximum forecast. Forecasting 200 years at 90% pnbe (I_{P200}) sees the intensity XI contour expand over the more northerly triple junction area between the FYR of Macedonia, Bulgaria and Serbia extending west to Skopje and Pristina.

The first order standard deviation of ω is between 0.4 (23.0°E, 39.5°N) and 243.3 (28.5°E, 44.0°/44.5°/45.0°N). Unsurprisingly the cell with the highest σ_ω is also that with the lowest curvature parameter, λ (0.04), and consequently the highest (that is, lowest negative) $\sigma^2_{\omega\lambda}$ of -59.0. Geographically, these cells are situated in the far northeast of the region, and are within a zone forecast with ω in excess of XII. This area is notable by an absence of retained extreme intensities in the immediate vicinity to constrain final extreme intensity forecasts. These three cells are also attached with the highest upper bound intensity estimate, ω, of 49.3. Covariance error matrices for each analysis cell used to contour regional intensity hazard are given in Appendix 14.

ω for regional intensity hazard is contoured in Figure 5.40(b), and it is immediately apparent how variation in $\sigma^2_{\omega\lambda}$ is governed by variation in ω. Both Figure 5.40(a) and (b) broadly adhere to the same contour patterns with highest estimates for ω generally found where higher [negative] $\sigma^2_{\omega\lambda}$ are found. Lower [negative] $\sigma^2_{\omega\lambda}$ are found towards the centre of the mapped area in north Greece, the Aegean extent, Albania and western Turkey; typically where higher seismicity – above the I_{CUT} value of VI – is most apparent. Certainly the denser distributions of lower intensity historical earthquakes (in the range considered) are predominantly found in areas where ω is forecast less than XII, and return period forecasts are within the bounds of the intensity scale. This suggests these moderate intensity earthquakes (VI and VII) – notably those intensities associated with the onset of damage and damage to reinforced structures respectively – help constrain distribution parameters to a greater degree.

Intensity hazard for the trans-frontier border region between FYROM, Greece and Bulgaria is shown in Figure 5.41 (and Appendix 15), with the $G^{(III)}$ distribution resulting from criteria of Table 5.17 given in Figure 5.37(b) and associated error matrices for each analysis cell given in Figure 5.40. Much of the zone is dominated by intensity XI at all return periods and probability levels of exceedance. All illustrations to Figure 5.41 are dominated by highest peak intensities in the northwest over southern Serbia and its border with the FYR of Macedonia.

The region immediately surrounding Sofia is forecast to be subject to [interpolated] peak intensities greater than XI in 50 years (maximum and at 90% pnbe). Orozova-Stanishkova and Slejko (1994) estimate lower values to intensity hazard for southwest Bulgaria, with the region surrounding Sofia subject to VII → VIII in 100 years using the three alternative methods of a $G^{(I)}$ distribution, $G^{(III)}$ distribution and using the envelopes of isointensity lines. Simeonova *et al.* (2006) forecast the 475-year return period intensity for the same area to be in the range I_{P50} = 7.5 → 8.5 (using the MSK-1964 scale). Forecasts are slightly up on estimates for intensity hazard to Sofia of Slavov *et al.* (2004), who assess specifically intensity hazard to Sofia.

Some previous studies also forecast intensity hazard of up to X for the region surrounding Sofia (Bončev *et al.* 1982; Stanishkova and Slejko, 1991; Solakov *et al.*, 2001). The main difference to be aware of between many of these studies and this is that intensities are forecast here by adopting an entirely statistical extreme values approach. Most previous studies (e.g. Simeonova *et al.*, 2006; Leydecker *et al.*, 2008) adopt more deterministic approaches reliant on approaches of Cornell (1968) and McGuire (1976) or other deterministic-orientated methods to incorporate knowledge of regional faulting systems and tectonics.

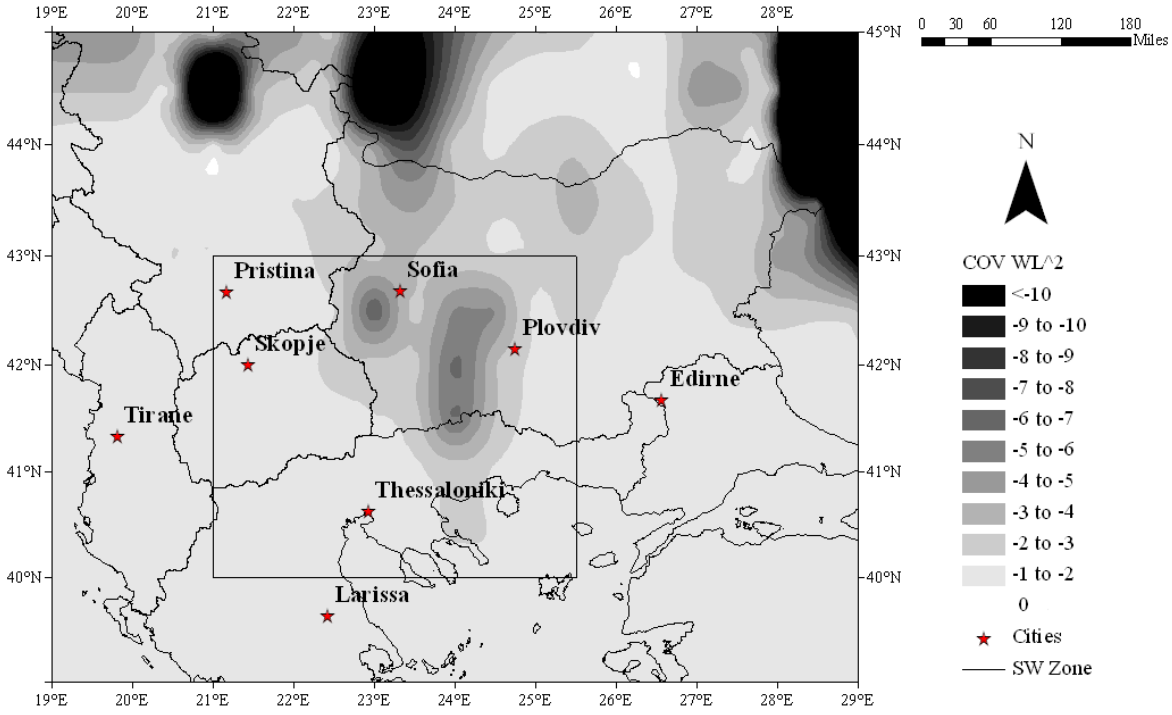

(a)

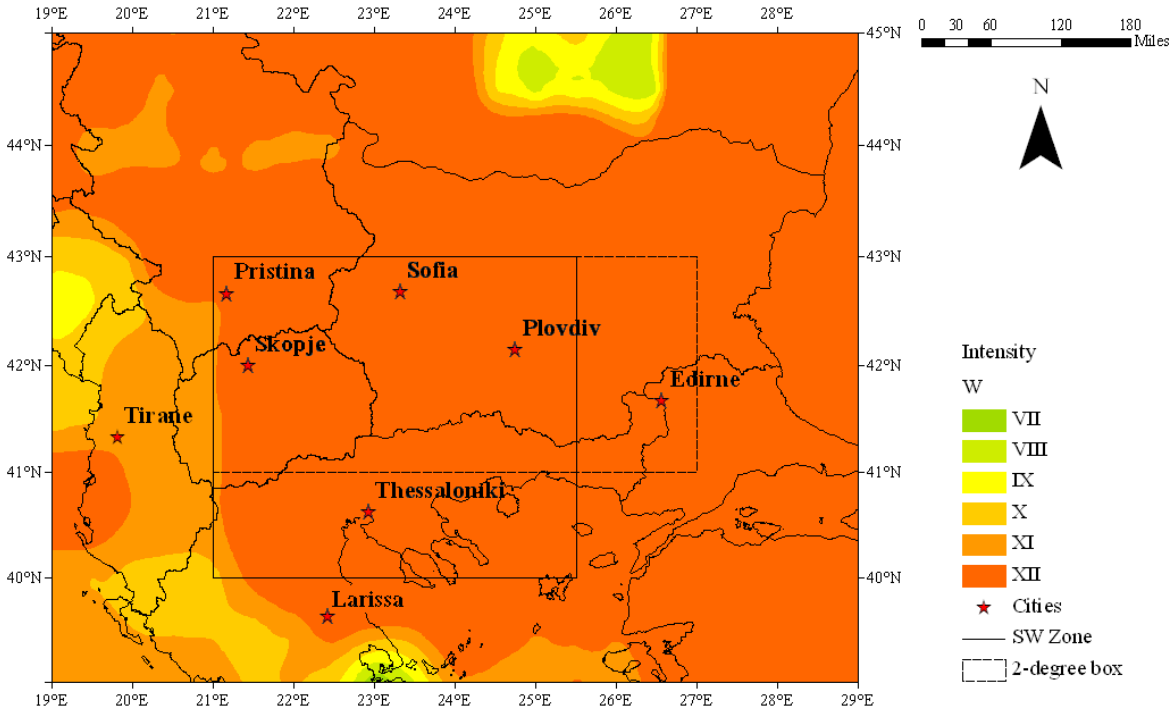

(b)

Figure 5.40 Covariance between ω and λ ($\sigma^2_{\omega\lambda}$) from error matrix ε of Gumbel's third distribution (all contours to (a) are at intervals of 1 unit up to -10); (b) the upper bound intensity, ω, of Gumbel's third extreme distribution for the broad Balkan region (all contours to (b) are at intervals of 1. Intensity contours above the acknowledged upper limit to intensity scales are classified as intensity XII)

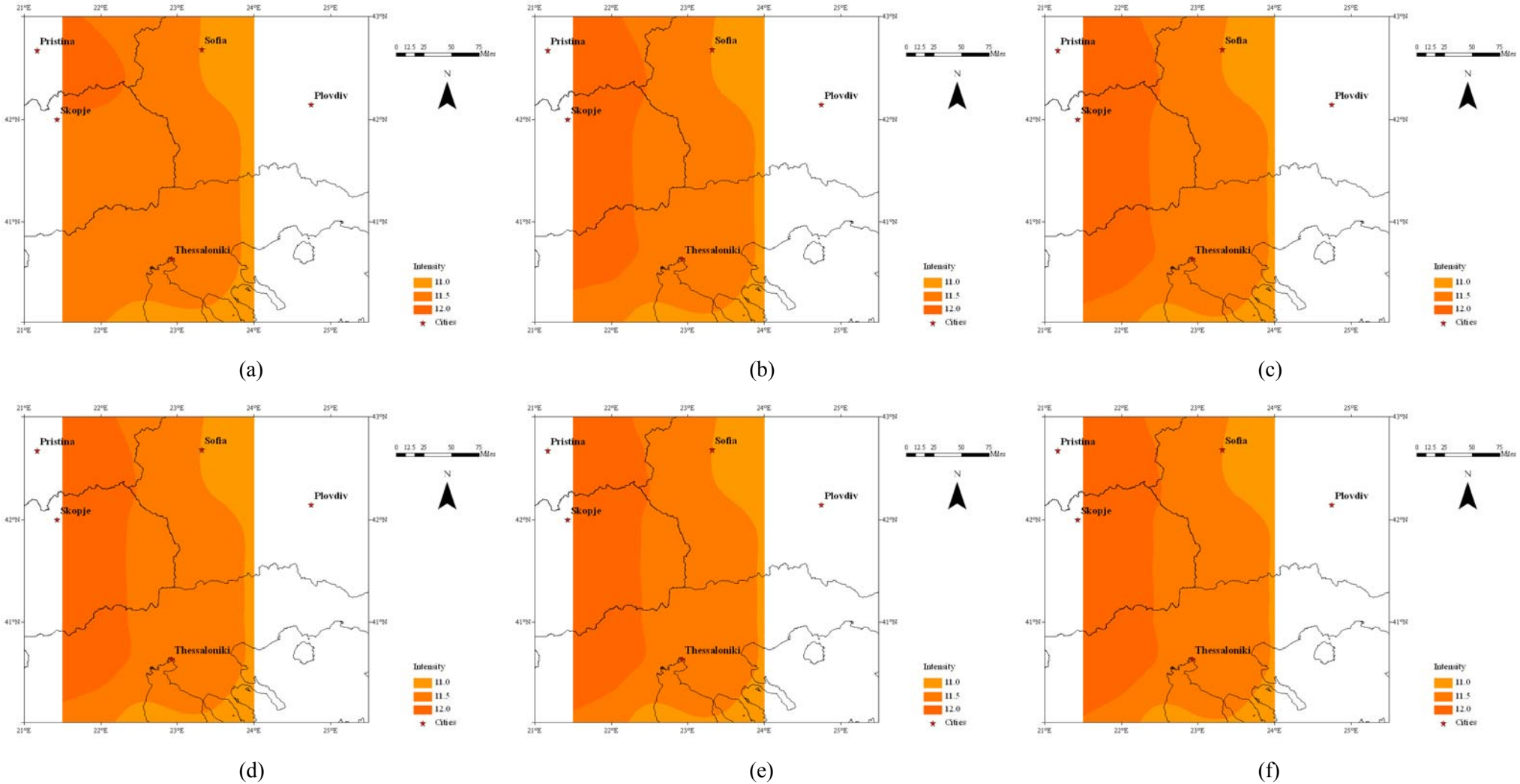

Figure 5.41 Macroseismic intensity hazard in southwest Bulgaria in (a) 50, (b) 100 and (c) 200 years and (d) 50, (e) 100 and (f) 200 years with 90% probability of not being exceeded (a 1 in 10 chance of being exceeded). Forecasts are obtained using Papazachos and Papaioannou (1997). Contours are at half-intensity intervals

21.0°E	21.5°E	22.0°E	22.5°E	23.0°E
---	$\begin{bmatrix} 0.639 & 3.023 & -0.363 \\ 3.023 & 24.783 & -2.445 \\ -0.363 & -2.445 & 0.261 \end{bmatrix}$	$\begin{bmatrix} 0.639 & 3.023 & -0.363 \\ 3.023 & 24.783 & -2.445 \\ -0.363 & -2.445 & 0.261 \end{bmatrix}$	---	---
---	$\begin{bmatrix} 3.402 & 4.307 & -0.825 \\ 4.307 & 7.669 & -1.224 \\ -0.825 & -1.224 & 0.216 \end{bmatrix}$	$\begin{bmatrix} 3.402 & 4.307 & -0.825 \\ 4.307 & 7.669 & -1.224 \\ -0.825 & -1.224 & 0.216 \end{bmatrix}$	$\begin{bmatrix} 0.635 & 1.760 & -0.333 \\ 1.760 & 8.875 & -1.312 \\ -0.333 & -1.312 & 0.217 \end{bmatrix}$	$\begin{bmatrix} 0.635 & 1.760 & -0.333 \\ 1.760 & 8.875 & -1.312 \\ -0.333 & -1.312 & 0.217 \end{bmatrix}$
---	$\begin{bmatrix} 2.367 & 2.461 & -0.656 \\ 2.461 & 3.923 & -0.827 \\ -0.656 & -0.827 & 0.200 \end{bmatrix}$	$\begin{bmatrix} 2.367 & 2.461 & -0.656 \\ 2.461 & 3.923 & -0.827 \\ -0.656 & -0.827 & 0.200 \end{bmatrix}$	$\begin{bmatrix} 0.643 & 1.087 & -0.318 \\ 1.087 & 3.561 & -0.765 \\ -0.318 & -0.765 & 0.192 \end{bmatrix}$	$\begin{bmatrix} 0.635 & 0.689 & -0.304 \\ 0.689 & 1.587 & -0.474 \\ -0.304 & -0.474 & 0.176 \end{bmatrix}$
---	$\begin{bmatrix} 2.367 & 2.461 & -0.656 \\ 2.461 & 3.923 & -0.827 \\ -0.656 & -0.827 & 0.200 \end{bmatrix}$	$\begin{bmatrix} 2.367 & 2.461 & -0.656 \\ 2.461 & 3.923 & -0.827 \\ -0.656 & -0.827 & 0.200 \end{bmatrix}$	$\begin{bmatrix} 0.643 & 1.087 & -0.318 \\ 1.087 & 3.561 & -0.765 \\ -0.318 & -0.765 & 0.192 \end{bmatrix}$	$\begin{bmatrix} 0.635 & 0.689 & -0.304 \\ 0.689 & 1.587 & -0.474 \\ -0.304 & -0.474 & 0.176 \end{bmatrix}$
---	$\begin{bmatrix} 2.367 & 2.461 & -0.656 \\ 2.461 & 3.923 & -0.827 \\ -0.656 & -0.827 & 0.200 \end{bmatrix}$	$\begin{bmatrix} 2.367 & 2.461 & -0.656 \\ 2.461 & 3.923 & -0.827 \\ -0.656 & -0.827 & 0.200 \end{bmatrix}$	$\begin{bmatrix} 0.643 & 1.087 & -0.318 \\ 1.087 & 3.561 & -0.765 \\ -0.318 & -0.765 & 0.192 \end{bmatrix}$	$\begin{bmatrix} 0.635 & 0.689 & -0.304 \\ 0.689 & 1.587 & -0.474 \\ -0.304 & -0.474 & 0.176 \end{bmatrix}$
---	$\begin{bmatrix} 2.367 & 2.461 & -0.656 \\ 2.461 & 3.923 & -0.827 \\ -0.656 & -0.827 & 0.200 \end{bmatrix}$	$\begin{bmatrix} 2.367 & 2.461 & -0.656 \\ 2.461 & 3.923 & -0.827 \\ -0.656 & -0.827 & 0.200 \end{bmatrix}$	$\begin{bmatrix} 0.643 & 1.087 & -0.318 \\ 1.087 & 3.561 & -0.765 \\ -0.318 & -0.765 & 0.192 \end{bmatrix}$	$\begin{bmatrix} 0.635 & 0.689 & -0.304 \\ 0.689 & 1.587 & -0.474 \\ -0.304 & -0.474 & 0.176 \end{bmatrix}$
---	$\begin{bmatrix} 0.358 & 3.182 & -0.388 \\ 3.182 & 55.309 & -5.559 \\ -0.388 & -5.559 & 0.595 \end{bmatrix}$	$\begin{bmatrix} 0.454 & 1.706 & -0.410 \\ 1.706 & 12.433 & -2.337 \\ -0.410 & -2.337 & 0.486 \end{bmatrix}$	$\begin{bmatrix} 0.454 & 1.706 & -0.410 \\ 1.706 & 12.433 & -2.337 \\ -0.410 & -2.337 & 0.486 \end{bmatrix}$	$\begin{bmatrix} 0.358 & 3.182 & -0.388 \\ 3.182 & 55.309 & -5.559 \\ -0.388 & -5.559 & 0.595 \end{bmatrix}$

23.5°E	24.0°E	24.5°E	25.0°E	25.5°E
---	---	---	---	---
$\begin{bmatrix} 0.358 & 3.182 & -0.388 \\ 3.182 & 55.309 & -5.559 \\ -0.388 & -5.559 & 0.595 \end{bmatrix}$	$\begin{bmatrix} 0.358 & 3.182 & -0.388 \\ 3.182 & 55.309 & -5.559 \\ -0.388 & -5.559 & 0.595 \end{bmatrix}$	---	---	---
$\begin{bmatrix} 0.698 & 1.108 & -0.454 \\ 1.108 & 3.365 & -1.011 \\ -0.454 & -1.011 & 0.356 \end{bmatrix}$	$\begin{bmatrix} 0.454 & 1.706 & -0.410 \\ 1.706 & 12.433 & -2.337 \\ -0.410 & -2.337 & 0.486 \end{bmatrix}$	---	---	---
$\begin{bmatrix} 0.698 & 1.108 & -0.454 \\ 1.108 & 3.365 & -1.011 \\ -0.454 & -1.011 & 0.356 \end{bmatrix}$	$\begin{bmatrix} 0.454 & 1.706 & -0.410 \\ 1.706 & 12.433 & -2.337 \\ -0.410 & -2.337 & 0.486 \end{bmatrix}$	---	---	---
$\begin{bmatrix} 0.698 & 1.108 & -0.454 \\ 1.108 & 3.365 & -1.011 \\ -0.454 & -1.011 & 0.356 \end{bmatrix}$	$\begin{bmatrix} 0.454 & 1.706 & -0.410 \\ 1.706 & 12.433 & -2.337 \\ -0.410 & -2.337 & 0.486 \end{bmatrix}$	---	---	---
$\begin{bmatrix} 0.698 & 1.108 & -0.454 \\ 1.108 & 3.365 & -1.011 \\ -0.454 & -1.011 & 0.356 \end{bmatrix}$	$\begin{bmatrix} 0.454 & 1.706 & -0.410 \\ 1.706 & 12.433 & -2.337 \\ -0.410 & -2.337 & 0.486 \end{bmatrix}$	---	---	---
---	---	---	---	---

Figure 5.42 Macroseismic intensity covariance error matrices, ε, for southwest Bulgaria. For presentation purposes, the geographic area represented has been split into two halves between the 23.0°E and 23.5°E meridians. The rows of each table represent – from bottom to top – parallels 40.0°N to 43.0°N at 0.5° steps. Cells with '*null*' forecasts are also given. Matrix elements of ε are:

$$\varepsilon = \begin{bmatrix} \sigma_{\omega}^{2} & \sigma_{\omega\mu}^{2} & \sigma_{\lambda\omega}^{2} \\ \sigma_{\omega\mu}^{2} & \sigma_{\mu}^{2} & \sigma_{\lambda}^{2} \\ \sigma_{\omega\lambda}^{2} & \sigma_{\mu\lambda}^{2} & \sigma_{\lambda}^{2} \end{bmatrix}$$

Observed macroseismic intensities from both pre-instrumental and instrumental periods of recording also support forecasts made here for the immediate vicinity to Sofia (e.g. 1818, I = VIII – IX, MSK; 1858, ~6.5 M_s, I = IX → X, MSK-64; 4th April 1904, I = X and I = 9.5, MSK-64).

Site-specific intensity hazard estimates are given in Table 5.20 for the eight urban centres considered throughout chapter 5. Estimates can then both be considered and adopted in isolation or in tandem with regional or local extreme intensity hazard maps from which interpolated estimates may be derived. Occasionally this resolves the issue of '*null*' areas of hazard forecasting (section 5.5.1) if a city falls inside such an area.

Plovdiv, Skopje and Pristina are cities that fall outside areas of forecast intensity hazard on the local scale by adopting distribution and data settings that cannot constrain forecasts at this level. Site-specific estimates afford opportunity to attach realistic estimates to these cities. Plovdiv is forecast a realistic ω (X; 10.3) but is attached with a large uncertainty (σ_ω = 1.1). Skopje and Pristina are also attached with a high uncertainty of ~1.0. These align with contoured intensity hazard of Figure 5.41, as each city is located within areas of '*null'* forecasts to the extreme west and east of the considered area. The important covariance element of ε, $\sigma^2_{\omega\lambda}$, is also negative and large for Plovdiv (relative to the other cities), at -0.77, while σ_λ (σ_λ = 0.77) is comparable to λ (0.79).

All other cities are forecast ω of X or XI, which is consistent with contoured regional intensity hazard. Sofia, Plovdiv and Thessaloniki are consistently forecast highest *maximum* intensities of XI for all return periods considered. Skopje and Edirne are also consistently forecast some of the higher extreme return period estimates of these eight cities. Viewing

Figure **5.38** and Figure 5.39 show these cities are found within the zone of higher intensity hazard forecasts (of at least intensity X) even for the shortest return periods considered. Further, Figure 5.40 illustrates these particular cities are in areas estimated highest values for ω (typically outside the standard intensity scale), and higher [negative] $\sigma^2_{\omega\lambda}$. $G^{(III)}$ distribution curve and covariance error matrix are given for Sofia in Figure 5.43 to complete the site-specific hazard forecasting for this city, while Appendix 16 provides these for the other cities considered.

Tirane is systematically forecast lowest peak intensities regardless of whether forecasts are maximum expected or at 90% confidence levels for any return period considered, and is in keeping with this city being situated to the west of the considered broader extent, and the prevalence of lower intensity observed extremes in this area (i.e. no historical earthquake with an assigned epicentral intensity X occurred within 3 degrees during the catalogued time interval).

City	ω	σ_ω	μ	σ_μ	λ	σ_λ	$\sigma^2_{\omega\mu}$	$\sigma^2_{\omega\lambda}$	$\sigma^2_{\mu\lambda}$	X^2	NMISS	I_M
Edirne	X (10.0)	0.6	VIII (8.2)	0.2	0.866	0.416	-0.064	-0.214	0.058	0.646	1	X (10.0)
Larissa	X (10.0)	0.9	VIII (8.2)	0.2	0.542	0.327	-0.093	-0.267	0.042	0.475	0	X (10.0)
Plovdiv	X (10.3)	1.1	VI (6.5)	1.6	0.790	0.769	1.277	-0.768	-1.138	0.432	8	X (10.0)
Pristina	X (10.4)	0.9	VI (6.7)	0.1	0.291	0.087	-0.039	-0.080	0.004	0.410	0	X (10.0)
Skopje	XI (11.0)	1.2	VI (6.3)	0.1	0.248	0.082	0.002	-0.093	-0.001	0.350	17	X (10.0)
Sofia	XI (11.2)	1.2	VII (7.0)	0.2	0.413	0.143	-0.116	-0.165	0.015	1.108	0	X (10.0)
Thessaloniki	X (10.4)	0.7	VII (7.8)	0.2	0.590	0.189	-0.066	-0.121	0.023	0.657	0	X (10.0)
Tirane	IX (9.3)	0.4	VI (6.3)	0.1	0.445	0.074	-0.011	-0.027	0.002	0.402	5	IX (9.0)

City	I_A	I_{25}	I_{50}	I_{100}	I_{200}	σ_I	I_{P25}	I_{P50}	I_{P100}	I_{P200}	σ_{IP}	I_M
Edirne	IX (9.7)	X (10.0)	X (10.0)	X (10.0)	X (10.0)	0.5	X (10.0)	X (10.0)	X (10.0)	X (10.0)	0.6	X (10.0)
Larissa	VIII (8.8)	IX (9.8)	IX (9.9)	IX (9.9)	IX (9.9)	0.7	IX (9.9)	IX (9.9)	IX (9.9)	X (10.0)	0.8	X (10.0)
Plovdiv	IX (9.2)	X (10.2)	X (10.3)	X (10.3)	X (10.3)	1.9	X (10.3)	X (10.3)	X (10.3)	X (10.3)	1.1	X (10.0)
Pristina	VII (7.0)	IX (9.1)	IX (9.3)	IX (9.5)	IX (9.7)	0.6	IX (9.7)	IX (9.8)	IX (9.9)	X (10.0)	0.8	X (10.0)
Skopje	VI (6.6)	IX (9.0)	IX (9.3)	IX (9.6)	IX (9.8)	0.7	IX (9.8)	X (10.0)	X (10.1)	X (10.2)	0.9	X (10.0)
Sofia	VII (7.8)	X (10.3)	X (10.5)	X (10.7)	X (10.8)	0.9	X (10.7)	X (10.9)	X (10.9)	XI (11.0)	1.1	X (10.0)
Thessaloniki	VIII (8.8)	X (10.1)	X (10.2)	X (10.3)	X (10.3)	0.6	X (10.3)	X (10.3)	X (10.3)	X (10.3)	0.7	X (10.0)
Tirane	VII (7.0)	VIII (8.8)	VIII (8.9)	IX (9.0)	IX (9.1)	0.3	IX (9.1)	IX (9.1)	IX (9.2)	IX (9.2)	0.4	IX (9.0)

Table 5.20 Parameters (ω, μ, λ) and their associated uncertainties of a $G^{(III)}$ distribution for selected urban centres in the catalogued region. I_M is the maximum observed intensity and I_A is the annual modal [or most probable] maximum event in each cell of analysis. I_{25}, I_{50}, I_{100} and I_{200} are the modal maximum intensities expected in 25-, 50-, 100- and 200-year return periods respectively. I_{P25}, I_{P50}, I_{P100} and I_{P200} are forecasts for intensities at 90% probability of non-exceedance in the time interval specified (a 1 in 10 chance of exceedance). σ_P and σ_{IP} are the respective uncertainties of maximum forecasts and those at 90% confidence levels. $\sigma^2_{\omega\mu}$, $\sigma^2_{\omega\lambda}$ and $\sigma^2_{\mu\lambda}$ are the off-diagonal elements of the covariance error matrix, ε. X^2 gives the reduced chi-square estimate for each cell of analysis, specifying the goodness of fit between observed extreme data values and Gumbel's third distribution. For each city, estimates derived from the distribution of seismicity present within a 2° half-width cell of the city are given. NMISS is the number of missing years of extreme data

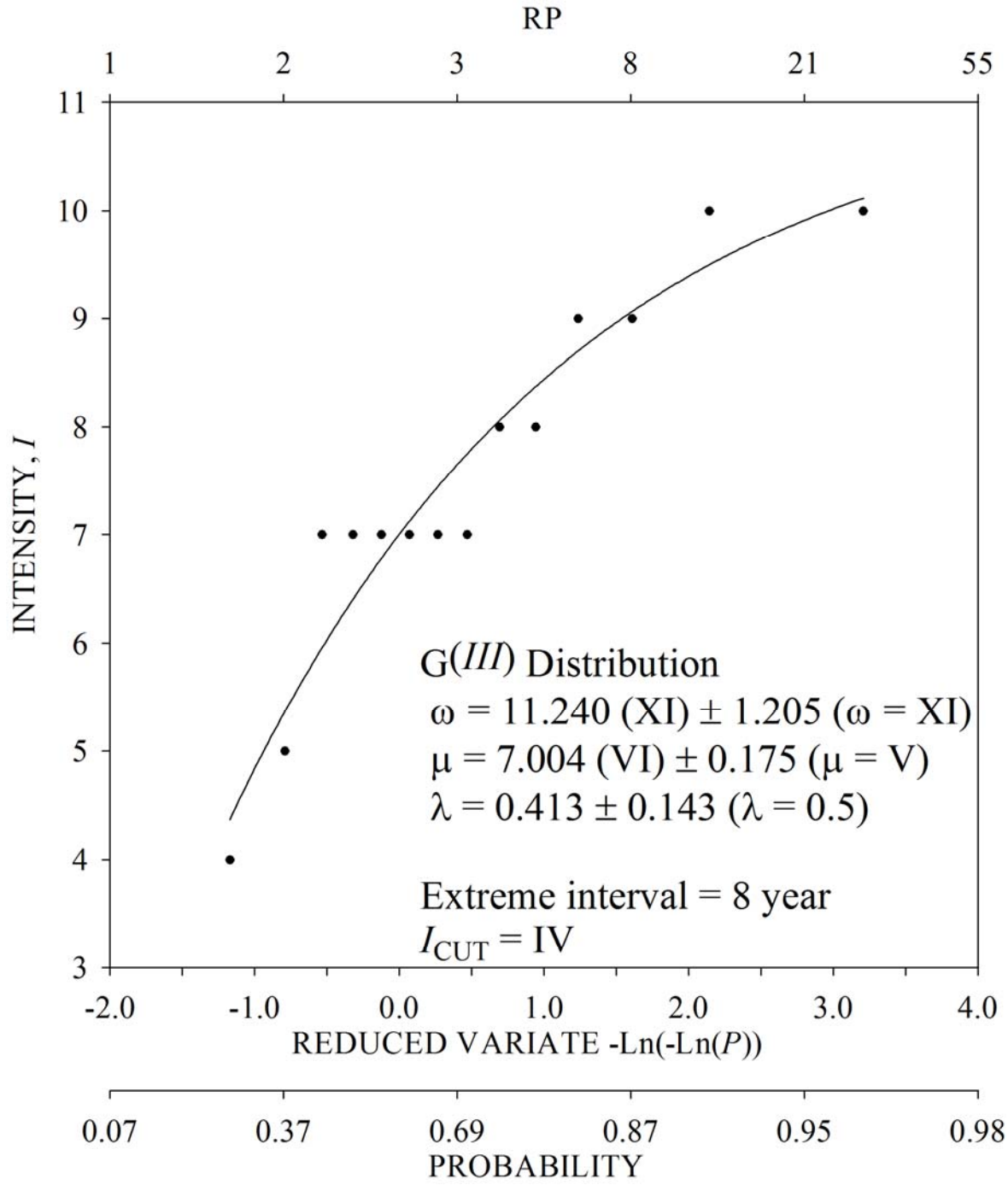

$$\varepsilon = \begin{bmatrix} 1.452 & -1.116 & -0.165 \\ -1.116 & 0.031 & -0.015 \\ -0.165 & -0.015 & 0.020 \end{bmatrix}$$

Figure 5.43 $G^{(III)}$ distribution curve of extreme value data and associated covariance error matrix, ε, for the area of 2° half width around Sofia for the time interval 1900 to 2004, using 8-yearly extreme intervals and epicentral intensities ≥IV

5.6 Discussion and summary

This chapter starts a new seismic hazard assessment for the Balkan region bounded by the 39.0°N, 45.0°N parallels and 19.0°E, 29.0°E meridians. This has been done with respect to extreme magnitude recurrence, peak ground acceleration (PGA), peak ground velocity (PGV) and macroseismic intensity statistics. Specific ground motion models have been adopted to estimate maximum ground motions expected in 50, 100 and 200 years, and also at 90% probability of not being exceeded (pnbe). These time intervals and confidence levels were also adopted for magnitude recurrence. Extreme earthquake hazard has been illustrated as a suite of contoured hazard maps across the region for each hazard descriptor considered. These practices were then extended to assess seismic hazard in the high hazard area of southwest Bulgaria and for eight cities.

An annual modal earthquake magnitude, m(1), of 6.89 M_s for the whole catalogued region has been calculated using Gumbel's third asymptotic extreme values distribution, compared with 6.67 M_s for southwest Bulgaria. These regions are forecast upper bound magnitudes, ω, of 7.69 M_s (± 0.56) and 7.84 M_s (± 0.76) respectively that are compatible with adopted and catalogued maximum magnitude seismicity. These estimates compare favourably to a number of previous studies for comparable – though not identical – areas. For example, Kárník and Schenková (1977) forecast ω = 8.87 M, Burton (1979) estimates ω = 6.87 M (± 0.80) → 9.38 M (± 2.86) for those analysis cells that cover geographic sub regions common to both hazard assessments. Makropoulos and Burton (1985a) estimates ω = 8.73 (± 0.65) for a region south of that considered here that includes more Greek and Aegean seismicity. Differences in these forecasts may be attributed to: using different parent earthquake datasets (e.g. fuller in size or differing in primary sources) to develop these statistics; adopting different magnitude scales for analysis or using different steps to homogenize magnitudes in the parent distribution, or; adopting different analysis cell geometries.

Estimates for the upper bound magnitude, ω, for both geographic areas are consistent with the *maximum* observed (homogenized) earthquake of 7.6 M_M, and also *maximum credible magnitudes*, M_3, from cumulative strain energy release techniques (M_3 = 7.82; considered in detail in chapter 6). Without a clear knowledge of previous work for comparison, ω for Southwest Bulgaria may appear artificially high compared with the full region. Possible reasons include: 1) superposition of multiple adjacent earthquake populations; 2) the sub-catalogue of earthquakes used to consider southwest Bulgaria may not represent [at least] one full cycle of seismicity, thus its content may be biased towards large magnitude events (whereas the broader region's full catalogue may represent a clearer cycle of seismicity), or adopting criteria of Table 5.5 may exclude more low-magnitude seismicity (that are possible extreme events) to inflate these estimates.

Bulgaria's capital Sofia is located north of the southwest Bulgaria zone considered, and is estimated an annual modal earthquake magnitude, m(1), of 6.88 M_s, and ω = 7.86 M_s ($\pm$ 0.75). Both are strikingly similar to estimates for southwest Bulgaria (Table 5.7), itself a sub zone of high forecasted magnitude hazard. This will be the result of seismicity producing the 1904 Kresna sequence that dominates the central region to Figure 5.17 and Figure 5.18. These figures, as well as Figure 5.20 and Figure 5.21, show the effect on magnitude hazard forecasts of the seismicity of one of the main geologic blocks in the border region of southwest Bulgaria and north Greece (the Serbomacedonian massif), and also how it helps constrain regional, local and site-specific magnitude hazard forecasts to realistic estimates.

All cities show good asymptotic behaviour, both visually by fitting a $G^{(III)}$ distribution curve to their respective extracted extreme values, and their site-specific estimates for ω (all are $\leq$7.9 M_s). Each also exhibit low chi-square, between 0.03 and 0.07. However, standard deviations on ω for Larissa, Plovdiv, Pristina, Skopje and Tirane are larger than 1.0 (1.21 to 1.70) and highlight a casual relationship between level of seismicity and an ability to constrain parameters of a statistical magnitude recurrence model such as Gumbel's extreme distribution. These cities tend to exhibit good asymptotic behaviour to some – but not all – elements of the third extreme distribution.

Extreme forecasts of ground acceleration and ground velocity are also estimated for Bulgaria and its surrounding region. These ground motion descriptors return contoured hazard maps consistent with each other in terms of the location of peak ground motion. Four areas of extreme ground acceleration of particular interest are consistently highlighted:

1. The Struma Valley adjacent to the border of southwest Bulgaria with the FYR of Macedonia and Greece (300+ cm s^{-2} for 50-year return period at 90% pnbe using Theodulidis and Papazachos);

2. West of Limnos, northern Aegean (500+ cm s^{-2} for 50-year return period at 90% pnbe using Theodulidis and Papazachos);

3. East of Plovdiv (500 cm s^{-2} for 50-year return period at 90% pnbe using Theodulidis and Papazachos);

4. West Turkey and Marmara Sea area (500+ cm s^{-2} for 50-year return period at 90% pnbe using Theodulidis and Papazachos).

Sofia is forecast maximum ground accelerations of 108 and 177 cm s^{-2} using Theodulidis and Papazachos. Hazard contours are such that the presence of the Serbomacedonian massif is highlighted clearly running northwest to southeast from the Struma Valley to immediately east of Thessaloniki. Each of these areas has experienced instances of high seismicity in the time interval catalogued.

Additional zones of high forecast ground motions – located outside the immediate border area between Bulgaria, the FYR of Macedonia and Greece – are in west Turkey, south of the Marmara Sea, central Albania, central Serbia, Serbia-FYR of Macedonia border and the Slovenia-Albania border to the extreme west of the study region. These particular zones of high hazard are consistent with results of Makropoulos and Burton (1985b) and Burton *et al.* (2003) for ground acceleration, with the latter work applying the attenuation model of Ambraseys (1995) to derive comparable estimates for ground motion. Contoured hazard levels are also similar to those proposed by Solakov *et al*. (2001), but have been translated here in a southerly direction from their zones of peak acceleration when considering hazard to Sofia.

The newer ground acceleration model of Ambraseys *et al*. (2005) has also been incorporated into this study to afford an updated view on estimated ground acceleration hazard in Bulgaria and the Balkans. Although it had to be simplified to accommodate limitations in the adopted input earthquake catalogue, it is still considered acceptable to adopt in this revised version of the model as it has been made reflect hazard produced by the dominant faulting mechanism (normal faulting) and soil type (stiff soil) of the region. Even after such simplifications, it systematically forecasts higher estimates regardless of the city area considered. However, which model of Ambraseys *et al*. (2005) and Theodulidis and Papazachos (1992) is most suited and indeed more likely to estimate realistic PGAs, is open to question and appears to be more site-dependent, reflecting general concern the latter model ($TP92_A$) over-estimates PGA in the near-field around large magnitude earthquakes, and is an obvious concern due to the region's seismicity predominantly being shallow focus in nature (section 2.5).

Intensity hazard has been assessed and illustrated for both geographic regions. Intensity ground motion hazard exhibits similar contour patterns to acceleration and velocity hazard in terms of the dominant regions of seismic hazard (i.e. west Turkey and north Aegean Sea extending into southwest Bulgaria tracing out the Serbomacedonian massif) with hazard estimates comparing favourably to other recent intensity hazard studies (e.g. Slavov *et al.*, 2004).

A major requirement of this work was to develop a comprehensive PSHA for a geographic region that could reasonably be considered overlooked in the past. This may be particularly true with respect to analytically forecasting extreme earthquake recurrence statistics against a standard PSHA framework. Whereas the majority of previous studies of southwest Bulgaria (the political triple junction, trans-frontier region between the FYR of Macedonia, Greece and Bulgaria) have concentrated upon integrating knowledge of localised seismicity, seismotectonics and geology together (Bončev *et al.*, 1982; Bončev, 1987b; Stanishkova and Slejko, 1991), this work extends consideration to include input of both near-field (Struma valley, Rhodopian and Rila mountain ranges) and far-field (Hellenic Arc-trench system, NAF, south Romania) seismic populations. Doing this provides insight into the seismic hazard potential specific to this localised area, across four initially considered core hazard descriptors. 475-year return period forecasts are also critical to consider if one is keen to relate any hazard analysis to EUROCODE 8 standards. The three ground motion hazard descriptors considered in this chapter meet current EUROCODE 8 requirements for reporting against the '475-year return period event'. Table 5.21 summarises EUROCODE 8 statistics for the two geographic extents considered as single entities and Sofia.

	Hazard descriptor			
Region	M_{P50}	A_{P50}[1]	V_{P50}[2]	I_{P50}[3]
Full region	8.20	n/a	n/a	XI (11.5)
SW Bulgaria	7.75	n/a	n/a	XI (11.3)
Sofia	7.83	177	27	XI (11.4)

[1] Using Theodulidis and Papazachos (1992; $TP92_A$) for stiff soil conditions (S = 0.5) at the 50th percentile (P = 0); [2] using Theodulidis and Papazachos (1992; $TP92_V$) for stiff soil conditions (S = 0.5) at the 50th percentile; [3] using Papazachos and Papaioannou (1997)

Table 5.21 Regional and site-specific hazard forecasts consistent with EUROCODE 8 requirements

This seismic hazard assessment for southwest Bulgaria, the surrounding region and urban centres continues in chapter 6 in terms of specific *design* and *scenario* earthquakes derived from cumulative strain energy techniques and earthquake perceptibility. These constitute a further four descriptors to defining seismic hazard for this region. Cumulative strain energy release techniques provide direct and analogous comparisons with statistical forecasts of Gumbel's extreme distributions. Earthquake perceptibility will also be modelled in terms of ground acceleration, ground velocity and macroseismic intensity, using relations discussed and selected in chapter 3 and already adopted in this chapter to source peak hazard estimates. Developing new sets of *design* or *scenario* earthquakes can be viewed a necessity for Bulgaria due to the region's apparent lack of instrumental records (Slavov *et al.*, 2004) providing alternative solutions to assessing regional and local seismic hazard.

Chapter 6 : Maximum credible magnitude and earthquake perceptibility hazard

6.1 Introduction

Earthquake hazard statistics are of significant interest to earthquake engineers designing civilian or critical structures to allow design of structures to withstand earthquakes and the resulting ground motions. Anti-seismic design criteria can benefit from cumulative strain energy release techniques or earthquake perceptibility theory, as they constitute specific measures of earthquake hazard. Each technique yields a specific *design* earthquake that can play a role in building collapse, economic loss, building usability (Goretti, 2003) and anti-seismic design in non-critical structures (Koravos *et al.*, 2003).

Cumulative strain energy release techniques yield an alternative but comparable maximum magnitude estimate to the upper bound magnitude of Gumbel's third asymptotic extreme values distribution. The former relies upon accessing the full parent distribution of seismicity, whereas the latter depends upon a filtered subset containing only pre-determined observed extremes. The return period, T_w, associated with cumulative energy release statistics will be equal to the time interval theoretically necessary for all strain energy to accumulate in a known area before being released instantaneously in the maximum earthquake associated to the statistical model. This assumes no other individual earthquakes occur in the meantime. These *whole process* maximum magnitude statistics differ in that they yield estimates that can be reconciled to a finite waiting time model. The comparable upper bound magnitude ω from an extreme values distribution more appropriately reconciles to an infinite return period model.

The maximum magnitude from cumulative energy release statistics, M_3, constitutes the *maximum credible earthquake magnitude* for the area considered, but will not be attached with probability levels of exceedance. Earthquake perceptibility does however yield probability estimates of experiencing a range of ground motions at different magnitudes, and so describes the earthquake most likely to cause a particular level of ground motion (e.g. Burton *et al.*, 2004b). This alternative *design* earthquake – or suite of *design* earthquakes – is taken as the *most perceptible earthquake magnitude,* $M_{P(max)}$. The *most perceptible magnitude* also benefits by allowing the user to relate recognised maximum earthquake magnitudes directly to resulting *design* ground motions and their probabilities of exceedance. This is not possible using cumulative strain energy release.

This chapter extends the evaluation of seismic hazard to Bulgaria, focusing upon cumulative strain energy release techniques (Figure 3.4) and earthquake perceptibility hazard (Figure 6.6). The same

catalogue adopted in chapter 5 is used again to consider each hazard technique and – where appropriate – the catalogue characteristics determined in section 5.3 will be adopted. This chapter will therefore develop four main areas of discussion relating to seismic hazard:

1. Cumulative strain energy release statistics will be determined and compared with comparable extreme hazard forecasts, taking into account each model's assumptions and limitations outlined in chapter 3. Discussion will extend to bring in knowledge of regional and localised historical observed seismicity listed by the catalogue. Although cumulative seismic moment release techniques is a newer approach to considering strain energy release statistics, a conscious decision is made here to concentrate solely upon the more traditional approach of strain energy release statistics.

2. Site-specific perceptibility and integrated perceptibility curves for horizontal ground acceleration, horizontal ground velocity and macroseismic intensity will be developed for the same urban centres – using elements of the same extreme earthquake distributions (appendix 4) – for which extreme earthquake hazard has already been considered. Estimates for the *most perceptible magnitude*, $M_{P(max)}$, and its associated annual probability of occurrence will be obtained for each city. These magnitudes are then related to maximum magnitudes from cumulative energy release hazard techniques and Gumbel's third extreme values distribution.

3. These earthquake perceptibility forecasts will allow site-specific hazard curves for the urban centres illustrated in Figure 5.1 to then be developed. These will estimate annual probabilities of exceedance for each ground motion hazard descriptor considered at each site.

4. Probability estimates from each city's perceptibility estimates and information extracted from the input earthquake catalogue will be combined to disaggregate the seismic source hazard to each city in terms of the most frequently occurring magnitudes at set distances from each urban centre.

The city of Sofia will continue to be used as a site-specific case study throughout this chapter for each hazard descriptor considered. Site-specific energy release plots, perceptibility and integrated perceptibility curves, probability of annual exceedance hazard curves and hazard disaggregation statistics are in the main text for Sofia, while equivalent illustrations for the other cities are in Appendices 17 to 30.

6.2 Maximum credible magnitude statistics

A key advantage to using cumulative energy release statistics to assess seismic hazard in a region is that they offer a means to examine the seismic cycle (cycle of periodicity), whether it has completed, its length, or estimate how long the time interval is before it is complete, i.e. the residual time. That is, the two important time intervals T_w (Makropoulos and Burton, 1983) and DT (Tsapanos, 1998). These estimates may then relate to key magnitude statistics of both techniques:

- M_2 – the magnitude that corresponds to the mean annual rate of energy release

- M_3 – the analytical upper bound earthquake magnitude for the region or location (the *maximum credible earthquake*)

This section will estimate T_w, DT, M_2 and M_3 (defined fully in section 3.7.1) for the two regions and each urban centre for which seismic hazard is considered using *whole process* seismicity illustrated in Figure 5.13 and Figure 5.14.

Cumulative strain energy release for the region bounded by 39°-45°N, 19°-29°E is illustrated in Figure 6.1, with the inset giving key hazard statistics for this magnitude recurrence model. These are the equivalent magnitudes M_2 and M_3, and energy releases associated to these. Estimates for M_1 from the cumulative frequency-magnitude distribution constants a and b are also be given (i.e. a/b). Cellular estimates for (a) M_2 and (b) M_3 using the same '*moving cell*' approach adopted for extreme hazard analysis to contour extreme hazard are given in Figure 6.2.

Key points can be determined from Figure 6.1, Figure 6.2 and Figure 5.19(a). The early part of the time interval considered is dominated by the earthquake sequences of 1904, 1905 and 1912. After 1912, the region's rate of strain energy release appears to be in a state of decrease throughout the rest of the 20th century, as the prevailing gradient of the energy release line decreases. This suggests strain energy is accumulating within the region. As line SS` approaches the lower bound line the likelihood increases for a large magnitude earthquake to occur. This seems to have been realised in 2000 when an earthquake (21st March, 2000, 41°N, 24°E, east of Thessaloniki; reported magnitude 6.5 m_b, homogenized magnitude of 7.6 M_s) occurred with a comparable homogenized magnitude to those of the early 20th century.

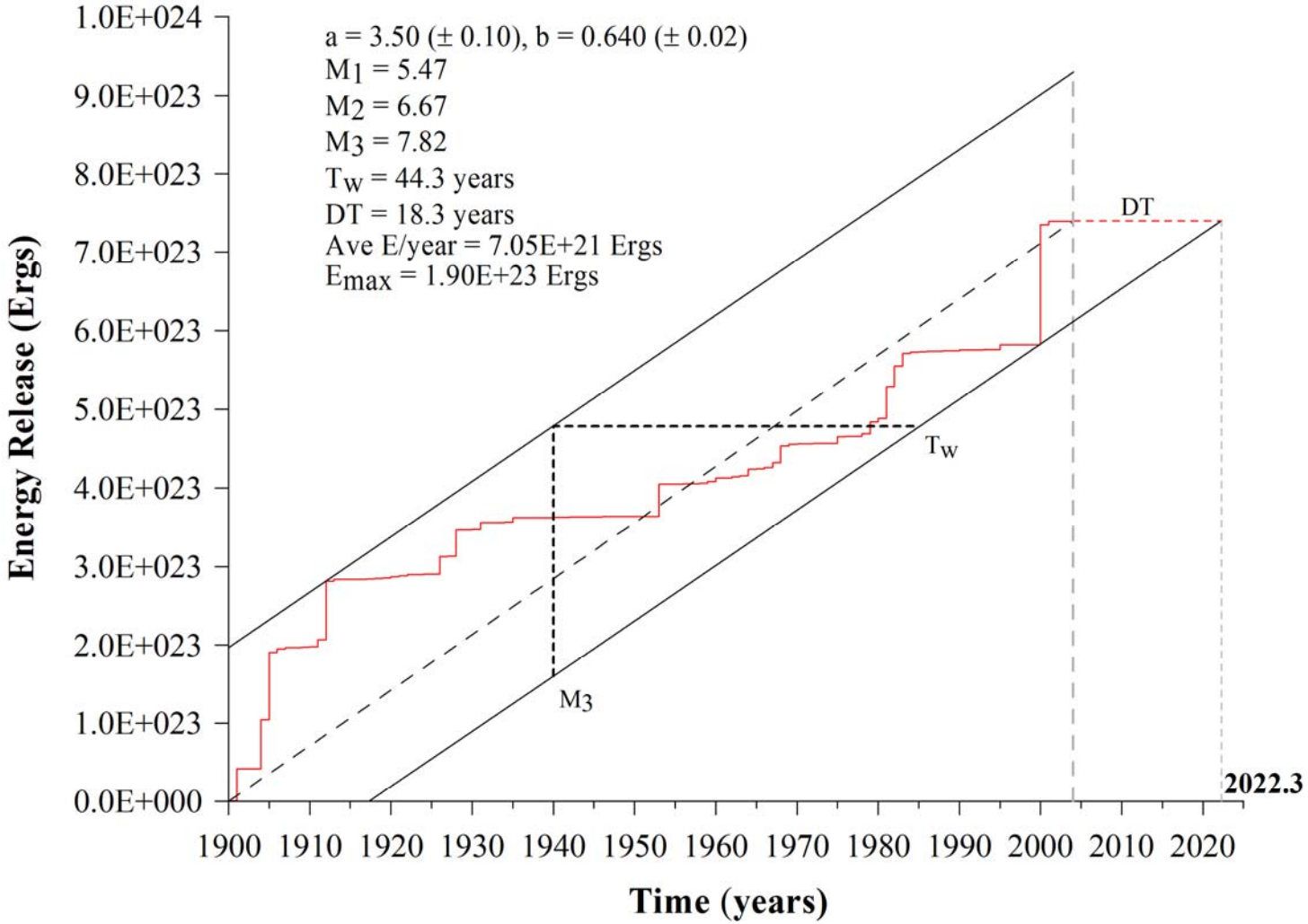

Figure 6.1 Cumulative strain energy release statistics considered as function of time (1900 to 2004 – marked by the vertical grey dashed line – plus the residual time, DT) for the full Balkan extent. The figure represents seismicity contained within the full geographic extent. The *maximum credible magnitude*, M_3 and the associated waiting times, T_w and DT are also indicated

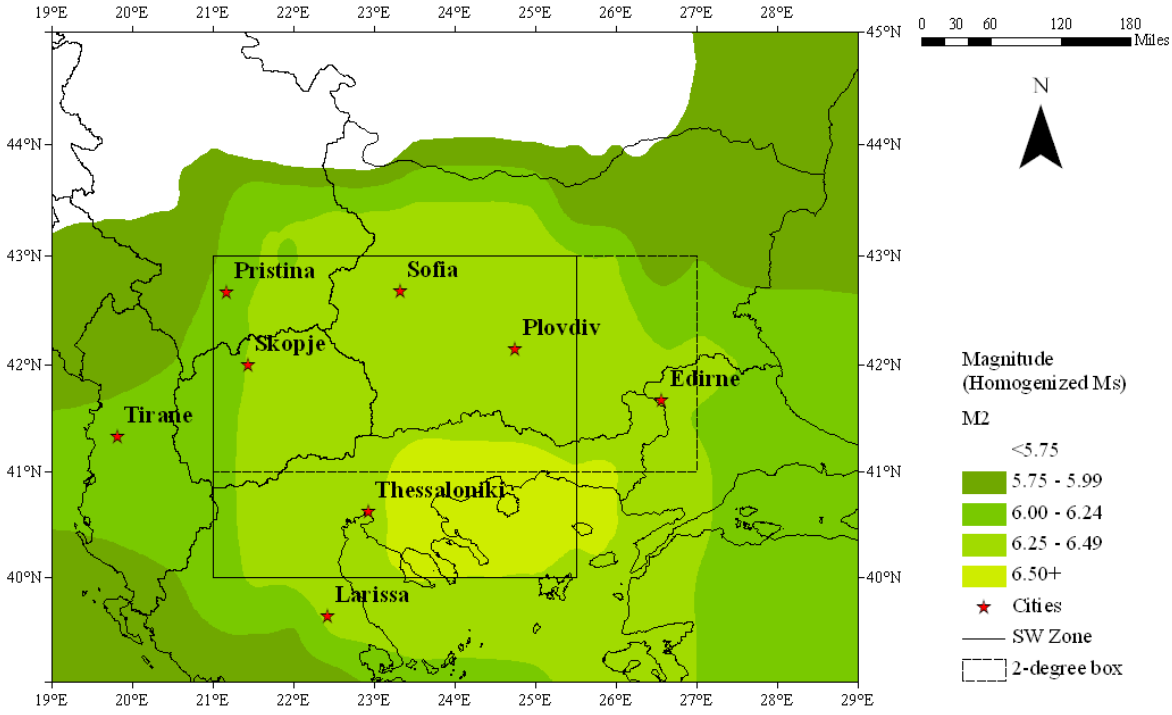

(a)

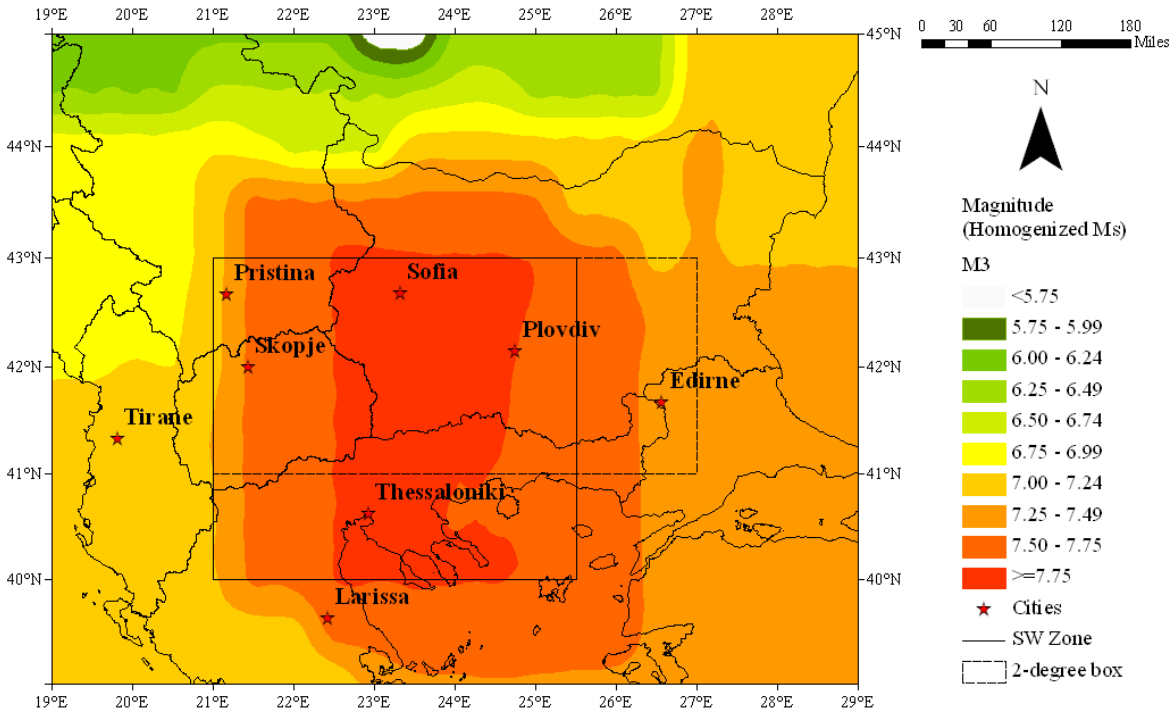

(b)

Figure 6.2 Magnitude hazard after adopting cumulative strain energy release analysis analogous to (a) the mean annual energy release (i.e. the magnitude estimate M_2) and (b) the analytical upper bound magnitude for each 2° analysis cell (i.e. the magnitude estimate M_3) during the time interval for which the broad Balkan region's seismicity has been catalogued. Contours for both are at intervals of 0.25 M_s

However, section 2.4.2 has already acknowledged that this large homogenized M_s magnitude estimate was the result of the steep gradient to the adopted magnitude conversion relation (Figure 4.2, Line 7) used on a moderate reported magnitude of 6.5 m_b; itself generated from the higher seismicity of the Hellenic Arc and Aegean area. Therefore it is unlikely this event does truly mark the end of the considered region's seismic cycle.

The reduced gradient of the energy release line SS` in the middle part of Figure 6.1 between approximately 1915 and 1980 suggests there is less large magnitude seismicity during this time interval. This apparent change in the region's seismic activity supports previous observations (Stanishkova and Slejko, 1991; Drakopoulos, 1976) that the majority of the region's seismic activity occurred towards the start of the 20th century.

The occurrence of the large magnitude event in 2000 suggests tentatively that this region has undergone at least one complete seismic cycle, possibly completing near the end of the 20th century. This implies approximately 100 years is required to accumulate the strain energy equivalent to the *maximum credible magnitude*, M_3. However, it is important to recognise that, with reference to only the catalogue used (as it is the sole input to this statistical model), it is not possible to determine with certainty if these large events at the start of the 20th century occurred at the start, middle or end of the then current seismic cycle. Indeed, as the earthquake of 2000 was not as large as the 1904 Kresna earthquake (reported body-wave magnitudes of 6.5 m_b and 7.8 m_b respectively) it is plausible that if the Kresna event defines the start of one seismic cycle, the Thessaloniki earthquake may simply represent a moderate mid-cycle earthquake.

Shebalin *et al.* (1998) is recognised as the most appropriate pre-instrumental catalogue to merge with this dataset to extend knowledge of regional Balkan seismicity back in time (Table 2.1). Although section 2.4.2 has already discussed some general points of pre-instrumental seismicity using this secondary data source, it is useful to consider it using data filtering criteria adopted in chapter 5. Filtering this fuller listing to cover only the catalogued area for magnitudes ≥4.0 M_w (homogenized moment magnitude), reveals a further 411 earthquakes to have occurred (between 342 BC and 1899 inclusive) and recorded sufficiently well enough by some means to warrant their listing. The largest magnitude is 8.2 M_s (±0.5; estimated from macroseismic intensity data) in 555 BC. There were 144 earthquakes recorded greater than 5.5 M_s (homogenized; the cut-off magnitude adopted for evaluating hazard using extreme statistics in chapter 5) with the last one of the 19th century occurring in 1897 (6.6 M_s ± 0.5; estimated from macroseismic intensity data). The most seismically active individual years of the 19th century – in terms of earthquakes above the 5.5 M_s cut-off – were 1895 (7 events, $5.5 \leq M_s \leq 7.3$), 1893 (7 events, $5.5 \leq M_s \leq 6.9$) and 1866 (7 events, $5.7 \leq M_s \leq 6.7$), with all these events being attached with uncertainties of ≥0.3 M_s.

Now knowing these comparative levels of seismicity in the late pre-instrumental period, one could suggest that this new catalogue does indeed commence in the middle of a significant period of seismic activity, as is demonstrated in Figure 2.11, with much of it focused in the confined southwest zone of interest (Figure 6.3) and along the Albanian coast to the west.

If one now considers statistics of the third extreme values distribution, Makropoulos and Burton (1985a) suggest that in places where one periodic cycle of strain energy release is not evident, large uncertainties will accompany the upper bound magnitude to Gumbel's third extreme values distribution. On its own a value for σ_ω of 0.562 is, although small, inconclusive evidence that the Balkan seismogenic region as a whole has experienced one full periodicity completing near the end of the 20th century.

Estimates for the *maximum credible magnitude*, M_3, of 7.82 M_s for the broad Balkan region is consistent with observed seismicity of the region. This is regardless of whether one considers the homogenized maximum magnitude, $M_{M,}$ of 7.6 M_s, the ten events of magnitude greater than 7.0 M_s during the catalogued period, or the reported unhomogenized maximum magnitude of 7.8 m_b.

The general rule $\omega - M_3 \geq 0$ does not hold here when adopting cumulative strain energy release techniques as $\omega - M_3 = -0.13\ M_{s,}$ contrary to the suggestion of Burton and Makropoulos (1985). One possible explanation for this discrepancy between ω and M_3 is that Burton and Makropoulos do not appear to adopt any method to refine their selected catalogue data (i.e. selecting suitable start year, extreme interval and magnitude threshold) used to determine ω. They stress that relationship $\omega - M_3 \geq 0$ results from a conceptual difference in waiting times for M_3 and ω to occur, and that large uncertainties usually attached to ω would likely encompass M_3. An alternative explanation may be that it is unlikely the adopted catalogue represents a full cycle of seismicity. If this is true, then not all 'extreme' events representative of this region's seismicity for a single cycle of periodicity will have been considered, thus compromising any extreme values statistics borne out of the analysis.

The last large magnitude earthquake occurred in the region in 2000. The waiting time T_w forecast for enough energy to accumulate equivalent to M_3 is 44.3 years. However, a value of 18.3 years for DT for the next seismic event of magnitude equal to or less than M_3 is indicative of a much shorter time interval, possibly for the completion of strain energy accumulation, until the next seismic event after 2004.

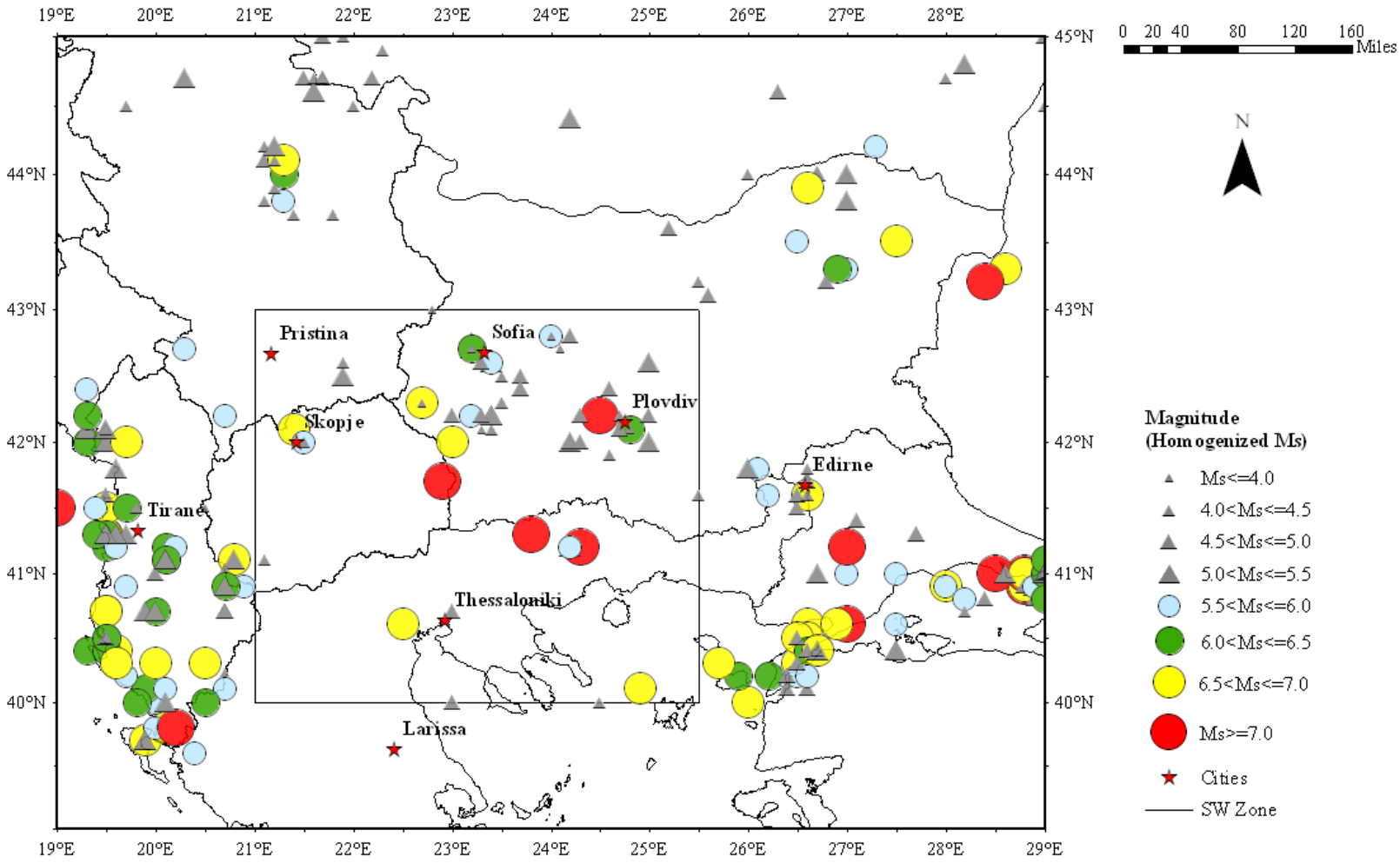

Figure 6.3 Pre-instrumental seismicity of the broader Balkan extent back to 342 BC (the start of the catalogue of Shebalin *et al.*, 1998) from 1899. Different symbols denote earthquakes below (triangles) and equal to or greater than 5.5 M_s (the cut-off magnitude, M_{CUT}; circles) for the full Balkan extent (all historical events illustrated have been homogenized using the same conversion scales and moment magnitude threshold described in chapter 4 as were applied to the events of the main catalogue)

This suggests a time interval of approximately 22 years until the next earthquake after the large 2000 earthquake, so approximately half of T_w. DT places the next seismic event sometime before 2022. This may mark the commencement of the next seismic cycle that is possibly more representative of the high seismicity experienced during the early stages of the 20th century, and suggests a cycle of seismic periodicity is approximately 115 to 120 years.

Gumbel's third distribution allows users to attach return periods to magnitude estimates from strain energy release techniques. The annual modal earthquake magnitude, M_1, of 5.47 M_s and derived from zone-dependent constants a and b of the cumulative frequency-magnitude distribution, closely agrees with estimates for return periods for magnitudes from the extreme values distribution. Here a magnitude 5.5 M is forecast with a return period of 1.1 years (Table 5.8). M_2, notionally equivalent to the mean annual rate of strain energy release, has a return period of about 2 years.

Regional hazard is forecast for M_2 and M_3 at a cellular level in Figure 6.2 using a '*moving cell*' approach identical to that used for contouring extreme hazard (2° half-width cells at 0.5° steps of latitude and longitude). These each approximate to the same contour patterns. Each is dominated by an extensive region of high magnitude hazard centred on southwest Bulgaria and north Greece. Maximum magnitudes for M_3 (Figure 6.2(b)) in excess of 7.75 M_s may occur in a region extending from the Chalkidiki Peninsula northwards to the Stara Planina mountain range north of Sofia, and from east FYR of Macedonia to Plovdiv. The majority of the region will be subject to maximum magnitudes in excess of 6.50 M_s with the lowest estimates in the northwest and the highest estimates are over the southwest area of interest.

The earlier energy accumulation illustration is repeated in Figure 6.4 for southwest Bulgaria. The same large increases representing significant seismic activity during 1904 and 2000 in Figure 6.1 are also present in Figure 6.4 and would initially suggest that this smaller region has experienced one full periodicity of strain accumulation and release, and that a large proportion of seismicity (i.e. strain energy) is contained in this sub region. The tendency for the prevailing gradient of each energy release line to decrease over time between the seismic sequences of 1904, 1905 and 2000 is again apparent.

Contouring cellular estimates for M_2 and M_3 indicate the majority of the southwest zone is dominated by *maximum credible magnitude*s greater than 7.0 M_s, with the highest magnitudes forecast over the centre and the east of the southwest zone, running in a north-south direction. Evidently, this sub region is dominated by seismicity of the Struma Valley and the tectonic region around Plovdiv.

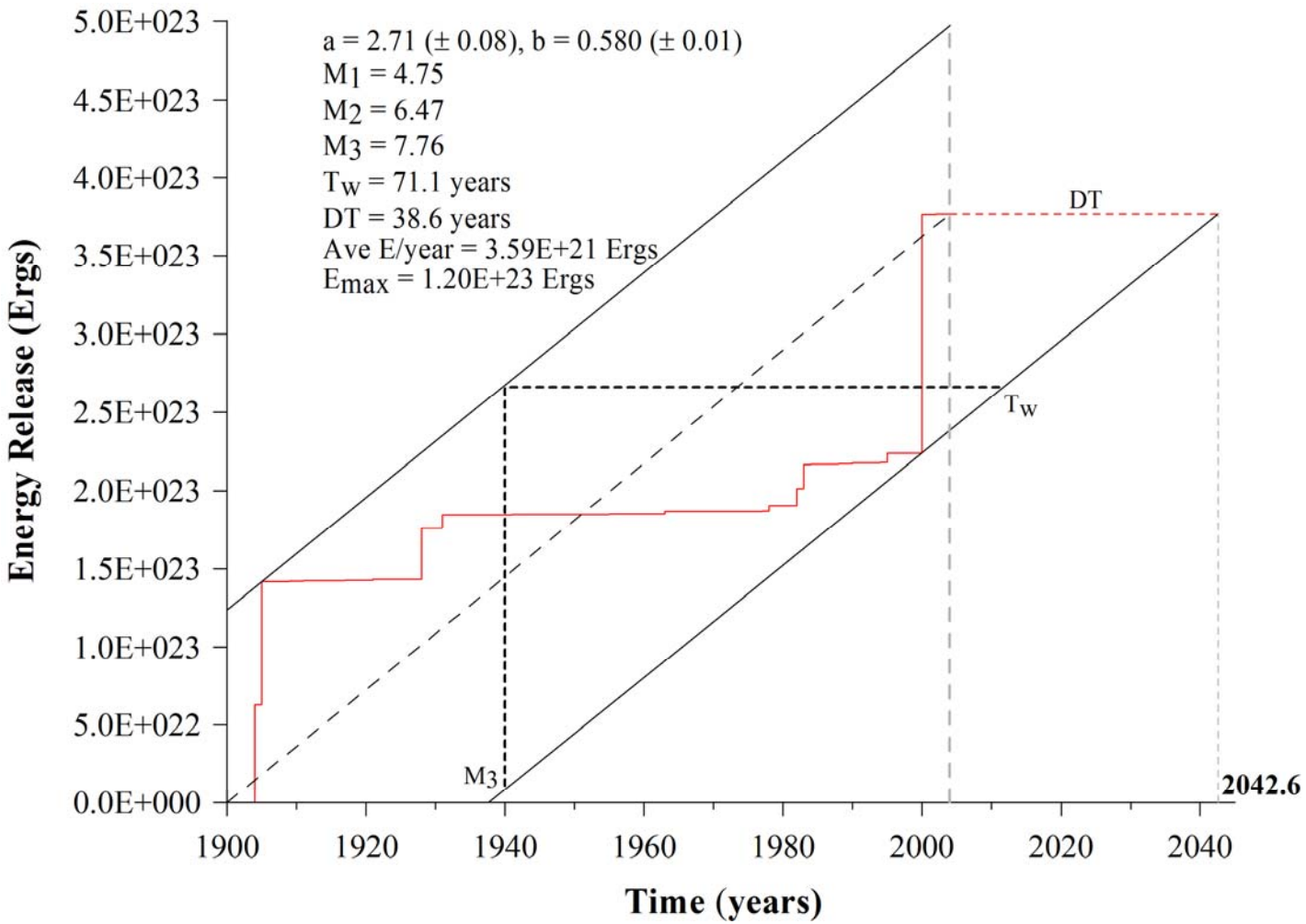

Figure 6.4 Cumulative strain energy release statistics considered as a function of time (1900 to 2004 – marked by the vertical grey dashed line – plus the residual time, DT) for southwest Bulgaria. The figure represents seismicity contained within southwest Bulgaria. The *maximum credible magnitude*, M_3 and the associated waiting times, T_w and DT are also indicated

The magnitude M_3 is estimated at 7.76 M_s for this southwest zone. As this is the region of the 1904 Kresna (homogenized 7.2 M_s), 1928 Plovdiv and 2000 Thessaloniki (homogenized 7.6 M_s) sequences, it is not surprising that this region returns an almost identical estimate for that of the broader region. This may be indicative of a large percentage of seismic energy being released within this confined region as a proportion of the fuller catalogued region. These also compare favourably to the region's value for ω of 7.84 M_s ($\pm$0.76). A higher estimate for the upper bound attached with a larger standard deviation also gives partial credence to the southwest region itself not having a completed cycle of seismicity within it.

DT is approximately 48% of the waiting time T_w for this southwest zone. Respecting that the equivalent value for the broader region is 32% goes some way to supporting earlier observations that most of the seismic loading and activity is to be found in this confined southwest zone of Bulgaria. The delay time DT until the next seismic event occurs within the southwest zone is 39 years, suggesting the next seismic event (after 2004) will likely occur before 2043.

This smaller region follows the ideal that $\omega - M_3 \geq 0$, with this difference being 0.09 M_s. Again, M_2 and M_3 differ by approximately one magnitude unit, with $M_3 - M_2$ giving 1.29 M_s but is larger than that for the broader region.

A site-specific *scenario* is illustrated in Figure 6.5 for Sofia. Equivalent plots for the other seven cities considered are in Appendix 17. Statistics resulting from each of these are summarised in Table 6.1, along with equivalent estimates for both regional geographic extents considered.

Statistics for each urban centre derive from *whole process* hypocentre distributions illustrated in Appendix 4, and represent seismicity present within 2° half-width cells centred on each city, which is the current standard practice in hazard analyses such as this (e.g. Makropoulos and Burton, 1985a, 1985b; Xu *et al.*, 2003; Burton *et al.*, 2004b). Justification for the analysis cell size and shape to adopt has already been made in section 5.3.5.

Larissa, Plovdiv, Pristina, Skopje, Sofia and Thessaloniki have M_3 estimates comparable to southwest Bulgaria (of 7.60 M_s, 7.75 M_s, 7.59 M_s, 7.59 M_s, 7.76 M_s and 7.76 M_s respectively, compared with 7.76 M_s) and also the full Balkan region (7.82 M_s). All these cities are within approximately 200 km of the 1904 and 2000 earthquakes. These two seismic sequences, along with that of Plovdiv (1928) to the east dominate local seismicity of this zone. Furthermore, Sofia is forecast acceptable and realistic estimates for M_3 (M_3 = 7.76 M_s) and ω (7.86 $M_s \pm 0.75$) based on observed catalogued seismicity of the 1904 and 2000 events (with homogenized and reported magnitudes of 7.2 M_s and 7.8 M_s, 7.6 M_s and 6.5 m_b respectively).

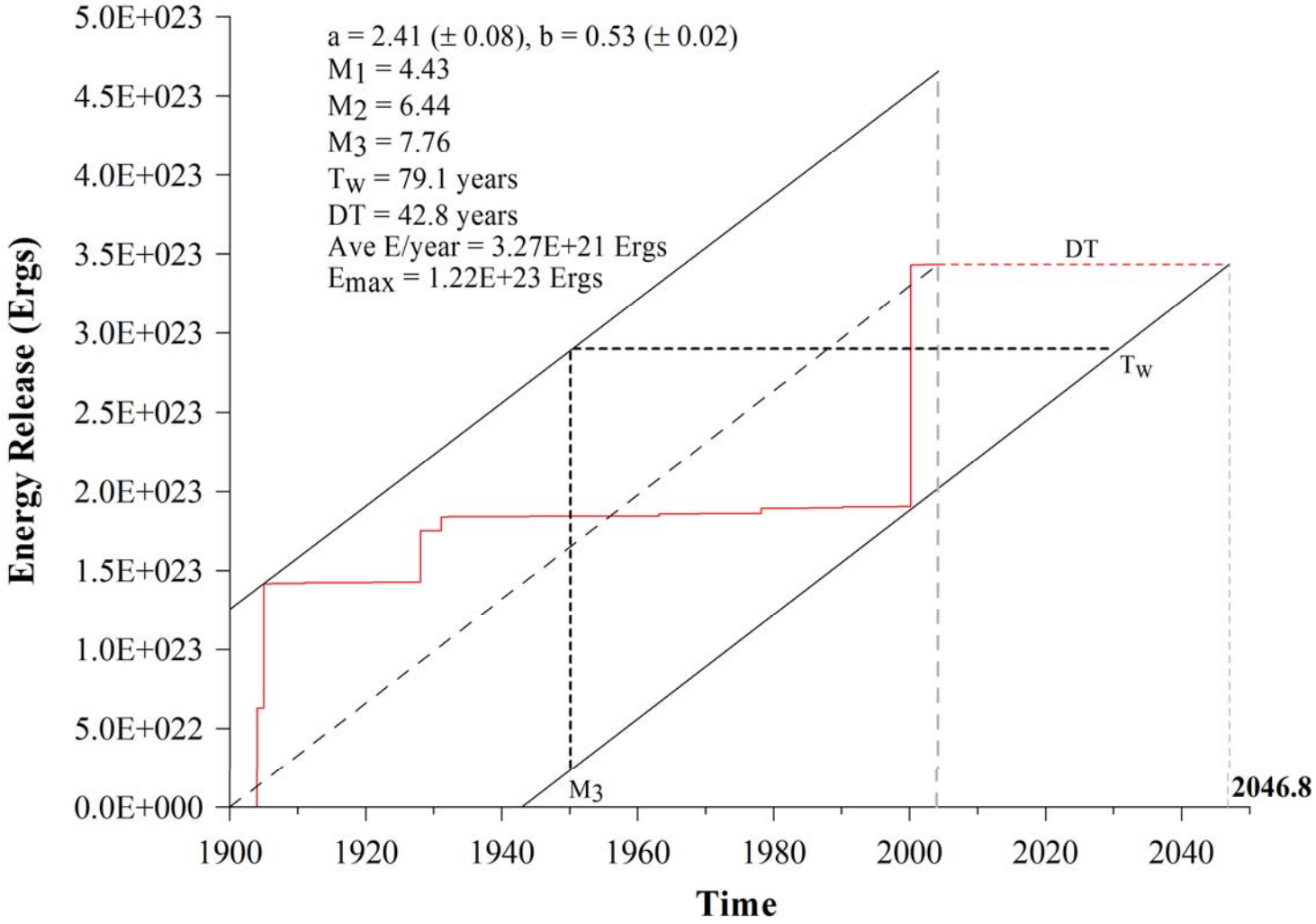

Figure 6.5 Cumulative strain energy release statistics considered as a function of time (1900 to 2004 – marked by the vertical grey dashed line – plus the residual time, DT) for Sofia. The figure represents seismicity contained in a 2° half-width cell centred on the city (Figure 5.15). The *maximum credible magnitude*, M_3 and the associated waiting times, T_w and DT are also indicated

Region	ω	a	b	M_1	M_2	TE/year	M_3	E_{max}	T_W/years	DT/years
Full region	7.686 (±0.562)	3.50 (± 0.10)	0.640 (± 0.02)	5.48	6.672	7.05E+21	7.815	1.90E+23	44.3	18.3
Southwest zone	7.840 (±0.759)	2.71 (± 0.08)	0.580 (± 0.01)	4.67	6.469	3.59E+21	7.755	1.20E+23	71.1	38.6
Edirne (41.67°N, 26.57°E)	7.571 (±0.706)	2.20 (± 0.07)	0.522 (± 0.01)	4.39	6.263	1.82E+21	7.401	5.84 E+22	43.6	12.4
Larissa (39.63°N, 22.42°E)	7.892 (±1.264)	3.10 (± 0.08)	0.674 (± 0.02)	4.60	6.304	2.08E+21	7.600	5.98E+21	73.6	71.7
Plovdiv 42.15°N, 24.75°E)	7.962 (±1.209)	2.53 (± 0.08)	0.563 (± 0.02)	4.49	6.439	3.25E+21	7.754	1.18E+23	78.4	43.1
Pristina (42.67°N, 21.17°E)	7.683 (±1.458)	3.04 (± 0.11)	0.634 (± 0.04)	4.79	6.265	1.82E+21	7.589	1.40E+23	80.7	4.9
Skopje (42.00°N, 21.43°E)	7.892 (±1.695)	3.20 (± 0.12)	0.650 (± 0.02)	4.92	6.291	1.99E+21	7.589	1.40E+23	74.0	4.9
Sofia (42.68°N, 23.32°E)	7.859 (±0.748)	2.41 (± 0.08)	0.530 (± 0.02)	4.43	6.441	3.27E+21	7.759	1.22E+23	79.1	42.8
Thessaloniki (40.63°N, 22.93°E)	7.896 (±0.940)	2.95 (± 0.07)	0.615 (± 0.07)	4.80	6.463	3.52E+21	7.756	1.17E+23	72.7	40.6
Tirane (41.33°N, 19.82°E)	7.349 (±1.288)	3.14 (± 0.12)	0.646 (± 0.02)	4.86	6.045	8.80E+20	7.112	2.59E+22	34.4	5.9

Table 6.1 Cumulative strain energy release statistics for seismicity within a 2° half-width cell of each (except for broad and southwest zones, where all seismicity in these zones is considered) for the time interval 1900 to 2004. a and b are least squares estimates for zone-dependent constants and used to derive M_1 (the modal earthquake magnitude, such that $M_1 = a/b$); TE/year is the mean annual rate of energy release, M_2 is the magnitude equivalent to TE/year. M_3 is the analytical upper bound magnitude and T_W is the waiting time for the all the energy in the region to accumulate if it were released in a single event. DT is the delay (or residual) time; i.e. the time between the upper bound enveloping line and the time since the last seismic activity. b-values given for the full catalogue region here are different to those given in Table 4.9 due to different data being adopted. All data are used here to be consistent with cumulative strain energy release statistics. Table 4.9 uses events with magnitudes ≥4.6 M_s, i.e. the notional lowest possible limit to the catalogue's magnitude completeness. However, smaller magnitudes have minor influence in estimating energy release statistics

Edirne is also forecast realistic estimates for ω (7.57 M_s ± 0.71) for the region within which it is located, and M_3 is within 0.1 M_s of ω. Estimates for ω for all other cities are below 8.0 M_s, compatible with homogenized and reported maximum magnitudes. Those cities are at greater distance from the large magnitude events of 1904 and 1928 (e.g. Edirne, Tirane, Pristina) have significantly reduced estimates for M_3, to reflect dominance of lower magnitude extremes in their immediate areas.

Pristina (DT = 4.9 years), Skopje (4.9 years) and Tirane (5.9 years) may be nearing completion of a cycle of localised seismicity. These cities are located geographically to the west in the broader study region, to the extreme west of – or outside of – the southwest zone of interest. As each city is forecast T_w and DT of less than 6 years, one might suggest that the localised seismicity of this confined area within which these cities are located may possibly be approaching the time of the next earthquake; that is, the strain energy accumulation is nearing its upper limit.

Pristina and Skopje are attached with estimates for DT that are less than 10% of T_w, again suggesting that these two cities are nearing completion of their seismic strain accumulation. Although Tirane is also forecast a low DT, this equates to approximately one-fifth of T_w, due to its significantly shorter T_w. T_w (34.4 years) is shortest for Tirane than any other city. This is perhaps a reflection of it being closest to the higher seismicity of the Adriatic subduction zone to the west. DT for Larissa is greater than 95% of T_w, suggesting that an accumulation cycle may have just completed. This suggests two scenarios: 1) there is a long waiting time before the next seismic cycle is completed, such that the M_3 event occurred recently in the past or, 2) the considered area immediately surrounding Larissa is dominated by low-level seismicity interspersed with rare moderate earthquakes to allow sufficient strain energy to accumulate to create the M_3 magnitude earthquake.

Although the concept of the seismic cycle is well understood and it is accepted this model can be measured using different methods, it is not well proven for Bulgaria and the immediate surrounding region (Ranguelov, pers. comm), unlike more seismically active counties such as China, Japan and Italy. This section goes some way support this claim. Adopting an input data set that represents a relatively short time interval as used here does not allow one to determine precisely or confidently where about in the seismic cycle the parent distribution used is located.

There is evident uncertainty about the legitimacy of the homogenized magnitude to the 2000 Thessaloniki event; an issue most probably borne out from applying a magnitude conversion relation generated from another region's [high seismicity] parent distribution of seismicity onto a region of small to moderate seismicity. Using a large number of magnitude conversion equations

(sections 4.6, 4.7 and 4.9) to generate the input catalogue further hides the ability to define the areas seismic cycle, since each will have a different gradient to converting magnitudes. Converting the moderate magnitude 6.5 m_b Thessaloniki earthquake to become the catalogue's largest homgenized event (7.6 M_s) masks the region's true largest magnitude events and may introduce misinterpretation of the region's seismic history.

The catalogue cannot be significantly extended forward in time; however investigating the pre-instrumental and historical records (Figure 6.3) in unison with the compiled catalogue shows that there are periods of high seismicity in very short periods of time. This task also shows the 7.2 M_s Kresna earthquake was not an anomalous event; both suggesting that the seismic cycle in this region may actually be shorter than 105 years. Additionally, the further one extends the complied record back into history, the greater proportion of smaller magnitude seismicity will be excluded, some of which may be true annual extreme events. Their exclusion may therefore adversely affect statistical recurrence distributions such as those adopted here. These uncertainties in assigned magnitude will therefore introduce larger uncertainty on hazard estimates presented in any resulting hazard maps.

6.3 Earthquake perceptibility

Understanding a region's ground motion and attenuation characteristics with respect to a specific form of ground motion provides benefits beyond developing earthquake hazard estimates in terms of absolute and expected levels of ground motion or ground motion spectra that may be experienced at a particular site or over a *source-to-site* distance. It also allows the user to determine probability levels of experiencing particular ground motion levels combined with region or site-specific probabilities of occurrence for a specific earthquake magnitude. Both of these are important to the earthquake engineer when approaching anti-seismic building design. Earthquake perceptibility theory provides such information by combining a chosen statistical magnitude distribution model with a ground motion model for an area of interest, as it affords a means to estimate the annual probability that a pre-selected level of ground motion will be generated by earthquakes of a known magnitude. This approach can then be extended to incorporate and develop relationships between perceptible magnitude hazard and maximum magnitude recurrence models with finite and infinite return period properties.

6.3.1 Earthquake perceptibility theory

Earthquake perceptibility is defined as the probability a site perceives ground shaking equal to or greater than a selected ground motion level, X, resulting from an earthquake of magnitude M, such that:

$$P(X \mid M) = P_c(X)\, P_e(M) \qquad (6\text{-}1)$$

$P_c(X)$ estimates the probability of perceiving ground motion level X from an earthquake of magnitude, M. $P_c(X)$ will increase at a non-linear rate with respect to M and can be considered as a ratio of the felt area at X to that of the considered area. $P_e(M)$ will be the derivative – probability density – of the specific statistical earthquake recurrence model applied (Burton, 1978b, 1981; Koravos *et al.*, 2003; Burton *et al.*, 2004b). In the instance of this work, $P_e(M)$ will estimate the probability of an event of magnitude M using Gumbel's third extreme values asymptotic distribution (Burton 1978b, 1981).

Earthquake perceptibility, Eq. (6-1), is a product of the probabilities from both $P_e(M)$ and a selected ground motion parameter, $P_c(X)$ (Figure 6.6). It is evident from Figure 6.6 that earthquake probabilities described by $P_e(M)$, are a decreasing function of M, such that $P_e(M) \rightarrow 0$ as the regional maximum magnitude defined by the adopted statistical distribution is approached.

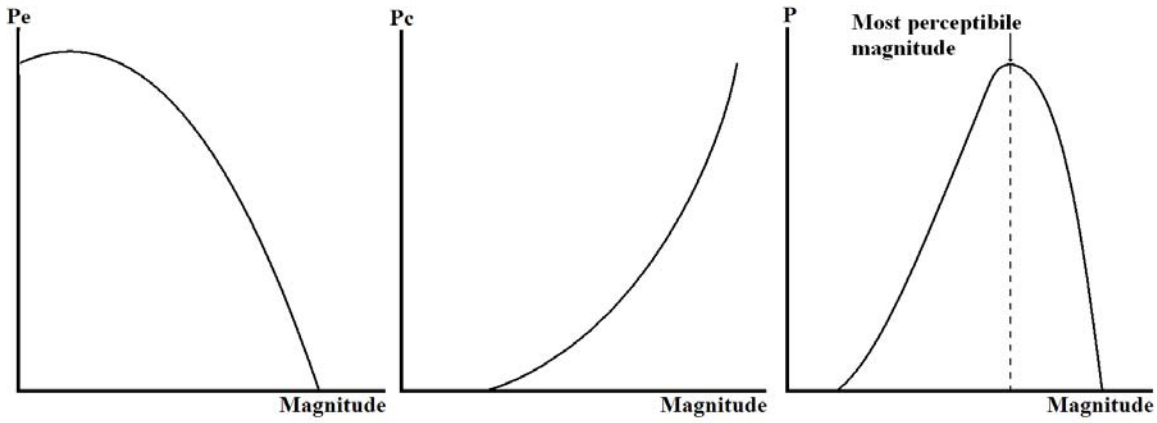

Figure 6.6 Magnitude perceptibility: (a) the probability density function of Gumbel's third extreme distribution ($P_e(M)$ of (Eq. 6-1)), (b) the probability of perceiving or feeling ground motion of level X or greater when a magnitude M earthquake has occurred ($P_c(X)$ of Eq. (6-1)), and (c) the perceptibility curve ($P(X \mid M)$ in Eq. (6-1); after: Burton *et al.*, 2004b)

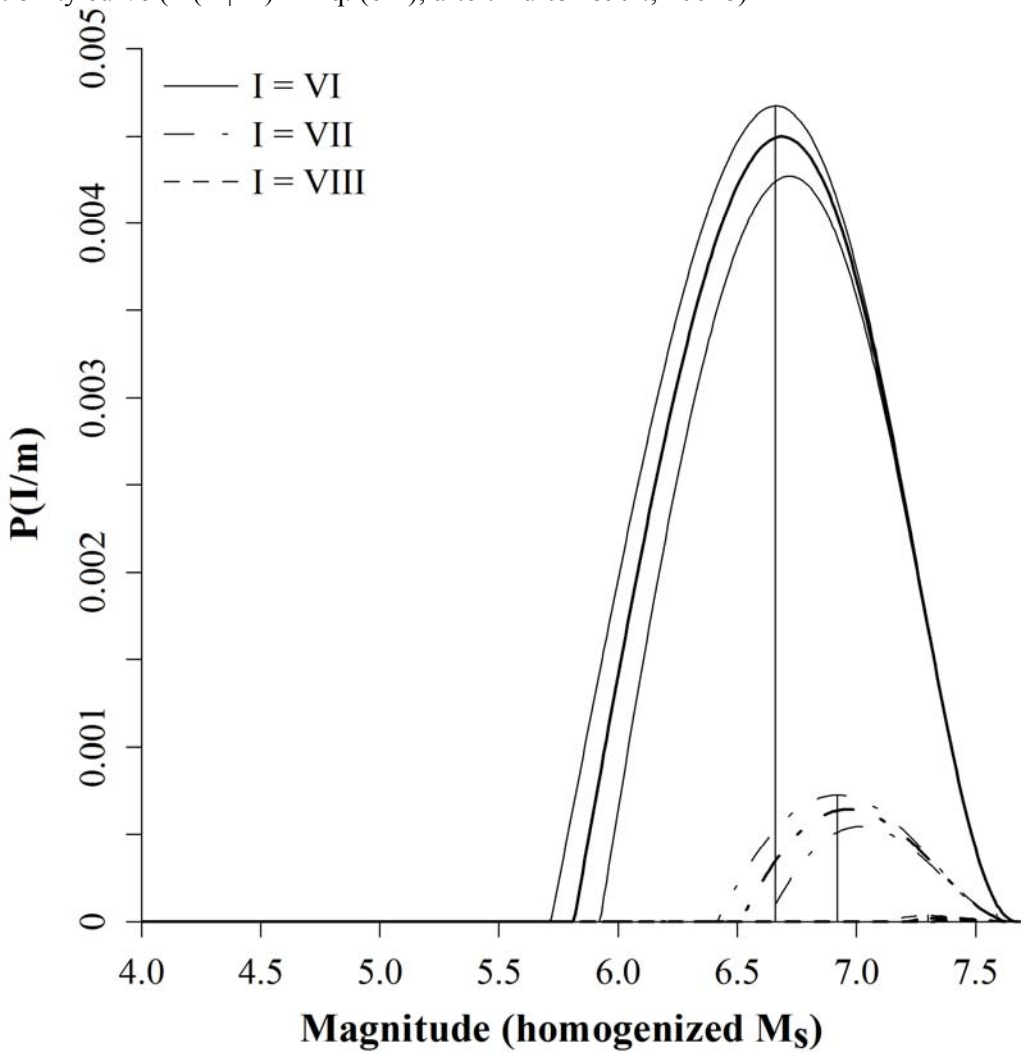

Figure 6.7 Earthquake macroseismic intensity perceptibility curves derived for intensity levels I = VI, VII and VIII. The vertical black lines are at the *most perceptible magnitude*, $M_{P(max)}$, for that particular level of ground motion (in this case, intensity)

$P_c(X)$ exhibits the opposite behaviour; $P_c(X) \rightarrow 1$ as M increases. Occurrences of small events have small probabilities of them being perceived; the probability of perceiving a large magnitude earthquake will be high. The resultant curve $P(X \mid M)$ 'falls away' after the *most perceptible magnitude*, $M_{P(max)}$, is reached at the peak of the curve, such that the bell-shaped curve in Figure 6.6(c) and Figure 6.7 is formed. The rate of this curve decay depends upon the ground motion model used and the seismicity of the tectonic regime considered. Modern ground motion models attempt to model site effects relevant to the region considered, e.g. *alluvium*, *soil*, *stiff soil*, or *rock* sites (listed in ascending order of 'stiffness') regardless of whether they forecast macroseismic intensity, ground acceleration or ground velocity. The *most perceptible magnitude*, $M_{P(max)}$, will increase – by varying amounts dependent upon the ground motion model adopted – for a nominal earthquake defined by a set magnitude and focal depth if the user considers increasing levels of ground motion.

Further, a set of curves describing a range of discrete, preselected ground motion levels will be nested and peak at $M_{P(max)}$ for each level of ground motion (Burton, 1990). These curves are 'nested' as lower probabilities are attached to higher levels of ground motion resulting from a given magnitude. Further, a set of $P(X \mid M)$ curves will be skewed towards higher magnitudes, such that $M_{P(max)}$ may increase for successive levels of ground motion X, dependent upon the form of the ground motion model used. The peak of a perceptibility curve is given by Eq. (6-2):

$$\frac{d\left[\left(X \middle| M\right)\right]}{dM} = 0 \tag{6-2}$$

This therefore defines the magnitude considered the '*most perceptible earthquake*' and constitutes a characteristic earthquake property for a region (Burton, 1990) due to its dependence on regional attenuation of the felt ground motion considered *and* the seismicity properties of the area.

A peak probability is achieved at $M_{P(max)}$ for each ground motion level. Peak probabilities for a suite of perceptibility curves derived for a range of ground motions (e.g. intensity VI, VII, and VIII) will decrease with increasing levels of ground motion (and therefore increasing $M_{P(max)}$). $M_{P(max)}$ associated to each peak probability is translated slightly to the right for each successive increment in ground motion. This translation of $M_{P(max)}$ is further enhanced right on the abscissa if a depth component function is introduced into the adopted ground motion model.

Curves exhibit an asymmetrical (or skewed) characteristic, falling away once a peak probability has been reached. Burton (1978b) attributes this to the effect from applying a $G^{(III)}$ distribution, and its near linear nature at intermediate magnitudes, but dropping away as a distribution tends towards its upper bound asymptote. This pattern may also occur if a *whole process* cumulative frequency-magnitude model is adopted. This form of magnitude occurrence distribution also shows a tendency to fall away at high and low magnitudes, resulting from under-reporting of small events and non-linear frequency of occurrence of larger events.

The behaviour of a set of peak perceptibility curves for a range of ground motions in relation to the maximum magnitude estimates from cumulative strain release techniques, M_3, and the upper bound magnitude of Gumbel's third distribution, ω, is illustrated in Figure 6.8. The curves $P_{(X-1)}$, $P_{(X)}$ and $P_{(X+1)}$ are probability curves relating to three discrete levels of ground motion, X (where $P_{(X)}$ is the middle level of ground motion considered). The discrete magnitude values $M_{P(X-1)}$, $M_{P(X)}$ and $M_{P(X+1)}$ represent the *most perceptible magnitude* for each perceptibility curve and are associated by the notation's suffix. It is evident from Figure 6.8 that when Gumbel's extreme values distribution is used as the statistical magnitude recurrence model, ω is a high-magnitude cut-off to each perceptibility curve $P(X \mid M)$ regardless of X and nominal focal depth, due to this distribution model having its own upper limit. M_3 from cumulative strain energy release statistics, being of finite waiting time, can be expected to be situated in between all instances of $M_{P(max)}$ (to the left) and ω on the abscissa of these plots (green line).

6.3.2 Integrated perceptibility

Magnitude perceptibility theory provides a basis with which to determine the probability of experiencing an earthquake of given magnitude, M, at a specified level of ground motion, X, such that Eq. (6-1) holds true. Integrated perceptibility however, provides the probability of a specific level of *perceptible* ground motion due to all earthquakes over the magnitude range extending from -∞ to a magnitude M_i, such that, after integrating the perceptibility curves through $-\infty \leq M \leq M_i$, using small intervals of this range (dM; Burton, 1981, 1990), one will obtain:

$$P_{ip}\left(X \mid M \leq M_i\right) = \int_{-\infty}^{M_i} P_p\left(X \mid M\right).dM \tag{6-3}$$

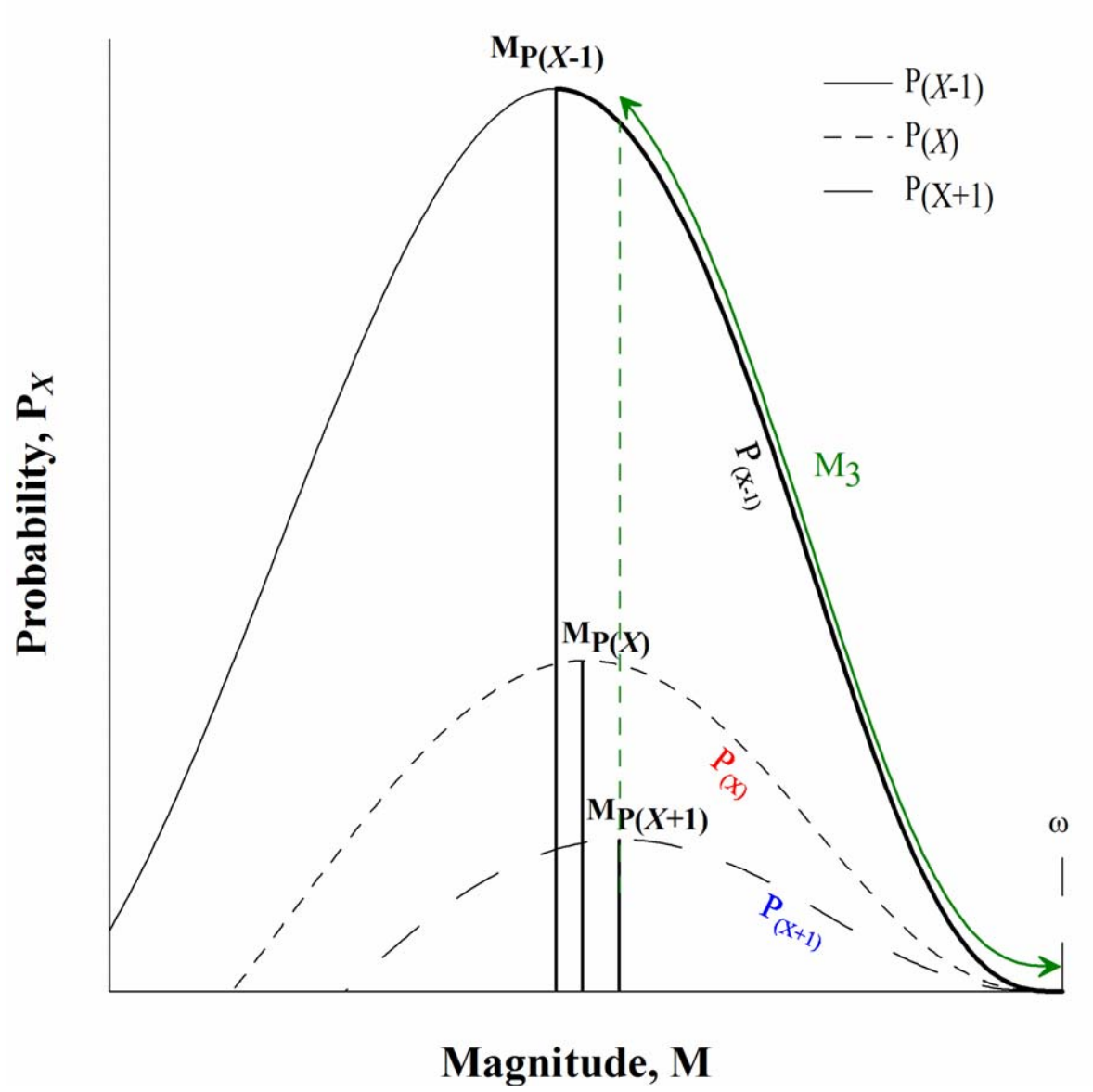

Figure 6.8 Relationship between the upper bound magnitude estimate M_3 the upper bound magnitude of Gumbel's third asymptotic extreme values distribution ω, and earthquake perceptibility curves for discrete values of a strong ground motion

This will constitute the annual probability of exceedance. Integration over the range $-\infty \leq M \leq M_i$ need only really consider intermediate magnitudes. Small magnitudes contribute negligible levels of perceptible hazard and the largest magnitudes approaching ω are rare. Contributions from intermediate magnitudes will determine the extent and gradient of the inflexion of the P_{ip} curve.

The value of P_{ip} at a specific level of ground shaking would then be obtained when the integration reaches $M = \omega$. This may be repeated for different levels of ground motion. Principles applied to magnitude perceptibility analysis, that a peak (or in this case, a specific) probability and magnitude can be obtained for a given site after considering attenuation using a selected ground motion law and regional seismicity combined with a magnitude recurrence model, can also be applied to integrated perceptibility for a range of discrete ground motion levels.

The difference in these two methods lies in the idea of *partitioned risk*. That is, considering probabilities of occurrence or exceedance only at discrete magnitudes versus over a defined magnitude interval. Perceptibility hazard at discrete levels of ground motion is examined under constraints of earthquake perceptibility. Integrated perceptibility effectively removes this partitioning. Thus, probabilities of occurrence or exceedance are relevant over a range of adjacent magnitudes. Two key ideas are observed using integrated perceptibility:

1. Probabilities associated to low magnitudes are negligible due to felt areas resulting from small magnitudes being small, and;

2. The probability of experiencing larger magnitude earthquakes become smaller as $M \rightarrow \omega$ due to the diminishing likelihood of these events occurring.

The annual probability of perceiving different levels of ground motion are obtained by integrating perceptibility curves throughout the magnitude range. In practice, integrated perceptibility possesses a lower limit characteristic that relates directly to either the magnitude of the smallest felt earthquake, or, a lower magnitude threshold, M_t, if one is applied to the catalogue used.

A practical *scenario* of integrated perceptibility (and perceptibility hazard) is considered for Sofia in sections 6.5.1 to 6.5.3 for each ground motion characteristic considered.

6.3.3 Previous work on earthquake perceptibility

Earthquake perceptibility is just one concept within the broader remit of seismic hazard and has been mentioned in some previous work (e.g. Azzaro and Barbano, 1995; Ambraseys and Adams, 1998; Musson, 1998; Gutdeutsch and Hammerl, 1999; Ambraseys, 2002; Dolce *et al.*, 2003). However, these examples are generally limited to quoting one-off estimates for the perceptible area resulting from a *scenario* earthquake for the ground motion characteristic reviewed and usually do not exploit the concept either analytically or graphically.

Although Burton (1978b, 1981) and Burton *et al.* (1983) set out the theory of – and example applications for – earthquake perceptibility, the geographic regions considered are seismically and geographically disparate to the Balkan extent of interest here. Recent work of Burton *et al.* (1984), Koravos *et al.* (2003) and Burton *et al.* (2004b) are more relevant to this study and are noteworthy as they consider earthquake perceptibility for geographic and seismotectonic regimes located closer to the catalogued area considered here, have compatible underlying aims or similar methodology.

Adoption by Koravos *et al.* (2003) of the same ground motion models from Theodulidis and Papazachos (1992) for peak ground acceleration and velocity ground motion models brings further compatibility between both studies. This is in addition to forecasting intensity-based perceptibility hazard. After applying this work to the 16 seismogenic regions of Holt *et al.* (2000), they suggest most of these 16 regions exhibit a *characteristic earthquake distribution* where $M_{P(max)}$ is equal to the maximum magnitude earthquake. Koravos *et al.* suggest a link between the seismotectonic nature of the area and regional variation of $M_{P(max)}$ by suggesting these magnitudes are located in the fastest-deforming region. Estimates are systematically lower to the west of the Aegean Sea region than the east, away from the high seismic activity of North Anatolian Fault. Their geographic area of interest is also close to that of this study. Due to strong parallels between Koravos *et al*. and this work a fuller discussion and comparison between them both will be made throughout section 6.5.

6.4 Seismic hazard disaggregation

Earthquake perceptibility is a form of hazard disaggregation reliant upon frequency of occurrence and probabilities of seismicity within a given area, and the likelihood specific levels of ground motion will arise from them. However, if a user needs to consider many levels of ground motion in a single instance it is constrained to consider only a single dimension of probability estimates in relation to magnitude.

For example, Figure 6.6 and Figure 6.7 considers earthquake perceptibility over a range of ground motions, but this consolidates the considered region's seismicity into just three perceptibility hazard curves, and three associated *design* earthquakes. It cannot consider and graphically represent geographic hazard across a broad seismotectonic regime. Earthquake perceptibility is hazard disaggregation with respect to magnitudes and their probabilities of occurrence. Conversely, contouring earthquake perceptibility is restricted to illustrating a single level of perceptibility hazard, but incorporates a visually broader geographic and seismotectonic review of this hazard.

Geographic disaggregation of seismic hazard is explored by McGuire (1995), Cramer and Petersen (1996), Bazzurro and Cornell (1999), Harmsen *et al.* (1999) and Harmsen and Frankel (2001) with respect to probabilistic ground motion hazard for various regions, and is another form of partitioned seismic hazard available to earthquake engineers. Seismic hazard disaggregation enables users to determine dominant sources of hazard within an area, and therefore provide alternative, realistic *scenario* or *design* earthquakes to those offered by earthquake perceptibility analysis, such as magnitudes at 10% probability of exceedance in 50 or 100 years at spectral accelerations of 0.2- and 0.3-sec (Cramer and Petersen, 1996; Harmsen *et al.*, 1999).

Geographic hazard disaggregation classifies contributions to the prevailing hazard at a point from near- and far-field tectonic regimes in terms of location (source-to-site azimuth, θ, and distance), magnitude and ground motion uncertainty. Magnitudes and epicentral distances for catalogued earthquakes in a known region are grouped together into pre-defined magnitude and distance intervals, covering the region's magnitude range and area of interest, in a process called *binning*.

Disaggregating a geographic region around a site of interest in such a manner allows one to determine the relative contribution of discrete geographic zones to the ground motion or magnitude hazard at a point or area using *binned* magnitude intervals, instead of a single discrete magnitudes. This can then be related to different time intervals and return periods for a specific real-time *scenario* (whether that is a lifeline infrastructure such as an oil or gas pipeline, critical buildings such as dams or nuclear power plants, or a specific urban centre, where each are concerned with different hazard return periods).

Binning magnitudes in this fashion and generalising earthquakes to standard statistics of magnitudes and distances based upon the content of these *bins* does however raise problems when deaggregating hazard in this fashion. The modal value can be used instead when the mean magnitude-distance distribution does not contribute a significant amount to the hazard. Although mean statistics provide usable summaries of magnitude seismicity, they do not describe the most likely earthquake magnitude or epicentral distance leading to defined levels of ground motion.

The mean magnitude may also not have physically occurred in the particular hazard cell to which it is calculated for. However, a number of previous authors (e.g. Chapman, 1995; Cramer and Petersen, 1996) show that taking modal estimates are not without risk as this value is reliant upon *bin* details (e.g. number of *bins*, *bin* size and increment), so bias results in favour of particular magnitudes. Adopting either statistical magnitude measure will therefore incur their individual pitfalls.

Limitations in geographic hazard disaggregation may also be experienced when and if magnitude conversions are required and used. Modern earthquake catalogues typically report on either the M_w or M_s magnitude scale depending upon their end need. After converting input magnitudes, a given *bin* size of resultant magnitudes may be the net result of a varied number of input magnitude increments and/or output magnitude calculations.

Sofia is explored later in this chapter as a site-specific *scenario* to consider its disaggregated seismogenic source. Discrete contributions to seismic sources will be investigated to determine those that dominate contribution to its prevailing seismic hazard. This will be based on the earthquake catalogue developed for this study and components of the probability density function (that is, Figure 6.6(a), the $P_e(M)$ component to the city's perceptibility curves) being classified in binned magnitude and distance classes using a joint magnitude-distance distribution.

6.5 Regional earthquake perceptibility hazard

The following sections discuss earthquake perceptibility hazard for the broad Balkan region, the political triple junction area, and the same urban centres for which extreme earthquake hazard and energy release statistics have already been considered. This will be done with respect to ground acceleration, velocity and macroseismic intensity. Before earthquake perceptibility hazard can be assessed, the levels of ground motion to be considered need to be defined and justified. Table 6.2 summarises these decisions for this work in light of previous studies and accepted definitions.

Perceptibility and integrated perceptibility curves are used to convey the level of perceived ground motion hazard for each urban centre considered. Sofia continues as a case study adopting *part process* seismicity plotted in Figure 5.15, with the remaining cities detailed in Appendices 18, 22 and 26 (using seismicity illustrated in Appendix 4).

- The topmost curve in each trio of curves in each perceptibility and integrated perceptibility plot represents the lowest level of ground motion (i.e. a = 50 cm s^{-2}, v = 5 cm s^{-1}, I = VI)

<table>
<tr><th>Ground motion</th><th>Range (increment)</th><th>Justification</th></tr>
<tr><td>Acceleration (cm s^{-2})</td><td>50 → 150 (50)</td><td>A number of previous studies correlate required intensity levels of interest to similar levels of ground acceleration e.g.:
<table>
<tr><th colspan="3">Intensity level</th><th></th></tr>
<tr><th>VI</th><th>VII</th><th>VIII</th><th>Source</th></tr>
<tr><td>12</td><td>50</td><td>144</td><td>Ishimoto (1932)</td></tr>
<tr><td>44</td><td>89</td><td>190</td><td>Kawasumi (1951)</td></tr>
<tr><td>47.9</td><td>128.8</td><td>346.7</td><td>Hershberger (1956)</td></tr>
<tr><td>64</td><td>130</td><td>265</td><td>Neumann (1954)</td></tr>
<tr><td>30</td><td>64</td><td>138</td><td>Richter (1958)</td></tr>
<tr><td>25-50</td><td>50-100</td><td>100-200</td><td>Medvedev and Sponheuer (1969)</td></tr>
<tr><td>21-44</td><td>44-94</td><td>94-202</td><td>JMA (Okamoto, 1973)</td></tr>
<tr><td>66</td><td>126</td><td>251</td><td>Trifunac and Brady (1975; for horizontal acceleration)</td></tr>
<tr><td>45</td><td>83</td><td>166</td><td>Trifunac and Brady (1975; for vertical acceleration)</td></tr>
<tr><td>25-50</td><td>50-100</td><td>100-200</td><td>Willmore (1979)</td></tr>
</table>
Correlated peak ground accelerations (in cm s^{-2}) by selected previous studies</td></tr>
<tr><td>Velocity (cm s^{-1})</td><td>5 → 15 (5)</td><td>A number of previous studies correlate required intensity levels of interest to similar levels of ground velocity e.g.:
<table>
<tr><th colspan="3">Intensity level</th><th></th></tr>
<tr><th>VI</th><th>VII</th><th>VIII</th><th>Source</th></tr>
<tr><td>7.57</td><td>16.48</td><td>18.95</td><td>Trifunac and Brady (1975)</td></tr>
<tr><td>4</td><td>18</td><td>16</td><td>Medvedev (1977)</td></tr>
<tr><td>0.6-0.8</td><td>1.0-1.2</td><td>2.1-2.5</td><td>Panza et al. (1997)[1]</td></tr>
<tr><td>8.1-16</td><td>16-31</td><td>31-60</td><td>Wald et al. (1999b)</td></tr>
</table>
Correlated peak ground velocities (in cm s^{-1}) from selected previous studies
Recent EC-COPERNICUS projects[2] forecast PGV for Bulgaria of ~4.0 → 60 cm s^{-1}.</td></tr>
<tr><td>Intensity (I)</td><td>VI → VIII (I)</td><td>VI is the threshold of damage to structures, as defined by EMS-98 intensity scale (Grünthal, 1998);
VII is threshold of damage to reinforced structures;
VIII represents onset of more severe damage.</td></tr>
</table>

[1] First value is for PGV versus *ISG* data. The second value is for PGV versus *ING* data. See text for fuller detail

[2] "Quantitative Seismic Zoning Of The Circum Pannonian Region (QSEZ-CIPAR)" and 'Earthquake hazard associated to the Vrancea region seismicity" and "Microzonation of Bucharest, Russe and Varna cities in connection with Vrancea Earthquakes"

Table 6.2 Justification for selected levels of ground motion considered for earthquake perceptibility hazard

- The central curve in each trio of curves in each perceptibility and integrated perceptibility plot represents the represents the middle level of ground motion (i.e. a = 100 cm s^{-2}, v = 10 cm s^{-1}, I = VII)

- The lower curve in each trio of curves in each perceptibility and integrated perceptibility plots represents the represents the highest level of ground motion (i.e. a = 150 cm s^{-2}, v = 15 cm s^{-1}, I = VIII)

The vertical dashed line on each plot is at M_3. The three vertical black lines on each plot are at the *most perceptible magnitude* for an earthquake of 10 km focal depth (i.e. the shallowest focal depth of the seismicity regime considered; Figure 2.14) for each level of each ground motion, as illustrated in Figure 6.8. The abscissa of each plot extends over the magnitude range $4.0 \leq M_s \leq \omega$. ω is the upper bound magnitude estimate to Gumbel's third extreme values distribution (Table 5.7(a)). This was derived from the seismicity present within a 2° half-width cell centred on each city after fitting Gumbel's third extreme values distribution to earthquake extreme data extracted using a site-specific extreme interval (NPER) and cut-off magnitude (M_{CUT}) for the time interval 1900 to 2004. In this situation ω should be related to the cellular region considered around each city, not specifically at the city itself.

Finally, where possible and practical to do so through section 6.5, emphasis is given to comparing these results with Koravos *et al.* (2003) for estimates of $M_{P(max)}$. It is important to remember when viewing comparison tables between these studies that Koravos *et al.* only provides one estimate for each seismogenic zone examined. With the smallest zone spanning approximately 1.5° of latitude and 3° longitude, each of the six zones considered cover large geographic areas, and span many hazard computation nodes and intervals of contoured forecast magnitude hazard in each regional hazard map developed here. Consequently, equivalent ranges for $M_{P(max)}$ are given for the ground motion models used in this work instead of discrete values. This is reflected in tables where $M_{P(max)}$ 'ranges' are given (i.e. '*in the range*' from X $\rightarrow$ Y). Specific zones of interest have geographic labels attached to further aid reader understanding; refer to Figure 2.17(b) for further clarification.

Cut-off magnitudes of 5.3 M_s and 5.5 M_s were selected (section 5.3.13) to develop extreme hazard estimates for southwest Bulgaria and the broader Balkan area respectively. The mean focal depth in the adopted catalogue for both these magnitudes is approximately 21 km (Figure 2.14), but this starts to decrease at higher magnitudes to never shallower than 10 km (mean focal depth at 6.9 M_s is 10.4 km). Seventy eight per cent of the catalogue has a focal depth of 21 km or less.

Therefore, contoured maps of earthquake perceptibility hazard will illustrate for a nominal earthquake of 15 km focal depth, while perceptibility and integrated perceptibility curves are presented for nominal focal depths of 10 km, 15 km and 20 km. These focal depths are physically realisable within the constraints of the adopted catalogue and are considered to best represent the regional seismogenic regime as the minimum, median and maximum mean focal depths in the catalogue at which the higher magnitudes that were used to develop extreme hazard estimates occur in (highlighted by the yellow hypocentre spheres in Figure 5.13, Figure 5.14, Figure 5.15 and Appendix 4).

6.5.1 Ground acceleration

The *most perceptible magnitudes* across the broad Balkan region – at ground accelerations of 50, 100 and 150 cm s^{-2} using Theodulidis and Papazachos (1992; $TP92_A$) for stiff soil conditions at the 50^{th} percentile are given in Figure 6.9(a)-(c) for a nominal focal depth of 15 km. Mention will also be made to the new ground acceleration model of Ambraseys *et al*. (2005; AM05) to afford an updated interpretation of perceptibility seismic hazard with respect to ground acceleration.

Theodulidis and Papazachos (1992) will generally forecast higher values for $M_{P(max)}$ than Ambraseys (1995). This is reasonable to expect as forecasts developed after allowing for depth control in Ambraseys' PGA model are typically more conservative than those derived from Theodulidis and Papazachos (1992). This concern has already been discussed earlier in the text and by Burton *et al.* (2003). Discussion of estimates for $M_{p(max)}$ from here on will tend to concentrate on those developed from $TP92_A$.

Three distinct areas of *most perceptible magnitudes* are seen in Figure 6.9. Firstly, a central zone of high perceptible magnitude hazard loosely bounded by 23°-26°E extends north-south across almost the entire area of interest, roughly approximating to west and central Bulgaria, northeast Greece and the north Aegean. This zone is dominated by estimates for $M_{P(max)}$ of 7.50 M_s at accelerations of 50 cm s^{-2}. Secondly, as ground motion increases to 150 cm s^{-2} a confined pocket of higher hazard delineated by the 7.75 M_s contour emerges in west-central Bulgaria centred on Sofia. Finally an outer belt of lower perceptible hazard appears in the west of the region and extends to cover Albania, northwest FYR of Macedonia, Yugoslavia and northwest Greece, and never exceeds 7.00 M_s.

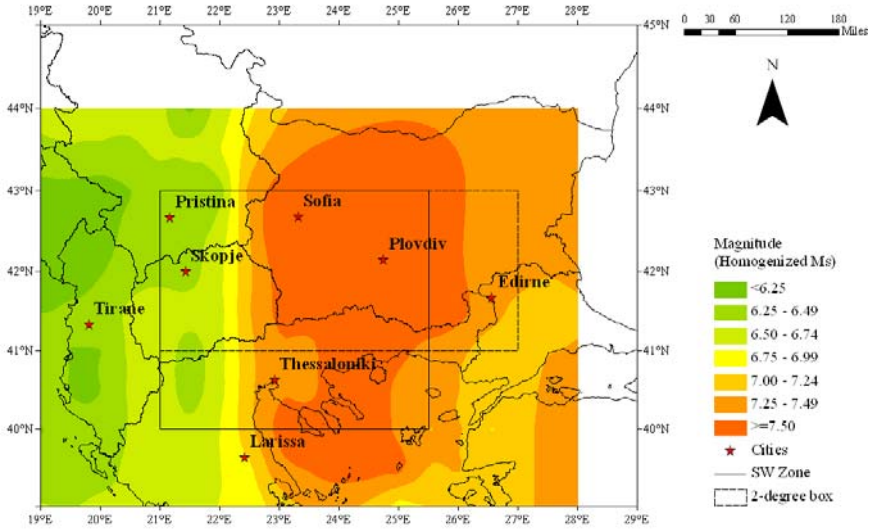

(a)

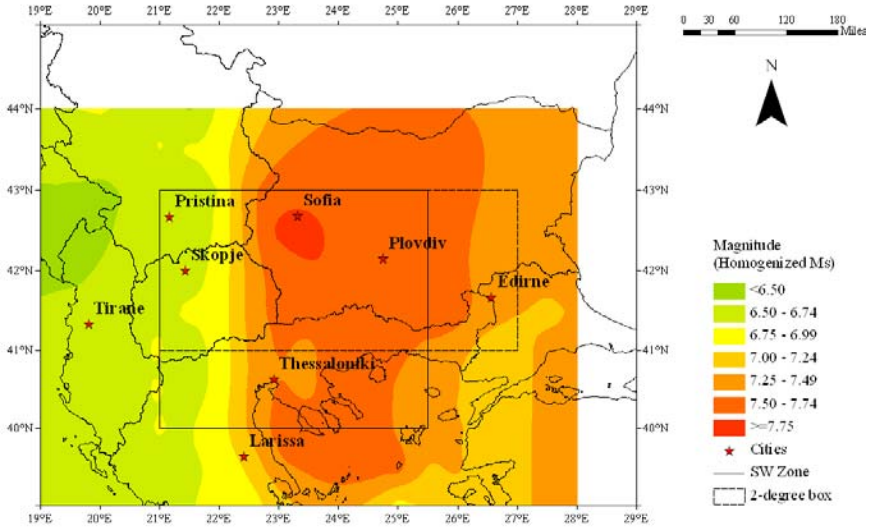

(b)

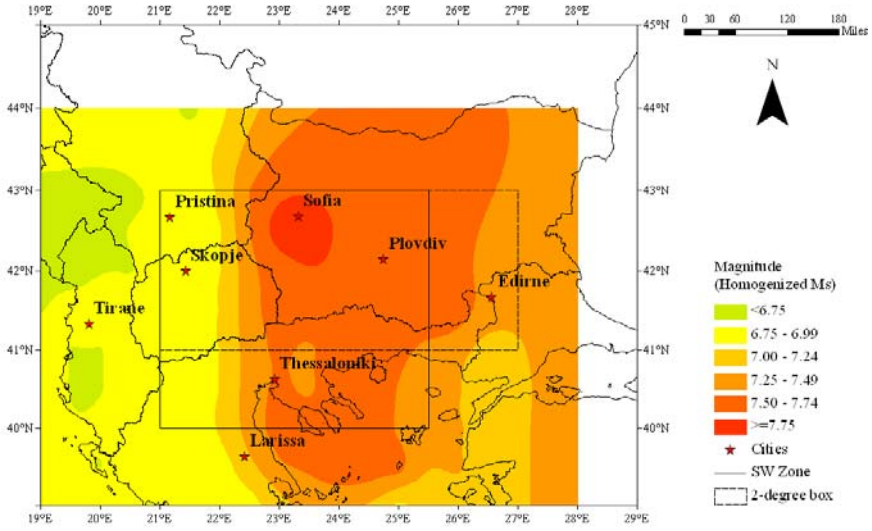

(c)

Figure 6.9 *Most perceptible magnitude* with respect to horizontal ground accelerations of (a) 50, (b) 100 and (c) 150 cm s^{-2} using Theodulidis and Papazachos (1992) for stiff soil conditions at the 50^{th} percentile for a nominal earthquake of 15 km focal depth. Contours are at intervals of 0.25 M_s

Koravos *et al.* (2003) assess earthquake perceptibility at an acceleration of 0.2 g for a nominal earthquake of 10 km focal depth. The closest comparison that can be made between those tectonic zones and this work is considering accelerations of 150 cm s^{-2} for an earthquake of the same nominal focal depth. Differences in forecast $M_{P(max)}$ are summarised in Table 6.3. Zone 14 is of most interest here, as it loosely covers the region of the political triple junction of Bulgaria, Greece and FYR of Macedonia. It approximates to a rectangular region bounded by the 22ºE, 25ºE meridians and 40.5ºE, 42.5ºN parallels. Comparable contoured perceptible hazard for this smaller region is in Figure 6.10 for a depth of 10 km. Figure 6.11(a)-(c) illustrate acceleration perceptibility hazard in southwest Bulgaria using Theodulidis and Papazachos (1992) for a nominal earthquake of 15 km focal depth. Koravos *et al.* assign only one perceptible magnitude estimate with respect to ground acceleration to this region of 7.1 M (± 0.2).

Seismogenic source zone[1] used by Koravos *et al.* (2003)	Ground acceleration perceptibility model	
	Koravos *et al.* (2003)[2]	This study; $TP92_A$[3, 4]
9 [east mainland Greece]	6.1 (± 0.1)	6.75 → <7.50
10 [north Aegean Sea]	6.2 (± 0.1)	7.00 → <7.75
11 [west Marmara Sea]	7.6 (± 0.2)	7.25 → <7.50
13 [Albania-Greece-FYROM border]	6.7 (± 0.2)	6.75 → <7.50
14 [Bulgaria-Greece-FYROM border]	7.1 (± 0.2)	7.25 → 7.75+

[1] Geographic labels have been attached in this text for benefit of the reader to provide a geographic reference. Refer to Figure 2.17(b) for further clarification; [2] Estimates for $M_{P(max)}$ at 0.2 g for a nominal earthquake of 10 km focal depth; [3] Estimates at 150 cm s^{-2} for a nominal focal depth of 10 km; [4] As seismogenic zones of Koravos *et al.* (2003) cover a wide geographic extent, it is not possible to assign a single comparable magnitude estimate from this study. Comparable estimates are given '*in the range*' from X → Y

Table 6.3 Empirical differences in forecasted *most perceptible magnitudes* for specific ground accelerations between regions common between Koravos *et al.* (2003) and this study

Koravos *et al.* forecast systematically lower perceptibility magnitudes for comparable zones than both laws considered here. Forecasts of Koravos *et al.* tend to be in the lower half [of the $M_{P(max)}$ range forecast here] or below the perceptible magnitude range forecast using Theodulidis and Papazachos (1992); some are substantially lower, by as much as ¾ magnitude unit. In two of the five areas compatible between both studies, Koravos *et al*. forecasts significantly lower estimates, by as much as one magnitude unit. Forecasts from Koravos *et al*. for the west Marmara Sea zone exceed that of this study; the Albania-Greece-FYROM border zone is within the range of forecasts from this study, whilst the three others are significantly lower and outside the perceptible magnitude ranges of this study.

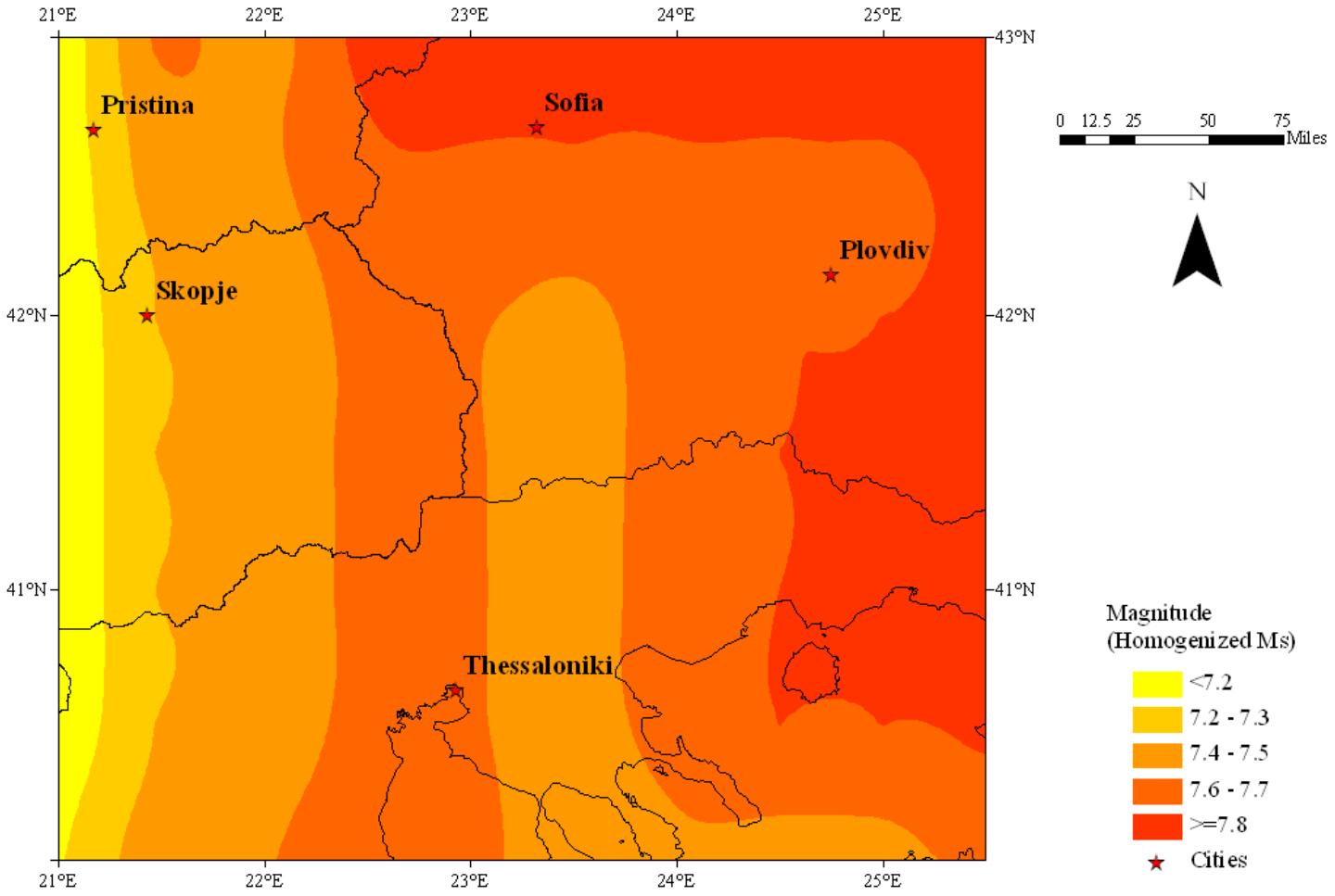

Figure 6.10 The *most perceptible magnitudes* in southwest Bulgaria for a ground acceleration of 150 cm s^{-2} and a nominal focal depth of 10 km using Theodulidis and Papazachos (1992) for stiff soil conditions at the 50th percentile. Contours are at intervals of 0.2 M_s

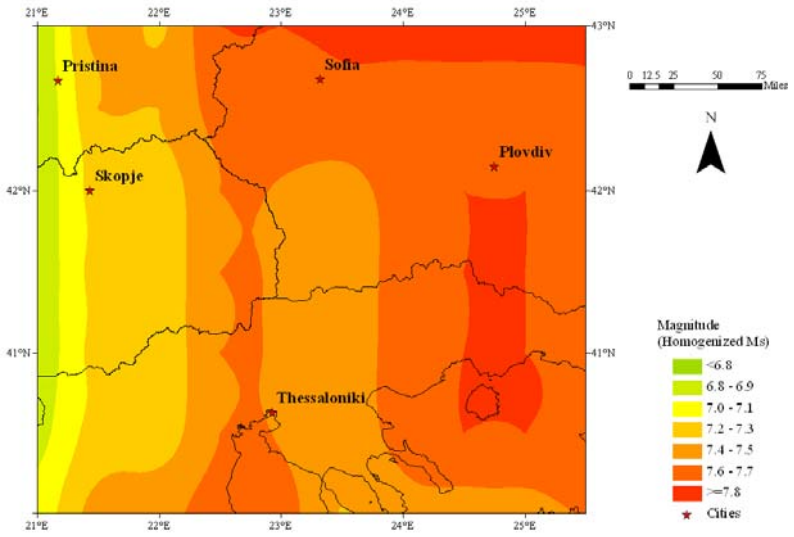

(a)

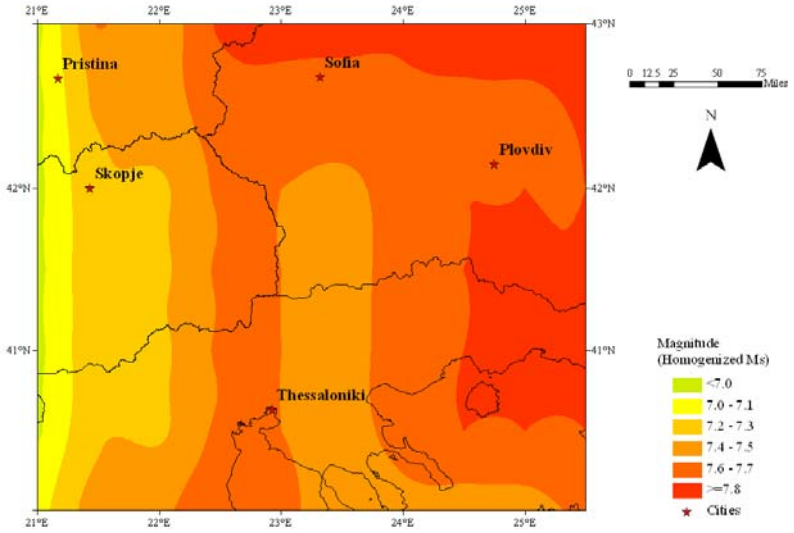

(b)

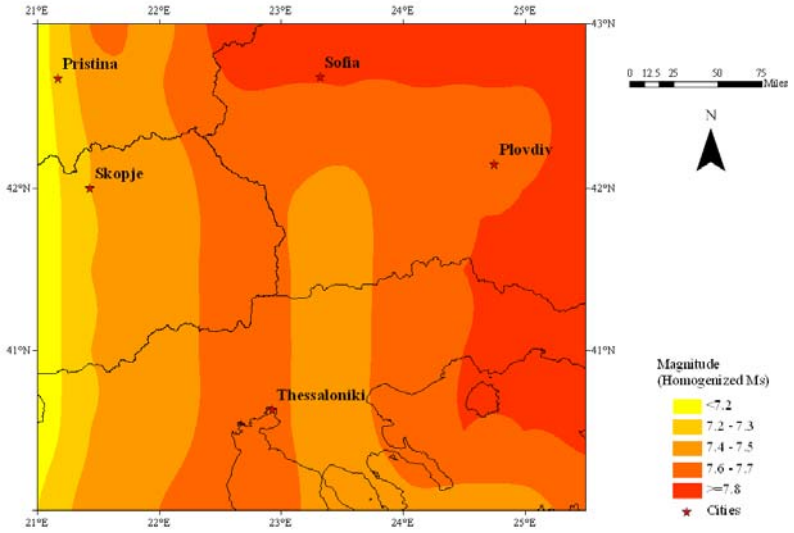

(c)

Figure 6.11 The *most perceptible magnitude* with respect ground accelerations of (a) 50, (b) 100 and (c) 150 cm s^{-2} using Theodulidis and Papazachos (1992) for stiff solid conditions at the 50th percentile for a nominal earthquake of 15 km focal depth. Contours are at intervals of 0.2 M_s

Forecasts that are significantly lower than this work are located over the mainland Greece-Bulgaria border region. Zones with estimates that are more compatible with this study exist at the two extremes of this region. However, as ground accelerations considered by both studies are different, due to concerns over *cell saturation* (section 6.7) it would be inappropriate to attach too much dependence on one aspect of the local seismicity of either evaluation for producing these empirical perceptibility estimates. Discussion of variability between Koravos *et al*. and this work will be reserved for ground velocity and macroseismic intensity perceptibility hazard as comparisons are more directly comparable.

Contoured hazard using Theodulidis and Papazachos (1992) have a high hazard zone located in the extreme east and north of the region and is characterised by lower hazard to the extreme east in central and east FYR of Macedonia. Theodulidis and Papazachos (1992) forecasts systematically higher perceptible hazard than Ambraseys (1995), which is likely due simply to the former relation forecasting noticeably higher ground motions in the near field than that of Ambraseys (sections 3.8.2 and 3.10; Burton *et al.*, 2003).

The *most perceptible magnitudes* for the area approximately covering the Bulgaria-Greece-FYROM border are in the range $M_{PA(150)} = 7.2 \rightarrow 7.8+$ using Theodulidis and Papazachos (1992) respectively (Figure 6.11). Tectonic zones governed estimates of Koravos *et al.* (2003). The Serbomacedonian massif runs directly through this region, and is the main source of its seismicity, shown by the epicentral distribution between Limnos, Thessaloniki and Blagoevgrad. So, if one acknowledges the slight difference between these analyses and ensuing hazard illustrations in terms of ground motions and focal depths considered, Figure 6.10 and Figure 6.11(c) suggests here that a zoned hazard analysis such as that adopted by Koravos *et al.* yields comparable results to those of a zone-free analysis adopted here as they both return similar perceptible magnitude hazard results.

Peak perceptibility and integrated perceptibility curves for Sofia using Theodulidis and Papazachos (1992) are in Figure 6.12, while curves for other cities considered are in Appendix 18. Estimates for $M_{p(max)}$, their associated peak probabilities and annual probabilities of occurrence at $M_{p(max)}$ for ground accelerations of 50 cm s^{-2}, 100 cm s^{-2} and 150 cm s^{-2} are in Table 6.4.

Accelerations of 50 cm s^{-2} are most likely to arise around Sofia from an $M_{PA(50)} = 7.70$ M_s using Theodulidis and Papazachos (1992) with a risk level of $P_{PA(50)} \approx 24.7\times10^{-3}$ per year, rising to $M_{PA(150)} = 7.72$ M_s at ground accelerations of 150 cm s^{-2}. Sofia can reasonably expect an earthquake of magnitude 6.5 M_s approximately every 4 years (so estimating 24 to 25 exceedances in a 100-year time interval; Table 5.8), a 7.0 M_s earthquake about every 10 years (10 to 11 exceedances), and a magnitude 7.5 M_s event about every 19 years (5 to 6 exceedances).

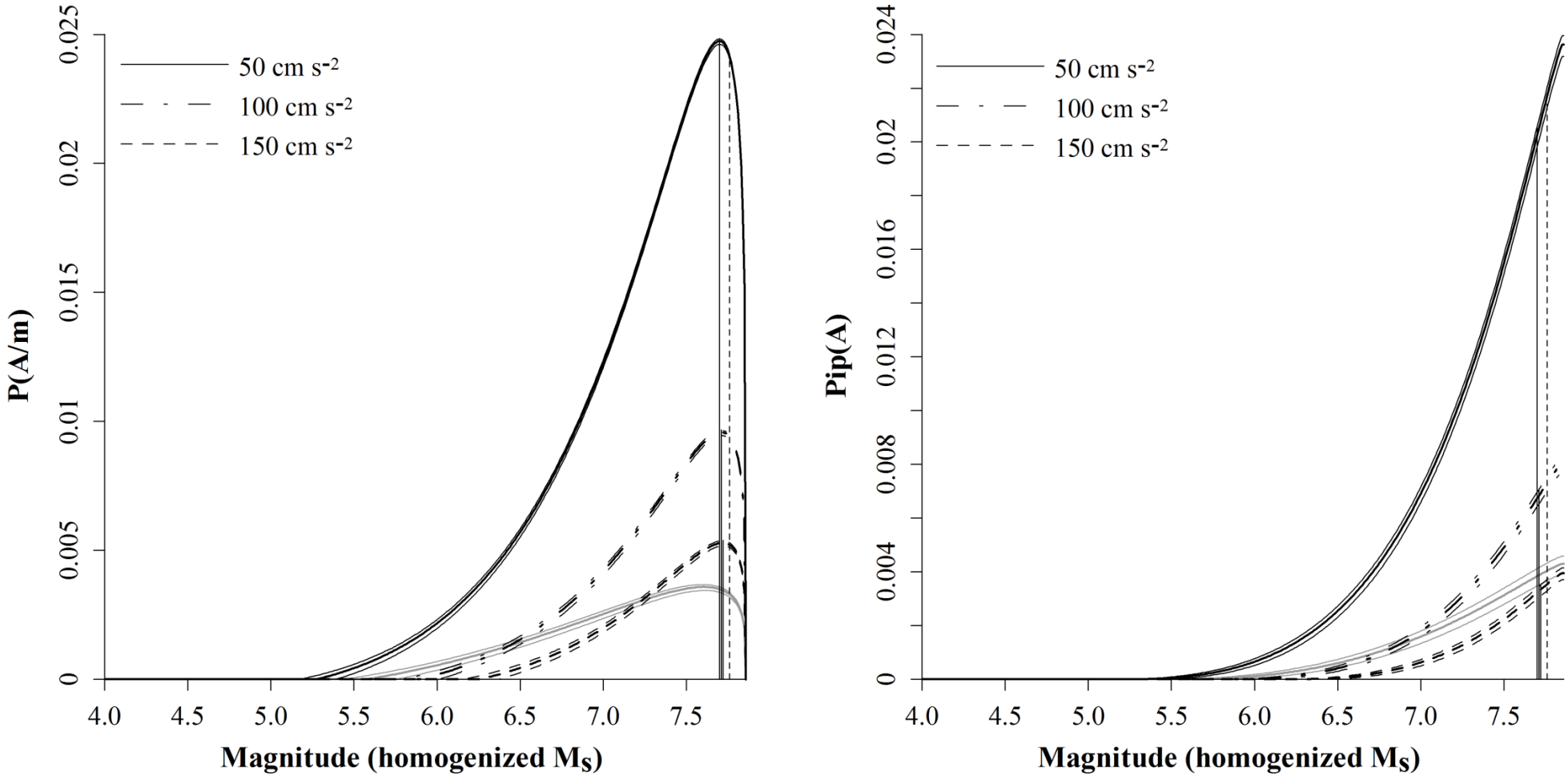

Figure 6.12 Ground acceleration (a) perceptibility and (b) integrated perceptibility curves for Sofia using Theodulidis and Papazachos (1992) for stiff soil conditions at the 50th percentile. The central heavy black curve of each set of three curves represents a nominal earthquake of 15 km focal depth, while the upper and lower curves represent 10 km and 20 km focal depth respectively. The grey sets of curves represent an earthquake of these focal depths from Ambraseys *et al*. (2005) for 50 cm s^{-2} only. Vertical black lines represent the *most perceptible magnitude* only for 10 km focal depth. The vertical dashed line represents M_3 from cumulative strain energy release techniques

	Horizontal ground acceleration (cm s^{-2})																	
	AM95_WDC									$TP92_A$ (S = 0.5, P = 0)								
	50 cm s^{-2}			100 cm s^{-2}			150 cm s^{-2}			50 cm s^{-2}			100 cm s^{-2}			150 cm s^{-2}		
City	$M_{P(max)}$[1]	P_p[1,2]	P_{ip}[1,3]	$M_{P(max)}$	P_p	P_{ip}	$M_{P(max)}$	P_p	P_{ip}	$M_{P(max)}$	P_p	P_{ip}	$M_{P(max)}$	P_p	P_{ip}	$M_{P(max)}$	P_p	P_{ip}
Edr	7.23	9.1	10.5	7.30	1.9	1.4	7.39	0.5	0.2	7.34	19.4	15.7	7.36	7.2	4.8	7.38	3.8	2.1
Lar	6.74	7.6	9.2	7.01	1.4	1.0	7.29	0.3	0.1	7.08	13.2	12.3	7.16	4.8	3.4	7.24	2.4	1.4
Plo	7.53	6.8	8.6	7.59	1.5	1.3	7.68	0.5	0.3	7.67	16.8	15.4	7.68	6.5	5.1	7.70	3.6	2.4
Pri	6.02	9.6	8.5	6.54	1.1	0.5	7.01	0.1	<0.1	6.44	10.7	7.5	6.65	3.0	1.5	6.81	1.2	0.5
Sko	5.99	11.4	9.7	6.53	1.3	0.6	7.04	0.1	<0.1	6.43	12.4	8.7	6.65	3.5	1.7	6.83	1.4	0.6
Sof	7.63	9.7	11.2	7.66	2.1	1.8	7.71	0.7	0.4	7.70	24.7	20.2	7.71	9.6	6.8	7.72	5.3	3.3
The	7.32	9.4	11.9	7.42	2.0	1.8	7.55	0.6	0.3	7.50	21.3	19.6	7.53	8.0	6.3	7.56	4.3	2.9
Tir	6.38	10.8	10.9	6.68	1.5	0.8	7.01	0.2	<0.1	6.66	14.7	11.0	6.77	4.6	2.4	6.87	2.0	0.8

[1] Estimates are given for an nominal earthquake with focal depth of 15 km. Probabilities are given at a factor of $\times 10^{-3}$; [2] Annual probability of perceiving ground motion arising from magnitude $M_{P(max)}$; [3] Annual probability of perceiving ground motion arising from all magnitudes up to and including $M_{P(max)}$

Table 6.4 The *most perceptible magnitude*, $M_{P(max)}$, with respect to horizontal ground accelerations of 50 cm s^{-2}, 100 cm s^{-2} and 150 cm s^{-2}, with the associated perceptibility probability, P_p and the annual probability of exceedance, P_{ip}, of perceiving these ground accelerations for urban centres considered. Estimates are derived from the distribution of seismicity present within a 2° half-width cell of the city are given, using the conditions outlined in section 5.3 using Theodulidis and Papazachos (1992) for stiff soil conditions at the 50th percentile for a nominal earthquake of 15 km focal depth

Data used to develop these estimates support the forecasts if one considers the catalogue's homogenized M_s magnitude estimates. The catalogue contains 27 events ≥6.5 M_s (so slightly underestimated), 10 earthquakes with 7.0 M_s (so approximating to a correct estimation) and one of ≥7.5 M_s (so slightly overestimated) during the catalogued time interval using this homogenized magnitude scale.

Introducing the ground motion model of Ambraseys *et al.* (2005) does not bring any major increase in estimated ground acceleration magnitude perceptibility hazard. On all figures (including those in Appendix 18) the model estimates significantly lower probability hazard for equivalent magnitude points than both older generation models considered by as much as 80% using $TP92_A$ when considering Sofia as the case example. Minimum threshold magnitudes to produce specific ground accelerations are higher using the newer model in every comparable instance.

Ambraseys (1995) generally forecasts lower $M_{P(max)}$ for each level of ground acceleration (Table 6.4). This is true for all cities and levels of ground motion except Pristina, Skopje and Tirane at 150 cm s^{-2}. Similarly, the associated probabilities are lower from Ambraseys (1995). The difference between equivalent estimates for $M_{P(max)}$ from each model at each level of ground motion decreases as ground motion level increases. $M_{P(max)}$ from Ambraseys (1995) for higher ground motion levels approach – and sometimes exceed – those of Theodulidis and Papazachos (1992). This suggests that Ambraseys (1995) may underestimate perceptible hazard at lower ground motions or Theodulidis and Papazachos (1992) may over-estimate hazard at lower ground motions.

Each model also consistently forecasts highest $M_{P(max)}$ for Plovdiv, Thessaloniki and Sofia. Edirne is also forecast high $M_{P(max)}$ for ground acceleration perceptible hazard. Some higher ground motions at Sofia and Plovdiv using Ambraseys (1995), and all ground motions using Theodulidis and Papazachos (1992), forecast higher $M_{P(max)}$ than the highest homogenized magnitude of 7.6 M_s.

This suggests these magnitudes are either beyond the scope of the area's seismicity, the proximity of large magnitude historical seismicity is having a dominating affect on these forecasts, or the adopted catalogue does not represent a full cycle of seismicity in the area around these particular cities. However, as the catalogue seems not to represent a full cycle of seismicity, it is possible a maximum magnitude of 7.6 M_s is not the maximum magnitude achievable in the region considered. A longer catalogue of seismicity would help refine further the estimates of the Gumbel distribution's parameters ω, λ and their uncertainties. It is then likely that both extreme and perceptible hazard forecasts would improve as a result.

Viewing pre-instrumental seismicity recorded in Shebalin *et al*. (1998), three magnitude 7.0 M+ earthquakes have occurred during the 19 century (1829; 1864; 1895). Extending back to the start of their catalogue highlights a further 11 events of magnitude 7.0 M+, with the largest reported at 8.2 $M_s \pm 0.5$ (555 AD at 10 km focal depth).

As surface wave magnitudes adopted from the catalogue were homogenized prior to analysis, it is perhaps unreasonable to compare values of $M_{P(max)}$ to individual reported large unhomogenized magnitude events. As magnitude homogenization involved two different geographic regions (north and south of 43°N) and conversion from four different magnitude scales onto the surface wave scale, a large amount of ambiguity may have been introduced. It is perhaps more reasonable to compare values of $M_{P(max)}$ to site-specific estimates for the *maximum credible earthquake magnitude*, M_3, as this is a measure of seismic energy retained in the local or regional seismogenic system. High values for *the most perceptible magnitude*, $M_{P(max)}$, are strongly correlated to high deformation velocities and strain rates (Koravos *et al.*, 2003), regardless of the form of ground motion considered.

The *most perceptible magnitude* never deviates from M_3 by more than ¼ M_s for the cities of Edirne, Thessaloniki, Sofia and Plovdiv using Theodulidis and Papazachos (1992). The latter two cities are located in the highest band of perceptible hazard (>7.5 M_s; Figure 6.9) while Thessaloniki and Edirne and in the next hazard band down. Many recent studies already discussed (e.g. Kahle *et al.*, 1995, 1998; Cocard *et al.*, 1999; Kotzev *et al.*, 2001, 2006; Tesauro *et al.*, 2006; Hollenstein *et al.*, 2008; Caparoli *et al.*, 2008) have studied strain rate and velocity field components of crustal deformation within specific sub regions of the eastern Mediterranean and Southern Europe. These highlight higher rates of deformation in the centre of the Aegean Sea, Macedonia and Southwest Bulgaria, especially compared with eastern Bulgaria and the Adriatic coast. Conversely, Pristina, Skopje, Tirane and Larissa exhibit larger variability between M_3 and $M_{P(max)}$ at each level of ground motion (typically 0.3 M_s to 1.2 M_s difference). These are in regions of noticeably lower strain energy (Figure 6.2) and earthquake perceptibility hazard (Figure 6.9).

Magnitude perceptibility estimates discussed in the previous paragraphs are site-specific to the area around Sofia as they are developed from seismicity found within a single analysis cell centred on this city. Interpolated estimates for cities can be derived from Figure 6.11, and afford the opportunity to develop hazard estimates for cities for which site-specific estimates cannot be developed directly, or hazard has not been considered throughout this work, such as Blagoevgrad to the south of Sofia.

These immediately highlight Blagoevgrad is forecast a marginally lower level of perceived hazard with respect to ground acceleration than Sofia. Blagoevgrad is found in a lower band of perceptible hazard than Sofia. For example, Ambraseys (1995) forecasts this city in the 7.4 $\rightarrow$ 7.6 M_s band for a ground acceleration of 150 cm s^{-2}, with Sofia in the next higher hazard band; Theodulidis and Papazachos (1992) increases these bands of hazard by an increment of 0.2 M_s.

This is reasonable to expect as: 1) Blagoevgrad is closer to the location of the 1904 Kresna event, and 2) the immediate area around Blagoevgrad contains higher seismic activity than Sofia; the analysis cell in which Blagoevgrad is located contains 872 earthquakes compared with 565 earthquakes local to Sofia. Consequently, as observations point to increased seismicity, forecasts for $M_{P(max)}$ at a range of ground motion levels will be lower than those of less seismically active locations. Estimates for $M_{P(max)}$ at like-for-like locations reflect this observation within the mapped area, with Theodulidis and Papazachos (1992) forecast systematically higher perceived magnitude hazard, over a narrower magnitude range, than Ambraseys (1995) (6.8 $\rightarrow$ 7.8+ M_s cf. 6.2 $\rightarrow$ 7.8+ M_s respectively).

Variation in $M_{P(max)}$ with respect to ground acceleration for Sofia is shown in Figure 6.13(a) for both ground motion models for test focal depths of 10, 15 and 20 km (with the other cities in Appendix 19). This shows a wider range to $M_{P(max)}$ using Ambraseys (1995) across the range of ground motion considered. Overall, $M_{P(max)}$ varies over a very small magnitude range (~0.3 M_s). Ambraseys (1995) also approaches ω earlier than equivalent curves of Theodulidis and Papazachos (1992), regardless of focal depth considered. For example, for a nominal earthquake of 10 km focal depth the *most perceptible magnitude* reaches this sub area's ω value at ground motions of 240 cm s^{-2} using Ambraseys (1995); Theodulidis and Papazachos (1992) does not forecast $M_{P(max)}$ that are near ω. At 15 km focal depth this is reached at 270 cm s^{-2}. ω is reached only at focal depths of 10 km and 15 km when using Ambraseys (1995). Curves also diverge from each other faster for Ambraseys (1995) than for Theodulidis and Papazachos (1992) with increased focal depth.

Two conclusions can be taken from Figure 6.13(a). First, Ambraseys (1995) predicts Sofia will never be subject to ground accelerations greater than 240 cm s^{-2} (Table 5.13(b) forecasts the 200-year return period ground motion to be only 150 cm s^{-2}), since ω is the theoretical maximum magnitude for the area but never reached in real-time scenarios. Secondly, Ambraseys (1995) forecasts magnitude perceptibility to saturate at these ground motions for all focal depths, while Theodulidis and Papazachos (1992) does not forecast saturation across the entire range considered.

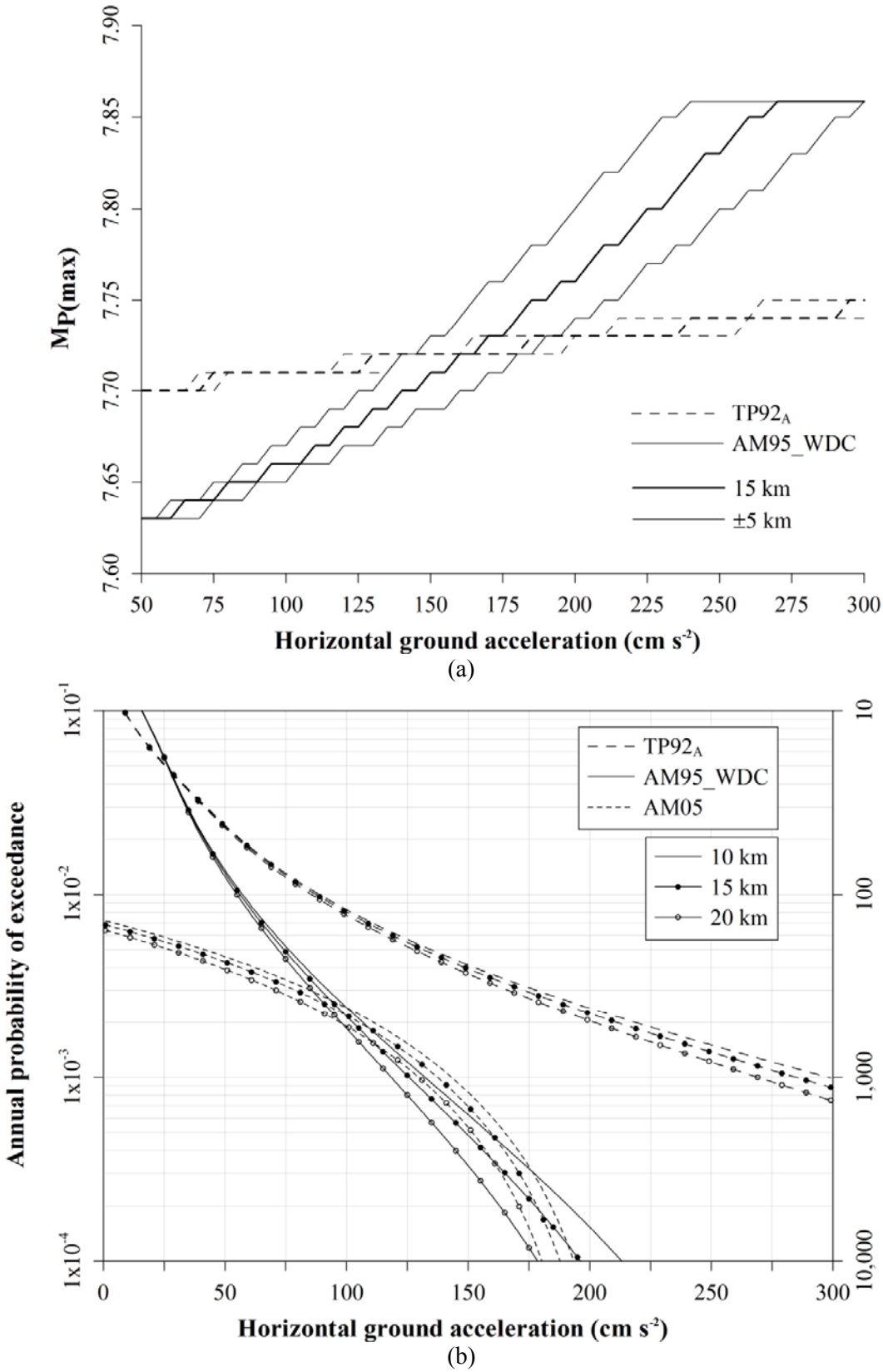

Figure 6.13 *Most perceptible magnitudes* for area around Sofia using Ambraseys (1995) with depth control at the 50th percentile and Theodulidis and Papazachos (1992) for stiff soil conditions at the 50th percentile for nominal earthquakes of focal depth 10, 15 and 20 km, and (b) ground acceleration hazard curves for Sofia for the same focal depths from integrated perceptibility curves with Ambraseys *et al*. (2005) added

Specimen ground acceleration hazard curves using Ambraseys (1995) and Theodulidis and Papazachos (1992) for horizontal ground acceleration around Sofia are given in Figure 6.13(b) for the same specimen focal depths, with equivalent hazard curves for the other cities presented in Appendix 20. Hazard curves for all eight urban centres are in Figure 6.14 for Theodulidis and Papazachos (1992) of 15 km focal depth, with Sofia highlighted as the reference case (red line).

Theodulidis and Papazachos (1992) leads to annual probabilities of exceedance that are systematically higher for Sofia by approximately a factor of two (Figure 6.13(b)) for comparable ground motions and focal depth. This characteristic is site-specific, as hazard curves for other cities exhibit much closer peak probabilities (e.g. Larissa) or even instances where accounting for focal depth with Ambraseys (1995) estimates higher probabilities than those from Theodulidis and Papazachos (1992) in the near-field region (at lower ground accelerations between 50 to 75 cm s^{-2} for Pristina, Skopje and Tirane; Appendix 20). Incorporating depth control with Ambraseys (1995) allows hazard curves to exhibit much faster rates of decay of probability levels than Theodulidis and Papazachos (1992) as ground acceleration increases.

Exceedance probabilities (at least once in *T*-years) for extreme ground accelerations estimated in Table 5.12 and Table 5.13, and therefore contributing to this site-specific hazard assessment of Sofia are in Table 6.5. These are for PGA extremes in return periods (*T*) of 25, 50, 100 and 200 year and *T*-years at 90% probability of non-exceedance. Ambraseys (1995) consistently estimates lower PGA extremes than Theodulidis and Papazachos (1992) (Table 5.12 and Table 5.13; other cities are in Appendix 21) for equivalent return periods. Annual exceedance probabilities reflect this with higher probabilities for each return period, *T* (or *T* at probability, *P*, of non-exceedance).

A qualitative assessment of these hazard curves suggests ground motions of about 120 cm s^{-2} and 225 cm s^{-2} will be exceeded at least once every 1,000 years using Ambraseys (1995) and Theodulidis and Papazachos (1992) respectively from seismicity at 15 km focal depth around Sofia. Estimates drop to 70 cm s^{-2} and 95 cm s^{-2} respectively to be exceeded at least once in 500 years, and 55 cm s^{-2} and 75 cm s^{-2} occur within 100 years (Table 6.6).

The magnitude at which a perceptibility curve departs the abscissa indicates the minimum magnitude that may produce a specific level of ground shaking. This assumes a finite focal depth system, as is the case here. These minimum magnitudes are in Table 6.7 for Sofia for $TP92_A$ at 10, 15, and 20 km focal depth. Koravos *et al*. consider this magnitude minimum to be 5.6 M for their southwest Bulgaria zone (at 0.2 g for a nominal event of 10 km focal depth using Theodulidis and Papazachos) in which Sofia is located. Although not directly comparable, this model forecasts a minimum magnitude of 6.16 M_s to produce PGAs of 150 cm s^{-2}.

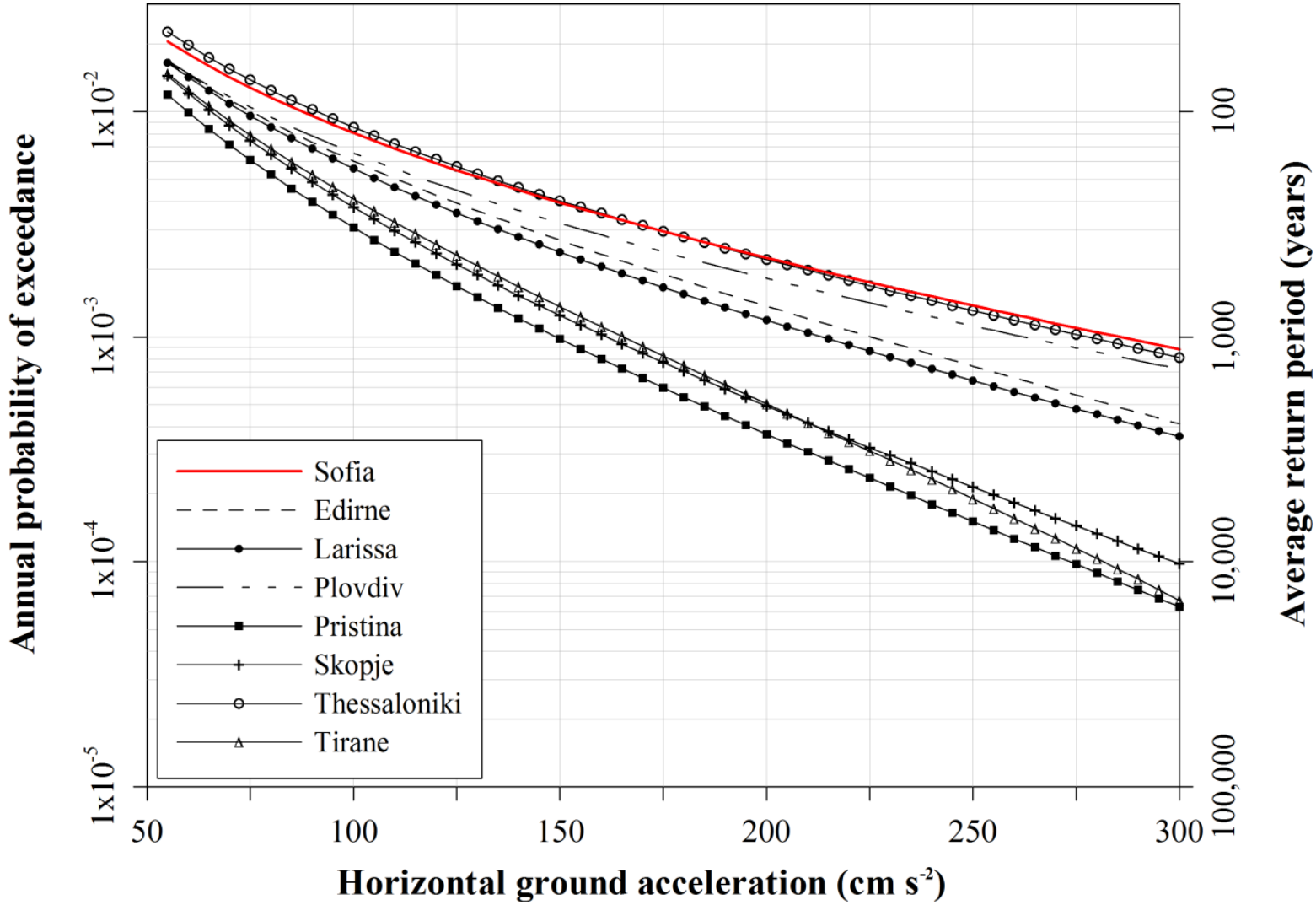

Figure 6.14 Ground acceleration hazard curves for all urban centres considered using Theodulidis and Papazachos (1992) for stiff soil conditions at the 50th percentile for a nominal earthquake of 15 km focal depth

		Annual probability of exceedance ($\times 10^{-3}$)							
Ground motion model	Focal depth (km)	A_{25} (**35.5**)	A_{50} (**42.7**)	A_{100} (**49.8**)	A_{200} (**57.0**)	A_{P25} (**58.8**)	A_{P50} (**65.9**)	A_{P100} (**73.1**)	A_{P200} (**80.2**)
Ambraseys (1995)	10	27.6	18.9	13.6	10.1	9.7	7.1	5.6	4.4
	15	27.1	18.4	13.1	9.7	8.9	6.8	5.2	4.1
	20	26.4	17.8	12.5	9.1	8.4	6.3	4.8	3.7

		Annual probability of exceedance ($\times 10^{-3}$)							
Ground motion model	Focal depth (km)	A_{25} (**86.0**)	A_{50} (**107.5**)	A_{100} (**129.0**)	A_{200} (**150.6**)	A_{P25} (**155.9**)	A_{P50} (**177.4**)	A_{P100} (**198.9**)	A_{P200} (**220.5**)
Theodulidis and Papazachos (1992)	10	10.5	7.3	5.4	4.1	3.8	3.0	2.4	2.0
	15	10.3	7.1	5.2	3.9	3.7	2.9	2.3	1.8
	20	9.9	6.7	4.9	3.6	3.5	2.6	2.1	1.6

Table 6.5 Annual probabilities ($\times 10^{-3}$ per annum) of experiencing extreme acceleration ground motions estimated for the 2° half-width cell centred on Sofia. Estimates are to the nearest cm s^{-2}. Values in brackets are the *T*-year (or *T*-year at 90% pnbe) estimates from Table 5.12 and Table 5.13 (to one decimal place)

		Annual probability of exceedance ($\times 10^{-3}$) in *T* years					
Ground motion model	Focal depth (km)	100	200	300	400	500	1,000
Ambraseys (1995)	10	57	60	63	67	71	132
	15	56	58	61	65	69	125
	20	54	57	60	63	67	118
Theodulidis and Papazachos (1992)	10	89	95	102	111	121	298
	15	87	93	100	108	119	285
	20	86	91	98	106	115	269

Table 6.6 Peak ground accelerations (in cm s^{-2}) expected to be exceeded at least once in *T* years for the 2° half-width cell centred on Sofia

	Theodulidis and Papazachos (1992)		
Focal Depth (km)	50 cm s^{-2}	100 cm s^{-2}	150 cm s^{-2}
10	5.18	5.80	6.16
15	5.28	5.90	6.26
20	5.40	6.02	6.38

Table 6.7 Minimum threshold magnitudes to produce specific levels of ground accelerations at Sofia

Solakov *et al*. (2001) provides a relatively recent comparable assessment of ground acceleration hazard to which they think Sofia may be subject. They investigate Sofia's PGA hazard using both synthetic Monte-Carlo and deterministic Cornell-McGuire PSHA approaches with a selection of ground acceleration models. Adopting Ambraseys *et al.* (1996) estimates Sofia's PGA hazard to be 0.30-0.35 g (294-343 cm s^{-2}) at least once in 1,000-years. Hazard curves they develop reinforce higher estimates expected using Theodulidis and Papazachos (1992), with forecasts approaching exceedances of 0.25-0.45 g at least once in a 1,000-year return period. Estimates here (Table 6.6) are to the lower end of their estimates, irrespective of the focal depth considered (Solakov *et al.* do not consider focal depth as a governing factor), and are aligned with estimates from other studies considered in this work (e.g. Bončev *et al.*, 1982; Stanishkova and Slejko, 1991).

The following sections will consider intensity and velocity hazard in a similar fashion, while correlated levels of acceleration, velocity and intensity ground motion is considered in detail in the Summary and Conclusions (section 6.7).

6.5.2 Ground velocity

Ground velocity is often considered to be more representative of a location's ground motion hazard than ground acceleration (Ambraseys, 1974) since velocity is related to the energy flux between ground and building. Previous work has investigated using ground velocity as an alternative measure to intensity, such that intensity may be determined as a function of PGV levels and earthquake damage statistics often give a much closer correlation with peak ground velocity than with peak ground acceleration (Panza *et al.*, 1996, 1997; Wu *et al.*, 2003).

Estimates for the *most perceptible magnitude*, $M_{P(max)}$, with respect to horizontal ground velocity of 5, 10 and 15 cm s^{-1}, using Theodulidis and Papazachos (1992; $TP92_V$) for stiff soil conditions (S = 0.5) at the 50^{th} percentile (P = 0) are illustrated in Figure 6.15(a)-(c) for a nominal earthquake of 15 km focal depth.

In the crudest sense, ground velocity hazard maps for $M_{P(max)}$ exhibit similar contour patterns to those of acceleration; lower magnitudes are forecast to the east and north, enclosing a region of higher magnitude hazard covering central and west Bulgaria, northeast Greece and the northern Aegean Sea area. At ground velocities of 5 cm s^{-1}, Yugoslavia, and Albania are forecast the lowest $M_{PV(5)}$ of below 6.50 M_s, with estimates increasing as one moves eastwards across the considered region. West Greece and the FYR of Macedonia are dominated by magnitudes 6.50-7.00 M_s, while west and central Bulgaria, east Greece and the north Aegean are encompassed by the 7.50 M_s contour. The highest *most perceptible magnitude* at this ground velocity is 7.75+ M_s in a single confined area east of the political triple junction between Greece, FYR of Macedonia and Bulgaria, extending south from Sofia.

As ground velocities rise to 15 cm s^{-1} in the broader region $M_{P(max)}$ increases by no more than 0.50 M_s in most areas, with the contour patterns remaining roughly consistent with lower velocity values. The area encompassed by the 7.75 M_s contour has now enlarged to cover more of west Bulgaria. The lowest $M_{PV(15)}$ is approximately. 6.75 M_s. Similarly, estimates for the *most perceptible magnitude* with respect to ground velocity across southwest Bulgaria are generally approximately 0.0-0.5 M_s greater than for acceleration perceptibility hazard at any geographic point (Figure 6.16). For example, arbitrarily taking the centre of the zone considered as the geographic point of reference (41.5ºN, 23.25ºE), $M_{PV(5)} \approx$ 7.4-7.6 cf. $M_{PA(50)} \approx$ 7.4-7.6; these estimates remain consistent through to the highest ground motions of 15 cm s^{-1} and 150 cm s^{-2} respectively. However, considering a second arbitrary point at the intersection of the political borders, $M_{P(max)}$ remains constant at 7.6-7.8 M_s throughout all ground velocities considered, while for acceleration, $M_{P(max)}$ increases marginally from 7.4-7.6 M_s to 7.6-7.8 M_s.

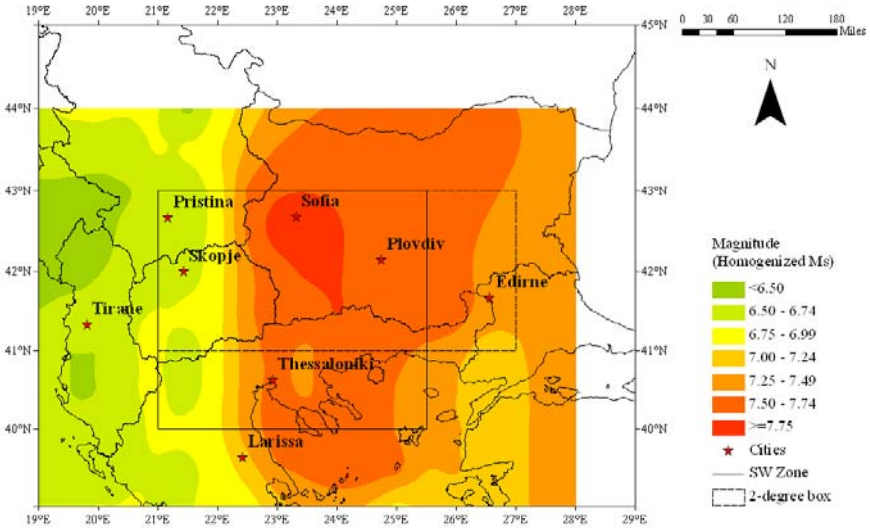

(a)

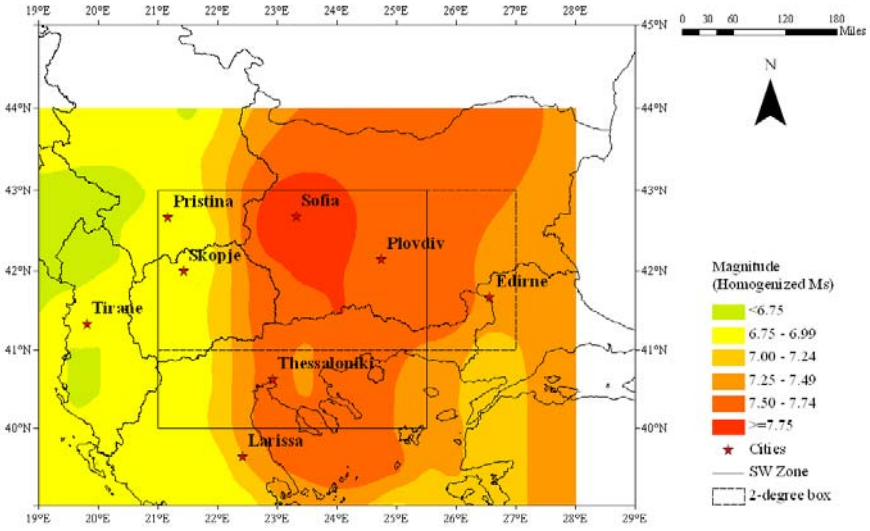

(b)

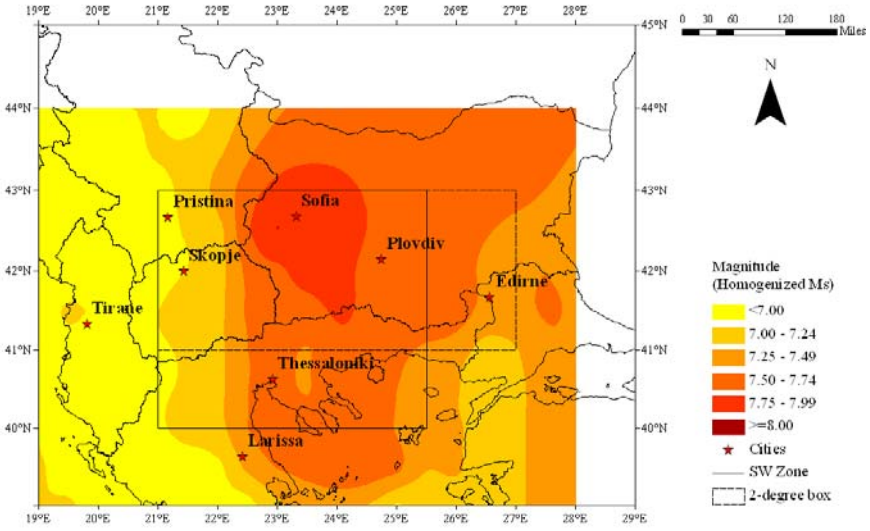

(c)

Figure 6.15 The *most perceptible magnitude* at ground velocities (a) 5, (b) 10 and (c) 15 cm s^{-1} using Theodulidis and Papazachos (1992) for stiff soil conditions at the 50th percentile for a nominal earthquake of 15 km focal depth. Contours are at intervals of 0.25 M_s

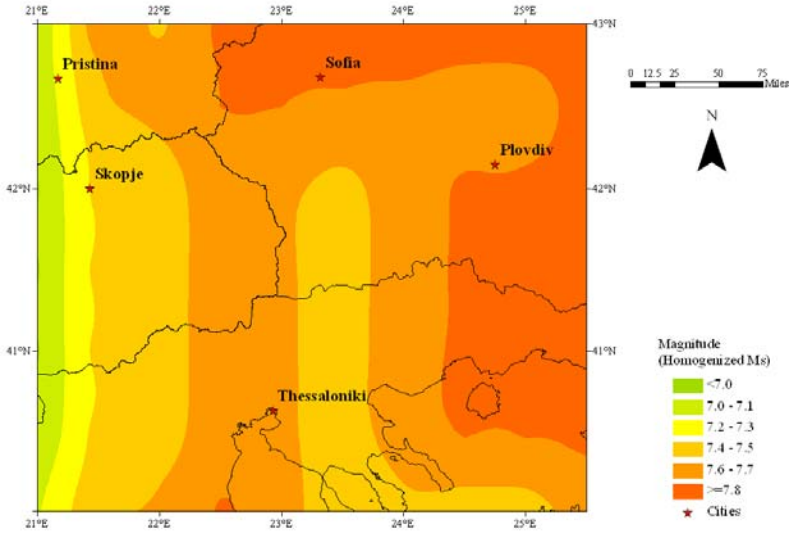

(a)

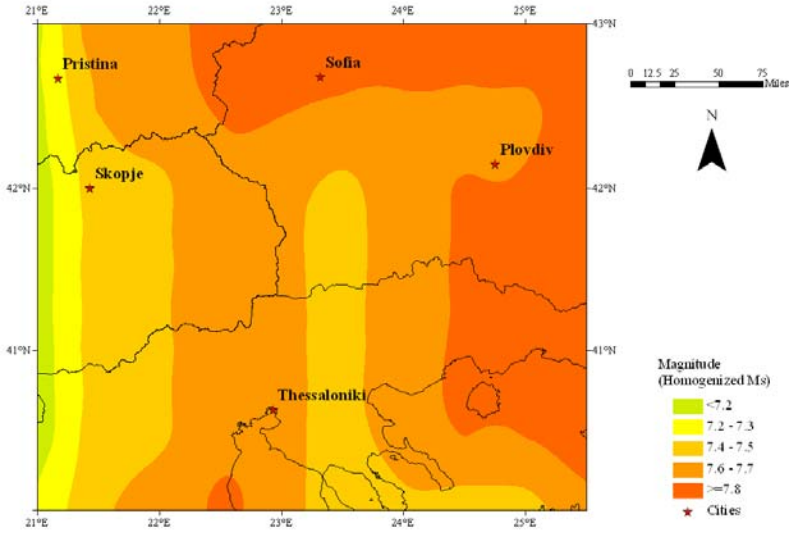

(b)

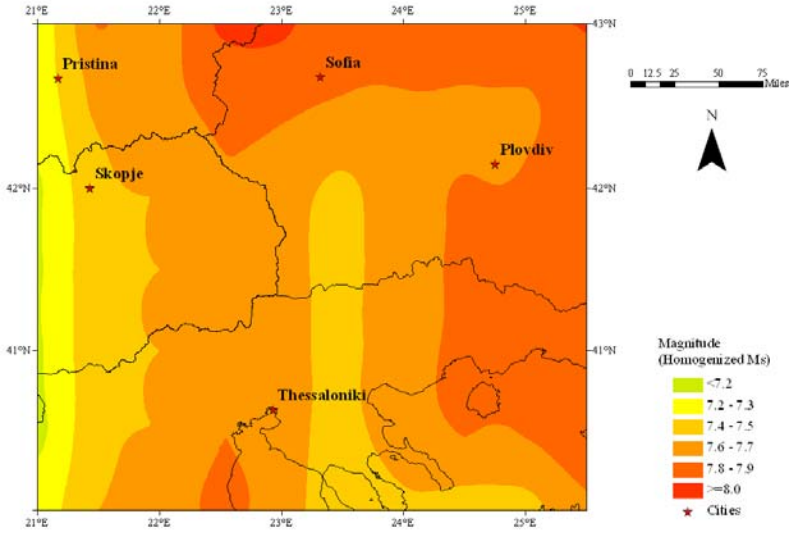

(c)

Figure 6.16 The *most perceptible magnitude* in southwest Bulgaria at ground velocities (a) 5, (b) 10 and (c) 15 cm s^{-1} using Theodulidis and Papazachos (1992) for stiff soil conditions at the 50^{th} percentile for a nominal earthquake of 15 km focal depth. Contours are at intervals of 0.2 M_s

Figure 6.17 provides perceptibility estimates for roughly the same region as Koravos *et al*. (2003), with observations of the approximate differences between each work given in Table 6.8.

Seismogenic source zone[1] used by Koravos *et al.* (2003)	Ground velocity perceptibility model	
	Koravos *et al.*[2]	This study; $TP92_V$[3, 4]
9 [east mainland Greece]	6.1 (± 0.1)	6.75 → <7.75
10 [north Aegean Sea]	6.2 (± 0.1)	7.25 → <7.75
11 [west Marmara Sea]	7.6 (± 0.2)	7.00 → <7.50
13 [Albania-Greece-FYROM border]	7.4 (± 0.1)	6.75 → <7.75
14 [Bulgaria-Greece-FYROM border]	6.7 (± 0.2)	7.25 → 7.75+

[1, 4] As for Table 6.3; [2, 3] Estimates for ground velocity of 10 cm s^{-1} at a nominal focal depth of 10 km

Table 6.8 Empirical differences in forecasted *most perceptible magnitudes* for specific ground velocities between regions common between Koravos *et al.* (2003) and this study

Patterns observed for ground acceleration perceptibility hazard – with regards to which zones are forecast higher, lower or 'in range' estimates by Koravos *et al*. compared with this work – are reproduced here. Any justification proposed for variability in ground acceleration perceptibility hazard between the two studies may also be attributable to velocity perceptibility hazard. However, '*like-for-like*' estimates are available from both studies, and allow more dependence to be attached to specific attributes of the regional seismicity or statistical methods adopted for this variability in forecasts:

1. The filtering out of lower-magnitude earthquakes from the catalogue had a significant effect of *weighting* magnitude forecasts in this central area towards the upper end of the magnitude range;

2. These differences are due to Koravos *et al.* using a seismogenic source model rather than a zone-free model;

3. Koravos *et al.* adopting a *whole process* model in-place of a *part process* model would likely reduce hazard estimates, in their work;

4. Koravos *et al*. adopting a different catalogue database (that of Papazachos *et al.,* 2000) to underpin their analysis.

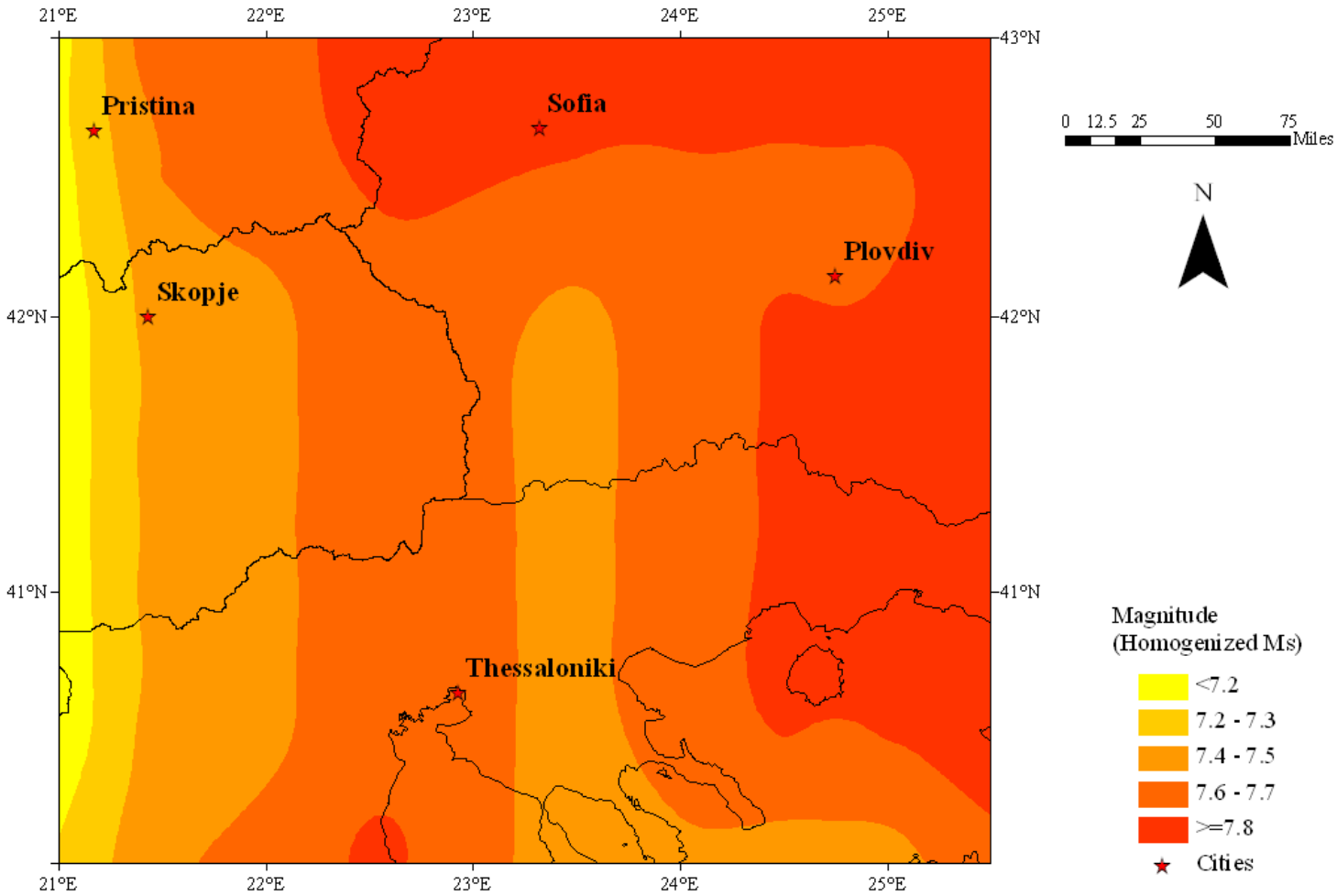

Figure 6.17 The *most perceptible magnitude* in southwest Bulgaria at ground velocity of 10 cm s^{-1} for a nominal focal depth of 10 km using Theodulidis and Papazachos (1992) for stiff soil conditions at the 50th percentile. Contours are at intervals of 0.2 M_s

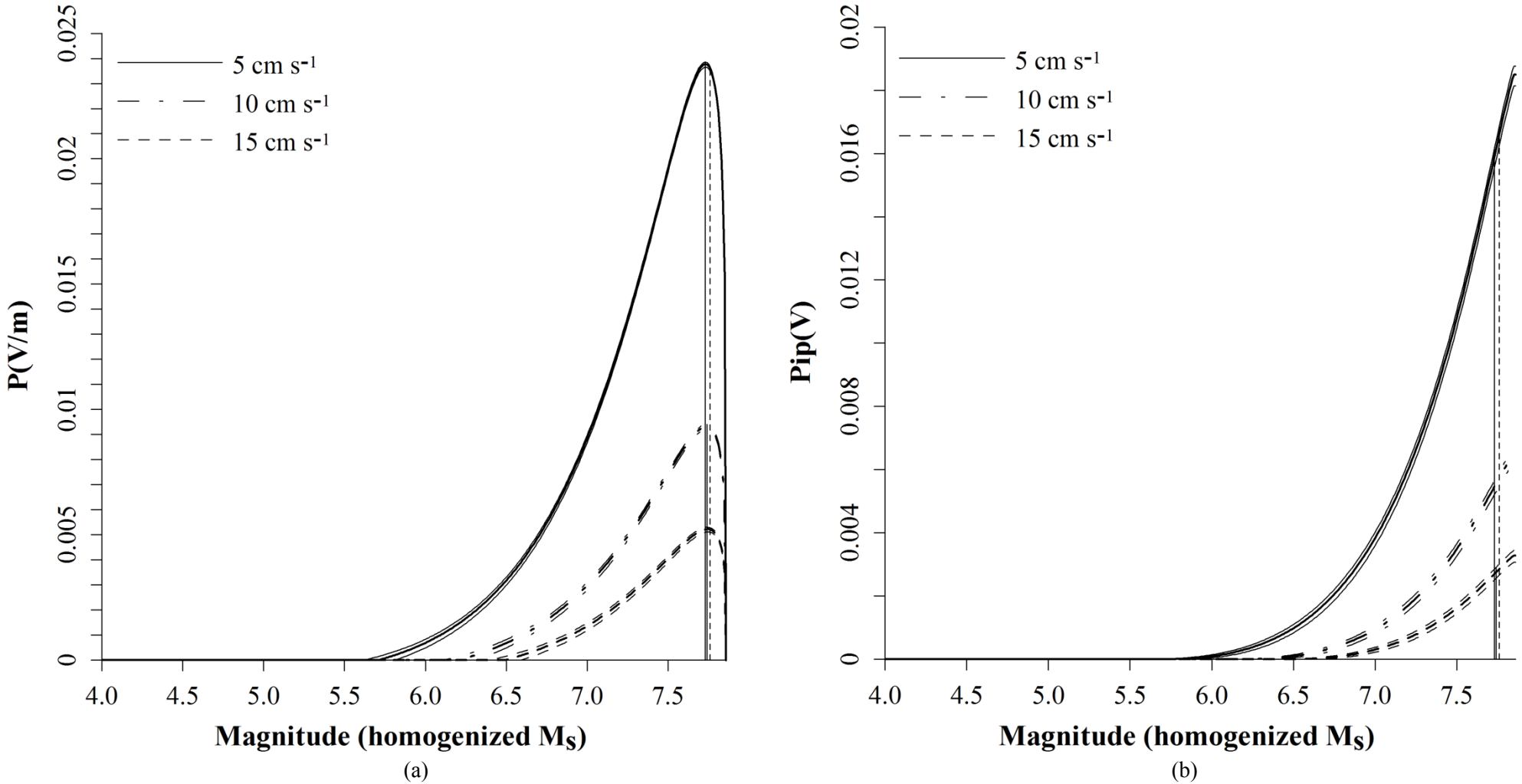

Figure 6.18 Ground velocity (a) perceptibility and (b) integrated perceptibility curves for Sofia using Theodulidis and Papazachos (1992) for stiff soil conditions at the 50th percentile. The central heavy black curve of each set of three curves represents a nominal earthquake of 15 km focal depth, while the upper and lower curves represent 10 km and 20 km focal depth respectively. Vertical black lines represent the *most perceptible magnitude* only for 10 km focal depth. The vertical dashed line represents M_3 from cumulative strain energy release techniques

	Horizontal ground velocity (cm s^{-1})								
	5 cm s^{-1}			10 cm s^{-1}			15 cm s^{-1}		
City	$M_{P(max)}$	P_p [1,2]	P_{ip} [1,3]	$M_{P(max)}$	P_p	P_{ip}	$M_{P(max)}$	P_p	P_{ip}
Edirne	7.38	16.2	10.7	7.40	6.1	3.3	7.41	3.2	1.5
Larissa	7.23	10.2	8.1	7.29	3.7	2.3	7.34	1.9	1.0
Plovdiv	7.72	16.0	12.0	7.74	6.2	4.2	7.75	3.5	2.1
Pristina	6.65	6.1	3.6	6.82	1.8	0.7	6.95	1.0	0.2
Skopje	6.66	7.1	4.3	6.84	2.1	0.9	6.98	1.0	<1.0
Sofia	7.73	23.8	15.9	7.74	9.3	5.6	7.74	5.2	2.8
Thessaloniki	7.57	19.1	14.5	7.59	7.4	4.8	7.61	4.1	2.3
Tirane	6.83	9.3	6.0	6.88	2.9	1.2	6.96	1.3	0.4

[1] Estimates are given for a nominal earthquake with focal depth of 15 km. Probabilities are given at a factor of $\times 10^{-3}$; [2] Annual probability of perceiving ground motion arising from magnitude $M_{P(max)}$; [3] Annual probability of perceiving ground motion arising from all magnitudes up to and including $M_{P(max)}$

Table 6.9 The most perceptible earthquake magnitude, $M_{P(max)}$, with respect to horizontal ground velocities of 5 cm s^{-1} 10 cm s^{-1} and 15 cm s^{-1}, with the associated perceptibility probability, P_p and the annual probability of exceedance, P_{ip}, of perceiving these ground velocities. Estimates are derived from the distribution of seismicity present within a 2° half-width cell of the city are given, using the conditions outlined in section 5.3 using Theodulidis and Papazachos (1992) for stiff soil conditions at the 50th percentile for a nominal earthquake of 15 km focal depth

Estimates for earthquake perceptibility and integrated perceptibility with respect to horizontal ground velocity at Sofia are in Figure 6.18(a) and (b) respectively and for the other urban centres in Table 6.9 and Appendix 22. The *most perceptible magnitude* with respect to ground velocity is 7.72 M_s at 5 cm s^{-1}, rising to 7.74 M_s at 15 cm s^{-1}. The small magnitude range reported is likely due to the small range in velocities considered for velocity perceptibility hazard. However, this range has been justified in Table 6.2 as suitable for the region considered. These are both outside the observed magnitude range of the adopted catalogue, giving more credence to the suggestion it may not fully report a complete seismic cycle. Due to this the number of exceedances expected in 50 or 100 years cannot be ascertained (Table 5.9). These however can be attributed to the same reasons as the high values for $M_{P(max)}$ for acceleration by relating them to variation in strain and velocity fields of the surrounding region (Pristina and Skopje again return larger differences between $M_{P(max)}$ and M_3, by as much as 0.9 M_s at lower ground motions). These perceptible magnitudes are at the lower and upper limits of ground velocity considered and come attached with perceptibility and integrated perceptibility probabilities of 23.8×10^{-3} and 16.0×10^{-3} per annum, dropping to 5.2×10^{-3} and 2.8×10^{-3} per annum respectively.

Minimum threshold magnitudes created by a finite focal depth system needed to produce the three ground velocities considered are in Table 6.10. Minimum magnitudes for velocity ground motion are consistently greater than correlated levels of acceleration hazard by between 0.22 and 0.44 M_s.

	Theodulidis and Papazachos (1992)		
Focal Depth (km)	5 cm s^{-1}	10 cm s^{-1}	15 cm s^{-1}
10	5.62	6.12	6.40
15	5.71	6.21	6.49
20	5.82	6.31	6.60

Table 6.10 Minimum magnitudes to produce specific levels of ground velocities around Sofia

Correlated levels of acceleration and velocity ground motion (using Theodulidis and Papazachos (1992) for both at the 50th percentile and for stiff soil conditions) show the ground acceleration model ($TP92_A$) systematically forecasts lower $M_{P(max)}$ than the ground velocity model ($TP92_V$) for all cities. However, no correlated pair of estimates is more than 0.2 M_s different (e.g. Skopje and Pristina at 5 cm s^{-1}). This results in associated peak probabilities for these estimates of $M_{P(max)}$ being higher for acceleration than for the equivalent velocities.

Variation in $M_{P(max)}$ for a nominal earthquake of 15 km focal depth is shown in Figure 6.19(a) for Sofia (Appendix 23 presents these for the other considered cities). This illustrates the *most perceptible magnitude* with respect to ground velocity is again confined to a very narrow magnitude range of ~0.2 M_s, regardless of the focal depth. As with a number of perceptible magnitudes with respect to acceleration hazard, Sofia's perceptibility hazard is forecast above the maximum observed earthquake in the adopted catalogue, and may be explained using the same reasons as ground acceleration perceptibility hazard.

Ground velocity hazard curves are in Figure 6.19(b) for Sofia, and for all other cities considered in Appendix 24. Each illustration adopts Theodulidis and Papazachos (1992) for stiff soil conditions at the 50th percentile. Sofia is estimated the highest levels of ground velocity hazard, and is nearly identical to Thessaloniki at low ground velocities (≤20 cm s^{-1}) and marginally more than Plovdiv. Each of these cities is located in the high seismicity southwest zone of interest. Sofia's 15 km hazard curve is once again illustrated in Figure 6.20 with equivalent curves for each other city considered. As is expected, due to its location in the high seismicity southwest Bulgaria zone, Sofia's curve is consistently estimating highest ground velocity hazard from seismicity of 15 km focal depth, as is Thessaloniki and Plovdiv.

Peak ground velocities estimated earlier have their annual probabilities of exceedance from these hazard curves in Table 6.11. This relatively high ground velocity hazard, when compared with the other cities considered, manifests itself in ground velocities of 27 cm s^{-1} expected to be exceeded in the local area to Sofia at least once in every 1,000 years, and 10 cm s^{-1} once in approximately 500 years (Table 6.12). Ground motion exceedances for the extreme ground velocity estimates of the other cities from chapter 5 and selected return periods are in Appendix 25.

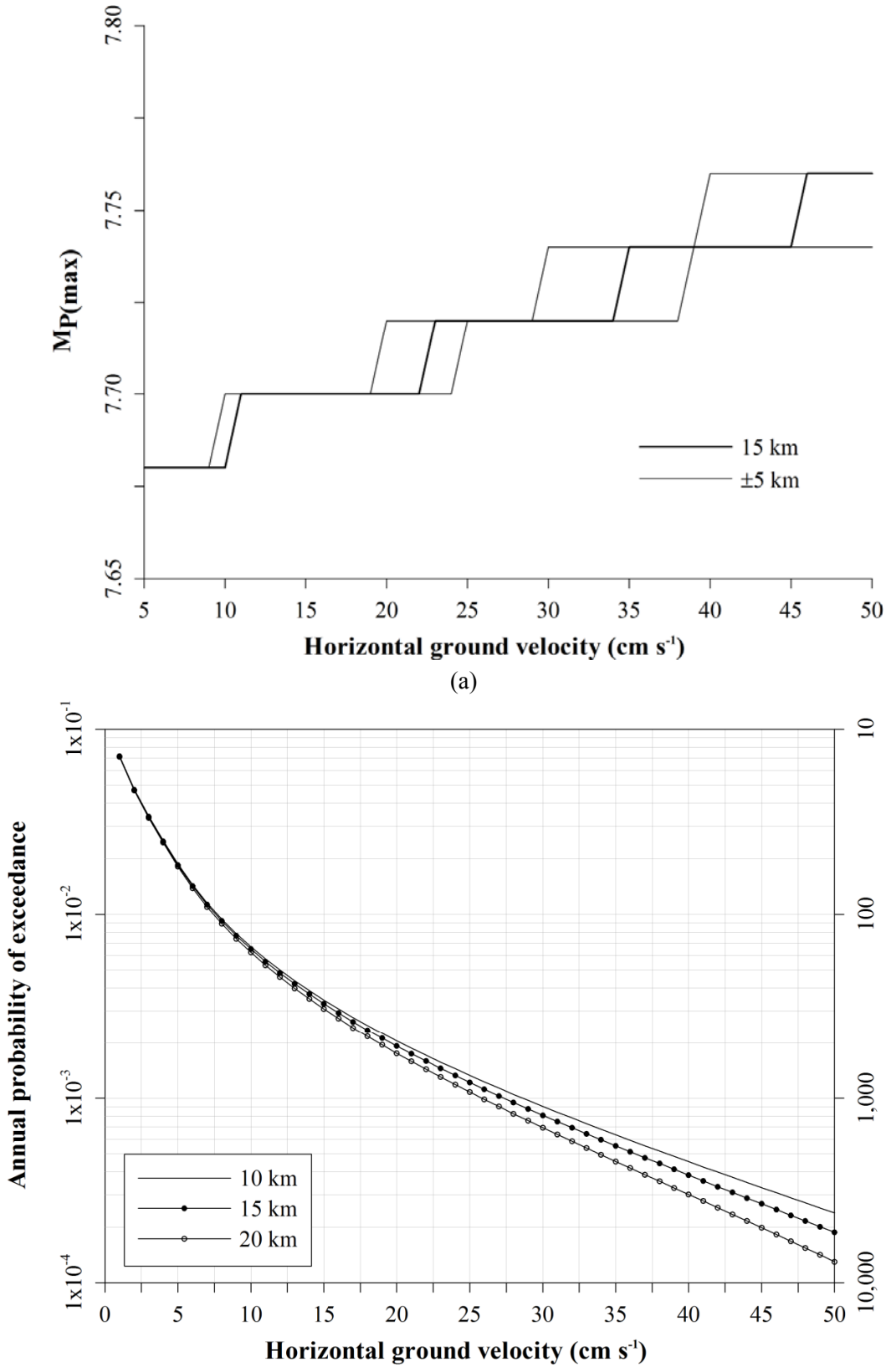

Figure 6.19 *Most perceptible magnitudes*, $M_{P(max)}$, for Sofia using Theodulidis and Papazachos (1992; $TP92_V$) for stiff soil conditions at the 50th percentile for nominal earthquakes of focal depth 10, 15 and 20 km, and (b) ground velocity hazard curves for Sofia for the same focal depth

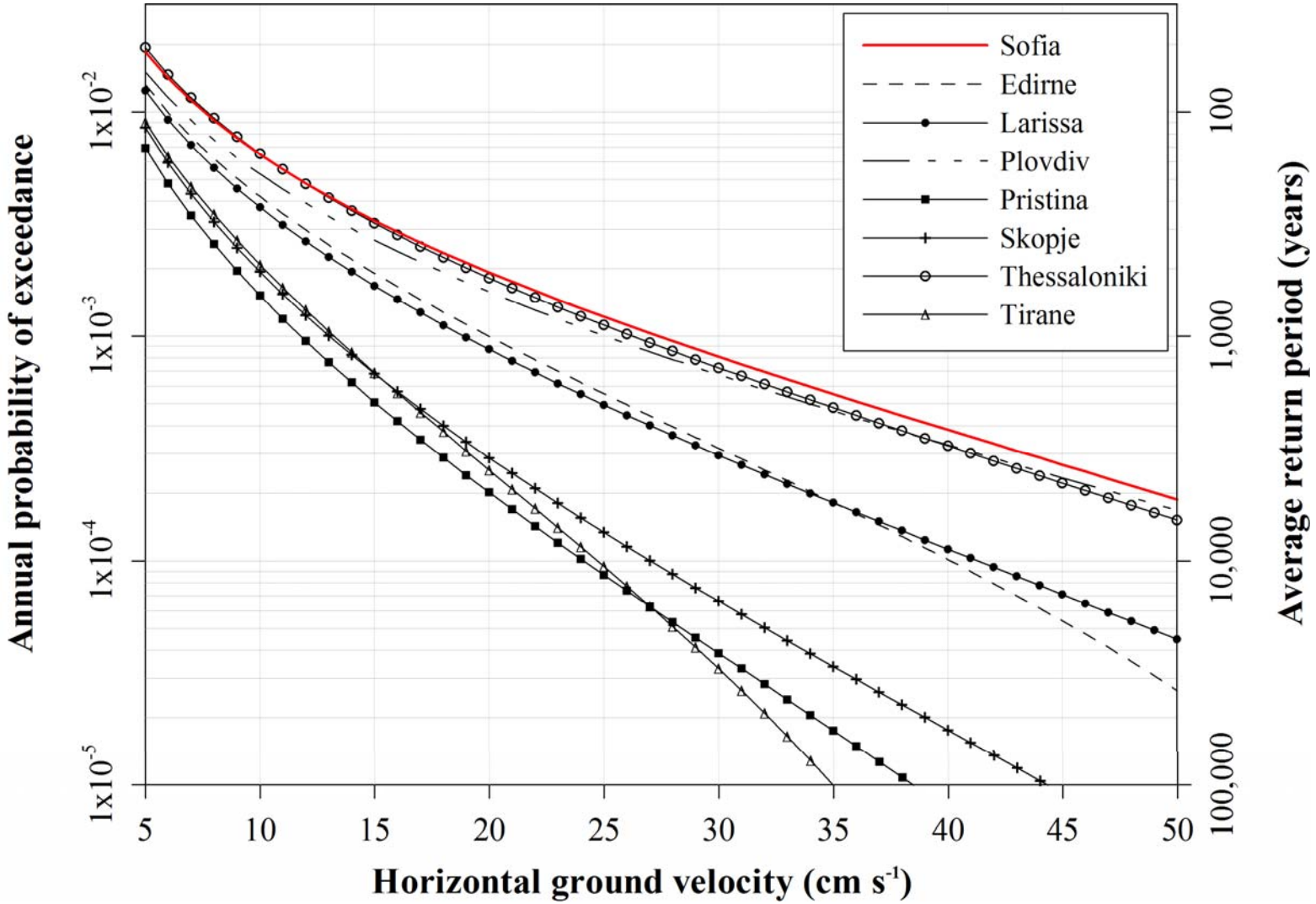

Figure 6.20 Horizontal ground velocity hazard curves for all urban centres considered using Theodulidis and Papazachos (1992) for stiff soil conditions at the 50th percentile for a nominal earthquake of 15 km focal depth

		Annual probability of exceedance ($\times 10^{-3}$)							
Ground motion model	Focal depth (km)	V_{25} (**12.8**)	V_{50} (**16.2**)	V_{100} (**19.6**)	V_{200} (**22.9**)	V_{P25} (**23.7**)	V_{P50} (**27.1**)	V_{P100} (**30.5**)	V_{P200} (**33.8**)
Theodulidis and Papazachos (1992)	10	4.5	3.0	2.1	1.6	1.5	1.1	0.9	0.7
	15	4.3	2.9	2.0	1.5	1.4	1.0	0.8	0.6
	20	4.1	2.7	1.8	1.3	1.2	0.9	0.7	0.5

Table 6.11 Annual probabilities ($\times 10^{-3}$) of experiencing extreme velocity ground motions estimated for the region surrounding Sofia. Values in brackets are the *T*-year (or *T* -year at 90% pnbe) estimates for Sofia from Table 5.13 (to one decimal place)

		Annual probability of exceedance ($\times 10^{-3}$) in *T* years					
Ground motion model	Focal depth (km)	100	200	300	400	500	1,000
Theodulidis and Papazachos (1992)	10	7.6	8.2	8.9	9.7	10.7	28.6
	15	7.5	8.1	8.8	9.5	10.5	27.4
	20	7.4	7.9	8.6	9.3	10.2	25.9

Table 6.12 Peak ground velocities (in cm s^{-1}) expected to be exceeded at least once in *T* years for the region surrounding Sofia

6.5.3 Macroseismic intensity

Ground motion models can provide estimates for low-magnitude thresholds below which no ground motion will be perceived. These cut-off magnitudes will be different for each model on which $P_c(X)$ – and therefore $P(X \mid M)$ – has dependence. Cut-off magnitudes based upon the intensity ground motion model of Papazachos and Papaioannou (1997), Eq. (3-23(a)), aggregated with three selected epicentral intensity equations (Eq. (3-17), (3-18) and (3-22)), are given in Table 6.13 and compared with those reported by Burton *et al.* (2004b) using the same intensity attenuation model specific to Greece. The main point to note from this table is that all three models return lower estimates for this cut-off magnitude than those reported by Burton *et al.* for Greece. Cut-off magnitudes generally reduce by between approximately 0.50 M and 0.75 M for the three models specific to Bulgaria and the Balkans. Figure 6.21 plots variation in epicentral intensity with magnitude for each of the four epicentral models considered in Table 6.13.

	Intensity		
Epicentral intensity model	VI	VII	VIII
Glavcheva (1997); Eq. (3-17)	4.07	4.80	5.53
Shebalin *et al.* (1998); Eq. (3-18)	3.87	4.54	5.21
Papazachos and Papaioannou (1997); for Bulgaria; Eq. (3-22)	4.03	4.73	5.43
Papazachos and Papaioannou (1997); for Greece; Eq. (3-21)	4.57	5.27	5.97

Table 6.13 Cut-off magnitudes based on Papazachos and Papaioannou (1997) combined with selected relations for epicentral intensity

Papazachos and Papaioannou (1997) for Bulgaria will be taken forward to contour regional intensity-based earthquake perceptibility hazard. The *most perceptible magnitudes* for intensities VI, VII and VIII are illustrated in Figure 6.22(a)-(c) across the Balkans, for a nominal earthquake at 15 km focal depth. The lowest intensity level was set at VI due to the onset of structural damage being ascribed for this level in the current EMS-98 macroseismic intensity scale (Grünthal, 1998). This is also true of the Medvedev-Sponheuer-Kárník (MSK) intensity scale, as EMS-98 is designed to be directly interchangeable with the MSK scale. The MSK intensity scale, being a derivative of the earlier Mercalli-Cancani-Sieberg (MCS), Modified Mercalli (MM-31 and MM-56) and Medvedev scales, provided the ground work on which the EMS scale was further developed. Recent updates to intensity scales also afford a period of dual running that allowed homogeneity between intensity scales. Figure 6.23(a)-(c) provides equivalent hazard maps for southwest Bulgaria.

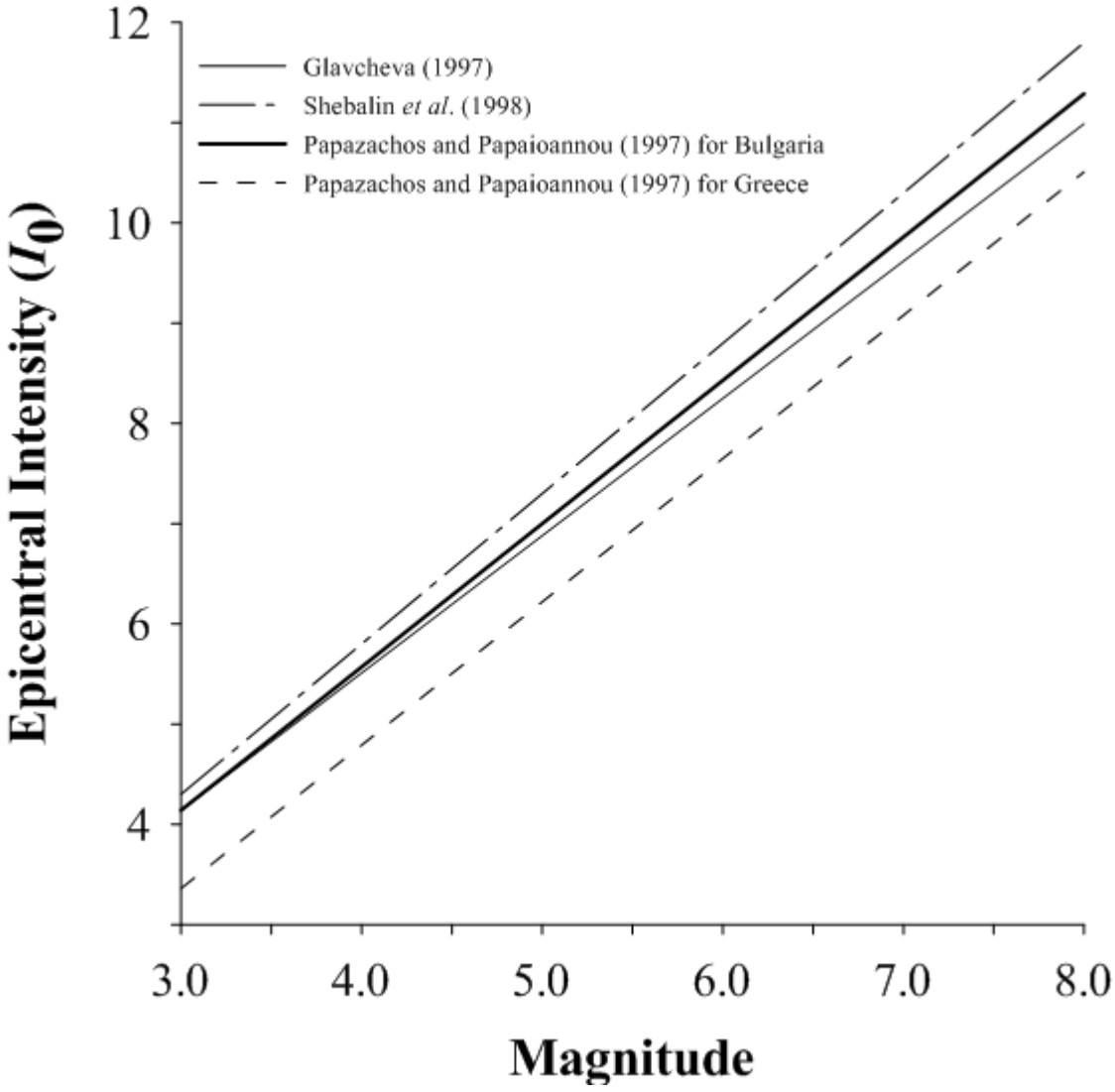

Figure 6.21 Four recent epicentral intensity relations developed for Balkan and Aegean seismicity. Papazachos and Papaioannou (1997) aggregated with their Bulgarian epicentral intensity model is highlighted by the solid line

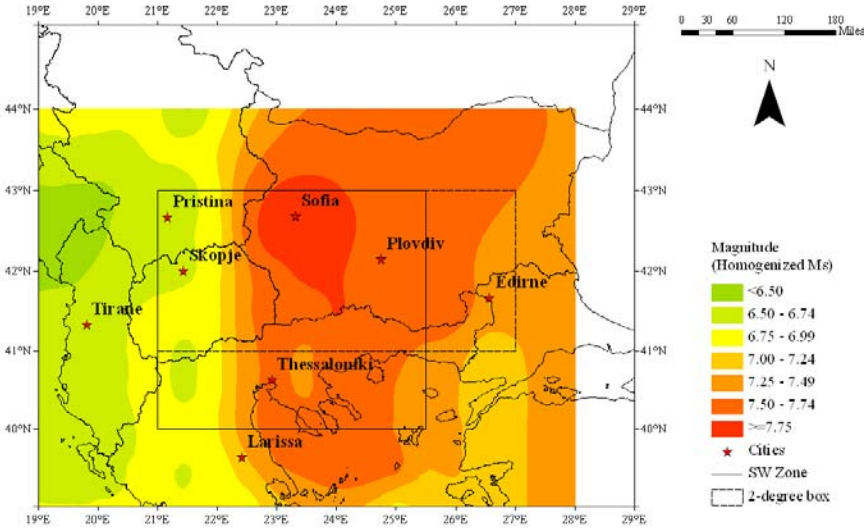

(a)

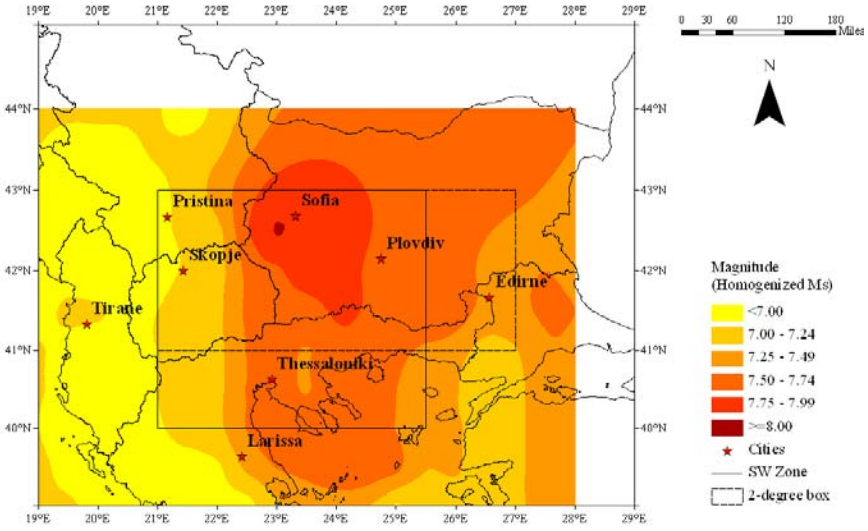

(b)

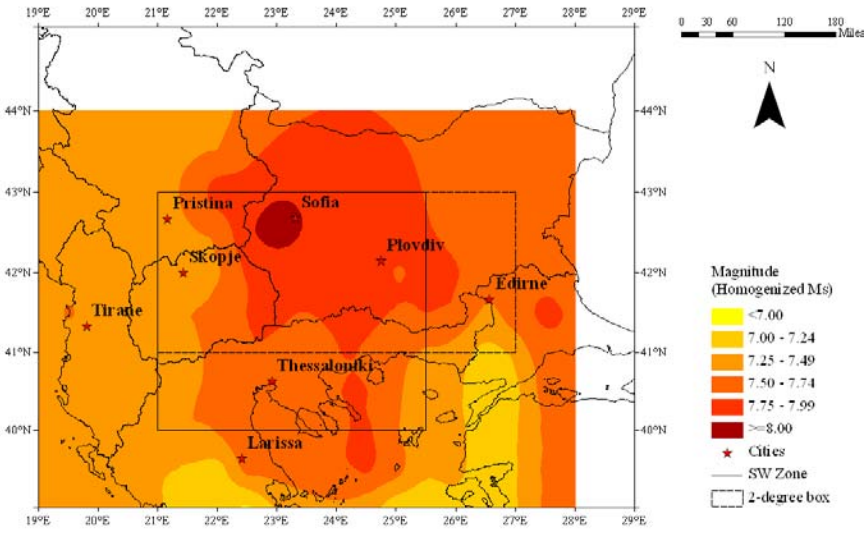

(c)

Figure 6.22 The most perceptible earthquake magnitude for I = (a) VI, (b) VII and (c) VIII. Estimates obtained using Eq. (3-23(b)) of Papazachos and Papaioannou (1997) across the broader Balkan region for a nominal earthquake of 15 km focal depth. Contours are at intervals of 0.25 M_s

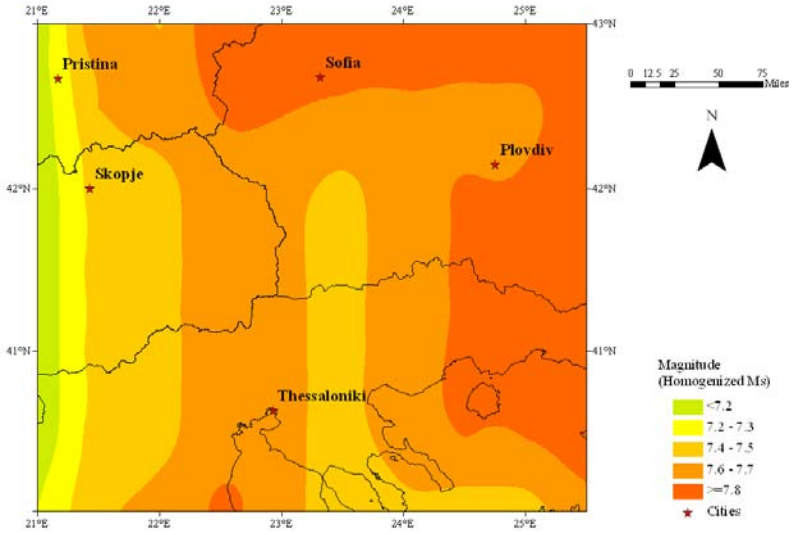

(a)

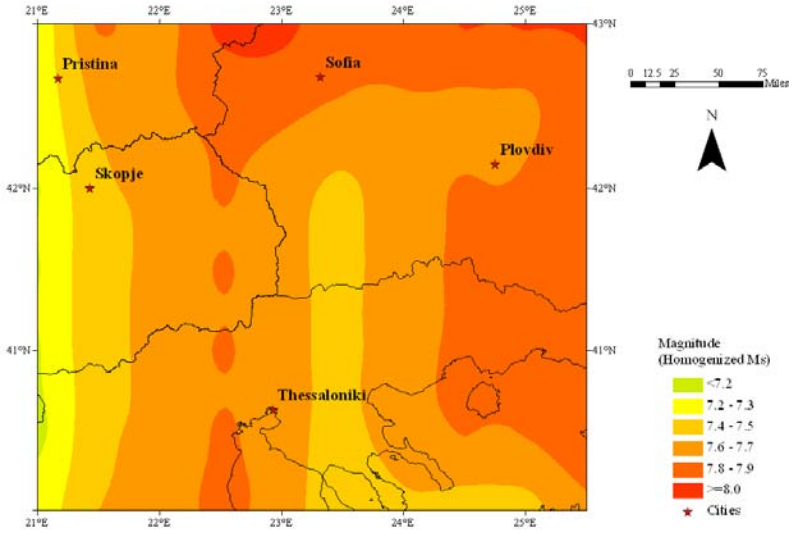

(b)

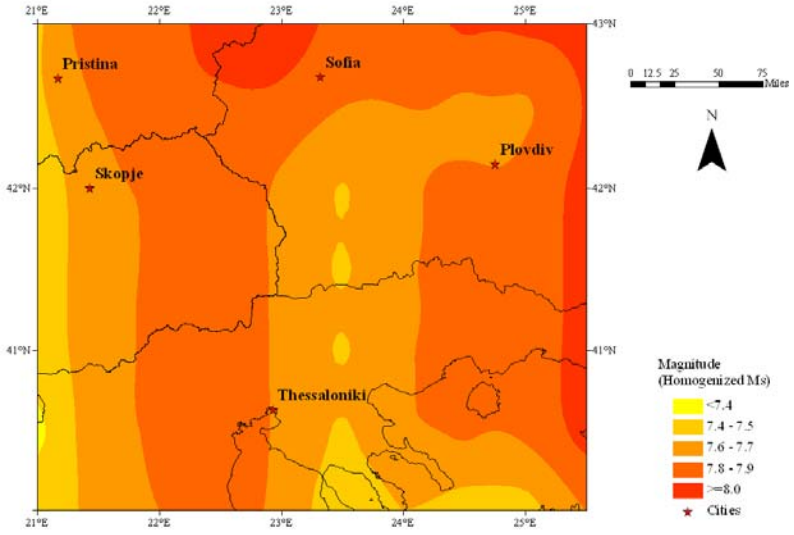

(c)

Figure 6.23 The most perceptible earthquake for I = (a) VI, (b) VII and (c) VIII using Papazachos and Papaioannou (1997) across southwest Bulgaria for an earthquake of 15 km focal depth. Contours are at intervals of 0.2 M_s

Similar contour patterns of hazard are seen across all intensity ground motion levels considered. Lower estimates of $M_{P(max)}$ are seen in the northwest corner of the region (<6.5 → 7.0 M_s at intensity VI), with forecasts increasing as one moves in a southeast direction towards the region's centre. The maximum $M_{P(max)}$ of 7.75+ M_s over Sofia is in west Bulgaria for I = VI, but is not seen to extend across the political borders between countries. A broader region bounded by the 7.50 M_s contour extends almost north to south across the entire region, encompassing over two-thirds of Bulgaria and much of north Greece and the north Aegean extent.

The highest $M_{P(max)}$ increases to 8.00+ M_s at I = VIII, and is confined to a small area centred on Sofia and extends westwards from here. The 7.75 M_s contour has extended north-south to the Bulgarian borders, and eastwards beyond Plovdiv, with additional confined zones at this hazard level extending south into the north Aegean area. The 7.50 M_s contour now extends into west Turkey as far as the 28° meridian. The lowest perceptible magnitude estimated is now 7.00 M_s running in a band of hazard east-west through the north Aegean into Turkey.

Burton *et al.* (2004b) find stable forecasts of 7.50 M_s at all intensity levels considered at this location. This work however expects stable estimates of $M_{P(max)}$ to be in the range 7.50-7.75 M_s at all intensities. With forecast magnitude extremes described earlier, for example, the 50-year return period event (section 5.5.3) and knowledge of this region's seismicity, earthquakes of [homogenized] 7.50 M_s to produce intensities of VIII are achievable and within the scope of seismicity in southwest Bulgaria.

$M_{P(max)}$ forecasts are consistent to each other for regions located central to both catalogued areas. For example, south of the political triple junction region into Greece both assessments suggest ≈7.0-7.5 M_s at intensities VI and VII respectively. The 7.0 M_s contour is consistently broader over northern Greece in this study than Burton *et al*. This broad similarity in estimates extends west to the Albanian coast where noticeably lower magnitudes are forecast compared with the north Aegean area and is likely due to the deeper subduction seismicity of this coastal region. However, this catalogue consistently produces forecasts marginally higher magnitudes (~0.50-0.75 M_s) to the west of the catalogued region. Unlike Burton *et al.* (2004b), hazard forecasts cease at the 28° meridian. This characteristic may be due to this study adopting a shorter extreme interval in this study, or truncating the adopted catalogue earlier in the easterly direction than their Greek catalogue; this characteristic excluded much of the Izmit earthquake sequence.

Although Table 6.14 and Figure 6.24 affords a direct comparison between Koravos *et al*. (2003) and this work for roughly the same broad geographic region, the connection between estimates for $M_{P(max)}$ at I = VIII is not as strong as for acceleration and velocity. Unlike ground acceleration or velocity hazard, Koravos *et al*. apply different ground motion models to this work. For the specific instance of hazard in southwest Bulgaria at intensity VIII from a nominal earthquake of 10 km focal depth the largest differences are found around the triple junction area of southwest Bulgaria (~0.9 M_s greater in this study). Magnitude estimates are closer between these studies as one extends into Greece and the north Aegean region from southwest Bulgaria, and then towards the edges of the study area for which hazard forecasts are available. This may be due to difference in the underlying methodology for hazard estimation. Koravos *et al*. adopt seismogenic source zones that are not only larger in comparison to the smaller, overlapping zone-free analysis cells adopted here that create a finer resolution of hazard forecasting, but also do not extend geographically as extensively as this studies, thus taking in a reduced amount of seismicity.

Burton *et al.* (1984) adopt a similar statistical approach to that used here for the Mediterranean, Aegean Sea and near Asian regions. Gumbel's third distribution is applied to cells that provide enough data for analytical purposes and estimates of $M(P_p$ max) are obtained using relevant regional intensity attenuation relations for Turkey. For the region centred on eastern Anatolia $M(P_p$ max) = 7.30.

Burton *et al.* (2004b) has already been discussed in detail earlier in this text. The salient points from that work are that it extends work done by Makropoulos and Burton (1985a) by considering earthquake perceptibility. Using data that may be construed as compatible with this work of $M \geq 5.5$ since 1900 and a compatible ground motion model, they forecast $M_{P(max)}$ at intensities VI, VII and VIII for broadly the same region as here. Although they do not state for which focal depth the specimen seismicity is set at to produce their estimates for $M_{P(max)}$, contoured hazard estimates are largely compatible between these studies. Typically, differences at identical points in each set of maps are no more than 0.25-0.50 M_s different. These variations may be accounted for if Burton *et al*. adopted a different focal depth for their hazard analysis.

Magnitude perceptibility and integrated perceptibility curves for Sofia are in Figure 6.25, with equivalent curves for the other cities considered in Appendix 26. From Figure 6.25 it is evident that with a finite focal depth the minimum magnitude that may produce ground shaking is 5.54 M_s at intensity VI, rising to 6.24 M_s at intensity VII and 6.94 M_s at intensity VIII at 15 km focal depth.

Seismogenic source zone[1] used by Koravos *et al.*	Macroseismic intensity perceptibility model	
	Koravos *et al.* (2003)[2]	This study; PP97[3, 4]
9 [east mainland Greece]	6.9 (± 0.1)	7.00 → <7.75
10 [north Aegean Sea]	7.4 (± 0.2)	7.00 → <7.75
11 [west Marmara Sea]	7.6 (± 0.2)	7.00 → <7.75
13 [Albania-Greece-FYROM border]	6.7 (± 0.2)	7.25 → <7.75
14 [Bulgaria-Greece-FYROM border]	7.1 (± 0.2)	7.50 → 8.00+

[1, 4] As for Table 6.3; [2] using the ground motion model of Musson (2000; Table 3.2) for an earthquake of 10 km focal depth; [3] using Eq. (3-22) for epicentral intensity for an earthquake of 10 km focal depth

Table 6.14 Empirical differences in forecasted *most perceptible magnitudes* at intensity VIII of 10 km focal depth in regions common to Koravos *et al.* (2003) and this study

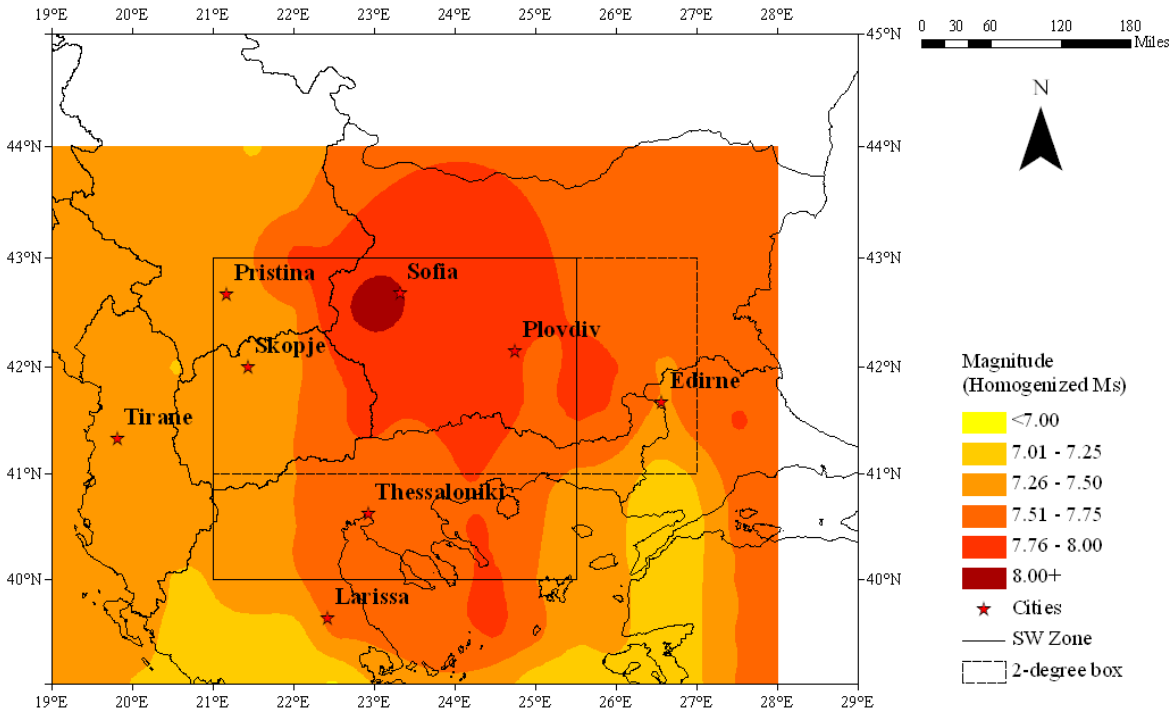

Figure 6.24 The *most perceptible magnitude* at intensity VIII for a nominal earthquake of 10 km focal depth using Papazachos and Papaioannou (1997) across the broad Balkan extent. Contours are at intervals of 0.25 M_s

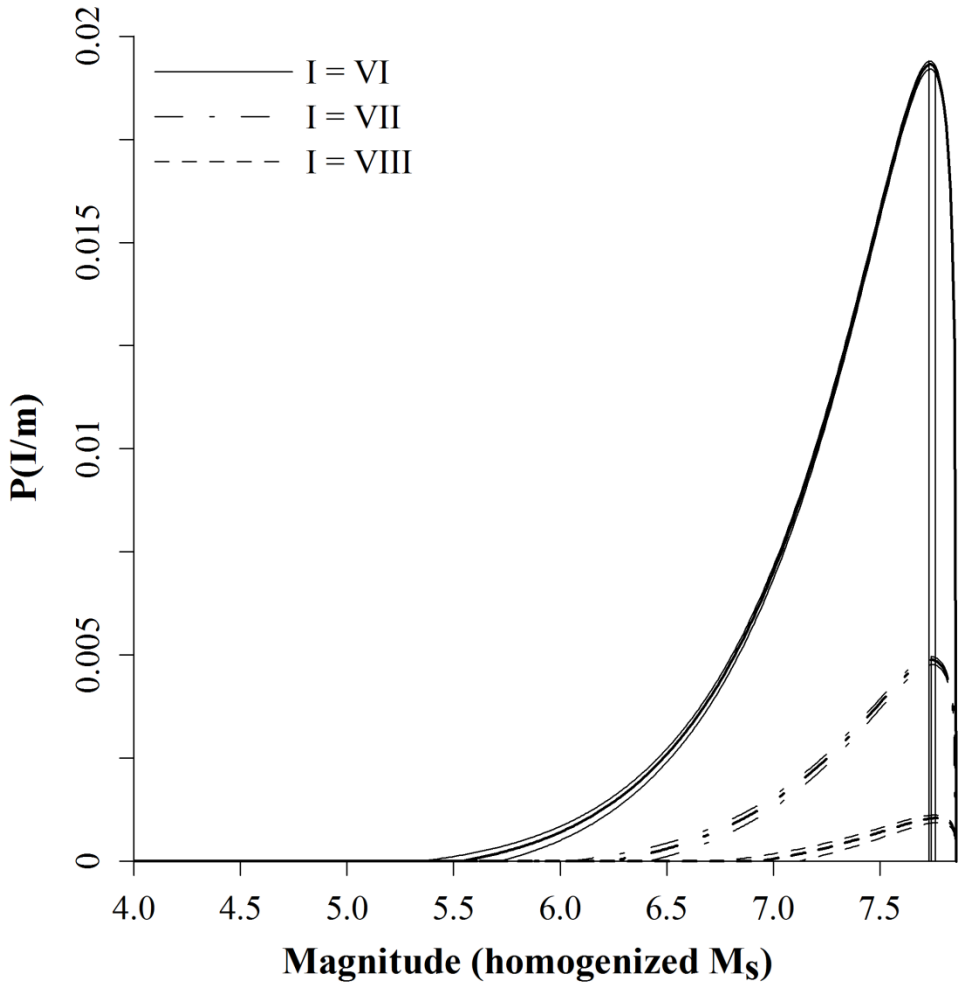

(a)

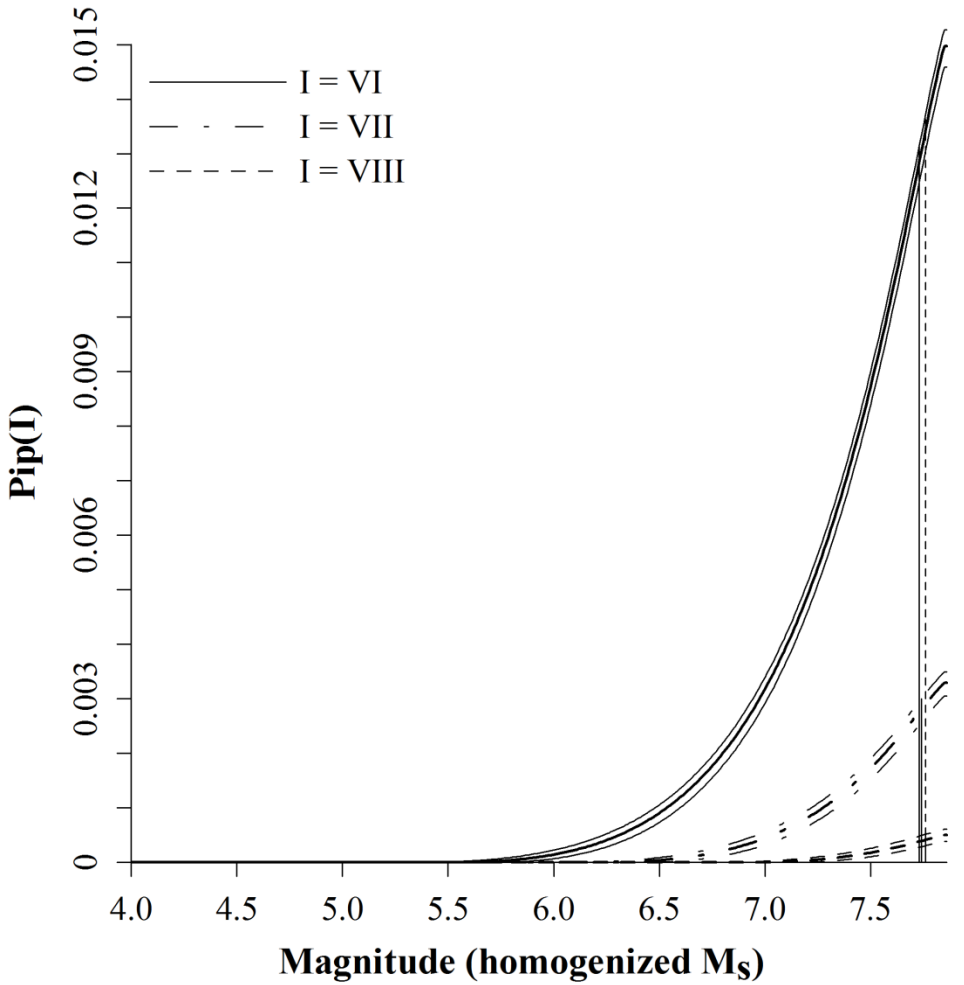

(b)

Figure 6.25 intensity (a) perceptibility and (b) integrated perceptibility curves for Sofia using Papazachos and Papaioannou (1997) at intensities VI, VII and VIII. The central heavy black curve of each set of three curves represents a nominal earthquake of 15 km focal depth, while the upper and lower curves represent 10 km and 20 km focal depth respectively. Vertical black lines represent the *most perceptible magnitude* only for 10 km focal depth. The vertical dashed line represents M_3 from cumulative strain energy release techniques

These magnitudes reduce to 5.35 M_s (VI), 6.05 M_s (VII) and 6.75 M_s (VIII) at the upper boundary to seismogenic activity (10 km), and rise to 5.72 M_s (VI), 6.42 M_s (VII) and 7.12 M_s (VIII) at the lower limit of 20 km. Koravos *et al*. forecast the minimum magnitude to be 6.4 M for a 10 km focal depth at intensity VIII (Table 6.15). The difference between this and 6.75 M_s estimated here may be due to their seismogenic source zone being about half the size of the analysis cell used here.

	Papazachos and Papaioannou (1997)		
Focal Depth (km)	VI	VII	VIII
10	5.35	6.05	6.75
15	5.54	6.24	6.94
20	5.72	6.42	7.12

Table 6.15 Minimum threshold magnitudes to produce specific levels of intensity at Sofia

The most perceptible magnitude at intensities VI, VII and VIII for Sofia and the other cities considered are in Table 6.16. Sofia, Plovdiv and Thessaloniki are again forecast highest $M_{P(max)}$ at each intensity, with each ground motion level forecast $M_{P(max)}$ approaching or marginally exceeding the catalogued homogenized magnitude of 7.6 M_s. These cities are consistently forecast $M_{P(max)}$ within 0.2 M_s of the *maximum credible magnitude*, M_3. Other cities such as Pristina, Larissa and Skopje have larger differences; on occasions these are as much as 0.9 M_s between $M_{P(max)}$ and M_3. The different regional and local seismotectonic environments in which these cities are located that help to explain variability in differences between $M_{P(max)}$ and M_3 has been discussed in section 6.5.1.

Sofia is estimated *most perceptible magnitudes* of $M_{PI(VI)}$ = 7.73 M_s to $M_{PI(VIII)}$ = 7.76 M_s (Table 6.16) and is estimated a modal extreme magnitude of 7.79 M_s in 25 years (Table 5.7). However, modal extreme forecasts are attached with reasonably large uncertainties, σ_M, of 1.17 M_s, which may help explain this discrepancy with a large extreme forecast for a relatively short return period, and also the occurrence of estimates for $M_{P(max)}$ that are outside the scope of the adopted catalogue.

	Macroseismic intensity								
	VI			VII			VIII		
City	$M_{P(max)}$	P_p [1,2]	P_{ip} [1,3]	$M_{P(max)}$	P_p	P_{ip}	$M_{P(max)}$	P_p	P_{ip}
Edirne	7.39	13.0	8.8	7.40	3.1	1.6	7.43	0.5	0.1
Larissa	7.23	8.1	6.7	7.30	1.9	1.1	7.46	0.3	0.1
Plovdiv	7.73	13.0	9.8	7.74	3.3	2.1	7.78	0.7	0.3
Pristina	6.69	4.5	2.5	6.96	0.6	0.2	7.36	<0.1	<0.1
Skopje	6.70	5.2	3.0	7.00	0.8	0.3	7.41	<0.1	<0.1
Sofia	7.73	19.3	12.9	7.74	4.9	2.8	7.76	1.0	0.4
Thessaloniki	7.59	15.2	11.2	7.62	3.6	2.0	7.70	0.6	0.2
Tirane	6.81	6.9	3.9	6.97	1.1	0.3	7.27	<0.1	<0.1

[1] Estimates are given for an nominal earthquake with focal depth of 15 km. Probabilities are given at a factor of $\times 10^{-3}$; [2] Annual probability of perceiving ground motion arising from magnitude $M_{P(max)}$; [3] Annual probability of perceiving ground motion arising from all magnitudes up to including $M_{P(max)}$

Table 6.16 The *most perceptible magnitude* at intensity of VI, VII and VIII with the associated perceptibility probability, P_p and the annual probability of exceedance, P_{ip}, of perceiving these macroseismic intensities. Estimates are derived from the distribution of seismicity present within a 2° half-width cell of the city are given, using the conditions outlined in section 5.4

The *most perceptible magnitude* for Sofia using Papazachos and Papaioannou (1997) at each focal depth is in Figure 6.26(a) (other cities are in Appendix 27). Each curve of $M_{P(max)}$ saturates to ω at intensity IX at all focal depths. Earlier sections outline Sofia is forecast significantly higher values for $M_{P(max)}$ due to being located in areas of higher crustal deformation. Figure 6.26(a) reflects this with the apex to this curve at approximately M_3. After this value, the curve plateaus in a zone of inflexion slightly below the forecasted annual maximum intensity for this city. All curves start to diverge between intensities VII and IX, and approach ω at intensity IX.

Hazard curves for Sofia using Papazachos and Papaioannou (1997) are in Figure 6.26(b) (other cities are in Appendix 28). Intensity IV is expected to be exceeded on an almost annual basis, while intensity VI is expected to be exceeded approximately once every 10 years. All eight cities are considered with respect to annual exceedances of intensities in Figure 6.27.

Curves are truncated at intensity VIII to highlight variability in hazard at these cities between low and moderate intensities, particularly in the interval that considers the change from onset of damage to inducing structural damage (VI to VIII). This highlights important differences between each city at lower intensities attributed with higher hazard. Both illustrations show these cities are forecast negligible annual hazard above of VIII.

It is evident that at lower intensities (I < V) Sofia and Plovdiv are forecast lower hazard levels relative to the other sites. Only above intensity V do these cities have higher probabilities associated to them than other cities considered. Thessaloniki appears to be forecast higher hazard than most sites across all intensities illustrated. The tendency for these cities to have higher hazard probabilities attached is likely a reflection of their central location within the high hazard area of southwest and central Bulgaria, and northern mainland Greece.

Finally, annual probabilities of exceedance for Sofia for specific intensities estimated using Gumbel's third distribution in chapter 5 are in Table 6.17, with annual probabilities of exceedance for Sofia in specific T-year time intervals in Table 6.18 at the three focal depths considered (with the other cities considered in Appendix 29). Due to the discrete and bounded nature of intensity scales, intensities expected to be exceeded at least once in each of the time intervals considered hover around VI and VII for 10 to 1,000 years.

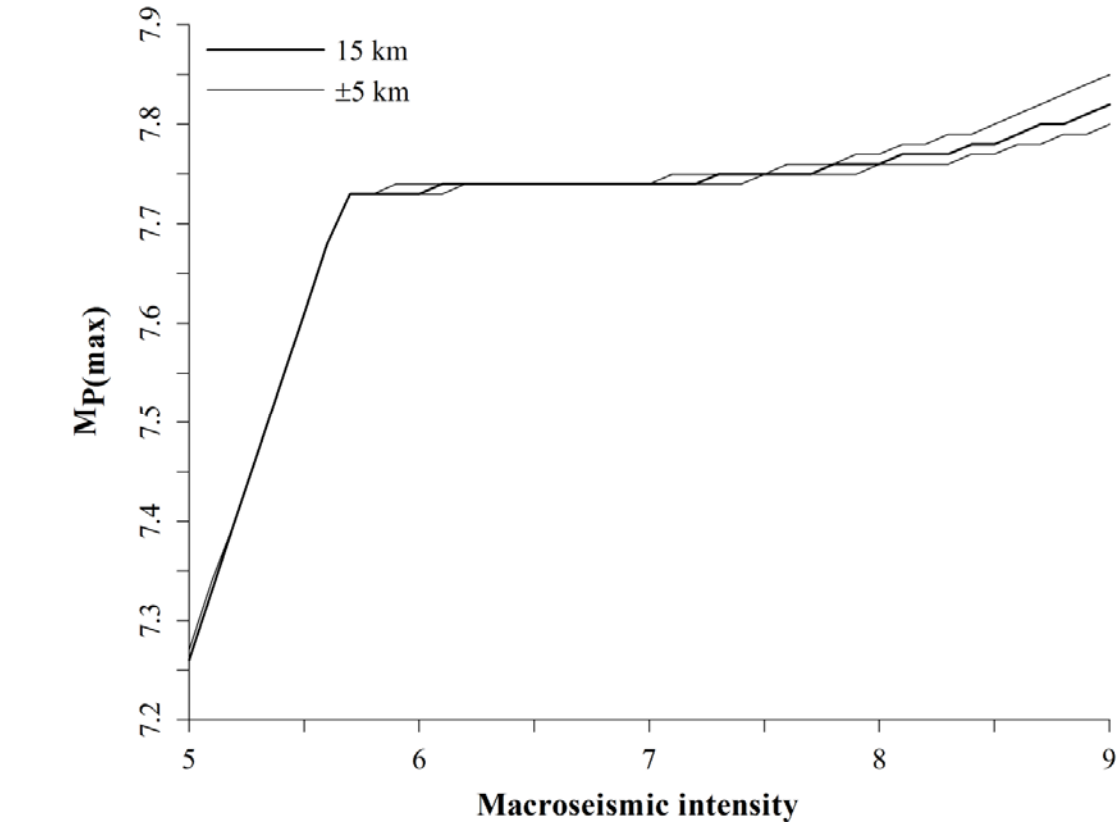

(a)

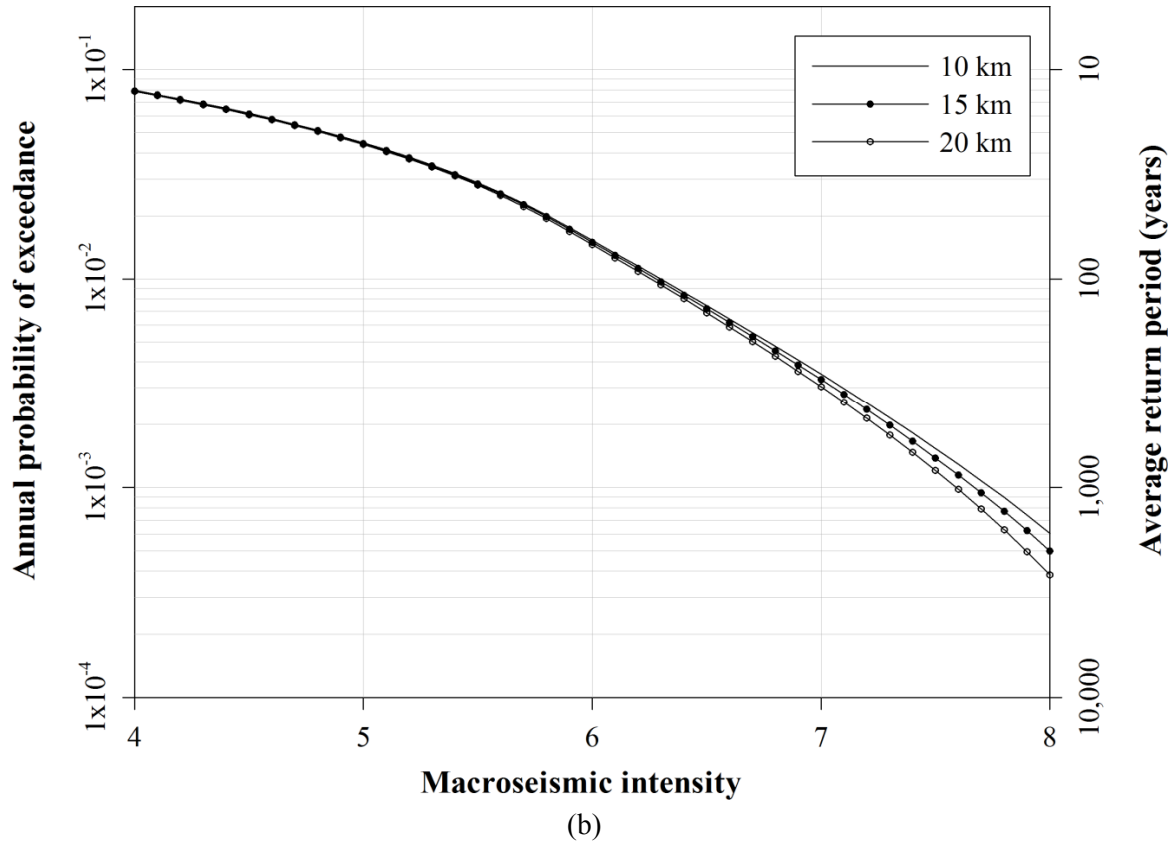

(b)

Figure 6.26 *Most perceptible magnitudes*, $M_{P(max)}$, for Sofia using Papazachos and Papaioannou (1997) for nominal earthquakes of focal depth 10 km, 15 km and 20 km (b) macroseismic intensity hazard curves for Sofia for the same focal depths

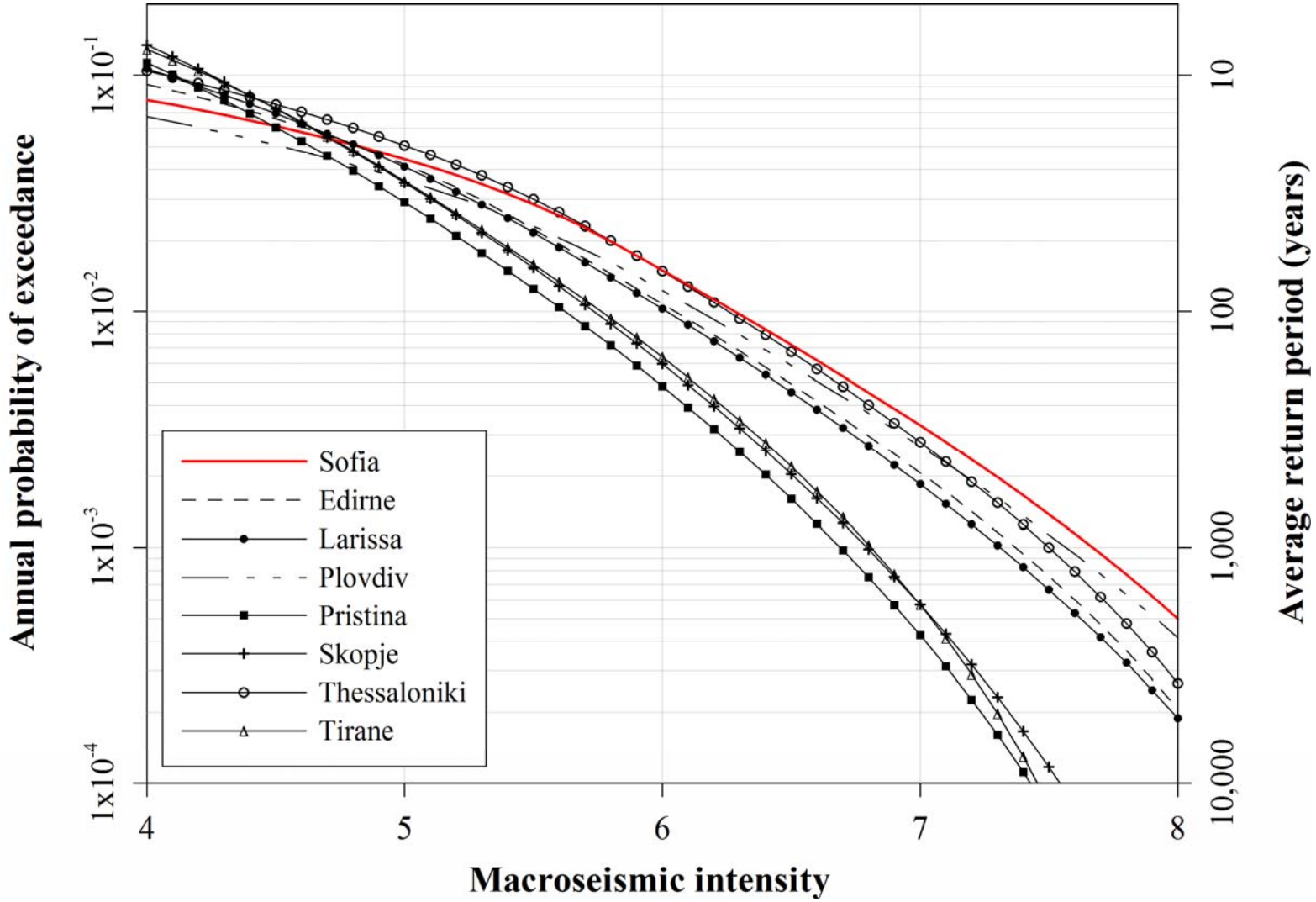

Figure 6.27 Macroseismic intensity hazard curves for all urban centres considered using Papazachos and Papaioannou (1997) for a nominal earthquake of 15 km focal depth

		Annual probability of exceedance ($\times 10^{-3}$)[1]							
Ground motion model	Focal depth (km)	I_μ **(VII: 7.0)**	I_A **(VII: 7.8)**	I_4	I_5	I_6	I_7	I_8	I_9
Papazachos and Papaioannou (1992)	10	3.5	0.9	80.0	44.7	15.3	3.5	0.6	<0.1
	15	3.3	0.8	79.3	44.4	15.0	3.3	0.5	<0.1
	20	3.0	0.6	78.8	43.9	14.6	3.0	0.4	<0.1

[1] Due to the discrete interval nature of intensity scales, annual probabilities of exceedance are given for parameter μ and the annual modal intensity of Gumbel's third extreme distribution (Table 5.19) and intensities IV to IX.

Table 6.17 Annual probabilities ($\times 10^{-3}$) of experiencing specific intensity ground motions estimated for the region surrounding Sofia

		Annual probability of exceedance ($\times 10^{-3}$) in T years					
Ground motion model	Focal depth (km)	100	200	300	400	500	1,000
Papazachos and Papaioannou (1992)	10	VI (6.3)	VI (6.4)	VI (6.4)	VI (6.5)	VI (6.6)	VII (7.7)
	15	VI (6.2)	VI (6.3)	VI (6.4)	VI (6.5)	VI (6.6)	VII (7.6)
	20	VI (6.6)	VI (6.6)	VI (6.6)	VI (6.6)	VI (6.6)	VII (7.5)

Table 6.18 Macroseismic intensities expected to be exceeded at least once in T years for the region surrounding Sofia

6.6 Seismic source disaggregation

Contributions to the prevailing seismic hazard of each city is now considered using modified seismic hazard disaggregation techniques (e.g. Cramer and Petersen, 1996; Harmsen *et al.*, 1999; Harmsen and Frankel, 2001). Hazard will be disaggregated into smaller contributory components characterised by set intervals of magnitude and epicentral distance, using data extracted from a subset of [*whole process*] seismicity present within a 2° half-width analysis cell centred on each city. The approach adopted by previous authors is used and adapted here to disaggregate the seismogenic source around Sofia as an example to determine values for the modal magnitude (M*) and modal distance (D*), and so create an alternative suite of '*design*' earthquakes, given in terms of an event's proximity to the city and its size. An example will be made of Sofia, with the other cities in Appendix 30 and discussed in section 6.6.2.

Modal values of the earthquake magnitude and source-to-site distance will be selected in place of mean equivalents as they better lend themselves to representing physically realisable earthquakes (Bazzurro and Cornell, 1999). Mean magnitudes of a suite of earthquakes in a confined zone may fall on a magnitude value that has not actually occurred in that specific zone. Further, a decision needs to be taken on whether uni-variate (e.g. M = 6.65 and D = 18 km obtained from a simple frequency analysis of the data used, thus potentially two earthquake parameters that may not actually occur in the same event) or bi-variate modal values (i.e. the most commonly occurring paired M-D values representing a real-time occurring earthquake) are accepted. Although Bazzurro and Cornell (1999) suggest bi-variate modal pairs are advantageous, uni-variate modal values will be extracted from data to disaggregate hazard to each city, as the subset of earthquakes extracted for each city will likely be relatively small compared with the parent catalogue of nearly 4,000 earthquakes. Each magnitude-distance '*bin*' will be defined by a small epicentral distance interval and magnitude interval. These could potentially contain small numbers of individual earthquakes, each characterised by a different M-D combination, thus not producing a unique modal M*-D* definition for that analysis cell. The number of events falling into each '*bin*' will be dependent upon their sizes. Seismicity extracted around each city to estimate extreme hazard will be used.

Disaggregating these data separates the earthquake inventory into discrete joint magnitude and distance '*bins*' of 0.25 M_s and 10 km respectively. M* and D* for each '*bin*' is then determined and the magnitude density value from the $P_e(M)$ distribution specific to Sofia is attached to M*. The full seismic hazard contribution to Sofia is in Figure 6.28(a). The interval containing the cut-off magnitude, M_{CUT}, adopted is in red. The interval containing the *maximum credible magnitude*, M_3, derived from energy release techniques is shaded yellow. The magnitude interval containing $M_{P(max)}$ for the lowest levels of each ground motion are highlighted by blue arrows.

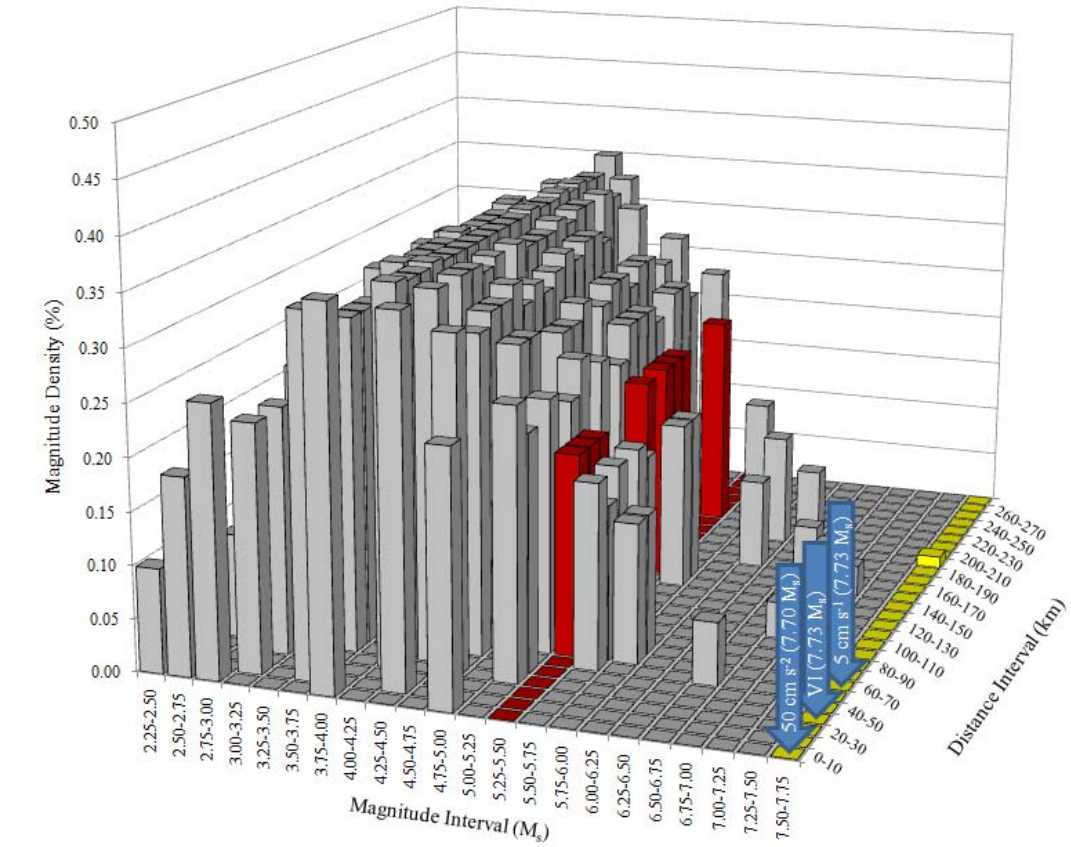

(a)

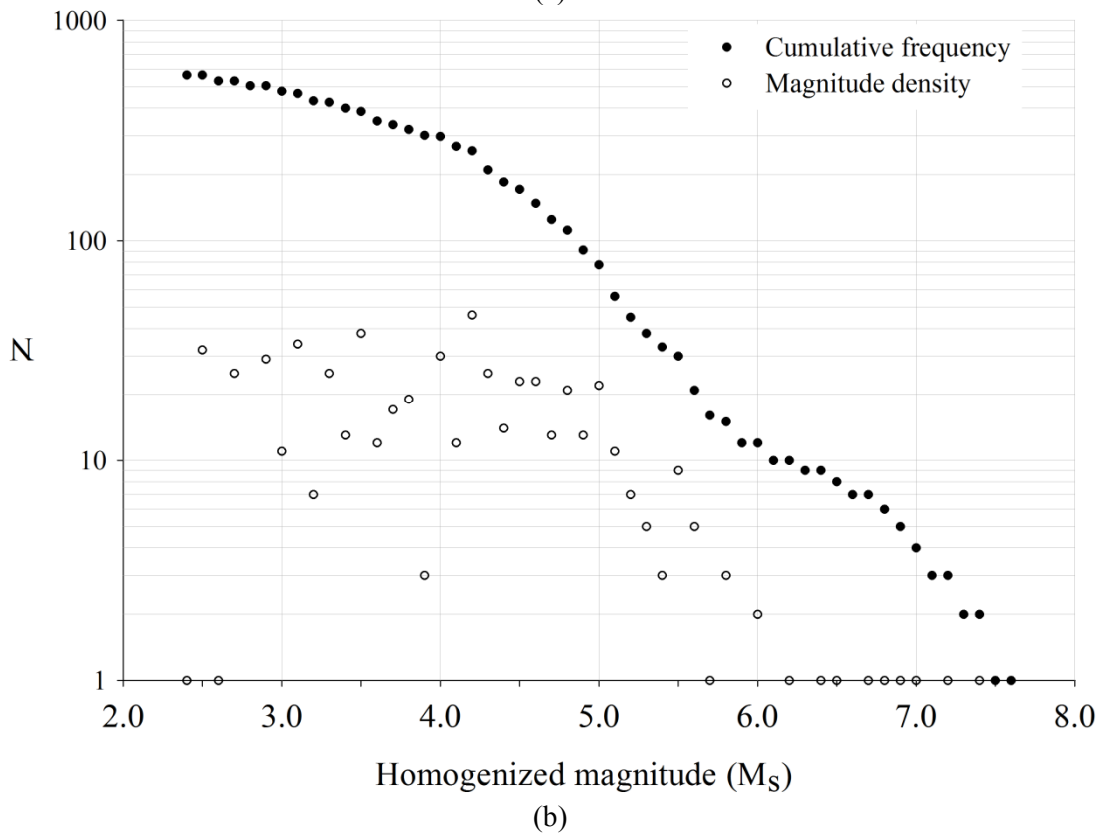

(b)

Figure 6.28 Seismic source disaggregation outlining contributions to the seismic hazard of Sofia from localised seismicity (considering all seismicity); (b) cumulative frequency and magnitude density distribution for Sofia using identical earthquake population to (a)

6.6.1 Disaggregating Sofia's hazard

Discussion here will concentrate remarks mainly with reference to magnitudes at and above the magnitude interval containing Sofia's cut-off threshold of 5.3 M_s adopted to develop extreme hazard estimates in chapter 5. The main contribution to Sofia's earthquake hazard appears confined to two regions of the joint distribution, from 5.25-6.00 M_s at 60-80 km, and 5.25-5.75 M_s at 140-180 km from Sofia (Figure 6.28(a)).

Sofia has had no large magnitude earthquake (≥5.25 M_s) within 50 km of it during the time span of the adopted catalogue. Larger magnitude earthquakes (≥6.50 M_s) are at distances greater than 50 km, but have small annual probabilities of occurrence. The largest homogenized magnitude of the adopted catalogue is located at over 190 km from Sofia, so poses little hazard.

Moderate magnitudes below the cut-off magnitude govern Sofia's local hazard, with seismicity between 4.25-4.50 M_s occurring within 10-20 km of the city, and earthquakes of 4.75-5.00 M_s within 10 km. The magnitude interval 4.25-5.50 M_s has the largest magnitude density attached to it of ~0.35 per annum, with seismicity between 5.00-5.25 M_s occurring between 30 and 50 km. Figure 6.28(b) illustrates site-specific cumulative frequency and magnitude density distributions for Sofia (other cities are given in Appendix 30). These adopt identical [*whole process*] catalogue content (Figure 5.15) used to develop Sofia's source disaggregation plots and from which [*part process*] extreme events (Figure 5.15) were extracted from to develop the related estimates. During the time span of the catalogue there were between 10 and 30 earthquakes at each 0.1 M_s interval between 4.0 M_s and 5.0 M_s. Above 5.0 M_s the number of occurrences begins to decrease, supporting the idea that Sofia is predominantly subject to moderate-magnitude seismicity.

M_3 is constrained to the same ¼ M_s magnitude interval as the largest homogenized catalogued earthquake. All estimates that are plotted for $M_{P(max)}$ and M_3 occupy the same magnitude interval due to its location in an area of high crustal deformation. Finally, with respect to extreme hazard estimates, only a small proportion of the sub-catalogue extracted for Sofia contributes to determining extreme hazard forecasts. For Sofia, this appears to have helped constrain $G^{(III)}$ distribution parameters resulting in a relatively small uncertainty, σ_ω, on the upper bound magnitude of 0.75, perhaps resulting from sufficient lower-magnitude '*dummy*' observations being excluded from consideration after Sofia's cut-off magnitude of 5.3 M_s is applied to catalogue data.

6.6.2 Disaggregating hazard to other cities

The other seven cities are subject to wide variation in earthquake hazard. This is largely due to the different sub areas of the broad seismogenic environment in which they are located. Site-specific disaggregation plots reflect this, derived from seismicity plotted in Appendix 4.

Moderate near-field seismicity dominates Plovdiv's hazard. There is bulk hazard between 3.50-5.25 M_s within 10 km and this has the highest magnitude density attached over a slightly broader magnitude interval than Sofia between ~3.75-4.50 M_s (~0.39 per annum). It does not appear subject to significant large magnitude hazard above its own cut-off magnitude of 5.6 M_s. Its most significant hazard comprises magnitude 5.50-6.00 M_s seismicity, although at a greater distance of 90-160 km. Such a high cut-off magnitude adopted for Plovdiv leaves a comparatively small amount of seismicity from which to develop extreme hazard estimates, resulting in estimates for $M_{P(max)}$ for the lowest levels of ground motion approximating to M_3, and a relatively large uncertainty on the city's upper bound, ω.

Edirne is located furthest from the high seismicity area of southwest Bulgaria. It has no large magnitude hazard (above its M_{CUT} of 5.2 M_s) within 30 km; the closest hazard of note is 5.00-5.25 M_s within 30-40 km. However, there is significant hazard in the magnitude interval containing M_{CUT} at greater distances from Edirne. Most of its bulk magnitude hazard is moderate and contained in the interval 5.00-6.00 M_s between 90 and 160 km. This is most likely to be hazard emanating from seismicity generated by the North Anatolian Fault (NAF) and western Turkey, and is reflected in this city's cumulative frequency and magnitude density distributions. These show Edirne subject to a larger number of higher magnitude ($M \geq 6.0$ M_s) earthquakes than Sofia.

Thessaloniki is subject to much more near-field seismicity than the other three cities already discussed. Being located closest of all cities considered to the Serbomacedonian massif, it will be most at risk to seismicity it produces (e.g. the homogenized 7.6 M_s earthquake of 2000). Magnitudes 5.75-6.00 M_s occur within 20-30 km ($P_e(M) \approx 0.21$ per annum) and 6.25-6.50 M_s occur within 30-40 km ($P_e(M) \approx 0.11$ per annum), with further seismicity found 6.00-6.25 M_s occur within 60-90 km ($P_e(M) \approx 0.17$ per annum). Thessaloniki's concentrated hazard is located between 5.25-6.00 M_s at 110-200 km.

Edirne and Thessaloniki also have extreme estimates developed from comparatively small amounts of seismicity; both having cut-off magnitudes ≥5.2 M_s. As with Sofia, this appears to have helped constrain uncertainty on the upper bound parameter ω to a higher degree. These cities are the only others with $\sigma_\omega < 1.0$ (0.71 and 0.94 respectively).

These illustrate that extreme hazard forecasts developed earlier derive from significantly different portions of each extracted catalogue, defined by $M_{\mathbf{CUT}}$ attached to each city (red banding). This affects relationships between $M_{\mathbf{CUT}}$, M_3, and [lowest] $M_{P(max)}$. Forecasts developed from smaller portions of a city's sub catalogue appear to result in estimates of the *most perceptible magnitude* that approach M_3 (e.g. Sofia, Edirne, Plovdiv, Thessaloniki), such that $M_{P(max)} \approx M_3$. For some cities, this also appears to help constrain ω and σ_ω.

Conversely, cities with extreme estimates derived from larger sub sections of the extracted catalogue exhibit estimates for $M_{P(max)}$ in the range $M_{\mathbf{CUT}} < M_{P(max)} < M_3$ (often $M_{P(max)} << M_3$). These cities also exhibit $M_{\mathbf{CUT}}$ approaching the magnitude with greatest probability density, $P_e(M)$. Typically $M_{\mathbf{CUT}}$ is closer to – or is contained within – the magnitude *bin* with greatest probability density the larger the difference between M_3 and $M_{P(max)}$.

These relationships between M_{CUT}, $M_{p(max)}$ and M_3 are consistent with hazard estimates for the four remaining cities. Larissa, Pristina, Skopje and Tirane are subject to localised hazard with the highest magnitude density (~0.50 per annum) of all cities at magnitudes around 5.00 M_s. These four cities each have M_{CUT} near to, or at, the maximum annual probability of occurrence, allowing estimates of $M_{P(max)}$ to be less constrained to M_3, and more realistic with respect to the larger magnitude seismicity of the full catalogue and each city's specific subset extracted from it.

6.7 Discussion and summary

This chapter completes the probabilistic seismic hazard assessment for southwest Bulgaria and the surrounding high hazard region. It extends well-known principles of cumulative strain energy release, earthquake perceptibility and integrated perceptibility to this seismic hazard assessment allowing additional and meaningful estimates of large earthquake potential to be developed. These have been compared with magnitude estimates obtained using Gumbel's asymptotic extreme value distributions. Energy release statistics afford alternative *maximum* magnitude scenarios to the probabilistic nature of Gumbel's extreme distributions. Perceptibility statistics allow ground motion hazard curves to be developed that suggest annual probabilities of exceedance for each of the ground motions considered. Ground motion models have been adopted that are directly comparable to those used in Burton *et al.* (2003, 2004b), differing in only the region considered. It is therefore acceptable to consider part of this work as a geographic extension to those studies.

Magnitude perceptibility and integrated perceptibility forecasts offer earthquake engineers means to partition seismic hazard to provide alternative earthquake scenarios and aid development of anti-seismic building codes. These consolidate principles of earthquake occurrence statistics with levels of felt ground motion resulting from regional seismicity. The ground motion interval considered is important, and varies depending on the ground motion characteristic and geographic region considered. For macroseismic intensity, scales adopted have a lower threshold to the onset of serious damage and hold for any seismic region of the world. This is because they are not dependant on geography, prevailing seismicity or methods of measuring this seismicity. The range and increment of ground accelerations and velocities considered may however depend upon both current building codes enforced (if any exist) in a particular location – with a view to their improvement – and designed in response to expected ground motions [estimated by previous studies] and consequently the building designs that are typical of the geographic region considered. For reviewing seismic hazard in this instance, ground accelerations of 50 cm s^{-2} to 150 cm s^{-2} (at intervals of 50 cm s^{-2}) ground velocities of 5 cm s^{-1} to 15 cm s^{-1} (at intervals of 5 cm s^{-1}) and intensity levels VI to VIII were selected as the *scenario* ground motions.

The most perceptible magnitude, $M_{P(max)}$, for high and low limits to each ground motion at each site considered in section 6.5 and sections therein are summarised in Table 6.19. Most forecasts of $M_{P(max)}$ are above 6.5 M_s, supporting conclusions of Koravos *et al.* (2003). For the broader regions the adopted statistical approaches forecast systematically lower *most perceptible magnitudes* to the west of this region regardless of the ground motion considered. Higher estimates are towards the east, where rarer larger events with magnitudes greater than 7.0 M_s dominate the hazard of this region, and are the product of a highly deforming tectonic environment.

	Most perceptible magnitude estimates for ground acceleration[1], ground velocity[2] and macroseismic intensity[3]					
City	50 cm s^{-2}	150cm s^{-2}	5 cm s^{-1}	15cm s^{-1}	VI	VIII
Edirne	7.34	7.38	7.38	7.41	7.39	7.43
Larissa	7.08	7.24	7.23	7.34	7.23	7.46
Plovdiv	7.67	7.70	7.72	7.75	7.73	7.78
Pristina	6.44	6.81	6.65	6.95	6.69	7.36
Skopje	6.43	6.83	6.66	6.98	6.70	7.41
Sofia	7.70	7.72	7.73	7.74	7.73	7.76
Thessaloniki	7.50	7.56	7.57	7.61	7.59	7.70
Tirane	6.66	6.87	6.83	6.96	6.81	7.27

[1, 2] Using Theodulidis and Papazachos (1992) for stiff soil conditions (S = 0.5) at the 50th percentile; [3] using Papazachos and Papaioannou (1997)

Table 6.19 The most perceptible earthquake magnitudes at each of the urban centres considered. For each ground motion, the lowest and highest ground motions considered are given

The majority of seismogenic zones studied by Koravos *et al.* (2003) returned *most perceptible magnitude* estimates that were identical for each ground motion considered. Although the largest difference was in zone 10 (loosely the central Aegean Sea area) with mp(I) forecast 1.2 magnitude units greater than mp(v) and mp(a), many zones exhibit differences of the order of ±0.1 between correlated levels of ground motion. The dominance of rare large magnitude earthquakes can account for this, and the ability for sub regions of high deformation strain rates and velocities to produce these large earthquakes. Illustrations in Appendix 30 highlight how cities within areas of apparent high deformation are forecast high *most perceptible magnitudes* that are compatible with the *maximum credible magnitude* it is forecast.

Each section that discusses earthquake perceptibility with respect to a form of ground motion provides a similar analysis, though using a zone-free cellular hazard model instead of a predefined framework of seismogenic source zones. Generally, higher $M_{P(max)}$ estimates are derived here than by Koravos *et al.* (2003), which may result from different input catalogues, magnitude homogenisation techniques, zoning of the region's seismicity or underlying statistical model adopted. Further difficulty arises for comparing these estimates due to the nature of the broad zones used by Koravos *et al.* spanning many computation nodes and magnitude intervals in the hazard maps created for section 6.5, so these findings need considering with due care.

It is also reasonable to consider differences in correlated estimates for $M_{P(max)}$ for individual urban centres from Table 6.19. This is not strictly the same practice as correlating actual estimates or measured values of PGA, PGV and intensity (e.g. Glavcheva, 1990; Wald *et al*., 1999b; Atkinson and Kaka, 2006). Edirne, Plovdiv and Sofia consistently exhibit the smallest differences between $M_{P(max)}$ for equivalent minimum and maximum levels of ground acceleration, ground velocity and intensity, with no difference being greater than ±0.08 M_s (between the highest levels of acceleration and intensity). Thessaloniki is also forecast correlated estimates for $M_{P(max)}$ with small differences between them ($0.02 \rightarrow 0.14$ M_s).

Figure 6.29 to Figure 6.31 correlate $M_{P(max)}$ for each minimum and maximum pair of ground motions considered (hollow circles). The dashed line on each plot is the linear best-fit line of these [city] data points. The solid grey line is at the adopted catalogue's maximum homogenized M_s magnitude, and bounds the magnitude range of the catalogue, while the *maximum credible magnitude*, M_3, for each city is also plotted (solid circles; with the black line being the best-fit line for the *maximum credible magnitudes*, and obviously will pass through each city point). The grey line highlights the perceptible magnitudes that are – in theory – outside the scope of the adopted catalogue by creating a boundary at the maximum homogenized M_s magnitude of the catalogue.

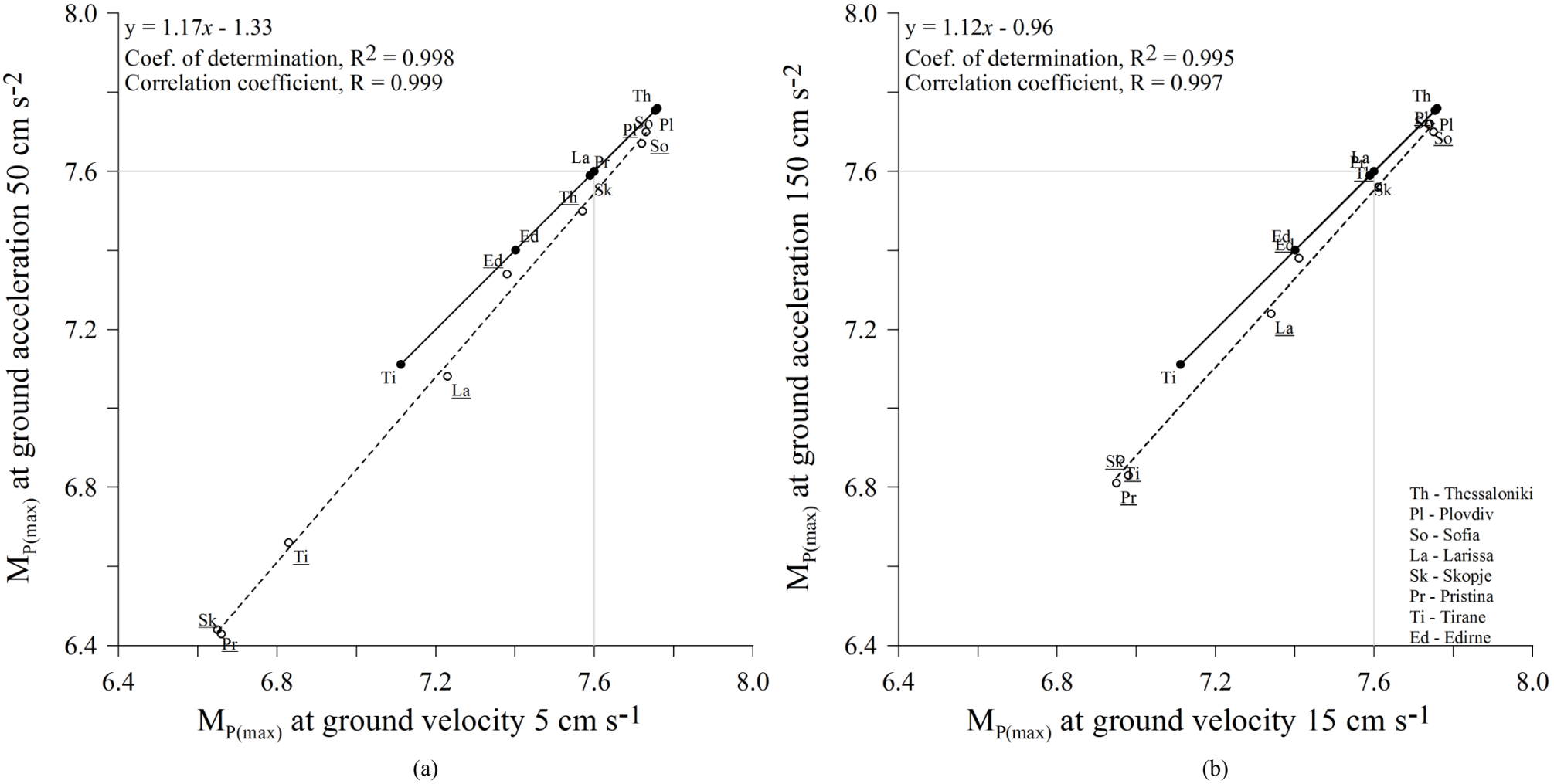

Figure 6.29 Linear correlation of (a) minimum and (b) maximum *most perceptible magnitudes* for horizontal ground acceleration and horizontal ground velocity for a nominal earthquake of 15 km focal depth. The solid line is the best-fit through *maximum credible magnitude* data points (M_3); dashed line is the best-fit through *most perceptible magnitude* ($M_{P(max)}$) data points

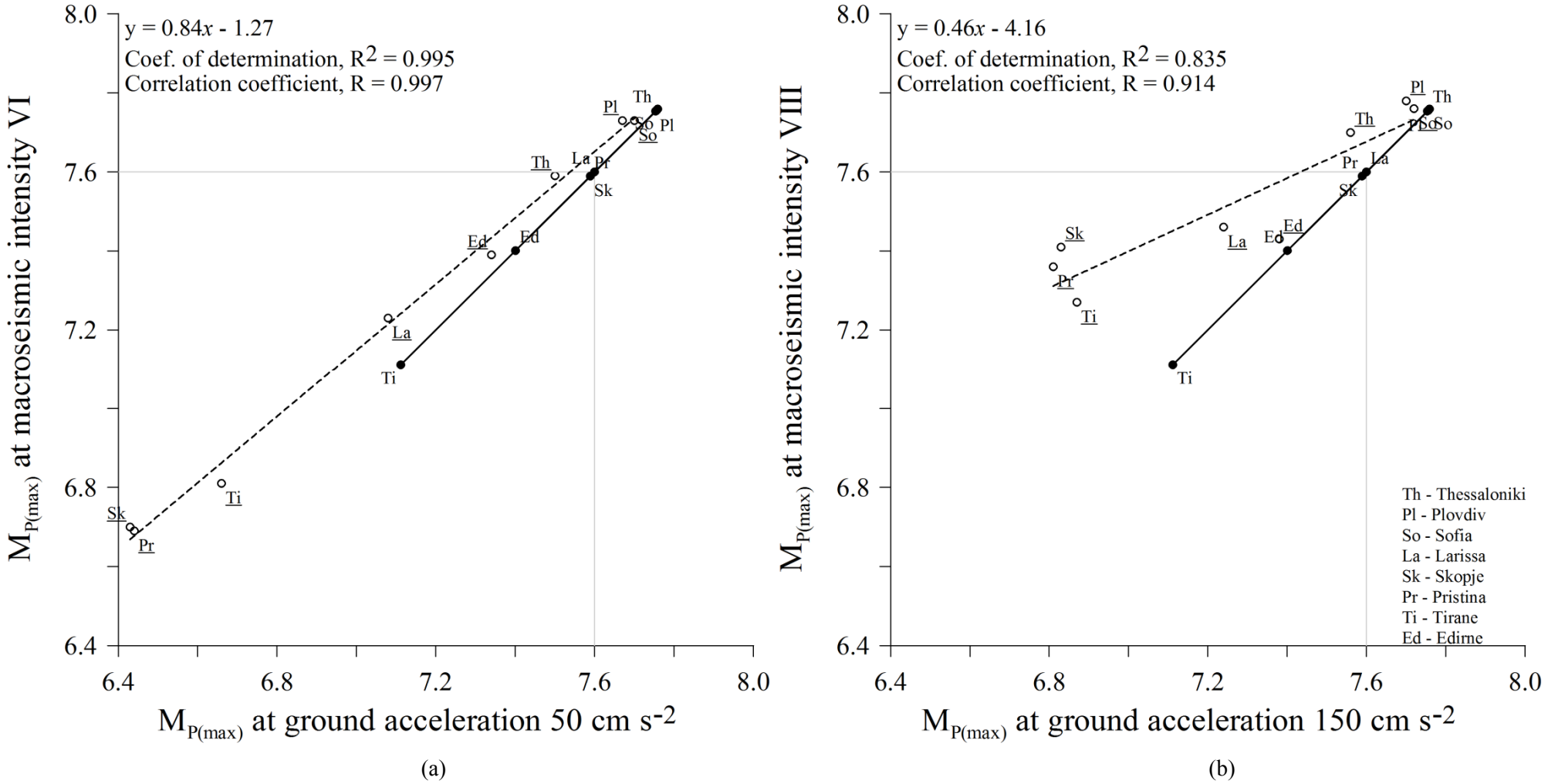

Figure 6.30 Linear correlation of (a) minimum and (b) maximum *most perceptible magnitudes* for horizontal ground acceleration and macroseismic intensity for a nominal earthquake of 15 km focal depth. The solid line is the best-fit through *maximum credible magnitude* data points (M_3); dashed line is the best-fit through *most perceptible magnitude* ($M_{P(max)}$) data points

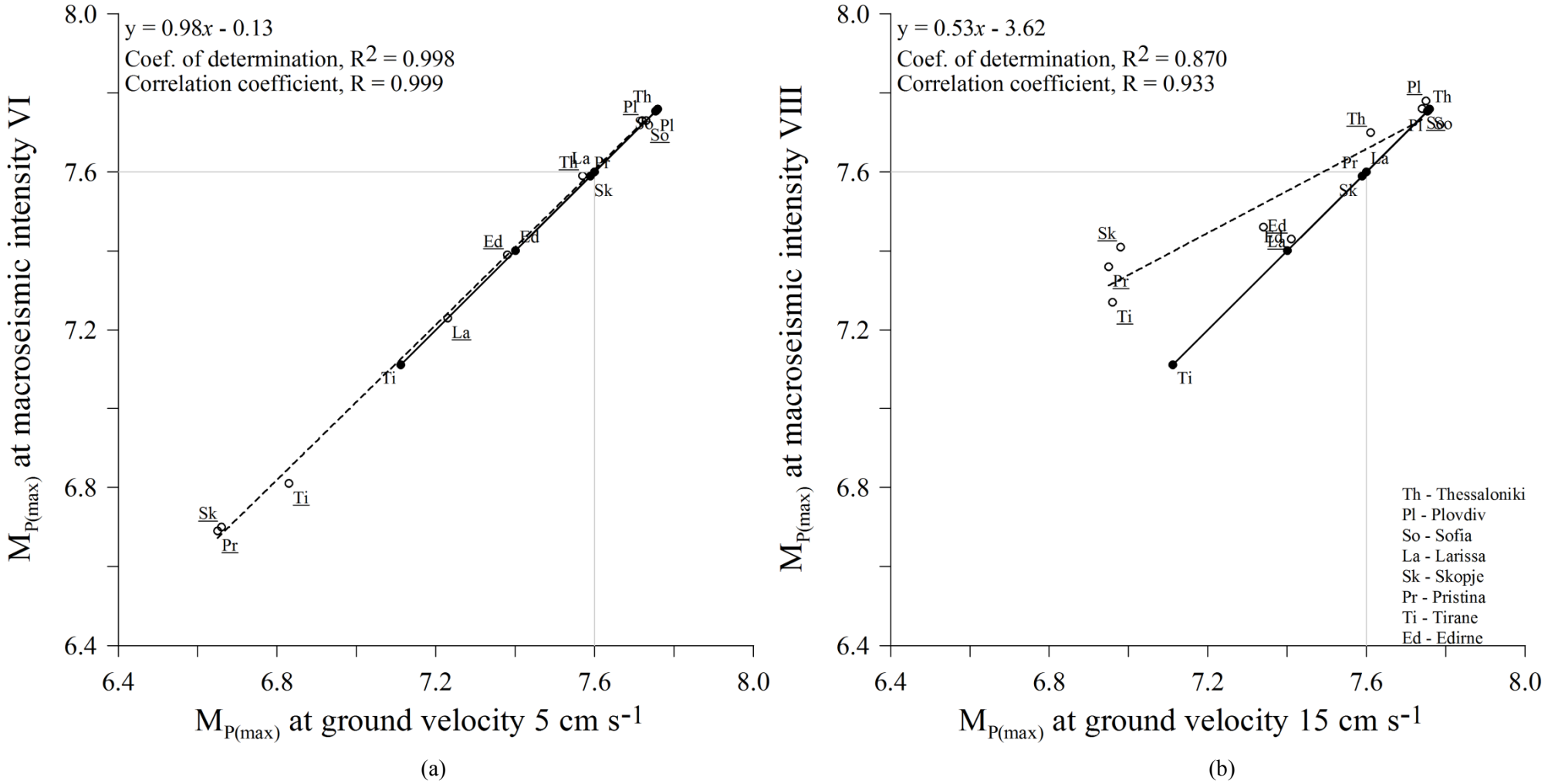

Figure 6.31 Linear correlation of (a) minimum and (b) maximum *most perceptible magnitudes* for horizontal ground velocity and macroseismic intensity for a nominal earthquake of 15 km focal depth. The solid line is the best-fit through *maximum credible magnitude* data points (M_3); dashed line is the best-fit through *most perceptible magnitude* ($M_{P(max)}$) data points

The general patterns for each city's position – with respect to the *most perceptible magnitudes* – are consistently the same. Thessaloniki, Sofia and Plovdiv are grouped together towards the upper magnitudes; Pristina, Skopje and Tirane occupy the lower end of the $M_{P(max)}$ range. Larissa and Edirne consistently occupy the centre of each plot. These groups of cities may also be grouped geographically and in a seismotectonic sense. Thessaloniki, Sofia and Plovdiv are towards the centre of the highly active southwest zone considered. Pristina, Skopje and Tirane are all located to the west of the considered region in the less seismically active portion. Larissa and Edirne, though not in the active southwest sub zone, are still both found in seismically active territories that are dominated by different tectonic regimes relevant to southwest Bulgaria (e.g. northern Aegean and NAF respectively).

The strongest correlation between paired ground motion levels is found to be 0.999 (Figure 6.29(a) and Figure 6.31(a)) between minimum levels of horizontal ground velocity with both macroseismic intensity and ground acceleration.

Correlating intensity with ground acceleration or ground velocity to determine relations between them is often used while designing anti-seismic structures (e.g. Berardi *et al.*, 1995; Panza *et al.*, 1997; Wald *et al.,* 1999a, 1999b; Boatwright *et al.*, 2001). Ambraseys (1974) even suggests velocity is more suitable than acceleration to predict seismic hazard to a region as it is a direct measure of the flux of energy between ground and building. It is therefore considered acceptable to correlate estimates of $M_{P(max)}$ developed for intensity with those from acceleration and velocity. Inspecting predictive correlations between $M_{P(max)}$ from intensity with those of another ground motion (Figure 6.30 and Figure 6.31) illustrates that lower ground motions considered exhibit very strong correlations, with a correlation coefficient, R, of 0.997 and 0.999 for acceleration and velocity respectively. As ground motions increase, R lessens to 0.914 and 0.933, suggesting this may be incorporated into possible measures of uncertainty with respect to the upper bound magnitude ω, as it is this magnitude that estimates of $M_{P(max)}$ are approaching for successive increments in ground motion.

This is reasonable to expect as peak velocity relates closely to kinetic energy, which in turn relates to damage, which is measured by intensity, albeit in a subjective fashion via intensity scales. Wald *et al.* (1999a, 1999b), Boatwright *et al.* (2001) and Atkinson and Kaka (2006) show that low intensities correlate well with PGA and PGV but high intensities correlate best only with PGV. Here we have been concerned solely with medium to moderately high levels of intensity ground shaking; i.e. those linked to the onset and initial increase of structural damage in current intensity scales adopted across Europe.

Preference to using PGA or PGV for predicting intensity is made typically around intensity VII for reproducing intensity patterns. Therefore, PGV provides a more suitable measure across a broader range for predicting intensity than PGA, if a single measure for correlating with intensity is required. Theodulidis and Papazachos (1992) also found stronger correlation between intensity and ground velocity, as did Trifunac and Brady (1975).

The magnitude range over which perceptible magnitudes are forecast reduces at higher ground motions, such that $M_3 - M_{P(max)}$ lessens as the ground motion considered increases for each city. This is likely due to adopting Gumbel's third extreme values distribution as the underlying statistical magnitude recurrence model, and its upper bound limiting characteristic for developing extreme and perceptible magnitude estimates. These statistics show that even though the sample set is relatively small (only eight cities are considered) relationships between acceleration and especially velocity with macroseismic intensity are very strong using this earthquake dataset. In theory, a city's correlated points for the *most perceptible magnitude* should plot to the lower-left of its own M_3 estimate. This ideal holds for all cities except for Edirne, Plovdiv and Tirane, when correlating maximum intensity and velocity, and is likely to reflect an incomplete cycle of seismicity in the catalogue.

Sofia has been used as a case study throughout this chapter due to its inherent importance as Bulgaria's capital, its central location in the southwest zone of interest and proximity to large magnitude historical earthquakes. Each section that considers earthquake perceptibility with respect to a ground motion presents example illustrations of earthquake perceptibility and integrated perceptibility curves that are site-specific to Sofia. Earthquake perceptibility curves for each ground motion characteristic highlight the peak probability occurs at a different magnitude for each ground motion level. Introducing a depth factor into the ground motion model necessarily displaces the *most perceptible magnitude* further to the right. This rightwards shift will also see a reduction in the probability of perception associated to $M_{P(max)}$.

Distributions of perceptibility are asymmetrical about the *most perceptible magnitude*. Perceptibility curves experience rapid fall-away after this magnitude resulting from an area's seismicity and – in the case of this work – adopting Gumbel's third extreme values distribution as the underlying magnitude recurrence model, which is near linear at moderate magnitudes and then falls away from this form as the magnitude approaches its asymptotic magnitude, ω.

The second required component of earthquake perceptibility hazard is the ground motion model. The model selected will largely depend upon a number of intrinsic factors. These include the geographic region considered, near-field, far-field and temporal seismicity patterns (i.e. data constraints on focal depth, magnitude range and time range), uncertainties on the catalogued seismicity adopted to model ground motion estimates and obviously the form of ground motion modelling required. The last point itself may be further divided into additional components that together force the model's functional form, e.g.; the form of historical hazard computation they follow; incorporating a focal depth control; adopting epicentral, hypocentral or other [source-to-site] distance; site conditions; magnitude scale adopted; percentile [level of confidence] value. Ground motion models used here vary greatly in how they model ground motion and their functional form (Table 6.20). Those fields that have been shaded are known to affect the *move out* - and thus the asymmetrical properties - of perceptibility curves and therefore estimates for $M_{P(max)}$.

The three lead ground motion models (one for each ground motion type and highlighted * in Table 6.20) are compatible with each other in that they do not have any focal depth function built into their functional form. On face value, this may be considered a significant shortfall in justifying their adoption for this hazard analysis. However, one needs to bear in mind the typical size of uncertainties on focal depth estimates attached to individual earthquakes. Focal depth is often difficult to determine accurately, especially in early periods of earthquake recording. So even in modern seismology and earthquake monitoring, practice often requires reporting agencies or cataloguing organisations to attach a nearest 'best guess' starting value at one of a set of predefined depths (section 4.8.2) for an individual earthquake for further revision later; a practice used for example on occasions by the ISC. This is usually determined with some underlying knowledge of the depth limits to the crust and its parent seismicity.

Models of Theodulidis and Papazachos (1992) for ground velocity and acceleration, and Papazachos and Papaioannou (1997) for macroseismic intensity resolve this concern by each excluding a depth function from their respective forms and adopting epicentral distance in place of hypocentral distance as the site-to-source distance function. Thus, the *move-out* of each perceptibility curve is solely dependent on the specimen focal depth taken for each curve to represent the seismogenic source depth in computing perceptibility, and not any single component of the ground motion model. As the regional seismicity is generally shallow focus in nature in the Balkans (section 2.5), and as some cities considered here are not subject to large magnitude hazard at shallow depth and close proximity (e.g. Sofia), this may help explain the rapid fall away of perceptibility curves after $M_{P(max)}$ is reached.

Source	Hazard computation model	Site conditions	Depth control function	Distance Function	Magnitude scale	Magnitude range	Faulting Model	Percentile
Ground acceleration								
Theodulidis and Papazachos (1992)*	No	Stiff soil	No	Epicentral	Surface-wave	Unspecified[1]	N o	50th
Ambraseys (1995)	No	No	Focal	Hypocentral	Surface-wave	$5.0 \leq M_s \leq 7.3$	N o	50th
Ambraseys *et al*. (2005)	No	Stiff soil[2]	No	Epicentral[3]	Moment	Unspecified[4]	Yes[5]	-
Ground velocity								
Theodulidis and Papazachos (1992) *	No	Stiff soil	No	Epicentral	Surface -wave	Unspecified[1]	N o	50th
Macroseismic intensity								
Papazachos and Papaioannou (1997) *	Cornell (1968)	No	No	Epicentral[6]	Moment	$6.0 \leq M_w \leq 8.0$	N o	-

* Ground motion model which should be taken as the final solution for the ground motion to which it relates; [1] Model was developed from data of earthquakes $4.5 \leq M_s \leq 7.0$; [2] Ground motion model was generalised to reflect this site condition, although other options are available (section 3.8.2.3); [3] Epicentral distance was enforced in this model as causative fault information was not available in the adopted earthquake catalogue; [4] Model was developed from data of earthquakes $M_w \geq 5.0$; [5] Model generalised to earthquakes generated by normal faulting mechanisms, although other alternative are available (section 3.8.2.3); [6] Defined as '*distance*' throughout original text, taken as epicentral distance here

Table 6.20 Summary of adopted ground motion models

Integrated perceptibility curves continue to illustrate ground motion seismic hazard that Sofia may experience. The abscissas of all perceptibility and integrated perceptibility curves for this city extend up to 7.86 M_s, the value for Gumbel's third distribution upper bound, ω, for the area immediately surrounding Sofia. Each integrated perceptibility plot shows roll-off at a particular magnitude for each level of ground motion. Above specific magnitude levels the plots level off until ω is reached. Additionally, each curve shows the inflexion (Burton, 1981) due to $P_c(X)$ decreasing faster than $\phi(M)$ increases at lower magnitudes, but at higher magnitudes, $\phi(M)$ decreases faster than $P_c(X)$ increases.

Earthquake perceptibility allows ground motion hazard curves to be developed on a site-specific basis; the primary aim from this section of work. Hazard curves developed for each ground motion model compare all cities for seismicity at 15 km focal depth (Figure 6.14, Figure 6.20 and Figure 6.27) and show annual probabilities of exceedance. Sofia, Thessaloniki and Plovdiv are consistently forecast the highest hazard, regardless of the ground motion. This is to be expected due to each city's proximity to large magnitude historical sequences and seismicity of the southwest zone. Sofia appears more prone to hazard than Thessaloniki in the medium to high range of ground motions (e.g. above accelerations of ~175 cm s^{-2}, velocities of ~10 cm s^{-1} and intensity VI); at these levels Sofia's curves cross those of Thessaloniki. Ground motions expected to be exceeded at least once in 100 and 1,000 years for Sofia, Thessaloniki and Plovdiv are in Table 6.21.

City	Acceleration[1] (cm s^{-2})		Velocity[2] (cm s^{-1})		Intensity (*I*)	
	100	1,000	100	1,000	100	1,000
Sofia	87	285	7.5	27.5	VI (6.3)	VII (7.7)
Thessaloniki	93	277	7.5	26.5	VI (6.3)	VII (7.5)
Plovdiv	77	263	6.5	25.0	VI (6.1)	VII (7.6)

[1] Using Theodulidis and Papazachos (1992) for stiff soil conditions (S = 0.5) at the 50th percentile; [2] Using Theodulidis and Papazachos (1992) for stiff soil conditions (S = 0.5) at the 50th percentile

Table 6.21 Ground motions expected to be exceeded at least once in 100 and 1,000 years at cities of southwest Bulgaria (for a nominal earthquake of 15 km focal depth)

Superimposed on each figure is the analytical *maximum credible magnitude*, M_3, (vertical dashed line) from cumulative strain energy statistics using the surface-wave magnitude as its input. Also shown is $M_{P(max)}$ (vertical solid black lines) for the three levels of ground motion considered at 10 km focal depth. Doing this highlights how estimates for $M_{P(max)}$, M_3, and ω for each urban centre considered in this work hold to the model's ideal discussed in section 6.3.1.

A small number of illustrations in Appendix 18 and Appendix 22 exhibit fall away of P (X | M) at magnitudes higher than the $M_{P(max)}$ for the lowest ground motion. This fall away occurs between 7.86 M_s and 7.89 M_s when considering ground velocity and acceleration using relations of Theodulidis and Papazachos for Plovdiv, Skopje and Thessaloniki (and also Larissa and Sofia with respect to ground velocity). Probabilities indicate these are magnitudes at which these cells reach *cell saturation*. That is, when $P_c(X)$ equals 1, indicating everywhere in that analysis cell reaches this level of ground vibration. In this work, only the lowest ground motion level exhibits this abrupt fall away. However, whether successive levels of ground motion will also exhibit such patterns for other regions or locations is governed by the range and increments of ground motion considered.

Moreover, it is important to remember that estimates of M_3 are developed from the full catalogue, whereas each $M_{P(max)}$ is a by-product of a *part process* magnitude recurrence model. These empirical observations further support the need to critically consider which ground motions levels are investigated at any given site, and that one does not adopt a static suite of arbitrary ground motions to apply in a broad region like the Balkans in the hope of getting realistic hazard estimates at all geographic points.

Adopting the levels of ground motion for acceleration, velocity and intensity considered in this chapter have been justified in Table 6.2 for the broad geographic region considered, yet these appear not to be truly appropriate for assessing seismic hazard for all urban centres and the areas immediately surrounding them listed in the previous paragraph. It appears more appropriate in some instances to investigate lower *'lowest levels'* of *scenario* ground motion [note: meaning with respect to those levels of ground motion proposed for this study in Table 6.2, and not the extreme ground motion forecasts already estimated in chapter 5 and listed in Table 5.12, Table 5.13 or Table 5.14] to investigate ground motion perceptibility hazard for the Balkans. Investigating higher *'lowest level' scenario* ground motions may potentially saturate hazard analysis cells and their ensuing forecasts to the point of providing no meaningful benefit to the end user. Adopting lower *scenario* ground motions in these instances will ensure a cell does not reach *cell saturation* across its entire area, but obtained hazard estimates that are realistic and realisable in the context of historical seismicity and meaningful and of use to earthquake engineers.

Introducing more modern ground motion models specifically for horizontal peak ground acceleration to update this aspect to the seismic hazard assessment – namely that of Ambraseys *et al*. (2005), after harmonizing it to reflect the prevailing faulting mechanism and soil type of the region – and to mitigate the age of the older models considered does not appear to elevate the hazard levels to Sofia (Figure 6.13(b) and Appendix 20) or indeed those that any of the other cities may be subject to. Each figure clearly shows this newer model to systematically estimate lower levels of ground acceleration hazard [over the full range considered] than Theodulidis and Papazachos (1992), and also over the lower range of acceleration ($0 \rightarrow \sim 100$ cm s^{-2}) than Ambraseys (1995) for all cities. At higher accelerations (>100 cm s^{-2}) both models by Ambraseys forecast comparable hazard.

The review of *maximum credible magnitude* hazard illustrates how southwest Bulgaria is dominated by a small number of large-magnitude earthquakes in recent history (e.g. 4th April 1904, 7.2 M_s and 6.8 M_s; 14th and 18th April 1928, 7.0 M_s and 6.8 M_s; 21st March 2000, 7.6 M_s). Cumulative energy release plots relating to both regions considered (Figure 6.1 and Figure 6.4) show the seismic cycle (cycle of periodicity) of both areas is dominated by these few large magnitude events, and the majority of strain energy release is accounted for by their occurrences.

Estimates for M_3 for both the full-catalogued Balkan region (M_3 = 7.82) and southwest Bulgaria (M_3 = 7.78) are compatible with the observed seismicity in the adopted catalogue. The 7.6 M_s homogenized earthquake of 2000 (reported magnitude 6.5 m_b) is the largest reported event in this dataset and is located within the southwest zone, so by definition it is also present in the larger area considered. This is also true of the 1904 Struma Valley sequence for which the main shock was estimated by Shebalin *et al.* (1998) and others at 7.8 m_b. It is apparent that estimates for maximum earthquake statistics (i.e. M_3) obtained using cumulative strain energy release techniques are more consistent with the observed seismicity than those derived using extreme values theory. *Maximum credible* statistics are achieved through adopting the full parent distribution (catalogue) as opposed to attempting to fit an extracted subset of extreme magnitude observations to an earthquake recurrence model. However, estimates for M_3 are disadvantaged, as they do not come with an associated uncertainty or probability of exceedance, unlike the asymptotic upper bound to Gumbel's distributions. It has been shown that this region holds to the $\omega - M_3 \geq 0$ ideal if one acknowledges the impact of σ_ω, but with $M_3 \approx \omega$.

A further but secondary objective was to determine whether a region or site-specific location has undergone a full cycle of seismicity. Previous authors (e.g. Burton and Makropoulos, 1985) have found applying cumulative strain energy release statistics in tandem with extreme values theory to high seismicity regions will return comparable estimates for the maximum magnitude earthquake.

This approach allows them to suggest these regions may have undergone at least one complete cycle of seismicity; these patterns are also observed here. This work achieves realistic estimates for M_3 for both study areas using strain energy release techniques. Markedly higher estimates than M_3 for the upper bound magnitude, ω, acknowledging the impact of σ_ω, of 7.69 M_s ± 0.56 and 7.84 M_s ± 0.76 for the Balkans and southwest Bulgaria suggest a full cycle has occurred due to small σ_ω.

Similarly, Appendix 17 provides cumulative strain energy release plots for the other urban centres considered. These suggest that Larissa, Pristina, Skopje and Tirane have either recently completed or are about to complete a full cycle of periodicity in terms of site-specific hazard in the time span of the applied catalogue, combined with short estimates for the waiting time, T_w, for all the energy equivalent to the maximum earthquake M_3 to accumulate. However, although Sofia is estimated relatively low standard deviation on ω, it is forecast long – and noticeable similar – time intervals for waiting times T_w and DT. These, together with its strain release plots indicate Sofia is some way from all seismic energy accumulating within the considered sub region.

No city is forecast estimates for M_3 and ω that are greater than 0.3 M_s different (Table 6.1). Each of the '*design*' earthquake estimates developed for the broader Balkan extent, the southwest border area and each of the eight urban centres are compared in Figure 6.32. No estimates of $M_{P(max)}$ have been calculated for either the Balkan and southwest Bulgaria zones. Those given for each urban centre are for the lowest ground motion level considered. Figure 6.32 supports observations that notionally, if one allows for uncertainty in ω:

- $M_3 \leq \omega$

- $M_{PA(max)}\{\text{Acceleration}\} \leq M_{PV(max)}\{\text{Velocity}\} \leq M_{PI(max)}\{\text{Intensity}\}$

Finally, an example of geographic seismic hazard disaggregation has been given that is specific to Sofia, and constitutes a further approach to partitioning this city's seismic hazard. An approach suggested by previous authors is adapted to suit size limitations of the input earthquake dataset. The procedure differs here in the manner the magnitude density is assigned from Gumbel's third distribution of extreme values to each characteristic magnitude value. This method illustrates that near field, moderate-magnitude seismicity between 4.25-4.50 M_s and 4.75-5.00 M_s with epicentral distances of less than 20 km has a large influence on Sofia's seismic hazard.

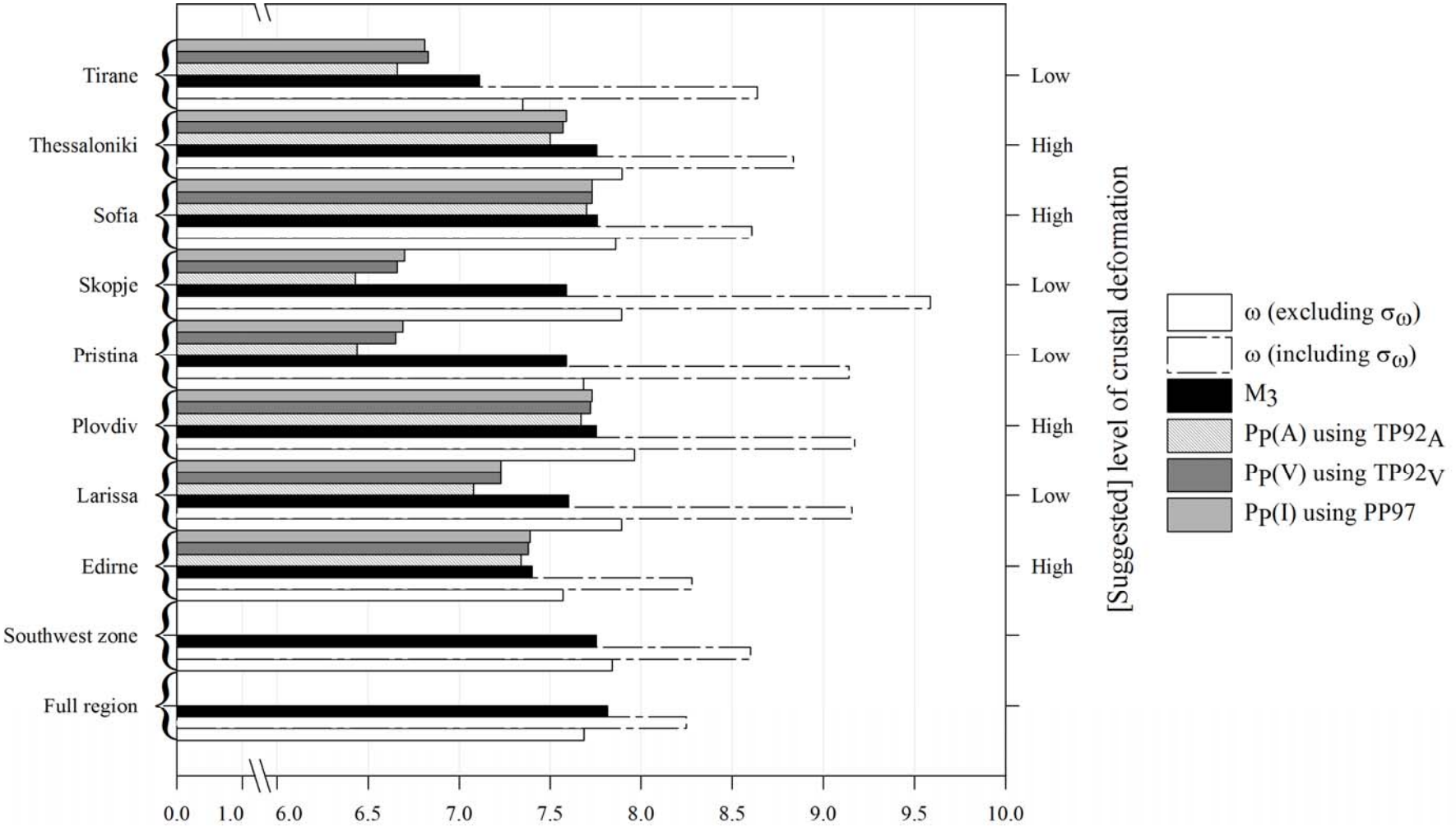

Figure 6.32 Design magnitudes for all regions and site-specific locations considered. $TP92_A$ is $M_{P(max)}$ at 50 cm s^{-2} for ground acceleration using Theodulidis and Papazachos (1992) for stiff soil conditions at the 50^{th} percentile. $TP92_V$ is $M_{P(max)}$ at 5 cm s^{-1} for ground velocity using Theodulidis and Papazachos (1992) for stiff soil conditions at the 50^{th} percentile. PP97 is $M_{P(max)}$ at intensity VI for macroseismic intensity using Papazachos and Papaioannou (1997)

However, hazard mentioned in the previous paragraph is fundamentally *near-field* hazard. Larger magnitude hazard found at greater distances from Sofia also needs to be recognised. Larger magnitude earthquakes (≥6.50 M_s) are only found at distances greater than 50 km, but have smaller annual probabilities of occurrence (Figure 6.29(a)), and obviously occur less frequently than small and moderate magnitude seismicity. However, Sofia has been subject to 78 earthquakes of magnitude 5.0+ M_s, 12 earthquakes of magnitude 6.0+ M_s and four earthquakes of magnitude 7.0+ M_s in the catalogued time span (including the maximum reported magnitude earthquake of the catalogue at a distance of 180-190 km).

Seismicity of magnitudes between 5.00-5.25 M_s at 30-50 km further increases hazard to Sofia. Relationships between regional crustal deformation strain and velocity rates, the *maximum credible magnitude* (M_3) and estimates for the *most perceptible magnitudes* are possible and illustrated in each site-specific seismic source disaggregation, such that:

- [Magnitude attached with] $P_{p[A/V/I](max)} \leq M_{CUT} \leq M_{P[A/V/I](max)} \leq M_3 \leq \omega$

Chapters 5 and 6 successfully demonstrate how a range of different statistical hazard models can be adopted and combined successfully to develop a wide-ranging suite of extreme and characteristic earthquake hazard estimates. These can sit mutually alongside and complement each other when assessing seismicity and seismic hazard for a given site-specific location or broader geographic extent. This work further supports previous authors in adopting these approaches to develop seismic hazard assessments, e.g.

- The finite waiting time models of cumulative strain energy release statistics compare favourably with infinite return period models of Gumbel's first and third extreme values distributions,

- The *whole process* cumulative frequency-magnitude distribution model against the *part process* models of Gumbel's first and third extreme values distributions

Although they differ in their fundamental approaches and underlying assumptions, each model is adopted constructively here in the same seismic hazard assessment to determine useful and usable seismic hazard statistics. No one recurrence model or statistical hazard approach adopted here is used in isolation:

- The zone-dependant parameters a and b of the *whole process* cumulative frequency-magnitude distribution model feed into cumulative strain energy release statistics;

- Specific components of Gumbel's third extreme values distribution are vital inputs to developing *characteristic magnitude* estimates through magnitude perceptibility, if one adopts the recurrence models of Gumbel (1958) as the statistical density distribution. However, adopting alternative magnitude recurrence models will require use of different specific components of the statistical model considered.

- Ground motion models used to achieve peak ground motion estimates are required in any related magnitude perceptibility or integrated perceptibility analysis to maintain compatibility of results.

These results confirm assessment of seismic hazard at a given location should ideally and intentionally incorporate a range of methods, that each ascertains different specific *design* magnitudes and aseismic design criteria such as those illustrated in Figure 6.32; no one result will offer a complete solution to assessing seismic hazard and mitigate the ensuing risk.

The key pattern to take from Figure 6.32 is that five cities – Larissa, Plovdiv, Skopje, Sofia and Thessaloniki – are forecast a greater value for ω than the fuller geographic region itself. This pattern ceases if one acknowledges σ_ω, both if σ_ω is added to each city's upper bound magnitude (uncertainties on ω are greater than 0.7 M_s for all cities) and onto ω of the full region, or if σ_ω is applied only to the upper bound magnitude of the full region.

This work provides insight into the seismic hazard to Bulgaria at regional, local and site-specific levels, and the quality of the earthquake catalogue as the main input adopted for this work. With these two aspects in mind, this work provides the following conclusions:

1. The 105-year time span of the developed catalogue does not represent a full cycle of seismicity within the region bounded by 19°-29°E, 39°-45°E.

2. It is important to accommodate uncertainty on the upper bound magnitude, ω, from Gumbel's third extreme values distribution on hazard forecasts if these estimates from *whole process* and *part process* statistical models are to adhere to acknowledged relationships outlined earlier in this chapter.

3. Having to accommodate often quite large values of σ_{ω} when comparing hazard estimates developed from different statistical recurrence models (see previous point) supports the view that the developed catalogue does not represent a full cycle of seismicity within the region considered.

4. Sub regions of highest crustal deformation – as indicated by their deformation strain and velocity rates – are characterised by estimates for the *most perceptible magnitude*, $M_{P(max)}$, that are similar to the *maximum credible magnitude*, M_3, for the same area. This is true regardless of the ground motion considered.

5. As the cut-off threshold approaches the magnitude with the greatest probability density from $P_e(M)$, the *most perceptible magnitudes*, $M_{P(max)}$, all reduce progressively further below the *maximum credible magnitude*, M_3, and indicate regions of lower crustal deformation (and therefore lower crustal deformation strain and velocity rates).

6. Edirne, Plovdiv, Sofia and Thessaloniki are located in sub regions of higher deformation strain and velocity rates than the other four cities considered.

7. Each statistical hazard model used here may be considered in isolation or in combination with others to qualitatively suggest if a full period of seismic loading has occurred in a given region in terms of the portion of the catalogue considered.

Chapter 7 : Summary and conclusions

7.1 Summary and conclusions

A new seismic hazard assessment has been detailed for Bulgaria and the Balkan area. Special attention has been given to southwest Bulgaria containing the political border region between Bulgaria, the FYR of Macedonia and Greece. This work also investigated hazard levels for selected urban centres located within the broader geographic extent considered.

The border region between these three countries needs detailed investigation as it is subject to multiple seismic populations and has large-scale faulting regimes (e.g. the Krupnik fault and Serbomacedonian massif) that cross borders between these countries. Many are capable of producing large-magnitude and destructive earthquakes. Seismicity is predominantly shallow focus in nature and these environmental considerations are compounded by the presence of a number of significant urban centres in each country present in the area considered. It is important that trans-frontier seismicity issues are considered holistically and not separately.

Seismic hazard may be considered an under-investigated area of study within the confined region of southwest Bulgaria and the adjacent political triple junction zone. Providing this contemporary seismic hazard analysis for these areas improves upon a number of deficiencies present in a number of previous studies (e.g. Bončev *et al.*, 1982; Orozova-Stanishkova and Slejko, 1994; Simeonova *et al.*, 2006). These include the date of the analysis work, timeliness of the adopted data, limitations in applied magnitude recurrence [or other] statistical models or the adoption of a restricted range of multiple seismic hazard descriptors investigated.

However, the main driver to justify this work is that it has allowed a seismic hazard analysis to cross the political borders between Bulgaria, the FYR of Macedonia and Greece, and consider the impact of multiple local and distant seismic populations on this exact area of concern. As an example of why this is considered such an important consideration, a nuclear power plant (NPP) is currently being constructed near Belene and Svishtov in northern Bulgaria. Acknowledging these different seismic provinces would allow *scenario* ground motion hazard estimates to be developed from appreciating the cross-border seismicity rather than just that defined by the borders of Bulgaria, with the expectation they would hopefully be more accurate with lower uncertainties.

This contemporary hazard assessment is also multi-disciplinary. It acts directly on benefits of a number of accepted and rigorously tested statistical earthquake hazard forecasting techniques to develop new estimates for a range of maximum *scenario* earthquakes and related ground motion

hazard descriptors for the broader Balkans area, a specified zone in southwest Bulgaria and particular site-specific locations (Figure 5.1).

The regions considered are typically of low to moderate magnitude seismicity, with earthquakes of shallow focal depths. However, they have been subject to notable large magnitude, destructive seismic sequences in the recent past which justifies this and all previous seismic hazard assessments. High seismicity – both in terms of the numbers of earthquakes and magnitudes experienced – was seen particularly in the first decades of the 20th century, after which the seismicity rate dropped away to predominantly lower levels in the middle of the 20th century. Also, a large percentage of Bulgaria's seismicity is found in the southwest. The new catalogue presented reflects these general patterns of seismicity, with a b-value from a cumulative frequency-magnitude distribution of 0.82 (±0.03), and lower b-values for the early instrumental period (0.76 ± 0.02) than the modern instrumental of reporting (0.79 ± 0.02), providing evidence that this early time interval is dominated, to some degree, by higher magnitude events.

The cut-off magnitude of the catalogue has been considered using Gumbel's third extreme values distribution in a *sensitivity analysis*. This allowed a subset of extracted extreme values to be refined to develop stable and consistent hazard estimates to be forecast. Adopting this approach suggests extreme data of magnitude ≥5.5 M_s and 4-year extreme intervals are most appropriate for forecasting hazard in general in this study whereas the values are ≥5.3 M_s and 5-year for the smaller southwest Bulgaria zone.

Although this new catalogue is considered to spatially cover the seismicity most influential to southwest Bulgaria (for that is the geographic area of most interest to this study) it has been shown using *cumulative strain energy release* statistics that the temporal cover provided by the 105-year time span may not necessarily represent a full cycle of periodicity in either geographic extent considered. However, hazard estimates developed specifically from this input catalogue suggest that a catalogue accounting for one full seismic cycle is not necessarily needed to obtain stable and compatible forecasts. This is likely due to adopting the extreme values distribution as the governing statistical magnitude recurrence model, and thus not needing the full parent distribution to represent the area's seismicity.

The upper bound magnitude, ω, for the larger geographic area is 7.69 M_s (±0.56; Figure 5.17(a)) derived from Gumbel's third extreme values distribution, compared with a *maximum credible magnitude*, M_3, of 7.82 M_s (Figure 6.1). These estimates equate to infinite return period magnitude and finite waiting time magnitude models respectively, and so differ in their underlying assumptions and magnitude statistics extracted from the earthquake database. The equivalent

estimates for southwest Bulgaria are 7.84 M_s (±0.76) (Figure 5.17(b)) and 7.76 M_s (Figure 6.4) respectively, and so each geographic extent adheres to the ideal that $\omega - M_3 \geq 0$ if one acknowledges influence of σ_ω. Extreme value statistics are calculated using data from the earthquake database under data conditions determined to ensure they are as statistically stable and as realistic as possible.

Further, as M_3 and ω are so similar to each other (Table 6.1) at a regional and southwest zone level, they could be considered to be converging towards each other; therefore their associated waiting times would be nearing convergence also. This is important since the former represents a theoretically infinite return period and the latter represents a maximum credible period. However, at a more localised level, site-specific estimates of ω differ from M_3 by between (-)0.1 and 0.3 M_s, occasionally with large σ_ω on the extreme upper bound magnitude. This therefore may suggest that particular sub regions of the geographic area considered are not represented by a complete cycle of seismicity in terms of the seismicity listed in the catalogue whereas others may be close to containing a full cycle.

The extreme north and east border regions of the broader area considered are not forecast as having significant hazard due to insufficient data, and lack of adequately large-magnitude earthquakes in recent history to allow hazard forecasts to be developed using either of the extreme distributions. These '*null*' areas with no hazard forecasts may be eradicated by extending the catalogued area northwards into Romania, Serbia and southern Russia. Doing this would also further refine hazard estimates for north Bulgaria/south Romania area that have been forecast, and would further benefit hazard estimates adopted for any 'critical structure' structure project such as the Belene NPP.

That is not to say these border areas simply have no seismic hazard. Figure 2.9, Figure 2.24 and Figure 6.3 attest to the fact that these areas are also prone to moderate and large magnitude earthquakes. However, these sized magnitude events may have far longer return periods – perhaps longer that the time span of the adopted catalogue – in this region than areas that are more central to the area considered. Consequently, the chosen magnitude recurrence model and its parameters may not be suitably tailored to highlight this hazard adequately.

These areas of '*null*' hazard forecasts – typically located around the edges of hazard maps – are one legacy of insufficient extreme seismicity from which to draw adequate hazard results. This is one form of '*edge effect*' that needs to be appreciated when mapping seismic hazard, and is a function of truncating the adopted earthquake database at the edge of the considered area.

A second result of insufficient extreme events – combined with analysis cells extending outside the limit of the catalogued area – is the poorer hazard forecasts that are often achieved. Those developed near the edge of the considered area will generally be attached with larger uncertainties and chi-square (X^2); these cells are highlighted as those located outside the central dashed rectangle on each hazard map, so any analysis cell whose centre is within 2° of the region's edge.

Earthquake ground motion hazard estimates that are compatible with the current European building code regulations of EUROCODE 8 prescribing building design for earthquake resistance have been developed. The main hazard measurement underpinning EUROCODE 8 standards is the 475-year return period ground motion – equivalent to the 50-year ground motion with 90% probability of non-exceedance – and is typically measured for peak ground acceleration or macroseismic intensity on the EMS-98 intensity scale. Applying Gumbel's third extreme distribution to the new earthquake catalogue estimates much of the broader catalogued region could be subject to intensities as high as XI. Although no earthquake in the catalogue is reported as having an epicentral intensity of XI (the highest is intensity X, after converting all event magnitudes) there is scope for other threads of analysis (e.g. strain energy release illustrations) to suggest the catalogue does not currently present a full cycle of seismic periodicity during the time interval detailed. Therefore, the region's maximum earthquake intensity may not have been experienced with its 105-year time span.

That said, both geographic extents considered are estimated upper bound intensities with relatively large uncertainties (XII (12.2) ± 0.8 and XI (11.4) ± 0.8; Figure 5.37). Acknowledging the lower bound to each of these estimates brings them within scope of the catalogued maximum epicentral intensity. Site-specific extreme intensity estimates (Table 5.20) present the same concern as extreme magnitude forecasts; perhaps an unsurprising situation since they are both point processes borne from the same earthquake size descriptor (in this instance extreme intensity hazard for both areas is developed from epicentral intensities, without adopting a ground motion model). For example, Edirne and Tirane exhibit $\sigma_I \approx 0.5$, while others (Sofia, Skopje and Plovdiv) are attached much higher uncertainties; again this suggests only some sub regions have a full cycle of seismicity present in the adopted catalogue whereas others may not.

Peak ground acceleration needs particular attention with respect to EUROCODE 8 requirements. Estimates obtained in this work using two alternative ground motion models provide compatibility to both historical work and to the large-scale SESAME (Jiménez *et al.*, 2001) and GSHAP (Giardini and Basham, 1993; Giardini, 1999) European seismic hazard projects. Both models suggest the broader area may be subject to highest PGA in the southwest Bulgaria '*triple-junction*' zone (highlighting the Krupnik fault and delineating the Serbomacedonian massif), south-central

Bulgaria local to Plovdiv, the north Aegean, and west Turkey (the latter two hazards being dominated by the North Anatolian Fault). Each of these localised areas may be subject to ground accelerations in excess of 500 cm s^{-2} (Figure 5.26; using Theodulidis and Papazachos (1992) attenuation after refining it to consider stiff-soil conditions). The specific area of high PGA hazard located in southwest Bulgaria is concentrated directly over the meizoseismal area of the destructive 1904 seismic sequence. Peak ground accelerations estimated here are broadly in line with those from both GSHAP and SESAME hazard assessments, if the ground motion model of Theodulidis and Papazachos for stiff soil site conditions is favoured. Hazard maps shown in Figure 5.26(a) and Figure 5.28(d) illustrate the 475-year return period PGA hazard (the preferred EUROCODE 8 hazard measure) and are therefore compatible with the afore mentioned European-wide seismic hazard projects.

Incorporating newer ground motion models to consider ground acceleration hazard does not appear to raise expected hazard levels above the maximum forecasts obtained from the earlier models. Typically, the more recent model of Ambraseys *et al*. (2005) – once refined to reflect prevailing regional faulting mechanisms and site soil types – estimates ground acceleration hazard in the middle range between equivalent estimates from Theodulidis and Papazachos (1992) and Ambraseys (1995).

Emphasis is often placed on the importance of ground velocity as a more suitable measure of ground motion hazard because of its causal relation between ground motions, energy transfer from the ground to structures and resultant building damage. Due to this, peak ground velocity (PGV) estimates have also been provided. As this is another form of ground motion hazard – and so being a field process, not a point process – regional hazard contours to comparable patterns of hazard as PGA. The same sub regions highlighted in the previous paragraph with respect to PGA hazard are also forecast PGVs of between 20 and 50 cm s^{-1} (the 475-year PGV hazard maps are shown in Figure 5.31(a) and Figure 5.32(d)).

Being situated within the high seismicity southwest zone, Bulgaria's capital, Sofia, is forecast to be subject to significant seismic hazard. In many instances, site-specific forecasts for individual cities are strikingly similar to those for the confined zone as a single considered area hazard estimate (Table 5.7 and Figure 5.19(b)). Indeed, estimates of the upper bound magnitude, ω, are within 0.02 M_s (7.86 $M_s \pm 0.75$ for Sofia compared with 7.84 $M_s \pm 0.76$ for southwest Bulgaria) of each other, with their uncertainty only 0.01 M_s different. Similarly, the extreme distribution's annual modal magnitude, m(1), is only 0.2 M_s different, but with slightly larger uncertainties attached to each (6.88 $M_s \pm 1.17$ for Sofia compared with 6.67 $M_s \pm 0.85$ for southwest Bulgaria). No return period magnitude estimated for Sofia is greater than 0.2 M_s different from the equivalent estimate for

southwest Bulgaria. These estimates converge as the return period forecasts increase. Sofia is also forecast comparatively high levels of ground motion hazard, regardless of the ground motion considered. The 475-year return period ground motions local to Sofia are 177 cm s^{-2} (σ_A = 0.45), 27 cm s^{-1} (σ_V = 0.45) and XI (±1.1) for acceleration, velocity – both from the ground motion models of Theodulidis and Papazachos (1992) – and intensity respectively.

Previous seismic hazard assessments have not investigated principles of, and sought benefit from, the concept of earthquake perceptibility. Earthquake perceptibility analysis has been introduced here as an alternative description of the hazard levels that may be related to both the finite waiting time model of cumulative strain energy release statistics and the infinite return period characteristic of extreme values. This is in terms of predefined *scenario* ground motions, and the magnitudes (with related probabilities of occurrence) at which these acceleration, intensity or velocity ground motions are most likely to be perceived, that is, the *most perceptible magnitude*, $M_{P(max)}$. Perceptibility and integrated perceptibility curves have been formed to estimate the probability of experiencing known ground motions from an earthquake of magnitude M, and for all magnitudes up to and including $M_{P(max)}$.

This hazard assessment has also shown how sub regions of highest crustal deformation are characterised by estimates for the *most perceptible magnitude*, $M_{P(max)}$, that are similar to the *maximum credible magnitude*, M_3, for the same area. This is true regardless of the ground motion considered, and suggests magnitude perceptibility is a hazard technique more suited to areas whose seismotectonic regimes create medium to low levels of deformation. This is borne out in estimates for $M_{P(max)}$ specifically for Sofia, with the lowest *scenario* ground motions considered returning estimates for $M_{P(max)}$ similar to the *maximum credible magnitude* of the site, and also above the maximum homogenized magnitude of the adopted catalogue of 7.6 M_s, while illustrations of crustal motion (Figure 2.20 to Figure 2.23) confirm this city is located in a sub region of high crustal deformation and velocity motions.

Site-specific hazard curves for each ground motion, created and investigated from each site's integrated perceptibility curves, allowed the annual probability of exceedance to be estimated for different ground motion models, focal depths and levels of ground motions. Hazard curves for all ground motions considered consistently show Sofia, Thessaloniki and Plovdiv to be subject to the highest ground motion probabilities of all eight cities considered.

Producing these sets of ground motion hazard curves 'closes the loop' in this probabilistic seismic hazard assessment for Bulgaria and the Balkans. It illustrates how specific elements of the extreme values discipline applied to hazard forecasting may be combined with suitable ground motion

models to develop site-specific ground motion hazard curves. These then allow annual probabilities of exceedance to be estimated for the extreme ground motions already forecast using the extreme values distribution in isolation.

In conclusion, this investigation and research may be considered as a significant contribution towards a contemporary understanding and appreciation of the seismic hazard generated by the *seismicity and large earthquake potential in southwest Bulgaria and the conterminous Balkan high hazard region*.

7.2 Further work

The catalogue developed for this probabilistic seismic hazard assessment is a directly compatible extension of the Greek catalogue developed by Burton *et al*. (2004a), both in functional form and its end use. Further work could consolidate both catalogues into a singular input tool facilitating a homogeneous PSHA study over a wider geographic area. This PSHA made no effort to incorporate the seismicity generated by the Hellenic Arc to the south, although this was ensured in the Greek hazard work. Likewise, only a percentage of the seismicity resulting from the high hazard southwest Bulgaria zone was involved in the work of Burton *et al*. (2004a). Consolidating both catalogues together would accommodate both these important seismicity regimes and mitigate loss of catalogued historical seismicity. Pursuing such a line of research would refine further extreme hazard estimates obtained independently by this study and that of Burton *et al*. (2004a), and allow comparison with other international seismic hazard projects (e.g. SESAME and GSHAP).

The analysis of urban-specific seismic hazard is arguably quite limited. Only eight cities were considered in the broader geographic extent for which adequate extreme magnitude data could be extracted from the catalogue. Attention has been paid to cities that allowed discussion of a wide range of geographic and seismotectonic regimes that produce varying levels of seismicity. Extending the catalogued area north into southern Romania would easily allow more cities to be incorporated, although at the extra effort of including the anomalous seismic sequences of Vrancea, southern Romania (Radulian *et al.*, 2002).

Incorporating this particular seismic sequence would be unlikely to affect the ability to apply *maximum credible magnitude* statistics. These *whole process* methods are unconcerned with the magnitudes and distributions they consider, and simply aim to sum the energy output of all earthquakes in a given region. However, Gumbel's third extreme distribution does require initialising of its distribution's parameters (ω, μ, λ). Adopting an ill-formed set could result in the sequence being excluded from consideration – either in terms of magnitude or the extreme interval

adopted – and the true hazard effects of this anomalous sequence. Incorporating this special sequence may result in adopting such a parameter set that adversely affects resultant hazard estimates.

Special consideration may also need to be paid to modelling ground motion attenuation if this seismicity were incorporated. Any new ground motion models developed and adopted would have to consider the directional nature of ground motion attenuation (e.g. geometric spreading and variation in speed of ground motion with epicentral distance and azimuthal direction; Lungu *et al.*, 1997; Musson, 1999).

Intensity ground motion models considered most relevant to Bulgaria and the Balkans are outlined in Table 3.2. No law is newer than 2003, and this most recent relation (Koravos *et al.,* 2003) only incorporates seismicity below 43°N. It would be useful to consider recorded macroseismic intensities resulting from large magnitude (above 6.0 M) historical earthquakes (possibly incorporating events from Romania, e.g. Vrancea). Macroseismic intensity estimated at known points in the field from selected earthquakes could be used to develop a contemporary macroseismic intensity ground motion model for this region of interest. Doing so would update knowledge on this element to seismic hazard analysis and further supplement the EUROCODE 8 hazard estimates.

A hazard assessment is one step towards facilitating reinsurance companies' endeavours to estimate extreme event losses from earthquakes. Performing a PSHA and understanding the related building vulnerability are prerequisites to understanding and assessing seismic risk in an area – risk to its building stock, infrastructures and even potential human loss (which arguably cannot be insured against). One major extension to this research, which would benefit city planners, earthquake engineers, hazard and risk modellers, reinsurance companies and governments of the countries covered in this study, would be to use these hazard statistics with an additional and detailed vulnerability data set, to estimate the total risk and its spatial variation for key urban centres such as Sofia, Plovdiv, Varna and Blagoevgrad and others in the region beyond the immediate area of the political triple junction between FYR of Macedonia, Greece and Bulgaria.

References

Abe, K., 1988. *Magnitudes and origin times from Milne seismograph data: Earthquakes in China and California, 1898-1912.* In: Lee, W.H.K., Meijers, H. And Shimazaki, K. (eds), Historical Seismograms and Earthquakes of the World, Academic Press, 37-50. [Not seen]

Abe, K., and Noguchi, S., 1983a. Determination of magnitudes for large shallow earthquakes 1898-1917. *Physics of the Earth and Planetary Interiors*, 32, 45-59.

Abe, K., and Noguchi, S., 1983b. Revision of magnitudes of large shallow earthquakes, 1897-1912: *Physics of the Earth and Planetary Interiors*, 33, 1-11.

Aki, K., 1965. Maximum Likelihood Estimate of b in the Formula log N = a-bM and its Confidence Limits. *Bull. Earthq. Res. Inst*., 43, 237-239.

Alsan, E., Tèzuçan, L. and Båth. M., 1975. An earthquake catalogue for Turkey for the interval 1913-1970. Common Rep. 75 Kandilli Turkey Obs., Seism. Inst. Uppsala, Sweden.

Ambraseys, N. N., 1974. Notes on engineering seismology, *Engineering seismology and Earthquake Engineering*, edited by J. Solnes, Nato Advanced Study, 33-54.

Ambraseys, N. N., 1985. Intensity-attenuation and magnitude-intensity relationships for northwest European earthquakes. *Earthquake Eng. Struct. Dynamics*. 13, 733-778.

Ambraseys, N. N., 1990. Uniform magnitude re-evaluation of European earthquakes associated with strong-motion records. *Earthquake Engineering and Structural Dynamics*, 19, 1-20.

Ambraseys, N. N., 1995. The prediction of earthquake peak ground acceleration in Europe. *Earth. Eng. Struct. Dyn*., 24, 467-490.

Ambraseys, N. N., 1997. Measurement of strong ground motion in Europe (MASGE). In: Ghazi, A., Yeroyanni, M., editors. Seismic Risk in the European Union. Proceedings of the review meetings in Brussels 2-3 and 23-24 May 1996, ECSC-EC-EAEC Brussels, Luxembourg, vol. 1. 195-217. [Not seen]

Ambraseys, N. N., 2001. The Kresna earthquake of 1904 in Bulgaria. *Annali di Geofisica*, 44, 1, 95-117.

Ambraseys, N. N., 2002. The Seismic Activity of the Marmara Sea Region over the Last 2000 Years. *Bull. Seism. Soc. Am.*, 92, 1-18. [Not seen]

Ambraseys, N. N. and Bommer, J. J., 1991. The attenuation of ground accelerations in Europe. *Earthquake Eng. Struct. Dynamics*. 20, 1179-1202.

Ambraseys, N. N. and Finkel, C. F., 1995. Seismicity of Turkey and Adjacent Areas, A Historical Review, 1500-1800. Publ. Muhittin Salih EREN, Istanbul. 240 pp. [Not seen]

Ambraseys, N. N. and Jackson, J. A., 1998. Faulting associated with historical and recent earthquakes in the Eastern Mediterranean region. *J. Geophys. Int.,* 133, 2, 390-406.

Ambraseys, N. N. and Adams, R. D., 1998. The Rhodes earthquake of 26 June 1926, *Journal of Seismology* 2, 267–292.

Ambraseys, N. N., Simpson, K. A. and Bommer, J. J., 1996. Prediction of horizontal response spectra in Europe. *Earthquake Engineering and Structural Dynamics*, 25, 371-400.

Ambraseys, N. N., Douglas, J., Sarma, S. K. and Smit, P.M., 2005. Equations for the Estimation of Strong Ground Motion from Shallow Earthquakes Using Data from Europe and The Middle East: Horizontal Peak Ground Acceleration and Spectral Acceleration. *Bull. Earth. Eng.*, 3, 1-53.

Ardeleanu, L., Leydecker, G., Bonjer, K-P., Busche, H., Kaiser, D. and Schmitt, T., 2005. Probabilistic seismic hazard map for Romania as a basis for a new building code. *Nat. Hazards Earth Syst. Sci*., 5, 679-684.

Armijo, R., Meyer, B., King, G. C. P., Rigo, A. and Papanastassiou, D., 1996. Quaternary evolution of the Corinth Rift and its implications for the evolution of the Aegean. *Geophys. J. Int*., 126, 11-53.

Atkinson, G. M. and Kaka, S. I., 2006. Relationships between Felt Intensity and Instrumental Ground Motion for New Madrid ShakeMaps. http://earthquake.usgs.gov/research/external/reports/05HQGR0039.pdf, 27 pp.

Azzaro, R. and Barbano, M. S., 1995. The Pollina (Northern Italy) earthquake of 26 June 1993: an application of the new European Macroseismic Scale 1992. *Natural Hazards*, 12, 3, 289-301. [Not seen]

Baba, A. B., Papadimitriou, E., Papazachos, B. C., Papaioannou, C. A., Karakostas, B. G., 2000. Unified local magnitude scale for earthquakes of south Balkan area. *Pure Appl. Geophys*., 157, 765-783.

Basham, P. and Giardini, D., 1993. Technical guidelines for global seismic hazard assessment. *Annali di Geofisica*, 36, 15-24.

Båth, M., 1973. *Introduction to Seismology*. Birkäuser-Verlag, Basle, 395 pp.

Båth, M., 1975. Seismicity of the Tanzania region. *Tectonophysics*, 27, 353-379.

Båth, M. and Benioff, H., 1958. The aftershock sequence of the Kamchatka earthquake of November 4, 1952. *Bull. Seism. Soc. Am*., 48, 1, 1-15.

Bazzurro, P. and Cornell, C. A., 1999. Disaggregation of Seismic Hazard. *Bull. Seism. Soc. Am*., 89, 2, 501-520.

Bender, B., 1983. Maximum Likelihood estimation of b-values for magnitude grouped data. *Bull. Seism. Soc. Am*., 73, 3, 831-851.

Benioff, H., 1951a. Earthquakes and Rock creep. *Bull. Seism. Soc. Am.*, 41, 1, 31-62.

Benioff, H., 1951b. Global Strain Accumulation and Release as Revealed by Great Earthquakes. *Bull. Seism. Soc. Am.*, 62, 331-338.

Benioff, H., 1955. Seismic evidence of crustal structure and tectonic activity. *Geol. Soc. Amer.,* Special Paper 62, 61-73.

Berardi, R., Mendez, A., Mucciarelli, M., Pacor, F., Longhi, G. And Petrungaro, C., 1995. On the modelling of strong motion parameters and correlation with historical macroseismic data: an application to the 1915 Avezzano earthquake. *Annali di Geofisicia*, 39, 5-5, 851-866.

Blake, A. 1941. On the estimation of focal depth from macroseismic data. *Bull. Seism. Soc. Am.*, 31, 225-231.

Boatwright, J., Thywissen, K. and Seekins, L. C., 2001. Correlation of Ground Motion and Intensity for the 17 January 1994 Northridge, California, Earthquake. *Bull. Seism. Soc. Am.*, 91, 4, 739-752.

Bončev, E., 1987a. *The Balkanides Geotectonic Position and Development*. Publ. House BAS, Sofia, 274 pp. [Not seen]

Bončev, E., 1987b. Main ideas in the tectonic synthesis of the Balkans I. The lithospheric plates and the collision space between them. *Geologica Balcanica*, 17, 4, 9-20.

Bončev, E., Bune, V. I., Christoskov, L., Karagjugleva, J., Kostadinov, V., Reisner, G. J., Rizhikova, S., Shebalin, N. V., Sholpo, V. N. and Sokerova, D., 1982. A method for compilation of seismic zoning prognostic maps for the territory of Bulgaria. *Geologica Balcanica*., 12, 2, 3-48.

Bondár, I., Yang, X., North, R. G., and Romney, C., 2001. Location Calibration Data for CTBT Monitoring at the Prototype International Data Center. *Pure Appl. Geophys*., 158, 19-34.

Bondár, I., Myers, S. C., Engdahl, E. R. and Bergman, E. A., 2004. Epicentre accuracy based on seismic network criteria. *Geophys. J. Int*., 156, 483-496.

Bormann, P., Baumbach, M. Bock, G., Grosser, H., Choy, G. L. and Boatwright, J., 2002. Chapter 3: Seismic Sources and Source Parameters. In: Bormann, P. (Ed.) (2002). *IASPEI New Manual of Seismological Observatory Practice*, GeoForschungsZentrum Potsdam, Vol. 1, 1-94.

Bungum, H., Lindholm, C. D. and Dahle, A., 2003. Long-period ground motions for large European earthquakes, 1905-1992, and comparisons with stochastic predictions. *J. Seism.*, 7, 377-396.

Burchfiel, B. C. R., Nakov, T., Tzankov, T. and Royden, L. H., 2000. Cenozoic extension in Bulgaria and Northern Greece: the northern part of the Aegean regime. In *Tectonics and Magmatism in Turkey and the Surrounding Area, Special Publications*, 173, E. Bozkvet, J. A. Winchester & J. D. A. Piper, Editors, 325-352, Geological Society, London.

Burchfiel, B. C., King, R. W., Todosov, A., Kotzev, V., Durmurdzanov, N., Serafimovski, T. and Nurce, B., 2006. GPS results for Macedonia and its importance for the tectonics of the Southern Balkan extensional regime. *Tectonophysics*, 413, 239-248.

Burton, P. W., 1977. The application of extreme value statistics to seismic hazard assessment in the European Area. *Proc. Int. Symp. Anal. Seismicity and Seismic Hazard, Liblice, Czech.*, 323-334.

Burton, P. W., 1978a. The IGS file of seismic activity and its use for hazard assessment. *Inst. Geol. Sci. Seismological Bulletin*, 6, 1-15.

Burton, P. W., 1978b. Perceptible earthquakes in the United Kingdom. *Geophys. J. R. astr. Soc*., 54, 475-479.

Burton, P. W., 1979. Seismic risk in southern Europe through to India examined using Gumbel's third distribution of extreme values. *Geophys. J. R. astr. Soc.,* 59, 249-280.

Burton, P. W., 1981. Variations in seismic risk parameters in Britain. In *Proceedings. 2nd Int. Symp. Anal. Seismicity and on Seismic Hazard*. Liblice (Czechoslovak Acad. Of Sciences), 2, 495-531.

Burton, P. W., 1990. Pathways to Seismic hazard Evaluation: Extreme and Characteristics Earthquakes in Areas of Low and High Seismicity. *Natural Hazards*, 3, 275-291.

Burton, P. W., 1996. Dicing with earthquakes. *Geophys Res. Lett*., 23, 11, 1379-1382.

Burton, P. W. and Neilson, G., 1978. Annual catalogues of British earthquakes recorded on LOWNET (1967-1976), *Inst. Geol. Sci., Glob. Seism. Unit*, Report No. 96, 60 pp. [Not seen]

Burton, P. W. and Neilson, G., 1980. Annual catalogues of British earthquakes recorded on LOWNET (1967-1978). *Seismol. Bull. Inst. Geol. Sci*., No. 4, HSMO.

Burton, P.W., Main, I.G. and Neilson, G., 1983. Seismic risk and the North Sea, in Proc. NATO Advanced Research Workshop, 1-4 June 1982, Utrecht, Holland, in Seismicity and Seismic Risk in the Offshore North Sea Area, eds A.R. Ritsema & A. Gurpinar, Reidel Publishing Company, Dordrecht, 347-364.

Burton, P. W., McGonigle, R., Makropoulos, K. C. and Üçer, S. C., 1984. Seismic risk in Turkey, the Aegean and the eastern Mediterranean: the occurrence of large magnitude earthquakes. *Geophys. J. R. astr*, 78, 475-506.

Burton, P. W. and Makropoulos, K. C., 1985. Seismic Risk of Circum-Pacific Earthquakes II. Extreme Values Using Gumbel's Third Distribution and the Relationship with Strain Energy Release. *PAGEOPH*, 123, 849-869.

Burton, P. W., McGonigle, R., Neilson, G., and Musson, R. M. W., 1985. Macroseismic focal depth and intensity attenuation for British earthquakes, in: *Earthquake engineering in Britain*, Telford, London, 91-110.

Burton, P. W., Makropoulos, K. C., McGonigle, R. W., Ritchie, m. E. A., Main, I. G., Kouskouna, V and Drakopoulos, J., 1991. Contemporary seismicity in eastern Greece from the Volos network (VOLNET): Fault parameters of major and minor earthquakes. Brit. Geol. Surv. Seismological Series, Report, WL/91/29, 106 pp.

Burton P. W., Xu Y., Tselentis G-A, Sokos E. and Aspinall, W., 2003. Strong ground acceleration seismic hazard in Greece and neighboring regions. *Soil Dynamics and Earthquake Engineering*, 23, 159-181.

Burton, P. W., Xu, Y., Qin, C., Tselentis, G-A and Sokos, E., 2004a. A catalogue of seismicity in Greece and the adjacent areas for the twentieth century. *Tectonophysics*, 390, 117-127.

Burton, P. W., Qin, C., Tselentis, G-A and Sokos, E., 2004b. Extreme Earthquake and Earthquake Perceptibility Study in Greece and its Surrounding Area. *Natural Hazards*, 32, 227-312.

Campbell, K. W. and Bozorgnia, Y., 2003. Updated near-source ground motion (attenuation) relations for the horizontal and vertical components of peak ground acceleration and acceleration response spectra. *Bull. Seism. Soc. Am*., 93, 1, 314-331.

Cancani, A., 1904. Sur l'emploi d'une double echelle seismique des intesites, empirique et absolue, *G. Beitr*. 2, 281-283. [Not seen]

Caporali, A, Aichhorn, C., Becker, M., Fejes, I., Gerhatova, L, Ghitau, D., Grenerczy, G., Hefty, J., Krauss, S., Medak, D., Milev, G., Mojzes, M., Mulic, M., Nardo, A., Pesec, P, Rus, T., Simek, J., Sledzinski, J., Solaric, M., Stangl, G., Vespe, F., Virag, G., Vodopivec, F. and Zablotskyi, F., 2008. Geokinematics of Central Europe: New insights from the CERGOP-2/Environment Project. *Jour. Geodynamics*, 45, 4-5, 246-256.

Cella, R., Zonna, G. and Meroni, F., 1996. Parameters estimation of intensity decay relationships. *Annali di Geofisicia*, 39, 5, 1095-1113.

Chapman, M. C., 1995. A Probabilistic Approach to Ground-Motion Selection for Engineering Design. *Bull. Seism. Soc. Am*., 85, 3, 937-942.

Christoskov, L., 1982. A method for estimating the seismological catalogues representativeness and its application to the central part of the Balkan region (in Bulgarian). *Bulg. Geophys. Jour*., 8, 66-76. [Not seen]

Christoskov, L. and Grigorova, E., 1968. Energetic and space-time characteristics of the destructive earthquakes in Bulgaria after 1900. *Bull. Inst. Geoph. Sofia*., XII, 79-107. [In Bulgarian with English summary]

Christoskov, L., Solakov, D., Simeonova, S. and Botev, E., 2003. Conception of making maps for seismic zoning regarding Eurocode 8 (EC8). *Bulgarian Academy of Sciences News*, No. 4, December 2003.

Cocard, M., Kahle, H.-G., Peter, Y., Geiger, A., Veis, G., Felekis, S., Paradissis, D. and Billiris, 1999. New constraints on the rapid crustal motion of the Aegean region: recent results inferred from GPS measurements (1993-1998) across ten West Hellenic Arc, *Greece. Earth and Planetary Science Letters*, 172, 39-47.

Contadakis, M. E. and Asteriadis, G., 2002. Recent results of the research for preseismic phenomena on the underground water and temperature in Pieria, northern Greece. *Natural Hazards and Earth System Sciences*, 1, 165-170.

Constantinescu, L. and Marza, V. I., 1980. A computer-compiled and computer-oriented catalogue of Romania's earthquakes during a millennium (984-1979). *Geophysique*, 24, 2, 193-234.

Corral, A., 2006. Dependence of earthquake recurrence times and independence of magnitudes on seismicity history. *Tectonophysics*, 424, 177-193.

Cornell, C. A., 1968. Engineering Seismic Risk Analysis. *Bull. Seism. Soc. Am*., 58, 5, 1583-1606.

Cvijic, J., 1904. Die Tektonik der Balkanhalbinsel usw., *C. R. IX Congr. Geol. Int. I*., Vienne. 247-270. [Not seen]

Cramer, C. H. And Petersen, M. D., 1996. Predominant Seismic Source Distance and magnitude Maps for Los Angeles, Orange, and Ventura Counties, California. *Bull. Seism. Soc. Am*., 86, 5, 1645-1649.

Dabovsky, Ch., 1991. Modern concepts on the evolution of the Alpine orogen in the Eastern Mediterranean and the Carpathian-Balkan area. A review and some problems of Bulgarian

geotectonics. Geotectonics, *Tectonophysics and Geodynamics*, 22, 45-79. [In Bulgarian; Not seen]

Dachev, H., Vaptzarov, I., Filipov, L., Solakov, D., Simeonova, S., and Nikolova, S, 1995. Investigations and activities for increasing of the seismic safety of the PNPP Belene site, Geophysical Institute Final Report, (unpublished), p250.

Dessokey, M. M., 1985. Extreme value models for seismic hazard analysis. *Bulletin of the International Institute of Seismology and Earthquake Engineering*, 21, 23-31.

Dick, I. D., 1964. Extreme value theory and earthquakes, *3rd ICEE, NZ*, 3, 45-53.

Dimitrov, D. S. and Ruegg, J-C., 1994. The 1928 Bulgarian earthquakes: fault geometry from geodetic and modelling. 1st International Symposium on Deformations in Turkey, Istanbul, 921-932.

Dimitrov, D. S., Chabalier, J-B., Ruegg, J-C., Armijo, R., Meyer, B. and Botev., 2004. The 1928 Plovdiv sequence (Bulgaria): fault model constrained from geodetic data and surface breaks. *Geophys. Jour. Int*. 9p

Dineva, S., Batllo, J., Mihaylov, D. and van Eck, T., 2002. Source parameters of four strong earthquakes in Bulgaria and Portugal at the beginning of the 20th Century. *J. Seism*., 6, 1, 99-123.

Dolce, M., Masi, A., Marino, M. and Vona, M., 2003. Earthquake Damage Scenarios of the Building Stock of Potenza (Southern Italy) Including Site Effects. *Bull. Earth. Eng.,* 1, 1, 115-140. [Not seen]

Donovan, N. C., 1973. A statistical evaluation of strong motion data including the February 9, 1971 San Fernando earthquake. *Proc. 5th World Conf. Earth. Eng. Rome*. [Not seen]

Douglas, A., 1967. Joint Epicentre Determination. *Nature*, 215, 5096, 47-48.

Douglas, J., 2003. Earthquake ground motion estimation using strong motion records: a review of equations for the estimation of peak ground acceleration and response spectral ordinates. *Earth Science Reviews*, 61, 43-104.

Drakopoulos, J. C., 1976. On the completeness of macroseismic data a) in the major area of Greece b) in the Balkan area. *Proc. Of the Seminar on seismic zoning maps UNESCO-Skopje*, 132-156.

Engdahl, E.R., R.D. van der Hilst, and R. Buland 1998. Global teleseismic earthquake relocation with improved travel times and procedures. *Bull. Seism. Soc. Am*., 88, 722-743

Epstein, B. and Lomnitz, C. 1966. A Model for the Occurrence of Large Earthquakes. *Nature*, 211, 954-956.

Esteva, L., 1974. Geology and probability in the assessment of seismic risk. *Proc. 2nd Int. Congr. Int. Assoc. Eng. Geol.*, Sao Paulo.

Esteva, L., 1976. Seismicity. In: *Seismic Risk and Engineering Decisions*. Lomnitz, C. and Rosenblueth, E. editors, Elsevier Science Publ. Comp. Amsterdam, 425 pp. [Not seen]

Esteva, L. and Rosenblueth, E., 1964. Espectos de temblores a distancias moderadas y grandes. *Bol. Soc. Mex. In. Sismica*, 2, 1-18. [Not seen]

EUROCODE 8, 2003. Design of structures for the earthquake resistance. Part 1: General Rules, seismic actions and rules for buildings. – Draft No. 6, Ref. No: prEN 1998-1:200X. European Committee for Standardisation, Central Secretariat: rue de Strassart, 36, B-1050 Brussels. [Not seen]

Evagelatou-Notara, Fl., 1993. The earthquakes in Byzantium, from the 13th till 15th century, historic examination. *Parousia*, Spec. Issue 24, 184 pp. [Not seen]

Flinn, E. A. and Engdahl, E. R., 1965. A proposal basis for geographical and seismic regionalization. *Rev. Geophys.,* 3, 123.

Flinn, E. A., Engdahl, E. R. and Hill, A. R., 1974. Seismic and geographical regionalization. *Bull. Seism. Soc. Am.*, 64, 3, 771-993.

Galanopoulos, A. G., 1941. Das erdbeben von Messenien vom 22 January 1899, "Prakt. Acad. Athens", 16, 127-134. [Not seen]

Galanopoulos, A. G., 1949. The Koroni (Messinia) earthquake of October 6, 1947. *Bull. Seism. Soc. Am.*, 39, 33-39.

Galanopoulos, A. G., 1950. Die beiden schadenbringenden Beben von Larissa aus den Jahren 1892 and 1941. "*Gerf Beitr. Z Geophys.",* 62, 27-38. [Not seen]

Galanopoulos, A. G., 1960. A *Catalogue of shocks with $I_0 \geq VI$ or $M \geq 5$ for the years 1801-1958*. Seismological Laboratory, Athens University, 119 pp. [Not seen]

Galanopoulos, A. G., 1961. A Catalogue of shocks with $I_0 \geq$ VII for the years prior to 1800. Seismological Laboratory, Athens University, 18 pp. [Not seen]

Galanopoulos, A. G., 1963. On mapping of seismic activity in Greece. *Ann. Di. Geof.*, 16, 37-100.

Galanopoulos, A. G., 1972. Annual and maximum possible strain accumulation in the major area of Greece. *Annls. geol. Pays Hell.*, 24, 467-480. [In Russian with English abstract].

García-Mayordomo, J. C., Faccioli, E. and Paolucci, R., 2004. Comparative Study of the Seismic Hazard Assessments in European National Seismic Codes. *Bulletin of Earthquake Engineering*, 2, 51-73.

Gardner, J. K. and Knopoff, L., 1974. Is the sequence of earthquakes in southern California, with aftershocks removed, Poissonian? *Bull. Seism. Soc. Am.*, 64, 5, 1363-1367.

Georgiev, I., Pashova, L., Nikolov, G., Botev, E., Dimitrov, D., Gospodinov. Sl., Zdravchev, I. and Alexandrov, B., 2002. Regional geodynamic GPS network in SW Bulgaria: geological and geophysical background, status and perspectives, *Bulgarian Geophysical Journal*, 28, 1-4, 78-90.

Giardini D., (editor), 1999. *The Global Seismic Hazard Assessment Program (GSHAP) 1992-1999*. Annali di Geofisica, 42, 6, 957-1,230.

Giardini, D. and Basham, P., 1993. The Global Seismic Hazard Assessment Program. *Annali di Geofisica*, 36, 3-13.

Glavcheva, R., 1984. Some characteristics of the mechanical process in the source of the April 1928 earthquake (M = 7), South Bulgaria. *Bulg. Geophys. J.,* 10, 53-61.

Glavcheva, R. P., 1990. On the optimization of the correlation between the macroseismic intensity and accelerogram characteristics. *Comptes rendus de l'Académie bulgare des Sciences*, 43, 11, 37-40.

Glavcheva, R., 1993. *Atlas of isoseismal maps. Bulgaria, 1981-1990*. Geophysical Institute Bulgarian Academy of Sciences. Sofia., 66 pp. [Not seen]

Glavcheva, R., 1997. Macroseismic area size and magnitude for the earthquakes in Bulgaria: empirical relations, *Bulg. Geophys. J.*, 23 (1-2), 96-106.

Glavcheva, R., Botev, B. and Ranguelov, B., 2003. Observations and monitoring of the seismicity in Bulgaria. *European-Mediterranean Seismological Centre Newsletter*, No. 19, 8-11.

Goldsworthy, M., Jackson, J. and Haines, J., 2002. The continuity of active fault systems in Greece. *Geophys. J. Int.,* 148, 596-618.

Goretti, A., 2003. The perceptibility in the selection of the reference earthquake. An application to the town of Potenza, In: M. Dolce, A. Masi, and M. Marino (eds.), *Proceedings of the International Workshop on the Seismic Risk and Earthquake Scenarios of Potenza*, European Commission XII Science Research and Development, Edizioni Lamisco della Spes sas, Potenza, Italy, pp. 71-82. [Not seen]

Grandori, G., Perotti, F. and Tagliani, A., 1987. On the attenuation of macroseismic intensity with epicentral distance. In: *3rd International Conference Soil Dynamics and Earthquake Engineering, Princeton* <<Ground Motion and Engineering Seismology>>, edited by A. S. Cakmak (Elsevier, Amsterdam), 581-594. [Not seen]

Grandori, G., Drei, A., Perotti, F. and Tagliani, A., 1991. Macroseismic intensity versus epicentral distance: the case for central Italy. In: M. Stucchi, D. Postpischl and D. Slejko (Editors), Investigation of Historical Earthquakes in Europe. *Tectonophysics*, 193, 165-171.

Grigorova, E. and Grigorov, B., 1964. *Epicenters and seismic lineaments in Bulgaria*. BAS, Sofia, 83 pp. [In Bulgarian with French abstract]

Gringorten, I., 1963. A plotting rule for extreme probability paper. *Journal of Geophysics Research*, 68, 813-814.

Grünthal, G., (ed.), 1998. "European *Macroseismic Scale 1998*", Cahiers du Centre Européen de Géodynamique et de Séismologie, Volume 15, Luxembourg, 99 pp.

Grünthal, G. and Wahlström, R., 2003. An M_w based earthquake catalogue for central, northern and northwestern Europe using a hierarchy of magnitude conversions. *Journal of Seismology*, 7, 507-531.

Guidoboni, E., Comastri, A. and Traina, G., 1994. *Catalogue of ancient earthquakes in the Mediterranean area up to the 10th century*. SGA Storia Geofisica Ambiente, Bologna. 504 pp. [Not seen]

Gumbel, E. J., 1935. Floods Les valeurs extrèmes des distribution statistiques, *Ann. Inst. Henri Poincaré*, 5, 115-158. [Not seen]

Gumbel, E. J. 1945a. Simplified plotting of statistical observations. *Trans. Am. Geophys. Union*, 126, 1, 71-83.

Gumbel, E. J., 1945b. Floods estimated by Probability Methods. *Eng. News Record,* 137, 97-101.

Gumbel, E. J., 1958. *Statistics of extremes*. Columbia Univ. Press, New York and London, 375 pp.

Gutdeutsch, R. and Hammerl, C., 1999. An uncertainty parameter of historical earthquakes – the record threshold. *J. Seism.,* 3, 4, 351-362. [Not seen]

Gutenberg, B. and Richter, C. F., 1936. On Seismic Waves (Third Paper). Gerlands Bietr. Z. Geophys., 47, 73-131. [Not seen]

Gutenberg, B. and Richter, C. F., 1942. Earthquake Magnitude, Intensity, Energy, and Acceleration. *Bull. Seism. Soc. Am.,* 32, 3, 163-191.

Gutenberg, B. and Richter, C. F., 1944. Frequency of Earthquakes in California. *Bull. Seism. Soc. Am*., 34, 185-188.

Gutenberg, B. and Richter, C. F., 1949. *Seismicity of the Earth and Associated Phenomena*. Princeton University Press. 273 pp.

Gutenberg, B. and Richter, C. F., 1956. Magnitude and Energy of Earthquakes. *Ann. Geofis*., 9, 1, 1-15.

Hadzievski, D., 1975. *Seismicity of the Territory of SR Macedonia*, Seismological Obs. Univ. Kiril and Metodij, Skopje. 199 pp. (in Macedonian). [Not seen]

Hanks, T. C. and Kanamori, H., 1979. A Moment Magnitude Scale. *Jour. Geo. Res*., 84, No. B5, 2348-2350.

Harmsen, S. and Frankel, A., 2001. Geographic Deaggregation of Seismic Hazard in the United States. *Bull. Seism. Soc. Am*., 91, 1, 13-26.

Harmsen, S., Perkins, D. and Frankel, A., 1999. Deaggregation of Probabilistic Ground Motions in the Central and Eastern United States. *Bull. Seism. Soc. Am*., 89, 1, 1-13.

Hershberger, J., 1956. A comparison of earthquake accelerations with intensity ratings. *Bull. Seism. Soc. Am*., 46, 317–320. [Not seen]

Hollenstein, Ch., Müller, M. D., Geiger, A. and Kahle, H.-G., 2008. Crustal motion and deformation in Greece from a decade of GPS measurements. *Tectonophysics*, 449, 17-40.

Holt, W. E., Shen-Tu, B., Haines, A. J. and Jackson, J. A., 2000. On the determination of self-consistent strain rate fields within zones of distributed continental deformation. *The History and Dynamics of Global Plate Motions. Geophysical Monograph, vol. 121. American Geophysical Union*, pp. 113-141.

Hudson, D. E., (editor) 1971. Unusual accelerograms recorded at Lima, Peru. *Bull. Seism. Soc. Am*., 57, 1179-1192.

Ishimoto, M., 1932, Echelle d'intensité sismique et acceleration maxima*, Bull. Earthq. Res. Inst.*, 10, 171, 614-626. [Not seen]

Jackson, J., 1994. Active tectonics of the Aegean region. *Annu. Rev. Earth Planet. Sci*., 22, 239-271.

Jackson, J. A. and Mckenzie, D. P., 1988. The relationship between plate motions and seismic tensors, and the rate of active deformation in the Mediterranean and Middle East. *Geophys. J. Int*., 93, 45-73.

Jánosi, I., 1907. Makroszeizmikus rengések feldolgozása a Cancani-féle egyenlet alapján, in Réthly, A., (Ed.) Az *1906 évi Magyarországi Földrengések, A. M. Kir. Orsz. Met. Föld. Int*., Budapest, 77-82. [Not seen]

Jefferys, H. and Bullen, K. E., 1988. *Seismological Tables*. British Association for the Advancement of Science, Black Bear Press Limited, Cambridge, 43 pp.

Jiménez, M. J., Giardini, D., Grünthal, G and SESAME Working Group (Erdik, M., García-Fernández, M., Lapajne, J., Makropoulos, K., Musson, R., Papaioannou, Ch., Rebez, A., Riad, S., Sellami, S., Shapira, A., Slejko, D., van Eck, T., El Sayed, A.), 2001. Unified seismic hazard modelling throughout the Mediterranean region. *Bollettino di Geofisicia Teorica ed Applicata*, 42, 1-2, 3-18.

Johnston, A. C. and Halchuk, S., 1993. The seismicity database for the Global Seismic Assessment Program. *Annali di Geofisica*, 36, 3-4, 133-151.

Joyner, W. B. and Boore, D. M., 1981. Peak horizontal acceleration and velocity from strong motion records including records from the 1979 Imperial Valley, California, earthquake. *Bull. Seism. Soc. Am*., 71, 2011-2038. [Not seen]

Kahle, H.-G., Müller, M. V., Geiger, A., Danuser, G., Mueller, S., Veis, G., Billiris, H. and Paradissis, D., 1995. The strain field in northwestern Greece and the Ionian Islands: results inferred from GPS measurements. *Tectonophysics*, 249, 41-52.

Kahle, H.-G., Straub, C., Reilinger, R., McClusky, S., King, R., Hurst, K., Veis, G., Kastens, K. And Cross., P., 1998. The strain rate field in the eastern Mediterranean region, estimated by repeated GPS measurements. *Tectonophysics*, 294, 237-252.

Kalafat, D., 2003. B.U. Kandilli Observatory and Earthquake Institute seismological Laboratory. *European-Mediterranean Seismological Centre Newsletter*, No. 19, 5-7.

Kanamori, H., 1977. The Energy Release in Great Earthquakes. *Jour. Geophys. Res.,* 82, 20, 2981-2987.

Kanamori, H., 1983. *Global Seismicity, in Earthquakes: Observation, theory and interpretation.* edited by H. Kanamori and E. Bosch, pp. 597, North Holland, New York.

Karakostas, V., Papadimitriou, E., Gospodinov, D. and Ranguelov, B.: Slip distribution of the 1928 Chirpan and Plovdiv main shocks and earthquake triggering. VIth International Conference of SGEM, 119-127, 2006.

Karastathis, V. K., Drakatos, G., Makris, J, Papoulia, J., Papanikolaou, M., Ganas, A. and Petrou, P., 2005. Microseismicity and passive tomography results in Attica region, Greece. *Geophys. Res. Abstracts*, 7, 2 pp. (abstract).

Kárník V., 1968. *Seismicity of the European Area. Part 1 (1900-1955).* Praha, 362 pp.

Kárník V., 1971. *Seismicity of the European Area. Part 2 (1801-1900).* Praha, 218 pp.

Kárník, V. and Hubnerová, Z., 1968. The Probability of Occurrence of Largest Earthquakes in the European Area. *PAGEOPH*, 70, 61-73.

Kárník, V. and Schenková, Z. 1977. The third asymptotic distribution in earthquake statistics. *Proc. Int. Symp. Anal. Seismicity and Seismic Hazard, Liblice, Czech.*, 335-350.

Kawasumi, H., 1951. Measures of earthquake danger and expectancy of maximum intensity throughout Japan as inferred from the seismic activity in historical times. Tokyo University Earthquake Research Institute Bulletin, 29, 3, 469-482. [Not seen]

Knopoff, L., 1971. A Stochastic Model for the Occurrence of Main Sequence Earthquakes. *Rev. Geophys*., 9, 175-188.

Kober, I., 1931. Das Alpine Europa und sein Rahmen. – Berlin. [Not seen]

Koravos, G. Ch., Main, I. G., Tsapanos, T. M. and Musson, R. M. W., 2003. Perceptible earthquakes in the broad Aegean area. *Tectonophysics*, 371, 175-186.

Kotzev, V., Nakov, R., Burchfiel, B. C., King, R. and Reilinger, R., 2001. GPS study of active tectonics in Bulgaria: results from 1996 to 1998. *Jour. Geophys*., 31, 189-200.

Kotzev, V., Nakov, R., Georgiev, Tz., Burchfiel, B. C. and King, R. W., 2006. Crustal motion and strain accumulation in western Bulgaria. *Tectonophysics*, 413, 127-145.

Kövesligethy, R., 1906. A makroszeizmikus rengések feldolgozása, *Math. És Természettudományi Értesítõ*, 24, 349-368. [Not seen]

Kövesligethy, R., 1907. Seismischer Stärkegrad und Intensität der Beben, *Beitr. zur Geoph*., 8, 363-366. [Not seen]

Lazarov, R. and Christoskov, L. 1981. Statistical aspects of the magnitude-frequency relation for Bulgaria. Proc. *2nd Int. Symp. Anal. Seismicity and Seismic Hazard, Liblice, Czech*., 56-66.

Leydecker, G., Busche, H., Bonjer, K.-P., Schmitt, T., Kaiser, D., Simeonova, S., Solakov, D. and Ardeleanu, L., 2008. Probabilistic seismic hazard in terms of intensities for Bulgaria and Romania – updated hazard maps. *Nat. Hazards Earth Syst. Sci*., 8, 1431-1439.

Lomnitz, C., 1966. Statistical Prediction of Earthquakes. *Rev. of Geop.*, 4, No. 3, 377-393.

Lomnitz, C., 1974. *Global tectonics and earthquake risk*. Elsev. Scient. Publ. Comp., Amsterdam, 320 pp.

Lomnitz, C., 1994. *Fundamentals of Earthquake Prediction*. Wiley and Sons, 326 pp.

Lungu, D., Cornea, T., Aldea, A. and Zaicenco, R. Y., 1997. Basic representation of seismic action in Design of structures in seismic zones (ed. Lungu, D., Mazzolani, F. and Savidis, S.) Bridgeman Ltd, Timisoara, 9-60. [Not seen]

Main, I. G., 1995. Earthquakes as critical phenomena: Implications for probabilistic seismic hazard analysis. *Bull. Seism. Soc. Am*., 85, 1299-1308.

Makris, J., Papoulia, J. and Drakatos, G., 2004. Tectonic Deformation and Microseismcity of the Saronikos Gulf, Greece. *Bull. Seism. Soc. Am*., 94, 3, 920-929.

Makropoulos, K. C., 1978. *The statistics of large earthquake magnitude and an evaluation of Greek seismicity*. PhD Thesis, University of Edinburgh, 193 pp.

Makropoulos, K. C. and Burton, P. W., 1981. A catalogue of seismicity in Greece and adjacent areas. *Geophys. J. R. astr. Soc*., 65, 741-762.

Makropoulos, K. C. and Burton, P. W., 1983. Seismic Risk of Circum-Pacific Earthquakes I. Strain Energy Release. *PAGEOPH*, 121, 2, 247-267.

Makropoulos, K. C. and Burton, P. W., 1984. Greek tectonics and seismicity. *Tectonophysics*, 106, 275-304. [Not seen]

Makropoulos, K. C. and Burton, P. W., 1985a. Seismic hazard in Greece. I. Magnitude Recurrence. *Tectonophysics*, 117, 205-257.

Makropoulos, K. C. and Burton, P. W., 1985b. Seismic hazard in Greece. II. Ground Acceleration. *Tectonophysics*, 117, 259-294.

Makropoulos, K. C., Drakopoulos, J. K. and Latousakis, J. B., 1989. A revised and extended earthquake catalogue for Greece since 1900. *Geophys. J. Int*., 98, 391-394.

Margaris, B. N. and Papazachos, C. B., 1999. Moment-magnitude relations based on strong motion records in Greece. *Bull. Seism. Soc. Am*., 89, 442-455.

McGuire, R. K., 1976. FORTRAN Computer Program for Seismic Risk Calculations, U.S. Geol. Surv. Open-File Rep. 76-67, 90.

McGuire, R.K., 1993. Computations of seismic hazard. *Annali Geofis.*, 36, 181-200.

McGuire, R. K., 1995. Probabilistic Seismic hazard Analysis and Design Earthquakes: Closing the Loop. *Bull. Seism. Soc. Am*., 85, 5, 1275-1284.

Medvedev, S. V., 1977. Seismic Intensity Scale MSK-76, *Publ. Inst. Geophys. Pol. Acad. C*., 117, 95-102.

Medvedev, S. and Sponheuer, W., 1969. "MSK Scale of Seismic Intensity", Proceedings of the Fourth World Conference on Earthquake Engineering, Santiago, Chile, 1, A2.

Meyer, B., Armijo, R. and Dimitrov, D., 2002. Active faulting in SW Bulgaria: possible surface rupture of the 1904 Struma earthquake. *Geophys. J. Int*., 148, 246-255.

Meyer, B., Sébrier, M. and Dimitrov, D., 2007. Rare destructive earthquakes in Europe: The 1904 Bulgaria event case. *Earth and Planetary Science Letters*, 253, 485–496.

Miyamura, S., 1962. Magnitude-frequency relations and its bearings to geotectonics. *Proc. Japan. Ac*., 38, 1, 27-30.

Muir-Wood R.; 1993. From global seismotectonics to global seismic hazard. *Annali Geofis*., 36, 153-168.

Murphy, J. R. and Lahoud, J. A., 1969. Analysis of seismic peak amplitudes from underground nuclear explosions. *Bull. Seism. Soc. Am*., 59, 2325-2342. [Not seen]

Musson, R. M. W., 1998. The Barrow-in-Furness Earthquake of 15 February 1865: Liquefaction from a Very Small Magnitude Event. *Pure and Applied Geophysics*, 152, 4, 733-745. [Not seen]

Musson, R. M. W., 1999. Probabilistic Seismic Hazard Maps for the North Balkan Region. *Annali di Geofisica*, 42, 1109-1124.

Musson, R. M. W., 2000. Intensity-based seismic risk assessment. *Soil Dynamics and Earthquake Engineering*, 20, 353-360.

Musson, R. M. W., 2002. Chapter 12: Intensity and Intensity Scales. In: Bormann, P. (Ed.) 2002. *IASPEI New Manual of Seismological Observatory Practice*, GeoForschungsZentrum Potsdam, Vol. 1, 20 pp.

Neumann, F., 1954. *Earthquake Intensity and Related Ground Motion*, University Press, Seattle, Washington, 77 pp. [Not seen]

Neunhofer, H. and Gueth, D., 1989. Detailed investigation of the great earthquake swarm in western Bohemia by the local Vogtland network. In: Bormann, P. (ed.), *Monitoring and Analysis of the earthquake swarm 1985/86 in the region Vogtland/Western Bohemia*, Veröffentlichung des Zentralinstitutt für Physik der Erde Nr. 110, Als Manuscripkt gedruckt, Potsdam. [Not seen]

Nikolova, S., Solakov, D. and Miloshev, N., 2005. Earthquake Forecasting and Earthquake Early Warning System in Bulgaria. *Bulgarian Academy of Sciences News*, No. 12 (28), December 2005.

Nocquet, J-M. and Calais, E., 2003. Crustal velocity field of western Europe from permanent GPS array solutions, 1996-2001. *Geophys. J. Int*., 154, 72-88.

Nordquist, J. M., 1945. Theory of large values applied to earthquake magnitudes. *Trans. Amer. Geophys. Union*, 26, 29-31.

Okamoto, S. 1973. *Introduction to Earthquake Engineering*, Wiley, New York. [Not seen]

Oncescu, M. C., Marza, V. I, Rizescu, M., Popa, M., 1999. The Romanian Earthquake Catalogue between 984-1997, in *Vrancea Earthquakes: Tectonics, Hazard and Risk Mitigation*. F. Wenzel, D. Lungu (eds.) and O. Novak (co-ed), Kluwer Academic Publishers, Dordrecht, Netherlands., 43-47.

Orozova-Stanishkova, I. and Slejko. D., 1994. Seismic Hazard of Bulgaria. *Natural Hazards,* 9, 247-271.

Orphal, D. L. and Lahoud, J. A., 1974. Prediction of peak ground motion from earthquakes. *Bull. Seism. Soc. Am*., 64, 5, 1563-1574.

Pacheco, J. F. and Sykes, L. R., 1992. Seismic moment catalog of large shallow earthquakes, 1900 to 1989. *Bull. Seism. Soc. Am*., 82, No. 3, 1306-1349.

Panza, G. F., Vaccari, F., Costa, G., Suhadolc, p. And Fäh, D. 1996. Seismic input modelling for zoning and microzoning. *Earthquake Spectra*, 12, 3, 529-566.

Panza, G. F., Cazzaro, R. and Vaccari, F., 1997. Correlation between macroseismic intensities and seismic ground motion parameters. *Annali di Geofisica*, 40, 5, 1371-1381.

Papadimitriou, E., Karakostas, V., Tranos, M., Ranguelov, B. And Gospodinov, D., 2007. Static stress changes associated with normal faulting earthquakes in south Balkan area. *Int. J. Earth. Sci.*, 96, 911-924.

Papaioannou, Ch. A., 1984. *Attenuation of seismic intensities and seismic hazard in Greece and surrounding area*. Ph.D. thesis, Univ. of Thessaloniki, 200 pp. [Not seen]

Papaioannou, Ch. A., 1986. Seismic Hazard Assessment and Long-Term Earthquake Prediction in Southern Balkan Region. *Proc. 2nd Int. Sem. In: Earthquake Prognostics*, [eds: A. Vogel & K. Brandes], Berlin FGR June 23-27, 1986, 223-241.

Papazachos, B. C., 1990. Seismicity of the Aegean and surrounding Area. *Tectonophysics*, 178, 287-308.

Papazachos, B. C., 1992. Anisotropic radiation modeling of macroseismic intensities for estimation of attenuation structure of the upper crust of Greece. *Pure. Appl. Geophys*. 138, 445-469.

Papazachos, B. C., and Comninakis, P. E., 1971. Geophysical and tectonic features of the Aegean Arc. *J. Geophys. Res*., 76, 8517-8533.

Papazachos, C. and Papaioannou, Ch., 1997. The macroseismic field of the Balkan region. *Journal of Seismology*, 1, 181-201.

Papazachos, B.C. and Papazachou, C., 1997. *The Earthquakes of Greece*. Ziti Publications, 304 pp.

Papazachos, B. C., Mountrakis, D., Psilovikos, A. and Leventakis, G., 1979. Surface fault traces and fault plane solutions of the May-June 1978 major shocks in the Thessaloniki area. *Tectonophysics*, 53, 171-183.

Papazachos, B. C., Comninakis, P. E., Hatzidimiriou, P. M., Kiriakidis, E. G., Kiratzi, A. A., Panagiotopoulos, D. G., Papadimitriou, E. E., Papaioannou, Ch. A., Pavlidis, S. B. and Tzanis, E. P., 1982. *Atlas of isoseismal maps for earthquakes in Greece 1902-1981*. "Publ. Geophys. Lab. Univ. Thessaloniki", 4, 126 pp. [Not seen]

Papazachos, B. C., Papaioannou, Ch., Papazachos, C. and Savvaidis, A., 1997a. *Atlas of isoseismal maps for strong shallow earthquakes in Greece and surrounding area (426BC-1995).* Ziti Publications, Thessaloniki, Greece, 176 pp.

Papazachos, B. C., Kiratzi, A. A. and Karakostas, B. G., 1997b. Towards a Homogenous Moment-Magnitude Determination for Earthquakes in Greece and the Surrounding Area. *Bull. Seism. Soc. Am*., 87, No. 2, 474-483.

Papazachos, B.C., Comninakis, P.E., Karakaisis, G.F., Karakostas, B.G., Papaioannou, Ch. A., Papazachos, C.B., Scordilis, E.M., 2000. A catalogue of earthquakes in Greece and surrounding area for the period 550BC– 1999. Publ. Geoph. Lab., Univ. Thessaloniki.

Papoulia, J. E. and Stavrakakis, G. N., 1990. Attenuation Laws and Seismic Hazard Assessment. *Natural Hazards*, 3, 49-58.

Pavlides, S. and Caputo, R., 2004. Magnitude versus faults' surface parameters: quantitative relationships from the Aegean Region. *Tectonophysics*, 380, 159-188.

Perez, O. J., 1999. Revised World Seismicity Catalog (1950-1977) for Strong (Ms ≥ 6) Shallow (h ≤ 70 km) Earthquakes. *Bull. Seism. Soc. Am*., 89, No. 2, 335-341.

Powell, J. A. and Duda, S. J., 1975. A statistical Study of Earthquake Occurrence. *Pageoph*, 113, 447-460.

Prochazkova, D., Schenkova, Z. and Kárník, V., 1977. *Catalogue of Earthquakes and Atlas of Isoseismals for the Bohemian Massif, the Carpathians and the Rhodope Mts*. Progress Report (1974-1975). Working Group 4.3.3 of the Commission of Academies of Sciences of Socialistic Countries for Planetary Geophysical Research.

Purcaru, G. and Berckhemer, H., 1978. A magnitude scale for very large earthquakes. *Tectonophysics*, 49, 189-198. [Not seen]

Purcaru, G., 1979. The Vrancea earthquake of March 4, 1977 – A quite successful prediction. *Phys. Ear. Plant. Int*., 18, 274-278.

Radu, C., 1979. Catalogue of Strong Earthquakes originated on the Romanian Territory: Part 1 – Before 1901; Part II – 1901-1979 (in Romanian). Cerc. Seism…., CFPS, Bucharest, 723-752. [Not seen]

Radu, C., 1991. Strong earthquakes occurred on the Romanian territory in the period 1901-1990. (in Romanian*). Vitralii*, 3, 12-13. [Not seen]

Radulian, M., Vaccari, F., Mandrescu, N., Moldoveanu, C. L. and Panza, G. F., 2002. *Seismic hazard in Romania associated to Vrancea subcrustal source: deterministic evaluation*. United Nations Educational Scientific and Cultural Organization and International Atomic Energy Agency, IC, 2002, 31, 23 pp.

Ranguelov, B., Rizhikova, S., Shanov, S., Gospodinov, D. and Toteva, T., 2000a. The seismic potential for the Kresna-Kroupnik zone - SW Bulgaria. In. *Reports on Geodesy* No. 4 (49), Warsaw, 237-241.

Ranguelov, B., van Eck, T., Papadopoulos, G., Pavlides, S., Shanov, S. and Shenk, V., 2000b. Initial data for the magnitude reevaluation of the strong earthquakes during 1904 in Kresna-Kroupnik zone (SW Bulgaria). In. *Reports on Geodesy*, No. 4 (49), Warsaw, 50-55.

Ranguelov, B., Rizhikova, S. and Toteva, T., 2001. *The earthquake (M7.8) source zone (South-West Bulgaria)*. Acad. Publ. House "M. Drinov", 279 pp. [Not seen]

Reasenberg, P., 1985. Second-order moment of central California seismicity. *Jour. Geophys. Res.*, 90, No. B7, 5479-5495.

Rezapour, M. and Pearce, R. G., 1998. Bias in Surface-Wave Magnitude M_s due to Inadequate Distance Corrections. *Bull. Seism. Soc. Am*., 88, 43-61.

Richter, C. F., 1935. An Instrumental Earthquake Magnitude Scale. *Bull. Seism. Soc. Am.,* 25, 1-32.

Richter, C. F., 1958. *Elementary Seismology*. Freeman, 768 pp.

Rizhikova, S., Toteva, T. and Ranguelov, B., 2000. Seismicity of the Kresna source zone for eighty-year post active period (1909-1989). In. *Reports on Geodesy*, No. 4 (49), Warsaw, 56-60.

Schenková, Z. and Kárník, V., 1978. The Third Asymptotic Distribution of Largest Magnitudes in the Balkan Earthquake Provinces. *PAGEOPH*, 116, 1314-1325.

Shanov, S., 2005. Post-Cretaceous to recent stress fields in the SE Moesian Platform (Bulgaria). *Tectonophysics*, 410, 217-233.

Shebalin N. V., Kárník, V. and Hadzvieski, D., (editors), 1974a. *Atlas of Isoseismal Maps*, UNDP/UNESCO Survey of the Seismicity of the Balkan Region. Skopje.

Shebalin, N. V., Kárník, V., Hadzievski, D., (editors), 1974b. *Catalogue of earthquakes, part 1, 1901- 1970*, UNDP/UNESCO Survey of the Seismicity of the Balkan Region. Skopje, 600 pp.

Shebalin, N. V., Leydecker, G., Mokrushina, N. G., Tatevossian, R. E., Erteleva, O. O. and Vassilev, V. Yu., 1998. *Earthquake Catalogue for Central and Southeastern Europe 342BC-1990AD*. Final report to contract ETNU-CT93-0087, 195 pp.

Sieberg, A., (editor) 1932a. Erdbebengeogrphie, "Outtenbergs Handbuch der Geophysik, Berlin", 4. [Not seen]

Sieberg, Al., 1932b. Untersuchungen uber erdbeben und bruchshollenbau imostlichen Mittelmeergebiet, "*Denkschr. Med. Naturw. Ges. Jena*", 18, 161-273. [Not seen]

Simeonova, S. D., Solakov, D. E., Leydecker, G., Busche, H., Schmitt, T. and Kaiser, D., 2006. Probabilistic seismic hazard map for Bulgaria as a basis for a new building code. *Nat. Hazards Earth Syst. Sci*., 6, 881-887.

Slavov, S., Paskaleva, I., Kouteva, M., Vaccari, F. And Panza, G. F., 2004. Deterministic Earthquake Scenarios for the City of Sofia. *Pure Appl. Geophys*, 161, 1221–1237.

Sledzinski, J., (editor), 2000. Reports on Geodesy. Warsaw University of Technology, Warsaw, Poland, 4, 49 pp. [Not seen]

Sokerova, D., Simeonova, S., Nikolova, S., Solakov, D. and Botev, E., 1992. *Geomorphology and Geology, Seismicity and Seismotectonics of the NPP "Kozloduy*". Final summary report. Publ. Geophys. Inst., 40 pp. [Not seen]

Solakov, D., Simeonova, S. and Christoskov, L., 2001. Seismic hazard assessment for the Sofia area. *Annali di Geophysics*, 44, 3, 541-555.

Stanishkova, I. and Slejko. D., 1991. Some seismotectonic characteristics of Bulgaria. *Boll. Geof. Teor. Appl.*, 33, 187-210.

Stepp, J. C., 1973. Analysis of completeness of the earthquake sample in the Puget Sound area. In Harding, S. T., editor, 1973, Contributions to seismic zoning: U.S. National Oceanic and Atmospheric Administration Technical Report ERL 267-ESL 30, 16-28.

Stille, H., 1924. *Grundfragen der vergleichenden Tektonik*. Berlin, 443 S. 9 [Not seen]

Stille, H., 1928. Über Europäisch-Zentralasiatische Gebirgszusammenhänge., *Nachr. Ges. Wiss. Göttingen, Math.phys*. K1. [Not seen]

Suess, Ed., 1885. *Das Antilitz der Erde*. I. 778 pp. [Not seen]

Tassos, S. T., 1984. *Static and dynamic properties of the upper mantle at the southern Aegean area*. PhD Thesis, Univ. of Thessaloniki, 155 pp. [Not seen]

Tesauro, M., Hollenstein. C., Egli, R., Geiger, A. and Kahle, H-G., 2006. Analysis of central western Europe deformation using GPS and seismic data. *Journal of Geodynamics*, 42, 194-206.

Thatcher, W. and Hanks, T. C., 1973. Source parameters of southern California earthquakes. *J. Geophys. Res*., 78, 8547-8576. [Not seen]

Theodulidis, N. P., 1991. *Contribution to the study of strong motion in Greece*. Ph.D. Thesis, Univ. Thessaloniki, 500 pp. [Not seen]

Theodulidis, N. P. and Papazachos, B. C., 1992. Dependence of strong ground motion on magnitude-distance, site geology and macroseismic intensity for shallow earthquakes in Greece: I, Peak horizontal acceleration, velocity and displacement. *Soil Dynamics and Earthquake Engineering*, 11, 387-402.

Toteva, T., Rizhikova, S. and Ranguelov, B., 2000. Recent seismicity in Kresna region and surroundings. In. *Reports on Geodesy*, No. 4 (49), Warsaw, 90-98.

Tranos, M. D., Papadimitriou, E. E. and Kilias, A. A., 2003. Thessaloniki–Gerakarou Fault Zone (TGFZ): the western extension of the 1978 Thessaloniki earthquake fault (Northern Greece) and seismic hazard assessment. *Journal of Structural Geology*, 25, 2109–2123.

Trifu, C. I. and Radulian, M., 1991. Depth-magnitude catalogue of Vrancea intermediate depth microearthquakes. *Rev. Roum. Geophys*., 35, 31-45.

Trifunac, M. D. and Brady, A. G., 1975. On the correlation of seismic intensity scales with the peaks of recorded strong motion, *Bull. Seism. Soc. Am*., 65, 139-162.

Tsapanos, T. M., 1998. Seismic hazard for some regions of the world examined using strain energy release. *Jour. Balkan. Geophys. Soc*., 1, 2, 19-24.

Tsapanos, T. M. and Burton, P. W., 1991. Seismic hazard evaluation for specific seismic regions of the world. *Tectonophysics*, 194, 153-169.

Tzankov, Tz., Angelova, D., Nakov, R., Burchfiel, B. C. and Royden, L. H., 1996. The Sub-Balkan graben system of central Bulgaria. *Basin Research*, 8, 125-142.

Utsu, T., 1966. A Statistical Significance Test of the Difference on b-value between Two Earthquake Groups. *Jour. Phys. Ear*., 14, 2, 37-40.

Utsu, T., 1971. Aftershocks and Earthquake Statistics (III) – Analysis of the distribution of Earthquake in Magnitude, Time and Space with Special Consideration to Clustering Characteristics of Earthquake Occurrence (1). *Jour. Faculty of Science, Hokkaido University. Series VII (Geophysics)*, 3, 5379-394.

van Eck, T. and Stoyanov, T., 1996. Seismotectonics and seismic hazard modelling for Southern Bulgaria. *Tectonophysics*, 262, 77-100.

Vanneste, K., Radulov, A., De Martini, P., Nikolov, G., Petermans, T., Verbeeck, K., Camelbeeck, T., Pantoti, D, Dimitrov, D. and Shanov, S., 2006. Paleoseismologic investigation of the fault rupture of the 14 April 1928 Chirpan earthquake (M6.8) southern Bulgaria. *Jour. Geophys. Res*., 111, 16 p.

Vere-Jones, D., 1970. Stochastic Models for Earthquake Occurrence. *Journal of Royal Statistical Society*, Series B, 32, 1-62.

Voutkov, V., Chanov, St. and Demirev, A. 1986. Evaluation de l'intensitié et de l'accélération maximale en zones séismiques. *Geologia Applicata ed Idrogeologia*, 21, 1, 13-22. [Not seen]

Wald, D. J., Quitoriano, V., Heaton, T. H., Kanamori, H., Scrivner, C. W. and Worden, C. B., 1999a. TriNet "ShakeMaps": Rapid Generation of Peak Ground Motion and Intensity Maps for Earthquakes in Southern California. *Earthquake Spectra,* 15, 3, 537-555

Wald, D. J., Quitoriano, V., Heaton, T. H. and Kanamori, H., 1999b. Relationships between Peak Ground Acceleration, Peak Ground Velocity, and Modified Mercalli Intensity in California. *Earthquake Spectra*, 15, 3, 557-564.

Wells, D. L. and Coppersmith, K. J., 1994. New Empirical Relationships among Magnitude, Rupture Length, Rupture Width, Rupture Area, and Surface Displacement. *Bull. Seism. Soc. Am*., 84, 4, 974-1002.

Wiggins, J. H., 1964. Construction of strong motion response spectra from magnitude and distance data. *Bull. Seism. Soc. Am*., 54, 1257-1269. [Not seen]

Willemann, R. J., 1999. Regional Thresholds of the ISC Bulletin. *Seismological Research Letters*, 70, 3, 313-321.

Willmore, P. L. (Ed.), 1979. Manual of Seismological Observatory Practice. World Data Center A for Solid Earth Geophysics, Report SE-20, September 1979, Boulder, Colorado, 165 pp. [Not seen]

Wilser, J., 1928. Die stratigraphische und tektonische Stellung der Dobrudscha und ihre Zugehörigkeit des Balkangebirges und zu den Nordanatolischen Ketten. *Geol. Rdsch.*, 19. [Not seen]

Wu, Y-M., Teng, T-L., Shin, T-C., and Hsiao, N-C., 2003. Relationship between Peak Ground Acceleration, Peak Ground Velocity, and Intensity in Taiwan. *Bull. Seism. Soc. Am*., 93, 1386-396.

Xu, Y., Burton, P. W. and Tselentis, G.-A., 2003. Regional seismic hazard for Revithoussa, Greece: an earthquake early warning Shield and selection of alert signals. *Nat. Hazards Earth Syst. Sci*., 3, 757-776.

Yegulalp, T. M., 1974. Forecasting for largest earthquakes. *Management Science*, 21, 4, 418-421.

Yegulalp, T. M. and Kuo, J. T., 1966. Application of extremal statistics to the maximum magnitude earthquakes (Abstract). *Trans. Am. Geophys. Union*, 47, 163.

Yegulalp, T. M. and Kuo, J. T., 1974. Statistical Prediction of the occurrence of maximum magnitude earthquakes. *Bull. Seism. Soc. Am*., 64, 2, 393-414.

Yilmaztürk, A., 1993. *Seismotectonics and seismic hazard in southern Turkey and the eastern Mediterranean Sea*. PhD Thesis, University of East Anglia, 252 pp.

Yilmaztürk, A. and Burton, P.W., 1999. An evaluation of seismic hazard parameters in southern Turkey. *Journal of Seismology*, 3, 61-81.

Yilmaztürk, A., Bayrak, Y. and Cakir, O., 1998. Crustal Seismicity In and Around Turkey. *Natural Hazards*, 18, 3, 253-266.

York, D., 1969. Least squares fitting of a straight line with correlated errors. *Earth and Planetary Science Letters*, 5, 320-324.

Zagorčhev, I. S., 1992a. Neotectonic of the central parts of the Balkan Peninsula: basic features and concepts. *Geol. Rundsch*., 81, 3, 635-654.

Zagorčhev, I. S., 1992b. Neotectonic development of the Struma (Kraistad) Lineament. South-west Bulgaria and northern Greece. *Geol Mag*., 129, 2, 197-222.

Zagorčhev, I. S., 1994. Structure and tectonic evolution of the Pirin-Pangaion structural zone (Rhodope massif, southern Bulgaria and northern Greece). *Geol Jour*., 29, 2, 241-268.

Other references

Wessel, P. and Smith, W. H. F., The Generic Mapping Tools, http://gmt.soest.hawaii.edu/

Surfer 8, Golden Software Inc., Golden, CO, USA, http://www.goldensoftware.com/products/surfer/surfer.shtml

Grapher 7, Golden Software Inc., Golden, CO, USA, http://www.goldensoftware.com/products/grapher/grapher.shtml

International Seismological Centre, On-line Bulletin, http://www.isc.ac.uk/Bull, Internatl. Seis. Cent., Thatcham, United Kingdom, 2006.

Stability Pact for south eastern Europe Disaster Preparedness and Prevention Initiative: Earthquake Monitoring in Support of Disaster Preparedness in South-Eastern Europe. Project Overview, December 2003.

Geodynamic map of the Mediterranean, http://ccgm.free.fr/mediterra_geodyn_gb.html, *Commission for the Geological Map of the World, http://www.cgmw.net*

Seismicity and large earthquake potential in southwest Bulgaria and the conterminous Balkan high hazard region

A thesis submitted for the degree of
Doctor of Philosophy

Volume 2 of 2

Thomas James Bayliss

School of Environmental Sciences,
University of East Anglia

March 2010

For my Grandfather,

There is no justice in Nature perhaps,
but the idea of justice must be sacred.

H. G. Wells (A Modern Utopia)

Abstract

A new probabilistic seismic hazard assessment is performed across southwest Bulgaria, the Balkans and selected cities. Previous analyses were limited by the age of the study, timeliness of data used, hazard maps typically stopped at political borders, they estimated hazard for a limited range of descriptors, had a different geographic coverage, or differed in the research discipline(s) that they investigated. This assessment uses these limitations as drivers for the work, and aims to mitigate these shortcomings.

A new historical earthquake catalogue is developed for the region's seismicity for moment magnitude 4 and above. This is adopted to illustrate seismic hazard for magnitude recurrence and ground motions in the region bounded by 39°-45°N, 19°-29°E, for return periods of 50, 100 and 200 years, and these time intervals at 90% probability of non-exceedance. Peak ground acceleration and macroseismic intensity are forecast to align with EUROCODE 8. Peak ground velocity is considered as it better represents energy flux between ground and building.

The 475-year return period hazard is estimated for each hazard descriptor, making this study compatible to EUROCODE 8 –with respect to ground acceleration hazard – and comparable to GSHAP and SESAME seismic hazard projects. Analysis is extended to consider *maximum credible magnitude* and *earthquake perceptibility* hazard. The latter combines extreme value distribution statistics with ground motion models to forecast the *most perceptible magnitude*, $M_{P(max)}$, for a range of *scenario* ground motions.

Southwest Bulgaria is dominated by the Serbomacedonian massif and Krupnik fault, both capable of generating large-magnitude earthquakes. It is consistently estimated highest levels of magnitude and ground motion hazard. Bulgaria's capital, Sofia, is estimated a regional upper bound magnitude of 7.86 M_s (±0.75) using an extreme value statistical model, compared with a *maximum credible magnitude* of 7.76 M_s using a cumulative strain energy release model. Importantly, the former model is asymptotic, relating the upper bound magnitude to an infinite waiting time; the latter reconciles a finite time for strain energy to accumulate equivalent to the maximum magnitude. The 475-year return period PGA for Sofia (from the lead peak ground acceleration model) is 177 cm s^{-2}.

Appendices

Appendix 1: Hazard nomenclature

A full nomenclature for seismic hazard terms adopted throughout chapters 5 and 6 follows, and covers magnitude and ground motion extreme, cumulative energy release and earthquake perceptibility hazard, as well as ground motion attenuation models adopted.

Cumulative frequency-magnitude hazard (*whole process*)

M_1	The annual modal magnitude derived from Gutenberg-Richter's cumulative frequency-magnitude distribution. Comparable to m(1) from Gumbel's third extreme values distribution

Extreme hazard (*part process*)

M_{25}, M_{50}, M_{100}, M_{200} A_{25}, A_{50}, A_{100}, A_{200} V_{25}, V_{50}, V_{100}, V_{200} I_{25}, I_{50}, I_{100}, I_{200}	The modal earthquake magnitude/acceleration/velocity/intensity expected within 25, 50, 100, 200 years
$\sigma_{M,}$ $\sigma_{A,}$ $\sigma_{V,}$ σ_I	The standard deviation [uncertainty] on the modal earthquake magnitude/acceleration/velocity/intensity expected within 25/50/100/200 years
M_{P25}, M_{P50}, M_{P100}, M_{P200} A_{P25}, A_{P50}, A_{P100}, A_{P200} V_{P25}, V_{P50}, V_{P100}, V_{P200} I_{P25}, I_{P50}, I_{P100}, I_{P200}	The modal earthquake magnitude/acceleration/velocity/intensity expected within 25, 50, 100, 200 years at 90% probability of not being exceeded
$\sigma_{MP,}$ σ_{IP}	The standard deviation [uncertainty] on the modal earthquake magnitude/intensity expected within 25/50/100/200 years at 90% probability of not being exceeded
m(1)	The annual modal magnitude derived from Gumbel's third extreme values distribution. Comparable to M_1 of cumulative energy release statistics
ω	The upper bound magnitude to Gumbel's third extreme values distribution
μ	The characteristic extreme magnitude to Gumbel's third extreme values distribution
λ	The curvature parameter to Gumbel's third extreme values distribution
$\sigma_{\omega,}$ $\sigma_{\mu,}$ σ_{λ}	Standard deviations of (ω,μ, λ)
T_{ave}	The average return period for *T*-year events
X^2	Chisq

Cumulative strain energy release techniques

M_2	The magnitude equivalent to the annual mean energy release for a region
M_3	The *maximum credible magnitude* earthquake for a region. Equivalent to all the strain energy released instantaneously in a single earthquake
T_W	*Waiting time.* Time necessary for strain energy to accumulative in a region equivalent to its *maximum credible magnitude*, M_3
DT	*Delay time*. Time estimated to wait for an earthquake of magnitude less than or equal to the *maximum credible magnitude*, M_3

Earthquake perceptibility

$M_{P(max)}$	The *most perceptible magnitude* (generic)
P_P	Peak probability attached to the *most perceptible magnitude* (generic)
P_{iP}	Integrated probability attached to the *most perceptible magnitude* (generic)
$M_{PA(50)}$, $M_{PA(100)}$, $M_{PA(150)}$	The [site-specific] *most perceptible magnitude* at horizontal ground accelerations of 50, 100 and 150 cm s^{-2} respectively (regardless of the model adopted)
$M_{PV(5)}$, $M_{PV(10)}$, $M_{PV(15)}$	The [site-specific] *most perceptible magnitude* at horizontal ground velocities of 5, 10 and 15 cm s^{-1} respectively (regardless of the model adopted)
$M_{PI(VI)}$, $M_{PI(VII)}$, $M_{PI(VIII)}$	The [site-specific] *most perceptible magnitude* at intensities of VI, VII and VII respectively (regardless of the model adopted)
$P_{PA(50)}$, $P_{PA(100)}$, $P_{PA(150)}$	The [site-specific] peak probability attached to the *most perceptible magnitude* at horizontal ground accelerations of 50, 100 and 150 cm s^{-2} respectively (regardless of the model adopted)
$P_{PV(5)}$, $P_{PV(10)}$, $P_{PV(15)}$	The [site-specific] peak probability attached to the *most perceptible magnitude* at horizontal ground velocities of 5, 10 and 15 cm s^{-1} respectively (regardless of the model adopted)
$P_{PI(VI)}$, $P_{PI(VII)}$, $P_{PI(VIII)}$	The [site-specific] peak probability attached to the *most perceptible magnitude* at intensities of VI, VII and VII respectively (regardless of the model adopted)
$P_{ipA(50)}$, $P_{ipA(100)}$, $P_{ipA(150)}$	The [site-specific] integrated probability attached to the *most perceptible magnitude* at horizontal ground accelerations of 50, 100 and 150 cm s^{-2} respectively (regardless of the model adopted)
$P_{ipV(5)}$, $P_{ipV(10)}$, $P_{ipV(15)}$	The [site-specific] integrated probability attached to the *most perceptible magnitude* at horizontal ground velocities of 5, 10 and 15 cm s^{-1} respectively (regardless of the model adopted)
$P_{ipI(VI)}$, $P_{ipI(VII)}$, $P_{ipI(VIII)}$	The [site-specific] integrated probability attached to the *most perceptible magnitude* at intensities of VI, VII and VII respectively (regardless of the model adopted)

Ground motion models

$TP92_A$	Horizontal peak ground accelerations estimated using Theodulidis and Papazachos (1992) for stiff soil conditions (S = 0.5) at the 50^{th} percentile (P = 0)
AM95_WDC	Horizontal peak ground accelerations estimated using Ambraseys (1995) with depth control at the 50^{th} percentile (P = 0) for rock sites
AM05	Horizontal peak ground accelerations estimated using Ambraseys *et al.* (2005) for stiff soil conditions (S_A = 1) and normal faulting mechanisms (F_N = 1)
$TP92_V$	Horizontal peak ground velocities estimated using Theodulidis and Papazachos (1992) for stiff soil conditions (S = 0.5) at the 50^{th} percentile (P = 0)
PP97	Macroseismic intensity estimated using Papazachos and Papaioannou (1997) with epicentral intensity relation for Bulgaria

Other

M_A	Annual maximum magnitude
M_c	Completeness threshold. Magnitude above which an earthquake dataset is considered complete (with respect to magnitude). Notionally related to *whole process* distributions
M_{CUT}	Cut-off magnitude. Lower magnitude at which an earthquake dataset is truncated to allow particular analysis to occur. Data below M_{CUT} is ignored in analysis. M_{CUT} may not equal M_c. Notionally related to *part process* distributions
M_M	Maximum reported [homogenized and catalogued] magnitude in region or area considered. In tables provided of hazard estimates, this will typically be the [homgenized] surface wave magnitude for the earthquake in question

Appendix 2: Gumbel's theory of extreme values

The statistical environment

Suppose one has a parent distribution of earthquake events, out of which is drawn a distributed subset containing only the largest instances of the parent distribution. Each extreme will be independent, and this derived subset of independent extremes is called the extreme values distribution. *Y* will be taken as the largest earthquake event in any given year, thus:

$$Y = \max (m_1, m_2, m_3, m_4, ..., m_N) \quad \text{(A2-1)}$$

With m_i forming a sequence of annual maximum earthquakes drawn randomly from the cumulative distribution F(m), the probability *Y* is the largest amongst *N* independent samples is:

$$\begin{aligned} \phi_N(Y) &= P(Y \leq y) \\ &= P(\text{all } m_i \leq y) \\ &= P(m_1 \leq y, m_2 \leq y, m_3 \leq y, ..., m_N \leq y) \end{aligned} \quad \text{(A2-2)}$$

As m_i are independent events, the probability of the largest event can be written using the multiplication rule as:

$$\begin{aligned} \phi_N(Y) &= P(Y \leq y) \\ &= P(m_1 \leq y)\, P(m_2 \leq y)\, P(m_3 \leq y) ... \, P(m_N \leq y) \\ &= Fm_1(y)\, Fm_2(y)\, Fm_3(y) ... \, Fm_N(y) \\ &= F_M^N(y) \end{aligned} \quad \text{(A2-3)}$$

The probability of a value being equal to or larger than y is:

$$1 - \phi_N(y) \quad \text{(A2-4)}$$

with its reciprocal value (below) providing the return period of *y*. This equates to the average number of intervals necessary for an extreme value greater than or equal to y being experienced.

$$T_N(y) = \frac{1}{1-\varphi_N(y)} \quad \text{(A2-5)}$$

When data is scarce, it may be necessary to resort to using k-year extremes. In this instance, the distribution $\phi_k(y)$ is related to $\phi_1(y)$ – one-year extreme intervals – by:

$$\varphi_k(y) = \varphi_1^k(y) \quad \text{(A2-6)}$$

Gumbel's first asymptotic extreme values distribution

Gumbel's first extreme distribution, $G^{(I)}$, is not governed by possessing an upper or lower bound to the data considered. So it is typically best suited to forecasting extremes of acceleration, velocity and displacement seismic hazard. A $G^{(I)}$ distribution takes the form of Eq. (7):

$$G^{(I)}(x) = \exp[-\exp(-\alpha(x-\mu))] \qquad \alpha > 0 \quad \text{(A2-7)}$$

Where x is the earthquake under consideration, α is the extremal intensity function, μ is the characteristic largest value such that $\phi^{(I)}(\mu) = 1/e$, and is also the mode of the largest values.

By replacing $G^{(I)}(x)$ with P and x with GM_P, the peak ground motion expected to be an annual maximum with probability P, in Eq. (A2-7), we get Eq. (A2-8):

$$GM_P = \mu - \frac{\ln(-\ln P)}{\alpha} \quad \text{(A2-8)}$$

Thus, the peak ground motion, GM_{PT}, which has probability P of not being exceeded in T years is:

$$GM_{PT} = \mu - \frac{\ln(-\ln P)}{\alpha} + \frac{\ln T}{\alpha} = a_P + \frac{\ln T}{\alpha} \quad \text{(A2-9)}$$

Gumbel's third asymptotic extreme values distribution

Gumbel's third extreme distribution, $G^{(III)}$, is more suited to modelling earthquake variate that are, or can be statistically bounded by an upper threshold. Earthquake magnitude and macroseismic intensity are examples of this, as the former is accepted to have an upper limit to it constrained by a

region's finite limit to strain rate accumulation, and the latter is a scale developed with a highest value in mind. Equation (10) gives Gumbel's third asymptotic distribution:

$$G^{(III)}(x) = \left[-\left(\frac{\omega-\mu}{\omega-x}\right)^{k}\right] \qquad k > 0,\ x \leq \omega,\ \mu < \omega \qquad \text{(A2-10)}$$

where $G^{(III)}(x)$ is the cumulative probability of the variate less than or equal to x; x takes on the same meaning as for the first distribution, by representing the variate considered. In the case of a $G^{(III)}(x)$ distribution though, x is typically magnitude or some other bounded descriptor, thus $G^{(III)}(x)$ becomes $G^{(III)}(m)$. k is a function of the curvature parameter, where $k = 1/\lambda$. μ is the characteristic largest value, and ω is the limiting upper bound value with,

$$\phi^{(III)}(\omega) = 1 \qquad \text{(A2-11)}$$

When *m* tends to its upper limit ω, the function $G^{(III)}(m) \rightarrow 1$, whereas when *m* decreases, $G^{(III)}(m) \rightarrow 0$. μ is the characteristic largest value and also being the mode of the largest values, such that:

$$\phi^{(I)}(\mu) = 1/e \qquad \text{(A2-12)}$$

Replacing *x* with *m* to denote magnitude as the chosen variate, the average return period in years, $T(m)$, for a magnitude *m* earthquake is:

$$T(m) = 1/(1\text{-}P(m)) \qquad \text{(A2-13)}$$

whilst the modal maximum, m(1), where 1 denotes the annual statistic – satisfying $d^2P/dm^2 = 0$ is:

$$m(1) = \omega - (\omega - \mu)(1 - \lambda)^{\lambda} \qquad \text{(A2-14)}$$

The *T*-year modal maximum earthquake magnitude is:

$$m(T) = \omega - (\omega - \mu)[((1 - \lambda)/T)]^{\lambda} \qquad \text{(A2-15)}$$

The magnitude with probability *P* of being a maximum or not being exceeded in next *T* years is:

$$m_P(T) = \omega - (\omega - \mu)[(-\ln P)/T)]^{\lambda} \quad \text{(A2-16)}$$

with a magnitude error:

$$\sigma_m^2 = \sigma_\omega^2\left(\frac{\partial M}{\partial \omega}\right)^2 + \sigma_\mu^2\left(\frac{\partial M}{\partial \mu}\right)^2 + \sigma_\lambda^2\left(\frac{\partial M}{\partial \lambda}\right)^2 + 2\sigma_{\omega\mu}^2\left(\frac{\partial M}{\partial \omega}\right)\left(\frac{\partial M}{\partial \mu}\right) + ... \quad \text{(A2-17)}$$

With a corresponding average return period of *T*' years:

$$T_{ave} = 1/(1\text{-}P^{1/T}) \quad \text{(A2-18)}$$

Uncertainties amongst the three parameters of the distribution (ω, μ, λ) are easily defined in the covariance error matrix, ε:

$$\varepsilon = \begin{bmatrix} \sigma_\omega^2 & \sigma_{\omega\mu}^2 & \sigma_{\lambda\omega}^2 \\ \sigma_{\omega\mu}^2 & \sigma_\mu^2 & \sigma_{\lambda\mu}^2 \\ \sigma_{\omega\lambda}^2 & \sigma_{\mu\lambda}^2 & \sigma_\lambda^2 \end{bmatrix} \quad \text{with } \sigma_\omega^2 \text{ being the variance on } \omega \text{ etc.} \quad \text{(A2-19)}$$

such that the partial derivatives are given by:

$$\frac{\partial m}{\partial \omega} = 1 - (-\ln P)^{\lambda} \quad \text{(A2-20)}$$

$$\frac{\partial m}{\partial \mu} = (-\ln P)^{\lambda} \quad \text{(A2-21)}$$

$$\frac{\partial m}{\partial \lambda} = -\left[(\omega - \mu)(-\ln P)^{\lambda}\ln(-\ln P)\right] \quad \text{(A2-22)}$$

Finally, Gumbel's first and third asymptotic distributions are related by:

$$\phi^{(I)}(\mu) = \phi^{(III)}(\mu) = \frac{1}{e} \quad \text{(A2-23)}$$

such that approximately 36% of the observations in all cases should be situated before the value $x = \mu$ (where x is the variate modelled by the extreme distribution).

Appendix 3: Earthquake catalogue (dimensions and listing)

Creation	July 2006	
Time interval	1900 to 2004 (inclusive)	
Geographical limits	39.0° - 45.0°N, 19.0° - 29.0°E	
Number of events	3,681	
Depth range	0.0 $\rightarrow$ 401.0 km	
M_w magnitude range	$4.0 \leq M_w \leq 7.2$	
M_s magnitude range	$2.4 \leq M_s \leq 7.6$	
Fields provided and format	**Fieldname**	**Field Format**
	Year	(F4.0)
	Month	(F3.0)
	Date	(F3.0)
	Hour	(F4.0)
	Minute	(F3.0)
	Second	(F7.2)
	Latitude	(F8.2)
	Longitude	(F8.2)
	Depth	(F7.1)
	Homogenized M_w	(F8.1)
	Homogenized M_s	(F8.1)
	Reported m_b	(F8.1)
	Reported M_s	(F8.1)
	Reported M_w	(F8.1)
	Reported M_L	(F8.1)

Note. The first column in the catalogue listing – Event Number – is not provided in the electronic version of the listing. It is provided here for reference.

										Homogenized magnitudes		Reported magnitudes			
Event Number	Year	Month	Date	Hour	Minute	Second	Latitude	Longitude	Depth	M_w	M_s	mb	M_s	M_w	ML
1	1900	1	14	9	53	0	43.5	27	45	4.5	4.5		4.5		
2	1900	2	0	0	0	0	40.9	26.9	20	5.1	4.3		4.3		
3	1900	6	14	1	0	0	42.1	19.6	20	5.5	5		5		
4	1900	10	26	15	45	0	43.7	27.5	70	5.9	5.9		5.9		
5	1901	3	31	7	10	24	43.5	28.7	14	7.2	7.2		7.2		
6	1901	3	31	11	30	0	43.6	27.8	32	5.1	5.1		5.1		
7	1901	4	25	22	25	0	43.4	28.5	18	5.2	5.2		5.2		
8	1901	4	26	1	10	0	43.3	27.5	20	4.9	4.9		4.9		
9	1901	7	6	23	28	0	43.4	28.3	10	5	5		5		
10	1901	7	30	3	30	0	43.4	28.7	14	5.8	5.8		5.8		
11	1901	8	18	7	44	0	44.2	20.7	5	4.6	4.6		4.6		
12	1901	8	29	7	29	36	44	21.3	8	4.3	4.3		4.3		
13	1901	10	27	20	10	42	44	19.5	10	4.9	4.9		4.9		
14	1902	1	29	16	58	0	42.6	21.9	5	4.7	3.7		3.7		
15	1902	1	30	1	0	0	42.5	21.8	7	4.5	3.3		3.3		
16	1902	5	2	19	0	0	43.5	28.5	18	4.8	4.8		4.8		
17	1902	5	25	22	30	0	43.5	28.5	10	4.2	4.2		4.2		
18	1902	6	26	20	45	0	42.2	23.6	5	5	4.2		4.2		
19	1902	11	18	22	6	0	42.2	23.1	10	4.6	3.5		3.5		
20	1903	4	2	6	50	0	43.5	28.5	20	4.7	4.7		4.7		
21	1903	7	27	17	10	0	42.2	22.5	5	4.6	3.5		3.5		
22	1903	11	25	23	16	42	42.13	23.1	10	5.6	5.4		5.4		
23	1903	11	27	15	13	0	42.1	23.2	14	5.3	4.8		4.8		
24	1903	11	30	2	34	0	42.1	23.2	12	5.5	5.1		5.1		
25	1903	12	1	13	34	0	42.1	23.4	14	5.3	4.8		4.8		
26	1903	12	5	10	46	0	42.13	23.3	7	4.9	4		4		
27	1903	12	5	12	7	0	42.1	23.4	10	4.6	3.5		3.5		
28	1903	12	5	14	0	0	42.1	23.4	10	4.6	3.5		3.5		
29	1904	1	1	1	48	0	44.9	21.4	25	5	5		5		
30	1904	2	1	1	45	0	41.1	21.7	15	5	4.1		4.1		
31	1904	2	8	6	16	0	43.5	28.5	19	4.8	4.8		4.8		
32	1904	4	4	10	2	34	41.78	22.9	18	6.8	6.9	7.1	6.9	6.8	
33	1904	4	4	10	5	0	41.8	23.1	20	5.5	5		5		
34	1904	4	4	10	6	0	41.8	23.1	20	5.7	5.5		5.5		
35	1904	4	4	10	7	0	41.8	23.1	20	5.5	5		5		
36	1904	4	4	10	9	0	41.8	23.2	20	5.7	5.5		5.5		
37	1904	4	4	10	11	0	41.8	23.1	20	5.5	5		5		
38	1904	4	4	10	13	0	42.1	23.4	6	5.4	4.9		4.9		
39	1904	4	4	10	19	0	41.8	23.2	20	5.7	5.5		5.5		
40	1904	4	4	10	25	55	41.8	23.1	24	7.1	7.2	7.8	7.2		
41	1904	4	4	10	30	0	42.1	23.4	28	5.9	5.7		5.7		
42	1904	4	4	10	39	0	42.1	23.4	29	5.8	5.6		5.6		
43	1904	4	4	10	49	0	41.8	23.2	13	5.5	5		5		
44	1904	4	4	10	54	0	41.8	23.1	20	5.6	5.2		5.2		
45	1904	4	4	11	4	0	42.1	23.4	17	5.3	4.8		4.8		
46	1904	4	4	11	9	0	42	23	39	5.7	5.5		5.5		
47	1904	4	4	12	49	0	41.8	23.1	20	5.8	5.6		5.6		
48	1904	4	5	5	19	0	41.8	23.2	8	5	4.2		4.2		
49	1904	4	9	5	35	0	42.2	23.7	26	5.1	4.3		4.3		
50	1904	4	10	2	24	0	42	23.5	30	5.7	5.5		5.5		
51	1904	4	10	8	52	46	42.8	22.7	27	6.5	6.5		6.5		
52	1904	4	11	0	50	0	42.5	21.8	12	5	4.2		4.2		
53	1904	4	11	4	18	0	42.8	22.8	24	5.6	5.2		5.2		
54	1904	4	13	9	55	0	42	23.1	41	5.7	5.5		5.5		
55	1904	4	13	21	30	0	42	21.4	10	4.6	3.5		3.5		
56	1904	4	15	11	41	0	41.8	23.2	10	4.6	3.5		3.5		
57	1904	4	19	18	14	0	42	23.1	14	5.9	5.8		5.8		
58	1904	4	20	1	32	0	42.5	22.3	17	5.3	4.7		4.7		
59	1904	4	21	13	0	0	42.1	23.2	25	5.9	5.8		5.8		
60	1904	4	25	20	2	0	42	23	30	5.7	5.5		5.5		
61	1904	5	7	23	44	0	41.8	23.1	20	5.5	5		5		
62	1904	5	8	17	57	0	41.8	23.1	20	5.5	5		5		
63	1904	5	12	17	14	0	41.8	23.1	20	5.5	5		5		
64	1904	5	16	1	58	0	44.45	19.1	8	4.2	4.2		4.2		
65	1904	6	6	14	25	0	44.1	27.3	36	5.2	5.2		5.2		
66	1904	6	10	17	38	54	42.2	23.1	13	5	4.1		4.1		
67	1904	6	21	13	10	0	41.7	23.3	28	5.8	5.6		5.6		
68	1904	6	28	2	15	0	41.65	24.7	30	5.5	5		5		
69	1904	7	1	22	14	0	42.1	23.2	4	4.8	3.9		3.9		
70	1904	7	24	6	33	0	42.2	23	17	5.3	4.7		4.7		
71	1904	8	1	7	30	0	42.1	23.2	28	5.5	5		5		
72	1904	8	4	8	39	0	42.6	21.9	5	4.8	3.8		3.8		
73	1904	8	9	6	22	0	42.1	23.4	5	4.6	3.4		3.4		
74	1904	10	11	18	55	0	43.6	20.8	17	4.2	4.2		4.2		
75	1904	10	29	16	12	30	41.9	23.2	28	5.5	5		5		
76	1905	1	5	18	22	36	44.5	19.3	9	4	4		4		
77	1905	1	6	3	34	6	44.44	19.3	11	5.2	5.2		5.2		
78	1905	1	16	4	49	18	44.37	19.4	7	4.7	4.7		4.7		
79	1905	1	17	15	8	0	42.1	23.4	17	5.1	4.3		4.3		
80	1905	2	2	22	45	0	42.2	23	24	5.3	4.7		4.7		
81	1905	2	28	9	12	0	42.3	23.4	5	4.6	3.4		3.4		
82	1905	4	4	10	24	48	41	21	27	5.5	5.3		5.3		

										Homogenized magnitudes		Reported magnitudes			
Event Number	Year	Month	Date	Hour	Minute	Second	Latitude	Longitude	Depth	M_w	M_s	mb	M_s	M_w	ML
83	1905	4	4	11	0	30	41	21	20	5.2	4.5		4.5		
84	1905	4	9	19	47	0	42.3	23.6	5	4.6	3.5		3.5		
85	1905	5	13	4	36	35	43.67	21.7	4	4.2	4.2		4.2		
86	1905	5	22	20	0	0	42.1	23.4	5	4.4	3.1		3.1		
87	1905	5	31	0	27	12	41.8	24	20	5.2	4.5		4.5		
88	1905	6	1	4	42	15	42.03	19.5	15	6.6	6.6		6.6		
89	1905	6	1	5	1	0	42	19.5	10	5	4.2		4.2		
90	1905	6	1	5	3	0	42	19.5	10	5	4.2		4.2		
91	1905	6	1	5	40	0	42	19.5	10	5	4.2		4.2		
92	1905	6	1	9	30	0	42	19.5	10	5.3	4.7		4.7		
93	1905	6	1	14	47	25	42	19.5	12	5.4	4.9		4.9		
94	1905	6	1	21	46	48	42.3	19.2	19	5.7	5.5		5.5		
95	1905	6	3	5	10	43	42.06	19.6	10	5.7	5.5		5.5		
96	1905	6	3	23	56	0	42.1	19.6	20	5	4.1		4.1		
97	1905	6	5	11	9	0	42.1	19.6	20	5.3	4.8		4.8		
98	1905	6	6	2	55	0	42.1	19.6	20	5.2	4.6		4.6		
99	1905	6	9	23	36	0	42.1	19.6	20	5.2	4.6		4.6		
100	1905	6	16	12	21	6	41.8	24.5	20	5	4.2		4.2		
101	1905	6	16	12	35	0	42.1	19.6	10	5.3	4.7		4.7		
102	1905	6	30	11	53	0	42.1	19.6	10	5.3	4.7		4.7		
103	1905	6	30	23	55	0	42.1	19.6	10	5.2	4.5		4.5		
104	1905	7	2	4	55	0	42.1	19.6	10	5	4.2		4.2		
105	1905	7	9	23	10	0	42	24.2	30	5.4	4.9		4.9		
106	1905	7	13	13	2	0	42.1	19.6	17	5.3	4.8		4.8		
107	1905	7	16	10	18	0	42.12	26.3	3	4.1	2.5		2.5		
108	1905	7	16	12	21	4	42.01	19.7	19	5.6	5.2		5.2		
109	1905	7	19	7	30	0	42.1	19.6	10	5	4.2		4.2		
110	1905	7	21	0	35	0	42.1	19.6	10	5	4.2		4.2		
111	1905	7	21	22	10	0	42.1	19.6	10	4.8	3.9		3.9		
112	1905	7	27	22	40	30	42.1	19.6	14	5.2	4.5		4.5		
113	1905	7	30	11	37	30	44.2	21.2	15	4	4		4		
114	1905	8	3	23	42	12	42.1	19.6	8	4.8	3.9		3.9		
115	1905	8	4	5	9	0	42.1	19.6	12	6.1	6		6		
116	1905	8	4	9	14	0	42.1	19.6	10	4.6	3.5		3.5		
117	1905	8	4	18	34	0	42.1	19.6	10	4.6	3.5		3.5		
118	1905	8	6	23	55	45	42.02	19.5	22	5.7	5.5		5.5		
119	1905	8	12	21	26	56	42.01	19.6	18	5.5	5.3		5.3		
120	1905	9	1	1	22	0	42.5	22.5	20	5.1	4.3		4.3		
121	1905	9	5	1	22	54	42.1	23.3	19	5.3	4.8		4.8		
122	1905	9	29	8	40	0	41	20.8	20	5.1	4.3		4.3		
123	1905	9	29	17	45	0	41	20.8	20	5.1	4.3		4.3		
124	1905	10	8	7	27	30	41.8	23.1	19	7.1	7.4	6.4			
125	1905	10	8	8	0	0	42.6	21.9	9	5.2	4.6		4.6		
126	1905	10	20	14	10	0	43.53	28.5	10	4.5	4.5		4.5		
127	1905	10	22	11	9	0	43	23.5	25	4.9	4		4		
128	1905	10	23	2	38	36	41.4	24	21	5.3	4.8		4.8		
129	1905	10	24	4	37	0	42.2	21.8	20	5.6	5.2		5.2		
130	1906	1	8	21	15	0	42.03	24	9	4.7	3.6		3.6		
131	1906	1	13	22	15	0	42.37	25.9	16	5	4.2		4.2		
132	1906	3	1	17	45	0	41.1	20.1	20	6.4	6.4		6.4		
133	1906	3	3	21	56	0	41	20	8	5.6	5.2		5.2		
134	1906	3	30	14	28	0	44.2	21.3	15	4.5	4.5		4.5		
135	1906	4	16	9	48	0	41.7	25.3	20	5.3	4.8		4.8		
136	1906	4	21	9	15	0	40.8	20.7	10	5.1	4.4		4.4		
137	1906	4	23	6	53	0	41.8	23.2	16	5.5	5.1		5.1		
138	1906	4	23	10	30	0	41.7	20.8	5	4.2	2.8		2.8		
139	1906	6	23	6	52	24	42.1	23.4	13	5.2	4.6		4.6		
140	1906	7	2	19	22	0	42.38	23.4	5	4.3	2.9		2.9		
141	1906	7	25	11	45	30	44.4	19.3	8	4.7	4.7		4.7		
142	1906	7	25	11	56	0	44.5	19.3	10	4.2	4.2		4.2		
143	1906	8	28	1	21	12	44.5	19.5	14	4	4		4		
144	1906	9	2	0	55	0	43.9	20.2	6	4	4		4		
145	1906	9	17	15	0	0	41.1	20.1	10	4.8	3.9		3.9		
146	1906	9	28	2	30	0	40.9	20.6	16	6.3	6.2		6.2		
147	1906	9	29	8	20	0	40.9	20.7	20	5.5	5		5		
148	1906	9	30	0	0	0	40.9	20.7	20	5.5	5		5		
149	1906	11	17	15	0	0	41.1	20.1	5	4.6	3.4		3.4		
150	1906	11	19	0	31	0	45	19.6	14	4.1	4.1		4.1		
151	1906	11	29	8	40	0	41	20.8	10	4.8	3.9		3.9		
152	1907	1	5	11	28	0	42.1	23.4	17	5.2	4.5		4.5		
153	1907	1	22	2	40	0	41	28	23	5.2	4.5		4.5		
154	1907	1	25	0	27	0	43.5	20.8	17	4.3	4.3		4.3		
155	1907	2	2	3	38	0	42.7	23.3	7	4.5	3.2		3.2		
156	1907	4	5	18	22	0	42.12	21.6	9	4.6	3.5		3.5		
157	1907	4	9	5	35	0	42.38	24	22	5.2	4.6		4.6		
158	1907	5	4	23	30	0	41.3	19.5	13	5.3	4.8		4.8		
159	1907	5	5	0	30	0	41.3	19.5	20	5.5	5		5		
160	1907	5	5	17	48	54	42.5	21.8	10	5	4.2		4.2		
161	1907	6	10	14	33	0	43.4	20.8	18	4.4	4.4		4.4		
162	1907	8	12	13	15	0	42.5	21.8	8	4.6	3.4		3.4		
163	1907	8	13	2	18	0	42.85	22.6	17	5.2	4.6		4.6		
164	1907	8	16	13	0	0	41.1	20.1	19	6.3	6.2		6.2		

										Homogenized magnitudes		Reported magnitudes			
Event Number	Year	Month	Date	Hour	Minute	Second	Latitude	Longitude	Depth	M_w	M_s	mb	M_s	M_w	ML
165	1907	8	17	5	10	0	44.1	21.2	15	4.2	4.2		4.2		
166	1907	8	17	11	51	0	41.3	22.5	9	5.3	4.8		4.8		
167	1907	9	17	16	20	0	42.18	25.2	3	4.5	3.3		3.3		
168	1908	1	5	21	49	0	42	19.5	20	5.1	4.3		4.3		
169	1908	6	14	4	23	0	42	23	30	5.2	4.5		4.5		
170	1908	10	23	7	20	0	43.9	21.3	10	4	4		4		
171	1908	10	26	20	36	0	43.4	20.8	10	4.2	4.2		4.2		
172	1908	11	16	20	31	36	41.5	26.5	30	5.2	4.5		4.5		
173	1908	12	25	21	58	0	44.15	19	9	5.3	5.3		5.3		
174	1908	12	27	22	41	0	44.1	19	10	4.7	4.7		4.7		
175	1909	1	20	19	57	0	42	24.5	60	5.2	4.6		4.6		
176	1909	2	14	22	28	0	42.5	26.5	22	5.6	5.2		5.2		
177	1909	2	15	9	34	0	42.54	26.4	11	6	5.9		5.9		
178	1909	2	15	9	41	0	42.2	26.1	52	5.3	4.8		4.8		
179	1909	2	15	14	8	0	42.7	26.3	26	5.3	4.7		4.7		
180	1909	2	15	15	16	0	42.5	26.5	32	5.4	4.9		4.9		
181	1909	2	15	20	0	0	42.5	26.5	29	5.1	4.4		4.4		
182	1909	2	16	0	14	0	42.12	26.4	24	5.3	4.8		4.8		
183	1909	3	1	7	1	0	42.62	26.2	10	4.8	3.8		3.8		
184	1909	3	1	7	13	0	42.53	26.4	22	5.1	4.4		4.4		
185	1909	3	2	20	15	0	42.5	24.3	40	5.2	4.5		4.5		
186	1909	3	7	15	1	0	42.2	24.8	60	5.2	4.5		4.5		
187	1909	3	10	16	36	0	42	23	14	5.2	4.6		4.6		
188	1909	3	10	16	56	0	42	25	50	5.3	4.8		4.8		
189	1909	3	10	22	36	0	42	24.5	42	5.3	4.8		4.8		
190	1909	3	11	0	6	0	42.4	23.3	22	5.2	4.6		4.6		
191	1909	3	11	2	2	0	42.1	24.5	19	5.2	4.5		4.5		
192	1909	3	12	18	59	0	42	25	42	5	4.1		4.1		
193	1909	4	1	0	18	0	42	24	62	5.2	4.6		4.6		
194	1909	4	1	2	4	0	42	24	58	5.2	4.5		4.5		
195	1909	4	15	18	49	0	42	24	45	5	4.2		4.2		
196	1909	4	25	2	34	0	42	24	48	5.1	4.3		4.3		
197	1909	4	27	18	24	0	42.63	23.3	3	4.1	2.5		2.5		
198	1909	5	15	7	35	0	44.2	20.8	15	4.2	4.2		4.2		
199	1909	6	9	1	33	0	42.57	26.3	23	5.3	4.7		4.7		
200	1909	6	19	17	45	54	43	26.5	60	5.6	5.2		5.2		
201	1909	7	6	5	48	0	41.87	24.6	32	5.5	5.1		5.1		
202	1909	9	19	21	53	0	41.9	24.7	52	5.5	5		5		
203	1909	10	10	20	27	0	43.02	28.3	27	4.5	4.5		4.5		
204	1910	1	29	12	5	0	42.53	26.3	8	4.7	3.6		3.6		
205	1910	2	19	19	6	0	42.7	23.2	2	4.7	3.7		3.7		
206	1910	2	20	3	32	0	42.6	23.2	5	4.6	3.5		3.5		
207	1910	2	23	7	52	0	41.8	23.4	14	5.6	5.2		5.2		
208	1910	2	28	1	15	0	42.12	25.3	8	4.6	3.5		3.5		
209	1910	3	10	17	15	0	42.57	26.3	3	4.3	3		3		
210	1910	3	14	6	47	18	43.8	20.4	11	4.1	4.1		4.1		
211	1910	3	22	2	6	24	41.26	21.9	8	5.5	5		5		
212	1910	3	29	16	9	0	42.6	23.3	6	4.9	4		4		
213	1910	4	0	0	0	0	40.15	26.4	20	5.1	4.3		4.3		
214	1910	4	6	1	36	0	42.1	23.2	12	5.2	4.6		4.6		
215	1910	5	15	10	43	0	42.2	24	6	4.3	3		3		
216	1910	5	28	23	25	0	44	20.9	12	4	4		4		
217	1910	10	11	12	53	0	44.9	22.4	11	4.3	4.3		4.3		
218	1910	12	3	8	15	54	44	21.2	8	4.5	4.5		4.5		
219	1910	12	19	4	29	0	42	23.1	11	5.3	4.8		4.8		
220	1910	12	20	4	57	0	41.5	21.4	5	4.6	3.4		3.4		
221	1911	2	18	21	35	15	40.89	20.7	17	6.7	6.7		6.7		
222	1911	2	18	21	38	0	41	20.7	8	5.8	5.6		5.6		
223	1911	2	18	22	59	0	41	20.7	15	5.6	5.2		5.2		
224	1911	2	20	3	45	0	40.9	20.7	15	5.6	5.2		5.2		
225	1911	2	20	15	15	0	41	20.7	6	5.2	4.6		4.6		
226	1911	2	21	13	46	0	42	20	20	5.4	4.9		4.9		
227	1911	2	22	2	8	0	40.9	20.8	20	6	5.9		5.9		
228	1911	2	23	2	57	0	41	20.7	10	5.1	4.4		4.4		
229	1911	2	23	3	59	0	40.9	20.8	10	5	4.2		4.2		
230	1911	2	23	4	12	0	41.5	20.5	10	5.2	4.6		4.6		
231	1911	2	23	11	34	0	40.9	20.8	20	5.6	5.4		5.4		
232	1911	3	5	0	55	0	41	20.7	12	5.1	4.4		4.4		
233	1911	3	5	3	33	0	42.5	22.5	42	5.6	5.4		5.4		
234	1911	3	11	19	15	0	41.6	22.4	30	5.3	4.8		4.8		
235	1911	3	11	20	40	18	42.2	23	52	5.7	5.5		5.5		
236	1911	3	16	3	14	0	41	22	30	5.2	4.5		4.5		
237	1911	3	16	12	8	0	42.55	22.9	6	4.4	3.1		3.1		
238	1911	6	19	15	40	0	42.2	21.7	8	4.7	3.7		3.7		
239	1911	6	21	1	27	0	42	21.4	10	4.6	3.5		3.5		
240	1911	8	20	23	47	0	41	20.8	13	5.3	4.7		4.7		
241	1911	9	8	12	9	15	43.4	28.1	16	4.8	4.8		4.8		
242	1911	9	24	6	5	0	41.5	20.8	16	5.3	4.7		4.7		
243	1912	2	13	8	3	54	40.9	20.6	14	6.1	6		6		
244	1912	2	15	9	30	0	41	20.5	10	5.5	5.1		5.1		
245	1912	2	15	17	30	0	42.57	26.3	2	4.1	2.6		2.6		
246	1912	2	24	14	41	48	41.8	19.6	5	5	4.1		4.1		

										Homogenized magnitudes		Reported magnitudes			
Event Number	Year	Month	Date	Hour	Minute	Second	Latitude	Longitude	Depth	M_w	M_s	mb	M_s	M_w	ML
247	1912	4	1	10	40	0	40.7	20.7	10	5.3	4.7		4.7		
248	1912	5	2	2	30	0	42.5	26.5	5	4.3	2.9		2.9		
249	1912	5	27	2	30	0	42.02	26.4	5	4.3	2.9		2.9		
250	1912	8	9	1	29	0	40.6	27	16	7.1	7.3		7.3		
251	1912	8	10	9	23	0	40.6	27.1	15	6.3	6.3		6.3		
252	1912	8	10	18	30	0	40.6	27.1	15	5.5	5.3		5.3		
253	1912	8	11	7	20	0	40.6	27.1	15	5.3	4.7		4.7		
254	1912	8	11	8	20	0	40.6	27.1	15	5.3	4.7		4.7		
255	1912	9	13	23	31	0	40.5	26.9	18	6.8	6.9		6.9		
256	1912	9	17	1	14	0	42.33	23.5	27	4.9	4		4		
257	1912	10	0	0	0	0	41.67	26.5	5	4.8	3.9		3.9		
258	1912	10	21	9	31	0	40.5	27	24	5.2	4.5		4.5		
259	1912	10	21	23	40	0	40.5	27	18	5.3	4.8		4.8		
260	1912	11	7	19	50	0	41.9	24	18	5.3	4.8		4.8		
261	1913	2	24	11	53	0	41.8	19.6	16	5.3	4.7		4.7		
262	1913	6	14	9	33	0	43.1	25.7	14	6.3	6.3		6.3		
263	1913	6	14	9	37	0	43.1	25.7	18	4.4	4.4		4.4		
264	1913	6	14	9	50	0	42.87	25.5	26	5.3	4.8		4.8		
265	1913	6	14	9	58	0	43.2	25.7	70	5.1	5.1		5.1		
266	1913	6	14	12	5	0	43.08	25.6	54	5.5	5.5		5.5		
267	1913	6	14	12	13	0	43	25.5	20	5.5	5		5		
268	1913	6	18	17	23	0	43.37	26.2	11	4.4	4.4		4.4		
269	1914	2	25	2	21	36	41	22	30	5.1	4.4		4.4		
270	1914	3	3	12	20	54	41.7	23	46	5.3	4.7		4.7		
271	1914	3	7	21	14	48	43.9	20.2	14	4	4		4		
272	1914	3	19	3	20	0	41.5	20.5	13	5.3	4.7		4.7		
273	1914	3	22	12	50	6	41.7	21.8	33	5.3	4.7		4.7		
274	1914	5	5	19	0	0	42.97	25.1	3	4.6	3.4		3.4		
275	1914	5	13	22	0	0	43	25.5	2	4.1	2.6		2.6		
276	1914	6	18	2	0	0	41.8	22.9	10	4.6	3.5		3.5		
277	1914	12	19	17	10	0	43.13	25.8	5	4.1	4.1		4.1		
278	1915	1	17	6	30	0	41.2	22.5	4	4.7	3.6		3.6		
279	1915	1	25	7	55	0	43.6	27.3	30	5.1	5.1		5.1		
280	1915	1	30	19	11	0	43.03	23.6	17	4.3	4.3		4.3		
281	1915	3	2	13	4	0	43.17	25.5	10	4.2	4.2		4.2		
282	1916	2	2	3	57	0	42.2	21.5	4	4.4	3.1		3.1		
283	1916	2	23	10	23	0	41.8	22.5	22	5.1	4.4		4.4		
284	1916	3	8	14	2	0	43.05	26.2	50	4.8	4.8		4.8		
285	1916	4	10	22	30	0	41.7	22	15	5.5	5		5		
286	1916	9	27	1	3	0	41.5	22.7	13	4.9	4		4		
287	1916	11	18	2	29	0	41.3	22.5	10	5	4.2		4.2		
288	1917	1	25	10	5	0	41.18	20.6	6	5	4.2		4.2		
289	1917	2	8	11	23	0	44.1	21.4	16	4	4		4		
290	1917	3	14	18	13	7	39.88	20.2	16	5.5	5.3		5.3		
291	1917	4	10	19	40	0	40.6	27.1	16	5.5	5.3		5.3		
292	1917	4	26	13	10	0	39.8	20.5	16	5.5	5		5		
293	1917	6	25	13	8	24	40	20	18	5.3	4.8		4.8		
294	1917	6	29	8	45	20	40	20	10	5.2	4.5		4.5		
295	1917	8	19	5	30	0	40.5	19.5	12	5.3	4.7		4.7		
296	1917	8	20	23	2	0	40	26	32	5.9	5.8		5.8		
297	1917	10	18	18	18	0	42.7	23.3	5	4.3	2.9		2.9		
298	1917	10	18	18	58	30	42.68	23.3	9	5.5	5.1		5.1		
299	1917	12	20	19	23	0	41.5	25.5	25	5.4	4.9		4.9		
300	1917	12	23	19	41	0	42.58	23.2	37	5.1	4.3		4.3		
301	1918	11	20	7	33	0	39.75	20	10	5.3	4.8		4.8		
302	1919	1	5	15	25	30	40	20	30	5.6	5.2		5.2		
303	1919	10	13	7	54	10	41.5	28	17	5.2	4.5		4.5		
304	1919	12	22	23	40	48	40.1	20.7	13	6.2	6.1		6.1		
305	1919	12	22	23	52	0	40.1	20.7	12	5.2	4.5		4.5		
306	1919	12	22	23	56	0	40.1	20.7	14	5.3	4.7		4.7		
307	1919	12	23	4	56	0	40.1	20.7	11	5.1	4.3		4.3		
308	1919	12	24	19	8	0	40.1	20.7	13	5	4.2		4.2		
309	1919	12	26	9	29	0	41.22	20.6	14	5.2	4.5		4.5		
310	1920	1	9	11	58	0	41.8	26.2	32	5.6	5.2		5.2		
311	1920	2	17	8	30	0	41.4	21	7	5.4	4.9		4.9		
312	1920	4	9	20	32	0	42.05	21.6	19	5.5	5		5		
313	1920	4	14	8	30	0	43.9	21.2	18	4.3	4.3		4.3		
314	1920	4	20	20	40	0	43.2	21.6	10	4.1	4.1		4.1		
315	1920	4	23	10	29	0	41.55	20.6	11	5.2	4.6		4.6		
316	1920	5	19	21	0	0	42.6	22	11	5	4.2		4.2		
317	1920	7	5	2	20	0	43.65	21.1	24	4.7	4.7		4.7		
318	1920	7	23	18	40	0	41.6	21.8	14	5.1	4.3		4.3		
319	1920	9	14	2	8	45	41.2	21.4	16	5.5	5.3		5.3		
320	1920	10	1	1	0	0	43.1	19.8	30	4.2	4.2		4.2		
321	1920	10	18	8	11	30	40	20.1	10	5.5	5.1		5.1		
322	1920	10	21	10	45	0	41.1	20.6	10	5.2	4.5		4.5		
323	1920	10	21	18	57	30	40.1	20.6	10	5.7	5.5		5.5		
324	1920	10	26	0	3	2	40	20	16	5.3	4.7		4.7		
325	1920	11	14	8	22	0	40.25	20.7	10	5	4.2		4.2		
326	1920	11	21	18	57	0	40.5	20	10	4.7	3.6		3.6		
327	1920	11	21	20	58	0	40.5	20	13	5.1	4.4		4.4		
328	1920	11	25	8	38	36	40.2	20.3	12	5.5	5		5		

										Homogenized magnitudes		Reported magnitudes			
Event Number	Year	Month	Date	Hour	Minute	Second	Latitude	Longitude	Depth	M_w	M_s	mb	M_s	M_w	ML
329	1920	11	26	8	51	0	40.27	19.9	9	6.1	6		6		
330	1920	11	28	8	5	0	40.3	20	5	5.1	4.3		4.3		
331	1920	11	29	15	48	0	40.45	20	14	5.7	5.5		5.5		
332	1920	11	29	20	14	0	40.5	20	12	5.1	4.3		4.3		
333	1920	12	6	13	44	0	40	20	14	5.4	4.9		4.9		
334	1920	12	6	14	30	0	41.45	22.4	14	5.2	4.5		4.5		
335	1920	12	8	3	55	20	40.8	20	13	5.5	5.1		5.1		
336	1920	12	10	13	42	0	40	20	13	5.5	5.1		5.1		
337	1920	12	17	20	28	0	41.33	20.6	10	4.8	3.8		3.8		
338	1920	12	18	2	1	24	41.1	20.1	12	5.8	5.6		5.6		
339	1920	12	23	3	10	0	41	19.7	10	5.3	4.7		4.7		
340	1920	12	27	0	0	0	41	19.7	10	5	4.1		4.1		
341	1921	3	15	1	40	0	41.43	21	7	4.9	4		4		
342	1921	3	15	1	42	0	41.4	21	10	4.8	3.9		3.9		
343	1921	3	15	1	45	0	41.4	21	10	4.8	3.8		3.8		
344	1921	3	29	16	50	0	41.7	20.5	10	5	4.2		4.2		
345	1921	3	30	12	30	0	41.7	20.3	20	4.9	4		4		
346	1921	3	30	15	5	30	41.72	20.4	13	5.9	5.8		5.8		
347	1921	3	31	16	4	0	41.75	20.5	20	5.2	4.6		4.6		
348	1921	4	2	5	4	0	41.4	21	11	5	4.2		4.2		
349	1921	4	16	22	14	0	41.75	20.5	20	5.2	4.6		4.6		
350	1921	4	17	4	15	0	41.75	20.5	20	5.2	4.6		4.6		
351	1921	4	18	9	10	0	41.5	22.1	10	4.8	3.8		3.8		
352	1921	5	4	17	35	36	42	22.8	50	5.5	5		5		
353	1921	5	15	7	59	0	43.4	20.1	16	4.6	4.6		4.6		
354	1921	6	10	1	10	30	41.1	20.1	21	5.5	5		5		
355	1921	7	1	11	48	17	43.96	21.2	10	4.5	4.5		4.5		
356	1921	7	6	11	4	0	41.75	20.5	6	5.2	4.5		4.5		
357	1921	8	2	11	55	0	41.47	21	14	5.3	4.8		4.8		
358	1921	8	3	16	37	0	43.05	20.1	5	4.2	4.2		4.2		
359	1921	8	10	14	10	31	42.35	21.3	12	5.9	5.7		5.7		
360	1921	8	10	14	40	55	42.3	21.4	18	5	4.2		4.2		
361	1921	8	11	17	34	20	41.75	20.5	14	5.1	4.3		4.3		
362	1921	8	12	16	25	0	41.21	21.1	9	5.1	4.4		4.4		
363	1921	8	15	8	23	34	42.33	21.4	9	5.3	4.7		4.7		
364	1921	8	20	19	28	0	42.08	21.4	4	5.1	4.3		4.3		
365	1921	8	23	14	20	0	42	21.5	10	5	4.2		4.2		
366	1921	9	2	9	41	20	42.38	21.4	6	5.2	4.5		4.5		
367	1921	9	10	3	20	0	42.1	21.4	7	4.8	3.8		3.8		
368	1921	9	11	15	47	0	42.12	21.4	7	5.1	4.4		4.4		
369	1921	9	12	6	33	30	41.7	22.8	20	5.3	4.7		4.7		
370	1921	9	13	15	38	0	42.1	21.4	7	4.8	3.8		3.8		
371	1921	9	21	9	38	0	42.2	21.2	14	5.1	4.4		4.4		
372	1921	10	3	2	30	0	41.2	20.7	18	5.1	4.3		4.3		
373	1921	10	3	12	30	0	42.12	21.3	6	5.1	4.4		4.4		
374	1921	10	5	12	25	48	42.3	21.4	8	5.2	4.6		4.6		
375	1921	10	7	4	57	0	41.7	20.5	10	5	4.2		4.2		
376	1921	10	14	17	10	0	42.3	21.4	10	5	4.2		4.2		
377	1921	10	21	2	6	10	41.1	20.1	14	5.5	5.1		5.1		
378	1921	10	22	4	58	30	42.5	22.5	18	5	4.1		4.1		
379	1921	11	7	22	23	0	42.08	21.4	8	5	4.2		4.2		
380	1921	11	8	2	57	0	42.1	21.4	9	5.2	4.6		4.6		
381	1921	11	23	5	15	0	42.4	19.3	5	4.9	4		4		
382	1921	12	28	6	53	19	44.4	20.4	10	4	4		4		
383	1922	1	6	5	53	26	43.96	20.4	9	4.1	4.1		4.1		
384	1922	1	12	10	42	0	40.1	20.1	12	5.5	5		5		
385	1922	2	7	12	29	0	42.2	21.2	10	4.7	3.6		3.6		
386	1922	2	24	13	24	0	42.4	21.1	14	5.2	4.6		4.6		
387	1922	3	5	10	8	45	44.18	21.3	7	4.6	4.6		4.6		
388	1922	3	24	12	22	14	44.4	20.5	8	6	6		6		
389	1922	3	24	12	26	0	44.4	20.4	20	4.3	4.3		4.3		
390	1922	3	25	2	38	48	44.3	20.6	22	4.4	4.4		4.4		
391	1922	3	25	2	53	54	44.4	20.2	32	4.3	4.3		4.3		
392	1922	3	29	7	58	0	44.4	20.4	28	4.7	4.7		4.7		
393	1922	4	1	16	10	36	44.6	20.3	18	4.9	4.9		4.9		
394	1922	4	3	14	48	0	41.3	20.7	16	5	4.1		4.1		
395	1922	4	11	4	35	10	40.5	19.2	13	5.8	5.6		5.6		
396	1922	5	31	17	33	8	43.8	21.1	11	4.1	4.1		4.1		
397	1922	6	9	15	36	24	41.8	20.5	8	5.3	4.8		4.8		
398	1922	6	9	16	13	20	41.8	20.5	16	5.5	5.1		5.1		
399	1922	6	9	16	59	0	41.8	20.5	14	5	4.2		4.2		
400	1922	6	13	0	43	0	41.7	21.8	20	5.2	4.5		4.5		
401	1922	6	22	13	22	0	40.1	20.1	10	4.8	3.8		3.8		
402	1922	6	29	10	30	20	40.2	20	14	5.5	5.1		5.1		
403	1922	7	1	8	5	10	40	20	12	5.1	4.4		4.4		
404	1922	7	2	20	1	48	40.25	20	14	5.4	4.9		4.9		
405	1922	7	3	8	21	45	40.1	20.1	12	5.1	4.4		4.4		
406	1922	9	3	3	11	12	42.45	20.4	14	5.5	5		5		
407	1922	9	5	15	56	49	41.3	22.6	15	5.2	4.5		4.5		
408	1922	9	30	0	20	12	44.4	20.4	14	4.3	4.3		4.3		
409	1922	10	5	0	0	0	42.7	23.1	2	4.2	2.7		2.7		
410	1922	12	7	16	22	10	41.78	20.5	17	5.9	5.7		5.7		

										Homogenized magnitudes		Reported magnitudes			
Event Number	Year	Month	Date	Hour	Minute	Second	Latitude	Longitude	Depth	M_w	M_s	mb	M_s	M_w	ML
411	1922	12	7	16	37	6	41.7	20.7	14	5.7	5.5		5.5		
412	1922	12	7	22	4	6	41.7	20.7	11	5.2	4.6		4.6		
413	1922	12	7	23	30	0	41.7	20.7	10	4.8	3.8		3.8		
414	1922	12	18	7	23	25	41.68	20.7	17	5.3	4.8		4.8		
415	1922	12	19	21	39	0	41.7	20.7	12	5.1	4.3		4.3		
416	1923	1	7	8	56	0	41	20	14	5.2	4.5		4.5		
417	1923	1	7	12	27	12	41.1	20.1	11	5.3	4.8		4.8		
418	1923	1	7	13	20	15	41.1	20.2	17	5.1	4.4		4.4		
419	1923	1	8	13	41	0	44.3	20.1	9	4	4		4		
420	1923	2	13	17	9	25	40.3	20	13	5.1	4.4		4.4		
421	1923	3	30	10	11	54	43.8	19.3	14	4.2	4.2		4.2		
422	1923	4	20	23	10	0	42.13	26.4	5	4.3	3		3		
423	1923	4	23	23	9	30	42.3	21.3	18	5	4.2		4.2		
424	1923	5	27	1	30	0	44.6	28.6	20	4	4		4		
425	1923	6	7	7	10	0	44.1	21.3	18	4.2	4.2		4.2		
426	1923	6	15	19	33	0	39.8	19.3	30	5	4.2		4.2		
427	1923	8	10	16	48	24	44.4	20.2	10	4	4		4		
428	1923	8	17	1	30	0	42.7	21.2	10	4.7	3.6		3.6		
429	1923	9	21	23	59	18	42.2	21.4	10	5	4.2		4.2		
430	1923	9	23	22	57	30	41.8	20.3	10	5.2	4.6		4.6		
431	1923	10	9	23	3	30	41.3	19.5	8	5	4.2		4.2		
432	1923	10	9	23	10	35	41.3	19.5	20	5.5	5.1		5.1		
433	1923	10	9	23	16	42	41.3	19.5	30	5.1	4.4		4.4		
434	1923	10	9	23	48	5	41.3	19.5	25	5.5	5.3		5.3		
435	1923	10	26	12	13	16	41.2	28.6	27	5.5	5		5		
436	1923	12	19	3	15	0	42.07	26.3	5	4.7	3.7		3.7		
437	1923	12	19	3	30	0	42.08	26.3	5	4.8	3.9		3.9		
438	1923	12	19	3	45	0	42.23	26.2	6	4.5	3.2		3.2		
439	1923	12	23	17	5	0	42.13	24.7	11	5.3	4.8		4.8		
440	1923	12	27	16	30	0	41	19.7	10	5.3	4.7		4.7		
441	1924	1	13	9	43	20	43.6	19.7	19	4.6	4.6		4.6		
442	1924	1	17	6	57	4	43.7	21	12	4.2	4.2		4.2		
443	1924	3	3	2	7	42	44.2	19.4	15	4	4		4		
444	1924	4	21	6	20	0	42.22	26.2	5	4.3	2.9		2.9		
445	1924	4	21	6	30	0	42.22	26.3	4	4.2	2.8		2.8		
446	1924	4	25	10	52	43	42.3	21.5	14	5.2	4.5		4.5		
447	1924	5	12	14	30	50	40	19.5	34	5.6	5.2		5.2		
448	1924	5	16	18	23	37	42.4	21.2	10	5.3	4.8		4.8		
449	1924	8	25	14	18	0	41.7	20.5	19	5.4	4.9		4.9		
450	1924	11	18	11	15	0	41.5	21	14	4.9	4		4		
451	1924	12	23	17	4	50	42.13	24.8	16	5.5	5.3		5.3		
452	1925	1	7	11	6	42	42	22.3	28	5.3	4.7		4.7		
453	1925	4	12	19	27	0	41.1	20.1	23	5.5	5.1		5.1		
454	1925	5	20	7	53	48	40.3	20	14	5.6	5.2		5.2		
455	1925	6	10	4	45	0	41	29	12	5.1	4.4		4.4		
456	1925	6	28	16	44	50	43.41	19.5	19	4.3	4.3		4.3		
457	1925	7	3	6	16	40	42.4	21.4	20	5.1	4.3		4.3		
458	1925	8	16	21	1	0	40.1	20.1	5	4.6	3.4		3.4		
459	1925	11	19	12	25	5	40.3	20	14	5.4	4.9		4.9		
460	1926	2	4	15	27	0	40.5	19.5	16	5.1	4.3		4.3		
461	1926	2	15	14	36	48	41.5	20	12	5.4	4.9		4.9		
462	1926	3	21	22	8	0	40.1	20.1	14	5.2	4.6		4.6		
463	1926	3	25	0	5	0	43.3	20.6	18	4.3	4.3		4.3		
464	1926	4	18	18	18	34	43.9	20.4	21	4.7	4.7		4.7		
465	1926	5	19	10	11	12	44.5	20.6	20	4.6	4.6		4.6		
466	1926	6	10	19	16	0	39.75	20	120	6.8	7	6.2			
467	1926	6	16	3	12	0	42	20.5	14	5.5	5.1		5.1		
468	1926	6	29	23	45	0	42.55	26.1	9	5.5	5		5		
469	1926	7	4	23	1	36	44.03	20.4	12	4.3	4.3		4.3		
470	1926	9	3	21	59	57	41.7	24.4	19	5.4	4.9		4.9		
471	1926	10	12	11	57	15	42.83	19.8	6	5.6	5.2		5.2		
472	1926	10	22	23	53	54	42.1	20.6	19	5.4	4.9		4.9		
473	1926	10	23	1	58	40	40	19.5	30	5.6	5.4		5.4		
474	1926	11	23	21	14	0	42.8	19.9	4	4.5	3.3		3.3		
475	1926	12	16	17	54	0	41.32	19.5	9	5.5	5		5		
476	1926	12	17	6	27	33	41.3	19.5	14	5.4	4.9		4.9		
477	1926	12	17	6	31	5	41.3	19.6	19	5.9	5.8		5.8		
478	1926	12	17	6	41	0	42.4	20.6	12	5.1	4.4		4.4		
479	1926	12	17	8	5	0	41.3	19.6	17	5	4.2		4.2		
480	1926	12	17	10	48	0	41.3	19.4	10	4.8	3.8		3.8		
481	1926	12	17	11	39	55	41.3	19.5	12	5.9	5.8		5.8		
482	1926	12	25	15	13	0	41.3	19.5	14	5.2	4.6		4.6		
483	1926	12	25	16	14	40	41.3	19.5	16	5.3	4.7		4.7		
484	1926	12	26	22	2	52	41.3	19.5	11	5	4.2		4.2		
485	1926	12	27	18	46	0	41.3	19.6	14	5.2	4.5		4.5		
486	1927	1	6	22	55	0	43	19.8	8	4.7	3.6		3.6		
487	1927	1	8	3	19	0	41.8	22.5	24	5.2	4.6		4.6		
488	1927	3	13	13	5	0	42.8	19.9	5	4.7	3.6		3.6		
489	1927	3	15	9	28	0	44.1	20.5	12	4	4		4		
490	1927	5	9	4	55	18	44.54	19.3	15	4.6	4.6		4.6		
491	1927	5	15	2	47	0	44.07	20.5	9	5.9	5.9		5.9		
492	1927	5	15	2	58	36	44.1	20.5	14	4.6	4.6		4.6		

										Homogenized magnitudes		Reported magnitudes			
Event Number	Year	Month	Date	Hour	Minute	Second	Latitude	Longitude	Depth	M_w	M_s	mb	M_s	M_w	ML
493	1927	5	15	3	12	0	44.2	20.5	19	5.2	5.2		5.2		
494	1927	5	15	3	19	18	44.1	20.6	14	4.6	4.6		4.6		
495	1927	5	15	3	24	48	44.4	20.2	18	4	4		4		
496	1927	5	15	5	48	42	44	20.6	20	4.3	4.3		4.3		
497	1927	5	15	7	53	54	44.05	20.6	26	4.8	4.8		4.8		
498	1927	5	15	8	28	30	44.1	20.5	15	4	4		4		
499	1927	5	15	16	55	0	44.1	20.5	14	4.2	4.2		4.2		
500	1927	5	15	17	22	12	44.1	20.5	12	4.1	4.1		4.1		
501	1927	5	15	21	31	30	44.1	20.5	17	4.9	4.9		4.9		
502	1927	5	17	17	38	12	44.1	20.4	25	4.9	4.9		4.9		
503	1927	5	27	10	58	0	44.1	20.5	14	4	4		4		
504	1927	5	31	22	58	15	44.9	21.7	12	4.4	4.4		4.4		
505	1927	5	31	23	10	0	44.05	20.9	12	4.9	4.9		4.9		
506	1927	6	1	2	39	12	44.1	20.6	14	4.2	4.2		4.2		
507	1927	6	13	6	3	0	44.1	20.6	12	4.1	4.1		4.1		
508	1927	6	18	4	11	0	44.1	20.6	17	4.2	4.2		4.2		
509	1927	6	18	6	26	48	43.9	20.6	14	4.9	4.9		4.9		
510	1927	6	18	9	26	39	43.8	20.6	17	4.2	4.2		4.2		
511	1927	6	18	10	37	0	43.8	20.7	10	4.1	4.1		4.1		
512	1927	6	18	12	21	54	43.8	20.5	20	4.3	4.3		4.3		
513	1927	7	8	12	16	42	43.8	20.6	13	4.2	4.2		4.2		
514	1927	7	21	3	32	12	43.8	20.6	14	4	4		4		
515	1927	7	21	23	35	48	44.1	20.5	14	4	4		4		
516	1927	7	22	10	3	0	41.3	20.8	15	4.9	4		4		
517	1927	7	23	16	52	0	40.5	19.5	10	4.8	3.9		3.9		
518	1927	7	23	19	14	24	41.7	22.8	17	5.4	4.9		4.9		
519	1927	7	24	4	33	48	44.1	20.8	12	4.2	4.2		4.2		
520	1927	7	24	20	17	5	45	28	32	4.9	4.9		4.9		
521	1927	8	7	5	25	0	42.4	20.5	29	5.3	4.8		4.8		
522	1927	8	7	6	33	50	42.45	19.4	16	5.6	5.2		5.2		
523	1927	8	11	1	34	18	41.79	22.1	7	5	4.2		4.2		
524	1927	9	17	13	45	28	44.2	20.6	21	4.7	4.7		4.7		
525	1927	10	11	15	29	1	44.13	20.6	7	4.4	4.4		4.4		
526	1927	10	12	7	20	15	44	21	30	4.8	4.8		4.8		
527	1927	10	24	7	33	6	44.05	20.5	14	4.2	4.2		4.2		
528	1927	11	2	0	45	48	44.05	20.4	12	4.2	4.2		4.2		
529	1928	3	10	12	17	42	42.2	21.4	12	5	4.2		4.2		
530	1928	3	17	19	40	54	41.8	20.5	20	5.3	4.8		4.8		
531	1928	4	14	8	59	57	42.14	25.2	16	6.7	6.8		6.8	6.7	
532	1928	4	14	9	23	36	42.2	25.3	31	5.5	5.1		5.1		
533	1928	4	14	10	23	35	42.2	25.3	54	5.5	5.3		5.3		
534	1928	4	16	9	30	6	42.4	25.3	60	5.2	4.5		4.5		
535	1928	4	17	5	47	26	42.2	25.3	9	5.3	4.7		4.7		
536	1928	4	17	7	35	0	42.1	25.3	10	5.3	4.8		4.8		
537	1928	4	18	6	47	24	42.1	25.5	14	5.2	4.5		4.5		
538	1928	4	18	19	23	47	42.14	25	14	6.8	7		7	6.8	
539	1928	4	18	19	34	0	42.37	24.2	40	5.6	5.2		5.2		
540	1928	4	18	19	40	58	42.17	25	41	5.8	5.6		5.6		
541	1928	4	18	19	51	11	42.2	25.1	44	5.2	4.6		4.6		
542	1928	4	18	19	57	56	42	25	40	5.2	4.5		4.5		
543	1928	4	18	20	5	52	42.17	25	31	5.5	5		5		
544	1928	4	18	20	49	56	42.7	23.7	16	5.5	5		5		
545	1928	4	18	21	58	18	42	24.3	19	5.1	4.3		4.3		
546	1928	4	18	22	48	56	42	24	34	5.1	4.3		4.3		
547	1928	4	18	23	14	39	42.17	25	10	5.7	5.5		5.5		
548	1928	4	19	1	1	18	42.2	24.7	30	5	4.2		4.2		
549	1928	4	19	1	10	0	42.1	24.5	40	5.3	4.8		4.8		
550	1928	4	19	4	59	22	42.1	25.2	18	5.3	4.8		4.8		
551	1928	4	19	5	23	57	42.1	25	30	5	4.2		4.2		
552	1928	4	19	5	55	18	42.2	25.1	16	5	4.2		4.2		
553	1928	4	19	6	32	16	42.2	25.1	21	5.1	4.4		4.4		
554	1928	4	19	6	46	27	42.2	25.1	19	5.1	4.3		4.3		
555	1928	4	19	7	46	1	42.1	25.2	21	5.1	4.4		4.4		
556	1928	4	19	9	10	0	41.92	25.1	12	5.2	4.5		4.5		
557	1928	4	19	9	57	15	42.1	24.9	21	5.1	4.4		4.4		
558	1928	4	19	13	0	0	42.27	25.5	20	5.2	4.5		4.5		
559	1928	4	19	22	21	8	42.2	25.1	26	5.6	5.2		5.2		
560	1928	4	19	22	40	18	41.58	24.6	39	5.3	4.8		4.8		
561	1928	4	20	6	15	11	41.92	25.5	31	5.5	5		5		
562	1928	4	20	6	16	18	42.2	25.1	12	5.1	4.3		4.3		
563	1928	4	22	8	22	0	42.1	25.4	5	4.9	4		4		
564	1928	4	23	10	50	0	42.37	25.7	6	4.8	3.9		3.9		
565	1928	4	24	1	14	48	42	25.5	13	5.5	5		5		
566	1928	4	24	14	30	0	42	25.5	10	5	4.2		4.2		
567	1928	4	25	9	25	43	42.03	25.9	10	5.8	5.6		5.6		
568	1928	4	25	9	36	0	41.9	25.9	10	5	4.2		4.2		
569	1928	4	27	0	0	30	41.95	24.2	31	5.4	4.9		4.9		
570	1928	4	28	3	7	0	42.1	25.3	13	5.3	4.7		4.7		
571	1928	4	28	17	59	25	42.1	25	52	5.5	5.3		5.3		
572	1928	5	3	1	25	13	40.65	26.8	6	5.1	4.3		4.3		
573	1928	5	25	21	25	0	42.2	25	2	4.4	3.1		3.1		
574	1928	5	26	5	54	27	40.2	19.7	14	5.4	4.9		4.9		

										Homogenized magnitudes		Reported magnitudes			
Event Number	Year	Month	Date	Hour	Minute	Second	Latitude	Longitude	Depth	M_w	M_s	mb	M_s	M_w	ML
575	1928	7	17	4	10	0	42.2	25	3	4.5	3.2		3.2		
576	1928	7	29	18	15	54	42.2	25	48	5.2	4.6		4.6		
577	1928	10	2	23	15	0	42.1	25.2	8	4.6	3.5		3.5		
578	1928	10	15	1	7	0	42.25	25.1	7	4.9	4		4		
579	1928	10	30	22	40	0	42.2	21.1	20	5.3	4.8		4.8		
580	1928	12	3	22	10	0	42.2	25.3	12	5.2	4.6		4.6		
581	1928	12	15	17	31	30	44.1	20.4	18	4	4		4		
582	1928	12	16	15	15	0	42.1	25.8	7	4.5	3.2		3.2		
583	1928	12	24	2	15	0	42.2	25.3	8	4.9	4		4		
584	1928	12	24	3	0	0	42.2	25.1	10	5.1	4.3		4.3		
585	1928	12	24	17	45	0	42.05	25.2	8	5.1	4.3		4.3		
586	1929	1	2	6	2	54	41.2	22.6	8	5	4.2		4.2		
587	1929	1	17	0	6	40	40.6	19.6	14	5.5	5.1		5.1		
588	1929	1	30	4	0	0	40.6	19.6	10	4.8	3.9		3.9		
589	1929	3	1	11	31	0	42.31	25.1	4	4.6	3.4		3.4		
590	1929	4	2	6	25	0	42.1	25.3	7	4.9	4		4		
591	1929	4	18	2	0	0	42.28	25.5	12	5.1	4.3		4.3		
592	1929	5	15	12	22	0	41.7	22.8	5	4.6	3.4		3.4		
593	1929	6	5	10	45	0	42.13	24.7	9	4.6	3.5		3.5		
594	1929	7	3	8	25	45	41.5	22	18	5.2	4.5		4.5		
595	1929	7	10	14	37	0	42.25	24.8	7	4.5	3.3		3.3		
596	1929	7	13	12	50	54	42.5	19	10	5.4	4.9		4.9		
597	1929	7	19	8	30	35	44.3	20.6	11	4.5	4.5		4.5		
598	1929	7	24	12	10	0	42.05	25.2	6	4.8	3.9		3.9		
599	1929	8	10	9	40	0	41.45	22.3	16	5.2	4.5		4.5		
600	1929	10	10	23	1	6	41.2	28.6	8	5.2	4.5		4.5		
601	1929	11	2	23	32	24	44.23	21.8	8	4	4		4		
602	1929	11	14	15	34	0	41.5	20.1	11	5.4	4.9		4.9		
603	1929	11	27	0	15	0	41.7	21.5	20	5.3	4.8		4.8		
604	1929	11	29	0	10	0	41.7	21.5	20	5.1	4.3		4.3		
605	1930	1	18	3	39	0	42.2	25.1	5	4.8	3.8		3.8		
606	1930	2	27	4	22	42	40.7	19.9	6	4.8	3.9		3.9		
607	1930	5	21	13	38	0	41.5	20.5	11	4.3	2.9		2.9		
608	1930	7	24	20	26	0	42.05	25.5	14	5	4.1		4.1		
609	1930	7	24	22	50	0	42.15	25.3	12	5.1	4.3		4.3		
610	1930	11	21	2	0	27	40.21	19.6	6	5.9	5.8		5.8		
611	1930	11	21	4	1	24	40.2	19.6	13	5.3	4.8		4.8		
612	1930	11	21	19	26	0	40.2	19.6	18	5.6	5.4		5.4		
613	1930	11	22	0	25	50	40.2	19.6	12	5.1	4.3		4.3		
614	1930	11	25	22	30	0	40.3	19.6	10	5.3	4.8		4.8		
615	1930	11	28	15	29	0	41.9	23.1	5	4.5	3.2		3.2		
616	1930	12	2	13	28	51	40.3	19.6	7	5.5	5		5		
617	1930	12	4	2	20	0	40.3	19.6	10	5.2	4.5		4.5		
618	1930	12	5	2	57	0	40.3	19.5	5	4.9	4		4		
619	1930	12	6	10	14	0	40.3	19.7	10	5.2	4.5		4.5		
620	1930	12	10	0	0	0	40.4	19.5	5	4.9	4		4		
621	1930	12	12	18	16	0	40.6	19.3	5	4.2	2.7		2.7		
622	1930	12	12	19	31	0	40.6	19.3	5	4.2	2.7		2.7		
623	1930	12	23	0	0	0	40.2	19.9	5	4.7	3.7		3.7		
624	1930	12	25	23	45	0	40.6	19.3	5	4.9	4		4		
625	1930	12	29	21	15	0	42.05	25.5	10	4.7	3.7		3.7		
626	1931	1	4	23	56	23	40.45	19.5	15	5.2	4.6		4.6		
627	1931	1	5	0	7	0	40.6	19.3	5	4.2	2.7		2.7		
628	1931	1	11	19	19	43	40.2	19.9	12	5.5	5		5		
629	1931	1	28	5	55	15	40.59	20.6	6	5.9	5.8		5.8		
630	1931	2	1	1	41	32	40.67	20.6	24	5.4	4.9		4.9		
631	1931	2	20	5	3	0	40.6	20.8	11	4.9	4		4		
632	1931	2	21	19	30	0	40.6	20.7	10	4.8	3.9		3.9		
633	1931	2	22	8	0	0	40.6	20.7	10	5.2	4.5		4.5		
634	1931	3	7	0	16	0	41.25	22.3	16	6.1	6		6		
635	1931	3	7	1	50	0	41.36	22.5	16	5.3	4.7		4.7		
636	1931	3	8	1	50	26	41.31	22.4	8	6.7	6.7		6.7		
637	1931	3	8	2	11	35	41.35	22.4	15	5.3	4.8		4.8		
638	1931	3	8	2	26	45	41.3	22.6	9	5.4	4.9		4.9		
639	1931	3	8	2	39	29	41.2	22.5	13	5	4.2		4.2		
640	1931	3	8	2	44	38	41.3	22.5	7	5	4.2		4.2		
641	1931	3	8	3	12	0	41.3	22.5	10	4.7	3.6		3.6		
642	1931	3	8	3	26	0	41.4	22.6	10	4.7	3.6		3.6		
643	1931	3	8	5	3	9	41.34	22.4	9	5.2	4.6		4.6		
644	1931	3	8	5	13	30	41.25	22.5	16	5.4	4.9		4.9		
645	1931	3	8	6	14	0	41.3	22.5	10	4.7	3.6		3.6		
646	1931	3	8	6	29	48	41.3	22.5	7	5.1	4.3		4.3		
647	1931	3	8	22	15	0	41.3	22.5	8	5	4.2		4.2		
648	1931	3	8	22	50	0	41.3	22.5	14	5.1	4.4		4.4		
649	1931	3	9	3	30	0	41.3	22.4	7	4.9	4		4		
650	1931	3	9	7	20	0	41.25	22.5	13	5.2	4.6		4.6		
651	1931	3	11	5	45	0	41.5	22.4	9	5	4.1		4.1		
652	1931	3	17	18	2	0	41.28	22.5	13	5.2	4.6		4.6		
653	1931	3	17	20	28	0	41.29	22.5	13	5.2	4.6		4.6		
654	1931	3	18	1	15	0	41.3	22.5	10	5.1	4.4		4.4		
655	1931	3	18	4	30	0	41.6	22.4	4	4.7	3.6		3.6		
656	1931	3	22	23	27	0	42.2	25.8	30	5	4.2		4.2		

										Homogenized magnitudes		Reported magnitudes			
Event Number	Year	Month	Date	Hour	Minute	Second	Latitude	Longitude	Depth	M_w	M_s	mb	M_s	M_w	ML
657	1931	3	25	2	30	0	41.4	22.7	7	5	4.2		4.2		
658	1931	4	17	19	30	0	41.4	22.7	4	4.6	3.5		3.5		
659	1931	4	27	22	15	0	41.3	22.5	9	5	4.2		4.2		
660	1931	5	4	11	12	0	40.2	19.6	9	5.5	5		5		
661	1931	7	23	3	8	44	41.65	22.4	12	5	4.1		4.1		
662	1931	8	27	1	21	18	44.1	20.8	9	4	4		4		
663	1931	9	23	13	28	3	40.38	19.5	3	5.5	5		5		
664	1931	10	12	16	58	12	44	20.6	16	4.2	4.2		4.2		
665	1931	10	15	23	25	0	42.13	25.5	42	5.2	4.5		4.5		
666	1931	11	15	10	17	0	40.1	19.9	14	5.2	4.5		4.5		
667	1931	11	26	21	26	48	42.8	20.7	13	5	4.2		4.2		
668	1931	11	28	11	58	36	42.9	20.8	12	5.1	4.3		4.3		
669	1931	12	3	7	50	0	42.13	25.3	9	4.7	3.7		3.7		
670	1931	12	14	6	7	0	41.3	22.5	7	4.9	4		4		
671	1932	1	17	5	50	0	40.7	20.7	5	4.4	3.1		3.1		
672	1932	1	17	13	0	0	40.7	20.7	5	4.4	3.1		3.1		
673	1932	2	22	5	20	0	41.3	22.5	8	4.9	4		4		
674	1932	4	19	2	3	6	42.8	20.7	14	5.1	4.3		4.3		
675	1932	4	23	9	58	0	41.3	22.7	21	5.5	5		5		
676	1932	5	20	2	30	0	40.9	20.7	5	4.4	3.1		3.1		
677	1932	5	20	4	17	17	40.9	20.7	9	4.9	4		4		
678	1932	6	17	23	45	0	42.07	26.2	7	4.5	3.2		3.2		
679	1932	7	22	4	55	0	42.07	26.2	5	4.3	3		3		
680	1932	8	3	11	42	39	39.9	19.9	14	5.2	4.6		4.6		
681	1932	12	1	10	15	0	42.5	19.5	16	5.3	4.8		4.8		
682	1932	12	1	15	0	0	42.75	19.4	11	5.1	4.4		4.4		
683	1932	12	11	21	46	9	42.45	19.3	18	5.5	5		5		
684	1933	1	2	7	56	52	41.7	24.2	28	5.2	4.6		4.6		
685	1933	1	7	13	10	0	42.17	25.2	6	4.4	3.1		3.1		
686	1933	1	18	2	35	21	44	20.2	14	4.5	4.5		4.5		
687	1933	2	4	9	35	0	41.6	19.4	5	4.6	3.4		3.4		
688	1933	3	21	3	55	0	41.3	22.5	6	4.9	4		4		
689	1933	5	8	1	13	48	41.5	24.2	32	5.4	4.9		4.9		
690	1933	5	9	22	10	0	42.18	25.3	14	5.4	4.9		4.9		
691	1933	7	27	1	3	5	40	20.1	12	5.4	4.9		4.9		
692	1933	9	8	15	10	2	43.4	19.2	28	4.7	4.7		4.7		
693	1933	9	10	9	35	0	42.12	25.6	14	5	4.2		4.2		
694	1934	2	4	9	35	22	41.25	19.6	11	5.8	5.6		5.6		
695	1934	2	10	10	1	0	41.3	19.6	5	4.6	3.4		3.4		
696	1934	6	7	10	1	0	42.7	22.9	6	4.4	3.1		3.1		
697	1934	9	13	4	5	0	41.35	20.8	8	5	4.2		4.2		
698	1934	10	15	1	40	12	44.41	19.4	8	4.3	4.3		4.3		
699	1934	11	14	16	24	0	42.23	23.6	7	4.3	3		3		
700	1934	12	5	18	0	0	42.1	19.5	5	4.7	3.7		3.7		
701	1934	12	10	10	47	0	41.4	19.6	5	4.6	3.4		3.4		
702	1935	1	4	14	41	0	40.6	27.5	11	6.4	6.4		6.4		
703	1935	1	4	15	18	57	40.5	27.5	10	5.2	4.6		4.6		
704	1935	1	4	15	19	24	40.5	27.5	26	5.8	5.6		5.6		
705	1935	1	4	16	20	0	40.3	27.6	21	6.3	6.3		6.3		
706	1935	3	31	3	21	31	41.25	20.2	12	5.9	5.7		5.7		
707	1935	3	31	3	44	55	41.1	20.4	14	5.4	4.9		4.9		
708	1935	6	19	13	25	0	42.18	23.6	4	4.3	2.9		2.9		
709	1935	6	22	11	29	0	41	21.2	10	4.8	3.9		3.9		
710	1935	11	7	4	37	28	41.3	20.3	17	5.6	5.4		5.4		
711	1936	1	29	15	55	33	41.3	20.3	14	5.5	5.1		5.1		
712	1936	3	5	4	12	18	42.3	21.4	10	4.9	4		4		
713	1936	3	27	19	41	0	42.35	24	14	4.9	4		4		
714	1936	3	29	21	27	14	42.2	20.7	15	5.4	4.9		4.9		
715	1936	6	8	9	17	0	41.8	23.2	16	5	4.2		4.2		
716	1936	8	28	1	57	0	41.63	25.3	16	5.1	4.3		4.3		
717	1936	9	12	16	3	0	41.7	24	36	5.1	4.4		4.4		
718	1936	9	13	3	3	1	44	20.6	28	4.4	4.4		4.4		
719	1937	2	12	12	0	0	42.15	25.2	7	4.5	3.3		3.3		
720	1937	2	23	23	37	39	41.7	20.4	10	5	4.2		4.2		
721	1937	2	25	9	27	44	44	20.6	12	4.4	4.4		4.4		
722	1937	2	28	9	40	0	41.3	20.6	7	4.9	4		4		
723	1937	3	5	13	2	6	43.9	20.7	9	4.2	4.2		4.2		
724	1937	3	6	0	54	30	39.8	19.9	16	5.3	4.7		4.7		
725	1937	9	8	2	51	11	41.6	24.1	23	5.1	4.4		4.4		
726	1937	9	29	3	30	0	42.17	25.4	17	5.2	4.5		4.5		
727	1937	12	11	0	30	0	42.23	23.6	7	4.5	3.2		3.2		
728	1938	4	19	1	55	0	42.83	19.8	8	4.9	4		4		
729	1938	8	15	11	2	4	40.33	20.6	11	5.4	4.9		4.9		
730	1938	9	16	2	6	0	41.5	23	30	5.2	4.5		4.5		
731	1939	2	17	3	24	24	42.1	23.4	44	5.5	5.1		5.1		
732	1939	5	3	10	9	0	41.68	24.6	5	5.1	4.3		4.3		
733	1939	5	20	9	35	24	41	19.5	16	5.5	5.3		5.3		
734	1939	7	27	0	0	0	42.2	25.3	7	4.4	3.1		3.1		
735	1939	8	2	9	25	17	41.5	24.7	53	5.4	4.9		4.9		
736	1939	8	9	3	30	24	40.62	19.7	11	5.5	5		5		
737	1939	8	9	12	29	41	42.12	25.2	8	5.3	4.8		4.8		
738	1939	11	29	4	52	0	42.18	23.6	6	4.6	3.5		3.5		

										Homogenized magnitudes		Reported magnitudes			
Event Number	Year	Month	Date	Hour	Minute	Second	Latitude	Longitude	Depth	M_w	M_s	mb	M_s	M_w	ML
739	1939	12	25	1	35	0	41.67	24.7	7	4.7	3.7		3.7		
740	1940	2	23	0	39	51	40.62	19.6	17	5.7	5.5		5.5		
741	1940	2	23	9	27	46	42.2	25	28	5.5	5		5		
742	1940	5	14	0	45	0	41.74	24.5	11	5.4	4.9		4.9		
743	1940	6	27	8	12	0	40	20.1	11	5.2	4.6		4.6		
744	1940	9	16	1	0	0	42.65	19.9	5	4.6	3.4		3.4		
745	1940	11	17	18	25	0	42	22.7	5	4.6	3.4		3.4		
746	1940	12	26	21	50	0	42.13	25	8	4.6	3.5		3.5		
747	1941	2	9	9	23	15	41	29	40	5.2	4.6		4.6		
748	1941	6	24	15	16	4	40.5	21	40	5.5	5		5		
749	1941	9	1	14	18	40	41.66	24.7	8	5.5	5.1		5.1		
750	1941	9	13	9	16	52	42	20.5	20	5.1	4.3		4.3		
751	1941	9	15	2	33	38	40.2	19.7	28	5.3	4.7		4.7		
752	1942	2	10	5	3	0	42.47	26.3	8	4.6	3.4		3.4		
753	1942	5	13	6	10	0	41.68	23.8	6	4.4	3.1		3.1		
754	1942	8	23	15	41	25	43.47	26.5	11	5.1	5.1		5.1		
755	1942	8	27	6	14	13	41.63	20.4	13	6.1	6		6		
756	1942	11	30	8	54	0	42.65	23.2	2	4.4	3.1		3.1		
757	1942	11	30	10	1	0	42.67	23.2	2	4.3	2.9		2.9		
758	1943	3	26	7	51	7	41.7	25.7	31	5.2	4.5		4.5		
759	1943	9	3	2	25	42	42.2	21.8	9	4.9	4		4		
760	1943	12	23	18	40	0	42.13	24.9	10	4.8	3.8		3.8		
761	1944	3	14	23	59	26	41.68	23.8	13	5.5	5.1		5.1		
762	1944	3	18	19	56	0	41.82	23.3	25	5.3	4.7		4.7		
763	1945	8	1	13	24	54	42.05	25.3	27	5	4.1		4.1		
764	1945	9	26	13	42	4	42.23	20.6	10	5.3	4.7		4.7		
765	1945	11	12	18	45	0	42.07	24	5	4.4	3.1		3.1		
766	1945	11	13	7	15	0	42.7	20.4	9	4.6	3.5		3.5		
767	1946	4	16	11	43	50	40.8	19.9	23	5.6	5.4		5.4		
768	1946	4	21	10	28	0	41	19	30	5.3	4.8		4.8		
769	1946	5	10	2	50	0	41	19	30	5.2	4.5		4.5		
770	1946	8	20	17	26	37	41.2	19.9	19	5.6	5.2		5.2		
771	1947	2	5	5	39	36	42.7	20.8	12	5.1	4.4		4.4		
772	1947	2	5	15	33	25	42.58	20.7	11	5.5	5		5		
773	1947	6	20	22	8	24	42.14	25.3	7	5.2	4.6		4.6		
774	1947	7	15	14	30	0	42	25.5	7	5.2	4.6		4.6		
775	1947	9	1	2	8	0	42.65	23.4	5	4.4	3.1		3.1		
776	1947	12	9	23	18	48	41.1	19.3	18	5.5	5.1		5.1		
777	1948	1	23	2	20	24	42.22	24.7	20	5.1	4.4		4.4		
778	1948	3	26	3	2	11	40.9	20.9	14	5.3	4.8		4.8		
779	1948	5	7	14	57	24	40	19	39	5.1	4.3		4.3		
780	1948	5	26	16	24	37	40	19	30	5	4.2		4.2		
781	1948	8	27	10	44	6	42.03	19.5	10	5.7	5.5		5.5		
782	1948	8	27	11	24	19	42.1	19.5	12	5.3	4.7		4.7		
783	1948	8	28	1	45	0	42.1	19.5	10	5	4.1		4.1		
784	1948	8	28	2	39	0	42.1	19.5	10	5	4.1		4.1		
785	1948	8	28	5	34	0	42	19.5	6	5	4.2		4.2		
786	1948	8	29	17	57	0	42.1	19.5	10	5.1	4.4		4.4		
787	1948	8	29	23	52	0	42.1	19.5	7	5.1	4.4		4.4		
788	1949	2	8	20	37	0	42.1	19.5	10	5.1	4.4		4.4		
789	1949	2	18	20	36	0	41.9	23.1	9	4.7	3.6		3.6		
790	1949	3	26	3	10	0	41.8	20.8	15	5	4.2		4.2		
791	1949	3	30	22	30	0	41.91	20.9	4	4.5	3.3		3.3		
792	1949	4	7	22	50	0	41.8	20.9	5	4.6	3.4		3.4		
793	1949	7	14	10	9	55	44.09	20.9	12	4.9	4.9		4.9		
794	1949	9	20	0	53	0	41.5	24.6	10	4.7	3.6		3.6		
795	1950	2	3	15	0	28	42.6	20.3	10	5.2	4.6		4.6		
796	1950	2	4	9	36	0	42.1	25.3	10	4.6	3.5		3.5		
797	1950	3	5	15	15	0	42.6	20.3	3	4.3	3		3		
798	1950	12	18	6	45	0	41.9	23.5	16	5	4.2		4.2		
799	1951	3	19	1	43	42	41.5	25	19	5	4.2		4.2		
800	1951	7	15	18	38	5	43.35	19.3	7	4	4		4		
801	1951	8	22	14	14	49	40	20	13	5.1	4.4		4.4		
802	1951	9	24	3	30	0	42	21.4	9	4.6	3.5		3.5		
803	1951	10	17	10	9	44	42.55	21.9	4	4.8	3.9		3.9		
804	1951	12	13	20	46	3	40.2	25.5	48	5.4	4.9		4.9		
805	1952	1	13	4	7	0	40.1	20.1	5	4.5	3.3		3.3		
806	1952	2	3	20	45	3	40.2	25.6	16	5.3	4.7		4.7		
807	1952	3	13	6	30	0	41	28.4	32	5.4	4.9		4.9		
808	1952	5	20	15	3	20	41.4	21	2	4.3	2.9		2.9		
809	1952	6	3	13	48	8	41.66	23.9	9	5.1	4.3		4.3		
810	1952	6	19	0	23	12	41.35	21	19	5.1	4.3		4.3		
811	1952	7	5	3	18	57	41.44	23.4	19	5	4.2		4.2		
812	1952	12	2	13	0	9	41.72	23.8	11	5.1	4.3		4.3		
813	1952	12	2	15	47	45	41.68	23.8	15	5	4.2		4.2		
814	1953	1	7	0	1	28	41.4	20.4	16	5.5	5.3		5.3		
815	1953	1	7	1	18	57	41.18	20.6	13	5.8	5.6		5.6		
816	1953	1	22	4	26	6	42.1	25.1	26	5	4.2		4.2		
817	1953	3	18	19	6	13	40	27.3	0	7.1	7.2		7.2		
818	1953	3	31	0	55	46	40.7	20	15	5.2	4.6		4.6		
819	1953	5	19	5	16	47	41.3	20.6	13	5.1	4.4		4.4		
820	1953	6	18	5	44	7	41.71	26.5	14	5.5	5.1		5.1		

										Homogenized magnitudes		Reported magnitudes			
Event Number	Year	Month	Date	Hour	Minute	Second	Latitude	Longitude	Depth	M_w	M_s	mb	M_s	M_w	ML
821	1953	9	4	2	29	54	41.9	23.2	50	5.6	5.2		5.2		
822	1954	3	19	2	14	44	40.5	20.3	13	5.2	4.5		4.5		
823	1954	3	23	12	58	46	40.5	27.5	100	5.3	4.8	5			
824	1954	4	19	5	37	0	41.2	20.7	8	4.9	4		4		
825	1954	4	25	23	30	0	41.2	20.6	7	4.5	3.2		3.2		
826	1954	5	8	22	5	45	40.3	20.3	16	5.1	4.4		4.4		
827	1954	5	8	22	27	36	40.3	20.3	18	5.3	4.8		4.8		
828	1954	6	7	12	49	41	42.08	25.2	9	5.1	4.4		4.4		
829	1954	9	2	1	54	34	42.1	19.8	14	5.3	4.8		4.8		
830	1955	2	20	20	27	18	42.7	22.5	15	5.4	4.9		4.9		
831	1955	3	1	6	2	0	41.4	20.9	9	4.6	3.5		3.5		
832	1955	3	2	20	34	24	41.7	23.5	35	4.8	3.8		3.8		
833	1955	6	2	23	34	33	40.3	25.5	24	5.7	5.5		5.5		
834	1955	6	28	7	14	7	44	20.4	24	4.4	4.4		4.4		
835	1955	7	6	10	7	55	40	20.5	10	5	4.2		4.2		
836	1955	7	9	16	54	40	42.65	19.3	30	5.1	4.4		4.4		
837	1955	10	2	17	57	54	39.8	20	16	5	4.1		4.1		
838	1956	1	4	12	20	39	39.75	20	17	5.5	5.1		5.1		
839	1956	1	6	12	15	42	40.45	26.1	19	5.7	5.5		5.5		
840	1956	6	30	1	50	22	43.5	28.5	30	4.8	4.8		4.8		
841	1956	7	8	10	40	42	42.4	21.5	8	5	4.1		4.1		
842	1957	2	23	22	13	28	39.8	19.9	14	5.4	4.9		4.9		
843	1957	4	7	9	59	46	42.1	19	30	5.1	4.3		4.3		
844	1957	7	7	14	37	0	41.9	20.8	14	4.8	3.9		3.9		
845	1957	9	6	20	22	10	40.5	19.7	11	5.2	4.6		4.6		
846	1957	11	14	14	16	37	39.8	19.7	12	5.2	4.6		4.6		
847	1957	11	18	15	3	18	39.8	20.2	14	5	4.2		4.2		
848	1957	12	16	4	50	0	43.7	20.6	9	4.1	4.1		4.1		
849	1958	2	9	2	40	0	42	21	5	4.2	2.7		2.7		
850	1958	3	15	6	27	7	41	21.2	16	5.5	5.3		5.3		
851	1958	4	3	2	23	41	41.32	19.5	16	5.8	5.6		5.6		
852	1958	4	4	4	4	20	41.3	19.5	12	5.2	4.6		4.6		
853	1958	4	4	9	18	52	41.3	19.5	14	5.3	4.8		4.8		
854	1958	5	1	21	15	30	41.1	20.1	12	5.3	4.7		4.7		
855	1958	6	10	8	28	52	41.5	19.2	12	5.3	4.7		4.7		
856	1958	7	16	20	29	54	41.9	23.4	10	5.1	4.4		4.4		
857	1958	8	9	9	34	24	43.2	20	12	4.4	4.4		4.4		
858	1958	10	31	23	1	0	41.4	20.9	9	4.6	3.5		3.5		
859	1959	3	8	11	17	10	40.21	19.8	13	5.3	4.7		4.7		
860	1959	4	25	3	10	0	41.7	21	5	4.3	3		3		
861	1959	6	6	11	31	0	42	21.5	5	4.2	2.7		2.7		
862	1959	6	9	17	32	0	42	21.5	6	4.7	3.7		3.7		
863	1959	6	16	0	32	17	42.19	24.1	14	5.2	4.5		4.5		
864	1959	6	17	12	32	6	42.6	20.2	13	5	4.2		4.2		
865	1959	7	26	17	7	3	40.85	27.5	32	5.5	5.1		5.1		
866	1959	8	11	23	28	7	41.14	22.7	20	5.1	4.3		4.3		
867	1959	8	17	1	33	14	40.89	19.8	16	6	5.9		5.9		
868	1959	8	17	4	29	1	40.58	19.6	7	5.3	4.7		4.7		
869	1959	8	18	22	4	2	41.04	19.8	16	5.3	4.7		4.7		
870	1959	8	18	23	36	0	40	20.3	14	4.8	3.9		3.9		
871	1959	9	1	11	37	41	40.87	19.8	14	6.3	6.2		6.2		
872	1959	9	3	4	2	2	40.75	19.7	0	5.2	4.6		4.6		
873	1959	10	5	20	34	6	40.82	19.9	11	5.5	5.3		5.3		
874	1959	10	7	8	30	41	40.9	19.6	12	5.8	5.6		5.6		
875	1959	10	7	9	34	55	41	19.8	9	5.1	4.3		4.3		
876	1959	10	10	16	11	1	40.5	19.5	12	5.1	4.4		4.4		
877	1959	11	6	7	37	24	41.6	20.4	18	5.3	4.8		4.8		
878	1960	1	4	12	51	55	44.8	26.9	25	4.5	4.5		4.5		
879	1960	1	6	13	39	0	39.8	20.2	30	5	4.1		4.1		
880	1960	3	6	20	37	6	41.3	26.5	27	5	4.1		4.1		
881	1960	3	9	8	35	48	40.5	26	30	5	4.1		4.1		
882	1960	3	12	11	54	1	41.89	20.9	11	5.9	5.7		5.7		
883	1960	3	12	12	2	32	41.95	20.9	8	4.9	4		4		
884	1960	4	19	18	4	27	39.7	19.9	3	4.7	3.7		3.7		
885	1960	5	26	0	48	0	39.6	19.9	14	4.9	4		4		
886	1960	5	26	0	54	44	40.6	20.6	8	5	4.2		4.2		
887	1960	5	26	5	10	11	40.6	20.6	9	6.5	6.5		6.5		
888	1960	5	26	5	37	58	40.6	20.6	14	5.2	4.5		4.5		
889	1960	6	9	8	24	1	40.5	20.3	13	5.3	4.8		4.8		
890	1960	6	12	23	10	8	42.85	28	30	4.9	4		4		
891	1960	7	9	22	42	54	41	21	12	5.3	4.7		4.7		
892	1960	9	28	22	23	30	39.8	20.2	14	5	4.1		4.1		
893	1960	11	1	16	13	59	41.1	21.3	16	5.3	4.8		4.8		
894	1960	11	4	6	43	48	40	20.7	7	4.6	3.4		3.4		
895	1961	6	22	0	56	3	42.4	19.3	13	5.4	4.9		4.9		
896	1961	6	22	1	13	0	42.3	19.2	10	4.8	3.9		3.9		
897	1961	8	17	8	37	48	42.5	26.3	8	4.9	4		4		
898	1961	11	23	6	46	0	42.6	22	8	4.6	3.5		3.5		
899	1961	11	28	8	58	0	40	26.2	100	5.5	5.2	5.2			
900	1961	12	12	4	36	0	42.2	19.3	13	5	4.1		4.1		
901	1962	3	18	15	30	33	40.7	19.6	24	6.3	6.2		6.2		
902	1962	4	6	18	48	0	40.8	19.8	50	5.1	4.3		4.3		

										Homogenized magnitudes		Reported magnitudes			
Event Number	Year	Month	Date	Hour	Minute	Second	Latitude	Longitude	Depth	M_w	M_s	mb	M_s	M_w	ML
903	1962	4	7	21	35	30	40.8	19.8	40	5.1	4.3		4.3		
904	1962	5	10	18	31	0	42.1	19.2	22	5.1	4.4		4.4		
905	1962	6	26	14	54	21	42.8	23.7	13	4.9	4		4		
906	1962	6	28	6	51	5	40.8	20.9	16	5.5	5		5		
907	1962	9	17	19	44	45	41.15	20.7	15	5.1	4.4		4.4		
908	1962	10	8	14	26	37	41.94	24.2	13	5.2	4.5		4.5		
909	1962	10	8	15	11	15	42	24.2	18	5.2	4.6		4.6		
910	1962	12	10	6	18	0	41.2	20.7	9	4.8	3.8		3.8		
911	1962	12	11	0	15	0	41.1	20.8	12	4.8	3.8		3.8		
912	1962	12	14	10	57	0	44.6	20.4	19	4	4		4		
913	1962	12	23	0	43	50	41.1	20.2	16	5.3	4.7		4.7		
914	1963	1	24	3	58	0	40	19.6	30	5.1	4.4		4.4		
915	1963	2	14	12	48	2	40.4	19.9	20	5.1	4.3		4.3		
916	1963	2	15	10	18	21	40.2	20.1	16	5.2	4.6		4.6		
917	1963	2	22	8	23	0	41.8	22.8	7	4.7	3.7		3.7		
918	1963	2	22	14	12	53	40.3	20	14	5.6	5.2		5.2		
919	1963	3	29	3	9	13	40.3	26.6	16	5.2	4.6		4.6		
920	1963	4	15	11	46	0	42	21.5	5	4.2	2.7		2.7		
921	1963	4	18	11	4	0	41.8	21.8	5	4.5	3.3		3.3		
922	1963	4	18	11	7	0	41.8	21.8	4	4.1	2.5		2.5		
923	1963	4	23	14	2	57	42.4	19.5	12	5.1	4.4		4.4		
924	1963	4	25	6	5	33	42.2	19.3	11	5	4.2		4.2		
925	1963	4	28	0	42	11	40.5	27.4	160	5.4	5	5.1			
926	1963	5	15	11	15	40	41.7	20.1	12	5.1	4.4		4.4		
927	1963	6	26	5	48	0	41.8	23.5	14	5	4.2		4.2		
928	1963	6	27	11	5	48	41.8	23.5	8	4.9	4		4		
929	1963	6	30	1	0	0	43.2	25.8	9	4	4		4		
930	1963	7	26	4	17	11	42.02	21.4	11	6.3	6.2		6.2		
931	1963	7	26	4	32	47	42.1	21.4	6	5	4.2		4.2		
932	1963	7	26	4	35	42	42.05	21.4	5	4.5	3.3		3.3		
933	1963	7	26	4	53	9	42.05	21.4	6	5	4.2		4.2		
934	1963	7	26	8	23	0	42.1	21.4	5	4.4	3.1		3.1		
935	1963	7	26	8	39	0	42.1	21.4	5	4.4	3.1		3.1		
936	1963	7	26	15	40	40	42.1	21.4	5	4.5	3.3		3.3		
937	1963	7	26	17	56	0	42.1	21.4	5	4.4	3.1		3.1		
938	1963	7	27	20	38	0	42	21.4	5	4.4	3.1		3.1		
939	1963	7	28	2	44	0	42	21.5	5	4.4	3.1		3.1		
940	1963	7	28	13	42	0	42	21.4	5	4.4	3.1		3.1		
941	1963	7	29	1	1	0	42	21.5	5	4.4	3.1		3.1		
942	1963	7	29	20	56	0	42.1	21.4	5	4.4	3.1		3.1		
943	1963	7	30	23	52	0	42.1	21.4	5	4.4	3.1		3.1		
944	1963	7	31	8	5	0	42	21.5	5	4.4	3.1		3.1		
945	1963	7	31	23	22	0	42.1	21.4	5	4.4	3.1		3.1		
946	1963	7	31	23	27	0	42	21.9	5	4.4	3.1		3.1		
947	1963	7	31	23	47	0	42	21.6	5	4.4	3.1		3.1		
948	1963	8	10	14	48	0	42	21.6	5	4.4	3.1		3.1		
949	1963	8	15	10	58	0	41.9	21.6	5	4.2	2.7		2.7		
950	1963	8	16	2	44	0	41.9	21.5	5	4.2	2.7		2.7		
951	1963	8	17	20	0	0	42	21.5	5	4.2	2.7		2.7		
952	1963	8	23	23	20	0	42	21.6	5	4.5	3.3		3.3		
953	1963	8	23	23	58	0	42	21.6	4	4.1	2.5		2.5		
954	1963	10	20	20	19	0	41.9	20.9	5	4.2	2.7		2.7		
955	1963	10	20	22	35	0	41.9	20.9	5	4.2	2.7		2.7		
956	1964	2	23	22	41	3.9	39.21	23.73	10	5.2	4.6	4.9			
957	1964	2	24	23	6	55.1	39.18	23.7	0	4.3	3.3	4.2			
958	1964	2	24	23	30	28	39.09	23.8	41	5.2	4.6	4.9			
959	1964	2	27	1	37	51.3	40.54	21.4	44	4.4	3.5	4.3			
960	1964	3	31	0	48	45.8	39.3	21.6	33	4.3	3.3	4.2			
961	1964	4	11	16	0	43	40.3	24.83	33	5.4	5	5.1			
962	1964	4	12	7	58	3	39.8	25	0	4.1	3.1	4.1			
963	1964	4	15	20	54	27.4	39.04	23.71	44	4.8	4	4.6			
964	1964	4	18	21	52	54	41.1	29	33	4.3	3.3	4.2			
965	1964	4	19	11	33	41.3	41.8	19.8	33	4.3	3.3	4.2			
966	1964	4	29	4	21	5.1	39.25	23.72	20	5.7	5.3	5.3			
967	1964	4	29	17	0	1.3	39.14	23.55	15	5.2	4.6	4.9			
968	1964	4	29	17	29	18.6	39.02	23.97	10	4.3	3.3	4.2			
969	1964	4	30	18	11	31.2	39.17	23.8	26	4.5	3.7	4.4			
970	1964	7	3	11	48	40	39	23.8	0	4.1	3.1	4.1			
971	1964	7	4	11	11	17.9	41.96	23.43	2	4.8	4	4.6			
972	1964	8	24	21	42	46.2	40.51	19.2	41	4.6	3.8	4.5			
973	1964	9	13	22	53	22.9	41.71	20.6	0	4	2.9	4			
974	1964	9	21	5	6	9.9	39.65	22.68	33	4.5	3.7	4.4			
975	1964	10	5	1	23	50.6	40.15	19.7	25	4.1	3.1	4.1			
976	1964	10	6	14	29	57.9	40.24	28.16	23	5.8	5.5	5.4			
977	1964	10	6	14	31	23	40.3	28.23	34	6.6	6.7	6			
978	1964	10	7	23	7	53.9	40.19	28.36	31	4.5	3.7	4.4			
979	1964	10	29	4	35	58.7	43.32	19.9	0	4.3	3.4	4.2			
980	1964	11	20	6	59	18.7	40.2	28.06	56	4.5	3.7	4.4			
981	1964	12	9	18	28	46	41.57	20.92	78	4.4	3.5	4.3			
982	1964	12	9	19	6	21.4	41.2	20.92	55	4.5	3.7	4.4			
983	1964	12	15	8	20	44	40.5	20.9	33	4.4	3.5	4.3			
984	1964	12	15	21	3	15.7	40.02	28.79	26	4.9	4.2	4.7			

										Homogenized magnitudes		Reported magnitudes			
Event Number	Year	Month	Date	Hour	Minute	Second	Latitude	Longitude	Depth	M_w	M_s	mb	M_s	M_w	ML
985	1964	12	21	0	50	10	40.5	27.5	0	4.8	4	4.6			
986	1964	12	23	21	3	3.5	41.09	20.77	40	4.1	3.1	4.1			
987	1965	1	28	23	10	46.8	42.5	23.1	77	4.4	3.5	4.3			
988	1965	3	9	17	57	54.5	39.34	23.82	18	6	5.9	5.6			
989	1965	3	9	18	37	54.6	39.28	23.93	33	5.4	5	5.1			
990	1965	3	9	19	46	58.7	39.12	23.86	19	5.2	4.6	4.9			
991	1965	3	9	21	20	4.5	39.19	23.87	7	4.6	3.8	4.5			
992	1965	3	9	22	19	6.4	39.17	23.96	13	4.5	3.7	4.4			
993	1965	3	9	22	35	15.3	39.26	23.84	18	4.9	4.2	4.7			
994	1965	3	10	0	4	32.9	39.19	23.76	0	4	2.9	4			
995	1965	3	10	1	36	5.8	39.08	23.77	18	5.3	4.8	5			
996	1965	3	10	21	50	19.8	39.35	23.94	37	4.8	4	4.6			
997	1965	3	13	4	8	40.6	39.11	23.97	11	4.9	4.2	4.7			
998	1965	3	13	4	9	37.9	39.03	23.68	33	5.4	5	5.1			
999	1965	3	13	9	9	29.5	39.1	24.1	0	4	2.9	4			
1000	1965	3	13	11	33	0.3	39.13	23.97	33	4.8	4	4.6			
1001	1965	3	13	15	42	16.5	39.14	23.9	18	4.8	4	4.6			
1002	1965	3	14	6	4	49.3	39.9	20.2	0	4.5	3.7	4.4			
1003	1965	3	15	23	8	30.9	39.16	24	33	4.9	4.2	4.7			
1004	1965	3	19	4	35	45.4	41.5	23.1	12	4.3	3.3	4.2			
1005	1965	3	19	23	37	31.9	41.39	22.88	33	4.4	3.5	4.3			
1006	1965	3	22	3	22	22.2	39.13	23.84	1	4.6	3.8	4.5			
1007	1965	3	31	20	8	25.5	39.2	24.1	33	4.6	3.8	4.5			
1008	1965	5	13	21	9	16.7	39.22	20.7	58	4.4	3.5	4.3			
1009	1965	5	31	18	29	41	42.8	22.2	0	4	2.9	4			
1010	1965	6	3	18	31	51	39.72	23.21	33	5	4.4	4.8			
1011	1965	6	24	23	36	14.5	39.46	21.95	0	4.3	3.3	4.2			
1012	1965	8	23	14	8	58.6	40.51	26.17	33	5.5	5.2	5.2			
1013	1965	8	24	23	57	35.4	40.39	26.2	18	4.3	3.3	4.2			
1014	1965	9	11	4	49	12.8	39.07	22.09	42	4.4	3.5	4.3			
1015	1965	10	28	14	39	28.5	41.67	19.3	28	4.5	3.7	4.4			
1016	1965	11	2	3	27	7.4	39.48	25.32	5	4.9	4.2	4.7			
1017	1965	11	20	19	58	10.9	39.6	22.4	105	4	2.9	4			
1018	1965	12	13	17	44	8.4	40.25	19.82	7	4.5	3.7	4.4			
1019	1965	12	20	0	8	16	40.21	24.82	33	5.4	5	5.1			
1020	1965	12	20	0	30	57.6	40.01	24.8	42	4.4	3.5	4.3			
1021	1965	12	25	10	18	10.2	44.06	19.97	0	4.3	3.4	4.2			
1022	1965	12	25	12	15	33.1	39.84	25	41	4.6	3.8	4.5			
1023	1966	1	17	8	39	42.6	40.09	20.57	46	4.5	3.7	4.4			
1024	1966	1	20	0	39	0.6	39.2	24.44	12	4.5	3.7	4.4			
1025	1966	1	22	5	1	38.1	39.08	21.6	0	4.5	3.7	4.4			
1026	1966	1	27	20	32	16	39.8	23.5	15	4.3	3.3	4.2			
1027	1966	1	31	4	30	57	39.05	21.9	51	4.6	3.8	4.5			
1028	1966	2	5	2	1	45.3	39.1	21.74	16	6.2	6.1	5.7			
1029	1966	2	5	2	11	8	39.17	21.89	21	5.2	4.6	4.9			
1030	1966	2	5	2	56	15.6	39.19	21.9	0	4.4	3.5	4.3			
1031	1966	2	5	2	58	1.2	39.11	21.91	50	5.4	5	5.1			
1032	1966	2	6	13	24	38.1	39.02	21.7	36	4.4	3.5	4.3			
1033	1966	2	8	20	8	4	41.08	24.97	21	4.9	4.2	4.7			
1034	1966	2	9	5	36	23.1	41.11	24.92	48	4.5	3.7	4.4			
1035	1966	2	11	6	49	37	39.15	21.45	24	4.5	3.7	4.4			
1036	1966	2	14	13	45	34	40.1	21	0	4.4	3.5	4.3			
1037	1966	2	17	7	37	45	39.03	21.6	25	4.4	3.5	4.3			
1038	1966	2	19	10	22	27	39.04	21.65	8	4.5	3.7	4.4			
1039	1966	2	22	10	5	30	39.4	21.1	0	6	5.9	5.6			
1040	1966	2	25	12	36	25	39.04	21.32	17	4.5	3.7	4.4			
1041	1966	3	14	14	8	41.2	39.07	21.36	45	4.9	4.2	4.7			
1042	1966	4	5	8	7	25	39.04	21.96	19	4.4	3.5	4.3			
1043	1966	4	18	8	37	8	39	21.4	1	4.4	3.5	4.3			
1044	1966	4	23	11	8	9.9	39.01	21.32	38	4.5	3.7	4.4			
1045	1966	5	25	9	6	57	40.32	19.82	21	4.8	4	4.6			
1046	1966	6	29	0	49	35	41.29	20.47	16	4.4	3.5	4.3			
1047	1966	6	30	19	21	29	41.18	20.85	19	4.6	3.8	4.5			
1048	1966	7	3	15	59	33	40.3	23.1	0	4.1	3.1	4.1			
1049	1966	7	31	11	3	21	41.2	21.2	31	4.3	3.3	4.2			
1050	1966	8	8	11	43	41	40.7	21.6	47	4.3	3.3	4.2			
1051	1966	8	9	3	34	15.1	40.22	19.86	38	5	4.4	4.8			
1052	1966	8	16	3	28	40	40	19.6	0	4.5	3.7	4.4			
1053	1966	8	16	3	53	41.7	40.16	19.75	20	4.9	4.2	4.7			
1054	1966	8	21	1	30	43.5	40.33	27.4	12	5	4.4	4.8			
1055	1966	9	6	22	41	5.7	39.35	25.1	33	4.9	4.2	4.7			
1056	1966	9	12	9	37	38	40.13	20.5	9	4.5	3.7	4.4			
1057	1966	9	22	20	14	39.4	39.83	23.92	35	4.9	4.2	4.7			
1058	1966	10	3	23	38	59	39.32	25.01	16	4.4	3.5	4.3			
1059	1966	10	11	2	55	40	41.4	19.7	49	4.3	3.3	4.2			
1060	1966	10	21	16	17	4	39.53	22.11	57	4.6	3.8	4.5			
1061	1966	10	22	5	38	24	41.96	23.09	13	4.8	4	4.6			
1062	1966	11	6	18	51	44.1	42.15	19.01	37	4.5	3.7	4.4			
1063	1966	11	9	15	12	28	39.18	20.54	35	4.8	4	4.6			
1064	1967	1	11	21	49	12	39.11	21.49	11	4.4	3.5	4.3			
1065	1967	2	9	14	8	18.2	39.92	20.26	1	5.8	5.5	5.4			
1066	1967	2	27	6	27	11.9	39.98	20.21	37	4.5	3.7	4.4			

										Homogenized magnitudes		Reported magnitudes			
Event Number	Year	Month	Date	Hour	Minute	Second	Latitude	Longitude	Depth	M_w	M_s	mb	M_s	M_w	ML
1067	1967	2	27	21	0	42	44.86	26.69	32	4.9	4.4	4.7			
1068	1967	3	1	5	17	13	40.33	22.35	1	4.4	3.5	4.3			
1069	1967	3	4	17	58	9	39.25	24.6	60	6.4	6.5	5.9			
1070	1967	3	16	22	24	54.8	39.35	24.27	0	5.2	4.6	4.9			
1071	1967	4	4	3	47	17	40.32	26.2	32	4.6	3.8	4.5			
1072	1967	4	4	9	48	33.8	40.31	26	0	4.5	3.7	4.4			
1073	1967	5	1	7	9	3	39.6	21.29	34	5.9	5.7	5.5			
1074	1967	5	1	8	15	46.9	39.75	21.42	38	4.6	3.8	4.5			
1075	1967	5	1	8	28	23	39.39	21.5	34	4.6	3.8	4.5			
1076	1967	5	1	9	47	40	39.46	21.23	10	4.6	3.8	4.5			
1077	1967	5	1	9	50	8.2	39.51	21.3	33	5	4.4	4.8			
1078	1967	5	1	14	38	2	39.36	21.31	21	4.6	3.8	4.5			
1079	1967	5	1	16	40	6	39.51	21.48	38	4.4	3.5	4.3			
1080	1967	5	2	1	27	20.4	39.56	21.2	35	4.5	3.7	4.4			
1081	1967	5	2	8	11	55.9	39.45	21.29	39	4.5	3.7	4.4			
1082	1967	5	2	13	51	26	39.9	21	0	4.1	3.1	4.1			
1083	1967	5	2	19	29	27.4	39.72	21.31	35	4.4	3.5	4.3			
1084	1967	5	3	18	41	47.2	39.53	21.34	37	4.9	4.2	4.7			
1085	1967	5	4	4	46	19.1	39.53	21.52	55	4.6	3.8	4.5			
1086	1967	5	4	8	53	17	39.9	22.1	74	4	2.9	4			
1087	1967	5	4	8	53	42	39.8	21.5	0	4.1	3.1	4.1			
1088	1967	5	4	8	55	58	40.6	19.5	33	4.4	3.5	4.3			
1089	1967	5	4	13	9	46.7	39.62	21.2	0	4.1	3.1	4.1			
1090	1967	5	4	13	13	35.8	39.78	21.52	60	4.5	3.7	4.4			
1091	1967	5	4	13	31	7.8	39.63	21.26	39	4.8	4	4.6			
1092	1967	5	4	17	11	3	39.8	21.1	0	4.5	3.7	4.4			
1093	1967	5	5	6	26	37.9	39.56	21.29	57	4.8	4	4.6			
1094	1967	5	5	14	50	3.3	39.42	21.15	45	4.4	3.5	4.3			
1095	1967	5	5	15	58	36	39.7	21.1	0	4.4	3.5	4.3			
1096	1967	5	5	20	18	32	39.56	21.25	20	4.1	3.1	4.1			
1097	1967	5	9	4	5	13	39.61	27.15	37	4.8	4	4.6			
1098	1967	5	9	8	0	47.3	39.72	21.39	53	5	4.4	4.8			
1099	1967	6	12	18	12	46.6	39.06	21.27	46	4.5	3.7	4.4			
1100	1967	7	2	1	14	8	44	19.1	33	4.3	3.4	4.2			
1101	1967	7	2	1	17	10	43.6	20.3	0	4.3	3.4	4.2			
1102	1967	7	3	2	53	43	44.02	19.18	1	4.8	4.2	4.6			
1103	1967	7	13	14	38	58.4	40.66	19.67	73	4.6	3.8	4.5			
1104	1967	7	20	19	3	30.4	40.72	19.88	58	4.5	3.7	4.4			
1105	1967	7	25	8	37	26	41.9	25	53	4.4	3.5	4.3			
1106	1967	7	31	7	12	5	40.6	27.62	4	4.3	3.3	4.2			
1107	1967	8	6	14	9	33	41	28.8	0	4.4	3.5	4.3			
1108	1967	9	7	0	32	22	40.75	19.58	13	4.5	3.7	4.4			
1109	1967	9	8	2	4	45	40.6	20.08	1	4.9	4.2	4.7			
1110	1967	9	8	9	51	42.8	39.08	21.4	40	4.5	3.7	4.4			
1111	1967	9	12	14	46	42	39.23	21.46	25	4.6	3.8	4.5			
1112	1967	9	24	22	11	20.4	40.86	19.7	35	4.5	3.7	4.4			
1113	1967	9	26	5	5	37.4	41.53	20.94	39	4.5	3.7	4.4			
1114	1967	10	7	17	36	45	39.09	23.34	6	4.8	4	4.6			
1115	1967	11	6	10	32	58	39.05	20.61	1	4.9	4.2	4.7			
1116	1967	11	9	10	12	5	41.5	22	0	4.6	3.8	4.5			
1117	1967	11	19	1	30	25	41.28	20.53	20	4.4	3.5	4.3			
1118	1967	11	26	3	24	57.4	39.4	20.49	37	4.9	4.2	4.7			
1119	1967	11	30	7	23	50.4	41.41	20.44	21	6.3	6.2	5.8	6.2		
1120	1967	11	30	7	42	52	41.43	20.49	21	4.9	4.2	4.7			
1121	1967	11	30	7	53	49.6	41.38	20.6	39	4.5	3.7	4.4			
1122	1967	11	30	8	11	29	41.45	20.56	12	4.5	3.7	4.4			
1123	1967	11	30	8	13	17.5	41.4	20.5	30	4.6	3.8	4.5			
1124	1967	11	30	9	21	0	42	21.7	124	4	2.9	4			
1125	1967	11	30	9	51	28	41.6	20.6	34	4.5	3.7	4.4			
1126	1967	11	30	9	55	27	41.1	20.3	33	4.4	3.5	4.3			
1127	1967	11	30	10	13	56	41.6	20.6	61	4.4	3.5	4.3			
1128	1967	11	30	11	57	33	41.4	20.2	37	4.1	3.1	4.1			
1129	1967	12	1	8	38	34.8	41.21	20.3	0	4.6	3.8	4.5			
1130	1967	12	1	9	15	26	41.12	19.8	40	4.4	3.5	4.3			
1131	1967	12	1	10	25	16	42.2	19.4	33	4.3	3.3	4.2			
1132	1967	12	1	18	30	57.1	41.37	20.27	0	4.6	3.8	4.5			
1133	1967	12	1	20	7	51	41.28	20.28	28	4.9	4.2	4.7			
1134	1967	12	2	0	24	13	41.31	20.34	8	5.7	5.3	5.3			
1135	1967	12	2	9	27	8	41.2	20.08	19	4.6	3.8	4.5			
1136	1967	12	2	12	44	42.7	41.32	20.29	16	5.5	5.2	5.2			
1137	1967	12	2	14	18	4	41.29	20.29	42	4.5	3.7	4.4			
1138	1967	12	2	14	18	57	40.7	21.4	33	4.6	3.8	4.5			
1139	1967	12	2	22	25	27	41.4	20.6	91	4.4	3.5	4.3			
1140	1967	12	3	17	59	25	41.25	20.2	25	4.4	3.5	4.3			
1141	1967	12	4	0	48	51	41.17	20.66	10	4.3	3.3	4.2			
1142	1967	12	6	0	1	56	41.3	20.4	42	4.4	3.5	4.3			
1143	1967	12	7	18	3	35	41.27	20.24	32	4.5	3.7	4.4			
1144	1967	12	8	7	8	31.2	41.45	20	33	4.4	3.5	4.3			
1145	1967	12	15	21	24	35	41.5	20.7	84	4.3	3.3	4.2			
1146	1967	12	19	8	32	32.3	41.49	20.43	29	5	4.4	4.8			
1147	1967	12	21	0	9	40	42.16	20.62	26	4.6	3.8	4.5			
1148	1967	12	22	7	21	57.8	41.21	20.4	0	4.4	3.5	4.3			

										Homogenized magnitudes		Reported magnitudes			
Event Number	Year	Month	Date	Hour	Minute	Second	Latitude	Longitude	Depth	M_w	M_s	mb	M_s	M_w	ML
1149	1967	12	29	19	49	24.1	41.41	20.27	46	4.9	4.2	4.7			
1150	1967	12	29	22	54	59	41.44	20.1	56	4.4	3.5	4.3			
1151	1967	12	30	21	27	20.3	40.66	21.47	34	4.5	3.7	4.4			
1152	1967	12	31	20	2	43	41.3	20.1	33	4.4	3.5	4.3			
1153	1968	1	12	15	5	25.9	41.37	20.3	0	4.4	3.5	4.3			
1154	1968	2	19	22	45	42.4	39.4	24.94	7	6.9	7	6	7		
1155	1968	2	19	23	9	46.4	39.36	24.7	0	4.8	4	4.6			
1156	1968	2	19	23	12	32	39.62	25.5	0	5	4.4	4.8			
1157	1968	2	19	23	21	2	39.8	26.4	0	5.5	5.2	5.2			
1158	1968	2	19	23	32	1	39.5	25.2	0	4.9	4.2	4.7			
1159	1968	2	19	23	34	42	40	24.9	186	4.4	3.5	4.3			
1160	1968	2	19	23	53	51	39.55	25.3	33	4.8	4	4.6			
1161	1968	2	20	0	21	51	39.5	25.4	0	5	4.4	4.8			
1162	1968	2	20	0	39	15.7	39.73	25.37	37	5.3	4.8	5			
1163	1968	2	20	1	28	29	39.4	25.6	46	4.6	3.8	4.5			
1164	1968	2	20	2	21	52	39.56	25.45	8	5.3	4.8	5			
1165	1968	2	20	2	29	28	39.3	24.9	33	4.8	4	4.6			
1166	1968	2	20	4	41	35	39.78	25.4	0	4.5	3.7	4.4			
1167	1968	2	20	6	15	46	39.3	25.5	32	4.5	3.7	4.4			
1168	1968	2	20	9	35	51.6	39.41	24.88	33	4.6	3.8	4.5			
1169	1968	2	20	9	41	9.9	39.35	24.95	33	4.9	4.2	4.7			
1170	1968	2	20	16	50	52.3	39.2	25.6	0	4.9	4.2	4.7			
1171	1968	2	20	21	5	23.6	39.25	25.05	33	5	4.4	4.8			
1172	1968	2	21	0	17	28	39.56	24.97	2	4.8	4	4.6			
1173	1968	2	21	1	0	41.9	40.6	21	0	4.5	3.7	4.4			
1174	1968	2	21	3	28	46.8	39.49	25.15	0	5	4.4	4.8			
1175	1968	2	21	5	38	12	39.41	25.1	6	4.3	3.3	4.2			
1176	1968	2	21	5	55	22.3	39.27	25.2	0	4.8	4	4.6			
1177	1968	2	21	7	18	50	39.3	25	6	4.5	3.7	4.4			
1178	1968	2	21	12	35	55.3	39.61	25.3	0	4.8	4	4.6			
1179	1968	2	21	17	16	42	41.8	19.1	401	4.3	3.3	4.2			
1180	1968	2	21	17	48	17	39.4	25.3	0	4.9	4.2	4.7			
1181	1968	2	22	2	16	39	39.66	25.72	6	4.6	3.8	4.5			
1182	1968	2	22	4	57	47	39.39	25.02	19	4.9	4.2	4.7			
1183	1968	2	22	12	22	50	41.7	20.13	46	4.3	3.3	4.2			
1184	1968	2	22	12	34	11	41.5	20	33	4.4	3.5	4.3			
1185	1968	2	22	15	7	25.8	39.45	24.91	0	4.1	3.1	4.1			
1186	1968	2	24	12	55	3	41.44	20.18	24	4.6	3.8	4.5			
1187	1968	2	26	5	43	30.4	39.39	24.79	0	4.6	3.8	4.5			
1188	1968	2	27	6	32	54	39.38	24.89	28	4.6	3.8	4.5			
1189	1968	2	27	13	20	15.7	39.59	25.51	36	4.8	4	4.6			
1190	1968	2	27	13	37	45.4	39.61	25.51	35	5	4.4	4.8			
1191	1968	2	28	0	31	43.8	39.48	25.03	0	4.5	3.7	4.4			
1192	1968	2	29	11	46	42	39.5	26	0	4.6	3.8	4.5			
1193	1968	2	29	12	47	33.5	39.12	24.32	18	4.5	3.7	4.4			
1194	1968	3	2	6	53	1	45	20.7	0	5.3	5	5			
1195	1968	3	4	14	48	39.7	39.53	25.9	0	4.1	3.1	4.1			
1196	1968	3	6	5	14	49	39.34	25.04	0	4.6	3.8	4.5			
1197	1968	3	7	17	5	0	39.2	21.6	59	4.5	3.7	4.4			
1198	1968	3	7	17	49	27	39.3	20	0	4.8	4	4.6			
1199	1968	3	10	6	48	17.1	39.1	24.36	33	4.6	3.8	4.5			
1200	1968	3	10	7	10	59	39.13	24.23	0	5.3	4.8	5			
1201	1968	3	10	8	5	22.2	39.05	24.5	0	4.8	4	4.6			
1202	1968	3	10	8	51	21.7	39.05	24.39	0	4.4	3.5	4.3			
1203	1968	3	11	17	32	46.9	39.5	25.56	0	4.9	4.2	4.7			
1204	1968	3	15	2	59	32.6	41.24	20.3	44	4.3	3.3	4.2			
1205	1968	3	15	22	56	36.9	43.89	20.35	43	4.3	3.4	4.2			
1206	1968	3	16	18	11	5.8	39.38	24.94	43	4.6	3.8	4.5			
1207	1968	3	21	16	1	30.1	39.8	25.6	0	4.3	3.3	4.2			
1208	1968	3	21	16	9	23.8	39.76	25.49	19	4.4	3.5	4.3			
1209	1968	3	23	13	11	10.3	39.83	25.5	0	4.1	3.1	4.1			
1210	1968	3	23	17	16	35.8	39.78	25.64	0	4.8	4	4.6			
1211	1968	3	23	17	25	55	39.76	25.48	33	4.8	4	4.6			
1212	1968	3	23	21	13	43.1	39.77	25.56	28	4.1	3.1	4.1			
1213	1968	3	23	21	52	37	39.75	25.3	3	4.1	3.1	4.1			
1214	1968	3	24	9	23	11.4	39.74	25.46	0	4.4	3.5	4.3			
1215	1968	3	26	17	9	30.7	39.57	25.46	36	4.4	3.5	4.3			
1216	1968	3	27	5	16	13	39.78	25.44	6	4.3	3.3	4.2			
1217	1968	3	28	16	37	47.3	39.49	20.38	18	4.9	4.2	4.7			
1218	1968	3	29	6	29	5	43.54	20.85	17	4.4	3.6	4.3			
1219	1968	3	29	7	8	31	39.6	20.6	0	4.4	3.5	4.3			
1220	1968	4	2	15	25	2	39.9	25.4	26	4.4	3.5	4.3			
1221	1968	4	5	15	54	32.7	39.76	25.55	18	4.6	3.8	4.5			
1222	1968	4	5	16	3	56.1	39.7	25.54	0	4.3	3.3	4.2			
1223	1968	4	5	16	10	9	39.3	25.9	0	4.5	3.7	4.4			
1224	1968	4	8	8	28	40.7	41.49	20.26	0	4.3	3.3	4.2			
1225	1968	4	8	8	59	9	39.68	25.5	9	4.5	3.7	4.4			
1226	1968	4	8	10	10	24	41.1	19.9	0	4.3	3.3	4.2			
1227	1968	4	10	7	15	38.7	39.71	25.49	0	4.3	3.3	4.2			
1228	1968	4	15	18	22	26	39.3	25.01	22	4.5	3.7	4.4			
1229	1968	4	18	3	8	3.4	41.25	20.22	36	4.5	3.7	4.4			
1230	1968	4	24	8	18	3.3	39.33	24.88	20	5.4	5	5.1			

										Homogenized magnitudes		Reported magnitudes			
Event Number	Year	Month	Date	Hour	Minute	Second	Latitude	Longitude	Depth	M_w	M_s	mb	M_s	M_w	ML
1231	1968	4	25	4	27	29	39.15	20.2	4	4.4	3.5	4.3			
1232	1968	5	3	3	28	12	39.06	21.33	0	4.5	3.7	4.4			
1233	1968	5	6	9	38	47	40.33	28.63	4	4.4	3.5	4.3			
1234	1968	7	22	9	22	5.9	39.67	25.66	0	4.4	3.5	4.3			
1235	1968	7	25	22	5	29	40.95	20.09	23	4.6	3.8	4.5			
1236	1968	8	4	0	53	3.1	39	22.15	89	4	2.9	4			
1237	1968	8	9	7	38	50	39.1	24.4	0	4.4	3.5	4.3			
1238	1968	8	14	18	23	20	39.08	21.81	0	4.4	3.5	4.3			
1239	1968	9	28	0	53	28	40.49	26.38	28	4.5	3.7	4.4			
1240	1968	10	3	18	18	34.8	40.13	19.85	58	4.9	4.2	4.7			
1241	1968	10	14	23	0	26	39.8	23.4	0	4.5	3.7	4.4			
1242	1968	11	3	4	49	33.7	42.1	19.35	28	5.5	5.3	5.1	5.3		
1243	1968	11	6	5	12	18	39	23.44	23	4.4	3.5	4.3			
1244	1968	11	6	14	49	42.9	39.68	25.45	0	4.3	3.3	4.2			
1245	1968	11	8	15	26	50.1	39.74	25.64	0	4.1	3.1	4.1			
1246	1968	11	9	12	38	58	40.15	28.35	24	4.3	3.3	4.2			
1247	1968	11	27	1	18	46.2	40.06	19.5	0	4.1	3.1	4.1			
1248	1969	1	10	4	32	3.4	39.23	19.97	37	4.6	3.8	4.5			
1249	1969	1	20	10	20	49	40.2	19.1	0	4.1	3.1	4.1			
1250	1969	1	31	15	34	28	39.1	20.43	4	4.8	4	4.6			
1251	1969	2	5	7	17	44.5	39.85	20.9	0	4.1	3.1	4.1			
1252	1969	2	5	22	44	16	41.1	22.8	37	4.8	4	4.6			
1253	1969	2	9	20	18	47	39.3	25.5	0	4.3	3.3	4.2			
1254	1969	2	21	18	39	57	39.14	21.87	33	4.8	4	4.6			
1255	1969	2	22	0	35	14.9	40.38	19.6	0	4.4	3.5	4.3			
1256	1969	2	24	9	8	45	39.3	21.6	0	4.5	3.7	4.4			
1257	1969	3	2	12	13	48	39.2	25.9	0	4.8	4	4.6			
1258	1969	3	3	0	59	10.5	40.08	27.5	6	5.9	5.8	5.6	5.8		
1259	1969	3	5	14	41	16.4	40.06	27.56	33	4.9	4.2	4.7			
1260	1969	3	22	18	0	55	39.1	28.67	28	4.9	4.2	4.7			
1261	1969	3	23	0	15	45	39.17	28.32	12	4.5	3.7	4.4			
1262	1969	3	23	3	50	58	39.3	28	10	4.8	4	4.6			
1263	1969	3	23	21	8	42.1	39.14	28.48	9	6.1	6	5.6	6		
1264	1969	3	24	1	59	34	39.11	28.51	30	5.5	5	5	5		
1265	1969	3	24	2	58	49	39.15	28.6	4	4.6	3.8	4.5			
1266	1969	3	24	8	13	5.4	39.02	28.41	43	5.2	4.5	4.7	4.5		
1267	1969	3	24	11	34	34	39.17	28.7	37	4.8	4	4.6			
1268	1969	3	24	12	13	17	39.08	28.65	20	4.9	4.2	4.7			
1269	1969	3	25	13	21	12	39.06	28.41	28	5.2	4.6	4.9			
1270	1969	3	25	13	21	34.2	39.25	28.44	37	6.1	6	5.5	6		
1271	1969	3	25	13	37	53	39	28	0	5.3	4.8	5			
1272	1969	3	25	14	18	52.1	39.17	28.49	34	5	4.4	4.8			
1273	1969	3	25	14	40	27	39.02	28.9	25	4.8	4	4.6			
1274	1969	3	25	16	13	30.4	39.08	28.44	42	4.9	4.2	4.7			
1275	1969	3	25	17	51	24	39.16	28	44	4.5	3.7	4.4			
1276	1969	3	26	3	31	26.5	39.03	28.27	37	4.8	4	4.6			
1277	1969	3	26	9	0	11	39.3	28.1	52	4.9	4.2	4.7			
1278	1969	3	26	13	50	41	39.3	28.2	0	4.4	3.5	4.3			
1279	1969	3	27	18	7	3	39.12	28.2	51	4.6	3.8	4.5			
1280	1969	3	28	10	2	17.4	39.13	28.45	37	5.2	4.5	4.9	4.5		
1281	1969	4	2	13	3	26.4	39.57	25.46	0	4.5	3.7	4.4			
1282	1969	4	3	22	12	21.9	40.66	19.98	21	5.7	5.5	5	5.5		
1283	1969	4	3	23	45	11.2	40.56	19.92	44	4.3	3.3	4.2			
1284	1969	4	4	4	20	46.3	40.48	19.7	33	4.1	3.1	4.1			
1285	1969	4	8	15	48	50.4	40.67	19.77	17	5	4.4	4.8			
1286	1969	4	12	15	33	6	39.33	28.1	0	4.4	3.5	4.3			
1287	1969	4	17	12	23	28.4	39.11	28.62	0	4.8	4	4.6			
1288	1969	4	20	4	59	29	39.2	28	0	4.1	3.1	4.1			
1289	1969	4	21	20	36	40	39.42	25.09	1	5.2	4.6	4.7	4.6		
1290	1969	4	30	20	20	32	39.12	28.52	8	5.6	5.2	5	5.2		
1291	1969	4	30	23	8	11	39.09	28.31	31	4.8	4	4.6			
1292	1969	5	3	16	7	59	39	28.6	25	4.9	4.2	4.7			
1293	1969	5	10	21	10	37.1	41.3	20.21	35	4	2.9	4			
1294	1969	5	13	17	48	2.1	39.03	28.57	35	4.8	4	4.6			
1295	1969	5	14	23	57	35.5	39.15	28.49	36	4.8	4	4.6			
1296	1969	5	15	4	49	5.6	40.51	19.71	0	4.4	3.5	4.3			
1297	1969	5	16	7	27	1.1	39.13	21.82	39	5.5	5	5.1	5		
1298	1969	5	31	14	20	24.8	41.21	24	0	4.3	3.3	4.2			
1299	1969	6	21	15	40	39.4	42.08	25.26	49	4.5	3.7	4.4			
1300	1969	6	22	17	27	32.8	39.12	28.6	0	4.6	3.8	4.5			
1301	1969	6	27	10	40	25	39.3	28.7	0	4.4	3.5	4.3			
1302	1969	7	7	18	12	27	40.49	19.78	42	4.1	3.1	4.1			
1303	1969	7	9	17	27	54	40.52	19.81	4	4.6	3.8	4.5			
1304	1969	8	9	16	25	35.9	42.33	19.22	30	5.5	5	4.5	5		
1305	1969	8	9	17	1	3	42.27	19.14	30	4.4	3.5	4.3			
1306	1969	8	14	21	51	5.3	39.52	27.87	21	5.2	4.6	4.7	4.6		
1307	1969	8	26	2	15	37.1	41.73	20.03	28	5.2	4.5	4.8	4.5		
1308	1969	10	7	5	9	12	39.2	28.4	13	5.5	5	4.9	5		
1309	1969	10	7	18	49	2.6	39.16	28.54	49	5.2	4.6	4.9			
1310	1969	10	12	13	34	19.9	39.76	20.55	46	5.4	4.9	5	4.9		
1311	1969	10	13	1	2	30.8	39.78	20.59	27	5.6	5.4	5.4	5.4		
1312	1969	10	13	3	24	26	39.17	28.38	9	5.2	4.6	4.9			

										Homogenized magnitudes		Reported magnitudes			
Event Number	Year	Month	Date	Hour	Minute	Second	Latitude	Longitude	Depth	M_w	M_s	mb	M_s	M_w	ML
1313	1969	10	27	8	42	19.3	39.82	20.43	54	4.5	3.7	4.4			
1314	1969	10	29	15	26	55.1	39.72	20.45	0	4.5	3.7	4.4			
1315	1969	11	14	13	49	39.3	41.2	19.8	0	4.4	3.5	4.3			
1316	1969	11	16	9	33	41	40.09	20.97	5	4.4	3.5	4.3			
1317	1969	11	17	0	49	42	40.1	21	39	4	2.9	4			
1318	1969	12	16	11	47	33.7	39.53	20.69	67	4.4	3.5	4.3			
1319	1969	12	23	2	13	49	39.37	23.8	6	5	4.4	4.8			
1320	1969	12	27	7	31	54.5	39.22	23.82	42	4.9	4.2	4.7			
1321	1969	12	28	17	39	36.6	39.13	23.4	0	4.6	3.8	4.5			
1322	1969	12	28	22	2	35.6	40.67	19.62	51	4.9	4.2	4.7			
1323	1970	1	17	6	30	28.4	41.86	19.48	33	4.1	3.1	4.1			
1324	1970	1	31	1	26	51	39	21.32	18	4.4	3.5	4.3			
1325	1970	2	9	2	4	17.3	39.88	20.62	55	4.3	3.3	4.2			
1326	1970	2	16	15	48	31.2	40.03	19.9	0	4.5	3.7	4.4			
1327	1970	2	17	0	16	28.3	39.34	20.62	53	4.8	4	4.6			
1328	1970	2	22	12	20	45.7	39.18	23.39	34	5.2	4.6	4.9			
1329	1970	2	24	18	8	22.3	39.11	23.4	0	4.4	3.5	4.3			
1330	1970	3	17	17	0	56.8	41.4	21.07	43	4.5	3.7	4.4			
1331	1970	3	19	6	19	40	41.4	19.8	0	4.1	3.1	4.1			
1332	1970	3	23	7	56	8	39.2	28.2	26	4.1	3.1	4.1			
1333	1970	3	23	20	56	1	39.04	20.49	7	5.3	4.7	4.5	4.7		
1334	1970	3	28	13	9	43	41.9	20	0	4.4	3.5	4.3			
1335	1970	3	28	22	59	34.1	39.13	29	0	4.1	3.1	4.1			
1336	1970	3	29	1	51	30.2	39.26	28.5	33	4.4	3.5	4.3			
1337	1970	4	1	3	46	43	39.3	28.7	25	4.5	3.7	4.4			
1338	1970	4	6	8	12	23.4	39.19	28.54	33	5.4	5	5.1			
1339	1970	4	7	10	55	2	39	27.8	48	4.3	3.3	4.2			
1340	1970	4	9	9	23	16	39.4	27.9	15	4.9	4.2	4.7			
1341	1970	4	11	8	36	38	39.1	28.8	49	4.9	4.2	4.7			
1342	1970	4	13	5	58	15	39.4	28	33	4.3	3.3	4.2			
1343	1970	4	16	22	39	31.3	40.67	23.45	20	5.5	5	4.9	5		
1344	1970	4	16	23	11	45	40.74	23.62	1	4.3	3.3	4.2			
1345	1970	4	23	9	1	26.6	39.13	28.65	28	5.5	5.3	5.2	5.3		
1346	1970	4	24	2	40	14	39.06	28.6	21	4.3	3.3	4.2			
1347	1970	4	24	11	17	12.2	39.91	19.61	41	4.5	3.7	4.4			
1348	1970	4	24	16	54	0	39.12	28.74	37	4.3	3.3	4.2			
1349	1970	4	26	18	24	34	39.37	28.79	46	4.1	3.1	4.1			
1350	1970	5	8	4	41	3	40.38	21.4	27	4.1	3.1	4.1			
1351	1970	5	22	7	7	34.5	39.13	21.68	44	4.5	3.7	4.4			
1352	1970	5	24	8	24	23	39.25	28.9	33	4.4	3.5	4.3			
1353	1970	5	30	19	49	52	39.4	28.8	0	4.4	3.5	4.3			
1354	1970	6	8	6	51	3	41.44	20.4	29	4.6	3.8	4.5			
1355	1970	6	13	11	25	25.6	39.32	23.16	0	5.2	4.6	4.9			
1356	1970	6	19	22	27	1.3	39.48	20.56	58	4.6	3.8	4.5			
1357	1970	6	27	18	57	15	41.49	19.39	48	5	4.4	4.8			
1358	1970	7	4	4	55	46.5	39.09	28.8	62	4	2.9	4			
1359	1970	7	10	5	36	20	39.16	28.6	12	4.3	3.3	4.2			
1360	1970	8	17	2	42	32.1	41.44	19.77	0	4.4	3.5	4.3			
1361	1970	8	17	4	22	14.3	41.34	19.63	0	4.1	3.1	4.1			
1362	1970	8	18	17	40	17.9	39.16	21.78	38	4.6	3.8	4.5			
1363	1970	8	19	2	1	51.6	41.08	19.77	21	5.9	5.7	4.9	5.7		
1364	1970	8	23	11	37	49.6	41.18	19.9	0	4.5	3.7	4.4			
1365	1970	8	29	10	42	17.2	41.49	19.45	33	4.4	3.5	4.3			
1366	1970	8	31	4	22	56.9	40.57	19.86	47	5	4.4	4.8			
1367	1970	9	8	7	29	23.2	41.1	19.55	25	4.1	3.1	4.1			
1368	1970	9	26	6	14	10.5	39.05	21.7	36	4.5	3.7	4.4			
1369	1970	9	27	15	56	35.5	39.18	20.4	53	4.3	3.3	4.2			
1370	1970	9	27	16	33	53.8	39.29	20.25	40	4.3	3.3	4.2			
1371	1970	10	22	23	57	12	39.16	21.9	12	5.2	4.6	4.9			
1372	1970	10	30	23	51	47	39.95	20.5	3	4.6	3.8	4.5			
1373	1970	10	31	4	36	11.4	39.92	26.16	0	4	2.9	4			
1374	1970	10	31	16	7	39.4	42.1	19.35	39	4.9	4	4.6	4		
1375	1970	11	9	6	42	16	39	28.9	64	4.1	3.1	4.1			
1376	1970	11	10	16	29	45.7	41	19.8	0	4.3	3.3	4.2			
1377	1970	11	19	23	31	49.3	39.07	21.8	0	4.4	3.5	4.3			
1378	1970	11	30	9	49	2.3	39.06	21.94	38	4.5	3.7	4.4			
1379	1970	12	4	18	2	42	39	21.13	24	4.3	3.3	4.2			
1380	1971	1	17	5	59	23.57	39.06	21.86	7.9	4.4	3.5	4.3			3.7
1381	1971	1	27	16	5	43.98	39.73	20.2	58.7	5.2	4.6	4.3	4.6		4.5
1382	1971	2	11	16	57	9.36	39.82	20.92	31.9	4.6	3.8	4.5			
1383	1971	2	23	19	41	23.03	39.62	27.32	9.6	5.6	5.4	5	5.4		
1384	1971	3	25	16	48	50.72	39.05	25.25	11	4.3	3.3	4.2			
1385	1971	4	10	2	58	7.23	42.48	20.15	37	4.5	3.7	4.4			
1386	1971	4	22	9	28	27.77	41.89	20.38	39.8	5.2	4.5	4.7	4.5		
1387	1971	5	1	13	45	27.38	40.95	27.99	13	4.8	4	4.6			
1388	1971	5	5	1	15	34.56	41.87	20.28	11.4	4.6	3.8	4.5			
1389	1971	6	20	2	4	7.39	39.06	21.85	34.6	4.4	3.5	4.3			
1390	1971	11	27	3	54	28.39	39.75	25.66	24.1	4.8	4	4.6			
1391	1971	12	2	6	0	28.59	39.28	22.24	0	4.4	3.5	4.3			
1392	1971	12	2	9	40	58.42	39.23	26.45	35	4.6	3.8	4.5			
1393	1972	2	21	23	2	52.48	41.05	22.11	0	4	2.9	4			3.8
1394	1972	2	28	2	4	35.23	40.4	29	6	4.6	3.5	4.1	3.5		4.4

										Homogenized magnitudes		Reported magnitudes			
Event Number	Year	Month	Date	Hour	Minute	Second	Latitude	Longitude	Depth	M_w	M_s	mb	M_s	M_w	ML
1395	1972	4	11	11	12	13.45	39.29	21.29	38.5	4.4	3.5	4.3			4
1396	1972	4	19	3	39	19.97	39.13	21.72	0.8	4.1	3.1	4.1			3.4
1397	1972	4	26	6	30	23.16	39.43	26.36	18.4	5.5	5	5	5		4.6
1398	1972	4	26	15	59	44.88	39.45	26.33	25.3	5.3	4.8	4.8	4.8		4.7
1399	1972	5	8	8	58	16.33	41.48	23.65	50.7	4.6	3.8	4.5			4.3
1400	1972	5	8	9	20	55.49	41.69	23.64	12.2	5.3	4.7	4.9	4.7		5
1401	1972	5	9	17	40	22.21	39.46	26.37	10.3	5.2	4.5	4.7	4.5		4.2
1402	1972	5	23	3	14	29.91	41.5	23.64	4.8	4.5	3.7	4.4			4.2
1403	1972	6	4	16	29	35.68	39.49	26.37	28.2	4	2.9	4			3.8
1404	1972	7	8	5	46	15.32	41.56	23.68	38.4	4.9	4.2	4.7			4.1
1405	1972	7	18	13	45	48.83	41.61	23.85	30.2	4	2.9	4			4.1
1406	1972	7	30	1	30	6.32	39.92	24.03	0	4.5	3.7	4.4			3.9
1407	1972	8	9	4	2	1.49	39.31	20.48	16.5	4.3	3.3	4.2			3.8
1408	1972	8	12	23	47	57.91	41.1	22.69	12	4.8	4	4.6			4.4
1409	1972	9	3	8	38	46.3	39.16	27.98	30.4	4.8	4	4.6			4.7
1410	1972	9	16	3	53	26.38	40.28	19.73	15	5.3	4.7	5	4.7		5.3
1411	1972	9	16	14	6	26.67	41.35	20.68	6	4.6	3.8	4.5			4.5
1412	1972	9	23	1	53	16.45	42.25	25.31	24.7	4.8	4	4.6			4.3
1413	1972	10	1	4	32	0.84	43.52	21.53	2	4.3	4.3	4.8	4.3		4.8
1414	1972	11	20	3	30	27.16	39.42	21.68	26	5	4.4	4.8			4.3
1415	1972	11	24	3	48	34.2	39.39	20.43	9.1	5.5	5.2	5.2			4.9
1416	1972	11	25	13	16	21.06	39.44	20.19	0	4.1	3.1	4.1			4.2
1417	1972	12	5	12	0	15.03	39.14	23.64	39.9	5.3	4.8	4.5	4.8		4.4
1418	1972	12	13	2	58	53.11	41.66	24.09	41.3	4.4	3.5	4.3			4.3
1419	1972	12	30	15	21	4.74	40.27	25.74	13.7	4.4	3.5	4.3			4.2
1420	1973	1	18	19	7	34.09	42.82	19.09	9.7	4.3	3.3	4.2			
1421	1973	2	8	14	33	14.13	39.25	28.73	38.3	4.3	3.3	4.2			4.2
1422	1973	2	26	22	23	11.79	39.84	20.3	44	4.6	3.8	4.5			4.2
1423	1973	3	7	6	35	12.86	41.87	20.15	48	4	2.9	4			4.2
1424	1973	4	7	19	30	8.55	41.47	19.9	19.6	4.6	3.8	4.5			4.5
1425	1973	7	2	12	14	9.76	39.68	23.73	33	4.1	3.1	4.1			3.9
1426	1973	7	5	22	21	18.83	41.78	19.95	52.2	4.3	3.3	4.2			3.8
1427	1973	8	6	1	11	13.47	39.77	20.6	33.6	4.1	3.1	4.1			4
1428	1973	8	8	8	23	48.73	41.69	19.43	39.2	4.6	3.8	4.5			4.5
1429	1973	9	12	9	36	50.46	40.72	21.01	91.2	4.6	3.8	4.5			4.5
1430	1973	9	18	3	54	29.59	39.84	23.69	1.2	4.4	3.5	4.3			3.8
1431	1973	11	20	13	2	34.17	39.31	23.8	0	5.4	4.9	4.6	4.9		4.9
1432	1973	12	27	17	45	44	39.3	20.5	100	4.3	3				3.9
1433	1974	1	3	7	39	47.94	39.74	26.82	28.8	4.3	3.3	4.2			4.3
1434	1974	1	6	23	24	16	40.08	24.57	33	4	2.9	4			3.8
1435	1974	1	11	21	15	7.45	40.11	24.52	45	4	2.9	4			3.9
1436	1974	1	18	10	57	14.25	40.5	28.94	18.4	4	2.9	4			4.5
1437	1974	2	7	8	46	51.95	39.7	26.88	37	4.3	3.3	4.2			4.3
1438	1974	3	10	21	51	5.99	40.88	21.1	32.1	4.4	3.5	4.3			4.1
1439	1974	3	14	20	57	35.57	41.83	19.39	45.5	4.4	3.5	4.3			3.9
1440	1974	3	22	17	2	20.17	40.65	20.55	27.5	4.6	3.8	4.5			4.3
1441	1974	5	30	15	39	40.62	39.33	24.86	38	4.4	3.5	4.3			4
1442	1974	6	22	23	30	12.11	41.25	23.05	7.8	5.1	4.4	5	4.4		4.7
1443	1974	7	21	5	24	22.91	40.07	19.76	36	4	2.9	4			3.8
1444	1974	9	8	19	9	56.73	39.66	24.39	0	4.4	3.5	4.3			4.5
1445	1974	9	11	5	12	56.59	40.03	19.64	27.9	4.6	3.8	4.5			4.1
1446	1974	9	13	18	24	57.37	40.48	23.39	7.6	4.5	3.7	4.4			4
1447	1974	9	17	4	18	11.12	40.22	20.61	49.2	4.5	3.7	4.4			4.1
1448	1974	9	17	5	10	31.82	40.29	20.63	17	5.5	5	4.9	5		4.9
1449	1974	9	18	9	7	2.34	40.21	20.78	3	4.5	3.7	4.4			4.2
1450	1974	10	15	9	56	49.19	40.67	22.99	0	4.3	3.3	4.2			4.1
1451	1974	11	1	16	39	16.13	39.49	20.34	0	4	2.9	4			3.8
1452	1974	12	1	11	20	12.58	39.53	26.36	0	4.3	3.3	4.2			3.6
1453	1974	12	1	12	9	29.51	39.48	26.35	36	4.6	3.8	4.5			4.3
1454	1974	12	2	14	15	44.13	41.13	23.07	21.7	4.1	3.1	4.1			3.8
1455	1974	12	18	21	30	54.76	39.95	23.86	33.4	4.6	3.8	4.5			3.9
1456	1974	12	20	15	9	32.65	39.67	20.53	47.3	5.5	5	4.7	5		4.8
1457	1974	12	20	16	2	6.2	39.71	20.74	47.3	4.5	3.7	4.4			4.2
1458	1975	1	24	16	33	4.41	41.14	19.77	45.5	4.6	3.8	4.5			4.5
1459	1975	2	2	21	12	20.24	40.48	21.39	40.1	4.6	3.8	4.5			4.3
1460	1975	2	12	1	48	23.23	39.14	29	15.1	4.3	3.3	4.2			
1461	1975	2	14	11	25	39.93	41.54	20.04	22.4	4.4	3.5	4.3			
1462	1975	2	28	19	51	9.21	40.66	22.52	29.2	4.5	3.7	4.4			4.1
1463	1975	3	16	8	37	16.32	40.36	26.14	5	4.4	3.5	4.3			4.4
1464	1975	3	17	2	6	39.06	40.48	26.03	2	4.6	3.8	4.5			4.2
1465	1975	3	17	5	11	16.49	40.48	25.95	22.5	5.5	5.3	4.9	5.3		4.8
1466	1975	3	17	5	17	47.11	40.4	26.24	5	5.7	5.5	4.8	5.5		5
1467	1975	3	17	5	35	17.62	40.48	26.08	17.6	6	5.9	5	5.9		5.2
1468	1975	3	27	5	15	7.94	40.45	26.12	15.4	6.7	6.7	5.5	6.7		5.7
1469	1975	3	27	6	15	45.9	40.41	26.23	21.7	4.9	4.2	4.7			4.5
1470	1975	3	27	19	42	42.5	40.48	26.08	5	4.6	3.8	4.5			4.5
1471	1975	3	29	2	6	5.03	40.42	26.03	33	5.7	5.3	5.3			
1472	1975	3	30	13	3	17.64	40.57	26.36	0	4.6	3.8	4.5			4.1
1473	1975	4	18	20	59	10.37	39.01	23.42	3.1	4.4	3.5	4.3			4.1
1474	1975	4	21	5	36	2.42	39.82	21.64	58.1	4.1	3.1	4.1			3.6
1475	1975	4	22	5	3	31.23	40.28	26.24	36.1	4	2.9	4			3.8
1476	1975	4	23	1	8	8.42	40.4	26.04	20	4.5	3.7	4.4			4.3

										Homogenized magnitudes		Reported magnitudes			
Event Number	Year	Month	Date	Hour	Minute	Second	Latitude	Longitude	Depth	M_w	M_s	mb	M_s	M_w	ML
1477	1975	5	19	23	25	40.9	39.61	19.74	47.3	4.8	4	4.6			4
1478	1975	8	21	15	29	18.46	40.14	19.8	46.2	4.4	3.5	4.3			4.2
1479	1975	9	16	0	27	38.12	41.54	19.31	39.2	4.3	3.3	4.2			3.9
1480	1975	9	16	5	6	19.06	41.54	19.33	25.1	5.5	5	5	5		5.1
1481	1975	9	16	18	45	48.21	41.52	19.28	46.4	4.8	4	4.6			4.5
1482	1975	9	16	18	55	1.64	41.49	19.29	70.2	4.3	3.3	4.2			4.5
1483	1975	10	2	15	59	45.09	40.16	20.49	40.4	4.1	3.1	4.1			4.1
1484	1975	11	22	10	6	8.38	39.92	20.11	33.5	5.3	4.8	5.1	4.8		5.1
1485	1975	12	16	8	8	29.36	39.44	20.45	49.6	4.6	3.8	4.5			4.1
1486	1976	2	2	12	13	1.01	39.78	20.56	35.6	4.6	3.8	4.5			3.8
1487	1976	2	11	7	35	46.74	40.53	24.5	10	5.4	5	5.1			
1488	1976	2	22	12	2	53.01	39.38	22.08	19	5.5	5.3	5	5.3		4.6
1489	1976	2	22	22	1	48.83	39.39	22.13	34.2	4.9	4.2	4.7			4.1
1490	1976	2	22	22	54	34.8	39.39	22.14	22.6	4.9	4.2	4.7			4.2
1491	1976	2	22	22	56	34.22	39.33	21.91	69.2	4.5	3.7	4.4			3.9
1492	1976	3	2	19	41	34.09	40.66	19.59	10.7	5.5	5	4.7	5		5
1493	1976	4	26	22	42	19.28	39.18	23.8	10	4	2.9	4			4
1494	1976	5	13	0	44	15.13	39.72	20.36	48.5	4.4	3.5	4.3			4.1
1495	1976	5	29	22	42	8.69	40.36	28.89	5.8	4	2.9	4			4.4
1496	1976	6	11	18	26	15.03	39.42	20.49	50.9	4.6	3.8	4.5			4.1
1497	1976	7	2	5	16	42.5	39.22	21.7	34	4.9	4.2	4.7			3.8
1498	1976	7	15	19	41	28.21	40.77	20.72	0.7	4	2.9	4			4
1499	1976	8	11	13	27	7.08	39.02	23.53	11	4	2.5				3.6
1500	1976	8	17	17	26	24.39	39.33	23.57	11	4	2.5				3.6
1501	1976	8	19	22	36	24.79	39.08	22.07	40.7	4.5	3.7	4.4			3.9
1502	1976	9	3	20	53	26.91	39.21	28.16	4	4.9	4.1				4.5
1503	1976	10	3	23	8	15.5	40.16	25.08	58	4.2	2.9				3.8
1504	1976	10	26	5	44	11.58	41.73	20	60.7	4.8	4	4.6			4
1505	1976	11	4	2	27	4.32	40.48	21.68	11	4.2	2.9				3.8
1506	1976	11	7	21	56	3.43	40.49	23.03	10	4	2.5				3.6
1507	1976	12	12	13	9	49.8	40.23	19.64	49.5	4.7	3.7				4.3
1508	1976	12	19	10	33	7.66	39.65	20.41	3.2	4.2	2.9				3.8
1509	1976	12	27	7	54	13.47	39.03	20.54	31.1	5.5	5	4.9	5		5
1510	1976	12	27	8	4	19.94	39.02	20.37	36	4.2	2.9				3.8
1511	1976	12	29	20	23	49.48	41.38	19.23	10	4.5	3.7	4.4			4.5
1512	1977	1	10	9	14	42.99	39.48	27.38	4	4.1	3.1	4.1			4.2
1513	1977	1	25	17	25	32.91	39.3	20.63	0.1	4.3	3				3.9
1514	1977	1	25	23	54	18.55	39.41	28.3	19.3	4.3	3.3	4.2			4.1
1515	1977	2	18	19	28	26.76	39.35	22.9	10	4.3	3				3.9
1516	1977	3	7	21	57	51.62	40.47	22.07	10	4.3	3				3.9
1517	1977	3	8	19	18	12.05	43.3	20.97	20.2	5	4.6	4.8			
1518	1977	3	11	6	6	5.8	41.16	24.08	10	4.1	2.7				3.7
1519	1977	3	13	20	42	22.96	39.16	26.27	10	4.4	3.2				4
1520	1977	3	14	8	46	54.52	39.47	20.5	42.9	4.2	2.9				3.8
1521	1977	3	14	10	2	40.29	39.47	19.86	54.5	4	2.5				3.6
1522	1977	3	19	20	49	13.54	41.7	23.84	9	4.1	2.7				3.7
1523	1977	3	23	11	55	53.81	39.63	28.65	22.8	4.3	3.3	4.2			4.5
1524	1977	3	28	8	16	44.49	41.83	20.23	4.5	4	2.5				3.6
1525	1977	4	5	17	15	8.89	39.28	23.3	43.4	4.3	3.3	4.2			4
1526	1977	4	5	17	16	48.71	39.46	23.12	8	4.2	2.9				3.8
1527	1977	4	5	17	47	12.01	39.24	23.36	10	4.1	2.7				3.7
1528	1977	5	13	16	14	33.8	39.06	23.69	22.7	4.9	4.2	4.7			4
1529	1977	5	13	18	17	44.48	39.13	23.52	0.2	5.3	4.7	4.8	4.7		4.6
1530	1977	5	13	19	2	49.54	39.12	23.38	10	4	2.5				3.6
1531	1977	5	18	17	24	41.19	40.41	26.44	9	4.1	2.7				3.7
1532	1977	5	25	12	52	35.55	39.11	20.56	10	4.2	2.9				3.8
1533	1977	6	21	11	31	44.69	39.48	27.63	10	4.5	3.4				4.1
1534	1977	7	1	12	40	39.04	40.7	20.74	37.5	4.5	3.7	4.4			4.2
1535	1977	7	18	10	9	14.17	41.71	20.3	10	5	4.4	4.8			
1536	1977	7	24	10	6	51.26	39.05	24.35	10	4.3	3				3.9
1537	1977	7	24	12	36	38.54	39.12	24.2	10	4.1	2.7				3.7
1538	1977	8	16	9	1	36.69	40.15	19.89	10	4.4	3.2				4
1539	1977	8	17	22	32	52.16	41.38	20.94	10	4.6	3.6				4.2
1540	1977	8	18	6	38	36.46	39.69	25.56	4.3	4.9	4.2	4.7			3.9
1541	1977	9	23	2	58	2.94	41.49	20.08	37.4	5.2	4.6	4.8	4.6		5.1
1542	1977	10	7	12	42	56.76	39.18	20.77	55.9	4.5	3.7	4.4			4.3
1543	1977	10	12	10	14	27.46	39.33	21.65	45	4.3	3.3	4.2			3.8
1544	1977	11	3	2	22	56	42.12	24.03	11	5.6	5.4	5.2	5.4		5.5
1545	1977	11	3	9	5	16.03	42.74	20.68	36.7	4.4	3.2				4
1546	1977	11	6	2	48	45.59	42.13	24.17	23	4.8	4	4.6			4.1
1547	1977	11	17	6	28	9.21	42.06	24.1	10	4.8	4	4.6			
1548	1977	12	3	5	39	30.73	40.15	19.89	42.1	5.2	4.6	4.9			4.4
1549	1978	1	26	8	29	48.1	39.27	22.99	54.8	4.3	3.3	4.2			3.4
1550	1978	1	31	6	39	19.27	39.34	22.91	38.6	4.5	3.2	4.5	3.2		4.1
1551	1978	2	2	11	11	42.01	39.9	21.48	41.2	4.1	3.1	4.1			4.1
1552	1978	2	8	9	3	40.04	39.25	22.98	3.7	4	2.9	4			3.4
1553	1978	4	13	18	5	23.72	43.3	20.99	10	4.8	4.8	4.9	4.8		4.9
1554	1978	4	14	14	30	31.42	39.91	25.61	10	4.2	2.9				3.8
1555	1978	4	16	17	22	47.64	39.93	25.67	6.1	4.1	2.7				3.7
1556	1978	4	16	23	19	33.75	43.25	20.89	10	4.4	3.6	4.3			
1557	1978	4	22	4	22	18.71	39.89	25.63	8.5	4.5	3.3	3.4	3.3		3.6
1558	1978	5	5	4	18	36.56	39.28	26.79	0	4.2	2.9				3.8

										Homogenized magnitudes		Reported magnitudes			
Event Number	Year	Month	Date	Hour	Minute	Second	Latitude	Longitude	Depth	M_w	M_s	mb	M_s	M_w	ML
1559	1978	5	8	14	38	59.58	40.71	23.38	39.9	4.6	3.5	4.4	3.5		4.2
1560	1978	5	8	15	0	8.51	40.74	23.39	10	4.7	3.6	4.1	3.6		3.4
1561	1978	5	10	13	12	52.04	40.71	23.38	28.6	4.8	4	4.6			4.3
1562	1978	5	11	10	6	34.12	40.3	21.96	10.5	4.1	2.7				3.7
1563	1978	5	11	23	5	42.73	40.72	23.37	20	4.1	2.7				3.7
1564	1978	5	13	8	35	36.38	40.68	23.45	16.4	4.1	3.1	4.1			4.1
1565	1978	5	18	2	37	5.48	43.3	20.96	0.1	4.4	3.6	4.3			
1566	1978	5	19	14	46	9.62	40.72	23.43	35.7	4	2.9	4			3.9
1567	1978	5	22	20	29	51.92	39	23.71	33	4	2.5				3.6
1568	1978	5	23	22	40	19.36	39.52	25.94	15	4.1	3.1	4.1			3.5
1569	1978	5	23	23	34	11.44	40.73	23.25	9.3	5.9	5.8	5.6	5.8		5.4
1570	1978	5	24	2	12	28.08	40.71	23.34	8.3	5.5	5	4.8	5		4.1
1571	1978	5	24	5	57	28.01	40.74	23.3	18.7	4.9	4.2	4.7			4.2
1572	1978	5	24	8	13	6.68	40.77	23.41	10	4.4	3.5	4.3			3.9
1573	1978	5	24	8	46	28.15	40.78	23.35	5.5	4.4	3.5	4.3			3.9
1574	1978	5	24	10	54	55.07	40.52	23.42	33	4	2.5				3.6
1575	1978	5	26	5	53	20.72	40.65	23.16	10	4.4	3.2				4
1576	1978	5	26	7	49	0.07	40.66	23.29	0.3	4.2	2.9				3.8
1577	1978	5	28	14	58	7.31	40.65	23.13	10	4	2.5				3.6
1578	1978	6	2	22	31	25.38	40.8	23.19	19	5	4.2	4.7	4.2		3.7
1579	1978	6	7	4	15	7.08	40.71	23.22	0	4.3	3				3.9
1580	1978	6	7	18	50	50.82	40.72	23.18	10	4	2.5				3.6
1581	1978	6	11	23	42	58.06	40.76	23.24	11	4.2	2.9				3.8
1582	1978	6	12	17	44	48.4	40.73	23.36	18.6	5	4.1	4.4	4.1		4.1
1583	1978	6	12	23	36	44.75	40.76	23.24	33.3	4.4	3.5	4.3			4.8
1584	1978	6	13	1	36	54.42	40.83	23.33	10	4.3	3.3	4.2			3.8
1585	1978	6	15	0	26	45.4	40.79	27.68	27.9	5	4.2	4.6	4.2		4.4
1586	1978	6	17	21	7	27.75	39.14	24.41	26.5	4	2.5				3.6
1587	1978	6	17	21	19	29.9	39.14	24.62	0	4.7	3.6	4.6	3.6		4.7
1588	1978	6	19	3	12	53.19	40.69	23.38	4.6	4.5	3.3	4	3.3		4.1
1589	1978	6	19	10	31	5.48	40.77	23.24	9.7	5.5	5.1	5.3	5.1		4.8
1590	1978	6	19	10	48	11.04	40.73	23.23	8.3	4.8	3.8	4.9	3.8		4.2
1591	1978	6	19	12	9	37.54	40.75	23.15	10	4	2.5				3.6
1592	1978	6	19	13	7	10.39	40.75	23.21	6.2	4	2.5				3.6
1593	1978	6	20	20	3	21.49	40.78	23.24	3	6.4	6.4	6.1	6.4		6
1594	1978	6	20	20	27	56.88	40.71	23.13	0	4.1	3.1	4.1			3.8
1595	1978	6	20	20	37	38.93	40.73	23.06	16.1	4	2.9	4			4
1596	1978	6	20	20	45	22.85	40.66	23.11	6.1	4.6	3.8	4.5			4.1
1597	1978	6	20	20	52	39.64	40.75	23.07	2.8	4.5	3.7	4.4			3.9
1598	1978	6	20	21	8	31.28	41.4	23.4	33	4.1	2.7				3.7
1599	1978	6	20	21	51	4.48	40.71	23.2	11.4	4.9	4.2	4.7			4.2
1600	1978	6	21	0	41	51.77	40.43	23.14	0	4.2	2.9				3.8
1601	1978	6	21	1	2	53.7	40.83	23.11	19.2	4.1	3.1	4.1			3.9
1602	1978	6	21	1	4	44.05	40.66	23.18	0	4.1	2.7				3.7
1603	1978	6	21	3	20	25.71	40.75	23.23	4.5	4.5	3.3	4.4	3.3		4
1604	1978	6	21	6	0	5.31	40.73	23.3	2.4	4.6	3.5	4.6	3.5		4.1
1605	1978	6	21	7	12	26.03	40.76	23.23	0	4	2.9	4			3.7
1606	1978	6	21	11	58	26.33	40.72	23.25	0	4	2.5				3.6
1607	1978	6	21	12	29	43.1	40.81	23.06	1.5	5.5	5	4.8	5		4.3
1608	1978	6	21	13	20	59.65	40.76	23.17	16.7	4.5	3.7	4.4			3.7
1609	1978	6	21	13	56	14.51	40.74	23.22	0	4.1	2.7				3.7
1610	1978	6	21	18	52	6.08	40.71	23.22	22.3	4.6	3.5	4.5	3.5		4
1611	1978	6	21	19	58	50.46	43.13	19.09	0	4.6	3.6				4.2
1612	1978	6	22	2	26	42.19	40.8	23.18	17.8	4	2.9	4			3.8
1613	1978	6	22	15	22	7.55	40.88	23.09	0	4.3	3				3.9
1614	1978	6	23	1	57	1.56	40.82	23.11	10	4.9	4	4.2	4		4.1
1615	1978	6	23	12	32	3.58	43.22	22.12	0	4.1	2.7				3.7
1616	1978	6	23	19	58	27.14	40.76	23.18	0	4.7	3.6	3.6	3.6		4
1617	1978	6	24	0	14	28.69	41.7	20.25	9.8	5	4.2	4.8	4.2		5.5
1618	1978	6	25	3	45	3.5	40.73	23.16	10	4	2.5				3.6
1619	1978	6	25	4	58	21.87	41.71	20.4	10	4.8	3.9				4.4
1620	1978	6	25	14	30	14	40.87	23.21	0	4	2.5				3.6
1621	1978	6	25	18	42	6.16	40.77	23.13	10	4	2.5				3.6
1622	1978	6	26	0	4	0.37	40.76	23.17	10.6	4.5	3.2	4.1	3.2		3.9
1623	1978	6	27	12	18	22.46	42.08	24.1	9.3	4.6	3.8	4.5			4.3
1624	1978	6	29	3	40	17.06	41.64	20.33	0	4.4	3.2				4
1625	1978	7	1	2	30	26.07	39.29	22.66	0	4.3	3.3	4.2			
1626	1978	7	3	20	9	48.82	40.61	23.36	0	4	2.9	4			3.8
1627	1978	7	3	20	11	13.58	40.69	23.26	0	4.5	3.3		3.3		
1628	1978	7	4	22	23	28.45	40.75	23.06	17.7	5.4	4.9	5	4.9		4.6
1629	1978	7	9	4	2	0.08	40.68	23.24	0	4.1	2.7				3.7
1630	1978	7	11	13	16	30.56	40.8	23.28	0	4.1	2.7				3.7
1631	1978	7	13	17	26	56.57	40.78	23.23	4.5	4.8	3.8	4.1	3.8		4
1632	1978	7	14	3	45	25.05	40.75	23.33	0	4.2	2.9				3.8
1633	1978	7	27	8	30	9.72	39.15	24.5	15.5	4	2.9	4			4.2
1634	1978	8	5	17	54	0.21	40.94	20.57	21	5.4	4.9				5
1635	1978	8	8	12	10	47.02	40.1	19.71	48.3	4.6	3.5	4.4	3.5		4.3
1636	1978	8	18	20	53	20.87	41.84	20.27	9.8	5.3	4.7	5.2	4.7		5.1
1637	1978	8	21	0	54	12.11	40.13	23.07	33	4.2	2.9				3.8
1638	1978	8	24	1	23	50.54	40.7	23.49	17.4	4.5	3.3	4.2	3.3		3.9
1639	1978	9	1	22	46	15.86	39.07	21.47	23.8	5	4.2	4.8	4.2		4.3
1640	1978	9	3	18	59	34.51	40.72	23.33	28	4.2	2.9				3.8

										Homogenized magnitudes		Reported magnitudes			
Event Number	Year	Month	Date	Hour	Minute	Second	Latitude	Longitude	Depth	M_w	M_s	mb	M_s	M_w	ML
1641	1978	9	10	2	44	46.61	40.78	24.16	10	4.1	2.7				3.7
1642	1978	9	16	21	54	13.49	40.42	25.59	33	4.3	3				3.9
1643	1978	9	16	23	17	2.8	40.37	25.59	10	4.1	2.7				3.7
1644	1978	9	18	2	55	35.22	40.27	25.63	0	4.3	3				3.9
1645	1978	9	18	20	37	33.18	39.97	23.51	10	4	2.5				3.6
1646	1978	10	2	14	18	15.14	40.56	23.22	0	4.2	2.9				3.8
1647	1978	10	21	5	12	19.17	40.68	25.46	10	4.4	3.2				4
1648	1978	11	4	9	17	26	40.73	23.26	10	4	2.5				3.6
1649	1978	11	19	19	59	19.44	40.67	23.33	10	4.1	2.7				3.7
1650	1978	11	23	19	42	11.25	39.08	21.24	42.5	4.4	3.5	4.3			3.9
1651	1978	11	25	7	34	34.28	39.1	26.65	0	4	2.5				3.6
1652	1978	11	28	17	42	12.28	41.83	20.04	11.9	4.8	4	4.6			
1653	1978	12	1	3	47	57.06	40.99	19.73	5.2	4.5	3.7	4.4			4.4
1654	1978	12	3	8	10	52.11	40.92	19.64	38.3	5.1	4.3	4.9	4.3		4.5
1655	1978	12	8	19	2	8.65	40.86	19.63	3.4	4.5	3.4				4.1
1656	1978	12	31	15	56	14.62	41.99	23.22	21.2	5.2	4.6	4.6	4.6		4.6
1657	1978	12	31	16	26	5.91	41.97	23.17	9.2	4.5	3.7	4.4			4.4
1658	1979	1	4	13	22	36.55	40.13	24.85	2	4	2.5				3.6
1659	1979	1	5	10	3	49.48	39.85	25.62	10	4.5	3.7	4.4			
1660	1979	2	7	10	16	48.31	39.56	23.26	42.1	4.6	3.5	4.7	3.5		4.3
1661	1979	2	22	17	37	18.8	40.46	22.51	3	4.4	3.5	4.3			4.2
1662	1979	2	26	22	9	46.15	41.52	20.06	28.2	4.8	4	4.6			4.6
1663	1979	2	26	22	35	59.21	41.47	20.18	10	5.2	4.6				4.8
1664	1979	3	1	2	50	32.79	39.29	23.28	0	4.3	3.3	4.2			3.7
1665	1979	3	9	15	55	32.21	43.58	20.12	10	4.7	3.7				4.3
1666	1979	3	10	16	36	49.99	40.98	20.54	10	4	2.5				3.6
1667	1979	4	9	2	10	21.1	41.95	19.04	12.7	5.6	5.2	5.2	5.2		5
1668	1979	4	11	2	25	44.28	41.99	19.07	14	4	2.5				3.6
1669	1979	4	11	11	41	20.17	41.9	19.15	21	4.1	2.7				3.7
1670	1979	4	12	1	2	21.06	39.09	25.99	10	4.3	3.3	4.2			3.9
1671	1979	4	12	23	9	12.45	39.14	24.24	10	4.9	4.2	4.7			4.8
1672	1979	4	15	5	58	41.6	41.95	19.14	10	4.6	3.6				4.2
1673	1979	4	15	6	19	41.41	42.04	19.05	3.8	6.8	6.9	6.1	6.9		6.8
1674	1979	4	15	7	1	36.08	41.97	19.75	10	4.5	3.7	4.4			
1675	1979	4	15	7	11	28.36	42.01	19.18	10	4.4	3.5	4.3			4.1
1676	1979	4	15	7	25	31.98	41.97	19.44	10	4	2.9	4			4.1
1677	1979	4	15	8	13	15.26	42.03	19.13	10	4.4	3.5	4.3			4.7
1678	1979	4	15	9	10	54.96	41.92	19.33	10	4.4	3.5	4.3			
1679	1979	4	15	10	25	24.31	41.88	19.28	10	5.1	4.4	5.1	4.4		4.9
1680	1979	4	15	12	43	46.11	41.96	19.11	6.4	4.6	3.8	4.5			4.6
1681	1979	4	15	14	11	10.13	42.65	19.03	3	4	2.9	4			4.5
1682	1979	4	15	17	20	39.97	41.87	19.32	10	4	2.9	4			4.3
1683	1979	4	15	20	49	46.26	41.98	19.11	8.5	4.4	3.5	4.3			4.6
1684	1979	4	16	7	56	0.93	41.83	19.4	8.4	5	4.4	4.8			4.7
1685	1979	4	16	9	43	42.69	41.86	19.43	6.8	4.8	4	4.6			4.4
1686	1979	4	16	10	4	39.6	41.94	19.23	21.1	5.3	4.7	5.2	4.7		4.9
1687	1979	4	16	15	51	7.81	41.85	19.32	10	4.8	4	4.6			4.2
1688	1979	4	16	23	0	26.88	41.91	19.37	10	4.8	4	4.6			4.8
1689	1979	4	17	1	32	26.93	42.01	19.21	10	4.9	4.2	4.7			
1690	1979	4	17	3	53	32.96	41.84	19.37	9.3	4.3	3.3	4.2			4.6
1691	1979	4	17	18	6	17.38	42.11	19.08	10	4.9	4.2	4.7			3.9
1692	1979	4	17	18	31	23.85	42.02	19.09	10	4.1	3.1	4.1			
1693	1979	4	18	3	50	5.99	41.93	19.11	17.4	4.9	4.2	4.7			4.4
1694	1979	4	18	19	51	12.59	42.09	19.01	2	5.2	4.6	4.9	4.6		4.5
1695	1979	4	19	0	17	35.58	41.93	19.12	11.7	5	4.4	4.8			4.6
1696	1979	4	20	19	32	56.5	41.99	19.34	10	5.3	4.8	5			
1697	1979	4	21	2	38	5.48	42	19.06	10	4.5	3.7	4.4			4.6
1698	1979	4	21	4	33	2.02	41.79	19.12	10	4.6	3.8	4.5			4.6
1699	1979	4	21	4	54	37.68	41.85	19.11	10	4.4	3.5	4.3			4.4
1700	1979	4	21	11	1	40.47	42.02	19.21	10	4.4	3.5	4.3			
1701	1979	4	21	20	18	56	42.49	19.09	10	4.1	2.7				3.7
1702	1979	4	22	6	32	12.73	41.95	19.14	4.3	5	4.1	4.6	4.1		4.7
1703	1979	4	25	6	36	50.14	41.91	19.24	47.4	4.8	4	4.6			4.6
1704	1979	4	26	11	12	10.93	42.05	19.15	10	4.1	2.7				3.7
1705	1979	4	29	10	24	18.71	41.97	19.26	10	4.5	3.7	4.4			
1706	1979	5	3	16	39	46.87	41.95	19.12	10	4.5	3.7	4.4			
1707	1979	5	11	1	46	26.78	40.74	23.27	5	5.2	4.5	4.7	4.5		4.3
1708	1979	5	12	18	49	11.56	41.77	19.51	10	4	2.5				3.6
1709	1979	5	14	9	53	7.45	41.94	19.16	8.9	5.1	4.4	4.7	4.4		4.7
1710	1979	5	18	2	42	59.1	42	19.23	20	4	2.5				3.6
1711	1979	5	30	5	38	0.44	41.85	19.06	10	4.5	3.7	4.4			4.3
1712	1979	6	1	19	4	30.65	40.33	24.22	0	4.5	3.3	3.6	3.3		3.8
1713	1979	6	1	21	3	34.39	39.22	20.51	46.8	4.8	4	4.6			4.1
1714	1979	6	2	3	11	59.04	40.3	24.14	10	4.8	3.8	4.4	3.8		5
1715	1979	6	21	2	9	52.64	39.03	22.21	23.9	4.4	3.5	4.3			3.7
1716	1979	6	26	3	34	34.32	39.15	24.4	0	4	2.9	4			4.4
1717	1979	7	4	23	44	14.56	42.01	19.1	0.7	4.5	3.7	4.4			4.9
1718	1979	7	18	13	12	2.28	39.66	28.65	7.1	5.4	4.9	5.2	4.9		5.2
1719	1979	7	25	22	43	10.08	41.81	19.46	10	4.1	2.7				3.7
1720	1979	7	29	13	23	50.69	39.75	20.63	48.9	4	2.9	4			3.9
1721	1979	8	2	14	41	47.48	42.06	19.04	10	4.9	4.1				4.5
1722	1979	8	13	21	9	12.72	40.88	20.25	13	4.4	3.5	4.3			4.2

										Homogenized magnitudes		Reported magnitudes			
Event Number	Year	Month	Date	Hour	Minute	Second	Latitude	Longitude	Depth	M_w	M_s	mb	M_s	M_w	ML
1723	1979	8	17	5	30	38.81	41.89	19.31	1.3	4.5	3.7	4.4			4.2
1724	1979	8	23	16	47	46.91	39.69	28.57	10	5.3	4.8	5			
1725	1979	8	31	17	24	10.16	40.73	23.36	10.5	5.2	4.5	4.5	4.5		4.4
1726	1979	9	2	13	54	29.05	40.53	20.94	4	4.5	3.3	3.9	3.3		4.2
1727	1979	9	9	16	10	13.21	39.32	28.83	7.8	4	2.9	4			4.2
1728	1979	9	13	12	6	43.06	42.15	25.29	16.3	4.9	4.2	4.7			4.3
1729	1979	9	21	5	10	26.86	41.91	19.25	7	4	2.5				3.6
1730	1979	9	21	12	2	42.46	41.97	19.38	10	4.5	3.7	4.4			4.5
1731	1979	9	25	1	41	29.68	40.87	22.35	3.1	4.6	3.5	4.6	3.5		4.2
1732	1979	10	4	9	19	32.06	39.39	20.28	54.7	4	2.9	4			4
1733	1979	10	6	6	40	0.86	41.55	20.86	8	4.7	3.7				4.3
1734	1979	10	12	12	28	37.23	41.43	19.48	1.2	4.5	3.4				4.1
1735	1979	10	14	15	0	16.09	40.18	21.52	40.9	4.5	3.2	4.1	3.2		3.9
1736	1979	10	21	11	31	8.48	41.14	19.94	2.1	5.3	4.8	5			4.5
1737	1979	11	2	5	30	34.65	39.51	20.2	41.6	4.7	3.7	4.8	3.7		4.4
1738	1979	11	2	21	7	22.86	41.18	20.03	10	4	2.9	4			4
1739	1979	11	6	5	26	15.98	39.56	20.32	26.2	5.5	5.1	5.4	5.1		5.1
1740	1979	11	6	8	5	27.24	41.95	19.32	10	4	2.9	4			3.6
1741	1979	11	6	15	19	42.84	39.48	20.32	49.3	4.3	3.3	4.2			4
1742	1979	11	8	2	3	54.63	41.12	19.65	12.7	5.2	4.6	4.9			4.3
1743	1979	11	8	4	30	20.19	39.49	20.25	56.4	4.5	3.3	4.6	3.3		4
1744	1979	11	8	10	7	47.95	39.46	20.31	4.1	4	2.9	4			4
1745	1979	11	9	1	48	49.68	41.85	19.16	11	4.5	3.7	4.4			4.4
1746	1979	11	10	4	19	34.33	41.89	19.19	10	4.5	3.7	4.4			
1747	1979	11	10	6	16	32.55	39.46	20.31	10.3	4.1	3.1	4.1			3.8
1748	1979	11	11	1	18	6.25	39.52	20.3	27.1	5.2	4.6	5.2	4.6		4.7
1749	1979	11	15	2	18	30.96	40.82	23.43	6.7	4.1	3.1	4.1			3.7
1750	1979	11	15	19	36	1.18	43.12	19.96	10	4.9	4.1				4.5
1751	1979	11	20	18	32	1.06	42.04	19.04	20	4.6	3.8	4.5			4.6
1752	1979	11	21	2	20	52.88	40.28	20.16	10	4.6	3.5	4.5	3.5		4.4
1753	1979	11	22	6	51	9.08	43.38	19.82	10	4.3	3.4	4.2			
1754	1979	11	22	9	28	12.96	39.4	20.32	8.3	4.3	3.3	4.2			3.9
1755	1979	11	23	1	26	59.05	40.83	19.83	2	4	2.5				3.6
1756	1979	11	24	9	48	42.37	41.03	19.56	0.5	4.5	3.7	4.4			4.4
1757	1979	11	26	10	32	6.56	41.27	21.07	24.1	4.1	3.1	4.1			
1758	1979	12	1	15	59	52.85	39.31	22.96	0.1	4.9	4.1				4.5
1759	1979	12	2	19	36	8.36	41.38	19.85	8	4	2.5				3.6
1760	1979	12	2	22	45	14.68	41.38	19.66	51.7	4.6	3.8	4.5			4.2
1761	1979	12	5	21	55	37.12	43.09	19.16	5	4.2	2.9				3.8
1762	1979	12	9	3	6	39.67	43.47	19.91	10	4.5	3.8	4.4			3.7
1763	1979	12	23	14	24	14.98	41.84	19.4	12	4.6	3.8	4.5			4.4
1764	1980	1	2	18	4	17.8	39.19	22.98	10	4.5	3.2	4.4	3.2		3.9
1765	1980	1	2	18	52	36.99	39.31	22.96	1.9	4.8	4	4.6			3.3
1766	1980	1	4	22	0	48.45	39.27	23.01	10	4.1	3.1	4.1			3.3
1767	1980	1	10	19	36	40.6	39.53	20.5	7.8	4.3	3.3	4.2			4.2
1768	1980	1	12	18	19	13.34	43.27	20.87	3	5.1	4.4				4.7
1769	1980	1	21	7	15	52.53	39.29	23.03	10	4.6	3.8	4.5			4
1770	1980	1	21	7	47	3.06	39.3	22.91	38.1	4.6	3.5	4.7	3.5		4.1
1771	1980	1	25	23	8	15.37	39.21	23.03	0	4.5	3.2	4.3	3.2		4.2
1772	1980	2	15	19	21	56.35	40.38	25.95	10	4.6	3.8	4.5			4
1773	1980	2	19	1	54	12.43	40.44	25.81	10	4.3	3.3	4.2			
1774	1980	2	20	22	55	23.49	40.42	26.04	10	4.3	3.3	4.2			3.8
1775	1980	3	9	16	52	23.78	43.04	23.36	9.5	4.2	4.2	4.5	4.2		
1776	1980	3	16	12	54	31.25	43.45	19.91	10	4.2	2.9				3.8
1777	1980	3	17	5	27	49.72	41.9	21.84	0	4.5	3.4				4.1
1778	1980	4	3	8	17	1.04	42.08	19.94	0	4.5	3.4				4.1
1779	1980	4	22	1	23	5.24	39.19	28.95	0	4.2	2.9				3.8
1780	1980	4	27	9	54	27.27	39.07	28.86	37.6	4.4	3.5	4.3			4.8
1781	1980	5	3	4	26	4.58	39.14	28.98	34.8	4.1	3.1	4.1			4.1
1782	1980	5	4	9	22	12.66	39.22	28.97	21.6	4.5	3.2	4.5	3.2		4.3
1783	1980	5	6	6	8	22.26	39.18	28.93	35.6	4.5	3.3	3.8	3.3		
1784	1980	5	7	11	24	1.85	39.44	20.25	7.5	4.3	3.3	4.2			3.9
1785	1980	5	8	22	6	58.69	39.2	28.9	0	4.9	4.1				4.5
1786	1980	5	9	12	33	42.63	42.3	24.2	71.2	4.6	3.6				4.2
1787	1980	5	18	20	2	56.55	43.31	20.87	0	5.9	5.9	5.7	5.9		5.6
1788	1980	5	18	20	18	58.63	43.26	20.9	10	4.8	4.2	4.6			
1789	1980	5	18	20	26	42.22	43.29	20.9	10.4	5.7	5.7	5.3	5.7		
1790	1980	5	18	20	41	28.82	43.29	20.89	0.6	5	4.6	4.8			
1791	1980	5	18	20	54	13.35	43.12	20.78	10	5	4.6	4.8			
1792	1980	5	19	2	56	44.98	43.32	20.89	10	4.8	3.9				4.4
1793	1980	5	19	4	0	38.62	43.32	20.95	0.2	4.4	3.6	4.3			
1794	1980	5	19	18	42	29.89	43.25	20.93	3	4.4	3.6	4.3			
1795	1980	5	23	12	26	23.9	43.34	20.96	3	4.6	4.6	4.5	4.6		4.4
1796	1980	5	25	7	8	51.01	43.25	20.79	10	4.6	3.6				4.2
1797	1980	6	2	3	39	51	40.88	22.37	1.7	4.5	3.3	3.9	3.3		3.9
1798	1980	6	2	4	22	52.5	40.83	22.29	7.6	4.6	3.5	4.6	3.5		4
1799	1980	6	3	19	8	4.89	43.23	20.97	10	4.1	2.7				3.7
1800	1980	6	10	21	25	0.05	43.32	20.93	10	4.3	3.4	4.2			4.5
1801	1980	6	12	2	48	37.04	40.06	20.4	59.9	5.5	5.2	5.2			4.5
1802	1980	6	13	8	6	33.54	43.18	20.52	10	5.2	4.8	4.9			
1803	1980	6	14	2	20	35.46	42.92	20.46	10	4	2.5				3.6
1804	1980	6	17	9	52	5.44	43.27	20.79	10	4.6	3.6				4.2

										Homogenized magnitudes		Reported magnitudes			
Event Number	Year	Month	Date	Hour	Minute	Second	Latitude	Longitude	Depth	M_w	M_s	mb	M_s	M_w	ML
1805	1980	6	17	22	14	37.71	43.27	20.86	10	4.5	3.8	4.4			
1806	1980	6	19	22	50	32.69	39.13	21.92	4.1	4.6	3.8	4.5			3.9
1807	1980	6	23	0	1	55.4	40.88	22.33	10	4.2	2.9				3.8
1808	1980	6	26	17	1	43.81	40.84	22.38	10	4	2.9	4			3.9
1809	1980	6	28	6	10	14.46	43.2	20.59	10	4.1	2.7				3.7
1810	1980	6	29	5	52	12.04	43.25	20.73	3	4.2	2.9				3.8
1811	1980	7	4	20	20	16.29	39.29	22.93	35.8	5.1	4.3	4.9	4.3		4.4
1812	1980	7	4	20	48	51.46	39.29	23.02	5.5	4.8	4	4.6			3.4
1813	1980	7	5	3	10	23.44	39.26	22.95	10	4.4	3.5	4.3			3.6
1814	1980	7	5	5	34	36.7	39.24	22.98	13	4.6	3.5	4.5	3.5		4
1815	1980	7	5	6	18	12.52	39.18	23	10	5	4.4	4.8			3.5
1816	1980	7	5	8	6	10.18	39.29	22.89	43.8	4.5	3.2	4.6	3.2		3.8
1817	1980	7	5	9	56	9.71	39.24	22.99	10	4.5	3.3	4.3	3.3		3.7
1818	1980	7	6	4	27	58.61	39.25	22.99	7.7	4.5	3.3	4	3.3		3.7
1819	1980	7	6	5	34	42.94	39.25	22.89	22.8	5.1	4.4	5	4.4		4.7
1820	1980	7	6	8	52	51.2	39.29	22.94	2.6	4.5	3.2	4.1	3.2		3.6
1821	1980	7	6	11	29	40.98	39.29	23.01	14.6	4	2.9	4			3.4
1822	1980	7	7	10	32	4.71	40.63	19.27	12.6	4.6	3.8	4.5			4.6
1823	1980	7	7	16	4	42.28	39.3	22.94	41	5.3	4.7	4.7	4.7		4.6
1824	1980	7	8	2	59	31.32	39.24	22.91	38.9	4.7	3.6	4.5	3.6		4.3
1825	1980	7	9	2	10	20.39	39.26	22.93	35.4	5.5	5.2	5.2			5.2
1826	1980	7	9	2	11	57.35	39.29	22.91	47.5	6.3	6.3	5.8	6.3		6
1827	1980	7	9	2	18	15.54	39.3	22.89	7.4	4.3	3.3	4.2			3.9
1828	1980	7	9	2	35	51.58	39.23	22.59	30.9	6.2	6.1	5.7	6.1		5.6
1829	1980	7	9	2	46	21.72	39.28	22.97	0.7	4	2.9	4			3.6
1830	1980	7	9	6	1	47.67	39.31	22.87	22.9	5.5	5	5.1	5		4.8
1831	1980	7	9	6	11	7.38	39.22	22.95	0.2	4.8	3.9	4.7	3.9		4.1
1832	1980	7	9	6	41	51.59	39.29	23.03	0	4.8	4	4.6			3.9
1833	1980	7	9	8	30	12.77	39.26	22.96	10	4.5	3.3	3.7	3.3		3.6
1834	1980	7	9	10	34	13.08	39.21	22.9	3.2	4.1	3.1	4.1			3.6
1835	1980	7	9	16	6	0.82	39.24	22.88	10	4.7	3.6	4.9	3.6		3.8
1836	1980	7	10	16	0	23.68	39.32	23.07	4.8	4.6	3.5	4.2	3.5		4.7
1837	1980	7	10	19	39	2.82	39.32	22.93	22.3	5.7	5.5	5.3	5.5		5
1838	1980	7	12	5	32	8.67	39.2	22.86	15.7	4	2.9	4			3.6
1839	1980	7	12	7	29	45.72	39.19	22.79	10	4	2.9	4			3.6
1840	1980	7	12	8	51	54.3	39.29	23.03	12.3	4.8	3.8	4.4	3.8		4
1841	1980	7	13	13	39	51.01	39.26	23.04	17.2	4	2.9	4			3.6
1842	1980	7	14	8	6	16.18	39.11	22.74	5.2	4	2.9	4			3.3
1843	1980	7	14	19	38	10.37	39.15	22.99	7.6	4.8	4	4.6			3.4
1844	1980	7	14	22	39	27.64	39.27	23.08	24.7	4.3	3.3	4.2			3.9
1845	1980	7	14	22	45	32.09	39.3	23.01	33	4.6	3.8	4.5			3.3
1846	1980	7	15	0	31	42.01	39.28	23.07	22.3	4.5	3.2	4.5	3.2		4.4
1847	1980	7	15	11	34	54.51	39.28	23.11	25.3	4.5	3.2	4.8	3.2		4.4
1848	1980	7	15	21	42	26.17	39.23	22.78	44.1	4.3	3.3	4.2			3.9
1849	1980	7	16	0	6	59.39	39.32	22.66	31	5.2	4.5	4.8	4.5		4.5
1850	1980	7	16	3	11	48.09	39.21	22.75	40.7	4.3	3.3	4.2			3.9
1851	1980	7	16	18	5	40.98	39.25	22.83	53	4.9	4.2	4.7			3.5
1852	1980	7	17	2	50	34.88	39.29	23.02	56.4	4.8	4	4.6			3.5
1853	1980	7	17	11	9	31.79	39.26	23.07	12.9	4.5	3.7	4.4			3.8
1854	1980	7	17	14	13	43.87	39.28	23.13	5.5	4.9	4.2	4.7			3.6
1855	1980	7	18	4	9	0.85	39.24	23.07	0	4.7	3.7	4.5	3.7		3.9
1856	1980	7	19	0	37	57.33	41.49	20.28	21.8	5.1	4.4	4.9	4.4		4.7
1857	1980	7	19	20	33	10.18	39.24	23.91	10	4.5	3.2	4.4	3.2		4.4
1858	1980	7	21	14	26	20.1	39.19	22.73	0	5	4.4	4.8			3.6
1859	1980	7	22	2	6	55.67	39.33	22.94	9.5	4.5	3.7	4.4			3.6
1860	1980	7	22	19	8	51.34	39.35	23.13	34.1	4.3	3.3	4.2			3.6
1861	1980	7	23	10	5	55.14	39.29	22.86	6.4	4	2.9	4			3.5
1862	1980	7	23	16	6	38.96	39.3	22.98	10	4.1	3.1	4.1			3.8
1863	1980	7	24	10	7	53.36	39.3	23.19	46.3	4.5	3.2	4.5	3.2		4
1864	1980	7	24	10	44	12.26	39.29	23.05	10.5	4.7	3.7	4.7	3.7		4.3
1865	1980	7	24	13	32	30.71	39.27	23.17	1.2	4.5	3.2	4.3	3.2		3.8
1866	1980	7	24	22	31	30.76	39.26	23.15	20.5	4.5	3.2	4.3	3.2		3.8
1867	1980	7	24	22	36	43.08	39.23	23.14	10	4.8	4	4.6			3.5
1868	1980	7	26	22	13	23.5	39.26	22.9	0	4.8	4	4.6			
1869	1980	7	28	20	39	6.97	39.26	23.08	36.6	4.1	3.1	4.1			3.7
1870	1980	7	29	20	41	31.22	39.31	23.01	33.7	5	4.2	5	4.2		4.5
1871	1980	7	30	9	38	36.36	39.31	23.12	12.3	4.1	3.1	4.1			3.8
1872	1980	8	5	10	3	4.58	39.19	22.79	9.8	4.5	3.3	4.6	3.3		3.9
1873	1980	8	11	9	15	59.7	39.26	22.72	26.7	5.3	4.8	5.2	4.8		4.7
1874	1980	8	11	10	2	39.95	39.25	22.82	10	4	2.9	4			3.5
1875	1980	8	12	1	41	5.46	39.29	22.72	30.8	4.7	3.6	4.7	3.6		4.3
1876	1980	8	12	3	15	30.17	39.25	22.83	5.4	4.5	3.2	4.2	3.2		3.7
1877	1980	8	12	13	11	18.42	39.24	22.86	2.3	4	2.9	4			3.7
1878	1980	9	26	4	19	20.6	39.27	22.76	41.9	4.9	4	4.7	4		4.4
1879	1980	10	21	2	35	43.35	39.29	23.05	3.9	5	4.1	4.5	4.1		4.3
1880	1980	10	21	4	7	18.39	39.29	23.05	7.3	5	4.1	4.7	4.1		4.5
1881	1980	10	21	19	43	10.2	43.27	20.81	10	4.5	3.4				4.1
1882	1980	10	24	2	4	6.44	40.02	24.91	10	4	2.9	4			3.9
1883	1980	11	12	15	35	41.55	39.05	24.31	0.9	5.1	4.4	4.6	4.4		4.7
1884	1980	11	12	16	4	46.85	39.1	24.3	0	4.8	4	4.6			3.6
1885	1980	11	14	11	12	52.11	39.28	23.09	10.9	4.8	4	4.6			3.4
1886	1980	11	14	18	4	28.41	39.1	24.29	1.3	4.7	3.7	4.4	3.7		4.4

										Homogenized magnitudes		Reported magnitudes			
Event Number	Year	Month	Date	Hour	Minute	Second	Latitude	Longitude	Depth	M_w	M_s	mb	M_s	M_w	ML
1887	1980	11	15	15	21	49.29	39.32	27.56	0	4.7	3.7				4.3
1888	1980	11	15	16	11	18.31	39.2	28.9	0	4.7	3.7				4.3
1889	1980	12	21	16	28	32.34	39.06	25.23	6.9	4.7	3.7	4.4	3.7		4
1890	1980	12	23	7	30	44.61	43.27	20.84	10	4	2.5				3.6
1891	1980	12	30	12	40	35.71	39.34	23.17	40.3	4.4	3.5	4.3			3.8
1892	1981	1	7	16	35	26.33	40.5	19.62	11.2	4.2	2.9				3.8
1893	1981	1	9	14	17	8.03	39.62	20.12	10	4.1	3.1	4.1			3.7
1894	1981	1	30	7	35	37.76	40.6	20.77	5.4	4.9	4.1				4.5
1895	1981	1	31	14	30	31.18	40.69	21.63	8.3	4	2.9	4			3.9
1896	1981	2	11	11	40	13.68	39.55	19.57	14.9	4.5	3.2	4.4	3.2		4
1897	1981	2	19	22	23	46.15	39.82	19.87	11.1	4.1	3.1	4.1			4
1898	1981	2	24	11	44	17.48	42.16	19.43	8.2	4.1	2.7				3.7
1899	1981	3	2	21	37	48.26	40.69	23.21	23.2	4.4	3.1	4.6	3.1		4.2
1900	1981	3	7	6	53	15	42.92	20.57	10	4.7	3.7				4.3
1901	1981	3	10	15	16	19.72	39.38	20.75	31.7	5.3	4.7	5.4	4.7		5.3
1902	1981	3	12	4	6	0.59	40.8	28.09	12.2	5.2	4.5	4.7	4.5		4.7
1903	1981	3	26	17	39	45.16	41.87	19.4	2.1	4.6	3.8	4.5			
1904	1981	4	3	18	36	30.98	39.13	24.56	10	4.7	3.6	4.2	3.6		4.4
1905	1981	4	23	11	8	50.02	40.48	21.35	28.1	4.6	3.8	4.5			4.3
1906	1981	5	3	20	41	12.2	40.79	28.09	24	4.7	3.7	4	3.7		4.4
1907	1981	5	6	0	18	25.01	39.26	22.78	32.4	5.1	4.3	4.8	4.3		4.4
1908	1981	5	6	17	12	7.03	39.1	21.77	6.4	4.3	3.3	4.2			3.7
1909	1981	5	10	10	3	47.03	44	19.05	16	4.4	3.2				4
1910	1981	5	18	20	40	57.53	40.71	22.29	24.7	4.5	3.4				4.1
1911	1981	5	23	21	0	41.73	39.11	24.45	10	5.2	4.6	4.5	4.6		4.9
1912	1981	5	24	0	3	44.56	39.23	24.63	35	4	2.9	4			3.8
1913	1981	6	2	19	7	16.29	39.41	27.96	6.5	4.6	3.5	4.1	3.5		4.5
1914	1981	6	21	18	49	14.13	39.47	20.58	59.6	4.6	3.5	4.4	3.5		4
1915	1981	6	21	20	11	42.33	39.34	20.5	30.3	4.3	3.3	4.2			3.9
1916	1981	6	30	23	5	32.19	41.33	19.47	10.5	4.5	3.7	4.4			
1917	1981	7	2	8	41	39.96	39.61	20.63	21.2	4.4	3.5	4.3			4.8
1918	1981	7	3	21	42	57.65	39.54	20.67	41.3	5.3	4.7	5.1	4.7		5.3
1919	1981	7	8	3	59	52.48	41.12	19.85	10.9	4.6	3.8	4.5			
1920	1981	7	15	0	50	37.54	42.16	19.22	10	4	2.5				3.6
1921	1981	7	21	9	43	37.22	40.23	28.86	1.2	4.1	3.1	4.1			4.6
1922	1981	7	22	22	2	45.93	40.27	28.9	2.1	4	2.9	4			4.5
1923	1981	7	25	3	21	41.88	39.44	20.67	57.1	4.7	3.6	4.3	3.6		4.7
1924	1981	7	25	9	17	38.32	39.4	20.6	25.7	4.1	2.6	3.9	2.6		3.9
1925	1981	8	8	15	10	58.97	40.71	28.26	3.3	4.4	3.2				4
1926	1981	8	12	8	31	25.11	39.51	26.99	0	4.7	3.7				4.3
1927	1981	8	18	9	49	26.17	41.86	19.96	0	5	4.2				4.6
1928	1981	8	21	22	42	37.25	39.73	27.81	2.1	4.5	3.2	3.7	3.2		4
1929	1981	8	22	9	33	52.19	39.27	23.78	5.4	4.8	4	4.6			3.6
1930	1981	8	26	10	42	10.28	42.02	20.18	17.8	4.5	3.7	4.4			4.5
1931	1981	8	30	15	40	37.93	42.18	25.4	19	4	2.9	4			
1932	1981	9	7	17	43	11.93	41.39	22.59	10	4.5	3.7	4.4			4.3
1933	1981	9	30	12	3	2.69	41.72	23.29	10	4.3	3.3	4.2			
1934	1981	10	14	10	58	26.61	39.28	25.46	10	4.8	3.9	4.6	3.9		4.2
1935	1981	10	24	6	40	19.08	42	20.5	10	4.8	4	4.6			
1936	1981	12	8	8	3	44.38	40.01	20.55	4.6	4	2.5				3.6
1937	1981	12	16	12	27	12.27	43.31	19.56	10	4.1	2.7				3.7
1938	1981	12	16	18	3	50.7	43.44	19.79	10	4	3	4			4.4
1939	1981	12	19	14	10	51.1	39.22	25.25	10	6.8	7.2	6	7.2	6.8	6.3
1940	1981	12	19	14	49	40.3	39.25	25.44	9.3	4.4	3.5	4.3			3.9
1941	1981	12	19	18	10	49.29	39.34	25.43	2.7	4.8	3.9	4.4	3.9		4.5
1942	1981	12	19	21	14	26.83	39.29	25.4	17.2	5.1	4.4	4.7	4.4		4.8
1943	1981	12	20	10	58	58.46	39	25.02	5.2	4.4	3.5	4.3			3.8
1944	1981	12	20	22	40	12.76	39.33	20.71	20	4.1	3.1	4.1			4.1
1945	1981	12	20	22	54	29.36	39.33	25.51	25.1	4.4	3.5	4.3			4
1946	1981	12	21	13	54	40.58	39.14	25.26	25.3	5	4.2	4.8	4.2		4.8
1947	1981	12	21	14	13	16.45	39.26	25.37	5.4	5.4	4.9	4.8	4.9		5
1948	1981	12	21	14	15	43.63	39.2	25.45	10.9	5.2	4.6	4.9			4.4
1949	1981	12	26	14	29	13.41	39.04	25.14	18.4	4.7	3.6	4.6	3.6		4.3
1950	1981	12	26	17	53	34.99	40.15	28.74	0	5.2	4.6	4.9			4.8
1951	1981	12	30	1	12	22.52	40.13	25.15	4	4.3	3.3	4.2			3.7
1952	1982	1	11	2	42	33.03	40.94	20.64	0	4.5	3.4				4.1
1953	1982	1	15	19	11	11.44	39.32	25.49	7.5	4	2.9	4			3.9
1954	1982	1	17	8	5	6.49	39.04	25.2	10	4.5	3.7	4.4			3.6
1955	1982	1	18	19	27	24.97	39.96	24.39	10	6.6	6.9	5.8	6.9	6.6	6.4
1956	1982	1	18	19	31	7.92	40.03	24.56	10	6.7	6.8	5.3	6.8		5.2
1957	1982	1	18	19	41	2	39.92	24.42	0	4	2.9	4			3.7
1958	1982	1	18	19	46	31.68	39.89	24.58	10.8	4.3	3.3	4.2			4
1959	1982	1	18	19	52	34.31	40.04	24.62	10	4.1	3.1	4.1			3.5
1960	1982	1	18	19	55	0.13	39.8	24.4	12.8	4.3	3.3	4.2			3.6
1961	1982	1	18	20	0	3.48	39.75	24.1	12.4	4.6	3.8	4.5			4.8
1962	1982	1	18	20	0	52.62	39.86	24.26	10	4.9	4.2	4.7			4.9
1963	1982	1	18	20	8	13.67	39.95	24.59	22	4.3	3.3	4.2			3.9
1964	1982	1	18	20	32	1.69	39.71	24.24	17	4.4	3.5	4.3			4.4
1965	1982	1	18	20	52	24.63	39.78	24.25	10.2	4	2.9	4			4.2
1966	1982	1	18	23	40	36.79	39.83	24.41	10	4.7	3.7	4.5	3.7		4.3
1967	1982	1	19	6	39	46.07	39.77	24.18	14.6	4	2.9	4			3.7
1968	1982	1	19	12	18	18.38	39.72	24.34	10	5.2	4.6	4.5	4.6		4.8

										Homogenized magnitudes		Reported magnitudes			
Event Number	Year	Month	Date	Hour	Minute	Second	Latitude	Longitude	Depth	M_w	M_s	mb	M_s	M_w	ML
1969	1982	1	19	16	17	56.61	39.59	23.69	16.6	5	4.2	4.7	4.2		4.4
1970	1982	1	19	17	35	33.16	39.89	24.42	7	4.1	3.1	4.1			3.6
1971	1982	1	20	17	4	32.22	39.48	24.08	10.5	4.4	3.5	4.3			3.8
1972	1982	1	23	22	58	9.66	39.89	24.48	8.3	4.7	3.7	4.1	3.7		4.3
1973	1982	1	26	22	40	55.16	39.73	24.24	0	4.8	3.9				4.4
1974	1982	1	27	9	21	37.05	39.87	24.49	0.7	5	4.4	4.8			3.5
1975	1982	2	7	12	48	15.66	39.76	24.23	16.6	4.3	3.3	4.2			3.9
1976	1982	2	8	9	1	46.15	42.12	19.16	12	4.4	3.5	4.3			4.3
1977	1982	2	9	2	44	24.32	39.7	24.26	6.2	4.8	3.8	4.5	3.8		4.5
1978	1982	2	28	13	1	21.25	41.28	20.44	9.5	5	4.4	4.8			4.4
1979	1982	3	9	23	11	35.56	39.83	19.85	24.5	4.5	3.7	4.4			3.9
1980	1982	3	11	6	13	50.49	40.08	20.05	0	4.7	3.7				4.3
1981	1982	3	15	20	15	59.23	40.84	22.99	10	4.9	4.1				4.5
1982	1982	3	18	7	33	31.57	39.06	25.14	3.8	5	4.1	4.5	4.1		4.3
1983	1982	3	22	23	12	59.42	40.03	19.76	14.3	4.4	3.5	4.3			3.2
1984	1982	4	4	10	36	46.37	39.87	24.56	22.4	4.7	3.6	4.2	3.6		4.1
1985	1982	4	10	4	50	51.12	39.95	24.58	2.1	5.6	5.2	5	5.2		5
1986	1982	4	10	11	38	5.19	39.43	25.54	11.7	5	4.1	4.8	4.1		4.5
1987	1982	4	11	12	51	53.93	43.32	20.97	0.6	4.6	4	4.5			3.9
1988	1982	4	12	3	39	28.44	40.54	23.69	3.8	4.1	3.1	4.1			3.9
1989	1982	4	16	4	48	22.51	39.54	26.08	0	4.1	3.1	4.1			3.7
1990	1982	4	17	15	12	37.23	40.6	27.34	21.6	5	4.2				4.6
1991	1982	5	1	16	0	27.83	41.91	19.16	5.4	4.6	3.8	4.5			3.6
1992	1982	5	2	3	27	45.18	41.86	20	13.4	4.8	3.8	4.4	3.8		4.6
1993	1982	5	3	0	55	55.91	40.37	19.56	14.8	4	2.5				3.6
1994	1982	5	6	2	32	39.16	39.23	22.04	10.1	4.5	3.7	4.4			3.4
1995	1982	5	16	7	50	58.42	39.73	20.35	29.9	4.3	3	4.3	3		3.8
1996	1982	5	20	2	42	48.94	40.4	28.98	10	4.6	3.5	3.9	3.5		4.5
1997	1982	6	2	5	42	25.86	43.35	20.94	2.3	4.6	4.6	4.9	4.6		4.4
1998	1982	6	6	5	32	58.07	39.29	25.5	7.3	4	2.9	4			3.7
1999	1982	6	9	4	13	36.6	40.14	28.89	10	4.5	3.7	4.4			4.8
2000	1982	6	11	2	57	14.3	39.55	23.68	7.8	4.5	3.7	4.4			4
2001	1982	6	20	13	57	11.24	40.34	25.31	19.8	4.7	3.7	4.3	3.7		4
2002	1982	6	22	23	38	9.89	40.31	25.36	11	4.5	3.3	4	3.3		4.3
2003	1982	7	8	10	35	23.57	39.08	25.13	3.8	5.1	4.3	4.6	4.3		4.3
2004	1982	7	8	18	28	13.05	43.41	20.07	10	4.5	3.8	4.4			4
2005	1982	7	12	14	46	13.59	41	27.83	25.1	4.7	3.6	4.6	3.6		4.3
2006	1982	7	14	16	14	51.98	42.17	21.32	6.4	4.6	3.8	4.5			4.4
2007	1982	7	18	13	41	54.02	39.19	25.32	0.2	5	4.2	4.5	4.2		4.3
2008	1982	7	22	12	38	32.86	39.04	25.14	10.6	4.8	3.9	4.4	3.9		4.1
2009	1982	7	22	19	57	21.35	39.01	25.24	5.5	4.1	3.1	4.1			3.7
2010	1982	7	23	0	38	48.38	39.05	25.21	22.3	4.7	3.7	4.7	3.7		4.3
2011	1982	7	27	4	14	18.17	40.15	19.48	35	4.6	3.5	4.4	3.5		4.4
2012	1982	7	27	10	23	14.58	40.38	28.95	11	4.6	3.4	4.3	3.4		4.6
2013	1982	8	4	22	38	52.96	39.72	20.52	21.6	5.2	4.5	4.9	4.5		4.8
2014	1982	8	5	8	55	47.87	39.12	23.39	7.2	4.5	3.3	4.3	3.3		3.8
2015	1982	8	5	11	5	43.99	39.28	22.95	28.1	4.7	3.6	4.5	3.6		4.3
2016	1982	8	6	13	3	17.2	39.23	25.38	7	4.6	3.5	4	3.5		3.6
2017	1982	8	7	0	11	33.23	39.6	20.52	10	4.2	2.9				3.8
2018	1982	8	8	8	28	33.05	39.32	22.87	38.4	5	4.2	4.4	4.2		4.1
2019	1982	8	10	14	38	46.75	39.29	22.9	11.1	4.8	4	4.6			3.6
2020	1982	8	22	9	28	26.78	39.43	20.41	25	4.6	3.8	4.5			4.2
2021	1982	8	26	18	18	35.64	39.06	21.84	5.7	4.3	3.3	4.2			3.6
2022	1982	8	27	9	58	56.77	43.67	26.07	42.6	4.9	4.4	4.7			
2023	1982	8	27	22	50	33.47	40.68	21.43	20.9	4.4	3.1	4.2	3.1		4.2
2024	1982	9	9	5	47	10.75	40.98	27.87	10	4.5	3.7	4.4			4.4
2025	1982	9	10	2	30	16.09	39.1	23.75	19.3	4.1	3.1	4.1			3.1
2026	1982	9	11	10	54	6.77	40.39	25.38	6	4.8	3.8	4.3	3.8		4.4
2027	1982	9	19	1	32	7.3	43.03	19.04	10	4.4	3.2				4
2028	1982	10	25	23	41	10.59	40.54	21.63	21.4	4.8	3.8	4.4	3.8		4.6
2029	1982	10	29	8	17	35.5	42.06	19.26	3.1	4.6	3.8	4.5			4.5
2030	1982	11	12	1	25	7.96	39.39	26.12	10.7	4	2.5				3.6
2031	1982	11	14	9	8	33.2	40.4	25.35	25	4.5	3.4				4.1
2032	1982	11	16	23	41	20.75	40.82	19.58	20.5	5.9	5.7	5.5	5.7		5.5
2033	1982	11	17	0	37	54.5	40.84	19.54	30	5	4.2	4.9	4.2		4.7
2034	1982	11	17	3	36	16.18	40.85	19.54	26.3	4.8	4	4.6			4.4
2035	1982	11	19	16	14	42.7	40.78	19.48	5	4.5	3.7	4.4			4.7
2036	1982	11	19	22	45	22.02	40.82	19.53	10	4.7	3.7				4.3
2037	1982	11	21	2	45	21.19	39.47	26.2	16.5	4.2	2.9				3.8
2038	1982	12	5	19	16	3.95	39.88	26.5	0	4.8	4	4.6			
2039	1982	12	26	17	48	1.04	39.32	28.26	4.6	5.2	4.6	4.9			
2040	1982	12	27	8	14	42.07	40.9	22.87	15	4.2	2.9				3.8
2041	1982	12	27	11	2	44.33	39.34	28.27	10.5	5	4.4	4.8			4.2
2042	1982	12	27	19	55	24.79	39.01	27.83	17	4.5	3.4				4.1
2043	1983	1	5	4	3	29.26	41.99	19.21	10	5	4.4	4.8			3.7
2044	1983	1	21	5	49	10.13	39.27	23.06	10	4.4	3.5	4.3			3.8
2045	1983	2	1	13	54	11.22	40.2	28.94	3.1	5	4.4	4.8			
2046	1983	2	6	5	59	40.06	40.07	24.8	13.8	4	2.5				3.6
2047	1983	2	12	18	34	26.24	39.24	25.54	28.4	4	2.5				3.6
2048	1983	2	15	2	21	45.72	39.07	28.71	7.3	4.8	4	4.6			
2049	1983	2	25	18	22	11.98	42	21.64	8.8	4.8	3.8	4.8	3.8		4.4
2050	1983	3	3	9	31	18.56	40.14	19.72	43	4.6	3.8	4.5			3.9

										Homogenized magnitudes		Reported magnitudes			
Event Number	Year	Month	Date	Hour	Minute	Second	Latitude	Longitude	Depth	M_w	M_s	mb	M_s	M_w	ML
2051	1983	3	4	12	5	49.96	39.2	25.39	1.2	4	2.5				3.6
2052	1983	3	6	9	53	25.56	39.1	28.68	11.5	4.7	3.7				4.3
2053	1983	3	8	15	31	22.04	39.76	20.25	8.6	4.1	3.1	4.1			4.1
2054	1983	3	10	7	24	12.3	39.48	26.39	10	4.1	2.7				3.7
2055	1983	3	11	22	55	50.21	40.16	24.87	9	4.3	3.3	4.2			4.2
2056	1983	3	12	4	17	5.49	40.16	24.85	27.2	4.4	3.5	4.3			4.1
2057	1983	3	18	18	25	34.42	41.45	19.8	31.4	4.1	3.1	4.1			3.8
2058	1983	3	22	2	1	59.5	39.8	19.96	4.5	4.1	2.7				3.7
2059	1983	3	23	8	0	0.2	42.71	21.89	7	4	2.5				3.6
2060	1983	4	6	4	55	26.6	40.85	22.96	4.4	4.3	3				3.9
2061	1983	4	21	0	32	29.89	39.31	25.48	10.5	4.1	2.7				3.7
2062	1983	4	26	0	54	22.12	39.63	28.7	10	4.3	3				3.9
2063	1983	4	29	5	36	45.35	39.67	26.43	1.2	5.6	5.3				5.2
2064	1983	5	3	4	37	50.2	39.36	23.02	10	4.3	3.3	4.2			3.8
2065	1983	5	14	2	29	8.95	39.75	21.69	3.6	4.1	2.7				3.7
2066	1983	5	25	18	8	52.42	39.57	23.64	1.9	4.3	3				3.9
2067	1983	5	27	10	4	38.58	39.6	23.7	13.5	4.1	2.7				3.7
2068	1983	5	28	2	40	15.21	40.02	26.89	8.6	4.5	3.7	4.4			
2069	1983	5	31	22	29	53.4	40.79	21.32	5	4.3	3				3.9
2070	1983	6	4	11	10	5.78	41.78	23.32	0	4.9	4.2	4.7			
2071	1983	6	5	23	51	34.5	40.46	21.74	5	4.1	2.7				3.7
2072	1983	6	11	23	31	30.66	39.28	21.58	11.7	4.9	4.2	4.7			3.7
2073	1983	6	14	4	40	42.82	40.47	24	12	4.6	3.5	4.3	3.5		3.9
2074	1983	6	15	13	45	8.86	39.46	28.24	10.2	4.6	3.6				4.2
2075	1983	7	2	16	16	47.18	40.81	20.71	22.6	5.1	4.3	4.7	4.3		4.6
2076	1983	7	2	16	38	51.42	40.85	20.73	21.7	5.2	4.5	4.9	4.5		4.6
2077	1983	7	5	12	1	27	40.33	27.21	6.9	5.9	5.8	5.5	5.8		5.9
2078	1983	7	5	17	30	43.11	40.26	27.16	4.3	4.8	3.8	4.1	3.8		4.4
2079	1983	7	8	2	55	1.11	40.23	27.18	17	4.5	3.3	3.8	3.3		4.2
2080	1983	7	13	3	50	39.44	39.42	25.73	10	4	2.5				3.6
2081	1983	7	22	8	2	27	43.26	20.84	13.7	4.9	4.4	4.7			4.3
2082	1983	8	1	3	40	26.33	39.5	23.61	3.5	4	2.5				3.6
2083	1983	8	6	15	43	51.87	40.14	24.74	2	6.7	6.9	6	6.9	6.7	6.6
2084	1983	8	6	16	15	16.58	39.95	24.49	7.4	4	2.5				3.6
2085	1983	8	6	16	34	20.88	40.29	24.76	47	4.2	2.9				3.8
2086	1983	8	6	16	46	22.96	39.85	24.55	6.9	4.5	3.7	4.4			4.4
2087	1983	8	6	17	15	44.8	39.87	24.45	37.9	4	2.9	4			3.7
2088	1983	8	6	17	30	47.31	40.08	24.86	10	4.2	2.9				3.8
2089	1983	8	6	18	40	6.88	39.9	24.46	12.7	4	2.5				3.6
2090	1983	8	6	18	46	44.68	39.97	24.62	18.2	4	2.9	4			4.1
2091	1983	8	6	18	58	35.38	40.11	24.8	7	4.1	3.1	4.1			4.2
2092	1983	8	6	19	15	41.31	40.07	24.74	10	4.3	3				3.9
2093	1983	8	6	19	44	28.97	40	24.86	5	4.1	2.7				3.7
2094	1983	8	6	20	6	36.54	40.12	24.61	7.8	4	2.5				3.6
2095	1983	8	6	21	3	50.64	40	24.65	10	4.1	2.7				3.7
2096	1983	8	6	21	9	15.65	40.14	24.98	5	4	2.5				3.6
2097	1983	8	6	22	10	43.43	40.15	24.89	10	4	2.5				3.6
2098	1983	8	6	22	12	49.87	40.16	24.82	5	4.1	2.7				3.7
2099	1983	8	7	0	11	31.67	40.05	24.78	10	4.1	2.7				3.7
2100	1983	8	7	1	44	10.73	40.09	24.76	2.8	5.1	4.4	4.1	4.4		4.3
2101	1983	8	7	4	35	59.36	39.93	24.83	10	4.3	3				3.9
2102	1983	8	7	5	29	23.15	40.2	24.83	10	4.2	2.9				3.8
2103	1983	8	7	5	55	55.01	40.11	24.81	9	4	2.5				3.6
2104	1983	8	7	6	12	6.09	39.95	24.39	9	4	2.5				3.6
2105	1983	8	7	7	13	34.75	39.88	24.55	14.9	4.2	2.9				3.8
2106	1983	8	7	9	17	26.53	39.99	24.47	10	4	2.5				3.6
2107	1983	8	7	9	39	20.65	40.05	24.78	18	4.2	2.9				3.8
2108	1983	8	7	10	44	14.03	40.02	24.92	10	4.2	2.9				3.8
2109	1983	8	7	14	6	47.06	40.04	24.8	15	4	2.5				3.6
2110	1983	8	7	14	21	13.76	39.9	24.2	19.2	4.1	2.7				3.7
2111	1983	8	7	20	45	24.62	39.39	23.83	2.2	4.3	3.3	4.2			3.7
2112	1983	8	7	21	23	34.99	40.05	24.83	40	4.1	2.7				3.7
2113	1983	8	8	0	36	53.13	40.14	24.83	25.8	4	2.5				3.6
2114	1983	8	8	1	56	42.57	40.06	24.77	10	4.7	3.6	4	3.6		4.1
2115	1983	8	8	3	31	16.57	40.1	24.86	10	4.2	2.9				3.8
2116	1983	8	8	8	9	37.86	40.02	24.79	5	5.2	4.6	4.2	4.6		5.1
2117	1983	8	8	9	5	34.96	40.09	24.82	22.3	4.3	3				3.9
2118	1983	8	8	11	12	4.03	39.72	24.36	10	4	2.5				3.6
2119	1983	8	8	12	45	55.47	39.88	24.65	5	4.2	2.9				3.8
2120	1983	8	8	16	39	17.3	39.98	24.87	5	4	2.5				3.6
2121	1983	8	9	23	41	58.55	40.07	24.82	32.3	4.2	2.9				3.8
2122	1983	8	10	5	14	13.54	40.04	24.9	5	4.1	2.7				3.7
2123	1983	8	10	22	30	13.88	40.02	24.9	10	4.2	2.9				3.8
2124	1983	8	11	1	4	36.7	40.1	24.82	9	5	4.1	4.5	4.1		4.4
2125	1983	8	11	20	22	29.2	40.1	24.76	17	4.2	2.9				3.8
2126	1983	8	12	7	28	47.58	40.15	24.86	10	4	2.5				3.6
2127	1983	8	12	18	41	18.67	39.77	24.92	5	4.1	2.7				3.7
2128	1983	8	13	14	59	35.16	40.09	24.83	4.1	4.2	2.9				3.8
2129	1983	8	17	1	38	41.91	39.44	24.2	6.5	4.1	2.7				3.7
2130	1983	8	18	13	10	54.01	40.08	24.82	14.5	4.5	3.4				4.1
2131	1983	8	19	4	43	19.34	40.1	24.79	28.8	4.1	3.1	4.1			4.2
2132	1983	8	20	6	46	12.61	40.07	24.63	10	4.3	3				3.9

										Homogenized magnitudes		Reported magnitudes			
Event Number	Year	Month	Date	Hour	Minute	Second	Latitude	Longitude	Depth	M_w	M_s	mb	M_s	M_w	ML
2133	1983	8	21	19	54	54.9	40.09	24.6	10	4.1	2.7				3.7
2134	1983	8	22	10	35	15.01	40.09	24.71	13	4.2	2.9				3.8
2135	1983	8	22	11	0	26.66	40.13	24.83	9.6	4.3	3				3.9
2136	1983	8	23	5	42	3.59	39.93	24.63	9	5.1	4.3	4.4	4.3		4
2137	1983	8	23	18	18	5.77	40.22	24.89	10	4.3	3				3.9
2138	1983	8	26	12	52	8.89	40.5	23.91	2.6	5.3	4.8	4.9	4.8		4.5
2139	1983	8	26	16	15	30.13	41.04	22.41	0.2	4.7	3.7	4.2	3.7		4.5
2140	1983	8	27	19	4	37.27	40.06	24.8	1	4.2	2.9				3.8
2141	1983	8	27	22	9	13.05	39.63	21.94	3.2	4.1	2.7				3.7
2142	1983	9	1	5	47	40.8	40.19	24.89	21.9	4.4	3.2				4
2143	1983	9	1	7	17	45.08	39.66	21.91	0.1	4	2.5				3.6
2144	1983	9	2	20	43	5.76	43.28	20.91	3.4	4.9	4.4	4.7			4.3
2145	1983	9	3	3	28	9.12	39.09	25.54	22.4	4.6	3.8	4.5			4.2
2146	1983	9	3	12	45	23.13	39.11	27.57	0	4.4	3.2				4
2147	1983	9	5	8	30	49.72	41.33	20.89	0	4.6	3.6				4.2
2148	1983	9	5	8	31	49.69	41.34	20.94	10	4.1	3.1	4.1			4
2149	1983	9	6	1	51	50.35	40.19	24.96	9	4.3	3				3.9
2150	1983	9	10	6	14	22.38	43.24	20.84	7.2	4.6	4.6	5	4.6		4.9
2151	1983	9	11	15	8	24.1	40.29	25.19	13.7	4.1	2.7				3.7
2152	1983	9	16	21	15	41.84	39.85	23.97	2.7	4.1	2.7				3.7
2153	1983	9	17	16	4	16.61	40.06	24.71	28.2	4.2	2.9				3.8
2154	1983	9	19	20	20	48.86	39.57	20.36	10	4.4	3.5	4.3			3.9
2155	1983	9	22	10	3	56.86	39.72	25.79	10	4.2	2.9				3.8
2156	1983	9	22	15	58	19.9	40.07	24.84	10	4.1	2.7				3.7
2157	1983	9	23	13	39	4.4	40.14	24.82	16	4.3	3				3.9
2158	1983	9	25	15	2	20.32	40.12	24.8	10	4.3	3				3.9
2159	1983	10	3	16	51	53.69	40.14	24.84	19	4.2	2.9				3.8
2160	1983	10	9	21	26	57.34	39.15	22.12	16.8	4	2.9	4			4.3
2161	1983	10	10	10	16	57.91	40.26	25.3	3.8	5.5	5.1	4.9	5.1		5.2
2162	1983	10	11	4	43	44.89	40.25	25.28	42	4.7	3.7				4.3
2163	1983	10	11	5	8	21.6	40.27	25.29	10	4.6	3.6				4.2
2164	1983	10	11	5	14	2.95	40.25	25.28	10	4.4	3.2				4
2165	1983	10	13	6	52	40.2	39.77	24.25	12	4.5	3.7	4.4			4.6
2166	1983	10	23	13	41	52.76	41.84	20.02	4.7	4	2.5				3.6
2167	1983	10	28	5	8	18.81	40.04	24.79	17	5.3	4.8	4.7	4.8		4.8
2168	1983	10	29	6	50	57.86	40.01	24.8	14.5	4	2.5				3.6
2169	1983	10	30	3	50	56.77	40.1	24.84	12	4.9	4	4.5	4		4.2
2170	1983	10	31	20	11	40.52	39.84	24.48	1.2	4.4	3.5	4.3			4.2
2171	1983	10	31	20	22	30.72	39.9	24.45	10	4	2.5				3.6
2172	1983	10	31	20	52	42.81	39.81	24.44	13	4.6	3.8	4.5			4
2173	1983	11	9	9	59	40.73	39.03	23.31	3.6	4.2	2.9				3.8
2174	1983	11	10	17	28	20.95	43.14	27.54	2.9	4	4	4.7	4		
2175	1983	11	16	5	56	28.59	39.87	24.41	10	4.4	3.5	4.3			4.5
2176	1983	11	21	18	26	16.03	40.1	24.8	5	4	2.5				3.6
2177	1983	11	25	22	8	32.16	40.1	24.83	11	4.1	2.7				3.7
2178	1983	11	28	7	50	52.98	39.86	24.75	5	4	2.5				3.6
2179	1983	12	9	2	55	23.04	40.43	25.49	10	4.7	3.7				4.3
2180	1983	12	20	23	43	13.82	40.35	25.5	0	4.3	3.3	4.2			
2181	1983	12	22	22	46	39.44	40	24.69	5	4.1	2.7				3.7
2182	1983	12	23	19	50	2.21	39.33	21.47	12.9	4.4	3.5	4.3			3.8
2183	1983	12	25	2	56	10.54	41.91	19.07	0	5.2	4.6	4.9			4.5
2184	1983	12	25	22	19	24.66	40.41	25.46	10	4.3	3				3.9
2185	1983	12	27	9	54	51.89	40.01	25.27	10	5.9	5.8				5.5
2186	1983	12	28	8	21	51.67	40.84	20.81	5	4.3	3.3	4.2			3.5
2187	1983	12	28	8	27	27.59	40.88	20.79	4.2	4	2.9	4			3.9
2188	1984	1	7	3	42	1.06	40.16	24.94	12	4.2	2.9				3.8
2189	1984	1	13	19	41	39.9	42	19.06	6.6	4.5	3.7	4.4			4.9
2190	1984	1	13	23	36	54.66	40.13	19.79	1.4	4.1	3.1	4.1			4
2191	1984	1	16	10	22	51.73	39.41	20.04	10	4.3	3				3.9
2192	1984	1	21	14	33	22.81	42	19.1	2.1	4.7	3.7				4.3
2193	1984	1	23	10	26	33.53	41.9	23.4	5.6	4.6	3.8	4.5			4.1
2194	1984	1	24	14	38	36.44	39.46	25.69	10	4.1	2.7				3.7
2195	1984	1	27	21	51	38.85	40.23	24.79	10	4.3	3				3.9
2196	1984	1	28	1	30	17.91	40.15	24.8	10	4.2	2.9				3.8
2197	1984	1	30	0	54	49.66	39.44	21.51	10	4.2	2.9				3.8
2198	1984	1	30	5	58	25.79	40.5	27.49	10	4.7	3.7	4.5	3.7		
2199	1984	2	4	4	39	22.39	39.54	28.76	12.2	5.6	5.3				5.2
2200	1984	2	5	23	11	17.79	39.89	24.29	24	4.1	2.7				3.7
2201	1984	2	7	18	28	18.23	40.5	21.67	5.5	4	2.5				3.6
2202	1984	2	9	1	51	6.67	40.41	21.58	12.5	4.7	3.6	4.7	3.6		4.6
2203	1984	2	11	9	25	28.54	42.6	19.21	2.6	4	2.9	4			4
2204	1984	2	17	21	19	53.62	39.21	23.46	6.2	4.6	3.8	4.5			3.9
2205	1984	2	19	2	53	0.75	40.62	23.37	7.9	4	2.9	4			3.7
2206	1984	2	19	3	47	22.51	40.67	23.36	24.5	5.1	4.3	4.9	4.3		4.3
2207	1984	2	19	3	59	59.59	40.56	23.38	15	4.1	2.7				3.7
2208	1984	2	20	14	1	39.44	43.69	20.55	4.9	4.4	3.2				4
2209	1984	2	25	22	1	0.88	39.38	27.88	9	4.4	3.2				4
2210	1984	3	2	15	50	43.35	39.01	21.61	39.4	4.9	4.2	4.7			4.3
2211	1984	3	3	8	32	15.08	43.33	20.99	6.2	4.8	4.2	4.6			4.2
2212	1984	3	4	21	39	25.45	39.95	24.74	5	4.1	2.7				3.7
2213	1984	3	11	21	19	59.41	39.17	20.51	45.2	4.6	3.8	4.5			4.1
2214	1984	3	11	23	28	20.32	39.14	20.49	45.4	4.3	3.3	4.2			4

										Homogenized magnitudes		Reported magnitudes			
Event Number	Year	Month	Date	Hour	Minute	Second	Latitude	Longitude	Depth	M_w	M_s	mb	M_s	M_w	ML
2215	1984	3	12	2	29	59.49	39.25	20.58	48.1	4.9	4	4.7	4		4.5
2216	1984	3	27	17	8	48.75	39.23	22.94	7.5	5.8	5.6				5.4
2217	1984	3	29	0	6	1.38	39.64	27.87	12	4.8	3.8	4.6	3.8		4.6
2218	1984	3	30	10	15	21.75	41.09	20	2.8	4.8	4	4.6			4.3
2219	1984	4	1	17	17	41.45	39.56	28.76	6.8	4.7	3.7	4.1	3.7		4.4
2220	1984	4	4	7	43	2.18	39.12	20.8	5	4.1	2.7				3.7
2221	1984	4	27	4	38	59.09	40.09	24.77	25.3	4.2	2.9				3.8
2222	1984	5	4	2	52	30.79	40.7	23.31	1.8	4	2.9	4			3.9
2223	1984	5	5	7	27	23.65	40.14	24.94	5	4	2.5				3.6
2224	1984	5	8	5	4	4.5	40.31	22.78	19	4.8	4	4.6			4.3
2225	1984	5	8	19	27	6.53	41.94	19.61	1.3	4.5	3.4				4.1
2226	1984	5	14	18	18	3.46	40.39	22.87	14	4.3	3.3	4.2			4.2
2227	1984	5	15	4	35	47.35	40.35	22.79	5	4	2.9	4			
2228	1984	5	17	16	33	27.03	39.86	24.76	5	4.1	2.7				3.7
2229	1984	5	24	11	34	3.49	40.04	20.12	12.6	4.3	3.3	4.2			4.5
2230	1984	5	30	23	44	40.08	39.18	24.36	2.3	4	2.5				3.6
2231	1984	6	12	0	10	32.95	40.08	24.92	20.3	4.3	3.3	4.2			3.9
2232	1984	6	23	21	11	1.09	40.37	25.46	15.5	4.4	3.2				4
2233	1984	6	25	8	37	48.18	42.1	19.68	3	4.6	3.6				4.2
2234	1984	6	26	14	48	47.9	39.45	21.66	31.5	5	4.4	4.8			4.1
2235	1984	6	29	23	18	34.29	41.2	19.72	28.2	4.6	3.8	4.5			4.2
2236	1984	6	30	6	4	28.57	40.45	25.37	10	4.2	2.9				3.8
2237	1984	6	30	16	44	52.1	40.27	25.32	10	4.1	2.7				3.7
2238	1984	7	4	18	44	42.83	39.03	22.07	21.5	4.4	3.5	4.3			3.4
2239	1984	7	8	3	31	39.48	41.16	22.55	2.8	4	2.9	4			4
2240	1984	7	8	7	18	52.78	40.06	24.61	5	4	2.5				3.6
2241	1984	7	9	18	57	13.08	40.69	21.85	36.2	5.5	5.1	5.1	5.1		5.2
2242	1984	7	11	13	54	41.04	40.19	24.86	10	4.1	2.7				3.7
2243	1984	7	12	7	48	37.76	40.83	20.46	6.9	4.7	3.6	4.1	3.6		3.9
2244	1984	7	15	17	47	2.54	39.22	27.72	10	4.5	3.4				4.1
2245	1984	7	16	13	52	45.41	39.99	23.71	10	4.1	2.7				3.7
2246	1984	7	29	1	58	43.31	40.45	25.91	21	5.2	4.6	5	4.6		4.9
2247	1984	7	29	2	21	11.73	40.4	26	10	5.3	4.7	4.8	4.7		4.3
2248	1984	7	29	2	27	3.27	40.45	26.05	10	4.1	2.7				3.7
2249	1984	7	29	2	30	46.31	40.37	26.12	10	4.1	2.7				3.7
2250	1984	7	29	4	30	55.86	40.46	26.02	5	4.3	3				3.9
2251	1984	7	29	9	48	23.82	40.43	25.93	27	5.1	4.3	4.5	4.3		4.6
2252	1984	7	29	12	17	37.16	40.44	26.02	2.4	4.2	2.9				3.8
2253	1984	7	29	12	22	57.63	40.44	25.96	0.7	4.1	2.7				3.7
2254	1984	7	29	12	58	29.16	40.4	25.96	4.6	4.2	2.9				3.8
2255	1984	7	29	22	22	25.91	40.39	25.99	10	4.9	4	4.2	4		4.3
2256	1984	7	30	0	12	56.63	40.4	26.19	10	4.2	2.9				3.8
2257	1984	8	2	5	15	35.18	40.11	24.67	11.3	4.1	2.7				3.7
2258	1984	8	3	15	3	43.06	40	21.73	5	4	2.5				3.6
2259	1984	8	19	4	8	6.32	41.63	20.8	5.5	4.6	3.8	4.5			4.3
2260	1984	9	4	1	6	5.69	39.4	20.57	54.9	4.7	3.6	4.6	3.6		4.1
2261	1984	9	7	0	44	40.78	43.32	20.97	5	4.7	4.7	5.1	4.7		5.3
2262	1984	9	15	23	31	27.13	39.29	20.53	14	4	2.5				3.6
2263	1984	9	25	6	58	14.13	40.71	23.44	2	4.1	2.7				3.7
2264	1984	9	29	11	14	3.09	41.52	20.16	7.2	4.1	2.7				3.7
2265	1984	10	3	4	23	44.03	40.06	24.7	9	4.8	3.9				4.4
2266	1984	10	3	4	41	52.2	39.98	24.71	10	4.6	3.6				4.2
2267	1984	10	5	14	22	47.68	40.93	23.48	7	4.3	3.3	4.2			4
2268	1984	10	5	20	58	48.64	39.15	25.26	8.7	5.1	4.4	5	4.4		5.2
2269	1984	10	22	14	51	28.11	39.81	20.63	11	4.1	2.7				3.7
2270	1984	10	25	14	38	30.3	40.11	21.62	40.1	5.5	5.3	5.2	5.3		5.1
2271	1984	10	27	0	57	34.05	39.08	25.2	28	4.7	3.6	4.4	3.6		3.9
2272	1984	10	29	2	5	40.29	39.05	22.03	25	4.1	3.1	4.1			3.8
2273	1984	11	9	5	13	55.72	41.06	19.91	6.5	4.8	3.9				4.4
2274	1984	11	14	14	24	24.94	40.33	27.23	5.7	4.1	3.1	4.1			
2275	1984	11	14	14	53	50.24	40.72	23.38	6.5	4.7	3.6	4.3	3.6		4
2276	1984	11	18	14	47	41.82	39.73	20.54	22.4	4.3	3	5.1	3		4.2
2277	1984	11	20	0	34	51.55	40.1	24.77	12.7	4.2	2.9				3.8
2278	1984	11	20	8	3	10.89	40.11	24.82	10	5.4	5	5.1			3.9
2279	1984	11	20	9	49	33.86	40.13	24.74	3.9	4.4	3.2				4
2280	1984	11	21	22	2	48.55	39.95	23.47	17	4	2.5				3.6
2281	1984	12	3	2	36	55.34	40.08	20.56	10	4.2	2.9				3.8
2282	1984	12	5	11	45	42.19	39.23	20.8	62.3	4.4	3.5	4.3			4.1
2283	1984	12	7	0	9	25.27	39.26	22.9	35.7	5	4.2	4.8	4.2		4.1
2284	1984	12	15	8	20	23.38	42.07	19.68	6.3	4.3	3.3	4.2			3.8
2285	1984	12	15	9	1	20.18	39.84	22.76	8.5	4.8	3.8	5	3.8		4.7
2286	1984	12	15	17	29	2.43	42.03	19.72	1.2	4.7	3.7	4.1	3.7		3.7
2287	1984	12	16	6	37	7.44	42.06	19.75	7	5	4.4	4.8			3
2288	1984	12	18	9	45	17.17	42.05	19.75	2	4	2.9	4			2.8
2289	1984	12	18	14	20	35.51	41.99	19.66	6	4	2.5				3.6
2290	1984	12	19	0	15	51.31	40.13	23.49	7	4	2.5				3.6
2291	1984	12	22	11	50	43.91	39.86	22.82	10	4.4	3.5	4.3			3.8
2292	1984	12	23	17	13	36.24	42.02	19.78	10.4	5	4.4	4.8			3
2293	1984	12	24	13	59	12.33	42.03	19.74	11.4	6.1	6.1				5.7
2294	1984	12	30	5	25	36.4	39.98	24.55	10	4.1	2.7				3.7
2295	1984	12	30	8	43	41.48	40.46	21.31	7	4.1	3.1	4.1			4
2296	1984	12	31	7	24	16.24	41.28	19.54	13.8	4	2.9	4			3.7

										Homogenized magnitudes		Reported magnitudes			
Event Number	Year	Month	Date	Hour	Minute	Second	Latitude	Longitude	Depth	M_w	M_s	mb	M_s	M_w	ML
2297	1985	1	5	13	6	33.23	42.58	22.13	18.9	4.9	4.2	4.7			4.5
2298	1985	1	16	23	35	58.02	40.69	19.22	13.7	5.5	5	5.1	5		5
2299	1985	1	26	17	25	32.61	39.38	25.37	41	4	2.5				3.6
2300	1985	2	5	23	31	57.9	39.93	24.56	18.9	4.1	2.7				3.7
2301	1985	2	16	6	33	41.49	42.05	23.68	11.2	4.9	4.2	4.7			3.9
2302	1985	2	21	3	3	32.94	39.83	24.4	4.4	4	2.9	4			4.3
2303	1985	2	21	6	21	37.41	41.55	20.4	5	4.3	3.3	4.2			4.1
2304	1985	3	12	9	51	7.15	39.44	23.98	6.4	5	4.4	4.8			4.5
2305	1985	3	20	13	10	35.98	40.86	23.59	1	4.1	2.7				3.7
2306	1985	3	29	19	50	25.87	39.38	20.62	5	4	2.5				3.6
2307	1985	4	9	4	53	20.36	41.42	23.04	3.5	5.5	5.1				5.1
2308	1985	4	16	0	40	24.24	39.68	20.57	10	4.7	3.6	4.5	3.6		3.8
2309	1985	4	16	12	46	45.26	39.74	20.58	11.9	4.5	3.3	4.6	3.3		4.3
2310	1985	4	16	13	8	3.52	39.74	20.58	23.8	4.1	3.1	4.1			3.7
2311	1985	4	16	19	0	36.4	39.8	20.64	10.8	4.7	3.6	4	3.6		3.8
2312	1985	4	25	12	5	35.5	40.8	20.37	6	4.5	3.7	4.4			4.2
2313	1985	4	27	12	33	6.89	40.74	27.38	9.1	5	4.2	4.4	4.2		4.6
2314	1985	4	30	18	14	12.89	39.26	22.81	25.5	5.7	5.5	5.4	5.5		5.3
2315	1985	5	3	22	13	55.78	39.3	22.98	15.7	4.6	3.4	3.6	3.4		3.5
2316	1985	5	10	23	45	27.41	43.34	20.93	0.6	4.6	4.6	5.2	4.6		5
2317	1985	5	11	7	29	59.52	39.17	20.71	13	4.3	3.3	4.2			4.2
2318	1985	5	14	4	52	18.49	39.71	26.09	25.7	4.4	3.2				4
2319	1985	5	21	23	27	1.56	39.95	20.09	5	4.8	3.8	4.5	3.8		4.2
2320	1985	5	30	21	41	33.86	39.7	20.38	4.3	4.1	2.7				3.7
2321	1985	6	4	1	5	58.46	40.86	27.84	10	4.1	3.1	4.1			
2322	1985	6	12	14	5	19.33	43.15	27.61	10	4.5	3.8	4.4			
2323	1985	6	13	0	53	13.01	39.01	25.95	28.8	5	4.1	4.4	4.1		4.2
2324	1985	6	20	2	58	31.46	39.24	22.97	43.7	4.6	3.5	4.3	3.5		4
2325	1985	6	26	4	48	52.63	41.16	19.89	23	4	2.9	4			4.2
2326	1985	6	28	4	36	51.17	39.14	23.41	10	4.1	2.7				3.7
2327	1985	7	6	8	53	41.02	40.19	23.71	8	4	2.5				3.6
2328	1985	7	28	12	33	52.06	39.34	27.62	18	4.3	3				3.9
2329	1985	7	30	18	53	16.13	40.39	22.79	10.3	5	4.4	4.8			
2330	1985	8	18	2	57	58.79	39.16	20.79	10	4.2	2.9				3.8
2331	1985	8	31	6	3	48.65	39.11	20.62	46.7	5.3	4.7	4.7	4.7		4.8
2332	1985	8	31	6	33	14.36	39.11	20.53	26.2	4.3	3.3	4.2			4
2333	1985	8	31	8	41	37.62	39.24	20.54	3.5	4.3	3				3.9
2334	1985	9	17	6	53	33.28	41.92	23.06	7.6	5	4.2				4.6
2335	1985	9	21	10	13	9.01	39.03	22.2	41.7	5.1	4.4	5	4.4		4.4
2336	1985	9	28	14	50	14.94	41.6	22.27	3.7	5.5	5	5	5		4.7
2337	1985	10	2	2	32	53.01	41.51	22.29	7.3	4.3	3.3	4.2			3.8
2338	1985	10	4	13	36	7.82	39.2	26.21	13.8	4.3	3.3	4.2			4.4
2339	1985	10	27	16	7	33.22	40.03	20.8	10	4.3	3.3	4.2			3.9
2340	1985	11	9	23	30	42.89	41.26	23.98	18.5	5.5	5.3	5.5	5.3		5.4
2341	1985	11	21	7	27	52.17	42.33	19.93	0.7	4.5	3.7	4.4			3.9
2342	1985	11	21	9	44	47.82	42.37	19.95	0	4.1	2.7				3.7
2343	1985	11	21	18	0	54.95	42.35	19.97	15	4	2.5				3.6
2344	1985	11	21	19	23	6.22	42.33	19.92	0	4.8	4	4.6			3.9
2345	1985	11	21	21	57	14.91	41.73	19.41	22.9	5.5	5.3	5.5	5.3		5.3
2346	1985	11	21	23	16	27.24	41.73	19.38	42.2	4.7	3.6	5	3.6		4.5
2347	1985	11	22	22	6	58.98	42.33	19.92	1.5	5	4.1	4.6	4.1		4.5
2348	1985	11	22	22	17	37.31	42.33	19.92	5.6	4.9	4.2	4.7			3.8
2349	1985	11	23	7	59	26.15	42.29	19.92	10	4.4	3.1	4.4	3.1		3.7
2350	1985	11	23	8	19	48.68	42.32	19.9	2.5	5.1	4.4	4.7	4.4		4.5
2351	1985	11	23	17	32	30.6	42.31	19.93	0	4.6	3.8	4.5			3.7
2352	1985	11	24	9	58	2.07	42.33	19.91	0	4.3	3.3	4.2			4.1
2353	1985	11	25	23	49	50.58	41.75	19.33	19	4.6	3.8	4.5			3.6
2354	1985	11	27	12	38	58.38	42.32	19.93	2.5	4.5	3.7	4.4			4.5
2355	1985	11	30	1	33	33.76	42.22	19.9	10	4.2	2.9				3.8
2356	1985	11	30	7	34	11.94	42.32	19.93	0.8	4	2.9	4			4
2357	1985	12	1	11	47	38.7	39.29	27.7	10	4.8	3.9	4.6	3.9		4.6
2358	1985	12	2	15	56	16.27	41.71	19.38	5	4.4	3.5	4.3			3.5
2359	1985	12	8	17	36	42.58	42.3	19.94	0.6	4.8	4	4.6			4.6
2360	1985	12	13	22	28	7.52	42.3	20	0	4	2.5				3.6
2361	1985	12	18	5	46	0.75	39.2	26.17	16.9	5.5	5.1	5	5.1		4.8
2362	1985	12	18	17	17	33.78	39.16	26.23	14.2	4.1	2.7				3.7
2363	1985	12	19	9	27	41.47	39.16	26.24	12.3	4.1	3.1	4.1			4.1
2364	1985	12	19	14	34	56.54	40.2	27.26	10	4.5	3.4				4.1
2365	1985	12	19	15	15	56.05	39.17	26.11	14.3	4	2.5				3.6
2366	1985	12	21	1	49	39.07	42.31	19.97	0.1	4.6	3.8	4.5			3.8
2367	1985	12	21	2	12	50.54	39.18	26.38	4.6	4.1	2.7				3.7
2368	1985	12	21	11	18	12.05	42.31	19.96	0	4.9	4.2	4.7			4
2369	1985	12	21	21	26	15.03	39.21	26.19	18.7	4.1	2.7				3.7
2370	1985	12	25	14	29	39.96	42.29	19.96	11	4.3	3.3	4.2			3.8
2371	1985	12	27	9	48	42.34	42.35	19.89	1	5	4.4	4.8			3.9
2372	1986	1	8	20	57	18.23	42.35	19.91	4.6	4.3	3.3	4.2			4
2373	1986	1	10	4	35	37.85	42.31	19.95	2.8	4.9	4.2	4.7			4.4
2374	1986	1	11	0	39	59.83	42.31	19.86	0	4.8	4	4.6			3.2
2375	1986	1	13	13	48	3.6	41.28	19.54	10	5	4.4	4.8			4.4
2376	1986	1	13	19	59	23.67	41	19.87	2.9	4	2.9	4			3.5
2377	1986	1	15	21	27	36.33	40.03	19.69	0	4.4	3.5	4.3			3.6
2378	1986	1	16	0	52	6.32	40.17	24.99	17.6	4.2	2.9				3.8

										Homogenized magnitudes		Reported magnitudes			
Event Number	Year	Month	Date	Hour	Minute	Second	Latitude	Longitude	Depth	M_w	M_s	mb	M_s	M_w	ML
2379	1986	1	16	2	10	37.34	39.99	19.48	16	4.8	3.9	4.1	3.9		3.7
2380	1986	1	21	21	22	23.02	42.37	20.11	0	5.2	4.6	4.9			3
2381	1986	2	18	14	34	3.56	40.79	22.07	19.9	5.3	4.8	5.1	4.8		4.6
2382	1986	2	18	21	55	35.02	40.68	23.2	10	4	2.5				3.6
2383	1986	2	21	5	39	55.27	43.3	25.96	10.7	5.5	5.5	4.9	5.5		5.2
2384	1986	2	22	9	11	33.44	39.06	22.11	10.7	4.7	3.6	4.4	3.6		3.9
2385	1986	3	3	1	24	4.27	42	20.3	7.1	5.5	5	4.9	5		4.7
2386	1986	3	3	4	25	51.77	41.98	20.31	1.9	4.6	3.8	4.5			4.2
2387	1986	3	3	12	35	49.5	41.96	20.31	3	4.8	4	4.6			3.8
2388	1986	3	7	6	23	27.77	41.96	20.29	7	4.6	3.5	3.8	3.5		3.6
2389	1986	3	9	3	6	41.63	42.34	19.98	7.3	4.2	2.7		2.7		2.3
2390	1986	3	11	5	38	30.25	41.98	20.31	0	4.3	3	4	3		3.1
2391	1986	3	13	12	26	21.2	41.68	19.44	10	4	2.4		2.4		2.4
2392	1986	3	15	8	46	56.59	41.15	20.17	6.6	5.2	4.6	4.9			4.2
2393	1986	3	24	2	1	36.1	41.19	19.87	10	4.2	2.7		2.7		2.8
2394	1986	4	12	16	57	34.52	39.39	20.52	10.5	4.1	3.1	4.1			4.1
2395	1986	5	2	10	19	23.95	42.33	19.96	0	4.1	3.1	4.1			3.8
2396	1986	5	4	0	30	11.2	42.33	19.96	0	4.5	3.7	4.4			3.7
2397	1986	5	4	21	16	26.21	42.33	19.95	0	4	2.5				3.6
2398	1986	5	14	3	1	25.44	39.49	28.42	7.7	4.8	3.8	4.5	3.8		
2399	1986	5	15	16	45	22.13	41.98	23.13	9.4	4.6	3.5	3.9	3.5		4
2400	1986	5	15	18	13	55.86	40.72	27.57	10	4.8	4	4.6			
2401	1986	5	17	13	16	39.21	39.03	26.15	12.5	4	2.5				3.6
2402	1986	5	27	8	54	58.19	39.46	28.44	11.1	4.6	3.5	4.4	3.5		4.5
2403	1986	6	3	19	35	53.75	39.46	28.36	9.4	4.4	3.5	4.3			
2404	1986	6	7	20	3	25.07	41.26	19.63	11.5	5	4.4	4.8			4.4
2405	1986	6	7	20	6	27.48	41.27	19.64	10.9	4.8	4	4.6			4.4
2406	1986	6	7	20	7	30.56	41.23	19.43	10	4.8	4	4.6			3.5
2407	1986	6	12	6	42	24.62	39.09	28.7	10	4.1	3.1	4.1			
2408	1986	6	16	10	26	44.31	40.07	19.68	1.8	4.4	3.5	4.3			3.8
2409	1986	6	25	11	48	22.51	39.46	28.36	5	4.7	3.7	3.9	3.7		4.2
2410	1986	6	26	20	44	24.26	41.26	19.61	10	5	4.1	5	4.1		4.3
2411	1986	6	27	18	33	36.65	40.89	28.35	5	4.1	3.1	4.1			4.4
2412	1986	8	18	1	48	48.54	41.61	20.12	10	4.7	3.7				4.3
2413	1986	8	19	4	5	42.22	43.16	26.04	5.3	4.2	2.9				3.8
2414	1986	8	19	6	3	54.39	39.04	28.79	10	4.9	4.2	4.7			4.2
2415	1986	8	30	4	47	10.9	39.11	27.84	10	4.5	3.4				4.1
2416	1986	9	3	18	42	53.3	40.24	25	10	4.2	2.9				3.8
2417	1986	9	12	10	34	50.49	40.25	27.32	5	4.5	3.4				4.1
2418	1986	9	23	8	41	25.1	39.09	27.75	14	4.6	3.6				4.2
2419	1986	9	29	17	38	3.86	39.07	27.79	11	4.5	3.4				4.1
2420	1986	10	5	8	55	22.05	43.6	20.85	10	4.4	3.2				4
2421	1986	10	12	11	13	40.03	39.66	28.97	11.3	4.5	3.7	4.4			
2422	1986	10	18	15	13	46.47	39.69	20.34	9.1	4.4	3.5	4.3			3.9
2423	1986	10	26	4	49	29.94	40.8	28.99	10	5	4.2				4.6
2424	1986	10	27	22	32	20.47	41.97	19.53	8	5.3	4.7	4.4	4.7		4.7
2425	1986	10	30	3	46	46.42	39.74	28.78	7.8	4	2.9	4			4.2
2426	1986	11	1	8	24	30.89	40.18	24.99	10	4.2	2.9				3.8
2427	1986	11	15	21	52	17.95	39.37	28.91	10	4.6	3.8	4.5			
2428	1986	11	22	16	28	44.97	40.13	25.11	3.6	4	2.5				3.6
2429	1986	11	22	17	49	7.82	40.22	25.2	9.2	4	2.5				3.6
2430	1986	12	4	20	31	57.43	39.63	20.52	0.2	4.2	2.9				3.8
2431	1986	12	7	14	17	8.1	43.29	25.94	7.5	5.7	5.7	5.1	5.7		
2432	1986	12	7	17	26	6.54	43.25	26.01	10	5	5	4.6	5		4.6
2433	1986	12	12	19	29	52.37	43.29	26.06	9.5	4.6	4	4.5			5
2434	1986	12	16	0	17	30.79	39.52	20.63	1	4.2	2.9				3.8
2435	1986	12	17	21	18	32.68	39.79	19.88	20	4.8	3.9	5	3.9		5.1
2436	1986	12	17	22	1	46.22	43.29	26.08	15	4.5	4.5	4.7	4.5		4.8
2437	1986	12	18	17	16	16.83	43.28	26.03	21.8	5.2	4.8	4.9			
2438	1986	12	29	3	59	33.14	41.05	20.02	27.1	4.8	4	4.6			3.7
2439	1987	1	7	0	39	27.47	40.44	20.61	9.8	4.7	3.6	4.7	3.6		4.7
2440	1987	1	7	0	44	52.19	40.46	20.65	10	4.3	3				3.9
2441	1987	1	31	1	29	14.18	40.48	24.04	10	4	2.5				3.6
2442	1987	2	7	1	21	17.38	39.79	24.35	10	4.1	2.7				3.7
2443	1987	2	13	13	58	6.21	40.22	19.87	0	5.2	4.5	4.9	4.5		4.9
2444	1987	2	13	17	36	48.92	40.2	20.79	1	4.4	3.2				4
2445	1987	2	19	22	41	22.93	40.2	21.48	10	4.1	3.1	4.1			4.2
2446	1987	2	25	12	20	46.7	43.32	20.91	4	4.8	4.2	4.6			3.2
2447	1987	3	1	12	17	46.22	39.01	22.28	46.3	4.5	3.7	4.4			3.7
2448	1987	3	8	17	38	33.76	39.4	20.58	10	4.8	3.8	4.1	3.8		4.1
2449	1987	3	8	17	42	20.93	39.48	20.59	33	4.7	3.7	4.8	3.7		4.5
2450	1987	3	9	19	50	21.84	39.4	20.65	33	4.4	3.5	4.3			3.6
2451	1987	4	24	16	34	30.41	40.45	25.97	4.6	4.4	3.2				4
2452	1987	4	25	22	10	59.91	39.3	27.92	3.3	4.3	3.3	4.2			4
2453	1987	5	16	0	2	19.08	39.35	21.5	10	4	2.5				3.6
2454	1987	6	17	11	0	54.49	41.44	20.07	3.3	4.1	2.7				3.7
2455	1987	7	6	6	34	29.08	42.5	19.4	10.6	4.1	2.7				3.7
2456	1987	7	11	23	9	19.47	43.72	20.44	10	4.5	3.8	4.4			
2457	1987	8	4	0	31	11.4	41.52	20.18	4.1	4	2.5				3.6
2458	1987	8	6	6	21	29.72	39.25	26.26	19.3	4.7	3.7	4.6	3.7		4.7
2459	1987	8	8	22	14	15.41	40.15	24.91	10	4.1	2.7				3.7
2460	1987	8	8	22	15	17.6	40.14	24.95	10	5	4.1	4.3	4.1		4.8

										Homogenized magnitudes		Reported magnitudes			
Event Number	Year	Month	Date	Hour	Minute	Second	Latitude	Longitude	Depth	M_w	M_s	mb	M_s	M_w	ML
2461	1987	8	14	6	24	4.28	43.71	20.38	10	4.3	4.3	5	4.3		4.6
2462	1987	8	23	16	43	16.15	41.99	20.36	8	4	2.5				3.6
2463	1987	8	23	23	32	3.21	39.42	27.87	8.4	4.2	2.9				3.8
2464	1987	9	10	16	9	17.5	41.99	20.95	10	4	2.5				3.6
2465	1987	9	28	21	15	30.4	39.55	24.19	10	4	2.5				3.6
2466	1987	10	2	14	52	26.68	42.02	20.52	10	4.2	2.9				3.8
2467	1987	10	5	15	21	1.3	39.71	26.89	1	4.3	3				3.9
2468	1987	10	14	9	49	34.99	39.72	25.56	3	4	2.5				3.6
2469	1987	10	27	3	15	30.58	40.42	28.46	17.7	4.7	3.7	4.4	3.7		4.7
2470	1987	11	24	19	35	14.9	40.33	25.56	3.3	4	2.5				3.6
2471	1987	11	30	4	19	26.91	39.29	22.82	45.3	4.7	3.6	4.6	3.6		3.9
2472	1987	12	18	4	51	17.57	42.1	19.09	2.7	4.3	3	4.3	3		4.5
2473	1987	12	21	20	55	43.96	39.48	19.97	10	4.5	3.7	4.4			4.1
2474	1987	12	31	21	49	53.83	39.43	27.98	26.2	4.5	3.4				4.1
2475	1988	1	4	18	51	54.02	39.64	20.29	4.9	4.4	3.5	4.3			4
2476	1988	1	9	1	2	47.39	41.25	19.66	30.4	5.9	5.7	5.2	5.7		5.1
2477	1988	1	9	7	10	52.72	41.19	19.68	30.8	5.2	4.6	4.9			3.7
2478	1988	1	14	23	47	0.16	39.72	20.21	9	4.1	3.1	4.1			3.8
2479	1988	1	17	21	6	51.16	40.26	21.2	10	4.1	2.7				3.7
2480	1988	2	18	11	11	34.21	39.09	23.47	12	4.7	3.7	4.6	3.7		3.8
2481	1988	2	19	2	18	0.42	39.3	22.97	46.2	4.4	3.5	4.3			3.4
2482	1988	3	3	22	28	23.08	40.44	19.08	6.1	4.1	3.1	4.1			3.6
2483	1988	3	16	20	2	5.38	40.11	19.73	1.3	4.8	4	4.6			4.2
2484	1988	3	19	11	52	35.48	42.1	19.24	7.3	4.4	3.5	4.3			3.6
2485	1988	3	26	20	35	9.5	40.12	19.92	5	5.2	4.5	5	4.5		4.9
2486	1988	4	3	8	56	38.98	39.31	20.52	10	4.5	3.3	4.5	3.3		3.4
2487	1988	4	4	0	27	17.24	40.03	19.98	5	4.3	3				3.9
2488	1988	4	23	17	54	45	39.1	28.1	33	4	2.9	4			
2489	1988	4	24	20	49	33.29	40.88	28.24	10.8	5.5	5.1	5	5.1		4.9
2490	1988	5	14	5	33	28.25	40.52	19.75	10	4	2.9	4			4.1
2491	1988	5	27	14	18	37.13	44.16	21.54	13.4	4.5	3.8	4.4			4.6
2492	1988	5	28	2	23	32.8	44.06	21.8	10	4	2.5				3.6
2493	1988	5	30	16	47	1.41	40.28	25.85	9.4	4.8	3.9	4.1	3.9		4.4
2494	1988	5	30	17	36	46.53	40.35	25.78	10	4.3	2.9	3.7	2.9		4.2
2495	1988	6	11	9	31	53.49	40.13	21.38	10	4.1	3.1	4.1			
2496	1988	6	23	11	55	13.37	39.73	23.75	10	4	2.5				3.6
2497	1988	7	16	17	56	28.5	39.98	23.85	13	4.9	4	3.9	4		3.5
2498	1988	7	29	13	37	48.22	40.74	23.11	10	4	2.5				3.6
2499	1988	8	11	12	45	52.47	39.89	23.89	5.4	4.3	3.3	4.2			3.8
2500	1988	8	13	7	26	20.99	39.96	24	11.5	5	4.2	4	4.2		4.1
2501	1988	8	14	5	51	40.06	40.06	23.92	9.1	4.3	3				3.9
2502	1988	8	16	21	34	8.35	39.93	23.99	8.6	4.9	4	4.4	4		4.2
2503	1988	8	20	18	10	57.73	39.96	24.05	4	4.1	2.7				3.7
2504	1988	8	27	0	19	10.4	39.94	23.99	10	4.6	3.4	3.5	3.4		3.6
2505	1988	9	10	7	7	17.55	39.83	25.44	9	4.2	2.9				3.8
2506	1988	9	10	12	47	40.12	39.45	21.45	10	4.4	3.2				4
2507	1988	9	19	9	29	49.41	39.57	21.69	10	4.2	2.9				3.8
2508	1988	10	14	16	12	20.19	40.17	19.77	10	4.7	3.6	4.8	3.6		4.6
2509	1988	10	20	14	0	59.14	40.52	22.9	27.3	5.1	4.3	4.7	4.3		4.2
2510	1988	10	20	18	54	38.56	39.38	23.7	0.8	4	2.5				3.6
2511	1988	10	21	2	18	21.39	41.3	20.89	10	4.4	3.1	4.6	3.1		4.4
2512	1988	11	19	16	11	55.76	39.64	26.04	11.9	4	2.5				3.6
2513	1988	11	23	5	17	48.1	40.14	19.85	10	4.2	2.9				3.8
2514	1988	11	29	5	24	2.3	44.33	20.19	10	4.1	2.7				3.7
2515	1988	12	2	17	43	4.55	40.47	22.69	1	4.6	3.5	4.5	3.5		4.1
2516	1988	12	8	9	26	14.37	40.65	22.5	8.7	4.6	3.8	4.5			4
2517	1988	12	11	6	12	28.84	40.71	22.48	1	4.4	3.2				4
2518	1988	12	14	9	45	5.35	39.69	20.37	24	4.7	3.7	4.8	3.7		4.6
2519	1988	12	17	16	50	18.92	40.67	22.49	9	4.1	3.1	4.1			3.8
2520	1988	12	24	23	8	49.97	41.23	23.3	6.7	4.2	2.9				3.8
2521	1988	12	26	17	49	49.4	39.14	26.48	3.5	4.1	2.7				3.7
2522	1989	1	8	13	15	21.36	41.71	19.4	7.7	4.4	3.2				4
2523	1989	1	26	15	15	13.55	40.18	19.57	10	4.6	3.8	4.5			4.3
2524	1989	1	28	15	28	38.31	41.98	20.13	5.1	4	2.5				3.6
2525	1989	2	6	11	37	36.3	39.16	24.55	10	4.3	3.3	4.2			3.9
2526	1989	2	19	1	50	45.76	40.26	21.81	14.1	4.2	2.9				3.8
2527	1989	2	19	8	52	31.05	40.25	21.83	8	4.1	2.7				3.7
2528	1989	2	26	23	54	36.81	39.14	24.52	10	5.2	4.6	4.9			4.3
2529	1989	3	5	16	44	27.03	39.93	19.66	17.1	4.6	3.8	4.5			4.2
2530	1989	3	8	5	56	43.38	40.2	19.56	5	4.4	3.5	4.3			4.2
2531	1989	3	13	17	30	11.39	41.11	23.96	6.3	4	2.5				3.6
2532	1989	3	17	0	50	52.96	41.25	19.87	22.6	5.2	4.5	4.8	4.5		4.9
2533	1989	3	18	8	40	52.97	41.64	19.66	10	4	2.5				3.6
2534	1989	3	18	21	27	39.42	39.24	23.53	8.6	5.1	4.3	4.5	4.3		4.3
2535	1989	3	19	0	19	20.63	39.25	23.53	6.9	4.9	4.2	4.7			3.6
2536	1989	3	19	5	36	59.21	39.24	23.5	10	5.6	5.4	5.2	5.4		5.3
2537	1989	3	19	5	41	45.28	39.26	23.62	27.1	4.8	4	4.6			4.6
2538	1989	3	19	5	48	53.44	39.28	23.58	47.7	4.1	3.1	4.1			4
2539	1989	3	19	5	49	37.34	39.33	23.6	24.6	4.5	3.7	4.4			4.2
2540	1989	3	19	5	57	43.91	39.29	23.57	38	4.3	3.3	4.2			4
2541	1989	3	19	6	35	53.05	39.27	23.59	6.9	4	2.5				3.6
2542	1989	3	19	7	41	51.15	39.25	23.62	22.2	4.3	3				3.9

										Homogenized magnitudes		Reported magnitudes			
Event Number	Year	Month	Date	Hour	Minute	Second	Latitude	Longitude	Depth	M_w	M_s	mb	M_s	M_w	ML
2543	1989	3	19	8	20	22.18	39.28	23.6	8.8	4	2.5				3.6
2544	1989	3	19	11	31	27.54	39.25	23.66	4.8	4.8	3.9	4.4	3.9		4.1
2545	1989	3	19	13	47	53.23	39.25	23.49	5.1	4	2.5				3.6
2546	1989	3	20	4	53	25.31	39.25	23.62	6.7	4.9	4.2	4.7			3.9
2547	1989	3	20	10	39	13.56	39.27	23.62	17.4	4.8	3.8	4.6	3.8		4.3
2548	1989	3	20	13	41	54.2	39.28	23.54	8.3	4	2.5				3.6
2549	1989	3	21	21	30	4.69	39.28	23.59	1.4	4.2	2.9				3.8
2550	1989	4	12	21	43	50.1	39.28	23.58	6.6	4.6	3.8	4.5			3.7
2551	1989	4	18	0	47	58.25	39.29	23.61	10.3	4.3	2.9	4.2	2.9		3.7
2552	1989	4	23	2	25	4.9	39.24	23.66	6.6	4.8	4	4.6			4.2
2553	1989	4	23	19	51	23.44	39.22	23.67	4.4	5.2	4.6	4.9			3.4
2554	1989	4	28	4	2	37.23	39.29	23.61	15.9	5.3	4.7	4.7	4.7		4.7
2555	1989	4	30	5	10	59.71	39.29	23.59	11.3	4.5	3.7	4.4			4.1
2556	1989	5	2	23	9	14.56	39.28	23.54	21.8	5.5	5.2	5.2			3.8
2557	1989	5	7	13	40	46.32	39.69	20.32	22.1	4.7	3.6	4.4	3.6		4.2
2558	1989	5	10	3	5	28.58	39.67	27.88	10	4.6	3.5	4.2	3.5		4.6
2559	1989	5	10	3	25	28.86	39.71	27.92	23.8	4.6	3.6				4.2
2560	1989	5	31	23	43	24.23	39.63	27.81	8.2	4.6	3.6				4.2
2561	1989	6	4	19	13	10.53	39.68	20.06	9.5	4.1	3.1	4.1			4
2562	1989	6	18	6	9	38.41	41.28	19.38	6.9	4.1	2.7				3.7
2563	1989	6	30	2	30	22.97	40.65	22.61	3.3	4	2.5				3.6
2564	1989	7	14	6	52	8.73	41.94	20.04	25.6	5.1	4.4	4.7	4.4		4.6
2565	1989	7	16	3	27	44.69	39.12	26.59	7.9	4.3	3				3.9
2566	1989	7	16	16	48	23.96	39.12	26.6	2.6	4.6	3.8	4.5			4
2567	1989	8	1	2	23	29.59	39.22	23.68	9.3	4.6	3.8	4.5			4.5
2568	1989	8	2	23	19	27.13	40.81	20.11	19.1	4	2.9	4			4.2
2569	1989	8	15	16	8	8.2	39.18	26.32	7.7	4.5	3.7	4.4			4.2
2570	1989	8	15	17	3	30.43	39.22	26.25	10	5.2	4.5	4.9	4.5		4.7
2571	1989	8	20	20	57	21.29	39.94	23.94	13.4	4.4	3.5	4.3			4
2572	1989	8	30	9	9	54.04	42	20.28	10	4.1	2.7				3.7
2573	1989	9	5	6	52	29.36	40.19	25.08	3.5	5.4	4.9	4.7	4.9		4.9
2574	1989	9	9	1	2	25.04	40.58	20.17	19.2	4.2	2.9				3.8
2575	1989	9	19	7	57	9.17	39.44	21.3	37.6	4.8	3.8	4.7	3.8		4.5
2576	1989	9	24	21	27	54.83	41.29	19.49	9.1	5.4	5	5.1			4.2
2577	1989	10	5	9	33	54.36	40.14	25.06	7.6	4.2	2.9				3.8
2578	1989	10	18	13	4	1.47	40.64	24.12	1	4.3	3				3.9
2579	1989	10	25	15	27	42.07	43	26.62	13.4	4.3	3.3	4.2			
2580	1989	11	6	10	40	33.5	39.2	21.55	1	4.6	3.8	4.5			3.8
2581	1989	12	6	22	34	40.71	40.48	21	3	4	2.5				3.6
2582	1989	12	17	21	22	33.06	39.3	28.27	10	4.6	3.6				4.2
2583	1989	12	22	19	19	19.73	40.69	21.7	1	4.1	2.7				3.7
2584	1989	12	29	20	43	39.4	40.21	24.48	2.8	4	2.5				3.6
2585	1989	12	31	1	4	56.59	40.72	21.57	10	4.3	3				3.9
2586	1990	1	5	4	2	41.47	39.39	20.53	1.5	4.2	2.9				3.8
2587	1990	1	29	3	51	55.97	40.82	23.23	0	4.1	2.7				3.7
2588	1990	1	29	13	1	45.51	39.97	23.94	13.5	4.3	3.3	4.2			4.1
2589	1990	1	31	10	16	14.21	41.41	22.67	11.3	4.6	3.8	4.5			4.2
2590	1990	1	31	15	0	31.19	39.48	26.09	10.4	4.4	3.5	4.3			3.7
2591	1990	1	31	19	58	30.37	39.11	25.92	21.3	4.1	3.1	4.1			3.8
2592	1990	2	8	7	47	28.42	39.15	23.71	1.7	5	4.4	4.8			4
2593	1990	2	10	19	48	1.08	39.57	27.94	10	4	2.9	4			
2594	1990	2	20	18	41	38.57	41.24	19.63	2.8	4.5	3.4				4.1
2595	1990	3	2	18	8	34	39.03	23.68	11.3	4.5	3.3	4.5	3.3		4.1
2596	1990	3	7	23	14	26.34	41.26	19.94	6.6	4.8	4	4.6			3.6
2597	1990	3	13	12	4	50.98	39.93	22.46	1.2	4.3	3.3	4.2			4
2598	1990	3	13	23	55	1.01	39.26	25.46	18	4.4	3.5	4.3			4.1
2599	1990	3	28	2	22	37.04	40.17	25.06	22.8	4.2	2.9				3.8
2600	1990	3	28	11	34	58.44	39.38	26.24	8	4	2.5				3.6
2601	1990	3	31	1	38	17.04	39.92	24.03	11.6	5	4.2	4.6	4.2		4.4
2602	1990	3	31	1	39	54.41	39.89	23.84	12.2	4.5	3.7	4.4			4
2603	1990	4	1	0	13	23.12	39.94	24.03	8.6	4.1	3.1	4.1			3.9
2604	1990	4	24	16	20	39.95	42.15	19.18	9.4	4.3	3				3.9
2605	1990	4	24	19	30	38.8	42.14	19.13	7.8	5	4.1	5	4.1		4.7
2606	1990	4	26	11	27	40.47	40.99	19.76	10	5.6	5.2	4.8	5.2		4.6
2607	1990	5	3	1	3	37.93	43.31	19.88	5	4.3	3.4	4.2			4.3
2608	1990	5	7	10	21	38.32	41.32	20.25	11.7	4.5	3.4				4.1
2609	1990	5	7	10	24	42.46	41.26	20.2	3	4.2	2.9				3.8
2610	1990	5	14	17	4	21.79	40.67	19.82	9.4	5.1	4.4	4.7	4.4		4.5
2611	1990	5	21	21	20	54.25	39.93	20.69	10	4.4	3.2				4
2612	1990	5	24	5	49	6.4	39.98	27.48	27.5	4.3	3.3	4.2			4.3
2613	1990	5	24	9	32	59.7	40.03	23.29	45	4.1	2.7				3.7
2614	1990	6	9	12	30	27.13	39.22	23.66	23.6	4.6	3.8	4.5			4.3
2615	1990	6	9	22	46	22.6	39.21	23.66	12.1	4.5	3.7	4.4			3.8
2616	1990	6	16	2	16	21.07	39.27	20.55	31.7	5.5	5.3	5.5	5.3		5.5
2617	1990	6	16	2	23	47.63	39.08	20.8	27	4	2.9	4			
2618	1990	6	16	2	44	7.61	39.14	20.56	2	4.1	2.7				3.7
2619	1990	6	16	21	39	51.93	39.13	20.52	1	4	2.9	4			
2620	1990	6	17	13	44	56.74	39.2	23.62	17.4	4.4	3.1	4	3.1		4.1
2621	1990	6	18	15	16	55.98	39.2	20.54	1	4.1	2.7				3.7
2622	1990	6	20	13	52	29.25	39.12	20.54	2	4	2.5				3.6
2623	1990	6	23	14	10	42.71	39.05	22.25	13.6	4.4	3.1	3.9	3.1		3.6
2624	1990	6	29	18	58	11.07	39.17	20.52	5.7	4.1	2.6	4.1	2.6		4.1

										Homogenized magnitudes		Reported magnitudes			
Event Number	Year	Month	Date	Hour	Minute	Second	Latitude	Longitude	Depth	M_w	M_s	mb	M_s	M_w	ML
2625	1990	7	4	21	35	24.04	39.54	23.59	4.6	4	2.5				3.6
2626	1990	8	1	9	42	23.9	44.64	27.97	10	4.1	2.7				3.7
2627	1990	8	4	7	29	26.04	39.26	20.49	38.3	5.1	4.3	4.9	4.3		4.5
2628	1990	8	5	0	45	46.1	39.48	20.95	0.4	4	2.9	4			3.7
2629	1990	8	6	3	26	9.69	39.16	20.58	2.7	4	2.5				3.6
2630	1990	8	11	6	45	46.41	40.88	22.71	4.4	4	2.5				3.6
2631	1990	8	18	14	47	50.56	40.14	19.77	11.3	5.5	5	4.2	5		4.2
2632	1990	8	19	11	7	0.64	40.16	19.78	8.5	4.4	3.5	4.3			4.1
2633	1990	9	1	21	30	3.42	40.73	21.63	10	4.1	2.7				3.7
2634	1990	9	3	5	35	48.86	39.93	24.01	5.4	4.6	3.8	4.5			4.1
2635	1990	9	9	19	0	38.58	39.91	24.03	8	5	4.4	4.8			4.5
2636	1990	9	13	22	5	13.2	39.54	28.53	10	4.4	3.5	4.3			4.2
2637	1990	10	8	22	47	27.61	39.01	23.63	4.4	4	2.5				3.6
2638	1990	10	8	23	42	42.5	44.11	19.32	10	4.2	2.9				3.8
2639	1990	10	13	4	12	7.36	40.7	23.41	3.6	4.4	3.5	4.3			3.9
2640	1990	10	13	14	6	34.49	40.68	23.4	1.7	4	2.5				3.6
2641	1990	10	30	8	27	47.56	39.1	20.6	13.6	4.2	2.9				3.8
2642	1990	11	26	21	37	33.75	39.37	23.9	7.4	4.4	3.1	3.8	3.1		3.8
2643	1990	12	19	15	43	6.78	40.24	19.54	23.8	4	2.9	4			4.3
2644	1990	12	21	6	57	43.18	41.01	22.3	13.3	6.1	6	5.7	6		5.4
2645	1990	12	21	13	12	52.82	39.26	19.86	58	4.3	3.3	4.2			4.2
2646	1990	12	21	16	19	48.35	41.03	22.32	10	4.3	3.3	4.2			3.9
2647	1991	1	6	3	51	8.32	43.3	19.13	10	4.4	3.6	4.3			3.5
2648	1991	1	7	14	3	42.61	43.29	19.11	6	4.4	3.6	4.3			4.6
2649	1991	1	19	17	32	37.73	39.43	28.03	19	4.4	3.2				4
2650	1991	1	23	10	35	1.05	39.95	24.05	10.2	4	2.9	4			3.8
2651	1991	1	27	19	50	49.49	39.61	23.81	22.6	4.3	3.3	4.2			4.2
2652	1991	1	27	23	23	19.39	39.62	23.78	10	4.1	3.1	4.1			3.5
2653	1991	1	28	4	7	26.71	39.57	23.77	10.8	4.5	3.3	4.1	3.3		4
2654	1991	2	12	9	54	58.93	40.8	28.82	10	5.3	4.8	4.8	4.8		4.5
2655	1991	2	20	5	34	11.66	39.43	20.71	2.3	4	2.5				3.6
2656	1991	2	23	22	38	8.56	39.29	23.63	6.8	4.2	2.9				3.8
2657	1991	2	25	7	25	57.77	41.33	20.25	17.7	4.6	3.8	4.5			4.2
2658	1991	3	2	7	6	55.18	40.27	25.2	3.9	4.2	2.9				3.8
2659	1991	3	3	8	39	25.45	40.63	29	10	5.1	4.3	4.6	4.3		
2660	1991	3	3	10	9	7.16	41.07	22.52	6.4	4.5	3.4				4.1
2661	1991	3	5	6	59	8.68	40.66	19.63	5	4.1	3.1	4.1			4
2662	1991	3	8	9	23	13.01	40.85	27.91	11	4.6	3.8	4.5			
2663	1991	3	15	13	30	19.34	39.27	20.54	10	4.6	3.5	4.7	3.5		4.3
2664	1991	3	16	5	51	17.42	41.48	19.5	10.8	5.2	4.6	4.9			3.5
2665	1991	3	17	4	24	10.94	39.28	20.49	24.5	4.3	2.9	3.9	2.9		4
2666	1991	3	17	19	22	10.62	39.31	20.51	10	4.9	4	4.7	4		4.4
2667	1991	3	18	23	28	52.99	39.28	20.47	10	4.4	3.1	4.3	3.1		4.7
2668	1991	3	19	2	37	3.64	39.21	20.52	10	4.7	3.6	4.7	3.6		4
2669	1991	3	19	2	51	25.61	39.28	20.46	10	4.6	3.8	4.5			4.2
2670	1991	3	20	4	45	38.19	39.28	20.56	10	4.1	2.6	3.4	2.6		
2671	1991	4	18	11	56	56.89	39.26	26.58	10	4.3	3.3	4.2			4
2672	1991	4	27	15	54	57.69	39.73	19.72	10	4.3	3.3	4.2			3.9
2673	1991	4	29	21	38	14.17	44.12	19.06	10	5.2	4.8	4.9			4.8
2674	1991	5	28	18	26	48.64	40.53	26.42	8.3	4.1	3.1	4.1			4.3
2675	1991	6	15	1	11	44.4	39.15	23.47	10	4.4	3.5	4.3			4
2676	1991	6	17	21	35	8.57	42.09	19.21	3.8	4.2	2.8	3.7	2.8		3.9
2677	1991	6	24	1	36	35.62	39.24	20.47	10	4.1	3.1	4.1			4
2678	1991	6	26	11	0	37.08	39.6	27.81	10.6	4.6	3.6				4.2
2679	1991	7	9	18	46	27.25	41.39	20.94	5	4.4	3.2				4
2680	1991	7	10	5	55	9.79	39.89	23.38	22.8	4.4	3.5	4.3			3.8
2681	1991	7	12	1	41	55.18	41.43	20.91	6.5	4	2.9	4			4
2682	1991	7	18	11	56	30.85	44.9	22.41	11.6	5.4	5.5	5.5	5.5	5.4	5.5
2683	1991	7	21	15	3	55.39	39.59	21	8.6	4.1	3.1	4.1			4.4
2684	1991	7	22	0	49	49.9	39.31	27.92	12.5	4	2.9	4			4.5
2685	1991	8	1	21	9	47.78	39.51	20.06	10	4.2	2.8	3.3	2.8		3.4
2686	1991	8	15	4	58	58.88	41.11	22.05	10.6	4.3	3	4.2	3		4.3
2687	1991	8	30	17	17	0.82	39.97	20.66	1.9	4	2.9	4			3.9
2688	1991	9	3	4	20	28.52	39.27	28.78	6.7	4	2.5				3.6
2689	1991	9	10	1	47	3.06	39.44	27.83	1.7	4.2	2.9				3.8
2690	1991	9	11	2	52	36.14	40.26	21.27	10.4	4.2	2.9				3.8
2691	1991	9	11	10	57	7.99	39.94	23.99	7.3	4.2	2.9				3.8
2692	1991	9	17	3	2	1.76	44.56	22.49	12.9	4.5	3.4				4.1
2693	1991	9	23	18	30	25.45	39.87	25.6	0.1	4	2.5				3.6
2694	1991	10	12	16	32	37.53	40.2	25.65	7.8	5.2	4.5	4.5	4.5		4.4
2695	1991	10	12	16	37	40.61	40.19	25.61	3.4	4.1	2.7				3.7
2696	1991	10	14	23	16	10.86	40.2	25.23	0.9	4	2.5				3.6
2697	1991	10	19	4	57	40.51	40.64	21.39	4.6	4.3	3				3.9
2698	1991	10	19	17	22	15.14	40.65	21.37	8	4.2	2.9				3.8
2699	1991	10	20	15	59	47.75	40.18	25.61	8.9	4	2.5				3.6
2700	1991	10	28	0	21	29.84	44.29	21.42	10	4.3	4.3	4.8	4.3		4.5
2701	1991	11	9	12	27	50.56	39.43	26.37	10	4.1	2.7				3.7
2702	1991	11	22	18	27	12.72	40.19	27.78	10.1	4.1	2.7				3.7
2703	1991	11	30	15	57	53.73	39.33	28.12	3.5	4.4	3.2				4
2704	1991	12	5	21	54	31.42	39.12	24.44	28.4	4.1	3.1	4.1			4
2705	1991	12	14	12	28	32.43	40.77	27.47	10	4	2.5				3.6
2706	1991	12	16	1	56	36.03	39.33	23.11	0.4	4.1	2.7				3.7

										Homogenized magnitudes		Reported magnitudes			
Event Number	Year	Month	Date	Hour	Minute	Second	Latitude	Longitude	Depth	M_w	M_s	mb	M_s	M_w	ML
2707	1991	12	26	23	44	57.76	41.27	20.22	6.9	4.4	3.5	4.3			4.1
2708	1991	12	28	19	56	14.59	41.25	20.27	2.2	4.2	2.9				3.8
2709	1992	2	17	11	1	0.94	44.66	22.63	10	4.1	2.7				3.7
2710	1992	2	18	0	16	27.09	39.83	24.35	10	4.4	3.5	4.3			4.3
2711	1992	2	25	23	54	3.44	39.39	27.84	9	4	2.5				3.6
2712	1992	3	1	14	44	16.69	39.08	26.03	8.9	4.1	3.1	4.1			3.9
2713	1992	3	1	16	43	46.78	39.04	25.94	10	4	2.5				3.6
2714	1992	3	1	17	59	36.14	39.06	26.01	9.3	4	2.5				3.6
2715	1992	3	2	1	36	44.66	39.05	25.96	0.1	4.1	2.7				3.7
2716	1992	3	2	18	45	22.41	39.09	25.97	8	4	2.5				3.6
2717	1992	3	2	18	48	32.97	39.03	26.01	3.8	4.1	2.7				3.7
2718	1992	3	5	14	33	58.7	44.9	25.67	5	4	2.5				3.6
2719	1992	3	7	12	51	37.55	39.09	25.94	10	4.1	2.7				3.7
2720	1992	3	11	1	54	42.57	39.11	26	2.8	4	2.9	4			4.1
2721	1992	3	11	20	24	9.25	39	26.01	10	4.1	2.7				3.7
2722	1992	3	12	19	40	22.56	39.03	25.96	7.1	4	2.5				3.6
2723	1992	3	16	6	33	45.37	39.71	26.04	7	4.2	2.9				3.8
2724	1992	3	16	10	34	43.95	39.03	26.1	5.2	4	2.5				3.6
2725	1992	3	22	16	52	24.99	40.2	28.35	24.5	5	4.1	4.9	4.1		4.9
2726	1992	3	30	19	32	2.25	41.1	20.96	12	5.2	4.6	4.4	4.6		4.9
2727	1992	3	31	22	1	3.45	41.12	20.99	5.4	5	4.4	4.8			4.1
2728	1992	4	1	0	13	33.19	41.1	21.04	3.1	4	2.5				3.6
2729	1992	4	1	12	23	40.07	39.4	28.68	11.6	4.2	2.8	3.6	2.8		4.1
2730	1992	4	1	12	36	9.75	39.39	28.7	9	4	2.5				3.6
2731	1992	4	4	12	50	8.94	39.5	26.02	7	4	2.5				3.6
2732	1992	4	5	0	48	1.89	40.8	27.93	5.6	4	2.9	4			2.9
2733	1992	4	15	21	51	48.05	41.34	20.81	10	4.4	3.5	4.3			4.2
2734	1992	5	5	10	18	24.46	39.41	19.26	1	4.1	2.7				3.7
2735	1992	5	6	13	52	58.29	39.21	20.52	6.8	4.2	2.9				3.8
2736	1992	5	8	5	15	50.51	40.12	19.76	22.1	4.5	3.3	4.6	3.3		4.4
2737	1992	5	11	0	54	8.07	39.42	25.59	10.6	4.3	3				3.9
2738	1992	5	24	6	44	52.05	39.03	20.05	53.1	4.5	3.2	4.3	3.2		4.3
2739	1992	6	8	2	52	10.65	42.06	25.65	10	4	2.5				3.6
2740	1992	6	16	23	24	38.56	39.27	26.2	13.3	4.2	2.9				3.8
2741	1992	6	21	18	59	5.59	39.19	19.74	39.6	5.6	5.4	5	5.4		4.8
2742	1992	6	24	16	12	8.4	42.05	21.21	13.7	4.7	3.7				4.3
2743	1992	6	28	2	7	24.64	39.67	25.36	5	4	2.5				3.6
2744	1992	6	28	2	13	34.62	39.58	25.36	10	4.5	3.3	4.6	3.3		4.3
2745	1992	6	30	10	37	15.02	41.91	20.53	10	4.7	3.7				4.3
2746	1992	6	30	12	31	21.66	39.04	26.06	10	4	2.5				3.6
2747	1992	7	8	1	36	46.86	40.01	24.59	11.9	4.1	2.7				3.7
2748	1992	7	14	22	57	17.61	39.93	24.52	10	4.2	2.9				3.8
2749	1992	7	23	20	12	44.58	39.86	24.38	19	5.5	5.1	5.1	5.1		4.8
2750	1992	7	23	20	24	52.5	40	24.34	13.2	4	2.5				3.6
2751	1992	7	24	23	55	14.94	39.99	24.43	13.2	4	2.5				3.6
2752	1992	7	31	11	36	39.12	39.91	24.56	0.5	4.3	3				3.9
2753	1992	8	13	4	52	29.31	40.98	20.94	3.4	4.8	3.8	4.2	3.8		4.2
2754	1992	8	13	5	2	59.45	40.96	21.02	10	4.2	2.9				3.8
2755	1992	8	17	6	48	48.68	39.35	20.81	13.1	4	2.5				3.6
2756	1992	8	26	15	7	45.22	39.13	20.39	56.3	4.6	3.4	4.8	3.4		4.5
2757	1992	8	26	18	42	1.57	42.4	19.34	28.2	5.2	4.6	4.8	4.6		4.5
2758	1992	9	9	11	11	2.86	39.78	25.62	5.2	4.2	2.9				3.8
2759	1992	9	24	1	47	46.16	43.13	19.44	10	4.2	2.9				3.8
2760	1992	9	26	8	18	10.98	42.44	19.15	11.8	4.1	2.7				3.7
2761	1992	10	3	11	11	21.78	39.34	25.56	11.7	4.2	2.9				3.8
2762	1992	10	24	19	36	45.73	39.3	25.47	9.1	4.3	3.3	4.2			4.1
2763	1992	10	30	5	38	28.18	42.42	19.04	26.5	4.8	3.9	4.7	3.9		4.6
2764	1992	11	5	20	41	11.25	39.58	25.37	9	4.1	2.7				3.7
2765	1992	11	10	17	39	43.17	40.56	27.1	3.8	4.2	2.9				3.8
2766	1992	11	11	10	10	45.46	42.38	20.89	10	4.3	3				3.9
2767	1992	12	22	22	15	48.14	39.29	28.8	10	4.1	2.7				3.7
2768	1992	12	25	22	36	32.21	39.25	28.79	6	4.1	2.7				3.7
2769	1992	12	28	21	59	7.83	39.31	28.8	9	4.2	2.9				3.8
2770	1992	12	31	12	21	27.07	39.26	28.77	3.4	4	2.5				3.6
2771	1993	1	3	7	15	49.51	39.29	20.76	5	4.5	3.7	4.4			4.3
2772	1993	1	5	20	37	22.32	39.62	25.38	10.4	4.1	2.7				3.7
2773	1993	1	5	22	53	38.29	43.96	20.56	10	4.2	2.9				3.8
2774	1993	1	12	18	50	52.58	42.51	22.05	10	4.3	3.3	4.2			3.7
2775	1993	1	18	19	19	9.87	41.62	19.61	27.7	4.1	3.1	4.1			4.2
2776	1993	1	21	13	1	34.2	40.37	27.44	3	4.3	3				3.9
2777	1993	1	22	0	23	55.22	40.5	24.4	1.9	4	2.5				3.6
2778	1993	1	22	3	7	25.72	39.43	20.46	22	4.3	3.3	4.2			3.9
2779	1993	1	23	0	20	12.98	39.34	24.91	18.8	4	2.5				3.6
2780	1993	1	23	15	32	44.85	40.78	28.76	6.3	4.5	3.4				4.1
2781	1993	2	12	2	53	8.21	41.44	25.24	14.6	4	2.5				3.6
2782	1993	2	24	11	14	45.73	40.13	24.11	4.4	4.3	3.3	4.2			3.9
2783	1993	3	2	7	12	52.29	39.79	25.59	10	4	2.5				3.6
2784	1993	3	9	9	41	22.02	39.16	28.8	0.8	4.5	3.4				4.1
2785	1993	3	18	1	36	16.95	40.44	28.05	6.2	4	2.5				3.6
2786	1993	3	18	7	19	39.03	40.4	28.01	9.8	4.1	3.1	4.1			4.3
2787	1993	3	18	7	22	44.78	40.46	27.98	9.5	4.5	3.7	4.4			4.1
2788	1993	3	18	7	51	37.82	40.43	28	8.5	4.7	3.7	4.4	3.7		4.3

										Homogenized magnitudes		Reported magnitudes			
Event Number	Year	Month	Date	Hour	Minute	Second	Latitude	Longitude	Depth	M_w	M_s	mb	M_s	M_w	ML
2789	1993	3	27	8	19	52.51	39.19	27.96	11	4.3	3				3.9
2790	1993	3	27	23	47	8	41.23	23.22	1.3	4.7	3.7	4.2	3.7		4.1
2791	1993	3	31	18	20	42.53	39.14	28.04	2	4.9	4	4.5	4		4.3
2792	1993	4	6	9	56	34.55	39.48	27.1	9	4.2	2.9				3.8
2793	1993	4	23	2	2	33.57	39.97	28.9	3.5	4.3	3				3.9
2794	1993	5	22	7	4	43.44	39.68	20.09	14.3	4	2.9	4			3.6
2795	1993	5	23	7	40	57.51	40.12	20.68	7.6	4.1	3.1	4.1			4
2796	1993	5	25	15	36	15.7	40.47	28.07	11.5	4.5	3.4				4.1
2797	1993	5	27	15	50	7.84	39.58	25.13	16.9	4.1	2.7				3.7
2798	1993	5	30	23	48	31.45	39.34	20.46	59.2	4.5	3.7	4.4			4.3
2799	1993	5	31	0	0	49.32	39.4	20.47	37	5.1	4.4	4.7	4.4		4.4
2800	1993	5	31	7	35	16.69	39.29	20.45	7.8	4	2.9	4			3.7
2801	1993	5	31	13	34	9.42	39.27	20.45	5.3	4.4	3.1	3.7	3.1		3
2802	1993	6	3	21	18	15.42	42.31	19.38	8.3	4	2.5				3.6
2803	1993	6	6	18	16	11.05	39.42	28.35	5.7	4.5	3.3	4	3.3		4.3
2804	1993	6	12	23	59	59.24	39.29	20.54	10	4.1	2.7				3.7
2805	1993	6	13	23	26	40.3	39.34	20.53	19.6	5.3	5.1	5.4	5.1	5.3	5.4
2806	1993	6	13	23	29	42.71	39.24	20.51	6.2	4	2.5				3.6
2807	1993	6	14	1	51	48.65	39.38	25.97	11.8	4.1	2.7				3.7
2808	1993	6	14	6	32	16.45	39.29	20.47	9.5	4.2	2.7	3.9	2.7		3.9
2809	1993	6	19	4	49	35.87	42.23	19.5	20.2	4.7	3.7	3.3	3.7		4.1
2810	1993	7	1	7	57	10.98	39.68	20.59	0	4.3	3				3.9
2811	1993	7	5	23	15	11.72	40.65	25.74	10.2	4.2	2.9				3.8
2812	1993	7	7	2	54	5.84	40.55	20.29	20.1	4.6	3.6				4.2
2813	1993	7	11	10	33	32.91	41.17	20.14	15	4.3	2.9	3.6	2.9		4.3
2814	1993	7	25	1	0	21.02	40.47	23.21	8.9	4	2.9	4			3.6
2815	1993	7	27	11	0	32.59	39.46	20.45	16.8	5.1	4.3	4	4.3		3.9
2816	1993	8	1	5	14	19.41	39.82	20.59	14.5	4.3	2.9	3.5	2.9		3.8
2817	1993	8	1	5	30	36.06	39.77	20.6	12.4	4	2.5				3.6
2818	1993	8	10	5	58	21.5	40.23	22.99	8.8	4.8	3.8	4.7	3.8		4.4
2819	1993	8	11	6	16	39.55	40.28	23.03	0.2	4.1	2.7				3.7
2820	1993	8	16	1	37	35.43	40.7	27.54	11	4.1	2.7				3.7
2821	1993	8	19	19	49	41.15	39.42	26.39	6.5	4.1	2.7				3.7
2822	1993	8	26	19	50	23.97	39.1	27.83	5	4.3	2.9	3.9	2.9		4.2
2823	1993	8	31	20	27	55.41	40.07	27.6	7.8	4	2.5				3.6
2824	1993	9	2	21	3	41.09	40.19	27.26	9.1	4.5	3.4				4.1
2825	1993	9	3	5	48	30.34	40.15	27.25	5.4	4.1	2.7				3.7
2826	1993	9	9	3	35	36.61	40.35	25.83	5.8	4.1	2.7				3.7
2827	1993	9	13	19	9	44.66	40.12	24.85	10	5.2	4.6	4.3	4.6		4.5
2828	1993	9	14	14	32	30.1	40.11	24.87	10	5.1	4.3	3.6	4.3		4.3
2829	1993	9	14	16	11	11.65	40.36	25.84	10	4	2.5				3.6
2830	1993	9	18	19	1	6.85	39.64	25.4	7	4	2.5				3.6
2831	1993	9	25	9	39	10.95	40.06	27.2	10.2	4.5	3.4				4.1
2832	1993	9	28	16	28	27.04	40.35	25.87	0.9	4	2.5				3.6
2833	1993	10	2	5	14	51.34	39.71	25.73	9.5	4	2.5				3.6
2834	1993	10	10	18	5	18.1	40.65	22.38	37.7	4.5	3.7	4.4			4
2835	1993	10	13	2	14	37.72	40.6	19.49	0.5	4	2.5				3.6
2836	1993	10	17	7	49	55.11	39.66	20.09	0.6	4	2.5				3.6
2837	1993	10	18	20	13	47.51	40.3	25.65	0	4.2	2.9				3.8
2838	1993	10	19	7	48	58.76	40.31	25.65	2.5	4.2	2.9				3.8
2839	1993	11	6	13	46	6.34	39.35	26.24	3.6	4	2.5				3.6
2840	1993	11	25	7	9	14.49	39.31	25.96	15.3	4.3	3				3.9
2841	1993	12	1	5	38	14.4	39.87	24.02	0	4	2.5				3.6
2842	1993	12	5	1	30	57.72	41.97	19.14	8.4	4.8	3.8	4.6	3.8		3.5
2843	1993	12	5	15	24	40.34	39.09	23.89	7.6	4	2.5				3.6
2844	1993	12	5	15	32	27.92	39	23.9	10	4.2	2.9				3.8
2845	1993	12	11	20	3	0.6	39.35	25.9	8	4.1	2.7				3.7
2846	1993	12	12	17	21	26.84	41.55	28.79	28.2	4.8	3.8	4.9	3.8		4.6
2847	1993	12	16	9	22	14.96	41.49	23.09	4	4.4	3.5	4.3			4.1
2848	1993	12	24	21	53	18.19	40.18	19.78	9.7	5.3	4.7	5.1	4.7		4.9
2849	1994	1	5	21	39	21.92	40.85	27.95	5.9	4.2	2.9				3.8
2850	1994	1	11	1	59	31.73	41.66	24.23	1.2	4.1	2.7				3.7
2851	1994	1	14	15	6	59.28	39.77	25.58	2	4.1	2.7				3.7
2852	1994	1	19	4	47	56.02	40.44	20.57	11	4.6	3.6				4.2
2853	1994	1	21	20	5	24.17	41.04	20.93	19	4.4	3.5	4.3			3.6
2854	1994	1	22	7	48	45.27	40.78	27.49	10.7	4.4	3.2				4
2855	1994	1	26	3	21	37.87	40.73	27.33	0.8	4.4	3.2				4
2856	1994	1	26	10	7	34.91	39.09	27.82	2.9	4.6	3.6				4.2
2857	1994	2	3	18	52	53.17	39.85	20.55	25.8	4.5	3.7	4.4			4.5
2858	1994	2	12	18	38	11.06	39.77	20.6	12.5	4.3	3				3.9
2859	1994	2	13	10	15	54.93	42.85	19.08	3	4.7	3.6	4.6	3.6		4.3
2860	1994	2	20	22	41	41.38	40.49	23.51	6.6	4	2.5				3.6
2861	1994	2	25	1	34	40.1	39.18	20.96	60.5	4.3	3	3.9	3		3.9
2862	1994	3	6	22	49	44.32	40.11	24.79	10.5	4.1	2.7				3.7
2863	1994	3	10	15	41	44.88	40.25	25.26	12	4.1	3.1	4.1			4.2
2864	1994	3	16	19	45	30.19	39.16	23.3	3.1	4	2.5				3.6
2865	1994	3	19	3	17	34.53	39.76	23.39	10.4	4	2.5				3.6
2866	1994	3	26	7	45	12.67	40.22	25.29	5.1	4	2.5				3.6
2867	1994	4	6	12	29	19.95	39.36	25.6	13.3	4.1	2.7				3.7
2868	1994	4	6	15	33	7.83	40.07	28.1	6.9	4.4	3.2				4
2869	1994	4	10	19	46	20.35	39.98	23.63	18	5.2	4.6	4.8	4.6		4.2
2870	1994	4	14	23	1	33.64	39.14	20.91	10	4.2	2.8	3.8	2.8		3.9

										Homogenized magnitudes		Reported magnitudes			
Event Number	Year	Month	Date	Hour	Minute	Second	Latitude	Longitude	Depth	M_w	M_s	mb	M_s	M_w	ML
2871	1994	5	6	1	12	48.23	39.13	26.42	6.8	4.5	3.2	3.4	3.2		3.8
2872	1994	5	27	2	23	58.57	41.89	19.03	5.2	4.2	2.9				3.8
2873	1994	5	30	19	8	28.28	40.17	25.09	3.3	4	2.5				3.6
2874	1994	5	30	23	24	13.09	40.14	19.67	10.4	4.6	3.4	4.8	3.4		4.4
2875	1994	6	4	15	10	9.5	44.82	22.52	2.8	4	2.5				3.6
2876	1994	6	4	19	2	6.84	39	26.61	10	4.1	2.7				3.7
2877	1994	6	12	1	22	38.39	39.52	28.34	8.1	4.4	3.2				4
2878	1994	6	14	18	58	13.97	39.8	24.47	5.7	4.1	3.1	4.1			3.6
2879	1994	6	20	1	36	15.97	40.57	27.34	11.6	4.5	3.2	4.1	3.2		4.2
2880	1994	6	20	15	59	48.58	44.53	20.96	10	4.2	2.9				3.8
2881	1994	6	22	16	43	58.95	40.17	27.43	8.6	4.3	3				3.9
2882	1994	6	28	10	22	51.31	41.12	20.02	27	4.6	3.8	4.5			4.3
2883	1994	7	16	3	9	15.81	40.8	27.41	7.7	4	2.5				3.6
2884	1994	7	16	20	11	3.58	40.14	24.79	1.4	4	2.5				3.6
2885	1994	7	17	22	19	55.55	40.25	24.48	13.7	4.2	2.9				3.8
2886	1994	8	7	15	41	34.08	39.45	20.28	24.1	4	2.9	4			3.2
2887	1994	8	17	10	57	54.85	42.79	19	9.3	4	2.9	4			3.6
2888	1994	8	19	9	2	14.4	40.4	25.78	10	4.1	3.1	4.1			4.1
2889	1994	9	1	16	12	40.71	41.18	21.2	12.4	5.8	5.6	5.6	5.6		5.2
2890	1994	9	1	16	23	12.7	41.14	21.25	24.9	5.4	5	5.1			4.8
2891	1994	9	1	16	45	54.57	41.16	21.31	2.6	4.1	3.1	4.1			3.4
2892	1994	9	1	19	42	31.44	41.2	21.28	5.6	4.5	3.4				4.1
2893	1994	9	1	20	49	13.59	41.17	21.23	0.9	4.1	2.7				3.7
2894	1994	9	2	0	32	58.51	41.14	21.19	9	4.2	2.9				3.8
2895	1994	9	2	16	32	56.35	41.16	21.24	3	4	2.5				3.6
2896	1994	9	5	11	25	51.23	39.1	27.77	11.2	4.3	3				3.9
2897	1994	9	7	6	2	23.62	40.16	27.27	9.2	4	2.5				3.6
2898	1994	9	23	11	37	29.71	40.64	23.52	7.4	4.3	3.3	4.2			4.1
2899	1994	9	28	3	23	7.91	41.9	20.64	9	4.4	3.5	4.3			4.4
2900	1994	10	12	21	23	37.39	40.94	25.19	29	4	2.5				3.6
2901	1994	10	18	16	45	13.82	40.02	20.31	13.1	4.5	3.4				4.1
2902	1994	10	22	22	19	48.57	39.04	27.87	8	4.3	3				3.9
2903	1994	11	1	10	6	30.39	39.46	20.32	28.9	4.3	3.3	4.2			3.9
2904	1994	11	2	9	50	45.03	40.58	26.05	2.2	4	2.5				3.6
2905	1994	11	2	13	15	55.43	40.58	26.06	6.1	4	2.5				3.6
2906	1994	11	5	11	12	46.17	40.76	27.45	2	4	2.5				3.6
2907	1994	11	6	2	12	39.11	39.16	23.48	7.2	4	2.5				3.6
2908	1994	11	8	8	11	46.57	40.85	20.82	6.4	4	2.9	4			3.6
2909	1994	11	21	0	11	25.17	39.21	26.27	13.3	4.1	2.7				3.7
2910	1994	11	23	13	24	12.06	42.21	24.2	10	4.1	2.7				3.7
2911	1994	11	29	10	18	43.12	42.16	25.19	14	4	2.5				3.6
2912	1994	12	4	14	51	18.93	41.9	20.23	13	4.1	3.1	4.1			4.2
2913	1994	12	7	3	17	7.08	41.09	24.6	11	4.3	3				3.9
2914	1994	12	9	6	18	59.32	40.88	20.78	1.2	4.5	3.7	4.4			3.5
2915	1994	12	9	16	56	35.33	39.34	25.52	5	4.1	2.7				3.7
2916	1994	12	16	5	45	9.71	44.1	21.29	7.6	4.3	3.4	4.2			4.1
2917	1994	12	21	22	44	54.6	43.33	22.06	1.8	4.2	2.9				3.8
2918	1995	1	5	4	48	3.2	40.83	23	7.5	4.2	2.9				3.8
2919	1995	1	5	4	48	30.05	40.82	22.9	10	4.1	2.7				3.7
2920	1995	1	5	20	57	42.62	39.76	25.71	10	4	2.9	4			3.9
2921	1995	1	8	13	8	53.07	39.33	25.53	8.3	4.6	3.4	4.2	3.4		4
2922	1995	1	22	22	27	28.09	40.62	23.43	1.6	4.4	3.2				4
2923	1995	1	22	22	35	23.99	40.61	23.48	1.5	4	2.5				3.6
2924	1995	1	30	18	27	3.53	39.36	21.52	43.1	4.5	3.7	4.4			3.7
2925	1995	2	8	21	24	52.38	40.8	27.77	10	4.5	3.7	4.4			4.5
2926	1995	2	11	23	8	34.61	39.83	24.32	9	4.6	3.8	4.5			3.3
2927	1995	2	13	13	16	34.58	40.7	22.68	10.3	4.9	4.2	4.7			4.1
2928	1995	2	23	12	13	57.6	39.4	20.33	10.3	4	2.9	4			3.6
2929	1995	2	24	18	0	8.08	40.52	20.64	10	4	2.9	4			3.4
2930	1995	3	13	2	41	41.29	39.2	20.56	10	4.1	3.1	4.1			3.8
2931	1995	4	4	17	10	9.87	40.55	23.6	22.8	4.1	3.1	4.1			4.1
2932	1995	4	4	17	27	4.78	40.57	23.69	5	5.5	5.1	3.8	5.1		4
2933	1995	4	13	4	8	2.29	40.85	27.65	26.7	5.1	4.4	4.8	4.4		4
2934	1995	4	14	17	59	5.43	41.65	19.6	8.8	4.3	3				3.9
2935	1995	4	18	5	36	3.53	40.86	27.75	22.3	4.9	4.2	4.7			4.1
2936	1995	4	28	20	3	14.85	39.16	20.44	5.2	4.1	3.1	4.1			3.3
2937	1995	4	30	7	50	32.12	40.44	21.84	5	4.2	2.9				3.8
2938	1995	5	3	15	39	54.92	40.59	23.72	7.2	4.8	3.8	4.1	3.8		4.2
2939	1995	5	3	21	36	54.06	40.58	23.6	20.2	5.3	4.7	4.6	4.7		4.4
2940	1995	5	3	21	43	27.35	40.59	23.58	23.6	5.3	4.7	4.7	4.7		4.6
2941	1995	5	4	0	34	9.69	40.59	23.56	13.7	5.3	5.1	5	5.1	5.3	4.8
2942	1995	5	4	0	43	40.3	40.58	23.7	0.5	4.1	2.7				3.7
2943	1995	5	7	9	26	26.43	40.58	23.67	10	4.2	2.9				3.8
2944	1995	5	9	1	14	37.05	40.82	20.74	8.9	5	4.2	4.8	4.2		4.7
2945	1995	5	9	1	22	38.34	40.7	20.87	18	4	2.5				3.6
2946	1995	5	9	1	41	5.41	40.79	20.79	8.2	4	2.9	4			4.3
2947	1995	5	12	7	25	12.23	39.11	24.47	29.3	4	2.5				3.6
2948	1995	5	13	8	42	11.22	40.11	21.73	6.6	4	2.9	4			3.9
2949	1995	5	13	8	43	16.39	40.15	21.63	11.4	4.3	3.3	4.2			4.5
2950	1995	5	13	8	47	1.19	40.07	21.72	5	4.1	2.7				3.7
2951	1995	5	13	8	47	13.06	40.17	21.69	13.9	6.4	6.6	6	6.6	6.4	6.1
2952	1995	5	13	9	1	5.22	40.12	21.97	13.6	4.1	3.1	4.1			4.2

										Homogenized magnitudes		Reported magnitudes			
Event Number	Year	Month	Date	Hour	Minute	Second	Latitude	Longitude	Depth	M_w	M_s	mb	M_s	M_w	ML
2953	1995	5	13	9	8	5.88	40.29	21.37	10	4	2.9	4			3.6
2954	1995	5	13	9	18	39.91	40.19	21.68	2.5	4	2.9	4			3.8
2955	1995	5	13	9	29	39.75	40.13	21.64	10	4.4	3.5	4.3			4.2
2956	1995	5	13	9	47	43.64	40.15	21.8	29.6	4.9	4.2	4.7			4.2
2957	1995	5	13	10	11	59.3	40.15	21.74	27.6	4	2.9	4			4.2
2958	1995	5	13	10	33	5.46	40.2	21.62	5	4.3	3.3	4.2			4.3
2959	1995	5	13	10	58	34.61	40.09	21.59	8.6	4.6	3.8	4.5			4
2960	1995	5	13	11	43	32.46	40.18	21.66	41.4	5.3	4.7	5	4.7		4.5
2961	1995	5	13	13	34	59.63	40.6	20.88	10	4.2	2.9				3.8
2962	1995	5	13	14	16	30.26	40.14	21.68	11.5	4	2.9	4			3.8
2963	1995	5	13	14	26	7.55	40.26	21.9	59.2	4	2.9	4			3.8
2964	1995	5	13	15	25	42.29	40.1	21.58	5	4.1	3.1	4.1			3.6
2965	1995	5	13	17	54	54.17	40.02	21.78	10.4	4.3	3.3	4.2			4.1
2966	1995	5	13	18	6	1.55	40.17	21.69	30.8	5.1	4.4	4.8	4.4		4.5
2967	1995	5	13	18	46	29.89	40.16	21.71	18.2	4	2.9	4			3.7
2968	1995	5	13	19	0	14.06	40.11	21.57	10	4.4	3.5	4.3			3.8
2969	1995	5	13	19	0	51.48	40.16	21.74	47.4	5	4.2	4.8	4.2		4.6
2970	1995	5	13	19	37	11.63	40.22	21.81	13.5	4.1	3.1	4.1			4.1
2971	1995	5	13	21	9	4.46	40.06	21.63	5	4.3	3.3	4.2			2.8
2972	1995	5	13	23	46	57.85	40.01	21.7	10	4.3	3.3	4.2			3.9
2973	1995	5	13	23	53	42.24	40.03	21.6	8.8	4.5	3.7	4.4			3.9
2974	1995	5	13	23	56	28.16	40.06	21.66	27.6	5	4.2	4.7	4.2		4.2
2975	1995	5	14	1	3	0.37	40.13	21.57	28.8	4.6	3.8	4.5			4.2
2976	1995	5	14	2	38	58	40.13	21.61	29	4.1	3.1	4.1			4
2977	1995	5	14	2	47	1.53	40.14	21.59	32.8	5.2	4.6	4.9	4.6		4.6
2978	1995	5	14	3	2	27.69	40.07	21.56	14.6	4.6	3.8	4.5			4.4
2979	1995	5	14	3	9	39.12	40.13	21.62	30.2	5.2	4.5	4.7	4.5		4.5
2980	1995	5	14	5	14	52.61	40.1	21.6	7.8	4	2.9	4			4
2981	1995	5	14	5	59	16.39	40.06	21.54	13.1	5.1	4.3	4.8	4.3		4.6
2982	1995	5	14	6	11	38.26	39.99	21.45	10	4.1	3.1	4.1			4
2983	1995	5	14	6	27	8.93	39.99	21.49	30.2	4	2.9	4			3.9
2984	1995	5	14	8	35	12.29	40.18	21.57	25.3	5.3	4.7	4.7	4.7		4.1
2985	1995	5	14	9	45	41.77	40.2	21.69	23.7	4.6	3.8	4.5			4.5
2986	1995	5	14	14	46	57.69	40.19	21.67	18.6	4.5	3.7	4.4			4.5
2987	1995	5	14	21	31	12.14	40.1	21.64	8.1	4.3	3.3	4.2			4.1
2988	1995	5	15	0	24	18.29	40.15	21.57	6.9	4.4	3.5	4.3			4
2989	1995	5	15	1	20	16.38	40.16	21.52	24.2	4.1	3.1	4.1			4.5
2990	1995	5	15	3	31	42.81	40.14	21.75	3	4.1	3.1	4.1			3.3
2991	1995	5	15	4	13	57.35	40.08	21.65	25.8	5.2	4.9	5.1	4.9	5.2	5.2
2992	1995	5	15	6	42	27.65	40.11	21.64	9.7	4.3	3.3	4.2			3.7
2993	1995	5	15	7	22	6.8	40.07	21.66	10	4.1	3.1	4.1			3.8
2994	1995	5	15	8	17	0.65	40.09	21.5	28.5	4.5	3.7	4.4			4.4
2995	1995	5	15	9	1	54.82	40.11	21.74	30.5	4.5	3.7	4.4			4.3
2996	1995	5	15	9	19	46.38	40.16	21.57	52.8	4.8	4	4.6			4.3
2997	1995	5	15	11	42	56.68	40.07	21.71	13.4	4.1	3.1	4.1			3.6
2998	1995	5	15	13	59	9.53	40.07	21.64	1	4	2.9	4			3.7
2999	1995	5	15	17	5	42.68	40.15	21.59	8.6	4.8	4	4.6			4.3
3000	1995	5	15	20	0	9.31	40.13	21.58	51.1	4	2.9	4			3.3
3001	1995	5	15	22	10	12.35	40.2	21.77	20	4.4	3.5	4.3			
3002	1995	5	15	22	47	34.49	40.2	21.66	25.8	4.4	3.5	4.3			4.2
3003	1995	5	16	4	37	28.15	40.01	21.58	9.3	5	4.4	4.8			4.5
3004	1995	5	16	4	38	38.22	40.14	21.72	21.2	4.5	3.7	4.4			3
3005	1995	5	16	5	4	14.63	40.13	21.65	23.7	4.1	3.1	4.1			3.7
3006	1995	5	16	7	17	23.72	40.05	21.6	1.5	4	2.9	4			3.8
3007	1995	5	16	12	31	21.03	40.14	21.62	10	4.1	3.1	4.1			3.2
3008	1995	5	16	17	57	51.28	40.09	21.62	11.1	4.8	4	4.6			4.2
3009	1995	5	16	21	54	17.23	40.01	21.62	10	4.5	3.7	4.4			4
3010	1995	5	16	23	0	41.6	40.05	21.6	14	5.2	4.6	4.9			4.6
3011	1995	5	16	23	57	28.78	40.16	21.63	24.9	5.2	4.6	4.9			4.7
3012	1995	5	17	3	54	52.99	40.06	21.65	7	4.3	3.3	4.2			3.9
3013	1995	5	17	4	14	26.16	40.15	21.62	20.7	5.5	5	5.1	5		5.1
3014	1995	5	17	4	37	45.48	40.13	21.65	2.1	4.5	3.7	4.4			
3015	1995	5	17	4	48	34.62	40.09	21.61	11.7	4.9	4.2	4.7			4.3
3016	1995	5	17	7	19	27.88	40.12	21.71	10	4.3	3.3	4.2			3.7
3017	1995	5	17	7	40	20.04	39.08	24.03	0	4	2.9	4			
3018	1995	5	17	9	45	7.42	40.02	21.57	8	5.3	4.8	5.1	4.8		4.9
3019	1995	5	17	10	18	43.2	40.02	21.6	4.2	4.5	3.7	4.4			3.8
3020	1995	5	17	11	25	28.52	40.01	21.65	10	4	2.9	4			3.8
3021	1995	5	17	11	28	38.41	40.03	21.65	11	4.3	3.3	4.2			3.8
3022	1995	5	17	11	30	18.89	40.05	21.54	8	4.4	3.5	4.3			3.3
3023	1995	5	17	11	36	49.08	39.93	21.63	10	4	2.9	4			3.8
3024	1995	5	17	15	37	59.6	40.04	21.62	2.8	4.3	3.3	4.2			3.8
3025	1995	5	17	16	20	2	40.01	21.64	10	4.1	3.1	4.1			3.7
3026	1995	5	17	23	51	47.32	40.02	21.65	3.7	4.3	3.3	4.2			3.8
3027	1995	5	18	3	49	2.08	40.1	21.66	22.6	4.3	3.3	4.2			3.8
3028	1995	5	18	6	22	54.93	40.05	21.6	8.9	4.6	3.8	4.5			4.5
3029	1995	5	18	15	8	42.61	40.07	21.69	10	4.3	3.3	4.2			3.7
3030	1995	5	18	15	26	41.84	40.23	21.87	12.9	4.5	3.7	4.4			3.6
3031	1995	5	19	1	3	42.09	40.07	21.67	5.7	4.3	3.3	4.2			3.8
3032	1995	5	19	1	30	24.27	40.06	21.66	6	4.3	3.3	4.2			3.9
3033	1995	5	19	1	33	55.28	40.06	21.7	1.9	4.3	3.3	4.2			3.8
3034	1995	5	19	6	48	49.9	40.09	21.6	10	5.1	4.9	5.1	4.9	5.1	5

										Homogenized magnitudes		Reported magnitudes			
Event Number	Year	Month	Date	Hour	Minute	Second	Latitude	Longitude	Depth	M_w	M_s	mb	M_s	M_w	ML
3035	1995	5	19	7	36	49.15	40.11	21.6	7.6	4.3	3.3	4.2			3.8
3036	1995	5	19	7	43	47.43	40.16	21.64	19.1	4.1	3.1	4.1			
3037	1995	5	19	12	29	53	40.11	21.76	9.4	4.8	3.9	4	3.9		3.8
3038	1995	5	19	13	7	47.56	39.99	21.58	5	4	2.5				3.6
3039	1995	5	19	21	44	50.55	39.98	21.63	1.4	4.8	3.8	4.1	3.8		3.6
3040	1995	5	20	17	4	45.06	40.05	21.66	28.6	4	2.9	4			3.6
3041	1995	5	20	20	9	31.2	40.01	21.6	11.1	4.6	3.8	4.5			4.3
3042	1995	5	20	20	11	57.12	39.99	21.68	62.1	4.3	3.3	4.2			4.1
3043	1995	5	20	20	35	45.86	40.03	21.64	2	4	2.9	4			3.6
3044	1995	5	20	21	6	25.91	40.02	21.62	26.9	5.3	4.8	4.5	4.8		4.4
3045	1995	5	20	22	25	0.41	40.03	21.65	10	4.1	3.1	4.1			3.4
3046	1995	5	21	4	4	22.67	40.02	21.6	5.8	4.7	3.7	4.2	3.7		4.2
3047	1995	5	21	20	38	26.63	40.16	21.52	4.3	4	2.9	4			3.7
3048	1995	5	22	12	22	21.74	40.12	21.63	12.5	4.1	3.1	4.1			3.4
3049	1995	5	22	20	21	34.1	40.12	21.6	7.6	4.3	3.3	4.2			4.1
3050	1995	5	22	21	10	33.77	40	21.63	10	4.1	3.1	4.1			4
3051	1995	5	22	22	30	40.53	40.08	21.74	9.3	4.3	3.3	4.2			3.6
3052	1995	5	23	4	37	39.94	40.12	21.56	8.2	4.4	3.5	4.3			4.1
3053	1995	5	23	5	51	58.78	40.18	21.83	12	5.4	4.9	4.1	4.9		3.8
3054	1995	5	23	20	9	53.32	40	21.58	10.6	4.6	3.8	4.5			4.4
3055	1995	5	23	20	59	50.21	39.97	21.62	12.4	4.1	3.1	4.1			4.2
3056	1995	5	24	1	0	37.28	39.99	21.65	10	4.1	3.1	4.1			3
3057	1995	5	24	5	22	43.33	40.08	21.64	7.1	4.4	3.5	4.3			3.6
3058	1995	5	24	6	24	8.77	39.97	21.63	8.8	4.5	3.7	4.4			4.3
3059	1995	5	24	7	0	1.99	39.98	21.59	4.4	4.4	3.5	4.3			3.7
3060	1995	5	24	14	45	21.84	39.99	21.61	0.4	4	2.9	4			4.1
3061	1995	5	24	17	34	26.47	40.09	21.66	1.2	4.1	3.1	4.1			3.5
3062	1995	5	25	4	5	44.4	40	21.62	3.3	4	2.9	4			3.1
3063	1995	5	30	6	21	6.58	40.09	21.6	6.8	4.4	3.5	4.3			3.1
3064	1995	5	30	6	46	0.4	40.1	21.55	4.3	5.3	4.7	4.1	4.7		3.7
3065	1995	5	30	12	6	42.89	40.03	21.71	12.9	4.8	4	4.6			4.1
3066	1995	5	30	14	30	2.16	39.99	21.63	10.9	4.5	3.7	4.4			4
3067	1995	6	2	0	27	27.12	40.41	26	32.5	4	2.5				3.6
3068	1995	6	2	7	47	16.1	40.06	21.64	10	4	2.9	4			3.1
3069	1995	6	3	10	20	15.94	40.18	21.67	27.7	4	2.9	4			3.8
3070	1995	6	5	5	20	20.96	39.4	20.24	24.4	4.7	3.7	4.7	3.7		4.4
3071	1995	6	6	4	36	0.17	40.18	21.64	23.6	5	4.4	4.8			4.2
3072	1995	6	6	21	19	43.12	39.27	20.78	63.8	4	2.9	4			3.8
3073	1995	6	7	8	37	34.29	40.13	21.67	5	5.3	4.7	4.1	4.7		3.9
3074	1995	6	8	4	54	27.58	40	21.9	5	4.1	2.7				3.7
3075	1995	6	9	15	20	48.37	40.17	21.66	9.1	4	2.9	4			3.9
3076	1995	6	11	18	51	48.97	40.01	21.62	27	5.1	4.3	4.8	4.3		4.3
3077	1995	6	11	20	38	21.36	39.99	21.63	1.8	4.1	3.1	4.1			3.7
3078	1995	6	17	6	14	52.54	40.02	21.56	4.3	4	2.9	4			3.9
3079	1995	6	18	17	28	9.4	40.02	21.43	20.9	4.6	3.8	4.5			4.1
3080	1995	6	19	3	53	59.1	40.07	21.84	11.2	4.8	3.9	4.6	3.9		4.4
3081	1995	6	19	4	41	32.81	40.21	21.72	20.5	4.5	3.2	4.4	3.2		4
3082	1995	6	19	7	7	3.51	40.09	21.69	10	4.1	3.1	4.1			3.9
3083	1995	6	19	15	0	21.75	40	21.87	23.2	4.8	4	4.6			4
3084	1995	6	21	13	3	18.27	40.21	21.7	5	4	2.9	4			3.2
3085	1995	6	26	19	41	55.59	40.21	21.7	5.1	4	2.9	4			2.8
3086	1995	7	13	12	13	25.23	41.67	20.8	2.6	4.6	3.8	4.5			4.3
3087	1995	7	14	21	19	39.09	40.06	21.69	9	4.5	3.7	4.4			3.8
3088	1995	7	17	23	18	16.06	40.21	21.55	21.7	5.2	4.8	5.3	4.8	5.2	4.9
3089	1995	7	18	3	9	7.81	40.17	21.58	12.1	4.7	3.7	4.6	3.7		3.9
3090	1995	7	18	5	5	32.98	40.12	21.63	11.9	4.5	3.7	4.4			4
3091	1995	7	18	5	13	27.33	40.13	21.68	5	4	2.9	4			3.6
3092	1995	7	18	7	42	56.76	40.14	21.66	47.4	5	4.2	4.8	4.2		4.2
3093	1995	7	18	20	19	8.92	40.13	21.61	10.7	4.3	3.3	4.2			4.2
3094	1995	7	18	23	29	56.85	42.69	27.88	58	4.5	3.3	3	3.3		3.9
3095	1995	7	19	18	23	15.51	40.14	21.63	27.1	5	4.1	4.8	4.1		4.7
3096	1995	7	21	13	27	47.75	40.03	21.56	55.5	4.1	3.1	4.1			3.9
3097	1995	7	28	22	43	30.4	40.18	21.66	9.5	4.5	3.2	4.2	3.2		4.2
3098	1995	7	30	9	28	11.84	40.15	21.74	21.3	4.1	3.1	4.1			3.5
3099	1995	8	5	18	14	41.53	40.13	21.61	0	5	4.2	4.2	4.2		3
3100	1995	8	13	8	32	53.05	41.18	19.92	17.5	4	2.9	4			3.3
3101	1995	8	14	17	57	4.09	40.16	21.67	10.1	4	2.9	4			3.9
3102	1995	8	20	19	21	25.01	40.23	21.84	30.7	4.6	3.8	4.5			4.2
3103	1995	8	20	19	27	51.85	40.23	21.82	13.6	4.1	3.1	4.1			3.9
3104	1995	9	4	4	9	24.14	40.1	21.75	8	4	2.9	4			3.9
3105	1995	9	8	12	57	28.37	39.09	26.19	10.4	4.1	2.7				3.7
3106	1995	9	10	12	53	8.39	39.97	20.65	9	4.6	3.5	3.4	3.5		3.3
3107	1995	9	14	1	26	38.8	40.15	21.53	6.9	4.4	3.5	4.3			4.3
3108	1995	9	21	8	46	54.41	39.69	20.5	23	4	2.9	4			4.2
3109	1995	10	5	6	21	50.31	39.29	21.66	26.3	4.1	3.1	4.1			3.9
3110	1995	10	11	5	35	42.89	39.4	23.9	16.5	4	2.5				3.6
3111	1995	10	18	9	36	44.32	43.03	24.84	10	4.5	3.4				4.1
3112	1995	10	24	13	12	23.92	40.69	19.84	3.1	4.1	3.1	4.1			3.7
3113	1995	10	26	16	41	55.57	39.39	23.96	17.1	4.1	2.7				3.7
3114	1995	10	28	10	45	1.06	40.84	27.97	24.8	4	2.9	4			
3115	1995	10	30	20	7	24.4	42.17	19.66	10	4.3	3.3	4.2			3.2
3116	1995	11	11	15	6	56.05	40.01	21.71	10	4	2.9	4			3.4

										Homogenized magnitudes		Reported magnitudes			
Event Number	Year	Month	Date	Hour	Minute	Second	Latitude	Longitude	Depth	M_w	M_s	mb	M_s	M_w	ML
3117	1995	11	13	13	40	33.24	40.07	21.8	7.6	4.3	3.3	4.2			3.9
3118	1995	12	22	19	4	34.7	39.2	28.08	5.1	4.2	2.9				3.8
3119	1996	1	22	18	4	43.58	39.01	27.89	14	4.3	3				3.9
3120	1996	2	25	22	0	47.72	44.19	19.84	0	4.3	3.4	4.2			3.5
3121	1996	2	26	21	39	12.56	40.64	21.6	13.2	4.7	3.6	4.4	3.6		4.5
3122	1996	3	14	9	28	26.95	39.05	27.58	12	4.7	3.7				4.3
3123	1996	3	23	11	59	18.92	40.3	25.86	9.1	4.2	2.9				3.8
3124	1996	3	27	22	21	1.45	40.56	27.37	6.6	4.1	2.7				3.7
3125	1996	3	31	9	33	43.99	41.98	20.08	26.7	4.1	3.1	4.1			3.5
3126	1996	4	14	8	31	7.01	40.79	27.47	19.9	4.9	4	4	4		4.3
3127	1996	4	20	20	2	45.96	42.62	23.59	10	4	2.5				3.6
3128	1996	5	2	18	8	54.32	39.47	20.42	10	4.6	3.8	4.5			4.2
3129	1996	5	5	4	58	9.28	39.03	27.83	10	4.2	2.9				3.8
3130	1996	5	9	8	26	39.22	42.42	19.44	11.3	4	2.5				3.6
3131	1996	7	16	2	41	24.38	43.01	20.62	10	4	2.5				3.6
3132	1996	7	23	7	42	58.6	39.03	26.1	12.7	4.1	2.7				3.7
3133	1996	7	26	18	55	49.79	40.08	20.61	5	5.3	5	5.1	5	5.3	4.8
3134	1996	7	28	1	12	4.15	40.02	20.64	4.7	4	2.9	4			3.8
3135	1996	8	5	22	46	42.49	40.09	20.63	8.5	5.4	5	5.1			5.1
3136	1996	8	11	7	57	16.92	40.03	20.69	11.1	4.4	3.5	4.3			4.2
3137	1996	8	19	1	5	37.14	39.36	25.97	18.8	4.8	3.9	4.6	3.9		4.2
3138	1996	8	20	1	26	50.31	40.04	20.63	7	5.2	4.6	4.9	4.6		4.8
3139	1996	8	25	4	48	19.86	39.56	26.11	25.4	4.7	3.7	3.9	3.7		4
3140	1996	9	1	9	50	59.24	40.79	19.48	55.1	4	2.9	4			4.4
3141	1996	9	4	9	24	16.24	40.24	27.86	8.2	4.2	2.9				3.8
3142	1996	9	4	9	42	41.66	40.25	27.9	11.9	4.2	2.9				3.8
3143	1996	9	18	13	55	17.38	39.35	25.52	5.6	4	2.5				3.6
3144	1996	9	26	12	31	50.04	40.01	20.73	11.7	4.3	3.3	4.2			4.2
3145	1996	9	28	15	21	0.75	42.97	20.65	10	4	2.9	4			4
3146	1996	10	4	0	16	16.5	41.96	20.25	4.4	4.5	3.2	4	3.2		4.1
3147	1996	10	5	7	49	0.6	39.37	21.78	5	4	2.5				3.6
3148	1996	10	10	15	48	1.7	42.88	21.79	0	4.7	3.7				4.3
3149	1996	10	10	19	7	46.75	40.16	21.52	8.5	4.3	3.3	4.2			4
3150	1996	11	2	0	11	42.77	39.98	20.68	5	4.2	2.9				3.8
3151	1996	11	14	3	3	37.11	40.02	20.59	10.7	5.1	4.4	4.6	4.4		4.8
3152	1996	12	3	18	5	10.29	39.95	20.03	30	4.1	3.1	4.1			4.3
3153	1996	12	10	20	14	53.24	41.4	19.83	7.5	4	2.9	4			4.5
3154	1996	12	12	10	6	26.18	40.48	23.22	7	4.3	3				3.9
3155	1997	1	6	14	17	4.09	40.49	23.67	1	4.1	2.7				3.7
3156	1997	1	12	12	10	51.48	40.82	19.69	18.2	4.8	4.7	4.6	4.7	4.8	5.2
3157	1997	1	19	19	42	39.57	40.77	19.71	20.3	4.7	4.6	4.7	4.6	4.7	4.9
3158	1997	2	13	20	10	23.67	40.15	21.7	47.9	4	2.9	4			4.1
3159	1997	2	18	8	43	47.87	39.42	26.29	11.4	4.5	3.3	3.8	3.3		3.8
3160	1997	2	19	4	3	27.65	40.07	20.7	10	4	2.5				3.6
3161	1997	3	21	6	17	7.27	39.31	23.78	5.3	4.9	4.5	4.5	4.5	4.9	4.5
3162	1997	3	21	6	32	21.09	39.22	23.72	11.1	4.9	4.1				4.5
3163	1997	3	24	21	21	9.96	42.02	20.15	6.7	4	2.9	4			3.5
3164	1997	4	7	12	32	21.79	40.23	22.65	26.2	4.6	3.5	3.7	3.5		3.4
3165	1997	5	2	8	45	12.63	39.67	28.59	7	4.6	3.4	3.7	3.4		4.2
3166	1997	5	16	7	0	49.55	41.02	20.19	21	5.4	5.3	5.1	5.3	5.4	4.9
3167	1997	5	18	3	2	9.1	41.05	20.2	8.5	4.4	3.1	4.3	3.1		4.4
3168	1997	5	19	20	16	12.05	41.04	20.18	10.3	4	2.9	4			4.4
3169	1997	5	28	10	50	44.22	39.88	27.11	2.2	4.5	3.4				4.1
3170	1997	6	3	1	13	45.38	40.18	19.75	22.7	4.1	2.5	4	2.5		4.3
3171	1997	6	23	18	40	27.37	40.38	26	8.1	4	2.5				3.6
3172	1997	6	25	20	25	42.23	40.59	24.01	2.5	4	2.5				3.6
3173	1997	6	27	15	0	30.89	40.96	20.23	2	4.1	2.6	3.8	2.6		3.4
3174	1997	7	16	10	6	6.59	39.09	25.2	6.1	4.9	4.4	4.5	4.4	4.9	4.6
3175	1997	7	20	3	39	10.24	41.23	19.85	24.9	4.6	4.5	4.5	4.5	4.6	4.7
3176	1997	7	20	3	43	45.28	41.29	19.82	12.6	4	2.9	4			4.5
3177	1997	7	20	9	24	32.78	41.29	19.89	27.3	4	2.9	4			4
3178	1997	7	20	9	48	24.87	41.35	19.91	19.7	4.5	3.7	4.4			3.9
3179	1997	7	29	21	14	45.76	39.26	22.17	26.3	4.3	3	3.9	3		3.9
3180	1997	8	3	6	37	37.39	41.27	19.89	27.2	4.1	2.6	3.7	2.6		4.4
3181	1997	8	8	10	36	16.62	43.08	27.47	10	4.3	3.4	4.2			3.3
3182	1997	8	16	9	14	23.99	40.67	21.75	5	4.4	3.1	3.8	3.1		4
3183	1997	8	17	21	52	13.62	40.7	27.58	10	4	2.5				3.6
3184	1997	8	19	19	3	46.85	40.05	21.66	0.9	4.3	2.9	3.9	2.9		3.9
3185	1997	8	22	3	17	47.31	40.15	21.57	23.2	4.4	3.5	4.3			4.2
3186	1997	9	19	12	0	26.7	40.05	21.34	4.8	4.9	4.5	4.8	4.5	4.9	4.9
3187	1997	9	29	1	10	25.32	39.49	25.97	3.9	4	2.5				3.6
3188	1997	10	18	9	18	52.91	39.8	28.67	4.7	4.6	3.4	3.9	3.4		4.5
3189	1997	10	18	10	18	26.99	39.81	28.62	6.5	4.4	3.2				4
3190	1997	10	20	23	53	46.12	39.34	25.91	10	4	2.5				3.6
3191	1997	10	21	5	6	24.63	39.38	25.89	4.7	4.2	2.9				3.8
3192	1997	10	21	17	57	46.19	39.04	22.06	25.9	4.7	4.4	4.7	4.4	4.7	4.2
3193	1997	10	21	21	33	40.96	39.35	25.88	9	4.1	2.7				3.7
3194	1997	10	28	8	18	49.34	39.81	23.84	9.7	4	2.9	4			4
3195	1997	10	30	21	37	26.51	41.37	20.75	8	4	2.5				3.6
3196	1997	11	11	3	32	21.62	40.43	26.27	12.3	4	2.5				3.6
3197	1997	11	12	16	26	56.86	39.22	20.25	20.9	4.9	4.5	4.8	4.5	4.9	4.8
3198	1997	11	13	0	48	45.08	43.33	20.37	3.8	4.5	3.7	4.3	3.7	4.5	4.4

										Homogenized magnitudes		Reported magnitudes			
Event Number	Year	Month	Date	Hour	Minute	Second	Latitude	Longitude	Depth	M_w	M_s	mb	M_s	M_w	ML
3199	1997	11	25	0	35	20.99	42.02	23.42	11	4	2.5				3.6
3200	1997	11	25	6	17	50.35	40.27	20.1	22	4.1	3.1	4.1			4.4
3201	1997	11	29	0	21	11.34	39.45	20.09	5.8	4.6	3.8	4.5			4.1
3202	1997	12	15	10	56	13.36	42.25	20.08	5.4	4	2.9	4			4.2
3203	1997	12	28	20	46	37.88	39.77	26.88	10	4.4	3.1	4.1	3.1		4.2
3204	1998	1	19	3	37	0.77	40.42	26.09	11.7	4.4	3.2				4
3205	1998	2	1	6	27	3.47	39.88	19.68	27.5	4.7	3.7	4.1	3.7		4.3
3206	1998	2	12	11	21	28.72	41.96	20.3	5	4	2.9	4			3.8
3207	1998	2	23	17	18	50.61	40.27	25.8	3.6	4.3	3				3.9
3208	1998	2	25	7	22	25.11	39.82	26.82	10	4.1	2.7				3.7
3209	1998	3	2	6	25	41.53	39.32	19.4	3.4	4.1	2.7				3.7
3210	1998	3	5	1	45	10.35	39.55	27.3	23	4.8	4.4	4.5	4.4	4.8	4.7
3211	1998	3	5	1	55	31.17	39.59	27.45	5	5.1	4.3	4.4	4.3		4.7
3212	1998	4	11	9	29	11.58	39.89	23.94	9.6	4.5	3.9	4.6	3.9	4.5	4.5
3213	1998	4	12	23	53	39.13	40.13	21.21	24.7	4.1	3.1	4.1			4.2
3214	1998	5	7	9	36	41.51	40.88	20.69	7.8	4.2	2.8	3.9	2.8		3.7
3215	1998	5	9	13	6	15.25	40.99	20.05	30.3	4.7	3.6	4.5	3.6		4.2
3216	1998	5	12	9	56	42.85	39.8	19.82	8.2	4.1	3.1	4.1			4.1
3217	1998	6	3	8	40	3.97	39.82	24.2	17	4.1	2.7				3.7
3218	1998	6	3	8	47	8.06	39.81	24.12	2.9	4.7	4.2	4.4	4.2	4.7	4.7
3219	1998	6	3	8	48	40.28	39.75	24.06	5.4	4.4	3.2				4
3220	1998	6	13	8	29	12.7	39.32	20.55	11.2	4.3	3	4	3		3.9
3221	1998	6	16	18	6	32.97	39.8	24.02	9.2	5	4.1	4.4	4.1		4.4
3222	1998	6	20	11	40	24.21	40.11	21.65	9.6	4.2	2.7	3.9	2.7		3.9
3223	1998	7	1	2	12	11.27	39.36	25.98	17.4	4.1	2.7				3.7
3224	1998	7	29	11	11	33.37	39.41	20.66	16	4	2.5				3.6
3225	1998	8	4	15	58	28.89	42.01	20.12	4.6	4.3	3.3	4.2			3.4
3226	1998	8	9	15	21	31.69	39.85	24.02	1	4.1	2.7				3.7
3227	1998	8	11	23	55	16.22	39.85	24.02	5.5	4	2.5				3.6
3228	1998	8	12	5	19	1.61	39.84	24.04	4.7	4	2.5				3.6
3229	1998	8	15	2	5	14.55	40.4	25.97	10	4.4	3.2				4
3230	1998	8	16	1	40	11.94	39.44	20.63	26.2	4.4	3.1	3.9	3.1		3.6
3231	1998	8	24	20	50	23.9	39.39	20.65	22.5	4.2	2.7	3.6	2.7		3.8
3232	1998	8	28	3	1	48.18	39.08	22.51	17.7	4.6	3.4	3.8	3.4		3.9
3233	1998	9	6	20	34	30.01	39.61	24.09	7	4.2	2.8	4	2.8		4.1
3234	1998	9	15	12	42	51.82	40.46	25.78	10	4	2.5				3.6
3235	1998	9	25	16	20	8.59	40.2	28.88	0.3	4.5	3.2	4	3.2		4
3236	1998	9	29	22	14	49.59	44.2	20.06	10	5.5	5.3	5.2	5.3	5.5	5.1
3237	1998	9	29	22	28	52.59	44.19	20.14	10	4.1	2.7				3.7
3238	1998	9	30	23	42	53.58	41.94	20.4	4.7	5.3	5	4.9	5	5.3	5.1
3239	1998	10	1	15	10	36.78	41.91	20.48	10	4	2.5				3.6
3240	1998	10	4	11	19	26.32	43.28	20.83	10	4.7	3.9	4.4	3.9	4.7	4.3
3241	1998	10	5	6	53	27.56	44.21	20.2	4.1	4	2.5				3.6
3242	1998	10	5	7	10	28.6	40.97	20.78	10	4	2.5				3.6
3243	1998	10	10	7	29	42.88	39.62	28.62	8.6	4.2	2.7	3.5	2.7		
3244	1998	10	11	5	33	26.51	39.77	23.8	11.3	4.6	3.5	3.6	3.5		3.6
3245	1998	11	2	0	44	23.97	39.26	28.29	9	4	2.5				3.6
3246	1998	11	2	20	27	50.19	39.27	21.51	18	4.5	3.3	4.1	3.3		3.9
3247	1998	11	5	21	52	2.48	39.25	26.73	5	4.2	2.9				3.8
3248	1998	11	25	2	0	17.31	39.37	25.52	10	4	2.5				3.6
3249	1998	12	11	15	9	19.01	42.22	25.28	6.2	4.5	4	4.7	4	4.5	4.5
3250	1998	12	25	4	32	57.08	39.01	26.35	5	4	2.5				3.6
3251	1999	1	10	0	17	24.96	40.51	23.97	5	4.1	2.7				3.7
3252	1999	1	12	7	26	10.94	40.02	20.5	11	4.1	3.1	4.1			4.2
3253	1999	1	27	11	20	17.92	42.8	23.31	7.4	4	2.5				3.6
3254	1999	2	2	16	24	14.88	40.88	27.63	5	4	2.5				3.6
3255	1999	2	7	15	19	5.72	39.02	20.68	11	4	2.5				3.6
3256	1999	2	7	22	28	36.75	39.01	23.19	22.6	4.8	4.2	4.7	4.2	4.8	4.7
3257	1999	2	7	22	31	50.7	39.04	23.32	14.3	4.2	2.9				3.8
3258	1999	2	7	22	32	46.62	39.12	23.39	14.4	4	2.5				3.6
3259	1999	2	7	22	33	29.67	39.06	23.15	5	4	2.5				3.6
3260	1999	2	19	0	19	18.81	39.34	20.75	49.3	4.2	2.8	4	2.8		4
3261	1999	2	25	10	21	54.57	42.97	20.59	5	4.1	3.1	4.1			3.2
3262	1999	2	28	7	5	8.16	40.42	25.92	6.3	4.4	3.2				4
3263	1999	3	5	22	58	21.98	40.43	26	4.8	4.2	2.9				3.8
3264	1999	3	31	0	0	23.25	39.67	20.81	74.4	4.5	3.2	4.2	3.2		4.3
3265	1999	4	8	10	12	54.64	40.19	27.33	2.9	4.4	3.2				4
3266	1999	4	8	20	32	44.65	40.37	25.94	10	4	2.5				3.6
3267	1999	4	18	12	50	2.96	39	23.17	3.7	4	2.4	3.7	2.4		3.9
3268	1999	4	19	5	37	51.48	39.06	23.23	7.7	4.1	2.6	4	2.6		4.2
3269	1999	4	20	16	1	12.79	39.53	23.98	12.7	4.6	4	4.5	4	4.6	4.9
3270	1999	4	21	4	20	14.45	39.54	24	8.9	4.3	3				3.9
3271	1999	4	30	3	30	37.36	44.18	20.07	10	5.4	4.8	5.1	4.8	5.4	5.2
3272	1999	4	30	7	41	0.3	44.19	20.12	3	4.3	3.2	4.2	3.2	4.3	4.2
3273	1999	5	7	23	3	54.14	39.05	21.63	10.4	4.5	3.3	4.1	3.3		3.9
3274	1999	5	8	5	6	57.6	39.07	21.64	36.8	4.6	3.5	3.9	3.5		3.7
3275	1999	5	8	6	33	43.73	39.01	21.67	10.4	4.5	3.3	4	3.3		3.8
3276	1999	5	8	7	21	28.52	40.23	20.65	9.7	4.7	3.6	4.1	3.6		4.2
3277	1999	5	17	7	35	36.49	43.57	21.05	10	4.4	3.6	4.3			
3278	1999	6	12	2	58	1.85	40.18	21.84	11	4.1	2.7				3.7
3279	1999	6	16	3	33	4.27	44.32	21.39	13.8	4	3	4			
3280	1999	6	27	8	43	1.72	41.29	20.01	9.7	4.1	2.6	3.8	2.6		4.2

										Homogenized magnitudes		Reported magnitudes			
Event Number	Year	Month	Date	Hour	Minute	Second	Latitude	Longitude	Depth	M_w	M_s	mb	M_s	M_w	ML
3281	1999	7	1	7	40	56.21	43.68	21.02	10	5.2	4.9	5.1	4.9	5.2	5.2
3282	1999	7	6	20	11	55.4	39	24.96	30	4	2.5				3.6
3283	1999	7	13	23	36	25.02	40.41	25.91	7.6	4.5	3.4				4.1
3284	1999	7	21	15	37	34.27	43.67	21.21	1.6	4.1	2.7				3.7
3285	1999	7	24	9	19	13.16	39.67	20.31	4	4.2	2.9				3.8
3286	1999	7	24	16	5	48.86	39.3	27.98	10	5	4.4	4.5	4.4	5	4.6
3287	1999	7	24	17	55	46.35	39.35	27.9	4.2	4.4	3.2				4
3288	1999	7	24	22	31	4.77	39.39	27.74	1	4.5	3.4				4.1
3289	1999	7	25	6	56	54.03	39.33	27.98	15.2	5.2	4.9	4.9	4.9	5.2	5
3290	1999	7	25	9	14	44.31	39.37	27.86	7.4	4.1	2.7				3.7
3291	1999	8	13	21	28	59.88	42.77	20.32	16	4.3	3				3.9
3292	1999	8	16	8	32	9.39	39.21	20.98	5	4.3	3.3	4.2			3.6
3293	1999	8	17	4	24	47.71	39.76	27.82	15	4.1	3.1	4.1			4
3294	1999	8	17	14	31	11.2	40.42	28.72	8	4.2	2.8	3.4	2.8		4.1
3295	1999	8	26	12	44	44.17	39.6	23.9	9.7	4.4	3.1	3.9	3.1		3.7
3296	1999	8	26	20	59	4.64	40.24	25.36	39	4	2.5				3.6
3297	1999	8	27	8	37	5.15	40.28	25.8	9.7	4.1	2.7				3.7
3298	1999	9	1	19	42	39.61	39.62	23.87	6.5	4.4	3.2				4
3299	1999	9	9	8	11	58.18	40.26	25.81	11	4.3	3	4.1	3		4.1
3300	1999	9	9	8	15	34.53	40.27	25.8	0	4.8	4.3	4.9	4.3	4.8	4.7
3301	1999	9	13	10	57	3.31	40.64	19.57	10.4	4	2.4	3.6	2.4		3.5
3302	1999	9	20	21	28	0.17	40.67	27.58	14.6	5.3	4.7	4.7	4.7		4.1
3303	1999	9	26	6	38	39.62	39.09	27.91	10.8	4.3	3	4.1	3		4.4
3304	1999	9	27	4	2	1.52	39.14	26.93	1.5	5	4.4	4.8			
3305	1999	9	29	16	46	31.12	39.1	29	3.3	4.1	2.6	4.1	2.6		3.9
3306	1999	9	30	10	30	2.48	43.07	19.04	10	4	2.5				3.6
3307	1999	11	2	3	42	49.88	39.8	20.62	54.5	4.5	4.2	4.4	4.2	4.5	4.4
3308	1999	11	2	9	26	49.79	39.77	20.68	10	4.1	3.1	4.1			2.7
3309	1999	11	13	2	7	37.59	40.22	25.01	10	4.2	2.9				3.8
3310	1999	11	16	0	29	22.97	40.45	27.04	10	4	2.5				3.6
3311	1999	11	16	9	33	29.52	41.51	19.49	9.9	4.2	2.8	3.9	2.8		3.4
3312	1999	11	20	2	1	17.06	40.4	26.08	10	4.2	2.9				3.8
3313	1999	11	20	2	5	37.14	40.39	26.06	9.9	4	2.5				3.6
3314	1999	11	21	13	46	12.62	40.34	25.94	2	4.2	2.9				3.8
3315	1999	11	21	17	52	23.04	40.44	26.13	35	4.6	3.6				4.2
3316	1999	11	23	0	47	54.21	41.88	25.06	10	4.9	4.1				4.5
3317	1999	11	24	3	38	51.24	39.67	20.56	10	4.8	4.4	4.8	4.4	4.8	4.6
3318	1999	11	24	21	10	51	40.17	19.71	29.2	4.3	3.9	4.4	3.9	4.3	4.5
3319	1999	11	28	0	59	47.11	41.54	19.44	41.8	4.8	4.5	4.8	4.5	4.8	3.2
3320	1999	12	12	13	26	2.61	39.21	21.43	6.5	4	2.9	4			3.6
3321	1999	12	12	19	25	57.53	40.57	23.63	14	4.9	4	4.4	4		4.3
3322	1999	12	22	8	40	26.11	41.06	20.39	8	4.2	2.7	3.9	2.7		3.8
3323	1999	12	22	9	6	11.43	41.92	20.55	2.9	5.1	4.6	4.8	4.6	5.1	4.8
3324	1999	12	22	9	10	34.31	42.02	20.63	3.9	4.8	4.2	4.5	4.2	4.8	4.5
3325	1999	12	22	9	41	4.68	41.93	20.56	2.5	4.6	4	4.6	4	4.6	4.2
3326	2000	1	1	1	19	26.31	41.93	20.55	4.6	4.7	4.2	4.5	4.2	4.7	4.8
3327	2000	1	4	17	2	9.83	39.88	20.27	7.7	4	2.4	3.6	2.4		3.3
3328	2000	1	8	23	9	51.85	43.69	21.13	10	4.2	2.9				3.8
3329	2000	1	27	0	3	21.35	40.7	25.58	8.5	4.2	2.7	3.8	2.7		3.9
3330	2000	2	23	14	46	13	40.04	23.52	5.7	4.1	2.6	3.4	2.6		3.3
3331	2000	3	10	9	1	33.66	40.97	20.23	4.4	4.8	3.9	4.1	3.9		4.3
3332	2000	3	12	18	26	23.4	39.81	20.62	5.1	4.3	3				3.9
3333	2000	3	14	7	2	44.63	39.02	23.25	0	4.2	2.9				3.8
3334	2000	3	21	4	2	25	41	24	0	7.2	7.6	6.5			
3335	2000	4	5	22	43	20.93	39.18	24.51	1.6	4.5	3.2	3.9	3.2		4.1
3336	2000	4	7	5	34	58.9	39.55	25.95	10	4	2.5				3.6
3337	2000	4	15	11	3	29.33	40.56	28.23	3.6	4	2.5				3.6
3338	2000	4	20	2	44	14.4	39.43	20.53	31.7	4.2	3.3	4.2	3.3	4.2	4.3
3339	2000	4	24	17	37	52.51	40.08	24.42	10	4.1	2.7				3.7
3340	2000	4	26	22	25	8.68	43.54	19.48	10	4.2	3.5	4	3.5	4.2	4.5
3341	2000	5	1	2	13	20.12	40.53	24.2	17.3	4.1	2.7				3.7
3342	2000	5	22	12	59	6.78	40.25	25.22	9	4.3	3				3.9
3343	2000	5	26	1	28	21.56	39.11	20.58	8.1	5.6	5.3	5.2	5.3	5.6	5.3
3344	2000	5	26	12	2	4.3	39.02	20.53	12.6	4.9	4	4.3	4		4.3
3345	2000	6	3	5	35	55.31	41.94	23.24	4	4	2.5				3.6
3346	2000	6	3	13	27	51.57	39.11	20.06	44.1	5.2	4.6	4.2	4.6		4.4
3347	2000	6	21	2	9	0.42	39.37	20.42	10	5	4.2	3.8	4.2		4
3348	2000	6	30	19	27	30.47	39.65	21.03	2.1	4.2	2.9				3.8
3349	2000	7	3	19	14	43.58	40.45	26.14	9.6	4.1	2.5	3.8	2.5		4.1
3350	2000	7	4	19	44	22.02	40.43	26.06	10.6	4.1	2.7				3.7
3351	2000	7	5	23	20	38.21	40.36	25.99	10.4	4.6	3.5	4	3.5		4.2
3352	2000	7	9	0	1	41.43	41.24	20.62	3.6	4.1	2.6	3.9	2.6		4.1
3353	2000	7	17	6	8	3.04	39.1	20.56	51.2	4.4	3.1	3.8	3.1		3.8
3354	2000	7	20	4	10	6.65	39.32	22.29	89	4.2	2.9				3.8
3355	2000	7	26	17	33	37.48	39.82	24.15	9.5	4	2.5				3.6
3356	2000	8	6	3	23	58.58	39.67	26.12	12.2	4.3	3				3.9
3357	2000	8	22	3	35	37.39	39.63	23.87	5.6	5	4.6	4.7	4.6	5	4.6
3358	2000	8	22	6	6	25.88	42.7	20.27	13.5	4.6	3.4	4.4	3.4		3.8
3359	2000	8	22	8	24	56.95	39.68	23.75	10	4	2.5				3.6
3360	2000	8	26	17	15	8.84	39.38	26.22	9.6	4.5	3.3	3.8	3.3		4.1
3361	2000	8	28	5	16	47.9	42.98	25.39	5.9	4.6	3.4	3.5	3.4		3.6
3362	2000	9	1	15	21	9.92	41.8	19.75	10	4.1	3.1	4.1			3.8

										Homogenized magnitudes		Reported magnitudes			
Event Number	Year	Month	Date	Hour	Minute	Second	Latitude	Longitude	Depth	M_w	M_s	mb	M_s	M_w	ML
3363	2000	9	8	5	46	46.79	39.4	27.67	5	4.7	3.8	4.3	3.8	4.7	4.7
3364	2000	9	9	8	18	48.58	39.39	27.66	5	4.3	3				3.9
3365	2000	9	12	16	28	40.98	39.4	26.31	13.3	4.3	3				3.9
3366	2000	10	22	0	58	48.97	39.82	20.12	16.6	4.2	2.8	3.6	2.8		4.2
3367	2000	10	25	23	6	4.55	42.85	22.87	4	4	2.5				3.6
3368	2000	11	7	21	13	57.84	39.41	26.28	10.1	4	2.9	4			4
3369	2000	11	13	15	40	15.09	39.32	25.52	8.5	4.1	2.7				3.7
3370	2000	11	29	17	16	56.41	39.88	22.95	14.2	4.4	3.5	4.3			3.9
3371	2001	1	7	11	58	11.42	39.49	26.3	26.7	4	2.5				3.6
3372	2001	1	24	5	19	42.9	39.59	26.08	8	4.4	3.2				4
3373	2001	2	1	9	58	47.34	40.08	27.77	7.5	4.4	3.2				4
3374	2001	2	14	6	36	25.74	39.32	20.27	13	4.4	3.1	4.4		4.4	4.5
3375	2001	2	15	15	10	17.3	39.24	22.16	92.2	4.4	3.2				4
3376	2001	2	20	8	15	19.77	39.13	24.33	14.7	4	2.9	4			3.8
3377	2001	2	21	17	20	6.74	44.18	20.33	0.7	4	3	4			3.9
3378	2001	2	27	4	10	47.63	39.01	26.67	9.8	4.3	3	3.8	3		4.1
3379	2001	2	27	6	14	55.95	39.07	26.73	21.1	4	2.9	4			4.1
3380	2001	2	27	13	48	22.79	42.47	21.32	0	4	2.5				3.6
3381	2001	3	26	8	27	59.92	39.36	21.69	5	4.7	3.7	4.2	3.7		4.1
3382	2001	4	9	17	38	36.2	40.07	20.44	10	5	4.5	4.7	4.5	5	5.3
3383	2001	4	17	0	42	38.3	40.6	19.48	18.9	4.3	3.2	4.2	3.2	4.3	4.5
3384	2001	4	29	0	15	7.23	39.3	22.35	4.9	4.1	2.7				3.7
3385	2001	5	18	20	32	34.1	41.36	20.3	7	4.2	2.7	3.9	2.7		4
3386	2001	5	19	3	11	14.89	39.16	22.54	14	4.4	3.4	4.5	3.4	4.4	4.3
3387	2001	5	24	3	18	8.73	39.32	27.9	7	4.5	3.7	4	3.7	4.5	4.5
3388	2001	5	24	6	25	54.58	39.36	27.89	6	4.5	3.3	3.8	3.3		4.4
3389	2001	5	31	19	39	50.78	39.42	26.36	10	4.4	3.2				4
3390	2001	6	14	17	22	58.53	39.17	20.73	11	4.3	2.9	4.1	2.9		4
3391	2001	6	22	11	54	50.78	39.34	27.91	7	5.1	4.7	4.6	4.7	5.1	4.8
3392	2001	6	23	12	18	22.25	39.39	27.88	8.4	4.8	4	4.2	4	4.8	4.7
3393	2001	6	23	16	1	26.15	40.24	25.21	8.4	4.3	3				3.9
3394	2001	6	24	13	33	2	39.35	27.86	9.9	4.3	3.3	4.2			
3395	2001	7	3	19	5	0.02	39.06	20.76	5	4.3	3				3.9
3396	2001	7	21	12	47	36.64	39.01	24.35	11.3	4.7	4	4.6	4	4.7	4.6
3397	2001	7	25	15	43	13.36	39.08	24.27	27.6	4.5	3.3	4.3	3.3		4.2
3398	2001	7	26	0	21	38.63	39.1	24.27	19	6.5	6.5	5.8	6.5	6.5	5.4
3399	2001	7	26	0	31	54.54	39.02	24.29	22.5	4	2.9	4			4.1
3400	2001	7	26	0	34	58.91	39	24.37	21.3	5.4	4.9	4.7	4.9		4.8
3401	2001	7	26	0	59	3.84	39.13	24.26	21	5	4.2	4.4	4.2		4.3
3402	2001	7	26	1	9	15.78	39.02	24.31	37	4	2.5				3.6
3403	2001	7	26	1	12	49.39	39.05	24.2	5	4.2	2.9				3.8
3404	2001	7	26	1	58	53.45	39.14	24.29	13	4.4	3.5	4.3			4.4
3405	2001	7	26	2	1	52.03	39.11	24.21	19.6	5	4.1	4.5	4.1		4.5
3406	2001	7	26	2	16	29.64	39.04	24.34	13.5	4	2.9	4			4.2
3407	2001	7	26	2	25	46.94	39.01	24.44	17.5	5.1	4.4				4.7
3408	2001	7	26	4	0	45.91	39.15	24.34	4.8	4	2.5				3.6
3409	2001	7	26	4	53	36.26	39.07	24.24	19.5	4.7	4	4.5	4	4.7	4.6
3410	2001	7	26	5	27	25.66	39.11	24.3	6.9	4.3	3				3.9
3411	2001	7	26	6	35	37.31	39.09	24.22	17	4	2.5				3.6
3412	2001	7	26	8	55	5.5	39.07	24.19	36	4.2	2.9				3.8
3413	2001	7	26	9	21	58.99	39.12	24.35	10	4.2	2.9				3.8
3414	2001	7	26	10	30	8.04	39.05	24.33	2.7	4.1	2.6	3.8	2.6		3.9
3415	2001	7	26	14	24	32.52	39.12	24.3	5.9	4.7	4	4.6	4	4.7	4.6
3416	2001	7	26	18	20	6.41	39.02	24.2	11.3	4.1	2.7				3.7
3417	2001	7	26	22	33	11.22	39.14	24.28	12.6	4	2.5				3.6
3418	2001	7	27	19	49	23.2	39.12	24.32	5	4.1	2.7				3.7
3419	2001	7	28	17	2	23.9	39.03	24.23	12.1	4	2.5				3.6
3420	2001	7	30	14	44	45	39.12	24.19	1.9	4.3	3				3.9
3421	2001	7	30	14	54	13.37	39.15	24.21	11.2	4.2	2.9				3.8
3422	2001	7	30	14	55	40.11	39.12	24.18	19.6	4.1	3.1	4.1			3.9
3423	2001	7	30	15	24	58.09	39.12	24.1	21	5	4.4	4.7	4.4	5	4.8
3424	2001	7	30	16	38	21.89	39.07	24.26	4.1	4.7	3.7	4.4	3.7		4.3
3425	2001	7	30	16	54	39.88	39.11	24.21	8.3	4	2.5				3.6
3426	2001	8	2	18	40	42.63	39.18	24.47	5.3	4.2	3.3	4	3.3	4.2	4.3
3427	2001	8	3	13	59	48.23	39.13	24.2	10.8	4.3	3				3.9
3428	2001	8	4	4	11	8.2	39.09	24.23	11.6	4	2.5				3.6
3429	2001	8	6	3	55	46.42	39.11	24.25	14	4.2	2.9				3.8
3430	2001	8	7	1	4	14.48	39.74	20.6	11.1	4.3	3				3.9
3431	2001	8	9	0	58	16.19	42.55	26.46	5	4.3	2.9	4.3	2.9		3.8
3432	2001	8	9	1	44	3.74	42.49	26.41	10	4.2	2.9				3.8
3433	2001	8	10	7	47	8.49	39.02	24.22	10	4.5	3.4				4.1
3434	2001	8	10	17	4	25.52	39.04	24.3	12	4.1	2.7				3.7
3435	2001	8	10	20	3	35.79	39.09	24.22	9.5	4.2	2.9				3.8
3436	2001	8	10	21	49	37.13	40.67	23.5	2	4.3	3				3.9
3437	2001	8	13	5	37	15.69	39.37	25.97	8.1	4.1	2.7				3.7
3438	2001	8	13	11	11	0.66	39.35	27.83	6	4.2	2.8	3.9	2.8		4
3439	2001	8	13	11	20	17.95	39.1	24.27	14.6	4.2	2.9				3.8
3440	2001	8	13	14	26	13.59	42.59	26.47	22.4	4.7	4	4.6	4	4.7	4.1
3441	2001	8	16	12	15	11.74	39.11	24.24	18.6	4.1	2.7				3.7
3442	2001	8	16	23	31	32.08	39.1	24.25	11.9	4.6	3.4	3.9	3.4		3.8
3443	2001	8	17	21	1	44.57	39	24.34	10.5	4.4	3.1	3.7	3.1		3.7
3444	2001	8	20	18	30	28.77	39.11	24.17	21.2	4.2	2.9				3.8

										Homogenized magnitudes		Reported magnitudes			
Event Number	Year	Month	Date	Hour	Minute	Second	Latitude	Longitude	Depth	M_w	M_s	mb	M_s	M_w	ML
3445	2001	8	27	21	43	43.06	39.12	24.2	19.2	4.5	3.2	4	3.2		4.3
3446	2001	9	7	17	57	20.53	39.02	24.18	10.3	4.3	3	4	3	4.3	4
3447	2001	9	10	19	51	36.89	39.03	24.14	8.8	4	2.5				3.6
3448	2001	9	26	1	29	34.33	40.22	25.23	12.5	4.3	2.9	3.9	2.9		4
3449	2001	9	26	6	21	43.62	40.17	25.2	20.5	4.4	3.2				4
3450	2001	9	26	8	15	33.56	40.24	25.18	6	4.2	2.9				3.8
3451	2001	10	2	13	4	9.8	39.1	24.24	9.9	4	2.5				3.6
3452	2001	10	6	7	25	55.4	40.87	20.74	10	4.8	3.9	4.3	3.9		4.4
3453	2001	10	8	4	50	19.75	40.57	23.2	11.4	4.4	3.2				4
3454	2001	10	8	5	32	14.65	40.58	23.15	10	4.4	3.2				4
3455	2001	10	12	22	54	50.21	39.14	24.2	8.5	4.2	2.9				3.8
3456	2001	10	17	2	27	13.39	39.87	26.82	5.9	4.3	3				3.9
3457	2001	10	25	9	36	30.47	39.2	23.81	7	4	2.5				3.6
3458	2001	11	3	11	58	35.12	39.13	24.22	10.3	4.1	2.7				3.7
3459	2001	11	3	17	32	51.94	39.03	24.16	10.6	4.2	2.9				3.8
3460	2001	11	5	12	10	50.11	40.17	24.95	2.9	4	2.5				3.6
3461	2001	12	1	1	54	43.37	41.33	20.49	22.3	4.3	3.3	4.3	3.3	4.3	5
3462	2001	12	3	20	40	18.3	39.5	25.96	10	4	2.5				3.6
3463	2001	12	7	19	44	49.82	39.39	23.78	5.8	5.1	5	4.8	5	5.1	5
3464	2001	12	7	20	28	55.31	39.29	23.64	7.2	4.3	3				3.9
3465	2001	12	8	4	31	34.54	39.34	23.77	11.6	4	2.5				3.6
3466	2001	12	8	5	31	1.4	39.33	23.73	6.9	4	2.5				3.6
3467	2001	12	10	19	19	25.46	39.18	24.21	9.8	4.3	3	3.7	3		4.4
3468	2001	12	11	16	34	2.91	39.02	24.32	11.2	4.8	3.8	4.2	3.8		4.4
3469	2002	1	3	0	17	50.33	39.72	23.03	10.2	4	2.9	4			3.5
3470	2002	1	16	18	24	39.19	41.37	19.79	18	4	2.9	4			4
3471	2002	1	18	12	52	48.64	39.1	24.21	17.7	4	2.5				3.6
3472	2002	2	28	8	37	51.92	40.8	28.14	11.5	4.7	3.6	4.1	3.6		3.4
3473	2002	3	5	5	23	42.96	40.7	25.57	9.1	4.6	3.6	4.3	3.6	4.6	4.3
3474	2002	3	23	2	36	10.46	40.86	27.83	7	4.4	3.3	4	3.3	4.4	3.7
3475	2002	4	5	13	13	58.14	42.11	24.84	3.5	4.6	3.8	4.8	3.8	4.6	4.6
3476	2002	4	6	5	47	9.54	42.05	24.79	21.4	4.4	3.1	4	3.1		3.7
3477	2002	4	6	7	48	47.85	41.96	24.9	7.1	4.1	2.6	3.7	2.6		3.6
3478	2002	4	8	1	20	48.45	42.46	19.77	11.1	4.4	3.5	4.4	3.5	4.4	3.8
3479	2002	4	9	4	26	34.92	42.43	19.76	3.5	4	2.5				3.6
3480	2002	4	10	21	15	11.37	42.43	19.79	5.7	4.1	2.6	3.8		4.1	3.9
3481	2002	4	12	14	55	55.31	40.2	25	9.2	4.5	3.2	3.6	3.2		4
3482	2002	4	24	10	51	49.98	42.45	21.5	2.5	5.6	5.6	5.7	5.6	5.6	5.5
3483	2002	4	24	11	24	21.6	42.45	21.48	1.8	4.6	3.5	4.4		4.6	3.8
3484	2002	4	24	11	33	14.72	42.5	21.57	8	4.1	3.1	4.1			3.7
3485	2002	4	24	16	4	29.09	42.47	21.55	5	4	2.9	4			3.5
3486	2002	4	24	23	37	56.95	42.49	21.56	3.9	4.6	3.5	4.4	3.5		3.9
3487	2002	4	25	3	43	33.82	42.49	21.58	0	4.5	3.3	4.2	3.3		3.9
3488	2002	4	25	7	28	9.16	40.6	20.83	10	4.2	2.7	3.9	2.7	4.2	4.2
3489	2002	4	26	0	21	31.47	42.45	21.55	1	4.6	3.5	4.1	3.5		4.1
3490	2002	4	26	6	31	3.11	42.49	21.59	5	4.5	3.2	4	3.2		3.6
3491	2002	4	29	10	10	51.62	42.49	21.6	2	4.5	3.3	4.2	3.3		3.9
3492	2002	5	2	3	31	29.97	42.43	21.49	3.5	4.1	2.5	3.8	2.5		3.5
3493	2002	5	5	9	22	9.99	40.55	28.3	8	4.4	3.1	3.9	3.1		3.6
3494	2002	5	24	20	42	26.29	44.73	21.65	7.3	4.5	3.8	4.7	3.8	4.5	4.1
3495	2002	5	28	19	45	11.74	42.43	19.79	8	4.4	3.9	4.3	3.9	4.4	3.9
3496	2002	6	14	10	52	53.69	42.47	21.57	10	4	2.9	4			3.3
3497	2002	6	24	17	8	47.51	42.18	20.59	5	4.3	3.3	4.2			3.7
3498	2002	7	9	22	39	15.12	39.34	27.81	1.1	4.7	3.7				4.3
3499	2002	7	13	3	13	32.53	39.24	26	21.4	4	2.5				3.6
3500	2002	7	22	4	51	19.48	39.07	24.26	11	4.4	3.2				4
3501	2002	7	31	4	5	52.8	41.24	23.07	9.2	4.3	2.9	4.1	2.9		4.2
3502	2002	8	2	9	37	19.25	44.72	21.62	16.9	4.2	3.7	4.3	3.7	4.2	4
3503	2002	8	11	21	49	43.53	42.47	21.57	10	4	2.4	3.7	2.4		3.3
3504	2002	8	18	8	33	10.49	42.48	21.66	3	4	2.5				3.6
3505	2002	8	31	14	30	42.86	39.19	24.22	7.5	4.3	3				3.9
3506	2002	9	1	2	39	38.36	39.34	24.08	14.4	4	2.5				3.6
3507	2002	9	2	18	56	1.29	41.23	20.31	23.8	4.4	3.5	4.3			4.3
3508	2002	9	5	2	19	7.24	39.3	20.82	12.2	4.2	2.9				3.8
3509	2002	9	7	4	48	41.08	39.32	24.02	21.4	4.5	3.2	3.8	3.2		4.3
3510	2002	9	18	11	10	9.55	39.09	24.24	13	4.2	2.9				3.8
3511	2002	9	19	12	12	22.33	39.16	20.53	11	4.2	2.9				3.8
3512	2002	9	25	18	46	5.73	41.18	20.28	1.1	4.1	3.1	4.1			2.9
3513	2002	10	8	4	40	47.6	40.01	20.42	22	4.5	3.8	4.6	3.8	4.5	4.5
3514	2002	10	8	9	46	3.35	39.93	20.44	15	4.8	3.9	4	3.9		4.1
3515	2002	10	24	11	0	54.58	39.96	19.73	12	4	2.9	4			3.2
3516	2002	10	24	15	15	37.57	39.98	19.61	10	4.3	3.3	4.2			4.3
3517	2002	10	29	5	52	8.75	39.09	24.24	17.9	4	2.9	4			3.9
3518	2002	11	9	17	1	57.92	41.08	19.83	15.1	4.5	3.2	3.6	3.2		3.8
3519	2002	11	10	6	48	44.97	40.02	25.45	8.3	4.2	2.9				3.8
3520	2002	11	10	8	17	30.71	39.08	24.52	15.8	4.5	3.2	3.6	3.2		4
3521	2002	11	17	18	24	58.61	40.06	19.56	14	5	4.1	4.5	4.1		4.4
3522	2002	11	25	11	58	7.09	39.55	25.22	10	4.1	2.7				3.7
3523	2002	12	23	4	2	36.02	39.08	20.19	55.7	4.3	3.6	4.3	3.6	4.3	4.3
3524	2002	12	31	20	29	33.61	39.13	21.25	10	5.1	4.3	4	4.3		4.4
3525	2003	1	3	5	47	3.1	39.01	23.24	23	4.3	3				3.9
3526	2003	1	25	23	2	11	41.38	20.36	8	4.4	3.2				4

										Homogenized magnitudes		Reported magnitudes			
Event Number	Year	Month	Date	Hour	Minute	Second	Latitude	Longitude	Depth	M_w	M_s	mb	M_s	M_w	ML
3527	2003	1	26	5	13	9.53	42.74	20.15	0	4	2.5				3.6
3528	2003	2	9	18	9	15.3	39.09	24.61	19	4.6	3.6				4.2
3529	2003	2	18	8	2	32.6	41.18	20.19	10	4.1	2.7				3.7
3530	2003	2	20	8	51	57.1	39.5	23.7	28	4.1	3.1	4.1			
3531	2003	2	20	17	33	15.12	40.94	19.9	10	4.2	2.9				3.8
3532	2003	2	21	0	30	44.8	39.12	24.28	34	4.4	3.5	4.3			
3533	2003	2	24	20	22	24.69	39.37	20.47	33	5	4.4	4.8			
3534	2003	3	20	12	25	34.83	40.04	28.82	10	4.1	3.1	4.1			
3535	2003	3	21	15	55	35.66	41.29	20.17	10	4.5	3.4				4.1
3536	2003	3	22	1	18	20.6	39.22	20.81	15	4.2	2.9				3.8
3537	2003	3	27	4	35	40.4	40.41	19.71	15	4.1	3.1	4.1			
3538	2003	5	3	21	3	6.82	41.88	22.97	15	4	2.5				3.6
3539	2003	5	9	22	5	54.6	39.16	27.39	5	4.3	3				3.9
3540	2003	5	13	17	13	24.5	39.82	25.66	18	4	2.5				3.6
3541	2003	5	21	7	44	18.7	39.34	21.56	5	4	2.5				3.6
3542	2003	5	29	11	38	9.33	39.55	20.39	10	4.6	3.8	4.5			
3543	2003	6	9	7	6	39.33	39.89	22.31	17	5.4	4.9				5
3544	2003	6	9	17	44	3.03	40.24	28.02	10	5.5	5.1				5.1
3545	2003	6	9	17	47	5.65	40.25	27.94	15	4.5	3.4				4.1
3546	2003	6	10	1	1	50.48	40.28	25.71	10	4.3	3				3.9
3547	2003	6	12	0	10	40.01	40.18	25.14	20	4.6	3.6				4.2
3548	2003	6	16	5	14	59	39.52	25.97	33	4.2	2.9				3.8
3549	2003	6	22	23	46	20.38	39.03	28.04	7	5	4.2				4.6
3550	2003	6	28	16	24	36.7	39.51	25.82	23	4.1	2.7				3.7
3551	2003	7	3	9	42	48	39.67	25.65	28	4	2.5				3.6
3552	2003	7	5	21	58	31.33	40.4	26.21	12	4.6	3.6				4.2
3553	2003	7	6	19	39	51.03	40.38	26.03	17	4.3	3				3.9
3554	2003	7	6	19	41	8.55	40.39	26.21	14	4.1	2.7				3.7
3555	2003	7	6	20	10	16.45	40.42	26.13	17	5.5	5		5		
3556	2003	7	6	22	5	47.13	40.33	26.06	10	4.3	3.3	4.2			
3557	2003	7	6	22	42	8.7	40.31	25.84	16	4.5	3.7	4.4			
3558	2003	7	9	22	1	58.34	40.41	25.9	13	4.4	3.2				4
3559	2003	7	9	22	31	41.22	40.35	25.93	18	4.9	4.2	4.7			
3560	2003	7	10	1	26	17.94	40.33	26.03	20	4.1	3.1	4.1			
3561	2003	7	10	6	58	47.9	41.11	20.33	12	4	2.5				3.6
3562	2003	7	10	9	1	18.64	40.13	25.41	20	4.4	3.5	4.3			
3563	2003	7	10	13	25	34	40.35	25.96	20	4	2.5				3.6
3564	2003	7	11	23	51	15.6	40.16	25.33	18	4.2	2.9				3.8
3565	2003	7	13	6	32	8.5	40.39	25.92	29	4.3	3				3.9
3566	2003	7	30	20	54	25.09	39.96	23.3	16	4	2.5				3.6
3567	2003	8	9	16	29	52.34	41.72	20.99	10	4	2.5				3.6
3568	2003	8	14	5	26	21.8	39.06	20.55	24	4.2	2.9				3.8
3569	2003	8	14	8	41	39.74	39	20.55	10	5.3	4.7				4.9
3570	2003	8	15	20	34	19.88	41.9	20.68	12	4.4	3.2				4
3571	2003	8	23	14	9	21	40.59	21.01	19	4.4	3.2				4
3572	2003	8	26	7	17	13.23	44.35	21.13	10	4.1	2.7				3.7
3573	2003	8	28	1	16	27.6	39.07	20.6	9	4.5	3.7	4.4			
3574	2003	8	31	7	50	57.2	40.4	25.97	33	4.4	3.2				4
3575	2003	9	28	12	0	25.1	40.08	22.35	28	4	2.5				3.6
3576	2003	10	16	11	28	9.6	43.33	19.95	12	4.5	3.4				4.1
3577	2003	10	20	5	36	32.5	41.2	20.72	15	4.4	3.2				4
3578	2003	10	29	21	15	47.6	40.71	22.83	25	4.8	4	4.6			
3579	2003	11	2	17	15	4.33	40.82	21.02	10	4.5	3.4				4.1
3580	2003	11	9	17	51	12.69	41.99	23.14	10	4	2.5				3.6
3581	2003	11	19	16	7	6.06	41.22	21.3	31	4.4	3.2				4
3582	2003	12	5	3	31	48.72	41.38	19.86	10	4.8	3.9				4.4
3583	2003	12	7	13	41	44.79	39.65	24.29	10	4.5	3.7	4.4			
3584	2003	12	7	15	40	17.98	39.84	20.74	72	4.4	3.5	4.3			
3585	2003	12	17	23	15	17.35	43.09	27.5	34	4.5	3.8	4.4			
3586	2004	1	18	12	43	35.9	39.88	24.4	30	4.2	2.9				3.8
3587	2004	1	27	6	24	5.4	40.14	19.61	19	4.2	2.9				3.8
3588	2004	1	30	10	42	24.5	41.93	19.12	6	4	2.5				3.6
3589	2004	2	4	5	36	11	40.12	19.38	26	4.7	3.7				4.3
3590	2004	2	5	2	51	39.6	40.26	19.58	5	4.2	2.9				3.8
3591	2004	2	8	12	20	59.3	39.92	19.89	11	4	2.5				3.6
3592	2004	2	12	21	50	6.6	39.86	20.35	25	4.4	3.2				4
3593	2004	2	13	0	39	19.5	40.58	20.68	36	4	2.5				3.6
3594	2004	2	18	3	20	53.1	40.11	19.81	13	4.7	3.7				4.3
3595	2004	2	27	6	46	34.6	40.11	19.84	5	4.1	2.7				3.7
3596	2004	3	14	5	0	18.5	41.92	20.38	5	4.3	3				3.9
3597	2004	3	18	1	13	0.6	41.01	22.07	16	4.2	2.9				3.8
3598	2004	3	18	1	57	13.3	40.91	22.19	15	4.1	2.7				3.7
3599	2004	3	20	19	50	2.4	40.51	26.47	16	4	2.5				3.6
3600	2004	3	21	3	18	53.4	41.64	19.7	33	5.1	4.4				4.7
3601	2004	3	27	0	0	39.1	40.31	26.8	10	4.1	2.7				3.7
3602	2004	3	27	10	39	24.6	40.5	23.8	5	4.2	2.9				3.8
3603	2004	3	30	8	7	34.4	39.28	24.13	38	4.6	3.6				4.2
3604	2004	4	4	1	9	43.8	39.4	20.52	5	4.1	2.7				3.7
3605	2004	4	7	1	32	28.3	40.65	20.38	90	5.1	4.4				4.7
3606	2004	4	19	15	27	12.6	40.73	27.9	19	4.7	3.7				4.3
3607	2004	4	21	1	5	0.4	39.49	26.42	5	4.2	2.9				3.8
3608	2004	4	26	11	58	12.9	41.92	23.22	23	4	2.5				3.6

										Homogenized magnitudes		Reported magnitudes			
Event Number	Year	Month	Date	Hour	Minute	Second	Latitude	Longitude	Depth	M_w	M_s	mb	M_s	M_w	ML
3609	2004	4	26	13	22	21.5	41.95	23.19	23	4.2	2.9				3.8
3610	2004	5	20	17	15	24.6	41.03	19.23	45	4.2	2.9				3.8
3611	2004	5	24	23	54	56.5	39.39	20.57	6	4.3	3				3.9
3612	2004	5	25	0	22	24.4	41.57	19.9	23	4	2.5				3.6
3613	2004	6	5	4	48	8.1	40.92	20.86	7	4	2.5				3.6
3614	2004	6	11	20	58	59.3	39.54	28.03	6	4	2.5				3.6
3615	2004	6	13	6	48	33.7	40.33	25.71	27	4.2	2.9				3.8
3616	2004	6	14	10	49	36.3	40.15	19.7	20	4	2.5				3.6
3617	2004	6	15	12	2	38.5	40.34	25.77	21	4.9	4.1				4.5
3618	2004	6	17	12	49	48.3	40.45	26.05	45	4	2.5				3.6
3619	2004	6	17	21	35	20.2	40.28	21.23	8	4.3	3				3.9
3620	2004	6	19	21	27	26.7	39.81	24.66	14	4.2	2.9				3.8
3621	2004	6	19	21	44	48.6	41.51	20.03	14	4.6	3.6				4.2
3622	2004	6	25	4	30	45	39.71	20.87	5	4.1	2.7				3.7
3623	2004	6	25	9	0	15.3	39.69	20.94	5	4.1	2.7				3.7
3624	2004	6	27	15	31	46.6	40.8	25.86	5	4.7	3.7				4.3
3625	2004	6	27	22	37	18.7	40.8	25.81	9	4.4	3.2				4
3626	2004	6	29	10	15	13.8	40.75	25.77	5	4.3	3				3.9
3627	2004	6	29	13	7	47.9	40.87	26.02	23	4	2.5				3.6
3628	2004	6	30	20	8	33.4	40.82	25.85	13	4.1	2.7				3.7
3629	2004	6	30	23	20	28.9	41.09	26.1	32	4.1	2.7				3.7
3630	2004	7	1	10	49	59.8	40.89	26.03	5	4.1	2.7				3.7
3631	2004	7	1	15	6	19.4	40.92	25.99	23	4	2.5				3.6
3632	2004	7	12	11	26	29	39.31	20.33	5	4.3	3				3.9
3633	2004	7	15	0	40	35.9	40.67	23.44	22	4.1	2.7				3.7
3634	2004	7	15	7	37	45.9	39.92	23.98	30	4.2	2.9				3.8
3635	2004	7	24	21	28	35.8	39.54	23.81	15	4	2.5				3.6
3636	2004	7	25	22	35	41.5	39.59	23.7	29	4.2	2.9				3.8
3637	2004	7	26	8	26	11.8	40.65	20.95	10	4.5	3.4				4.1
3638	2004	8	7	3	51	45.7	39.4	20.5	5	4.1	2.7				3.7
3639	2004	8	7	23	11	30.6	41.25	20.3	5	4	2.5				3.6
3640	2004	8	13	15	13	44.4	40.84	26.4	29	4.3	3				3.9
3641	2004	8	21	12	54	3.2	40.82	21.04	18	4.6	3.6				4.2
3642	2004	8	25	10	34	13.5	39.4	27.86	13	4	2.5				3.6
3643	2004	8	25	22	41	18.7	41.34	19.75	2	4.2	2.9				3.8
3644	2004	8	25	23	26	32.7	39.37	20.48	10	4	2.5				3.6
3645	2004	8	28	22	16	47.2	41.34	19.46	37	4.8	3.9				4.4
3646	2004	9	9	9	33	21.7	41.99	20.08	36	4.2	2.9				3.8
3647	2004	9	10	17	46	10.9	41.8	24.76	26	4.3	3				3.9
3648	2004	9	12	10	42	44.2	39.16	20.89	13	4	2.5				3.6
3649	2004	9	12	16	41	18.9	39.12	20.59	4	4.5	3.4				4.1
3650	2004	9	14	21	37	20.6	39.64	20.37	7	4	2.5				3.6
3651	2004	9	16	1	24	16.8	39.8	20.65	24	4.7	3.7				4.3
3652	2004	9	17	16	45	9.9	39.52	24.04	39	4.1	2.7				3.7
3653	2004	9	22	3	51	1.7	40.48	23.42	15	4	2.5				3.6
3654	2004	10	8	0	47	51.7	41.42	21.1	24	5	4.2				4.6
3655	2004	10	10	12	58	24.3	39.11	23.29	20	4.1	2.7				3.7
3656	2004	10	26	2	33	38.2	39.66	20.42	19	4	2.5				3.6
3657	2004	10	28	0	46	34.7	40.18	21.82	12	4.1	2.7				3.7
3658	2004	10	28	17	15	33.5	39.08	26.97	4	4.3	3				3.9
3659	2004	10	29	23	30	34.8	41.17	19.46	29	4.1	2.7				3.7
3660	2004	11	5	17	30	19.4	39.23	27.97	5	4.9	4.1				4.5
3661	2004	11	8	4	6	55.7	40.25	19.38	7	4.1	2.7				3.7
3662	2004	11	10	22	39	57.5	41.42	20.31	5	4	2.5				3.6
3663	2004	11	21	20	49	46.4	41.11	19.54	39	4.2	2.9				3.8
3664	2004	11	23	2	26	12.5	40.35	20.6	11	5.8	5.6				5.4
3665	2004	11	23	2	59	17.6	40.2	20.67	11	4.5	3.4				4.1
3666	2004	11	23	8	9	27.8	40.22	20.71	3	4	2.5				3.6
3667	2004	11	23	16	1	2.5	40.36	21.28	22	4	2.5				3.6
3668	2004	11	27	23	57	36	41.25	20.15	7	4.2	2.9				3.8
3669	2004	11	30	10	51	34.8	39.38	20.55	9	4	2.5				3.6
3670	2004	12	2	15	51	49.1	39.2	27.94	30	4.7	3.7				4.3
3671	2004	12	3	10	57	19	39.24	20.75	10	4	2.5				3.6
3672	2004	12	4	19	36	24.7	39.64	19.92	8	4	2.5				3.6
3673	2004	12	5	17	10	37.4	39.28	25.47	30	4	2.5				3.6
3674	2004	12	7	14	32	45.9	39.94	19.67	15	5	4.2				4.6
3675	2004	12	7	14	59	1.2	39.76	19.65	21	4.5	3.4				4.1
3676	2004	12	11	21	3	19	39.24	21.68	15	4.6	3.6				4.2
3677	2004	12	14	21	35	27.5	40.3	20.66	5	4.1	2.7				3.7
3678	2004	12	15	4	27	13.5	40.77	27.78	10	4.3	3				3.9
3679	2004	12	20	13	32	5.1	40.35	26.37	10	4	2.5				3.6
3680	2004	12	24	7	35	5.5	39.38	24.82	25	4	2.5				3.6
3681	2004	12	30	7	35	35.5	39.12	22.29	98	4.7	3.7				4.3

Appendix 4 Hypocentres considered for *whole* and *part process* hazard estimates

This Appendix provides 4-dimensional (latitude, longitude, depth and magnitude) plots of the hypocentral distributions in the 2° half-width area around each urban centre for which seismic hazard has been considered in the assessment.

Seismicity shown is that considered to estimate hazard forecasts for (a) *whole process* (cumulative frequency-magnitude and magnitude density distributions and cumulative strain energy release statistics) and (b) *part process* (Gumbel's extreme values theory and earthquake perceptibility) hazard estimates.

Green sphere's represent seismicity h <10 km focal depth

Yellow sphere's represent seismicity 10 km $\leq h \leq$ 20 km focal depth

Grey sphere's represent seismicity 20 km $< h <$ 30 km focal depth

Red sphere's represent seismicity $h \geq$ 30 km focal depth

The most significant depth range to appreciate is that which represents seismicity in the focal depth range of 10 km $\leq h \leq$ 20 km. This encompasses seismicity considered to contribute the majority of the extreme seismic hazard. Consequently, these are the maximum and minimum *scenario* focal depths considered in all earthquake perceptibility and integrated perceptibility plots in Chapter 6 and Appendices 20 to 31 (inc).

Due the region's seismicity predominantly being shallow focal depth (<60 km), each hypocentre plot covers the top 100 km. There may be small numbers of earthquakes at focal depths greater than this depth. Epicentres in all plots are drawn using the sizing scale.

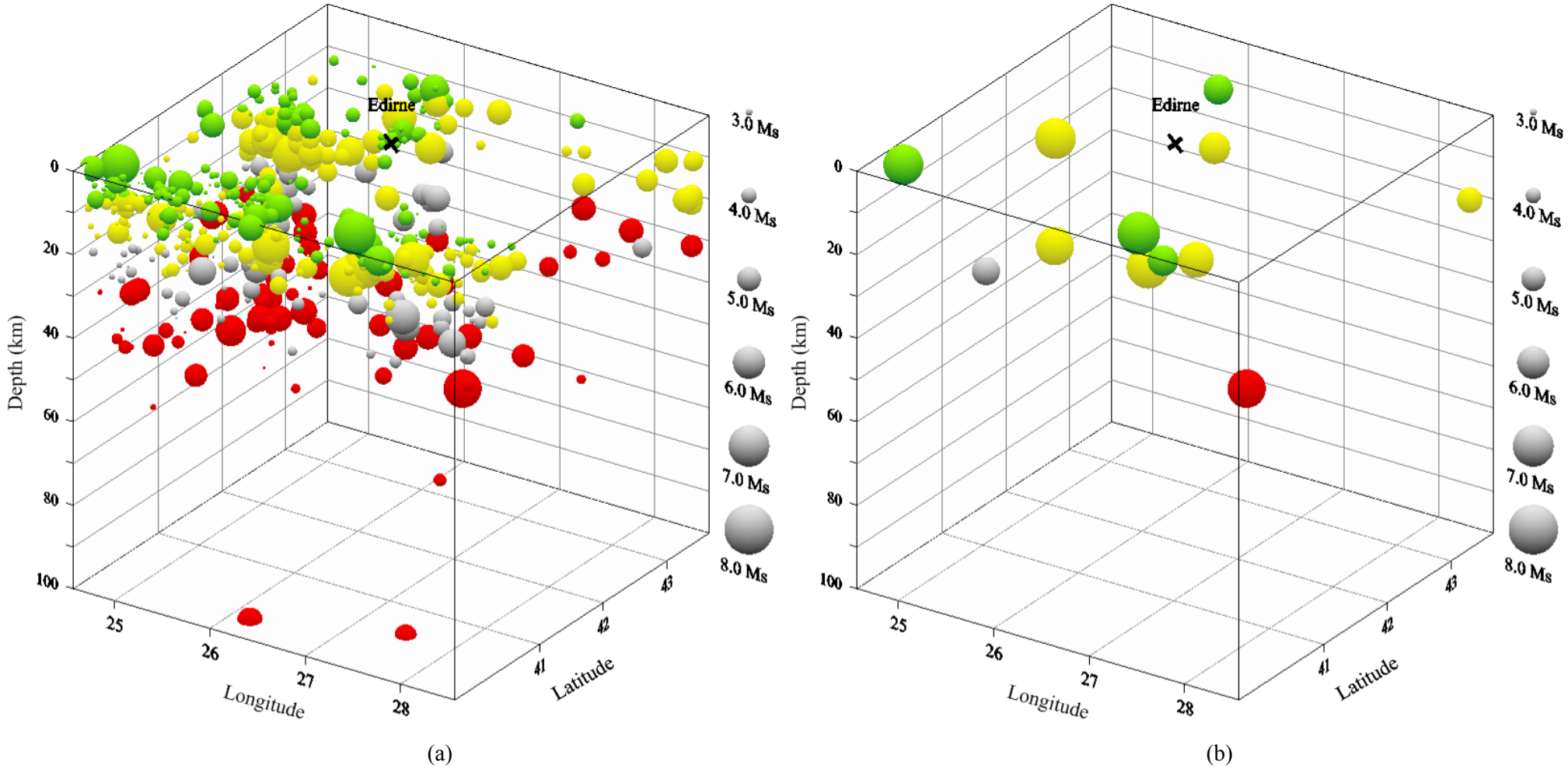

(a) (b)

Site-specific hypocentral distributions contributing to (a) *whole process* and (b) *part process* seismic hazard statistics for Edirne

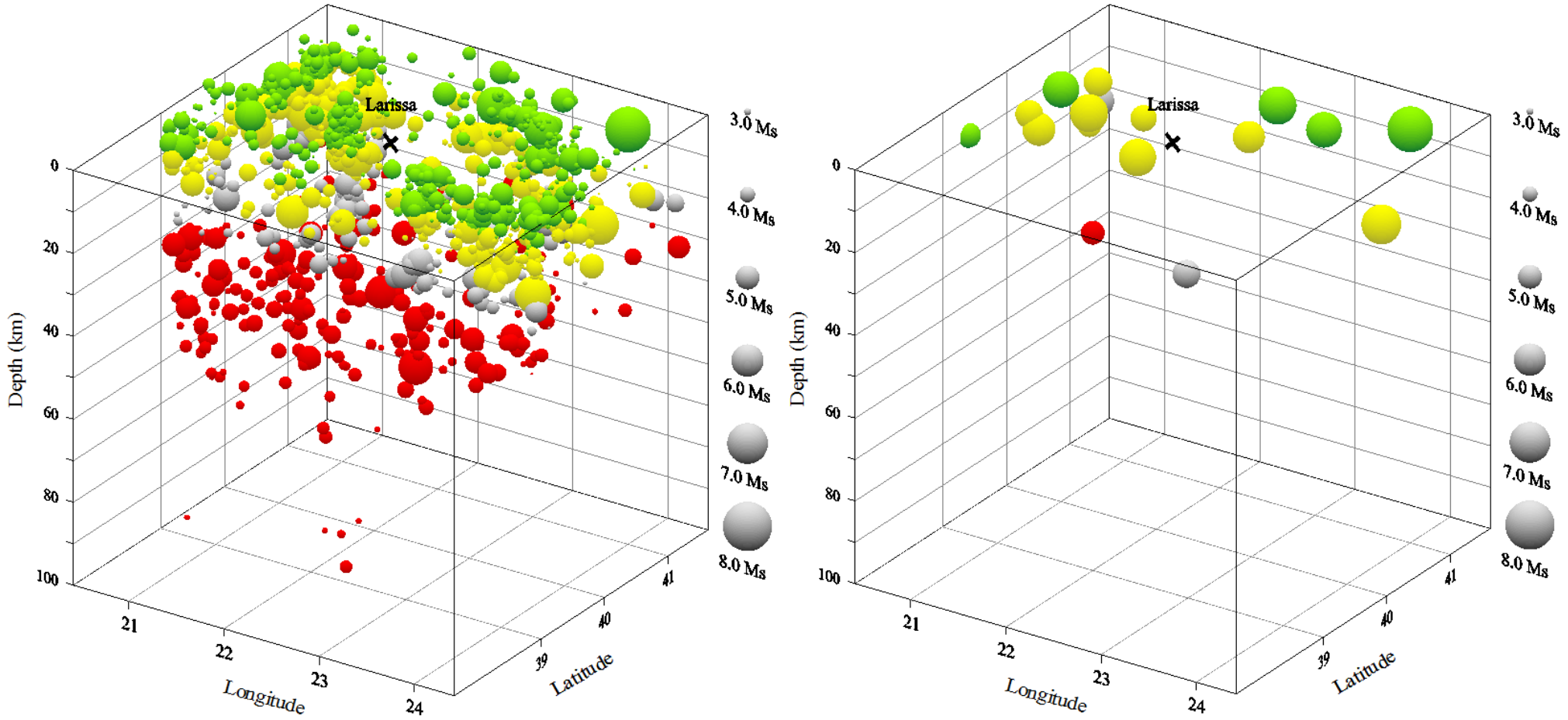

(a) (b)

Site-specific hypocentral distributions contributing to (a) *whole process* and (b) *part process* seismic hazard statistics for Larissa

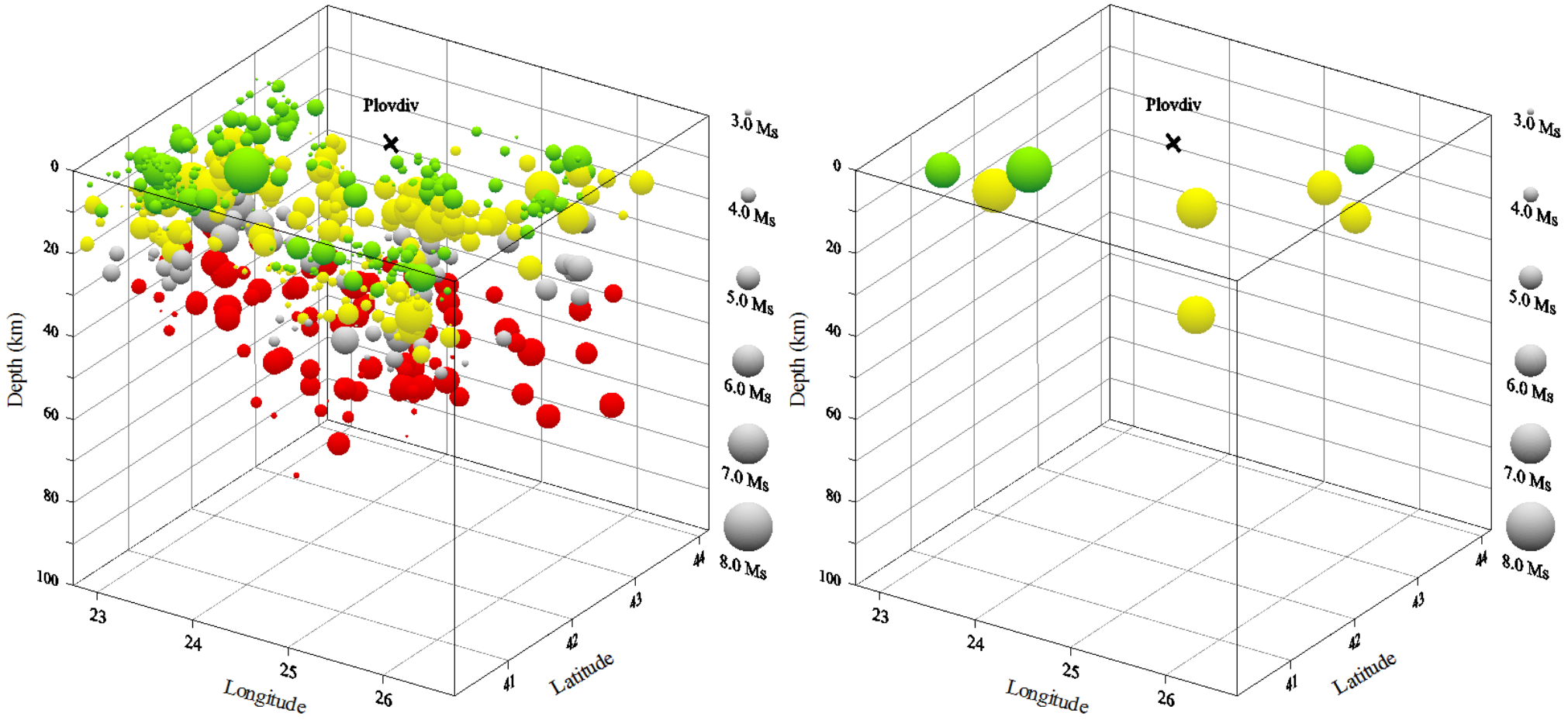

(a) (b)

Site-specific hypocentral distributions contributing to (a) *whole process* and (b) *part process* seismic hazard statistics for Plovdiv

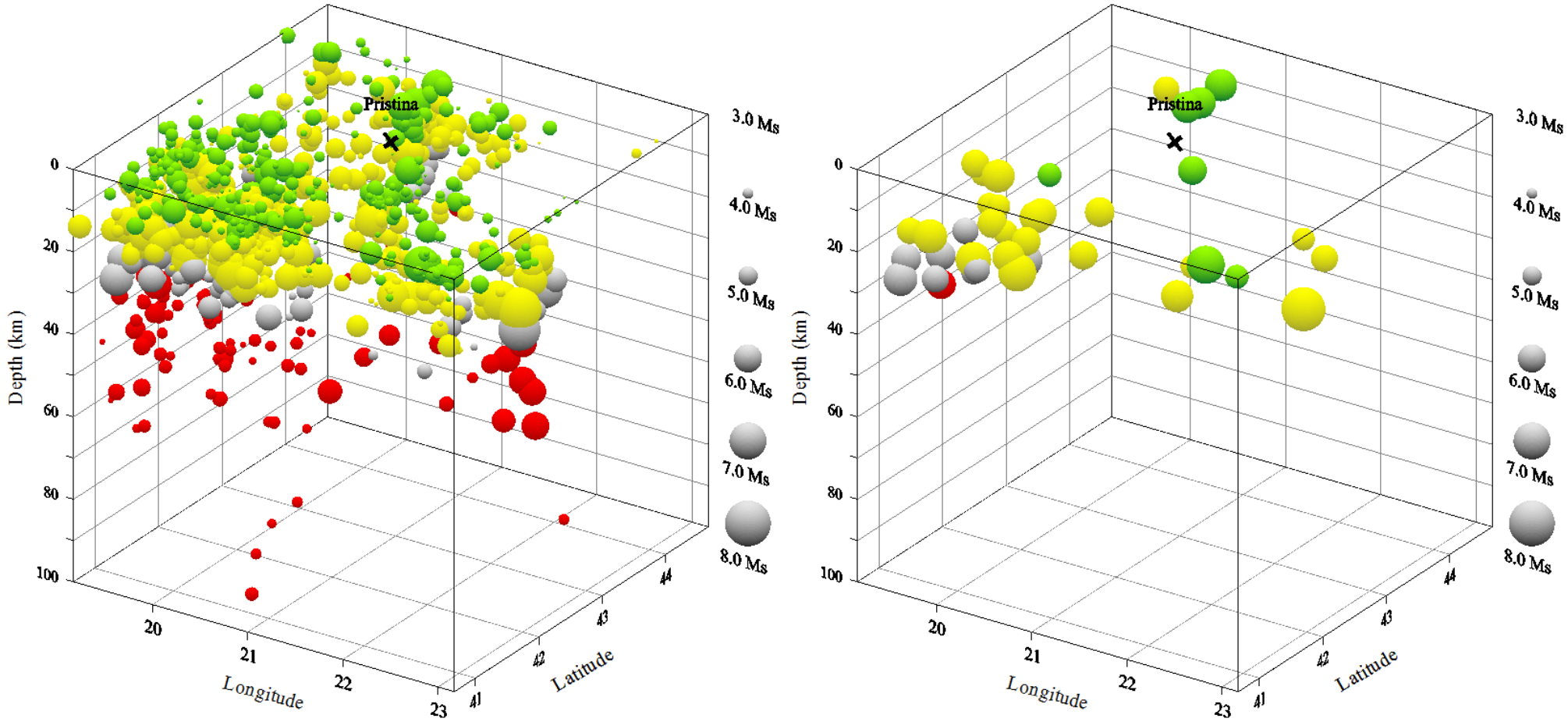

(a) (b)

Site-specific hypocentral distributions contributing to (a) *whole process* and (b) *part process* seismic hazard statistics for Pristina

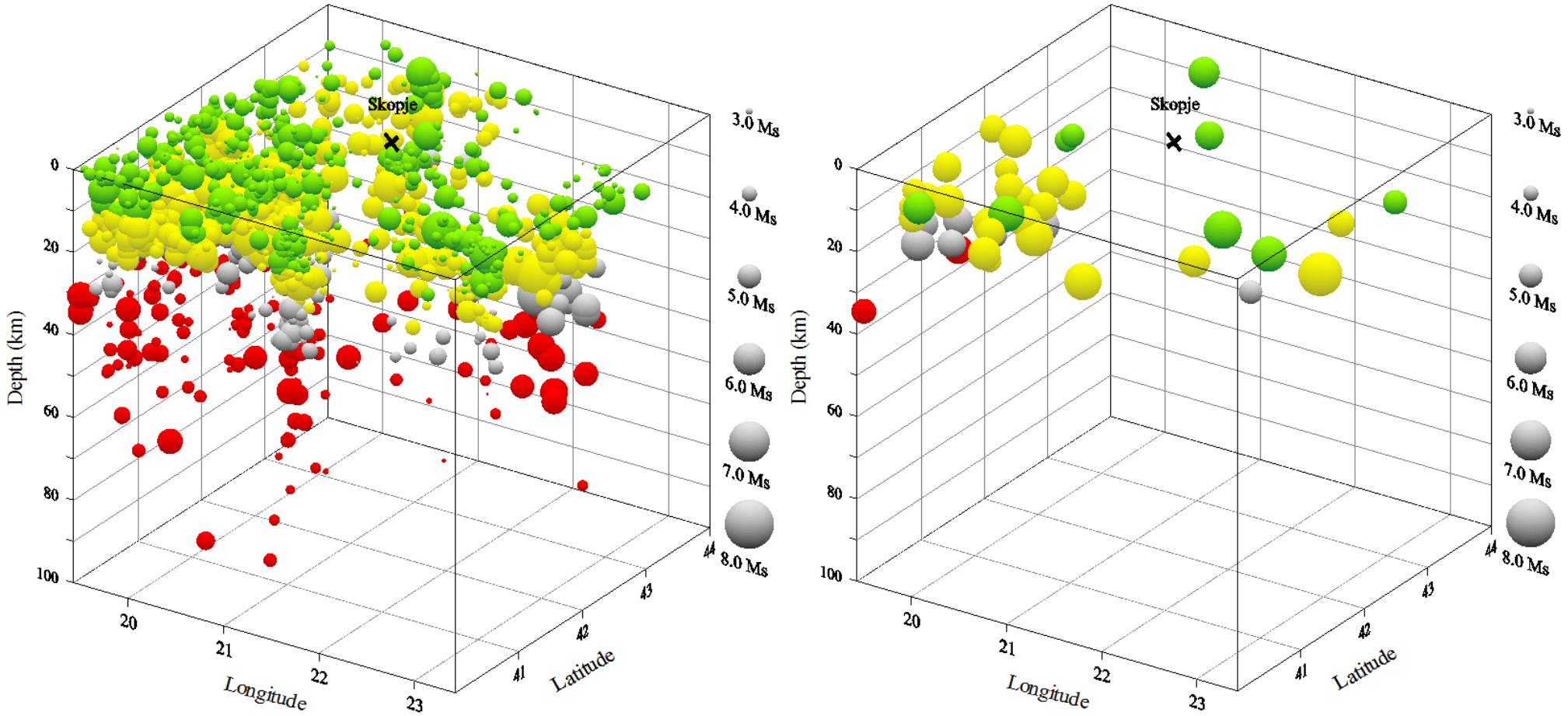

(a) (b)

Site-specific hypocentral distributions contributing to (a) *whole process* and (b) *part process* seismic hazard statistics for Skopje

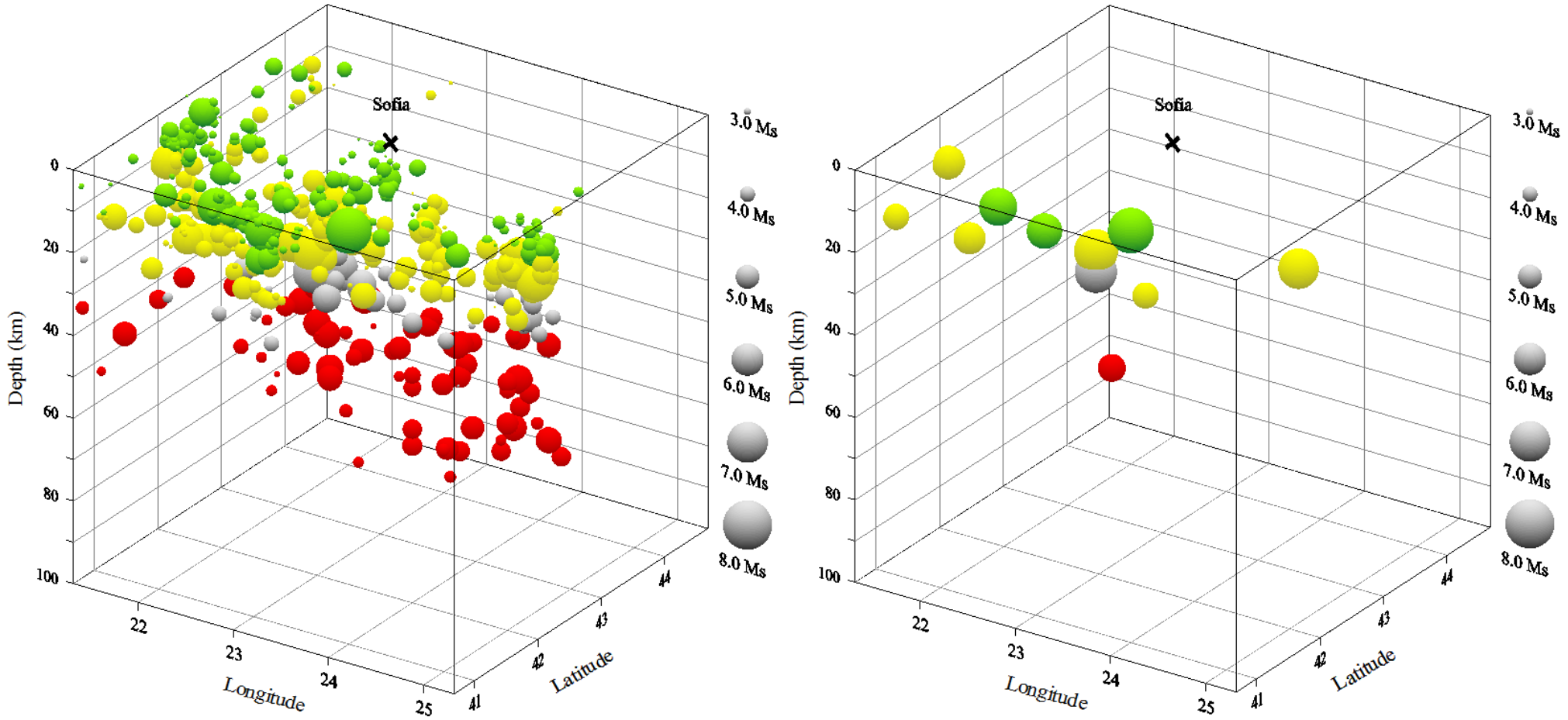

(a) (b)

Site-specific hypocentral distributions contributing to (a) *whole process* and (b) *part process* seismic hazard statistics for Sofia

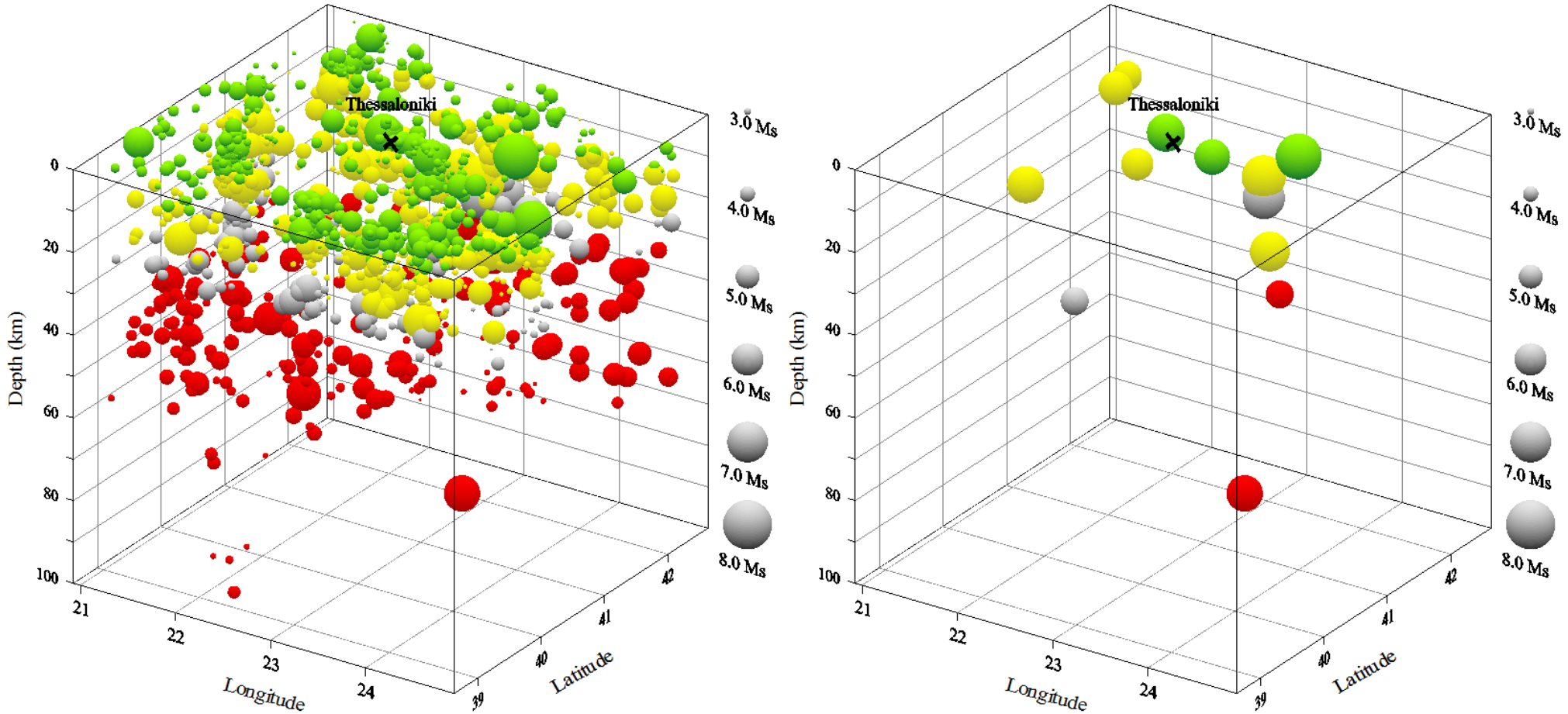

(a) (b)

Site-specific hypocentral distributions contributing to (a) *whole process* and (b) *part process* seismic hazard statistics for Thessaloniki

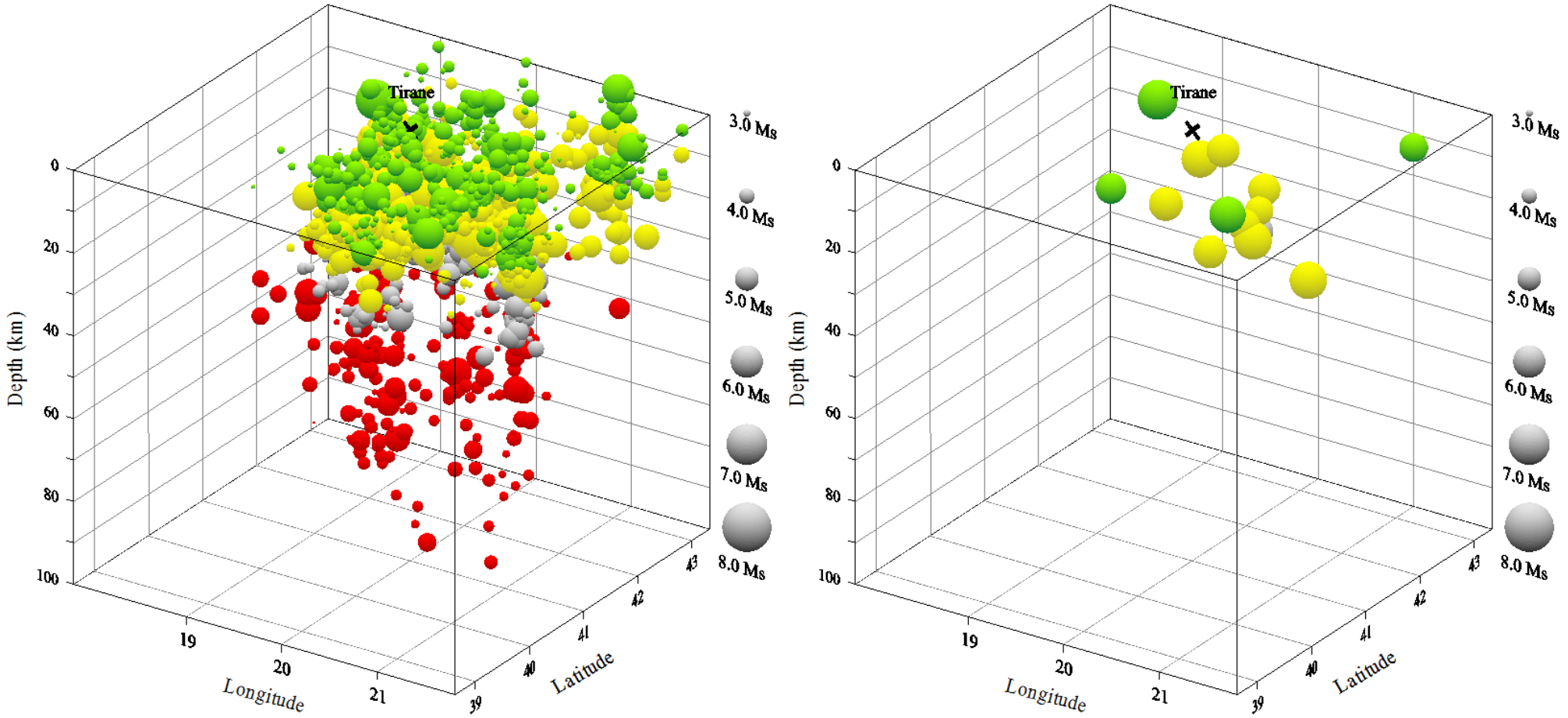

(a) (b)

Site-specific hypocentral distributions contributing to (a) *whole process* and (b) *part process* seismic hazard statistics for Tirane

Appendix 5: Regional cellular $G^{(III)}$ magnitude recurrence estimates

Parameters (ω, μ, λ) and their associated uncertainties of a $G^{(III)}$ distribution for each cell used to contour magnitude hazard over the catalogued region. M_M is the maximum observed magnitude and m(1) is the annual modal [or most probable] maximum event in each cell of analysis. $M_{50,}$ M_{100} and M_{200} are the modal maximum magnitudes expected in 50-, 100- and 200-year time intervals respectively. M_{P50}, M_{P100} and M_{P200} are the magnitudes expected to be extremes with 90% probability of non-exceedance in the 50-, 100- and 200-year time intervals (a 1 in 10 chance of exceedance). σ_M and σ_{MP} are the uncertainties in these forecasts. Forecasts were obtained using earthquake data of 4-year extreme intervals, $M_s \geq 5.5$ and time interval 1900 to 2004. $\sigma^2_{\omega\mu}$, $\sigma^2_{\omega\lambda}$ and $\sigma^2_{\mu\lambda}$ are the off-diagonal elements of the covariance (error) matrix, ε.

Lat	Lon	ω	σ_ω	μ	σ_μ	λ	σ_λ	$\sigma^2_{\omega\mu}$	$\sigma^2_{\omega\lambda}$	$\sigma^2_{\mu\lambda}$	M_M	M_A	M_{50}	M_{100}	M_{200}	σ_M	M_{p50}	M_{p100}	M_{p200}	σ_{Mp}
39.0	19.0	7.71	2.97	5.13	0.54	0.31	0.62	1.19	-1.81	-0.28	7.0	5.41	7.03	7.16	7.27	2.37	7.33	7.41	7.47	2.61
39.0	19.5	7.84	3.54	5.22	0.53	0.28	0.63	1.40	-2.21	-0.28	7.0	5.45	7.05	7.19	7.30	2.60	7.38	7.46	7.53	3.00
39.0	20.0	7.42	1.77	5.26	0.47	0.40	0.63	0.56	-1.08	-0.24	7.0	5.66	7.06	7.15	7.21	1.68	7.24	7.29	7.32	1.65
39.0	20.5	7.42	1.77	5.26	0.47	0.40	0.63	0.56	-1.08	-0.24	7.0	5.66	7.06	7.15	7.21	1.68	7.24	7.29	7.32	1.65
39.0	21.0	7.32	1.43	5.34	0.39	0.44	0.61	0.34	-0.85	-0.18	7.0	5.78	7.04	7.11	7.17	1.40	7.18	7.22	7.25	1.36
39.0	21.5	7.20	1.13	5.42	0.33	0.49	0.61	0.20	-0.66	-0.14	7.0	5.92	7.01	7.07	7.11	1.15	7.12	7.14	7.16	1.09
39.0	22.0	7.13	0.97	5.10	0.68	0.61	0.74	0.44	-0.67	-0.43	7.0	5.97	7.02	7.05	7.08	1.27	7.08	7.09	7.10	0.95
39.0	22.5	6.94	0.64	4.96	0.80	0.81	0.84	0.32	-0.49	-0.58	6.9	6.43	6.92	6.93	6.94	1.02	6.93	6.94	6.94	0.64
39.0	24.5	7.36	0.88	3.53	2.28	0.78	0.77	1.52	-0.62	-1.65	7.2	6.19	7.31	7.33	7.34	1.93	7.33	7.34	7.35	0.89
39.0	25.0	7.06	0.56	2.69	3.52	0.76	0.96	1.40	-0.47	-3.24	7.2	5.56	6.99	7.02	7.04	1.74	7.02	7.04	7.05	0.58
39.0	25.5	7.08	0.49	0.22	7.20	0.90	1.08	2.43	-0.43	-7.57	7.3	6.17	7.05	7.06	7.07	2.25	7.05	7.06	7.07	0.51
39.0	26.0	7.15	0.49	2.23	4.36	0.84	1.04	1.46	-0.43	-4.36	7.3	6.13	7.11	7.13	7.14	1.76	7.12	7.14	7.14	0.50
39.0	26.5	7.05	0.47	-0.19	7.68	0.92	1.09	2.49	-0.42	-8.15	7.3	6.31	7.03	7.04	7.04	2.28	7.02	7.03	7.04	0.49
39.0	27.0	7.22	0.58	1.36	5.31	0.81	0.96	2.20	-0.47	-4.90	7.3	5.70	7.16	7.19	7.20	2.15	7.18	7.20	7.21	0.60
39.0	27.5	7.62	1.05	3.27	2.84	0.73	0.77	2.38	-0.76	-2.09	7.3	5.95	7.52	7.56	7.58	2.37	7.57	7.59	7.60	1.07
39.0	28.0	7.62	1.05	3.27	2.84	0.73	0.77	2.38	-0.76	-2.09	7.3	5.95	7.52	7.56	7.58	2.37	7.57	7.59	7.60	1.07
39.5	19.0	8.48	6.55	5.45	0.29	0.18	0.53	1.21	-3.47	-0.11	7.0	5.56	7.05	7.22	7.37	3.21	7.50	7.61	7.72	4.51
39.5	19.5	7.76	3.22	5.46	0.25	0.26	0.53	0.44	-1.69	-0.08	7.0	5.63	6.98	7.11	7.22	2.09	7.29	7.37	7.43	2.61
39.5	20.0	7.83	3.90	5.50	0.25	0.23	0.55	0.53	-2.13	-0.09	7.0	5.64	6.95	7.08	7.20	2.33	7.28	7.36	7.43	3.02
39.5	20.5	7.37	1.41	5.50	0.26	0.41	0.55	0.17	-0.74	-0.09	7.0	5.87	7.07	7.15	7.20	1.26	7.22	7.26	7.29	1.31
39.5	21.0	7.30	1.22	5.57	0.22	0.44	0.53	0.10	-0.62	-0.06	7.0	5.95	7.05	7.12	7.16	1.10	7.18	7.21	7.23	1.14
39.5	21.5	7.22	1.04	5.65	0.19	0.47	0.53	0.04	-0.52	-0.04	7.0	6.04	7.03	7.08	7.12	0.94	7.13	7.15	7.17	0.98
39.5	22.0	7.12	0.85	5.42	0.34	0.59	0.63	0.14	-0.50	-0.15	7.0	6.12	7.02	7.06	7.08	0.94	7.08	7.09	7.10	0.83
39.5	22.5	8.16	2.37	5.35	0.37	0.33	0.47	0.57	-1.08	-0.13	7.6	5.69	7.47	7.61	7.72	1.89	7.78	7.86	7.92	2.10

Appendix 5. Continued.

Lat	Lon	ω	σ_ω	μ	σ_μ	λ	σ_λ	$\sigma^2_{\omega\mu}$	$\sigma^2_{\omega\lambda}$	$\sigma^2_{\mu\lambda}$	M_M	M_A	M_{50}	M_{100}	M_{200}	σ_M	M_{p50}	M_{p100}	M_{p200}	σ_{Mp}
39.5	23.0	7.73	1.20	4.04	2.62	0.67	0.86	2.53	-0.97	-2.14	7.6	5.99	7.61	7.65	7.68	2.46	7.67	7.70	7.71	1.22
39.5	23.5	7.74	1.03	3.72	2.88	0.74	0.84	2.36	-0.81	-2.31	7.6	6.26	7.66	7.69	7.71	2.36	7.70	7.72	7.73	1.05
39.5	24.0	7.77	0.89	2.66	3.24	0.82	0.72	2.23	-0.59	-2.23	7.6	6.54	7.72	7.74	7.75	2.27	7.74	7.75	7.76	0.90
39.5	24.5	8.01	1.23	3.50	1.86	0.63	0.58	1.81	-0.67	-1.00	7.6	5.57	7.80	7.88	7.92	2.15	7.92	7.95	7.97	1.23
39.5	25.0	7.62	0.65	2.59	2.97	0.98	0.72	1.40	-0.42	-2.04	7.6	7.52	7.62	7.62	7.62	1.79	7.61	7.61	7.62	0.65
39.5	25.5	7.29	0.48	-0.47	7.29	0.93	0.97	2.44	-0.38	-6.85	7.6	6.59	7.27	7.28	7.29	2.26	7.27	7.28	7.29	0.50
39.5	26.0	7.38	0.49	1.77	4.34	0.87	0.91	1.46	-0.37	-3.79	7.6	6.47	7.35	7.37	7.37	1.77	7.36	7.37	7.37	0.50
39.5	26.5	7.05	0.47	-0.19	7.68	0.92	1.09	2.49	-0.42	-8.15	7.3	6.31	7.03	7.04	7.04	2.28	7.02	7.03	7.04	0.49
39.5	27.0	7.22	0.58	1.36	5.31	0.81	0.96	2.20	-0.47	-4.90	7.3	5.70	7.16	7.19	7.20	2.15	7.18	7.20	7.21	0.60
39.5	27.5	7.62	1.05	3.27	2.84	0.73	0.77	2.38	-0.76	-2.09	7.3	5.95	7.52	7.56	7.58	2.37	7.57	7.59	7.60	1.07
39.5	28.0	7.62	1.05	3.27	2.84	0.73	0.77	2.38	-0.76	-2.09	7.3	5.95	7.52	7.56	7.58	2.37	7.57	7.59	7.60	1.07
40.0	19.0	8.56	7.69	5.51	0.29	0.17	0.56	1.42	-4.27	-0.11	7.0	5.60	7.03	7.20	7.35	3.49	7.48	7.60	7.71	5.05
40.0	19.5	7.72	3.24	5.51	0.25	0.26	0.55	0.44	-1.77	-0.09	7.0	5.67	6.97	7.09	7.19	2.10	7.26	7.34	7.40	2.62
40.0	20.0	8.09	4.75	5.56	0.25	0.21	0.54	0.66	-2.55	-0.09	7.0	5.68	7.03	7.18	7.30	2.60	7.40	7.49	7.57	3.50
40.0	20.5	7.42	1.68	5.58	0.26	0.37	0.57	0.21	-0.94	-0.09	7.0	5.87	7.06	7.14	7.20	1.41	7.23	7.27	7.31	1.53
40.0	21.0	7.43	1.37	5.62	0.22	0.41	0.52	0.11	-0.69	-0.06	7.0	5.97	7.13	7.20	7.26	1.19	7.28	7.32	7.34	1.27
40.0	21.5	8.17	3.26	5.70	0.19	0.24	0.44	0.21	-1.41	-0.04	7.4	5.86	7.27	7.41	7.52	1.97	7.61	7.70	7.77	2.54
40.0	22.0	8.03	2.42	5.56	0.26	0.30	0.46	0.32	-1.09	-0.07	7.4	5.81	7.35	7.48	7.58	1.77	7.65	7.72	7.78	2.07
40.0	22.5	8.34	2.12	5.33	0.37	0.35	0.42	0.51	-0.88	-0.12	7.6	5.75	7.68	7.82	7.94	1.77	7.99	8.07	8.13	1.90
40.0	23.0	7.69	0.77	3.78	2.52	0.86	0.82	1.45	-0.57	-1.94	7.6	6.96	7.66	7.67	7.68	1.86	7.67	7.68	7.68	0.78
40.0	23.5	7.67	0.65	3.31	2.96	0.98	0.83	1.40	-0.48	-2.34	7.6	7.56	7.66	7.67	7.67	1.80	7.66	7.66	7.66	0.66
40.0	24.0	7.70	0.62	2.42	3.11	0.98	0.72	1.40	-0.39	-2.12	7.6	7.60	7.70	7.70	7.70	1.78	7.69	7.69	7.70	0.63
40.0	24.5	7.86	0.79	3.35	1.77	0.80	0.56	1.02	-0.41	-0.93	7.6	6.62	7.81	7.83	7.85	1.61	7.83	7.85	7.85	0.79

Appendix 5. Continued.

Lat	Lon	ω	σ_ω	μ	σ_μ	λ	σ_λ	$\sigma^2_{\omega\mu}$	$\sigma^2_{\omega\lambda}$	$\sigma^2_{\mu\lambda}$	M_M	M_A	M_{50}	M_{100}	M_{200}	σ_M	M_{p50}	M_{p100}	M_{p200}	σ_{Mp}
40.0	25.0	7.57	0.56	2.89	2.41	0.82	0.70	0.92	-0.34	-1.60	7.6	6.40	7.52	7.54	7.55	1.45	7.54	7.55	7.56	0.56
40.0	25.5	7.29	0.48	-0.47	7.29	0.93	0.97	2.44	-0.38	-6.85	7.6	6.59	7.27	7.28	7.29	2.26	7.27	7.28	7.29	0.50
40.0	26.0	7.38	0.49	1.77	4.34	0.87	0.91	1.46	-0.37	-3.79	7.6	6.47	7.35	7.37	7.37	1.77	7.36	7.37	7.37	0.50
40.0	26.5	7.05	0.47	-0.19	7.68	0.92	1.09	2.49	-0.42	-8.15	7.3	6.31	7.03	7.04	7.04	2.28	7.02	7.03	7.04	0.49
40.0	27.0	7.22	0.58	1.36	5.31	0.81	0.96	2.20	-0.47	-4.90	7.3	5.70	7.16	7.19	7.20	2.15	7.18	7.20	7.21	0.60
40.0	27.5	7.62	1.05	3.27	2.84	0.73	0.77	2.38	-0.76	-2.09	7.3	5.95	7.52	7.56	7.58	2.37	7.57	7.59	7.60	1.07
40.0	28.0	7.62	1.05	3.27	2.84	0.73	0.77	2.38	-0.76	-2.09	7.3	5.95	7.52	7.56	7.58	2.37	7.57	7.59	7.60	1.07
40.5	19.0	8.28	4.49	5.61	0.18	0.20	0.45	0.31	-2.01	-0.04	7.0	5.73	7.13	7.28	7.41	2.36	7.52	7.62	7.70	3.23
40.5	19.5	8.03	4.19	5.64	0.16	0.20	0.47	0.18	-1.94	-0.03	7.0	5.75	7.00	7.13	7.25	2.21	7.35	7.44	7.51	3.02
40.5	20.0	7.97	3.77	5.70	0.15	0.21	0.45	0.07	-1.67	-0.01	7.0	5.81	7.01	7.14	7.25	2.02	7.34	7.43	7.50	2.75
40.5	20.5	7.59	1.63	5.74	0.14	0.33	0.43	0.01	-0.67	-0.01	7.0	5.97	7.15	7.24	7.31	1.20	7.35	7.40	7.44	1.42
40.5	21.0	7.48	1.27	5.77	0.14	0.39	0.43	0.00	-0.53	-0.01	7.0	6.06	7.17	7.24	7.29	1.01	7.32	7.36	7.39	1.15
40.5	21.5	8.25	3.76	5.76	0.15	0.21	0.41	0.07	-1.52	-0.01	7.4	5.88	7.20	7.34	7.47	2.01	7.56	7.66	7.74	2.74
40.5	22.0	8.17	2.89	5.59	0.22	0.27	0.43	0.28	-1.23	-0.05	7.4	5.79	7.33	7.47	7.59	1.90	7.67	7.75	7.82	2.36
40.5	22.5	8.34	2.12	5.33	0.37	0.35	0.42	0.51	-0.88	-0.12	7.6	5.75	7.68	7.82	7.94	1.77	7.99	8.07	8.13	1.90
40.5	23.0	7.84	0.94	4.64	0.89	0.65	0.54	0.59	-0.47	-0.42	7.6	6.20	7.71	7.76	7.79	1.37	7.78	7.80	7.82	0.93
40.5	23.5	7.57	0.57	3.11	2.36	0.80	0.73	0.92	-0.36	-1.61	7.6	6.34	7.51	7.54	7.55	1.45	7.53	7.55	7.56	0.57
40.5	24.0	7.76	0.65	3.00	2.07	0.93	0.61	0.95	-0.35	-1.17	7.6	7.37	7.75	7.76	7.76	1.52	7.75	7.75	7.76	0.65
40.5	24.5	7.86	0.75	4.13	0.99	0.75	0.49	0.51	-0.34	-0.43	7.6	6.54	7.79	7.82	7.84	1.23	7.83	7.84	7.85	0.75
40.5	25.0	7.60	0.52	3.88	1.26	0.81	0.60	0.42	-0.27	-0.68	7.6	6.65	7.56	7.57	7.58	1.04	7.57	7.58	7.59	0.53
40.5	25.5	7.38	0.43	1.81	3.42	0.95	0.82	0.97	-0.29	-2.67	7.6	7.05	7.38	7.38	7.38	1.46	7.37	7.37	7.38	0.44
40.5	26.0	7.33	0.44	2.63	3.32	0.89	0.94	0.96	-0.34	-2.97	7.6	6.66	7.31	7.32	7.33	1.45	7.31	7.32	7.33	0.45
40.5	26.5	7.03	0.42	0.95	5.94	0.95	1.14	1.64	-0.38	-6.52	7.3	6.65	7.02	7.02	7.02	1.86	7.01	7.02	7.02	0.43

Appendix 5. Continued.

Lat	Lon	ω	σ_ω	μ	σ_μ	λ	σ_λ	$\sigma^2_{\omega\mu}$	$\sigma^2_{\omega\lambda}$	$\sigma^2_{\mu\lambda}$	M_M	M_A	M_{50}	M_{100}	M_{200}	σ_M	M_{p50}	M_{p100}	M_{p200}	σ_{Mp}
40.5	27.0	7.18	0.48	1.83	4.43	0.87	0.98	1.47	-0.39	-4.15	7.3	6.29	7.15	7.16	7.17	1.77	7.15	7.16	7.17	0.50
40.5	27.5	7.79	1.39	3.93	1.75	0.58	0.65	1.95	-0.86	-1.07	7.3	5.45	7.55	7.63	7.69	2.26	7.69	7.72	7.75	1.39
40.5	28.0	7.62	1.05	3.27	2.84	0.73	0.77	2.38	-0.76	-2.09	7.3	5.95	7.52	7.56	7.58	2.37	7.57	7.59	7.60	1.07
41.0	19.0	8.28	4.49	5.61	0.18	0.20	0.45	0.31	-2.01	-0.04	7.0	5.73	7.13	7.28	7.41	2.36	7.52	7.62	7.70	3.23
41.0	19.5	8.03	4.19	5.64	0.16	0.20	0.47	0.18	-1.94	-0.03	7.0	5.75	7.00	7.13	7.25	2.21	7.35	7.44	7.51	3.02
41.0	20.0	7.97	3.77	5.70	0.15	0.21	0.45	0.07	-1.67	-0.01	7.0	5.81	7.01	7.14	7.25	2.02	7.34	7.43	7.50	2.75
41.0	20.5	7.59	1.63	5.74	0.14	0.33	0.43	0.01	-0.67	-0.01	7.0	5.97	7.15	7.24	7.31	1.20	7.35	7.40	7.44	1.42
41.0	21.0	7.48	1.27	5.77	0.14	0.39	0.43	0.00	-0.53	-0.01	7.0	6.06	7.17	7.24	7.29	1.01	7.32	7.36	7.39	1.15
41.0	21.5	8.25	3.76	5.76	0.15	0.21	0.41	0.07	-1.52	-0.01	7.4	5.88	7.20	7.34	7.47	2.01	7.56	7.66	7.74	2.74
41.0	22.0	8.17	2.89	5.59	0.22	0.27	0.43	0.28	-1.23	-0.05	7.4	5.79	7.33	7.47	7.59	1.90	7.67	7.75	7.82	2.36
41.0	22.5	8.34	2.12	5.33	0.37	0.35	0.42	0.51	-0.88	-0.12	7.6	5.75	7.68	7.82	7.94	1.77	7.99	8.07	8.13	1.90
41.0	23.0	7.84	0.94	4.64	0.89	0.65	0.54	0.59	-0.47	-0.42	7.6	6.20	7.71	7.76	7.79	1.37	7.78	7.80	7.82	0.93
41.0	23.5	7.57	0.57	3.11	2.36	0.80	0.73	0.92	-0.36	-1.61	7.6	6.34	7.51	7.54	7.55	1.45	7.53	7.55	7.56	0.57
41.0	24.0	7.76	0.65	3.00	2.07	0.93	0.61	0.95	-0.35	-1.17	7.6	7.37	7.75	7.76	7.76	1.52	7.75	7.75	7.76	0.65
41.0	24.5	7.82	0.73	4.20	1.00	0.77	0.51	0.49	-0.34	-0.46	7.6	6.65	7.76	7.79	7.80	1.21	7.79	7.80	7.81	0.73
41.0	25.0	7.58	0.53	4.04	1.25	1.00	0.63	0.42	-0.29	-0.71	7.6	7.57	7.58	7.58	7.58	1.06	7.57	7.57	7.58	0.53
41.0	25.5	7.50	0.47	3.07	2.03	0.89	0.70	0.61	-0.28	-1.33	7.6	6.88	7.48	7.48	7.49	1.19	7.48	7.49	7.49	0.47
41.0	26.0	7.43	0.46	3.47	2.06	0.86	0.80	0.61	-0.31	-1.53	7.6	6.68	7.41	7.42	7.43	1.19	7.41	7.42	7.43	0.47
41.0	26.5	7.14	0.42	2.38	3.56	0.92	0.99	0.98	-0.34	-3.36	7.3	6.66	7.13	7.14	7.14	1.46	7.13	7.14	7.14	0.43
41.0	27.0	7.31	0.53	3.18	2.53	0.81	0.83	0.92	-0.38	-1.99	7.3	6.23	7.26	7.28	7.29	1.44	7.28	7.29	7.30	0.54
41.0	27.5	8.03	1.99	4.48	1.16	0.44	0.59	1.87	-1.14	-0.63	7.3	5.29	7.55	7.68	7.77	2.37	7.80	7.86	7.91	1.93
41.0	28.0	7.83	1.54	4.16	1.68	0.54	0.67	2.09	-0.99	-1.05	7.3	5.43	7.54	7.63	7.69	2.35	7.70	7.74	7.77	1.53
41.5	19.0	7.95	4.17	5.63	0.18	0.21	0.51	0.29	-2.09	-0.04	7.0	5.74	6.98	7.12	7.23	2.27	7.32	7.40	7.48	3.06

Appendix 5. Continued.

Lat	Lon	ω	σ_ω	μ	σ_μ	λ	σ_λ	$\sigma^2_{\omega\mu}$	$\sigma^2_{\omega\lambda}$	$\sigma^2_{\mu\lambda}$	M_M	M_A	M_{50}	M_{100}	M_{200}	σ_M	M_{p50}	M_{p100}	M_{p200}	σ_{Mp}
41.5	19.5	8.61	5.64	5.65	0.16	0.17	0.42	0.26	-2.35	-0.02	7.0	5.75	7.16	7.33	7.47	2.60	7.60	7.71	7.82	3.74
41.5	20.0	8.10	3.30	5.71	0.15	0.22	0.41	0.06	-1.33	-0.01	7.0	5.84	7.16	7.30	7.41	1.87	7.50	7.59	7.66	2.49
41.5	20.5	7.56	1.58	5.76	0.14	0.34	0.43	0.01	-0.66	-0.01	7.0	5.99	7.14	7.23	7.30	1.17	7.33	7.38	7.42	1.39
41.5	21.0	7.61	1.54	5.75	0.14	0.34	0.42	0.00	-0.63	-0.01	7.0	6.00	7.19	7.28	7.35	1.16	7.38	7.43	7.47	1.36
41.5	21.5	8.13	2.67	5.74	0.14	0.25	0.38	0.04	-1.00	-0.01	7.4	5.91	7.30	7.44	7.55	1.64	7.63	7.71	7.78	2.11
41.5	22.0	8.23	3.16	5.54	0.25	0.26	0.45	0.43	-1.41	-0.07	7.4	5.75	7.33	7.48	7.61	2.07	7.69	7.78	7.85	2.57
41.5	22.5	8.35	2.13	5.23	0.46	0.36	0.45	0.67	-0.93	-0.16	7.6	5.69	7.70	7.84	7.96	1.87	8.01	8.09	8.14	1.94
41.5	23.0	8.14	1.50	4.28	1.27	0.52	0.55	1.51	-0.79	-0.64	7.6	5.53	7.81	7.91	7.98	2.09	7.99	8.04	8.07	1.49
41.5	24.0	8.03	1.13	3.38	1.94	0.66	0.57	1.72	-0.61	-1.04	7.6	5.74	7.86	7.92	7.96	2.09	7.95	7.98	8.00	1.14
41.5	24.5	8.11	1.27	4.31	1.04	0.55	0.50	0.99	-0.60	-0.46	7.6	5.68	7.83	7.92	7.98	1.75	7.98	8.02	8.05	1.25
41.5	25.0	7.86	0.85	4.01	1.24	0.72	0.54	0.76	-0.42	-0.60	7.6	6.32	7.76	7.80	7.82	1.46	7.81	7.83	7.84	0.85
41.5	25.5	7.84	0.77	3.31	1.79	0.81	0.57	1.01	-0.40	-0.95	7.6	6.67	7.79	7.81	7.82	1.60	7.81	7.82	7.83	0.78
41.5	26.0	7.85	0.83	4.10	1.25	0.73	0.55	0.75	-0.43	-0.63	7.6	6.41	7.76	7.80	7.82	1.45	7.80	7.82	7.83	0.84
41.5	26.5	7.50	0.69	4.10	1.40	0.84	0.66	0.68	-0.41	-0.85	7.3	6.76	7.47	7.48	7.49	1.34	7.48	7.49	7.49	0.69
41.5	27.0	8.09	1.96	4.88	0.72	0.41	0.52	1.06	-0.99	-0.32	7.3	5.50	7.57	7.70	7.79	2.01	7.83	7.89	7.94	1.85
41.5	27.5	8.87	4.80	4.99	0.62	0.25	0.50	2.37	-2.36	-0.27	7.3	5.26	7.51	7.73	7.91	3.21	8.04	8.17	8.28	3.90
41.5	28.0	8.31	3.03	4.68	1.05	0.35	0.59	2.62	-1.77	-0.56	7.3	5.19	7.52	7.69	7.83	2.90	7.89	7.98	8.05	2.80
42.0	19.0	8.23	6.54	5.63	0.18	0.17	0.53	0.48	-3.44	-0.05	6.9	5.71	6.91	7.06	7.18	2.91	7.30	7.40	7.49	4.24
42.0	19.5	8.59	9.76	5.65	0.16	0.13	0.52	0.51	-5.05	-0.03	6.9	5.70	6.86	7.01	7.14	3.50	7.27	7.39	7.49	5.45
42.0	20.0	8.08	4.25	5.70	0.15	0.20	0.45	0.09	-1.88	-0.01	6.9	5.80	7.02	7.15	7.27	2.16	7.37	7.46	7.53	3.00
42.0	20.5	7.45	1.75	5.73	0.14	0.32	0.47	0.01	-0.80	-0.01	6.9	5.93	7.02	7.10	7.17	1.26	7.21	7.26	7.30	1.51
42.0	21.0	7.65	2.04	5.73	0.14	0.29	0.44	0.02	-0.87	-0.01	6.9	5.92	7.10	7.20	7.28	1.39	7.33	7.39	7.44	1.71
42.0	21.5	8.09	3.16	5.72	0.15	0.23	0.41	0.05	-1.26	-0.01	7.4	5.85	7.18	7.31	7.43	1.82	7.51	7.60	7.67	2.41

Appendix 5. Continued.

Lat	Lon	ω	σ_ω	μ	σ_μ	λ	σ_λ	$\sigma^2_{\omega\mu}$	$\sigma^2_{\omega\lambda}$	$\sigma^2_{\mu\lambda}$	M_M	M_A	M_{50}	M_{100}	M_{200}	σ_M	M_{p50}	M_{p100}	M_{p200}	σ_{Mp}
42.0	22.0	7.92	2.47	5.46	0.31	0.31	0.50	0.44	-1.20	-0.11	7.4	5.72	7.26	7.39	7.49	1.86	7.55	7.62	7.68	2.13
42.0	22.5	8.48	2.70	5.15	0.55	0.33	0.47	1.08	-1.25	-0.21	7.6	5.56	7.67	7.84	7.97	2.25	8.04	8.13	8.20	2.40
42.0	23.0	7.95	1.17	3.83	1.91	0.65	0.64	1.76	-0.70	-1.14	7.6	5.84	7.78	7.84	7.88	2.12	7.87	7.90	7.92	1.18
42.0	24.0	8.03	1.13	3.38	1.94	0.66	0.57	1.72	-0.61	-1.04	7.6	5.74	7.86	7.92	7.96	2.09	7.95	7.98	8.00	1.14
42.0	24.5	8.11	1.27	4.31	1.04	0.55	0.50	0.99	-0.60	-0.46	7.6	5.68	7.83	7.92	7.98	1.75	7.98	8.02	8.05	1.25
42.0	25.0	7.86	0.85	4.01	1.24	0.72	0.54	0.76	-0.42	-0.60	7.6	6.32	7.76	7.80	7.82	1.46	7.81	7.83	7.84	0.85
42.0	25.5	7.84	0.77	3.31	1.79	0.81	0.57	1.01	-0.40	-0.95	7.6	6.67	7.79	7.81	7.82	1.60	7.81	7.82	7.83	0.78
42.0	26.0	8.02	1.10	4.59	0.84	0.58	0.49	0.66	-0.51	-0.36	7.6	5.95	7.81	7.88	7.93	1.49	7.93	7.96	7.98	1.09
42.0	26.5	7.60	0.87	4.61	0.92	0.68	0.59	0.55	-0.47	-0.48	7.3	6.22	7.51	7.54	7.57	1.32	7.56	7.58	7.59	0.86
42.0	27.0	7.65	0.84	4.52	0.94	0.70	0.57	0.54	-0.44	-0.47	7.3	6.29	7.56	7.59	7.62	1.30	7.61	7.62	7.63	0.83
42.0	27.5	8.00	1.56	4.73	0.76	0.47	0.50	0.87	-0.76	-0.33	7.3	5.56	7.61	7.72	7.80	1.78	7.82	7.87	7.91	1.51
42.0	28.0	7.63	0.90	3.97	1.62	0.73	0.65	1.09	-0.55	-0.98	7.3	6.20	7.55	7.58	7.60	1.69	7.59	7.60	7.61	0.91
42.5	19.0	7.71	4.40	5.56	0.25	0.22	0.62	0.61	-2.72	-0.10	6.9	5.67	6.84	6.96	7.07	2.49	7.15	7.23	7.29	3.30
42.5	19.5	8.16	5.85	5.58	0.21	0.18	0.54	0.61	-3.13	-0.06	6.9	5.67	6.94	7.08	7.21	2.82	7.32	7.42	7.51	3.99
42.5	20.0	8.51	8.58	5.60	0.18	0.14	0.52	0.66	-4.48	-0.05	6.9	5.67	6.89	7.05	7.18	3.37	7.31	7.43	7.53	5.11
42.5	20.5	7.60	2.32	5.62	0.19	0.29	0.50	0.14	-1.13	-0.04	6.9	5.81	7.02	7.13	7.22	1.61	7.27	7.33	7.38	1.95
42.5	21.0	7.78	2.56	5.62	0.19	0.27	0.47	0.16	-1.18	-0.04	6.9	5.80	7.10	7.22	7.32	1.71	7.38	7.45	7.51	2.11
42.5	21.5	8.06	3.30	5.60	0.19	0.24	0.44	0.22	-1.44	-0.04	7.4	5.76	7.16	7.30	7.41	1.98	7.50	7.59	7.66	2.57
42.5	22.0	8.14	3.54	5.40	0.36	0.26	0.52	0.84	-1.83	-0.14	7.4	5.61	7.23	7.39	7.51	2.38	7.60	7.69	7.76	2.90
42.5	22.5	9.16	4.86	5.10	0.62	0.25	0.48	2.40	-2.30	-0.25	7.6	5.38	7.73	7.95	8.14	3.23	8.28	8.42	8.53	3.94
42.5	23.0	8.87	3.34	3.90	1.73	0.37	0.57	5.01	-1.86	-0.92	7.6	4.69	7.90	8.12	8.29	3.63	8.37	8.49	8.57	3.17
43.0	19.0	7.83	5.45	5.37	0.35	0.21	0.66	1.29	-3.54	-0.17	6.9	5.48	6.79	6.93	7.05	3.01	7.15	7.24	7.32	4.03
43.0	19.5	7.68	4.31	5.41	0.30	0.23	0.62	0.79	-2.65	-0.13	6.9	5.54	6.81	6.94	7.05	2.55	7.13	7.21	7.28	3.31

Appendix 5. Continued.

Lat	Lon	ω	σ_ω	μ	σ_μ	λ	σ_λ	$\sigma^2_{\omega\mu}$	$\sigma^2_{\omega\lambda}$	$\sigma^2_{\mu\lambda}$	M_M	M_A	M_{50}	M_{100}	M_{200}	σ_M	M_{p50}	M_{p100}	M_{p200}	σ_{Mp}
43.0	20.5	7.68	3.33	5.50	0.21	0.25	0.53	0.33	-1.76	-0.06	6.9	5.65	6.90	7.02	7.13	2.06	7.20	7.28	7.34	2.63
43.0	21.0	7.86	3.54	5.49	0.21	0.24	0.50	0.35	-1.75	-0.06	6.9	5.64	6.98	7.11	7.23	2.13	7.31	7.39	7.46	2.75
43.0	21.5	9.05	9.48	5.43	0.25	0.15	0.48	1.36	-4.54	-0.08	7.4	5.51	7.05	7.24	7.42	3.78	7.58	7.72	7.85	5.71
43.0	22.0	12.46	45.29	5.27	0.45	0.08	0.55	16.36	-25.1	-0.21	7.4	5.31	7.15	7.42	7.68	9.72	7.96	8.19	8.41	17.25
43.0	22.5	8.41	2.70	4.44	1.07	0.38	0.54	2.38	-1.42	-0.52	7.6	5.08	7.64	7.81	7.95	2.74	8.01	8.10	8.17	2.53
43.5	19.0	7.77	5.42	4.84	1.55	0.29	1.02	7.41	-5.45	-1.47	6.9	5.11	6.91	7.06	7.19	4.48	7.27	7.36	7.43	4.75
43.5	19.5	7.61	4.45	4.92	1.61	0.32	1.08	6.30	-4.73	-1.62	6.9	5.23	6.92	7.06	7.17	4.11	7.23	7.31	7.36	4.05
43.5	20.0	7.59	3.95	4.93	1.27	0.32	0.94	4.29	-3.67	-1.10	6.9	5.24	6.92	7.05	7.16	3.56	7.22	7.29	7.35	3.57
43.5	20.5	7.60	3.73	4.95	1.00	0.31	0.83	3.12	-3.07	-0.76	6.9	5.25	6.91	7.05	7.16	3.20	7.22	7.29	7.36	3.33
43.5	21.0	7.71	3.41	4.87	1.02	0.33	0.77	2.89	-2.58	-0.71	6.9	5.22	7.02	7.16	7.27	3.06	7.34	7.41	7.47	3.09
43.5	21.5	7.86	3.99	4.75	0.99	0.30	0.72	3.30	-2.83	-0.64	7.4	5.08	7.01	7.17	7.30	3.30	7.38	7.47	7.55	3.51
43.5	22.0	7.95	4.29	4.40	1.63	0.33	0.81	6.12	-3.44	-1.24	7.4	4.83	7.08	7.25	7.39	4.05	7.47	7.57	7.65	3.93
44.0	20.0	7.57	3.48	4.67	1.71	0.36	0.97	5.18	-3.33	-1.56	6.9	5.11	6.98	7.11	7.21	3.69	7.26	7.33	7.38	3.28
44.0	20.5	7.63	3.55	4.74	1.30	0.34	0.86	3.93	-2.99	-1.02	6.9	5.12	6.96	7.10	7.21	3.39	7.27	7.35	7.41	3.27
44.0	21.0	7.63	3.55	4.74	1.30	0.34	0.86	3.93	-2.99	-1.02	6.9	5.12	6.96	7.10	7.21	3.39	7.27	7.35	7.41	3.27
44.0	21.5	7.45	5.54	4.94	1.19	0.27	1.06	5.72	-5.80	-1.16	6.6	5.14	6.64	6.78	6.89	4.17	6.97	7.05	7.12	4.70

Appendix 6: Regional magnitude hazard $G^{(III)}$ covariance error matrices

Magnitude covariance error matrices, ε, for the broad Balkan area considered between 39.0°N and 45.0°N, 19.0°E and 29.0°E (inclusive). For ease of reference each matrix is arranged with respect to the geographic co-ordinates of the centre of the analysis cell it represents. The first sheet gives covariance error matrices, ε, for the Balkans between meridians 19.0°E and 23.5°E (inclusive). The second sheet gives covariance error matrices, ε, for the Balkans between meridians 24.0°E and 29.0°E (inclusive). Cells with '*null'* forecasts are also given. Matrix elements of ε are:

$$\varepsilon = \begin{bmatrix} \sigma_{\omega}^{2} & \sigma_{\omega\mu}^{2} & \sigma_{\lambda\omega}^{2} \\ \sigma_{\omega\mu}^{2} & \sigma_{\mu}^{2} & \sigma_{\lambda\mu}^{2} \\ \sigma_{\omega\lambda}^{2} & \sigma_{\mu\lambda}^{2} & \sigma_{\lambda}^{2} \end{bmatrix}$$

19.0°E	19.5°E	20.0°E	20.5°E	21.0°E	21.5°E	22.0°E	22.5°E	23.0°E	23.5°E	
---	---	---	---	---	---	---	---	---	---	45.0°N
---	---	---	---	---	---	---	---	---	---	44.5°N
---	---	$\begin{bmatrix} 12.089 & 5.175 & -3.327 \\ 5.175 & 2.929 & -1.562 \\ -3.327 & -1.562 & 0.947 \end{bmatrix}$	$\begin{bmatrix} 12.614 & 3.930 & -2.989 \\ 3.930 & 1.684 & -1.024 \\ -2.989 & -1.024 & 0.731 \end{bmatrix}$	$\begin{bmatrix} 12.614 & 3.930 & -2.989 \\ 3.930 & 1.684 & -1.024 \\ -2.989 & -1.024 & 0.731 \end{bmatrix}$	$\begin{bmatrix} 30.703 & 5.716 & -5.795 \\ 5.716 & 1.416 & -1.157 \\ -5.795 & -1.157 & 1.115 \end{bmatrix}$	---	---	---	---	44.0°N
$\begin{bmatrix} 29.328 & 7.407 & -5.453 \\ 7.407 & 1.416 & -1.157 \\ -5.453 & -1.473 & 1.034 \end{bmatrix}$	$\begin{bmatrix} 19.819 & 6.303 & -4.728 \\ 6.303 & 2.600 & -1.624 \\ -4.728 & -1.624 & 1.157 \end{bmatrix}$	$\begin{bmatrix} 15.609 & 4.292 & -3.672 \\ 4.292 & 1.608 & -1.102 \\ -3.672 & -1.102 & 0.888 \end{bmatrix}$	$\begin{bmatrix} 13.912 & 3.121 & -3.066 \\ 3.121 & 1.608 & -0.757 \\ -3.066 & -0.757 & 0.695 \end{bmatrix}$	$\begin{bmatrix} 11.627 & 2.892 & -2.577 \\ 2.892 & 1.041 & -0.710 \\ -2.577 & -0.710 & 0.590 \end{bmatrix}$	$\begin{bmatrix} 15.887 & 3.304 & -2.828 \\ 3.304 & 0.981 & -0.644 \\ -2.828 & -0.644 & 0.517 \end{bmatrix}$	$\begin{bmatrix} 18.441 & 6.122 & -3.438 \\ 6.122 & 2.642 & -1.235 \\ -3.438 & -1.235 & 0.658 \end{bmatrix}$	---	---	---	43.5°N
$\begin{bmatrix} 29.668 & 1.293 & -3.540 \\ 1.293 & 0.121 & -0.171 \\ -3.540 & -0.171 & 0.429 \end{bmatrix}$	$\begin{bmatrix} 18.557 & 0.788 & -2.654 \\ 0.788 & 0.087 & -0.128 \\ -2.654 & -0.128 & 0.387 \end{bmatrix}$	$\begin{bmatrix} 23.058 & 0.666 & -2.831 \\ 0.666 & 0.062 & -0.093 \\ -2.831 & -0.093 & 0.354 \end{bmatrix}$	$\begin{bmatrix} 11.112 & 0.325 & -1.755 \\ 0.325 & 0.046 & -0.062 \\ -1.755 & -0.062 & 0.284 \end{bmatrix}$	$\begin{bmatrix} 12.511 & 0.347 & -1.748 \\ 0.347 & 0.046 & -0.058 \\ -1.748 & -0.058 & 0.250 \end{bmatrix}$	$\begin{bmatrix} 89.854 & 1.357 & -4.543 \\ 1.357 & 0.060 & -0.075 \\ -4.543 & -0.075 & 0.232 \end{bmatrix}$	$\begin{bmatrix} 2051.5 & 16.364 & -25.05 \\ 16.364 & 0.202 & -0.205 \\ -25.05 & -0.205 & 0.306 \end{bmatrix}$	$\begin{bmatrix} 7.265 & 2.376 & -1.417 \\ 2.376 & 1.152 & -0.523 \\ -1.417 & -0.523 & 0.288 \end{bmatrix}$	---	---	43.0°N
$\begin{bmatrix} 19.343 & 0.607 & -2.717 \\ 0.607 & 0.062 & -0.098 \\ -2.717 & -0.098 & 0.389 \end{bmatrix}$	$\begin{bmatrix} 34.164 & 0.606 & -3.133 \\ 0.606 & 0.045 & -0.063 \\ -3.133 & -0.063 & 0.291 \end{bmatrix}$	$\begin{bmatrix} 73.625 & 0.657 & -4.478 \\ 0.657 & 0.034 & -0.045 \\ -4.478 & -0.045 & 0.275 \end{bmatrix}$	$\begin{bmatrix} 5.373 & 0.139 & -1.134 \\ 0.139 & 0.034 & -0.039 \\ -1.134 & -0.039 & 0.248 \end{bmatrix}$	$\begin{bmatrix} 6.562 & 0.158 & -1.181 \\ 0.158 & 0.034 & -0.037 \\ -1.181 & -0.037 & 0.219 \end{bmatrix}$	$\begin{bmatrix} 10.862 & 0.217 & -1.442 \\ 0.217 & 0.034 & -0.036 \\ -1.442 & -0.036 & 0.196 \end{bmatrix}$	$\begin{bmatrix} 12.511 & 0.842 & -1.825 \\ 0.842 & 0.128 & -0.140 \\ -1.825 & -0.140 & 0.273 \end{bmatrix}$	$\begin{bmatrix} 23.652 & 2.396 & -2.296 \\ 2.396 & 0.385 & -0.254 \\ -2.296 & -0.254 & 0.227 \end{bmatrix}$	$\begin{bmatrix} 11.140 & 5.013 & -1.858 \\ 5.013 & 2.993 & -0.920 \\ -1.858 & -0.920 & 0.321 \end{bmatrix}$	---	42.5°N
$\begin{bmatrix} 42.739 & 0.484 & -3.436 \\ 0.484 & 0.034 & -0.045 \\ -3.436 & -0.045 & 0.279 \end{bmatrix}$	$\begin{bmatrix} 95.322 & 0.508 & -3.436 \\ 0.508 & 0.026 & -0.031 \\ -5.048 & -0.031 & 0.269 \end{bmatrix}$	$\begin{bmatrix} 18.046 & 0.089 & -1.877 \\ 0.089 & 0.021 & -0.014 \\ -1.877 & -0.014 & 0.199 \end{bmatrix}$	$\begin{bmatrix} 3.078 & 0.010 & -1.877 \\ 0.010 & 0.021 & -0.009 \\ -0.797 & -0.009 & 0.217 \end{bmatrix}$	$\begin{bmatrix} 4.146 & 0.010 & -0.871 \\ 0.010 & 0.021 & -0.009 \\ -0.871 & -0.009 & 0.190 \end{bmatrix}$	$\begin{bmatrix} 10.009 & 0.052 & -1.264 \\ 0.052 & 0.021 & -0.011 \\ -1.264 & -0.011 & 0.164 \end{bmatrix}$	$\begin{bmatrix} 6.080 & 0.443 & -1.204 \\ 0.443 & 0.093 & -0.105 \\ -1.204 & -0.105 & 0.248 \end{bmatrix}$	$\begin{bmatrix} 7.261 & 1.084 & -1.247 \\ 1.084 & 0.297 & -0.214 \\ -1.247 & -0.214 & 0.222 \end{bmatrix}$	$\begin{bmatrix} 1.362 & 1.756 & -0.702 \\ 1.756 & 3.643 & -1.139 \\ -0.702 & -1.139 & 0.407 \end{bmatrix}$	---	42.0°N
$\begin{bmatrix} 17.383 & 0.288 & -2.091 \\ 0.288 & 0.034 & -0.042 \\ -2.091 & -0.042 & 0.256 \end{bmatrix}$	$\begin{bmatrix} 31.806 & 0.263 & -2.345 \\ 0.263 & 0.026 & -0.024 \\ -2.345 & -0.024 & 0.175 \end{bmatrix}$	$\begin{bmatrix} 10.893 & 0.057 & -1.328 \\ 0.057 & 0.021 & -0.011 \\ -1.328 & -0.011 & 0.166 \end{bmatrix}$	$\begin{bmatrix} 2.483 & 0.005 & -0.663 \\ 0.005 & 0.021 & -0.007 \\ -0.663 & -0.007 & 0.187 \end{bmatrix}$	$\begin{bmatrix} 2.384 & 0.004 & -0.627 \\ 0.004 & 0.021 & -0.007 \\ -0.627 & -0.007 & 0.174 \end{bmatrix}$	$\begin{bmatrix} 7.107 & 0.036 & -0.995 \\ 0.036 & 0.021 & -0.010 \\ -0.995 & -0.010 & 0.144 \end{bmatrix}$	$\begin{bmatrix} 9.993 & 0.427 & -1.413 \\ 0.427 & 0.064 & -0.072 \\ -1.413 & -0.072 & 0.205 \end{bmatrix}$	$\begin{bmatrix} 4.523 & 0.669 & -0.925 \\ 0.669 & 0.210 & -0.163 \\ -0.925 & -0.163 & 0.198 \end{bmatrix}$	$\begin{bmatrix} 2.250 & 1.506 & -0.794 \\ 1.506 & 1.623 & -0.643 \\ -0.794 & -0.643 & 0.304 \end{bmatrix}$	---	41.5°N
$\begin{bmatrix} 20.126 & 0.314 & -2.009 \\ 0.314 & 0.034 & -0.038 \\ -2.009 & -0.038 & 0.204 \end{bmatrix}$	$\begin{bmatrix} 17.585 & 0.180 & -1.938 \\ 0.180 & 0.026 & -0.026 \\ -1.938 & -0.026 & 0.218 \end{bmatrix}$	$\begin{bmatrix} 14.220 & 0.072 & -1.673 \\ 0.072 & 0.021 & -0.013 \\ -1.673 & -0.013 & 0.201 \end{bmatrix}$	$\begin{bmatrix} 2.641 & 0.006 & -0.672 \\ 0.006 & 0.021 & -0.008 \\ -0.672 & -0.008 & 0.180 \end{bmatrix}$	$\begin{bmatrix} 1.606 & -0.003 & -0.529 \\ -0.003 & 0.021 & -0.005 \\ -0.529 & -0.005 & 0.186 \end{bmatrix}$	$\begin{bmatrix} 14.112 & 0.072 & -1.520 \\ 0.072 & 0.021 & -0.012 \\ -1.520 & -0.012 & 0.167 \end{bmatrix}$	$\begin{bmatrix} 8.358 & 0.276 & -1.229 \\ 0.276 & 0.021 & -0.050 \\ -1.229 & -0.050 & 0.186 \end{bmatrix}$	$\begin{bmatrix} 4.477 & 0.505 & -0.878 \\ 0.505 & 0.140 & -0.119 \\ -0.878 & -0.119 & 0.180 \end{bmatrix}$	$\begin{bmatrix} 0.875 & 0.585 & -0.471 \\ 0.585 & 0.797 & -0.423 \\ -0.471 & -0.423 & 0.290 \end{bmatrix}$	$\begin{bmatrix} 0.319 & 0.923 & -0.357 \\ 0.923 & 5.586 & -1.612 \\ -0.357 & -1.612 & 0.528 \end{bmatrix}$	41.0°N
$\begin{bmatrix} 20.126 & 0.314 & -2.009 \\ 0.314 & 0.034 & -0.038 \\ -2.009 & -0.038 & 0.204 \end{bmatrix}$	$\begin{bmatrix} 17.585 & 0.180 & -1.938 \\ 0.180 & 0.026 & -0.026 \\ -1.938 & -0.026 & 0.218 \end{bmatrix}$	$\begin{bmatrix} 14.220 & 0.072 & -1.673 \\ 0.072 & 0.021 & -0.013 \\ -1.673 & -0.013 & 0.201 \end{bmatrix}$	$\begin{bmatrix} 2.641 & 0.006 & -0.672 \\ 0.006 & 0.021 & -0.008 \\ -0.672 & -0.008 & 0.180 \end{bmatrix}$	$\begin{bmatrix} 1.606 & -0.003 & -0.529 \\ -0.003 & 0.021 & -0.005 \\ -0.529 & -0.005 & 0.186 \end{bmatrix}$	$\begin{bmatrix} 14.112 & 0.072 & -1.520 \\ 0.072 & 0.021 & -0.012 \\ -1.520 & -0.012 & 0.167 \end{bmatrix}$	$\begin{bmatrix} 8.358 & 0.276 & -1.229 \\ 0.276 & 0.021 & -0.050 \\ -1.229 & -0.050 & 0.186 \end{bmatrix}$	$\begin{bmatrix} 4.477 & 0.505 & -0.878 \\ 0.505 & 0.140 & -0.119 \\ -0.878 & -0.119 & 0.180 \end{bmatrix}$	$\begin{bmatrix} 0.875 & 0.585 & -0.471 \\ 0.585 & 0.797 & -0.423 \\ -0.471 & -0.423 & 0.290 \end{bmatrix}$	$\begin{bmatrix} 0.319 & 0.923 & -0.357 \\ 0.923 & 5.586 & -1.612 \\ -0.357 & -1.612 & 0.528 \end{bmatrix}$	40.5°N
$\begin{bmatrix} 59.076 & 1.422 & -4.270 \\ 1.422 & 0.083 & -0.112 \\ -4.270 & -0.112 & 0.312 \end{bmatrix}$	$\begin{bmatrix} 10.505 & 0.438 & -1.772 \\ 0.438 & 0.064 & -0.087 \\ -1.772 & -0.087 & 0.307 \end{bmatrix}$	$\begin{bmatrix} 22.539 & 0.658 & -2.551 \\ 0.658 & 0.062 & -0.085 \\ -2.551 & -0.085 & 0.294 \end{bmatrix}$	$\begin{bmatrix} 2.834 & 0.213 & -0.935 \\ 0.213 & 0.067 & -0.091 \\ -0.935 & -0.091 & 0.326 \end{bmatrix}$	$\begin{bmatrix} 1.878 & 0.112 & -0.687 \\ 0.112 & 0.048 & -0.058 \\ -0.687 & -0.058 & 0.269 \end{bmatrix}$	$\begin{bmatrix} 10.608 & 0.214 & -1.413 \\ 0.214 & 0.034 & -0.036 \\ -1.413 & -0.036 & 0.193 \end{bmatrix}$	$\begin{bmatrix} 5.865 & 0.319 & -1.091 \\ 0.319 & 0.065 & -0.073 \\ -1.091 & -0.073 & 0.211 \end{bmatrix}$	$\begin{bmatrix} 4.477 & 0.505 & -0.878 \\ 0.505 & 0.140 & -0.119 \\ -0.878 & -0.119 & 0.180 \end{bmatrix}$	$\begin{bmatrix} 0.594 & 1.451 & -0.568 \\ 1.451 & 6.370 & -1.942 \\ -0.568 & -1.942 & 0.664 \end{bmatrix}$	$\begin{bmatrix} 0.426 & 1.400 & -0.480 \\ 1.400 & 8.747 & -2.336 \\ -0.480 & -2.336 & 0.693 \end{bmatrix}$	40.0°N
$\begin{bmatrix} 42.956 & 1.209 & -3.467 \\ 1.209 & 0.084 & -0.108 \\ -3.467 & -0.108 & 0.283 \end{bmatrix}$	$\begin{bmatrix} 10.390 & 0.436 & -1.685 \\ 0.436 & 0.064 & -0.084 \\ -1.685 & -0.084 & 0.281 \end{bmatrix}$	$\begin{bmatrix} 15.177 & 0.534 & -2.134 \\ 0.534 & 0.063 & -0.087 \\ -2.134 & -0.087 & 0.304 \end{bmatrix}$	$\begin{bmatrix} 1.977 & 0.174 & -0.741 \\ 0.174 & 0.069 & -0.088 \\ -0.741 & -0.088 & 0.297 \end{bmatrix}$	$\begin{bmatrix} 1.486 & 0.097 & -0.624 \\ 0.097 & 0.048 & -0.059 \\ -0.624 & -0.059 & 0.283 \end{bmatrix}$	$\begin{bmatrix} 1.078 & 0.043 & -0.523 \\ 0.043 & 0.034 & -0.036 \\ -0.523 & -0.036 & 0.278 \end{bmatrix}$	$\begin{bmatrix} 0.716 & 0.143 & -0.503 \\ 0.143 & 0.115 & -0.149 \\ -0.503 & -0.149 & 0.401 \end{bmatrix}$	$\begin{bmatrix} 5.627 & 0.566 & -1.081 \\ 0.566 & 0.137 & -0.129 \\ -1.081 & -0.129 & 0.216 \end{bmatrix}$	$\begin{bmatrix} 1.436 & 2.529 & -0.973 \\ 2.529 & 6.846 & -2.142 \\ -0.973 & -2.142 & 0.745 \end{bmatrix}$	$\begin{bmatrix} 1.068 & 2.362 & -0.808 \\ 2.362 & 8.309 & -2.306 \\ -0.808 & -2.306 & 0.708 \end{bmatrix}$	39.5°N
$\begin{bmatrix} 8.836 & 1.188 & -1.812 \\ 1.188 & 0.289 & -0.277 \\ -1.812 & -0.277 & 0.384 \end{bmatrix}$	$\begin{bmatrix} 12.542 & 2.213 & -2.213 \\ 1.398 & 0.277 & -0.277 \\ -2.213 & -0.277 & 0.401 \end{bmatrix}$	$\begin{bmatrix} 3.129 & 0.562 & -1.077 \\ 0.562 & 0.221 & -0.236 \\ -1.077 & -0.236 & 0.393 \end{bmatrix}$	$\begin{bmatrix} 3.129 & 0.562 & -1.077 \\ 0.562 & 0.221 & -0.236 \\ -1.077 & -0.236 & 0.393 \end{bmatrix}$	$\begin{bmatrix} 2.057 & 0.344 & -0.847 \\ 0.344 & 0.154 & -0.181 \\ -0.847 & -0.181 & 0.375 \end{bmatrix}$	$\begin{bmatrix} 1.286 & 0.196 & -0.661 \\ 0.196 & 0.107 & -0.138 \\ -0.661 & -0.138 & 0.372 \end{bmatrix}$	$\begin{bmatrix} 0.930 & 0.143 & -0.673 \\ 0.439 & 0.462 & -0.428 \\ -0.673 & -0.428 & 0.551 \end{bmatrix}$	$\begin{bmatrix} 0.411 & 0.324 & -0.485 \\ 0.324 & 0.646 & -0.580 \\ -0.485 & -0.580 & 0.705 \end{bmatrix}$	---	---	39.0°N

---	---	---	---	---	---	---	---	---	---	---
---	---	---	---	---	---	---	---	---	---	---
---	---	---	---	---	---	---	---	---	---	---
---	---	---	---	---	---	---	---	---	---	---
---	---	---	---	---	---	---	---	---	---	---
---	---	---	---	---	---	---	---	---	---	---
$\begin{bmatrix} 1.275 & 1.723 & -0.607 \\ 1.723 & 3.777 & -1.040 \\ -0.607 & -1.040 & 0.327 \end{bmatrix}$	$\begin{bmatrix} 1.604 & 0.988 & -0.598 \\ 0.988 & 1.074 & -0.461 \\ -0.598 & -0.461 & 0.246 \end{bmatrix}$	$\begin{bmatrix} 0.726 & 0.756 & -0.422 \\ 0.756 & 1.525 & -0.600 \\ -0.422 & -0.600 & 0.287 \end{bmatrix}$	$\begin{bmatrix} 0.595 & 1.007 & -0.399 \\ 1.007 & 3.120 & -0.945 \\ -0.399 & -0.945 & 0.323 \end{bmatrix}$	$\begin{bmatrix} 1.210 & 0.660 & -0.510 \\ 0.660 & 0.705 & -0.360 \\ -0.510 & -0.360 & 0.240 \end{bmatrix}$	$\begin{bmatrix} 0.751 & 0.554 & -0.472 \\ 0.554 & 0.851 & -0.477 \\ -0.472 & -0.477 & 0.344 \end{bmatrix}$	$\begin{bmatrix} 0.698 & 0.540 & -0.439 \\ 0.540 & 0.879 & -0.469 \\ -0.439 & -0.469 & 0.322 \end{bmatrix}$	$\begin{bmatrix} 2.425 & 0.872 & -0.755 \\ 0.872 & 0.573 & -0.331 \\ -0.755 & -0.331 & 0.252 \end{bmatrix}$	$\begin{bmatrix} 0.816 & 1.088 & -0.547 \\ 1.088 & 2.608 & -0.976 \\ -0.547 & -0.976 & 0.428 \end{bmatrix}$	---	---
$\begin{bmatrix} 1.275 & 1.723 & -0.607 \\ 1.723 & 3.777 & -1.040 \\ -0.607 & -1.040 & 0.327 \end{bmatrix}$	$\begin{bmatrix} 1.604 & 0.988 & -0.598 \\ 0.988 & 1.074 & -0.461 \\ -0.598 & -0.461 & 0.246 \end{bmatrix}$	$\begin{bmatrix} 0.726 & 0.756 & -0.422 \\ 0.756 & 1.525 & -0.600 \\ -0.422 & -0.600 & 0.287 \end{bmatrix}$	$\begin{bmatrix} 0.595 & 1.007 & -0.399 \\ 1.007 & 3.120 & -0.945 \\ -0.399 & -0.945 & 0.323 \end{bmatrix}$	$\begin{bmatrix} 0.696 & 0.746 & -0.426 \\ 0.746 & 1.561 & -0.628 \\ -0.426 & -0.628 & 0.307 \end{bmatrix}$	$\begin{bmatrix} 0.479 & 0.675 & -0.414 \\ 0.675 & 1.969 & -0.850 \\ -0.414 & -0.850 & 0.441 \end{bmatrix}$	$\begin{bmatrix} 2.830 & 1.058 & -0.985 \\ 1.058 & 0.515 & -0.322 \\ -0.985 & -0.322 & 0.268 \end{bmatrix}$	$\begin{bmatrix} 23.014 & 2.366 & -2.361 \\ 2.366 & 0.387 & -0.265 \\ -2.361 & -0.265 & 0.247 \end{bmatrix}$	$\begin{bmatrix} 9.205 & 2.621 & -1.768 \\ 1.088 & 1.092 & -0.563 \\ -1.768 & -0.563 & 0.352 \end{bmatrix}$	---	---
$\begin{bmatrix} 0.418 & 0.946 & -0.348 \\ 0.946 & 4.270 & -1.170 \\ -0.348 & -1.170 & 0.367 \end{bmatrix}$	$\begin{bmatrix} 0.531 & 0.494 & -0.341 \\ 0.494 & 1.008 & -0.457 \\ -0.341 & -0.457 & 0.263 \end{bmatrix}$	$\begin{bmatrix} 0.278 & 0.420 & -0.288 \\ 0.420 & 1.525 & -0.705 \\ -0.288 & -0.705 & 0.393 \end{bmatrix}$	$\begin{bmatrix} 0.217 & 0.611 & -0.276 \\ 0.611 & 4.117 & -1.328 \\ -0.276 & -1.328 & 0.495 \end{bmatrix}$	$\begin{bmatrix} 0.212 & 0.611 & -0.308 \\ 0.611 & 4.245 & -1.530 \\ -0.308 & -1.530 & 0.637 \end{bmatrix}$	$\begin{bmatrix} 0.179 & 0.979 & -0.342 \\ 0.979 & 12.641 & -3.358 \\ -0.342 & -3.358 & 0.984 \end{bmatrix}$	$\begin{bmatrix} 0.283 & 0.921 & -0.381 \\ 0.921 & 6.419 & -1.990 \\ -0.381 & -1.990 & 0.696 \end{bmatrix}$	$\begin{bmatrix} 3.972 & 1.865 & -1.144 \\ 1.865 & 0.387 & -0.625 \\ -1.144 & -0.625 & 0.349 \end{bmatrix}$	$\begin{bmatrix} 2.360 & 2.085 & -0.994 \\ 2.085 & 2.811 & -1.053 \\ -0.994 & -1.053 & 0.455 \end{bmatrix}$	---	---
$\begin{bmatrix} 0.418 & 0.946 & -0.348 \\ 0.946 & 4.270 & -1.170 \\ -0.348 & -1.170 & 0.367 \end{bmatrix}$	$\begin{bmatrix} 0.569 & 0.505 & -0.339 \\ 0.505 & 1.008 & -0.428 \\ -0.339 & -0.428 & 0.241 \end{bmatrix}$	$\begin{bmatrix} 0.274 & 0.419 & -0.273 \\ 0.419 & 1.575 & -0.678 \\ -0.273 & -0.678 & 0.360 \end{bmatrix}$	$\begin{bmatrix} 0.187 & 0.968 & -0.290 \\ 0.611 & 11.725 & -2.667 \\ -0.290 & -2.667 & 0.670 \end{bmatrix}$	$\begin{bmatrix} 0.194 & 0.959 & -0.341 \\ 0.959 & 11.009 & -2.966 \\ -0.341 & -2.966 & 0.885 \end{bmatrix}$	$\begin{bmatrix} 0.175 & 1.638 & -0.379 \\ 1.638 & 35.307 & -6.518 \\ -0.379 & -6.518 & 1.290 \end{bmatrix}$	$\begin{bmatrix} 0.234 & 1.466 & -0.393 \\ 1.466 & 19.660 & -4.153 \\ -0.393 & -4.153 & 0.953 \end{bmatrix}$	$\begin{bmatrix} 1.925 & 1.951 & -0.864 \\ 1.951 & 0.387 & -1.068 \\ -0.864 & -1.068 & 0.427 \end{bmatrix}$	$\begin{bmatrix} 1.111 & 2.382 & -0.758 \\ 2.382 & 8.080 & -2.085 \\ -0.758 & -2.085 & 0.595 \end{bmatrix}$	---	---
$\begin{bmatrix} 0.388 & 1.395 & -0.391 \\ 1.395 & 9.688 & -2.120 \\ -0.391 & -2.120 & 0.514 \end{bmatrix}$	$\begin{bmatrix} 0.619 & 1.016 & -0.405 \\ 1.016 & 3.122 & -0.925 \\ -0.405 & -0.925 & 0.319 \end{bmatrix}$	$\begin{bmatrix} 0.308 & 0.922 & -0.338 \\ 0.922 & 5.827 & -1.597 \\ -0.338 & -1.597 & 0.496 \end{bmatrix}$	$\begin{bmatrix} 0.233 & 2.438 & -0.384 \\ 2.438 & 53.143 & -6.851 \\ -0.384 & -6.851 & 0.939 \end{bmatrix}$	$\begin{bmatrix} 0.240 & 1.457 & -0.373 \\ 1.457 & 18.820 & -3.793 \\ -0.373 & -3.793 & 0.832 \end{bmatrix}$	$\begin{bmatrix} 0.222 & 2.493 & -0.419 \\ 2.493 & 59.006 & -8.146 \\ -0.419 & -8.146 & 1.193 \end{bmatrix}$	$\begin{bmatrix} 0.330 & 2.199 & -0.470 \\ 2.199 & 28.243 & -4.920 \\ -0.470 & -4.920 & 0.915 \end{bmatrix}$	$\begin{bmatrix} 1.111 & 2.382 & -0.758 \\ 2.382 & 8.080 & -2.085 \\ -0.758 & -2.085 & 0.595 \end{bmatrix}$	$\begin{bmatrix} 1.111 & 2.382 & -0.758 \\ 2.382 & 8.080 & -2.085 \\ -0.758 & -2.085 & 0.595 \end{bmatrix}$	---	---
$\begin{bmatrix} 0.788 & 2.234 & -0.586 \\ 2.234 & 10.500 & -2.231 \\ -0.586 & -2.231 & 0.521 \end{bmatrix}$	$\begin{bmatrix} 1.500 & 1.016 & -0.666 \\ 1.016 & 3.465 & -1.000 \\ -0.666 & -1.000 & 0.331 \end{bmatrix}$	$\begin{bmatrix} 0.422 & 1.399 & -0.415 \\ 1.399 & 8.824 & -2.039 \\ -0.415 & -2.039 & 0.523 \end{bmatrix}$	$\begin{bmatrix} 0.233 & 2.438 & -0.384 \\ 2.438 & 53.143 & -6.851 \\ -0.384 & -6.851 & 0.939 \end{bmatrix}$	$\begin{bmatrix} 0.240 & 1.457 & -0.373 \\ 1.457 & 18.820 & -3.793 \\ -0.373 & -3.793 & 0.832 \end{bmatrix}$	$\begin{bmatrix} 0.222 & 2.493 & -0.419 \\ 2.493 & 59.006 & -8.146 \\ -0.419 & -8.146 & 1.193 \end{bmatrix}$	$\begin{bmatrix} 0.330 & 2.199 & -0.470 \\ 2.199 & 28.243 & -4.920 \\ -0.470 & -4.920 & 0.915 \end{bmatrix}$	$\begin{bmatrix} 1.111 & 2.382 & -0.758 \\ 2.382 & 8.080 & -2.085 \\ -0.758 & -2.085 & 0.595 \end{bmatrix}$	$\begin{bmatrix} 1.111 & 2.382 & -0.758 \\ 2.382 & 8.080 & -2.085 \\ -0.758 & -2.085 & 0.595 \end{bmatrix}$	---	---
---	$\begin{bmatrix} 0.772 & 1.522 & -0.622 \\ 1.522 & 5.189 & -1.650 \\ -0.622 & -1.650 & 0.593 \end{bmatrix}$	$\begin{bmatrix} 0.318 & 1.400 & -0.468 \\ 1.400 & 12.388 & -3.236 \\ -0.468 & -3.236 & 0.930 \end{bmatrix}$	$\begin{bmatrix} 0.236 & 2.425 & -0.432 \\ 2.425 & 51.848 & -7.570 \\ -0.432 & -7.570 & 1.175 \end{bmatrix}$	$\begin{bmatrix} 0.239 & 1.459 & -0.425 \\ 1.459 & 18.972 & -4.358 \\ -0.425 & -4.358 & 1.089 \end{bmatrix}$	$\begin{bmatrix} 0.222 & 2.493 & -0.419 \\ 2.493 & 59.006 & -8.146 \\ -0.419 & -8.146 & 1.193 \end{bmatrix}$	$\begin{bmatrix} 0.330 & 2.199 & -0.470 \\ 2.199 & 28.243 & -4.920 \\ -0.470 & -4.920 & 0.915 \end{bmatrix}$	$\begin{bmatrix} 1.111 & 2.382 & -0.758 \\ 2.382 & 8.080 & -2.085 \\ -0.758 & -2.085 & 0.595 \end{bmatrix}$	$\begin{bmatrix} 1.111 & 2.382 & -0.758 \\ 2.382 & 8.080 & -2.085 \\ -0.758 & -2.085 & 0.595 \end{bmatrix}$	---	---
24.0°E	24.5°E	25.0°E	25.5°E	26.0°E	26.5°E	27.0°E	27.5°E	28.0°E	28.5°E	29.0°E

Appendix 7: Southwest zone cellular $G^{(III)}$ magnitude recurrence estimates

Parameters (ω, μ, λ) and their associated uncertainties of a $G^{(III)}$ distribution for each cell used to contour magnitude hazard over the southwest zone. M_M is the maximum observed magnitude and m(1) is the annual modal [or most probable] maximum event in each cell of analysis. $M_{50,}$ M_{100} and M_{200} are the modal maximum magnitudes expected in 50-, 100- and 200 year time intervals respectively. M_{P50}, M_{P100} and M_{P200} are the magnitudes expected to be extremes with 90% probability of non-exceedance in the 50-, 100- and 200-year time intervals (a 1 in 10 chance of exceedance). σ_M and σ_{Mp} are the uncertainties in these forecasts. Forecasts were obtained using earthquake data of 5-year extreme intervals, $M_s \geq 5.3$ and time interval 1900 to 2004. $\sigma^2_{\omega\mu}$, $\sigma^2_{\omega\lambda}$ and $\sigma^2_{\mu\lambda}$ are the off-diagonal elements of the covariance error matrix, ε.

Lat	Lon	ω	σ_ω	μ	σ_μ	λ	σ_λ	$\sigma^2_{\omega\mu}$	$\sigma^2_{\omega\lambda}$	$\sigma^2_{\mu\lambda}$	M_M	M_A	M_{50}	M_{100}	M_{200}	σ_M	M_{p50}	M_{p100}	M_{p200}	σ_{Mp}
40.0	21.0	7.72	2.29	3.79	1.71	0.48	0.72	3.26	-1.60	-1.15	6.9	4.85	7.28	7.41	7.49	3.03	7.52	7.57	7.62	2.25
40.0	21.5	7.77	1.02	3.44	1.63	0.73	0.60	1.24	-0.57	-0.90	7.4	6.12	7.67	7.71	7.73	1.83	7.72	7.74	7.75	1.02
40.0	22.0	8.10	1.56	4.11	0.96	0.53	0.50	1.12	-0.75	-0.43	7.4	5.41	7.76	7.86	7.94	1.97	7.95	7.99	8.03	1.53
40.0	22.5	8.19	1.16	4.23	0.76	0.60	0.44	0.60	-0.48	-0.28	7.6	5.88	7.97	8.04	8.09	1.50	8.09	8.12	8.15	1.15
40.0	23.0	7.78	0.66	4.04	0.95	0.89	0.54	0.39	-0.31	-0.44	7.6	7.26	7.76	7.77	7.77	1.09	7.76	7.77	7.77	0.66
40.0	23.5	7.50	0.55	3.07	2.68	0.85	0.88	0.99	-0.41	-2.21	7.6	6.64	7.47	7.48	7.49	1.50	7.48	7.49	7.49	0.56
40.0	24.0	7.63	0.59	2.58	2.49	0.88	0.72	0.99	-0.36	-1.68	7.6	6.86	7.60	7.61	7.62	1.52	7.60	7.61	7.62	0.59
40.0	24.5	7.51	0.57	-2.20	8.03	0.98	0.86	3.26	-0.41	-6.68	7.6	7.34	7.51	7.51	7.51	2.62	7.49	7.50	7.50	0.59
40.0	25.0	7.51	0.57	-2.20	8.03	0.98	0.86	3.26	-0.41	-6.68	7.6	7.34	7.51	7.51	7.51	2.62	7.49	7.50	7.50	0.59
40.5	21.0	7.45	1.59	4.43	0.96	0.52	0.67	1.14	-1.02	-0.56	6.9	5.39	7.18	7.26	7.32	1.99	7.32	7.36	7.39	1.56
40.5	21.5	8.21	1.97	4.87	0.50	0.41	0.46	0.66	-0.89	-0.18	7.4	5.53	7.67	7.81	7.91	1.88	7.94	8.01	8.06	1.85
40.5	22.0	8.57	2.83	5.01	0.37	0.32	0.42	0.65	-1.15	-0.11	7.4	5.42	7.67	7.85	8.00	2.20	8.08	8.18	8.25	2.48
40.5	22.5	8.39	1.55	4.93	0.39	0.45	0.39	0.35	-0.58	-0.11	7.6	5.75	7.94	8.06	8.15	1.52	8.17	8.23	8.27	1.48
40.5	23.0	7.94	0.89	4.96	0.42	0.64	0.44	0.20	-0.37	-0.13	7.6	6.40	7.81	7.86	7.89	1.04	7.88	7.90	7.92	0.88
40.5	23.5	7.63	0.53	4.47	0.71	0.84	0.57	0.20	-0.26	-0.33	7.6	6.95	7.60	7.61	7.62	0.82	7.61	7.62	7.62	0.53
40.5	24.0	7.86	0.72	4.49	0.63	0.79	0.47	0.26	-0.31	-0.24	7.6	6.88	7.82	7.84	7.85	1.00	7.84	7.85	7.85	0.71
40.5	24.5	7.90	0.73	3.41	1.33	0.87	0.53	0.65	-0.35	-0.64	7.6	7.15	7.87	7.88	7.89	1.35	7.88	7.88	7.89	0.73
40.5	25.0	7.90	0.73	3.41	1.33	0.87	0.53	0.65	-0.35	-0.64	7.6	7.15	7.87	7.88	7.89	1.35	7.88	7.88	7.89	0.73
40.5	25.5	8.72	3.06	3.49	1.57	0.41	0.54	4.08	-1.63	-0.79	7.6	4.50	7.87	8.08	8.24	3.45	8.30	8.41	8.48	2.93
41.0	21.0	7.78	2.53	4.72	0.64	0.38	0.59	1.19	-1.46	-0.32	6.9	5.22	7.20	7.33	7.44	2.34	7.48	7.55	7.61	2.34
41.0	21.5	8.21	1.97	4.87	0.50	0.41	0.46	0.66	-0.89	-0.18	7.4	5.53	7.67	7.81	7.91	1.88	7.94	8.01	8.06	1.85
41.0	22.0	8.57	2.83	5.01	0.37	0.32	0.42	0.65	-1.15	-0.11	7.4	5.42	7.67	7.85	8.00	2.20	8.08	8.18	8.25	2.48
41.0	22.5	8.39	1.55	4.93	0.39	0.45	0.39	0.35	-0.58	-0.11	7.6	5.75	7.94	8.06	8.15	1.52	8.17	8.23	8.27	1.48
41.0	23.0	7.94	0.89	4.96	0.42	0.64	0.44	0.20	-0.37	-0.13	7.6	6.40	7.81	7.86	7.89	1.04	7.88	7.90	7.92	0.88

Appendix 7. Continued.

Lat	Lon	ω	σ_ω	μ	σ_μ	λ	σ_λ	$\sigma^2_{\omega\mu}$	$\sigma^2_{\omega\lambda}$	$\sigma^2_{\mu\lambda}$	M_M	M_A	M_{50}	M_{100}	M_{200}	σ_M	M_{p50}	M_{p100}	M_{p200}	σ_{Mp}
41.0	23.5	7.63	0.53	4.47	0.71	0.84	0.57	0.20	-0.26	-0.33	7.6	6.95	7.60	7.61	7.62	0.82	7.61	7.62	7.62	0.53
41.0	24.0	7.86	0.72	4.49	0.63	0.79	0.47	0.26	-0.31	-0.24	7.6	6.88	7.82	7.84	7.85	1.00	7.84	7.85	7.85	0.71
41.0	24.5	7.90	0.73	3.41	1.33	0.87	0.53	0.65	-0.35	-0.64	7.6	7.15	7.87	7.88	7.89	1.35	7.88	7.88	7.89	0.73
41.0	25.0	7.90	0.73	3.41	1.33	0.87	0.53	0.65	-0.35	-0.64	7.6	7.15	7.87	7.88	7.89	1.35	7.88	7.88	7.89	0.73
41.0	25.5	8.72	3.06	3.49	1.57	0.41	0.54	4.08	-1.63	-0.79	7.6	4.50	7.87	8.08	8.24	3.45	8.30	8.41	8.48	2.93
41.5	21.0	7.78	2.53	4.72	0.64	0.38	0.59	1.19	-1.46	-0.32	6.9	5.22	7.20	7.33	7.44	2.34	7.48	7.55	7.61	2.34
41.5	21.5	8.21	1.97	4.87	0.50	0.41	0.46	0.66	-0.89	-0.18	7.4	5.53	7.67	7.81	7.91	1.88	7.94	8.01	8.06	1.85
41.5	22.0	8.57	2.83	5.01	0.37	0.32	0.42	0.65	-1.15	-0.11	7.4	5.42	7.67	7.85	8.00	2.20	8.08	8.18	8.25	2.48
41.5	22.5	8.39	1.55	4.93	0.39	0.45	0.39	0.35	-0.58	-0.11	7.6	5.75	7.94	8.06	8.15	1.52	8.17	8.23	8.27	1.48
41.5	23.0	7.94	0.89	4.96	0.42	0.64	0.44	0.20	-0.37	-0.13	7.6	6.40	7.81	7.86	7.89	1.04	7.88	7.90	7.92	0.88
41.5	23.5	7.63	0.53	4.47	0.71	0.84	0.57	0.20	-0.26	-0.33	7.6	6.95	7.60	7.61	7.62	0.82	7.61	7.62	7.62	0.53
41.5	24.0	7.86	0.72	4.49	0.63	0.79	0.47	0.26	-0.31	-0.24	7.6	6.88	7.82	7.84	7.85	1.00	7.84	7.85	7.85	0.71
41.5	24.5	7.90	0.73	3.41	1.33	0.87	0.53	0.65	-0.35	-0.64	7.6	7.15	7.87	7.88	7.89	1.35	7.88	7.88	7.89	0.73
41.5	25.0	7.90	0.73	3.41	1.33	0.87	0.53	0.65	-0.35	-0.64	7.6	7.15	7.87	7.88	7.89	1.35	7.88	7.88	7.89	0.73
41.5	25.5	8.72	3.06	3.49	1.57	0.41	0.54	4.08	-1.63	-0.79	7.6	4.50	7.87	8.08	8.24	3.45	8.30	8.41	8.48	2.93
42.0	21.0	7.78	2.53	4.72	0.64	0.38	0.59	1.19	-1.46	-0.32	6.9	5.22	7.20	7.33	7.44	2.34	7.48	7.55	7.61	2.34
42.0	21.5	8.21	1.97	4.87	0.50	0.41	0.46	0.66	-0.89	-0.18	7.4	5.53	7.67	7.81	7.91	1.88	7.94	8.01	8.06	1.85
42.0	22.0	8.57	2.83	5.01	0.37	0.32	0.42	0.65	-1.15	-0.11	7.4	5.42	7.67	7.85	8.00	2.20	8.08	8.18	8.25	2.48
42.0	22.5	8.39	1.55	4.93	0.39	0.45	0.39	0.35	-0.58	-0.11	7.6	5.75	7.94	8.06	8.15	1.52	8.17	8.23	8.27	1.48
42.0	23.0	7.94	0.89	4.96	0.42	0.64	0.44	0.20	-0.37	-0.13	7.6	6.40	7.81	7.86	7.89	1.04	7.88	7.90	7.92	0.88
42.0	23.5	7.63	0.53	4.47	0.71	0.84	0.57	0.20	-0.26	-0.33	7.6	6.95	7.60	7.61	7.62	0.82	7.61	7.62	7.62	0.53
42.0	24.0	7.86	0.72	4.49	0.63	0.79	0.47	0.26	-0.31	-0.24	7.6	6.88	7.82	7.84	7.85	1.00	7.84	7.85	7.85	0.71
42.0	24.5	7.90	0.73	3.41	1.33	0.87	0.53	0.65	-0.35	-0.64	7.6	7.15	7.87	7.88	7.89	1.35	7.88	7.88	7.89	0.73

Appendix 7. Continued.

Lat	Lon	ω	σ_ω	μ	σ_μ	λ	σ_λ	$\sigma^2_{\omega\mu}$	$\sigma^2_{\omega\lambda}$	$\sigma^2_{\mu\lambda}$	M_M	M_A	M_{50}	M_{100}	M_{200}	σ_M	M_{p50}	M_{p100}	M_{p200}	σ_{Mp}
42.0	25.0	7.90	0.73	3.41	1.33	0.87	0.53	0.65	-0.35	-0.64	7.6	7.15	7.87	7.88	7.89	1.35	7.88	7.88	7.89	0.73
42.0	25.5	8.72	3.06	3.49	1.57	0.41	0.54	4.08	-1.63	-0.79	7.6	4.50	7.87	8.08	8.24	3.45	8.30	8.41	8.48	2.93
42.5	21.0	8.17	4.94	4.52	1.03	0.30	0.71	4.27	-3.48	-0.66	6.9	4.88	7.14	7.33	7.48	3.93	7.58	7.69	7.78	4.30
42.5	21.5	8.34	2.44	4.55	0.86	0.41	0.54	1.64	-1.28	-0.41	7.4	5.27	7.71	7.87	7.98	2.49	8.03	8.10	8.16	2.30
42.5	22.0	8.73	3.27	4.72	0.62	0.33	0.47	1.51	-1.51	-0.24	7.4	5.21	7.75	7.95	8.11	2.70	8.20	8.31	8.39	2.91
42.5	22.5	8.28	1.40	4.45	0.72	0.53	0.45	0.70	-0.60	-0.27	7.6	5.71	7.96	8.06	8.13	1.67	8.13	8.18	8.21	1.37
42.5	23.0	8.28	1.40	4.45	0.72	0.53	0.45	0.70	-0.60	-0.27	7.6	5.71	7.96	8.06	8.13	1.67	8.13	8.18	8.21	1.37
42.5	23.5	7.83	0.69	3.45	1.38	0.92	0.56	0.63	-0.34	-0.70	7.6	7.37	7.82	7.82	7.82	1.31	7.81	7.82	7.82	0.69
42.5	24.0	7.83	0.69	3.45	1.38	0.92	0.56	0.63	-0.34	-0.70	7.6	7.37	7.82	7.82	7.82	1.31	7.81	7.82	7.82	0.69
42.5	24.5	7.79	0.67	1.09	3.52	0.90	0.66	1.71	-0.39	-2.21	7.6	6.98	7.77	7.78	7.79	1.96	7.77	7.78	7.79	0.68
42.5	25.0	7.79	0.67	1.09	3.52	0.90	0.66	1.71	-0.39	-2.21	7.6	6.98	7.77	7.78	7.79	1.96	7.77	7.78	7.79	0.68
43.0	21.0	8.17	4.94	4.52	1.03	0.30	0.71	4.27	-3.48	-0.66	6.9	4.88	7.14	7.33	7.48	3.93	7.58	7.69	7.78	4.30
43.0	21.5	8.66	3.24	4.29	1.11	0.37	0.56	2.97	-1.77	-0.56	7.4	4.98	7.79	7.99	8.14	3.18	8.21	8.31	8.39	3.02
43.0	22.0	8.52	3.15	4.43	0.82	0.35	0.52	2.05	-1.60	-0.37	7.4	5.02	7.64	7.83	7.98	2.86	8.06	8.16	8.23	2.88
43.0	22.5	8.78	2.24	4.46	0.65	0.40	0.41	1.07	-0.90	-0.23	7.6	5.28	8.06	8.24	8.37	2.19	8.42	8.51	8.58	2.10
43.0	23.0	8.78	2.24	4.46	0.65	0.40	0.41	1.07	-0.90	-0.23	7.6	5.28	8.06	8.24	8.37	2.19	8.42	8.51	8.58	2.10
43.0	23.5	8.08	0.95	3.64	1.15	0.72	0.49	0.77	-0.43	-0.50	7.6	6.30	7.97	8.01	8.04	1.53	8.02	8.04	8.06	0.95
43.0	24.0	8.08	0.95	3.64	1.15	0.72	0.49	0.77	-0.43	-0.50	7.6	6.30	7.97	8.01	8.04	1.53	8.02	8.04	8.06	0.95
43.0	24.5	8.17	1.09	2.25	2.37	0.75	0.55	2.00	-0.56	-1.23	7.6	6.09	8.06	8.11	8.14	2.23	8.12	8.14	8.15	1.10
43.0	25.0	8.17	1.09	2.25	2.37	0.75	0.55	2.00	-0.56	-1.23	7.6	6.09	8.06	8.11	8.14	2.23	8.12	8.14	8.15	1.10

Appendix 8: Site-specific magnitude $G^{(III)}$ distribution curves

Site-specific Gumbel third extreme values distribution curves and covariance error matrices, ε, for urban centres for which magnitude seismic hazard is considered for in chapters 5 and 6. Graphs show return periods, reduced variates and associated probabilities for estimated intensity extreme values.

Each figure represents seismicity contained in a 2° half-width cell centred on the city, and adopting a cut-off magnitude, M_{CUT}, extreme interval, NPER, that are specific for that city.

City	Co-ordinates	NPER	M_{CUT}	ω	σ_ω	μ	σ_μ	λ	σ_λ	$\sigma^2_{\omega\mu}$	$\sigma^2_{\omega\lambda}$	$\sigma^2_{\mu\lambda}$	X^2	NMISS	M_M
Edirne	41.67°N, 26.57°E	6	5.2	7.57	0.71	5.31	0.25	0.73	0.47	0.032	-0.305	-0.044	0.07	5	7.3
Larissa	39.63°N, 22.42°E	5	5.0	7.89	1.26	5.51	0.17	0.43	0.35	-0.006	-0.428	-0.005	0.06	4	7.6
Plovdiv	42.15°N, 24.75°E	6	5.6	7.96	1.21	4.47	1.54	0.69	0.76	1.398	-0.866	-1.070	0.03	10	7.6
Pristina	42.67°N, 21.17°E	2	4.9	7.68	1.46	5.08	0.13	0.29	0.24	0.049	-0.341	-0.011	0.04	13	7.4
Skopje	42.00°N, 21.43°E	2	5.0	7.89	1.70	5.25	0.10	0.26	0.22	0.019	-0.373	-0.005	0.03	10	7.4
Sofia	42.68°N, 23.32°E	5	5.3	7.86	0.75	4.18	0.89	0.81	0.52	0.423	-0.351	-0.394	0.05	10	7.6
Thessaloniki	40.63°N, 22.93°E	5	5.4	7.90	0.94	5.26	0.42	0.62	0.50	0.208	-0.436	-0.149	0.03	8	7.6
Tirane	41.33°N, 19.82°E	6	5.6	7.35	1.29	5.91	0.17	0.44	0.60	-0.030	-0.741	0.005	0.03	3	7.0

City	Co-ordinates	NPER	M_{CUT}	M_A	M_{25}	M_{50}	M_{100}	M_{200}	σ_M	M_{P25}	M_{P50}	M_{P100}	M_{P200}	σ_{MP}
Edirne	41.67°N, 26.57°E	6	5.2	6.70	7.49	7.52	7.54	7.55	0.73	7.53	7.55	7.56	7.56	0.70
Larissa	39.63°N, 22.42°E	5	5.0	6.01	7.42	7.54	7.63	7.70	1.06	7.66	7.72	7.77	7.80	1.18
Plovdiv	42.15°N, 24.75°E	6	5.6	6.40	7.79	7.86	7.90	7.92	2.00	7.88	7.91	7.93	7.94	1.21
Pristina	42.67°N, 21.17°E	2	4.9	5.33	6.76	6.93	7.07	7.18	1.01	7.15	7.25	7.33	7.39	1.23
Skopje	42.00°N, 21.43°E	2	5.0	5.44	6.81	6.99	7.13	7.26	1.06	7.24	7.34	7.43	7.51	1.35
Sofia	42.68°N, 23.32°E	5	5.3	6.88	7.79	7.82	7.84	7.85	1.17	7.81	7.83	7.84	7.85	0.75
Thessaloniki	40.63°N, 22.93°E	5	5.4	6.44	7.70	7.77	7.81	7.84	1.08	7.81	7.84	7.86	7.87	0.93
Tirane	41.33°N, 19.82°E	6	5.6	6.23	7.08	7.15	7.20	7.24	1.07	7.22	7.25	7.28	7.30	1.20

(ω, μ, λ) and uncertainties for a $G^{(III)}$ distribution for selected cities. M_M is maximum observed magnitude; m(1) is annual modal magnitude; M_{25}, M_{50}, M_{100} and M_{200} are modal maximums in 25, 50, 100 and 200 years. M_{P25}, M_{P50}, M_{P100} and M_{P200} are these at 90% probability of non-exceedance (σ_M and σ_{MP} are their uncertainties). $\sigma^2_{\omega\mu}$, $\sigma^2_{\omega\lambda}$ and $\sigma^2_{\mu\lambda}$ are off-diagonal elements of the covariance error matrix, ε. NMISS is number of extreme intervals of missing extreme data; X^2 is goodness of fit measure

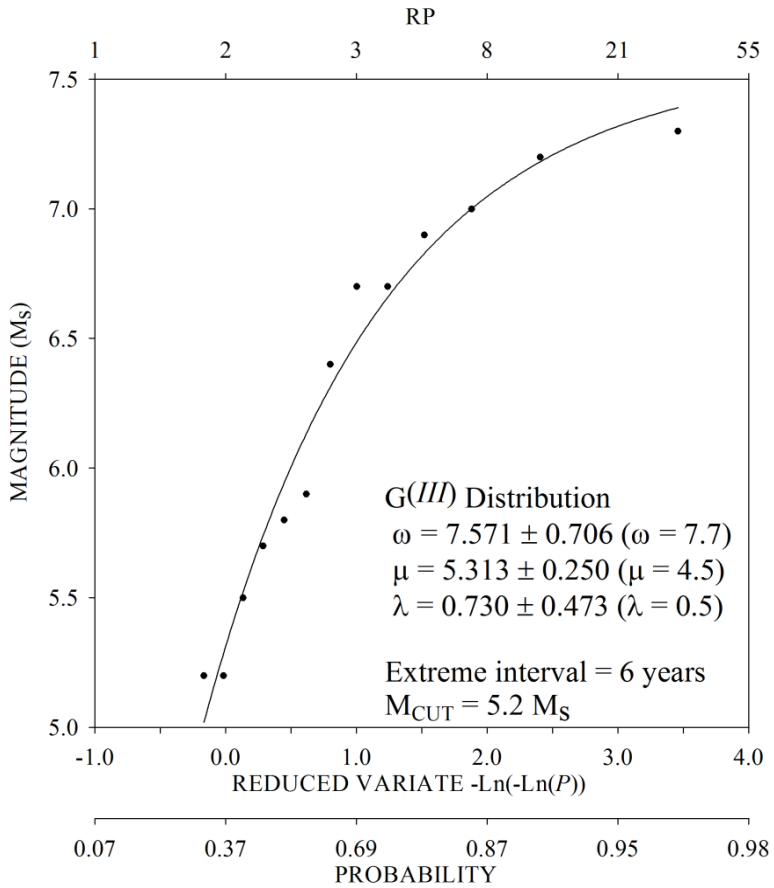

$$\varepsilon = \begin{bmatrix} 0.498 & 0.032 & -0.305 \\ 0.032 & 0.062 & -0.044 \\ -0.305 & -0.044 & 0.224 \end{bmatrix}$$

(a)

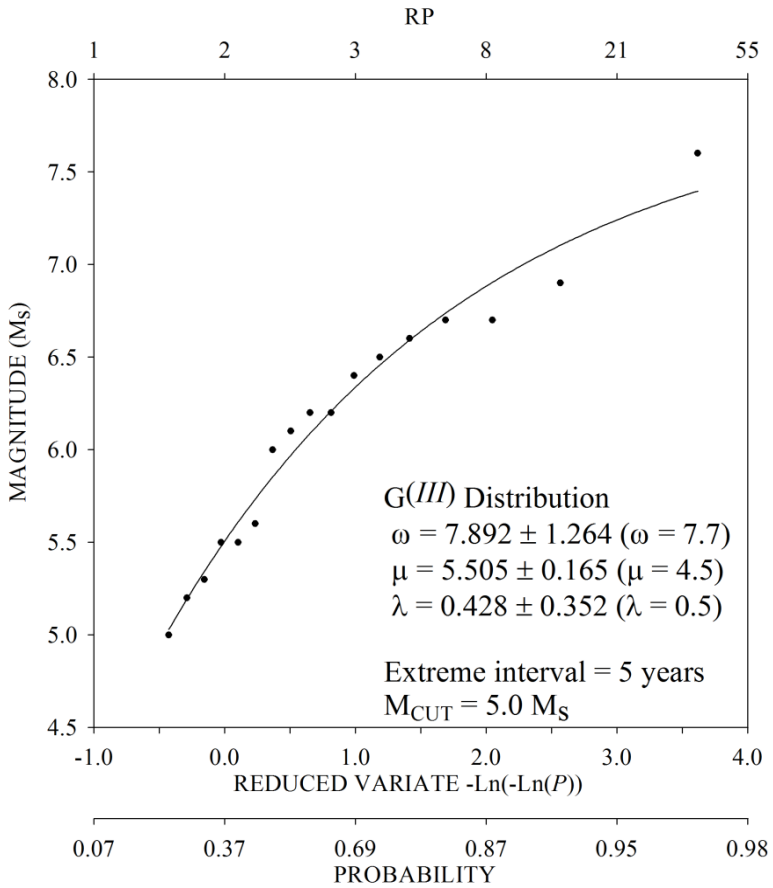

$$\varepsilon = \begin{bmatrix} 1.597 & -0.006 & -0.428 \\ -0.006 & 0.027 & -0.005 \\ -0.428 & -0.005 & 0.124 \end{bmatrix}$$

(b)

$G^{(III)}$ asymptotic extreme values distribution curves for (a) Edirne and (b) Larissa

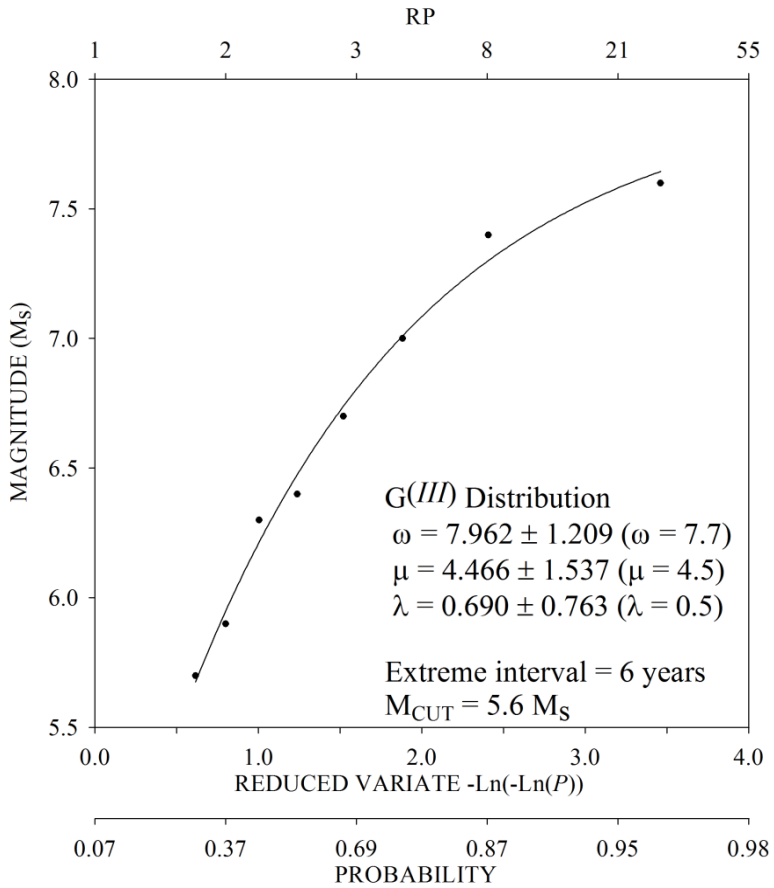

$$\varepsilon = \begin{bmatrix} 1.461 & 1.398 & -0.866 \\ 1.398 & 2.363 & -1.070 \\ -0.866 & -1.070 & 0.582 \end{bmatrix}$$

(a)

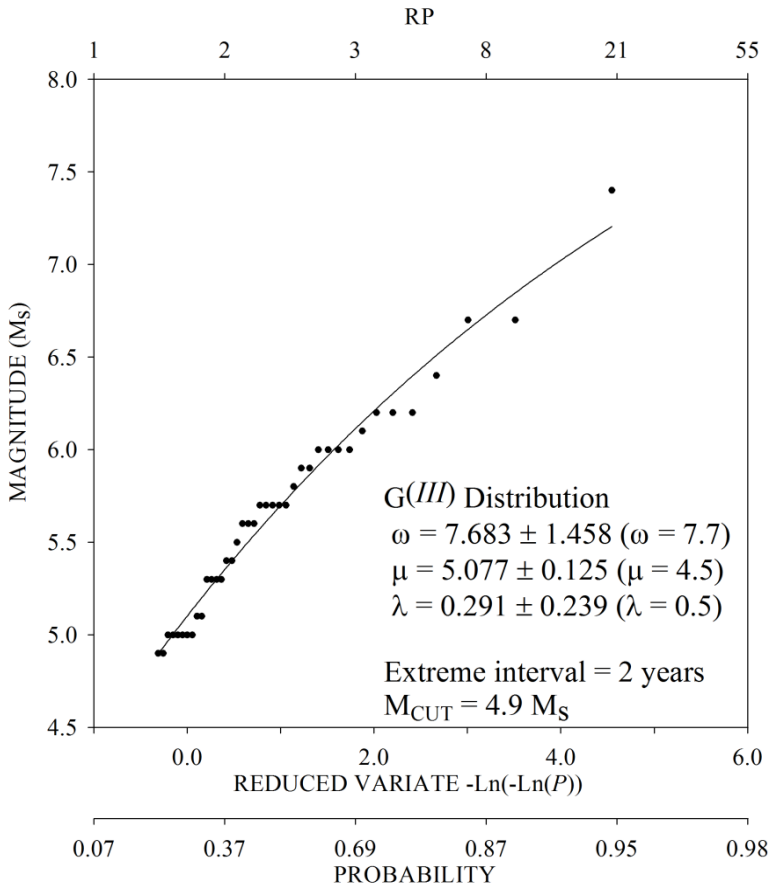

$$\varepsilon = \begin{bmatrix} 2.125 & 0.049 & -0.341 \\ 0.049 & 0.016 & -0.011 \\ -0.341 & -0.011 & 0.057 \end{bmatrix}$$

(b)

$G^{(III)}$ asymptotic extreme values distribution curves for (a) Plovdiv and (b) Pristina

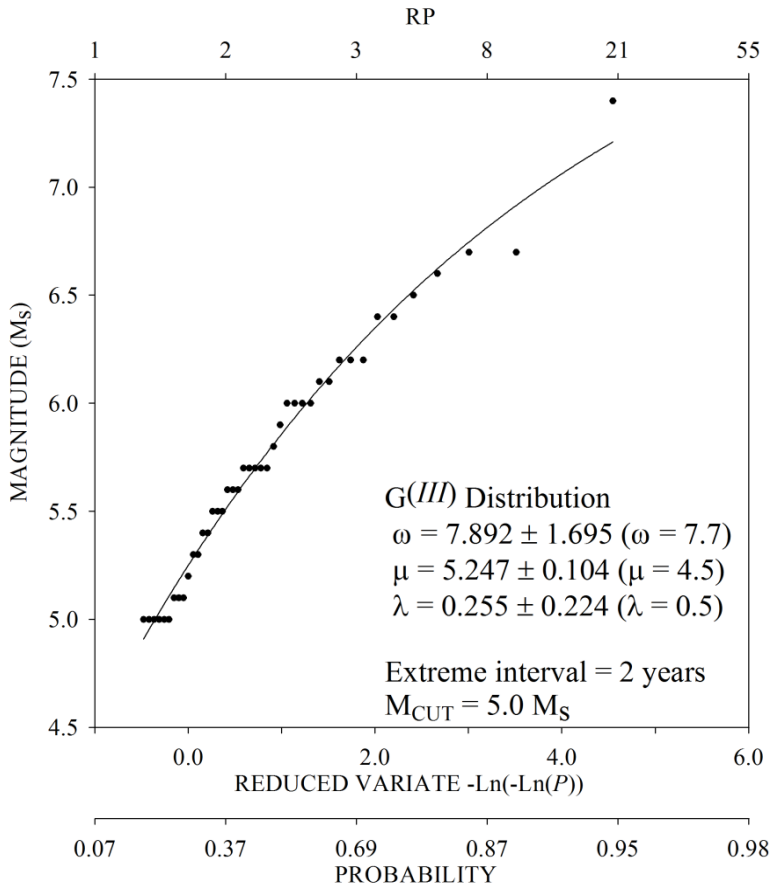

$$\varepsilon = \begin{bmatrix} 2.871 & 0.019 & -0.373 \\ 0.019 & 0.011 & -0.005 \\ -0.373 & -0.005 & 0.050 \end{bmatrix}$$

(a)

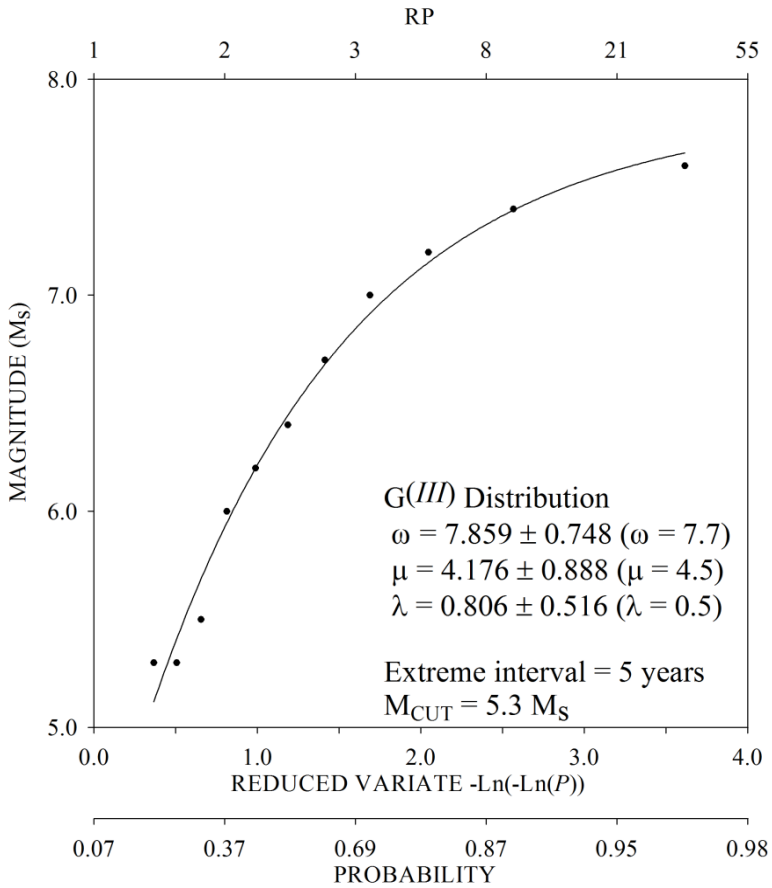

$$\varepsilon = \begin{bmatrix} 0.560 & 0.423 & -0.351 \\ 0.423 & 0.788 & -0.394 \\ -0.351 & -0.394 & 0.267 \end{bmatrix}$$

(b)

$G^{(III)}$ asymptotic extreme values distribution curves for (a) Skopje and (b) Sofia

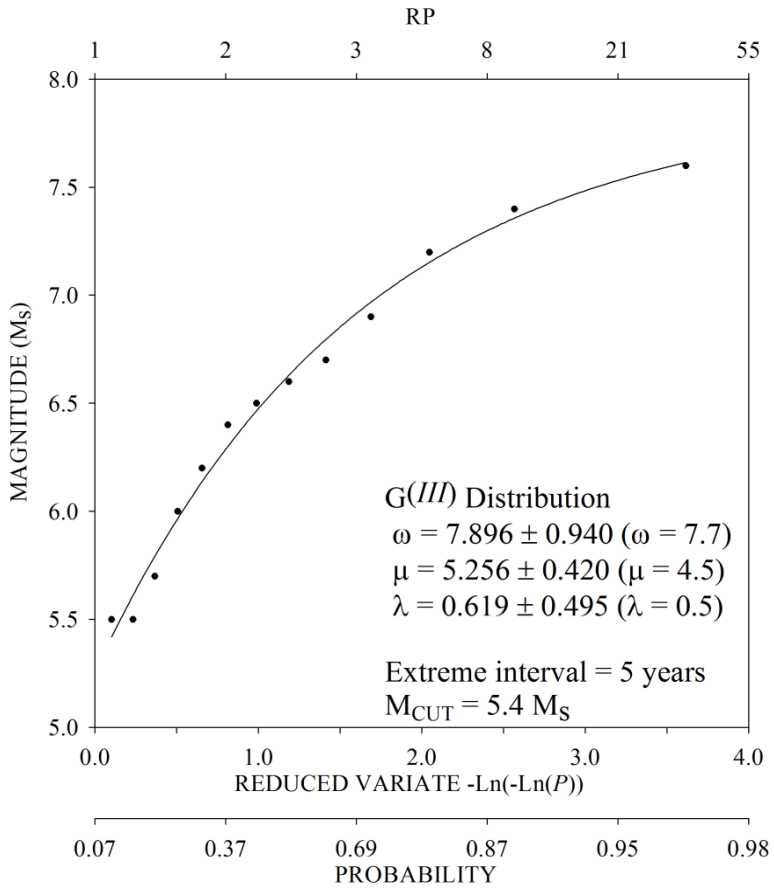

$$\varepsilon = \begin{bmatrix} 0.883 & 0.208 & -0.436 \\ 0.208 & 0.176 & -0.149 \\ -0.436 & -0.149 & 0.245 \end{bmatrix}$$

(a)

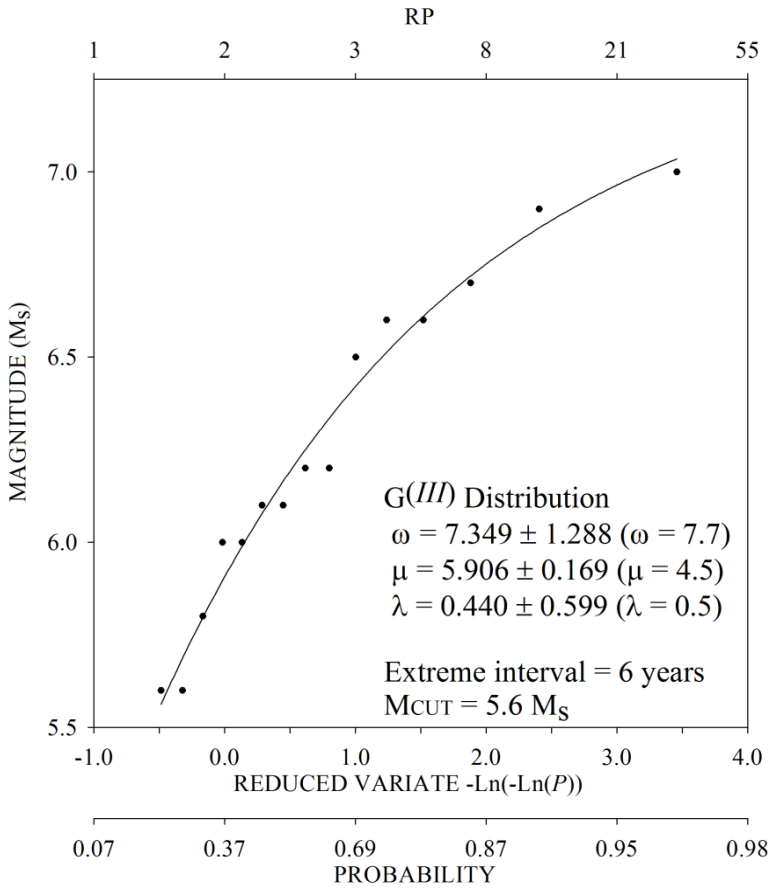

$$\varepsilon = \begin{bmatrix} 1.660 & -0.030 & -0.741 \\ -0.030 & 0.029 & 0.005 \\ -0.741 & 0.005 & 0.359 \end{bmatrix}$$

(b)

$G^{(III)}$ asymptotic extreme values distribution curves for (a) Thessaloniki and (b) Tirane

Appendix 9: Regional cellular $G^{(I)}$ peak ground acceleration estimates ($TP92_A$)

Parameters (α, μ) and uncertainties of a $G^{(I)}$ distribution for each cell used to contour ground acceleration hazard over the catalogued region. $A_{50,}$ A_{100} and A_{200} are the maximum accelerations expected in 50-, 100- and 200-year time intervals respectively. A_{P50}, A_{P100} and A_{P200} are the ground accelerations expected to be extremes with 90% probability of non-exceedance in the 50-, 100- and 200-year time intervals (a 1 in 10 chance of exceedance). σ_{PA} is uncertainty on A_{P50} only. Forecasts were obtained using earthquake data of 4-year extreme intervals, $M_s \geq 5.5$ and time interval 1900 to 2004. Estimates are obtained using Theodulidis and Papazachos (1992) for stiff soil conditions (S = 0.5) at the 50^{th} percentile (P = 0). Forecasted accelerations are given in units of cm s^{-2}.

Lat	Lon	α	σ_α	μ	σ_μ	A_{50}	A_{100}	A_{200}	A_{P50}	σ_{PA}	A_{P100}	A_{P200}
39.0	19.0	-3.300	0.243	0.112	0.139	31.775	37.990	44.205	51.952	0.363	58.167	64.381
39.0	19.5	-6.214	0.243	0.079	0.139	43.614	52.442	61.271	72.277	0.358	81.105	89.934
39.0	20.0	-6.031	0.224	0.068	0.132	51.547	61.749	71.951	84.669	0.337	94.871	105.073
39.0	20.5	-5.205	0.224	0.069	0.132	51.270	61.277	71.283	83.757	0.356	93.764	103.770
39.0	21.0	-2.550	0.207	0.076	0.126	49.166	58.329	67.492	78.915	0.338	88.079	97.242
39.0	21.5	-11.717	0.192	0.041	0.121	84.435	101.472	118.508	139.746	0.298	156.782	173.819
39.0	22.0	-19.878	0.243	0.035	0.139	92.086	111.924	131.762	156.492	0.376	176.330	196.169
39.0	22.5	-19.085	0.243	0.036	0.139	88.410	107.457	126.503	150.246	0.379	169.293	188.339
39.0	24.5	-81.503	0.359	0.012	0.176	238.415	295.100	351.784	422.446	0.537	479.130	535.815
39.0	25.0	-123.206	0.359	0.009	0.176	295.173	369.303	443.433	535.843	0.543	609.973	684.103
39.0	25.5	-125.067	0.404	0.010	0.189	260.851	329.230	397.608	482.849	0.586	551.227	619.606
39.0	26.0	-31.338	0.359	0.028	0.176	109.983	135.023	160.062	191.277	0.542	216.317	241.357
39.0	26.5	-13.004	0.404	0.047	0.189	69.943	84.640	99.337	117.658	0.608	132.355	147.052
39.0	27.0	-13.699	0.404	0.051	0.189	62.710	76.249	89.787	106.664	0.608	120.203	133.741
39.0	27.5	-16.065	0.404	0.051	0.189	60.162	73.668	87.174	104.011	0.608	117.517	131.023
39.0	28.0	-18.069	0.404	0.047	0.189	65.794	80.653	95.512	114.035	0.604	128.894	143.753
39.5	19.0	-2.179	0.192	0.081	0.121	45.954	54.482	63.011	73.642	0.300	82.170	90.699
39.5	19.5	-9.160	0.179	0.041	0.116	86.260	103.167	120.073	141.149	0.271	158.056	174.963
39.5	20.0	-25.056	0.179	0.021	0.116	163.101	196.439	229.777	271.337	0.263	304.675	338.013
39.5	20.5	-8.284	0.179	0.036	0.116	98.961	117.963	136.965	160.653	0.286	179.655	198.657
39.5	21.0	-9.414	0.167	0.031	0.111	115.608	137.760	159.911	187.526	0.274	209.677	231.829
39.5	21.5	-0.429	0.156	0.052	0.107	74.603	87.897	101.192	117.765	0.267	131.059	144.353
39.5	22.0	-0.331	0.192	0.064	0.121	60.876	71.720	82.565	96.085	0.320	106.929	117.774
39.5	22.5	-7.672	0.207	0.044	0.126	81.037	96.755	112.472	132.066	0.338	147.784	163.501

Appendix 9. Continued.

Lat	Lon	α	σ_α	μ	σ_μ	A_{50}	A_{100}	A_{200}	A_{P50}	σ_{PA}	A_{P100}	A_{P200}
39.5	23.0	-48.061	0.404	0.021	0.189	135.171	167.636	200.102	240.573	0.594	273.039	305.505
39.5	23.5	-13.295	0.404	0.040	0.189	84.202	101.477	118.752	140.286	0.603	157.561	174.836
39.5	24.0	-36.725	0.404	0.023	0.189	134.367	164.682	194.997	232.787	0.581	263.102	293.417
39.5	24.5	-77.356	0.359	0.013	0.176	228.883	283.144	337.405	405.046	0.541	459.307	513.567
39.5	25.0	-247.871	0.359	0.005	0.176	529.582	667.334	805.087	976.808	0.531	1114.560	1252.312
39.5	25.5	-94.959	0.404	0.012	0.189	242.649	302.467	362.286	436.855	0.593	496.674	556.492
39.5	26.0	-16.266	0.359	0.030	0.176	113.786	136.830	159.873	188.599	0.548	211.642	234.685
39.5	26.5	-13.415	0.404	0.036	0.189	94.666	113.816	132.966	156.838	0.609	175.988	195.139
39.5	27.0	-42.283	0.404	0.023	0.189	127.987	158.156	188.325	225.934	0.596	256.103	286.272
39.5	27.5	-50.942	0.404	0.021	0.189	134.614	167.491	200.369	241.354	0.594	274.231	307.108
39.5	28.0	-27.638	0.404	0.031	0.189	99.801	122.381	144.961	173.110	0.607	195.690	218.270
40.0	19.0	0.481	0.192	0.069	0.121	56.850	66.838	76.826	89.277	0.319	99.265	109.253
40.0	19.5	-7.076	0.179	0.031	0.116	119.214	141.590	163.967	191.861	0.297	214.238	236.614
40.0	20.0	-19.217	0.179	0.018	0.116	199.601	238.372	277.143	325.475	0.284	364.246	403.017
40.0	20.5	-4.676	0.179	0.023	0.116	164.919	194.969	225.019	262.478	0.303	292.528	322.577
40.0	21.0	2.254	0.167	0.037	0.111	107.251	125.855	144.459	167.650	0.290	186.254	204.857
40.0	21.5	-6.111	0.156	0.029	0.107	128.357	152.182	176.008	205.709	0.246	229.534	253.360
40.0	22.0	-6.717	0.179	0.037	0.116	99.328	118.117	136.906	160.329	0.274	179.118	197.908
40.0	22.5	0.672	0.207	0.062	0.126	64.270	75.538	86.807	100.854	0.345	112.122	123.391
40.0	23.0	-1.653	0.359	0.056	0.176	68.463	80.886	93.309	108.796	0.547	121.219	133.643
40.0	23.5	-15.149	0.359	0.035	0.176	95.114	114.651	134.187	158.542	0.543	178.079	197.616
40.0	24.0	-71.742	0.359	0.015	0.176	191.340	237.954	284.568	342.676	0.539	389.290	435.904
40.0	24.5	-235.942	0.322	0.005	0.164	527.298	662.532	797.766	966.347	0.457	1101.581	1236.815

Appendix 9. Continued.

Lat	Lon	α	σ_α	μ	σ_μ	A_{50}	A_{100}	A_{200}	A_{P50}	σ_{PA}	A_{P100}	A_{P200}
40.0	25.0	-71.746	0.322	0.013	0.164	225.604	278.289	330.975	396.652	0.483	449.338	502.024
40.0	25.5	-1.230	0.404	0.034	0.189	114.904	135.481	156.058	181.709	0.606	202.286	222.863
40.0	26.0	-7.268	0.404	0.032	0.189	113.441	134.829	156.216	182.878	0.605	204.265	225.653
40.5	19.0	4.611	0.156	0.049	0.107	84.176	98.274	112.371	129.945	0.270	144.043	158.141
40.5	19.5	8.691	0.147	0.031	0.102	135.773	158.290	180.807	208.877	0.260	231.394	253.910
40.5	20.0	12.276	0.138	0.027	0.099	155.331	180.678	206.025	237.623	0.245	262.970	288.317
40.5	20.5	1.789	0.138	0.016	0.099	243.780	286.657	329.534	382.984	0.240	425.861	468.738
40.5	21.0	9.118	0.138	0.033	0.099	126.848	147.708	168.568	194.571	0.247	215.431	236.291
40.5	21.5	4.728	0.138	0.043	0.099	94.753	110.704	126.655	146.539	0.240	162.490	178.441
40.5	22.0	-0.251	0.167	0.045	0.111	86.741	102.155	117.569	136.783	0.283	152.197	167.610
40.5	22.5	-0.041	0.207	0.048	0.126	82.193	96.764	111.335	129.498	0.341	144.069	158.639
40.5	23.0	-21.012	0.265	0.027	0.146	124.759	150.587	176.415	208.612	0.419	234.441	260.269
40.5	23.5	-51.596	0.322	0.017	0.164	174.990	215.137	255.285	305.332	0.495	345.479	385.627
40.5	24.0	-74.938	0.322	0.014	0.164	208.526	258.751	308.976	371.586	0.483	421.811	472.036
40.5	24.5	-50.647	0.291	0.017	0.155	182.428	223.726	265.023	316.504	0.445	357.801	399.098
40.5	25.0	-28.795	0.291	0.022	0.155	145.211	176.042	206.873	245.307	0.452	276.138	306.969
40.5	25.5	-8.689	0.359	0.031	0.176	116.759	138.986	161.213	188.922	0.537	211.149	233.376
40.5	26.0	-150.225	0.359	0.007	0.176	376.644	469.996	563.349	679.721	0.526	773.074	866.427
40.5	26.5	-90.457	0.404	0.011	0.189	251.279	311.829	372.379	447.860	0.602	508.410	568.960
40.5	27.0	-385.439	0.404	0.004	0.189	719.493	915.269	1111.045	1355.098	0.569	1550.874	1746.650
40.5	27.5	-138.631	0.404	0.008	0.189	366.582	456.098	545.613	657.203	0.608	746.718	836.234
41.0	19.0	12.452	0.156	0.087	0.107	57.277	65.219	73.162	83.062	0.272	91.005	98.947
41.0	19.5	15.816	0.147	0.032	0.102	136.855	158.302	179.748	206.482	0.261	227.929	249.375

Appendix 9. Continued.

Lat	Lon	α	σ_α	μ	σ_μ	A_{50}	A_{100}	A_{200}	A_{P50}	σ_{PA}	A_{P100}	A_{P200}
41.0	20.0	10.048	0.138	0.018	0.099	229.731	268.656	307.580	356.103	0.242	395.027	433.951
41.0	20.5	5.860	0.138	0.015	0.099	263.860	309.574	355.287	412.273	0.242	457.987	503.700
41.0	21.0	5.743	0.138	0.026	0.099	159.087	186.257	213.427	247.298	0.240	274.468	301.638
41.0	21.5	9.244	0.138	0.059	0.099	75.405	87.128	98.850	113.464	0.248	125.186	136.909
41.0	22.0	-3.716	0.167	0.033	0.111	113.176	133.887	154.598	180.417	0.284	201.128	221.840
41.0	22.5	-23.287	0.207	0.019	0.126	177.620	213.218	248.815	293.191	0.340	328.789	364.386
41.0	23.0	-32.364	0.265	0.019	0.146	171.378	207.477	243.577	288.579	0.419	324.678	360.778
41.0	23.5	-112.774	0.322	0.010	0.164	298.985	371.942	444.899	535.846	0.484	608.803	681.760
41.0	24.0	-16.341	0.322	0.042	0.164	77.901	94.600	111.298	132.114	0.500	148.812	165.511
41.0	24.5	-7.341	0.291	0.054	0.155	64.703	77.468	90.233	106.146	0.456	118.911	131.676
41.0	25.0	-1.521	0.291	0.063	0.155	60.573	71.575	82.577	96.292	0.458	107.294	118.295
41.0	25.5	-6.784	0.322	0.051	0.164	69.974	83.574	97.174	114.128	0.493	127.728	141.328
41.0	26.0	-15.911	0.322	0.035	0.164	95.638	115.402	135.167	159.805	0.494	179.570	199.334
41.0	26.5	-42.243	0.359	0.021	0.176	141.292	173.811	206.331	246.869	0.537	279.389	311.908
41.0	27.0	-73.953	0.359	0.014	0.176	195.974	243.800	291.627	351.247	0.526	399.074	446.901
41.0	27.5	-52.146	0.359	0.019	0.176	155.471	192.257	229.043	274.901	0.548	311.687	348.473
41.0	28.0	-25.130	0.404	0.032	0.189	97.839	119.628	141.416	168.577	0.600	190.365	212.153
41.5	19.0	4.389	0.156	0.048	0.107	86.156	100.644	115.132	133.193	0.269	147.680	162.168
41.5	19.5	13.136	0.147	0.037	0.102	117.536	136.034	154.532	177.591	0.259	196.089	214.587
41.5	20.0	19.021	0.138	0.045	0.099	105.394	120.698	136.002	155.079	0.247	170.383	185.687
41.5	20.5	3.295	0.138	0.019	0.099	205.566	241.406	277.245	321.922	0.238	357.761	393.600
41.5	21.0	13.780	0.138	0.061	0.099	77.429	88.706	99.984	114.042	0.248	125.320	136.597
41.5	21.5	9.045	0.138	0.065	0.099	68.970	79.588	90.205	103.441	0.246	114.059	124.677

Appendix 9. Continued.

Lat	Lon	α	σ_α	μ	σ_μ	A_{50}	A_{100}	A_{200}	A_{P50}	σ_{PA}	A_{P100}	A_{P200}
41.5	22.0	-8.926	0.179	0.031	0.116	116.458	138.674	160.890	188.584	0.295	210.800	233.016
41.5	22.5	-50.405	0.224	0.015	0.132	216.651	263.970	311.288	370.274	0.349	417.592	464.910
41.5	23.0	-115.317	0.322	0.010	0.164	274.441	343.500	412.558	498.647	0.469	567.705	636.764
41.5	24.0	-47.866	0.404	0.025	0.189	108.826	136.589	164.353	198.962	0.599	226.726	254.489
41.5	24.5	-26.655	0.359	0.036	0.176	83.397	102.896	122.396	146.704	0.540	166.203	185.703
41.5	25.0	-27.285	0.359	0.035	0.176	85.842	105.886	125.931	150.918	0.543	170.962	191.006
41.5	25.5	-23.803	0.404	0.039	0.189	75.250	92.800	110.351	132.230	0.608	149.780	167.331
41.5	26.0	-11.387	0.359	0.052	0.176	64.514	77.962	91.411	108.175	0.546	121.624	135.072
41.5	26.5	-11.164	0.322	0.049	0.164	68.255	82.326	96.398	113.940	0.496	128.011	142.083
41.5	27.0	-13.523	0.291	0.046	0.155	71.662	86.755	101.849	120.664	0.451	135.757	150.851
41.5	27.5	-13.761	0.291	0.049	0.155	66.214	80.384	94.555	112.219	0.455	126.389	140.560
41.5	28.0	-12.829	0.359	0.057	0.176	56.000	68.195	80.390	95.593	0.547	107.788	119.983
42.0	19.0	-66.282	0.156	0.008	0.107	428.312	515.946	603.580	712.824	0.232	800.458	888.092
42.0	19.5	-49.669	0.147	0.008	0.102	470.677	562.874	655.070	770.002	0.236	862.199	954.396
42.0	20.0	4.146	0.138	0.032	0.099	128.063	150.018	171.974	199.345	0.242	221.300	243.256
42.0	20.5	10.029	0.138	0.054	0.099	83.067	96.008	108.949	125.082	0.247	138.023	150.964
42.0	21.0	5.439	0.138	0.049	0.099	85.209	99.343	113.477	131.096	0.232	145.230	159.364
42.0	21.5	-9.748	0.138	0.021	0.099	174.114	206.691	239.268	279.879	0.216	312.456	345.034
42.0	22.0	-6.226	0.192	0.041	0.121	88.268	105.011	121.753	142.625	0.318	159.368	176.110
42.0	22.5	-38.150	0.243	0.021	0.139	147.655	180.576	213.498	254.537	0.368	287.459	320.380
42.0	23.0	-198.642	0.359	0.007	0.176	392.124	496.798	601.472	731.958	0.504	836.632	941.306
42.0	24.0	-55.119	0.404	0.022	0.189	119.836	150.836	181.835	220.478	0.594	251.478	282.477
42.0	24.5	-63.901	0.359	0.019	0.176	144.003	180.840	217.678	263.599	0.527	300.436	337.273

Appendix 9. Continued.

Lat	Lon	α	σ_α	μ	σ_μ	A_{50}	A_{100}	A_{200}	A_{P50}	σ_{PA}	A_{P100}	A_{P200}
42.0	25.0	-188.385	0.359	0.007	0.176	357.717	454.477	551.238	671.859	0.497	768.619	865.379
42.0	26.0	-44.670	0.322	0.023	0.164	122.523	152.147	181.771	218.700	0.470	248.324	277.947
42.0	26.5	-4.465	0.291	0.071	0.155	50.556	60.305	70.054	82.207	0.454	91.955	101.704
42.0	27.0	-1.829	0.291	0.084	0.155	44.877	53.152	61.428	71.744	0.457	80.020	88.295
42.0	27.5	-3.461	0.291	0.087	0.155	41.407	49.357	57.307	67.218	0.459	75.168	83.117
42.0	28.0	-5.737	0.359	0.085	0.176	40.414	48.591	56.769	66.962	0.547	75.139	83.317
42.5	19.0	-10.168	0.179	0.038	0.116	92.734	110.967	129.199	151.928	0.287	170.160	188.393
42.5	19.5	-4.617	0.167	0.041	0.111	90.413	107.250	124.088	145.078	0.277	161.916	178.753
42.5	20.0	2.746	0.156	0.064	0.107	64.145	75.024	85.903	99.465	0.267	110.344	121.223
42.5	20.5	7.382	0.156	0.107	0.107	44.040	50.535	57.030	65.127	0.275	71.622	78.117
42.5	21.0	4.152	0.156	0.069	0.107	60.570	70.566	80.562	93.023	0.272	103.020	113.016
42.5	21.5	-11.827	0.156	0.025	0.107	142.396	169.722	197.048	231.112	0.257	258.438	285.764
42.5	22.0	-4.201	0.207	0.057	0.126	64.894	77.136	89.379	104.640	0.342	116.883	129.125
42.5	22.5	-22.424	0.265	0.035	0.146	89.669	109.530	129.391	154.149	0.398	174.010	193.871
42.5	23.0	-50.079	0.404	0.025	0.189	109.623	137.919	166.216	201.490	0.589	229.786	258.083
43.0	19.0	-3.440	0.207	0.091	0.126	39.758	47.412	55.066	64.607	0.333	72.261	79.915
43.0	19.5	-1.270	0.192	0.094	0.121	40.168	47.510	54.852	64.005	0.319	71.347	78.689
43.0	20.0	1.460	0.179	0.111	0.116	36.814	43.078	49.342	57.151	0.305	63.415	69.680
43.0	20.5	1.686	0.167	0.097	0.111	41.998	49.140	56.282	65.186	0.286	72.329	79.471
43.0	21.0	0.354	0.167	0.081	0.111	48.590	57.137	65.683	76.338	0.277	84.884	93.431
43.0	21.5	0.900	0.179	0.099	0.116	40.315	47.298	54.282	62.988	0.305	69.972	76.955
43.0	22.0	-6.847	0.243	0.068	0.139	50.674	60.866	71.058	83.763	0.376	93.955	104.146
43.0	22.5	-47.676	0.322	0.024	0.164	116.352	145.415	174.478	210.708	0.451	239.771	268.834

Appendix 9. Continued.

Lat	Lon	α	σ_α	μ	σ_μ	A_{50}	A_{100}	A_{200}	A_{P50}	σ_{PA}	A_{P100}	A_{P200}
43.5	19.0	-3.581	0.404	0.133	0.189	25.820	31.029	36.239	42.733	0.607	47.942	53.151
43.5	19.5	-0.279	0.404	0.144	0.189	26.892	31.707	36.521	42.523	0.605	47.337	52.151
43.5	20.0	-0.666	0.359	0.118	0.176	32.443	38.309	44.175	51.488	0.535	57.355	63.221
43.5	20.5	-13.712	0.322	0.055	0.164	57.534	70.158	82.782	98.518	0.494	111.142	123.765
43.5	21.0	-25.410	0.322	0.038	0.164	78.778	97.239	115.699	138.712	0.471	157.172	175.633
43.5	21.5	-6.879	0.322	0.086	0.164	38.422	46.449	54.475	64.481	0.500	72.508	80.535
43.5	22.0	-7.235	0.404	0.098	0.189	32.685	39.758	46.832	55.649	0.600	62.722	69.796
44.0	20.0	-19.970	0.404	0.051	0.189	56.514	70.066	83.618	100.512	0.604	114.064	127.615
44.0	20.5	-90.378	0.359	0.014	0.176	184.762	233.513	282.263	343.035	0.515	391.785	440.536
44.0	21.0	-16.874	0.359	0.053	0.176	56.760	69.807	82.853	99.117	0.546	112.164	125.211
44.0	21.5	-3.602	0.359	0.121	0.176	28.600	34.305	40.011	47.123	0.536	52.829	58.535

Appendix 10: Southwest zone cellular $G^{(I)}$ peak ground acceleration estimates ($TP92_A$)

Parameters (α, μ) and uncertainties of a $G^{(I)}$ distribution for each cell used to contour ground acceleration hazard over the southwest zone. $A_{50,}$ A_{100} and A_{200} are the maximum accelerations expected in 50-, 100- and 200-year time intervals respectively. A_{P50}, A_{P100} and A_{P200} are the ground accelerations expected to be extremes with 90% probability of non-exceedance in the 50-, 100- and 200-year time intervals (a 1 in 10 chance of exceedance). σ_{PA} is uncertainty on A_{P50} only. Forecasts were obtained using earthquake data of 5-year extreme intervals, $M_s \geq 5.3$ and time interval 1900 to 2004. Estimates are obtained using Theodulidis and Papazachos (1992) stiff soil conditions (S = 0.5) at the 50^{th} percentile P = 0). Forecasted accelerations are given in units of cm s^{-2}.

Lat	Lon	α	σ_α	μ	σ_μ	A_{50}	A_{100}	A_{200}	A_{P50}	σ_{PA}	A_{P100}	A_{P200}
40.0	21.0	-8.467	0.351	0.056	0.186	61.929	74.402	86.875	80.480	0.363	92.953	105.426
40.0	21.5	-10.960	0.470	0.051	0.223	65.672	79.251	92.829	85.867	0.471	99.445	113.023
40.0	22.0	-15.404	0.470	0.042	0.223	78.271	94.869	111.466	102.957	0.469	119.555	136.152
40.0	22.5	-8.467	0.351	0.056	0.186	61.929	74.402	86.875	80.480	0.363	92.953	105.426
40.0	23.0	-10.960	0.470	0.051	0.223	65.672	79.251	92.829	85.867	0.471	99.445	113.023
40.0	23.5	-15.404	0.470	0.042	0.223	78.271	94.869	111.466	102.957	0.469	119.555	136.152
40.0	24.0	-8.467	0.351	0.056	0.186	61.929	74.402	86.875	80.480	0.363	92.953	105.426
40.0	24.5	-10.960	0.470	0.051	0.223	65.672	79.251	92.829	85.867	0.471	99.445	113.023
40.0	25.0	-15.404	0.470	0.042	0.223	78.271	94.869	111.466	102.957	0.469	119.555	136.152
40.0	25.5	-8.467	0.351	0.056	0.186	61.929	74.402	86.875	80.480	0.363	92.953	105.426
40.5	21.0	-10.960	0.470	0.051	0.223	65.672	79.251	92.829	85.867	0.471	99.445	113.023
40.5	21.5	-15.404	0.470	0.042	0.223	78.271	94.869	111.466	102.957	0.469	119.555	136.152
40.5	22.0	-8.467	0.351	0.056	0.186	61.929	74.402	86.875	80.480	0.363	92.953	105.426
40.5	22.5	-10.960	0.470	0.051	0.223	65.672	79.251	92.829	85.867	0.471	99.445	113.023
40.5	23.0	-15.404	0.470	0.042	0.223	78.271	94.869	111.466	102.957	0.469	119.555	136.152
40.5	23.5	-8.467	0.351	0.056	0.186	61.929	74.402	86.875	80.480	0.363	92.953	105.426
40.5	24.0	-10.960	0.470	0.051	0.223	65.672	79.251	92.829	85.867	0.471	99.445	113.023
40.5	24.5	-15.404	0.470	0.042	0.223	78.271	94.869	111.466	102.957	0.469	119.555	136.152
40.5	25.0	-8.467	0.351	0.056	0.186	61.929	74.402	86.875	80.480	0.363	92.953	105.426
40.5	25.5	-10.960	0.470	0.051	0.223	65.672	79.251	92.829	85.867	0.471	99.445	113.023
41.0	21.0	24.913	0.120	0.029	0.091	158.943	182.691	206.439	194.264	0.143	218.012	241.760
41.0	21.5	20.959	0.120	0.062	0.091	83.762	94.889	106.017	100.312	0.149	111.440	122.567
41.0	22.0	11.754	0.137	0.036	0.103	119.898	139.059	158.221	148.397	0.167	167.558	186.720
41.0	22.5	0.451	0.172	0.021	0.120	190.907	224.652	258.398	241.097	0.204	274.843	308.588

Appendix 10. Continued.

Lat	Lon	α	σ_α	μ	σ_μ	A_{50}	A_{100}	A_{200}	A_{P50}	σ_{PA}	A_{P100}	A_{P200}
41.0	23.0	-4.871	0.204	0.021	0.134	185.502	219.233	252.965	235.671	0.235	269.402	303.133
41.0	23.5	-35.298	0.204	0.012	0.134	299.039	358.278	417.517	387.146	0.227	446.385	505.624
41.0	24.0	3.182	0.204	0.045	0.134	89.969	105.346	120.723	112.840	0.237	128.217	143.594
41.0	24.5	1.377	0.224	0.056	0.141	71.502	83.927	96.353	89.982	0.253	102.408	114.833
41.0	25.0	4.244	0.224	0.064	0.141	65.473	76.321	87.170	81.608	0.254	92.457	103.306
41.0	25.5	1.873	0.187	0.055	0.127	72.610	85.143	97.677	91.251	0.219	103.784	116.318
41.5	21.0	21.590	0.120	0.070	0.091	77.705	87.648	97.590	92.493	0.150	102.435	112.378
41.5	21.5	17.914	0.120	0.070	0.091	74.021	83.962	93.904	88.807	0.149	98.748	108.689
41.5	22.0	8.630	0.137	0.033	0.103	128.215	149.403	170.592	159.729	0.166	180.917	202.106
41.5	22.5	-16.228	0.172	0.015	0.120	251.411	298.833	346.254	321.942	0.198	369.363	416.784
41.5	23.0	-51.575	0.204	0.010	0.134	353.222	424.946	496.669	459.898	0.226	531.621	603.345
41.5	23.5	-45.157	0.248	0.013	0.150	254.990	308.171	361.352	334.087	0.267	387.268	440.449
41.5	24.0	-16.073	0.276	0.026	0.160	137.142	164.290	191.437	177.519	0.302	204.667	231.814
41.5	24.5	-11.372	0.309	0.036	0.172	96.780	115.943	135.106	125.281	0.330	144.444	163.607
41.5	25.0	-13.332	0.309	0.036	0.172	94.135	113.176	132.217	122.455	0.331	141.496	160.538
41.5	25.5	-7.931	0.248	0.047	0.150	76.024	90.899	105.775	98.148	0.276	113.024	127.899
42.0	21.0	15.179	0.120	0.055	0.091	85.902	98.433	110.964	104.540	0.139	117.071	129.602
42.0	21.5	11.448	0.120	0.023	0.091	178.752	208.396	238.040	222.842	0.130	252.486	282.129
42.0	22.0	6.278	0.147	0.040	0.108	103.805	121.085	138.365	129.506	0.178	146.786	164.067
42.0	22.5	-18.403	0.187	0.018	0.127	199.098	237.635	276.173	256.415	0.211	294.953	333.491
42.0	23.0	-102.902	0.224	0.006	0.141	522.496	633.307	744.117	687.307	0.241	798.117	908.927
42.0	23.5	-61.707	0.248	0.011	0.150	306.271	371.471	436.671	403.244	0.264	468.444	533.644
42.0	24.0	-20.279	0.276	0.022	0.160	161.178	193.329	225.481	208.997	0.298	241.149	273.300

Appendix 10. Continued.

Lat	Lon	α	σ_α	μ	σ_μ	A_{50}	A_{100}	A_{200}	A_{P50}	σ_{PA}	A_{P100}	A_{P200}
42.0	24.5	-38.358	0.309	0.019	0.172	170.054	206.982	243.909	224.977	0.330	261.904	298.832
42.0	25.0	-139.041	0.309	0.007	0.172	401.739	497.556	593.374	544.250	0.304	640.067	735.885
42.0	25.5	-52.832	0.309	0.017	0.172	174.067	214.270	254.473	233.862	0.303	274.065	314.267
42.5	21.0	10.268	0.129	0.075	0.098	62.559	71.824	81.089	76.339	0.159	85.604	94.869
42.5	21.5	6.391	0.129	0.028	0.098	146.872	171.763	196.653	183.892	0.149	208.783	233.674
42.5	22.0	5.993	0.147	0.054	0.108	77.872	90.607	103.343	96.814	0.180	109.550	122.285
42.5	22.5	-11.805	0.204	0.029	0.134	121.935	145.631	169.328	157.179	0.228	180.876	204.572
42.5	23.0	-28.488	0.276	0.023	0.160	142.307	172.570	202.832	187.317	0.297	217.579	247.841
42.5	23.5	-26.967	0.309	0.025	0.172	130.052	157.874	185.695	171.432	0.329	199.253	227.074
42.5	24.0	-16.830	0.351	0.032	0.186	103.629	124.972	146.315	135.373	0.363	156.716	178.060
42.5	24.5	-40.374	0.470	0.023	0.223	131.153	161.544	191.936	176.355	0.471	206.746	237.138
42.5	25.0	-76.358	0.470	0.015	0.223	183.009	228.965	274.920	251.360	0.452	297.315	343.271
42.5	25.5	-56.942	0.470	0.021	0.223	129.835	162.929	196.023	179.057	0.466	212.151	245.245
43.0	21.0	6.681	0.129	0.093	0.098	48.871	56.347	63.823	59.990	0.152	67.466	74.941
43.0	21.5	6.144	0.137	0.101	0.103	44.901	51.768	58.635	55.114	0.168	61.981	68.848
43.0	22.0	1.628	0.159	0.067	0.114	59.996	70.338	80.680	75.378	0.188	85.720	96.061
43.0	22.5	-18.791	0.204	0.027	0.134	126.483	152.223	177.964	164.767	0.218	190.507	216.248
43.0	23.0	-30.692	0.276	0.026	0.160	121.996	149.049	176.103	162.233	0.289	189.287	216.341
43.0	23.5	-12.548	0.309	0.047	0.172	70.513	85.231	99.948	92.402	0.327	107.120	121.837
43.0	24.0	-8.467	0.351	0.056	0.186	61.929	74.402	86.875	80.480	0.363	92.953	105.426
43.0	24.5	-10.960	0.470	0.051	0.223	65.672	79.251	92.829	85.867	0.471	99.445	113.023
43.0	25.0	-15.404	0.470	0.042	0.223	78.271	94.869	111.466	102.957	0.469	119.555	136.152

Appendix 11: Regional cellular $G^{(I)}$ peak ground velocity estimates ($TP92_V$)

Parameters (α, μ) and uncertainties of a $G^{(I)}$ distribution for each cell used to contour ground velocity hazard over the catalogued region.. $V_{50,}$ V_{100} and V_{200} are the maximum velocities expected in 50-, 100- and 200-year time intervals respectively. V_{P50}, V_{P100} and V_{P200} are the ground velocities expected to be extremes with 90% probability of non-exceedance in the 50-, 100- and 200-year time intervals (a 1 in 10 chance of exceedance). σ_{PV} is uncertainty on V_{P50} only. Forecasts were obtained using earthquake data of 4-year extreme intervals, $M_s \geq 5.5$ and time interval 1900 to 2004. Estimates are obtained using Theodulidis and Papazachos (1992) for stiff soil conditions (S = 0.5) at the 50^{th} percentile (P = 0). Forecasted velocities are given in units of cm s^{-1}.

Lat	Lon	α	σ_α	μ	σ_μ	V_{50}	V_{100}	V_{200}	V_{P50}	σ_{PV}	V_{P100}	V_{P200}
39.0	19.0	-0.097	0.243	2.736	0.139	1.333	1.586	1.839	2.155	0.378	2.408	2.662
39.0	19.5	-0.110	0.243	2.324	0.139	1.574	1.872	2.170	2.542	0.378	2.841	3.139
39.0	20.0	-0.036	0.224	2.188	0.132	1.751	2.068	2.385	2.780	0.357	3.096	3.413
39.0	20.5	-0.069	0.224	1.922	0.132	1.967	2.327	2.688	3.138	0.369	3.499	3.859
39.0	21.0	-0.115	0.207	1.607	0.126	2.320	2.751	3.183	3.720	0.344	4.152	4.583
39.0	21.5	-0.509	0.192	0.890	0.121	3.885	4.664	5.442	6.413	0.301	7.192	7.970
39.0	22.0	-0.866	0.243	0.771	0.139	4.208	5.108	6.007	7.127	0.378	8.026	8.925
39.0	22.5	-0.527	0.243	1.028	0.139	3.279	3.954	4.628	5.469	0.391	6.143	6.818
39.0	24.5	-4.055	0.359	0.251	0.176	11.560	14.327	17.094	20.543	0.533	23.310	26.077
39.0	25.0	-8.840	0.359	0.139	0.176	19.398	24.401	29.404	35.641	0.535	40.645	45.648
39.0	25.5	-9.019	0.404	0.146	0.189	17.798	22.550	27.301	33.225	0.582	37.976	42.728
39.0	26.0	-2.471	0.359	0.394	0.176	7.461	9.221	10.981	13.175	0.542	14.935	16.695
39.0	26.5	-1.200	0.404	0.655	0.189	4.771	5.829	6.886	8.205	0.607	9.263	10.321
39.0	27.0	-1.256	0.404	0.705	0.189	4.292	5.275	6.259	7.484	0.607	8.467	9.450
39.0	27.5	-1.383	0.404	0.725	0.189	4.012	4.967	5.923	7.115	0.605	8.071	9.026
39.0	28.0	-1.216	0.404	0.754	0.189	3.969	4.888	5.807	6.952	0.608	7.871	8.790
39.5	19.0	0.032	0.192	2.402	0.121	1.661	1.949	2.238	2.598	0.315	2.886	3.175
39.5	19.5	0.055	0.179	1.918	0.116	2.094	2.455	2.817	3.267	0.299	3.629	3.990
39.5	20.0	0.138	0.179	1.704	0.116	2.434	2.841	3.248	3.755	0.301	4.162	4.569
39.5	20.5	0.108	0.179	1.469	0.116	2.772	3.244	3.716	4.304	0.306	4.776	5.249
39.5	21.0	-0.562	0.167	0.598	0.111	5.982	7.142	8.301	9.747	0.267	10.906	12.066
39.5	21.5	0.060	0.156	1.245	0.107	3.203	3.760	4.316	5.011	0.269	5.567	6.124
39.5	22.0	-0.064	0.192	1.235	0.121	3.105	3.667	4.228	4.928	0.322	5.490	6.051
39.5	22.5	-0.219	0.207	1.028	0.126	3.586	4.260	4.935	5.775	0.345	6.450	7.124

Appendix 11. Continued.

Lat	Lon	α	σ_α	μ	σ_μ	V_{50}	V_{100}	V_{200}	V_{P50}	σ_{PV}	V_{P100}	V_{P200}
39.5	23.0	-0.474	0.404	0.850	0.189	4.127	4.942	5.757	6.774	0.598	7.589	8.404
39.5	23.5	-0.758	0.404	0.704	0.189	4.798	5.782	6.767	7.994	0.591	8.978	9.963
39.5	24.0	-2.388	0.404	0.389	0.189	7.656	9.436	11.216	13.434	0.593	15.214	16.993
39.5	24.5	-5.239	0.359	0.213	0.176	13.098	16.347	19.596	23.646	0.545	26.895	30.144
39.5	25.0	-17.673	0.359	0.073	0.176	36.124	45.656	55.188	67.070	0.526	76.602	86.134
39.5	25.5	-7.217	0.404	0.163	0.189	16.792	21.046	25.300	30.603	0.595	34.857	39.111
39.5	26.0	-1.616	0.359	0.416	0.176	7.787	9.453	11.119	13.196	0.549	14.862	16.529
39.5	26.5	-1.465	0.404	0.489	0.189	6.537	7.955	9.373	11.141	0.607	12.558	13.976
39.5	27.0	-3.564	0.404	0.312	0.189	8.970	11.190	13.411	16.180	0.598	18.400	20.621
39.5	27.5	-4.099	0.404	0.293	0.189	9.272	11.641	14.010	16.963	0.592	19.332	21.702
39.5	28.0	-2.292	0.404	0.449	0.189	6.415	7.958	9.500	11.424	0.607	12.966	14.509
40.0	19.0	0.154	0.192	1.941	0.121	2.169	2.526	2.883	3.329	0.326	3.686	4.043
40.0	19.5	0.001	0.179	0.971	0.116	4.031	4.745	5.459	6.349	0.305	7.063	7.777
40.0	20.0	0.295	0.179	0.920	0.116	4.547	5.301	6.054	6.993	0.307	7.746	8.500
40.0	20.5	-0.067	0.179	0.585	0.116	6.622	7.808	8.993	10.470	0.306	11.655	12.841
40.0	21.0	0.041	0.167	0.756	0.111	5.219	6.136	7.054	8.197	0.290	9.115	10.032
40.0	21.5	-0.418	0.156	0.539	0.107	6.842	8.128	9.415	11.018	0.245	12.304	13.591
40.0	22.0	-0.513	0.179	0.633	0.116	5.665	6.760	7.854	9.219	0.278	10.313	11.408
40.0	22.5	-0.195	0.207	0.900	0.126	4.150	4.919	5.689	6.649	0.345	7.419	8.188
40.0	23.0	-0.720	0.359	0.690	0.176	4.948	5.952	6.956	8.208	0.543	9.212	10.216
40.0	23.5	-1.656	0.359	0.463	0.176	6.792	8.288	9.785	11.651	0.546	13.148	14.645
40.0	24.0	-5.024	0.359	0.221	0.176	12.695	15.834	18.974	22.888	0.541	26.027	29.166
40.0	24.5	-12.409	0.322	0.097	0.164	28.119	35.300	42.481	51.433	0.464	58.614	65.795

Appendix 11. Continued.

Lat	Lon	α	σ_α	μ	σ_μ	V_{50}	V_{100}	V_{200}	V_{P50}	σ_{PV}	V_{P100}	V_{P200}
40.0	25.0	-5.469	0.322	0.187	0.164	15.504	19.221	22.937	27.569	0.483	31.286	35.002
40.0	25.5	-0.291	0.404	0.552	0.189	6.800	8.056	9.312	10.878	0.598	12.134	13.391
40.0	26.0	-0.466	0.404	0.515	0.189	7.131	8.477	9.823	11.501	0.590	12.847	14.193
40.5	19.0	0.282	0.156	1.183	0.107	3.588	4.174	4.760	5.490	0.273	6.076	6.662
40.5	19.5	0.505	0.147	0.809	0.102	5.344	6.201	7.058	8.127	0.260	8.984	9.842
40.5	20.0	0.747	0.138	0.789	0.099	5.702	6.580	7.459	8.553	0.248	9.431	10.309
40.5	20.5	-0.157	0.138	0.295	0.099	13.087	15.434	17.780	20.706	0.237	23.052	25.399
40.5	21.0	0.299	0.138	0.588	0.099	6.950	8.129	9.307	10.776	0.246	11.955	13.133
40.5	21.5	0.142	0.138	0.745	0.099	5.395	6.326	7.256	8.417	0.241	9.348	10.278
40.5	22.0	-0.151	0.167	0.751	0.111	5.061	5.984	6.908	8.059	0.285	8.982	9.905
40.5	22.5	-0.340	0.207	0.663	0.126	5.559	6.605	7.650	8.953	0.345	9.998	11.043
40.5	23.0	-1.814	0.265	0.376	0.146	8.591	10.435	12.278	14.576	0.423	16.420	18.263
40.5	23.5	-4.273	0.322	0.231	0.164	12.645	15.643	18.640	22.377	0.490	25.375	28.372
40.5	24.0	-6.216	0.322	0.178	0.164	15.701	19.584	23.467	28.308	0.477	32.191	36.075
40.5	24.5	-4.219	0.291	0.222	0.155	13.368	16.484	19.600	23.484	0.446	26.600	29.716
40.5	25.0	-2.347	0.291	0.318	0.155	9.951	12.130	14.309	17.026	0.448	19.205	21.384
40.5	25.5	-0.882	0.359	0.481	0.176	7.245	8.685	10.125	11.921	0.536	13.361	14.801
40.5	26.0	-6.149	0.359	0.167	0.176	17.226	21.367	25.509	30.672	0.528	34.813	38.955
40.5	26.5	-6.332	0.404	0.173	0.189	16.239	20.238	24.237	29.222	0.601	33.221	37.220
40.5	27.0	-20.028	0.404	0.068	0.189	37.849	48.104	58.359	71.143	0.575	81.398	91.653
40.5	27.5	-7.442	0.404	0.140	0.189	20.524	25.479	30.434	36.611	0.596	41.566	46.521
41.0	19.0	0.500	0.156	1.578	0.107	2.979	3.418	3.858	4.405	0.275	4.844	5.284
41.0	19.5	0.695	0.147	0.736	0.102	6.012	6.953	7.895	9.070	0.261	10.012	10.954

Appendix 11. Continued.

Lat	Lon	α	σ_α	μ	σ_μ	V_{50}	V_{100}	V_{200}	V_{P50}	σ_{PV}	V_{P100}	V_{P200}
41.0	20.0	0.611	0.138	0.447	0.099	9.355	10.904	12.454	14.385	0.246	15.934	17.484
41.0	20.5	0.243	0.138	0.327	0.099	12.221	14.344	16.466	19.112	0.243	21.234	23.357
41.0	21.0	0.173	0.138	0.486	0.099	8.230	9.657	11.085	12.865	0.238	14.292	15.720
41.0	21.5	0.377	0.138	1.001	0.099	4.287	4.980	5.672	6.536	0.247	7.229	7.922
41.0	22.0	-0.326	0.167	0.573	0.111	6.501	7.710	8.920	10.427	0.285	11.637	12.846
41.0	22.5	-1.384	0.207	0.333	0.126	10.380	12.465	14.549	17.148	0.341	19.233	21.317
41.0	23.0	-2.665	0.265	0.269	0.146	11.861	14.435	17.009	20.218	0.420	22.791	25.365
41.0	23.5	-9.305	0.322	0.122	0.164	22.785	28.471	34.156	41.244	0.476	46.930	52.616
41.0	24.0	-1.321	0.322	0.606	0.164	5.131	6.274	7.417	8.842	0.499	9.986	11.129
41.0	24.5	-0.713	0.291	0.785	0.155	4.273	5.157	6.040	7.142	0.457	8.025	8.909
41.0	25.0	-0.308	0.291	0.927	0.155	3.911	4.659	5.406	6.338	0.456	7.085	7.833
41.0	25.5	-0.596	0.322	0.770	0.164	4.482	5.382	6.282	7.403	0.492	8.303	9.203
41.0	26.0	-1.337	0.322	0.513	0.164	6.282	7.632	8.982	10.665	0.499	12.015	13.365
41.0	26.5	-3.169	0.359	0.310	0.176	9.442	11.676	13.911	16.696	0.534	18.931	21.165
41.0	27.0	-5.398	0.359	0.211	0.176	13.132	16.415	19.698	23.791	0.524	27.074	30.357
41.0	27.5	-3.822	0.359	0.280	0.176	10.165	12.643	15.121	18.211	0.544	20.689	23.167
41.0	28.0	-2.051	0.404	0.465	0.189	6.366	7.857	9.348	11.207	0.605	12.699	14.190
41.5	19.0	0.010	0.156	0.791	0.107	4.955	5.831	6.708	7.800	0.262	8.676	9.552
41.5	19.5	0.503	0.147	0.733	0.102	5.841	6.787	7.733	8.912	0.261	9.858	10.804
41.5	20.0	0.854	0.138	0.902	0.099	5.190	5.958	6.726	7.684	0.248	8.452	9.220
41.5	20.5	0.461	0.138	0.532	0.099	7.819	9.123	10.427	12.053	0.245	13.356	14.660
41.5	21.0	0.619	0.138	1.169	0.099	3.965	4.558	5.150	5.889	0.248	6.482	7.075
41.5	21.5	0.324	0.138	1.034	0.099	4.108	4.778	5.448	6.284	0.246	6.955	7.625

Appendix 11. Continued.

Lat	Lon	α	σ_α	μ	σ_μ	V_{50}	V_{100}	V_{200}	V_{P50}	σ_{PV}	V_{P100}	V_{P200}
41.5	22.0	-0.749	0.179	0.491	0.116	7.212	8.622	10.032	11.791	0.292	13.201	14.611
41.5	22.5	-3.375	0.224	0.228	0.132	13.767	16.804	19.841	23.627	0.346	26.664	29.701
41.5	23.0	-7.784	0.322	0.154	0.164	17.695	22.209	26.724	32.351	0.467	36.866	41.380
41.5	24.0	-3.583	0.404	0.356	0.189	7.407	9.355	11.302	13.730	0.595	15.677	17.625
41.5	24.5	-1.921	0.359	0.530	0.176	5.461	6.769	8.077	9.708	0.535	11.016	12.324
41.5	25.0	-1.964	0.359	0.518	0.176	5.584	6.922	8.259	9.926	0.545	11.264	12.601
41.5	25.5	-1.710	0.404	0.595	0.189	4.862	6.026	7.190	8.642	0.608	9.806	10.970
41.5	26.0	-1.026	0.359	0.735	0.176	4.298	5.241	6.184	7.360	0.547	8.304	9.247
41.5	26.5	-1.037	0.322	0.694	0.164	4.600	5.599	6.598	7.843	0.495	8.842	9.841
41.5	27.0	-1.179	0.291	0.652	0.155	4.817	5.879	6.942	8.266	0.450	9.328	10.391
41.5	27.5	-1.164	0.291	0.703	0.155	4.398	5.384	6.369	7.598	0.452	8.583	9.569
41.5	28.0	-1.124	0.359	0.805	0.176	3.734	4.594	5.455	6.528	0.548	7.389	8.249
42.0	19.0	-5.346	0.156	0.106	0.107	31.620	38.170	44.719	52.884	0.228	59.434	65.984
42.0	19.5	-1.413	0.147	0.218	0.102	16.564	19.749	22.935	26.906	0.245	30.091	33.276
42.0	20.0	0.137	0.138	0.595	0.099	6.710	7.874	9.039	10.491	0.240	11.655	12.820
42.0	20.5	0.526	0.138	1.167	0.099	3.879	4.473	5.067	5.808	0.243	6.402	6.997
42.0	21.0	0.315	0.138	1.087	0.099	3.914	4.552	5.189	5.984	0.236	6.622	7.260
42.0	21.5	-0.425	0.138	0.449	0.099	8.283	9.826	11.369	13.293	0.223	14.836	16.379
42.0	22.0	-0.623	0.192	0.635	0.121	5.536	6.627	7.718	9.079	0.313	10.170	11.261
42.0	22.5	-2.813	0.243	0.314	0.139	9.634	11.839	14.044	16.793	0.361	18.999	21.204
42.0	23.0	-12.011	0.359	0.112	0.176	22.827	29.000	35.173	42.868	0.495	49.040	55.213
42.0	24.0	-4.102	0.404	0.319	0.189	8.172	10.347	12.522	15.233	0.592	17.408	19.583
42.0	24.5	-4.279	0.359	0.288	0.176	9.318	11.727	14.136	17.139	0.528	19.548	21.957

Appendix 11. Continued.

Lat	Lon	α	σ_α	μ	σ_μ	V_{50}	V_{100}	V_{200}	V_{P50}	σ_{PV}	V_{P100}	V_{P200}
42.0	25.0	-10.786	0.359	0.125	0.176	20.418	25.947	31.476	38.368	0.500	43.897	49.426
42.0	26.0	-1.728	0.322	0.553	0.164	5.346	6.599	7.853	9.415	0.486	10.669	11.922
42.0	26.5	-0.452	0.291	1.066	0.155	3.217	3.867	4.517	5.327	0.457	5.977	6.627
42.0	27.0	-0.339	0.291	1.175	0.155	2.990	3.580	4.170	4.905	0.459	5.495	6.085
42.0	27.5	-0.465	0.291	1.196	0.155	2.806	3.385	3.965	4.687	0.459	5.267	5.846
42.0	28.0	-0.608	0.359	1.165	0.176	2.751	3.346	3.942	4.684	0.547	5.279	5.874
42.5	19.0	-0.783	0.179	0.608	0.116	5.648	6.788	7.927	9.348	0.283	10.487	11.627
42.5	19.5	-0.430	0.167	0.684	0.111	5.291	6.304	7.318	8.582	0.275	9.595	10.609
42.5	20.0	0.028	0.156	1.094	0.107	3.605	4.239	4.872	5.662	0.265	6.296	6.930
42.5	20.5	0.290	0.156	1.817	0.107	2.444	2.825	3.207	3.683	0.273	4.064	4.446
42.5	21.0	0.218	0.156	1.433	0.107	2.947	3.430	3.914	4.517	0.275	5.000	5.484
42.5	21.5	-0.712	0.156	0.459	0.107	7.808	9.318	10.827	12.709	0.256	14.219	15.728
42.5	22.0	-0.453	0.207	0.886	0.126	3.963	4.745	5.527	6.502	0.335	7.285	8.067
42.5	22.5	-1.438	0.265	0.604	0.146	5.040	6.188	7.336	8.767	0.393	9.915	11.063
42.5	23.0	-3.581	0.404	0.375	0.189	6.865	8.716	10.567	12.874	0.568	14.725	16.576
43.0	19.0	-0.311	0.207	1.479	0.126	2.333	2.801	3.270	3.854	0.329	4.323	4.791
43.0	19.5	-0.184	0.192	1.561	0.121	2.323	2.767	3.211	3.764	0.315	4.209	4.653
43.0	20.0	-0.025	0.179	1.856	0.116	2.082	2.456	2.829	3.294	0.304	3.668	4.041
43.0	20.5	0.038	0.167	1.804	0.111	2.206	2.591	2.975	3.454	0.287	3.838	4.222
43.0	21.0	-0.025	0.167	1.545	0.111	2.507	2.955	3.404	3.963	0.280	4.412	4.860
43.0	21.5	-0.067	0.179	1.643	0.116	2.314	2.736	3.158	3.684	0.304	4.105	4.527
43.0	22.0	-0.392	0.243	1.335	0.139	2.539	3.059	3.578	4.225	0.376	4.745	5.264
43.0	22.5	-1.945	0.322	0.576	0.164	4.847	6.051	7.254	8.754	0.456	9.958	11.161

Appendix 11. Continued.

Lat	Lon	α	σ_α	μ	σ_μ	V_{50}	V_{100}	V_{200}	V_{P50}	σ_{PV}	V_{P100}	V_{P200}
43.5	19.0	-0.369	0.404	2.061	0.189	1.529	1.866	2.202	2.621	0.604	2.958	3.294
43.5	19.5	-0.195	0.404	2.219	0.189	1.568	1.880	2.193	2.582	0.610	2.894	3.207
43.5	20.0	-0.076	0.359	2.226	0.176	1.681	1.992	2.304	2.692	0.533	3.003	3.315
43.5	20.5	-0.708	0.322	1.082	0.164	2.907	3.547	4.188	4.986	0.496	5.626	6.267
43.5	21.0	-1.380	0.322	0.711	0.164	4.123	5.098	6.073	7.288	0.471	8.263	9.238
43.5	21.5	-0.434	0.322	1.563	0.164	2.069	2.512	2.956	3.509	0.490	3.952	4.395
43.5	22.0	-0.593	0.404	1.580	0.189	1.883	2.322	2.760	3.307	0.594	3.746	4.185
44.0	20.0	-0.952	0.404	1.052	0.189	2.767	3.427	4.086	4.907	0.607	5.566	6.225
44.0	20.5	-3.995	0.359	0.317	0.176	8.331	10.515	12.699	15.422	0.519	17.606	19.790
44.0	21.0	-0.812	0.359	1.094	0.176	2.763	3.396	4.029	4.819	0.548	5.452	6.085
44.0	21.5	-0.182	0.359	2.526	0.176	1.367	1.641	1.916	2.258	0.531	2.532	2.807

Appendix 12: Southwest zone cellular $G^{(I)}$ peak ground velocity estimates ($TP92_V$)

Parameters (α, μ) and uncertainties of a $G^{(I)}$ distribution for each cell used to contour ground velocity hazard over the southwest zone. $V_{50,}$ V_{100} and V_{200} are the maximum velocities expected in 50-, 100- and 200-year time intervals respectively. V_{P50}, V_{P100} and V_{P200} are the ground velocities expected to be extremes with 90% probability of non-exceedance in the 50-, 100- and 200-year time intervals (a 1 in 10 chance of exceedance). σ_{PV} is uncertainty on V_{P50} only. Forecasts were obtained using earthquake data of 5-year extreme intervals, $M_s \geq 5.3$ and time interval 1900 to 2004. Estimates are obtained using Theodulidis and Papazachos (1992) for stiff soil conditions (S = 0.5) at the 50^{th} percentile (P = 0). Forecasted velocities are given in units of cm s^{-1}.

Lat	Lon	α	σ_α	μ	σ_μ	V_{50}	V_{100}	V_{200}	V_{P50}	σ_{PV}	V_{P100}	V_{P200}
40.0	21.0	0.759	0.120	0.910	0.091	5.056	5.817	6.578	7.527	0.219	8.289	9.050
40.0	21.5	0.617	0.120	0.652	0.091	6.621	7.684	8.748	10.074	0.194	11.138	12.201
40.0	22.0	0.300	0.137	0.721	0.103	5.726	6.688	7.649	8.848	0.227	9.809	10.771
40.0	22.5	0.304	0.172	0.955	0.120	4.399	5.125	5.850	6.755	0.306	7.481	8.206
40.0	23.0	-0.101	0.224	0.732	0.141	5.241	6.188	7.134	8.314	0.378	9.261	10.207
40.0	23.5	-0.737	0.276	0.493	0.160	7.191	8.596	10.000	11.751	0.452	13.156	14.561
40.0	24.0	-2.951	0.276	0.241	0.160	13.289	16.166	19.044	22.631	0.445	25.508	28.386
40.0	24.5	-10.853	0.309	0.092	0.172	31.586	39.105	46.625	55.998	0.467	63.518	71.037
40.0	25.0	-3.912	0.276	0.189	0.160	16.763	20.426	24.089	28.656	0.439	32.319	35.983
40.0	25.5	-0.209	0.276	0.503	0.160	7.563	8.941	10.318	12.035	0.446	13.412	14.789
40.5	21.0	1.029	0.120	0.666	0.091	6.899	7.939	8.979	10.276	0.217	11.316	12.356
40.5	21.5	0.774	0.120	0.831	0.091	5.480	6.314	7.148	8.187	0.214	9.021	9.855
40.5	22.0	0.502	0.137	0.814	0.103	5.306	6.157	7.008	8.069	0.248	8.920	9.771
40.5	22.5	0.377	0.172	0.705	0.120	5.926	6.910	7.893	9.118	0.306	10.102	11.085
40.5	23.0	-0.538	0.204	0.406	0.134	9.107	10.816	12.525	14.656	0.353	16.365	18.074
40.5	23.5	-1.337	0.204	0.280	0.134	12.619	15.092	17.564	20.647	0.343	23.119	25.592
40.5	24.0	-2.209	0.204	0.223	0.134	15.339	18.448	21.558	25.434	0.331	28.543	31.652
40.5	24.5	-2.257	0.224	0.241	0.141	13.969	16.844	19.719	23.303	0.370	26.178	29.053
40.5	25.0	-1.063	0.224	0.339	0.141	10.462	12.504	14.546	17.092	0.373	19.134	21.176
40.5	25.5	-0.078	0.204	0.502	0.134	7.720	9.101	10.483	12.205	0.349	13.587	14.969
41.0	21.0	1.148	0.120	0.565	0.091	8.068	9.294	10.521	12.049	0.209	13.275	14.501
41.0	21.5	1.008	0.120	1.077	0.091	4.639	5.283	5.926	6.728	0.222	7.371	8.015
41.0	22.0	0.560	0.137	0.609	0.103	6.982	8.120	9.258	10.677	0.250	11.815	12.953
41.0	22.5	0.003	0.172	0.348	0.120	11.261	13.256	15.250	17.737	0.304	19.731	21.726

Appendix 12. Continued.

Lat	Lon	α	σ_α	μ	σ_μ	V_{50}	V_{100}	V_{200}	V_{P50}	σ_{PV}	V_{P100}	V_{P200}
41.0	23.0	-0.754	0.204	0.287	0.134	12.873	15.288	17.702	20.712	0.351	23.127	25.541
41.0	23.5	-3.258	0.204	0.151	0.134	22.605	27.188	31.770	37.483	0.332	42.066	46.648
41.0	24.0	-0.072	0.204	0.659	0.134	5.860	6.911	7.963	9.273	0.354	10.324	11.375
41.0	24.5	-0.156	0.224	0.796	0.141	4.761	5.632	6.504	7.590	0.379	8.461	9.332
41.0	25.0	0.103	0.224	0.944	0.141	4.248	4.983	5.717	6.633	0.377	7.367	8.102
41.0	25.5	-0.016	0.187	0.842	0.127	4.631	5.454	6.277	7.304	0.325	8.127	8.951
41.5	21.0	1.049	0.120	1.325	0.091	4.002	4.525	5.048	5.700	0.223	6.223	6.747
41.5	21.5	0.856	0.120	1.076	0.091	4.491	5.135	5.779	6.582	0.220	7.226	7.871
41.5	22.0	0.348	0.137	0.508	0.103	8.050	9.414	10.779	12.480	0.244	13.844	15.209
41.5	22.5	-1.209	0.172	0.227	0.120	16.000	19.049	22.098	25.899	0.293	28.949	31.998
41.5	23.0	-3.509	0.204	0.153	0.134	22.035	26.561	31.087	36.729	0.337	41.255	45.781
41.5	23.5	-3.346	0.248	0.195	0.150	16.718	20.274	23.829	28.260	0.399	31.815	35.371
41.5	24.0	-1.497	0.276	0.369	0.160	9.116	10.997	12.878	15.222	0.449	17.102	18.983
41.5	24.5	-1.044	0.309	0.525	0.172	6.403	7.722	9.042	10.687	0.491	12.006	13.326
41.5	25.0	-1.116	0.309	0.534	0.172	6.206	7.503	8.800	10.417	0.500	11.715	13.012
41.5	25.5	-0.679	0.248	0.700	0.150	4.912	5.902	6.893	8.128	0.412	9.118	10.109
42.0	21.0	0.770	0.120	1.221	0.091	3.975	4.543	5.111	5.819	0.210	6.387	6.955
42.0	21.5	0.601	0.120	0.484	0.091	8.691	10.124	11.557	13.344	0.200	14.778	16.211
42.0	22.0	0.175	0.147	0.602	0.108	6.669	7.820	8.971	10.405	0.262	11.556	12.707
42.0	22.5	-1.495	0.187	0.272	0.127	12.903	15.454	18.005	21.186	0.311	23.737	26.288
42.0	23.0	-6.177	0.224	0.110	0.141	29.313	35.602	41.890	49.729	0.357	56.017	62.305
42.0	23.5	-4.393	0.248	0.163	0.150	19.648	23.908	28.168	33.478	0.396	37.738	41.998
42.0	24.0	-1.804	0.276	0.321	0.160	10.394	12.556	14.717	17.411	0.452	19.572	21.734

Appendix 12. Continued.

Lat	Lon	α	σ_α	μ	σ_μ	V_{50}	V_{100}	V_{200}	V_{P50}	σ_{PV}	V_{P100}	V_{P200}
42.0	24.5	-2.801	0.309	0.286	0.172	10.865	13.286	15.707	18.726	0.494	21.147	23.568
42.0	25.0	-7.891	0.309	0.128	0.172	22.620	28.026	33.432	40.171	0.459	45.578	50.984
42.0	25.5	-3.153	0.309	0.296	0.172	10.073	12.417	14.760	17.681	0.462	20.025	22.368
42.5	21.0	0.522	0.129	1.530	0.098	3.078	3.531	3.984	4.549	0.237	5.002	5.455
42.5	21.5	0.314	0.129	0.501	0.098	8.122	9.506	10.889	12.614	0.221	13.997	15.381
42.5	22.0	0.153	0.147	0.853	0.108	4.741	5.554	6.366	7.380	0.264	8.193	9.006
42.5	22.5	-0.819	0.204	0.511	0.134	6.830	8.186	9.541	11.230	0.338	12.586	13.941
42.5	23.0	-2.204	0.276	0.346	0.160	9.089	11.089	13.090	15.584	0.437	17.585	19.586
42.5	23.5	-2.277	0.309	0.353	0.172	8.810	10.774	12.739	15.187	0.492	17.152	19.116
42.5	24.0	-1.559	0.351	0.456	0.186	7.027	8.549	10.070	11.967	0.548	13.488	15.010
42.5	24.5	-3.143	0.470	0.332	0.223	8.632	10.718	12.804	15.405	0.720	17.491	19.577
42.5	25.0	-5.397	0.470	0.227	0.223	11.824	14.875	17.927	21.731	0.697	24.782	27.833
42.5	25.5	-3.768	0.470	0.339	0.223	7.781	9.827	11.873	14.424	0.705	16.470	18.516
43.0	21.0	0.309	0.129	1.754	0.098	2.540	2.935	3.330	3.823	0.228	4.218	4.613
43.0	21.5	0.246	0.137	1.644	0.103	2.626	3.048	3.470	3.995	0.251	4.417	4.839
43.0	22.0	0.025	0.159	1.189	0.114	3.316	3.899	4.483	5.210	0.275	5.793	6.376
43.0	22.5	-0.824	0.204	0.589	0.134	5.816	6.992	8.168	9.635	0.334	10.811	11.988
43.0	23.0	-1.470	0.276	0.525	0.160	5.978	7.298	8.617	10.262	0.436	11.582	12.901
43.0	23.5	-1.051	0.309	0.697	0.172	4.563	5.558	6.552	7.792	0.495	8.787	9.781
43.0	24.0	-0.857	0.351	0.767	0.186	4.240	5.143	6.047	7.172	0.548	8.076	8.979
43.0	24.5	-1.068	0.470	0.719	0.223	4.370	5.334	6.297	7.498	0.715	8.462	9.426
43.0	25.0	-1.170	0.470	0.651	0.223	4.836	5.901	6.965	8.292	0.720	9.356	10.420

Appendix 13: Regional cellular $G^{(III)}$ intensity recurrence estimates (PP97)

Parameters (ω, μ, λ) and their associated uncertainties of a $G^{(III)}$ distribution for each cell used to contour intensity hazard over the catalogued region. I_M is the maximum observed intensity and $I(1)$ is the annual modal [or most probable] maximum event in each cell of analysis. $I_{50,}$ I_{100} and I_{200} are the modal maximum intensities expected in 50-, 100- and 200-year time intervals respectively. I_{P50}, I_{P100} and I_{P200} are the intensities expected to be extremes with 90% probability of non-exceedance in the 50-, 100- and 200-year time intervals (a 1 in 10 chance of exceedance). σ_I and σ_{IP} are the uncertainties in these forecasts. Forecasts were obtained using earthquake data of 4-year extreme intervals, cut-off intensity of $I_{CUT} \geq$ VI and time interval 1900 to 2004. $\sigma^2_{\omega\mu}$, $\sigma^2_{\omega\lambda}$ and $\sigma^2_{\mu\lambda}$ are the off-diagonal elements of the covariance (error) matrix, ε.

Lat	Lon	ω	σ_ω	μ	σ_μ	λ	σ_λ	$\sigma^2_{\omega\mu}$	$\sigma^2_{\omega\lambda}$	$\sigma^2_{\mu\lambda}$	I_M	I (1)	I_{50}	I_{100}	I_{200}	σ_I	I_{P50}	I_{P100}	I_{P200}	σ_{IP}
39.0	19.0	XI (11.8)	9.6	VII (7.0)	1.1	0.20	0.63	9.28	-0.41	-0.64	IX (9.4)	VII (7.2)	IX (9.7)	X (10.0)	X (10.2)	5.4	X (10.4)	X (10.6)	X (10.7)	7.1
39.0	19.5	XII (12.6)	16.3	VII (7.2)	0.8	0.15	0.60	11.80	-0.41	-0.45	IX (9.4)	VII (7.3)	IX (9.6)	IX (9.9)	X (10.2)	6.6	X (10.4)	X (10.6)	X (10.8)	10.0
39.0	20.0	XI (11.2)	5.3	VII (7.2)	0.8	0.25	0.54	3.31	-0.41	-0.36	IX (9.4)	VII (7.5)	IX (9.8)	X (10.0)	X (10.2)	3.6	X (10.3)	X (10.4)	X (10.5)	4.3
39.0	20.5	XI (11.2)	5.3	VII (7.2)	0.8	0.25	0.54	3.31	-0.41	-0.36	IX (9.4)	VII (7.5)	IX (9.8)	X (10.0)	X (10.2)	3.6	X (10.3)	X (10.4)	X (10.5)	4.3
39.0	21.0	XI (11.2)	5.3	VII (7.2)	0.8	0.25	0.54	3.31	-0.41	-0.36	IX (9.4)	VII (7.5)	IX (9.8)	X (10.0)	X (10.2)	3.6	X (10.3)	X (10.4)	X (10.5)	4.3
39.0	21.5	X (10.3)	1.8	VII (7.1)	0.7	0.43	0.52	0.99	-0.41	-0.33	IX (9.4)	VII (7.8)	IX (9.8)	X (10.0)	X (10.1)	1.9	X (10.1)	X (10.1)	X (10.2)	1.7
39.0	22.0	IX (9.9)	0.9	VI (6.1)	1.7	0.76	0.66	1.06	-0.52	-1.03	IX (9.4)	VIII (8.6)	IX (9.8)	IX (9.8)	IX (9.8)	1.7	IX (9.8)	IX (9.8)	IX (9.8)	0.9
39.0	22.5	IX (9.3)	0.5	V (5.0)	3.0	0.72	0.94	0.93	-0.37	-2.61	IX (9.4)	VII (7.6)	IX (9.2)	IX (9.2)	IX (9.2)	1.4	IX (9.2)	IX (9.2)	IX (9.3)	0.5
39.0	26.0	XI (11.2)	0.8	IV (4.8)	3.5	0.88	0.62	2.18	-0.41	-2.09	X (10.9)	X (10.2)	XI (11.2)	XI (11.2)	XI (11.2)	2.2	XI (11.2)	XI (11.2)	XI (11.2)	0.8
39.5	19.0	XII (12.4)	11.9	VII (7.5)	0.5	0.15	0.48	4.43	-0.41	-0.19	IX (9.4)	VII (7.6)	IX (9.7)	X (10.0)	X (10.2)	4.9	X (10.5)	X (10.6)	X (10.8)	7.4
39.5	19.5	XII (12.4)	11.9	VII (7.5)	0.5	0.15	0.48	4.43	-0.41	-0.19	IX (9.4)	VII (7.6)	IX (9.7)	X (10.0)	X (10.2)	4.9	X (10.5)	X (10.6)	X (10.8)	7.4
39.5	20.0	XI (11.1)	6.4	VII (7.5)	0.4	0.20	0.51	1.92	-0.41	-0.17	IX (9.4)	VII (7.7)	IX (9.5)	IX (9.7)	IX (9.9)	3.4	X (10.0)	X (10.2)	X (10.3)	4.6
39.5	20.5	X (10.2)	1.4	VII (7.4)	0.5	0.47	0.47	0.44	-0.41	-0.18	IX (9.4)	VIII (8.1)	IX (9.9)	IX (9.9)	X (10.0)	1.4	X (10.0)	X (10.1)	X (10.1)	1.3
39.5	21.0	X (10.2)	1.4	VII (7.4)	0.5	0.47	0.47	0.44	-0.41	-0.18	IX (9.4)	VIII (8.1)	IX (9.9)	IX (9.9)	X (10.0)	1.4	X (10.0)	X (10.1)	X (10.1)	1.3
39.5	21.5	X (10.0)	0.9	VII (7.4)	0.4	0.58	0.47	0.22	-0.41	-0.15	IX (9.4)	VIII (8.4)	IX (9.8)	IX (9.9)	IX (9.9)	1.1	IX (9.9)	X (10.0)	X (10.0)	0.9
39.5	22.0	IX (9.4)	0.4	VI (6.2)	1.5	0.72	0.82	0.40	-0.30	-1.12	IX (9.4)	VIII (8.1)	IX (9.3)	IX (9.3)	IX (9.3)	1.0	IX (9.3)	IX (9.4)	IX (9.4)	0.4
39.5	22.5	XI (11.3)	1.9	VI (6.8)	0.9	0.43	0.41	1.37	-0.41	-0.33	X (10.9)	VII (7.8)	X (10.7)	X (10.9)	XI (11.0)	2.1	XI (11.0)	XI (11.1)	XI (11.2)	1.9
39.5	26.0	X (10.7)	0.5	I (1.4)	6.3	0.85	0.70	2.30	-0.41	-4.28	X (10.9)	VIII (8.9)	X (10.6)	X (10.7)	X (10.7)	2.2	X (10.6)	X (10.7)	X (10.7)	0.5
40.0	19.0	XII (13.4)	19.6	VII (7.6)	0.4	0.11	0.46	5.78	-0.41	-0.14	IX (9.4)	VII (7.6)	IX (9.7)	X (10.0)	X (10.2)	6.1	X (10.5)	X (10.7)	X (10.9)	9.9
40.0	19.5	XII (13.4)	19.6	VII (7.6)	0.4	0.11	0.46	5.78	-0.41	-0.14	IX (9.4)	VII (7.6)	IX (9.7)	X (10.0)	X (10.2)	6.1	X (10.5)	X (10.7)	X (10.9)	9.9
40.0	20.0	XI (11.9)	7.2	VII (7.6)	0.3	0.18	0.41	1.70	-0.41	-0.11	IX (9.4)	VII (7.8)	IX (9.8)	X (10.1)	X (10.3)	3.5	X (10.5)	X (10.6)	X (10.8)	4.9
40.0	20.5	X (10.3)	1.7	VII (7.5)	0.4	0.40	0.44	0.41	-0.41	-0.13	IX (9.4)	VIII (8)	IX (9.8)	X (10.0)	X (10.0)	1.6	X (10.1)	X (10.1)	X (10.2)	1.6
40.0	21.0	X (10.3)	1.7	VII (7.5)	0.4	0.40	0.44	0.41	-0.41	-0.13	IX (9.4)	VIII (8)	IX (9.8)	X (10.0)	X (10.0)	1.6	X (10.1)	X (10.1)	X (10.2)	1.6
40.0	21.5	XII (12.3)	4.0	VII (7.6)	0.3	0.24	0.29	0.74	-0.41	-0.06	X (10.9)	VII (7.9)	X (10.5)	X (10.8)	XI (11.0)	2.5	XI (11.2)	XI (11.4)	XI (11.5)	3.2

Appendix 13. Continued.

Lat	Lon	ω	σ_ω	μ	σ_μ	λ	σ_λ	$\sigma^2_{\omega\mu}$	$\sigma^2_{\omega\lambda}$	$\sigma^2_{\mu\lambda}$	I_M	I (1)	I_{50}	I_{100}	I_{200}	σ_I	I_{P50}	I_{P100}	I_{P200}	σ_{IP}
40.0	22.0	XII (12.2)	4.6	VII (7.4)	0.4	0.24	0.34	1.39	-0.41	-0.11	X (10.9)	VII (7.7)	X (10.4)	X (10.7)	X (10.9)	2.8	XI (11.1)	XI (11.3)	XI (11.4)	3.6
40.0	22.5	XI (11.8)	1.7	VI (6.9)	0.7	0.44	0.34	0.96	-0.41	-0.21	X (10.9)	VII (7.9)	XI (11.1)	XI (11.3)	XI (11.4)	1.9	XI (11.4)	XI (11.5)	XI (11.6)	1.7
40.0	23.0	XI (11.8)	3.0	VII (7.2)	1.8	0.40	0.61	4.57	-0.41	-1.02	X (10.9)	VIII (8.0)	XI (11.0)	XI (11.2)	XI (11.3)	3.5	XI (11.4)	XI (11.5)	XI (11.6)	2.8
40.0	23.5	XI (11.2)	0.8	IV (4.8)	3.5	0.88	0.62	2.18	-0.41	-2.09	X (10.9)	X (10.2)	XI (11.2)	XI (11.2)	XI (11.2)	2.2	XI (11.2)	XI (11.2)	XI (11.2)	0.8
40.0	25.0	XI (11.2)	0.8	IV (4.8)	3.5	0.88	0.62	2.18	-0.41	-2.09	X (10.9)	X (10.2)	XI (11.2)	XI (11.2)	XI (11.2)	2.2	XI (11.2)	XI (11.2)	XI (11.2)	0.8
40.0	26.0	X (10.7)	0.5	I (1.4)	6.3	0.85	0.70	2.30	-0.41	-4.28	X (10.9)	VIII (8.9)	X (10.6)	X (10.7)	X (10.7)	2.2	X (10.6)	X (10.7)	X (10.7)	0.5
40.5	19.0	XII (13.5)	16.7	VII (7.7)	0.3	0.11	0.39	3.13	-0.41	-0.08	IX (9.4)	VII (7.8)	IX (9.8)	X (10.1)	X (10.4)	5.3	X (10.6)	X (10.8)	XI (11.0)	8.5
40.5	19.5	XII (13.5)	16.7	VII (7.7)	0.3	0.11	0.39	3.13	-0.41	-0.08	IX (9.4)	VII (7.8)	IX (9.8)	X (10.1)	X (10.4)	5.3	X (10.6)	X (10.8)	XI (11.0)	8.5
40.5	20.0	XI (11.3)	4.4	VII (7.7)	0.3	0.22	0.38	0.60	-0.41	-0.06	IX (9.4)	VII (7.9)	IX (9.9)	X (10.1)	X (10.2)	2.5	X (10.4)	X (10.5)	X (10.6)	3.3
40.5	20.5	X (10.3)	1.4	VII (7.7)	0.3	0.41	0.40	0.18	-0.41	-0.06	IX (9.4)	VIII (8.2)	IX (9.9)	X (10.0)	X (10.0)	1.3	X (10.1)	X (10.1)	X (10.2)	1.3
40.5	21.0	X (10.3)	1.4	VII (7.7)	0.3	0.41	0.40	0.18	-0.41	-0.06	IX (9.4)	VIII (8.2)	IX (9.9)	X (10.0)	X (10.0)	1.3	X (10.1)	X (10.1)	X (10.2)	1.3
40.5	21.5	XII (12.6)	4.9	VII (7.6)	0.2	0.21	0.28	0.68	-0.41	-0.04	X (10.9)	VII (7.9)	X (10.5)	X (10.8)	XI (11.0)	2.6	XI (11.2)	XI (11.4)	XI (11.6)	3.6
40.5	22.0	XII (12.2)	4.6	VII (7.4)	0.4	0.24	0.34	1.39	-0.41	-0.11	X (10.9)	VII (7.7)	X (10.4)	X (10.7)	X (10.9)	2.8	XI (11.1)	XI (11.3)	XI (11.4)	3.6
40.5	22.5	XI (11.8)	1.7	VI (6.9)	0.7	0.44	0.34	0.96	-0.41	-0.21	X (10.9)	VII (7.9)	XI (11.1)	XI (11.3)	XI (11.4)	1.9	XI (11.4)	XI (11.5)	XI (11.6)	1.7
40.5	23.0	XI (11.3)	1.1	VI (6.2)	1.4	0.62	0.44	1.25	-0.41	-0.57	X (10.9)	VIII (8.5)	XI (11.0)	XI (11.1)	XI (11.2)	1.9	XI (11.2)	XI (11.2)	XI (11.2)	1.1
40.5	23.5	XI (11.2)	0.8	IV (4.8)	3.5	0.88	0.62	2.18	-0.41	-2.09	X (10.9)	X (10.2)	XI (11.2)	XI (11.2)	XI (11.2)	2.2	XI (11.2)	XI (11.2)	XI (11.2)	0.8
40.5	24.5	XI (11.2)	0.8	IV (4.8)	3.5	0.88	0.62	2.18	-0.41	-2.09	X (10.9)	X (10.2)	XI (11.2)	XI (11.2)	XI (11.2)	2.2	XI (11.2)	XI (11.2)	XI (11.2)	0.8
40.5	25.0	XI (11.4)	1.1	VI (6.5)	2.0	0.67	0.55	1.71	-0.41	-1.02	X (10.9)	IX (9.0)	XI (11.2)	XI (11.3)	XI (11.3)	2.1	XI (11.3)	XI (11.3)	XI (11.3)	1.1
40.5	25.5	X (10.7)	0.5	I (1.4)	6.3	0.85	0.70	2.30	-0.41	-4.28	X (10.9)	VIII (8.9)	X (10.6)	X (10.7)	X (10.7)	2.2	X (10.6)	X (10.7)	X (10.7)	0.5
40.5	26.0	X (10.9)	0.6	IV (4.5)	3.5	0.78	0.65	1.40	-0.41	-2.12	X (10.9)	VIII (8.9)	X (10.8)	X (10.8)	X (10.9)	1.7	X (10.8)	X (10.9)	X (10.9)	0.6
40.5	26.5	XI (11.2)	0.8	IV (4.8)	3.5	0.88	0.62	2.18	-0.41	-2.09	X (10.9)	X (10.2)	XI (11.2)	XI (11.2)	XI (11.2)	2.2	XI (11.2)	XI (11.2)	XI (11.2)	0.8
40.5	27.0	X (10.9)	0.7	II (2.4)	4.4	0.77	0.55	2.14	-0.41	-2.35	X (10.9)	VIII (8.1)	X (10.8)	X (10.9)	X (10.9)	2.1	X (10.9)	X (10.9)	X (10.9)	0.7
41.0	19.0	XII (13.5)	16.7	VII (7.7)	0.3	0.11	0.39	3.13	-0.41	-0.08	IX (9.4)	VII (7.8)	IX (9.8)	X (10.1)	X (10.4)	5.3	X (10.6)	X (10.8)	XI (11.0)	8.5

Appendix 13. Continued.

Lat	Lon	ω	σ_ω	μ	σ_μ	λ	σ_λ	$\sigma^2_{\omega\mu}$	$\sigma^2_{\omega\lambda}$	$\sigma^2_{\mu\lambda}$	I_M	I (1)	I_{50}	I_{100}	I_{200}	σ_I	I_{P50}	I_{P100}	I_{P200}	σ_{IP}
41.0	19.5	XII (13.5)	16.7	VII (7.7)	0.3	0.11	0.39	3.13	-0.41	-0.08	IX (9.4)	VII (7.8)	IX (9.8)	X (10.1)	X (10.4)	5.3	X (10.6)	X (10.8)	XI (11.0)	8.5
41.0	20.0	XI (11.3)	4.4	VII (7.7)	0.3	0.22	0.38	0.60	-0.41	-0.06	IX (9.4)	VII (7.9)	IX (9.9)	X (10.1)	X (10.2)	2.5	X (10.4)	X (10.5)	X (10.6)	3.3
41.0	20.5	X (10.3)	1.4	VII (7.7)	0.3	0.41	0.40	0.18	-0.41	-0.06	IX (9.4)	VIII (8.2)	IX (9.9)	X (10.0)	X (10.0)	1.3	X (10.1)	X (10.1)	X (10.2)	1.3
41.0	21.0	X (10.3)	1.4	VII (7.7)	0.3	0.41	0.40	0.18	-0.41	-0.06	IX (9.4)	VIII (8.2)	IX (9.9)	X (10.0)	X (10.0)	1.3	X (10.1)	X (10.1)	X (10.2)	1.3
41.0	21.5	XII (12.6)	4.9	VII (7.6)	0.2	0.21	0.28	0.68	-0.41	-0.04	X (10.9)	VII (7.9)	X (10.5)	X (10.8)	XI (11.0)	2.6	XI (11.2)	XI (11.4)	XI (11.6)	3.6
41.0	22.0	XII (12.2)	4.6	VII (7.4)	0.4	0.24	0.34	1.39	-0.41	-0.11	X (10.9)	VII (7.7)	X (10.4)	X (10.7)	X (10.9)	2.8	XI (11.1)	XI (11.3)	XI (11.4)	3.6
41.0	22.5	XI (11.8)	1.7	VI (6.9)	0.7	0.44	0.34	0.96	-0.41	-0.21	X (10.9)	VII (7.9)	XI (11.1)	XI (11.3)	XI (11.4)	1.9	XI (11.4)	XI (11.5)	XI (11.6)	1.7
41.0	23.0	XI (11.3)	1.1	VI (6.2)	1.4	0.62	0.44	1.25	-0.41	-0.57	X (10.9)	VIII (8.5)	XI (11.0)	XI (11.1)	XI (11.2)	1.9	XI (11.2)	XI (11.2)	XI (11.2)	1.1
41.0	23.5	XI (11.2)	0.8	IV (4.8)	3.5	0.88	0.62	2.18	-0.41	-2.09	X (10.9)	X (10.2)	XI (11.2)	XI (11.2)	XI (11.2)	2.2	XI (11.2)	XI (11.2)	XI (11.2)	0.8
41.0	24.5	XI (11.1)	0.7	IV (4.4)	2.8	0.95	0.52	1.41	-0.41	-1.39	X (10.9)	X (10.7)	XI (11.1)	XI (11.1)	XI (11.1)	1.8	XI (11.1)	XI (11.1)	XI (11.1)	0.7
41.0	25.0	XI (11.2)	0.8	V (5.8)	1.8	0.82	0.48	1.01	-0.41	-0.81	X (10.9)	IX (9.8)	XI (11.1)	XI (11.1)	XI (11.2)	1.6	XI (11.1)	XI (11.2)	XI (11.2)	0.8
41.0	25.5	X (10.8)	0.5	II (2.1)	4.2	0.87	0.56	1.44	-0.41	-2.25	X (10.9)	IX (9.4)	X (10.8)	X (10.8)	X (10.8)	1.8	X (10.8)	X (10.8)	X (10.8)	0.5
41.0	26.0	X (10.9)	0.5	IV (4.4)	2.6	0.81	0.53	0.92	-0.41	-1.27	X (10.9)	IX (9.2)	X (10.9)	X (10.9)	X (10.9)	1.4	X (10.9)	X (10.9)	X (10.9)	0.5
41.0	26.5	XI (11.1)	0.7	IV (4.4)	2.8	0.95	0.52	1.41	-0.41	-1.39	X (10.9)	X (10.7)	XI (11.1)	XI (11.1)	XI (11.1)	1.8	XI (11.1)	XI (11.1)	XI (11.1)	0.7
41.0	27.0	XI (11.3)	0.8	III (3.9)	2.6	0.88	0.44	1.44	-0.41	-1.07	X (10.9)	X (10.1)	XI (11.3)	XI (11.3)	XI (11.3)	1.8	XI (11.3)	XI (11.3)	XI (11.3)	0.8
41.0	27.5	XII (12.3)	2.4	V (5.2)	1.9	0.44	0.39	3.97	-0.41	-0.70	X (10.9)	VI (6.8)	XI (11.3)	XI (11.6)	XI (11.8)	3.2	XI (11.9)	XII (12)	XII (12.1)	2.4
41.0	28.0	XII (12.3)	2.4	V (5.2)	1.9	0.44	0.39	3.97	-0.41	-0.70	X (10.9)	VI (6.8)	XI (11.3)	XI (11.6)	XI (11.8)	3.2	XI (11.9)	XII (12)	XII (12.1)	2.4
41.5	19.0	XII (13.5)	16.7	VII (7.7)	0.3	0.11	0.39	3.13	-0.41	-0.08	IX (9.4)	VII (7.8)	IX (9.8)	X (10.1)	X (10.4)	5.3	X (10.6)	X (10.8)	XI (11.0)	8.5
41.5	19.5	XII (13.5)	16.7	VII (7.7)	0.3	0.11	0.39	3.13	-0.41	-0.08	IX (9.4)	VII (7.8)	IX (9.8)	X (10.1)	X (10.4)	5.3	X (10.6)	X (10.8)	XI (11.0)	8.5
41.5	20.0	XI (11.3)	4.4	VII (7.7)	0.3	0.22	0.38	0.60	-0.41	-0.06	IX (9.4)	VII (7.9)	IX (9.9)	X (10.1)	X (10.2)	2.5	X (10.4)	X (10.5)	X (10.6)	3.3
41.5	20.5	X (10.3)	1.4	VII (7.7)	0.3	0.41	0.40	0.18	-0.41	-0.06	IX (9.4)	VIII (8.2)	IX (9.9)	X (10.0)	X (10.0)	1.3	X (10.1)	X (10.1)	X (10.2)	1.3
41.5	21.0	X (10.3)	1.4	VII (7.7)	0.3	0.41	0.40	0.18	-0.41	-0.06	IX (9.4)	VIII (8.2)	IX (9.9)	X (10.0)	X (10.0)	1.3	X (10.1)	X (10.1)	X (10.2)	1.3
41.5	21.5	XII (12.6)	4.9	VII (7.6)	0.2	0.21	0.28	0.68	-0.41	-0.04	X (10.9)	VII (7.9)	X (10.5)	X (10.8)	XI (11.0)	2.6	XI (11.2)	XI (11.4)	XI (11.6)	3.6

Appendix 13. Continued.

Lat	Lon	ω	σ_ω	μ	σ_μ	λ	σ_λ	$\sigma^2_{\omega\mu}$	$\sigma^2_{\omega\lambda}$	$\sigma^2_{\mu\lambda}$	I_M	I (1)	I_{50}	I_{100}	I_{200}	σ_I	I_{P50}	I_{P100}	I_{P200}	σ_{IP}
41.5	22.0	XII (12.2)	4.6	VII (7.4)	0.4	0.24	0.34	1.39	-0.41	-0.11	X (10.9)	VII (7.7)	X (10.4)	X (10.7)	X (10.9)	2.8	XI (11.1)	XI (11.3)	XI (11.4)	3.6
41.5	22.5	XI (11.8)	1.7	VI (6.9)	0.7	0.44	0.34	0.96	-0.41	-0.21	X (10.9)	VII (7.9)	XI (11.1)	XI (11.3)	XI (11.4)	1.9	XI (11.4)	XI (11.5)	XI (11.6)	1.7
41.5	23.0	XII (12.0)	1.9	V (5.6)	1.6	0.49	0.38	2.39	-0.41	-0.55	X (10.9)	VII (7.4)	XI (11.3)	XI (11.5)	XI (11.6)	2.6	XI (11.6)	XI (11.7)	XI (11.8)	1.8
41.5	24.5	XII (12.0)	1.9	V (5.6)	1.6	0.49	0.38	2.39	-0.41	-0.55	X (10.9)	VII (7.4)	XI (11.3)	XI (11.5)	XI (11.6)	2.6	XI (11.6)	XI (11.7)	XI (11.8)	1.8
41.5	25.0	XI (11.4)	1.2	V (5.5)	1.9	0.64	0.44	1.78	-0.41	-0.78	X (10.9)	VIII (8.3)	XI (11.1)	XI (11.2)	XI (11.3)	2.1	XI (11.3)	XI (11.3)	XI (11.3)	1.2
41.5	25.5	XI (11.3)	0.8	II (2.2)	3.8	0.93	0.46	2.15	-0.41	-1.66	X (10.9)	X (10.6)	XI (11.3)	XI (11.3)	XI (11.3)	2.2	XI (11.3)	XI (11.3)	XI (11.3)	0.8
41.5	26.0	XI (11.5)	1.0	V (5.2)	1.6	0.69	0.37	1.13	-0.41	-0.53	X (10.9)	VIII (8.7)	XI (11.4)	XI (11.4)	XI (11.5)	1.7	XI (11.5)	XI (11.5)	XI (11.5)	1.0
41.5	26.5	XI (11.7)	1.5	VI (6.1)	1.3	0.52	0.38	1.54	-0.41	-0.44	X (10.9)	VII (7.8)	XI (11.2)	XI (11.3)	XI (11.4)	2.1	XI (11.4)	XI (11.5)	XI (11.6)	1.5
41.5	27.0	XII (13.3)	4.2	VI (6.6)	0.8	0.28	0.31	2.67	-0.41	-0.21	X (10.9)	VII (7.2)	XI (11.3)	XI (11.6)	XI (11.9)	3.2	XII (12.1)	XII (12.3)	XII (12.5)	3.6
41.5	27.5	XII (14.1)	6.1	VI (6.4)	0.9	0.24	0.32	4.81	-0.41	-0.27	X (10.9)	VI (6.9)	XI (11.3)	XI (11.7)	XII (12.1)	4.1	XII (12.3)	XII (12.6)	XII (12.8)	4.9
41.5	28.0	XII (12.9)	3.4	V (5.8)	1.3	0.35	0.35	3.77	-0.41	-0.42	X (10.9)	VI (6.8)	XI (11.3)	XI (11.6)	XI (11.9)	3.3	XII (12.0)	XII (12.2)	XII (12.4)	3.1
42.0	19.0	XI (11.3)	6.7	VII (7.7)	0.3	0.18	0.45	1.24	-0.41	-0.09	IX (9.4)	VII (7.8)	IX (9.5)	IX (9.7)	IX (9.9)	3.2	X (10.1)	X (10.2)	X (10.3)	4.6
42.0	19.5	XI (11.3)	6.7	VII (7.7)	0.3	0.18	0.45	1.24	-0.41	-0.09	IX (9.4)	VII (7.8)	IX (9.5)	IX (9.7)	IX (9.9)	3.2	X (10.1)	X (10.2)	X (10.3)	4.6
42.0	20.0	XI (11.0)	4.4	VII (7.7)	0.3	0.22	0.41	0.61	-0.41	-0.06	IX (9.4)	VII (7.9)	IX (9.7)	IX (9.9)	X (10.0)	2.5	X (10.2)	X (10.3)	X (10.4)	3.3
42.0	20.5	XI (11.3)	4.4	VII (7.7)	0.3	0.22	0.38	0.60	-0.41	-0.06	IX (9.4)	VII (7.9)	IX (9.9)	X (10.1)	X (10.2)	2.5	X (10.4)	X (10.5)	X (10.6)	3.3
42.0	21.0	XI (11.3)	4.4	VII (7.7)	0.3	0.22	0.38	0.60	-0.41	-0.06	IX (9.4)	VII (7.9)	IX (9.9)	X (10.1)	X (10.2)	2.5	X (10.4)	X (10.5)	X (10.6)	3.3
42.0	21.5	XII (14.0)	9.5	VII (7.6)	0.2	0.15	0.28	1.36	-0.41	-0.04	X (10.9)	VII (7.8)	X (10.5)	X (10.8)	XI (11.1)	3.8	XI (11.4)	XI (11.6)	XI (11.8)	5.7
42.0	22.0	XII (12.2)	3.8	VII (7.2)	0.5	0.27	0.33	1.50	-0.41	-0.14	X (10.9)	VII (7.6)	X (10.6)	X (10.9)	XI (11.1)	2.7	XI (11.3)	XI (11.4)	XI (11.6)	3.2
42.0	22.5	XI (11.9)	1.8	VI (6.5)	0.9	0.44	0.34	1.32	-0.41	-0.28	X (10.9)	VII (7.7)	XI (11.1)	XI (11.3)	XI (11.5)	2.1	XI (11.5)	XI (11.6)	XI (11.7)	1.8
42.0	23.0	XI (11.5)	1.3	IV (4.6)	2.5	0.64	0.45	2.64	-0.41	-1.07	X (10.9)	VII (7.9)	XI (11.2)	XI (11.3)	XI (11.4)	2.5	XI (11.4)	XI (11.4)	XI (11.5)	1.3
42.0	24.5	XII (12.0)	1.9	V (5.6)	1.6	0.49	0.38	2.39	-0.41	-0.55	X (10.9)	VII (7.4)	XI (11.3)	XI (11.5)	XI (11.6)	2.6	XI (11.6)	XI (11.7)	XI (11.8)	1.8
42.0	25.0	XI (11.4)	1.2	V (5.5)	1.9	0.64	0.44	1.78	-0.41	-0.78	X (10.9)	VIII (8.3)	XI (11.1)	XI (11.2)	XI (11.3)	2.1	XI (11.3)	XI (11.3)	XI (11.3)	1.2
42.0	25.5	XI (11.3)	0.8	II (2.2)	3.8	0.93	0.46	2.15	-0.41	-1.66	X (10.9)	X (10.6)	XI (11.3)	XI (11.3)	XI (11.3)	2.2	XI (11.3)	XI (11.3)	XI (11.3)	0.8

Appendix 13. Continued.

Lat	Lon	ω	σ_ω	μ	σ_μ	λ	σ_λ	$\sigma^2_{\omega\mu}$	$\sigma^2_{\omega\lambda}$	$\sigma^2_{\mu\lambda}$	I_M	I (1)	I_{50}	I_{100}	I_{200}	σ_I	I_{P50}	I_{P100}	I_{P200}	σ_{IP}
42.0	26.0	XI (11.9)	1.3	VI (6)	1.0	0.54	0.32	1.02	-0.41	-0.29	X (10.9)	VIII (8.0)	XI (11.4)	XI (11.6)	XI (11.7)	1.8	XI (11.7)	XI (11.7)	XI (11.8)	1.3
42.0	26.5	XI (11.9)	1.8	VI (6.5)	0.9	0.44	0.34	1.32	-0.41	-0.28	X (10.9)	VII (7.7)	XI (11.1)	XI (11.3)	XI (11.5)	2.1	XI (11.5)	XI (11.6)	XI (11.7)	1.8
42.0	27.0	XI (11.9)	1.3	VI (6)	1.0	0.54	0.32	1.02	-0.41	-0.29	X (10.9)	VIII (8.0)	XI (11.4)	XI (11.6)	XI (11.7)	1.8	XI (11.7)	XI (11.7)	XI (11.8)	1.3
42.0	27.5	XII (12.1)	1.5	V (5.5)	1.3	0.52	0.33	1.51	-0.41	-0.38	X (10.9)	VII (7.6)	XI (11.5)	XI (11.7)	XI (11.8)	2.1	XI (11.8)	XI (11.9)	XI (11.9)	1.5
42.0	28.0	XI (11.7)	1.0	IV (4.4)	2.1	0.70	0.38	1.64	-0.41	-0.73	X (10.9)	VIII (8.5)	XI (11.4)	XI (11.5)	XI (11.6)	2.0	XI (11.6)	XI (11.6)	XI (11.6)	1.0
42.5	19.0	XI (11.1)	5.8	VII (7.6)	0.3	0.20	0.47	1.38	-0.41	-0.12	IX (9.4)	VII (7.7)	IX (9.6)	IX (9.8)	X (10.0)	3.1	X (10.1)	X (10.2)	X (10.4)	4.2
42.5	19.5	XI (11.1)	5.8	VII (7.6)	0.3	0.20	0.47	1.38	-0.41	-0.12	IX (9.4)	VII (7.7)	IX (9.6)	IX (9.8)	X (10.0)	3.1	X (10.1)	X (10.2)	X (10.4)	4.2
42.5	20.0	XI (11.1)	5.8	VII (7.6)	0.3	0.20	0.47	1.38	-0.41	-0.12	IX (9.4)	VII (7.7)	IX (9.6)	IX (9.8)	X (10.0)	3.1	X (10.1)	X (10.2)	X (10.4)	4.2
42.5	20.5	XI (11.9)	7.2	VII (7.6)	0.3	0.18	0.41	1.70	-0.41	-0.11	IX (9.4)	VII (7.8)	IX (9.8)	X (10.1)	X (10.3)	3.5	X (10.5)	X (10.6)	X (10.8)	4.9
42.5	21.0	XI (11.9)	7.2	VII (7.6)	0.3	0.18	0.41	1.70	-0.41	-0.11	IX (9.4)	VII (7.8)	IX (9.8)	X (10.1)	X (10.3)	3.5	X (10.5)	X (10.6)	X (10.8)	4.9
42.5	21.5	XII (26.3)	112.4	VII (7.5)	0.3	0.04	0.29	26.40	-0.41	-0.07	X (10.9)	VII (7.5)	X (10.5)	XI (11.0)	XI (11.5)	14.3	XII (12.0)	XII (12.4)	XII (12.8)	27.3
42.5	22.0	XII (13.1)	6.4	VII (7.0)	0.6	0.21	0.34	3.11	-0.41	-0.18	X (10.9)	VII (7.3)	X (10.6)	XI (11.0)	XI (11.3)	3.7	XI (11.5)	XI (11.7)	XI (11.9)	4.9
42.5	22.5	XII (12.6)	3.0	VI (6.3)	1.0	0.35	0.34	2.61	-0.41	-0.32	X (10.9)	VII (7.2)	XI (11.2)	XI (11.5)	XI (11.8)	2.9	XI (11.9)	XII (12.1)	XII (12.2)	2.8
43.0	19.0	XI (11.5)	15.5	VII (7.4)	0.7	0.14	0.72	8.95	-0.41	-0.43	IX (9.4)	VII (7.5)	IX (9.2)	IX (9.4)	IX (9.6)	6.1	IX (9.8)	X (10.0)	X (10.1)	9.4
43.0	19.5	XI (11.5)	15.5	VII (7.4)	0.7	0.14	0.72	8.95	-0.41	-0.43	IX (9.4)	VII (7.5)	IX (9.2)	IX (9.4)	IX (9.6)	6.1	IX (9.8)	X (10.0)	X (10.1)	9.4
43.0	20.0	XI (11.5)	15.5	VII (7.4)	0.7	0.14	0.72	8.95	-0.41	-0.43	IX (9.4)	VII (7.5)	IX (9.2)	IX (9.4)	IX (9.6)	6.1	IX (9.8)	X (10.0)	X (10.1)	9.4
43.0	20.5	XI (11.1)	7.3	VII (7.4)	0.6	0.20	0.58	3.52	-0.41	-0.30	IX (9.4)	VII (7.5)	IX (9.5)	IX (9.7)	IX (9.9)	4.0	X (10.0)	X (10.2)	X (10.3)	5.4
43.0	21.0	XI (11.1)	7.3	VII (7.4)	0.6	0.20	0.58	3.52	-0.41	-0.30	IX (9.4)	VII (7.5)	IX (9.5)	IX (9.7)	IX (9.9)	4.0	X (10.0)	X (10.2)	X (10.3)	5.4
43.0	21.5	XII (15.8)	28.6	VII (7.0)	0.7	0.10	0.42	16.05	-0.41	-0.25	X (10.9)	VII (7.1)	X (10.0)	X (10.4)	X (10.8)	8.4	XI (11.2)	XI (11.5)	XI (11.8)	13.9
43.0	22.0	XII (15.6)	24.4	VI (6.6)	1.0	0.13	0.45	21.90	-0.41	-0.41	X (10.9)	VI (6.8)	X (10.2)	X (10.7)	XI (11.1)	8.6	XI (11.5)	XI (11.8)	XII (12.1)	13.6

Appendix 14: Regional intensity hazard $G^{(III)}$ covariance error matrices (PP97)

Macroseismic intensity covariance error matrices, ε, for the broad Balkan area considered between 39.0°N and 45.0°N, 19.0°E and 29.0°E (inclusive). For ease of reference each matrix is arranged with respect to the geographic co-ordinates of the centre of the analysis cell it represents. The first sheet gives covariance error matrices, ε, for the Balkans between meridians 19.0°E and 23.5°E (inclusive). The second sheet gives covariance error matrices, ε, for the Balkans between meridians 24.0°E and 29.0°E (inclusive). Cells with '*null'* forecasts are also given. Matrix elements of ε are:

$$\varepsilon = \begin{bmatrix} \sigma_{\omega}^{2} & \sigma_{\omega\mu}^{2} & \sigma_{\lambda\omega}^{2} \\ \sigma_{\omega\mu}^{2} & \sigma_{\mu}^{2} & \sigma_{\lambda\mu}^{2} \\ \sigma_{\omega\lambda}^{2} & \sigma_{\mu\lambda}^{2} & \sigma_{\lambda}^{2} \end{bmatrix}$$

$\begin{bmatrix} 322.61 & 3.359 & -3.754 \\ 3.359 & 0.079 & -0.041 \\ -3.754 & -0.041 & 0.044 \end{bmatrix}$	$\begin{bmatrix} 322.61 & 3.359 & -3.754 \\ 3.359 & 0.079 & -0.041 \\ -3.754 & -0.041 & 0.044 \end{bmatrix}$	$\begin{bmatrix} 322.61 & 3.359 & -3.754 \\ 3.359 & 0.079 & -0.041 \\ -3.754 & -0.041 & 0.044 \end{bmatrix}$	$\begin{bmatrix} 30.623 & 1.018 & -1.197 \\ 1.018 & 0.085 & -0.044 \\ -1.197 & -0.044 & 0.047 \end{bmatrix}$	$\begin{bmatrix} 30.623 & 1.018 & -1.197 \\ 1.018 & 0.085 & -0.044 \\ -1.197 & -0.044 & 0.047 \end{bmatrix}$	$\begin{bmatrix} 322.61 & 3.359 & -3.754 \\ 3.359 & 0.079 & -0.041 \\ -3.754 & -0.041 & 0.044 \end{bmatrix}$	$\begin{bmatrix} 322.61 & 3.359 & -3.754 \\ 3.359 & 0.079 & -0.041 \\ -3.754 & -0.041 & 0.044 \end{bmatrix}$	$\begin{bmatrix} 44.566 & 2.546 & -1.627 \\ 2.546 & 0.245 & -0.100 \\ -1.627 & -0.100 & 0.060 \end{bmatrix}$	---	---	45.0°N
$\begin{bmatrix} 112.07 & 1.521 & -2.160 \\ 1.521 & 0.060 & -0.032 \\ -2.160 & -0.032 & 0.042 \end{bmatrix}$	$\begin{bmatrix} 112.07 & 1.521 & -2.160 \\ 1.521 & 0.060 & -0.032 \\ -2.160 & -0.032 & 0.042 \end{bmatrix}$	$\begin{bmatrix} 112.07 & 1.521 & -2.160 \\ 1.521 & 0.060 & -0.032 \\ -2.160 & -0.032 & 0.042 \end{bmatrix}$	$\begin{bmatrix} 20.712 & 0.629 & -1.000 \\ 0.629 & 0.062 & -0.035 \\ -1.000 & -0.035 & 0.049 \end{bmatrix}$	$\begin{bmatrix} 26911. & 24.666 & -25.78 \\ 24.666 & 0.056 & -0.024 \\ -25.78 & -0.024 & 0.025 \end{bmatrix}$	$\begin{bmatrix} 326.76 & 2.011 & -2.853 \\ 2.011 & 0.044 & -0.019 \\ -2.853 & -0.019 & 0.025 \end{bmatrix}$	$\begin{bmatrix} 105.64 & 1.110 & -1.681 \\ 1.110 & 0.044 & -0.019 \\ -1.681 & -0.019 & 0.027 \end{bmatrix}$	$\begin{bmatrix} 139.76 & 2.201 & -2.051 \\ 2.201 & 0.081 & -0.035 \\ -2.051 & -0.035 & 0.030 \end{bmatrix}$	$\begin{bmatrix} 3714.8 & 66.664 & -19.09 \\ 66.664 & 1.425 & -0.348 \\ -19.09 & -0.348 & 0.098 \end{bmatrix}$	---	44.5°N
$\begin{bmatrix} 11.948 & 0.230 & -0.496 \\ 0.230 & 0.034 & -0.012 \\ -0.496 & -0.012 & 0.021 \end{bmatrix}$	$\begin{bmatrix} 3.173 & 0.098 & -0.272 \\ 0.098 & 0.034 & -0.012 \\ -0.272 & -0.012 & 0.025 \end{bmatrix}$	$\begin{bmatrix} 4.473 & 0.067 & -0.315 \\ 0.067 & 0.026 & -0.007 \\ -0.315 & -0.007 & 0.023 \end{bmatrix}$	$\begin{bmatrix} 4.483 & 0.067 & -0.331 \\ 0.067 & 0.026 & -0.008 \\ -0.331 & -0.008 & 0.025 \end{bmatrix}$	$\begin{bmatrix} 4.483 & 0.067 & -0.331 \\ 0.067 & 0.026 & -0.008 \\ -0.331 & -0.008 & 0.025 \end{bmatrix}$	$\begin{bmatrix} 5.317 & 0.077 & -0.398 \\ 0.077 & 0.026 & -0.009 \\ -0.398 & -0.009 & 0.031 \end{bmatrix}$	$\begin{bmatrix} 10.128 & 0.124 & -0.595 \\ 0.124 & 0.026 & -0.010 \\ -0.595 & -0.010 & 0.036 \end{bmatrix}$	$\begin{bmatrix} 7.889 & 0.178 & -0.526 \\ 0.178 & 0.034 & -0.015 \\ -0.526 & -0.015 & 0.036 \end{bmatrix}$	$\begin{bmatrix} 201.39 & 3.355 & -3.091 \\ 3.355 & 0.111 & -0.055 \\ -3.091 & -0.055 & 0.048 \end{bmatrix}$	$\begin{bmatrix} 1311.7 & 5.357 & -6.504 \\ 5.357 & 0.057 & -0.028 \\ -6.504 & -0.028 & 0.032 \end{bmatrix}$	44.0°N
$\begin{bmatrix} 8.156 & -0.056 & -0.350 \\ -0.056 & 0.015 & 0.002 \\ -0.350 & 0.002 & 0.015 \end{bmatrix}$	$\begin{bmatrix} 8.156 & -0.056 & -0.350 \\ -0.056 & 0.015 & 0.002 \\ -0.350 & 0.002 & 0.015 \end{bmatrix}$	$\begin{bmatrix} 14.238 & -0.111 & -0.442 \\ -0.111 & 0.014 & 0.003 \\ -0.442 & 0.003 & 0.014 \end{bmatrix}$	$\begin{bmatrix} 26.993 & -0.197 & -0.596 \\ -0.197 & 0.013 & 0.003 \\ -0.596 & 0.003 & 0.013 \end{bmatrix}$	$\begin{bmatrix} 26.993 & -0.197 & -0.596 \\ -0.197 & 0.013 & 0.003 \\ -0.596 & 0.003 & 0.013 \end{bmatrix}$	$\begin{bmatrix} 31.065 & -0.060 & -0.706 \\ -0.060 & 0.015 & 0.001 \\ -0.706 & 0.001 & 0.016 \end{bmatrix}$	$\begin{bmatrix} 69.295 & -0.056 & -1.067 \\ -0.056 & 0.015 & 0.000 \\ -1.067 & 0.000 & 0.017 \end{bmatrix}$	$\begin{bmatrix} 109.10 & 0.122 & -1.407 \\ 0.122 & 0.018 & -0.002 \\ -1.407 & -0.002 & 0.018 \end{bmatrix}$	$\begin{bmatrix} 335.24 & 0.122 & -2.743 \\ 0.636 & 0.021 & -0.006 \\ -2.743 & -0.006 & 0.023 \end{bmatrix}$	$\begin{bmatrix} 561.57 & 1.374 & -3.488 \\ 1.374 & 0.026 & -0.009 \\ -3.488 & -0.009 & 0.022 \end{bmatrix}$	43.5°N
$\begin{bmatrix} 1.009 & -0.059 & -0.137 \\ -0.059 & 0.015 & 0.008 \\ -0.137 & 0.008 & 0.020 \end{bmatrix}$	$\begin{bmatrix} 1.466 & -0.068 & -0.173 \\ -0.068 & 0.015 & 0.008 \\ -0.173 & 0.008 & 0.022 \end{bmatrix}$	$\begin{bmatrix} 3.827 & -0.113 & -0.248 \\ -0.113 & 0.014 & 0.007 \\ -0.248 & 0.007 & 0.017 \end{bmatrix}$	$\begin{bmatrix} 66.799 & -0.372 & -1.063 \\ -0.372 & 0.013 & 0.006 \\ -1.063 & 0.006 & 0.017 \end{bmatrix}$	$\begin{bmatrix} 66.799 & -0.372 & -1.063 \\ -0.372 & 0.013 & 0.006 \\ -1.063 & 0.006 & 0.017 \end{bmatrix}$	$\begin{bmatrix} 19.698 & -0.222 & -0.493 \\ -0.222 & 0.013 & 0.005 \\ -0.493 & 0.005 & 0.013 \end{bmatrix}$	$\begin{bmatrix} 25.150 & -0.192 & -0.570 \\ -0.192 & 0.013 & 0.004 \\ -0.570 & 0.004 & 0.013 \end{bmatrix}$	$\begin{bmatrix} 253.42 & 0.237 & -1.775 \\ 0.237 & 0.018 & -0.002 \\ -1.775 & -0.002 & 0.012 \end{bmatrix}$	$\begin{bmatrix} 205.68 & 0.203 & -1.594 \\ 0.203 & 0.018 & -0.002 \\ -1.594 & -0.002 & 0.012 \end{bmatrix}$	$\begin{bmatrix} 280.98 & 0.938 & -1.966 \\ 0.938 & 0.026 & -0.007 \\ -1.966 & -0.007 & 0.014 \end{bmatrix}$	43.0°N
$\begin{bmatrix} 0.341 & -0.038 & -0.082 \\ -0.038 & 0.017 & 0.011 \\ -0.082 & 0.011 & 0.023 \end{bmatrix}$	$\begin{bmatrix} 0.389 & -0.038 & -0.102 \\ -0.044 & 0.016 & 0.011 \\ -0.102 & 0.011 & 0.024 \end{bmatrix}$	$\begin{bmatrix} 1.021 & -0.038 & -0.128 \\ -0.064 & 0.015 & 0.009 \\ -0.128 & 0.009 & 0.017 \end{bmatrix}$	$\begin{bmatrix} 2.578 & -0.096 & -0.203 \\ -0.096 & 0.014 & 0.008 \\ -0.203 & 0.008 & 0.017 \end{bmatrix}$	$\begin{bmatrix} 2.578 & -0.096 & -0.203 \\ -0.096 & 0.014 & 0.008 \\ -0.203 & 0.008 & 0.017 \end{bmatrix}$	$\begin{bmatrix} 18.061 & -0.214 & -0.432 \\ -0.214 & 0.013 & 0.005 \\ -0.432 & 0.005 & 0.011 \end{bmatrix}$	$\begin{bmatrix} 10.740 & -0.173 & -0.315 \\ -0.173 & 0.013 & 0.005 \\ -0.315 & 0.005 & 0.009 \end{bmatrix}$	$\begin{bmatrix} 58.096 & -0.167 & -0.716 \\ -0.167 & 0.014 & 0.002 \\ -0.716 & 0.002 & 0.009 \end{bmatrix}$	$\begin{bmatrix} 4457.9 & -0.642 & -6.257 \\ -0.642 & 0.014 & 0.001 \\ -6.257 & 0.002 & 0.009 \end{bmatrix}$	$\begin{bmatrix} 211.65 & -0.033 & -1.446 \\ -0.033 & 0.015 & 0.000 \\ -1.446 & 0.000 & 0.001 \end{bmatrix}$	42.5°N
$\begin{bmatrix} 0.626 & -0.051 & -0.103 \\ -0.051 & 0.015 & 0.010 \\ -0.103 & 0.010 & 0.019 \end{bmatrix}$	$\begin{bmatrix} 1.579 & -0.051 & -0.173 \\ -0.078 & 0.014 & 0.009 \\ -0.173 & 0.009 & 0.020 \end{bmatrix}$	$\begin{bmatrix} 8.424 & -0.156 & -0.412 \\ -0.156 & 0.013 & 0.007 \\ -0.412 & 0.007 & 0.021 \end{bmatrix}$	$\begin{bmatrix} 5.163 & -0.128 & -0.310 \\ -0.128 & 0.014 & 0.008 \\ -0.310 & 0.008 & 0.019 \end{bmatrix}$	$\begin{bmatrix} 5.163 & -0.128 & -0.310 \\ -0.128 & 0.014 & 0.008 \\ -0.310 & 0.008 & 0.019 \end{bmatrix}$	$\begin{bmatrix} 21.443 & -0.230 & -0.552 \\ -0.230 & 0.013 & 0.006 \\ -0.552 & 0.006 & 0.014 \end{bmatrix}$	$\begin{bmatrix} 19.612 & -0.222 & -0.459 \\ -0.222 & 0.013 & 0.005 \\ -0.459 & 0.005 & 0.011 \end{bmatrix}$	$\begin{bmatrix} 272.58 & -0.480 & -1.597 \\ -0.480 & 0.013 & 0.003 \\ -1.597 & 0.003 & 0.009 \end{bmatrix}$	$\begin{bmatrix} 310.92 & -0.506 & -1.545 \\ -0.506 & 0.013 & 0.002 \\ -1.545 & 0.002 & 0.008 \end{bmatrix}$	$\begin{bmatrix} 243.72 & -0.255 & -1.450 \\ -0.255 & 0.014 & 0.001 \\ -1.450 & 0.001 & 0.009 \end{bmatrix}$	42.0°N
$\begin{bmatrix} 0.667 & -0.053 & -0.101 \\ -0.053 & 0.015 & 0.009 \\ -0.101 & 0.009 & 0.017 \end{bmatrix}$	$\begin{bmatrix} 1.508 & -0.076 & -0.160 \\ -0.076 & 0.014 & 0.009 \\ -0.160 & 0.009 & 0.018 \end{bmatrix}$	$\begin{bmatrix} 5.163 & -0.128 & -0.310 \\ -0.128 & 0.014 & 0.008 \\ -0.310 & 0.008 & 0.019 \end{bmatrix}$	$\begin{bmatrix} 3.211 & -0.105 & -0.238 \\ -0.105 & 0.014 & 0.008 \\ -0.238 & 0.008 & 0.018 \end{bmatrix}$	$\begin{bmatrix} 3.211 & -0.105 & -0.238 \\ -0.105 & 0.014 & 0.008 \\ -0.238 & 0.008 & 0.018 \end{bmatrix}$	$\begin{bmatrix} 12.000 & -0.105 & -0.404 \\ -0.181 & 0.013 & 0.006 \\ -0.404 & 0.006 & 0.014 \end{bmatrix}$	$\begin{bmatrix} 18.351 & -0.216 & -0.521 \\ -0.216 & 0.013 & 0.006 \\ -0.521 & 0.006 & 0.015 \end{bmatrix}$	$\begin{bmatrix} 30.005 & -0.265 & -0.497 \\ -0.265 & 0.013 & 0.004 \\ -0.497 & 0.004 & 0.008 \end{bmatrix}$	$\begin{bmatrix} 127.97 & -0.356 & -0.986 \\ -0.356 & 0.013 & 0.002 \\ -0.986 & 0.002 & 0.008 \end{bmatrix}$	$\begin{bmatrix} 243.72 & -0.255 & -1.450 \\ -0.255 & 0.014 & 0.001 \\ -1.450 & 0.001 & 0.009 \end{bmatrix}$	41.5°N
$\begin{bmatrix} 16.043 & -0.204 & -0.547 \\ -0.204 & 0.013 & 0.007 \\ -0.547 & 0.007 & 0.019 \end{bmatrix}$	$\begin{bmatrix} 16.043 & -0.204 & -0.547 \\ -0.204 & 0.013 & 0.007 \\ -0.547 & 0.007 & 0.019 \end{bmatrix}$	$\begin{bmatrix} 5.163 & -0.128 & -0.310 \\ -0.128 & 0.014 & 0.008 \\ -0.310 & 0.008 & 0.019 \end{bmatrix}$	$\begin{bmatrix} 3.211 & -0.105 & -0.238 \\ -0.105 & 0.014 & 0.008 \\ -0.238 & 0.008 & 0.018 \end{bmatrix}$	$\begin{bmatrix} 3.211 & -0.105 & -0.238 \\ -0.105 & 0.014 & 0.008 \\ -0.238 & 0.008 & 0.018 \end{bmatrix}$	$\begin{bmatrix} 12.000 & -0.105 & -0.404 \\ -0.181 & 0.013 & 0.006 \\ -0.404 & 0.006 & 0.014 \end{bmatrix}$	$\begin{bmatrix} 18.351 & -0.216 & -0.521 \\ -0.216 & 0.013 & 0.006 \\ -0.521 & 0.006 & 0.015 \end{bmatrix}$	$\begin{bmatrix} 30.005 & -0.265 & -0.497 \\ -0.265 & 0.013 & 0.004 \\ -0.497 & 0.004 & 0.008 \end{bmatrix}$	$\begin{bmatrix} 21.184 & -0.180 & -0.449 \\ -0.180 & 0.013 & 0.003 \\ -0.449 & 0.003 & 0.010 \end{bmatrix}$	$\begin{bmatrix} 54.840 & -0.257 & -0.566 \\ -0.257 & 0.013 & 0.002 \\ -0.566 & 0.002 & 0.006 \end{bmatrix}$	41.0°N
$\begin{bmatrix} 16.043 & -0.204 & -0.547 \\ -0.204 & 0.013 & 0.007 \\ -0.547 & 0.007 & 0.019 \end{bmatrix}$	$\begin{bmatrix} 16.043 & -0.204 & -0.547 \\ -0.204 & 0.013 & 0.007 \\ -0.547 & 0.007 & 0.019 \end{bmatrix}$	$\begin{bmatrix} 5.163 & -0.128 & -0.310 \\ -0.128 & 0.014 & 0.008 \\ -0.310 & 0.008 & 0.019 \end{bmatrix}$	$\begin{bmatrix} 3.211 & -0.105 & -0.238 \\ -0.105 & 0.014 & 0.008 \\ -0.238 & 0.008 & 0.018 \end{bmatrix}$	$\begin{bmatrix} 3.211 & -0.105 & -0.238 \\ -0.105 & 0.014 & 0.008 \\ -0.238 & 0.008 & 0.018 \end{bmatrix}$	$\begin{bmatrix} 12.000 & -0.105 & -0.404 \\ -0.181 & 0.013 & 0.006 \\ -0.404 & 0.006 & 0.014 \end{bmatrix}$	$\begin{bmatrix} 18.351 & -0.216 & -0.521 \\ -0.216 & 0.013 & 0.006 \\ -0.521 & 0.006 & 0.015 \end{bmatrix}$	$\begin{bmatrix} 30.005 & -0.265 & -0.497 \\ -0.265 & 0.013 & 0.004 \\ -0.497 & 0.004 & 0.008 \end{bmatrix}$	$\begin{bmatrix} 21.184 & -0.180 & -0.449 \\ -0.180 & 0.013 & 0.003 \\ -0.449 & 0.003 & 0.010 \end{bmatrix}$	$\begin{bmatrix} 54.840 & -0.257 & -0.566 \\ -0.257 & 0.013 & 0.002 \\ -0.566 & 0.002 & 0.006 \end{bmatrix}$	40.5°N
$\begin{bmatrix} 2.276 & -0.080 & -0.218 \\ -0.080 & 0.014 & 0.007 \\ -0.218 & 0.007 & 0.022 \end{bmatrix}$	$\begin{bmatrix} 2.276 & -0.080 & -0.218 \\ -0.080 & 0.014 & 0.007 \\ -0.218 & 0.007 & 0.022 \end{bmatrix}$	$\begin{bmatrix} 1.113 & -0.061 & -0.151 \\ -0.061 & 0.015 & 0.009 \\ -0.151 & 0.009 & 0.022 \end{bmatrix}$	$\begin{bmatrix} 0.891 & -0.056 & -0.131 \\ -0.056 & 0.015 & 0.009 \\ -0.131 & 0.009 & 0.021 \end{bmatrix}$	$\begin{bmatrix} 0.891 & -0.056 & -0.131 \\ -0.056 & 0.015 & 0.009 \\ -0.131 & 0.009 & 0.021 \end{bmatrix}$	$\begin{bmatrix} 3.413 & -0.092 & -0.216 \\ -0.092 & 0.014 & 0.006 \\ -0.216 & 0.006 & 0.014 \end{bmatrix}$	$\begin{bmatrix} 10.520 & -0.139 & -0.356 \\ -0.139 & 0.014 & 0.004 \\ -0.356 & 0.004 & 0.012 \end{bmatrix}$	$\begin{bmatrix} 7.450 & -0.123 & -0.265 \\ -0.123 & 0.014 & 0.004 \\ -0.265 & 0.004 & 0.010 \end{bmatrix}$	$\begin{bmatrix} 6.368 & -0.054 & -0.226 \\ -0.054 & 0.015 & 0.001 \\ -0.226 & 0.001 & 0.008 \end{bmatrix}$	$\begin{bmatrix} 9.852 & -0.057 & -0.259 \\ -0.057 & 0.015 & 0.001 \\ -0.259 & 0.001 & 0.007 \end{bmatrix}$	40.0°N
$\begin{bmatrix} 4.593 & -0.103 & -0.299 \\ -0.103 & 0.014 & 0.006 \\ -0.299 & 0.006 & 0.020 \end{bmatrix}$	$\begin{bmatrix} 4.593 & -0.103 & -0.299 \\ -0.103 & 0.014 & 0.006 \\ -0.299 & 0.006 & 0.020 \end{bmatrix}$	$\begin{bmatrix} 1.851 & -0.103 & -0.188 \\ -0.074 & 0.014 & 0.007 \\ -0.188 & 0.007 & 0.020 \end{bmatrix}$	$\begin{bmatrix} 1.371 & -0.066 & -0.157 \\ -0.066 & 0.015 & 0.008 \\ -0.157 & 0.008 & 0.019 \end{bmatrix}$	$\begin{bmatrix} 1.371 & -0.066 & -0.157 \\ -0.066 & 0.015 & 0.008 \\ -0.157 & 0.008 & 0.019 \end{bmatrix}$	$\begin{bmatrix} 0.688 & -0.051 & -0.113 \\ -0.051 & 0.015 & 0.009 \\ -0.113 & 0.009 & 0.020 \end{bmatrix}$	$\begin{bmatrix} 1.284 & -0.055 & -0.153 \\ -0.055 & 0.015 & 0.006 \\ -0.153 & 0.006 & 0.020 \end{bmatrix}$	$\begin{bmatrix} 3.813 & -0.051 & -0.230 \\ -0.051 & 0.016 & 0.002 \\ -0.230 & 0.002 & 0.014 \end{bmatrix}$	$\begin{bmatrix} 1.038 & 0.076 & -0.133 \\ 0.076 & 0.049 & -0.015 \\ -0.133 & -0.015 & 0.019 \end{bmatrix}$	$\begin{bmatrix} 0.591 & -0.187 & -0.104 \\ 0.187 & 0.193 & -0.049 \\ -0.104 & -0.049 & 0.021 \end{bmatrix}$	39.5°N
$\begin{bmatrix} 13.988 & -0.154 & -0.553 \\ -0.154 & 0.013 & 0.006 \\ -0.553 & 0.006 & 0.022 \end{bmatrix}$	$\begin{bmatrix} 5.738 & -0.111 & -0.305 \\ -0.111 & 0.014 & 0.006 \\ -0.305 & 0.006 & 0.017 \end{bmatrix}$	$\begin{bmatrix} 2.536 & -0.083 & -0.196 \\ -0.083 & 0.014 & 0.006 \\ -0.196 & 0.006 & 0.016 \end{bmatrix}$	$\begin{bmatrix} 2.536 & -0.083 & -0.196 \\ -0.083 & 0.014 & 0.006 \\ -0.196 & 0.006 & 0.016 \end{bmatrix}$	$\begin{bmatrix} 2.536 & -0.083 & -0.196 \\ -0.083 & 0.014 & 0.006 \\ -0.196 & 0.006 & 0.016 \end{bmatrix}$	$\begin{bmatrix} 1.234 & -0.063 & -0.134 \\ -0.063 & 0.015 & 0.007 \\ -0.134 & 0.007 & 0.016 \end{bmatrix}$	$\begin{bmatrix} 1.423 & -0.056 & -0.144 \\ -0.056 & 0.015 & 0.005 \\ -0.144 & 0.005 & 0.016 \end{bmatrix}$	$\begin{bmatrix} 0.414 & -0.002 & -0.105 \\ -0.002 & 0.025 & -0.003 \\ -0.105 & -0.003 & 0.031 \end{bmatrix}$	$\begin{bmatrix} 0.154 & 1.035 & -0.169 \\ 1.035 & 17.120 & -2.146 \\ -0.169 & -2.146 & 0.294 \end{bmatrix}$	$\begin{bmatrix} 0.266 & 1.428 & -0.159 \\ 1.428 & 15.982 & -1.395 \\ -0.159 & -1.395 & 0.133 \end{bmatrix}$	39.0°N
19.0°E	19.5°E	20.0°E	20.5°E	21.0°E	21.5°E	22.0°E	22.5°E	23.0°E	23.5°E	

---	---	---	$\begin{bmatrix}21.556 & 4.914 & -1.571\\ 4.914 & 1.508 & -0.387\\ -1.571 & -0.387 & 0.117\end{bmatrix}$	$\begin{bmatrix}1.072 & 1.644 & -0.364\\ 1.644 & 1.508 & -0.722\\ -0.364 & -0.722 & 0.142\end{bmatrix}$	$\begin{bmatrix}2.009 & 1.446 & -0.447\\ 1.446 & 1.694 & -0.393\\ -0.447 & -0.393 & 0.109\end{bmatrix}$	$\begin{bmatrix}233.39 & 8.829 & -2.765\\ 8.829 & 0.467 & -0.109\\ -2.765 & -0.109 & 0.033\end{bmatrix}$	$\begin{bmatrix}233.39 & 8.829 & -2.765\\ 8.829 & 0.467 & -0.109\\ -2.765 & -0.109 & 0.033\end{bmatrix}$	$\begin{bmatrix}873.92 & 16.589 & -6.250\\ 16.589 & 0.432 & -0.122\\ -6.250 & -0.122 & 0.045\end{bmatrix}$	$\begin{bmatrix}59197. & 254.29 & -59.04\\ 254.29 & 1.286 & -0.255\\ -59.04 & -0.255 & 0.059\end{bmatrix}$	---
---	$\begin{bmatrix}1.616 & 2.608 & -0.425\\ 2.608 & 6.386 & -0.848\\ -0.425 & -0.848 & 0.125\end{bmatrix}$	$\begin{bmatrix}0.563 & 1.440 & -0.298\\ 1.440 & 6.677 & -1.075\\ -0.298 & -1.075 & 0.194\end{bmatrix}$	$\begin{bmatrix}1.623 & 0.992 & -0.390\\ 0.992 & 1.069 & -0.298\\ -0.390 & -0.298 & 0.103\end{bmatrix}$	$\begin{bmatrix}0.452 & 0.957 & -0.229\\ 0.957 & 3.987 & -0.710\\ -0.229 & -0.710 & 0.145\end{bmatrix}$	$\begin{bmatrix}0.452 & 0.957 & -0.229\\ 0.957 & 3.987 & -0.710\\ -0.229 & -0.710 & 0.145\end{bmatrix}$	$\begin{bmatrix}500.55 & 12.696 & -3.993\\ 12.696 & 0.445 & -0.105\\ -3.993 & -0.105 & 0.032\end{bmatrix}$	$\begin{bmatrix}500.55 & 12.696 & -3.993\\ 12.696 & 0.445 & -0.105\\ -3.993 & -0.105 & 0.032\end{bmatrix}$	$\begin{bmatrix}354.44 & 10.768 & -3.705\\ 10.768 & 0.455 & -0.117\\ -3.705 & -0.117 & 0.039\end{bmatrix}$	$\begin{bmatrix}59197. & 254.29 & -59.04\\ 254.29 & 1.286 & -0.255\\ -59.04 & -0.255 & 0.059\end{bmatrix}$	---
$\begin{bmatrix}83.754 & 0.982 & -1.445\\ 0.982 & 0.044 & -0.019\\ -1.445 & -0.019 & 0.025\end{bmatrix}$	$\begin{bmatrix}39.695 & 0.657 & -0.927\\ 0.657 & 0.045 & -0.017\\ -0.927 & -0.017 & 0.022\end{bmatrix}$	$\begin{bmatrix}123.48 & 0.875 & -1.649\\ 0.875 & 0.034 & -0.013\\ -1.649 & -0.013 & 0.022\end{bmatrix}$	$\begin{bmatrix}152.90 & 0.981 & -1.881\\ 0.981 & 0.034 & -0.013\\ -1.881 & -0.013 & 0.023\end{bmatrix}$	$\begin{bmatrix}31.826 & 0.409 & -0.845\\ 0.409 & 0.034 & -0.013\\ -1.845 & -0.013 & 0.023\end{bmatrix}$	$\begin{bmatrix}21.808 & 0.647 & -0.753\\ 0.647 & 0.062 & -0.026\\ -0.753 & -0.013 & 0.027\end{bmatrix}$	$\begin{bmatrix}134.56 & 2.159 & -1.502\\ 2.159 & 0.081 & -0.026\\ -1.502 & -0.026 & 0.017\end{bmatrix}$	$\begin{bmatrix}63.134 & 3.008 & -1.328\\ 3.008 & 0.238 & -0.068\\ -1.328 & -0.068 & 0.028\end{bmatrix}$	$\begin{bmatrix}354.44 & 10.768 & -3.705\\ 10.768 & 0.455 & -0.117\\ -3.705 & -0.117 & 0.039\end{bmatrix}$	$\begin{bmatrix}59197. & 254.29 & -59.04\\ 254.29 & 1.286 & -0.255\\ -59.04 & -0.255 & 0.059\end{bmatrix}$	---
$\begin{bmatrix}218.55 & 1.191 & -2.502\\ 1.191 & 0.034 & -0.012\\ -2.052 & -0.012 & 0.019\end{bmatrix}$	$\begin{bmatrix}77.624 & 0.676 & -1.151\\ 0.676 & 0.034 & -0.011\\ -1.151 & -0.011 & 0.017\end{bmatrix}$	$\begin{bmatrix}117.54 & 0.573 & -1.338\\ 0.573 & 0.026 & -0.007\\ -1.338 & -0.007 & 0.015\end{bmatrix}$	$\begin{bmatrix}282.65 & 0.942 & -2.570\\ 0.942 & 0.026 & -0.010\\ -2.570 & -0.010 & 0.023\end{bmatrix}$	$\begin{bmatrix}123.48 & 0.873 & -1.649\\ 0.873 & 0.034 & -0.013\\ -1.649 & -0.013 & 0.022\end{bmatrix}$	$\begin{bmatrix}33.623 & 0.813 & -0.940\\ 0.813 & 0.061 & -0.026\\ -0.940 & -0.026 & 0.027\end{bmatrix}$	$\begin{bmatrix}84.707 & 1.316 & -1.184\\ 1.316 & 0.060 & -0.020\\ -1.184 & -0.020 & 0.017\end{bmatrix}$	$\begin{bmatrix}74.949 & 2.051 & -1.379\\ 2.051 & 0.115 & -0.041\\ -1.379 & -0.041 & 0.026\end{bmatrix}$	$\begin{bmatrix}348.28 & 6.870 & -3.528\\ 6.870 & 0.216 & -0.073\\ -3.528 & -0.073 & 0.036\end{bmatrix}$	$\begin{bmatrix}678.772 & 18.399 & -5.839\\ 18.399 & 0.653 & -0.163\\ -5.839 & -0.163 & 0.050\end{bmatrix}$	---
$\begin{bmatrix}95.530 & 0.508 & -1.140\\ 0.508 & 0.026 & -0.007\\ -1.140 & -0.007 & 0.014\end{bmatrix}$	$\begin{bmatrix}64.075 & 0.402 & -0.904\\ 0.402 & 0.026 & -0.007\\ -0.904 & -0.007 & 0.013\end{bmatrix}$	$\begin{bmatrix}90.340 & 0.283 & -0.985\\ 0.283 & 0.021 & -0.004\\ -0.985 & -0.004 & 0.011\end{bmatrix}$	$\begin{bmatrix}272.77 & 0.563 & -1.856\\ 0.563 & 0.021 & -0.004\\ -1.856 & -0.004 & 0.013\end{bmatrix}$	$\begin{bmatrix}78.703 & 0.454 & -1.027\\ 0.454 & 0.026 & -0.007\\ -1.027 & -0.007 & 0.014\end{bmatrix}$	$\begin{bmatrix}33.623 & 0.813 & -0.940\\ 0.813 & 0.061 & -0.026\\ -0.940 & -0.026 & 0.027\end{bmatrix}$	$\begin{bmatrix}84.707 & 1.316 & -1.184\\ 1.316 & 0.060 & -0.020\\ -1.184 & -0.020 & 0.017\end{bmatrix}$	$\begin{bmatrix}74.949 & 2.051 & -1.379\\ 2.051 & 0.115 & -0.041\\ -1.379 & -0.041 & 0.026\end{bmatrix}$	$\begin{bmatrix}393.71 & 5.858 & -3.541\\ 5.858 & 0.152 & -0.055\\ -3.541 & -0.055 & 0.032\end{bmatrix}$	$\begin{bmatrix}699.17 & 11.976 & -5.457\\ 11.976 & 0.300 & -0.097\\ -5.457 & -0.097 & 0.043\end{bmatrix}$	$\begin{bmatrix}2616.5 & 35.122 & -11.08\\ 35.122 & 0.609 & -0.152\\ -11.08 & -0.152 & 0.047\end{bmatrix}$
$\begin{bmatrix}1934.2 & 0.162 & -4.239\\ 0.162 & 0.015 & -0.001\\ -4.239 & -0.001 & 0.009\end{bmatrix}$	$\begin{bmatrix}1934.2 & 0.162 & -4.239\\ 0.162 & 0.015 & -0.001\\ -4.239 & -0.001 & 0.009\end{bmatrix}$	$\begin{bmatrix}44.554 & -0.060 & -0.626\\ -0.060 & 0.015 & 0.000\\ -0.626 & 0.000 & 0.009\end{bmatrix}$	$\begin{bmatrix}231.15 & 0.221 & -1.564\\ 0.221 & 0.018 & -0.002\\ -1.564 & -0.002 & 0.011\end{bmatrix}$	$\begin{bmatrix}43.844 & 0.049 & -0.658\\ 0.049 & 0.018 & -0.001\\ -0.658 & -0.001 & 0.010\end{bmatrix}$	$\begin{bmatrix}73.347 & 0.085 & -0.968\\ 0.085 & 0.018 & -0.002\\ -0.968 & -0.002 & 0.013\end{bmatrix}$	$\begin{bmatrix}38.396 & 0.295 & -0.677\\ 0.295 & 0.026 & -0.006\\ -0.677 & -0.006 & 0.012\end{bmatrix}$	$\begin{bmatrix}129.39 & 0.896 & -1.379\\ 0.896 & 0.034 & -0.011\\ -1.379 & -0.011 & 0.015\end{bmatrix}$	$\begin{bmatrix}174.57 & 1.448 & -1.677\\ 1.448 & 0.044 & -0.015\\ -1.677 & -0.015 & 0.016\end{bmatrix}$	$\begin{bmatrix}131.59 & 2.135 & -1.514\\ 2.135 & 0.081 & -0.026\\ -1.514 & -0.026 & 0.018\end{bmatrix}$	$\begin{bmatrix}232.12 & 2.844 & -1.849\\ 2.844 & 0.080 & -0.024\\ -1.849 & -0.024 & 0.015\end{bmatrix}$
$\begin{bmatrix}3169.6 & -0.573 & -5.418\\ -0.573 & 0.014 & 0.001\\ -5.418 & 0.001 & 0.009\end{bmatrix}$	$\begin{bmatrix}380.95 & -0.293 & -1.900\\ -0.293 & 0.014 & 0.001\\ -1.900 & 0.001 & 0.001\end{bmatrix}$	$\begin{bmatrix}56.187 & -0.165 & -0.692\\ -0.165 & 0.014 & 0.002\\ -0.692 & 0.002 & 0.009\end{bmatrix}$	$\begin{bmatrix}36.344 & -0.060 & -0.527\\ -0.060 & 0.015 & 0.000\\ -0.527 & 0.000 & 0.008\end{bmatrix}$	$\begin{bmatrix}11.959 & -0.146 & -0.271\\ -0.146 & 0.014 & 0.003\\ -0.271 & 0.003 & 0.006\end{bmatrix}$	$\begin{bmatrix}10.614 & -0.139 & -0.275\\ -0.139 & 0.014 & 0.003\\ -0.275 & 0.003 & 0.007\end{bmatrix}$	$\begin{bmatrix}4.889 & -0.081 & -0.185\\ -0.081 & 0.014 & 0.003\\ -0.185 & 0.003 & 0.007\end{bmatrix}$	$\begin{bmatrix}7.699 & -0.056 & -0.249\\ -0.056 & 0.015 & 0.001\\ -0.249 & 0.001 & 0.008\end{bmatrix}$	$\begin{bmatrix}4.882 & -0.023 & -0.221\\ -0.023 & 0.021 & 0.002\\ -0.221 & 0.002 & 0.010\end{bmatrix}$	$\begin{bmatrix}2.449 & 0.375 & -0.204\\ 0.375 & 0.150 & -0.039\\ -0.204 & -0.039 & 0.018\end{bmatrix}$	$\begin{bmatrix}13.171 & 0.244 & -0.368\\ 0.244 & 0.034 & -0.008\\ -0.368 & -0.008 & 0.011\end{bmatrix}$
$\begin{bmatrix}3169.6 & -0.573 & -5.418\\ -0.573 & 0.014 & 0.001\\ -5.418 & 0.001 & 0.009\end{bmatrix}$	$\begin{bmatrix}380.95 & -0.293 & -1.900\\ -0.293 & 0.014 & 0.001\\ -1.900 & 0.001 & 0.001\end{bmatrix}$	$\begin{bmatrix}56.187 & -0.165 & -0.692\\ -0.165 & 0.014 & 0.002\\ -0.692 & 0.002 & 0.009\end{bmatrix}$	$\begin{bmatrix}125.86 & -0.209 & -0.938\\ -0.209 & 0.014 & 0.001\\ -0.938 & 0.001 & 0.007\end{bmatrix}$	$\begin{bmatrix}23.310 & -0.186 & -0.374\\ -0.186 & 0.013 & 0.003\\ -0.374 & 0.003 & 0.006\end{bmatrix}$	$\begin{bmatrix}21.687 & -0.181 & -0.388\\ -0.181 & 0.013 & 0.003\\ -0.388 & 0.003 & 0.007\end{bmatrix}$	$\begin{bmatrix}18.089 & -0.170 & -0.344\\ -0.170 & 0.013 & 0.003\\ -0.344 & 0.003 & 0.007\end{bmatrix}$	$\begin{bmatrix}27.583 & -0.134 & -0.463\\ -0.134 & 0.014 & 0.002\\ -0.463 & 0.002 & 0.008\end{bmatrix}$	$\begin{bmatrix}13.995 & 0.001 & -0.368\\ 0.001 & 0.018 & -0.001\\ -0.368 & -0.001 & 0.010\end{bmatrix}$	$\begin{bmatrix}26.527 & 0.120 & -0.528\\ 0.120 & 0.021 & -0.003\\ -0.528 & -0.003 & 0.011\end{bmatrix}$	$\begin{bmatrix}33.627 & 0.144 & -0.564\\ 0.144 & 0.021 & -0.003\\ -0.564 & -0.003 & 0.010\end{bmatrix}$
$\begin{bmatrix}276.50 & -0.482 & -0.320\\ -0.482 & 0.013 & 0.002\\ -1.320 & 0.002 & 0.006\end{bmatrix}$	$\begin{bmatrix}91.129 & -0.312 & -0.787\\ -0.312 & 0.013 & 0.002\\ -0.787 & 0.002 & 0.007\end{bmatrix}$	$\begin{bmatrix}15.493 & -0.160 & -0.328\\ -0.160 & 0.013 & 0.003\\ -0.328 & 0.003 & 0.007\end{bmatrix}$	$\begin{bmatrix}10.290 & -0.101 & -0.266\\ -0.101 & 0.014 & 0.002\\ -0.266 & 0.002 & 0.007\end{bmatrix}$	$\begin{bmatrix}3.129 & -0.071 & -0.145\\ -0.071 & 0.015 & 0.003\\ -0.145 & 0.003 & 0.007\end{bmatrix}$	$\begin{bmatrix}9.440 & -0.098 & -0.257\\ -0.098 & 0.014 & 0.002\\ -0.257 & 0.002 & 0.007\end{bmatrix}$	$\begin{bmatrix}16.212 & -0.056 & -0.321\\ -0.115 & 0.014 & 0.002\\ -0.321 & 0.002 & 0.006\end{bmatrix}$	$\begin{bmatrix}75.215 & -0.056 & -0.763\\ -0.056 & 0.015 & 0.000\\ -0.763 & 0.000 & 0.008\end{bmatrix}$	$\begin{bmatrix}13.729 & 0.364 & -0.763\\ 0.070 & 0.021 & -0.003\\ -0.364 & -0.003 & 0.010\end{bmatrix}$	$\begin{bmatrix}35.676 & 0.282 & -0.616\\ 0.282 & 0.026 & -0.006\\ -0.616 & -0.006 & 0.011\end{bmatrix}$	$\begin{bmatrix}26.170 & 0.366 & -0.542\\ 0.366 & 0.034 & -0.009\\ -0.542 & -0.009 & 0.011\end{bmatrix}$
$\begin{bmatrix}276.50 & -0.482 & -0.320\\ -0.482 & 0.013 & 0.002\\ -1.320 & 0.002 & 0.006\end{bmatrix}$	$\begin{bmatrix}126.11 & -0.354 & -0.938\\ -0.354 & 0.013 & 0.002\\ -0.938 & 0.002 & 0.007\end{bmatrix}$	$\begin{bmatrix}35.561 & -0.218 & -0.497\\ -0.218 & 0.013 & 0.003\\ -0.497 & 0.003 & 0.007\end{bmatrix}$	$\begin{bmatrix}20.310 & -0.081 & -0.370\\ -0.081 & 0.014 & 0.003\\ -0.370 & 0.003 & 0.007\end{bmatrix}$	$\begin{bmatrix}4.903 & -0.081 & -0.180\\ -0.081 & 0.014 & 0.003\\ -0.180 & 0.003 & 0.007\end{bmatrix}$	$\begin{bmatrix}18.779 & -0.120 & -0.359\\ -0.120 & 0.014 & 0.002\\ -0.359 & 0.002 & 0.007\end{bmatrix}$	$\begin{bmatrix}19.257 & -0.060 & -0.367\\ -0.060 & 0.015 & 0.001\\ -0.367 & 0.001 & 0.007\end{bmatrix}$	$\begin{bmatrix}29.764 & -0.061 & -0.476\\ -0.061 & 0.015 & 0.000\\ -0.476 & 0.000 & 0.008\end{bmatrix}$	$\begin{bmatrix}23.532 & 0.110 & -0.469\\ 0.110 & 0.021 & -0.001\\ -0.469 & -0.001 & 0.010\end{bmatrix}$	$\begin{bmatrix}45.409 & 0.327 & -0.677\\ 0.327 & 0.026 & -0.006\\ -0.677 & -0.006 & 0.010\end{bmatrix}$	$\begin{bmatrix}26.170 & 0.366 & -0.542\\ 0.366 & 0.034 & -0.009\\ -0.542 & -0.009 & 0.011\end{bmatrix}$
$\begin{bmatrix}17.340 & -0.117 & -0.332\\ -0.117 & 0.014 & 0.002\\ -0.332 & 0.002 & 0.006\end{bmatrix}$	$\begin{bmatrix}141.21 & -0.217 & -0.982\\ -0.217 & 0.014 & 0.001\\ -0.982 & 0.001 & 0.007\end{bmatrix}$	$\begin{bmatrix}18.779 & -0.120 & -0.359\\ -0.120 & 0.014 & 0.002\\ -0.359 & 0.001 & 0.007\end{bmatrix}$	$\begin{bmatrix}82.227 & -0.185 & -0.728\\ -0.185 & 0.014 & 0.002\\ -0.728 & 0.001 & 0.006\end{bmatrix}$	$\begin{bmatrix}6.906 & -0.055 & -0.223\\ -0.055 & 0.015 & 0.001\\ -0.223 & 0.001 & 0.007\end{bmatrix}$	$\begin{bmatrix}22.020 & 0.016 & -0.436\\ 0.016 & 0.018 & -0.001\\ -0.436 & -0.001 & 0.006\end{bmatrix}$	$\begin{bmatrix}10.680 & 0.056 & -0.305\\ 0.056 & 0.018 & -0.003\\ -0.305 & -0.003 & 0.009\end{bmatrix}$	$\begin{bmatrix}16.162 & 0.005 & -0.372\\ 0.005 & 0.018 & -0.001\\ -0.372 & -0.001 & 0.009\end{bmatrix}$	$\begin{bmatrix}23.532 & 0.110 & -0.469\\ 0.110 & 0.021 & -0.001\\ -0.469 & -0.001 & 0.010\end{bmatrix}$	$\begin{bmatrix}45.409 & 0.327 & -0.677\\ 0.327 & 0.026 & -0.006\\ -0.677 & -0.006 & 0.010\end{bmatrix}$	$\begin{bmatrix}26.170 & 0.366 & -0.542\\ 0.366 & 0.034 & -0.009\\ -0.542 & -0.009 & 0.011\end{bmatrix}$
$\begin{bmatrix}3.609 & 0.244 & -0.214\\ 0.244 & 0.067 & -0.018\\ -0.214 & -0.018 & 0.013\end{bmatrix}$	$\begin{bmatrix}4.463 & 0.192 & -0.248\\ 0.192 & 0.047 & -0.014\\ -0.248 & -0.014 & 0.014\end{bmatrix}$	$\begin{bmatrix}0.840 & 0.156 & -0.126\\ 0.156 & 0.113 & -0.034\\ -0.126 & -0.034 & 0.021\end{bmatrix}$	$\begin{bmatrix}0.698 & 0.141 & -0.106\\ 0.141 & 0.113 & -0.032\\ -0.106 & -0.032 & 0.018\end{bmatrix}$	$\begin{bmatrix}0.479 & 0.074 & -0.084\\ 0.074 & 0.077 & -0.022\\ -0.084 & -0.022 & 0.017\end{bmatrix}$	$\begin{bmatrix}1.161 & 0.128 & -0.128\\ 0.128 & 0.071 & -0.002\\ -0.128 & -0.002 & 0.015\end{bmatrix}$	$\begin{bmatrix}4.556 & 0.125 & -0.214\\ 0.125 & 0.034 & -0.008\\ -0.214 & -0.008 & 0.011\end{bmatrix}$	$\begin{bmatrix}23.532 & 0.110 & -0.469\\ 0.110 & 0.021 & -0.003\\ -0.469 & -0.003 & 0.010\end{bmatrix}$	$\begin{bmatrix}11.982 & 0.139 & -0.356\\ 0.139 & 0.026 & -0.006\\ -0.356 & -0.006 & 0.011\end{bmatrix}$	$\begin{bmatrix}26.170 & 0.366 & -0.542\\ 0.366 & 0.034 & -0.009\\ -0.542 & -0.009 & 0.011\end{bmatrix}$	$\begin{bmatrix}26.170 & 0.366 & -0.542\\ 0.366 & 0.034 & -0.009\\ -0.542 & -0.009 & 0.011\end{bmatrix}$
$\begin{bmatrix}1.385 & 0.937 & -0.222\\ 0.937 & 1.135 & -0.191\\ -0.222 & -0.191 & 0.040\end{bmatrix}$	$\begin{bmatrix}0.853 & 0.310 & -0.157\\ 0.310 & 0.288 & -0.079\\ -0.157 & -0.079 & 0.033\end{bmatrix}$	$\begin{bmatrix}0.453 & 0.165 & -0.115\\ 0.165 & 0.207 & -0.065\\ -0.115 & -0.065 & 0.035\end{bmatrix}$	$\begin{bmatrix}0.704 & 0.204 & -0.121\\ 0.204 & 0.185 & -0.050\\ -0.121 & -0.050 & 0.024\end{bmatrix}$	$\begin{bmatrix}0.401 & 0.105 & -0.087\\ 0.105 & 0.127 & -0.037\\ -0.087 & -0.037 & 0.023\end{bmatrix}$	$\begin{bmatrix}0.839 & 0.156 & -0.119\\ 0.156 & 0.127 & -0.032\\ -0.119 & -0.032 & 0.019\end{bmatrix}$	$\begin{bmatrix}1.225 & 0.191 & -0.136\\ 0.191 & 0.107 & -0.029\\ -0.136 & -0.029 & 0.017\end{bmatrix}$	$\begin{bmatrix}2.132 & 0.256 & -0.187\\ 0.256 & 0.101 & -0.029\\ -0.187 & -0.029 & 0.018\end{bmatrix}$	$\begin{bmatrix}1.599 & 0.304 & -0.178\\ 0.304 & 0.159 & -0.044\\ -0.178 & -0.044 & 0.022\end{bmatrix}$	$\begin{bmatrix}9.474 & 0.952 & -0.428\\ 0.952 & 0.192 & -0.049\\ -0.428 & -0.049 & 0.020\end{bmatrix}$	$\begin{bmatrix}9.474 & 0.952 & -0.428\\ 0.952 & 0.192 & -0.049\\ -0.428 & -0.049 & 0.020\end{bmatrix}$
24.0°E	24.5°E	25.0°E	25.5°E	26.0°E	26.5°E	27.0°E	27.5°E	28.0°E	28.5°E	29.0°E

Appendix 15: Southwest zone cellular $G^{(III)}$ intensity recurrence estimates (PP97)

Parameters (ω, μ, λ) and their associated uncertainties of a $G^{(III)}$ distribution for each cell used to contour intensity hazard over southwest Bulgaria. I_M is the maximum observed intensity and $I(1)$ is the annual modal [or most probable] maximum event in each cell of analysis. $I_{50,}$ I_{100} and I_{200} are the modal maximum intensities expected in 50-, 100- and 200-year time intervals respectively. I_{P50}, I_{P100} and I_{P200} are the intensities expected to be extremes with 90% probability of non-exceedance in the 50-, 100- and 200-year time intervals (a 1 in 10 chance of exceedance). σ_I and σ_{IP} are the uncertainties in these forecasts. Forecasts were obtained using earthquake data of 5-year extreme intervals, cut-off intensity $I_{CUT} \geq$ VIII and time interval 1900 to 2004. $\sigma^2_{\omega\mu}$, $\sigma^2_{\omega\lambda}$ and $\sigma^2_{\mu\lambda}$ are the off-diagonal elements of the covariance (error) matrix, ε.

Lat	Lon	ω	σ_ω	μ	σ_μ	λ	σ_λ	$\sigma^2_{\omega\mu}$	$\sigma^2_{\omega\lambda}$	$\sigma^2_{\mu\lambda}$	I_M	I (1)	I_{50}	I_{100}	I_{200}	σ_I	I_{P50}	I_{P100}	I_{P200}	σ_{IP}
40.0	22.5	X (10.7)	0.6	0 (0.6)	7.4	0.85	0.77	3.18	-0.39	-5.56	X (10.9)	VIII (8.7)	X (10.6)	X (10.6)	X (10.6)	2.6	X (10.6)	X (10.6)	X (10.6)	0.6
40.0	23.0	X (10.9)	0.7	IV (4.6)	3.5	0.77	0.70	1.71	-0.41	-2.34	X (10.9)	VIII (8.8)	X (10.8)	X (10.9)	X (10.9)	1.9	X (10.9)	X (10.9)	X (10.9)	0.7
40.0	23.5	X (10.9)	0.7	IV (4.6)	3.5	0.77	0.70	1.71	-0.41	-2.34	X (10.9)	VIII (8.8)	X (10.8)	X (10.9)	X (10.9)	1.9	X (10.9)	X (10.9)	X (10.9)	0.7
40.0	24.0	X (10.7)	0.6	0 (0.6)	7.4	0.85	0.77	3.18	-0.39	-5.56	X (10.9)	VIII (8.7)	X (10.6)	X (10.6)	X (10.6)	2.6	X (10.6)	X (10.6)	X (10.6)	0.6
40.5	21.5	XI (11.8)	1.5	V (5.2)	2.0	0.60	0.45	2.46	-0.66	-0.83	X (10.9)	VIII (8.0)	XI (11.4)	XI (11.5)	XI (11.6)	2.6	XI (11.6)	XI (11.7)	XI (11.7)	1.5
40.5	22.0	XI (11.8)	1.5	V (5.2)	2.0	0.60	0.45	2.46	-0.66	-0.83	X (10.9)	VIII (8.0)	XI (11.4)	XI (11.5)	XI (11.6)	2.6	XI (11.6)	XI (11.7)	XI (11.7)	1.5
40.5	22.5	XI (11.4)	0.8	IV (4.8)	1.9	0.87	0.44	1.09	-0.32	-0.77	X (10.9)	X (10.2)	XI (11.4)	XI (11.4)	XI (11.4)	1.7	XI (11.4)	XI (11.4)	XI (11.4)	0.8
40.5	23.0	XI (11.3)	0.8	V (5.9)	1.3	0.82	0.42	0.69	-0.30	-0.47	X (10.9)	X (10.0)	XI (11.3)	XI (11.3)	XI (11.3)	1.4	XI (11.3)	XI (11.3)	XI (11.3)	0.8
40.5	23.5	XI (11.2)	0.8	VI (6.5)	1.8	0.84	0.60	1.11	-0.45	-1.01	X (10.9)	X (10.2)	XI (11.2)	XI (11.2)	XI (11.2)	1.7	XI (11.2)	XI (11.2)	XI (11.2)	0.8
40.5	24.0	X (10.9)	0.7	IV (4.6)	3.5	0.77	0.70	1.71	-0.41	-2.34	X (10.9)	VIII (8.8)	X (10.8)	X (10.9)	X (10.9)	1.9	X (10.9)	X (10.9)	X (10.9)	0.7
41.0	21.5	XI (11.8)	1.5	V (5.2)	2.0	0.60	0.45	2.46	-0.66	-0.83	X (10.9)	VIII (8.0)	XI (11.4)	XI (11.5)	XI (11.6)	2.6	XI (11.6)	XI (11.7)	XI (11.7)	1.5
41.0	22.0	XI (11.8)	1.5	V (5.2)	2.0	0.60	0.45	2.46	-0.66	-0.83	X (10.9)	VIII (8.0)	XI (11.4)	XI (11.5)	XI (11.6)	2.6	XI (11.6)	XI (11.7)	XI (11.7)	1.5
41.0	22.5	XI (11.4)	0.8	IV (4.8)	1.9	0.87	0.44	1.09	-0.32	-0.77	X (10.9)	X (10.2)	XI (11.4)	XI (11.4)	XI (11.4)	1.7	XI (11.4)	XI (11.4)	XI (11.4)	0.8
41.0	23.0	XI (11.3)	0.8	V (5.9)	1.3	0.82	0.42	0.69	-0.30	-0.47	X (10.9)	X (10.0)	XI (11.3)	XI (11.3)	XI (11.3)	1.4	XI (11.3)	XI (11.3)	XI (11.3)	0.8
41.0	23.5	XI (11.2)	0.8	VI (6.5)	1.8	0.84	0.60	1.11	-0.45	-1.01	X (10.9)	X (10.2)	XI (11.2)	XI (11.2)	XI (11.2)	1.7	XI (11.2)	XI (11.2)	XI (11.2)	0.8
41.0	24.0	X (10.9)	0.7	IV (4.6)	3.5	0.77	0.70	1.71	-0.41	-2.34	X (10.9)	VIII (8.8)	X (10.8)	X (10.9)	X (10.9)	1.9	X (10.9)	X (10.9)	X (10.9)	0.7
41.5	21.5	XI (11.8)	1.5	V (5.2)	2.0	0.60	0.45	2.46	-0.66	-0.83	X (10.9)	VIII (8.0)	XI (11.4)	XI (11.5)	XI (11.6)	2.6	XI (11.6)	XI (11.7)	XI (11.7)	1.5
41.5	22.0	XI (11.8)	1.5	V (5.2)	2.0	0.60	0.45	2.46	-0.66	-0.83	X (10.9)	VIII (8.0)	XI (11.4)	XI (11.5)	XI (11.6)	2.6	XI (11.6)	XI (11.7)	XI (11.7)	1.5
41.5	22.5	XI (11.4)	0.8	IV (4.8)	1.9	0.87	0.44	1.09	-0.32	-0.77	X (10.9)	X (10.2)	XI (11.4)	XI (11.4)	XI (11.4)	1.7	XI (11.4)	XI (11.4)	XI (11.4)	0.8
41.5	23.0	XI (11.3)	0.8	V (5.9)	1.3	0.82	0.42	0.69	-0.30	-0.47	X (10.9)	X (10.0)	XI (11.3)	XI (11.3)	XI (11.3)	1.4	XI (11.3)	XI (11.3)	XI (11.3)	0.8
41.5	23.5	XI (11.2)	0.8	VI (6.5)	1.8	0.84	0.60	1.11	-0.45	-1.01	X (10.9)	X (10.2)	XI (11.2)	XI (11.2)	XI (11.2)	1.7	XI (11.2)	XI (11.2)	XI (11.2)	0.8
41.5	24.0	X (10.9)	0.7	IV (4.6)	3.5	0.77	0.70	1.71	-0.41	-2.34	X (10.9)	VIII (8.8)	X (10.8)	X (10.9)	X (10.9)	1.9	X (10.9)	X (10.9)	X (10.9)	0.7
42.0	21.5	XI (11.8)	1.5	V (5.2)	2.0	0.60	0.45	2.46	-0.66	-0.83	X (10.9)	VIII (8.0)	XI (11.4)	XI (11.5)	XI (11.6)	2.6	XI (11.6)	XI (11.7)	XI (11.7)	1.5
42.0	22.0	XI (11.8)	1.5	V (5.2)	2.0	0.60	0.45	2.46	-0.66	-0.83	X (10.9)	VIII (8.0)	XI (11.4)	XI (11.5)	XI (11.6)	2.6	XI (11.6)	XI (11.7)	XI (11.7)	1.5

Appendix 15. Continued.

Lat	Lon	ω	σ_ω	μ	σ_μ	λ	σ_λ	$\sigma^2_{\omega\mu}$	$\sigma^2_{\omega\lambda}$	$\sigma^2_{\mu\lambda}$	I_M	I (1)	I_{50}	I_{100}	I_{200}	σ_I	I_{P50}	I_{P100}	I_{P200}	σ_{IP}
42.0	22.5	XI (11.4)	0.8	IV (4.8)	1.9	0.87	0.44	1.09	-0.32	-0.77	X (10.9)	X (10.2)	XI (11.4)	XI (11.4)	XI (11.4)	1.7	XI (11.4)	XI (11.4)	XI (11.4)	0.8
42.0	23.0	XI (11.3)	0.8	V (5.9)	1.3	0.82	0.42	0.69	-0.30	-0.47	X (10.9)	X (10.0)	XI (11.3)	XI (11.3)	XI (11.3)	1.4	XI (11.3)	XI (11.3)	XI (11.3)	0.8
42.0	23.5	XI (11.2)	0.8	VI (6.5)	1.8	0.84	0.60	1.11	-0.45	-1.01	X (10.9)	X (10.2)	XI (11.2)	XI (11.2)	XI (11.2)	1.7	XI (11.2)	XI (11.2)	XI (11.2)	0.8
42.0	24.0	X (10.9)	0.7	IV (4.6)	3.5	0.77	0.70	1.71	-0.41	-2.34	X (10.9)	VIII (8.8)	X (10.8)	X (10.9)	X (10.9)	1.9	X (10.9)	X (10.9)	X (10.9)	0.7
42.5	21.5	XII (12.0)	1.8	IV (4.2)	2.8	0.59	0.47	4.31	-0.83	-1.22	X (10.9)	VII (7.4)	XI (11.6)	XI (11.7)	XI (11.8)	3.3	XI (11.8)	XI (11.9)	XI (11.9)	1.9
42.5	22.0	XII (12.0)	1.8	IV (4.2)	2.8	0.59	0.47	4.31	-0.83	-1.22	X (10.9)	VII (7.4)	XI (11.6)	XI (11.7)	XI (11.8)	3.3	XI (11.8)	XI (11.9)	XI (11.9)	1.9
42.5	22.5	XI (11.4)	0.8	III (3.2)	3.0	0.93	0.47	1.76	-0.33	-1.31	X (10.9)	X (10.8)	XI (11.4)	XI (11.4)	XI (11.4)	2.0	XI (11.4)	XI (11.4)	XI (11.4)	0.8
42.5	23.0	XI (11.4)	0.8	III (3.2)	3.0	0.93	0.47	1.76	-0.33	-1.31	X (10.9)	X (10.8)	XI (11.4)	XI (11.4)	XI (11.4)	2.0	XI (11.4)	XI (11.4)	XI (11.4)	0.8
42.5	23.5	X (10.7)	0.6	0 (0.6)	7.4	0.85	0.77	3.18	-0.39	-5.56	X (10.9)	VIII (8.7)	X (10.6)	X (10.6)	X (10.6)	2.6	X (10.6)	X (10.6)	X (10.6)	0.6
42.5	24.0	X (10.7)	0.6	0 (0.6)	7.4	0.85	0.77	3.18	-0.39	-5.56	X (10.9)	VIII (8.7)	X (10.6)	X (10.6)	X (10.6)	2.6	X (10.6)	X (10.6)	X (10.6)	0.6
43.0	22.5	XI (11.3)	0.8	0 (0.7)	5.0	0.82	0.51	3.02	-0.36	-2.45	X (10.9)	VIII (8.6)	XI (11.2)	XI (11.2)	XI (11.3)	2.6	XI (11.2)	XI (11.3)	XI (11.3)	0.8
43.0	23.0	XI (11.3)	0.8	0 (0.7)	5.0	0.82	0.51	3.02	-0.36	-2.45	X (10.9)	VIII (8.6)	XI (11.2)	XI (11.2)	XI (11.3)	2.6	XI (11.2)	XI (11.3)	XI (11.3)	0.8

Appendix 16: Site-specific intensity $G^{(III)}$ distribution curves (PP97)

Site-specific Gumbel third extreme values distribution curves and covariance error matrices, ε, for urban centres for which intensity seismic hazard is considered for in chapter 5 and 6. Graphs show return periods, reduced variates and associated probabilities for estimated intensity extreme values.

Each figure represents seismicity contained in a 2° half-width cell centred on the city, and adopting a cut-off intensity, I_{CUT}, and extreme interval specific to the site and its immediate surrounding area.

City	Co-ordinates	NPER	I_{CUT}	ω	σ_ω	μ	σ_μ	λ	σ_λ	$\sigma^2_{\omega\mu}$	$\sigma^2_{\omega\lambda}$	$\sigma^2_{\mu\lambda}$	X^2	NMISS	I_M
Edirne	41.67°N, 26.57°E	10	7	X (10.0)	0.6	VIII (8.2)	0.2	0.866	0.416	-0.064	-0.214	0.058	0.646	1	X (10.0)
Larissa	39.63°N, 22.42°E	9	4	X (10.0)	0.9	VIII (8.2)	0.2	0.542	0.327	-0.093	-0.267	0.042	0.475	0	X (10.0)
Plovdiv	42.15°N, 24.75°E	7	8	X (10.3)	1.1	VI (6.5)	1.6	0.790	0.769	1.277	-0.768	-1.138	0.432	8	X (10.0)
Pristina	42.67°N, 21.17°E	2	5	X (10.4)	0.9	VI (6.7)	0.1	0.291	0.087	-0.039	-0.080	0.004	0.410	0	X (10.0)
Skopje	42.00°N, 21.43°E	1	6	XI (11.0)	1.2	VI (6.3)	0.1	0.248	0.082	0.002	-0.093	-0.001	0.350	17	X (10.0)
Sofia	42.68°N, 23.32°E	8	4	XI (11.2)	1.2	VII (7.0)	0.2	0.413	0.143	-0.116	-0.165	0.015	1.108	0	X (10.0)
Thessa'	40.63°N, 22.93°E	8	4	X (10.4)	0.7	VII (7.8)	0.2	0.590	0.189	-0.066	-0.121	0.023	0.657	0	X (10.0)
Tirane	41.33°N, 19.82°E	1	4	IX (9.3)	0.4	VI (6.3)	0.1	0.445	0.074	-0.011	-0.027	0.002	0.402	5	IX (9.0)

City	Co-ordinates	NPER	I_{CUT}	I_A	I_{25}	I_{50}	I_{100}	I_{200}	σ_I	I_{P25}	I_{P50}	I_{P100}	I_{P200}	σ_{IP}
Edirne	41.67°N, 26.57°E	10	7	IX (9.7)	X (10.0)	X (10.0)	X (10.0)	X (10.0)	0.5	X (10.0)	X (10.0)	X (10.0)	X (10.0)	0.6
Larissa	39.63°N, 22.42°E	9	4	VIII (8.8)	IX (9.8)	IX (9.9)	IX (9.9)	IX (9.9)	0.7	IX (9.9)	IX (9.9)	IX (9.9)	X (10.0)	0.8
Plovdiv	42.15°N, 24.75°E	7	8	IX (9.2)	X (10.2)	X (10.3)	X (10.3)	X (10.3)	1.9	X (10.3)	X (10.3)	X (10.3)	X (10.3)	1.1
Pristina	42.67°N, 21.17°E	2	5	VII (7.0)	IX (9.1)	IX (9.3)	IX (9.5)	IX (9.7)	0.6	IX (9.7)	IX (9.8)	IX (9.9)	X (10.0)	0.8
Skopje	42.00°N, 21.43°E	1	6	VI (6.6)	IX (9.0)	IX (9.3)	IX (9.6)	IX (9.8)	0.7	IX (9.8)	X (10.0)	X (10.1)	X (10.2)	0.9
Sofia	42.68°N, 23.32°E	8	4	VII (7.8)	X (10.3)	X (10.5)	X (10.7)	X (10.8)	0.9	X (10.7)	X (10.9)	X (10.9)	XI (11.0)	1.1
Thessa'	40.63°N, 22.93°E	8	4	VIII (8.8)	X (10.1)	X (10.2)	X (10.3)	X (10.3)	0.6	X (10.3)	X (10.3)	X (10.3)	X (10.3)	0.7
Tirane	41.33°N, 19.82°E	1	4	VII (7.0)	VIII (8.8)	VIII (8.9)	IX (9.0)	IX (9.1)	0.3	IX (9.1)	IX (9.1)	IX (9.2)	IX (9.2)	0.4

Parameters (ω, μ, λ) and their associated uncertainties of a $G^{(III)}$ distribution for selected urban centres in the catalogued region. I_M is the maximum observed intensity and I_A is the annual modal [or most probable] maximum event in each cell of analysis. I_{25}, I_{50}, I_{100} and I_{200} are the modal maximum intensities expected in 25-, 50-, 100- and 200-year return periods respectively. I_{P25}, I_{P50}, I_{P100} and I_{P200} are forecasts for intensities at 90% probability of non-exceedance in the time interval specified (a 1 in 10 chance of exceedance). σ_P and σ_{IP} are the respective uncertainties of maximum forecasts and those at 90% confidence levels. $\sigma^2_{\omega\mu}$, $\sigma^2_{\omega\lambda}$ and $\sigma^2_{\mu\lambda}$ are the off-diagonal elements of the covariance error matrix, ε. X^2 gives the reduced chi-square estimate for each cell of analysis, specifying the goodness of fit between observed extreme data values and Gumbel's third distribution. For each city, estimates derived from the distribution of seismicity present within a 2° half-width cell of the city are given. NMISS is the number of missing years of extreme data

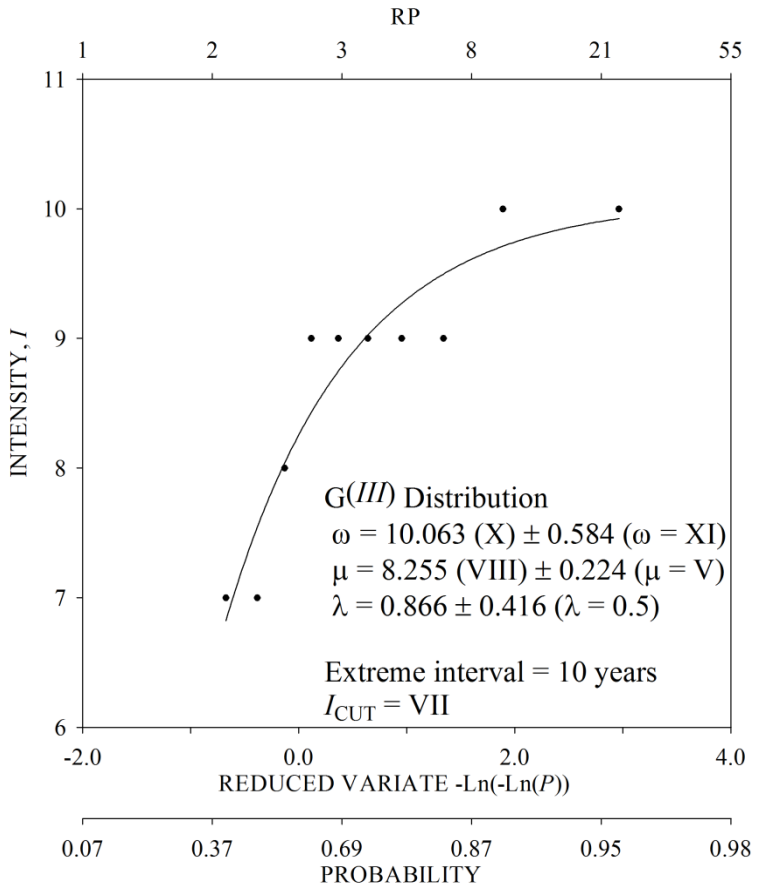

$$\varepsilon = \begin{bmatrix} 0.341 & -0.064 & -0.214 \\ -0.064 & 0.050 & -0.058 \\ -0.214 & -0.058 & 0.173 \end{bmatrix}$$

(a)

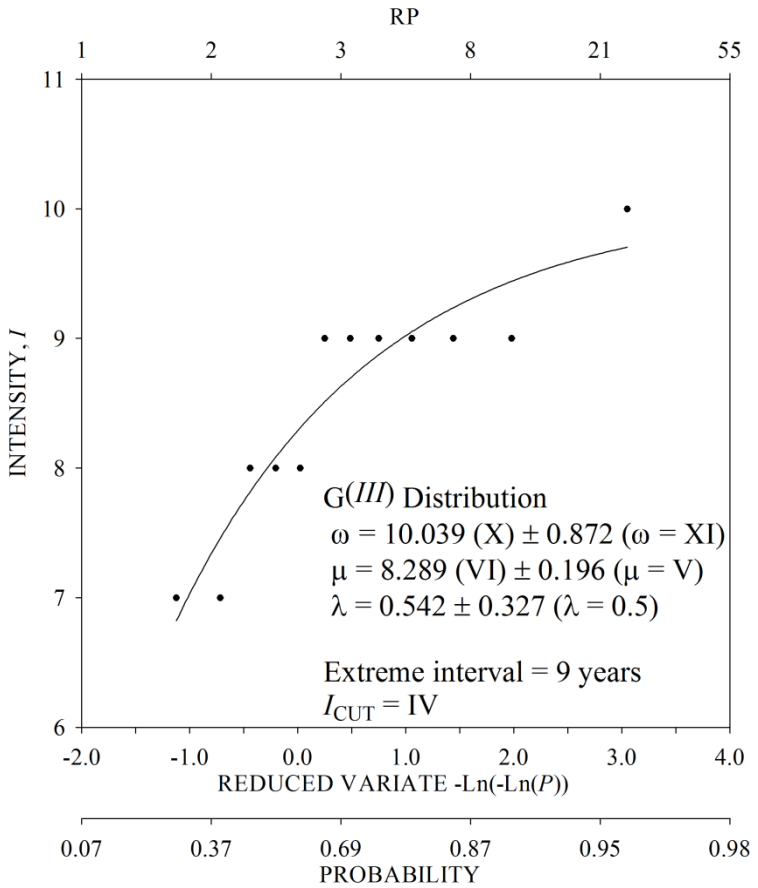

$$\varepsilon = \begin{bmatrix} 0.760 & -0.093 & -0.267 \\ -0.093 & 0.038 & -0.042 \\ -0.267 & -0.042 & 0.107 \end{bmatrix}$$

(b)

Gumbel III asymptotic extreme values distribution curves for (a) Edirne and (b) Larissa

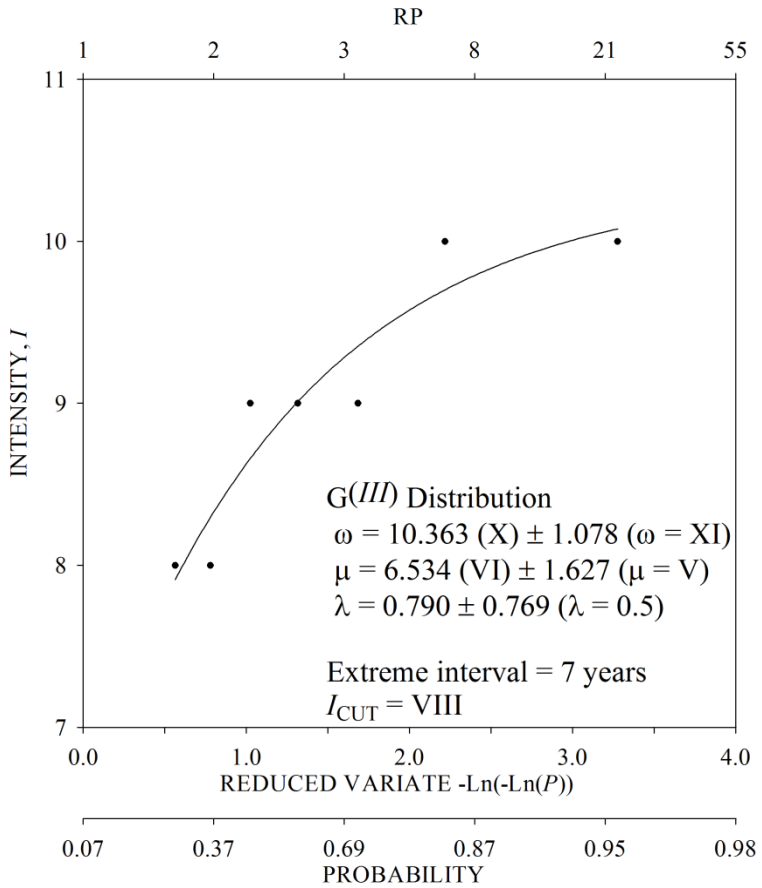

$$\varepsilon = \begin{bmatrix} 0.760 & -0.093 & -0.267 \\ -0.093 & 0.038 & -0.042 \\ -0.267 & -0.042 & 0.107 \end{bmatrix}$$

(a)

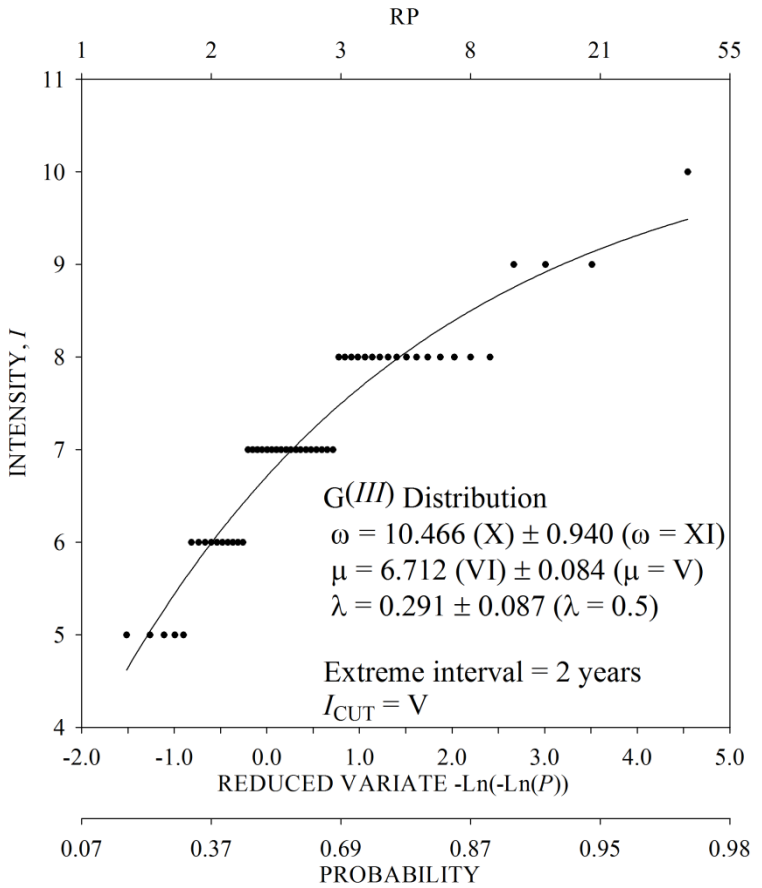

$$\varepsilon = \begin{bmatrix} 0.760 & -0.093 & -0.267 \\ -0.093 & 0.038 & -0.042 \\ -0.267 & -0.042 & 0.107 \end{bmatrix}$$

(b)

$G^{(III)}$ asymptotic extreme values distribution curves for (a) Plovdiv and (b) Pristina

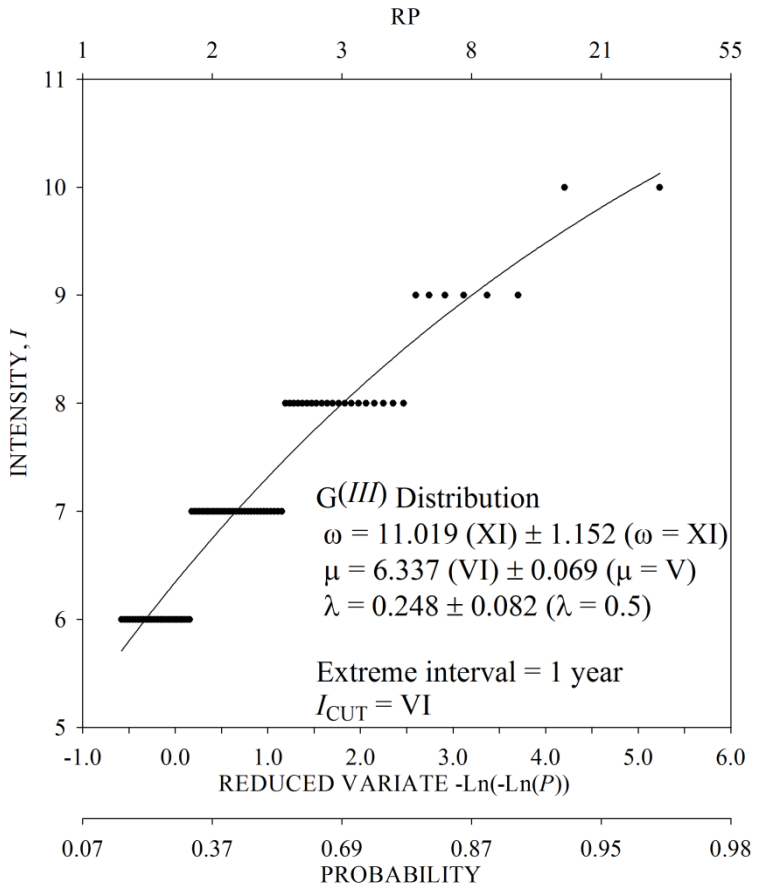

$$\varepsilon = \begin{bmatrix} 1.328 & 0.002 & -0.093 \\ 0.002 & 0.005 & -0.001 \\ -0.093 & -0.001 & 0.007 \end{bmatrix}$$

(a)

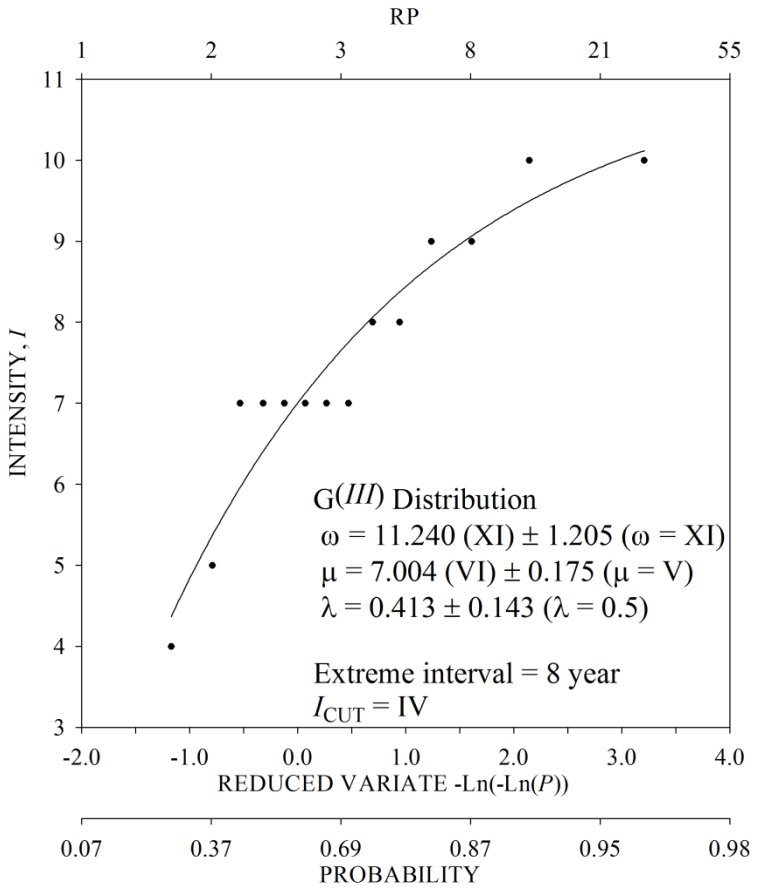

$$\varepsilon = \begin{bmatrix} 1.452 & -1.116 & -0.165 \\ -1.116 & 0.031 & -0.015 \\ -0.165 & -0.015 & 0.020 \end{bmatrix}$$

(b)

$G^{(III)}$ asymptotic extreme values distribution curves for (a) Skopje and (b) Sofia

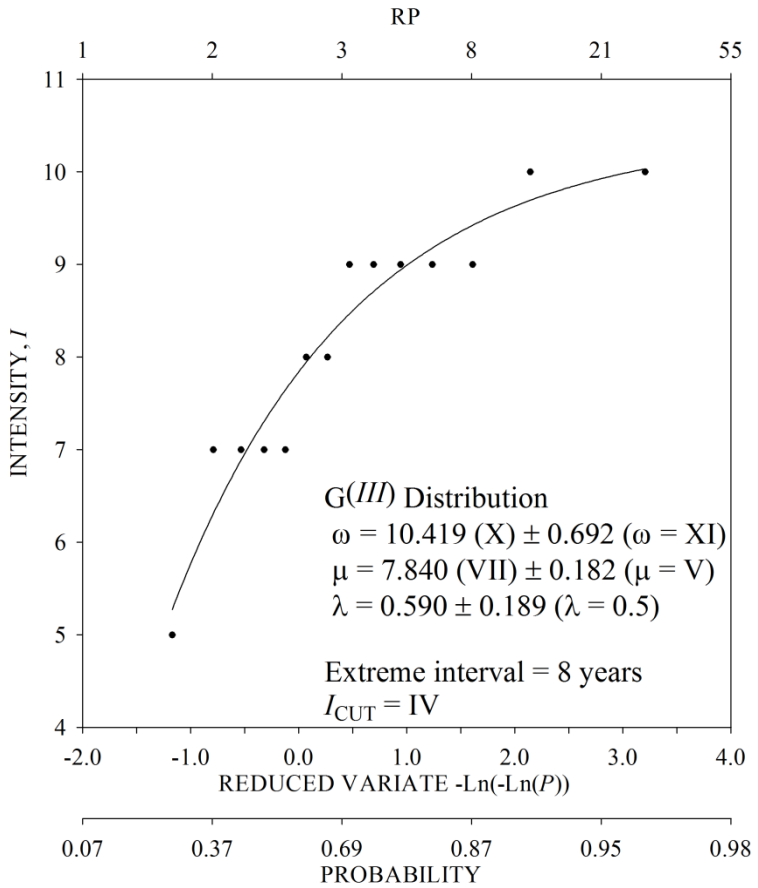

$$\varepsilon = \begin{bmatrix} 0.479 & -0.066 & -0.121 \\ -0.066 & 0.033 & 0.023 \\ -0.121 & 0.023 & 0.036 \end{bmatrix}$$

(a)

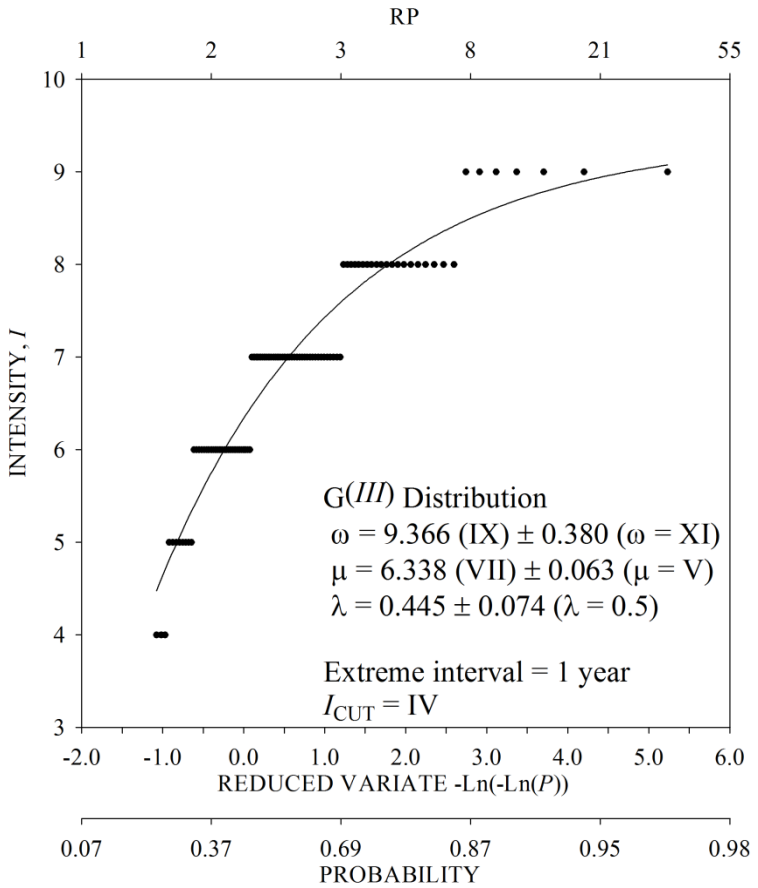

$$\varepsilon = \begin{bmatrix} 0.144 & -0.011 & -0.027 \\ -0.011 & 0.004 & 0.002 \\ -0.027 & 0.002 & 0.006 \end{bmatrix}$$

(b)

$G^{(III)}$ asymptotic extreme values distribution curves for (a) Thessaloniki and (b) Tirane

Appendix 17: Site-specific cumulative strain energy release graphs

Cumulative strain energy release plots for the urban centres listed for which seismic hazard is forecast. Each figure represents seismicity contained in a 2° half-width cell centred on the city.

Each graph illustrates the waiting times DT, T_w, M_2, M_3 as well as the year that ends the waiting time period DT (when the energy line SS' (Figure 3.4) meets the lower bound energy release envelope CC'), along with *whole process* statistics from the cumulative frequency-magnitude distribution (M_1, a-value, b-value)

Region	ω	a	b	M_1	M_2	TE/year	M_3	E_{max}	T_W/years	DT/years
Full region	7.686 (±0.562)	3.50 (± 0.10)	0.640 (± 0.02)	5.48	6.672	7.05E+21	7.815	1.90E+23	44.3	18.3
Southwest zone	7.840 (±0.759)	2.71 (± 0.08)	0.580 (± 0.01)	4.67	6.469	3.59E+21	7.755	1.20E+23	71.1	38.6
Edirne (41.67°N, 26.57°E)	7.571 (±0.706)	2.20 (± 0.07)	0.522 (± 0.01)	4.39	6.263	1.82E+21	7.401	5.84 E+22	43.6	12.4
Larissa (39.63°N, 22.42°E)	7.892 (±1.264)	3.10 (± 0.08)	0.674 (± 0.02)	4.60	6.304	2.08E+21	7.600	5.98E+21	73.6	71.7
Plovdiv 42.15°N, 24.75°E)	7.962 (±1.209)	2.53 (± 0.08)	0.563 (± 0.02)	4.49	6.439	3.25E+21	7.754	1.18E+23	78.4	43.1
Pristina (42.67°N, 21.17°E)	7.683 (±1.458)	3.04 (± 0.11)	0.634 (± 0.04)	4.79	6.265	1.82E+21	7.589	1.40E+23	80.7	4.9
Skopje (42.00°N, 21.43°E)	7.892 (±1.695)	3.20 (± 0.12)	0.650 (± 0.02)	4.92	6.291	1.99E+21	7.589	1.40E+23	74.0	4.9
Sofia (42.68°N, 23.32°E)	7.859 (±0.748)	2.41 (± 0.08)	0.530 (± 0.02)	4.43	6.441	3.27E+21	7.759	1.22E+23	79.1	42.8
Thessaloniki (40.63°N, 22.93°E)	7.896 (±0.940)	2.95 (± 0.07)	0.615 (± 0.07)	4.80	6.463	3.52E+21	7.756	1.17E+23	72.7	40.6
Tirane (41.33°N, 19.82°E)	7.349 (±1.288)	3.14 (± 0.12)	0.646 (± 0.02)	4.86	6.045	8.80E+20	7.112	2.59E+22	34.4	5.9

Cumulative strain energy release statistics for seismicity within a 2° half-width cell of each (except for broad and southwest zones, where all seismicity in these zones is considered) for the time interval 1900 to 2004. a and b are least squares estimates for zone-dependent constants and used to derive M_1 (the modal earthquake magnitude, such that $M_1 = a/b$); TE/year is the mean annual rate of energy release, M_2 is the magnitude equivalent to TE/year. M_3 is the analytical upper bound magnitude and T_W is the waiting time for the all the energy in the region to accumulate if it were released in a single event. DT is the delay (or residual) time; i.e. the time between the upper bound enveloping line and the time since the last seismic activity. b-values given for the full catalogue region here are different to those given in Table 4.9 due to different data being adopted. All data are used here to be consistent with cumulative strain energy release statistics. Table 4.9 uses events with magnitudes ≥4.6 M_s, i.e. the notional lowest possible limit to the catalogue's magnitude completeness. However, smaller magnitudes have minor influence in estimating energy release statistics

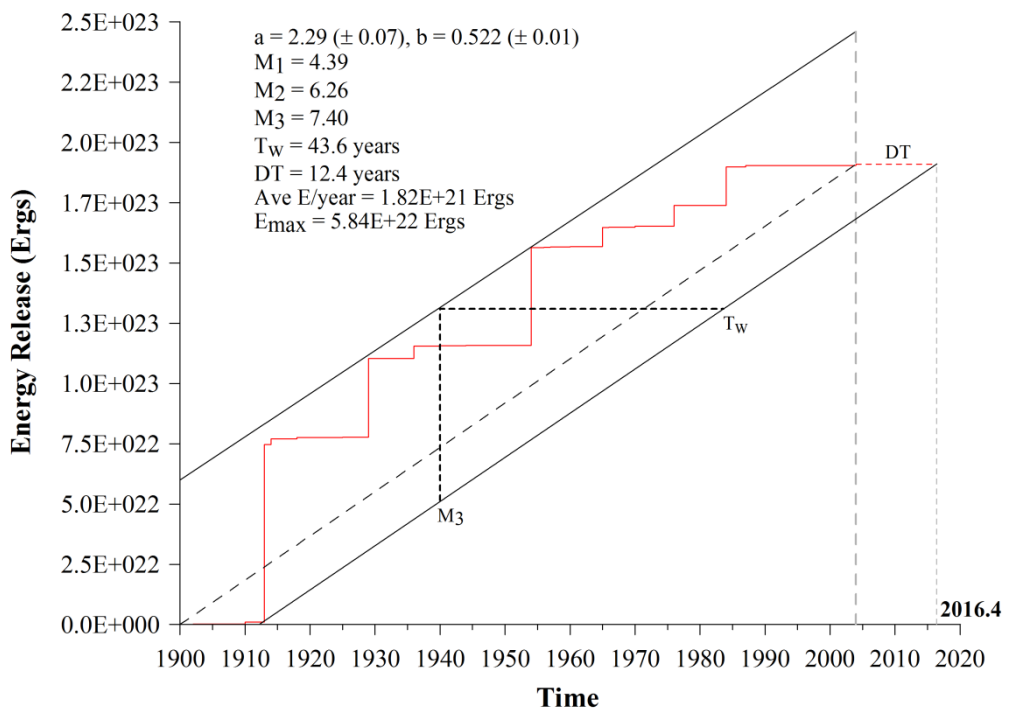

(a)

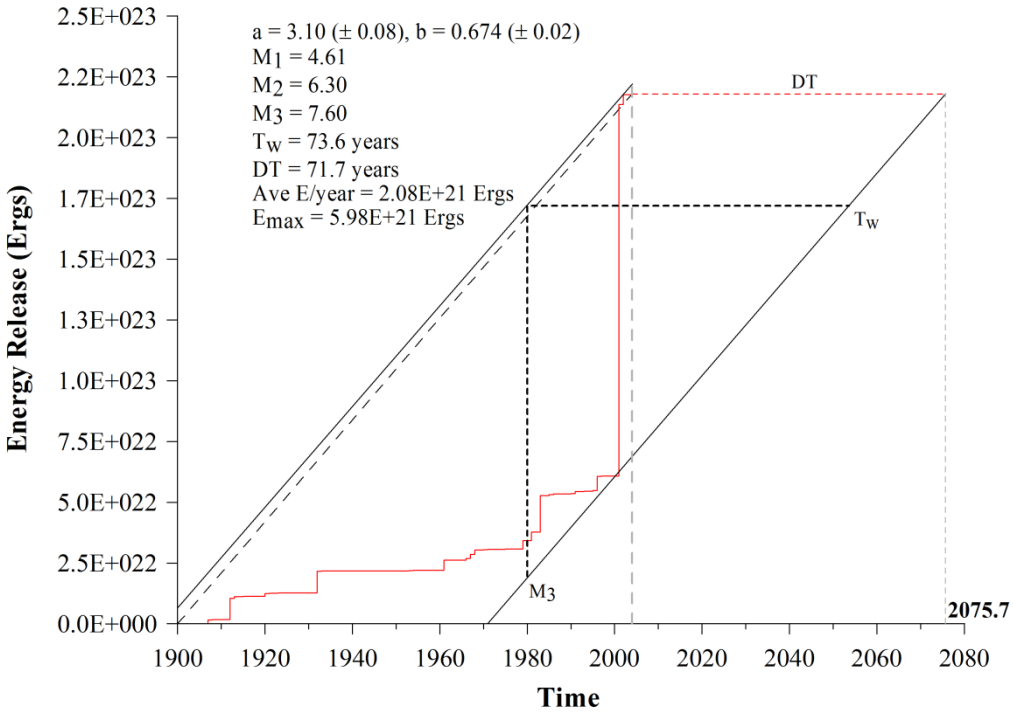

(b)

Cumulative strain energy release statistics for (a) Edirne and (b) Larissa considered as a function of time (1900 to 2004)

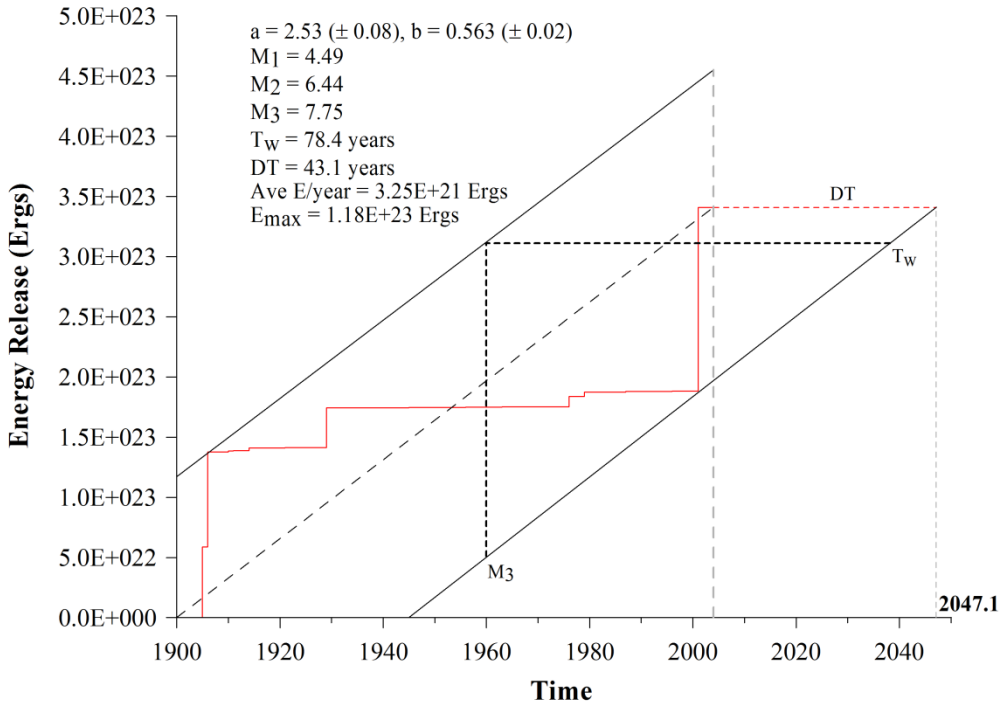

(a)

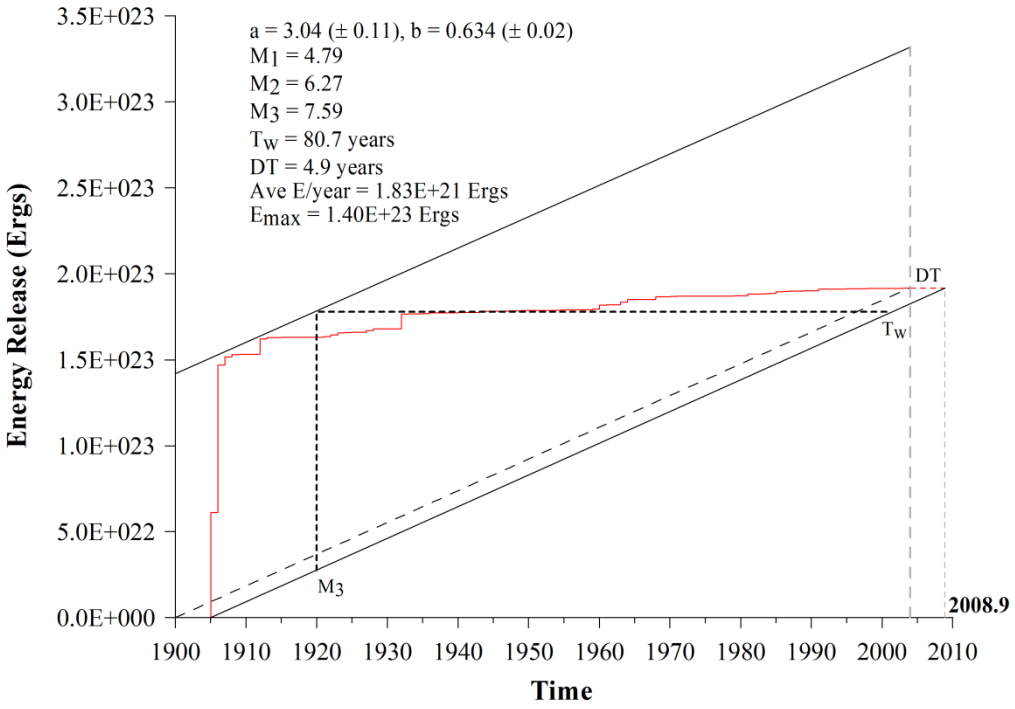

(b)

Cumulative strain energy release statistics for (a) Plovdiv and (b) Pristina considered as a function of time (1900 to 2004)

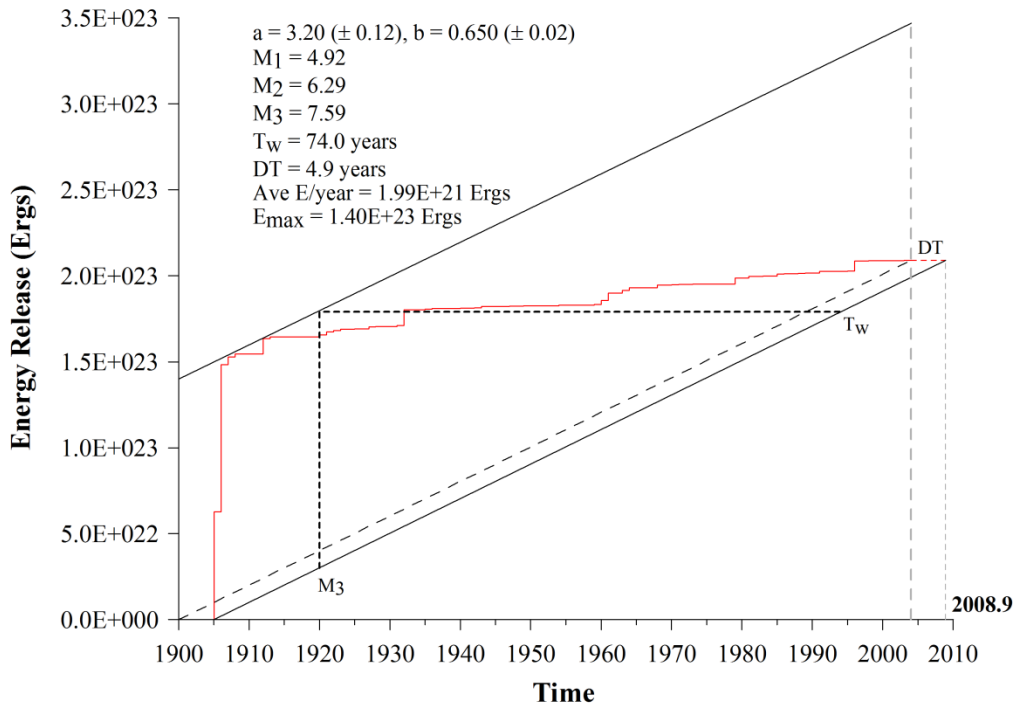

(a)

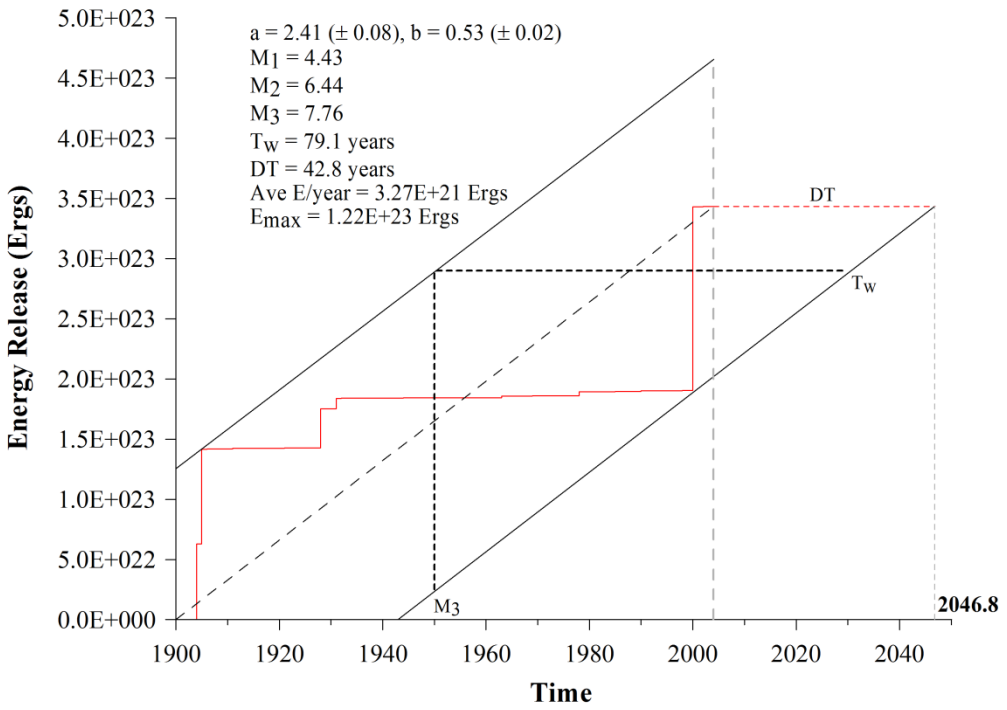

(b)

Cumulative strain energy release statistics for (a) Skopje and (b) Sofia considered as a function of time (1900 to 2004)

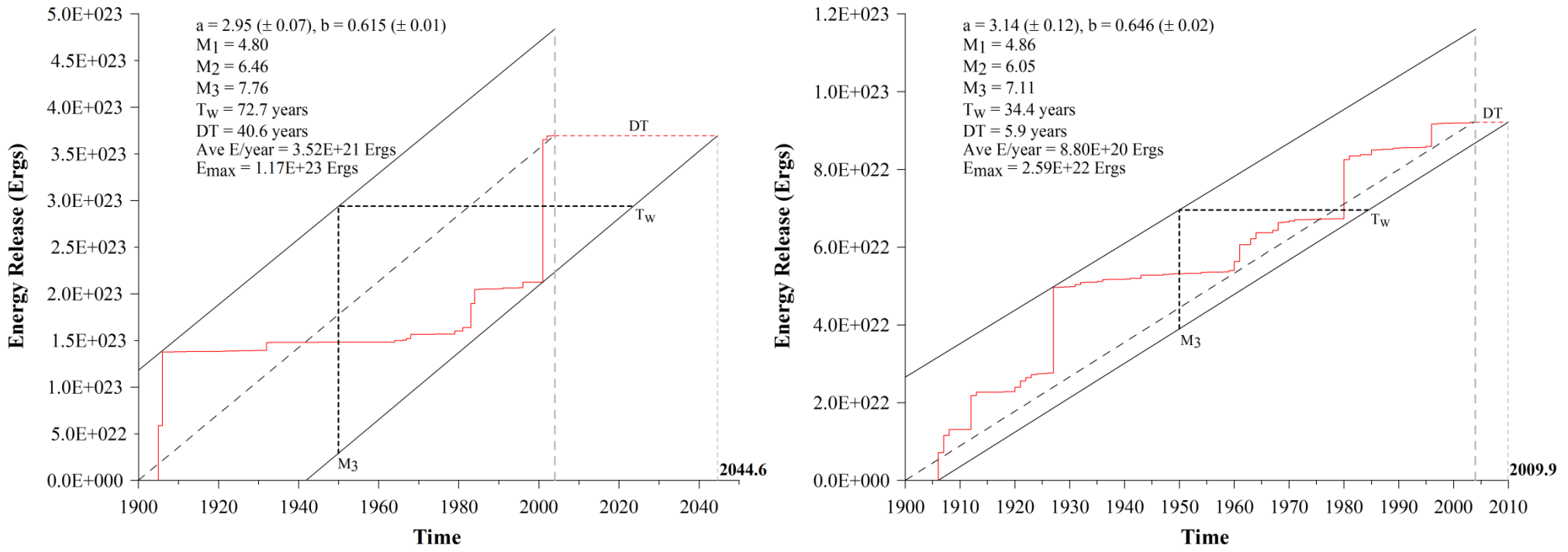

(a) (b)

Cumulative strain energy release statistics for (a) Thessaloniki and (b) Tirane considered as a function of time (1900 to 2004)

Appendix 18: Site-specific acceleration perceptibility/integrated perceptibility curves

Ground acceleration (a) perceptibility and (b) integrated perceptibility curves Theodulidis and Papazachos (1992; $TP92_A$) for stiff soil (S = 0.5) at the 50^{th} percentile (P = 0) for the urban centres for which seismic hazard is forecast.

In each set of three curves on these graphs, the central bold line represents an earthquake at a nominal focal depth of 15 km (approximating to the mean seismogenic depth for historical seismicity above M_{CUT} for the broader region of 5.5 M_S; Figure 2.14). Thinner curves above and below each bold curve represent earthquakes at nominal focal depths of 10 km and 20 km respectively. Vertical black lines are at *the most perceptible magnitude,* $M_{P(max)}$, only for 10 km focal depth estimates. The vertical dashed line represents M_3 from cumulative strain energy release techniques (chapter 6 and Appendix 17).

The set of grey lines on each graph represents the 50 cm s^{-2} ground acceleration at each focal depth considered, estimated using the modern ground motion model of Ambraseys *et al*. (2005).

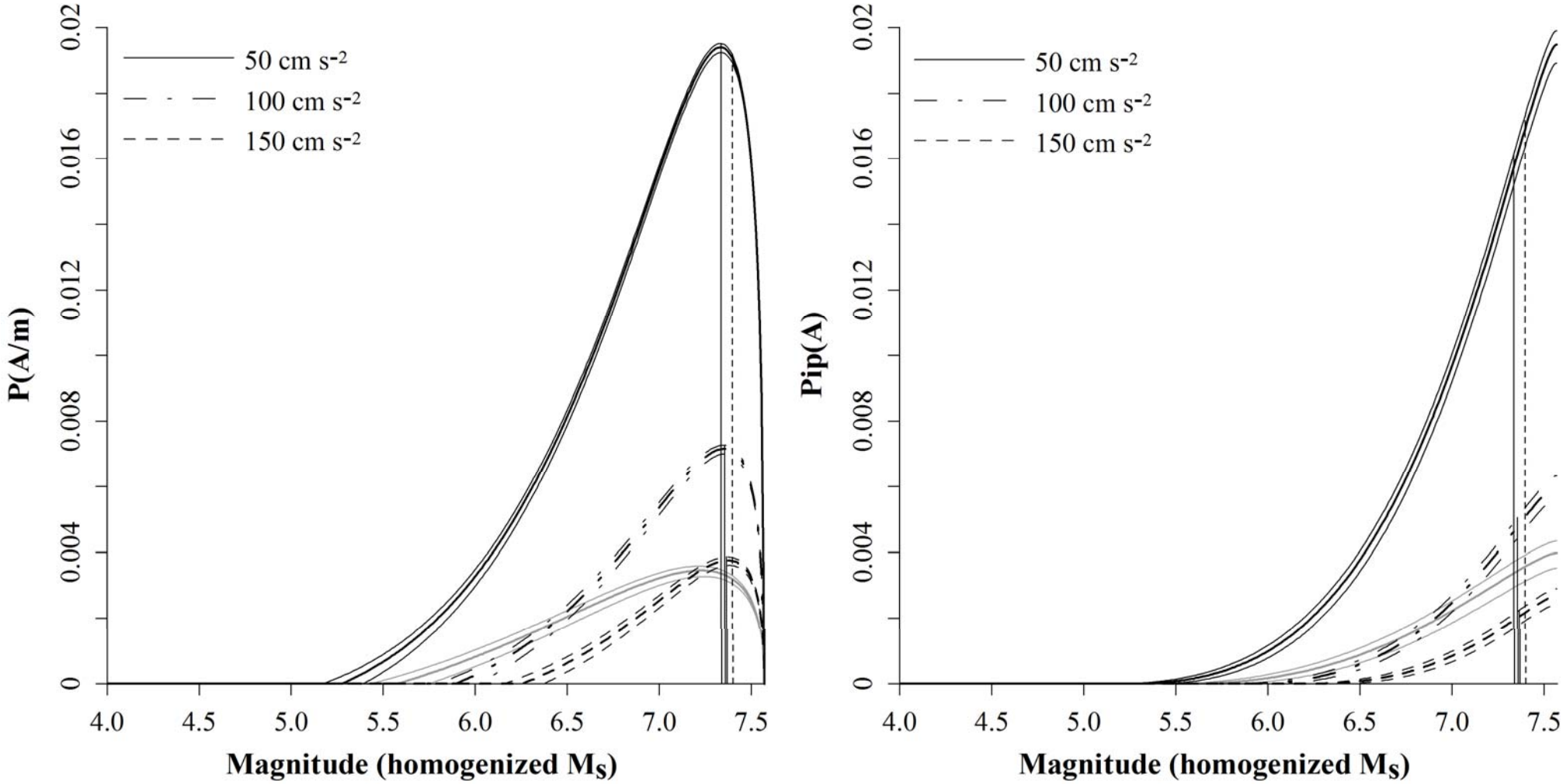

(a) (b)

Ground acceleration (a) perceptibility and (b) integrated perceptibility curves for Edirne using Theodulidis and Papazachos (1992; $TP92_A$)

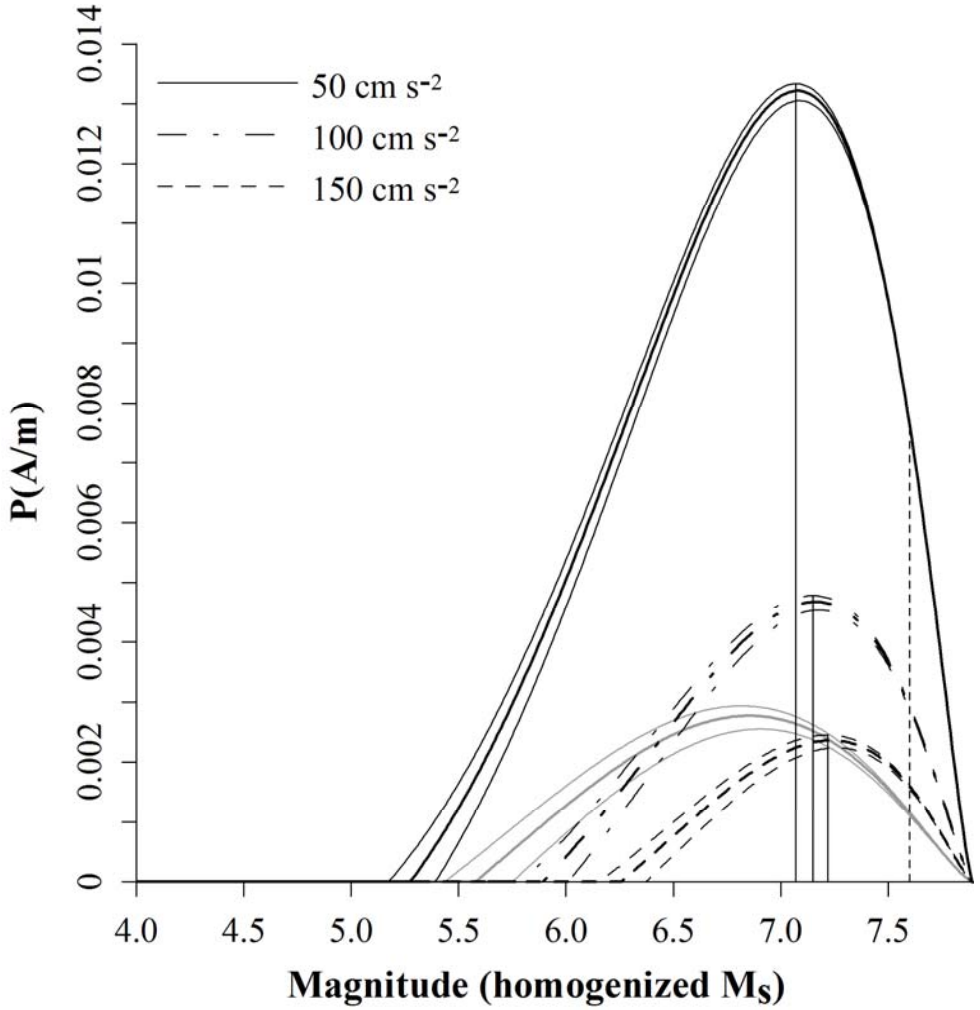

(a)

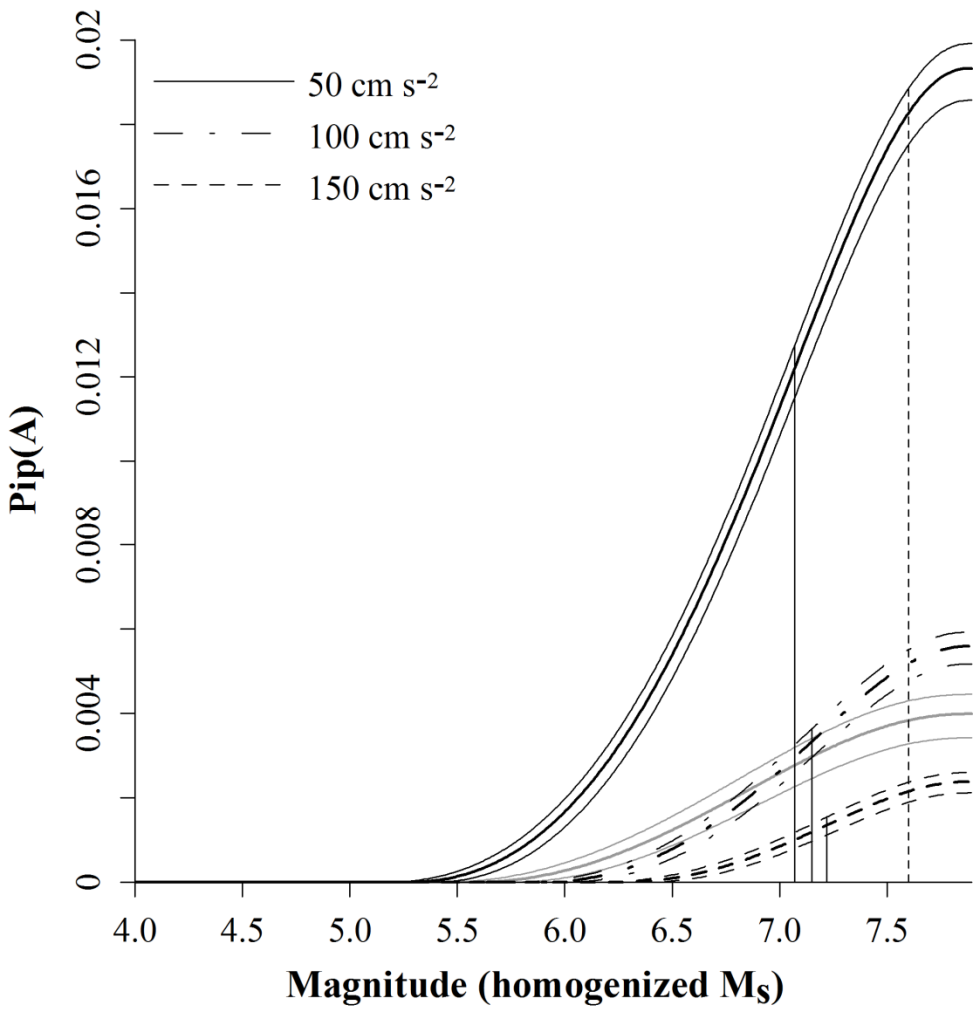

(b)

Ground acceleration (a) perceptibility and (b) integrated perceptibility curves for Larissa using Theodulidis and Papazachos (1992; $TP92_A$)

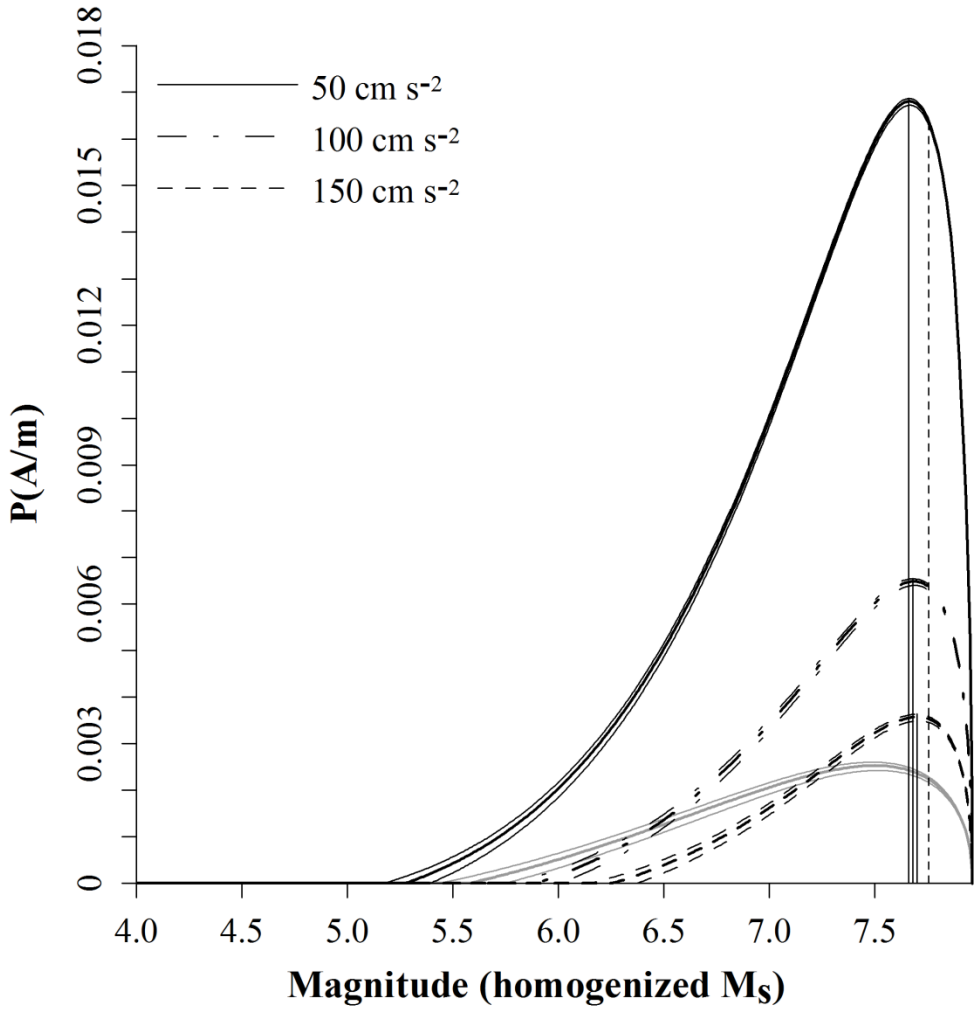

(a)

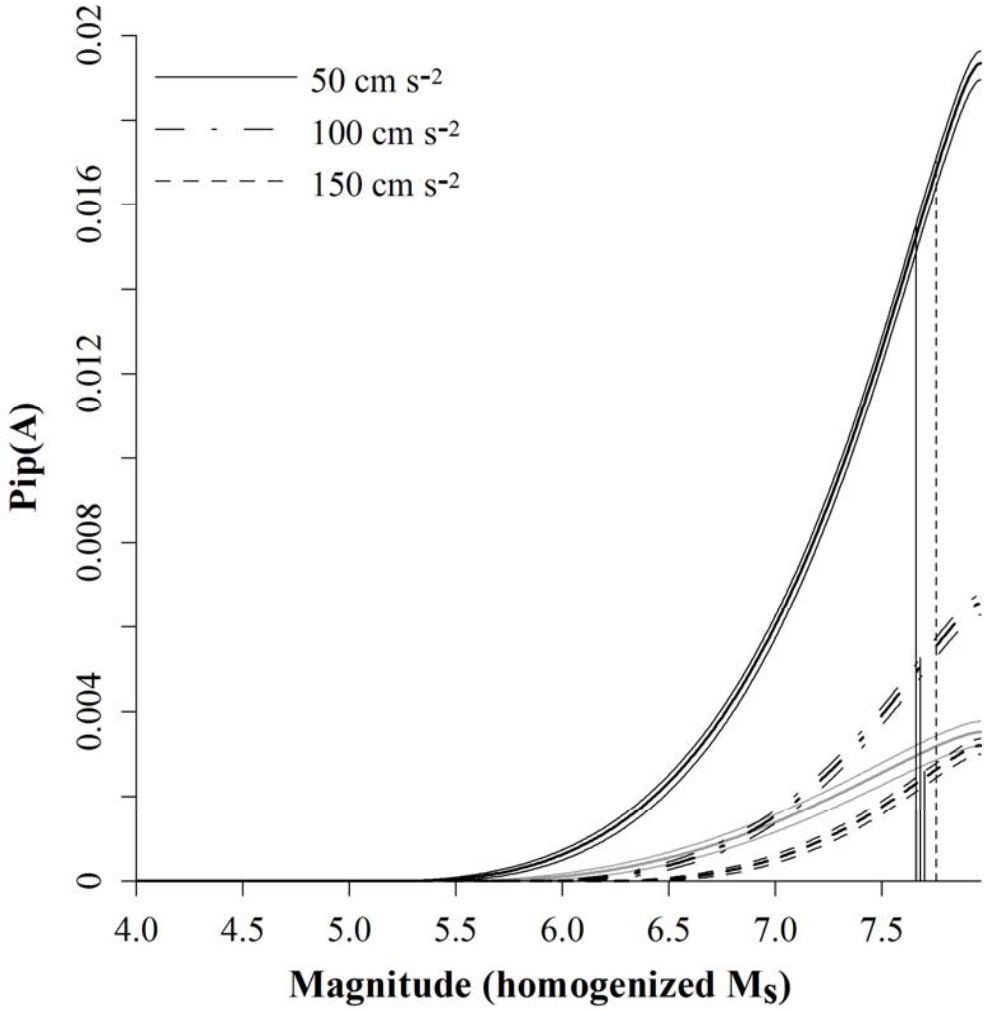

(b)

Ground acceleration (a) perceptibility and (b) integrated perceptibility curves for Plovdiv using Theodulidis and Papazachos (1992; $TP92_A$)

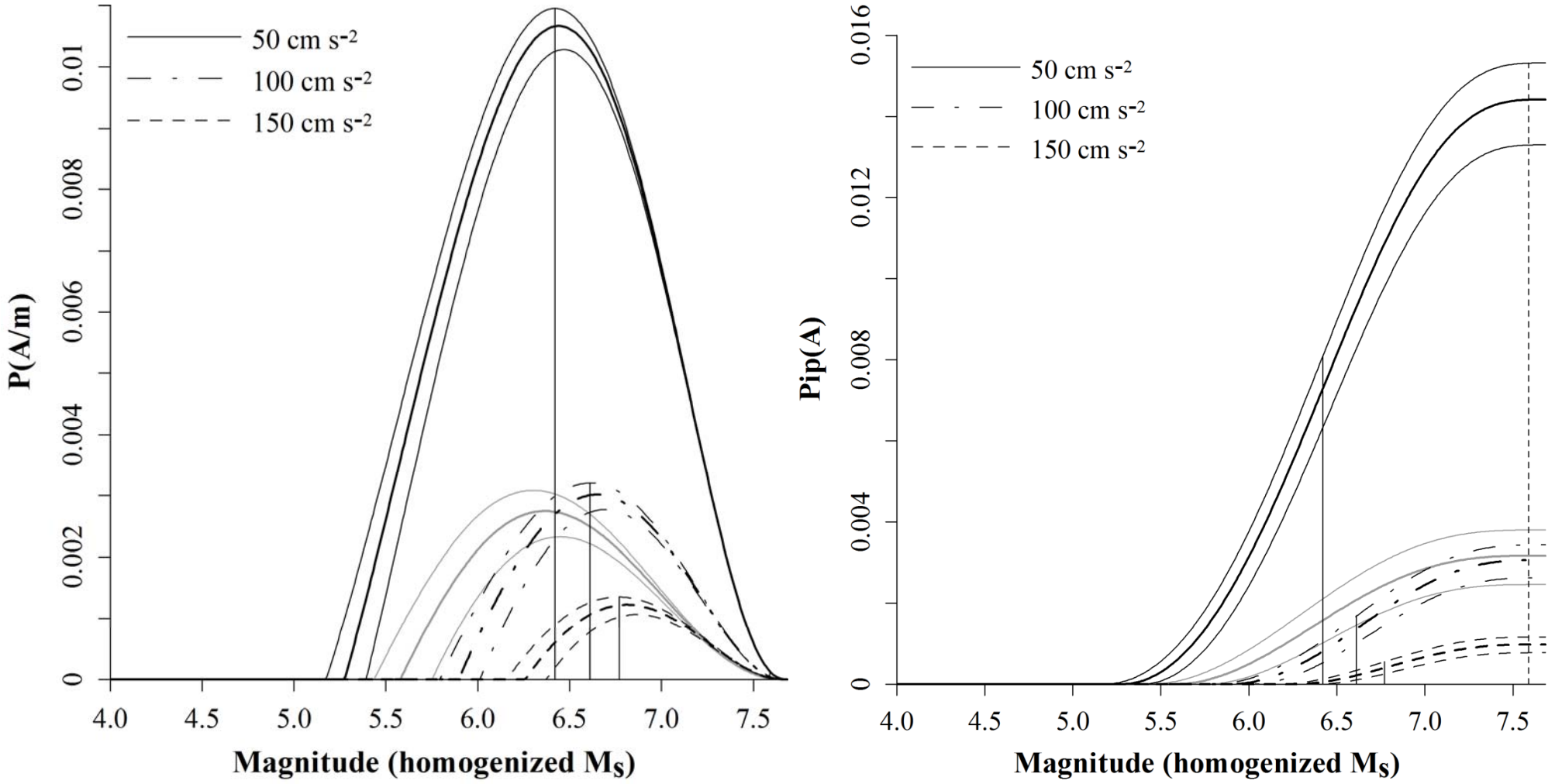

Ground acceleration (a) perceptibility and (b) integrated perceptibility curves for Pristina using Theodulidis and Papazachos (1992; $TP92_A$)

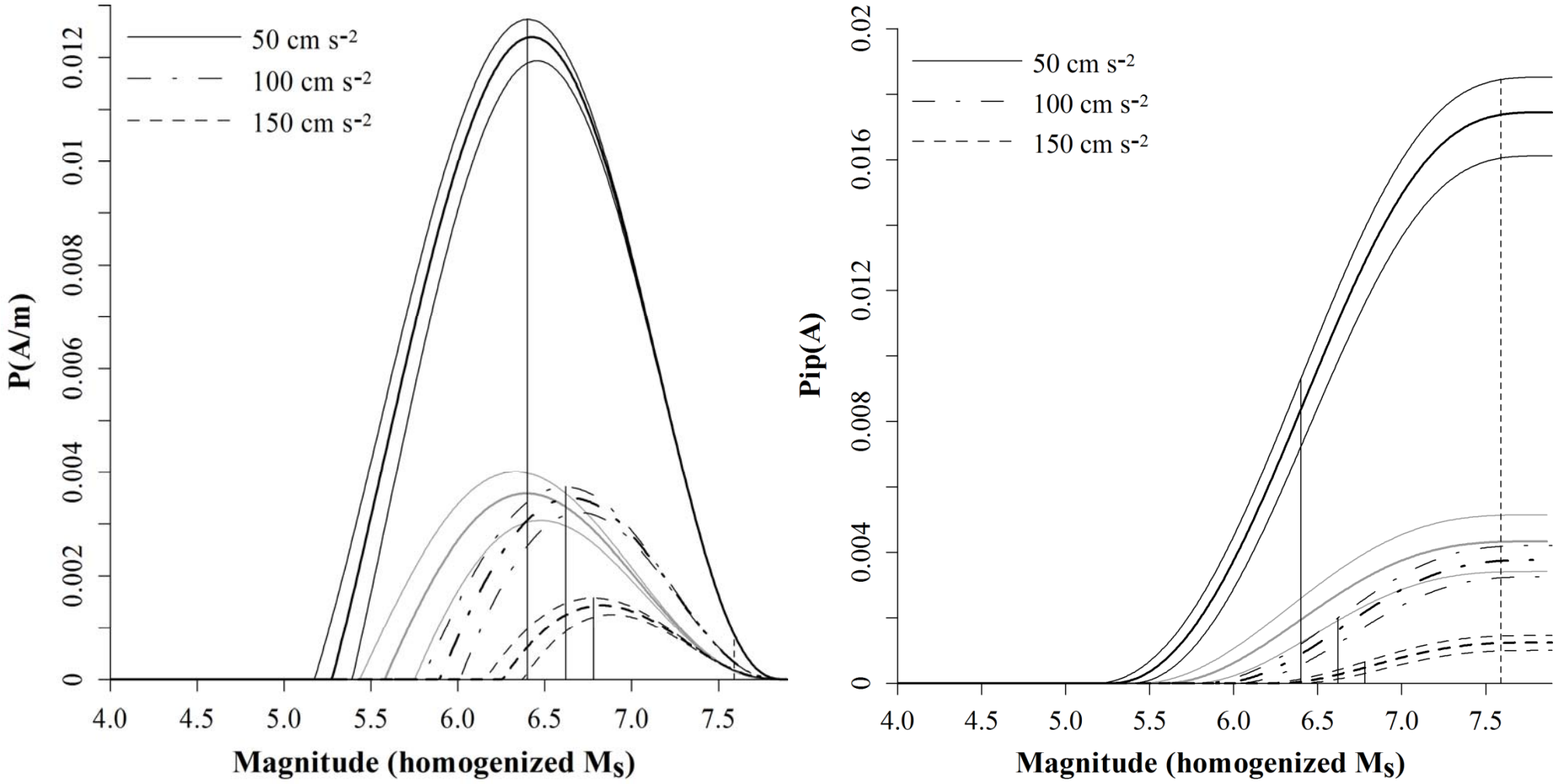

(a) (b)

Ground acceleration (a) perceptibility and (b) integrated perceptibility curves for Skopje using Theodulidis and Papazachos (1992; $TP92_A$)

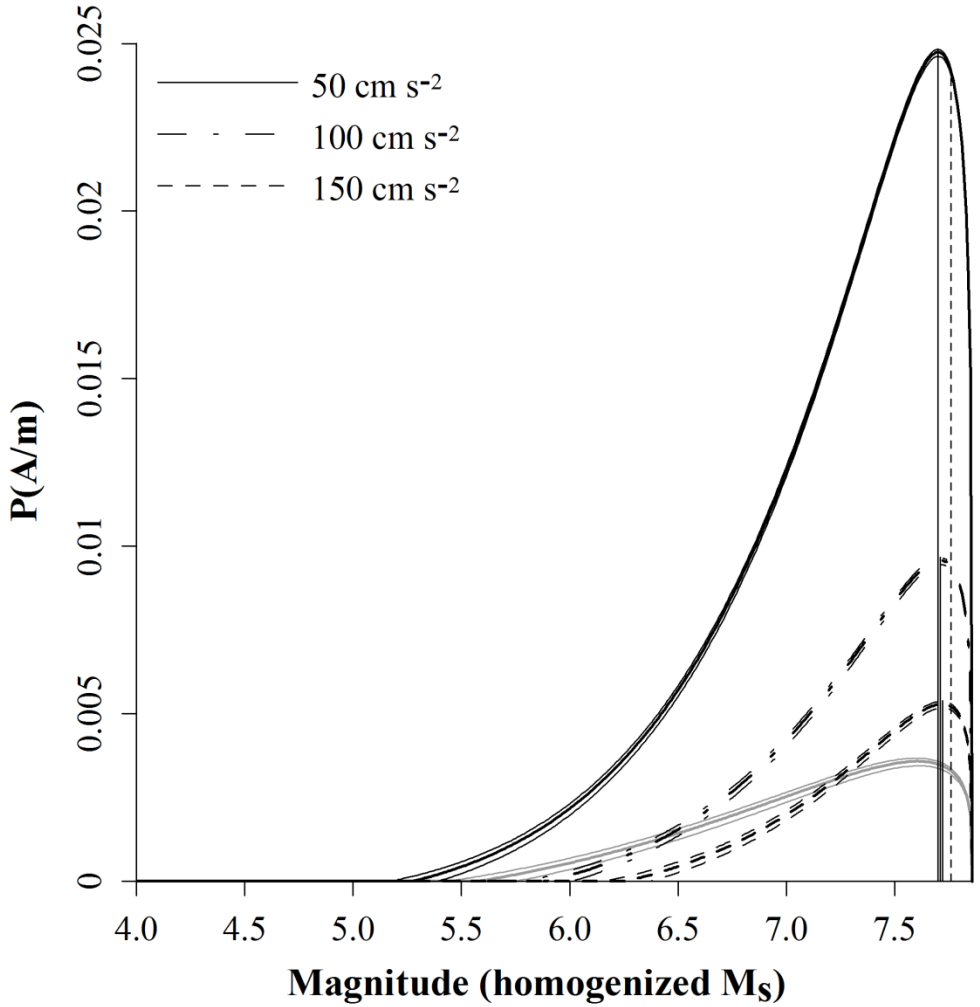

(a)

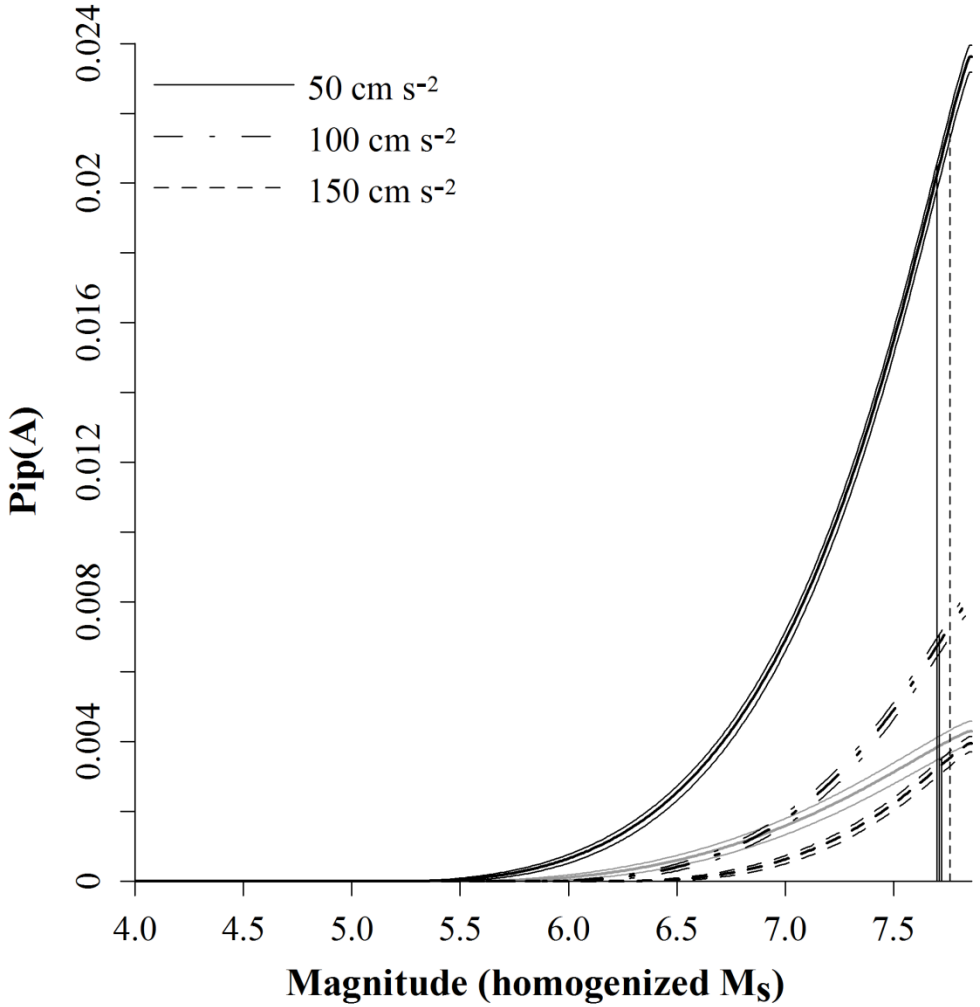

(b)

Ground acceleration (a) perceptibility and (b) integrated perceptibility curves for Sofia using Theodulidis and Papazachos (1992; $TP92_A$)

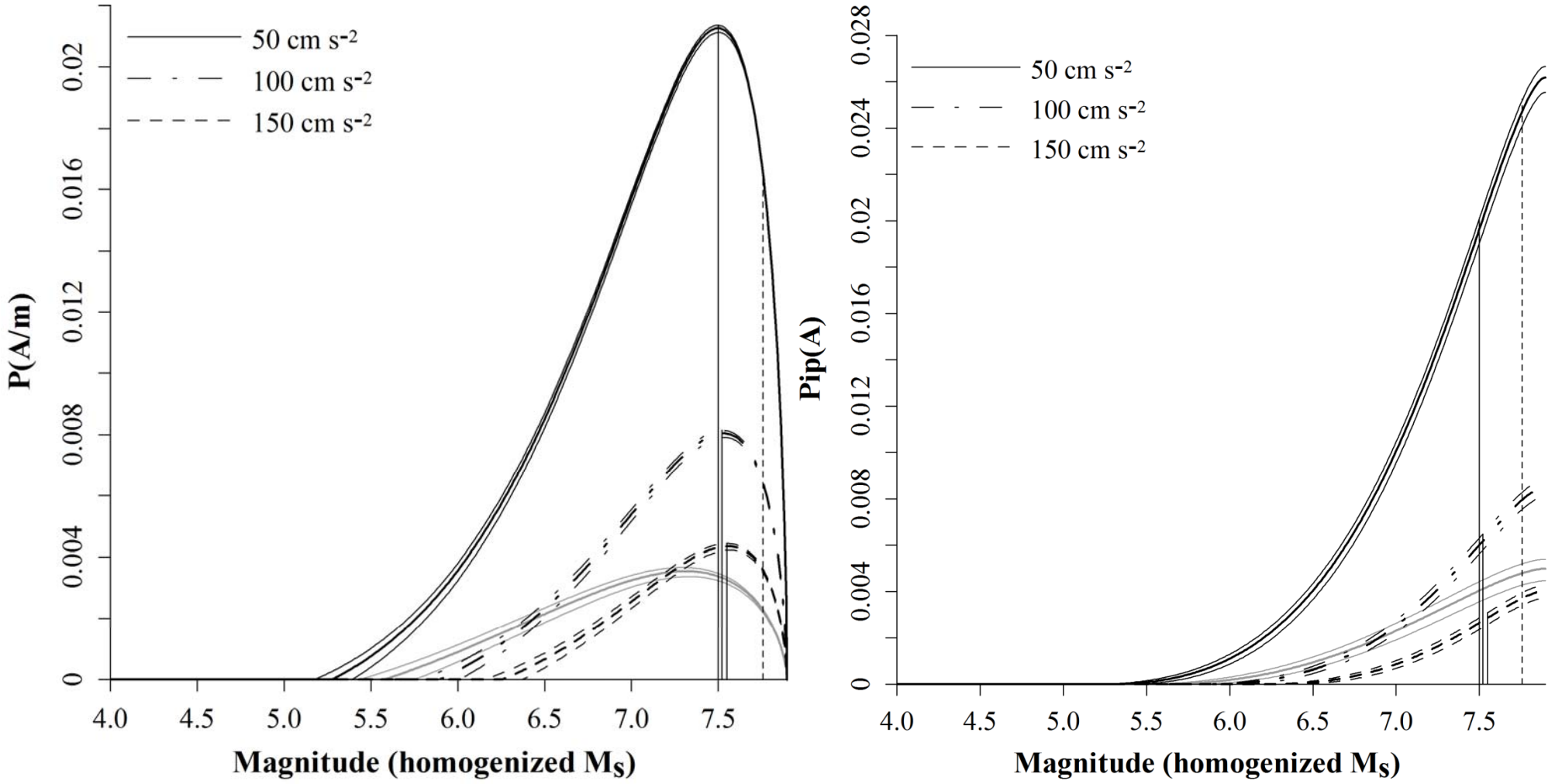

(a) (b)

Ground acceleration (a) perceptibility and (b) integrated perceptibility curves for Thessaloniki using Theodulidis and Papazachos (1992; $TP92_A$)

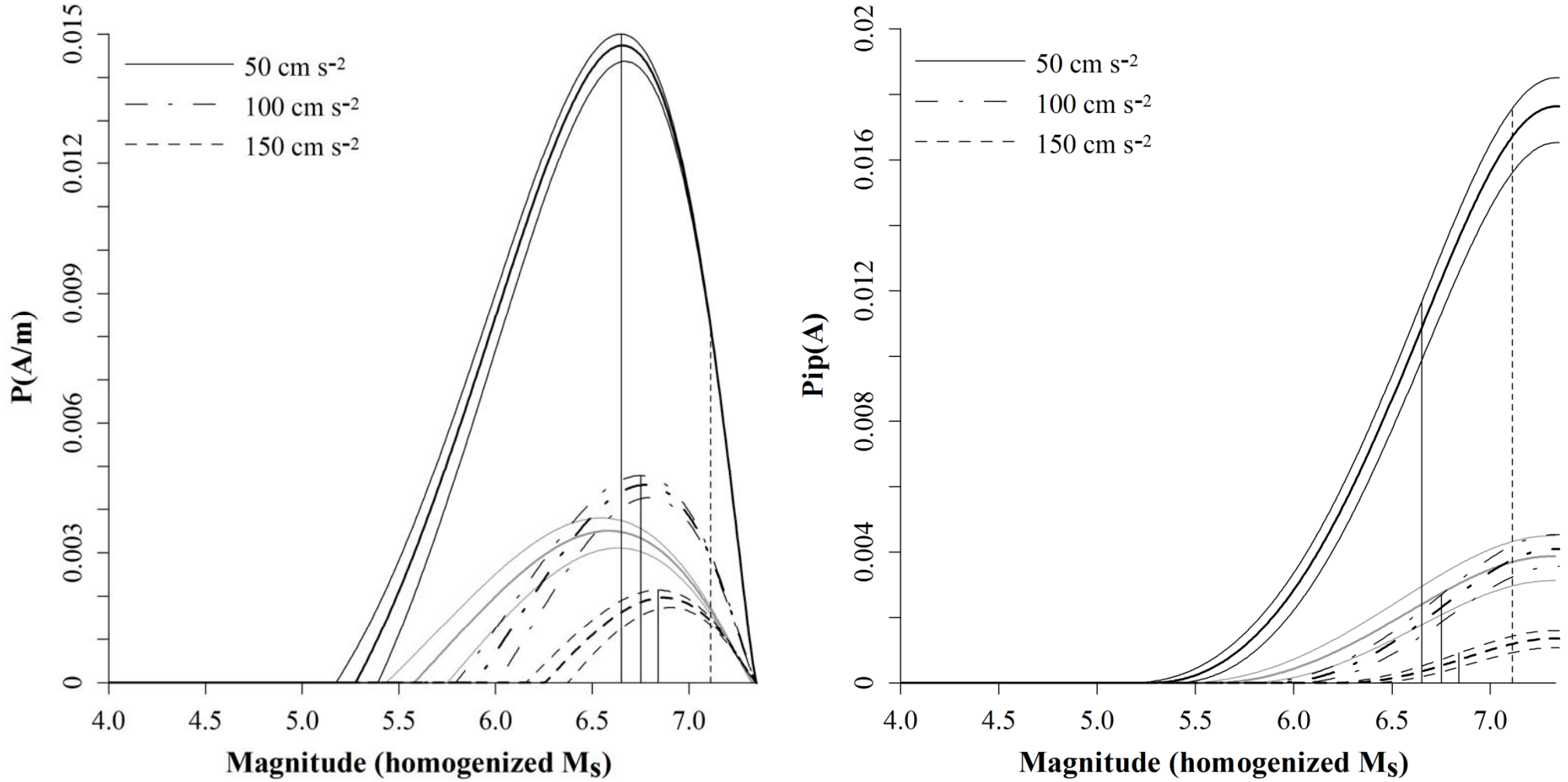

(a) (b)

Ground acceleration (a) perceptibility and (b) integrated perceptibility curves for Tirane using Theodulidis and Papazachos (1992; $TP92_A$)

Appendix 19: $M_{P(max)}$ curves for ground acceleration perceptibility

Most perceptible magnitude curves for ground acceleration perceptibility using Ambraseys (1995; AM95_WDC) for rock sites with depth control at the 50th percentile (P = 0) and Theodulidis and Papazachos (1992; $TP92_A$) for stiff soil (S = 0.5) at the 50th percentile (P = 0) for the urban centres listed for which seismic hazard is forecast.

In each set of three curves on these graphs, the central bold line represents an earthquake at a nominal focal depth of 15 km (approximating to the mean seismogenic depth for historical seismicity above M_{CUT} for the broader region of 5.5 M_S; Figure 2.14. Thinner curves above and below each bold curve represent earthquakes at nominal focal depths of 10 km and 20 km respectively.

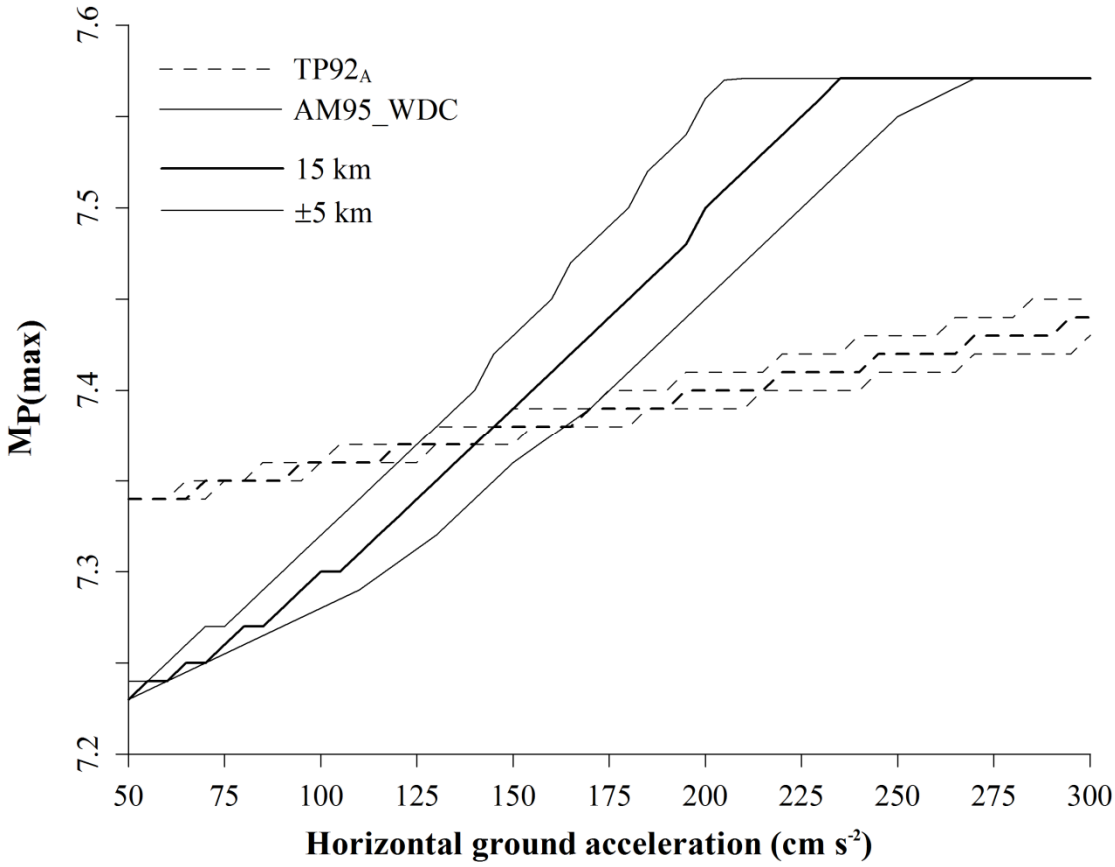

(a)

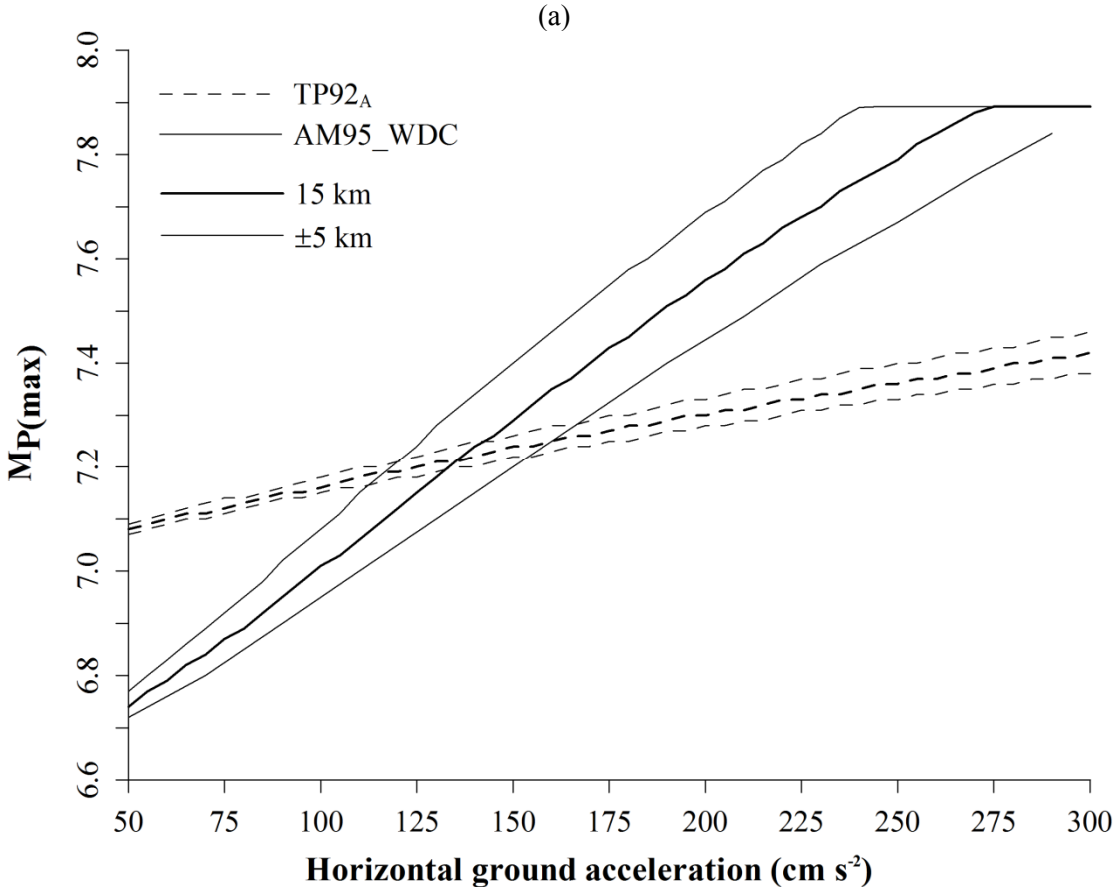

(b)

Most perceptible magnitudes for (a) Edirne and (b) Larissa

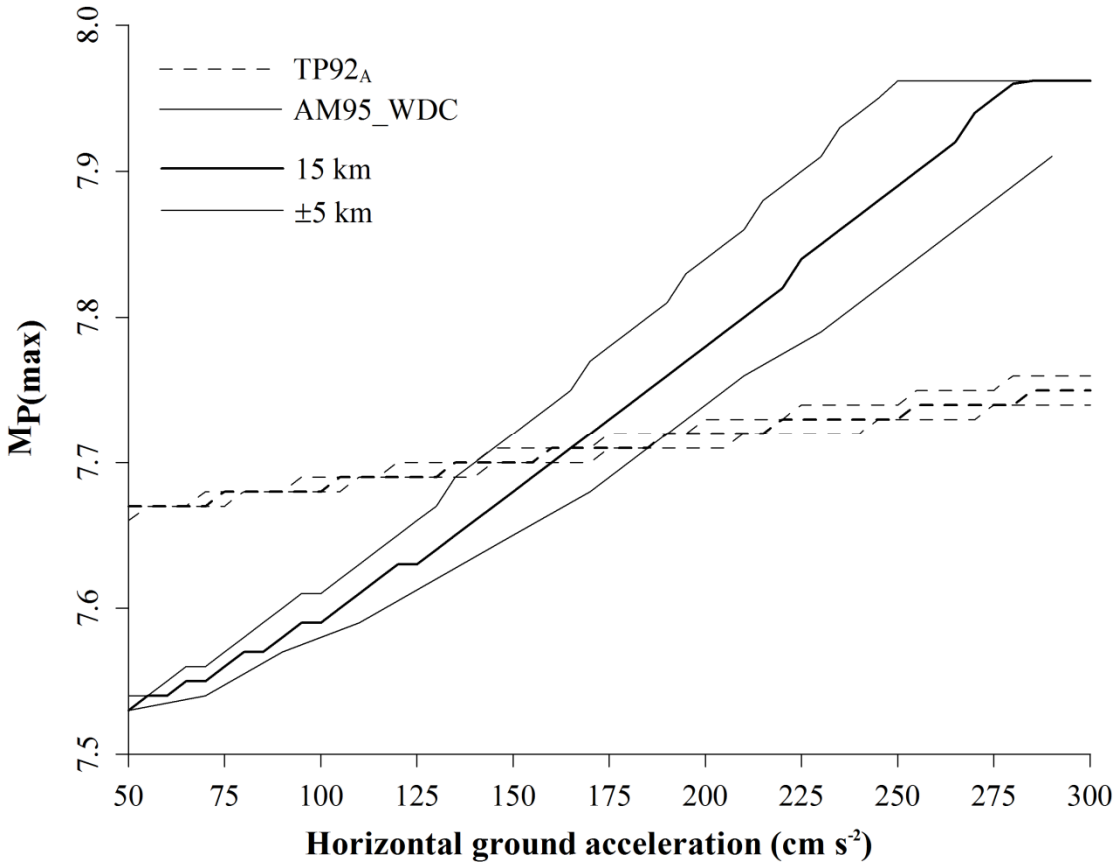

(a)

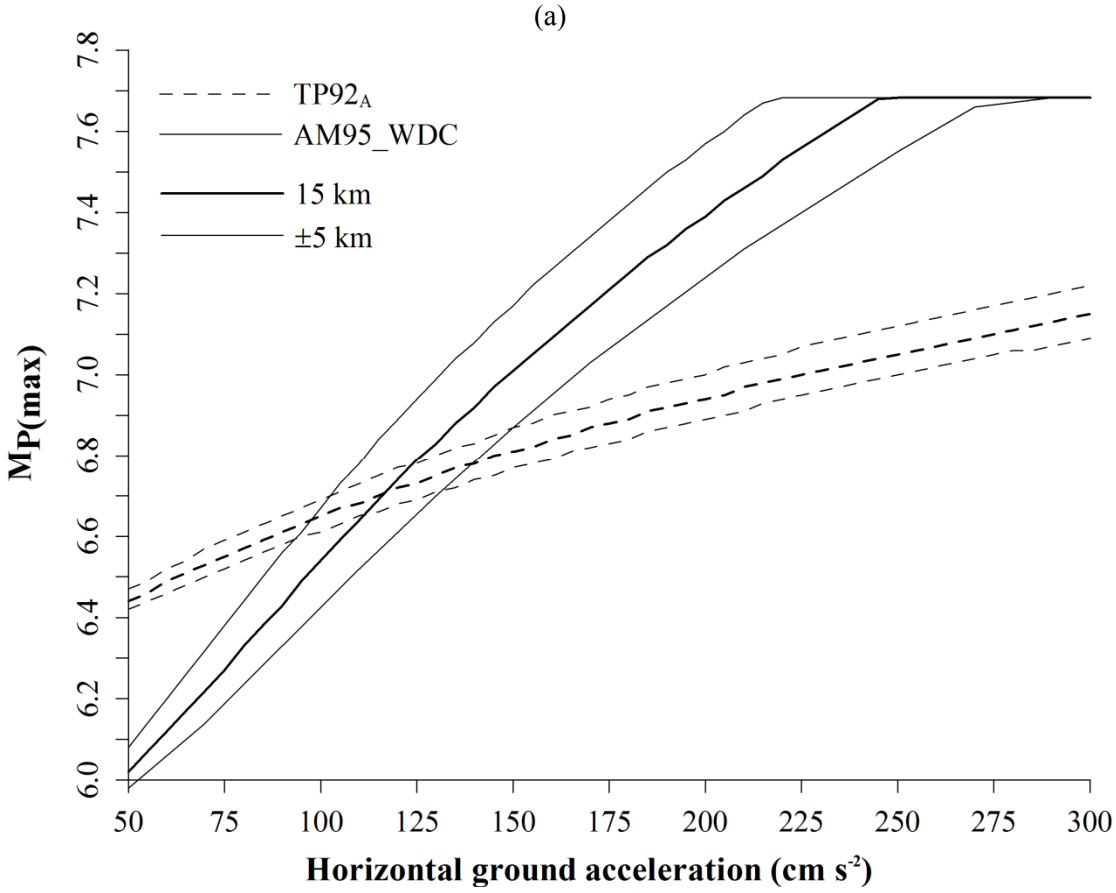

(b)

Most perceptible magnitudes for (a) Plovdiv and (b) Pristina

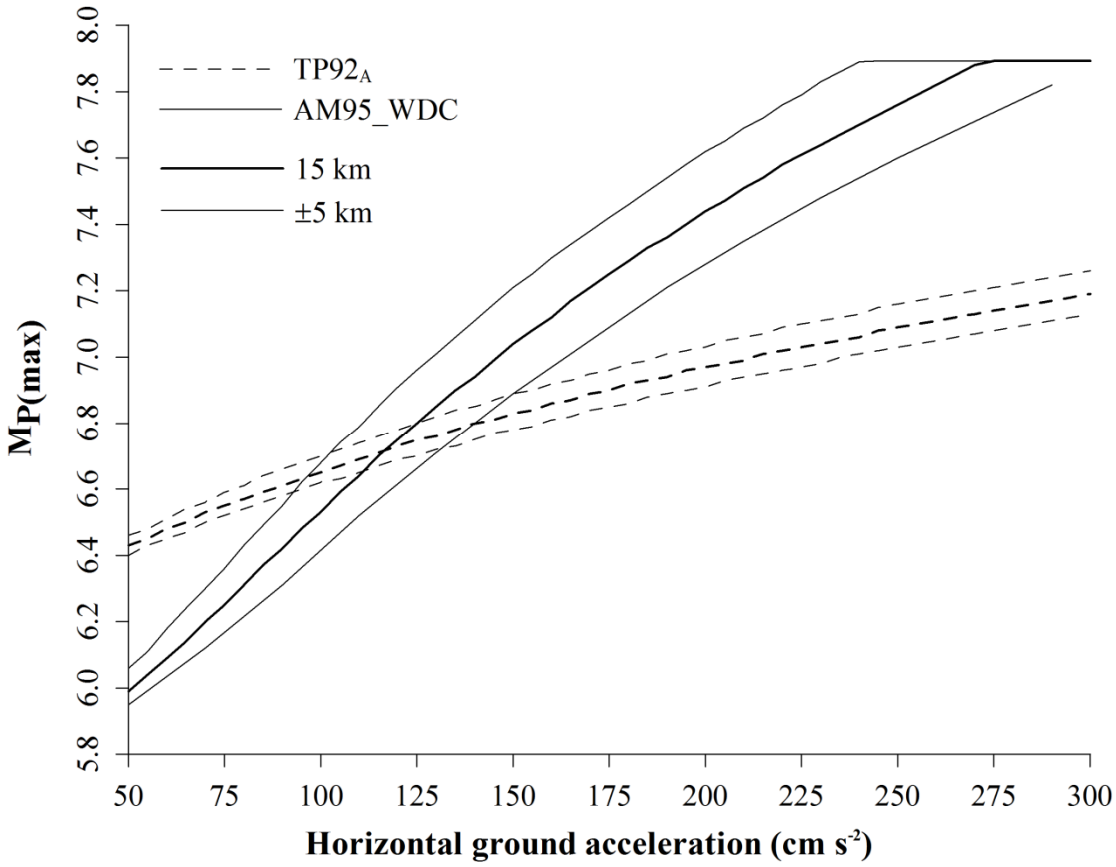

(a)

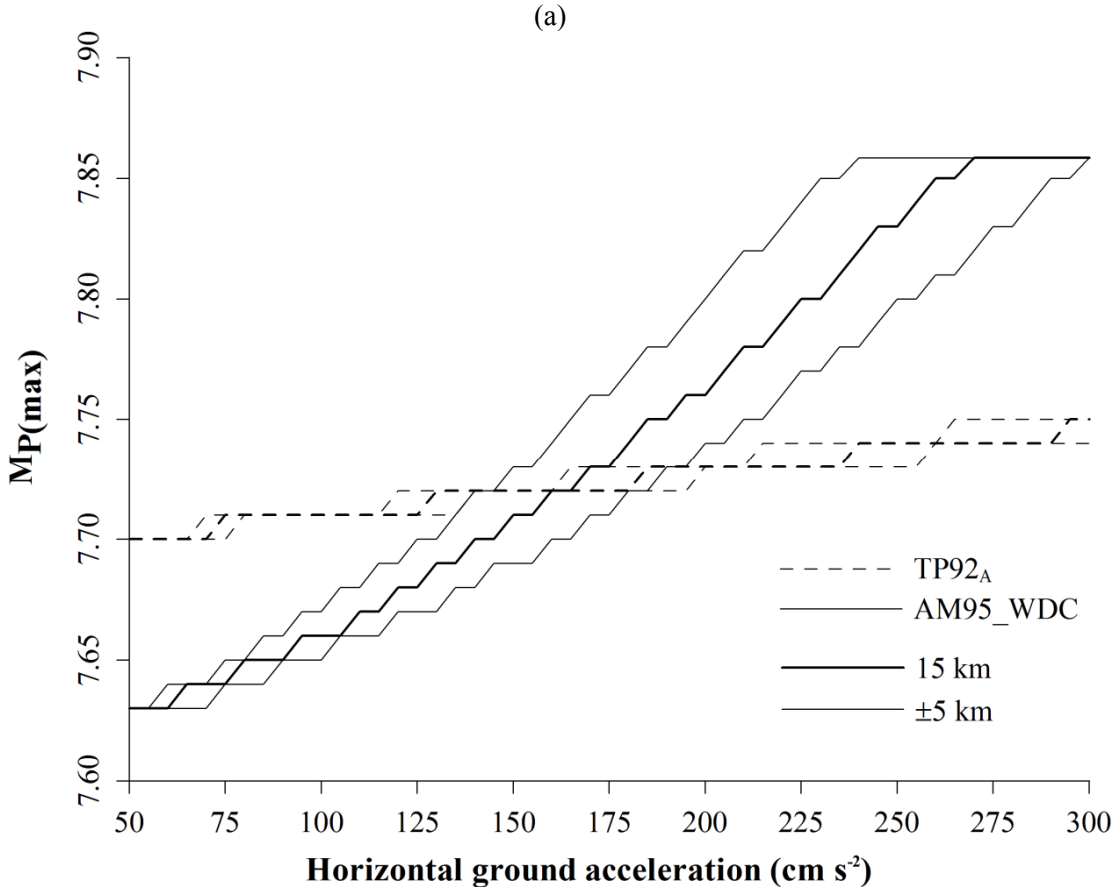

(b)

Most perceptible magnitudes for (a) Skopje and (b) Sofia

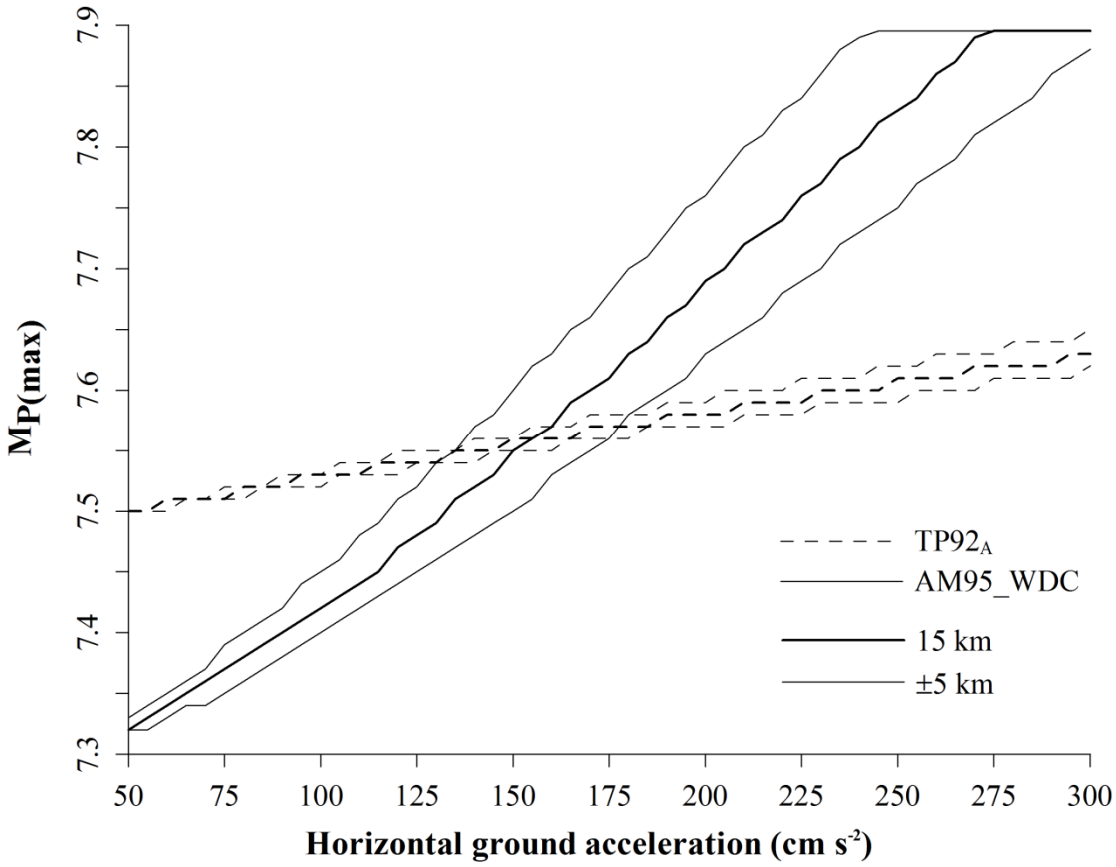

(a)

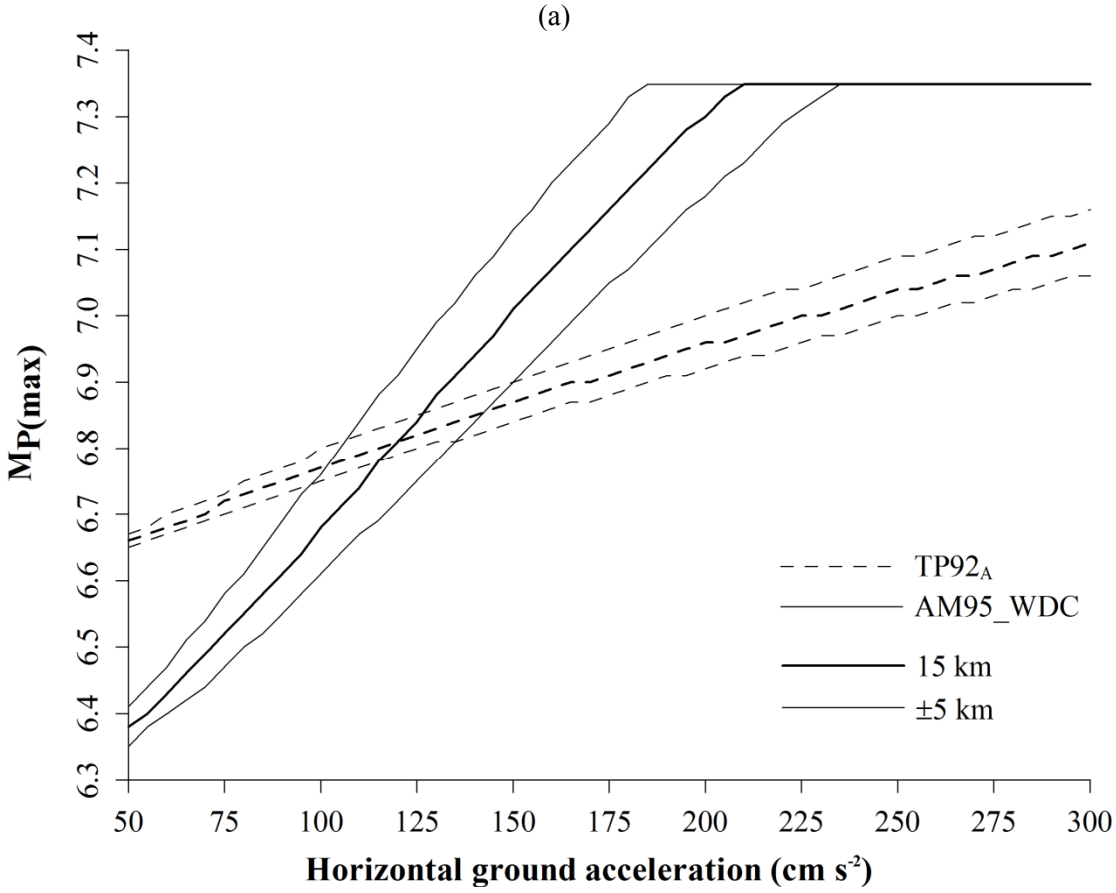

(b)

Most perceptible magnitudes for (a) Thessaloniki and (b) Tirane

Appendix 20: Site-specific horizontal ground acceleration hazard curves

Horizontal ground acceleration hazard curves for the urban centres for which seismic hazard is forecast using:

- Ambraseys (1995; AM95_WDC) for rock sites with depth control at the 50^{th} percentile (P = 0)

- Theodulidis and Papazachos (1992; $TP92_A$) for stiff soil conditions (S = 0.5) at the 50^{th} percentile (P = 0)

- Ambraseys *et al*. (2005; AM05) for normal faulting mechanism earthquakes (F*N* = 1) and stiff soil conditions (S*A* = 1)

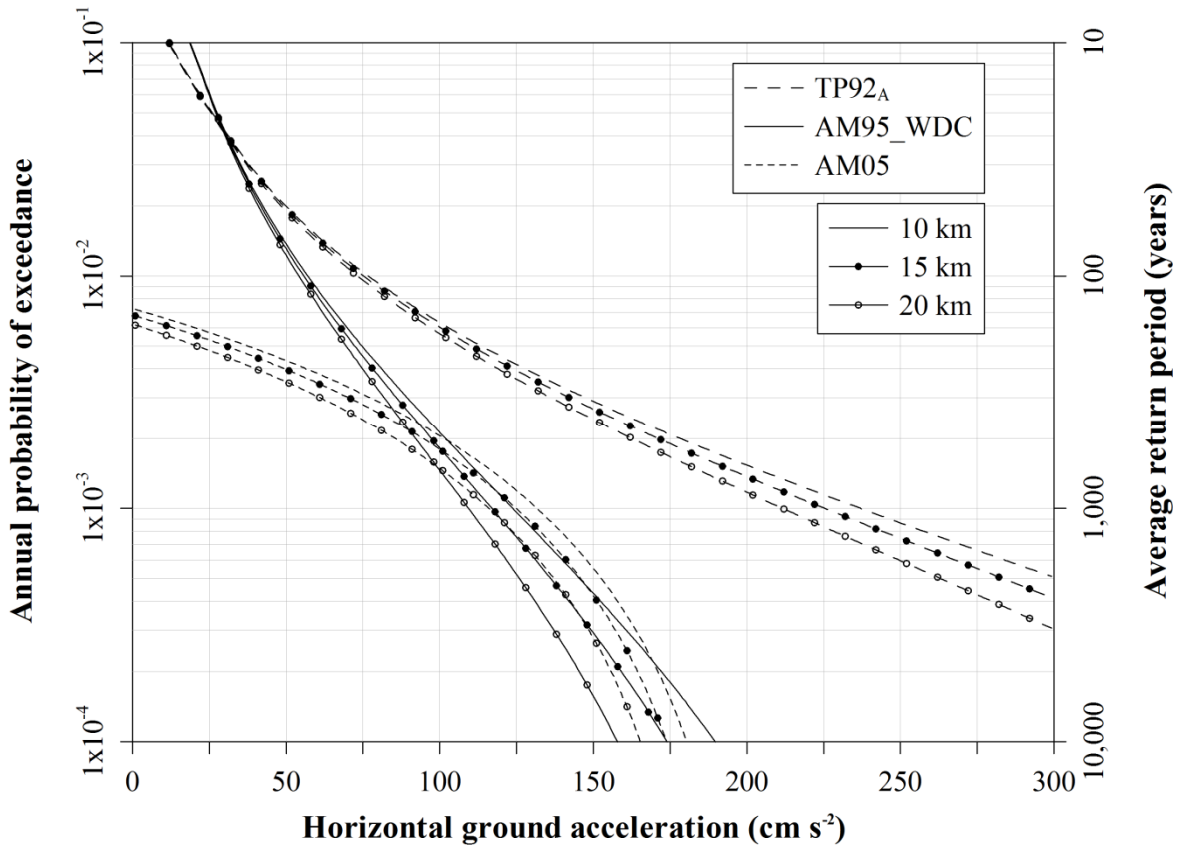

(a)

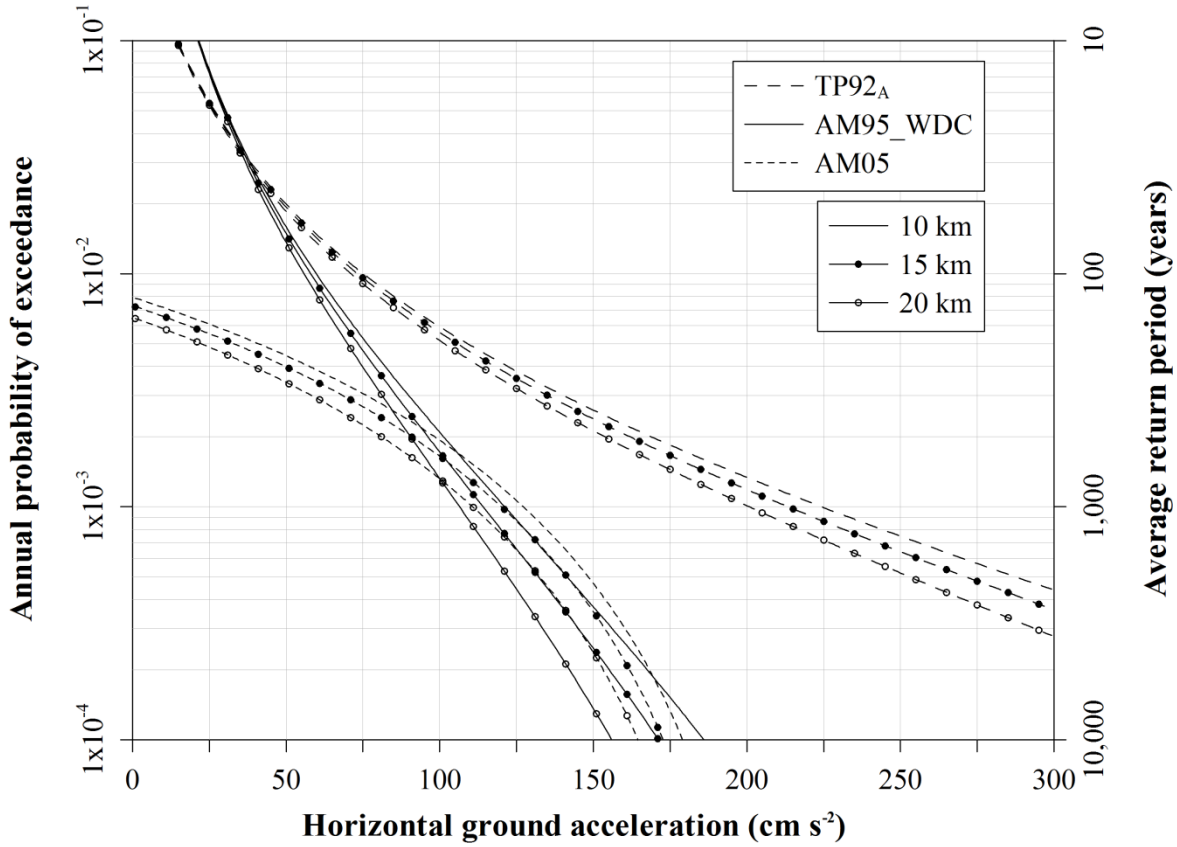

(b)

Ground acceleration hazard curves for (a) Edirne and (b) Larissa

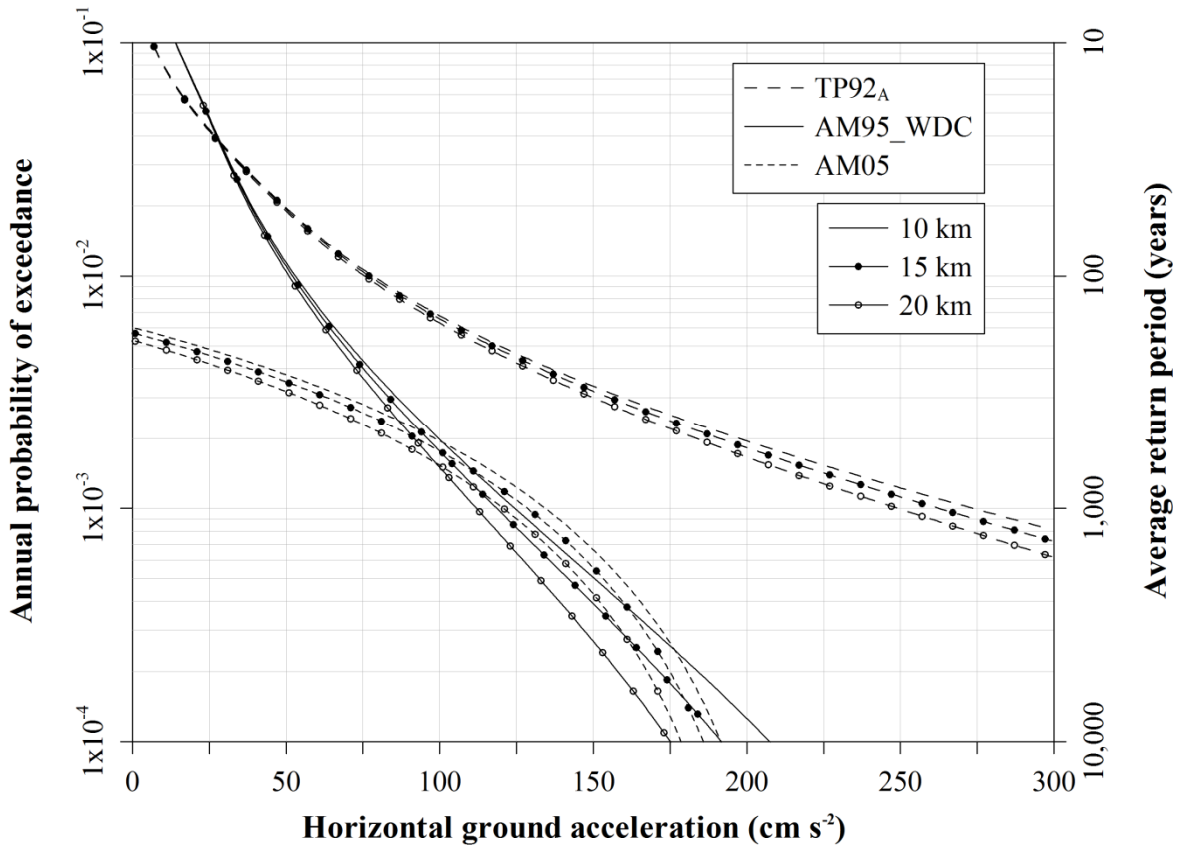

(a)

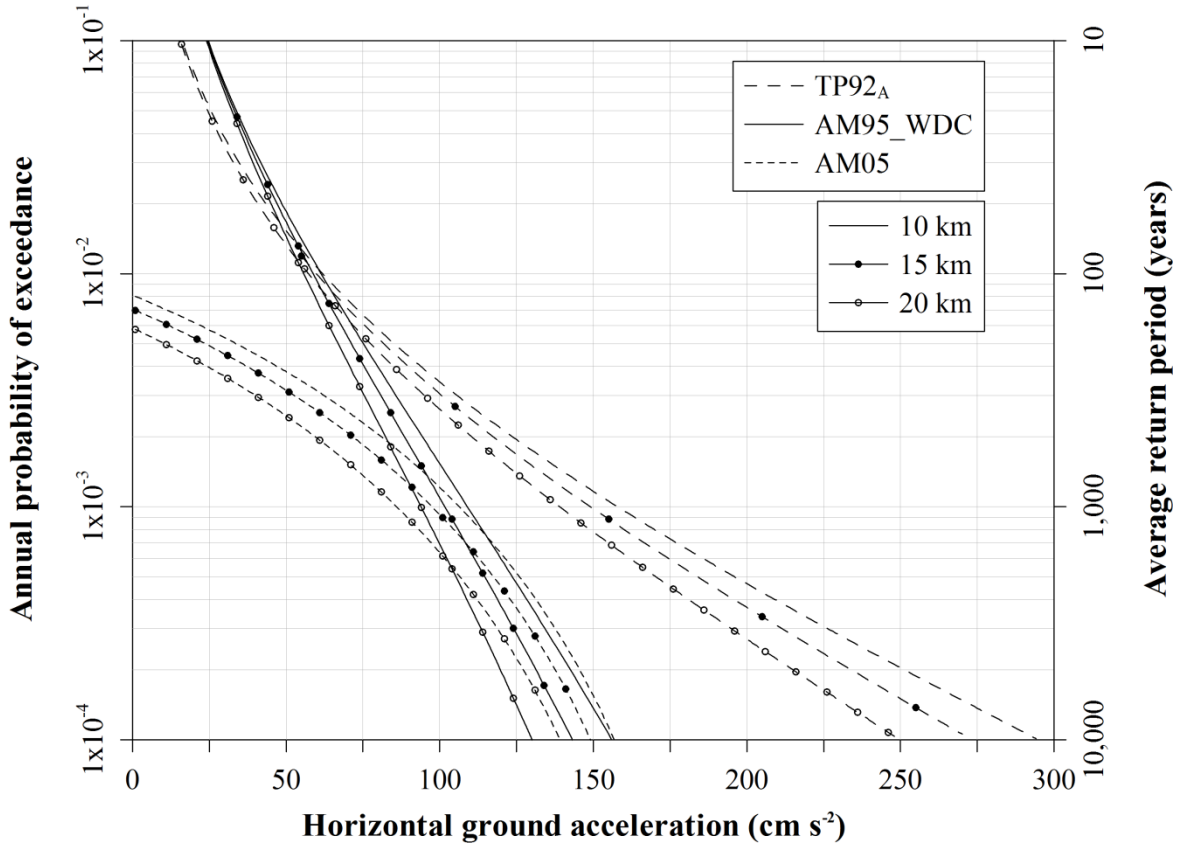

(b)

Ground acceleration hazard curves for (a) Plovdiv and (b) Pristina

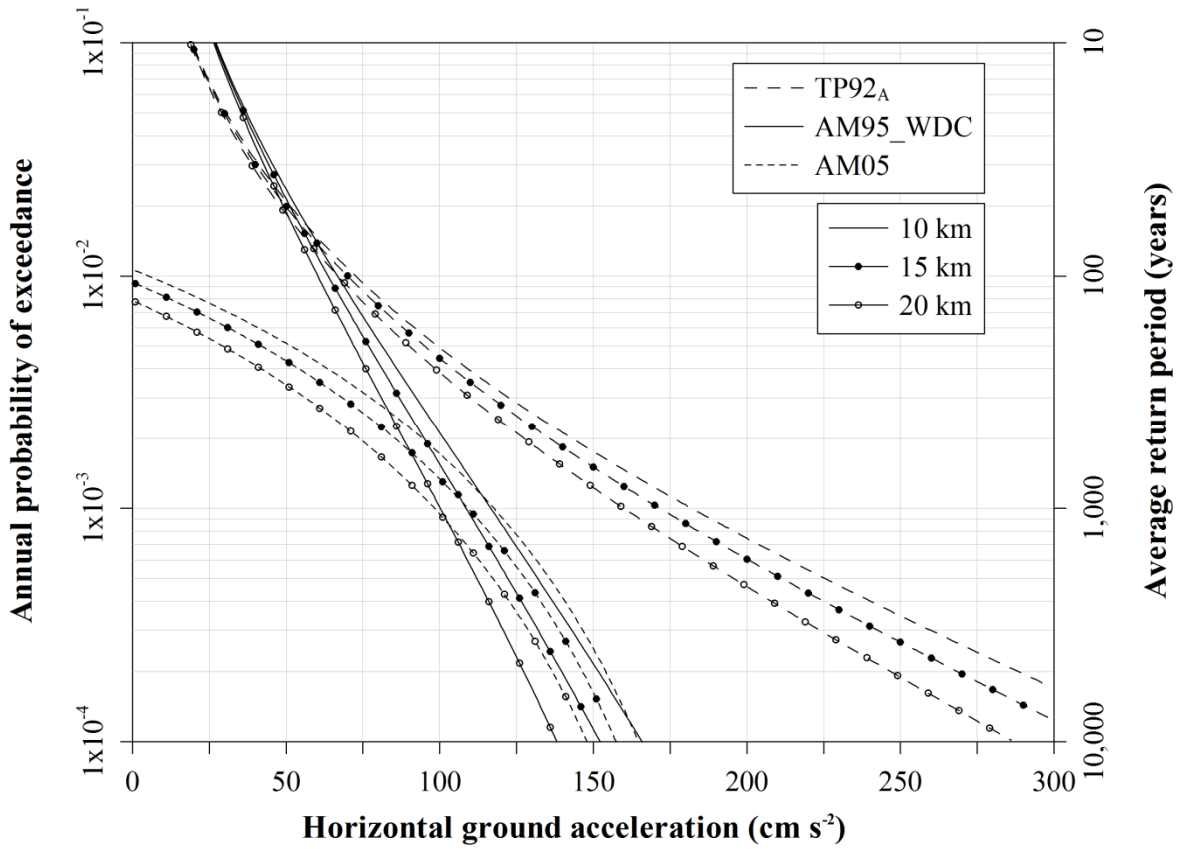

(a)

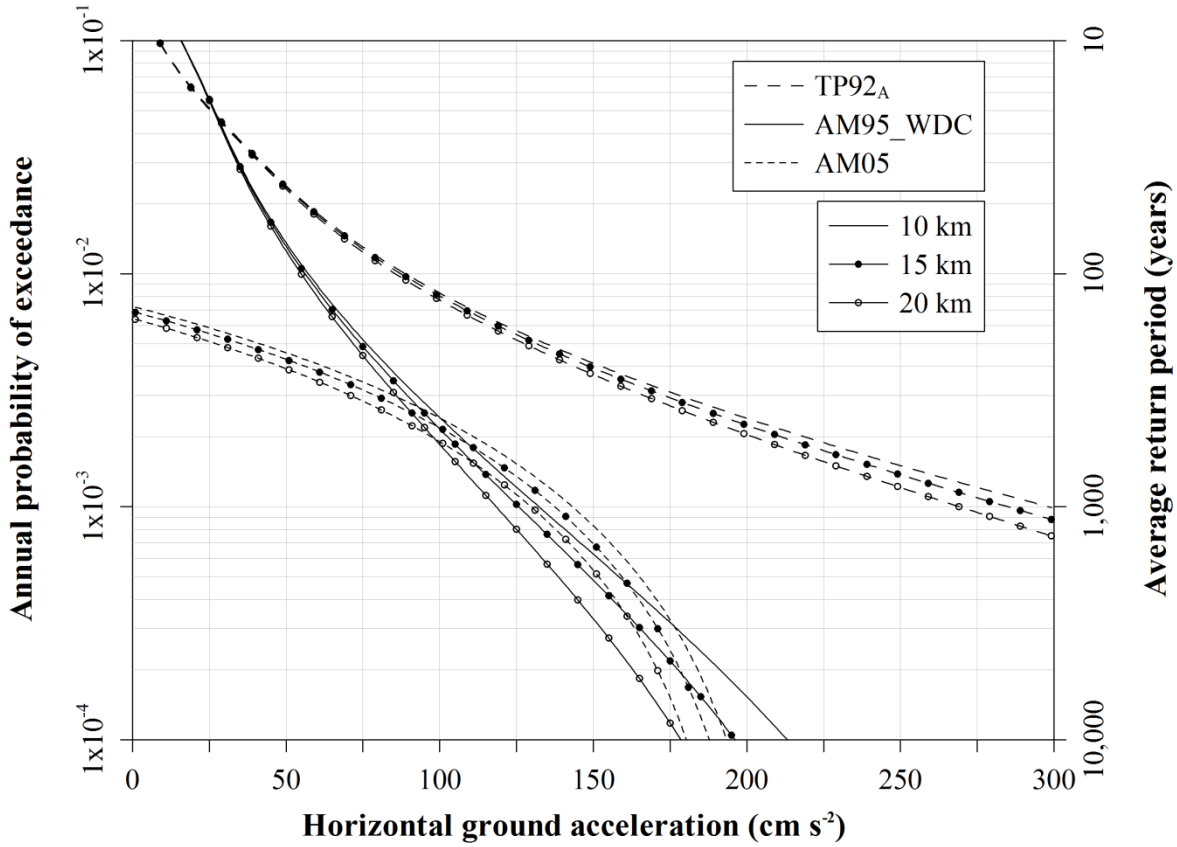

(b)

Ground acceleration hazard curves for (a) Skopje and (b) Sofia

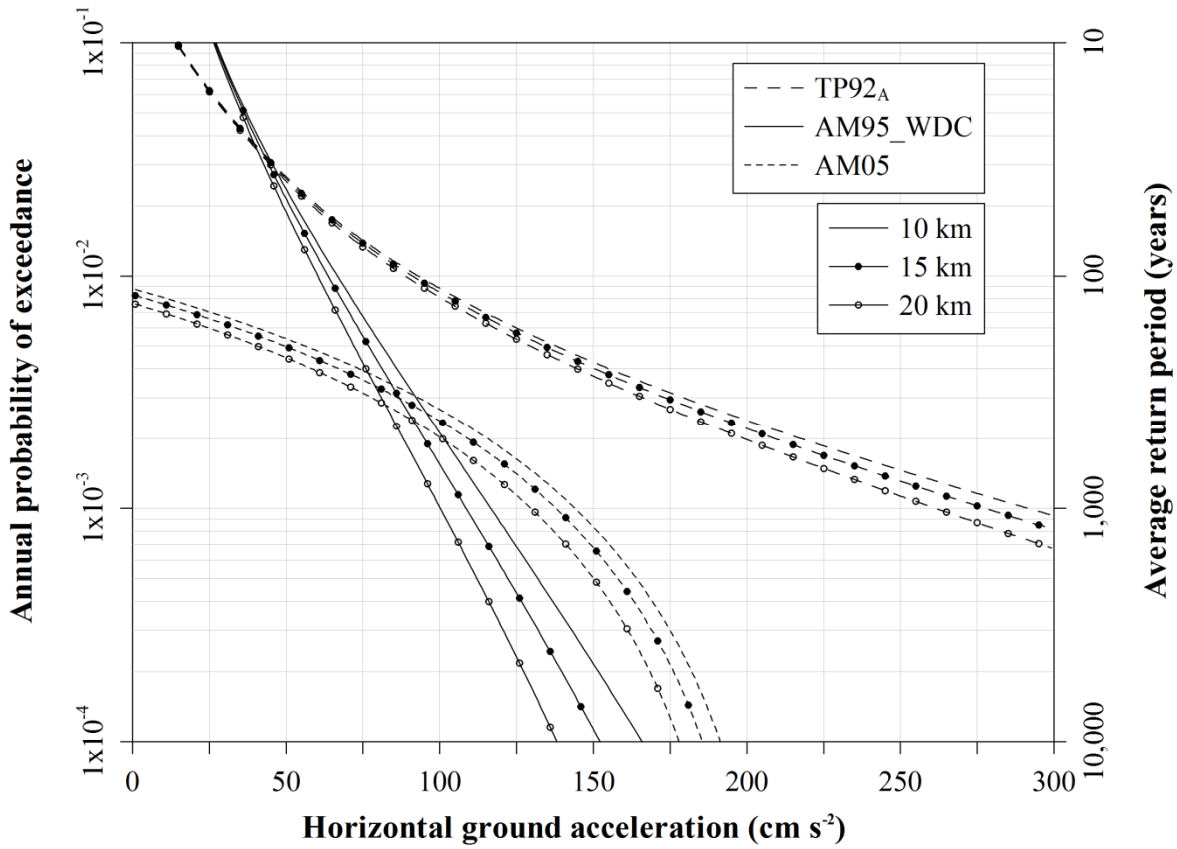

(a)

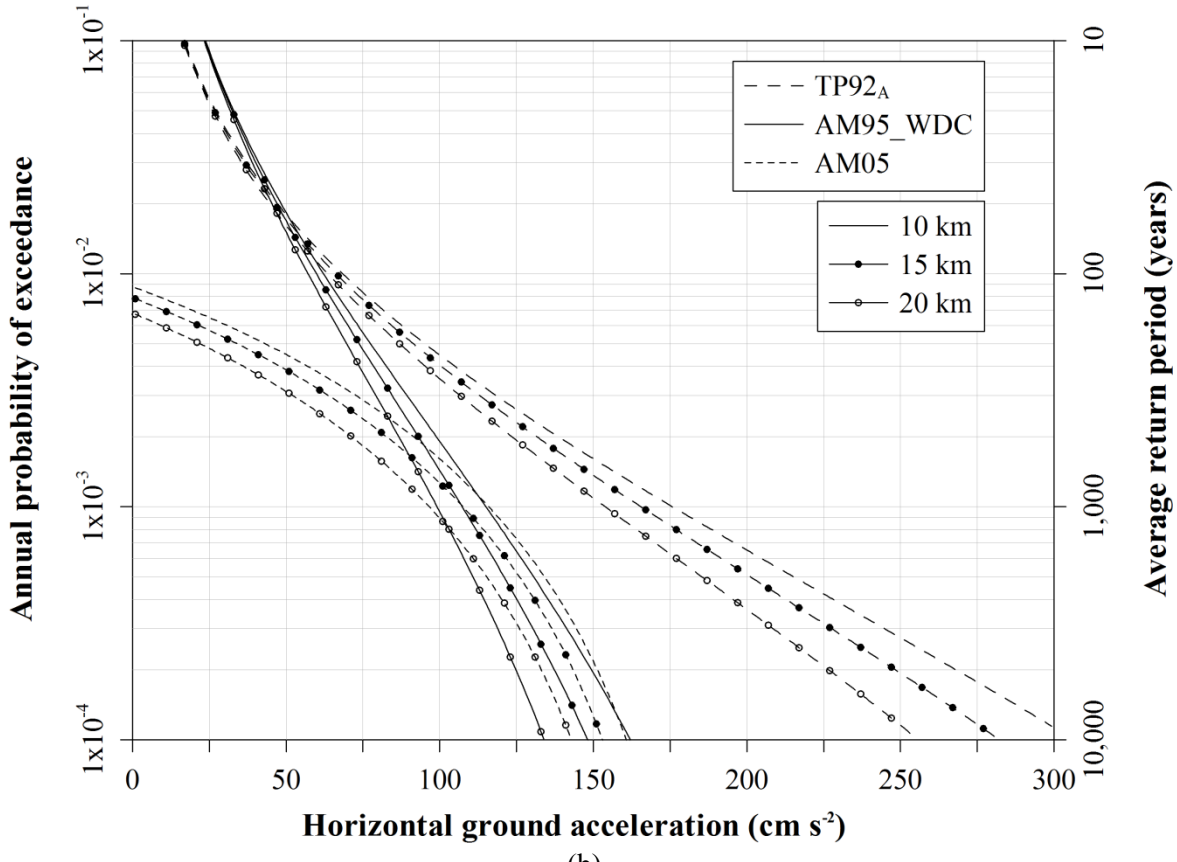

(b)

Ground acceleration hazard curves for (a) Thessaloniki and (b) Tirane

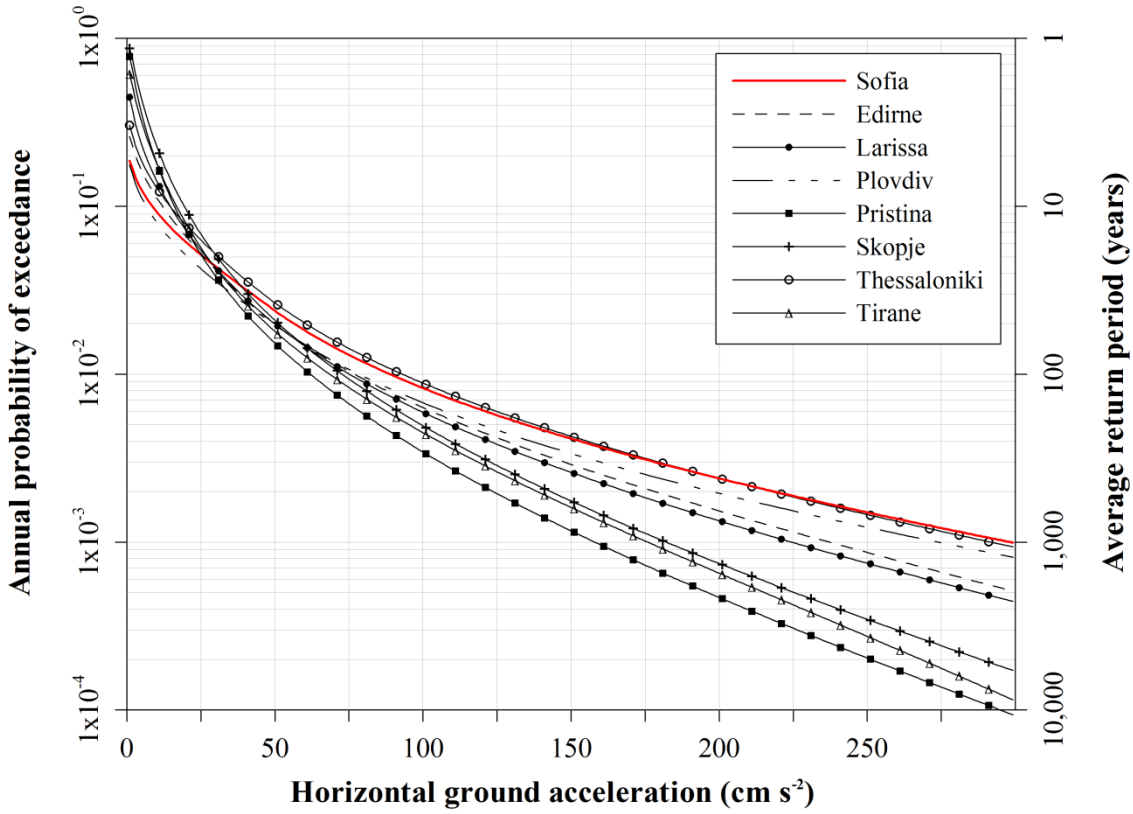

(a)

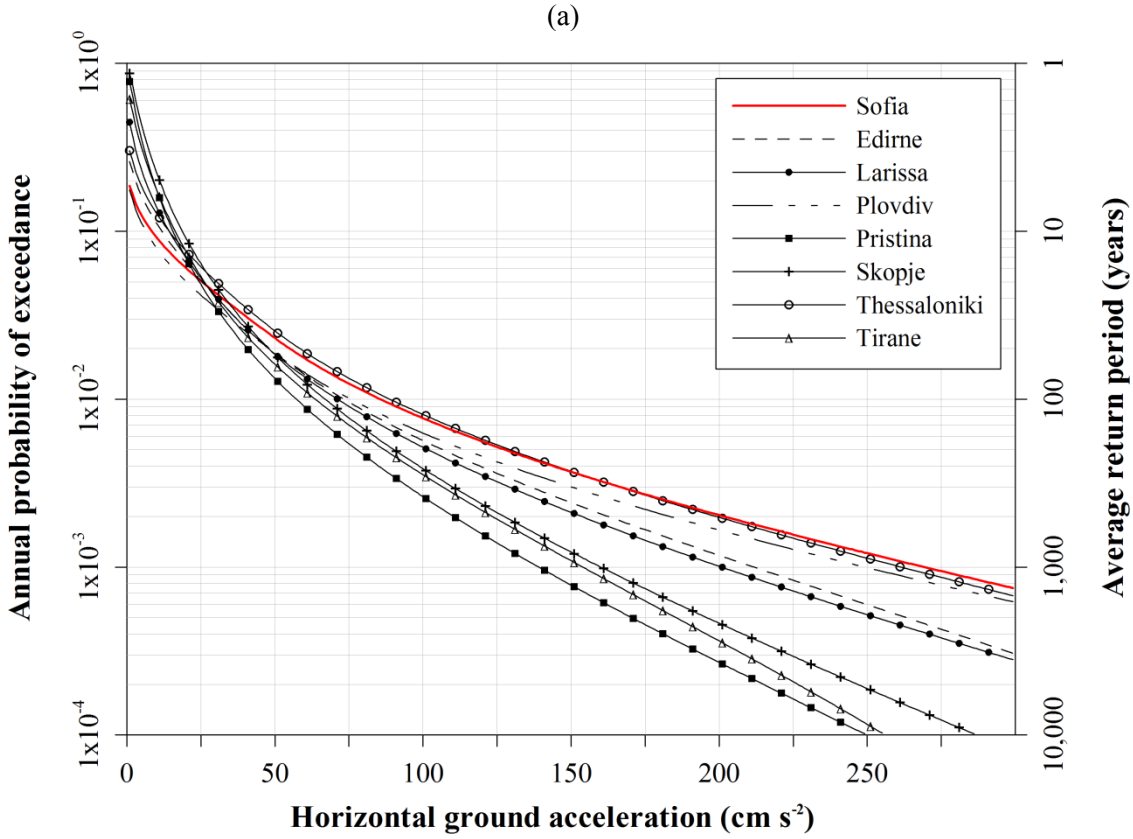

(b)

Ground acceleration hazard curves for urban centres considered using Theodulidis and Papazachos (1992; $TP92_A$) for stiff soil conditions (S = 0.5) at the 50th percentile (P = 0) for a nominal earthquake with focal depth of (a) 10 km and (b) 20 km. In each case, Sofia is highlighted in red as the reference case

Appendix 21: Annual exceedance probabilities of site-specific PGA

Site-specific probabilities for annual exceedance for horizontal peak ground acceleration hazard and in *T*-years for the urban centres listed in Table 5.5 for which seismic hazard is forecast using:

- Ambraseys (1995; AM95_WDC) for rock sites with depth control at the 50th percentile (P = 0)

- Theodulidis and Papazachos (1992; $TP92_A$) for stiff soil conditions (S = 0.5) at the 50th percentile (P = 0)

- Ambraseys *et al*. (2005; AM05) for normal faulting mechanism earthquakes (F_N = 1) and stiff soil conditions (S_A = 1)

City	Focal Depth (km)	Annual probability of exceedance ($\times 10^{-3}$)							
		A_{25}	A_{50}	A_{100}	A_{200}	A_{P25}	A_{P50}	A_{P100}	A_{P200}
Edirne	10	17.2	13.2	10.2	8.1	7.8	6.3	5.2	4.4
	15	16.8	12.8	9.8	7.8	7.5	6.0	5.0	4.2
	20	16.2	12.3	9.4	7.4	7.1	5.7	4.6	3.9
Larissa	10	16.5	12.2	9.4	7.5	7.1	5.7	4.8	3.9
	15	16.0	11.7	8.9	7.1	6.7	5.5	4.4	3.6
	20	15.3	11.1	8.4	6.7	6.3	5.0	4.0	3.3
Plovdiv	10	1.0	---	---	---	---	---	---	---
	15	1.0	---	---	---	---	---	---	---
	20	1.0	---	---	---	---	---	---	---
Pristina	10	29.5	21.3	15.3	11.8	11.1	8.8	6.9	5.6
	15	28.2	20.2	14.4	11.1	10.3	8.1	6.3	5.1
	20	26.7	18.9	13.3	10.1	9.4	7.3	5.6	4.5
Skopje	10	2.8	1.5	1.0	1.0	<1.0	<1.0	<1.0	---
	15	2.5	1.3	1.0	<1.0	<1.0	<1.0	<1.0	---
	20	2.1	1.1	1.0	<1.0	<1.0	<1.0	<1.0	---
Thessaloniki	10	6.0	4.1	2.9	2.1	2.0	1.5	1.1	---
	15	5.7	3.8	2.7	1.9	1.8	1.3	1.0	---
	20	5.4	3.5	2.4	1.7	1.6	1.2	1.0	---
Tirane	10	2.0	1.3	1.0	1.0	<1.0	<1.0	<1.0	<1.0
	15	1.7	1.1	1.0	<1.0	<1.0	<1.0	<1.0	<1.0
	20	1.4	1.0	1.0	<1.0	<1.0	<1.0	<1.0	<1.0

Annual probabilities ($\times 10^{-3}$) of experiencing extreme acceleration ground motions estimated for the region surrounding each urban centre using Theodulidis and Papazachos (1992) for stiff soil conditions at the 50th percentile. '---' is outside the range of the hazard curve

City	Focal Depth (km)	Time interval (*T*-year)					
		100	200	300	400	500	1,000
Edirne	10	77	82	87	95	103	237
	15	75	80	86	92	100	225
	20	73	78	83	90	97	211
Larissa	10	75	80	85	91	99	224
	15	73	78	83	89	96	213
	20	71	75	80	86	93	200
Plovdiv	10	78	84	90	98	107	274
	15	77	82	89	96	105	262
	20	75	81	87	94	102	249
Pristina	10	62	65	69	73	79	157
	15	59	63	66	71	76	149
	20	57	60	63	67	72	139
Skopje	10	73	76	81	86	92	182
	15	70	73	77	82	88	171
	20	67	70	74	78	84	160
Thessaloniki	10	93	99	106	114	125	291
	15	91	97	104	112	121	277
	20	89	94	101	108	118	261
Tirane	10	68	72	76	82	88	176
	15	66	70	74	79	84	165
	20	63	67	71	75	80	153

Peak ground accelerations (in cm s^{-2}) expected within a *T*-year time interval for the region surrounding each urban centre using Theodulidis and Papazachos (1992) for stiff soil conditions at the 50^{th} percentile

Appendix 22: Site-specific velocity perceptibility/integrated perceptibility curves

Ground velocity (a) perceptibility and (b) integrated perceptibility curves for the urban centres for which seismic hazard is forecast, using Theodulidis and Papazachos (1992; $TP92_V$) for stiff soil conditions (S = 0.5) at the 50^{th} percentile (P = 0).

In each set of three curves on these graphs, the central bold line represents an earthquake at a nominal focal depth of 15 km (approximating to the mean seismogenic depth for historical seismicity above M_{CUT} for the broader region of 5.5 M_S; Figure 2.14). Thinner curves above and below each bold curve represent earthquakes at nominal focal depths of 10 km and 20 km respectively. Vertical black lines are at *the most perceptible magnitude,* $M_{P(max)}$, only for 10 km focal depth estimates. The vertical dashed line represents M_3 from cumulative strain energy release techniques (chapter 6 and Appendix 17).

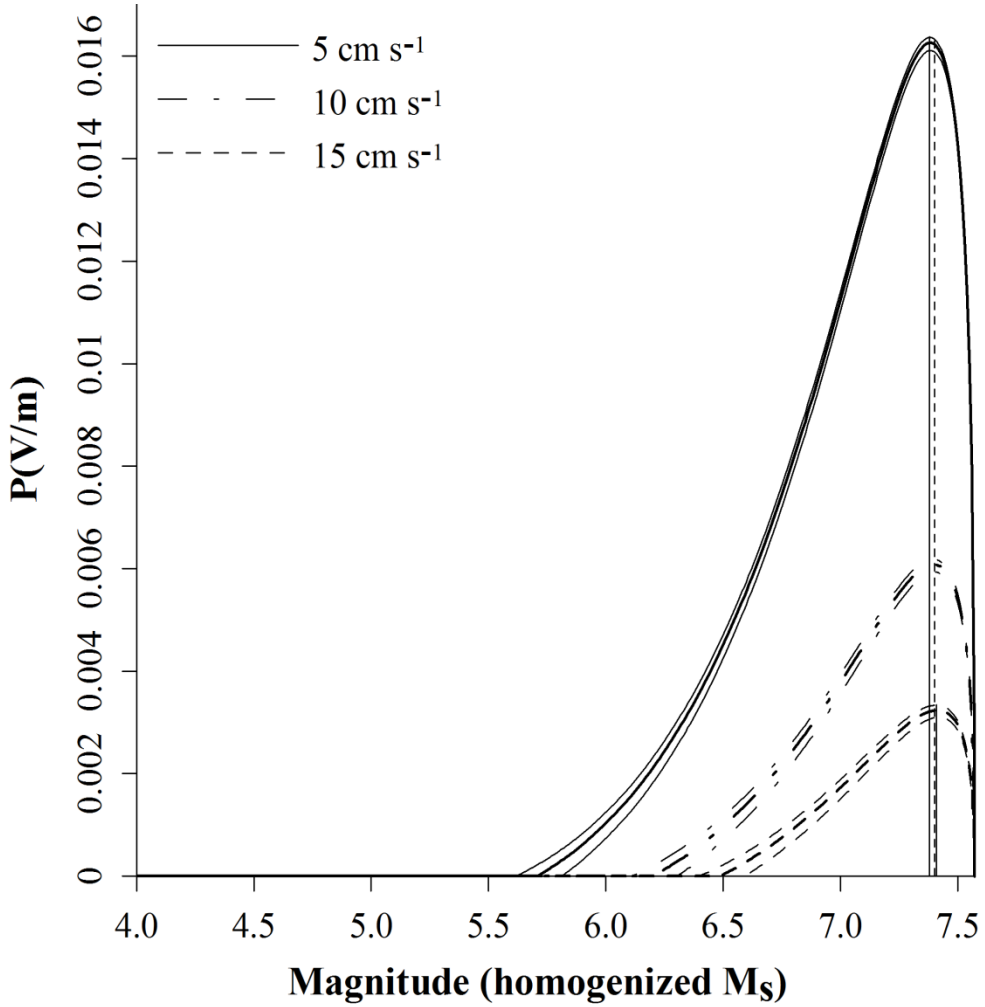

(a)

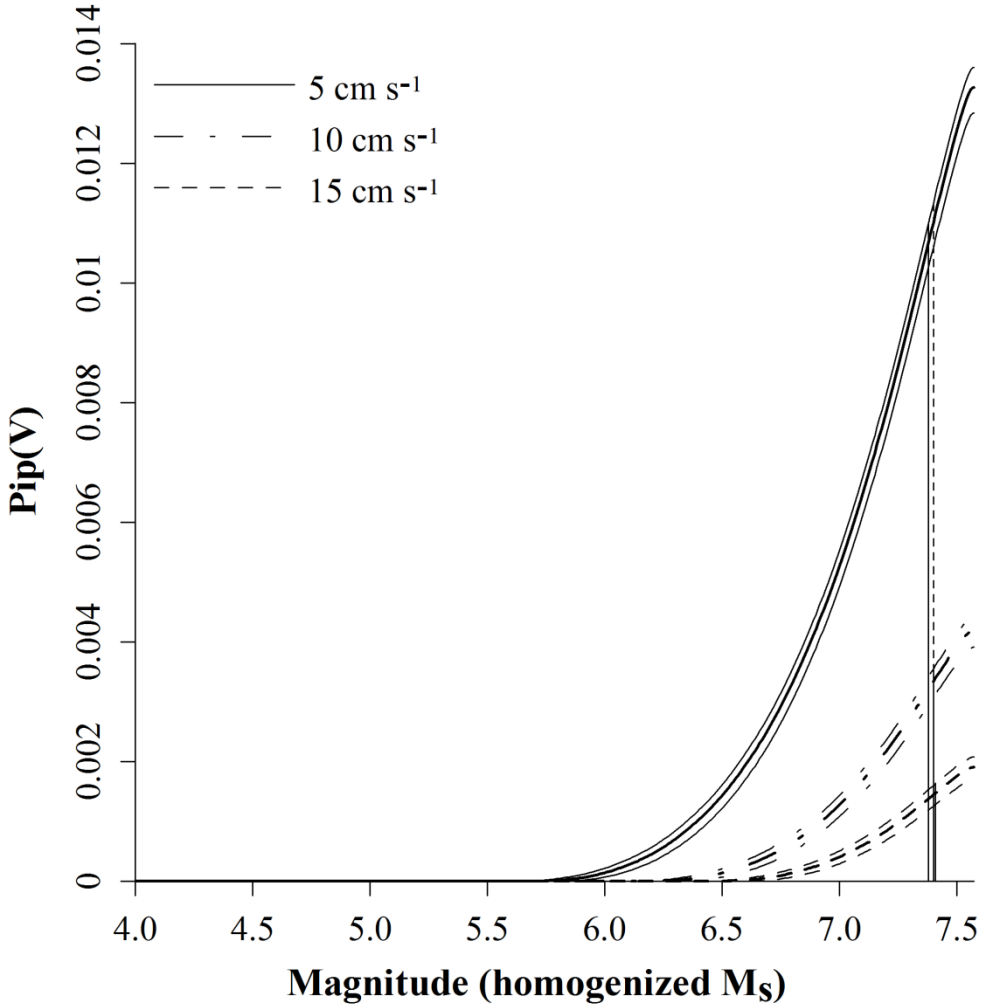

(b)

Ground velocity (a) perceptibility and (b) integrated perceptibility curves for Edirne

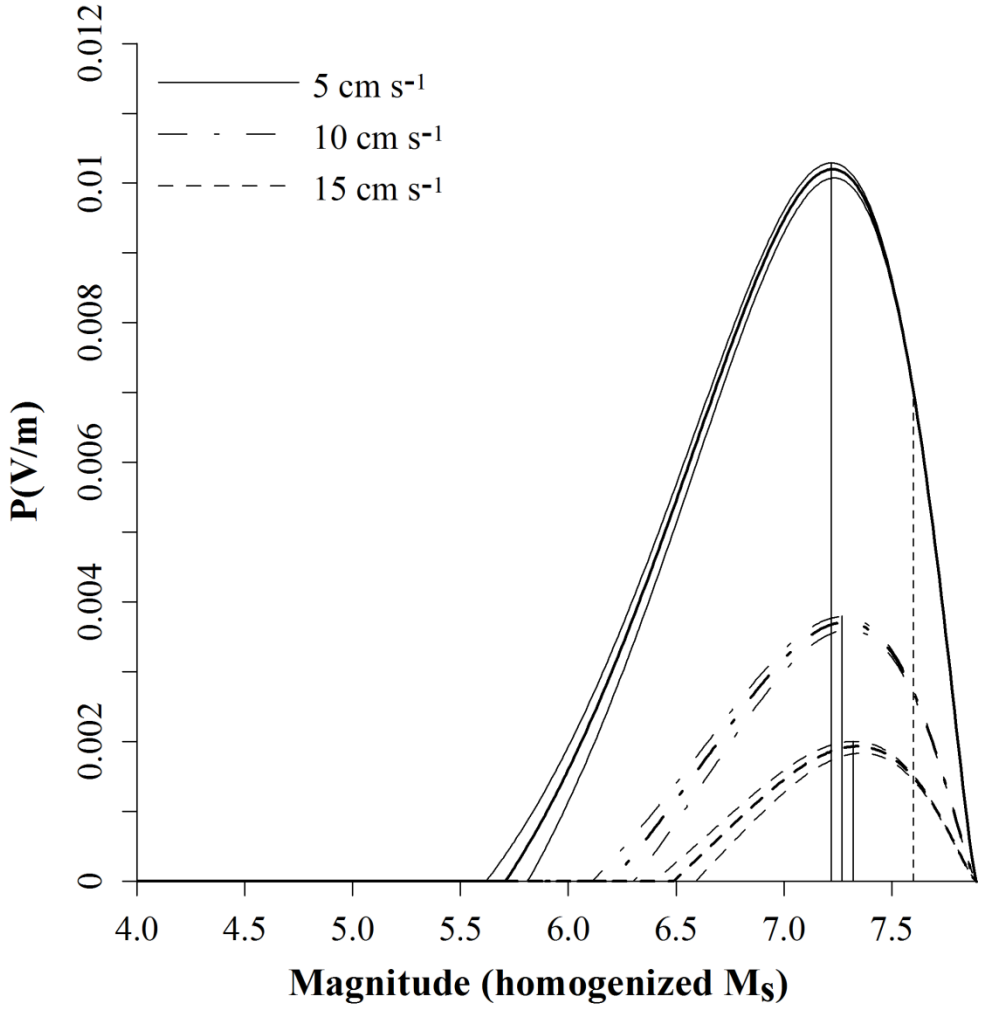

(a)

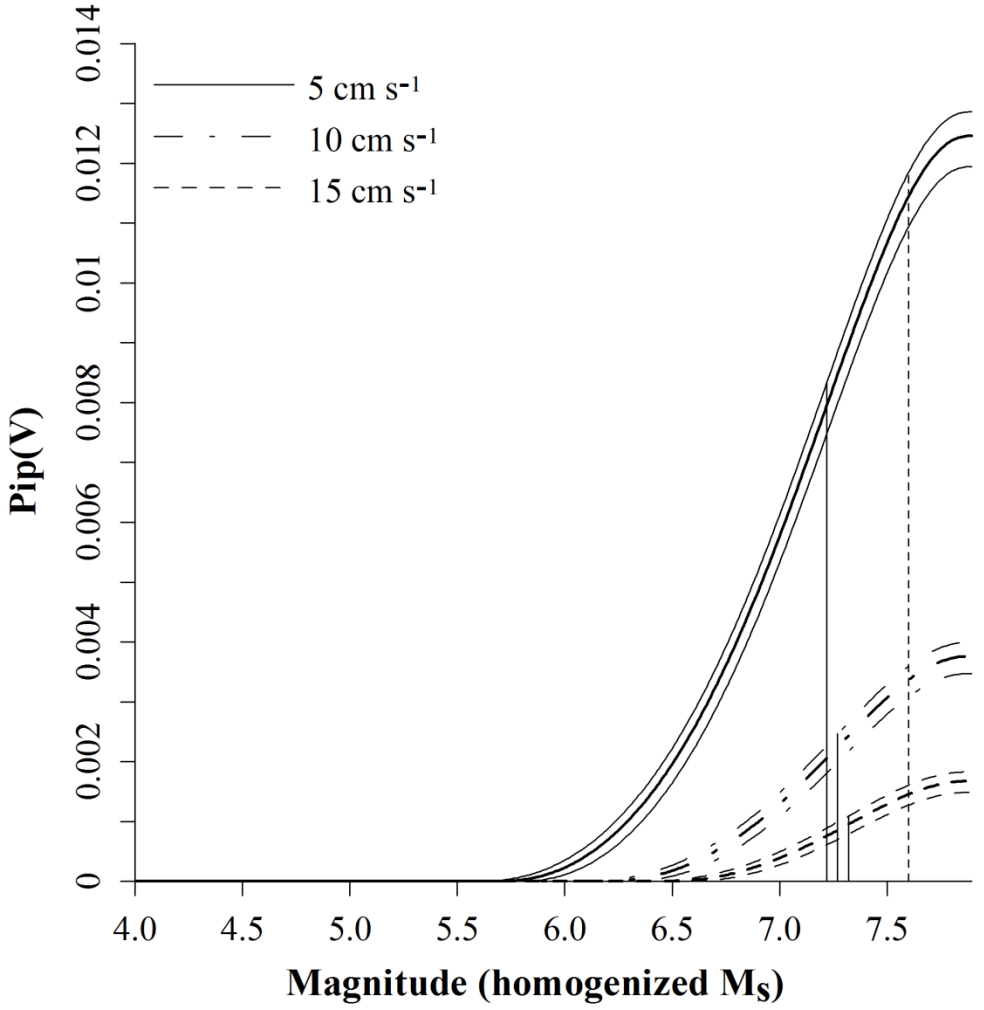

(b)

Ground velocity (a) perceptibility and (b) integrated perceptibility curves for Larissa

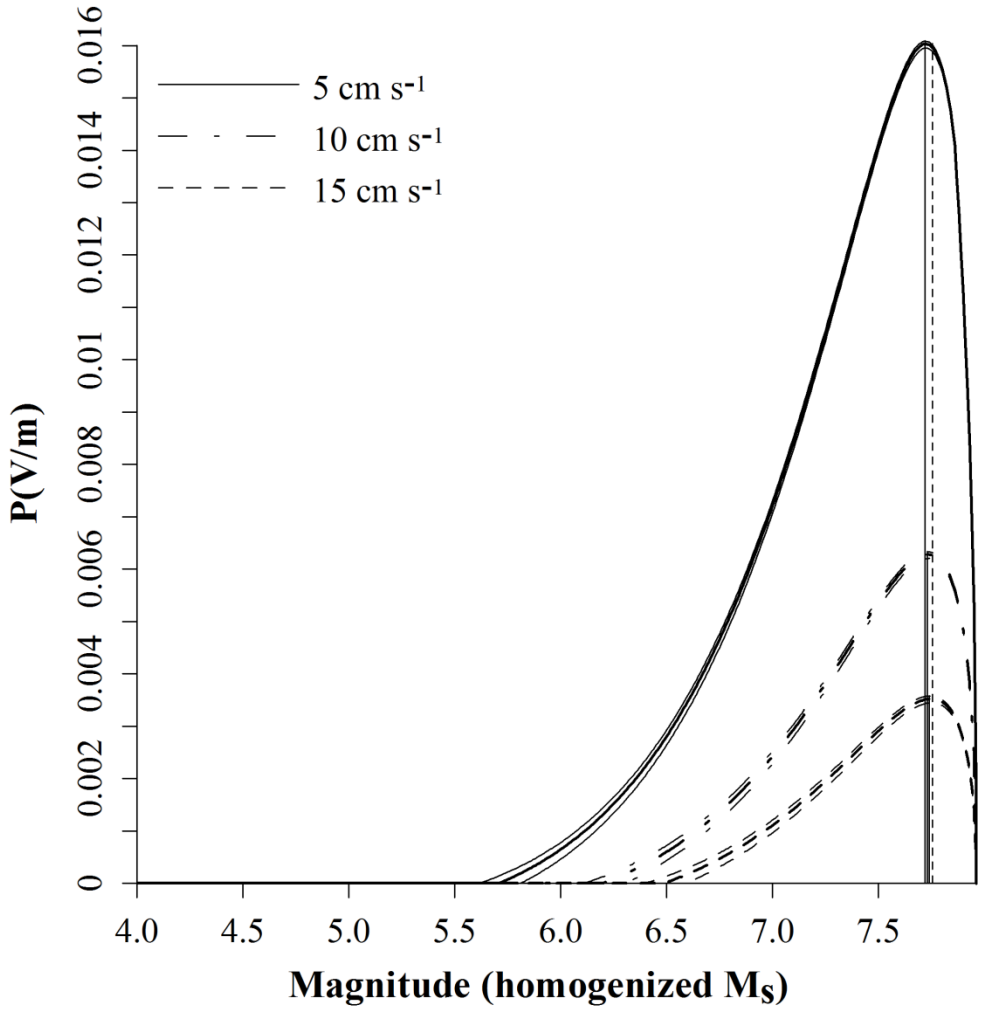

(a)

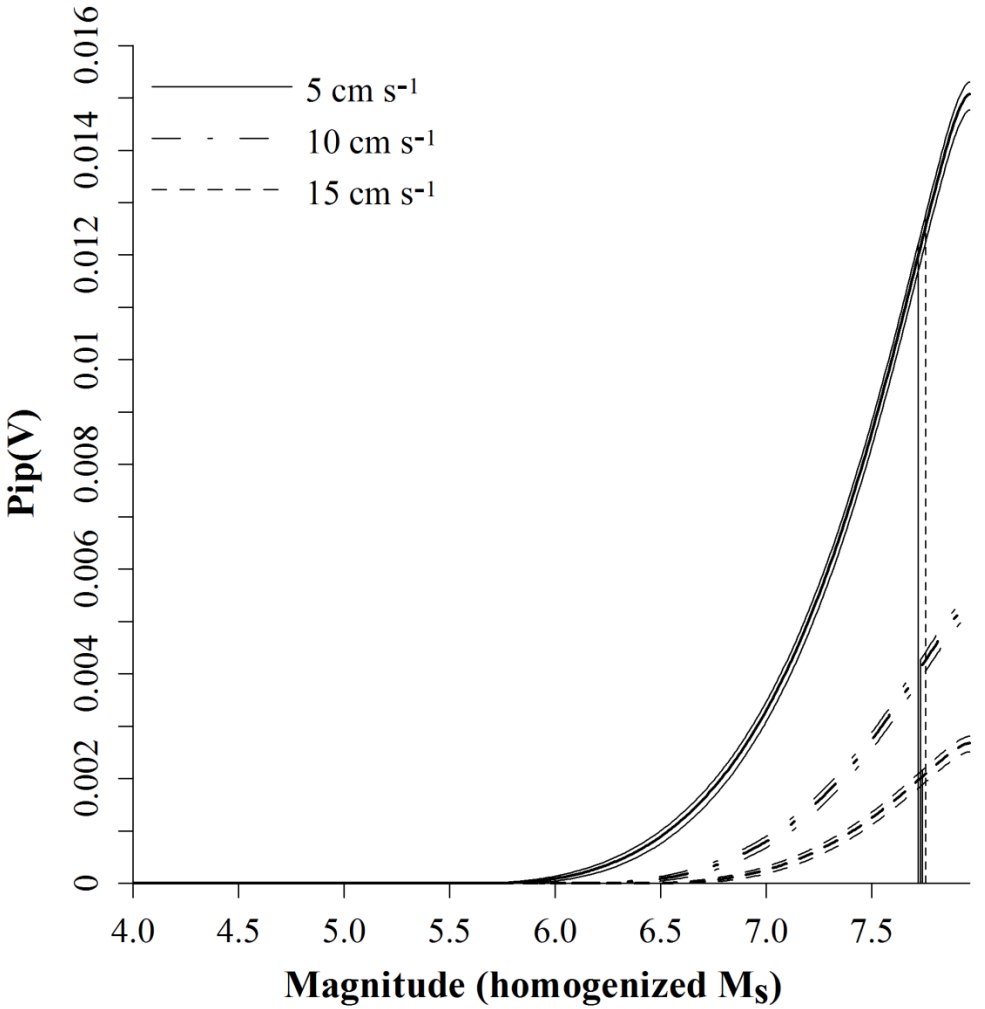

(b)

Ground velocity (a) perceptibility and (b) integrated perceptibility curves for Plovdiv

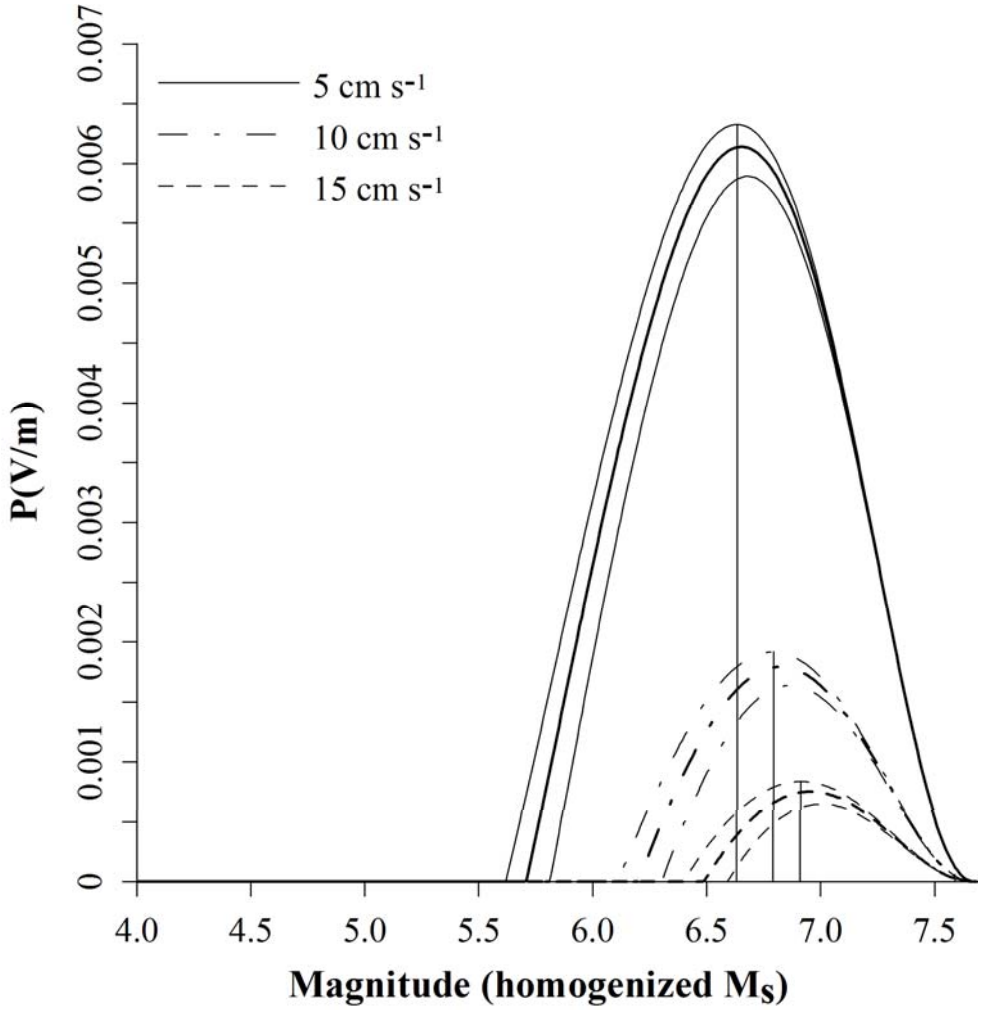

(a)

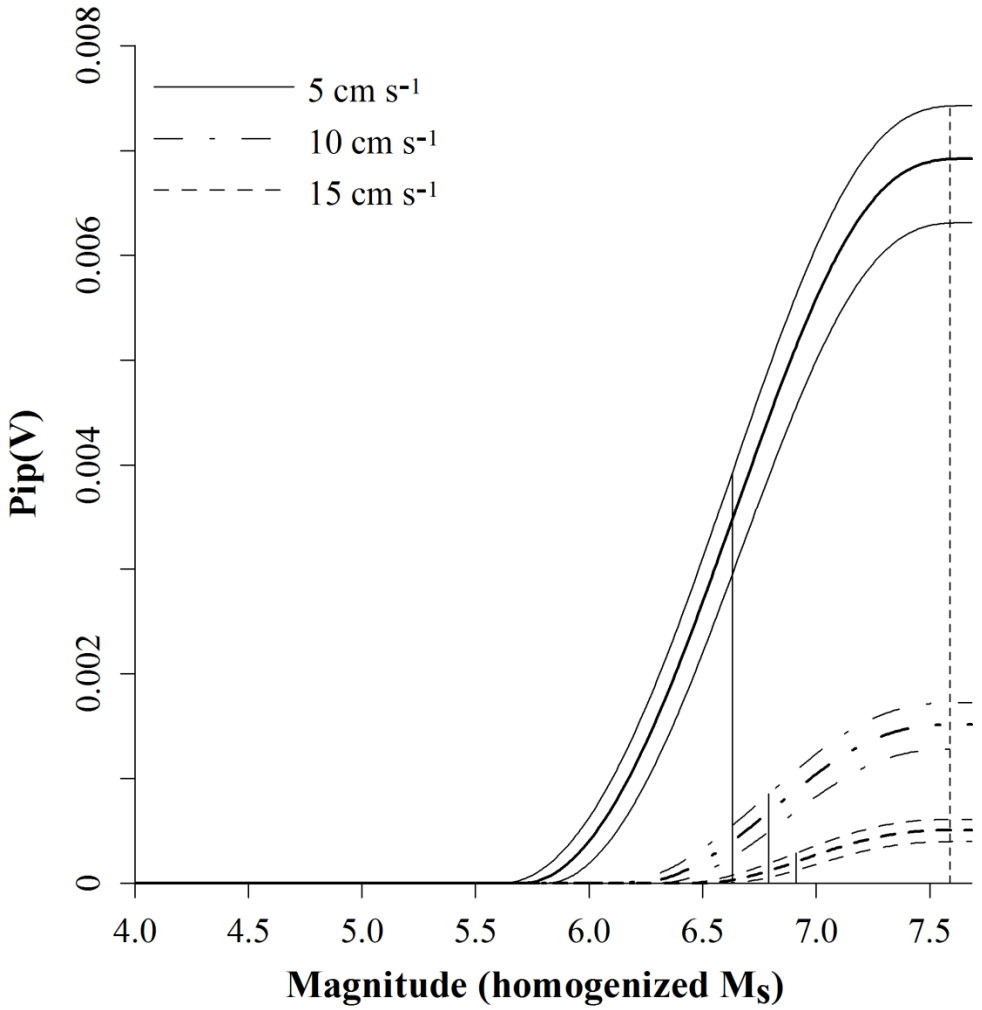

(b)

Ground velocity (a) perceptibility and (b) integrated perceptibility curves for Pristina

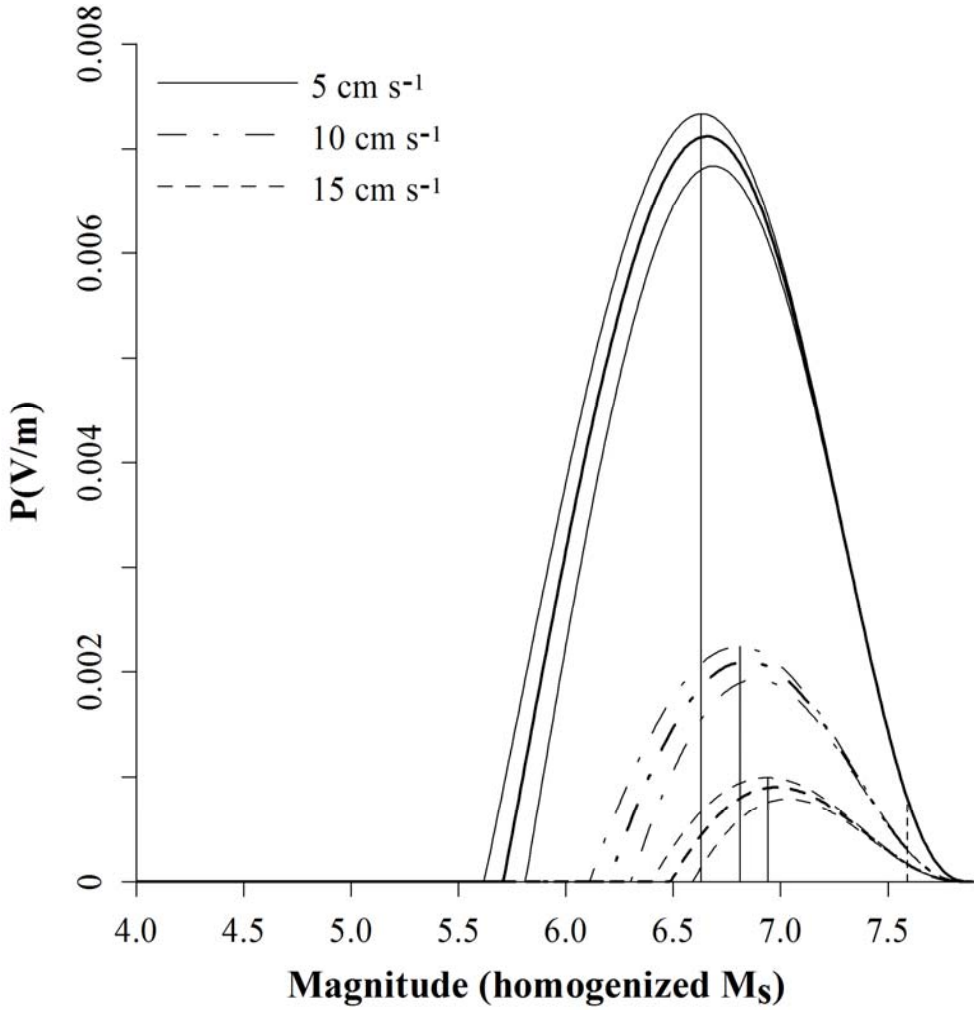

(a)

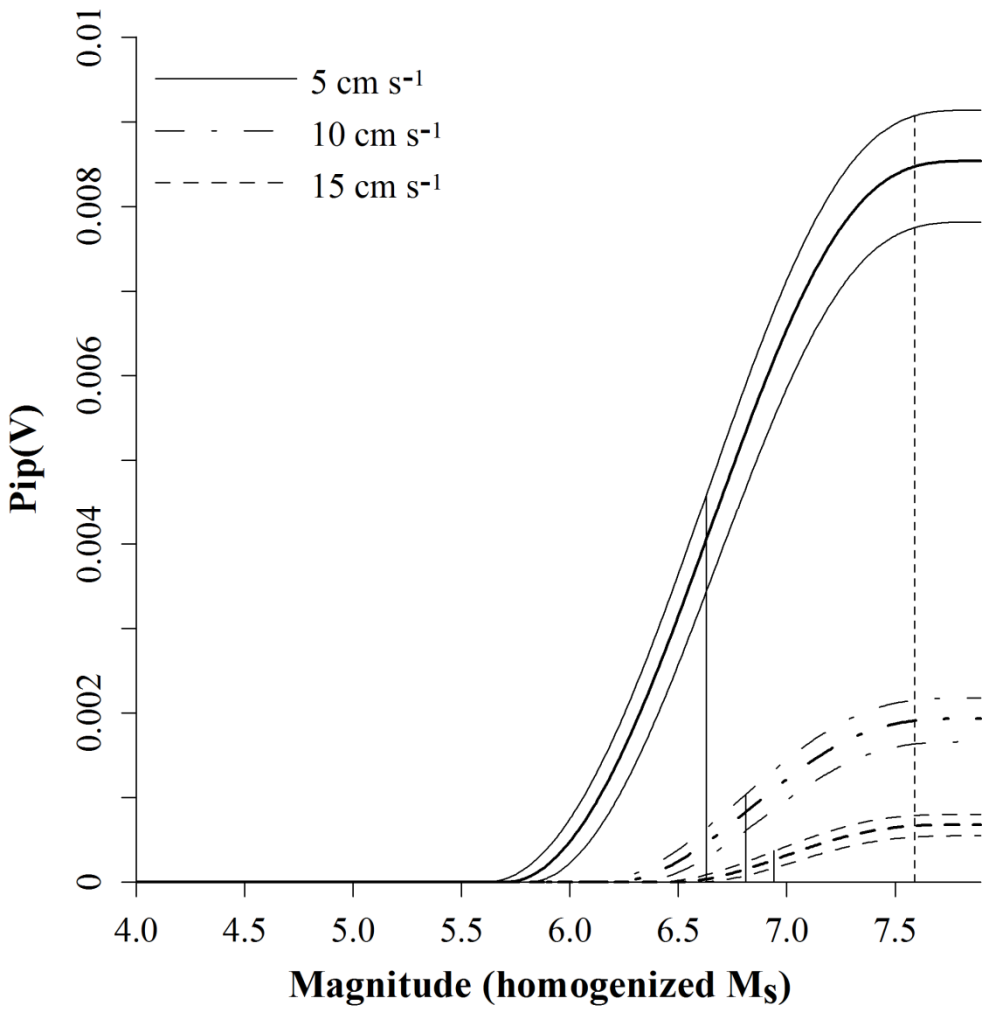

(b)

Ground velocity (a) perceptibility and (b) integrated perceptibility curves for Skopje

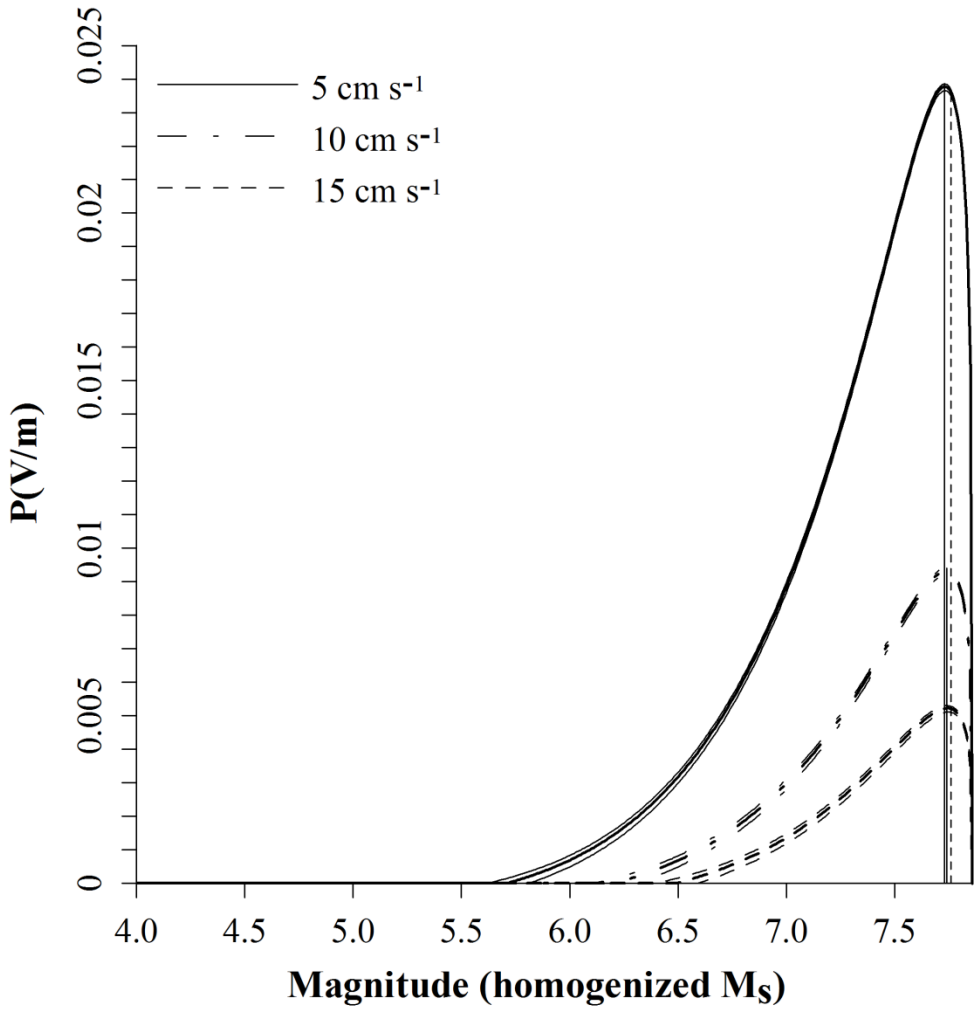

(a)

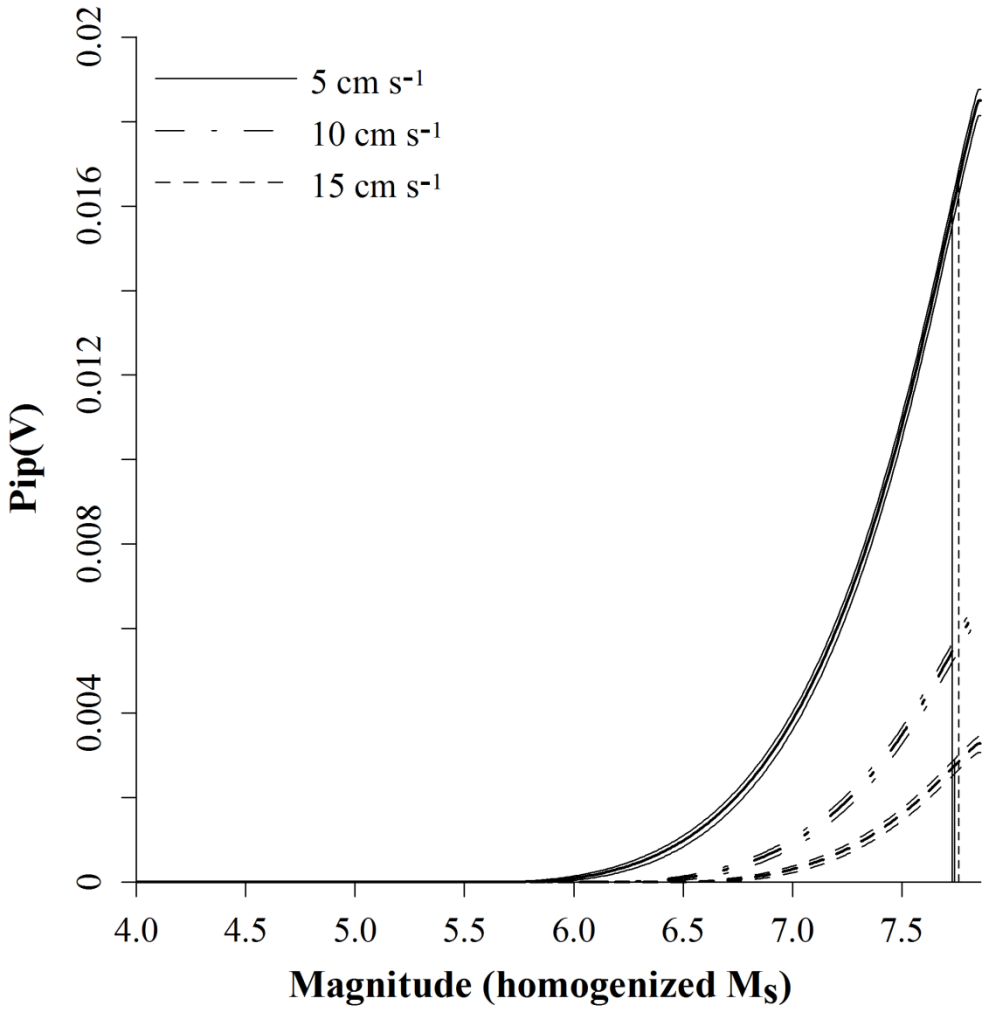

(b)

Ground velocity (a) perceptibility and (b) integrated perceptibility curves for Sofia

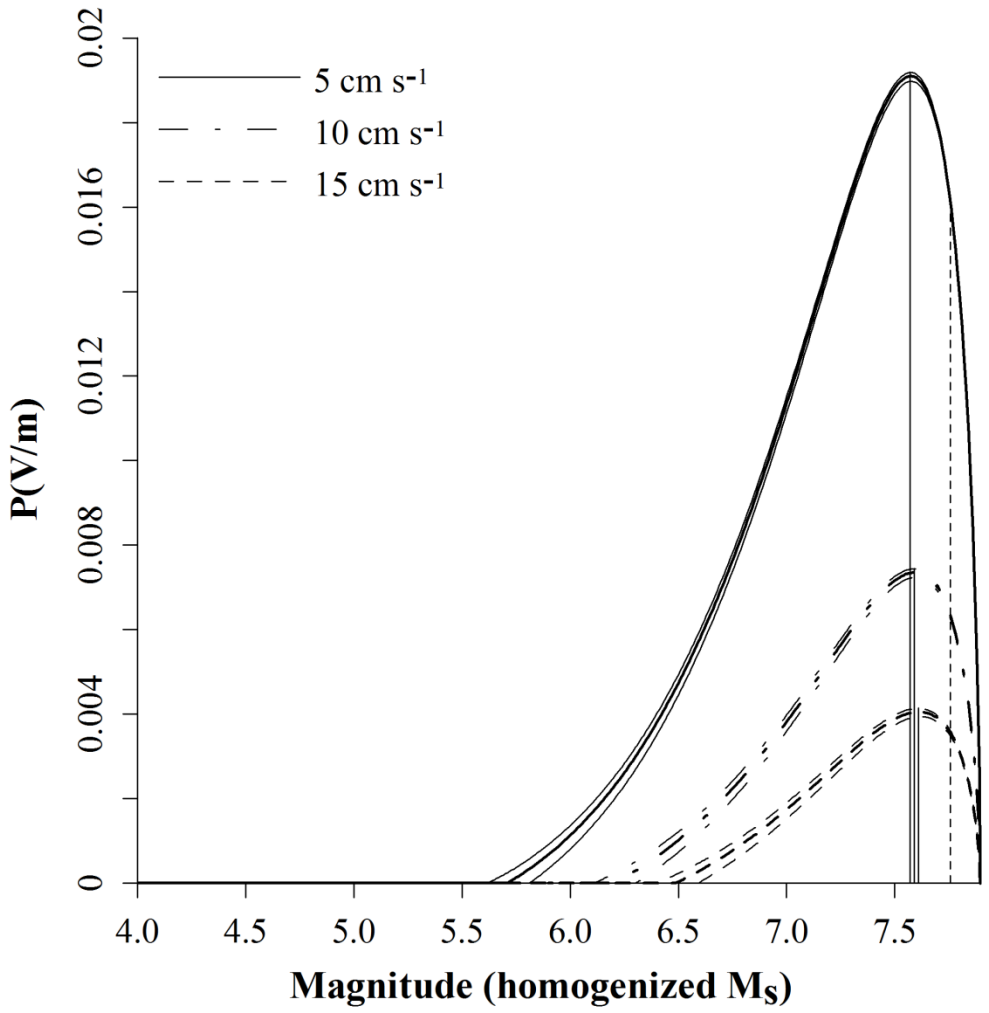

(a)

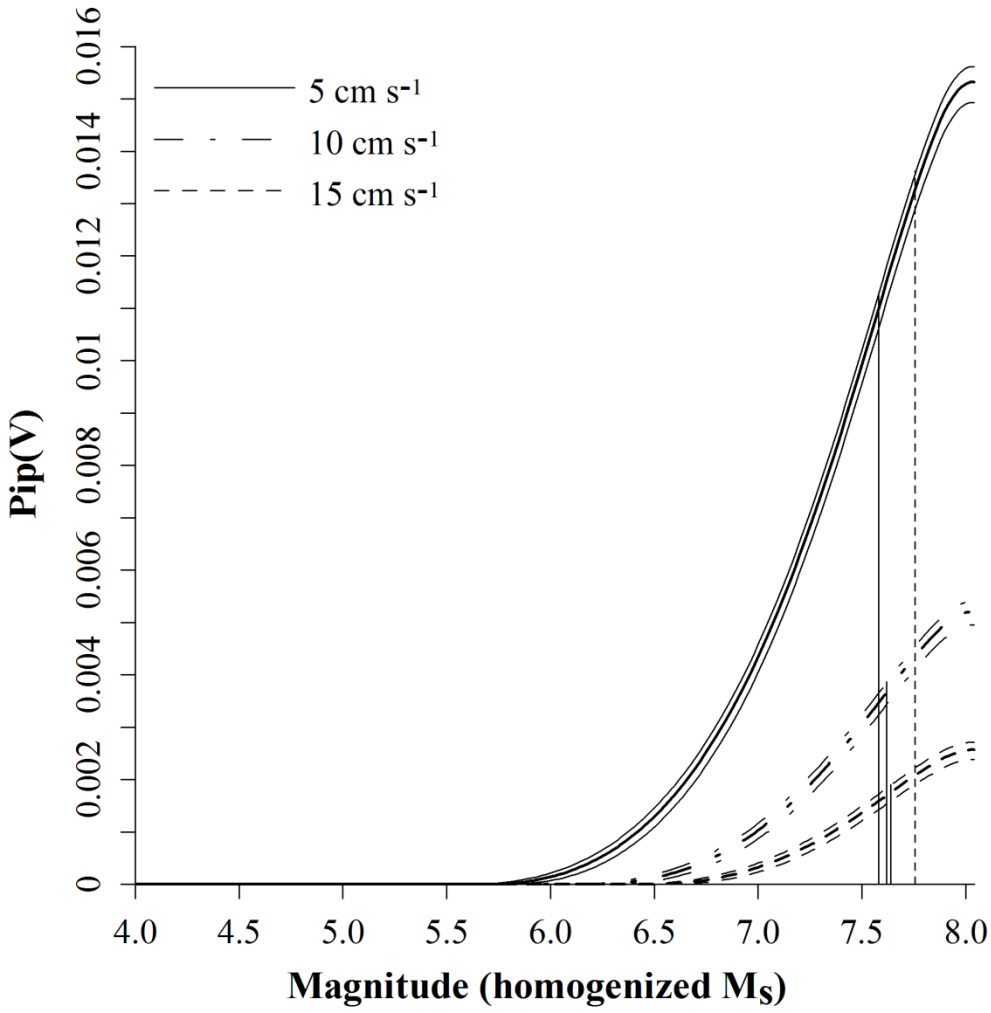

(b)

Ground velocity (a) perceptibility and (b) integrated perceptibility curves for Thessaloniki

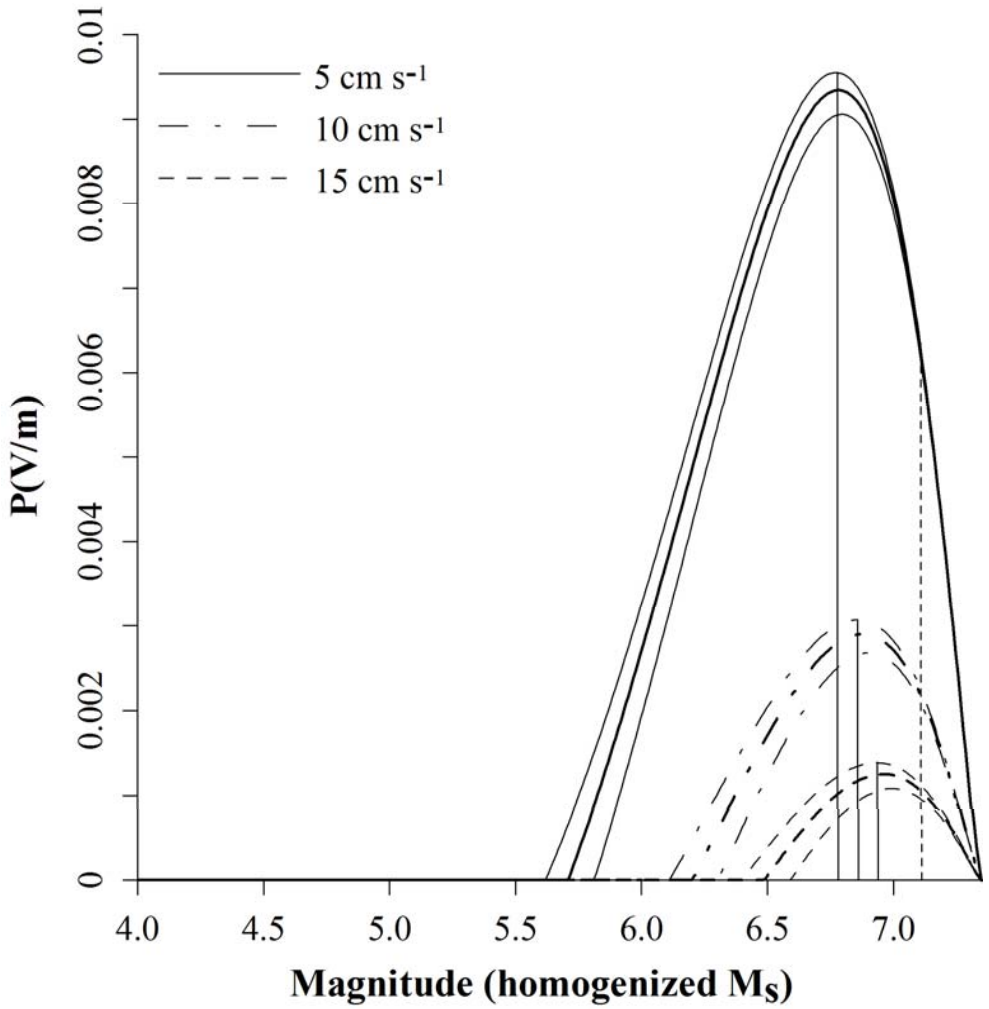

(a)

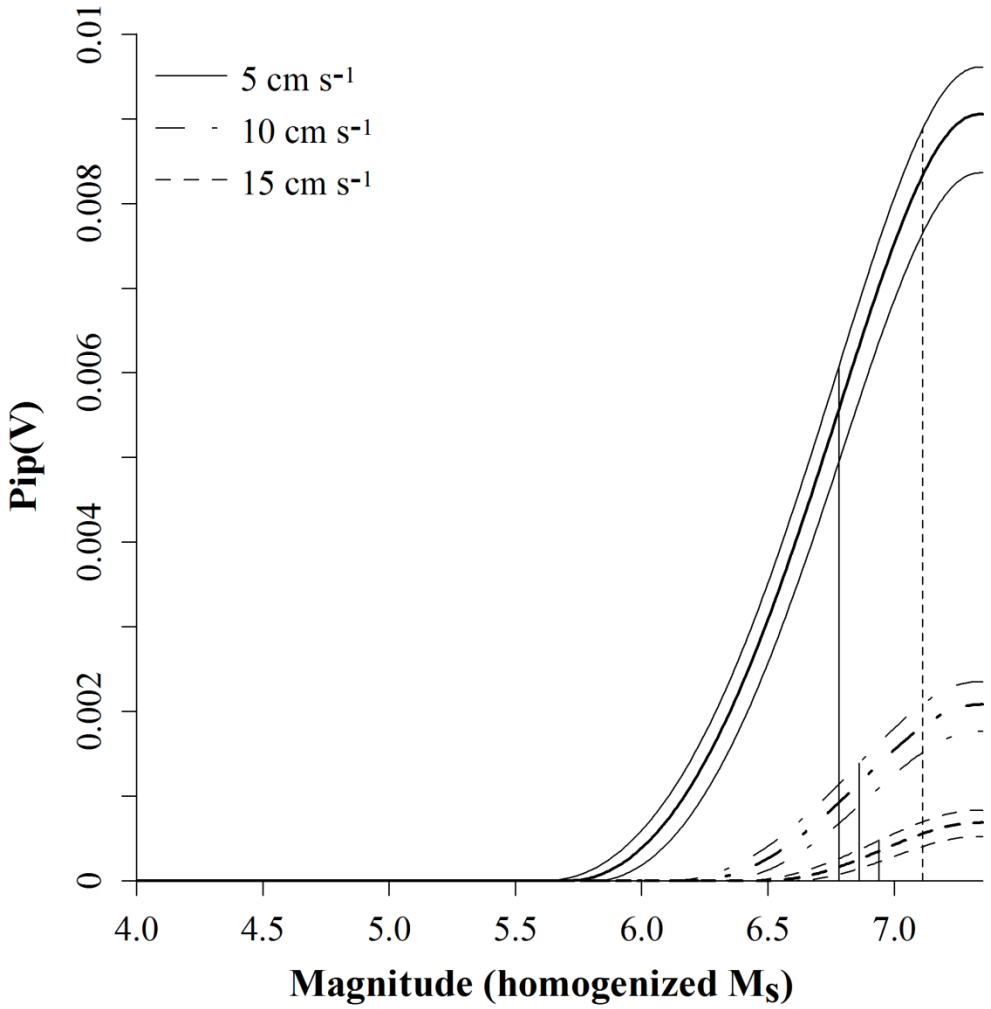

(b)

Ground velocity (a) perceptibility and (b) integrated perceptibility curves for Tirane

Appendix 23: $M_{P(max)}$ curves for ground velocity perceptibility

Most perceptible magnitude curves for ground velocity perceptibility for all urban centres for which seismic hazard is forecast using Papazachos (1992; $TP92_v$) for stiff soil conditions (S = 0.5) at the 50^{th} percentile (P = 0).

In each set of three curves on these graphs, the central bold line represents an earthquake at a nominal focal depth of 15 km (approximating to the mean seismogenic depth for historical seismicity above M_{CUT} for the broader region of 5.5 M_S; Figure 2.14). Thinner curves above and below each bold curve represent earthquakes at nominal focal depths of 10 km and 20 km respectively.

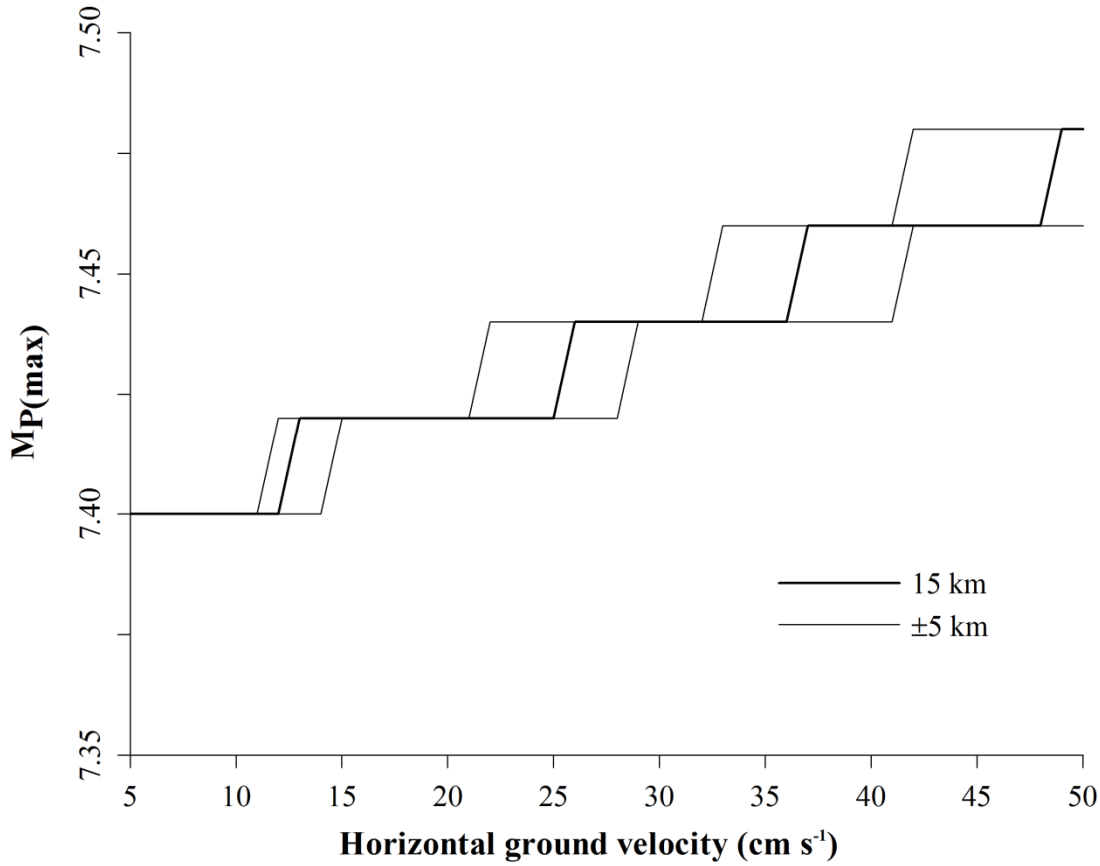

(a)

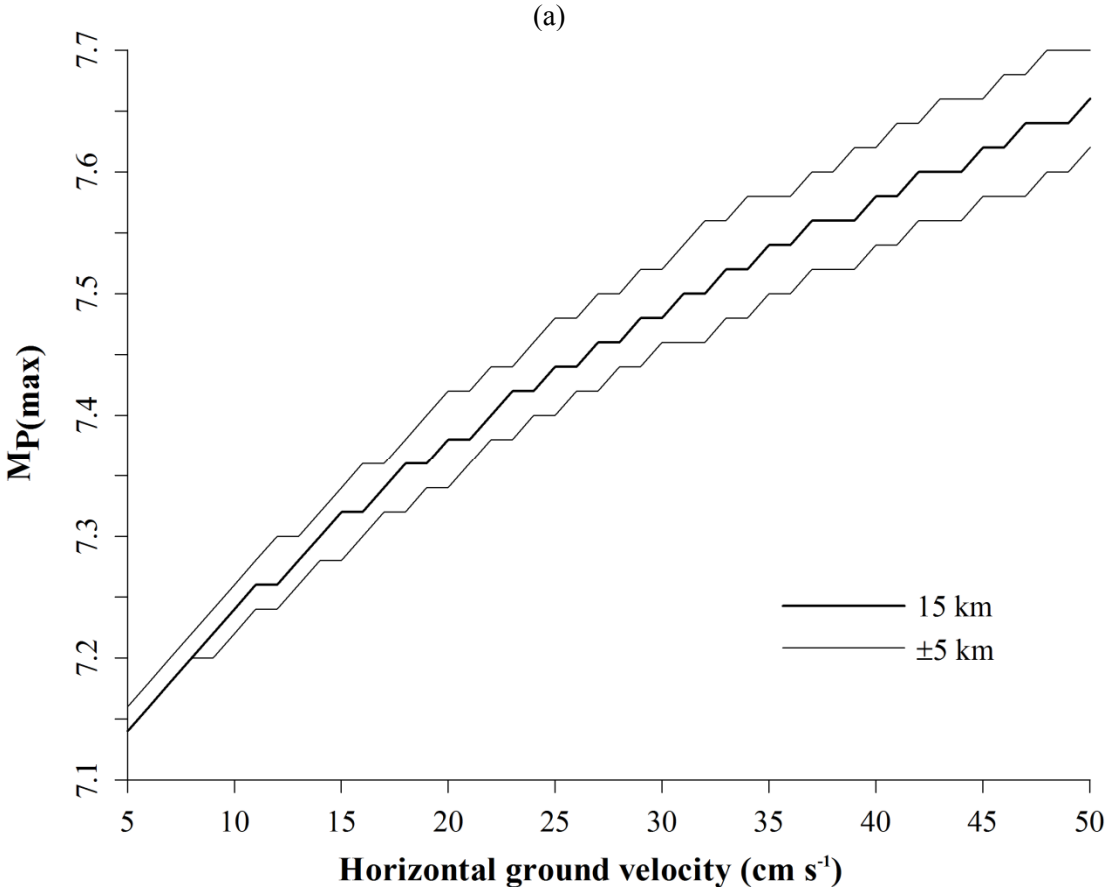

(b)

Most perceptible magnitudes for (a) Edirne and (b) Larissa

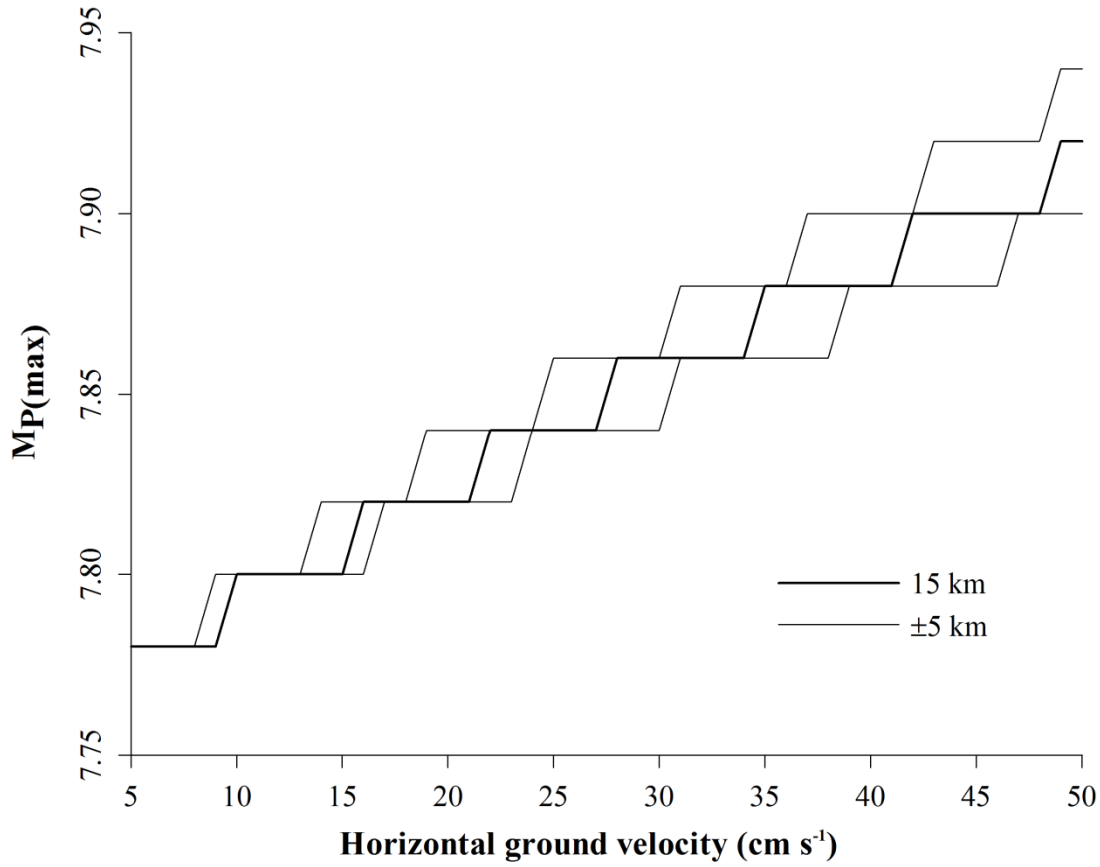

(a)

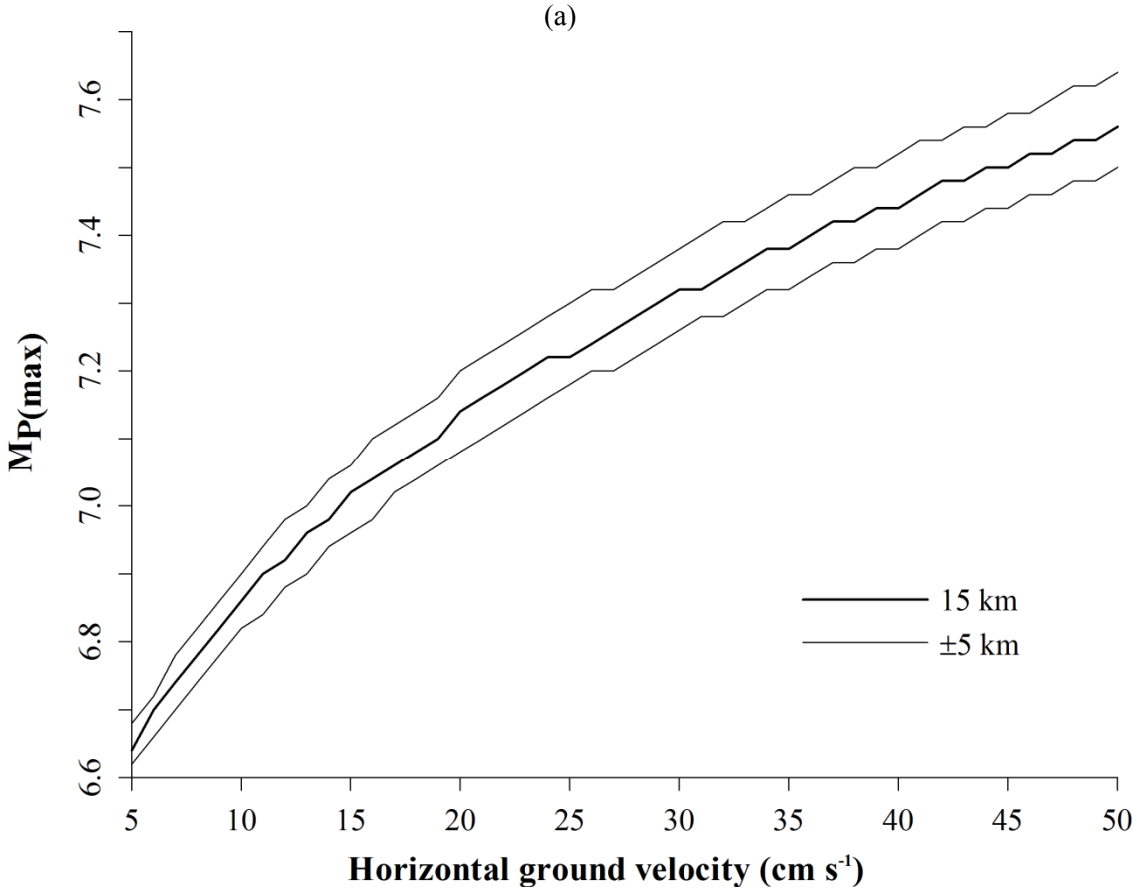

(b)

Most perceptible magnitudes for (a) Plovdiv and (b) Pristina

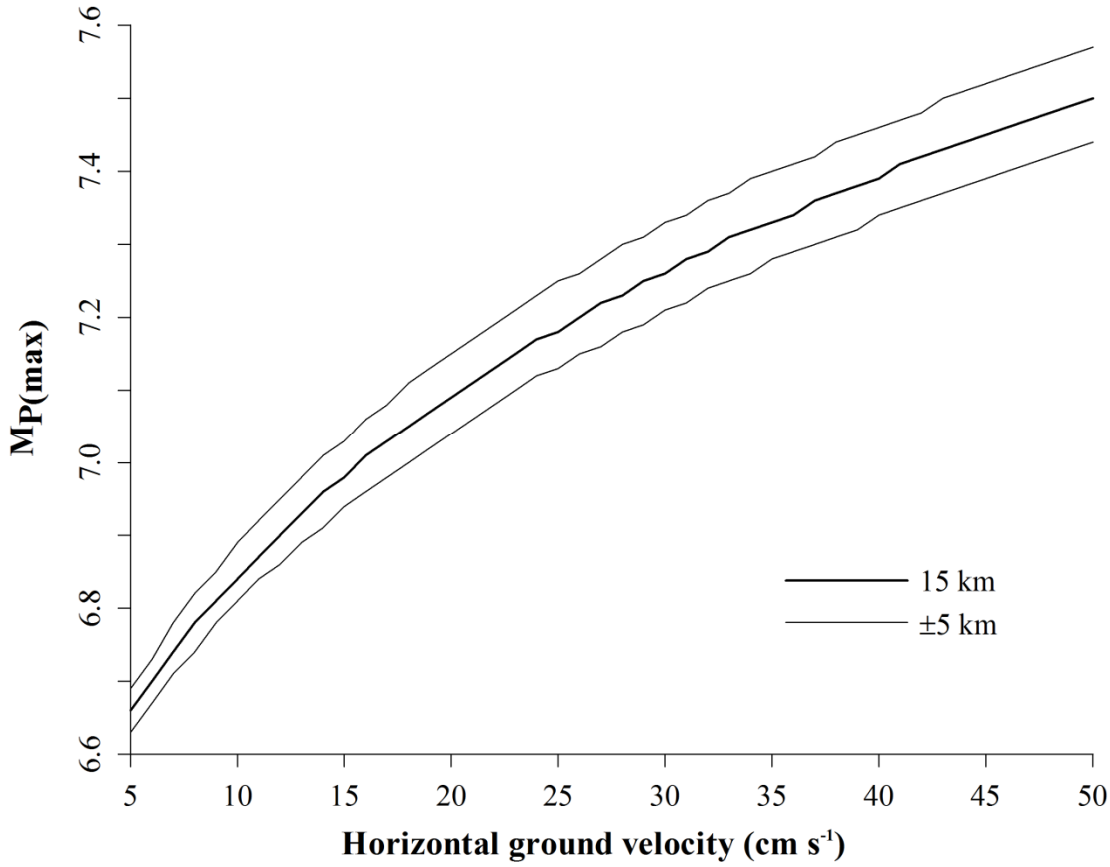

(a)

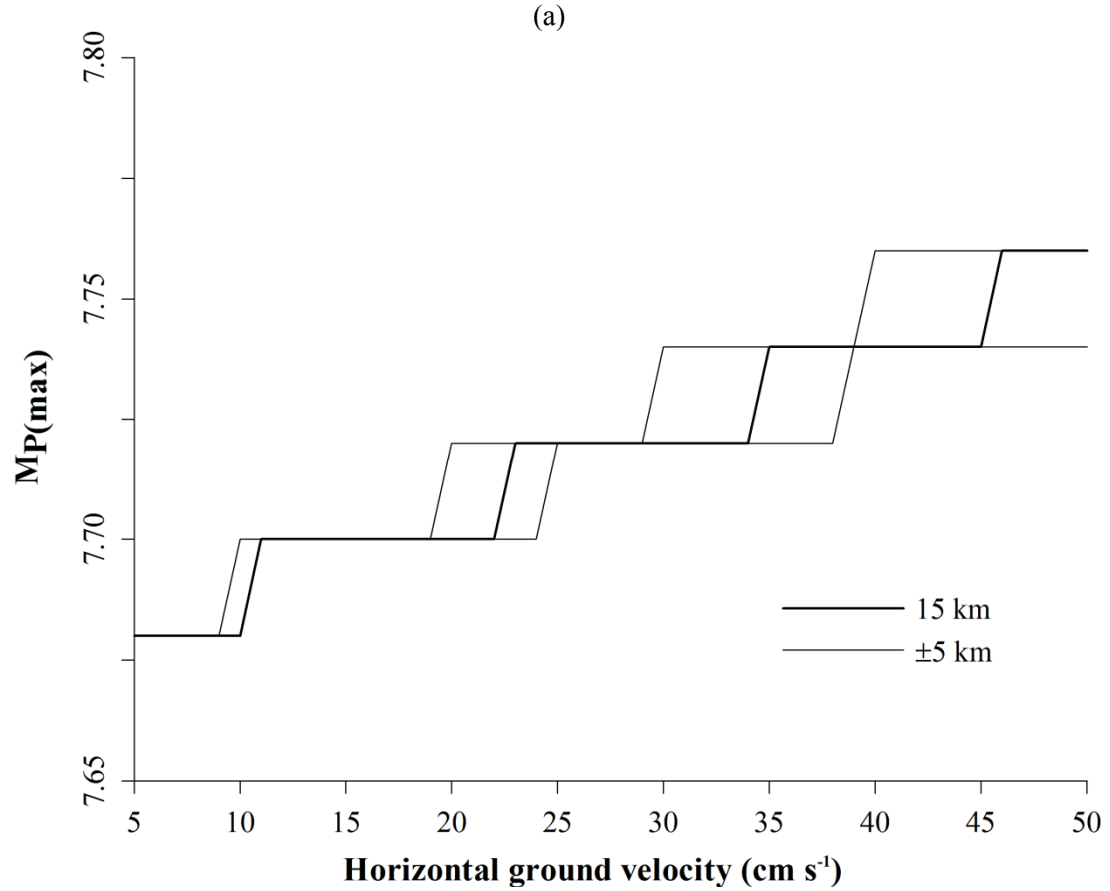

(b)

Most perceptible magnitudes for (a) Skopje and (b) Sofia

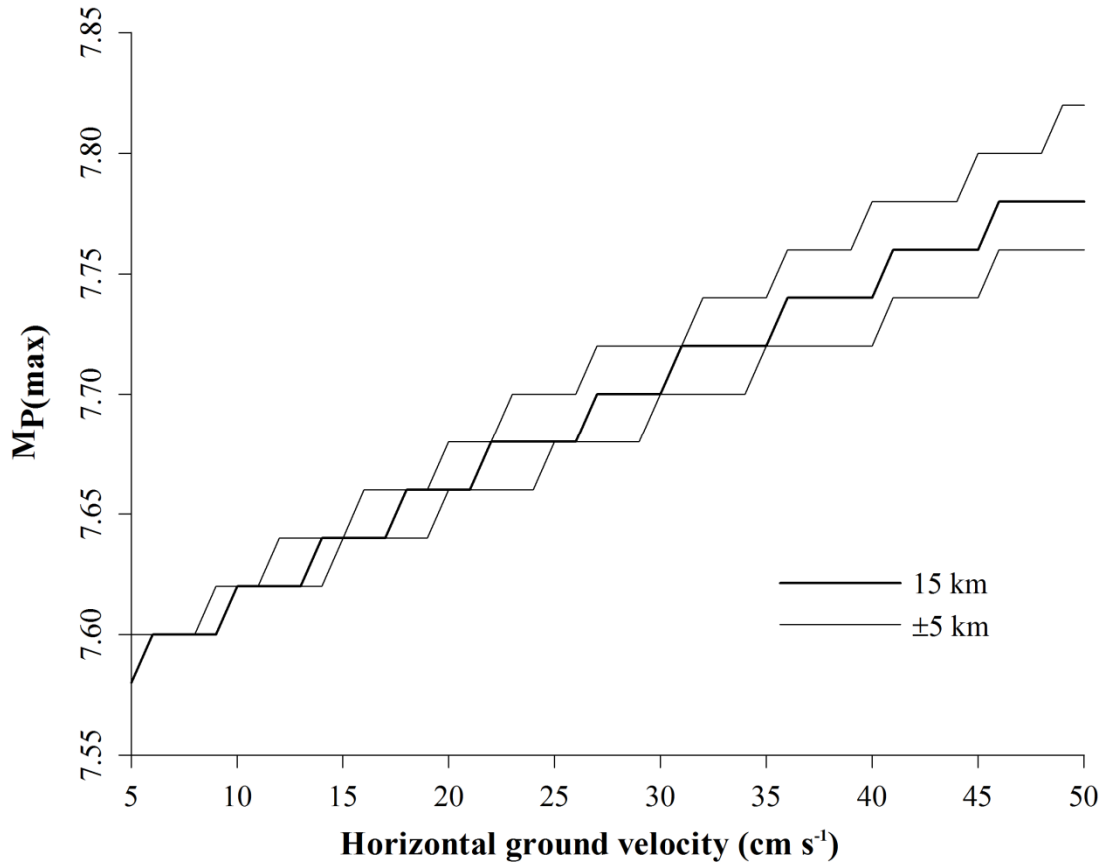

(a)

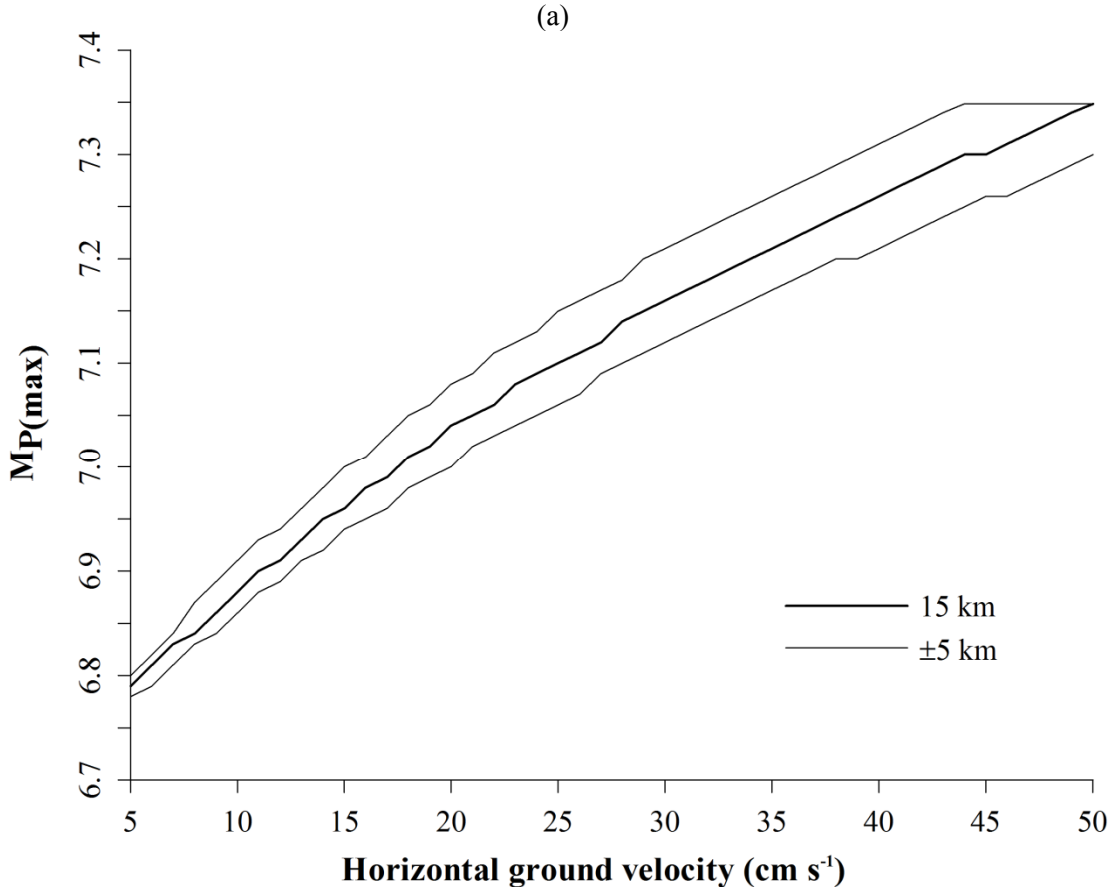

(b)

Most perceptible magnitudes for (a) Thessaloniki and (b) Tirane

Appendix 24: Site-specific horizontal ground velocity hazard curves

Horizontal ground velocity hazard curves for the urban centres for which seismic hazard is forecast using Papazachos (1992; $TP92_v$) for stiff soil conditions (S = 0.5) at the 50^{th} percentile (P = 0).

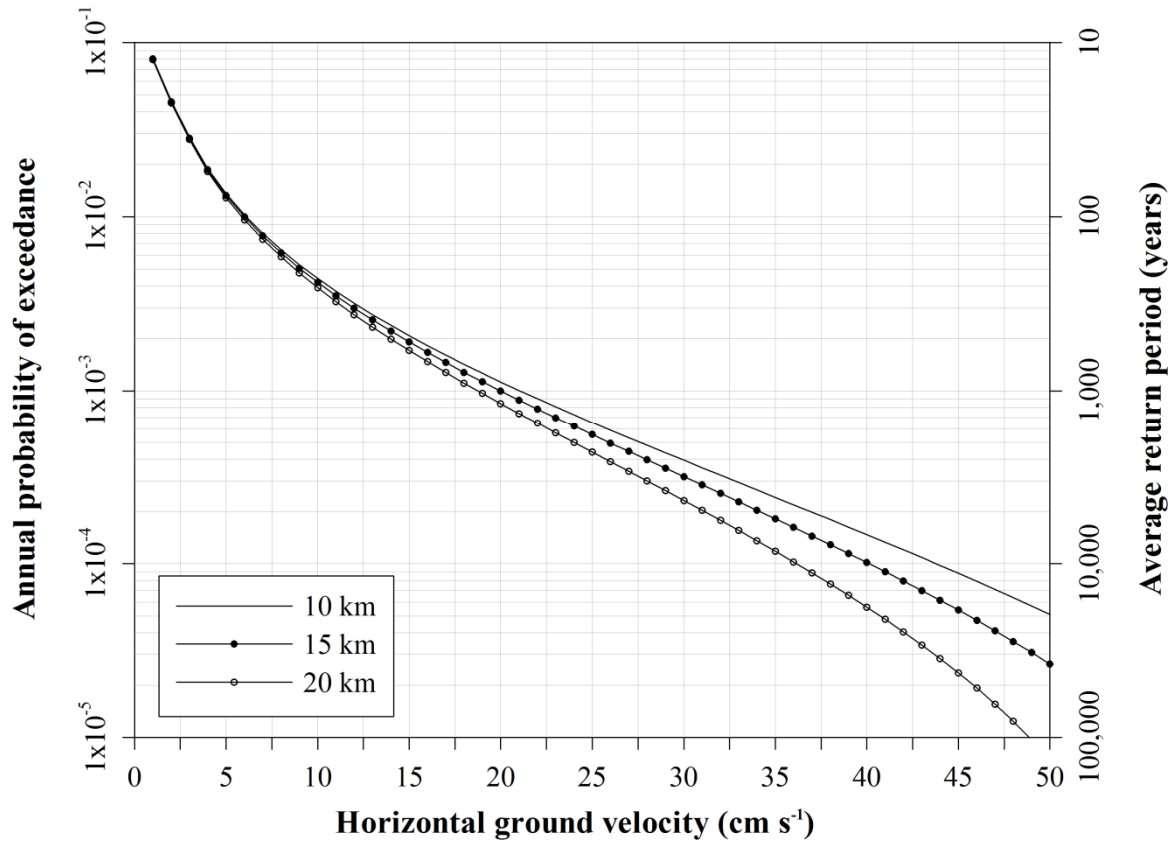

(a)

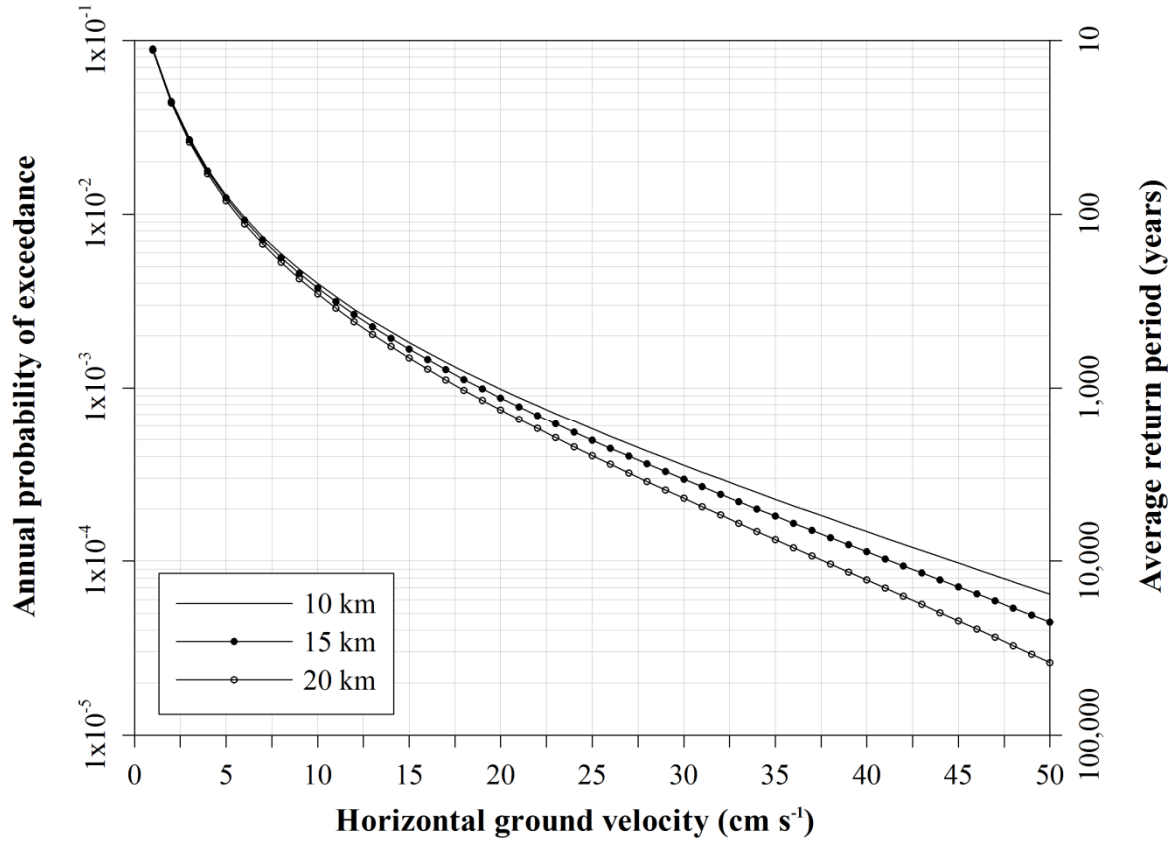

(b)

Ground velocity hazard curves for (a) Edirne and (b) Larissa

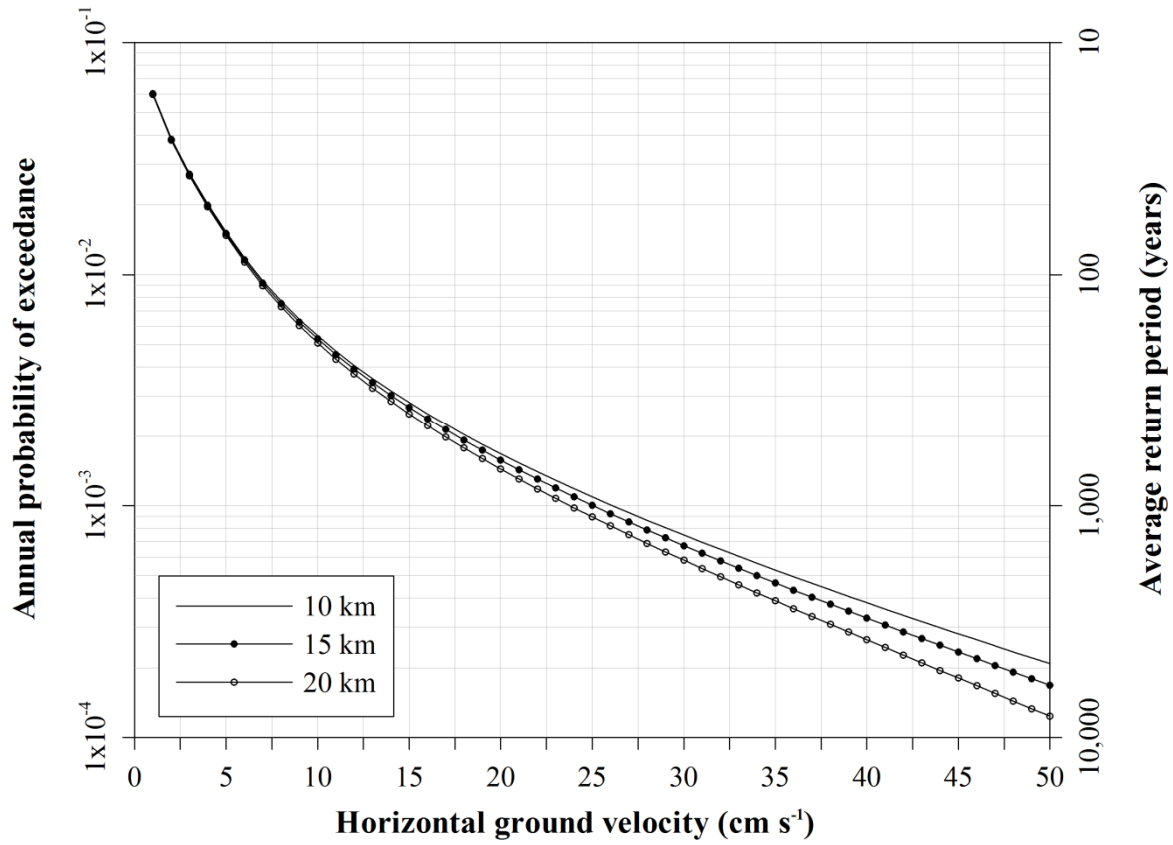

(a)

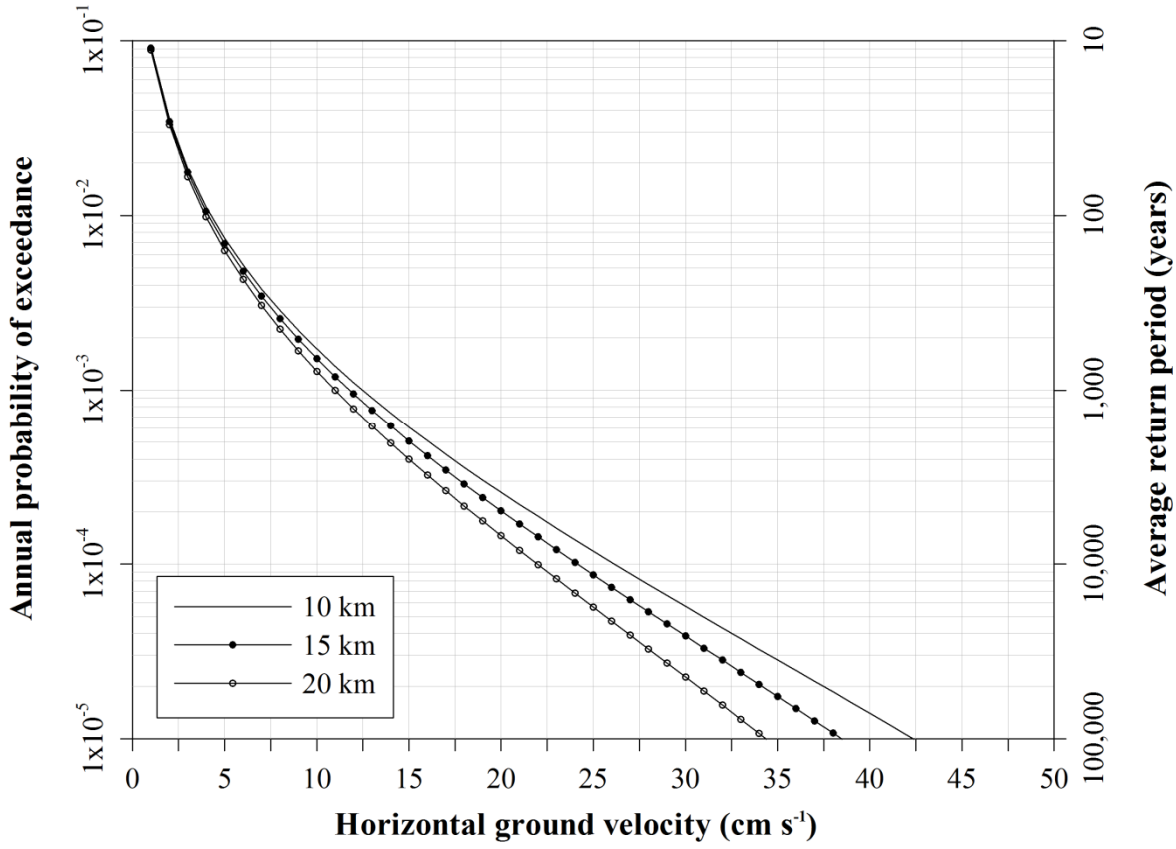

(b)

Ground velocity hazard curves for (a) Plovdiv and (b) Pristina

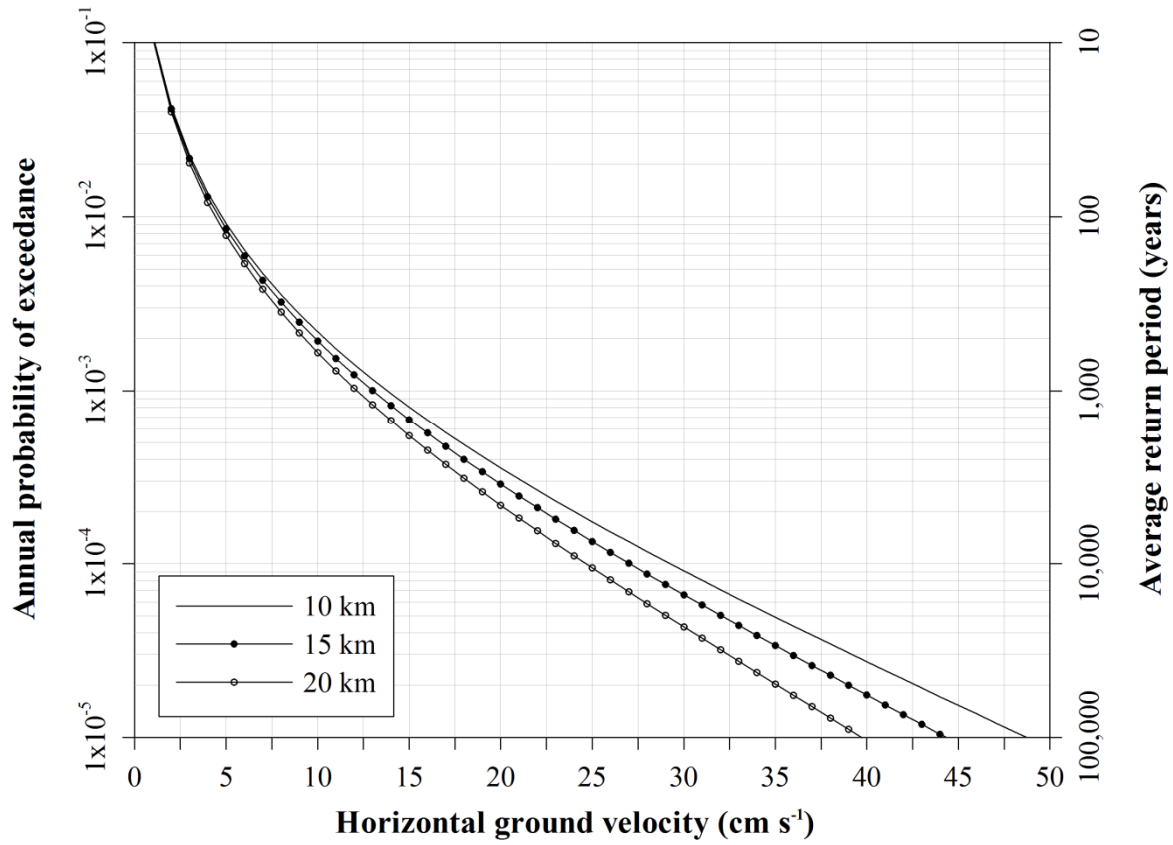

(a)

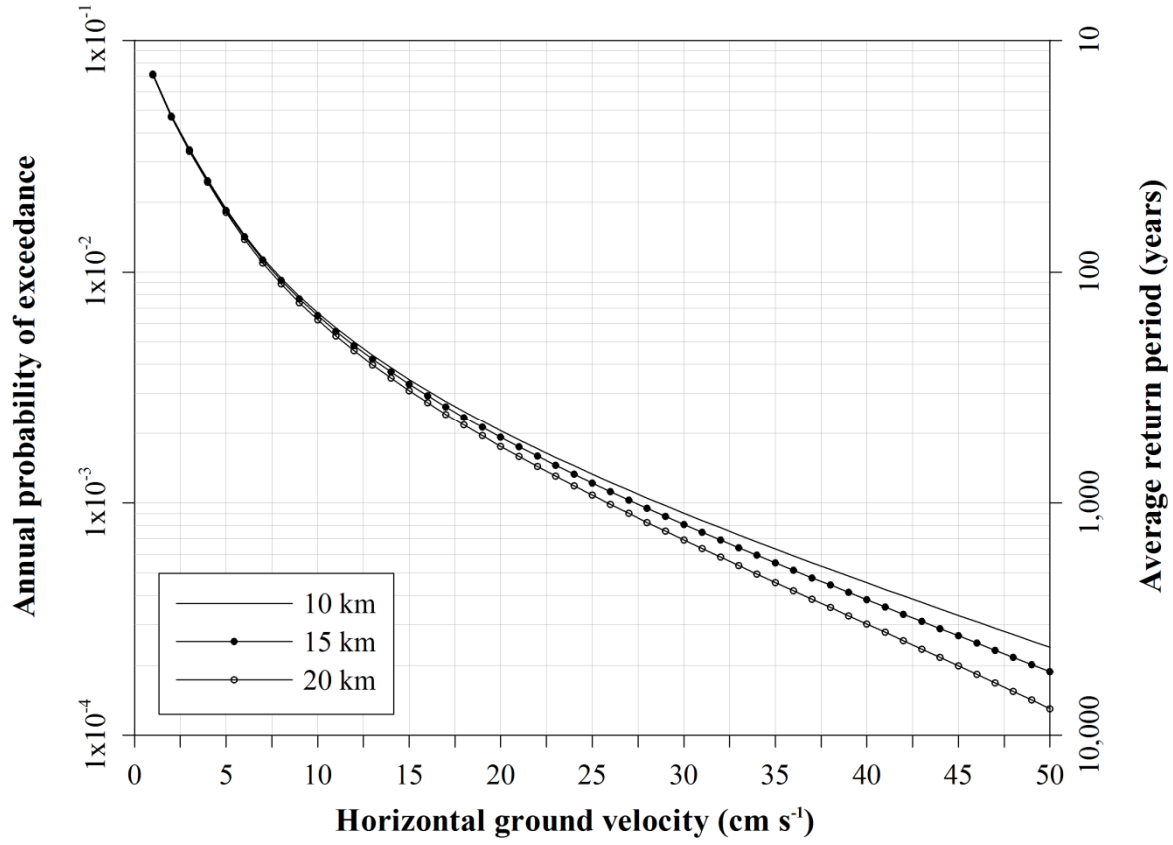

(b)

Ground velocity hazard curves for (a) Skopje and (b) Sofia

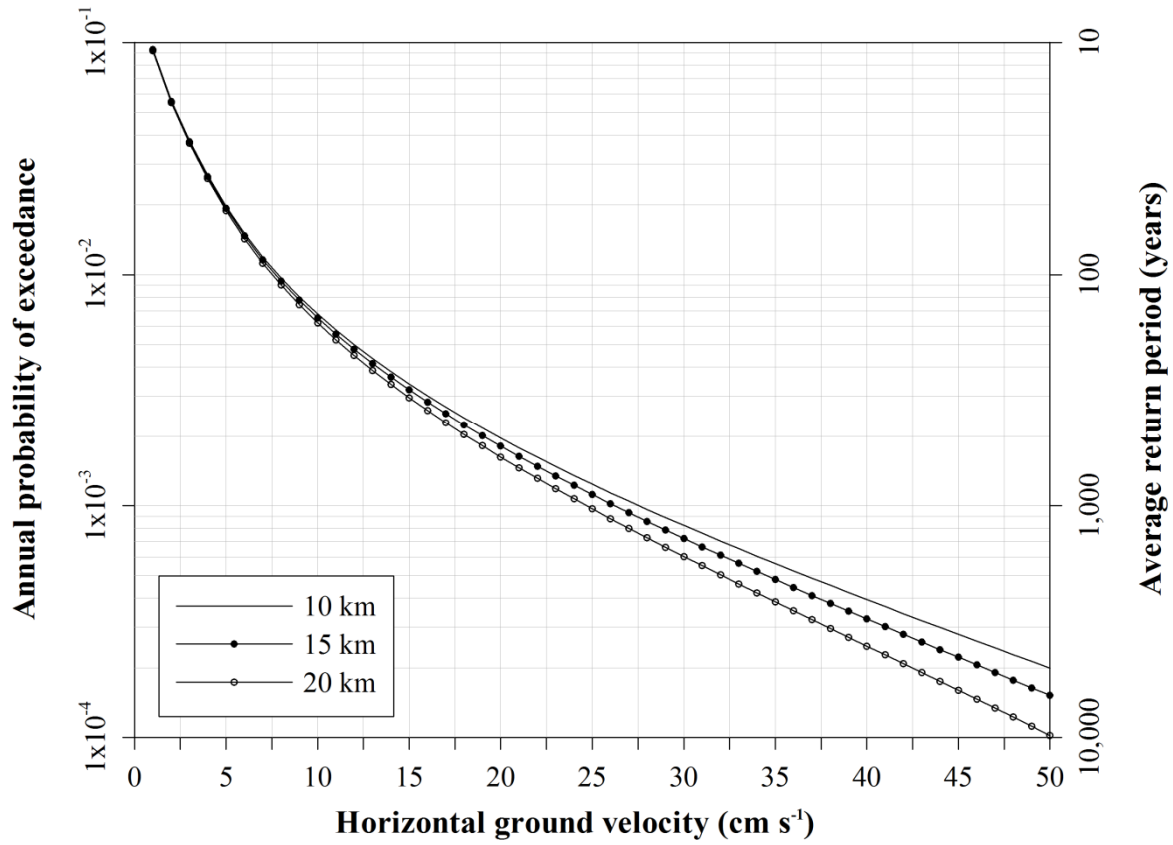

(a)

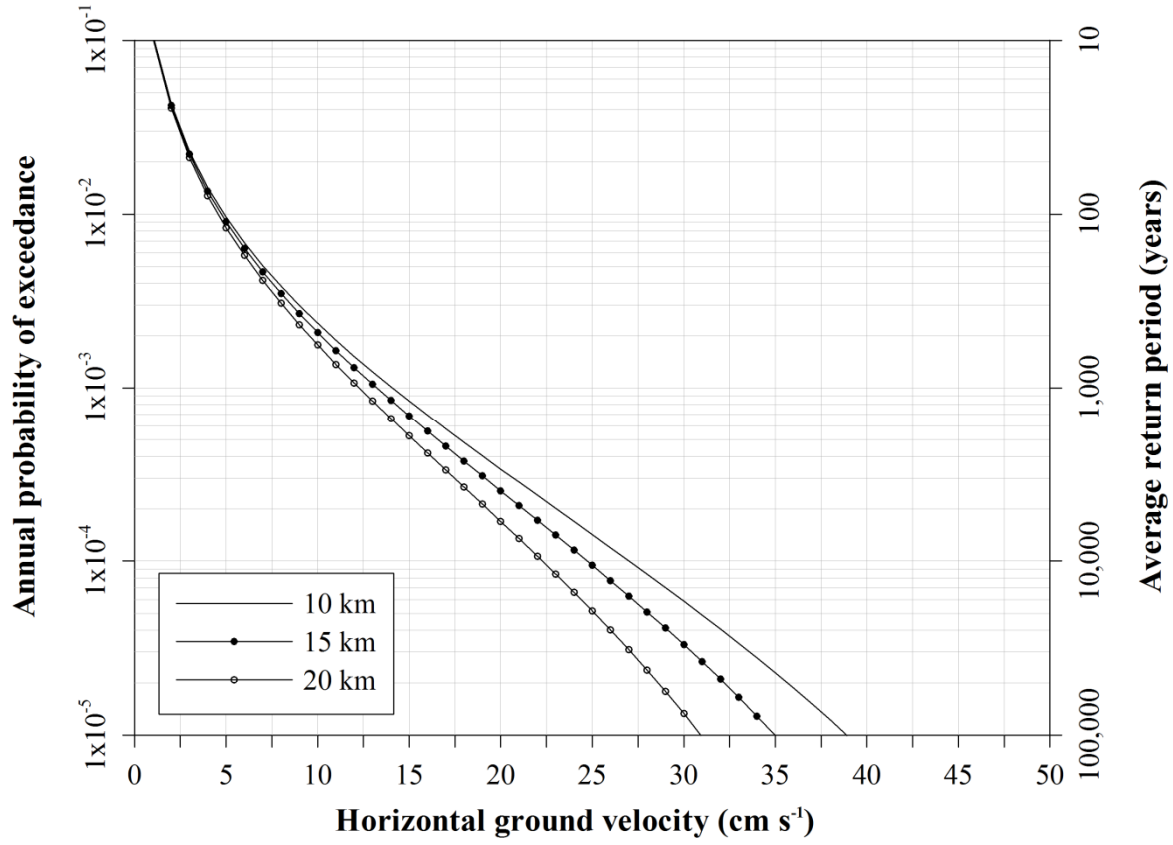

(b)

Ground velocity hazard curves for (a) Thessaloniki and (b) Tirane

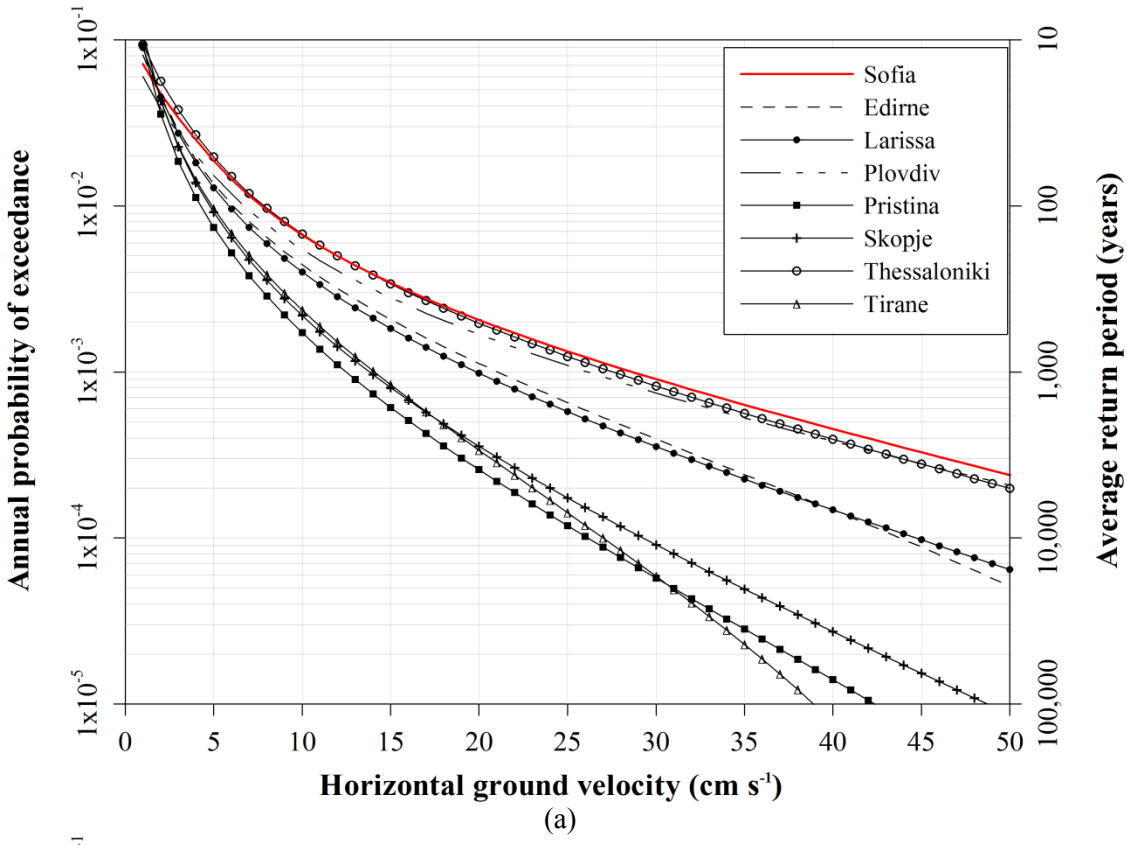

(a)

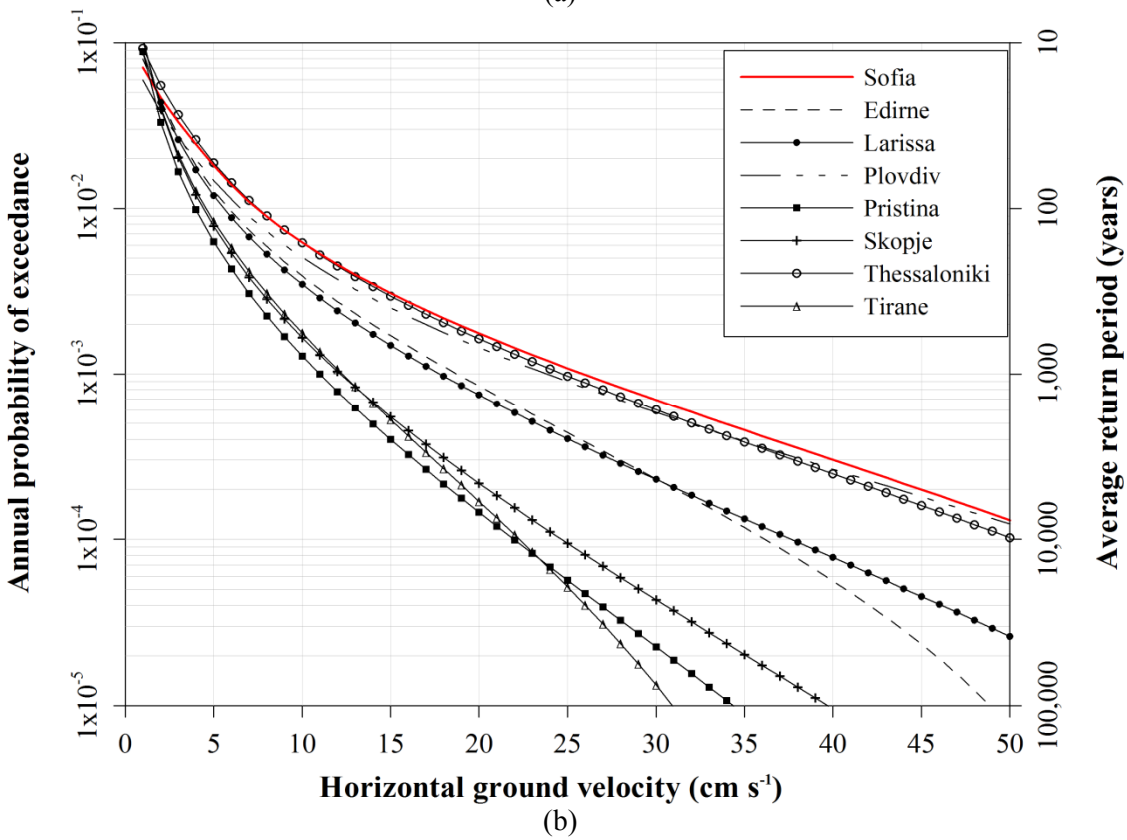

(b)

Ground velocity hazard curves for urban centres considered using Theodulidis and Papazachos (1992; $TP92_V$) for stiff soil conditions (S = 0.5) at the 50th percentile (P = 0) for a nominal earthquake with focal depth of (a) 10 km and (b) 20 km. In each case, Sofia is highlighted in red as the reference case

Appendix 25: Annual exceedance probabilities of site-specific PGV

Site-specific probabilities for annual exceedance for horizontal peak ground velocity hazard and in *T*-years for the urban centres for which seismic hazard is forecast using Theodulidis and Papazachos (1992; $TP92_V$) for stiff soil conditions (S = 0.5) at the 50^{th} percentile (P = 0).

City	Focal Depth (km)	Annual probability of exceedance ($\times 10^{-3}$)							
		V_{25}	V_{50}	V_{100}	V_{200}	V_{P25}	V_{P50}	V_{P100}	V_{P200}
Edirne	10	7.2	5.1	3.7	2.9	2.7	2.1	1.7	1.4
	15	6.9	4.9	3.5	2.7	2.5	1.9	1.5	1.2
	20	6.6	4.6	3.3	2.4	2.2	1.7	1.3	1.0
Larissa	10	8.2	5.9	4.6	3.5	3.3	2.7	2.2	1.8
	15	7.9	5.6	4.3	3.3	3.1	2.5	2.0	1.6
	20	7.5	5.3	4.0	3.0	2.9	2.2	1.8	1.5
Plovdiv	10	0.5	0.2	---	---	---	---	---	---
	15	0.4	0.2	---	---	---	---	---	---
	20	0.4	0.1	---	---	---	---	---	---
Pristina	10	11.8	8.0	5.8	4.4	4.2	3.2	2.6	2.0
	15	11.1	7.5	5.3	4.1	3.8	3.0	2.3	1.8
	20	10.3	6.9	4.8	3.6	3.4	2.5	2.0	1.5
Skopje	10	2.1	1.3	0.8	0.5	0.5	0.3	0.2	0.1
	15	1.9	1.1	0.7	0.4	0.4	0.3	0.2	0.1
	20	1.6	0.9	0.5	0.3	0.3	0.2	0.1	0.1
Thessaloniki	10	2.3	1.5	1.0	0.7	0.7	0.5	0.4	0.3
	15	2.1	1.4	0.9	0.6	0.6	0.4	0.3	0.2
	20	1.9	1.2	0.8	0.5	0.5	0.3	0.2	0.1
Tirane	10	1.3	0.9	0.6	0.4	0.4	0.3	0.2	0.1
	15	1.2	0.8	0.5	0.3	0.3	0.2	0.1	0.1
	20	0.9	0.6	0.4	0.2	0.2	0.1	0.1	<0.1

Annual probabilities ($\times 10^{-3}$ per annum) of experiencing extreme velocity ground motions estimated for the region surrounding each urban centre using Theodulidis and Papazachos (1992) for stiff soil conditions at the 50th percentile. '---' is outside the range of the hazard curve

City	Focal Depth (km)	Time interval (*T*-year)					
		100	200	300	400	500	1,000
Edirne	10	6.1	6.5	7.0	7.6	8.4	21.0
	15	6.0	6.4	6.9	7.4	8.1	19.9
	20	5.8	6.2	6.7	7.2	7.9	18.7
Larissa	10	5.8	6.2	6.7	7.3	7.9	19.8
	15	5.7	6.1	6.5	7.1	7.7	18.8
	20	5.5	5.9	6.3	6.9	7.5	17.7
Plovdiv	10	6.7	7.2	7.8	8.5	9.4	26.1
	15	6.6	7.1	7.7	8.4	9.2	25.0
	20	6.5	7.0	7.5	8.2	9.0	23.7
Pristina	10	4.2	4.5	4.8	5.1	5.6	12.4
	15	4.1	4.4	4.6	5.0	5.4	11.7
	20	3.9	4.2	4.4	4.8	5.1	10.9
Skopje	10	5.2	5.5	5.8	6.2	6.7	14.9
	15	5.0	5.3	5.6	6.0	6.5	14.0
	20	4.7	5.0	5.4	5.7	6.2	13.0
Thessaloniki	10	7.8	8.4	9.0	9.8	10.7	27.5
	15	7.6	8.2	8.8	9.6	10.5	26.2
	20	7.4	8.0	8.6	9.3	10.1	24.6
Tirane	10	4.8	5.1	5.5	5.9	6.4	14.1
	15	4.7	5.0	5.3	5.7	6.2	13.2
	20	4.5	4.8	5.1	5.4	5.9	12.3

Peak ground velocities (in cm s^{-1}) expected within a *T*-year time interval for the region surrounding each urban centre using Theodulidis and Papazachos (1992) for stiff soil conditions at the 50^{th} percentile

Appendix 26: Site-specific intensity perceptibility/integrated perceptibility curves

Macroseismic intensity (a) perceptibility and (b) integrated perceptibility curves for the eight urban centres for which seismic hazard is forecast using Papazachos and Papaioannou (1997; PP97).

In each set of three curves on these graphs, the central bold line represents an earthquake at a nominal focal depth of 15 km (approximating to the mean seismogenic depth for historical seismicity above M_{CUT} for the broader region of 5.5 M_S; Figure 2.14). Thinner curves above and below each bold curve represent earthquakes at nominal focal depths of 10 km and 20 km respectively. Vertical black lines are at *the most perceptible magnitude,* $M_{P(max)}$, only for 10 km focal depth estimates. The vertical dashed line represents M_3 from cumulative strain energy release techniques (chapter 6 and Appendix 17).

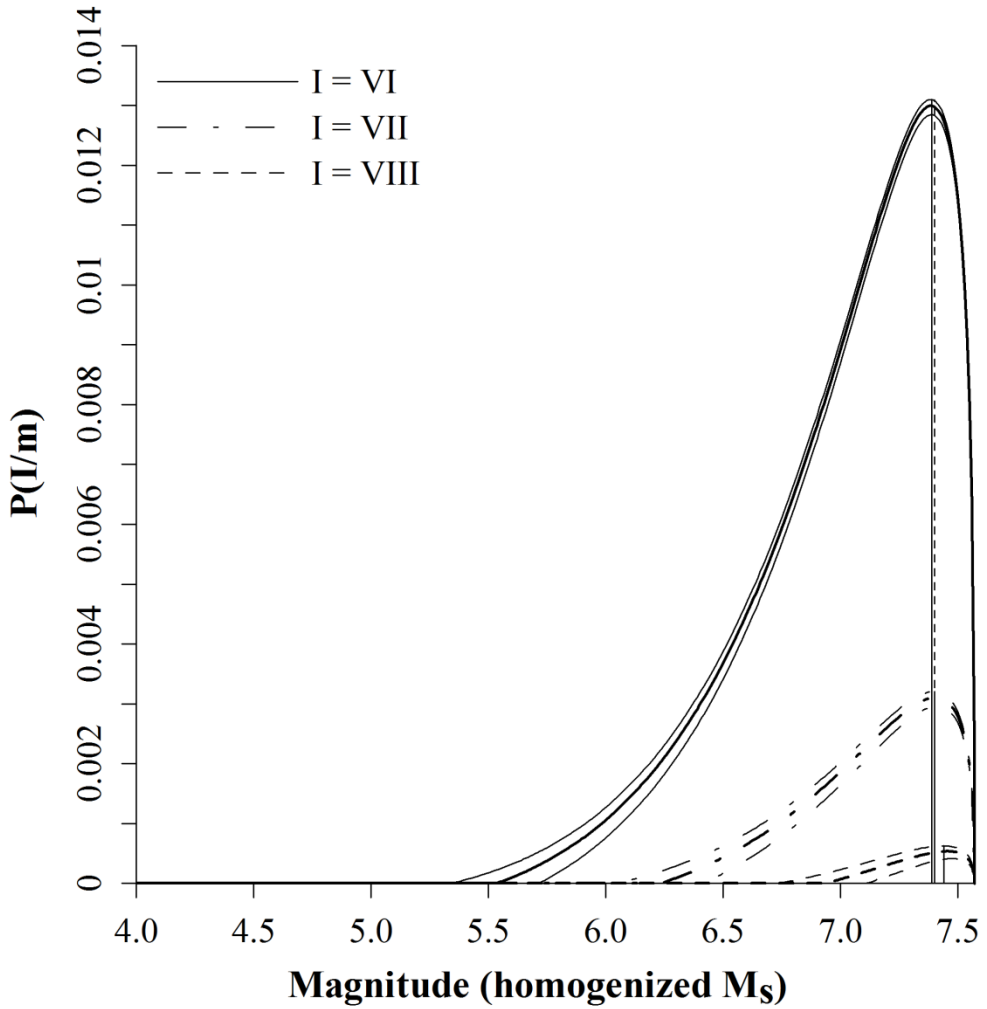

(a)

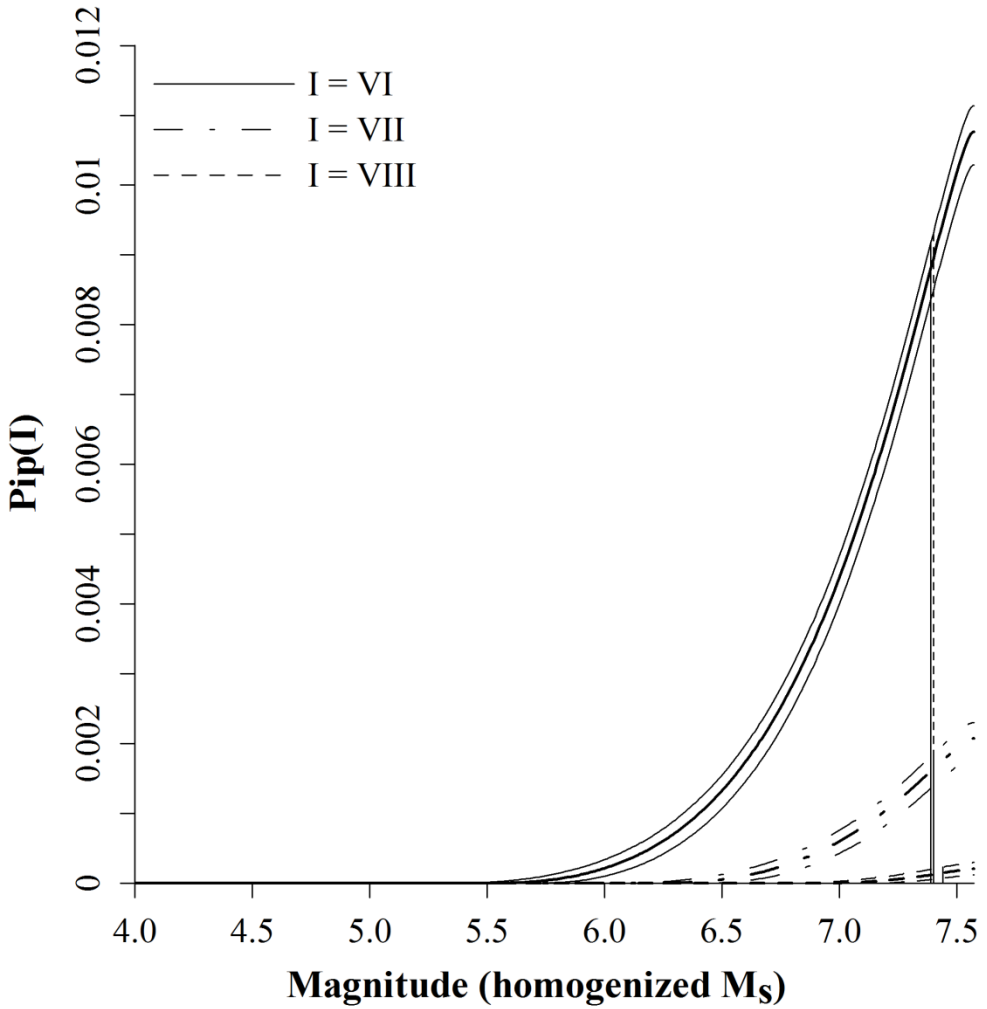

(b)

Macroseismic intensity (a) perceptibility and (b) integrated perceptibility curves for Edirne

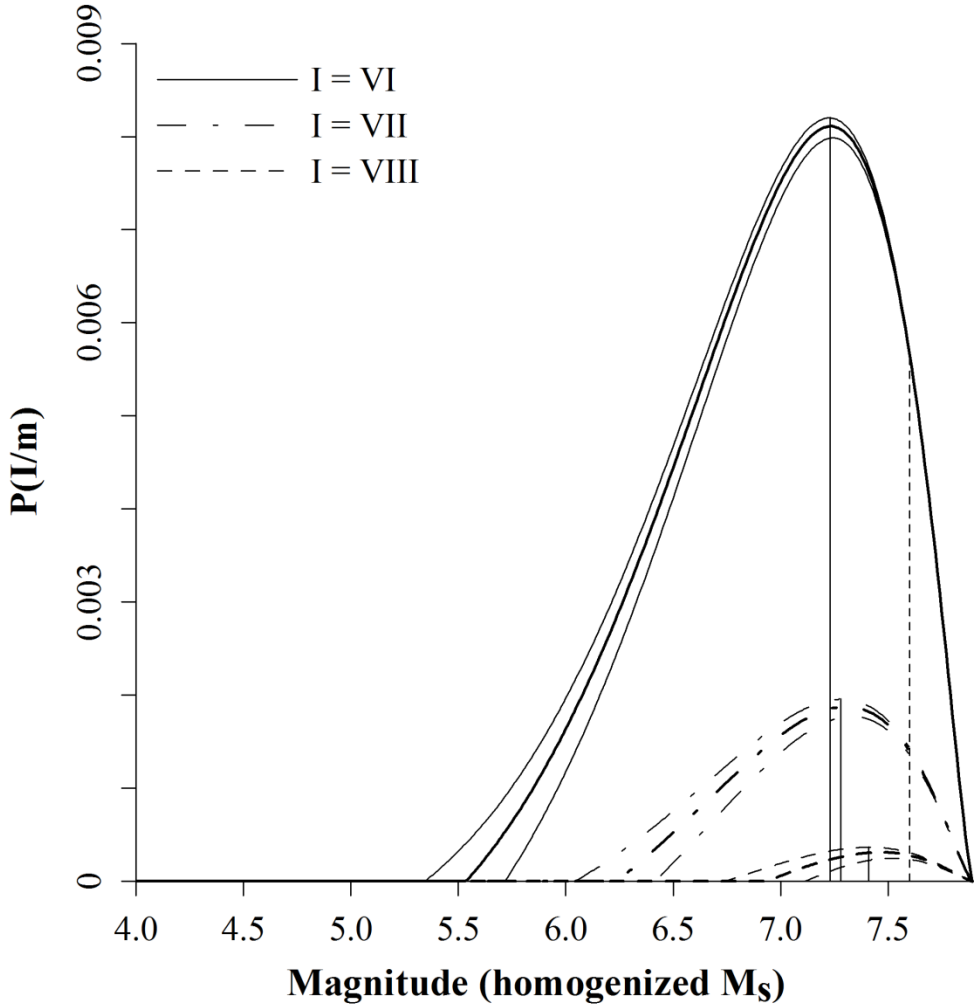

(a)

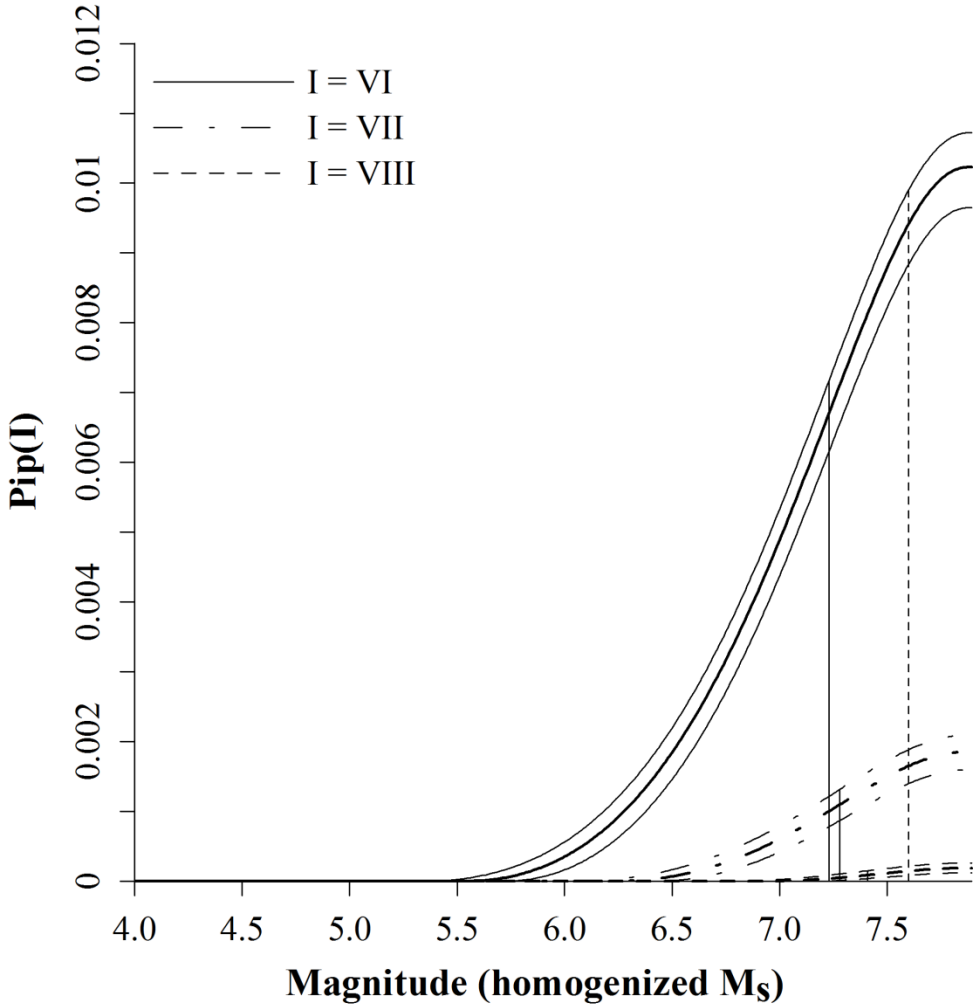

(b)

Macroseismic intensity (a) perceptibility and (b) integrated perceptibility curves for Larissa

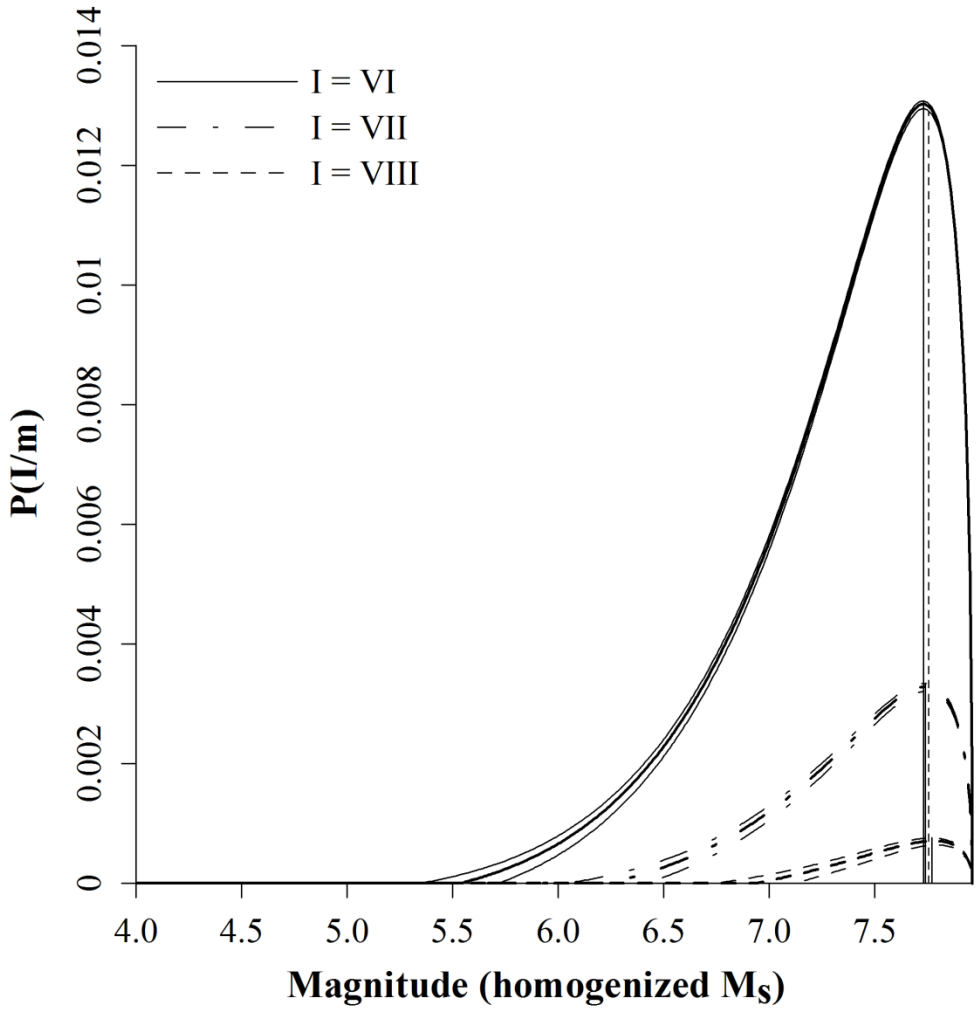

(a)

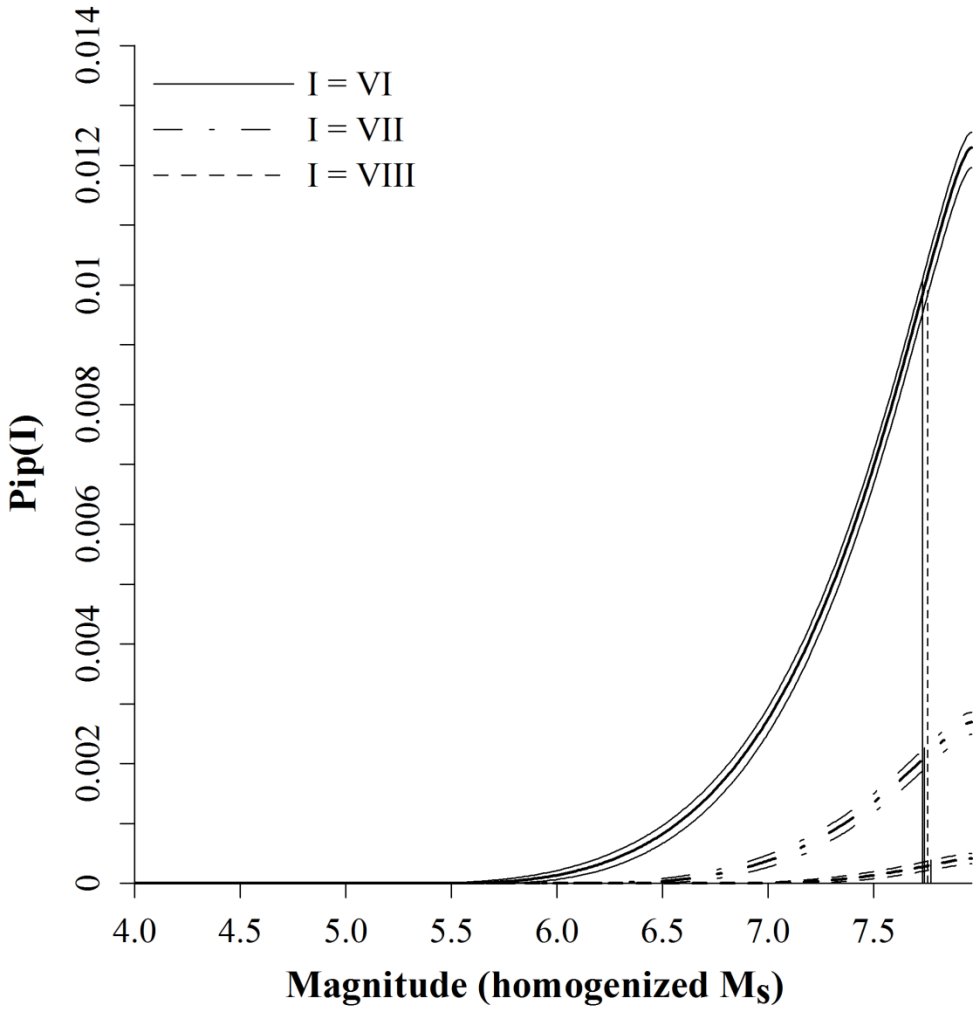

(b)

Macroseismic intensity (a) perceptibility and (b) integrated perceptibility curves for Plovdiv

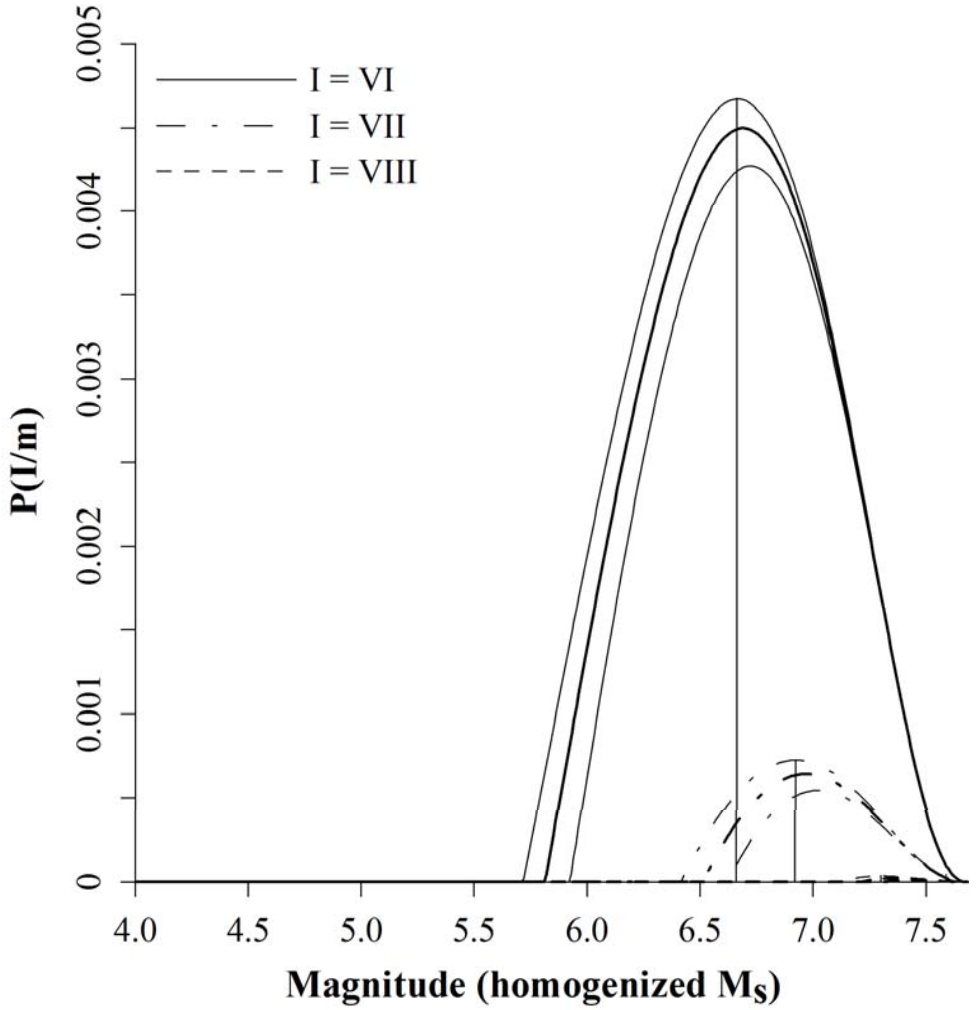

(a)

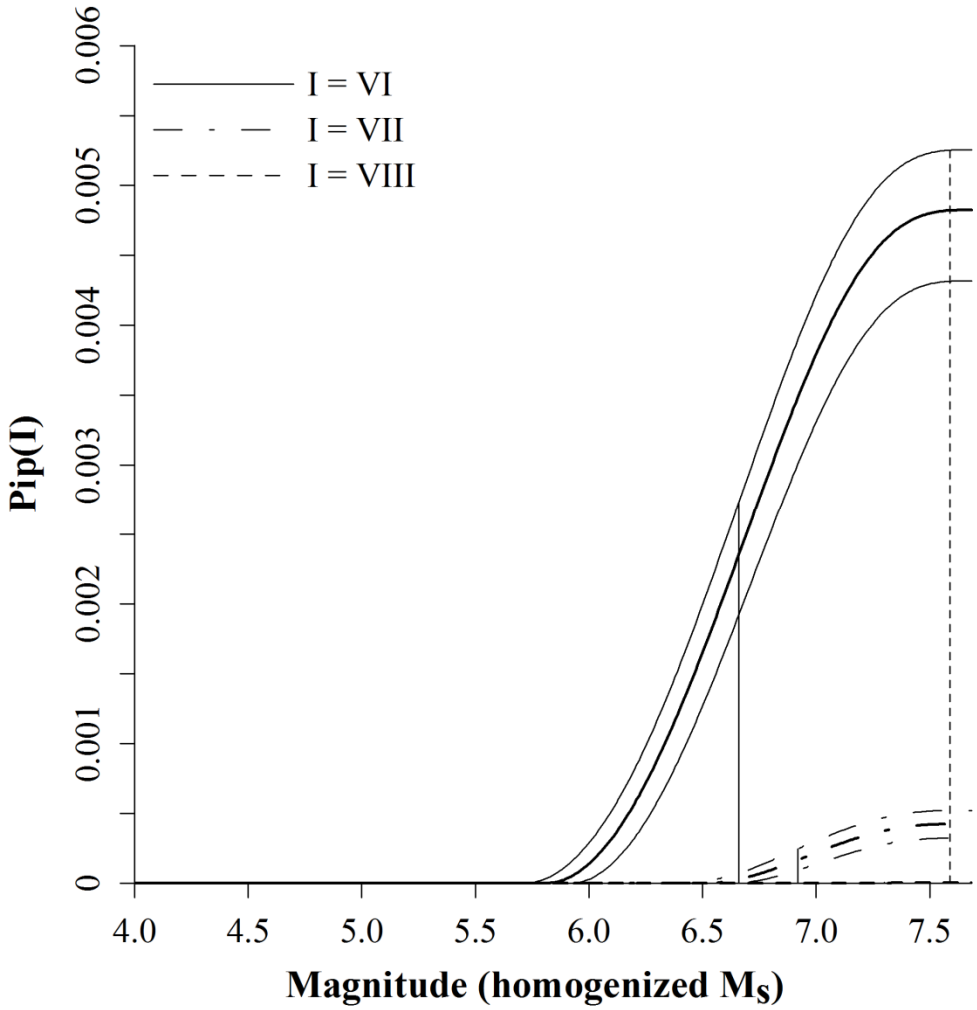

(b)

Macroseismic intensity (a) perceptibility and (b) integrated perceptibility curves for Pristina

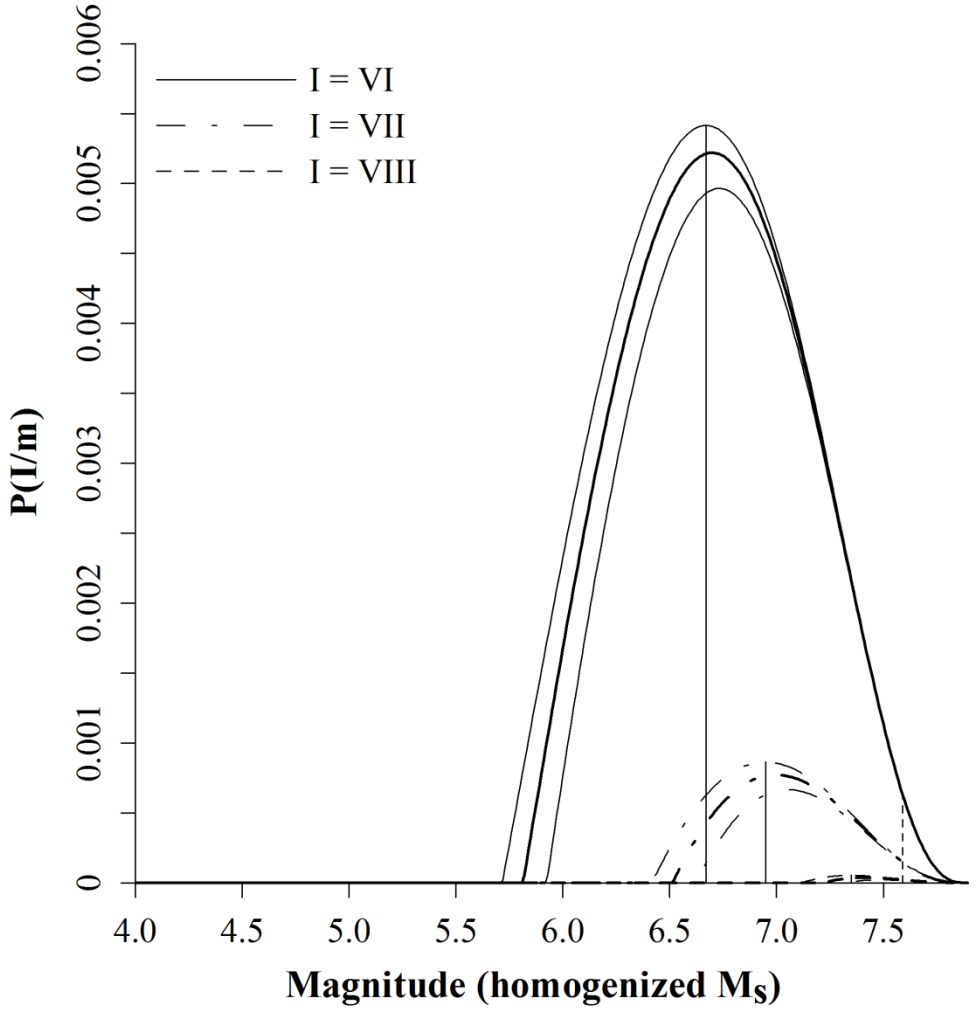

(a)

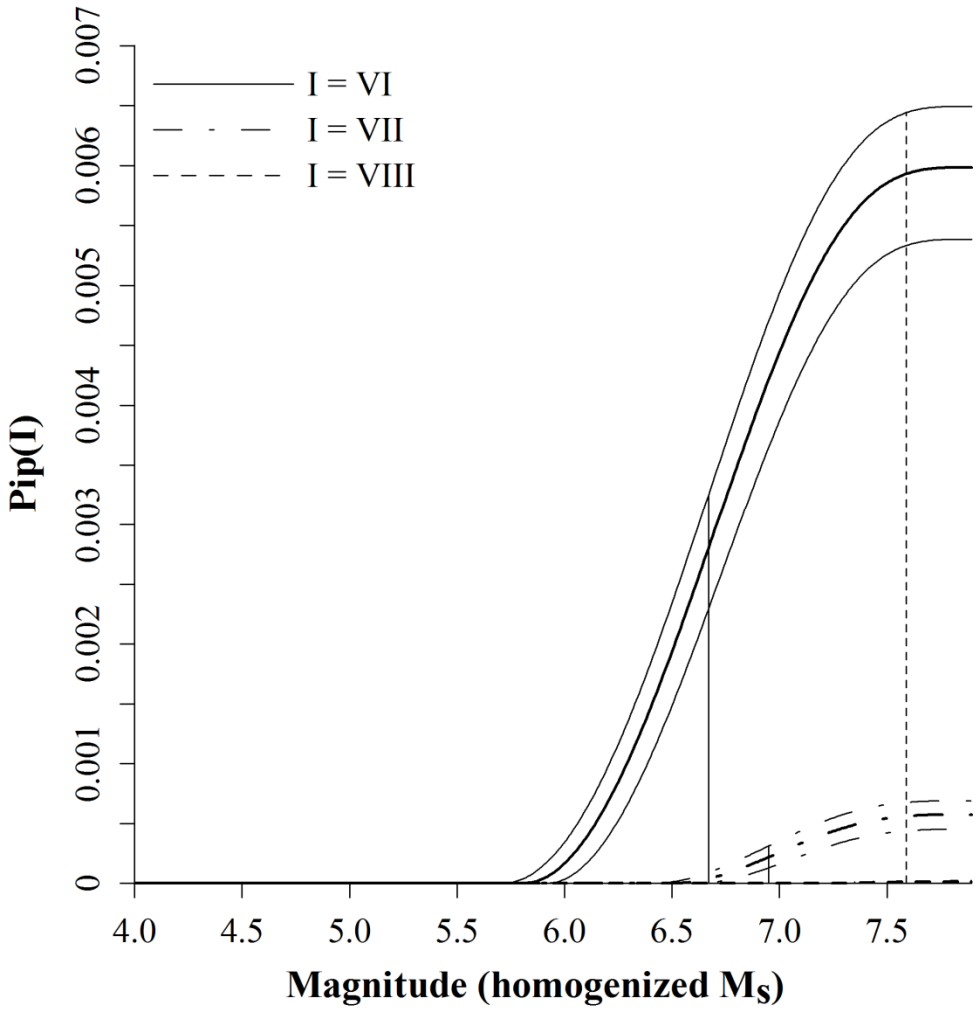

(b)

Macroseismic intensity (a) perceptibility and (b) integrated perceptibility curves for Skopje

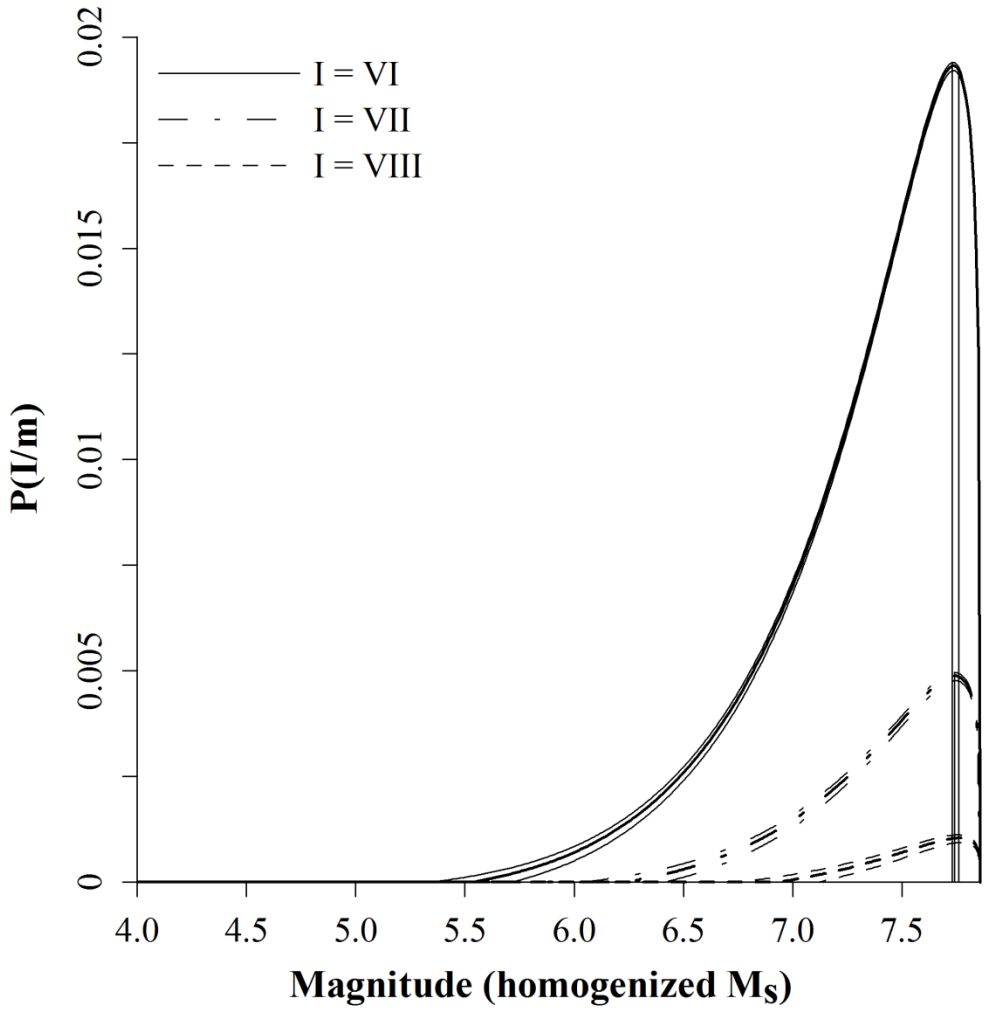

(a)

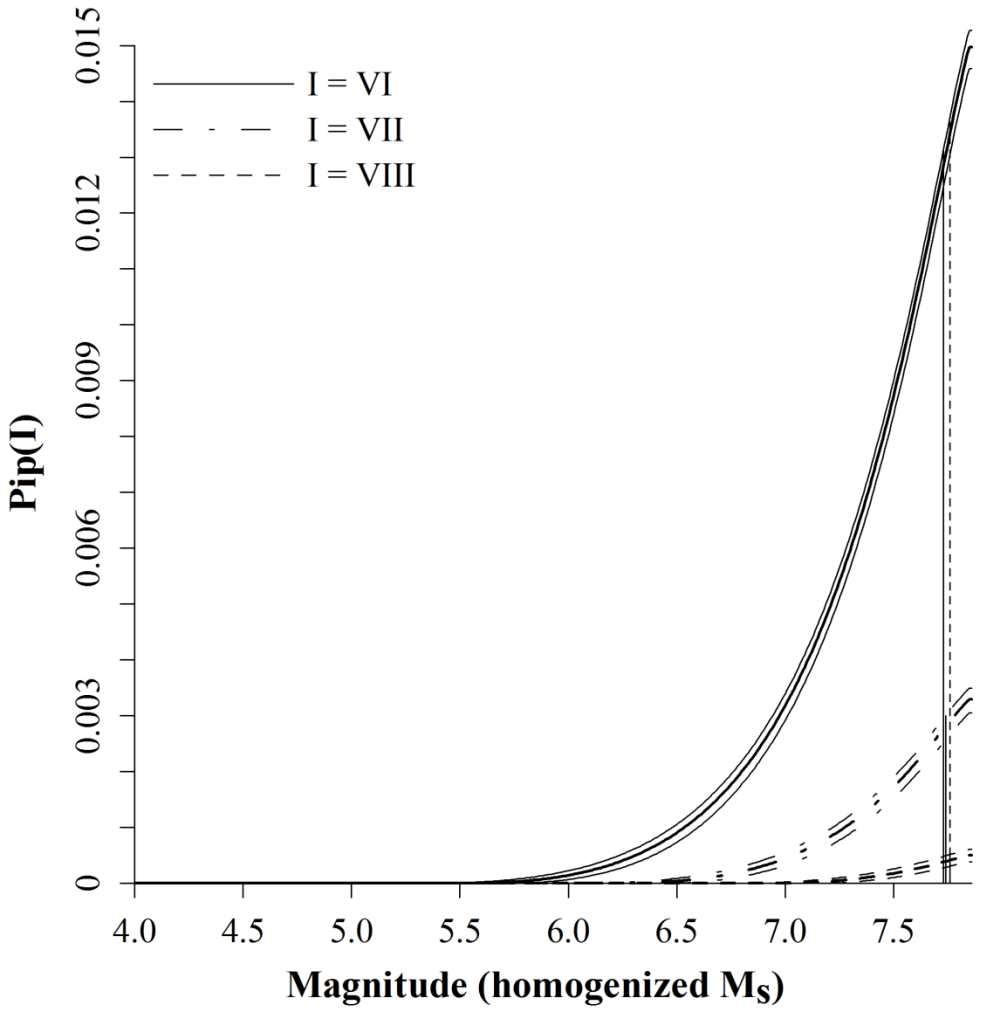

(b)

Macroseismic intensity (a) perceptibility and (b) integrated perceptibility curves for Sofia

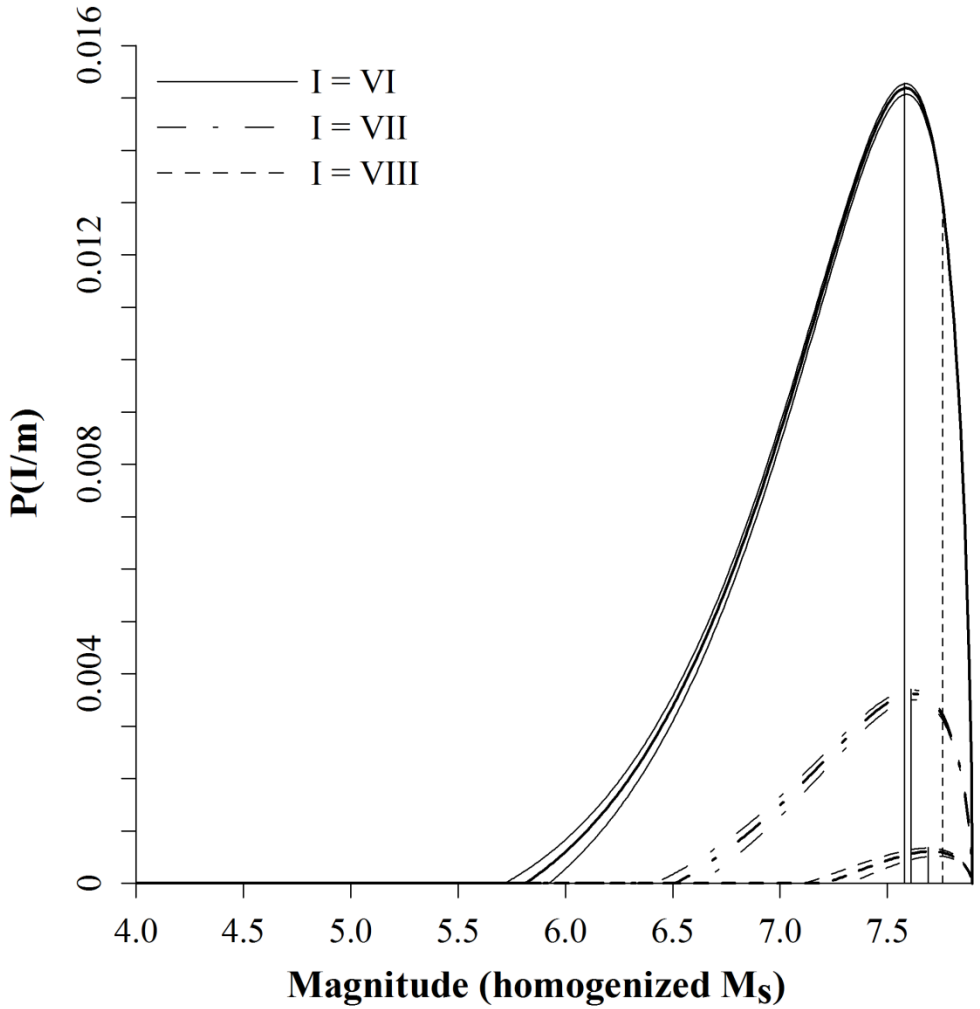

(a)

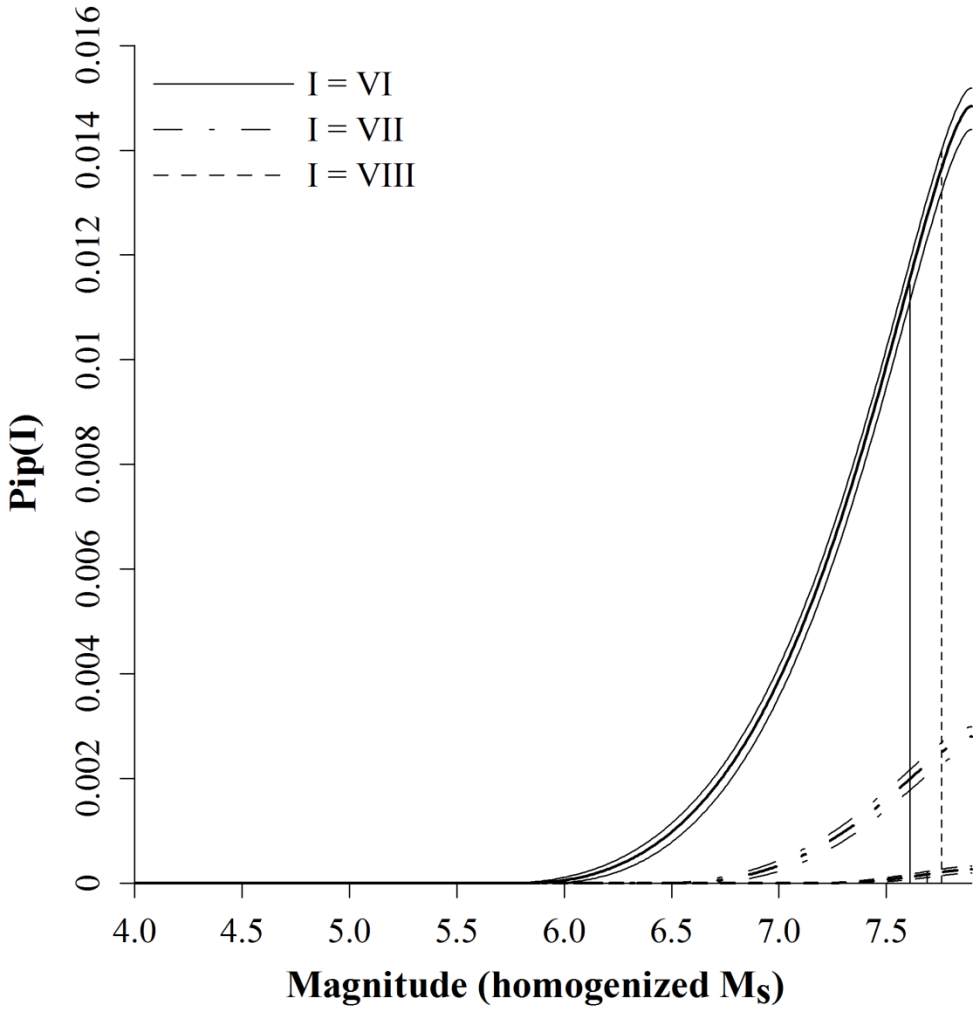

(b)

Macroseismic intensity (a) perceptibility and (b) integrated perceptibility curves for Thessaloniki

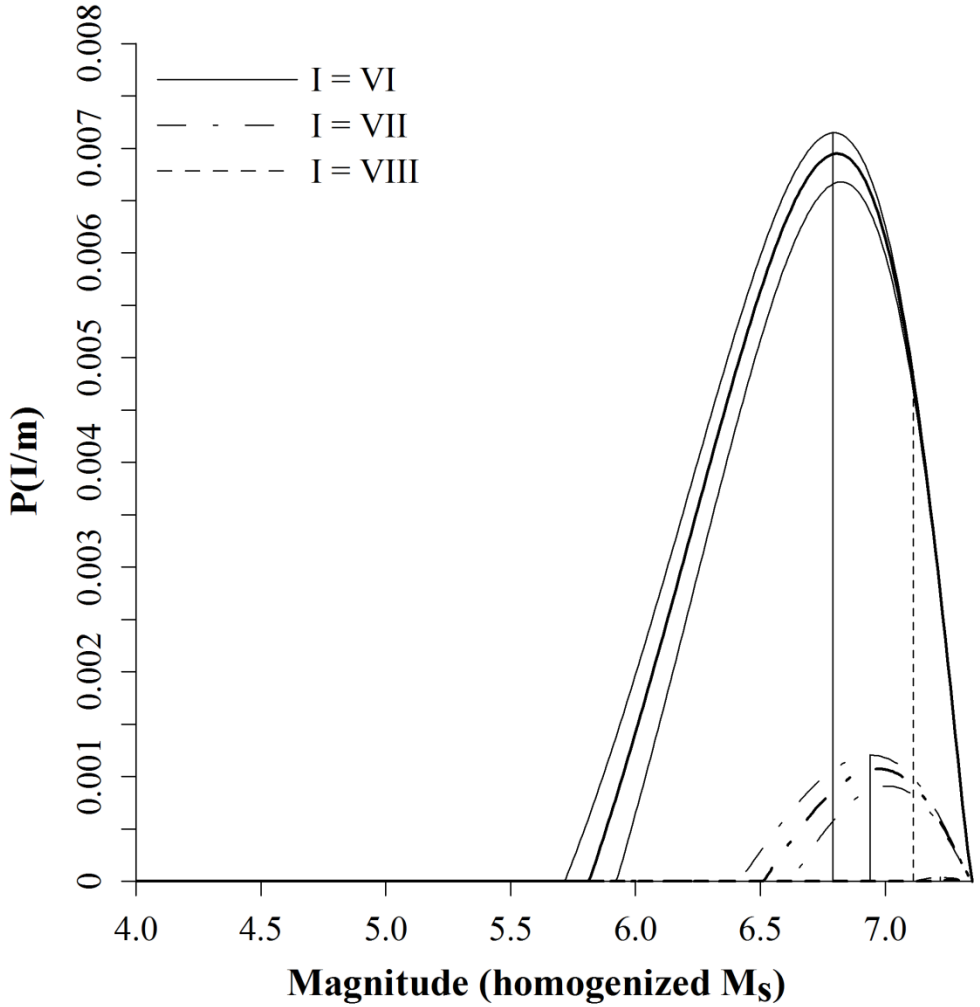

(a)

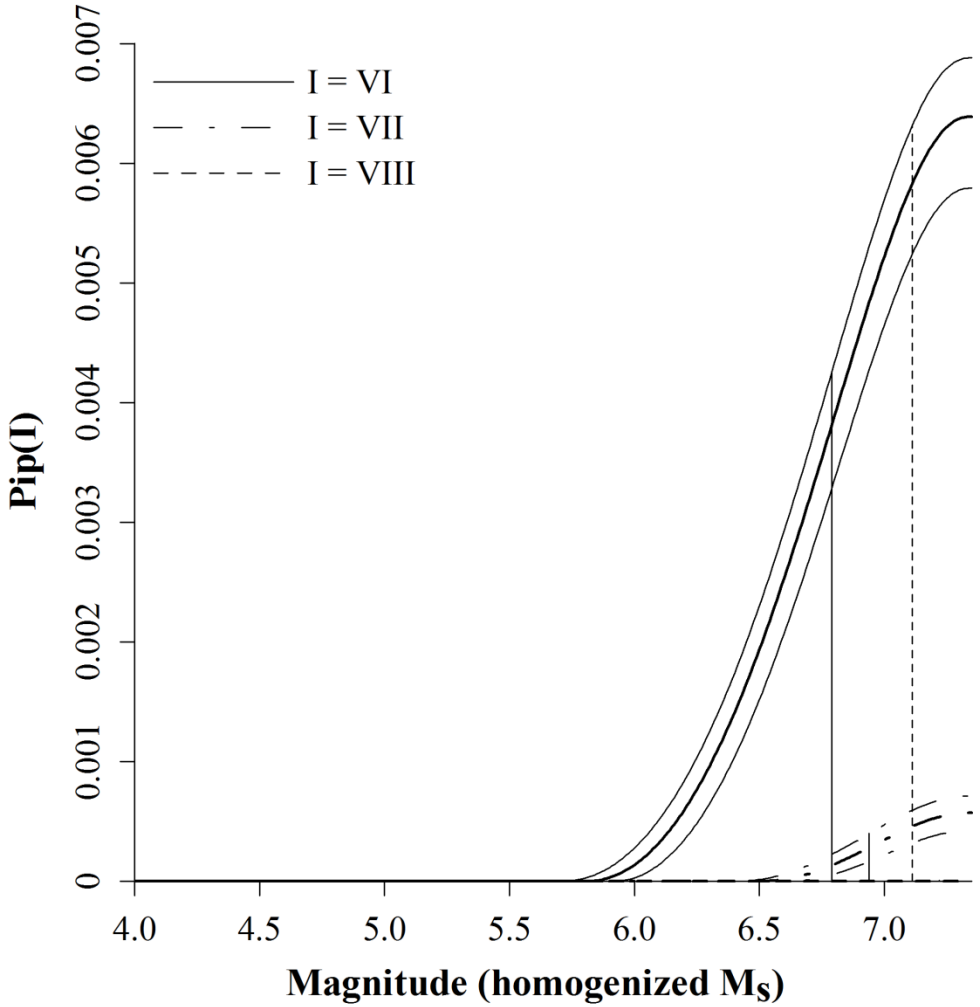

(b)

Macroseismic intensity (a) perceptibility and (b) integrated perceptibility curves for Tirane

Appendix 27: $M_{P(max)}$ curves for intensity perceptibility

Most perceptible magnitude curves for each city considered. In each set of three curves on these graphs, the central bold line represents an earthquake at a nominal focal depth of 15 km (approximating to the mean seismogenic depth for historical seismicity above M_{CUT} for the broader region of 5.5 M_S; Figure 2.14). Thinner curves above and below each bold curve represent earthquakes at nominal focal depths of 10 km and 20 km respectively.

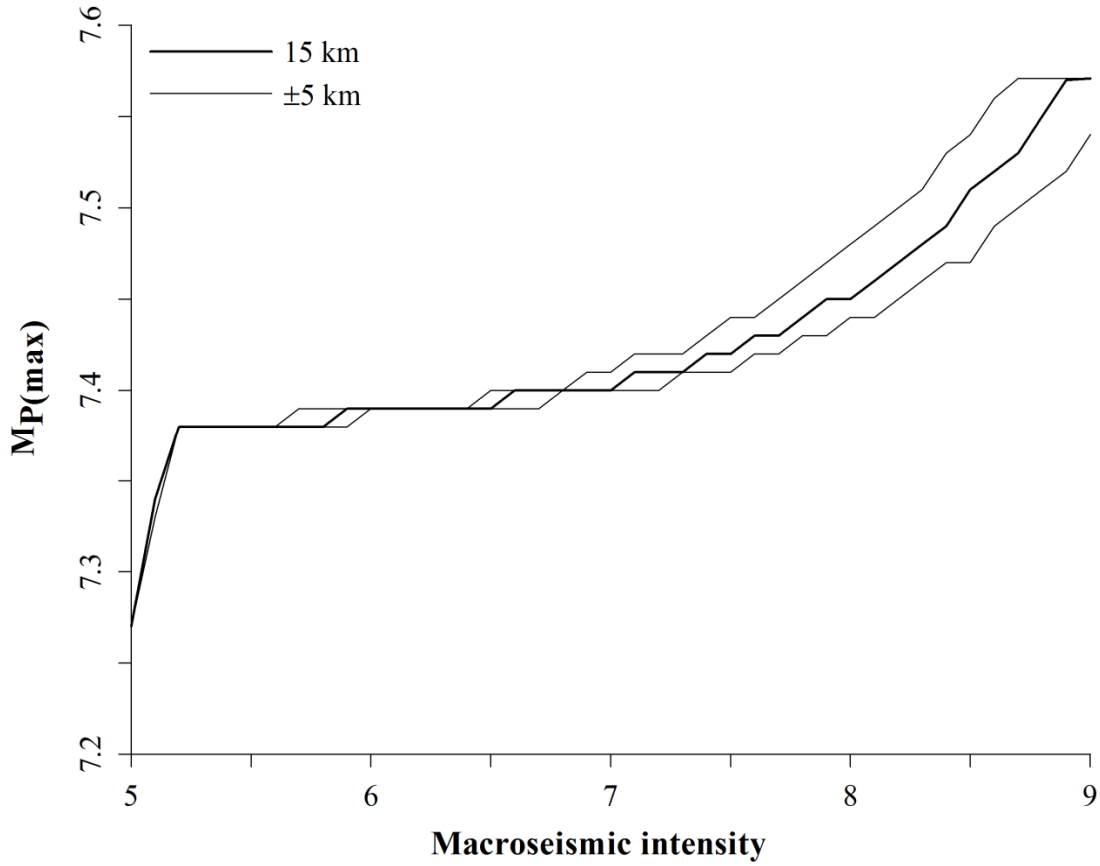

(a)

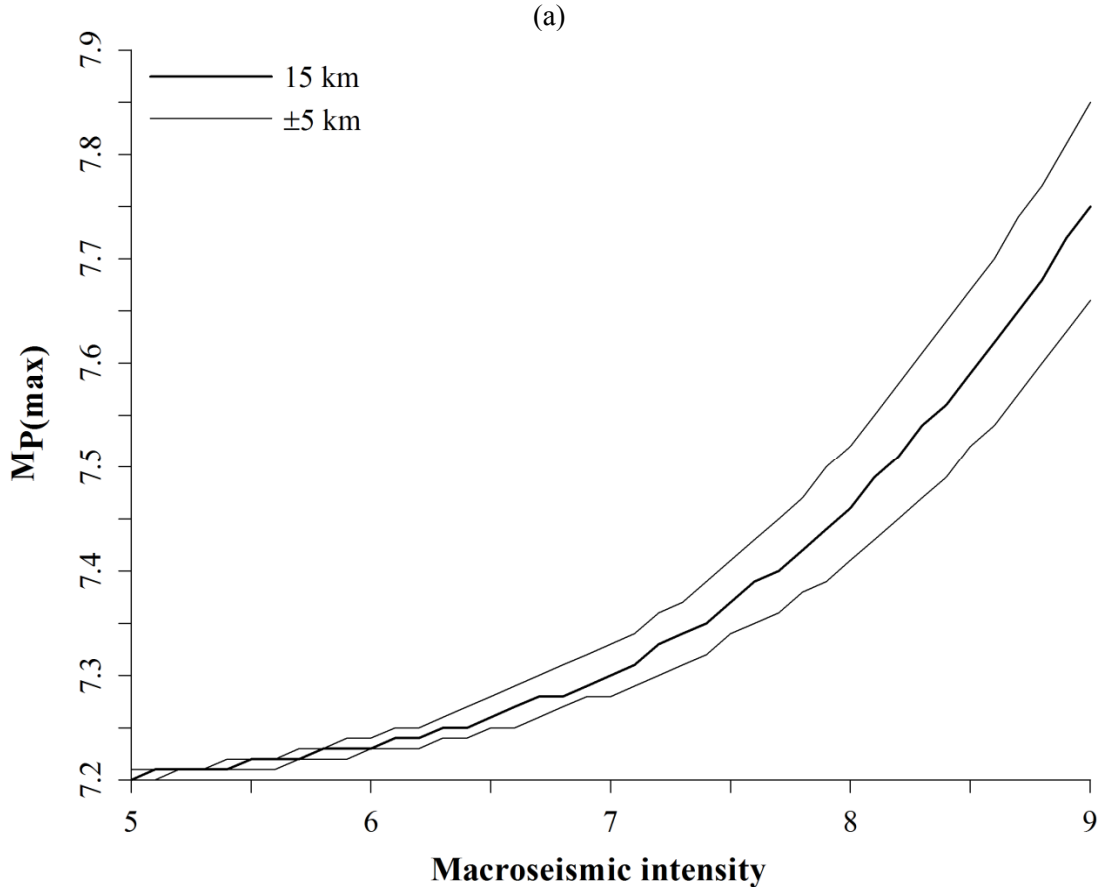

(b)

Most perceptible magnitudes for (a) Edirne and (b) Larissa

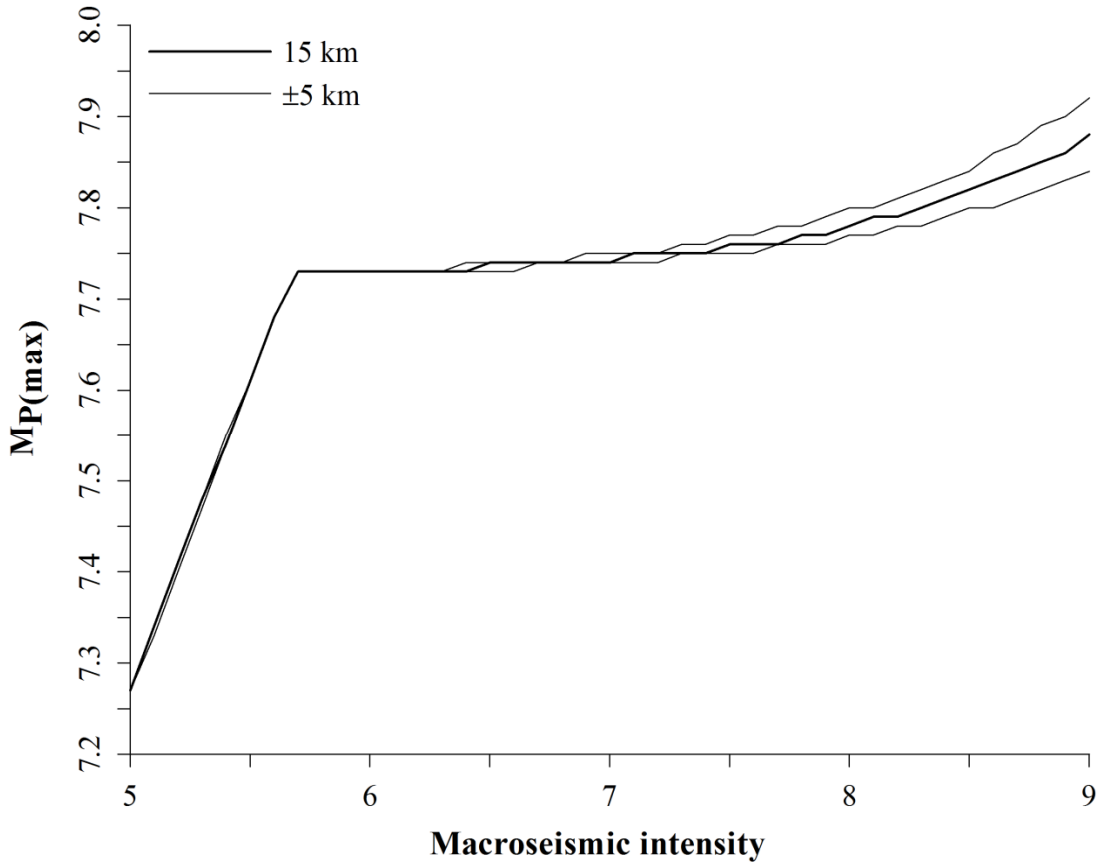

(a)

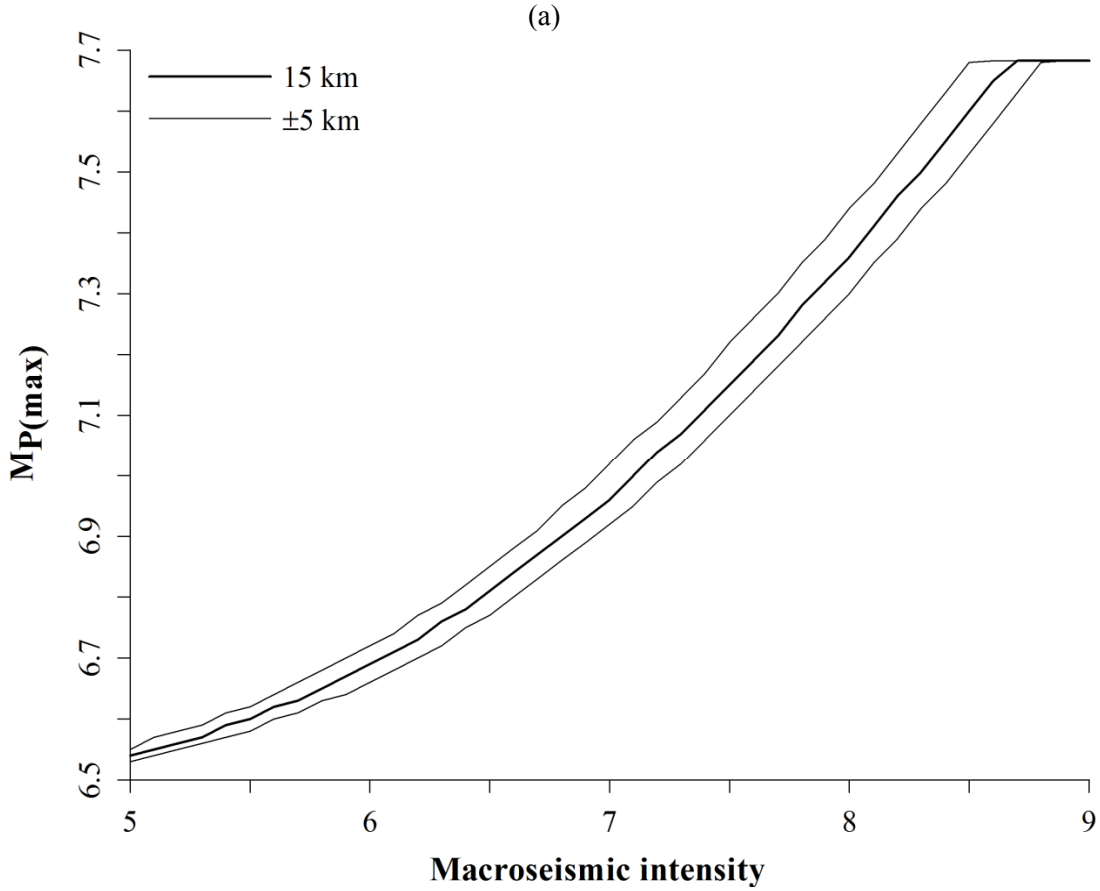

(b)

Most perceptible magnitudes for (a) Plovdiv and (b) Pristina

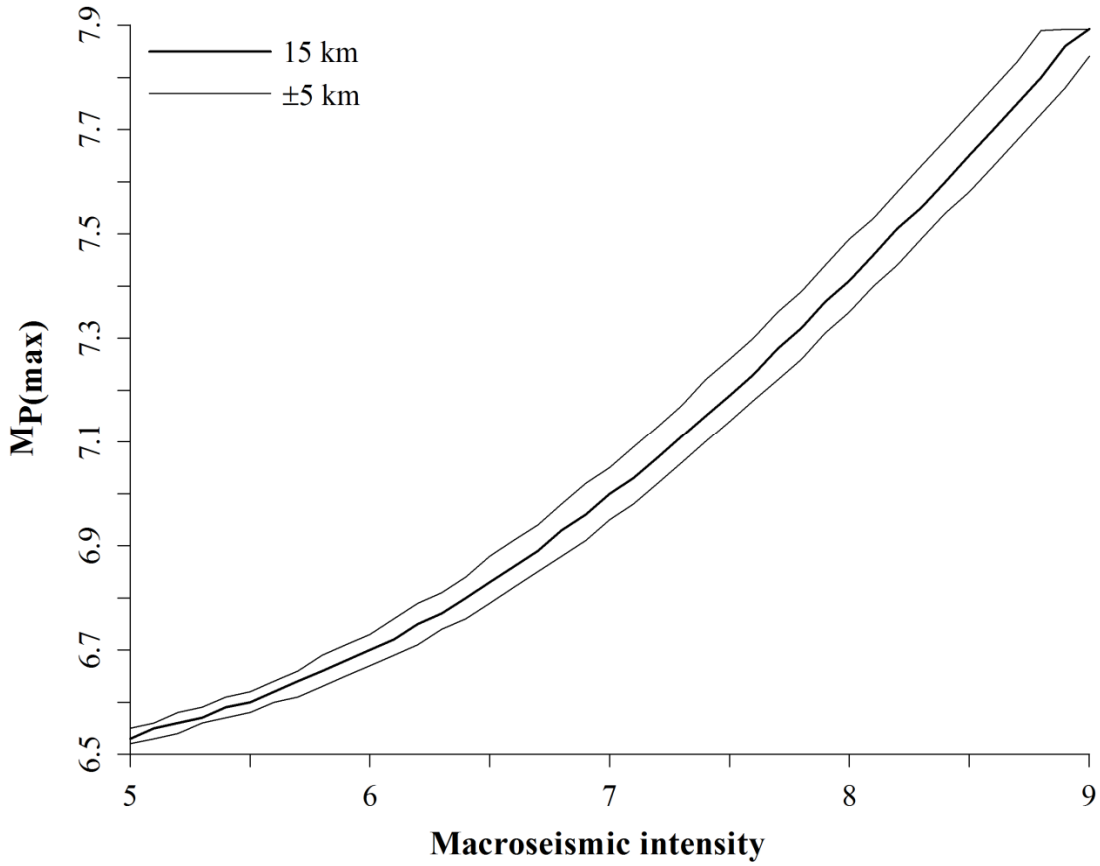

(a)

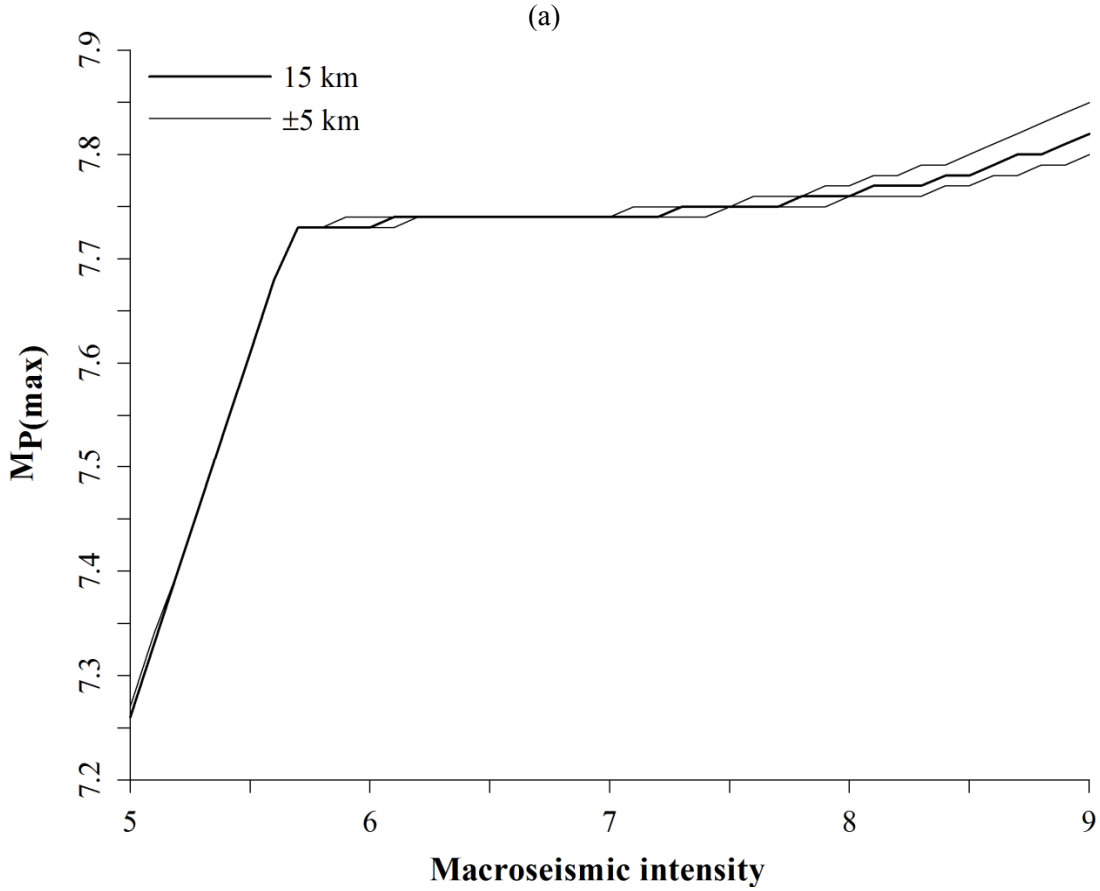

(b)

Most perceptible magnitudes for (a) Skopje and (b) Sofia

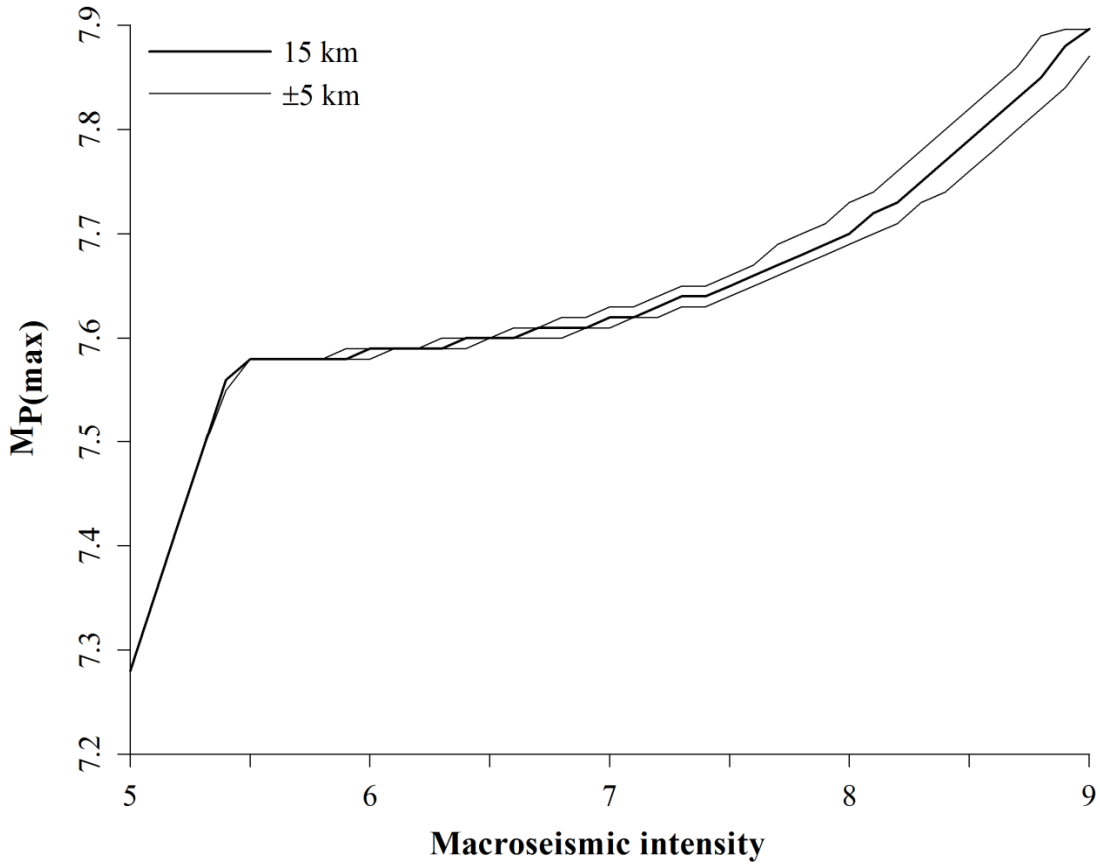

(a)

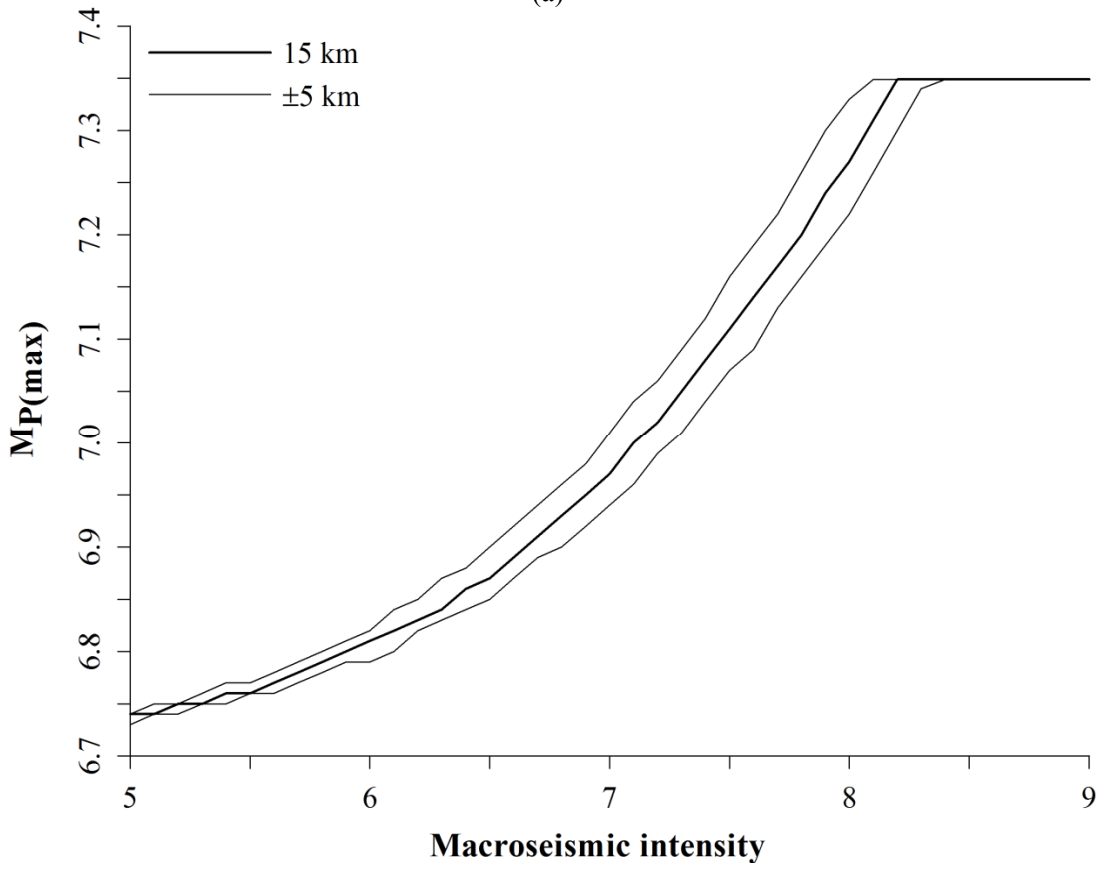

(b)

Most perceptible magnitudes for (a) Thessaloniki and (b) Tirane

Appendix 28: Site-specific intensity hazard curves

Macroseismic intensity hazard curves for the urban centres for which seismic hazard is forecast, using Papazachos and Papaioannou (1997; PP97).

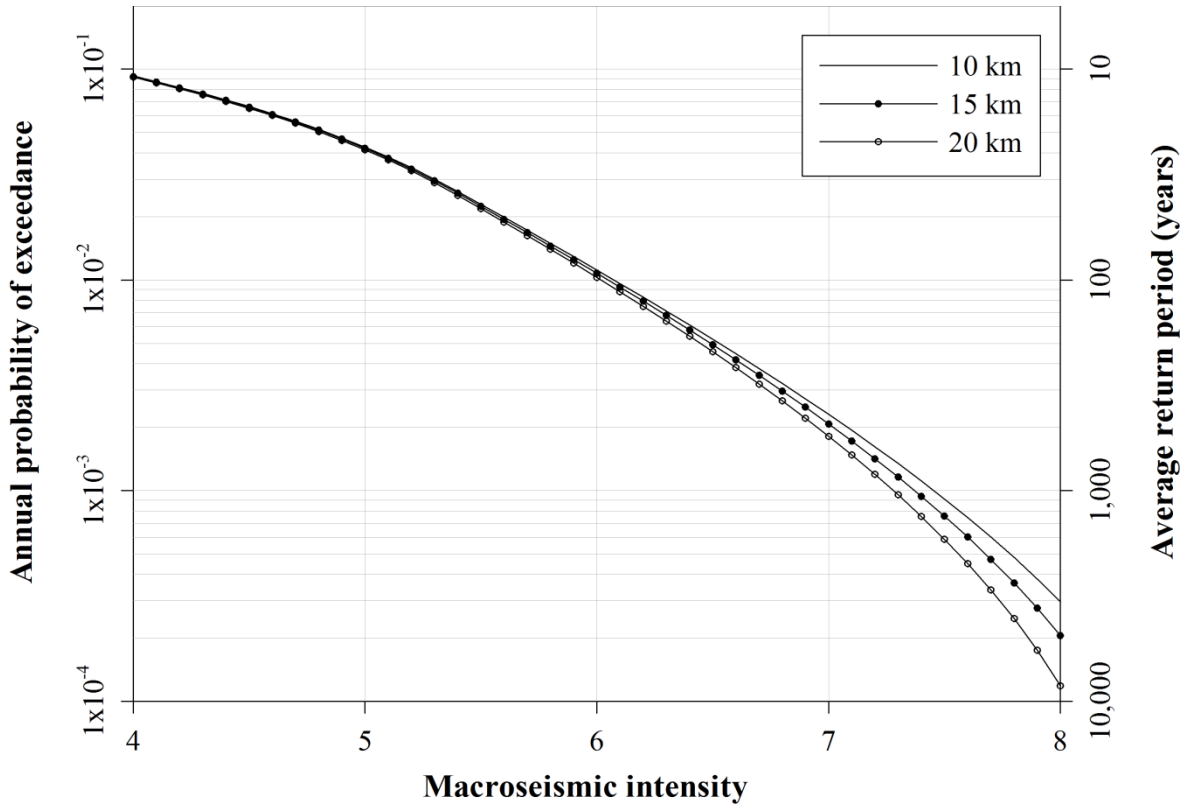

(a)

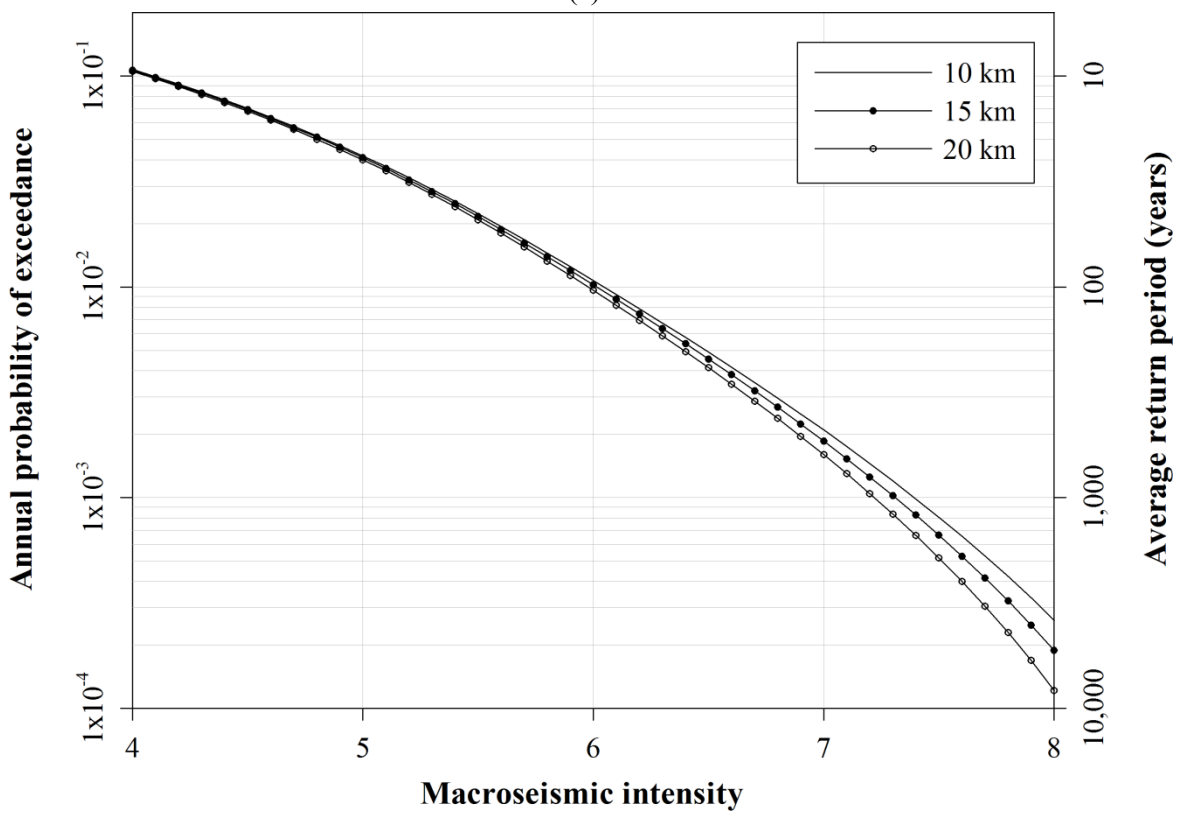

(b)

Macroseismic intensity hazard curves for (a) Edirne and (b) Larissa

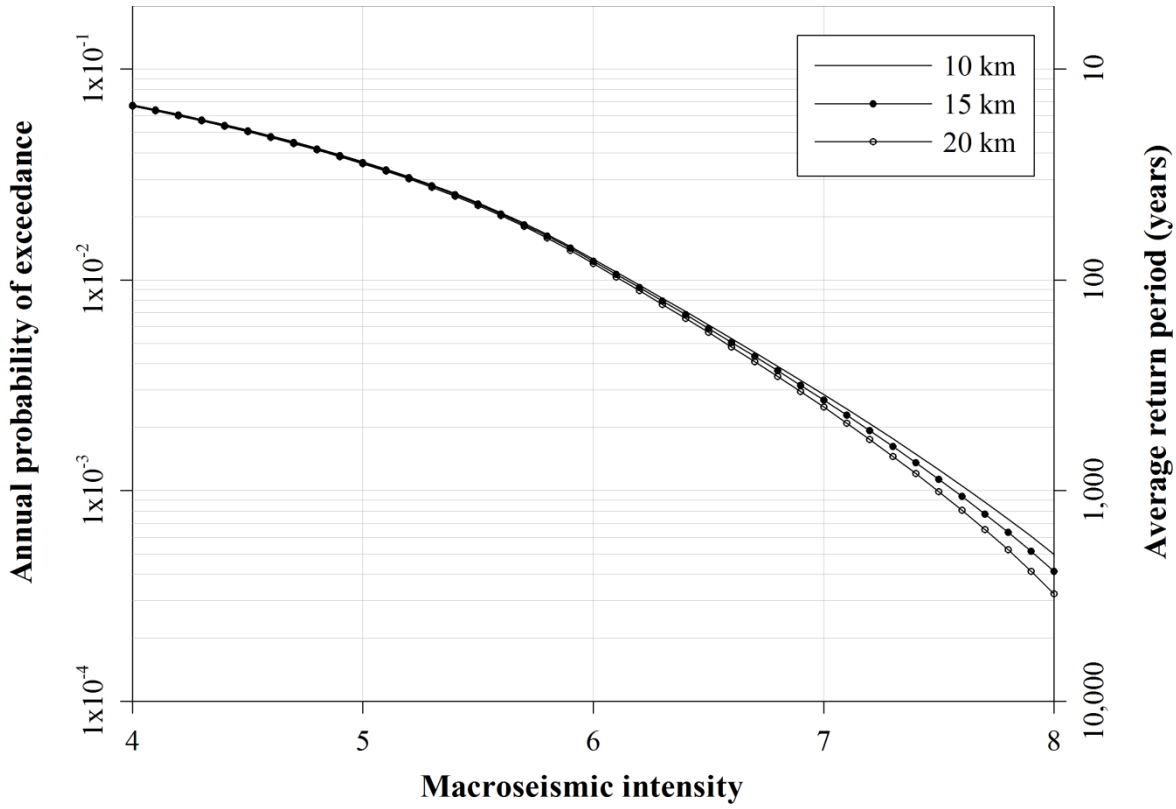

(a)

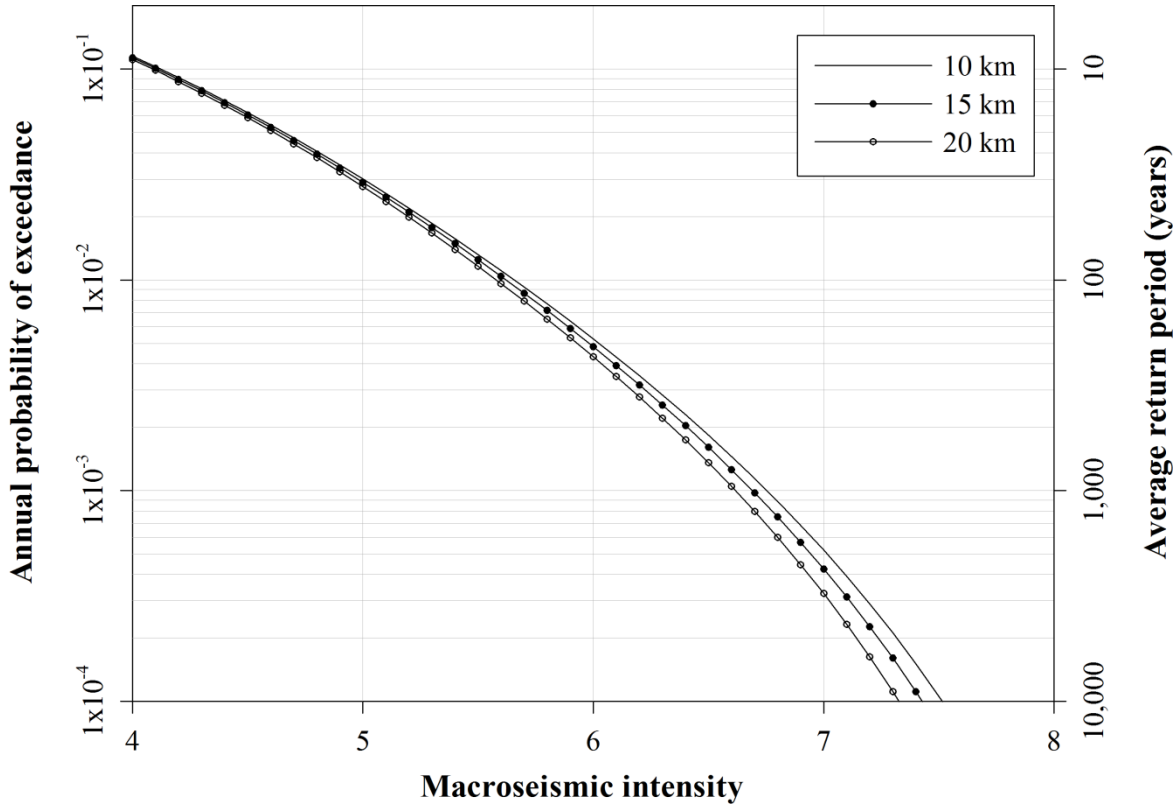

(b)

Macroseismic intensity hazard curves for (a) Plovdiv and (b) Pristina

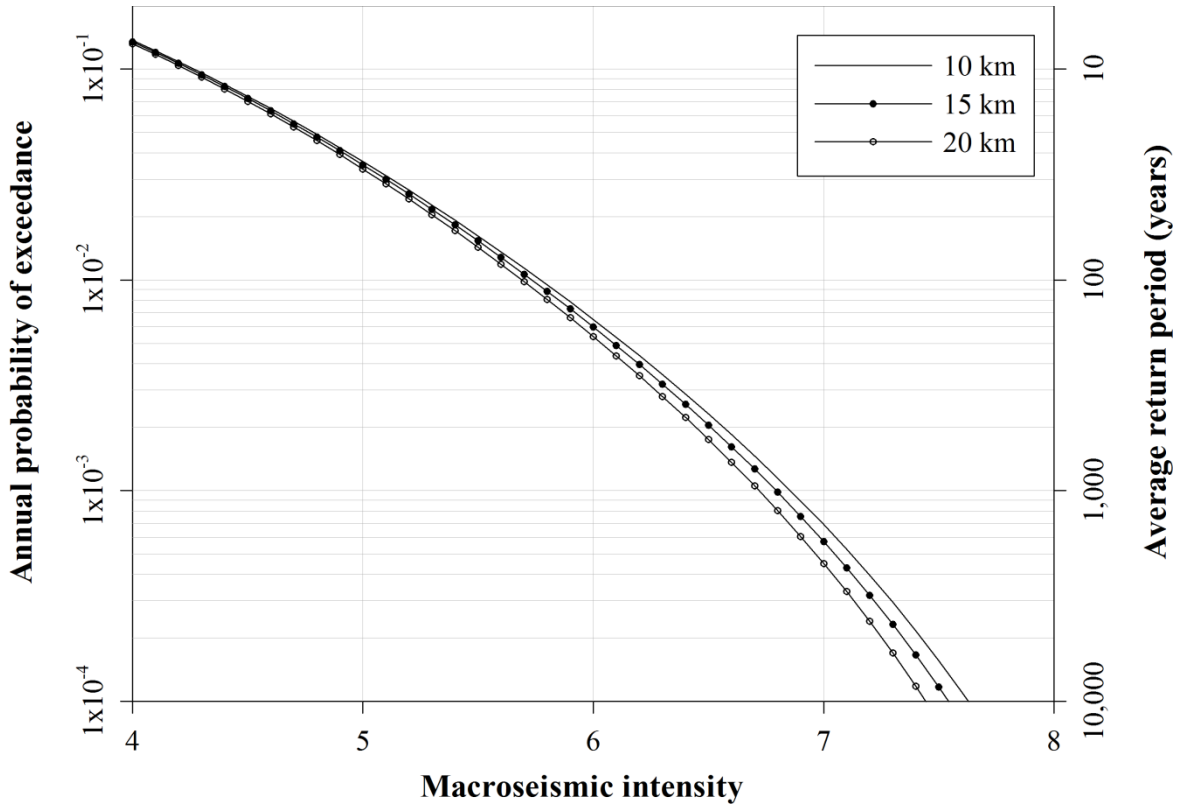

(a)

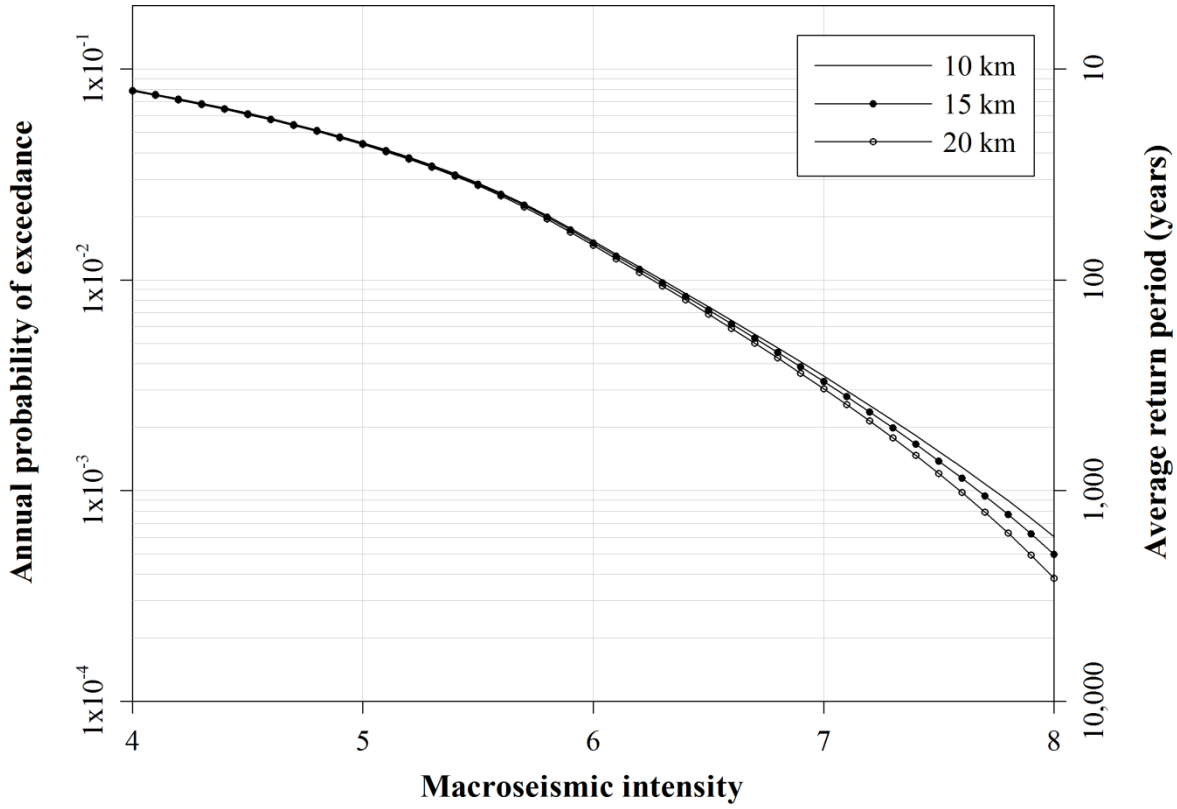

(b)

Macroseismic hazard curves for (a) Skopje and (b) Sofia

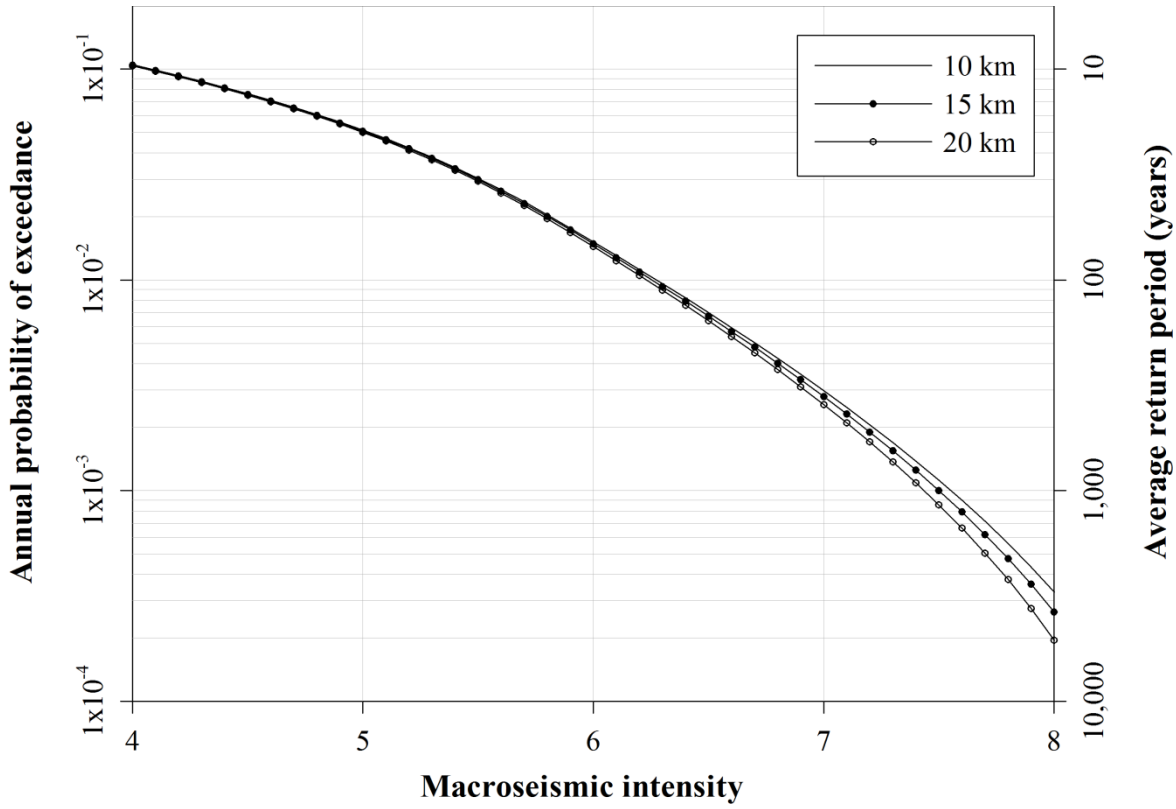

(a)

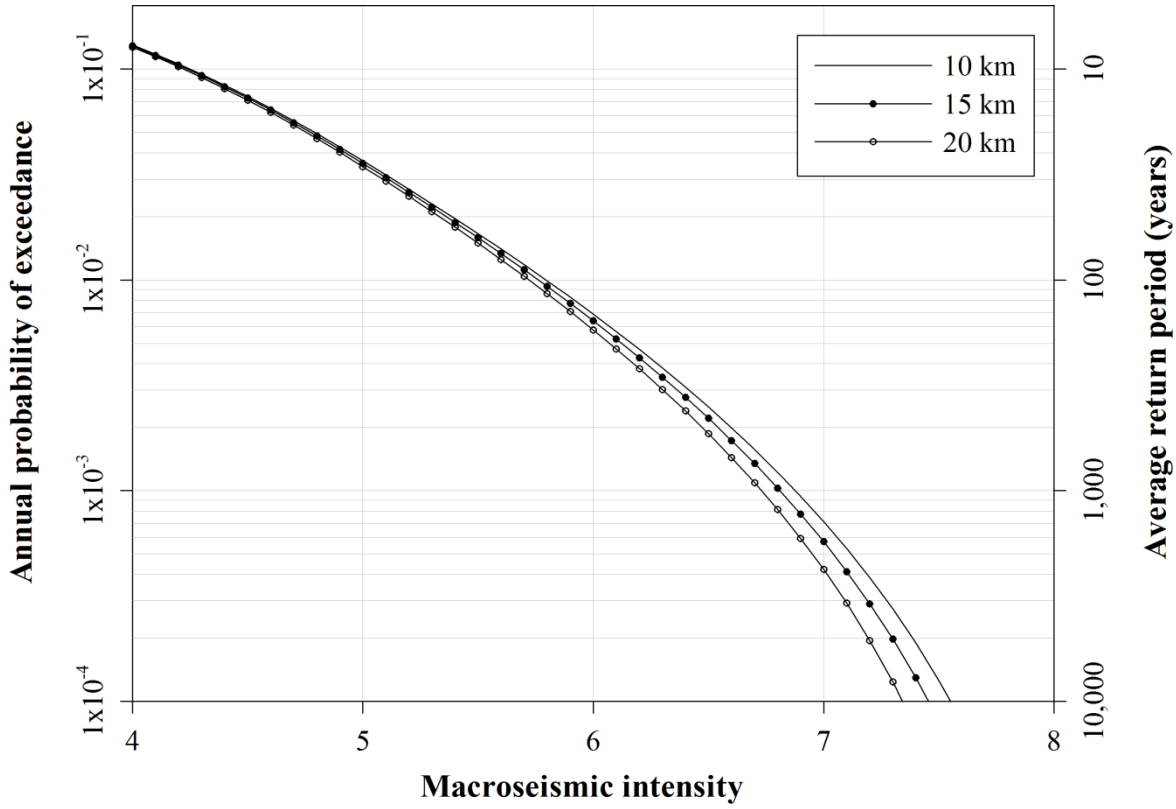

(b)

Macroseismic hazard curves for (a) Thessaloniki and (b) Tirane

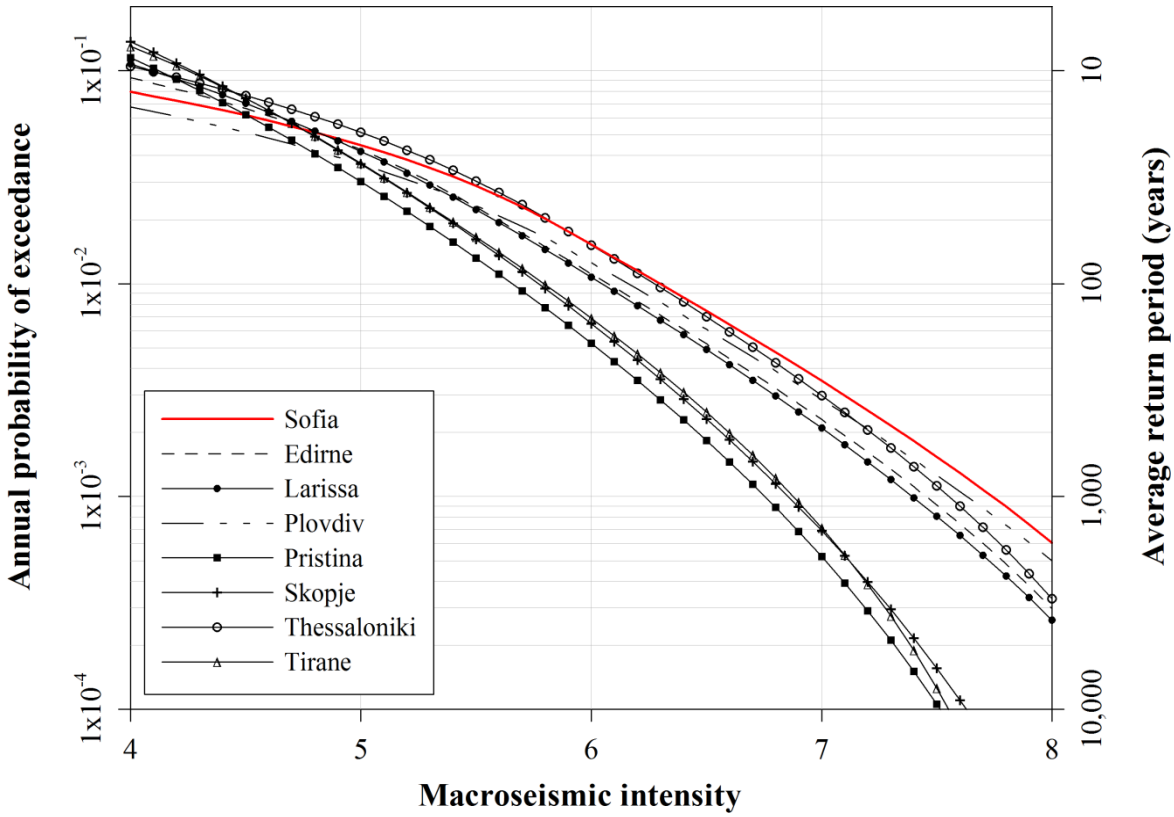

(a)

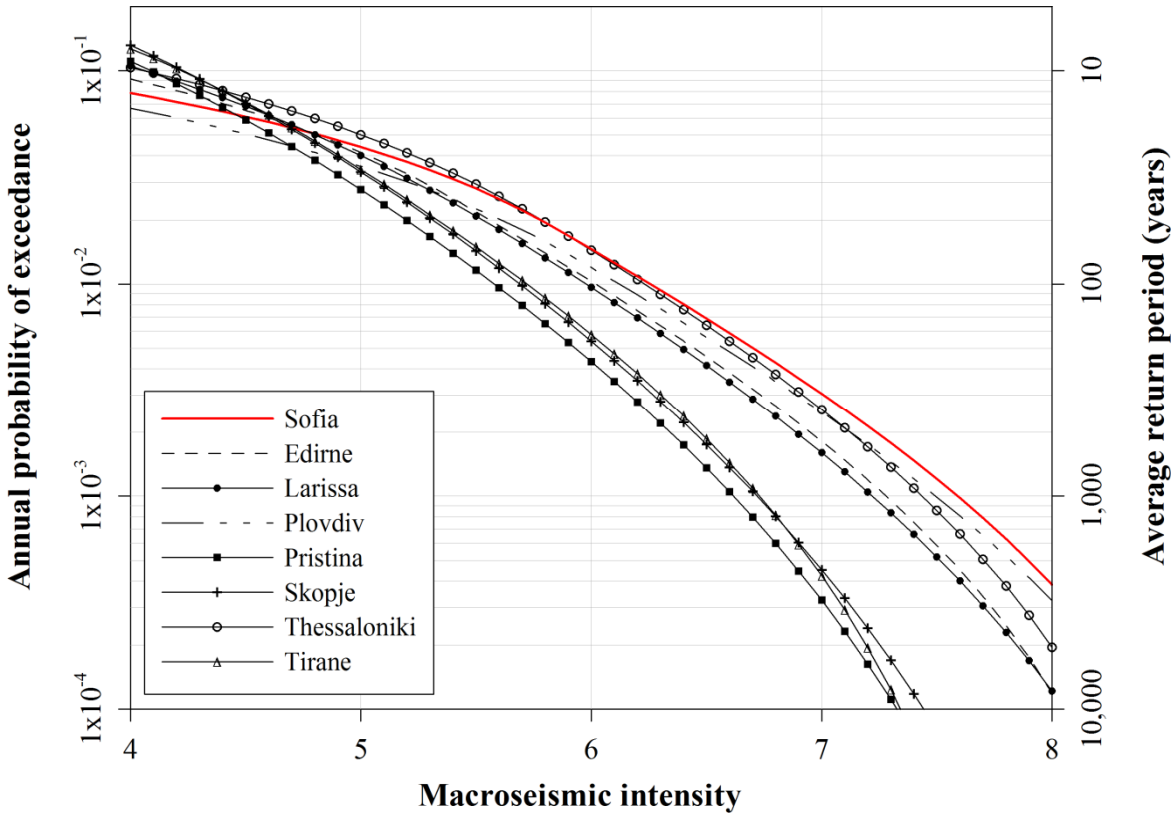

(b)

Macroseismic intensity hazard curves for urban centres considered using and Papaioannou (1997; PP97) for a nominal earthquake with focal depth of (a) 10 km and (b) 20 km. In each case, Sofia is highlighted in red as the reference case

Appendix 29: Annual exceedance probabilities of site-specific intensities

Site-specific probabilities for annual exceedance for macroseismic intensity hazard and in *T* years for the urban centres for which seismic hazard is forecast using Papazachos and Papazachos (1997).

City	Focal Depth (km)	Annual probability of exceedance ($\times 10^{-3}$)							
		I_{μ}	I_A	I_4	I_5	I_6	I_7	I_8	I_9
Edirne	10	0.3	<0.1	92.8	42.6	11.1	2.3	0.3	<0.1
	15	0.1	<0.1	92.2	42.1	10.8	2.1	0.2	<0.1
	20	<0.1	<0.1	91.5	41.5	10.3	1.8	0.1	<0.1
Larissa	10	0.2	<0.1	107.7	41.9	10.7	2.1	0.3	<0.1
	15	0.1	<0.1	106.6	41.1	10.2	1.9	0.2	<0.1
	20	0.1	<0.1	105.5	40.1	9.6	1.3	0.1	<0.1
Plovdiv	10	6.1	<0.1	67.7	36.4	12.6	2.9	0.5	<0.1
	15	5.6	<0.1	67.4	36.1	12.3	2.7	0.4	<0.1
	20	5.6	<0.1	66.9	35.6	12.0	2.5	0.3	<0.1
Pristina	10	1.1	0.5	115.2	30.2	5.3	0.5	<0.1	<0.1
	15	1.0	0.3	113.5	29.1	4.8	0.3	<0.1	<0.1
	20	0.9	0.3	111.1	27.7	4.3	0.3	<0.1	<0.1
Skopje	10	3.6	1.5	136.7	36.5	6.5	0.7	<0.1	<0.1
	15	3.2	1.3	134.7	35.2	6.0	0.6	<0.1	<0.1
	20	2.8	1.1	132.0	33.6	5.4	0.5	<0.1	<0.1
Thessaloniki	10	0.6	<0.1	105.1	51.3	15.2	3.0	0.3	<0.1
	15	0.5	<0.1	104.5	50.9	14.8	2.8	0.3	<0.1
	20	0.4	<0.1	103.8	50.2	14.3	2.6	0.2	<0.1
Tirane	10	3.8	0.7	130.5	36.8	6.9	0.7	<0.1	<0.1
	15	3.5	0.6	129.1	35.8	6.4	0.6	<0.1	<0.1
	20	3.0	0.4	127.2	34.5	5.8	0.3	<0.1	<0.1

Annual probabilities ($\times 10^{-3}$) of experiencing specific intensities estimated for the region surrounding each city using Papazachos and Papaioannou (1997)

City	Focal Depth (km)	Time interval (*T*-year)					
		100	200	300	400	500	1,000
Edirne	10	6.0	6.1	6.2	6.3	6.4	7.5
	15	6.0	6.1	6.2	6.3	6.4	7.4
	20	6.0	6.1	6.2	6.3	6.4	7.3
Larissa	10	6.0	6.1	6.2	6.3	6.4	7.4
	15	6.0	6.1	6.2	6.2	6.3	7.3
	20	5.9	6.0	6.1	6.2	6.3	7.2
Plovdiv	10	6.1	6.2	6.3	6.4	6.5	7.6
	15	6.1	6.2	6.3	6.4	6.5	7.5
	20	6.1	6.2	6.3	6.4	6.5	7.5
Pristina	10	5.7	5.7	5.8	5.8	5.9	6.7
	15	5.6	5.7	5.7	5.8	5.9	6.6
	20	5.6	5.6	5.7	5.8	5.8	6.6
Skopje	10	5.8	5.8	5.9	6.0	6.0	6.8
	15	5.7	5.8	5.9	5.9	6.0	6.8
	20	5.7	5.7	5.8	5.9	5.9	6.7
Thessaloniki	10	6.3	6.3	6.4	6.5	6.6	7.6
	15	6.2	6.3	6.4	6.5	6.6	7.5
	20	6.2	6.3	6.4	6.4	6.5	7.4
Tirane	10	5.8	5.9	5.9	6.0	6.1	6.9
	15	5.8	5.8	5.9	5.9	6.0	6.8
	20	5.7	5.8	5.8	5.9	6.0	6.7

Macroseismic intensities expected within a *T*-year time interval for the region surrounding each urban centre in using Papazachos and Papaioannou (1997)

Appendix 30: Site-specific seismic source disaggregation/*whole process* distributions

(a) Site-specific seismic source disaggregation plots for the urban centres for which seismic hazard is considered. On each graph:

- The magnitude interval shaded red contains the cut-off magnitude, M_{CUT}, adopted in chapter 5 to develop all extreme forecasts;

- The magnitude interval shaded yellow contains the *maximum credible magnitude*, M_3;

- The three blue arrows indicate the *most perceptible magnitude*, $M_{p(max)}$, for the lowest level of each form of ground motion considered (as labelled) in chapter 6. Ground acceleration is for Theodulidis and Papazachos (1992; $TP92_A$) for stiff soil conditions (S = 0.5) at the 50^{th} percentile; ground acceleration is for Theodulidis and Papazachos (1992; $TP92_V$) for stiff soil conditions (S = 0.5) at the 50^{th} percentile); macroseismic intensity is for Papazachos and Papaioannou (1997; PP97).

(b) Cumulative frequency and magnitude density distribution for the area immediately surrounding the city

Each graph considers seismicity within a 2° half-width rectangular cell centred on the city in question.

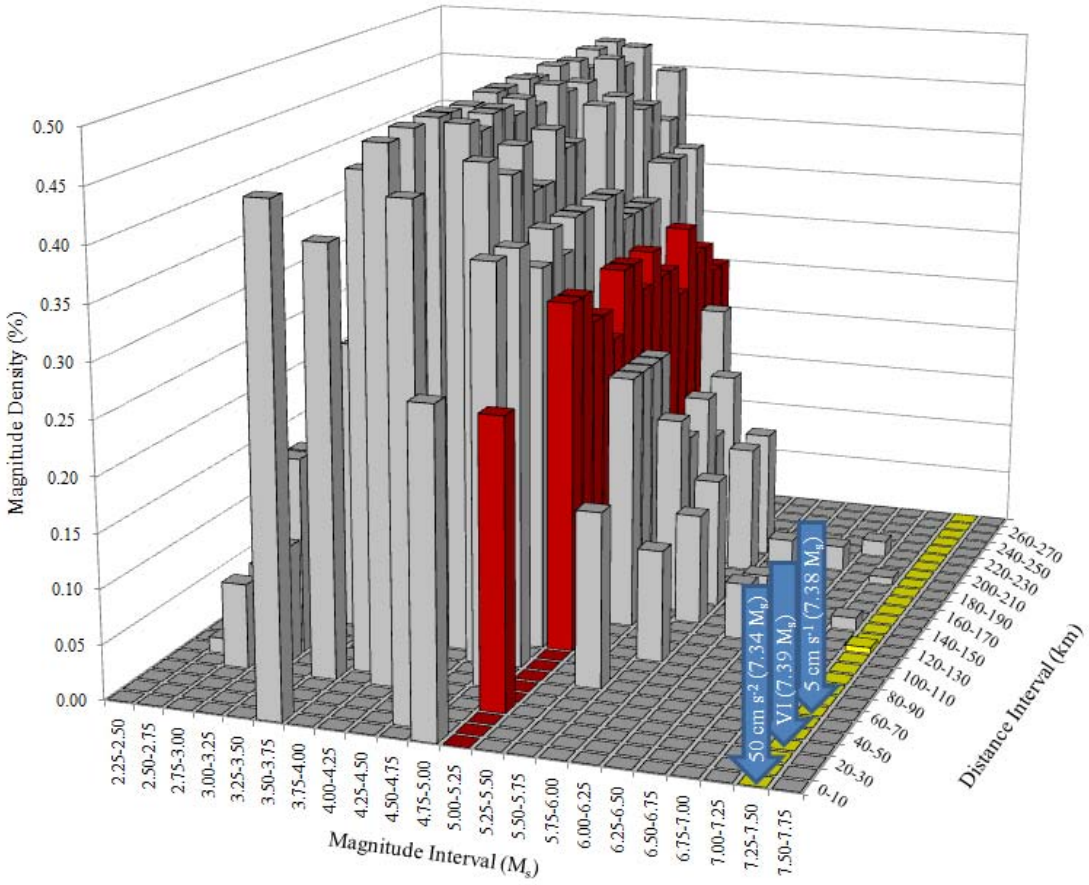

(a)

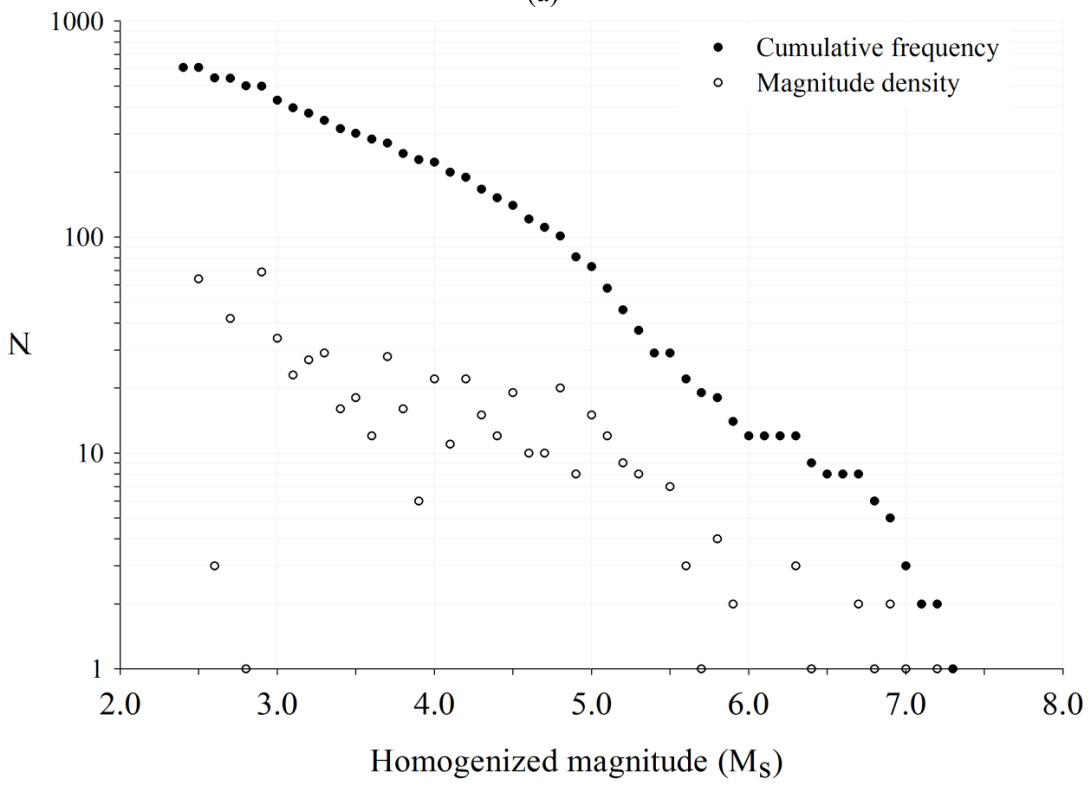

(b)

(a) Seismic source disaggregation and
(b) cumulative frequency and magnitude density distribution around Edirne

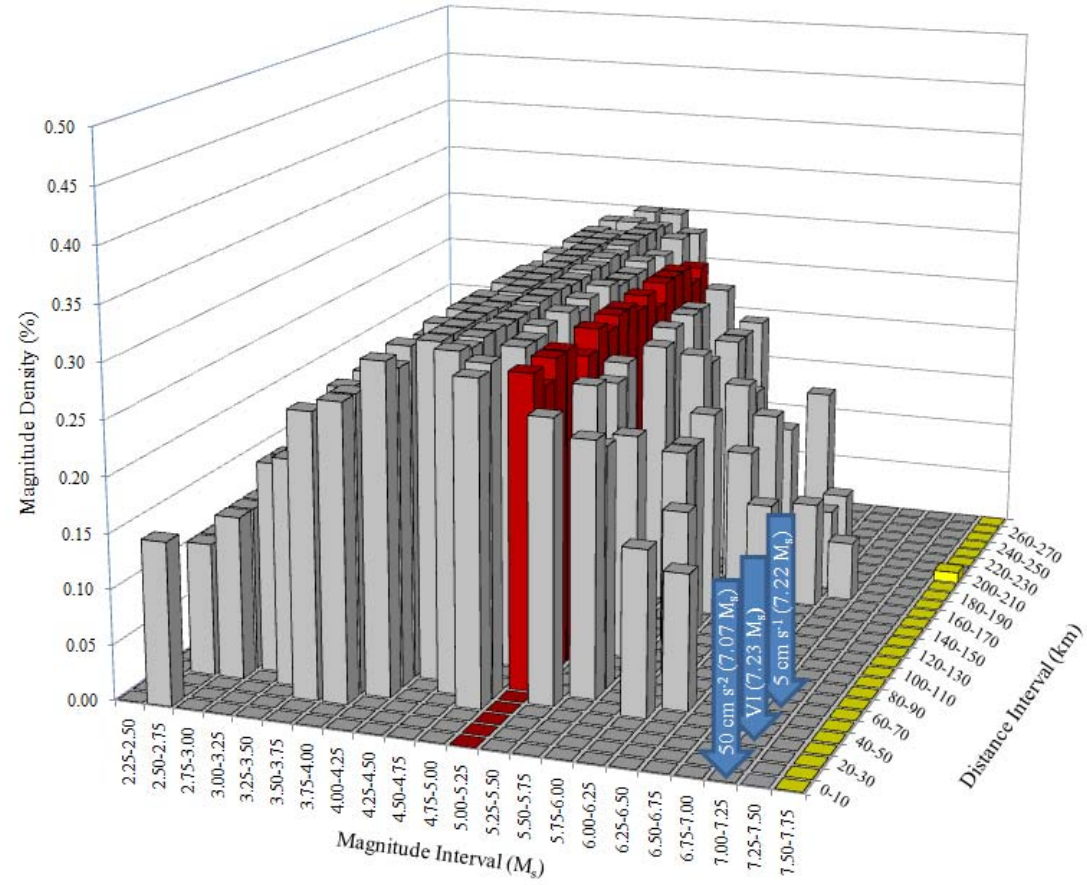

(a)

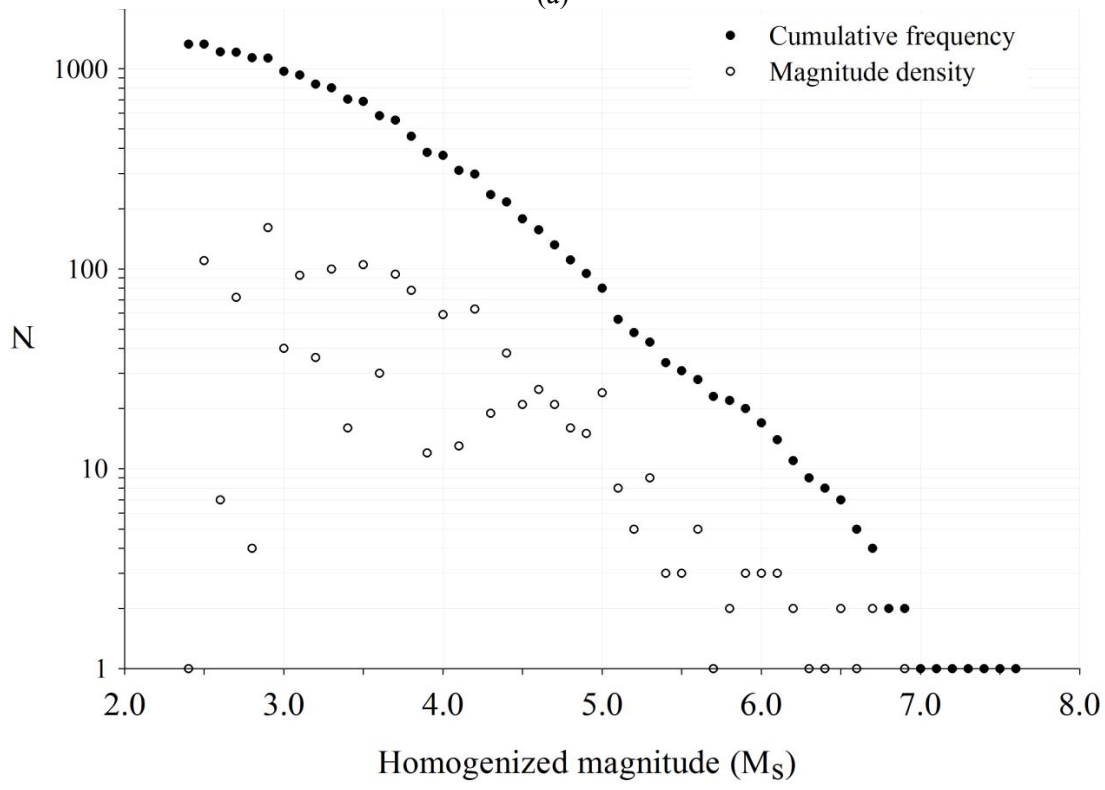

(b)

(a) Seismic source disaggregation and
(b) cumulative frequency and magnitude density distribution around Larissa

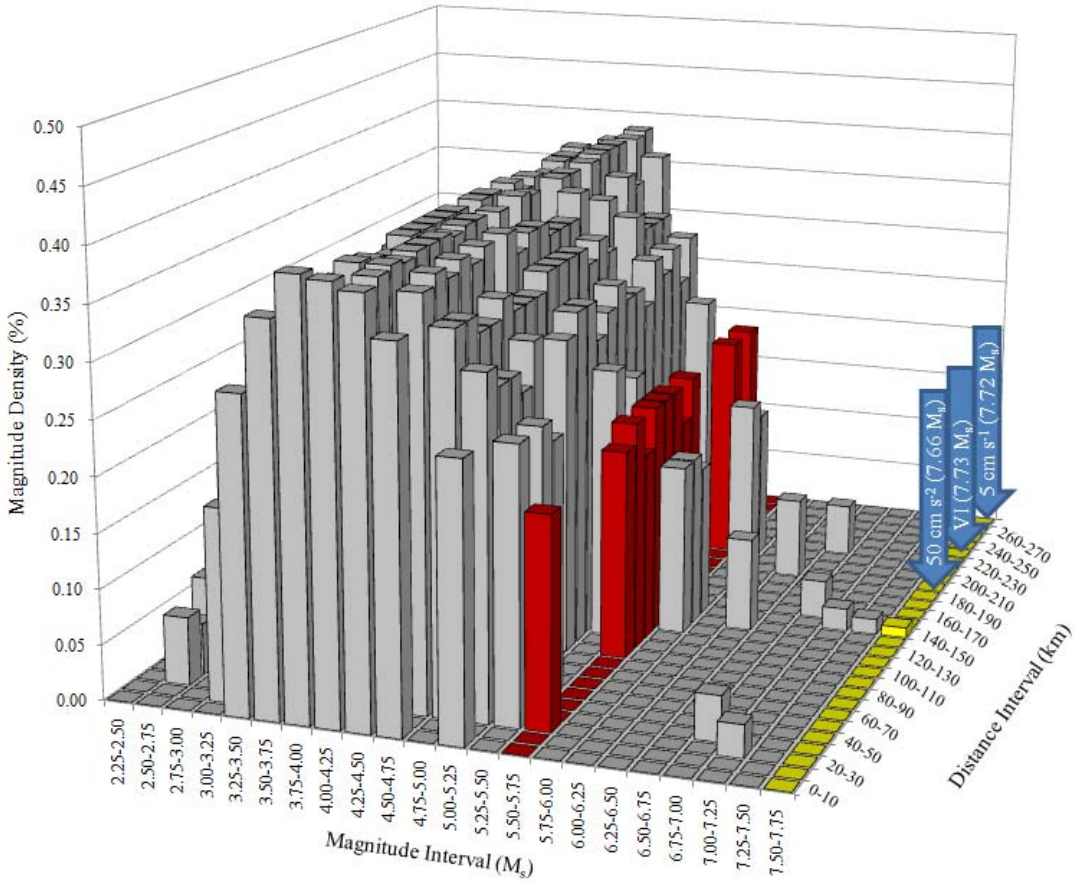

(a)

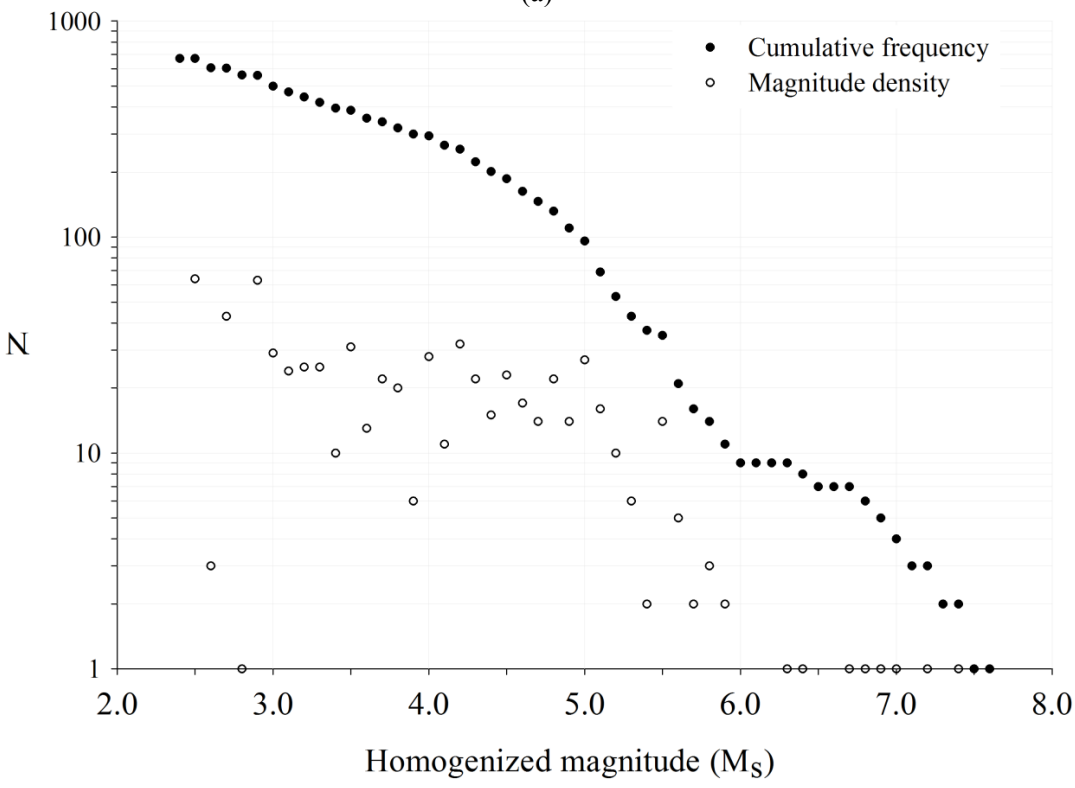

(b)

(a) Seismic source disaggregation and
(b) cumulative frequency and magnitude density distribution around Plovdiv

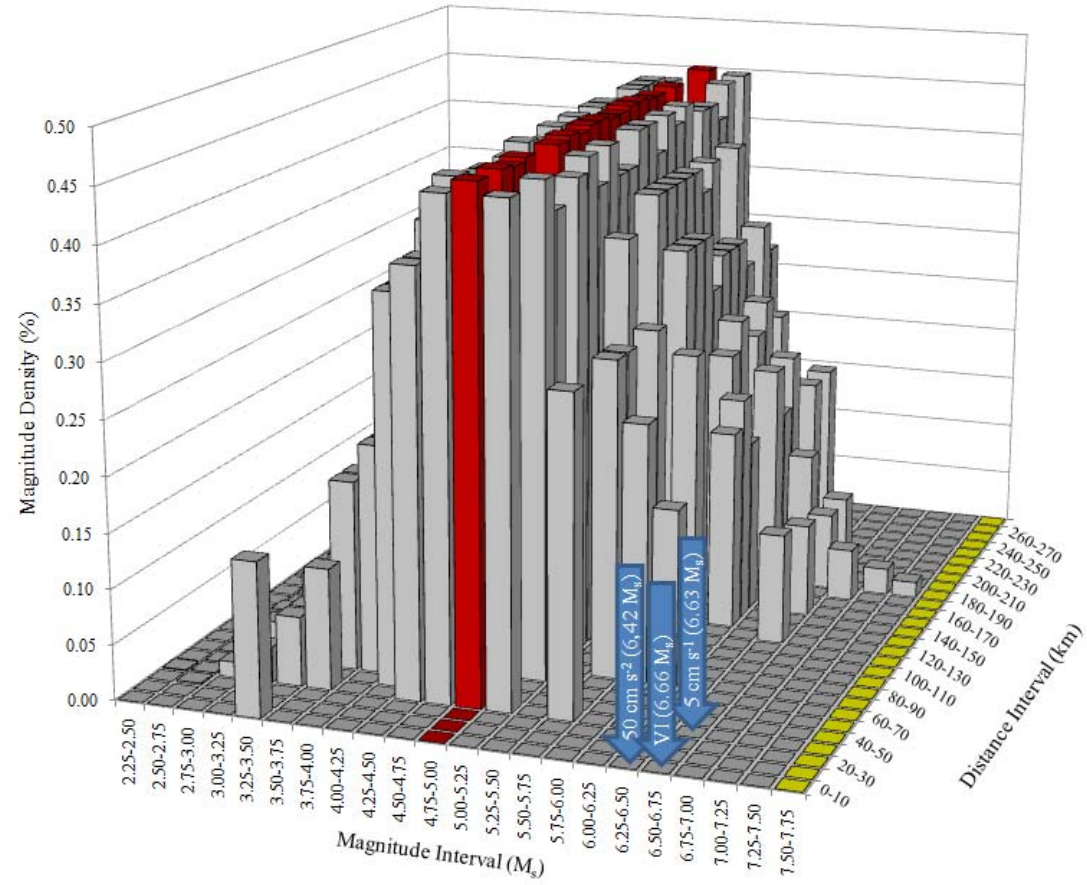

(a)

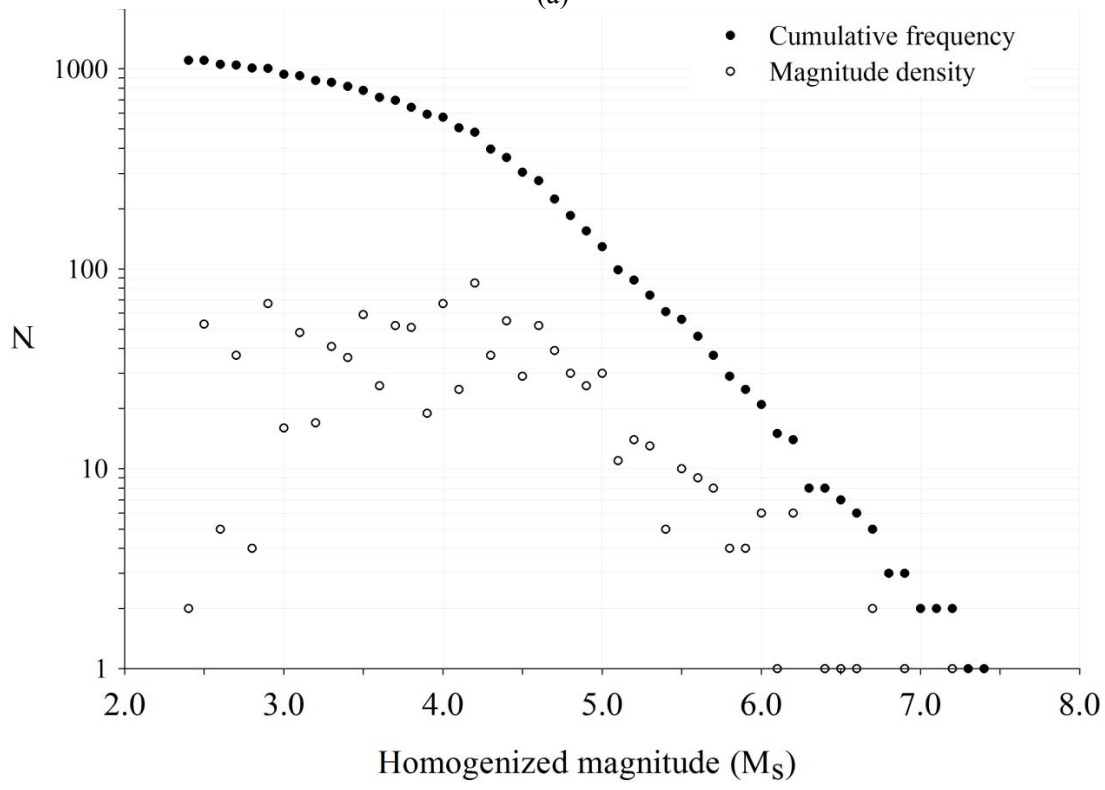

(b)

(a) Seismic source disaggregation and
(b) cumulative frequency and magnitude density distribution around Pristina

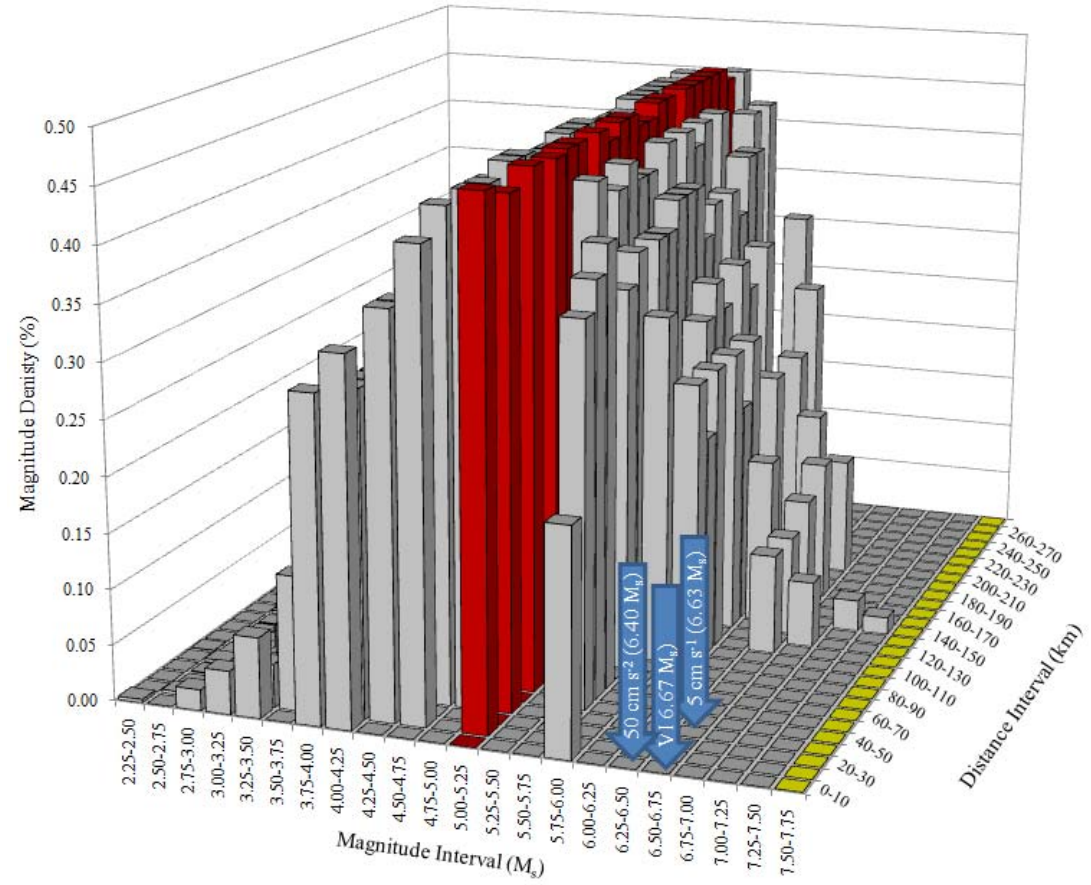

(a)

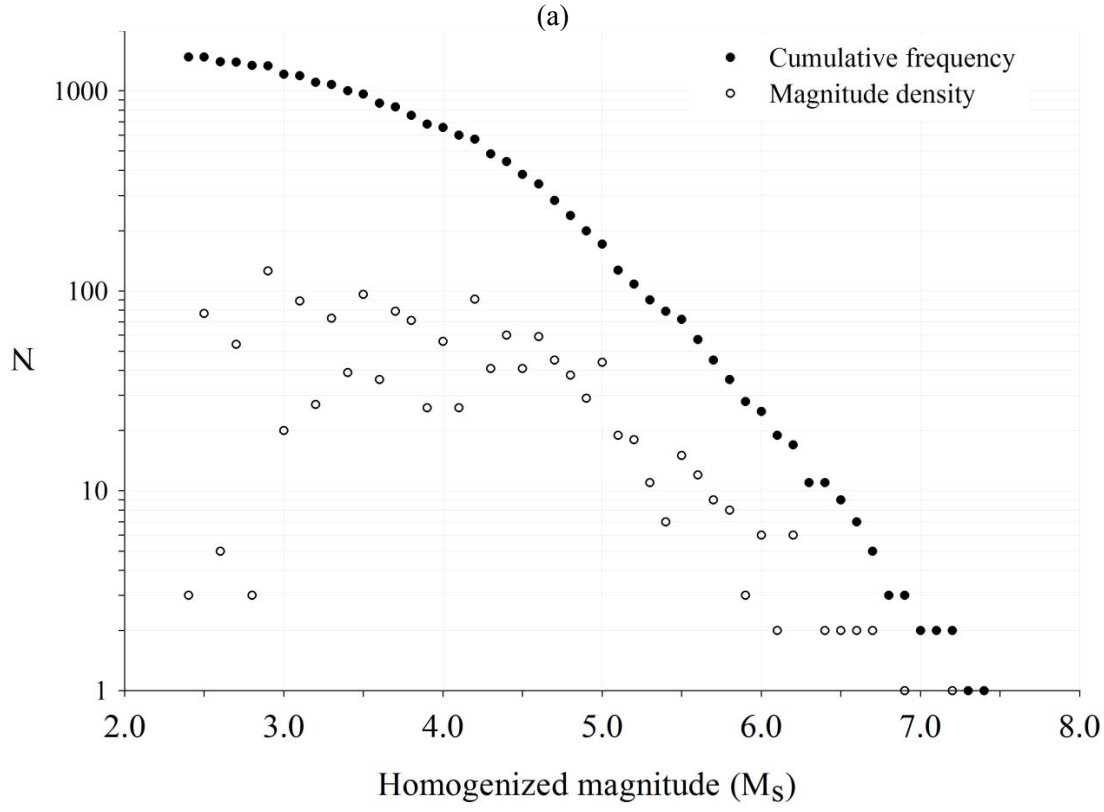

(b)

(a) Seismic source disaggregation and
(b) cumulative frequency and magnitude density distribution around Skopje

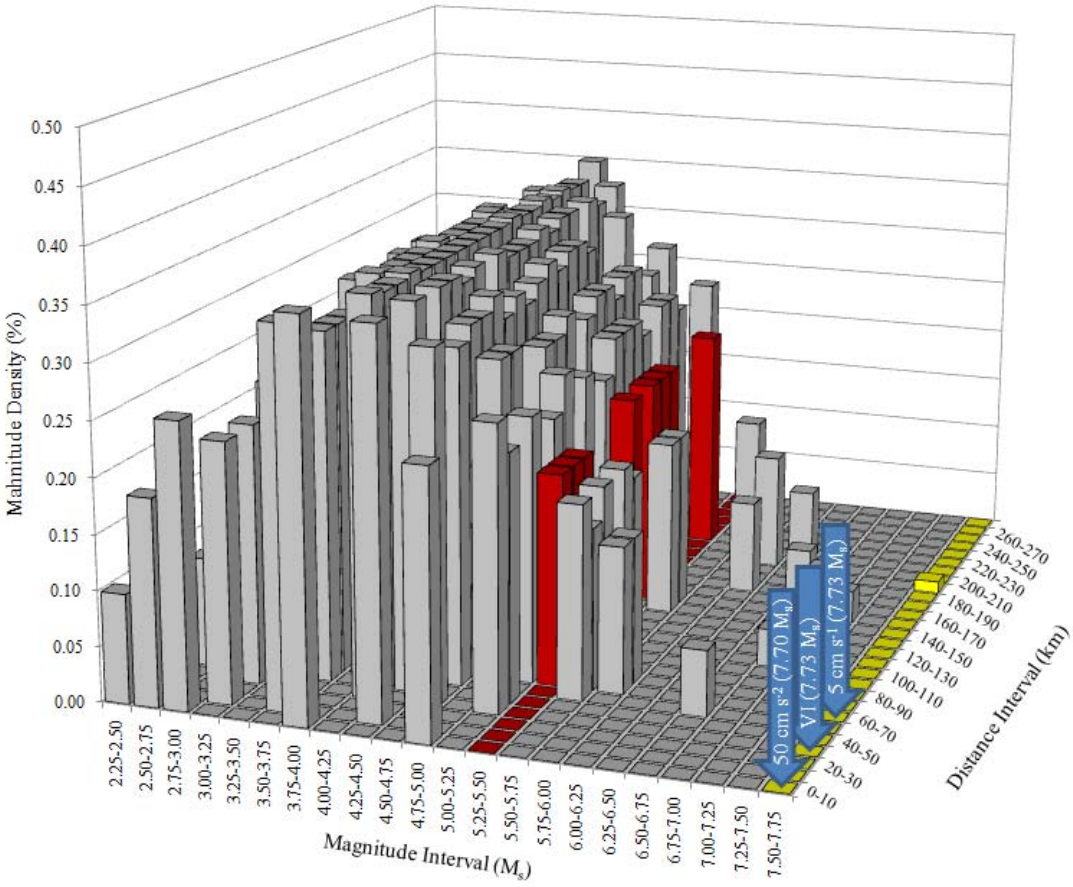

(a)

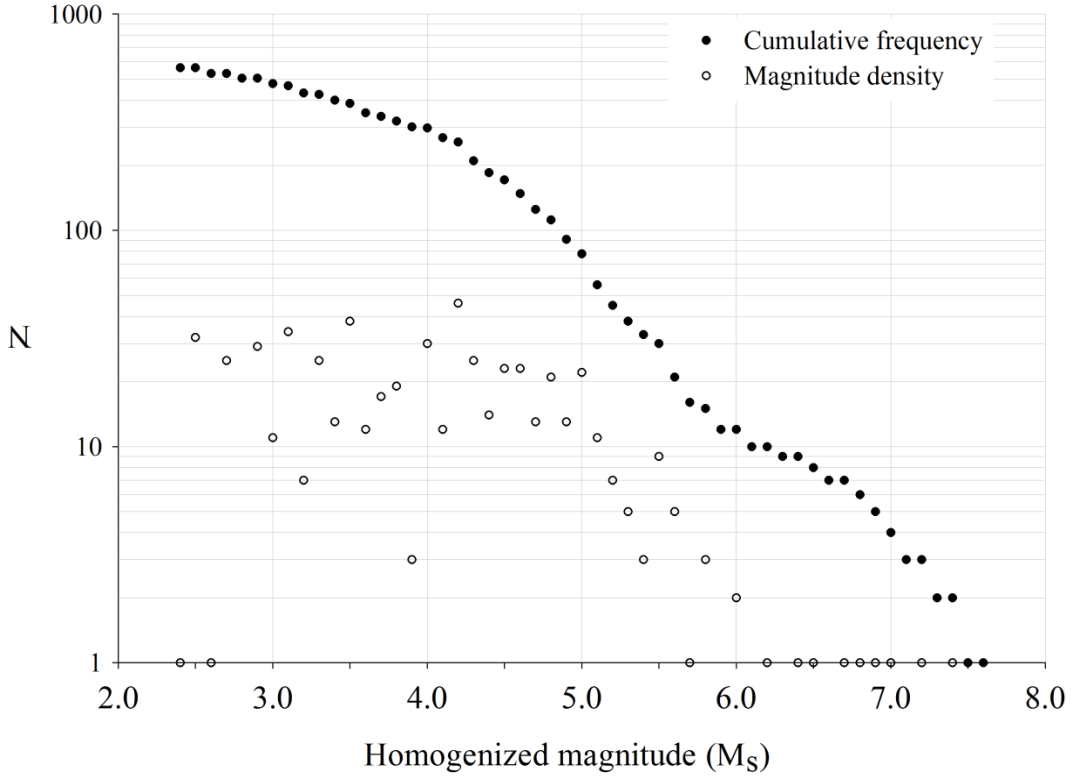

(b)

(a) Seismic source disaggregation and
(b) cumulative frequency and magnitude density distribution around Sofia

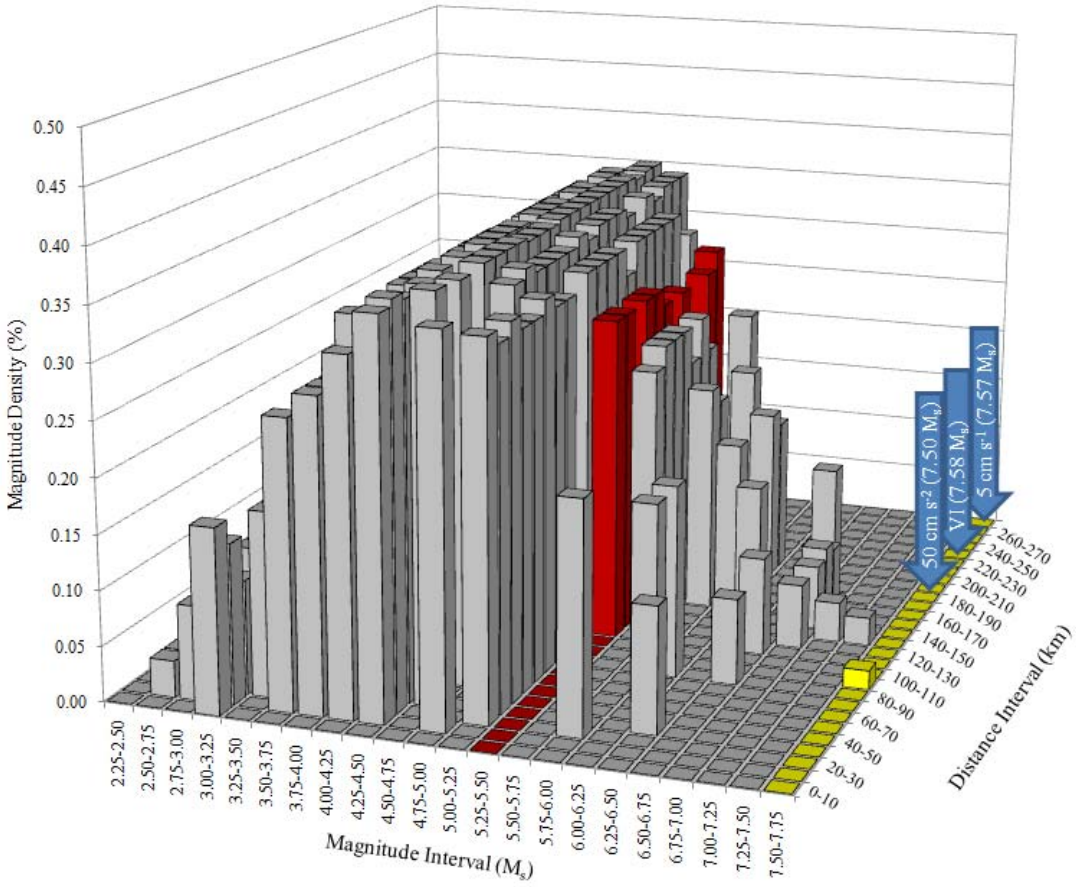

(a)

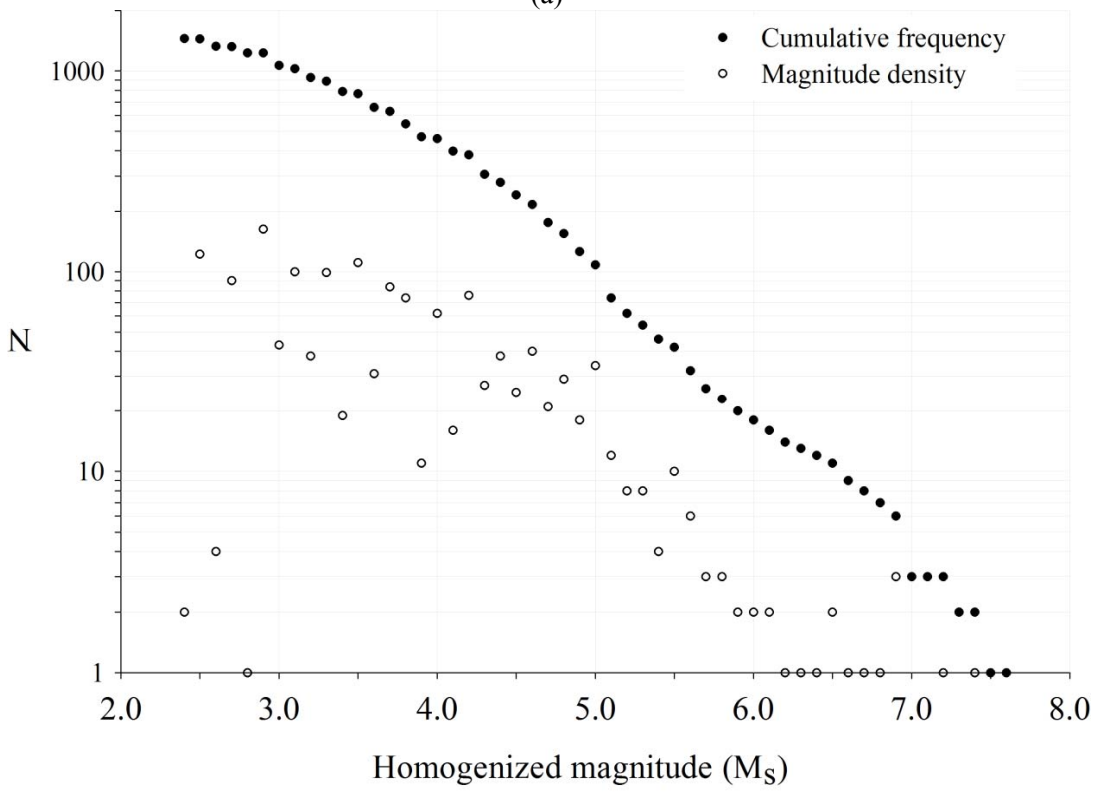

(b)

(a) Seismic source disaggregation and
(b) cumulative frequency and magnitude density distribution around Thessaloniki

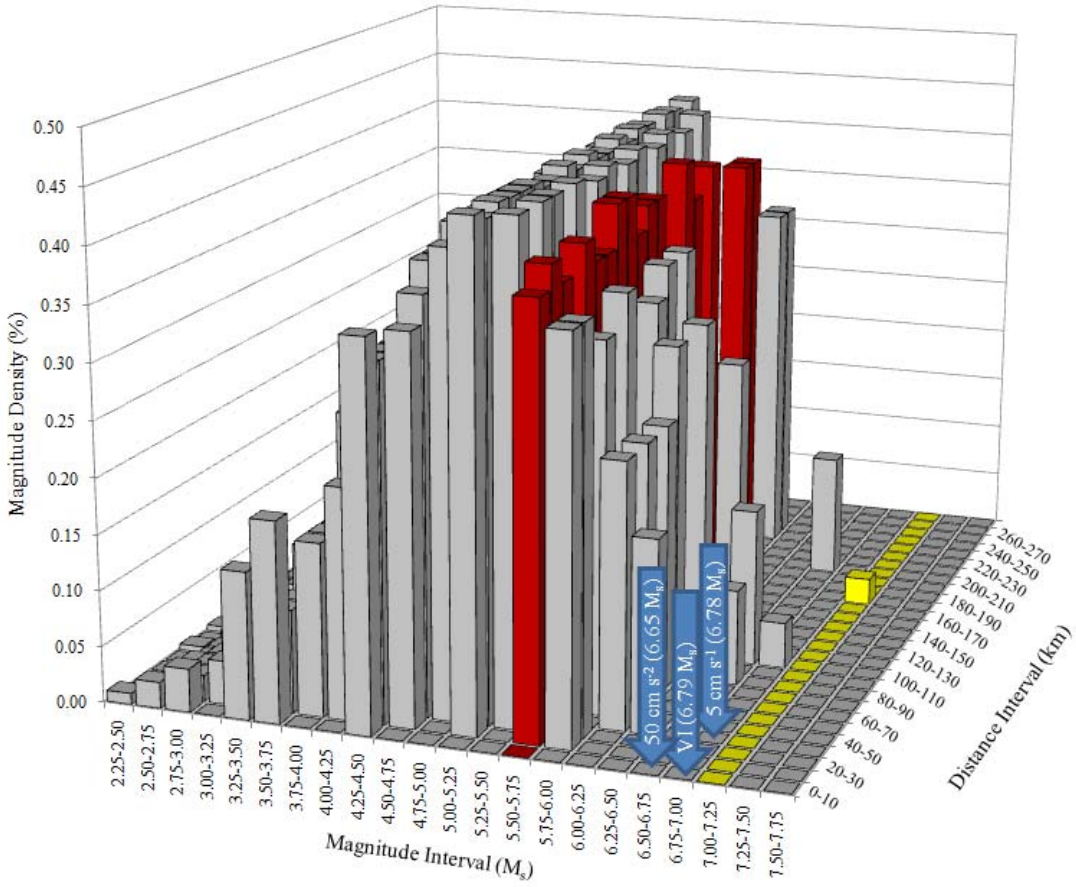

(a)

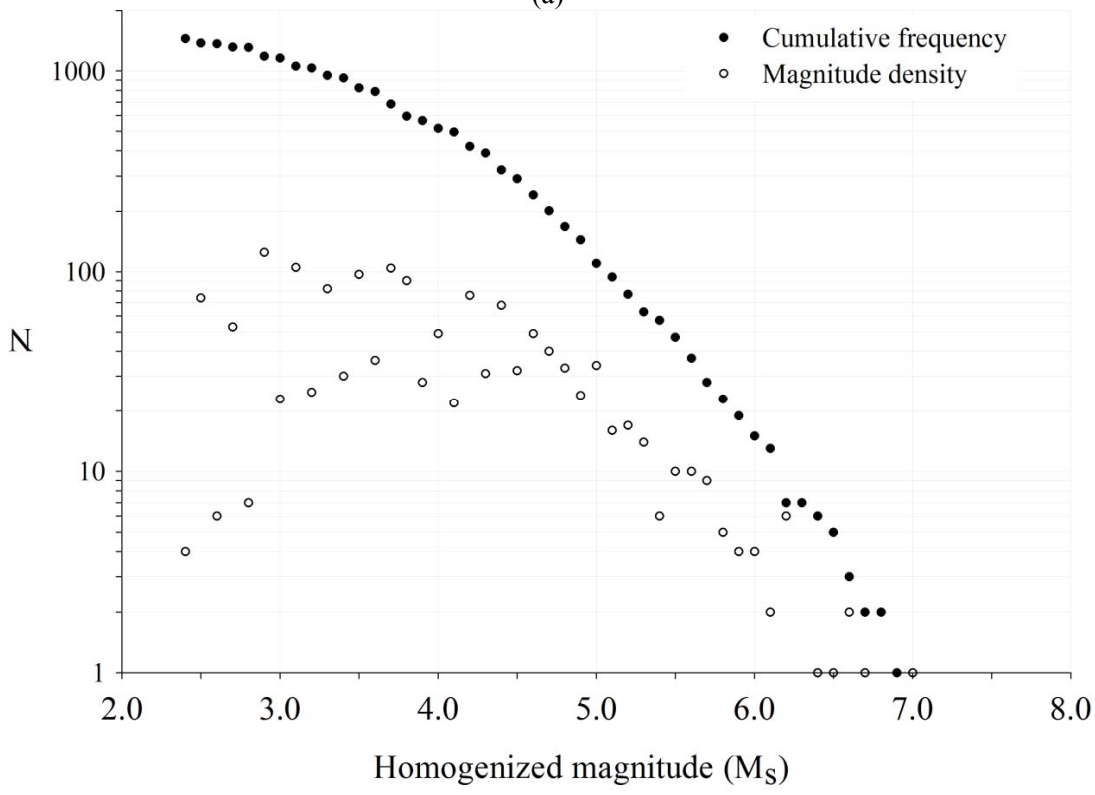

(b)

(a) Seismic source disaggregation and
(b) cumulative frequency and magnitude density distribution around Tirane